# THERMODYNAMICS,

## STATISTICAL THERMODYNAMICS, & KINETICS

THIRD EDITION

THOMAS ENGEL | PHILIP REID

# Thermodynamics, Statistical Thermodynamics, & Kinetics

**THIRD EDITION**

## Thomas Engel
*University of Washington*

## Philip Reid
*University of Washington*

To Walter and Juliane,
my first teachers,
and to Gloria,
Alex,
and Gabrielle.
*Thomas Engel*


To my family.
*Philip Reid*

# Brief Contents

# Contents

# About the Authors

**Thomas Engel** has taught chemistry at the University of Washington for more than 20 years, where he is currently professor emeritus of chemistry. Professor Engel received his bachelor's and master's degrees in chemistry from the Johns Hopkins University, and his Ph.D. in chemistry from the University of Chicago. He then spent 11 years as a researcher in Germany and Switzerland, in which time he received the Dr. rer. nat. habil. degree from the Ludwig Maximilians University in Munich. In 1980, he left the IBM research laboratory in Zurich to become a faculty member at the University of Washington.

Professor Engel's research interests are in the area of surface chemistry, and he has published more than 80 articles and book chapters in this field. He has received the Surface Chemistry or Colloids Award from the American Chemical Society and a Senior Humboldt Research Award from the Alexander von Humboldt Foundation.

**Philip Reid** has taught chemistry at the University of Washington since 1995. Professor Reid received his bachelor's degree from the University of Puget Sound in 1986, and his Ph.D. from the University of California, Berkeley in 1992. He performed postdoctoral research at the University of Minnesota, Twin Cities before moving to Washington.

Professor Reid's research interests are in the areas of atmospheric chemistry, ultrafast condensed-phase reaction dynamics, and organic electronics. He has published more than 100 articles in these fields. Professor Reid is the recipient of a CAREER Award from the National Science Foundation, is a Cottrell Scholar of the Research Corporation, and is a Sloan Fellow. He received the University of Washington Distinguished Teaching Award in 2005.

*This page intentionally left blank*

The third edition of this book builds on user and reviewer comments on the previous editions. Our goal remains to provide students with an accessible overview of the whole field of physical chemistry while focusing on basic principles that unite the subdisciplines of the field. We continue to present new research developments in the field to emphasize the vibrancy of physical chemistry. Many chapters have been extensively revised as described below. We include additional end-of-chapter concept problems and most of the numerical problems have been revised. The target audience remains undergraduate students majoring in chemistry, biochemistry, and chemical engineering, as well as many students majoring in the atmospheric sciences and the biological sciences. The following objectives, illustrated with brief examples, outline our approach to teaching physical chemistry.

- **Focus on teaching core concepts.** The central principles of physical chemistry are explored by focusing on core ideas, and then extending these ideas to a variety of problems. The goal is to build a solid foundation of student understanding rather than cover a wide variety of topics in modest detail.

- **Illustrate the relevance of physical chemistry to the world around us.** Many students struggle to connect physical chemistry concepts to the world around them. To address this issue, example problems and specific topics are tied together to help the student develop this connection. Fuel cells, refrigerators, heat pumps, and real engines are discussed in connection with the second law of thermodynamics. The particle in the box model is used to explain why metals conduct electricity and why valence electrons rather than core electrons are important in chemical bond formation. Examples are used to show the applications of chemical spectroscopies. Every attempt is made to connect fundamental ideas to applications that are familiar to the

U.S. 2002 Carbon Dioxide Emissions from Energy
Consumption – 5,682* Million Metric Tons of $CO_2$**
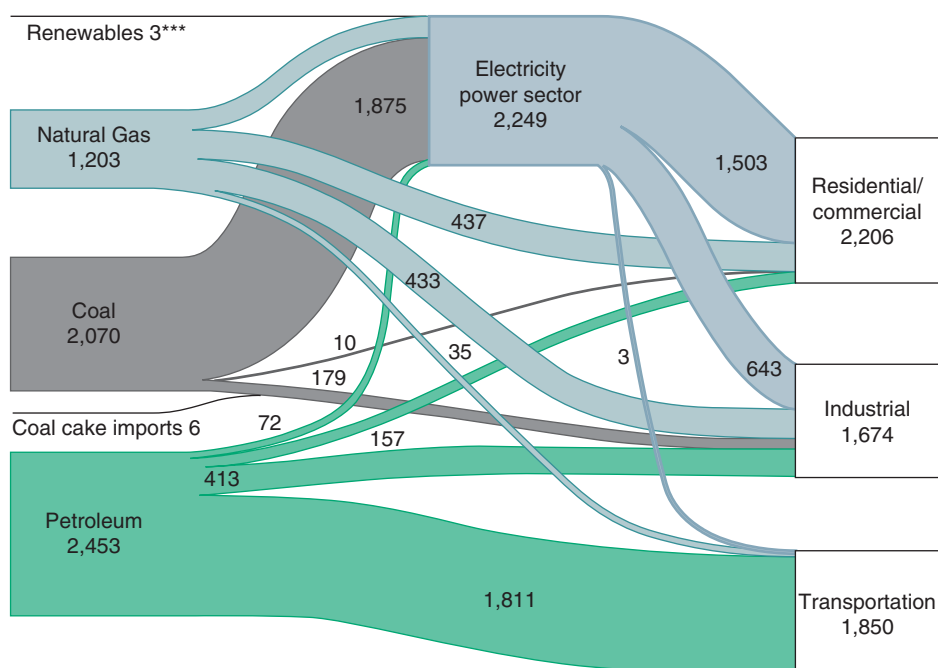


Source: Energy Information Administration. *Emissions of Greenhouse Gases in the United States 2002*. Tables 4–10.
*Includes adjustments of 42.9 million metric tons of carbon dioxide from U.S. territories, less 90.2 $MtCO_2$ from international and military bunker fuels.
**Previous versions of this chart showed emissions in metric tons of carbon, not of $CO_2$.
***Municipal solid waste and geothermal energy.
Note: Numbers may not equal sum of components because of independent rounding.

student. Art is used to convey complex information in an accessible manner as in the images here of U.S. carbon dioxide emissions.

- **Present exciting new science in the field of physical chemistry.** Physical chemistry lies at the forefront of many emerging areas of modern chemical research. Recent applications of quantum behavior include band-gap engineering, quantum dots, quantum wells, teleportation, and quantum computing. Single-molecule spectroscopy has led to a deeper understanding of chemical kinetics, and heterogeneous catalysis has benefited greatly from mechanistic studies carried out using the techniques of modern surface science. Atomic scale electrochemistry has become possible through scanning tunneling microscopy. The role of physical chemistry in these and other emerging areas is highlighted throughout the text. The following figure shows working principles for different types of fuel cells.

**Types of fuel cells**

Direct methanol fuel cell

Polymer electrolyte fuel cell

Proton exchange membrane fuel cells (PEMFC)

Enzymatic fuel cell

Alkaline fuel cell

Phosphoric acid fuel cell

Molten carbonate fuel cell

Solid oxide fuel cell

Legend of components:
A = anode
E = electrolyte
C = cathode
PEM = proton exchange membrane
YSZ = yttria-stabilized zirconia
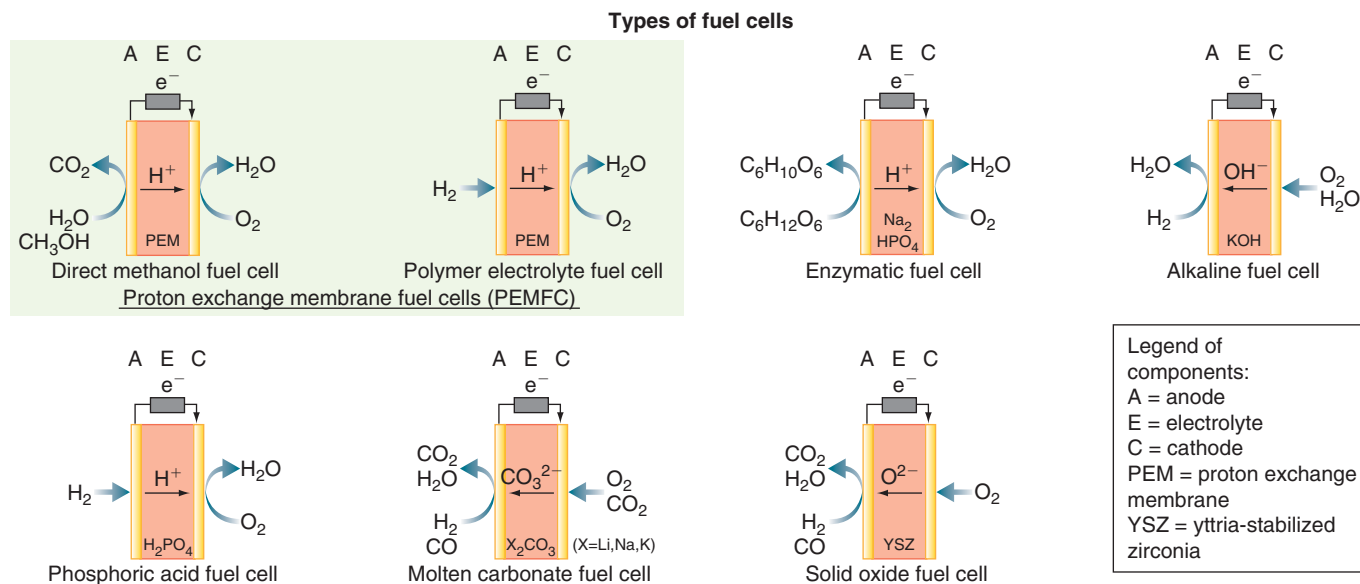
- **Web-based simulations illustrate the concepts being explored and avoid math overload.** Mathematics is central to physical chemistry; however, the mathematics can distract the student from "seeing" the underlying concepts. To circumvent this problem, web-based simulations have been incorporated as end-of-chapter problems throughout the book so that the student can focus on the science and avoid a math overload. These web-based simulations can also be used by instructors during lecture. An important feature of the simulations is that each problem has been designed as an assignable exercise with a printable answer sheet that the student can submit to the instructor. The Study Area in MasteringChemistry® also includes a graphing routine with a curve-fitting capability, which allows students to print and submit graphical data. The 50 web-based simulations listed in the end-of-chapter
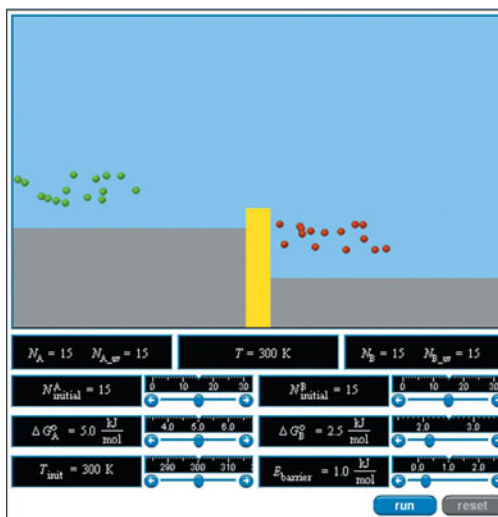
problems are available in the Study Area of MasteringChemistry® for Physical Chemistry. MasteringChemistry® also includes a broad selection of end-of-chapter problems with answer-specific feedback.

- **Show that learning problem-solving skills is an essential part of physical chemistry.**   Many example problems are worked through in each chapter. They introduce the student to a useful method to solve physical chemistry problems.

---

**EXAMPLE PROBLEM 2.5**

A system containing 2.50 mol of an ideal gas for which $C_{V,m} = 20.79$ J mol$^{-1}$ K$^{-1}$ is taken through the cycle in the following diagram in the direction indicated by the arrows. The curved path corresponds to $PV = nRT$, where $T = T_1 = T_3$.
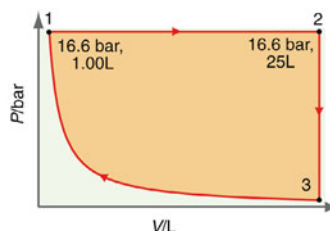
a. Calculate $q$, $w$, $\Delta U$, and $\Delta H$ for each segment and for the cycle assuming that the heat capacity is independent of temperature.

b. Calculate $q$, $w$, $\Delta U$, and $\Delta H$ for each segment and for the cycle in which the direction of each process is reversed.



- **The End-of-Chapter Problems cover a range of difficulties suitable for students at all levels.**

**P8.6**   A $P-T$ phase diagram for potassium is shown next.
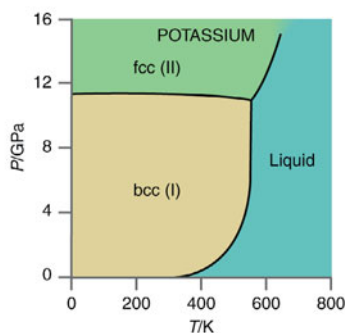


*Source: Phase Diagrams of the Elements* by David A. Young. © 1991 Regents of the University of California. Published by the University of California Press.

a. Which phase has the higher density, the fcc or the bcc phase? Explain your answer.

b. Indicate the range of $P$ and $T$ in the phase diagram for which fcc and liquid potassium are in equilibrium. Does fcc potassium float on or sink in liquid potassium? Explain your answer.

c. Redraw this diagram for a different pressure range and indicate where you expect to find the vapor phase. Explain how you chose the slope of your liquid–vapor coexistence line.

- **Conceptual questions at the end of each chapter ensure that students learn to express their ideas in the language of science.**

---

## Conceptual Problems

**Q5.1**   Under what conditions is $\Delta S < 0$ for a spontaneous process?

**Q5.2**   Why are $\Delta S_{fusion}$ and $\Delta S_{vaporization}$ always positive?

**Q5.3**   An ideal gas in thermal contact with the surroundings is cooled in an irreversible process at constant pressure. Are $\Delta S$, $\Delta S_{surroundings}$, and $\Delta S_{total}$ positive, negative, or zero? Explain your reasoning.

**Q5.4**   The amplitude of a pendulum consisting of a mass on a long wire is initially adjusted to have a very small value. The amplitude is found to decrease slowly with time. Is this process reversible? Would the process be reversible if the amplitude did not decrease with time?

**Q5.5**   A process involving an ideal gas and in which the temperature changes at constant volume is carried out. For a fixed value of $\Delta T$, the mass of the gas is doubled. The process is repeated with the same initial mass and $\Delta T$ is doubled. For which of these processes is $\Delta S$ greater? Why?

**Q5.6**   You are told that $\Delta S = 0$ for a process in which the system is coupled to its surroundings. Can you conclude that the process is reversible? Justify your answer.

**Q5.12**   An ideal gas undergoes an adiabatic expansion into a vacuum. Are $\Delta S$, $\Delta S_{surroundings}$, and $\Delta S_{total}$ positive, negative, or zero? Explain your reasoning.

**Q5.13**   When a saturated solution of a salt is cooled, a precipitate crystallizes out. Is the entropy of the crystalline precipitate greater or less than the dissolved solute? Explain why this process is spontaneous.

**Q5.14**   A system undergoes a change from one state to another along two different pathways, one of which is reversible and the other of which is irreversible. What can you say about the relative magnitudes of $q_{reversible}$ and $q_{irreversible}$?

**Q5.15**   An ideal gas in a piston and cylinder assembly with adiabatic walls undergoes an expansion against a constant external pressure. Are $\Delta S$, $\Delta S_{surroundings}$, and $\Delta S_{total}$ positive, negative, or zero? Explain your reasoning.

**Q5.16**   Is the equation

$$\Delta S = \int_{T_i}^{T_f} \frac{C_V}{T}\, dT + \int_{V_i}^{V_f} \frac{\beta}{\kappa}\, dV = C_V \ln \frac{T_f}{T_i} + \frac{\beta}{\kappa}(V_f - V_i)$$

- **Integrate computational chemistry into the standard curriculum.** The teaching of quantum mechanics has not taken advantage of the widespread availability of Ab Initio Software. Many chapters include computational problems for which detailed instructions for the student are available in the Study Area in MasteringChemistry®. It is our experience that students welcome this material, (see L. Johnson and T. Engel, *Journal of Chemical Education* 2011, 88 [569-573]) which transforms the teaching of chemical bonding and molecular structure from being qualitative to quantitative. For example, in computational problem C18.1, students calculate a portion of the ground state potential surface for CF3Cl in order to understand the dissociation of the C-Cl bond in this molecule.

- **Key equations.** Physical chemistry is a chemistry subdiscipline that is mathematics intensive in nature. Key equations that summarize fundamental relationships between variables are colored in red for emphasis.

- **Green boxes.** Fundamental principles such as the laws of thermodynamics and the quantum mechanical postulates are displayed in green boxes.

- **Updated graph design.** Color is used in graphs to clearly display different relationships in a single figure as shown in the heat capacity for oxygen as a function of temperature and the cell potential of a lithium ion battery versus the energy density for a number of electrode materials.
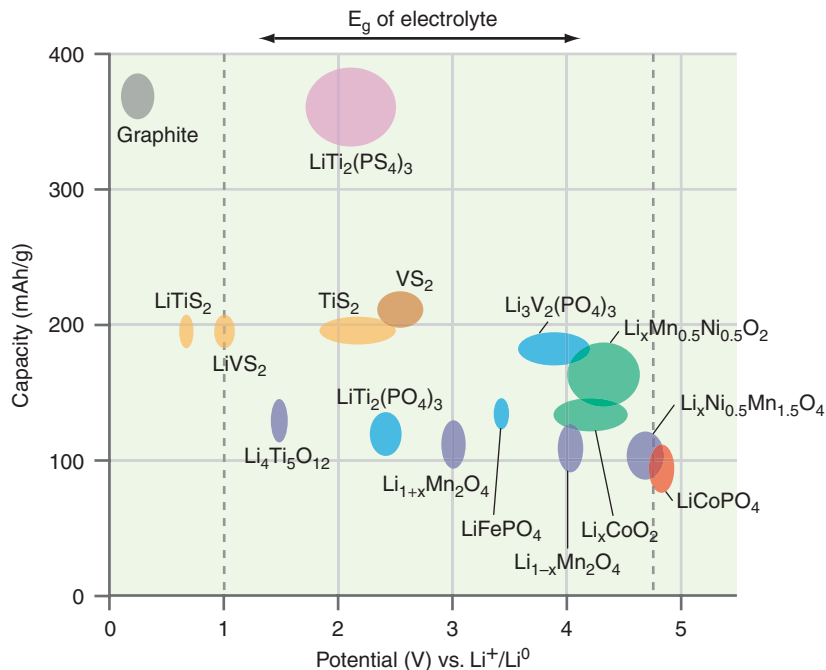
This text contains more material than can be covered in an academic year, and this is entirely intentional. Effective use of the text does not require a class to proceed sequentially through the chapters, or to include all sections. Some topics are discussed in supplemental sections that can be omitted if they are not viewed as essential to the course. Also, many sections are self contained so that they can be readily omitted if they do not serve the needs of the instructor. This text is constructed to be flexible to your needs, not the other way around. We welcome the comments of both students and instructors on how the material was used and how the presentation can be improved.

Thomas Engel
*University of Washington*

Philip Reid
*University of Washington*

# New to This Edition

The third edition of *Thermodynamics, Statistical Thermodynamics, & Kinetics* includes changes at several levels. The most far-reaching change is the introduction of MasteringChemistry® for Physical Chemistry. Over 460 tutorials will augment the example problems in the book and enhance active learning and problem solving. Selected end-of-chapter problems are now assignable within MasteringChemistry® and numerical, equation, and symbolic answer types are automatically graded.

The art program has been updated and expanded, and several levels of accuracy checking have been incorporated to increase accuracy throughout the text. Many new conceptual problems have been added to the book and most of the numerical problems have been revised. Significant content updates include moving part of the kinetic gas theory to Chapter 1 to allow a molecular level discussion of $P$ and $T$. The heat capacity discussion previously in sections 2.5 and 3.2 have been consolidated in Chapter 2, and a new section on doing work and changing the system energy from a molecular level perspective has been added. The discussion of differential scanning calorimetry in Chapter 4 has been expanded and a molecular level discussion of entropy has been added to Chapter 5. The discussion of batteries and fuel cells in Chapter 11 has been revised and updated. The content on transition state theory in Chapter 15 has been updated. A discussion of oscillating reactions has been added to Chapter 19 and the material on electron transfer has been expanded.

# Acknowledgments

### 3RD EDITION

### MANUSCRIPT REVIEWERS

Nathan Hammer,
*The University of Mississippi*
Geoffrey Hutchinson,
*University of Pittsburgh*
George Kaminski,
*Central Michigan University*

Herve Marand,
*Virginia Polytechnic Institute and
State University*
Paul Siders,
*University of Minnesota–Duluth*

### ACCURACY REVIEWERS

Alexander Angerhofer,
*University of Florida*
Clayton Baum,
*Florida Institute of Technology*

Jennifer Mihalik,
*University of Wisconsin–Oshkosh*
David Zax,
*Cornell University*

### PRESCRIPTIVE REVIEWERS

Geoffrey Hutchinson,
*University of Pittsburgh*
William Lester,
*University of California–Berkeley*
Herve Marand,
*Virginia Polytechnic Institute and
State University*

Thomas Mason,
*University of California–Los Angeles*
Paul Siders,
*University of Minnesota–Duluth*

### 2ND EDITION

### PRESCRIPTIVE REVIEWERS

David L. Cedeño,
*Illinois State University*
Rosemarie Chinni,
*Alvernia College*
Allen Clabo,
*Francis Marion University*
Lorrie Comeford,
*Salem State College*
John M. Jean,
*Regis University*
Martina Kaledin,
*Kennesaw State University*
Daniel Lawson,
*University of Michigan–Dearborn*
Dmitrii E. Makarov,
*University of Texas at Austin*

Enrique Peacock-López,
*Williams College*
Anthony K. Rappe,
*Colorado State University*
Markku Räsänen,
*University of Helsinki*
Richard W. Schwenz,
*University of Northern Colorado*
Jie Song,
*University of Michigan–Flint*
Michael E. Starzak,
*Binghamton University*
Liliya Vugmeyster,
*University of Alaska–Anchorage*
James E. Whitten,
*University of Massachusetts–Lowell*

## ART REVIEWER

Lorrie Comeford,
*Salem State College*

## MATH REVIEWER

Leon Gerber,
*St. John's University*

## MANUSCRIPT REVIEWERS

Alexander Angerhofer,
*University of Florida*

Martha Bruch,
*State University of New York at Oswego*

Stephen Cooke,
*University of North Texas*

Douglas English,
*University of Maryland–College Park*

Sophya Garashchuk,
*University of South Carolina*

Cynthia Hartzell,
*Northern Arizona University*

George Kaminski,
*Central Michigan University*

Herve Marand,
*Virginia Polytechnic Institute and State University*

Thomas Pentecost,
*University of Colorado*

Rajeev Prabhakar,
*University of Miami*

Sanford Safron,
*Florida State University*

Ali Sezer,
*California University of Pennsylvania*

Andrew Teplyakov,
*University of Delaware*

Daniel Zeroka,
*Lehigh University*

# Mastering Chemistry®

## www.masteringchemistry.com

MasteringChemistry® is designed with a single purpose: to help students reach the moment of understanding. The Mastering online homework and tutoring system delivers self-paced tutorials that provide students with individualized coaching set to your course objectives. MasteringChemistry® helps students arrive better prepared for lecture and lab.

## Engaging Experiences

MasteringChemistry® promotes interactivity in Physical Chemistry. Research shows that Mastering's immediate feedback and tutorial assistance helps students understand and master concepts and skills in Chemistry—allowing them to retain more knowledge and perform better in this course and beyond.



### STUDENT TUTORIALS

MasteringChemistry® is the only system to provide instantaneous feedback specific to individual student entries. Students can submit an answer and receive immediate, error-specific feedback. Simpler sub-problems—hints—help students think through the problem. Over 460 tutorials will be available with MasteringChemistry® for Physical Chemistry including new ones on The Cyclic Rule, Particle in a Box, and Components of *U*.

### END-OF-CHAPTER CONTENT AVAILABLE IN MASTERINGCHEMISTRY®:

Selected end-of-chapter problems are assignable within MasteringChemistry®, including:

• **Numerical answers** with hints and feedback

• **Equation and Symbolic answer types** so that the results of a self-derivation can be entered to check for correctness, feedback, and assistance

• A **Solution View** that allows students to see intermediate steps involved in calculations of the final numerical result

# Trusted Partner

The Mastering platform was developed by scientists for science students and instructors, and has a proven history with over 10 years of student use. Mastering currently has more than 1.5 million active registrations with active users in all 50 states and in 41 countries. The Mastering platform has 99.8% server reliability.



## PEARSON ETEXT

Pearson eText provides access to the text when and wherever students have access to the Internet. eText pages look exactly like the printed text, offering powerful new functionality. Users can create notes, highlight the text in different colors, create bookmarks, zoom, click hyperlinked words and phrases to view definitions, view as single or two-pages. Pearson eText also links students to associated media files, enabling them to view an animation as they read the text, and offers a full text search and the ability to save and export notes.

## GRADEBOOK

Every assignment is automatically graded. Shades of red highlight vulnerable students and challenging assignments.



## GRADEBOOK DIAGNOSTICS

This screen provides you with your favorite diagnostics. With a single click, charts summarize the most difficult problems, vulnerable students, grade distribution, and even score improvement over the course.

*This page intentionally left blank*

# Fundamental Concepts of Thermodynamics

Thermodynamics provides a description of matter on a macroscopic scale using bulk properties such as pressure, density, volume, and temperature. This chapter introduces the basic concepts employed in thermodynamics including system, surroundings, intensive and extensive variables, adiabatic and diathermal walls, equilibrium, temperature, and thermometry. The macroscopic variables pressure and temperature are also discussed in terms of a molecular level model. The usefulness of equations of state, which relate the state variables of pressure, volume, and temperature, is also discussed for real and ideal gases.

## 1.1 What Is Thermodynamics and Why Is It Useful?

Thermodynamics is the branch of science that describes the behavior of matter and the transformation between different forms of energy on a **macroscopic scale,** or the human scale and larger. Thermodynamics describes a system of interest in terms of its bulk properties. Only a few such variables are needed to describe the system, and the variables are generally directly accessible through measurements. A thermodynamic description of matter does not make reference to its structure and behavior at the microscopic level. For example, 1 mol of gaseous water at a sufficiently low density is completely described by two of the three **macroscopic variables** of pressure, volume, and temperature. By contrast, the microscopic scale refers to dimensions on the order of the size of molecules. At the microscopic level, water would be described as a dipolar triatomic molecule, $H_2O$, with a bond angle of 104.5° that forms a network of hydrogen bonds.

In this book, we first discuss thermodynamics and then statistical thermodynamics. Statistical thermodynamics (Chapters 14 and 15) uses atomic and molecular properties to calculate the macroscopic properties of matter. For example, statistical thermodynamics can show that liquid water is the stable form of aggregation at a pressure of 1 bar and a temperature of 90°C, whereas gaseous water is the stable form at 1 bar and 110°C. Using statistical thermodynamics, the macroscopic properties of matter are calculated from underlying molecular properties.

Given that the microscopic nature of matter is becoming increasingly well understood using theories such as quantum mechanics, why is a macroscopic science like thermodynamics relevant today? The usefulness of thermodynamics can be illustrated by describing four applications of thermodynamics which you will have mastered after working through this book:

- You have built a plant to synthesize $NH_3$ gas from $N_2$ and $H_2$. You find that the yield is insufficient to make the process profitable and decide to try to improve the $NH_3$ output by changing the temperature and/or the pressure. However, you do not know whether to increase or decrease the values of these variables. As will be shown in Chapter 6, the ammonia yield will be higher at equilibrium if the temperature is decreased and the pressure is increased.

- You wish to use methanol to power a car. One engineer provides a design for an internal combustion engine that will burn methanol efficiently according to the reaction $CH_3OH(l) + 3/2 O_2(g) \rightarrow CO_2(g) + 2H_2O(l)$. A second engineer designs an electrochemical fuel cell that carries out the same reaction. He claims that the vehicle will travel much farther if powered by the fuel cell than by the internal combustion engine. As will be shown in Chapter 5, this assertion is correct, and an estimate of the relative efficiencies of the two propulsion systems can be made.

- You are asked to design a new battery that will be used to power a hybrid car. Because the voltage required by the driving motors is much higher than can be generated in a single electrochemical cell, many cells must be connected in series. Because the space for the battery is limited, as few cells as possible should be used. You are given a list of possible cell reactions and told to determine the number of cells needed to generate the required voltage. As you will learn in Chapter 11, this problem can be solved using tabulated values of thermodynamic functions.

- Your attempts to synthesize a new and potentially very marketable compound have consistently led to yields that make it unprofitable to begin production. A supervisor suggests a major effort to make the compound by first synthesizing a catalyst that promotes the reaction. How can you decide if this effort is worth the required investment? As will be shown in Chapter 6, the maximum yield expected under equilibrium conditions should be calculated first. If this yield is insufficient, a catalyst is useless.

---

## 1.2 The Macroscopic Variables Volume, Pressure, and Temperature

We begin our discussion of thermodynamics by considering a bottle of a gas such as He or $CH_4$. At a macroscopic level, the sample of known chemical composition is completely described by the measurable quantities volume, pressure, and temperature for which we use the symbols $V$, $P$, and $T$. The volume $V$ is just that of the bottle. What physical association do we have with $P$ and $T$?

Pressure is the force exerted by the gas per unit area of the container. It is most easily understood by considering a microscopic model of the gas known as the kinetic theory of gases. The gas is described by two assumptions: the atoms or molecules of an ideal gas do not interact with one another, and the atoms or molecules can be treated as point masses. The pressure exerted by a gas on the container confining the gas arises from collisions of randomly moving gas molecules with the container walls. Because the number of molecules in a small volume of the gas is on the order of Avogadro's number $N_A$, the number of collisions between molecules is also large. To describe pressure, a molecule is envisioned as traveling through space with a velocity vector $\mathbf{v}$ that can be decomposed into three Cartesian components: $\mathbf{v}_x$, $\mathbf{v}_y$, and $\mathbf{v}_z$ as illustrated in Figure 1.1.

The square of the magnitude of the velocity $v^2$ in terms of the three velocity components is
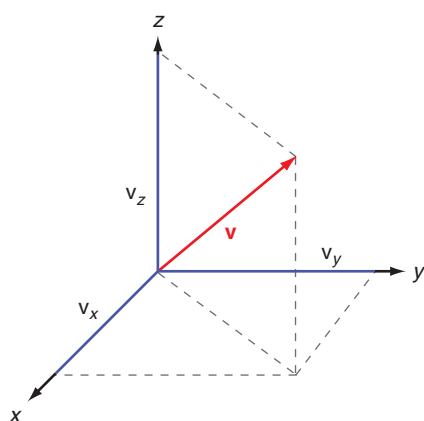


**FIGURE 1.1**

Cartesian components of velocity. The particle velocity $\mathbf{v}$ can be decomposed into three velocity components: $\mathbf{v}_x$, $\mathbf{v}_y$, and $\mathbf{v}_z$.

$$v^2 = \mathbf{v} \cdot \mathbf{v} = v_x^2 + v_y^2 + v_z^2 \qquad \textbf{(1.1)}$$

The particle kinetic energy is $1/2\ mv^2$ such that

$$\varepsilon_{Tr} = \frac{1}{2}mv^2 = \frac{1}{2}mv_x^2 + \frac{1}{2}mv_y^2 + \frac{1}{2}mv_z^2 = \varepsilon_{Tr_x} + \varepsilon_{Tr_y} + \varepsilon_{Tr_z} \quad \textbf{(1.2)}$$

where the subscript $Tr$ indicates that the energy corresponds to translational motion of the particle. Furthermore, this equation states that the total translational energy is the sum of translational energy along each Cartesian dimension.

Pressure arises from the collisions of gas particles with the walls of the container; therefore, to describe pressure we must consider what occurs when a gas particle collides with the wall. First, we assume that the collisions with the wall are **elastic collisions,** meaning that translational energy of the particle is conserved. Although the collision is elastic, this does not mean that nothing happens. As a result of the collision, linear momentum is imparted to the wall, which results in pressure. The definition of pressure is force per unit area and, by Newton's second law, force is equal to the product of mass and acceleration. Using these two definitions, the pressure arising from the collision of a single molecule with the wall is expressed as

$$P = \frac{F}{A} = \frac{ma_i}{A} = \frac{m}{A}\left(\frac{dv_i}{dt}\right) = \frac{1}{A}\left(\frac{dmv_i}{dt}\right) = \frac{1}{A}\left(\frac{dp_i}{dt}\right) \quad \textbf{(1.3)}$$

In Equation (1.3), $F$ is the force of the collision, $A$ is the area of the wall with which the particle has collided, $m$ is the mass of the particle, $v_i$ is the velocity component along the $i$ direction ($i = x$, $y$, or $z$), and $p_i$ is the particle linear momentum in the $i$ direction. Equation (1.3) illustrates that pressure is related to the change in linear momentum with respect to time that occurs during a collision. Due to conservation of momentum, any change in particle linear momentum must result in an equal and opposite change in momentum of the container wall. A single collision is depicted in Figure 1.2. This figure illustrates that the particle linear momentum change in the $x$ direction is $-2mv_x$ (note there is no change in momentum in the $y$ or $z$ direction). Given this, a corresponding momentum change of $2mv_x$ must occur for the wall.

The pressure measured at the container wall corresponds to the sum of collisions involving a large number of particles that occur per unit time. Therefore, the total momentum change that gives rise to the pressure is equal to the product of the momentum change from a single particle collision and the total number of particles that collide with the wall:

$$\Delta p_{Total} = \frac{\Delta p}{\text{molecule}} \times (\text{number of molecules}) \quad \textbf{(1.4)}$$

How many molecules strike the side of the container in a given period of time? To answer this question, the time over which collisions are counted must be considered. Consider a volume element defined by the area of the wall $A$ times length $\Delta x$ as illustrated in Figure 1.3. The collisional volume element depicted in Figure 1.3 is given by

$$V = A\Delta x \quad \textbf{(1.5)}$$

The length of the box $\Delta x$ is related to the time period over which collisions will be counted $\Delta t$ and the component of particle velocity parallel to the side of the box (taken to be the $x$ direction):

$$\Delta x = v_x\Delta t \quad \textbf{(1.6)}$$

In this expression, $v_x$ is for a single particle; however, an average of this quantity will be used when describing the collisions from a collection of particles. Finally, the number of particles that will collide with the container wall $N_{coll}$ in the time interval $\Delta t$ is equal to the number density $\tilde{N}$. This quantity is equal to the number of particles in the container $N$ divided by the container volume $V$ and multiplied by the collisional volume element depicted in Figure 1.3:

$$N_{coll} = \tilde{N} \times (Av_x\Delta t)\left(\frac{1}{2}\right) = \frac{nN_A}{V}(Av_x\Delta t)\left(\frac{1}{2}\right) \quad \textbf{(1.7)}$$
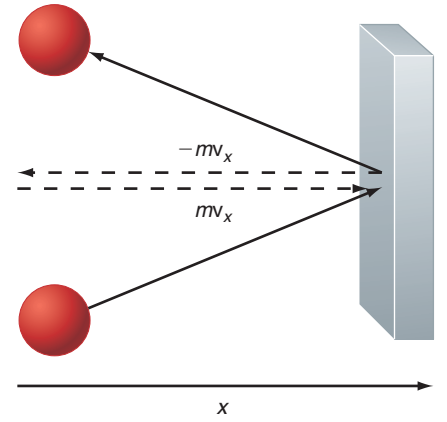


**FIGURE 1.2**
Collision between a gas particle and a wall. Before the collision, the particle has a momentum of $mv_x$ in the $x$ direction, and after the collision the momentum is $-mv_x$. Therefore, the change in particle momentum resulting from the collision is $-2mv_x$. By conservation of momentum, the change in momentum of the wall must be $2mv_x$. The incoming and outgoing trajectories are offset to show the individual momentum components.
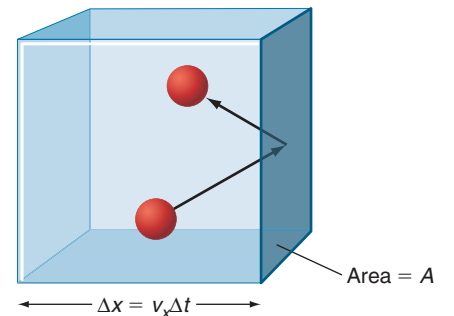


**FIGURE 1.3**
Volume element used to determine the number of collisions with the wall per unit time.

We have used the equality $N = n\,N_A$ where $N_A$ is Avogadro's number and $n$ is the number of moles of gas in the second part of Equation (1.7). Because particles travel in either the $+x$ or $-x$ direction with equal probability, only those molecules traveling in the $+x$ direction will strike the area of interest. Therefore, the total number of collisions is divided by two to take the direction of particle motion into account. Employing Equation (1.7), the total change in linear momentum of the container wall imparted by particle collisions is given by

$$\Delta p_{Total} = (2m\mathrm{v}_x)(N_{coll})$$

$$= (2m\mathrm{v}_x)\left(\frac{nN_A}{V}\,\frac{A\mathrm{v}_x\Delta t}{2}\right)$$

$$= \frac{nN_A}{V}\,A\Delta t\,m\langle\mathrm{v}_x^2\rangle \tag{1.8}$$

In Equation (1.8), angle brackets appear around $\mathrm{v}_x{}^2$ to indicate that this quantity represents an average value since the particles will demonstrate a distribution of velocities. This distribution is considered in detail later in Chapter 13. With the total change in linear momentum provided in Equation (1.8), the force and corresponding pressure exerted by the gas on the container wall [Equation (1.3)] are as follows:

$$F = \frac{\Delta p_{Total}}{\Delta t} = \frac{nN_A}{V}\,Am\langle\mathrm{v}_x^2\rangle$$

$$P = \frac{F}{A} = \frac{nN_A}{V}\,m\langle\mathrm{v}_x^2\rangle \tag{1.9}$$

Equation (1.9) can be converted into a more familiar expression once $1/2\,m\langle\mathrm{v}_x^2\rangle$ is recognized as the translational energy in the $x$ direction. In Chapter 14, it will be shown that the average translational energy for an individual particle in one dimension is

$$\frac{m\langle\mathrm{v}_x^2\rangle}{2} = \frac{k_BT}{2} \tag{1.10}$$

where $T$ is the gas temperature.

Substituting this result into Equation (1.9) results in the following expression for pressure:

$$P = \frac{nN_A}{V}\,m\langle\mathrm{v}_x^2\rangle = \frac{nN_A}{V}\,kT = \frac{nRT}{V} \tag{1.11}$$

We have used the equality $N_A\,k_B = R$ where $k_B$ is the **Boltzmann constant** and $R$ is the **ideal gas constant** in the last part of Equation (1.11). Equation (1.11) is the **ideal gas law.** Although this relationship is familiar, we have derived it by employing a classical description of a single molecular collision with the container wall and then scaling this result up to macroscopic proportions. We see that the origin of the pressure exerted by a gas on its container is the momentum exchange of the randomly moving gas molecules with the container walls.

What physical association can we make with the temperature $T$? At the microscopic level, temperature is related to the mean kinetic energy of molecules as shown by Equation (1.10). We defer the discussion of temperature at the microscopic level until Chapter 13 and focus on a macroscopic level discussion here. Although each of us has a sense of a "temperature scale" based on the qualitative descriptors *hot* and *cold*, a more quantitative and transferable measure of temperature that is not grounded in individual experience is needed. The quantitative measurement of temperature is accomplished using a **thermometer.** For any useful thermometer, the measured temperature, $T$, must be a single-valued, continuous, and monotonic function of some thermometric system property such as the volume of mercury confined to a narrow capillary, the electromotive force generated at the junction of two dissimilar metals, or the electrical resistance of a platinum wire.

The simplest case that one can imagine is when $T$ is linearly related to the value of the thermometric property $x$:

$$T(x) = a + bx \qquad (1.12)$$

Equation (1.12) defines a **temperature scale** in terms of a specific thermometric property, once the constants $a$ and $b$ are determined. The constant $a$ determines the zero of the temperature scale because $T(0) = a$ and the constant $b$ determines the size of a unit of temperature, called a degree.

One of the first practical thermometers was the mercury-in-glass thermometer. This thermometer utilizes the thermometric property that the volume of mercury increases monotonically over the temperature range –38.8°C to 356.7°C in which Hg is a liquid. In 1745, Carolus Linnaeus gave this thermometer a standardized scale by arbitrarily assigning the values 0 and 100 to the freezing and boiling points of water, respectively. Because there are 100 degrees between the two calibration points, this scale is known as the **centigrade scale.**

The centigrade scale has been superseded by the **Celsius scale.** The Celsius scale (denoted in units of °C) is similar to the centigrade scale. However, rather than being determined by two fixed points, the Celsius scale is determined by one fixed reference point at which ice, liquid water, and gaseous water are in equilibrium. This point is called the triple point (see Section 8.2) and is assigned the value 0.01°C. On the Celsius scale, the boiling point of water at a pressure of 1 atmosphere is 99.975°C. The size of the degree is chosen to be the same as on the centigrade scale.

Although the Celsius scale is used widely throughout the world today, the numerical values for this temperature scale are completely arbitrary, because a liquid other than water could have been chosen as a reference. It would be preferable to have a temperature scale derived directly from physical principles. There is such a scale, called the **thermodynamic temperature scale** or **absolute temperature scale.** For such a scale, the temperature is independent of the substance used in the thermometer, and the constant $a$ in Equation (1.12) is zero. The **gas thermometer** is a practical thermometer with which the absolute temperature can be measured. A gas thermometer contains a dilute gas under conditions in which the ideal gas law of Equation (1.11) describes the relationship among $P$, $T$, and the molar density $\rho_m = n/V$ with sufficient accuracy:

$$P = \rho_m RT \qquad (1.13)$$

Equation (1.13) can be rewritten as

$$T = \frac{P}{\rho_m R} \qquad (1.14)$$

showing that for a gas thermometer, the thermometric property is the temperature dependence of $P$ for a dilute gas at constant $V$. The gas thermometer provides the international standard for thermometry at very low temperatures. At intermediate temperatures, the electrical resistance of platinum wire is the standard, and at higher temperatures the radiated energy emitted from glowing silver is the standard. The absolute temperature is shown in Figure 1.4 on a logarithmic scale together with associated physical phenomena.

Equation (1.14) implies that as $T \to 0$, $P \to 0$. Measurements carried out by Guillaume Amontons in the 17th century demonstrated that the pressure exerted by a fixed amount of gas at constant $V$ varies linearly with temperature as shown in Figure 1.5. At the time of these experiments, temperatures below –30°C were not attainable in the laboratory. However, the $P$ versus $T_C$ data can be extrapolated to the limiting $T_C$ value at which $P \to 0$. It is found that these straight lines obtained for different values of $V$ intersect at a common point on the $T_C$ axis that lies near –273°C.

The data in Figure 1.5 show that at constant $V$, the thermometric property $P$ varies with temperature as

$$P = a + bT_C \qquad (1.15)$$

where $T_C$ is the temperature on the Celsius scale, and $a$ and $b$ are experimentally obtained proportionality constants. Figure 1.5 shows that all lines intersect at a single
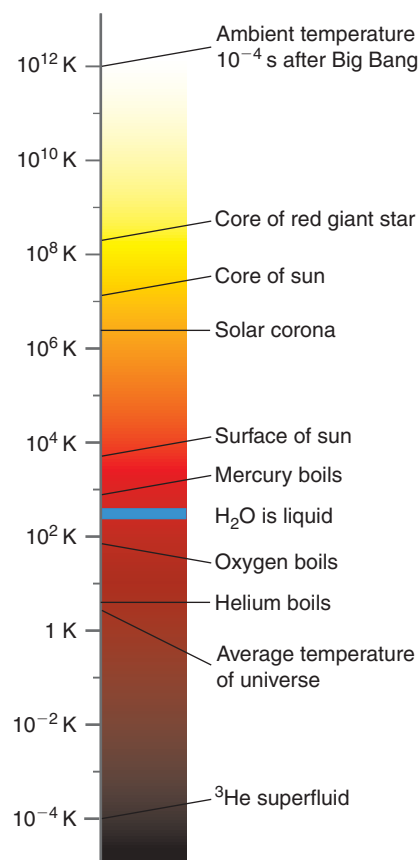


**FIGURE 1.4**

The absolute temperature is shown on a logarithmic scale together with the temperature of a number of physical phenomena.
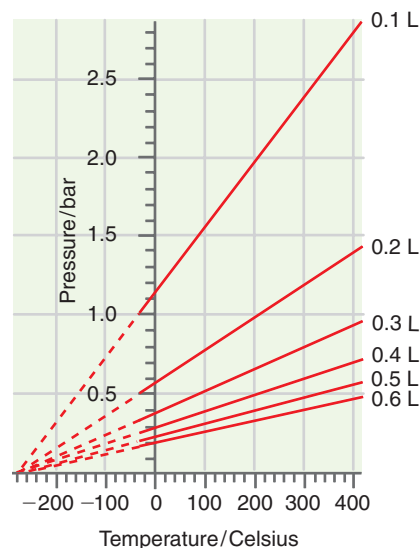


**FIGURE 1.5**

The pressure exerted by $5.00 \times 10^{-3}$ mol of a dilute gas is shown as a function of the temperature measured on the Celsius scale for different fixed volumes. The dashed portion indicates that the data are extrapolated to lower temperatures than could be achieved experimentally by early investigators.

point, even for different gases. This suggests a unique reference point for temperature, rather than the two reference points used in constructing the centigrade scale. The value zero is given to the temperature at which $P \rightarrow 0$, so that $a = 0$. However, this choice is not sufficient to define the temperature scale, because the size of the degree is undefined. By convention, the size of the degree on the absolute temperature scale is set equal to the size of the degree on the Celsius scale. With these two choices, the absolute and Celsius temperature scales are related by Equation (1.16). The scale measured by the ideal gas thermometer is the absolute temperature scale used in thermodynamics. The unit of temperature on this scale is called the kelvin, abbreviated K (without a degree sign):

$$T/K = T_C/°C + 273.15 \qquad \textbf{(1.16)}$$

## 1.3 Basic Definitions Needed to Describe Thermodynamic Systems

Having discussed the macroscopic variables pressure, volume, and temperature, we introduce some important concepts used in thermodynamics. A thermodynamic **system** consists of all the materials involved in the process under study. This material could be the contents of an open beaker containing reagents, the electrolyte solution within an electrochemical cell, or the contents of a cylinder and movable piston assembly in an engine. In thermodynamics, the rest of the universe is referred to as the **surroundings.** If a system can exchange matter with the surroundings, it is called an **open system;** if not, it is a **closed system.** Living cells are open systems (see Figure 1.6). Both open and closed systems can exchange energy with the surroundings. Systems that can exchange neither matter nor energy with the surroundings are called **isolated systems.**

The interface between the system and its surroundings is called the **boundary.** Boundaries determine if energy and mass can be transferred between the system and the surroundings and lead to the distinction between open, closed, and isolated systems. Consider Earth's oceans as a system, with the rest of the universe being the surroundings. The system–surroundings boundary consists of the solid–liquid interface between the continents and the ocean floor and the water–air interface at the ocean surface. For an open beaker in which the system is the contents, the boundary surface is just inside the inner wall of the beaker, and it passes across the open top of the beaker. In this case, energy can be exchanged freely between the system and surroundings through the side and bottom walls, and both matter and energy can be exchanged between the system and surroundings through the open top boundary. The portion of the boundary formed by the beaker in the previous example is called a **wall.** Walls can be rigid or movable and permeable or nonpermeable. An example of a movable wall is the surface of a balloon. An example of a selectively permeable wall is the fabric used in raingear, which is permeable to water vapor, but not liquid water.

The exchange of energy and matter across the boundary between system and surroundings is central to the important concept of **equilibrium.** The system and surroundings can be in equilibrium with respect to one or more of several different **system variables** such as pressure ($P$), temperature ($T$), and concentration. **Thermodynamic equilibrium** refers to a condition in which equilibrium exists with respect to $P$, $T$, and concentration. What conditions are necessary for a system to come to equilibrium with its surroundings? Equilibrium is established with respect to a given variable only if that variable does not change with time, and if it has the same value in all parts of the system and surroundings. For example, the interior of a soap bubble[1] (the system) and the surroundings (the room) are in equilibrium with respect to $P$ because the movable wall (the bubble) can reach a position where $P$ on both sides of the wall is the same, and because $P$ has the same value throughout the system and surroundings. Equilibrium with respect to concentration exists only if transport of all species across the boundary in both directions is possible. If the boundary is a movable wall that is not permeable to



**Nucleus**

Vacuole

Cell wall    Chloroplast    Mitochondrion

**Plant cell**



Nucleus

Mitochondrion    Plasma membrane
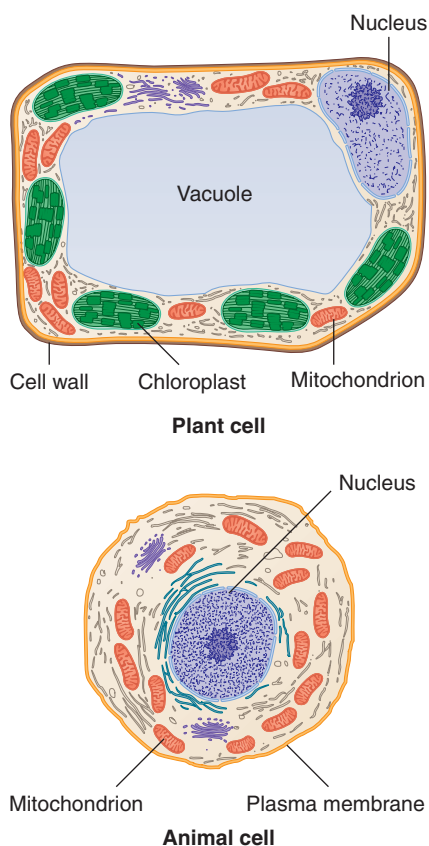
**Animal cell**

**FIGURE 1.6**

Animal and plant cells are open systems. The contents of the animal cell include the cytosol fluid and the numerous organelles (e.g., nucleus, mitochondria, etc.) that are separated from the surroundings by a lipid-rich plasma membrane. The plasma membrane acts as a boundary layer that can transmit energy and is selectively permeable to ions and various metabolites. A plant cell is surrounded by a cell wall that similarly encases the cytosol and organelles, including chloroplasts, that are the sites of photosynthesis.

---

[1]For this example, the surface tension of the bubble is assumed to be so small that it can be set equal to zero. This is in keeping with the thermodynamic tradition of weightless pistons and frictionless pulleys.

all species, equilibrium can exist with respect to $P$, but not with respect to concentration. Because $N_2$ and $O_2$ cannot diffuse through the (idealized) bubble, the system and surroundings are in equilibrium with respect to $P$, but not to concentration. Equilibrium with respect to temperature is a special case that is discussed next.

Two systems that have the same temperature are in **thermal equilibrium.** We use the concepts of temperature and thermal equilibrium to characterize the walls between a system and its surroundings. Consider the two systems with rigid walls shown in Figure 1.7a. Each system has the same molar density and is equipped with a pressure gauge. If we bring the two systems into direct contact, two limiting behaviors are observed. If neither pressure gauge changes, as in Figure 1.7b, we refer to the walls as being **adiabatic.** Because $P_1 \neq P_2$, the systems are not in thermal equilibrium and, therefore, have different temperatures. An example of a system surrounded by adiabatic walls is coffee in a Styrofoam cup with a Styrofoam lid.[2] Experience shows that it is not possible to bring two systems enclosed by adiabatic walls into thermal equilibrium by bringing them into contact, because adiabatic walls insulate against the transfer of "heat." If we push a Styrofoam cup containing hot coffee against one containing ice water, they will not reach the same temperature. Rely on experience at this point regarding the meaning of heat; a thermodynamic definition will be given in Chapter 2.

The second limiting case is shown in Figure 1.7c. In bringing the systems into intimate contact, both pressures change and reach the same value after some time. We conclude that the systems have the same temperature, $T_1 = T_2$, and say that they are in thermal equilibrium. We refer to the walls as being **diathermal.** Two systems in contact separated by diathermal walls reach thermal equilibrium because diathermal walls conduct heat. Hot coffee stored in a copper cup is an example of a system surrounded by diathermal walls. Because the walls are diathermal, the coffee will quickly reach room temperature.

The **zeroth law of thermodynamics** generalizes the experiment illustrated in Figure 1.7 and asserts the existence of an objective temperature that can be used to define the condition of thermal equilibrium. The formal statement of this law is as follows:

> Two systems that are separately in thermal equilibrium with a third system are also in thermal equilibrium with one another.

The unfortunate name assigned to the "zeroth" law is due to the fact that it was formulated after the first law of thermodynamics, but logically precedes it. The zeroth law tells us that we can determine if two systems are in thermal equilibrium without bringing them into contact. Imagine the third system to be a thermometer, which is defined more precisely in the next section. The third system can be used to compare the temperatures of the other two systems; if they have the same temperature, they will be in thermal equilibrium if placed in contact.



**(a)**

**(b)**

**(c)**
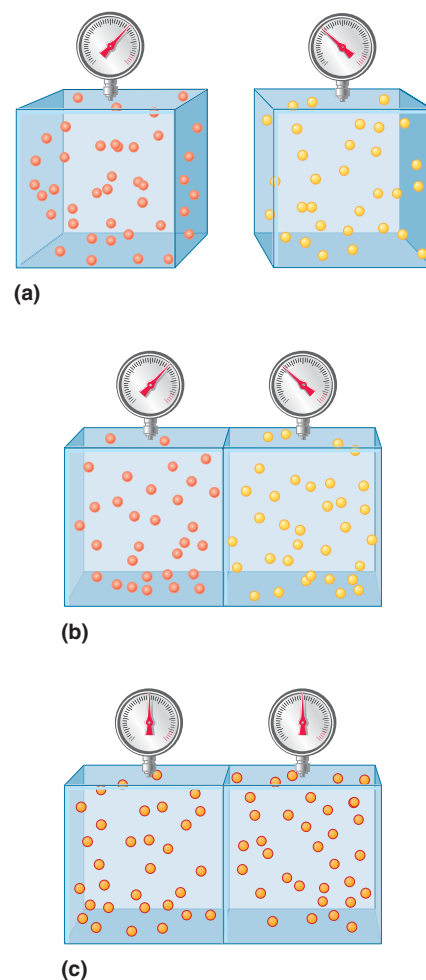
**FIGURE 1.7**
**(a)** Two separated systems with rigid walls and the same molar density have different temperatures. **(b)** Two systems are brought together so that their adiabatic walls are in intimate contact. The pressure in each system will not change unless heat transfer is possible. **(c)** As in part (b), two systems are brought together so that their diathermal walls are in intimate contact. The pressures become equal.

# 1.4 Equations of State and the Ideal Gas Law

Macroscopic models in which the system is described by a set of variables are based on experience. It is particularly useful to formulate an **equation of state,** which relates the state variables. A dilute gas can be modeled as consisting of point masses that do not interact with one another; we call this an **ideal gas.** The equation of state for an ideal gas was first determined from experiments by the English chemist Robert Boyle. If the pressure of He is measured as a function of the volume for different values of temperature, the set of nonintersecting hyperbolas as shown in Figure 1.8 is obtained. The curves in this figure can be quantitatively fit by the functional form

$$PV = \alpha T \qquad \textbf{(1.17)}$$

[2]In this discussion, Styrofoam is assumed to be a perfect insulator.
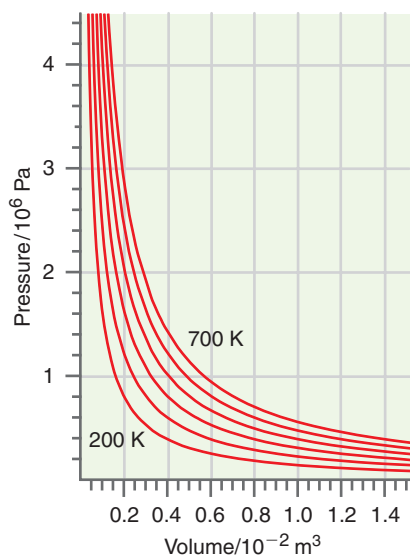
**FIGURE 1.8**

Illustration of the relationship between pressure and volume of 0.010 mol of He for fixed values of temperature, which differ by 100 K.

where $T$ is the absolute temperature as defined by Equation (1.16), allowing $\alpha$ to be determined. The constant $\alpha$ is found to be directly proportional to the mass of gas used. It is useful to separate this dependence by writing $\alpha = nR$, where $n$ is the number of moles of the gas, and $R$ is a constant that is independent of the size of the system. The result is the ideal gas equation of state

$$PV = Nk_BT = nRT \tag{1.18}$$

as derived in Equation (1.11). The equation of state given in Equation (1.18) is familiar as the ideal gas law. Because the four variables $P$, $V$, $T$, and $n$ are related through the equation of state, any three of these variables is sufficient to completely describe the ideal gas.

Of these four variables, $P$ and $T$ are independent of the amount of gas, whereas $V$ and $n$ are proportional to the amount of gas. A variable that is independent of the size of the system (for example, $P$ and $T$) is referred to as an **intensive variable,** and one that is proportional to the size of the system (for example, $V$) is referred to as an **extensive variable.** Equation (1.18) can be written in terms of intensive variables exclusively:

$$P = \rho_m RT \tag{1.13}$$

For a fixed number of moles, the ideal gas equation of state has only two independent intensive variables: any two of $P$, $T$, and $\rho_m$.

For an ideal gas mixture

$$PV = \sum_i n_i RT \tag{1.19}$$

because the gas molecules do not interact with one another. Equation (1.19) can be rewritten in the form

$$P = \sum_i \frac{n_i RT}{V} = \sum_i P_i = P_1 + P_2 + P_3 + ... \tag{1.20}$$

In Equation (1.20), $P_i$ is the **partial pressure** of each gas. This equation states that each ideal gas exerts a pressure that is independent of the other gases in the mixture. We also have

$$\frac{P_i}{P} = \frac{\dfrac{n_i RT}{V}}{\displaystyle\sum_i \dfrac{n_i RT}{V}} = \frac{\dfrac{n_i RT}{V}}{\dfrac{nRT}{V}} = \frac{n_i}{n} = x_i \tag{1.21}$$

which relates the partial pressure of a component in the mixture $P_i$ with its **mole fraction,** $x_i = n_i/n$, and the total pressure $P$.

In the SI system of units, pressure is measured in Pascal (Pa) units, where $1 \text{ Pa} = 1 \text{ N/m}^2$. The volume is measured in cubic meters, and the temperature is measured in kelvin. However, other units of pressure are frequently used, and these units are related to the Pascal as indicated in Table 1.1. In this table, numbers that are not exact have been given to five significant figures. The other commonly used unit of volume is the liter (L), where $1 \text{ m}^3 = 10^3 \text{ L}$ and $1 \text{ L} = 1 \text{ dm}^3 = 10^{-3} \text{ m}^3$.

**TABLE 1.1    Units of Pressure and Conversion Factors**

| Unit of Pressure | Symbol | Numerical Value |
|---|---|---|
| Pascal | Pa | $1 \text{ N m}^{-2} = 1 \text{ kg m}^{-1}\text{s}^{-2}$ |
| Atmosphere | atm | $1 \text{ atm} = 101{,}325 \text{ Pa (exactly)}$ |
| Bar | bar | $1 \text{ bar} = 10^5 \text{ Pa}$ |
| Torr or millimeters of Hg | Torr | $1 \text{ Torr} = 101{,}325/760 = 133.32 \text{ Pa}$ |
| Pounds per square inch | psi | $1 \text{ psi} = 6{,}894.8 \text{ Pa}$ |

## EXAMPLE PROBLEM 1.1

Starting out on a trip into the mountains, you inflate the tires on your automobile to a recommended pressure of $3.21 \times 10^5$ Pa on a day when the temperature is –5.00°C. You drive to the beach, where the temperature is 28.0°C. (a) What is the final pressure in the tires, assuming constant volume? (b) Derive a formula for the final pressure, assuming more realistically that the volume of the tires increases with increasing pressure as $V_f = V_i\left(1 + \gamma\left[P_f - P_i\right]\right)$ where $\gamma$ is an experimentally determined constant.

### Solution

**a.** Because the number of moles is constant,

$$\frac{P_i V_i}{T_i} = \frac{P_f V_f}{T_f}; \quad P_f = \frac{P_i V_i T_f}{V_f T_i};$$

$$P_f = \frac{P_i V_i T_f}{V_f T_i} = 3.21 \times 10^5 \text{Pa} \times \frac{V_i}{V_i} \times \frac{(273.15 + 28.0)}{(273.15 - 5.00)} = 3.61 \times 10^5 \text{Pa}$$

**b.**
$$\frac{P_i V_i}{T_i} = \frac{P_f V_i\left(1 + \gamma\left[P_f - P_i\right]\right)}{T_f};$$

$$P_i T_f = P_f T_i\left(1 + \gamma\left[P_f - P_i\right]\right)$$

$$P_f^2 T_i \gamma + P_f T_i(1 - P_i\gamma) - P_i T_f = 0$$

$$P_f = \frac{-T_i(1 - P_i\gamma) \pm \sqrt{T_i^2(1 - P_i\gamma)^2 + 4T_i T_f \gamma P_i}}{2T_i \gamma}$$

We leave it to the end-of-chapter problems to show that this expression for $P_f$ has the correct limit as $\gamma \to 0$.

In the SI system, the constant $R$ that appears in the ideal gas law has the value $8.314$ J K$^{-1}$ mol$^{-1}$, where the joule (J) is the unit of energy in the SI system. To simplify calculations for other units of pressure and volume, values of the constant $R$ with different combinations of units are given in Table 1.2.

## EXAMPLE PROBLEM 1.2

Consider the composite system, which is held at 298 K, shown in the following figure. Assuming ideal gas behavior, calculate the total pressure and the partial pressure of each component if the barriers separating the compartments are removed. Assume that the volume of the barriers is negligible.

**TABLE 1.2  The Ideal Gas Constant, $R$, in Various Units**

$R = 8.314$ J K$^{-1}$ mol$^{-1}$

$R = 8.314$ Pa m$^3$ K$^{-1}$ mol$^{-1}$

$R = 8.314 \times 10^{-2}$ L bar K$^{-1}$ mol$^{-1}$

$R = 8.206 \times 10^{-2}$ L atm K$^{-1}$ mol$^{-1}$

$R = 62.36$ L Torr K$^{-1}$ mol$^{-1}$



| He | Ne | Xe |
|---|---|---|
| 2.00 L | 3.00 L | 1.00 L |
| 1.50 bar | 2.50 bar | 1.00 bar |
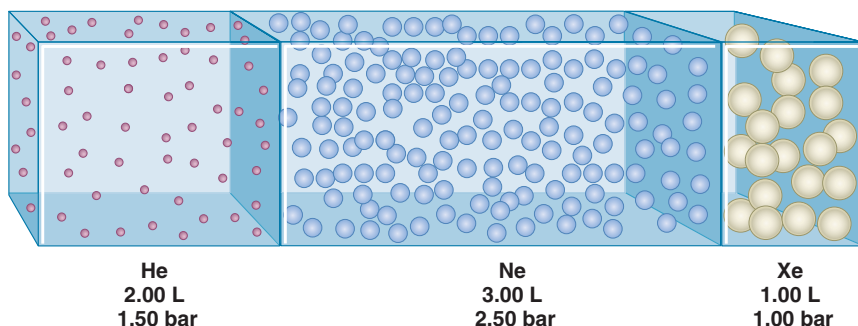
**Solution**

The number of moles of He, Ne, and Xe is given by

$$n_{He} = \frac{PV}{RT} = \frac{1.50\,\text{bar} \times 2.00\,\text{L}}{8.314 \times 10^{-2}\,\text{L bar K}^{-1}\,\text{mol}^{-1} \times 298\,\text{K}} = 0.121\,\text{mol}$$

$$n_{Ne} = \frac{PV}{RT} = \frac{2.50\,\text{bar} \times 3.00\,\text{L}}{8.314 \times 10^{-2}\,\text{L bar K}^{-1}\,\text{mol}^{-1} \times 298\,\text{K}} = 0.303\,\text{mol}$$

$$n_{Xe} = \frac{PV}{RT} = \frac{1.00\,\text{bar} \times 1.00\,\text{L}}{8.314 \times 10^{-2}\,\text{L bar K}^{-1}\,\text{mol}^{-1} \times 298\,\text{K}} = 0.0403\,\text{mol}$$

$$n = n_{He} + n_{Ne} + n_{Xe} = 0.464$$

The mole fractions are

$$x_{He} = \frac{n_{He}}{n} = \frac{0.121}{0.464} = 0.261$$

$$x_{Ne} = \frac{n_{Ne}}{n} = \frac{0.303}{0.464} = 0.653$$

$$x_{Xe} = \frac{n_{Xe}}{n} = \frac{0.0403}{0.464} = 0.0860$$

The total pressure is given by

$$P = \frac{(n_{He} + n_{Ne} + n_{Xe})RT}{V}$$

$$= \frac{0.464\,\text{mol} \times 8.314 \times 10^{-2}\,\text{L bar K}^{-1}\,\text{mol}^{-1} \times 298\,\text{K}}{6.00\,\text{L}}$$

$$= 1.92\,\text{bar}$$

The partial pressures are given by

$$P_{He} = x_{He}P = 0.261 \times 1.92\,\text{bar} = 0.501\,\text{bar}$$
$$P_{Ne} = x_{Ne}P = 0.653 \times 1.92\,\text{bar} = 1.25\,\text{bar}$$
$$P_{Xe} = x_{Xe}P = 0.0860 \times 1.92\,\text{bar} = 0.165\,\text{bar}$$

# 1.5 A Brief Introduction to Real Gases

The ideal gas law provides a first look at the usefulness of describing a system in terms of macroscopic parameters. However, we should also emphasize the downside of not taking the microscopic nature of the system into account. For example, the ideal gas law only holds for gases at low densities. In practice, deviations from the ideal gas law that occur for real gases must be taken into account in such applications as a gas thermometer. If data were obtained from a gas thermometer using He, Ar, and $N_2$ for a temperature very near the temperature at which the gas condenses to form a liquid, they would exhibit the behavior shown in Figure 1.9. We see that the temperature only becomes independent of $P$ and of the gas used in the thermometer if the data are extrapolated to zero pressure. It is in this limit that the gas thermometer provides a measure of the thermodynamic temperature. In practice, gas-independent $T$ values are only obtained below $P \sim 0.01$ bar.

For most applications, calculations based on the ideal gas law are valid to much higher pressures. Real gases will be discussed in detail in Chapter 7. However, because we need to take nonideal gas behavior into account in Chapters 2 through 6, we introduce an equation of state that is valid to higher densities in this section.



**FIGURE 1.9**
The temperature measured in a gas thermometer is independent of the gas used only in the limit that $P \rightarrow 0$.

The ideal gas assumptions that the atoms or molecules of a gas do not interact with one another and can be treated as point masses have a limited range of validity, which can be discussed using the potential energy function typical for a real gas, as shown in Figure 1.10. This figure shows the potential energy of interaction of two gas molecules as a function of the distance between them. The intermolecular potential can be divided into regions in which the potential energy is essentially zero ($r > r_{transition}$), negative (attractive interaction) ($r_{transition} > r > r_{V=0}$), and positive (repulsive interaction) ($r < r_{V=0}$). The distance $r_{transition}$ is not uniquely defined and depends on the energy of the molecule. It is on the order of the molecular size.

As the density is increased from very low values, molecules approach one another to within a few molecular diameters and experience a long-range attractive van der Waals force due to time-fluctuating dipole moments in each molecule. This strength of the attractive interaction is proportional to the polarizability of the electron charge in a molecule and is, therefore, substance dependent. In the attractive region, $P$ is lower than that calculated using the ideal gas law. This is the case because the attractive interaction brings the atoms or molecules closer than they would be if they did not interact. At sufficiently high densities, the atoms or molecules experience a short-range repulsive interaction due to the overlap of the electron charge distributions. Because of this interaction, $P$ is higher than that calculated using the ideal gas law. We see that for a real gas, $P$ can be either greater or less than the ideal gas value. Note that the potential becomes repulsive for a value of $r$ greater than zero. As a consequence, the volume of a gas even well above its boiling temperature approaches a finite limiting value as $P$ increases. By contrast, the ideal gas law predicts that $V \to 0$ as $P \to \infty$.

Given the potential energy function depicted in Figure 1.10, under what conditions is the ideal gas equation of state valid? A real gas behaves ideally only at low densities for which $r > r_{transition}$, and the value of $r_{transition}$ is substance dependent. The **van der Waals equation of state** takes both the finite size of molecules and the attractive potential into account. It has the form

$$P = \frac{nRT}{V - nb} - \frac{n^2 a}{V^2} \qquad (1.22)$$

This equation of state has two parameters that are substance dependent and must be experimentally determined. The parameters $b$ and $a$ take the finite size of the molecules and the strength of the attractive interaction into account, respectively. (Values of $a$ and $b$ for selected gases are listed in Table 7.4.) The van der Waals equation of state is more accurate in calculating the relationship between $P$, $V$, and $T$ for gases than the ideal gas law because $a$ and $b$ have been optimized using experimental results. However, there are other more accurate equations of state that are valid over a wider range than the van der Waals equation, as will be discussed in Chapter 7.
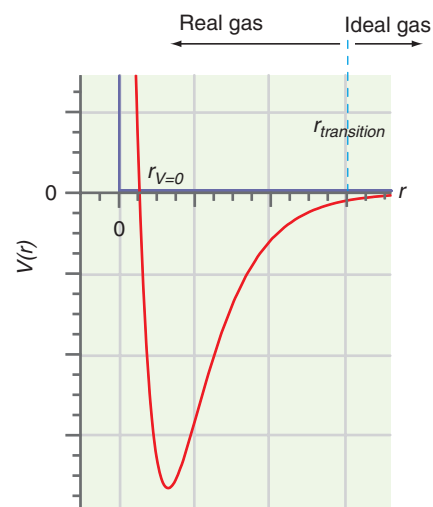


**FIGURE 1.10**
The potential energy of interaction of two molecules or atoms is shown as a function of their separation $r$. The red curve shows the potential energy function for an ideal gas. The dashed blue line indicates an approximate $r$ value below which a more nearly exact equation of state than the ideal gas law should be used. $V(r) = 0$ at $r = r_{V=0}$ and as $r \to \infty$.

**EXAMPLE PROBLEM 1.3**

Van der Waals parameters are generally tabulated with either of two sets of units:
  **a.** Pa m$^6$ mol$^{-2}$ or bar dm$^6$ mol$^{-2}$
  **b.** m$^3$ mol$^{-1}$ or dm$^3$ mol$^{-1}$
Determine the conversion factor to convert one system of units to the other. Note that $1 \text{ dm}^3 = 10^{-3} \text{ m}^3 = 1 \text{ L}$.

**Solution**

$$\text{Pa m}^6 \text{ mol}^{-2} \times \frac{\text{bar}}{10^5 \text{ Pa}} \times \frac{10^6 \text{ dm}^6}{\text{m}^6} = 10 \text{ bar dm}^6 \text{ mol}^{-2}$$

$$\text{m}^3 \text{ mol}^{-1} \times \frac{10^3 \text{ dm}^3}{\text{m}^3} = 10^3 \text{ dm}^3 \text{ mol}^{-1}$$

In Example Problem 1.4, a comparison is made of the molar volume for $N_2$ calculated at low and high pressures, using the ideal gas and van der Waals equations of state.

### EXAMPLE PROBLEM 1.4

a. Calculate the pressure exerted by $N_2$ at 300. K for molar volumes of 250. L mol$^{-1}$ and 0.100 L mol$^{-1}$ using the ideal gas and the van der Waals equations of state. The values of parameters $a$ and $b$ for $N_2$ are 1.370 bar dm$^6$ mol$^{-2}$ and 0.0387 dm$^3$ mol$^{-1}$, respectively.

b. Compare the results of your calculations at the two pressures. If $P$ calculated using the van der Waals equation of state is greater than those calculated with the ideal gas law, we can conclude that the repulsive interaction of the $N_2$ molecules outweighs the attractive interaction for the calculated value of the density. A similar statement can be made regarding the attractive interaction. Is the attractive or repulsive interaction greater for $N_2$ at 300. K and $V_m = 0.100$ L?

### Solution

a. The pressures calculated from the ideal gas equation of state are

$$P = \frac{nRT}{V} = \frac{1\,\text{mol} \times 8.314 \times 10^{-2}\,\text{L bar mol}^{-1}\text{K}^{-1} \times 300.\,\text{K}}{250.\,\text{L}} = 9.98 \times 10^{-2}\,\text{bar}$$

$$P = \frac{nRT}{V} = \frac{1\,\text{mol} \times 8.314 \times 10^{-2}\,\text{L bar mol}^{-1}\text{K}^{-1} \times 300.\,\text{K}}{0.100\,\text{L}} = 249\,\text{bar}$$

The pressures calculated from the van der Waals equation of state are

$$P = \frac{nRT}{V - nb} - \frac{n^2 a}{V^2}$$

$$= \frac{1\,\text{mol} \times 8.314 \times 10^{-2}\,\text{L bar mol}^{-1}\text{K}^{-1} \times 300.\,\text{K}}{250.\,\text{L} - 1\,\text{mol} \times 0.0387\,\text{dm}^3\,\text{mol}^{-1}}$$

$$- \frac{(1\,\text{mol})^2 \times 1.370\,\text{bar dm}^6\,\text{mol}^{-2}}{(250.\,\text{L})^2}$$

$$= 9.98 \times 10^{-2}\,\text{bar}$$

$$P = \frac{1\,\text{mol} \times 8.314 \times 10^{-2}\,\text{L bar mol}^{-1}\text{K}^{-1} \times 300\,\text{K}}{0.100\,\text{L} - 1\,\text{mol} \times 0.0387\,\text{dm}^3\,\text{mol}^{-1}}$$

$$- \frac{(1\,\text{mol})^2 \times 1.370\,\text{bar dm}^6\,\text{mol}^{-2}}{(0.100\,\text{L})^2}$$

$$= 270.\,\text{bar}$$

b. Note that the result is identical with that for the ideal gas law for $V_m = 250.$ L, and that the result calculated for $V_m = 0.100$ L deviates from the ideal gas law result. Because $P^{real} > P^{ideal}$, we conclude that the repulsive interaction is more important than the attractive interaction for this specific value of molar volume and temperature.

# Vocabulary

| | | |
|---|---|---|
| absolute temperature scale | Celsius scale | elastic collision |
| adiabatic | centigrade scale | equation of state |
| Boltzmann constant | closed system | equilibrium |
| boundary | diathermal | extensive variable |

| | | |
|---|---|---|
| gas thermometer | macroscopic variables | temperature scale |
| ideal gas | mole fraction | thermal equilibrium |
| ideal gas constant | open system | thermodynamic equilibrium |
| ideal gas law | partial pressure | thermodynamic temperature scale |
| intensive variable | surroundings | thermometer |
| isolated system | system | van der Waals equation of state |
| kelvin | system variables | wall |
| macroscopic scale | temperature | zeroth law of thermodynamics |

# Conceptual Problems

**Q1.1**  Real walls are never totally adiabatic. Use your experience to order the following walls in increasing order with respect to their being diathermal: 1-cm-thick concrete, 1-cm-thick vacuum, 1-cm-thick copper, 1-cm-thick cork.

**Q1.2**  The parameter $a$ in the van der Waals equation is greater for $H_2O$ than for He. What does this say about the difference in the form of the potential function in Figure 1.10 for the two gases?

**Q1.3**  Give an example based on molecule–molecule interactions excluding chemical reactions, illustrating how the total pressure upon mixing two real gases could be different from the sum of the partial pressures.

**Q1.4**  Can temperature be measured directly? Explain your answer.

**Q1.5**  Explain how the ideal gas law can be deduced for the measurements shown in Figures 1.5 and 1.8.

**Q1.6**  The location of the boundary between the system and the surroundings is a choice that must be made by the thermodynamicist. Consider a beaker of boiling water in an airtight room. Is the system open or closed if you place the boundary just outside the liquid water? Is the system open or closed if you place the boundary just inside the walls of the room?

**Q1.7**  Give an example of two systems that are in equilibrium with respect to only one of two state variables.

**Q1.8**  At sufficiently high temperatures, the van der Waals equation has the form $P \approx RT/(V_m - b)$. Note that the attractive part of the potential has no influence in this expression. Justify this behavior using the potential energy diagram of Figure 1.10.

**Q1.9**  Give an example of two systems separated by a wall that are in thermal but not chemical equilibrium.

**Q1.10**  Which of the following systems are open? (a) a dog, (b) an incandescent light bulb, (c) a tomato plant, (d) a can of tomatoes. Explain your answers.

**Q1.11**  Which of the following systems are isolated? (a) a bottle of wine, (b) a tightly sealed, perfectly insulated thermos bottle, (c) a tube of toothpaste, (d) our solar system. Explain your answers.

**Q1.12**  Why do the $z$ and $y$ components of the velocity not change in the collision depicted in Figure 1.2?

**Q1.13**  If the wall depicted in Figure 1.2 were a movable piston, under what conditions would it move as a result of the molecular collisions?

**Q1.14**  The mass of a He atom is less than that of an Ar atom. Does that mean that because of its larger mass, Argon exerts a higher pressure on the container walls than He at the same molar density, volume, and temperature? Explain your answer.

**Q1.15**  Explain why attractive interactions between molecules in gas make the pressure less than that predicted by the ideal gas equation of state.

# Numerical Problems

Problem numbers in **red** indicate that the solution to the problem is given in the *Student's Solutions Manual*.

**P1.1**  Approximately how many oxygen molecules arrive each second at the mitochondrion of an active person with a mass of 84 kg? The following data are available: Oxygen consumption is about 40. mL of $O_2$ per minute per kilogram of body weight, measured at $T = 300.$ K and $P = 1.00$ atm. In an adult there are about $1.6 \times 10^{10}$ cells per kg body mass. Each cell contains about 800. mitochondria.

**P1.2**  A compressed cylinder of gas contains $2.74 \times 10^3$ g of $N_2$ gas at a pressure of $3.75 \times 10^7$ Pa and a temperature of 18.7°C. What volume of gas has been released into the atmosphere if the final pressure in the cylinder is $1.80 \times 10^5$ Pa? Assume ideal behavior and that the gas temperature is unchanged.

**P1.3**  Calculate the pressure exerted by Ar for a molar volume of 1.31 L mol$^{-1}$ at 426 K using the van der Waals equation of state. The van der Waals parameters $a$ and $b$ for Ar are 1.355 bar dm$^6$ mol$^{-2}$ and 0.0320 dm$^3$ mol$^{-1}$, respectively. Is the attractive or repulsive portion of the potential dominant under these conditions?

**P1.4**  A sample of propane $(C_3H_8)$ is placed in a closed vessel together with an amount of $O_2$ that is 2.15 times the amount needed to completely oxidize the propane to $CO_2$ and

$H_2O$ at constant temperature. Calculate the mole fraction of each component in the resulting mixture after oxidation, assuming that the $H_2O$ is present as a gas.

**P1.5**    A gas sample is known to be a mixture of ethane and butane. A bulb having a 230.0 $cm^3$ capacity is filled with the gas to a pressure of $97.5 \times 10^3$ Pa at 23.1°C. If the mass of the gas in the bulb is 0.3554 g, what is the mole percent of butane in the mixture?

**P1.6**    One liter of fully oxygenated blood can carry 0.18 liters of $O_2$ measured at $T = 298$ K and $P = 1.00$ atm. Calculate the number of moles of $O_2$ carried per liter of blood. Hemoglobin, the oxygen transport protein in blood has four oxygen binding sites. How many hemoglobin molecules are required to transport the $O_2$ in 1.0 L of fully oxygenated blood?

**P1.7**    Yeast and other organisms can convert glucose ($C_6H_{12}O_6$) to ethanol ($CH_3CH_2OH$) by a process called alchoholic fermentation. The net reaction is

$$C_6H_{12}O_6(s) \rightarrow 2C_2H_5OH(l) + 2CO_2(g)$$

Calculate the mass of glucose required to produce 2.25 L of $CO_2$ measured at $P = 1.00$ atm and $T = 295$ K.

**P1.8**    A vessel contains 1.15 g liq $H_2O$ in equilibrium with water vapor at 30.°C. At this temperature, the vapor pressure of $H_2O$ is 31.82 torr. What volume increase is necessary for all the water to evaporate?

**P1.9**    Consider a 31.0 L sample of moist air at 60.°C and one atm in which the partial pressure of water vapor is 0.131 atm. Assume that dry air has the composition 78.0 mole percent $N_2$, 21.0 mole percent $O_2$, and 1.00 mole percent Ar.

**a.** What are the mole percentages of each of the gases in the sample?

**b.** The percent relative humidity is defined as %RH = $P_{H_2O}/P^*_{H_2O}$ where $P_{H_2O}$ is the partial pressure of water in the sample and $P^*_{H_2O} = 0.197$ atm is the equilibrium vapor pressure of water at 60.°C. The gas is compressed at 60.°C until the relative humidity is 100.%. What volume does the mixture contain now?

**c.** What fraction of the water will be condensed if the total pressure of the mixture is isothermally increased to 81.0 atm?

**P1.10**    A typical diver inhales 0.450 liters of air per breath and carries a 25 L breathing tank containing air at a pressure of 300. bar. As she dives deeper, the pressure increases by 1 bar for every 10.08 m. How many breaths can the diver take from this tank at a depth of 35 m? Assume that the temperature remains constant.

**P1.11**    Use the ideal gas and van der Waals equations to calculate the pressure when 2.25 mol $H_2$ are confined to a volume of 1.65 L at 298 K. Is the gas in the repulsive or attractive region of the molecule–molecule potential?

**P1.12**    A rigid vessel of volume 0.400 $m^3$ containing $H_2$ at 21.25°C and a pressure of $715 \times 10^3$ Pa is connected to a second rigid vessel of volume 0.750 $m^3$ containing Ar at 30.15°C at a pressure of $203 \times 10^3$ Pa. A valve separating the two

vessels is opened and both are cooled to a temperature of 12.2°C. What is the final pressure in the vessels?

**P1.13**    A mixture of oxygen and hydrogen is analyzed by passing it over hot copper oxide and through a drying tube. Hydrogen reduces the CuO according to the reaction $CuO(s) + H_2(g) \rightarrow Cu(s) + H_2O(l)$, and oxygen reoxidizes the copper formed according to $Cu(s) + 1/2\ O_2(g) \rightarrow CuO(s)$. At 25°C and 750. Torr, 172.0 $cm^3$ of the mixture yields 77.5 $cm^3$ of dry oxygen measured at 25°C and 750. Torr after passage over CuO and the drying agent. What is the original composition of the mixture?

**P1.14**    An athlete at high performance inhales ~3.75 L of air at 1.00 atm and 298 K. The inhaled and exhaled air contain 0.50 and 6.2% by volume of water, respectively. For a respiration rate of 32 breaths per minute, how many moles of water per minute are expelled from the body through the lungs?

**P1.15**    Devise a temperature scale, abbreviated G, for which the magnitude of the ideal gas constant is 5.52 J $G^{-1}$ $mol^{-1}$.

**P1.16**    Aerobic cells metabolize glucose in the respiratory system. This reaction proceeds according to the overall reaction

$$6O_2(g) + C_6H_{12}O_6(s) \rightarrow 6CO_2(g) + 6H_2O(l)$$
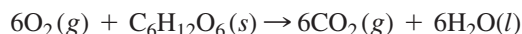
Calculate the volume of oxygen required at STP to metabolize 0.025 kg of glucose ($C_6H_{12}O_6$). STP refers to standard temperature and pressure, that is, $T = 273$ K and $P = 1.00$ atm. Assume oxygen behaves ideally at STP.

**P1.17**    An athlete at high performance inhales ~3.75 L of air at 1.0 atm and 298 K at a respiration rate of 32 breaths per minute. If the exhaled and inhaled air contain 15.3 and 20.9% by volume of oxygen respectively, how many moles of oxygen per minute are absorbed by the athlete's body?

**P1.18**    A mixture of $2.10 \times 10^{-3}$ g of $O_2$, $3.88 \times 10^{-3}$ mol of $N_2$, and $5.25 \times 10^{20}$ molecules of CO are placed into a vessel of volume 5.25 L at 12.5°C.

**a.** Calculate the total pressure in the vessel.

**b.** Calculate the mole fractions and partial pressures of each gas.

**P1.19**    Calculate the pressure exerted by benzene for a molar volume of 2.00 L at 595 K using the Redlich-Kwong equation of state:

$$P = \frac{RT}{V_m - b} - \frac{a}{\sqrt{T}} \frac{1}{V_m (V_m + b)}$$
$$= \frac{nRT}{V - nb} - \frac{n^2 a}{\sqrt{T}} \frac{1}{V(V + nb)}$$

The Redlich-Kwong parameters $a$ and $b$ for benzene are 452.0 bar $dm^6$ $mol^{-2}$ $K^{1/2}$ and 0.08271 $dm^3$ $mol^{-1}$, respectively. Is the attractive or repulsive portion of the potential dominant under these conditions?

**P1.20**    In the absence of turbulent mixing, the partial pressure of each constituent of air would fall off with height above sea level in Earth's atmosphere as $P_i = P^0_i e^{-M_i gz/RT}$ where $P_i$ is the partial pressure at the height $z$, $P^0_i$ is the partial pressure of component $i$ at sea level, $g$ is the acceleration of

gravity, $R$ is the gas constant, $T$ is the absolute temperature, and $M_i$ is the molecular mass of the gas. As a result of turbulent mixing, the composition of Earth's atmosphere is constant below an altitude of 100 km, but the total pressure decreases with altitude as $P = P^0 e^{-M_{ave}gz/RT}$ where $M_{ave}$ is the mean molecular weight of air. At sea level, $x_{N_2} = 0.78084$ and $x_{He} = 0.00000524$ and $T = 300.$ K.

**a.** Calculate the total pressure at 8.5 km, assuming a mean molecular mass of 28.9 g mol⁻¹ and that $T = 300.$ K throughout this altitude range.

**b.** Calculate the value that $x_{N_2}/x_{He}$ would have at 8.5 km in the absence of turbulent mixing. Compare your answer with the correct value.

**P1.21**  An initial step in the biosynthesis of glucose $C_6H_{12}O_6$ is the carboxylation of pyruvic acid $CH_3COCOOH$ to form oxaloacetic acid $HOOCCOCH_2COOH$

$$CH_3COCOOH(s) + CO_2(g) \rightarrow HOOCCOCH_2COOH(s)$$
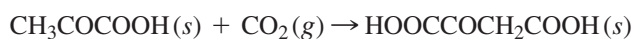
If you knew nothing else about the intervening reactions involved in glucose biosynthesis other than no further carboxylations occur, what volume of $CO_2$ is required to produce 1.10 g of glucose? Assume $P = 1$ atm and $T = 298$ K.

**P1.22**  Consider the oxidation of the amino acid glycine $NH_2CH_2COOH$ to produce water, carbon dioxide, and urea $NH_2CONH_2$:

$$NH_2CH_2COOH(s) + 3O_2(g) \rightarrow$$
$$NH_2CONH_2(s) + 3CO_2(g) + 3H_2O(l)$$
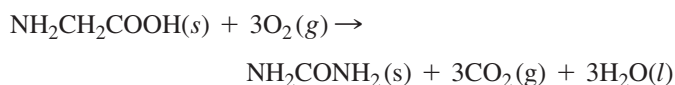
Calculate the volume of carbon dioxide evolved at $P = 1.00$ atm and $T = 305$ K from the oxidation of 0.022 g of glycine.

**P1.23**  Assume that air has a mean molar mass of 28.9 g mol⁻¹ and that the atmosphere has a uniform temperature of 25.0°C. Calculate the barometric pressure in Pa in Santa Fe, for which $z = 7000.$ ft. Use the information contained in Problem P1.20.

**P1.24**  When Julius Caesar expired, his last exhalation had a volume of 450. cm³ and contained 1.00 mole percent argon. Assume that $T = 300.$ K and $P = 1.00$ atm at the location of his demise. Assume further that $T$ has the same value throughout Earth's atmosphere. If all of his exhaled Ar atoms are now uniformly distributed throughout the atmosphere, how many inhalations of 450. cm³ must we make to inhale one of the Ar atoms exhaled in Caesar's last breath? Assume the radius of Earth to be $6.37 \times 10^6$ m. [*Hint:* Calculate the number of Ar atoms in the atmosphere in the simplified geometry of a plane of area equal to that of Earth's surface. See Problem P1.20 for the dependence of the barometric pressure and the composition of air on the height above Earth's surface.

**P1.25**  Calculate the number of molecules per m³ in an ideal gas at the standard temperature and pressure conditions of 0.00°C and 1.00 atm.

**P1.26**  Consider a gas mixture in a 1.50 dm³ flask at 22.0°C. For each of the following mixtures, calculate the partial pressure of each gas, the total pressure, and the composition of the mixture in mole percent:

**a.** 3.06 g $H_2$ and 2.98 g $O_2$

**b.** 2.30 g $N_2$ and 1.61 g $O_2$

**c.** 2.02 g $CH_4$ and 1.70 g $NH_3$

**P1.27**  A mixture of $H_2$ and $NH_3$ has a volume of 139.0 cm³ at 0.00°C and 1 atm. The mixture is cooled to the temperature of liquid nitrogen at which ammonia freezes out and the remaining gas is removed from the vessel. Upon warming the vessel to 0.00°C and 1 atm, the volume is 77.4 cm³. Calculate the mole fraction of $NH_3$ in the original mixture.

**P1.28**  A sealed flask with a capacity of 1.22 dm³ contains 4.50 g of carbon dioxide. The flask is so weak that it will burst if the pressure exceeds $9.500 \times 10^5$ Pa. At what temperature will the pressure of the gas exceed the bursting pressure?

**P1.29**  A balloon filled with 11.50 L of Ar at 18.7°C and 1 atm rises to a height in the atmosphere where the pressure is 207 Torr and the temperature is –32.4°C. What is the final volume of the balloon? Assume that the pressure inside and outside the balloon have the same value.

**P1.30**  Carbon monoxide competes with oxygen for binding sites on the transport protein hemoglobin. CO can be poisonous if inhaled in large quantities. A safe level of CO in air is 50. parts per million (ppm). When the CO level increases to 800. ppm, dizziness, nausea, and unconsciousness occur, followed by death. Assuming the partial pressure of oxygen in air at sea level is 0.20 atm, what proportion of CO to $O_2$ is fatal?

**P1.31**  The total pressure of a mixture of oxygen and hydrogen is 1.65 atm. The mixture is ignited and the water is removed. The remaining gas is pure hydrogen and exerts a pressure of 0.190 atm when measured at the same values of $T$ and $V$ as the original mixture. What was the composition of the original mixture in mole percent?

**P1.32**  Suppose that you measured the product $PV$ of 1 mol of a dilute gas and found that $PV = 24.35$ L atm at 0.00°C and 33.54 L atm at 100.°C. Assume that the ideal gas law is valid, with $T = t(°C) + a$, and that the values of $R$ and $a$ are not known. Determine $R$ and $a$ from the measurements provided.

**P1.33**  Liquid $N_2$ has a density of 875.4 kg m⁻³ at its normal boiling point. What volume does a balloon occupy at 298 K and a pressure of 1.00 atm if $3.10 \times 10^{-3}$ L of liquid $N_2$ is injected into it? Assume that there is no pressure difference between the inside and outside of the balloon.

**P1.34**  Calculate the volume of all gases evolved by the complete oxidation of 0.375 g of the amino acid alanine $CH3CH(NH_2)COOH$ if the products are liquid water, nitrogen gas, and carbon dioxide gas; the total pressure is 1.00 atm; and $T = 298$ K.

**P1.35**  As a result of photosynthesis, an acre of forest (1 acre = 4047 square meters) can take up 1000. kg of $CO_2$. Assuming air is 0.0314% $CO_2$ by volume, what volume of air is required to provide 350. kg of $CO_2$? Assume $T = 310$ K and $P = 1.00$ atm.

**P1.36** A glass bulb of volume 0.198 L contains 0.457 g of gas at 759.0 Torr and 134.0°C. What is the molar mass of the gas?

**P1.37** Use L'Hôpital's rule, $\lim\left[f(x)/g(x)\right]_{x\to 0} = \lim\left[\dfrac{df(x)/dx}{dg(x)/dx}\right]_{x\to 0}$ to show that the expression derived for $P_f$ in part (b) of Example Problem 1.1 has the correct limit as $\gamma \to 0$.

**P1.38** A 455 cm$^3$ vessel contains a mixture of Ar and Xe. If the mass of the gas mixture is 2.245 g at 25.0°C and the pressure is 760. Torr, calculate the mole fraction of Xe in the mixture.

**P1.39** Many processes such as the fabrication of integrated circuits are carried out in a vacuum chamber to avoid reaction of the material with oxygen in the atmosphere. It is difficult to routinely lower the pressure in a vacuum chamber below $1.0 \times 10^{-10}$ Torr. Calculate the molar density at this pressure at 300. K. What fraction of the gas phase molecules initially present for 1.0 atm in the chamber are present at $1.0 \times 10^{-10}$ Torr?

**P1.40** Rewrite the van der Waals equation using the molar volume rather than $V$ and $n$.

# Heat, Work, Internal Energy, Enthalpy, and the First Law of Thermodynamics

In this chapter, the internal energy $U$ is introduced. The first law of thermodynamics relates $\Delta U$ to the heat ($q$) and work ($w$) that flows across the boundary between the system and the surroundings. Other important concepts introduced include heat capacity, the difference between state and path functions, and reversible versus irreversible processes. The enthalpy $H$ is introduced as a form of energy that can be directly measured by the heat flow in a constant pressure process. We show how $\Delta U$, $\Delta H$, $q$, and $w$ can be calculated for processes involving ideal gases.

## 2.1 The Internal Energy and the First Law of Thermodynamics

This section focuses on the change in energy of the system and surroundings during a thermodynamic process such as an expansion or compression of a gas. In thermodynamics, we are interested in the internal energy of the system, as opposed to the energy associated with the system relative to a particular frame of reference. For example, a container of gas in an airplane has a kinetic energy relative to an observer on the ground. However, the internal energy of the gas is defined relative to a coordinate system fixed on the container. Viewed at a molecular level, the internal energy can take on a number of forms such as

- the translational energy of the molecules.
- the potential energy of the constituents of the system; for example, a crystal consisting of polarizable molecules will experience a change in its potential energy as an electric field is applied to the system.
- the internal energy stored in the form of molecular vibrations and rotations.
- the internal energy stored in the form of chemical bonds that can be released through a chemical reaction.
- the potential energy of interaction between molecules.

The total of all these forms of energy for the system of interest is given the symbol $U$ and is called the **internal energy.**[1]

The **first law of thermodynamics** is based on our experience that energy can be neither created nor destroyed, if the energies of both the system and the surroundings are taken into account. This law can be formulated in a number of equivalent forms. Our initial formulation of this law is as follows:

> The internal energy $U$ of an isolated system is constant.

This form of the first law looks uninteresting because it suggests that nothing happens in an isolated system when viewed from outside the system. How can the first law tell us anything about thermodynamic processes such as chemical reactions? Consider separating an isolated system into two subsystems, the system and the surroundings. When changes in $U$ occur in a system in contact with its surroundings, $\Delta U_{total}$ is given by

$$\Delta U_{total} = \Delta U_{system} + \Delta U_{surroundings} = 0 \tag{2.1}$$

Therefore, the first law becomes

$$\Delta U_{system} = -\Delta U_{surroundings} \tag{2.2}$$

For any decrease of $U_{system}$, $U_{surroundings}$ must increase by exactly the same amount. For example, if a gas (the system) is cooled, the temperature of the surroundings must increase.

How can the energy of a system be changed? There are many ways to alter $U$, several of which are discussed in this chapter. Experience has shown that all changes in a closed system in which no chemical reactions or phase changes occur can be classified only as heat, work, or a combination of both. Therefore, the internal energy of such a system can only be changed by the flow of heat or work across the boundary between the system and surroundings. For example, $U$ for a gas can be increased by putting it in an oven or by compressing it. In both cases, the temperature of the system increases. This important recognition leads to a second and more useful formulation of the first law:

$$\Delta U = q + w \tag{2.3}$$

where $q$ and $w$ designate heat and work, respectively. We use $\Delta U$ without a subscript to indicate the change in internal energy of the system. What do we mean by heat and work? In the following two sections, we define these important concepts and discuss how they differ.

The symbol $\Delta$ is used to indicate a change that occurs as a result of an arbitrary process. The simplest processes are those in which one of $P$, $V$, or $T$ remains constant. A constant temperature process is referred to as **isothermal,** and the corresponding terms for constants $P$ and $V$ are **isobaric** and **isochoric,** respectively.

# 2.2 **Work**

In this and the next section, we discuss the two ways in which the internal energy of a system can be changed. **Work** in thermodynamics is defined as any quantity of energy that "flows" across the boundary between the system and surroundings as a result of a force acting through a distance. Examples are moving an ion in a solution from one region of electrical potential to another, inflating a balloon, or climbing stairs. In each of these examples, there is a force along the direction of motion. Consider another example, a gas in a piston and cylinder assembly as shown in Figure 2.1. In this example, the system is defined as the gas alone. Everything else shown in the figure is in the surroundings. As the gas is compressed, the height of the mass in the surroundings is lowered and the initial and final volumes are defined by the mechanical stops indicated in the figure.



**FIGURE 2.1**
A system is shown in which compression work is being done on a gas. The walls are adiabatic.

---

[1]We could include other terms such as the binding energy of the atomic nuclei but choose to include only the forms of energy that are likely to change in simple chemical reactions.

Work has several important characteristics:

- Work is transitory in that it only appears during a change in state of the system and surroundings. Only energy, and not work, is associated with the initial and final states of the systems.
- The net effect of work is to change $U$ of the system and surroundings in accordance with the first law. If the only change in the system results from a force acting through a distance (as for example the movement of the mass in Figure 2.1), work has flowed between the system and the surroundings. Work can usually be represented by a mass in the surroundings that has been raised or lowered in Earth's gravitational field.
- The quantity of work can be calculated using the definition

$$w = \int_{x_i}^{x_f} \mathbf{F} \cdot d\mathbf{x} \tag{2.4}$$

Note that because of the scalar product in the integral, the work will be zero unless the force has a component along the displacement direction.

- The sign of the work follows from evaluating the preceding integral. If $w > 0$, $\Delta U > 0$ for an adiabatic process. It is common usage to say that if $w$ is positive, work is done on the system by the surroundings. If $w$ is negative, work is done by the system on the surroundings. The quantity of work can also be calculated from the change in potential energy of the mass in the surroundings, $\Delta E_{potential} = mg\Delta h = -w$, where $g$ is the gravitational acceleration and $\Delta h$ is the change in the height of the mass $m$.

Using the definition of pressure as the force per unit area ($A$), the work done in moving the mass in Figure 2.1 is given by

$$w = \int_{x_i}^{x_f} \mathbf{F} \cdot d\mathbf{x} = -\int_{x_i}^{x_f} P_{external}A dx = -\int_{V_i}^{V_f} P_{external} dV \tag{2.5}$$

The minus sign appears because $\mathbf{F}$ and $d\mathbf{x}$ are vectors that point in opposite directions. Note that the pressure that appears in this expression is the external pressure $P_{external}$ which need not equal the system pressure $P$.

An example of another important kind of work, electrical work, is shown in Figure 2.2, in which the content of the cylinder is the system. Electrical current flows through a conductive aqueous solution and water undergoes electrolysis to produce $H_2$ and $O_2$ gas. The current is produced by a generator, like that used to power a light on a bicycle through the mechanical work of pedaling. As current flows, the mass that drives the generator is lowered. In this case, the surroundings do the electrical work on the system. As a result, some of the liquid water is transformed to $H_2$ and $O_2$. From electrostatics, the work done in transporting a charge $Q$ through an electrical potential difference $\phi$ is

$$w_{electrical} = Q\phi \tag{2.6}$$

For a constant current $I$ that flows for a time $t$, $Q = It$. Therefore,

$$w_{electrical} = I\phi t \tag{2.7}$$

The system also does work on the surroundings through the increase in the volume of the gas phase at the constant external pressure $P_i$, as shown by the raised mass on the piston. The total work done is

$$w = w_{P-V} + w_{electrical} = I\phi t - \int_{V_i}^{V_f} P_{external} dV = I\phi t - P_{external}(V_f - V_i) \tag{2.8}$$

Other forms of work include the work of expanding a surface, such as a soap bubble, against the surface tension. Table 2.1 shows the expressions for work for four different cases. Each of these different types of work poses a requirement on the walls separating the system and surroundings. To be able to carry out the first three types of work, the walls must be movable, whereas for electrical work, they must be conductive. Several examples of work calculations are given in Example Problem 2.1.
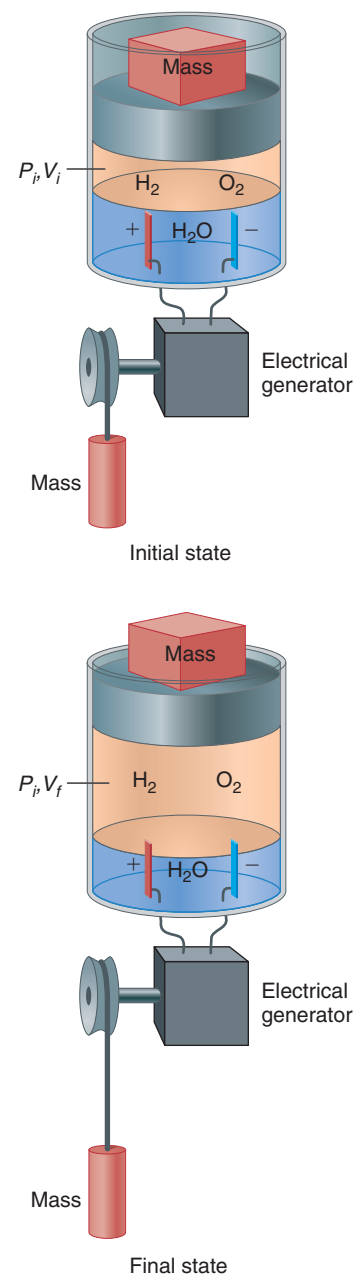


**FIGURE 2.2**
Current produced by a generator is used to electrolyze water and thereby do work on the system as shown by the lowered mass linked to the generator.

**TABLE 2.1    Types of Work**

| Types of Work | Variables | Equation for Work | Conventional Units |
|---|---|---|---|
| Volume expansion | Pressure ($P$), volume ($V$) | $w = -\displaystyle\int_{V_i}^{V_f} P_{external}\, dV$ | Pa m$^3$ = J |
| Stretching | Force ($F$), length ($l$) | $w = \displaystyle\int_{x_i}^{x_f} \mathbf{F} \cdot d\mathbf{l}$ | N m = J |
| Surface expansion | Surface tension ($\gamma$), area ($\sigma$) | $w = \displaystyle\int_{\sigma_i}^{\sigma_f} \boldsymbol{\gamma} \cdot d\boldsymbol{\sigma}$ | (N m$^{-1}$)(m$^2$) = J |
| Electrical | Electrical potential ($\phi$), electrical charge ($Q$) | $w = \displaystyle\int_{0}^{Q} \phi\, dQ'$ | V C = J |

### EXAMPLE PROBLEM 2.1

**a.** Calculate the work involved in expanding 20.0 L of an ideal gas to a final volume of 85.0 L against a constant external pressure of 2.50 bar.

**b.** A bubble is expanded from a radius of 1.00 cm to a radius of 3.25 cm. The surface tension of water is 71.99 N m$^{-1}$. How much work is done in increasing the area of the bubble?

**c.** A current of 3.20 A is passed through a heating coil for 30.0 s. The electrical potential across the resistor is 14.5 V. Calculate the work done on the coil.

**d.** If the force to stretch a fiber a distance $x$ is given by $F = -kx$ with k = 100. N cm$^{-1}$, how much work is done to stretch the fiber 0.15 cm?

**Solution**

**a.** $w = -\displaystyle\int_{V_i}^{V_f} P_{external}\, dV = -P_{external}(V_f - V_i)$

$$= -2.50 \text{ bar} \times \frac{10^5 \text{ Pa}}{\text{bar}} \times (85.0 \text{ L} - 20.0 \text{ L}) \times \frac{10^{-3} \text{ m}^3}{\text{L}} = -16.3 \text{ kJ}$$

**b.** A factor of 2 is included in the following calculation because a bubble has an inner and an outer surface. We consider the bubble and its contents to be the system. The vectors $\boldsymbol{\gamma}$ and $\boldsymbol{\sigma}$ point in opposite directions, giving rise to the negative sign in the second integral.

$$w = \int_{\sigma_i}^{\sigma_f} \boldsymbol{\gamma} \cdot d\boldsymbol{\sigma} = -\int_{\sigma_i}^{\sigma_f} \gamma d\sigma = 2\gamma 4\pi(r_f^2 - r_i^2)$$

$$= -8\pi \times 71.99 \text{ N m}^{-1}(3.25^2 \text{ cm}^2 - 1.00^2 \text{ cm}^2) \times \frac{10^{-4} \text{ m}^2}{\text{cm}^2}$$

$$= -1.73 \text{ J}$$

**c.** $w = \displaystyle\int_{0}^{Q} \phi\, dQ' = \phi Q = I\phi t = 14.5 \text{ V} \times 3.20 \text{ A} \times 30.0 \text{ s} = 1.39 \text{ kJ}$

**d.** We must distinguish between $\mathbf{F}$, the restoring force on the fiber, and $\mathbf{F'}$, the force exerted by the person stretching the fiber. They are related by $\mathbf{F} = -\mathbf{F'}$. If we calculate the work done on the fiber, $\mathbf{F'} \cdot d\mathbf{l} = F' dl$ because the vectors $\mathbf{F'}$ and $d\mathbf{l}$ point in the same direction

$$w = \int_{x_0}^{x_f} \mathbf{F'} \cdot d\mathbf{l} = \int kx\,dx = \left[\frac{kx^2}{2}\right]_{x_0}^{x_f} = \left[\frac{100. \text{ N m}^{-1} \times x^2}{2}\right]_{0}^{0.15} = 1.1 \text{ J}$$

If we calculate the work done by the fiber, the sign of $w$ is reversed because $\mathbf{F}$ and $d\mathbf{l}$ point in opposite directions.

# 2.3 Heat

**Heat**[2] is defined in thermodynamics as the quantity of energy that flows across the boundary between the system and surroundings because of a temperature difference between the system and the surroundings. Heat always flows spontaneously from regions of high temperature to regions of low temperature. Just as for work, several important characteristics of heat are of importance:

- Heat is transitory, in that it only appears during a change in state of the system and surroundings. Heat is not associated with the initial and final states of the system and the surroundings.
- The net effect of heat is to change the internal energy of the system and surroundings in accordance with the first law. If the only change in the surroundings is a change in temperature of a reservoir, heat has flowed between the system and the surroundings. The quantity of heat that has flowed is directly proportional to the change in temperature of the reservoir.
- The sign convention for heat is as follows. If the temperature of the system is raised, $q$ is positive; if it is lowered, $q$ is negative. It is common usage to say that if $q$ is positive, heat is withdrawn from the surroundings and deposited in the system. If $q$ is negative, heat is withdrawn from the system and deposited in the surroundings.

Defining the surroundings as the rest of the universe is impractical because it is not realistic to search through the whole universe to see if a mass has been raised or lowered and if the temperature of a reservoir has changed. Experience shows that in general only those parts of the universe close to the system interact with the system. Experiments can be constructed to ensure that this is the case, as shown in Figure 2.3. Imagine that we are interested in an exothermic chemical reaction that is carried out in a rigid sealed container with diathermal walls. We define the system as consisting solely of the reactant and product mixture. The vessel containing the system is immersed in an inner water bath separated from an outer water bath by a container with rigid diathermal walls. During the reaction, heat flows out of the system ($q < 0$), and the temperature of the inner water bath increases to $T_f$. Using an electrical heater, the temperature of the outer water bath is increased so that at all times, $T_{outer} = T_{inner}$. Because of this condition, no heat flows across the boundary between the two water baths, and because the container enclosing the inner water bath is rigid, no work flows across this boundary. Therefore, $\Delta U = q + w = 0 + 0 = 0$ *for the composite system* made up of the inner water bath and everything within it. Therefore, this composite system is an isolated system that does not interact with the rest of the universe. To determine $q$ and $w$ for the reactant and product mixture, we need to examine only the composite system and can disregard the rest of the universe.

To emphasize the distinction between $q$ and $w$ and the relationship between $q$, $w$, and $\Delta U$, we discuss the two processes shown in Figure 2.4. They are each carried out in an isolated system, divided into two subsystems, I and II. In both cases, system I consists solely of the liquid in the beaker, and everything else including the rigid adiabatic walls is in system II. We refer to system I as the system and system II as the surroundings in the following discussion. We assume that the temperature of the liquid is well below its boiling point so that its vapor pressure is negligibly small. This ensures that no liquid is vaporized in the process, and the system is closed. We also assume that the change in temperature of the system is very small. System II can be viewed as the surroundings for system I and vice versa.
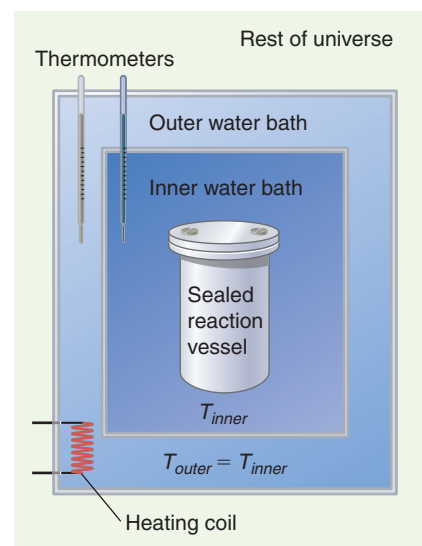


**FIGURE 2.3**

An isolated composite system is created in which the surroundings to the system of interest are limited in extent. The walls surrounding the inner water bath are rigid.

---

[2]Heat is perhaps the most misused term in thermodynamics as discussed by Robert Romer ["Heat is not a Noun." *American Journal of Physics*, 69 (2001), 107–109]. In common usage, it is incorrectly referred to as a substance as in the phrase "Close the door; you're letting the heat out!" An equally inappropriate term is heat capacity (discussed in Section 2.5), because it implies that materials have the capacity to hold heat, rather than the capacity to store energy. We use the terms *heat flow* or *heat transfer* to emphasize the transitory nature of heat. However, you should not think of heat as a fluid or a substance.

**FIGURE 2.4**
Two subsystems, I and II, are enclosed in a rigid adiabatic enclosure. System I consists solely of the liquid in the beaker for each case. System II consists of everything else in the enclosure, and is the surroundings for system I. **(a)** The liquid is heated using a flame. **(b)** The liquid is heated using a resistive coil through which an electrical current flows.



(a)        (b)
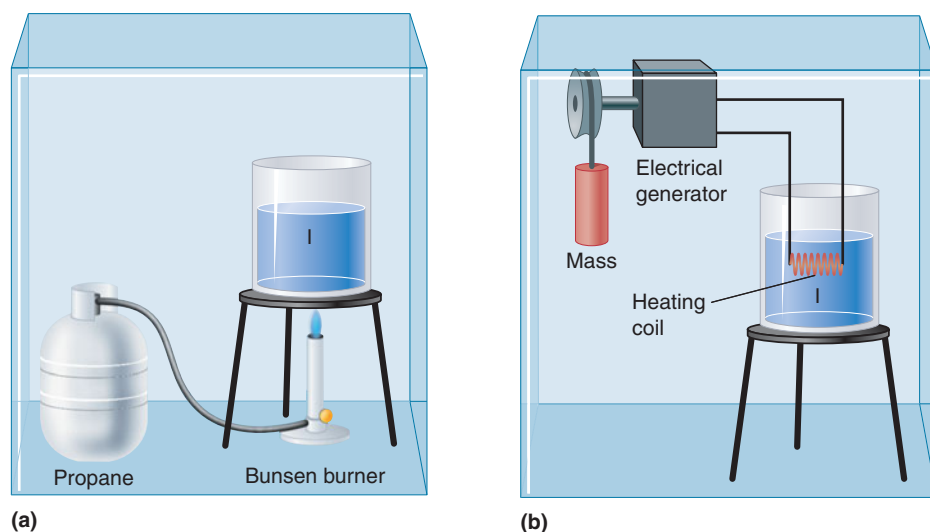
In Figure 2.4a, a Bunsen burner fueled by a propane canister is used to heat the liquid (system). The boundary between system and surroundings is the surface that encloses the liquid, and heat can flow all across this boundary. It is observed that the temperature of the liquid increases in the process. The temperature of the surroundings also increases because the system and surroundings are in thermal equilibrium. From Section 1.2, we know that the internal energy of a monatomic gas increases linearly with $T$. This result can be generalized to state that $U$ is a monotonically increasing function of $T$ for a uniform single-phase system of constant composition. Therefore, because $\Delta T > 0$, $\Delta U > 0$.

We next consider the changes in the surroundings. From the first law, $\Delta U_{surroundings} = -\Delta U < 0$. No forces oppose changes in the system. We conclude that $w = 0$. Therefore, if $\Delta U > 0$, $q > 0$ and $q_{surroundings} < 0$.

We now consider Figure 2.4b. In this case, the boundary between system and surroundings lies just inside the inner wall of the beaker, across the open top of the beaker, and just outside of the surface of the heating coil. Note that the heating coil is entirely in the surroundings. Heat can flow across the boundary surface. Upon letting the mass in the surroundings fall, electricity flows through the heating coil. It is our experience that the temperature of the liquid (system) will increase. We again conclude that $\Delta U > 0$. What values do $q$ and $w$ have for the process?

To answer this question, consider the changes in the surroundings. From the first law, $\Delta U_{surroundings} = -\Delta U < 0$. We see that a mass has been lowered in the surroundings. Can we conclude that $w > 0$? *No, because work is being done only on the heating coil, which is in the surroundings. The current flow never crosses the boundary between system and surroundings.* Therefore, $w = 0$ because no work is done on the system. However, $\Delta U > 0$, so if $w = 0$ we conclude that $q > 0$. The increase in $U$ is due to heat flow from the surroundings to the system caused by the difference between the temperature of the heating filament and the liquid and not by the electrical work done on the filament. Note that because $\Delta U + \Delta U_{surroundings} = 0$, the heat flow from the surroundings to the system can be calculated from the electrical work done entirely within the surroundings, $q = -w_{surroundings} = I\phi t$.

These examples show that the distinction between heat and work must be made carefully with a clear knowledge of the position and nature of the boundary between the system and the surroundings.

**EXAMPLE PROBLEM 2.2**

A heating coil is immersed in a 100. g sample of $H_2O$ liquid which boils at 99.61°C in an open insulated beaker on a laboratory bench at 1 bar pressure. In this process, 10.0% of the liquid is converted to the gaseous form at a pressure of 1 bar. A current of 2.00 A flows through the heater from a 12.0 V battery for $1.00 \times 10^3$ s to

effect the transformation. The densities of liquid and gaseous water under these conditions are 997 and 0.590 kg m$^{-3}$, respectively.

a. It is often useful to replace a real process by a model that exhibits the important features of the process. Design a model system and surroundings, like those shown in Figures 2.1 and 2.2, that would allow you to measure the heat and work associated with this transformation. For the model system, define the system and surroundings as well as the boundary between them.

b. How can you define the system for the open insulated beaker on the laboratory bench such that the work is properly described?

c. Calculate $q$ and $w$ for the process.

### Solution

a. The model system is shown in the following figure. The cylinder walls and the piston form adiabatic walls. The external pressure is held constant by a suitable weight.

b. Define the system as the liquid in the beaker and the volume containing only molecules of $H_2O$ in the gas phase. This volume will consist of disconnected volume elements dispersed in the air above the laboratory bench.

c. In the system shown, the heat input to the liquid water can be equated with the work done on the heating coil. Therefore,

$$q = I\phi t = 2.00 \text{ A} \times 12.0 \text{ V} \times 1.00 \times 10^3 \text{ s} = 24.0 \text{ kJ}$$

As the liquid is vaporized, the volume of the system increases at a constant external pressure. Therefore, the work done by the system on the surroundings is

$$w = -P_{external}(V_f - V_i) = -10^5 \text{ Pa}$$
$$\times \left( \frac{10.0 \times 10^{-3} \text{ kg}}{0.590 \text{ kg m}^{-3}} + \frac{90.0 \times 10^{-3} \text{ kg}}{997 \text{ kg m}^{-3}} - \frac{100.0 \times 10^{-3} \text{ kg}}{997 \text{ kg m}^{-3}} \right)$$
$$= -1.70 \text{ kJ}$$

Note that the electrical work done on the heating coil is much larger than the $P$–$V$ work done in the expansion.



$P_{external} = 1.00$ atm

Mass

Heating coil

$H_2O$ (g)

12 V

$H_2O$ (l)
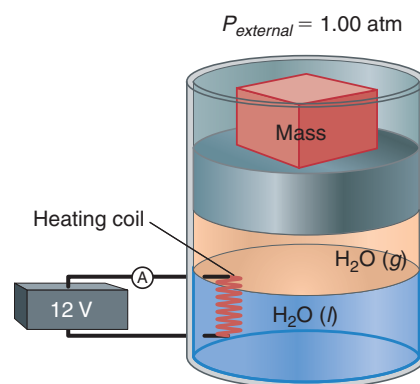
# 2.4 Doing Work on the System and Changing the System Energy from a Molecular Level Perspective

Our discussion so far has involved changes in energy for macroscopic systems, but what happens at the molecular level if energy is added to the system? In shifting to a molecular perspective, we move from a classical to a quantum mechanical description of matter. For this discussion, we need two results that will be discussed elsewhere in this textbook. First, (as discussed in Chapter 4 in Engel, *Quantum Chemistry & Spectroscopy*) in general the energy levels of quantum mechanical systems are discrete and molecules can only possess amounts of energy that correspond to these values. By contrast, in classical mechanics the energy is a continuous variable. Second, we use a result from statistical mechanics that the relative probability of a molecule being in a state corresponding to the allowed energy values $\varepsilon_1$ and $\varepsilon_2$ at temperature $T$ is given by $e^{-([\varepsilon_2-\varepsilon_1]/k_BT)}$. This result will be discussed in Chapter 13.

To keep the mathematics simple, consider a very basic model system: a gas consisting of a single He atom confined in a one-dimensional container with a length of 10. nm. Quantum mechanics tells us that the translational energy of the He atom confined in this box can only have the discrete values shown in Figure 2.5a. We lower the temperature of this one-dimensional He gas to 0.20 K. The calculated probability of the atom being in a given energy level is shown in Figure 2.5a. If we now do work on the system by compressing the box to half its original length at constant temperature, the energy levels will change to those shown in Figure 2.5b. Note

**FIGURE 2.5**
Energy levels are shown for the box of length **(a)** 10. nm, and **(b)** 5.0 nm. The circles indicate the probability that the He atom has an energy corresponding to each of the energy levels at 0.2 K. Each circle indicates a probability of 0.010. For example, the probability that the energy of the He atom corresponds to the lowest energy level in Figure 2.5a is 0.22. Note the different scales for energy in each graph.
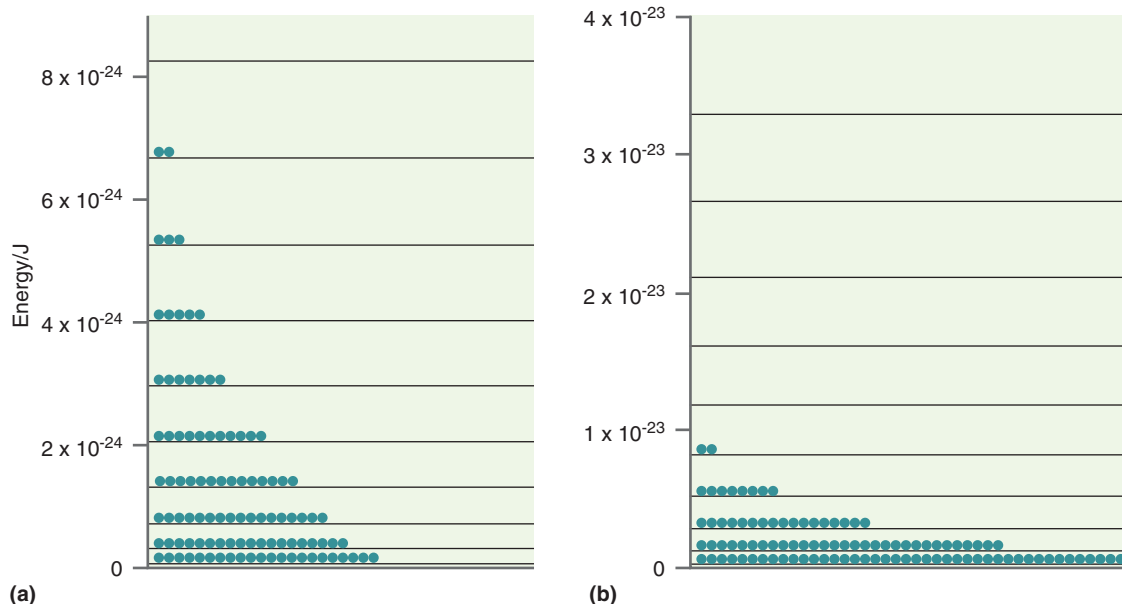
that all the energy levels are shifted to higher values as the container is made smaller (an effect that is fully explored in Chapter 4 in Engel, *Quantum Chemistry & Spectroscopy*). If we keep the temperature constant at 0.20 K during this compression, the distribution of the atoms among the energy levels changes to that shown in Figure 2.5b. This redistribution occurs because the total translational energy of the He atom remains constant in the compression if the temperature is kept constant, assuming ideal gas behavior.

What happens if we keep the container at the smaller length and raise the system energy by increasing $T$ to 0.40 K? In this case, the energy levels are unchanged because they depend on the container length, but not on the temperature of the gas. However, the energy of the system increases and as shown in Figure 2.6, this occurs by a redistribution of the probability of finding the He atom in the energy levels. The increase in system energy comes from an increase in the probability of the He atom populating higher-energy levels and a corresponding decrease in the probability of populating lower-energy levels.

Just as for a calculation of the energy of a gas using classical mechanics, the quantum mechanical system energy increases through an increase in the translational energy

**FIGURE 2.6**
Energy levels are shown for the 5.0 nm box. The circles indicate the probability that a He atom has an energy corresponding to each of the energy levels at **(a)** 0.20 K and **(b)** 0.40 K.
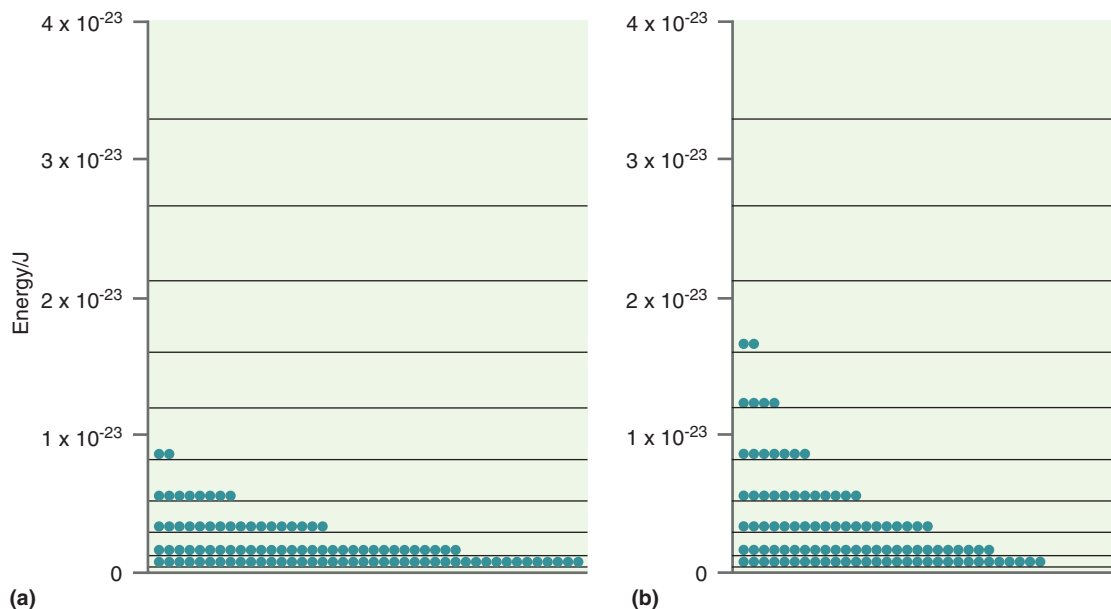
of the atom. However, the discrete energy level structure influences how the system can take up energy. This will become clearer in the next section when we consider how molecules can take up energy through rotation and vibration.

# 2.5 Heat Capacity

The process shown in Figure 2.4b provides a way to quantify heat flow in terms of the easily measured electrical work done on the heating coil, $w = I\phi t$. The response of a single-phase system of constant composition to heat input is an increase in $T$ as long as the system does not undergo a phase change such as the vaporization of a liquid.

The thermal response of the system to heat flow is described by a very important thermodynamic property called the **heat capacity,** which is a measure of energy needed to change the temperature of a substance by a given amount. The name heat capacity is unfortunate because it implies that a substance has the capacity to take up heat. A much better name would be energy capacity.

Heat capacity is a material-dependent property, as will be discussed later. Mathematically, heat capacity is defined by the relation

$$C = \lim_{\Delta T \to 0} \frac{q}{T_f - T_i} = \frac{\bar{d}q}{dT} \tag{2.9}$$

where $C$ is in the SI unit of J K$^{-1}$. It is an extensive quantity that doubles as the mass of the system is doubled. Often, the molar heat capacity $C_m$ is used in calculations. It is an intensive quantity with the units of J K$^{-1}$ mol$^{-1}$. Experimentally, the heat capacity of fluids is measured by immersing a heating coil in the gas or liquid and equating the electrical work done on the coil with the heat flow into the sample. For solids, the heating coil is wrapped around the solid. The significance of the notation $\bar{d}q$ for an incremental amount of heat is explained in the next section.

The value of the heat capacity depends on the experimental conditions under which it is determined. The most common conditions are constant $V$ or $P$, for which the heat capacity is denoted $C_V$ and $C_P$, respectively. Values of $C_{P,m}$ at 298.15 K for pure substances are tabulated in Tables 2.2 and 2.3 (see Appendix A, Data Tables), and formulas for calculating $C_{P,m}$ at other temperatures for gases and solids are listed in Tables 2.4 and 2.5, respectively.

We next discuss heat capacities using a molecular level model, beginning with gases. Figure 2.7 illustrates the energy level structure for a molecular gas. Molecules can take up energy by moving faster, by rotating in three-dimensional space, by periodic oscillations (known as vibrations) of the atoms around their equilibrium structure, and by electronic excitations. These energetic **degrees of freedom** are referred to as
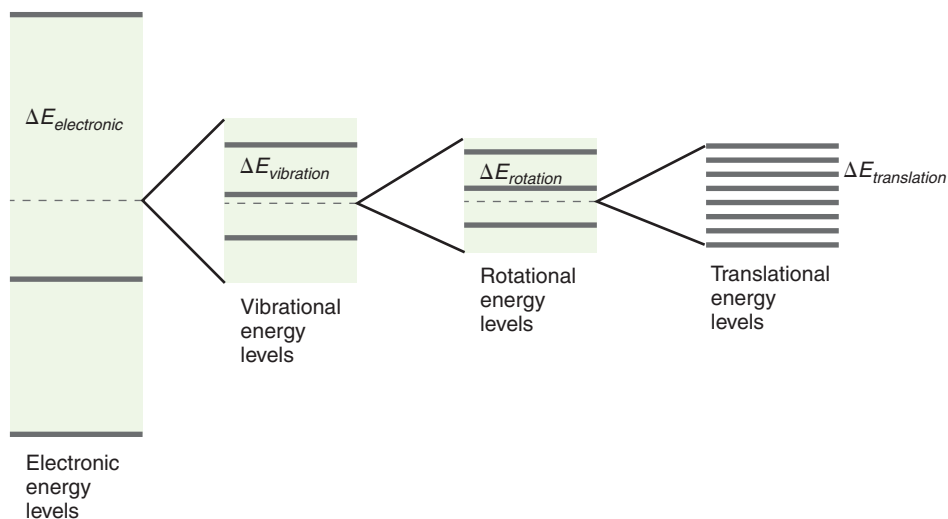


**FIGURE 2.7**
Energy levels are shown schematically for each degree of freedom. The gray area between electronic energy levels on the left indicates what appear to be a continuous range of allowed energies. However, as the energy scale is magnified stepwise, discrete energy levels for vibration, rotation, and translation can be resolved.

**TABLE 2.2** Energy Level Spacings for Different Degrees of Freedom

| Degree of Freedom | Energy Level Spacing |
|---|---|
| Electronic | $5 \times 10^{-19}$ J |
| Vibration | $2 \times 10^{-20}$ J |
| Rotation | $2 \times 10^{-23}$ J |
| Translation | $2 \times 10^{-41}$ J |

translation, rotation, vibration, and electronic excitation. Each of the degrees of freedom has its own set of energy levels and the probability of an individual molecule occupying a higher energy level increases as it gains energy. Except for translation, the energy levels for atoms and molecules are independent of the container size.

The amount of energy needed to move up the ladder of energy levels is very different for the different degrees of freedom: $\Delta E_{\text{electronic}} \gg \Delta E_{\text{vibration}} \gg \Delta E_{\text{rotation}} \gg \Delta E_{\text{translation}}$. Values for these $\Delta E$ are molecule dependent, but order of magnitude numbers are shown in Table 2.2.

Energy is gained or lost by a molecule through collisions with other molecules. An order of magnitude estimate of the energy that can be gained or lost by a molecule in a collision is $k_B T$, where $k = R/N_A$ is the Boltzmann constant, and $T$ is the absolute temperature. A given degree of freedom in a molecule can only take up energy through molecular collisions if the spacing between adjacent energy levels and the temperature satisfies the relationship $\Delta E \approx k_B T$, which has the value $4.1 \times 10^{-21}$ J at 300 K. At 300 K, $\Delta E \approx k_B T$ is always satisfied for translation and rotation, but not for vibration and electronic excitation. We formulate the following general rule relating the heat capacity $C_{V,m}$ and the degrees of freedom in a molecule, which will be discussed in more detail in Chapter 15.

> The heat capacity $C_{V,m}$ for a gas at temperature $T$ not much lower than 300 K is $R/2$ for each translation and rotational degree of freedom, where $R$ is the ideal gas constant. Each vibrational degree of freedom for which the relation $\Delta E/kT < 0.1$ is obeyed contributes $R$ to $C_{V,m}$. If $\Delta E/k_B T > 10$, the degree of freedom does not contribute to $C_{V,m}$. For $10 > \Delta E/k_B T > 0.1$, the degree of freedom contributes partially to $C_{V,m}$.

Figure 2.8 shows the variation of $C_{V,m}$ for a monatomic gas and several molecular gases. Atoms only have three translational degrees of freedom. Linear molecules have an additional 2 rotational degrees of freedom and $3n$-5 vibrational degrees of freedom where $n$ is the number of atoms in the molecule. Nonlinear molecules have 3 translational degrees of freedom, 3 rotational degrees of freedom, and $3n$-6 vibrational degrees of freedom. A He atom has only 3 translational degrees of freedom, and all electronic transitions are of high energy compared to $kT$. Therefore, $C_{V,m} = 3R/2$ over the entire temperature range as shown in the figure. CO is a linear diatomic molecule that has two rotational degrees of freedom for which $\Delta E/k_B T < 0.1$ at 200. K. Therefore, $C_{V,m} = 5R/2$ at 200. K. The single vibrational degree of freedom begins to contribute to $C_{V,m}$ above 200. K, but does not contribute fully for $T < 1000$. K because $10 > \Delta E/k_B T$ below 1000. K. $CO_2$ has 4 vibrational degrees of freedom, some of which contribute to $C_{V,m}$ near 200. K. However, $C_{V,m}$ does not reach its maximum value of $13R/2$ below 1000. K. Similarly, $C_{V,m}$ for $C_2H_4$, which has 12 vibrational degrees of freedom, does not reach its maximum value of 15 R below 1000. K, because $10 > \Delta E/k_B T$ for some vibrational degrees of freedom. Electronic energy levels are too far apart for any of the molecular gases to give a contribution to $C_{V,m}$.

To this point, we have only discussed $C_{V,m}$ for gases. It is easier to measure $C_{P,m}$ than $C_{V,m}$ for liquids and solids because liquids and solids generally expand with increasing temperature and exert enormous pressure on a container at constant volume (see Example Problem 3.2.) An example of how $C_{P,m}$ depends on $T$ for solids and liquids is illustrated in Figure 2.9 for $Cl_2$. To make the functional form of $C_{P,m}(T)$ understandable, we briefly discuss the relative magnitudes of $C_{P,m}$ in the solid, liquid, and gaseous phases using a molecular level model. A solid can be thought of as a set of interconnected harmonic oscillators, and heat uptake leads to the excitations of the collective vibrations of the solid. At very low temperatures these vibrations cannot be activated, because the spacing of the vibrational energy levels is large compared to $k_B T$. As a consequence, energy cannot be taken up by the solid. Hence, $C_{P,m}$ approaches zero as $T$ approaches zero. For the solid, $C_{P,m}$ rises rapidly with $T$ because the thermal energy available as $T$ increases is sufficient to activate the vibrations of



**FIGURE 2.8**
Molar heat capacities $C_{V,m}$ are shown for a number of gases. Atoms have only translational degrees of freedom and, therefore, have comparatively low values for $C_{V,m}$ that are independent of temperature. Molecules with vibrational degrees of freedom have higher values of $C_{V,m}$ at temperatures sufficiently high to activate the vibrations.

the solid. The heat capacity increases discontinuously as the solid melts to form a liquid. This is the case because the liquid retains all the local vibrational modes of the solid, and more low-energy modes become available upon melting. Therefore, the heat capacity of the liquid is greater than that of the solid. As the liquid vaporizes, the local vibrational modes present in the liquid are converted to translations that cannot take up as much energy as vibrations. Therefore, $C_{P,m}$ decreases discontinuously at the vaporization temperature. The heat capacity in the gaseous state increases slowly with temperature as the vibrational modes of the individual molecules are activated as discussed previously. These changes in $C_{P,m}$ can be calculated for a specific substance using a microscopic model and statistical thermodynamics, as will be discussed in detail in Chapter 15.

Once the heat capacity of a variety of different substances has been determined, we have a convenient way to quantify heat flow. For example, at constant pressure, the heat flow between the system and surroundings can be written as

$$q_P = \int_{T_{sts,i}}^{T_{sys,f}} C_P^{system}(T)dT = -\int_{T_{surr,i}}^{T_{surr,f}} C_P^{surroundings}(T)dT \qquad \textbf{(2.10)}$$

By measuring the temperature change of a thermal reservoir in the surroundings at constant pressure, $q_P$ can be determined. In Equation (2.10), the heat flow at constant pressure has been expressed both from the perspective of the system and from the perspective of the surroundings. A similar equation can be written for a constant volume process. Water is a convenient choice of material for a heat bath in experiments because $C_P$ is nearly constant at the value 4.18 J g$^{-1}$ K$^{-1}$ or 75.3 J mol$^{-1}$ K$^{-1}$ over the range from 0°C to 100.°C.
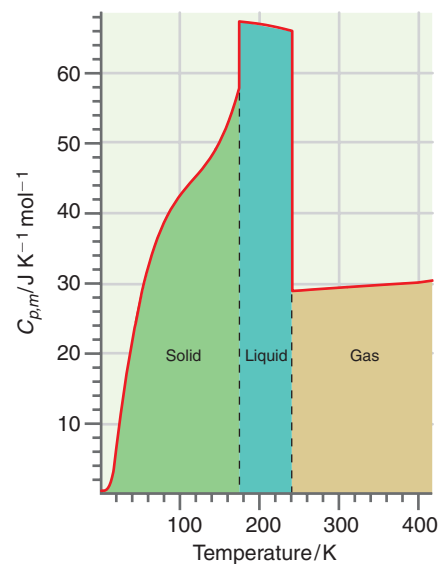


**FIGURE 2.9**
The variation of $C_{P,m}$ with temperature is shown for $Cl_2$.

---

**EXAMPLE PROBLEM 2.3**

The volume of a system consisting of an ideal gas decreases at constant pressure. As a result, the temperature of a 1.50 kg water bath in the surroundings increases by 14.2°C. Calculate $q_P$ for the system.

**Solution**

$$q_P = \int_{T_{surr,i}}^{T_{surr,f}} C_P^{surroundings}(T)dT = -C_P^{surroundings}\Delta T$$

$$= -1.50 \text{ kg} \times 4.18 \text{ J g}^{-1} \text{ K}^{-1} \times 14.2 \text{ K} = -89.1 \text{ kJ}$$



Constant pressure heating

Initial state      Final state

How are $C_P$ and $C_V$ related for a gas? Consider the processes shown in Figure 2.10 in which a fixed amount of heat flows from the surroundings into a gas. In the constant pressure process, the gas expands as its temperature increases. Therefore, the system does work on the surroundings. As a consequence, not all the heat flow into the system can be used to increase $\Delta U$. No such work occurs for the corresponding constant volume process, and all the heat flow into the system can be used to increase $\Delta U$. Therefore, $dT_P < dT_V$ for the same heat flow $dq$. For this reason, $C_P > C_V$ for gases.

The same argument applies to liquids and solids as long as $V$ increases with $T$. Nearly all substances follow this behavior, although notable exceptions occur, such as liquid water between 0°C and 4°C, for which the volume increases as $T$ decreases. However, because $\Delta V_m$ upon heating is much smaller than for a gas, the difference between $C_{P,m}$ and $C_{V,m}$ for a liquid or solid is much smaller than for a gas.

Constant volume heating

Initial state      Final state
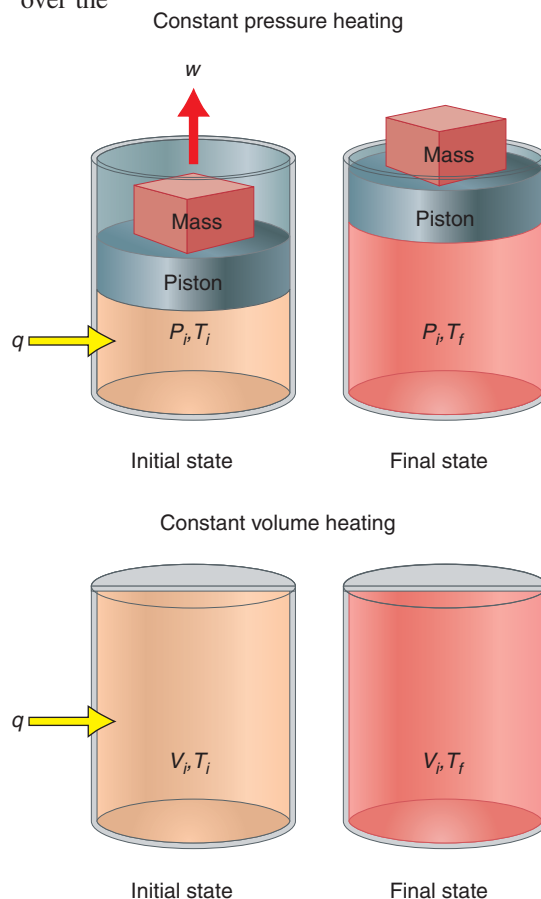
**FIGURE 2.10**
Not all the heat flow into the system can be used to increase $\Delta U$ in a constant pressure process, because the system does work on the surroundings as it expands. However, no work is done for constant volume heating.

The preceding remarks about the difference between $C_P$ and $C_V$ have been qualitative in nature. However, the following quantitative relationship, which will be proved in Chapter 3, holds for an ideal gas:

$$C_P - C_V = nR \quad \text{or} \quad C_{P,m} - C_{V,m} = R \tag{2.11}$$

## 2.6 State Functions and Path Functions

An alternate statement of the first law is that $\Delta U$ is independent of the path connecting the initial and final states, and depends only on the initial and final states. We make this statement plausible for the kinetic energy, and the argument can be extended to the other forms of energy listed in Section 2.1. Consider a single molecule in the system. Imagine that the molecule of mass $m$ initially has the speed $v_1$. We now change its speed incrementally following the sequence $v_1 \rightarrow v_2 \rightarrow v_3 \rightarrow v_4$. The change in the kinetic energy along this sequence is given by

$$\Delta E_{kinetic} = \left( \frac{1}{2} m(v_2)^2 - \frac{1}{2} m(v_1)^2 \right) + \left( \frac{1}{2} m(v_3)^2 - \frac{1}{2} m(v_2)^2 \right)$$

$$+ \left( \frac{1}{2} m(v_4)^2 - \frac{1}{2} m(v_3)^2 \right)$$

$$= \left( \frac{1}{2} m(v_4)^2 - \frac{1}{2} m(v_1)^2 \right) \tag{2.12}$$

Even though $v_2$ and $v_3$ can take on any arbitrary values, they still do not influence the result. We conclude that the change in the kinetic energy depends only on the initial and final speed and that it is independent of the path between these values. Our conclusion remains the same if we increase the number of speed increments in the interval between $v_1$ and $v_2$ to an arbitrarily large number. Because this conclusion holds for all molecules in the system, it also holds for $\Delta U$.

This example supports the assertion that $\Delta U$ depends only on the final and initial states and not on the path connecting these states. Any function that satisfies this condition is called a **state function,** because it depends only on the state of the system and not the path taken to reach the state. This property can be expressed in a mathematical form. Any state function, for example $U$, must satisfy the equation

$$\Delta U = \int_i^f dU = U_f - U_i \tag{2.13}$$

where $i$ and $f$ denote the initial and final states. This equation states that in order for $\Delta U$ to depend only on the initial and final states characterized here by $i$ and $f$, the value of the integral must be independent of the path. If this is the case, $U$ can be expressed as an infinitesimal quantity, $dU$, that when integrated, depends only on the initial and final states. The quantity $dU$ is called an **exact differential.** We defer a discussion of exact differentials to Chapter 3.

It is useful to define a cyclic integral, denoted by the symbol $\oint$, as applying to a **cyclic path** such that the initial and final states are identical. For $U$ or any other state function,

$$\oint dU = U_f - U_f = 0 \tag{2.14}$$

because the initial and final states are the same in a cyclic process.

We next show that $q$ and $w$ are not state functions. The state of a single-phase system at fixed composition is characterized by any two of the three variables $P$, $T$, and $V$. The same is true of $U$. Therefore, for a system of fixed mass, $U$ can be written in any of the three forms $U(V,T)$, $U(P,T)$, or $U(P,V)$. Imagine that a gas characterized by $V_1$ and $T_1$ is confined in a piston and cylinder system that is isolated from the surroundings. There is a thermal reservoir in the surroundings at a temperature $T_3 < T_1$. We do compression work on the system starting from an initial state in which the volume is $V_1$ to

an intermediate state in which the volume is $V_2$ using a constant external pressure $P_{external}$ where $V_2 < V_1$. The work is given by

$$w = -\int_{V_i}^{V_f} P_{external}\, dV = -P_{external}\int_{V_i}^{V_f} dV = -P_{external}(V_f - V_i) = -P_{external}\Delta V \quad \textbf{(2.15)}$$

Because work is done on the system in the compression (see Figure 2.11), $w$ is positive and $U$ increases. Because the system consists of a uniform single phase, $U$ is a monotonic function of $T$, and $T$ also increases. The change in volume $\Delta V$ has been chosen such that the temperature of the system $T_2$ in the intermediate state after the compression satisfies the inequality $T_1 < T_2 < T_3$.

We next lock the piston in place and let an amount of heat $q$ flow between the system and surroundings at constant $V$ by bringing the system into contact with the reservoir at temperature $T_3$. The final state values of $T$ and $V$ after these two steps are $T_3$ and $V_2$.

This two-step process is repeated for different values of the external pressure by changing the mass resting on the piston. In each case the system is in the same final state characterized by the variables $V_2$ and $T_3$. The sequence of steps that takes the system from the initial state $V_1,T_1$ to the final state $V_2,T_3$ is referred to as a **path.** By changing the mass, a set of different paths is generated, all of which originate from the state $V_1,T_1$, and end in the state $V_2,T_3$. According to the first law, $\Delta U$ for this two-step process is

$$\Delta U = U(T_3,V_2) - U(T_1,V_1) = q + w \quad \textbf{(2.16)}$$

Because $\Delta U$ is a state function, its value for the two-step process just described is the same for each of the different values of the mass.

Are $q$ and $w$ also state functions? For this two step process,

$$w = -P_{external}\Delta V \quad \textbf{(2.17)}$$

and $P_{external}$ is different for each value of the mass or for each path, whereas $\Delta V$ is constant. Therefore, $w$ is also different for each path; we can choose one path from $V_1,T_1$ to $V_2,T_3$ and a different path from $V_2,T_3$ back to $V_1,T_1$. Because the work is different along these paths, the cyclic integral of work is not equal to zero. Therefore, $w$ is not a state function.

Using the first law to calculate $q$ for each of the paths, we obtain the result

$$q = \Delta U - w = \Delta U + P_{external}\Delta V \quad \textbf{(2.18)}$$

Because $\Delta U$ is the same for each path, and $w$ is different for each path, we conclude that $q$ is also different for each path. Just as for work, the cyclic integral of heat is not equal to zero. Therefore, neither $q$ nor $w$ are state functions, and they are called **path functions.**

Because both $q$ and $w$ are path functions, there are no exact differentials for work and heat unless the path is specified. Incremental amounts of these quantities are denoted by $\text{\dj}q$ and $\text{\dj}w$, rather than $dq$ and $dw$, to emphasize the fact that incremental amounts of work and heat are not exact differentials. Because $\text{\dj}q$ and $\text{\dj}w$ are not exact differentials, there are no such quantities as $\Delta q$, $q_f$, $q_i$ and $\Delta w$, $w_f$, $w_i$. One cannot refer to the work or heat possessed by a system or to the change in work or heat associated with a process. After a transfer of heat and/or work between the system and surroundings is completed, the system and surroundings possess internal energy, but not heat or work.

The preceding discussion emphasizes that it is important to use the terms *work* and *heat* in a way that reflects the fact that they are not state functions. Examples of systems of interest to us are batteries, fuel cells, refrigerators, and internal combustion engines. In each case, the utility of these systems is that work and/or heat flows between the system and surroundings. For example, in a refrigerator, electrical energy is used to extract heat from the inside of the device and to release it in the surroundings. One can speak of the refrigerator as having the capacity to extract heat, but it would be wrong to speak of it as having heat. In the internal combustion engine, chemical energy contained in the bonds of the fuel molecules and in $O_2$ is released in forming $CO_2$ and $H_2O$. This change in internal energy can be used to rotate the wheels of the vehicle, thereby inducing a flow of work between the vehicle and the surroundings. One can refer to the capability of the engine to do work, but it would be incorrect to refer to the vehicle or the engine as containing or having work.
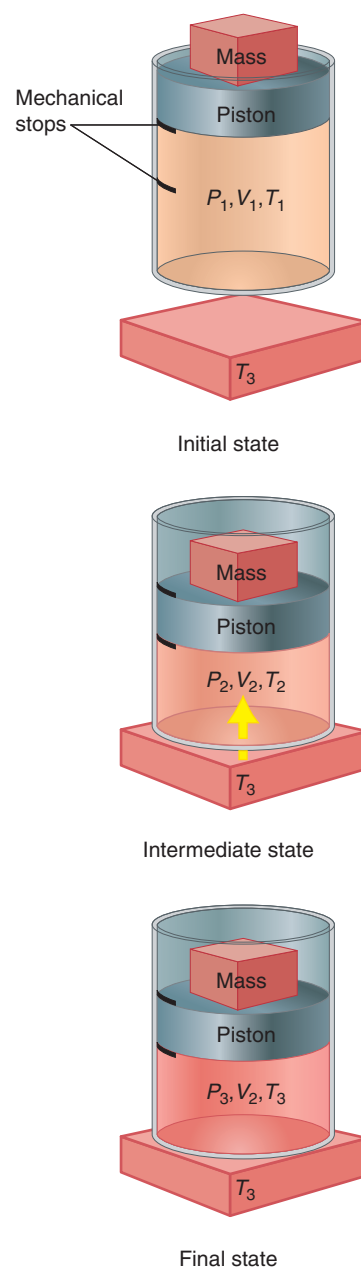


**FIGURE 2.11**
A system consisting of an ideal gas is contained in a piston and cylinder assembly. An external pressure is generated by the mass resting on the piston. The gas in the initial state $V_1,T_1$ is compressed to an intermediate state, whereby the temperature increases to the value $T_2$. It is then brought into contact with a thermal reservoir at $T_3$, leading to a further rise in temperature. The final state is $V_2,T_3$. The mechanical stops allow the system volume to be only $V_1$ or $V_2$.
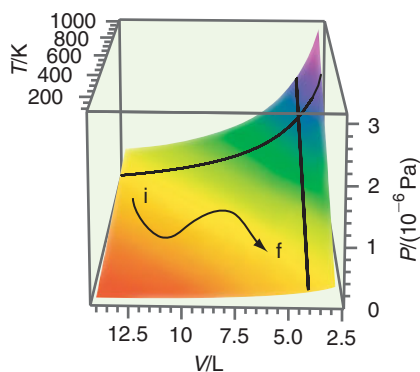
**FIGURE 2.12**

All combinations of pressure, volume, and temperature consistent with 1 mol of an ideal gas lie on the colored surface. All combinations of pressure and volume consistent with $T = 800$ K and all combinations of pressure and temperature consistent with a volume of 4.0 L are shown as black curves that lie in the $P$–$V$–$T$ surface. The third curve corresponds to a path between an initial state $i$ and a final state $f$ that is neither a constant temperature nor a constant volume path.
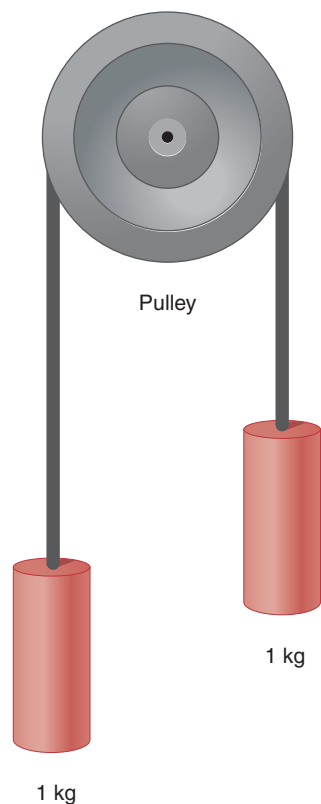
## 2.7 Equilibrium, Change, and Reversibility

Thermodynamics can only be applied to systems in internal equilibrium, and a requirement for equilibrium is that the overall rate of change of all processes such as diffusion or chemical reaction be zero. How do we reconcile these statements with our calculations of $q$, $w$, and $\Delta U$ associated with processes in which there is a macroscopic change in the system? To answer this question, it is important to distinguish between the system and surroundings each being in internal equilibrium, and the system and surroundings being in equilibrium with one another.

We first discuss the issue of internal equilibrium. Consider a system made up of an ideal gas, which satisfies the equation of state, $P = nRT/V$. All combinations of $P$, $V$, and $T$ consistent with this equation of state form a surface in $P$–$V$–$T$ space as shown in Figure 2.12. All points on the surface correspond to states of internal equilibrium, meaning that the system is uniform on all length scales and is characterized by single values of $T$, $P$, and concentration. Points that are not on the surface do not correspond to any equilibrium state of the system because the equation of state is not satisfied. Nonequilibrium situations cannot be represented on such a plot, because $T$, $P$, and concentration do not have unique values for a system that is not in equilibrium. An example of a system that is not in internal equilibrium is a gas that is expanding so rapidly that different regions of the gas have different values for the density, pressure, and temperature.

Next, consider a process in which the system changes from an initial state characterized by $P_i$, $V_i$, and $T_i$ to a final state characterized by $P_f$, $V_f$, and $T_f$ as shown in Figure 2.12. If the rate of change of the macroscopic variables is negligibly small, the system passes through a succession of states of internal equilibrium as it goes from the initial to the final state. Such a process is called a **quasi-static process,** in which internal equilibrium is maintained in the system. If the rate of change is large, the rates of diffusion and intermolecular collisions may not be high enough to maintain the system in a state of internal equilibrium. Thermodynamic calculations for such a process are valid only if it is meaningful to assign a single value of the macroscopic variables $P$, $V$, $T$, and concentration to the system undergoing change. The same considerations hold for the surroundings. We only consider quasi-static processes in this text.

We now visualize a process in which the system undergoes a major change in terms of a directed path consisting of a sequence of quasi-static processes, and distinguish between two very important classes of quasi-static processes, namely reversible and irreversible processes. It is useful to consider the mechanical system shown in Figure 2.13 when discussing reversible and irreversible processes. Because the two masses have the same value, the net force acting on each end of the wire is zero, and the masses will not move. If an additional mass is placed on either of the two masses, the system is no longer in mechanical equilibrium, and the masses will move. In the limit in which the incremental mass approaches zero, the velocity at which the initial masses move approaches zero. In this case, one refers to the process as being **reversible,** meaning that the direction of the process can be reversed by placing the infinitesimal mass on the other side of the pulley.

Reversibility in a chemical system can be illustrated by a system consisting of liquid water in equilibrium with gaseous water that is surrounded by a thermal reservoir. The system and surroundings are both at temperature $T$. An infinitesimally small increase in $T$ results in a small increase of the amount of water in the gaseous phase, and a small decrease in the liquid phase. An equally small decrease in the temperature has the opposite effect. Therefore, fluctuations in $T$ give rise to corresponding fluctuations in the composition of the system. If an infinitesimal opposing change in the variable that drives the process (temperature in this case) causes a reversal in the direction of the process, the process is reversible.

If an infinitesimal change in the driving variable does not change the direction of the process, one says that the process is **irreversible.** For example, if a large stepwise temperature increase is induced in the system using a heat pulse, the amount of water in the gas phase increases abruptly. In this case, the composition of the system cannot be



**FIGURE 2.13**

Two masses of exactly 1 kg each are connected by a wire of zero mass running over a frictionless pulley. The system is in mechanical equilibrium and the masses are stationary.

returned to its initial value by an infinitesimal temperature decrease. This relationship is characteristic of an irreversible process. Although any process that takes place at a rapid rate in the real world is irreversible, real processes can approach reversibility in the appropriate limit. For example, a slow increase in the electrical potential in an electrochemical cell can convert reactants to products in a nearly reversible process.

# 2.8 Comparing Work for Reversible and Irreversible Processes

We concluded in Section 2.6 that $w$ is not a state function and that the work associated with a process is path dependent. This statement can be put on a quantitative footing by comparing the work associated with the reversible and irreversible expansion and the compression of an ideal gas. This process is discussed next and illustrated in Figure 2.14.

Consider the following irreversible process, meaning that the internal and external pressures are not equal. A quantity of an ideal gas is confined in a cylinder with a weightless movable piston. The walls of the system are diathermal, allowing heat to flow between the system and surroundings. Therefore, the process is isothermal at the temperature of the surroundings, $T$. The system is initially defined by the variables $T$, $P_1$, and $V_1$. The position of the piston is determined by $P_{external} = P_1$, which can be changed by adding or removing weights from the piston. Because the weights are moved horizontally, no work is done in adding or removing them. The gas is first expanded at constant temperature by decreasing $P_{external}$ abruptly to the value $P_2$ (weights are removed), where $P_2 < P_1$. A sufficient amount of heat flows into the system through the diathermal walls to keep the temperature at the constant value $T$. The system is now in the state defined by $T$, $P_2$, and $V_2$, where $V_2 > V_1$. The system is then returned to its original state in an **isothermal process** by increasing $P_{external}$ abruptly to its original value $P_1$ (weights are added). Heat flows out of the system into the surroundings in this step. The system has been restored to its original state and, because this is a cyclic process, $\Delta U = 0$. Are $q_{total}$ and $w_{total}$ also zero for the cyclic process? The total work associated with this cyclic process is given by the sum of the work for each individual step:

$$w_{total} = \sum_i - P_{external,i} \Delta V_i = w_{expansion} + w_{compression}$$

$$= -P_2(V_2 - V_1) - P_1(V_1 - V_2)$$

$$= -(P_2 - P_1) \times (V_2 - V_1) > 0 \quad \text{because } P_2 < P_1 \quad \text{and } V_2 > V_1 \quad \textbf{(2.19)}$$

The relationship between $P$ and $V$ for the process under consideration is shown graphically in Figure 2.14, in what is called an **indicator diagram.** An indicator diagram is useful because the work done in the expansion and contraction steps can be evaluated from the appropriate area in the figure, which is equivalent to evaluating the integral $w = -\int P_{external} \, dV$. Note that the work done in the expansion is negative because $\Delta V > 0$, and that done in the compression is positive because $\Delta V < 0$. Because $P_2 < P_1$, the magnitude of the work done in the compression process is more than that done in the expansion process and $w_{total} > 0$. What can one say about $q_{total}$? The first law states that because $\Delta U = q_{total} + w_{total} = 0$, $q_{total} < 0$.

The same cyclical process is carried out in a reversible cycle. A necessary condition for reversibility is that $P = P_{external}$ at every step of the cycle. This means that $P$ changes during the expansion and compression steps. The work associated with the expansion is

$$w_{expansion} = -\int P_{external} \, dV = -\int P \, dV = -nRT \int \frac{dV}{V} = -nRT \ln \frac{V_2}{V_1} \quad \textbf{(2.20)}$$

This work is shown schematically as the red area in the indicator diagram of Figure 2.15.

If this process is reversed and the compression work is calculated, the following result is obtained:

$$w_{compression} = -nRT \ln \frac{V_1}{V_2} \quad \textbf{(2.21)}$$
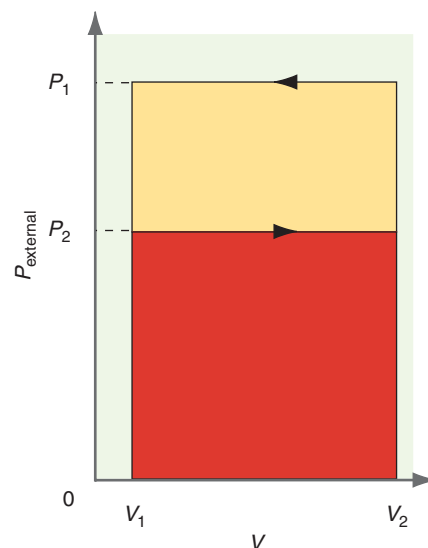


**FIGURE 2.14**
The work for each step and the total work can be obtained from an indicator diagram. For the compression step, $w$ is given by the total area in red and yellow; for the expansion step, $w$ is given by the red area. The arrows indicate the direction of change in $V$ in the two steps. The sign of $w$ is opposite for these two processes. The total work in the cycle is the yellow area.
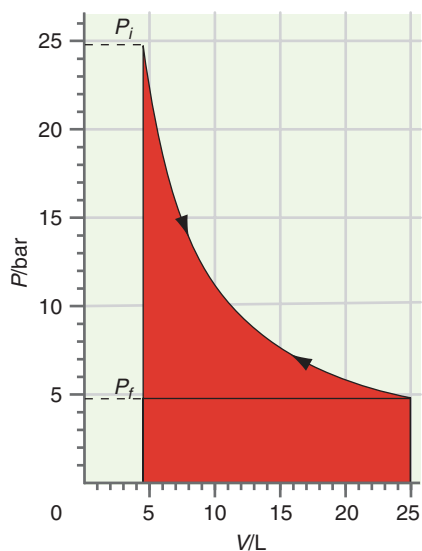
**FIGURE 2.15**
Indicator diagram for a reversible process. Unlike Figure 2.14, the areas under the P–V curves are the same in the forward and reverse directions.

The magnitudes of the work in the forward and reverse processes are equal. The total work done in this cyclical process is given by

$$w = w_{expansion} + w_{compression} = -nRT \ln \frac{V_2}{V_1} - nRT \ln \frac{V_1}{V_2}$$

$$= -nRT \ln \frac{V_2}{V_1} + nRT \ln \frac{V_2}{V_1} = 0 \tag{2.22}$$

Therefore, the work done in a reversible isothermal cycle is zero. Because $\Delta U = q + w$ is a state function, $q = -w = 0$ for this reversible isothermal process. Looking at the heights of the weights in the surroundings at the end of the process, we find that they are the same as at the beginning of the process. To compare the work for reversible and irreversible processes, the state variables need to be given specific values as is done in Example Problem 2.4.

## EXAMPLE PROBLEM 2.4

In this example, 2.00 mol of an ideal gas undergoes isothermal expansion along three different paths: (1) reversible expansion from $P_i = 25.0$ bar and $V_i = 4.50$ L to $P_f = 4.50$ bar, (2) a single-step irreversible expansion against a constant external pressure of 4.50 bar, and (3) a two-step irreversible expansion consisting initially of an expansion against a constant external pressure of 11.0 bar until $P = P_{external}$, followed by an expansion against a constant external pressure of 4.50 bar until $P = P_{external}$.

Calculate the work for each of these processes. For which of the irreversible processes is the magnitude of the work greater?

### Solution

The processes are depicted in the following indicator diagram:
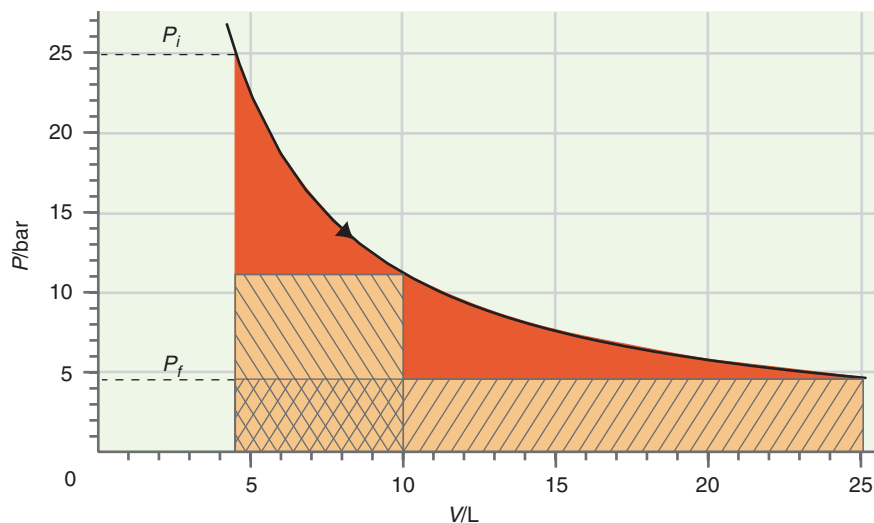


We first calculate the constant temperature at which the process is carried out, the final volume, and the intermediate volume in the two-step expansion:

$$T = \frac{P_i V_i}{nR} = \frac{25.0 \text{ bar} \times 4.50 \text{ L}}{8.314 \times 10^{-2} \text{ L bar mol}^{-1} \text{ K}^{-1} \times 2.00 \text{ mol}} = 677 \text{ K}$$

$$V_f = \frac{nRT}{P_f} = \frac{8.314 \times 10^{-2} \text{ L bar mol}^{-1} \text{ K}^{-1} \times 2.00 \text{ mol} \times 677 \text{ K}}{4.50 \text{ bar}} = 25.0 \text{ L}$$

$$V_{int} = \frac{nRT}{P_{int}} = \frac{8.314 \times 10^{-2} \text{ L bar mol}^{-1} \text{ K}^{-1} \times 2.00 \text{ mol} \times 677 \text{ K}}{11.0 \text{ bar}} = 10.2 \text{ L}$$

The work of the reversible process is given by

$$w = -nRT_1 \ln \frac{V_f}{V_i}$$

$$= -2.00 \text{ mol} \times 8.314 \text{ J mol}^{-1} \text{ K}^{-1} \times 677 \text{ K} \times \ln \frac{25.0 \text{ L}}{4.50 \text{ L}} = -19.3 \times 10^3 \text{ J}$$

We next calculate the work of the single-step and two-step irreversible processes:

$$w_{single} = -P_{external}\Delta V = -4.50 \text{ bar} \times \frac{10^5 \text{ Pa}}{\text{bar}} \times (25.0 \text{ L} - 4.50 \text{ L}) \times \frac{10^{-3} \text{ m}^3}{\text{L}}$$

$$= -9.23 \times 10^3 \text{ J}$$

$$w_{two\text{-}step} = -P_{external}\Delta V = -11.0 \text{ bar} \times \frac{10^5 \text{ Pa}}{\text{bar}} \times (10.2 \text{ L} - 4.50 \text{ L}) \times \frac{10^{-3} \text{ m}^3}{\text{L}}$$

$$-4.50 \text{ bar} \times \frac{10^5 \text{ Pa}}{\text{bar}} \times (25.0 \text{ L} - 10.2 \text{ L}) \times \frac{10^{-3} \text{ m}^3}{\text{L}}$$

$$= -12.9 \times 10^3 \text{ J}$$

The magnitude of the work is greater for the two-step process than for the single-step process, but less than that for the reversible process.

Example Problem 2.4 shows that the magnitude of $w$ for the irreversible expansion is less than that for the reversible expansion, but also suggests that the magnitude of $w$ for a multistep expansion process increases with the number of steps. This is indeed the case, as shown in Figure 2.16. Imagine that the number of steps $n$ increases indefinitely.
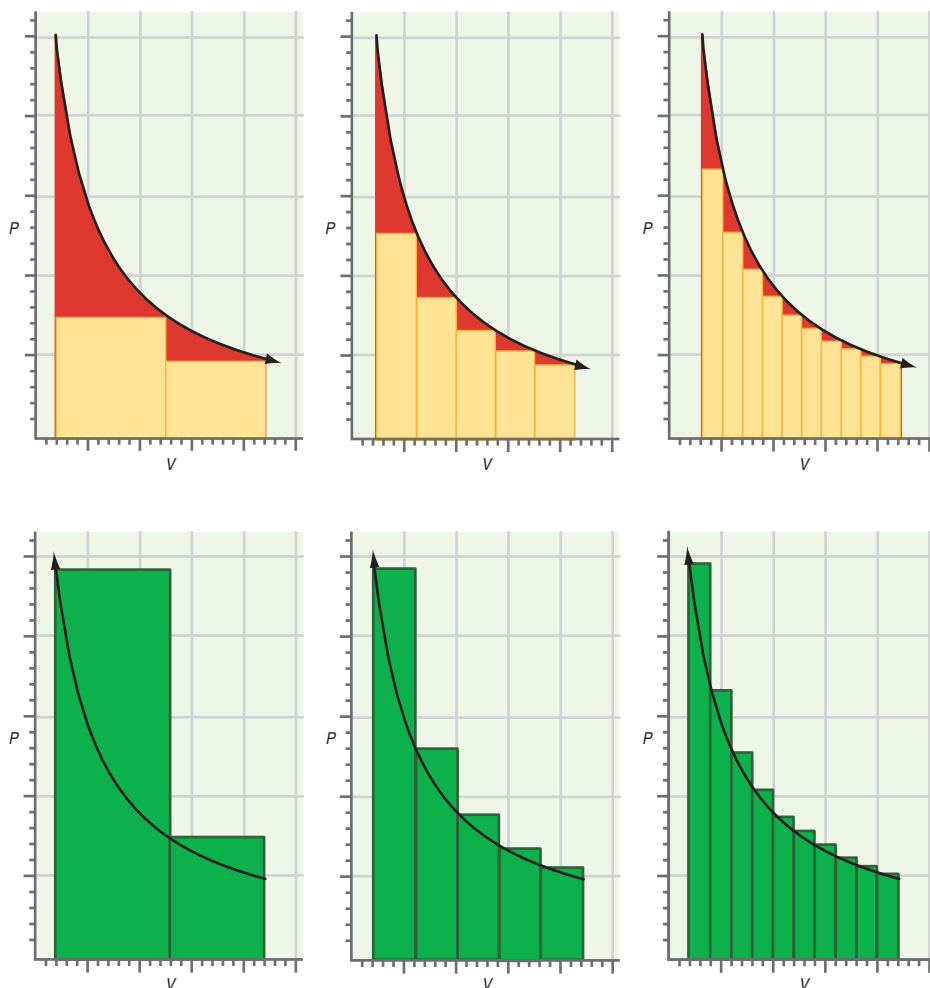


**FIGURE 2.16**
The work done in an expansion (red plus yellow areas) is compared with the work done in a multistep series of irreversible expansion processes at constant pressure (yellow area) in the top panel. The bottom panel shows analogous results for the compression, where the area under the black curve is the reversible compression work. Note that the total work done in the irreversible expansion and compression processes approaches that of the reversible process as the number of steps becomes large.

As $n$ increases, the pressure difference $P_{external} - P$ for each individual step decreases. In the limit that $n \rightarrow \infty$, the pressure difference $P_{external} - P \rightarrow 0$, and the total area of the rectangles in the indicator diagram approaches the area under the reversible curve. In this limit, the irreversible process becomes reversible and the value of the work equals that of the reversible process.

By contrast, the magnitude of the irreversible compression work exceeds that of the reversible process for finite values of $n$ and becomes equal to that of the reversible process as $n \rightarrow \infty$. The difference between the expansion and compression processes results from the requirement that $P_{external} < P$ at the beginning of each expansion step, whereas $P_{external} > P$ at the beginning of each compression step.

On the basis of these calculations for the reversible and irreversible cycles, we introduce another criterion to distinguish between reversible and irreversible processes. Suppose that a system undergoes a change through one or more individual steps, and that the system is restored to its initial state by following the same steps in reverse order. The system is restored to its initial state because the process is cyclical. If the surroundings are also returned to their original state (all masses at the same height and all reservoirs at their original temperatures), the process is reversible. If the surroundings are not restored to their original state, the process is irreversible.

We are often interested in extracting work from a system. For example, it is the expansion of the fuel–air mixture in an automobile engine upon ignition that provides the torque that eventually drives the wheels. Is the capacity to do work similar for reversible and irreversible processes? This question is answered using the indicator diagrams of Figures 2.14 and 2.15 for the specific case of isothermal expansion work, noting that the work can be calculated from the area under the $P$–$V$ curve. We compare the work for expansion from $V_1$ to $V_2$ in a single stage at constant pressure to that for the reversible case. For the single-stage expansion, the constant external pressure is given by $P_{external} = nRT/V_2$. However, if the expansion is carried out reversibly, the system pressure is always greater than this value. By comparing the areas in the indicator diagrams of Figure 2.16, it is seen that

$$\left|w_{reversible}\right| \geq \left|w_{irreversible}\right| \tag{2.23}$$

By contrast, for the compression step,

$$\left|w_{reversible}\right| \leq \left|w_{irreversible}\right| \tag{2.24}$$

The reversible work is the lower bound for the compression work and the upper bound for the expansion work. This result for the expansion work can be generalized to an important statement that holds for all forms of work: *The maximum work that can be extracted from a process between the same initial and final states is that obtained under reversible conditions.*

Although the preceding statement is true, it suggests that it would be optimal to operate an automobile engine under conditions in which the pressure inside the cylinders differs only infinitesimally from the external atmospheric pressure. This is clearly not possible. A practical engine must generate torque on the drive shaft, and this can only occur if the cylinder pressure is appreciably greater than the external pressure. Similarly, a battery is only useful if one can extract a sizable rather than an infinitesimal current. To operate such devices under useful irreversible conditions, the work output is less than the theoretically possible limit set by the reversible process.[3]

## 2.9 Determining $\Delta U$ and Introducing Enthalpy, a New State Function

Measuring the energy taken up or released in a chemical reaction is of particular interest to chemists. How can the $\Delta U$ for a thermodynamic process be measured? This will be the topic of Chapter 4. However, this topic is briefly discussed here in order to enable you to carry out calculations on ideal gas systems in the end-of-chapter

---

[3]For a more detailed discussion of irreversible work, see D. Kivelson and I. Oppenheim, "Work in Irreversible Expansions," *Journal of Chemical Education* 43 (1966): 233.

problems. The first law states that $\Delta U = q + w$. Imagine that the process is carried out under constant volume conditions and that nonexpansion work is not possible. Because under these conditions $w = -\int P_{external} dV = 0$,

$$\Delta U = q_V \tag{2.25}$$

Equation (2.25) states that $\Delta U$ can be experimentally determined by measuring the heat flow between the system and surroundings in a constant volume process.

Chemical reactions are generally carried out under constant pressure rather than constant volume conditions. It would be useful to have an energy state function that has a relationship analogous to Equation (2.25), but at constant pressure conditions. Under constant pressure conditions, we can write

$$dU = đq_P - P_{external} dV = đq_P - P \, dV \tag{2.26}$$

Integrating this expression between the initial and final states:

$$\int_i^f dU = U_f - U_i = \int đq_P - \int P \, dV = q_P - P(V_f - V_i)$$

$$= q_P - \left( P_f V_f - P_i V_i \right) \tag{2.27}$$

Note that in order to evaluate the integral involving $P$, we must know the functional relationship $P(V)$, which in this case is $P_i = P_f = P$ where $P$ is constant. Rearranging the last equation, we obtain

$$(U_f + P_f V_f) - (U_i + P_i V_i) = q_P \tag{2.28}$$

Because $P$, $V$, and $U$ are all state functions, $U + PV$ is a state function. This new state function is called **enthalpy** and is given the symbol $H$.

$$H \equiv U + PV \tag{2.29}$$

As is the case for $U$, $H$ has the units of energy, and it is an extensive property. As shown in Equation (2.30), $\Delta H$ for a process involving only $P$–$V$ work can be determined by measuring the heat flow between the system and surroundings at constant pressure:

$$\Delta H = q_P \tag{2.30}$$

This equation is the constant pressure analogue of Equation (2.25). Because chemical reactions are much more frequently carried out at constant $P$ than constant $V$, the energy change measured experimentally by monitoring the heat flow is $\Delta H$ rather than $\Delta U$. When we classify a reaction as being exothermic or endothermic, we are talking about $\Delta H$, not $\Delta U$.

# 2.10 Calculating $q$, $w$, $\Delta U$, and $\Delta H$ for Processes Involving Ideal Gases

In this section we discuss how $\Delta U$ and $\Delta H$, as well as $q$ and $w$, can be calculated from the initial and final state variables if the path between the initial and final state is known. The problems at the end of this chapter ask you to calculate $q$, $w$, $\Delta U$, and $\Delta H$ for simple and multistep processes. Because an equation of state is often needed to carry out such calculations, the system will generally be an ideal gas. Using an ideal gas as a surrogate for more complex systems has the significant advantage that the mathematics is simplified, allowing one to concentrate on the process rather than the manipulation of equations and the evaluation of integrals.

What does one need to know to calculate $\Delta U$? The following discussion is restricted to processes that do not involve chemical reactions or changes in phase. Because $U$ is a state function, $\Delta U$ is independent of the path between the initial and final states. To describe a fixed amount of an ideal gas (i.e., $n$ is constant), the values of two of the variables $P$, $V$, and $T$ must be known. Is this also true for $\Delta U$ for processes involving ideal gases? To answer this question, consider the expansion of an ideal gas

from an initial state $V_1, T_1$ to a final state $V_2, T_2$. We first assume that $U$ is a function of both $V$ and $T$. Is this assumption correct? Because ideal gas atoms or molecules do not interact with one another, $U$ will not depend on the distance between the atoms or molecules. Therefore, $U$ is not a function of $V$, and we conclude that $\Delta U$ must be a function of $T$ only for an ideal gas, $\Delta U = \Delta U(T)$.

We also know that for a temperature range over which $C_V$ is constant,

$$\Delta U = q_V = C_V(T_f - T_i) \tag{2.31}$$

Is this equation only valid for constant $V$? Because $U$ is a function of only $T$ for an ideal gas, Equation (2.31) is also valid for processes involving ideal gases in which $V$ is not constant. Therefore, if one knows $C_V$, $T_1$, and $T_2$, $\Delta U$ can be calculated, regardless of the path between the initial and final states.

How many variables are required to define $\Delta H$ for an ideal gas? We write

$$\Delta H = \Delta U(T) + \Delta(PV) = \Delta U(T) + \Delta(nRT) = \Delta H(T) \tag{2.32}$$

We see that $\Delta H$ is also a function of only $T$ for an ideal gas. In analogy to Equation (2.31),

$$\Delta H = q_P = C_P(T_f - T_i) \tag{2.33}$$

Because $\Delta H$ is a function of only $T$ for an ideal gas, Equation (2.33) holds for all processes involving ideal gases, whether $P$ is constant or not, as long as it is reasonable to assume that $C_P$ is constant. Therefore, if the initial and final temperatures are known or can be calculated, and if $C_V$ and $C_P$ are known, $\Delta U$ and $\Delta H$ can be calculated *regardless of the path* for processes involving ideal gases using Equations (2.31) and (2.33), as long as no chemical reactions or phase changes occur. Because $U$ and $H$ are state functions, the previous statement is true for both reversible and irreversible processes. Recall that for an ideal gas $C_P - C_V = nR$, so that if one of $C_V$ and $C_P$ is known, the other can be readily determined.

We next note that the first law links $q$, $w$, and $\Delta U$. If any two of these quantities are known, the first law can be used to calculate the third. In calculating work, often only expansion work takes place. In this case one always proceeds from the equation

$$w = -\int P_{external}\, dV \tag{2.34}$$

This integral can only be evaluated if the functional relationship between $P_{external}$ and $V$ is known. A frequently encountered case is $P_{external} = $ constant, such that

$$w = -P_{external}(V_f - V_i) \tag{2.35}$$

Because $P_{external} \neq P$, the work considered in Equation (2.35) is for an irreversible process.

A second frequently encountered case is that the system and external pressure differ only by an infinitesimal amount. In this case, it is sufficiently accurate to write $P_{external} = P$, and the process is reversible:

$$w = -\int \frac{nRT}{V}\, dV \tag{2.36}$$

This integral can only be evaluated if $T$ is known as a function of $V$. The most commonly encountered case is an isothermal process, in which $T$ is constant. As was seen in Section 2.2, for this case

$$w = -nRT \int \frac{dV}{V} = -nRT \ln \frac{V_f}{V_i} \tag{2.37}$$

In solving thermodynamic problems, it is very helpful to understand the process thoroughly before starting the calculation, because it is often possible to obtain the value of one or more of $q$, $w$, $\Delta U$, and $\Delta H$ without a calculation. For example, $\Delta U = \Delta H = 0$ for an isothermal process because $\Delta U$ and $\Delta H$ depend only on $T$. For an adiabatic process, $q = 0$ by definition. If only expansion work is possible, $w = 0$ for a constant volume process. These guidelines are illustrated in the following two example problems.

## EXAMPLE PROBLEM 2.5

A system containing 2.50 mol of an ideal gas for which $C_{V,m} = 20.79$ J mol$^{-1}$ K$^{-1}$ is taken through the cycle in the following diagram in the direction indicated by the arrows. The curved path corresponds to $PV = nRT$, where $T = T_1 = T_3$.

a. Calculate $q$, $w$, $\Delta U$, and $\Delta H$ for each segment and for the cycle assuming that the heat capacity is independent of temperature.

b. Calculate $q$, $w$, $\Delta U$, and $\Delta H$ for each segment and for the cycle in which the direction of each process is reversed.

*P/bar* vs *V/L* diagram: 1 (16.6 bar, 1.00L), 2 (16.6 bar, 25L), 3.
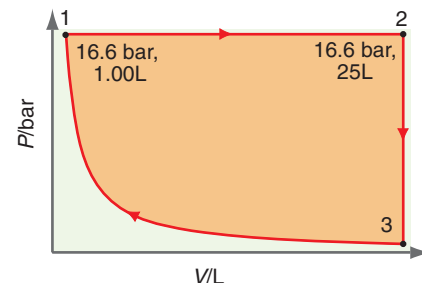
## Solution

We begin by asking whether we can evaluate $q$, $w$, $\Delta U$, or $\Delta H$ for any of the segments without any calculations. Because the path between states 1 and 3 is isothermal, $\Delta U$ and $\Delta H$ are zero for this segment. Therefore, from the first law, $q_{3\to1} = -w_{3\to1}$. For this reason, we only need to calculate one of these two quantities. Because $\Delta V = 0$ along the path between states 2 and 3, $w_{2\to3} = 0$. Therefore, $\Delta U_{2\to3} = q_{2\to3}$. Again, we only need to calculate one of these two quantities. Because the total process is cyclic, the change in any state function is zero. Therefore, $\Delta U = \Delta H = 0$ for the cycle, no matter which direction is chosen. We now deal with each segment individually.

## Segment 1→2

The values of $n$, $P_1$ and $V_1$, and $P_2$ and $V_2$ are known. Therefore, $T_1$ and $T_2$ can be calculated using the ideal gas law. We use these temperatures to calculate $\Delta U$ as follows:

$$\Delta U_{1\to2} = nC_{V,m}(T_2 - T_1) = \frac{nC_{V,m}}{nR}(P_2V_2 - P_1V_1)$$

$$= \frac{20.79 \text{ J mol}^{-1}\text{ K}^{-1}}{0.08314 \text{ L bar K}^{-1}\text{ mol}^{-1}}$$

$$\times (16.6 \text{ bar} \times 25.0 \text{ L} - 16.6\text{ bar} \times 1.00 \text{ L})$$

$$= 99.6\text{ kJ}$$

The process takes place at constant pressure, so

$$w = -P_{external}(V_2 - V_1) = -16.6\text{ bar} \times \frac{10^5\text{ N m}^{-2}}{\text{bar}}$$

$$\times (25.0 \times 10^{-3}\text{ m}^3 - 1.00 \times 10^{-3}\text{ m}^3)$$

$$= -39.8\text{ kJ}$$

Using the first law,

$$q = \Delta U - w = 99.6 \text{ kJ} + 39.8 \text{ kJ} = 139.4 \text{ kJ}$$

We next calculate $T_2$:

$$T_2 = \frac{P_2V_2}{nR} = \frac{16.6\text{ bar} \times 25.0\text{L}}{2.50\text{ mol} \times 0.08314\text{L bar K}^{-1}\text{ mol}^{-1}} = 2.00 \times 10^3 \text{ K}$$

We next calculate $T_3 = T_1$ and then $\Delta H_{1\to2}$:

$$T_1 = \frac{P_1V_1}{nR} = \frac{16.6\text{ bar} \times 1.00\text{L}}{2.50\text{ mol} \times 0.08314\text{L bar K}^{-1}\text{mol}^{-1}} = 79.9 \text{ K}$$

$$\Delta H_{1\to2} = \Delta U_{1\to2} + \Delta(PV) = \Delta U_{1\to2} + nR(T_2 - T_1)$$

$$= 99.6 \times 10^3 \text{ J} + 2.5\text{ mol} \times 8.314\text{ J mol}^{-1}\text{K}^{-1}$$

$$\times (2000\text{ K} - 79.9\text{ K}) = 139.4\text{ kJ}$$

### Segment 2 → 3

As previously noted, $w = 0$, and

$$\Delta U_{2 \to 3} = q_{2 \to 3} = C_V(T_3 - T_2)$$
$$= 2.50 \, \text{mol} \times 20.79 \, \text{J mol}^{-1} \text{K}^{-1}(79.9 \, \text{K} - 2000 \, \text{K})$$
$$= -99.6 \, \text{kJ}$$

The numerical result is equal in magnitude, but opposite in sign to $\Delta U_{1 \to 2}$ because $T_3 = T_1$. For the same reason, $\Delta H_{2 \to 3} = -\Delta H_{1 \to 2}$.

### Segment 3 → 1

For this segment, $\Delta U_{3 \to 1} = 0$ and $\Delta H_{3 \to 1} = 0$ as noted earlier, and $w_{3 \to 1} = -q_{3 \to 1}$. Because this is a reversible isothermal compression,

$$w_{3 \to 1} = -nRT \ln \frac{V_1}{V_3} = -2.50 \, \text{mol} \times 8.314 \, \text{J mol}^{-1} \text{K}^{-1} \times 79.9 \, \text{K}$$
$$\times \ln \frac{1.00 \times 10^{-3} \, \text{m}^3}{25.0 \times 10^{-3} \, \text{m}^3}$$
$$= 5.35 \, \text{kJ}$$

The results for the individual segments and for the cycle in the indicated direction are given in the following table. If the cycle is traversed in the reverse fashion, the magnitudes of all quantities in the table remain the same, but all signs change.

| Path | $q$ (kJ) | $w$ (kJ) | $\Delta U$ (kJ) | $\Delta H$ (kJ) |
|---|---|---|---|---|
| 1 → 2 | 139.4 | − 39.8 | 99.6 | 139.4 |
| 2 → 3 | − 99.6 | 0 | − 99.6 | − 139.4 |
| 3 → 1 | − 5.35 | 5.35 | 0 | 0 |
| Cycle | 34.5 | − 34.5 | 0 | 0 |

### EXAMPLE PROBLEM 2.6

In this example, 2.50 mol of an ideal gas with $C_{V,m} = 12.47 \, \text{J mol}^{-1} \text{K}^{-1}$ is expanded adiabatically against a constant external pressure of 1.00 bar. The initial temperature and pressure of the gas are 325 K and 2.50 bar, respectively. The final pressure is 1.25 bar. Calculate the final temperature, $q$, $w$, $\Delta U$, and $\Delta H$.

### Solution

Because the process is adiabatic, $q = 0$, and $\Delta U = w$. Therefore,

$$\Delta U = nC_{v,m}(T_f - T_i) = -P_{external}(V_f - V_i)$$

Using the ideal gas law,

$$nC_{v,m}(T_f - T_i) = -nRP_{external}\left(\frac{T_f}{P_f} - \frac{T_i}{P_i}\right)$$

$$T_f\left(nC_{v,m} + \frac{nRP_{external}}{P_f}\right) = T_i\left(nC_{v,m} + \frac{nRP_{external}}{P_i}\right)$$

$$T_f = T_i\left(\frac{C_{v,m} + \dfrac{RP_{external}}{P_i}}{C_{v,m} + \dfrac{RP_{external}}{P_f}}\right)$$

$$= 325 \, \text{K} \times \left(\frac{12.47 \, \text{J mol}^{-1} \text{K}^{-1} + \dfrac{8.314 \, \text{J mol}^{-1} \text{K}^{-1} \times 1.00 \, \text{bar}}{2.50 \, \text{bar}}}{12.47 \, \text{J mol}^{-1} \text{K}^{-1} + \dfrac{8.314 \, \text{J mol}^{-1} \text{K}^{-1} \times 1.00 \, \text{bar}}{1.25 \, \text{bar}}}\right) = 268 \, \text{K}$$

We calculate $\Delta U = w$ from

$$\Delta U = nC_{V,m}(T_f - T_i) = 2.5 \text{ mol} \times 12.47 \text{ J mol}^{-1}\text{K}^{-1} \times (268 \text{ K} - 325 \text{ K})$$

$$= -1.78 \text{ kJ}$$

Because the temperature falls in the expansion, the internal energy and enthalpy decreases:

$$\Delta H = \Delta U + \Delta(PV) = \Delta U + nR(T_2 - T_1)$$

$$= -1.78 \times 10^3 \text{ J} + 2.5 \text{ mol} \times 8.314 \text{ J mol}^{-1}\text{K}^{-1}$$

$$\times (268 \text{ K} - 325 \text{ K}) = -2.96 \text{ kJ}$$

# 2.11 The Reversible Adiabatic Expansion and Compression of an Ideal Gas

The adiabatic expansion and compression of gases is an important meteorological process. For example, the cooling of a cloud as it moves upward in the atmosphere can be modeled as an adiabatic process because the heat transfer between the cloud and the rest of the atmosphere is slow on the timescale of its upward motion.

Consider the adiabatic expansion of an ideal gas. Because $q = 0$, the first law takes the form

$$\Delta U = w \quad \text{or} \quad C_V dT = -P_{external}dV \qquad (2.38)$$

For a reversible adiabatic process, $P = P_{external}$, and

$$C_V dT = -nRT \frac{dV}{V} \quad \text{or, equivalently,} \quad C_V \frac{dT}{T} = -nR \frac{dV}{V} \qquad (2.39)$$

Integrating both sides of this equation between the initial and final states,

$$\int_{T_i}^{T_f} C_V \frac{dT}{T} = -nR \int_{V_i}^{V_f} \frac{dV}{V} \qquad (2.40)$$

If $C_V$ is constant over the temperature interval $T_f - T_i$, then

$$C_V \ln \frac{T_f}{T_i} = -nR \ln \frac{V_f}{V_i} \qquad (2.41)$$

Because $C_P - C_V = nR$ for an ideal gas, Equation (2.41) can be written in the form

$$\ln\left(\frac{T_f}{T_i}\right) = -(\gamma - 1) \ln\left(\frac{V_f}{V_i}\right) \quad \text{or, equivalently,} \quad \frac{T_f}{T_i} = \left(\frac{V_f}{V_i}\right)^{1-\gamma} \qquad (2.42)$$

where $\gamma = C_{P,m}/C_{V,m}$. Substituting $T_f/T_i = P_f V_f / P_i V_i$ in the previous equation, we obtain

$$P_i V_i^\gamma = P_f V_f^\gamma \qquad (2.43)$$

for the adiabatic reversible expansion or compression of an ideal gas. Note that our derivation is only applicable to a reversible process, because we have assumed that $P = P_{external}$.

Reversible adiabatic compression of a gas leads to heating, and reversible adiabatic expansion leads to cooling. Adiabatic and isothermal expansion and compression are compared in Figure 2.17, in which two systems containing 1 mol of an ideal gas have the same volume at $P = 1$ atm. One system undergoes adiabatic compression or expansion, and the other undergoes isothermal compression or expansion. Under isothermal conditions, heat flows out of the system as it is compressed to $P > 1$ atm, and heat flows into the system as it is expanded to $P < 1$ atm to keep $T$ constant. Because no heat flows into or out of the system under adiabatic conditions, its temperature increases in compression and decreases in expansion. Because $T > T_{isothermal}$ for a compression starting at 1 atm, $P_{adiabatic} > P_{isothermal}$ for a given volume of
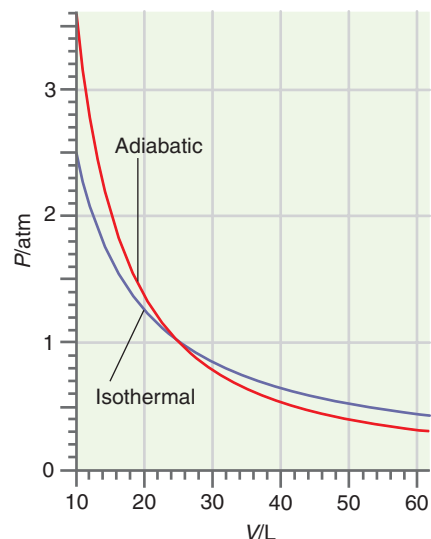


**FIGURE 2.17**
Two systems containing 1 mol of $N_2$ have the same $P$ and $V$ values at 1 atm. The red curve corresponds to reversible expansion and compression under adiabatic conditions. The blue curve corresponds to reversible expansion and compression under isothermal conditions.

the gas. Similarly, in a reversible adiabatic expansion originating at 1 atm, $P_{adiabatic} < P_{isothermal}$ for a given volume of the gas.

## EXAMPLE PROBLEM 2.7

A cloud mass moving across the ocean at an altitude of 2000. m encounters a coastal mountain range. As it rises to a height of 3500. m to pass over the mountains, it undergoes an adiabatic expansion. The pressure at 2000. m and 3500. m is 0.802 and 0.602 atm, respectively. If the initial temperature of the cloud mass is 288 K, what is the cloud temperature as it passes over the mountains? Assume that $C_{P,m}$ for air is 28.86 J K$^{-1}$ mol$^{-1}$ and that air obeys the ideal gas law. If you are on the mountain, should you expect rain or snow?

### Solution

$$\ln\left(\frac{T_f}{T_i}\right) = -(\gamma - 1)\ln\left(\frac{V_f}{V_i}\right)$$

$$= -(\gamma - 1)\ln\left(\frac{T_f}{T_i}\frac{P_i}{P_f}\right) = -(\gamma - 1)\ln\left(\frac{T_f}{T_i}\right) - (\gamma - 1)\ln\left(\frac{P_i}{P_f}\right)$$

$$= -\frac{(\gamma - 1)}{\gamma}\ln\left(\frac{P_i}{P_f}\right) = -\frac{\left(\dfrac{C_{P,m}}{C_{P,m} - R} - 1\right)}{\dfrac{C_{P,m}}{C_{P,m} - R}}\ln\left(\frac{P_i}{P_f}\right)$$

$$= -\frac{\left(\dfrac{28.86 \text{ J K}^{-1} \text{ mol}^{-1}}{28.86 \text{ J K}^{-1} \text{ mol}^{-1} - 8.314 \text{ J K}^{-1} \text{ mol}^{-1}} - 1\right)}{\dfrac{28.86 \text{ J K}^{-1} \text{ mol}^{-1}}{28.86 \text{ J K}^{-1} \text{ mol}^{-1} - 8.314 \text{ J K}^{-1} \text{ mol}^{-1}}} \times \ln\left(\frac{0.802 \text{ atm}}{0.602 \text{ atm}}\right)$$

$$= -0.0826$$

$$T_f = 0.9207 \, T_i = 265 \text{ K}$$

You can expect snow.
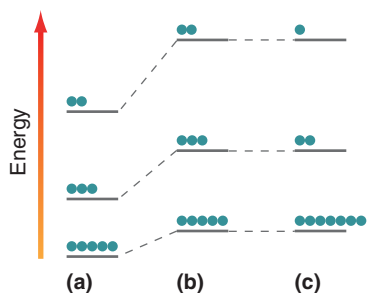


**FIGURE 2.18**
(a) A system has the translational energy levels shown before undergoing an adiabatic compression. (b) After the compression, the energy levels are shifted upward but the occupation probability of the levels shown on the horizontal axis is unchanged. (c) Subsequent cooling to the original temperature at constant $V$ restores the energy to its original value by decreasing the probability of occupying higher energy states. Each circle corresponds to a probability of 0.10.

It is instructive to consider an adiabatic compression or expansion from a microscopic point of view. In an adiabatic compression, the energy levels are all raised, but the probability that a given level is accessed is unchanged. This behavior is observed in contrast to that shown in Figure 2.5 because in an adiabatic compression, $T$ and therefore $U$ increases. For more details, see R. E. Dickerson, *Molecular Thermodynamics*, W.A. Benjamin, Menlo Park, 1969. If the gas is subsequently cooled at constant V, the energy levels remain unchanged, but the probability that higher energy states are populated decreases as shown in Figure 2.18c.

# Vocabulary

cyclic path

degrees of freedom

enthalpy

exact differential

first law of thermodynamics

heat

heat capacity

indicator diagram

internal energy

irreversible

isobaric

isochoric

isothermal

path

path function

quasi-static process

reversible

state function

work

# Conceptual Problems

**Q2.1**  Electrical current is passed through a resistor immersed in a liquid in an adiabatic container. The temperature of the liquid is varied by 1°C. The system consists solely of the liquid. Does heat or work flow across the boundary between the system and surroundings? Justify your answer.

**Q2.2**  Two ideal gas systems undergo reversible expansion under different conditions starting from the same $P$ and $V$. At the end of the expansion, the two systems have the same volume. The pressure in the system that has undergone adiabatic expansion is lower than in the system that has undergone isothermal expansion. Explain this result without using equations.

**Q2.3**  You have a liquid and its gaseous form in equilibrium in a piston and cylinder assembly in a constant temperature bath. Give an example of a reversible process.

**Q2.4**  Describe how reversible and irreversible expansions differ by discussing the degree to which equilibrium is maintained between the system and the surroundings.

**Q2.5**  For a constant pressure process, $\Delta H = q_P$. Does it follow that $q_P$ is a state function? Explain.

**Q2.6**  A cup of water at 278 K (the system) is placed in a microwave oven and the oven is turned on for 1 minute during which the water begins to boil. State whether each of $q$, $w$, and $\Delta U$ is positive, negative, or zero.

**Q2.7**  In the experiments shown in Figure 2.4a and 2.4b, $\Delta U_{surroundings} < 0$, but $\Delta T_{surroundings} > 0$. Explain how this is possible.

**Q2.8**  What is wrong with the following statement? *Burns caused by steam at 100°C can be more severe than those caused by water at 100°C because steam contains more heat than water.* Rewrite the sentence to convey the same information in a correct way.

**Q2.9**  Why is it incorrect to speak of the heat or work associated with a system?

**Q2.10**  You have a liquid and its gaseous form in equilibrium in a piston and cylinder assembly in a constant temperature bath. Give an example of an irreversible process.

**Q2.11**  What is wrong with the following statement? *Because the well-insulated house stored a lot of heat, the temperature didn't fall much when the furnace failed.* Rewrite the sentence to convey the same information in a correct way.

**Q2.12**  Explain how a mass of water in the surroundings can be used to determine $q$ for a process. Calculate $q$ if the temperature of a 1.00 kg water bath in the surroundings increases by 1.25°C. Assume that the surroundings are at a constant pressure.

**Q2.13**  A chemical reaction occurs in a constant volume enclosure separated from the surroundings by diathermal walls. Can you say whether the temperature of the surroundings increases, decreases, or remains the same in this process? Explain.

**Q2.14**  Explain the relationship between the terms *exact differential* and *state function.*

**Q2.15**  In the experiment shown in Figure 2.4b, the weight drops in a very short time. How will the temperature of the water change with time?

**Q2.16**  Discuss the following statement: If the temperature of the system increased, heat must have been added to it.

**Q2.17**  Discuss the following statement: Heating an object causes its temperature to increase.

**Q2.18**  An ideal gas is expanded reversibly and adiabatically. Decide which of $q$, $w$, $\Delta U$, and $\Delta H$ are positive, negative, or zero.

**Q2.19**  An ideal gas is expanded reversibly and isothermally. Decide which of $q$, $w$, $\Delta U$, and $\Delta H$ are positive, negative, or zero.

**Q2.20**  An ideal gas is expanded adiabatically into a vacuum. Decide which of $q$, $w$, $\Delta U$, and $\Delta H$ are positive, negative, or zero.

**Q2.21**  A bowling ball (a) rolls across a table, and (b) falls on the floor. Is the work associated with each part of this process positive, negative, or zero?

**Q2.22**  A perfectly insulating box is partially filled with water in which an electrical resistor is immersed. An external electrical generator converts the change in potential energy of a mass m that falls by a vertical distance $h$ into electrical energy that is dissipated in the resistor. What value do $q$, $w$, and $\Delta U$ have if the system is defined as the resistor and the water? Everything else is in the surroundings.

**Q2.23**  A student gets up from her chair and pushes a stack of books across the table. They fall to the floor. Is the work associated with each part of this process positive, negative, or zero?

**Q2.24**  Explain why ethene has a higher value for $C_{V,m}$ at 800 K than CO.

**Q2.25**  Explain why $C_{P,m}$ is a function of temperature for ethane, but not for argon in a temperature range in which electronic excitations do not occur.

**Q2.26**  What is the difference between a quasi-static process and a reversible process?

# Numerical Problems

Problem numbers in **red** indicate that the solution to the problem is given in the *Student's Solutions Manual.*

**P2.1**  A 3.75 mole sample of an ideal gas with $C_{V,m} = 3R/2$ initially at a temperature $T_i = 298$ K and $P_i = 1.00$ bar is enclosed in an adiabatic piston and cylinder assembly. The gas is compressed by placing a 725 kg mass on the piston of diameter 25.4 cm. Calculate the work done in this process and the distance that the piston travels. Assume that the mass of the piston is negligible.

**P2.2** The temperature of 1.75 moles of an ideal gas increases from 10.2°C to 48.6°C as the gas is compressed adiabatically. Calculate $q$, $w$, $\Delta U$, and $\Delta H$ for this process, assuming that $C_{V,m} = 3R/2$.

**P2.3** A 2.50 mole sample of an ideal gas, for which $C_{V,m} = 3R/2$, is subjected to two successive changes in state: (1) From 25.0°C and $125 \times 10^3$ Pa, the gas is expanded isothermally against a constant pressure of $15.2 \times 10^3$ Pa to twice the initial volume. (2) At the end of the previous process, the gas is cooled at constant volume from 25.0°C to –29.0°C. Calculate $q$, $w$, $\Delta U$, and $\Delta H$ for each of the stages. Also calculate $q$, $w$, $\Delta U$, and $\Delta H$ for the complete process.

**P2.4** A hiker caught in a thunderstorm loses heat when her clothing becomes wet. She is packing emergency rations that if completely metabolized will release 35 kJ of heat per gram of rations consumed. How much rations must the hiker consume to avoid a reduction in body temperature of 2.5 K as a result of heat loss? Assume the heat capacity of the body equals that of water and that the hiker weighs 51 kg. State any additional assumptions.

**P2.5** Count Rumford observed that using cannon boring machinery a single horse could heat 11.6 kg of ice water $(T = 273\text{ K})$ to $T = 355$ K in 2.5 hours. Assuming the same rate of work, how high could a horse raise a 225 kg weight in 2.5 minutes? Assume the heat capacity of water is $4.18\text{ J K}^{-1}\text{ g}^{-1}$.

**P2.6** A 1.50 mole sample of an ideal gas at 28.5°C expands isothermally from an initial volume of 22.5 dm³ to a final volume of 75.5 dm³. Calculate $w$ for this process (a) for expansion against an external pressure of $0.498 \times 10^5$ Pa, and (b) for a reversible expansion.

**P2.7** Calculate $q$, $w$, $\Delta U$, and $\Delta H$ if 2.25 mol of an ideal gas with $C_{V,m} = 3R/2$ undergoes a reversible adiabatic expansion from an initial volume $V_i = 5.50\text{ m}^3$ to a final volume $V_f = 25.0\text{ m}^3$. The initial temperature is 275 K.

**P2.8** Calculate $w$ for the adiabatic expansion of 2.50 mol of an ideal gas at an initial pressure of 2.25 bar from an initial temperature of 450. K to a final temperature of 300. K. Write an expression for the work done in the isothermal reversible expansion of the gas at 300. K from an initial pressure of 2.25 bar. What value of the final pressure would give the same value of $w$ as the first part of this problem? Assume that $C_{P,m} = 5R/2$.

**P2.9** At 298 K and 1 bar pressure, the density of water is $0.9970\text{ g cm}^{-3}$, and $C_{P,m} = 75.3\text{ J K}^{-1}\text{ mol}^{-1}$. The change in volume with temperature is given by $\Delta V = V_{initial}\beta \Delta T$ where $\beta$, the coefficient of thermal expansion, is $2.07 \times 10^{-4}\text{ K}^{-1}$. If the temperature of 325 g of water is increased by 25.5 K, calculate $w$, $q$, $\Delta H$, and $\Delta U$.

**P2.10** A muscle fiber contracts by 3.5 cm and in doing so lifts a weight. Calculate the work performed by the fiber. Assume the muscle fiber obeys Hooke's law $F = -k\,x$ with a force constant $k$ of $750.\text{ N m}^{-1}$.

**P2.11** A cylindrical vessel with rigid adiabatic walls is separated into two parts by a frictionless adiabatic piston. Each part contains 45.0 L of an ideal monatomic gas with $C_{V,m} = 3R/2$. Initially, $T_i = 300.$ K and $P_i = 1.75 \times 10^5$ Pa in each part. Heat is slowly introduced into the left part using an electrical heater until the piston has moved sufficiently to

the right to result in a final pressure $P_f = 4.00$ bar in the right part. Consider the compression of the gas in the right part to be a reversible process.

**a.** Calculate the work done on the right part in this process and the final temperature in the right part.

**b.** Calculate the final temperature in the left part and the amount of heat that flowed into this part.

**P2.12** In the reversible adiabatic expansion of 1.75 mol of an ideal gas from an initial temperature of 27.0°C, the work done on the surroundings is 1300. J. If $C_{V,m} = 3R/2$, calculate $q$, $w$, $\Delta U$, and $\Delta H$.

**P2.13** A system consisting of 82.5 g of liquid water at 300. K is heated using an immersion heater at a constant pressure of 1.00 bar. If a current of 1.75 A passes through the 25.0 ohm resistor for 100. s, what is the final temperature of the water?

**P2.14** A 1.25 mole sample of an ideal gas is expanded from 320. K and an initial pressure of 3.10 bar to a final pressure of 1.00 bar, and $C_{P,m} = 5R/2$. Calculate $w$ for the following two cases:

**a.** The expansion is isothermal and reversible.

**b.** The expansion is adiabatic and reversible.

Without resorting to equations, explain why the result to part (b) is greater than or less than the result to part (a).

**P2.15** A bottle at 325 K contains an ideal gas at a pressure of $162.5 \times 10^3$ Pa. The rubber stopper closing the bottle is removed. The gas expands adiabatically against $P_{external} = 120.0 \times 10^3$ Pa, and some gas is expelled from the bottle in the process. When $P = P_{external}$, the stopper is quickly replaced. The gas remaining in the bottle slowly warms up to 325 K. What is the final pressure in the bottle for a monatomic gas, for which $C_{V,m} = 3R/2$, and a diatomic gas, for which $C_{V,m} = 5R/2$?

**P2.16** A 2.25 mole sample of an ideal gas with $C_{V,m} = 3R/2$ initially at 310. K and $1.25 \times 10^5$ Pa undergoes a reversible adiabatic compression. At the end of the process, the pressure is $3.10 \times 10^6$ Pa. Calculate the final temperature of the gas. Calculate $q$, $w$, $\Delta U$, and $\Delta H$ for this process.

**P2.17** A vessel containing 1.50 mol of an ideal gas with $P_i = 1.00$ bar and $C_{P,m} = 5R/2$ is in thermal contact with a water bath. Treat the vessel, gas, and water bath as being in thermal equilibrium, initially at 298 K, and as separated by adiabatic walls from the rest of the universe. The vessel, gas, and water bath have an average heat capacity of $C_P = 2450.\text{ J K}^{-1}$. The gas is compressed reversibly to $P_f = 20.5$ bar. What is the temperature of the system after thermal equilibrium has been established?

**P2.18** An ideal gas undergoes an expansion from the initial state described by $P_i$, $V_i$, $T$ to a final state described by $P_f$, $V_f$, $T$ in (a) a process at the constant external pressure $P_f$, and (b) in a reversible process. Derive expressions for the largest mass that can be lifted through a height $h$ in the surroundings in these processes.

**P2.19** An ideal gas described by $T_i = 275$ K, $P_i = 1.10$ bar, and $V_i = 10.0$ L is heated at constant volume until $P = 10.0$ bar. It then undergoes a reversible isothermal expansion until $P = 1.10$ bar. It is then restored to its original state by the extraction of heat at constant pressure. Depict this closed-cycle

process in a P–V diagram. Calculate w for each step and for the total process. What values for w would you calculate if the cycle were traversed in the opposite direction?

**P2.20** In an adiabatic compression of one mole of an ideal gas with $C_{V,m} = 5R/2$, the temperature rises from 278 K to 450. K. Calculate $q$, $w$, $\Delta H$, and $\Delta U$.

**P2.21** The heat capacity of solid lead oxide is given by

$$C_{P,m} = 44.35 + 1.47 \times 10^{-3}\frac{T}{K} \text{ in units of J K}^{-1}\text{ mol}^{-1}$$

Calculate the change in enthalpy of 1.75 mol of PbO(s) if it is cooled from 825 K to 375 K at constant pressure.

**P2.22** A 2.25 mole sample of carbon dioxide, for which $C_{P,m} = 37.1$ J K$^{-1}$ mol$^{-1}$ at 298 K, is expanded reversibly and adiabatically from a volume of 4.50 L and a temperature of 298 K to a final volume of 32.5 L. Calculate the final temperature, $q$, $w$, $\Delta H$, and $\Delta U$. Assume that $C_{P,m}$ is constant over the temperature interval.

**P2.23** A 1.75 mole sample of an ideal gas for which $P = 2.50$ bar and $T = 335$ K is expanded adiabatically against an external pressure of 0.225 bar until the final pressure is 0.225 bar. Calculate the final temperature, $q$, $w$, $\Delta H$, and $\Delta U$ for (a) $C_{V,m} = 3R/2$, and (b) $C_{V,m} = 5R/2$.

**P2.24** A 3.50 mole sample of $N_2$ in a state defined by $T_i = 250$. K and $V_i = 3.25$ L undergoes an isothermal reversible expansion until $V_f = 35.5$ L Calculate $w$, assuming (a) that the gas is described by the ideal gas law, and (b) that the gas is described by the van der Waals equation of state. What is the percent error in using the ideal gas law instead of the van der Waals equation? The van der Waals parameters for $N_2$ are listed in Table 7.4.

**P2.25** A major league pitcher throws a baseball with a speed of 162 kilometers per hour. If the baseball weighs 235 grams and its heat capacity is 1.7 J g$^{-1}$ K$^{-1}$, calculate the temperature rise of the ball when it is stopped by the catcher's mitt. Assume no heat is transferred to the catcher's mitt and that the catcher's arm does not recoil when he or she catches the ball. Also assume that the kinetic energy of the ball is completely converted into thermal energy.

**P2.26** A 2.50 mol sample of an ideal gas for which $C_{V,m} = 3R/2$ undergoes the following two-step process: (1) From an initial state of the gas described by $T = 13.1°C$ and $P = 1.75 \times 10^5$ Pa, the gas undergoes an isothermal expansion against a constant external pressure of $3.75 \times 10^4$ Pa until the volume has doubled. (2) Subsequently, the gas is cooled at constant volume. The temperature falls to $-23.6°C$. Calculate $q$, $w$, $\Delta U$, and $\Delta H$ for each step and for the overall process.

**P2.27** A 2.35 mole sample of an ideal gas, for which $C_{V,m} = 3R/2$, initially at 27.0°C and $1.75 \times 10^6$ Pa, undergoes a two-stage transformation. For each of the stages described in the following list, calculate the final pressure, as well as $q$, $w$, $\Delta U$, and $\Delta H$. Also calculate $q$, $w$, $\Delta U$, and $\Delta H$ for the complete process.

a. The gas is expanded isothermally and reversibly until the volume triples.

b. Beginning at the end of the first stage, the temperature is raised to 105°C at constant volume.

**P2.28** A 3.50 mole sample of an ideal gas with $C_{V,m} = 3R/2$ is expanded adiabatically against a constant external pressure of 1.45 bar. The initial temperature and pressure are $T_i = 310$. K and $P_i = 15.2$ bar. The final pressure is $P_f = 1.45$ bar. Calculate $q$, $w$, $\Delta U$, and $\Delta H$ for the process.

**P2.29** A nearly flat bicycle tire becomes noticeably warmer after it has been pumped up. Approximate this process as a reversible adiabatic compression. Assume the initial pressure and temperature of the air before it is put in the tire to be $P_i = 1.00$ bar and $T_i = 280$. K The final pressure in the tire is $P_f = 3.75$ bar. Calculate the final temperature of the air in the tire. Assume that $C_{V,m} = 5R/2$.

**P2.30** For 1.25 mol of an ideal gas, $P_{external} = P = 350. \times 10^3$ Pa. The temperature is changed from 135°C to 21.2°C, and $C_{V,m} = 3R/2$. Calculate $q$, $w$, $\Delta U$, and $\Delta H$.

**P2.31** Suppose an adult is encased in a thermally insulating barrier so that all the heat evolved by metabolism of food-stuffs is retained by the body. What is her temperature increase after 2.5 hours? Assume the heat capacity of the body is 4.18 J g$^{-1}$K$^{-1}$ and that the heat produced by metabolism is 9.4 kJ kg$^{-1}$hr$^{-1}$.

**P2.32** Consider the isothermal expansion of 2.35 mol of an ideal gas at 415 K from an initial pressure of 18.0 bar to a final pressure of 1.75 bar. Describe the process that will result in the greatest amount of work being done by the system with $P_{external} \geq 1.75$ bar, and calculate $w$. Describe the process that will result in the least amount of work being done by the system with $P_{external} \geq 1.75$ bar, and calculate $w$. What is the least amount of work done without restrictions on the external pressure?

**P2.33** An automobile tire contains air at $225 \times 10^3$ Pa at 25.0°C. The stem valve is removed and the air is allowed to expand adiabatically against the constant external pressure of one bar until $P = P_{external}$. For air, $C_{V,m} = 5R/2$. Calculate the final temperature. Assume ideal gas behavior.

**P2.34** One mole of an ideal gas is subjected to the following changes. Calculate the change in temperature for each case if $C_{V,m} = 3R/2$.

a. $q = -425$ J, $w = 185$ J

b. $q = 315$. J, $w = -315$ J

c. $q = 0$, $w = 225$ J

**P2.35** Consider the adiabatic expansion of 0.500 mol of an ideal monatomic gas with $C_{V,m} = 3R/2$. The initial state is described by $P = 6.25$ bar and $T = 300$. K.

a. Calculate the final temperature if the gas undergoes a reversible adiabatic expansion to a final pressure of $P = 1.25$ bar.

b. Calculate the final temperature if the same gas undergoes an adiabatic expansion against an external pressure of $P = 1.25$ bar to a final pressure $P = 1.25$ bar.

Explain the difference in your results for parts (a) and (b).

**P2.36** A pellet of Zn of mass 31.2 g is dropped into a flask containing dilute $H_2SO_4$ at a pressure of $P = 1.00$ bar and a temperature of $T = 300$. K. What is the reaction that occurs? Calculate $w$ for the process.

**P2.37**    Calculate $\Delta H$ and $\Delta U$ for the transformation of 2.50 mol of an ideal gas from 19.0°C and 1.00 atm to 550.°C and 19.5 atm if $C_{P,m} = 20.9 + 0.042 \dfrac{T}{K}$ in units of J K$^{-1}$ mol$^{-1}$.

**P2.38**    A 1.75 mole sample of an ideal gas for which $C_{V,m} = 20.8$ J K$^{-1}$ mol$^{-1}$ is heated from an initial temperature of 21.2°C to a final temperature of 380.°C at constant volume. Calculate $q$, $w$, $\Delta U$, and $\Delta H$ for this process.

**P2.39**    An ideal gas undergoes a single-stage expansion against a constant external pressure $P_{external} = P_f$ at constant temperature from $T$, $P_i$, $V_i$, to $T$, $P_f$, $V_f$.

**a.** What is the largest mass $m$ that can be lifted through the height $h$ in this expansion?

**b.** The system is restored to its initial state in a single-state compression. What is the smallest mass $m'$ that must fall through the height $h$ to restore the system to its initial state?

**c.** If $h = 15.5$ cm, $P_i = 1.75 \times 10^6$ Pa, $P_f = 1.25 \times 10^6$ Pa, $T = 280.$ K, and $n = 2.25$ mol, calculate the values of the masses in parts (a) and (b).

**P2.40**    The formalism of the Young's modulus is sometimes used to calculate the reversible work involved in extending or compressing an elastic material. Assume a force $F$ is applied to an elastic rod of cross-sectional area $A_0$ and length $L_0$. As a result of this force the rod changes in length by $\Delta L$. The Young's modulus $E$ is defined as

$$E = \frac{\text{tensile stress}}{\text{tensile strain}} = \frac{F/A_0}{\Delta L/L_0} = \frac{FL_0}{A_0 \Delta L}$$

**a.** Relate $k$ in Hooke's Law to the Young's modulus expression just given.

**b.** Using your result in part (a) show that the magnitude of the reversible work involved in changing the length $L_0$ of an elastic cylinder of cross-sectional area $A_0$ by $\Delta L$ is

$$w = \frac{1}{2}\left(\frac{\Delta L}{L_0}\right)^2 EA_0L_0.$$

**P2.41**    The Young's modulus (see Problem P2.40) of muscle fiber is approximately $2.80 \times 10^7$ Pa. A muscle fiber 3.25 cm in length and 0.125 cm in diameter is suspended with a mass $M$ hanging at its end. Calculate the mass required to extend the length of the fiber by 10%.

**P2.42**    DNA can be modeled as an elastic rod that can be twisted or bent. Suppose a DNA molecule of length $L$ is bent such that it lies on the arc of a circle of radius $R_c$. The reversible work involved in bending DNA without twisting is $w_{bend} = \dfrac{BL}{2R_c^2}$ where $B$ is the bending force constant. The DNA in a nucleosome particle is about 680. Å in length. Nucleosomal DNA is bent around a protein complex called the histone octamer into a circle of radius 55 Å. Calculate the reversible work involved in bending the DNA around the histone octamer if the force constant $B = 2.00 \times 10^{-28}$ J m.

**P2.43**    A 1.75 mole sample of an ideal gas is compressed isothermally from 62.0 L to 19.0 L using a constant external pressure of 2.80 atm. Calculate $q$, $w$, $\Delta U$, and $\Delta H$.

**P2.44**    Assume the following simplified dependence of the pressure in a ventricle of the human heart as a function of the volume of blood pumped.
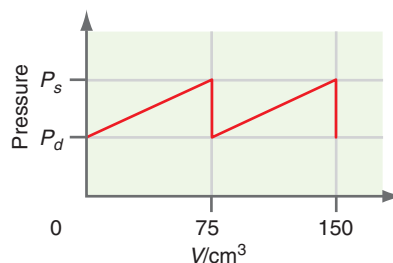


$P_s$, the systolic pressure, is 120. mm Hg, corresponding to 0.158 atm. $P_d$, the diastolic pressure, is 80.0 mm Hg, corresponding to 0.105 atm. If the volume of blood pumped in one heartbeat is 75.0 cm$^3$, calculate the work done in a heartbeat.

# Web-Based Simulations, Animations, and Problems

**W2.1**    A simulation is carried out in which an ideal gas is heated under constant pressure or constant volume conditions. The quantities $\Delta V$ (or $\Delta P$), $w$, $\Delta U$, and $\Delta T$ are determined as a function of the heat input. The heat taken up by the gas under constant $P$ or $V$ is calculated and compared with $\Delta U$ and $\Delta H$.

**W2.2**    The reversible isothermal compression and expansion of an ideal gas is simulated for different values of $T$. The work $w$ is calculated from the $T$ and $V$ values obtained in the simulation. The heat $q$ and the number of moles of gas in the system are calculated from the results.

**W2.3**    The reversible isobaric compression and expansion of an ideal gas is simulated for different values of pressure gas as heat flows to/from the surroundings. The quantities $q$, $w$, and $\Delta U$ are calculated from the $\Delta T$ and $\Delta V$ values obtained in the simulation.

**W2.4**    The isochoric heating and cooling of an ideal gas is simulated for different values of volume. The number of moles of gas and $\Delta U$ are calculated from the constant $V$ value and from the $T$ and $P$ values obtained in the simulation.

**W2.5**    Reversible cyclic processes are simulated in which the cycle is either rectangular or triangular on a $P$–$V$ plot. For each segment and for the cycle, $\Delta U$, $q$, and $w$ are determined. For a given cycle type, the ratio of work done on the surroundings to the heat absorbed from the surroundings is determined for different $P$ and $V$ values.

**W2.6**    The reversible adiabatic heating and cooling of an ideal gas is simulated for different values of the initial temperature. The quantity $\gamma = C_{P,m}/C_{V,m}$ as well as $C_{Pm}$ and $C_{Vm}$ are determined from the $P$, $V$ values of the simulation; $\Delta U$ and $\Delta U$ are calculated from the $V$, $T$, and $P$ values obtained in the simulation.

# The Importance of State Functions: Internal Energy and Enthalpy

T he mathematical properties of state functions are utilized to express the infinitesimal quantities *dU* and *dH* as exact differentials. By doing so, expressions can be derived that relate the change of *U* with *T* and *V* and the change in *H* with *T* and *P* to experimentally accessible quantities such as the heat capacity and the coefficient of thermal expansion. Although both *U* and *H* are functions of any two of the variables *P*, *V*, and *T*, the dependence of *U* and *H* on temperature is generally far greater than the dependence on *P* or *V*. As a result, for most processes involving gases, liquids, and solids, *U* and *H* can be regarded as functions of *T* only. An exception to this statement is the cooling on the isenthalpic expansion of real gases, which is commercially used in the liquefaction of $N_2$, $O_2$, He, and Ar.

## 3.1 The Mathematical Properties of State Functions

In Chapter 2 we demonstrated that *U* and *H* are state functions and that *w* and *q* are path functions. We also discussed how to calculate changes in these quantities for an ideal gas. In this chapter, the path independence of state functions is exploited to derive relationships with which $\Delta U$ and $\Delta H$ can be calculated as functions of *P*, *V*, and *T* for real gases, liquids, and solids. In doing so, we develop the formal aspects of thermodynamics. We will show that the formal structure of thermodynamics provides a powerful aid in linking theory and experiment. However, before these topics are discussed, the mathematical properties of state functions need to be outlined.

The thermodynamic state functions of interest here are defined by two variables from the set *P*, *V*, and *T*. In formulating changes in state functions, we will make extensive use of partial derivatives, which are reviewed in the Math Supplement (Appendix B). The following discussion does not apply to path functions such as *w* and *q* because a functional
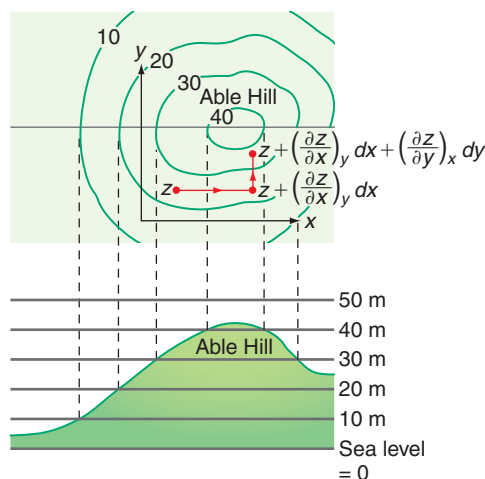
**FIGURE 3.1**
Starting at the point labeled $z$ on the hill, a person first moves in the positive $x$ direction and then along the $y$ direction. If $dx$ and $dy$ are sufficiently small, the change in height $dz$ is given by

$$dz = \left(\frac{\partial z}{\partial x}\right)_y dx + \left(\frac{\partial z}{\partial y}\right)_x dy.$$

relationship such as Equation (3.1) does not exist for path-dependent functions. Consider 1 mole of an ideal gas for which

$$P = f(V,T) = \frac{RT}{V} \tag{3.1}$$

Note that $P$ can be written as a function of the two variables $V$ and $T$. The change in $P$ resulting from a change in $V$ or $T$ is proportional to the following **partial derivatives:**

$$\left(\frac{\partial P}{\partial V}\right)_T = \lim_{\Delta V \to 0} \frac{P(V + \Delta V,T) - P(V,T)}{\Delta V} = -\frac{RT}{V^2}$$

$$\left(\frac{\partial P}{\partial T}\right)_V = \lim_{\Delta T \to 0} \frac{P(V,T + \Delta T) - P(V,T)}{\Delta T} = \frac{R}{V} \tag{3.2}$$

The subscript $T$ in $(\partial P/\partial V)_T$ indicates that $T$ is being held constant in the differentiation with respect to $V$. The partial derivatives in Equation (3.2) allow one to determine how a function changes when the variables change. For example, what is the change in $P$ if the values of $T$ and $V$ both change? In this case, $P$ changes to $P +$ $dP$ where

$$dP = \left(\frac{\partial P}{\partial T}\right)_V dT + \left(\frac{\partial P}{\partial V}\right)_T dV \tag{3.3}$$

Consider the following practical illustration of Equation (3.3). A person is on a hill and has determined his or her altitude above sea level. How much will the altitude (denoted by $z$) change if the person moves a small distance east (denoted by $x$) and north (denoted by $y$)? The change in $z$ as the person moves east is the slope of the hill in that direction, $(\partial z/\partial x)_y$, multiplied by the distance $dx$ that he or she moves. A similar expression can be written for the change in altitude as the person moves north. Therefore, the total change in altitude is the sum of these two changes or

$$dz = \left(\frac{\partial z}{\partial x}\right)_y dx + \left(\frac{\partial z}{\partial y}\right)_x dy$$

These changes in the height $z$ as the person moves first along the $x$ direction and then along the $y$ direction are illustrated in Figure 3.1. Because the slope of the hill is a nonlinear function of $x$ and $y$, this expression for $dz$ is only valid for small changes $dx$ and $dy$. Otherwise, higher order derivatives need to be considered.

Second or higher derivatives with respect to either variable can also be taken. The mixed second partial derivatives are of particular interest. Consider the mixed partial derivatives of $P$:

$$\left(\frac{\partial}{\partial T}\left(\frac{\partial P}{\partial V}\right)_T\right)_V = \frac{\partial^2 P}{\partial T \partial V} = \left(\partial\left(\frac{\partial\left[\frac{RT}{V}\right]}{\partial V}\right)_T \middle/ \partial T\right)_V = \left(\partial\left[-\frac{RT}{V^2}\right]\middle/\partial T\right)_V = -\frac{R}{V^2}$$

$$\left(\frac{\partial}{\partial V}\left(\frac{\partial P}{\partial T}\right)_V\right)_T = \frac{\partial^2 P}{\partial V \partial T} = \left(\partial\left(\frac{\partial\left[\frac{RT}{V}\right]}{\partial T}\right)_V \middle/ \partial V\right)_T = \left(\partial\left[\frac{R}{V}\right]\middle/\partial V\right)_T = -\frac{R}{V^2} \tag{3.4}$$

For all state functions $f$ and for our specific case of $P$, the order in which the function is differentiated does not affect the outcome. For this reason,

$$\left(\frac{\partial}{\partial T}\left(\frac{\partial f(V,T)}{\partial V}\right)_T\right)_V = \left(\frac{\partial}{\partial V}\left(\frac{\partial f(V,T)}{\partial T}\right)_V\right)_T \tag{3.5}$$

Because Equation (3.5) is only satisfied by state functions $f$, it can be used to determine if a function $f$ is a state function. If $f$ is a state function, one can write $\Delta f = \int_i^f df = f_{final} - f_{initial}$. This equation states that $f$ can be expressed as an infinitesimal quantity $df$ that when integrated depends only on the initial and final states; $df$ is called an **exact differential.** An example of a state function and its exact differential is $U$ and $dU = đq - P_{external}\, dV$.

**EXAMPLE PROBLEM 3.1**

**a.** Calculate

$$\left(\frac{\partial f}{\partial x}\right)_y, \left(\frac{\partial f}{\partial y}\right)_x, \left(\frac{\partial^2 f}{\partial x^2}\right)_y, \left(\frac{\partial^2 f}{\partial y^2}\right)_x, \left(\frac{\partial\left(\frac{\partial f}{\partial x}\right)_y}{\partial y}\right)_x, \text{ and } \left(\frac{\partial\left(\frac{\partial f}{\partial y}\right)_x}{\partial x}\right)_y$$

for the function $f(x, y) = ye^x + xy + x \ln y$.

**b.** Determine if $f(x, y)$ is a state function of the variables $x$ and $y$.

**c.** If $f(x, y)$ is a state function of the variables $x$ and $y$, what is the total differential $df$?

**Solution**

**a.** $\left(\dfrac{\partial f}{\partial x}\right)_y = ye^x + y + \ln y,$     $\left(\dfrac{\partial f}{\partial y}\right)_x = e^x + x + \dfrac{x}{y}$

$\left(\dfrac{\partial^2 f}{\partial x^2}\right)_y = ye^x,$     $\left(\dfrac{\partial^2 f}{\partial y^2}\right)_x = -\dfrac{x}{y^2}$

$\left(\dfrac{\partial\left(\frac{\partial f}{\partial x}\right)_y}{\partial y}\right)_x = e^x + 1 + \dfrac{1}{y},$     $\left(\dfrac{\partial\left(\frac{\partial f}{\partial y}\right)_x}{\partial x}\right)_y = e^x + 1 + \dfrac{1}{y}$

**b.** Because we have shown that

$$\left(\frac{\partial\left(\frac{\partial f}{\partial x}\right)_y}{\partial y}\right)_x = \left(\frac{\partial\left(\frac{\partial f}{\partial y}\right)_x}{\partial x}\right)_y$$

$f(x, y)$ is a state function of the variables $x$ and $y$. Generalizing this result, any well-behaved function that can be expressed in analytical form is a state function.

**c.** The total differential is given by

$$df = \left(\frac{\partial f}{\partial x}\right)_y dx + \left(\frac{\partial f}{\partial y}\right)_x dy$$

$$= (ye^x + y + \ln y)dx + \left(e^x + x + \frac{x}{y}\right)dy$$

Two other important results from differential calculus will be used frequently. Consider a function $z = f(x, y)$ that can be rearranged to $x = g(y, z)$ or $y = h(x, z)$. For example, if $P = nRT/V$, then $V = nRT/P$ and $T = PV/nR$. In this case

$$\left(\frac{\partial x}{\partial y}\right)_z = \frac{1}{\left(\frac{\partial y}{\partial x}\right)_z} \tag{3.6}$$

The **cyclic rule** will also be used:

$$\left(\frac{\partial x}{\partial y}\right)_z \left(\frac{\partial y}{\partial z}\right)_x \left(\frac{\partial z}{\partial x}\right)_y = -1 \tag{3.7}$$

It is called the cyclic rule because $x$, $y$, and $z$ in the three terms follow the orders $x, y, z$; $y, z, x$; and $z, x, y$. Equations (3.6) and (3.7) can be used to reformulate Equation (3.3) shown next below:

$$dP = \left(\frac{\partial P}{\partial T}\right)_V dT + \left(\frac{\partial P}{\partial V}\right)_T dV$$

Suppose this expression needs to be evaluated for a specific substance, such as $N_2$ gas. What quantities must be measured in the laboratory in order to obtain numerical values for $(\partial P/\partial T)_V$ and $(\partial P/\partial V)_T$? Using Equations (3.6) and (3.7),

$$\left(\frac{\partial P}{\partial V}\right)_T \left(\frac{\partial V}{\partial T}\right)_P \left(\frac{\partial T}{\partial P}\right)_V = -1$$

$$\left(\frac{\partial P}{\partial T}\right)_V = -\left(\frac{\partial P}{\partial V}\right)_T \left(\frac{\partial V}{\partial T}\right)_P = -\frac{\left(\frac{\partial V}{\partial T}\right)_P}{\left(\frac{\partial V}{\partial P}\right)_T} = \frac{\beta}{\kappa} \quad \text{and}$$

$$\left(\frac{\partial P}{\partial V}\right)_T = -\frac{1}{\kappa V} \tag{3.8}$$

where $\beta$ and $\kappa$ are the readily measured **isobaric volumetric thermal expansion coefficient** and the **isothermal compressibility,** respectively, defined by

$$\beta = \frac{1}{V}\left(\frac{\partial V}{\partial T}\right)_P \quad \text{and} \quad \kappa = -\frac{1}{V}\left(\frac{\partial V}{\partial P}\right)_T \tag{3.9}$$

Both $(\partial V/\partial T)_P$ and $(\partial V/\partial P)_T$ can be measured by determining the change in volume of the system when the pressure or temperature is varied, while keeping the second variable constant.

The minus sign in the equation for $\kappa$ is chosen so that values of the isothermal compressibility are positive. For small changes in $T$ and $P$, Equations (3.9) can be written in the more compact form: $V(T_2) = V(T_1)(1 + \beta[T_2 - T_1])$ and $V(P_2) = V(P_1)(1 - \kappa[P_2 - P_1])$. Values for $\beta$ and $\kappa$ for selected solids and liquids are shown in Tables 3.1 and 3.2, respectively.

Equation (3.8) is an example of how seemingly abstract partial derivatives can be directly linked to experimentally determined quantities using the mathematical properties of state functions. Using the definitions of $\beta$ and $\kappa$, Equation (3.3) can be written in the form

$$dP = \frac{\beta}{\kappa} dT - \frac{1}{\kappa V} dV \tag{3.10}$$

which can be integrated to give

$$\Delta P = \int_{T_i}^{T_f} \frac{\beta}{\kappa} dT - \int_{V_i}^{V_f} \frac{1}{\kappa V} dV \approx \frac{\beta}{\kappa}(T_f - T_i) - \frac{1}{\kappa}\ln\frac{V_f}{V_i} \tag{3.11}$$

**TABLE 3.1    Volumetric Thermal Expansion Coefficient for Solids and Liquids at 298 K**

| Element | $10^6 \, \beta/(\text{K}^{-1})$ | Element or Compound | $10^4 \, \beta/(\text{K}^{-1})$ |
|---------|------|------|------|
| Ag(s) | 57.6 | Hg(l) | 1.81 |
| Al(s) | 69.3 | CCl$_4$(l) | 11.4 |
| Au(s) | 42.6 | CH$_3$COCH$_3$(l) | 14.6 |
| Cu(s) | 49.5 | CH$_3$OH(l) | 14.9 |
| Fe(s) | 36.9 | C$_2$H$_5$OH(l) | 11.2 |
| Mg(s) | 78.3 | C$_6$H$_5$CH$_3$(l) | 10.5 |
| Si(s) | 7.5 | C$_6$H$_6$(l) | 11.4 |
| W(s) | 13.8 | H$_2$O(l) | 2.04 |
| Zn(s) | 90.6 | H$_2$O(s) | 1.66 |

*Sources:* Benenson, W., Harris, J. W., Stocker, H., and Lutz, H. *Handbook of Physics.* New York: Springer, 2002; Lide, D. R., ed. *Handbook of Chemistry and Physics.* 83rd ed. Boca Raton, FL: CRC Press, 2002; Blachnik, R., ed. *D'Ans Lax Taschenbuch für Chemiker und Physiker.* 4th ed. Berlin: Springer, 1998.

**TABLE 3.2** Isothermal Compressibility at 298 K

| Substance | $10^6 \, \kappa/\text{bar}^{-1}$ | Substance | $10^6 \, \kappa/\text{bar}^{-1}$ |
|---|---|---|---|
| Al(s) | 1.33 | Br$_2$(l) | 64 |
| SiO$_2$(s) | 2.57 | C$_2$H$_5$OH(l) | 110 |
| Ni(s) | 0.513 | C$_6$H$_5$OH(l) | 61 |
| TiO$_2$(s) | 0.56 | C$_6$H$_6$(l) | 94 |
| Na(s) | 13.4 | CCl$_4$(l) | 103 |
| Cu(s) | 0.702 | CH$_3$COCH$_3$(l) | 125 |
| C(graphite) | 0.156 | CH$_3$OH(l) | 120 |
| Mn(s) | 0.716 | CS$_2$(l) | 92.7 |
| Co(s) | 0.525 | H$_2$O(l) | 45.9 |
| Au(s) | 0.563 | Hg(l) | 3.91 |
| Pb(s) | 2.37 | SiCl$_4$(l) | 165 |
| Fe(s) | 0.56 | TiCl$_4$(l) | 89 |
| Ge(s) | 1.38 | | |

*Sources:* Benenson, W., Harris, J. W., Stocker, H., and Lutz, H. *Handbook of Physics*. New York: Springer, 2002; Lide, D. R., ed. *Handbook of Chemistry and Physics*. 83rd ed. Boca Raton FL: CRC Press, 2002; Blachnik, R., ed. *D'Ans Lax Taschenbuch für Chemiker und Physiker*. 4th ed. Berlin: Springer, 1998.

The second expression in Equation (3.11) holds if $\Delta T$ and $\Delta V$ are small enough that $\beta$ and $\kappa$ are constant over the range of integration. Example Problem 3.2 shows a useful application of this equation.

---

**EXAMPLE PROBLEM 3.2**

You have accidentally arrived at the end of the range of an ethanol-in-glass thermometer so that the entire volume of the glass capillary is filled. By how much will the pressure in the capillary increase if the temperature is increased by another $10.0°C$? $\beta_{glass} = 2.00 \times 10^{-5}(°C)^{-1}$, $\beta_{ethanol} = 11.2 \times 10^{-4}(°C)^{-1}$, and $\kappa_{ethanol} = 11.0 \times 10^{-5}(\text{bar})^{-1}$. Will the thermometer survive your experiment?

**Solution**

Using Equation (3.11),

$$\Delta P = \int \frac{\beta_{ethanol}}{\kappa} \, dT - \int \frac{1}{\kappa V} \, dV \approx \frac{\beta_{ethanol}}{\kappa} \Delta T - \frac{1}{\kappa} \ln \frac{V_f}{V_i}$$

$$= \frac{\beta_{ethanol}}{\kappa} \Delta T - \frac{1}{\kappa} \ln \frac{V_i(1 + \beta_{glass}\Delta T)}{V_i} \approx \frac{\beta_{ethanol}}{\kappa} \Delta T - \frac{1}{\kappa} \frac{V_i \beta_{glass}\Delta T}{V_i}$$

$$= \frac{(\beta_{ethanol} - \beta_{glass})}{\kappa} \Delta T$$

$$= \frac{(11.2 - 0.200) \times 10^{-4}(°C)^{-1}}{11.0 \times 10^{-5}(\text{bar})^{-1}} \times 10.0°C = 100. \text{ bar}$$

In this calculation, we have used the relations $V(T_2) = V(T_1)(1 + \beta[T_2 - T_1])$ and $\ln(1 + x) \approx x$ if $x \ll 1$.

The glass is unlikely to withstand such a large increase in pressure.

# 3.2 The Dependence of *U* on *V* and *T*

In this section, the fact that $dU$ is an exact differential is used to establish how $U$ varies with $T$ and $V$. For a given amount of a pure substance or a mixture of fixed composition, $U$ is determined by any two of the three variables $P$, $V$, and $T$. One could choose other combinations of variables to discuss changes in $U$. However, the following discussion will demonstrate that it is particularly convenient to choose the variables $T$ and $V$. Because $U$ is a state function, an infinitesimal change in $U$ can be written as

$$dU = \left(\frac{\partial U}{\partial T}\right)_V dT + \left(\frac{\partial U}{\partial V}\right)_T dV \tag{3.12}$$

This expression says that if the state variables change from $T$, $V$ to $T + dT$, $V + dV$, the change in $U$, $dU$, can be determined in the following way. We determine the slopes of $U(T,V)$ with respect to $T$ and $V$ and evaluate them at $T$, $V$. Next, these slopes are multiplied by the increments $dT$ and $dV$, respectively, and the two terms are added. As long as $dT$ and $dV$ are infinitesimal quantities, higher order derivatives can be neglected.

How can numerical values for $(\partial U/\partial T)_V$ and $(\partial U/\partial V)_T$ be obtained? In the following, we only consider $P$–$V$ work. Combining Equation (3.12) and the differential expression of the first law,

$$dq - P_{external}dV = \left(\frac{\partial U}{\partial T}\right)_V dT + \left(\frac{\partial U}{\partial V}\right)_T dV \tag{3.13}$$

The symbol $dq$ is used for an infinitesimal amount of heat as a reminder that heat is not a state function. We first consider processes at constant volume for which $dV = 0$, so that Equation (3.13) becomes

$$dq_V = \left(\frac{\partial U}{\partial T}\right)_V dT \tag{3.14}$$

Note that in the previous equation, $dq_V$ is the product of a state function and an exact differential. Therefore, $dq_V$ behaves like a state function, but only because the path (constant $V$) is specified. The quantity $dq$ is *not* a state function.

Although the quantity $(\partial U/\partial T)_V$ looks very abstract, it can be readily measured. For example, imagine immersing a container with rigid diathermal walls in a water bath, where the contents of the container are the system. A process such as a chemical reaction is carried out in the container and the heat flow to the surroundings is measured. If heat flow $dq_V$ occurs, a temperature increase or decrease $dT$ is observed in the system and the water bath surroundings. Both of these quantities can be measured. Their ratio, $dq_V/dT$, is a special form of the heat capacity discussed in Section 2.5:

$$\frac{dq_V}{dT} = \left(\frac{\partial U}{\partial T}\right)_V = C_V \tag{3.15}$$

where $dq_V/dT$ corresponds to a constant volume path and is called the **heat capacity at constant volume.**

The quantity $C_V$ is extensive and depends on the size of the system, whereas $C_{V, m}$ is an intensive quantity. As discussed in Section 2.5, $C_{V, m}$ is different for different substances under the same conditions. Observations show that $C_{V, m}$ is always positive for a single-phase, pure substance or for a mixture of fixed composition, as long as no chemical reactions or phase changes take place in the system. For processes subject to these constraints, $U$ increases monotonically with $T$.

With the definition of $C_V$, we now have a way to experimentally determine changes in $U$ with $T$ at constant $V$ for systems of pure substances or for mixtures of constant composition in the absence of chemical reactions or phase changes. After $C_V$ has been

determined as a function of $T$ as discussed in Section 2.5, the following integral is numerically evaluated:

$$\Delta U_V = \int_{T_1}^{T_2} C_V dT = n \int_{T_1}^{T_2} C_{V,m} \, dT \qquad (3.16)$$

Over a limited temperature range, $C_{V,m}$ can often be regarded as a constant. If this is the case, Equation (3.16) simplifies to

$$\Delta U_V = \int_{T_1}^{T_2} C_V dT = C_V \Delta T = n C_{V,m} \Delta T \qquad (3.17)$$

which can be written in a different form to explicitly relate $q_V$ and $\Delta U$:

$$\int_i^f đq_V = \int_i^f \left(\frac{\partial U}{\partial T}\right)_V dT \ \text{ or } \ q_V = \Delta U \qquad (3.18)$$

Although $đq$ is not an exact differential, the integral has a unique value if the path is defined, as it is in this case (constant volume). Equation (3.18) shows that $\Delta U$ for an arbitrary process in a closed system in which only $P$–$V$ work occurs can be determined by measuring $q$ under constant volume conditions. As discussed in Chapter 4, the technique of bomb calorimetry uses this approach to determine $\Delta U$ for chemical reactions.

Next consider the dependence of $U$ on $V$ at constant $T$, or $(\partial U/\partial V)_T$. This quantity has the units of $\text{J/m}^3 = (\text{J/m})/\text{m}^2 = \text{kg ms}^{-2}/\text{m}^2 = \text{force/area} = \text{pressure}$ and is called the **internal pressure.** To explicitly evaluate the internal pressure for different substances, a result will be used that is derived in the discussion of the second law of thermodynamics in Section 5.12:

$$\left(\frac{\partial U}{\partial V}\right)_T = T\left(\frac{\partial P}{\partial T}\right)_V - P \qquad (3.19)$$

Using this equation, the total differential of the internal energy can be written as

$$dU = dU_V + dU_T = C_V \, dT + \left[ T\left(\frac{\partial P}{\partial T}\right)_V - P \right] dV \qquad (3.20)$$

In this equation, the symbols $dU_V$ and $dU_T$ have been used, where the subscript indicates which variable is constant. Equation (3.20) is an important result that applies to systems containing gases, liquids, or solids in a single phase (or mixed phases at a constant composition) if no chemical reactions or phase changes occur. The advantage of writing $dU$ in the form given by Equation (3.20) over that in Equation (3.12) is that $(\partial U/\partial V)_T$ can be evaluated in terms of the system variables $P$, $V$, and $T$ and their derivatives, all of which are experimentally accessible.

Once $(\partial U/\partial V)_T$ and $(\partial U/\partial T)_V$ are known, these quantities can be used to determine $dU$. Because $U$ is a state function, the path taken between the initial and final states is unimportant. Three different paths are shown in Figure 3.2, and $dU$ is the same for these and any other paths connecting $V_i$, $T_i$ and $V_f$, $T_f$. To simplify the calculation, the path chosen consists of two segments, in which only one of the variables changes in a given path segment. An example of such a path is $V_i, T_i \rightarrow V_f, T_i \rightarrow V_f, T_f$. Because $T$ is constant in the first segment,

$$dU = dU_T = \left[ T\left(\frac{\partial P}{\partial T}\right)_V - P \right] dV$$

Because $V$ is constant in the second segment, $dU = dU_V = C_V dT$. Finally, the total change in $U$ is the sum of the changes in the two segments, $dU_{total} = dU_V + dU_T$.
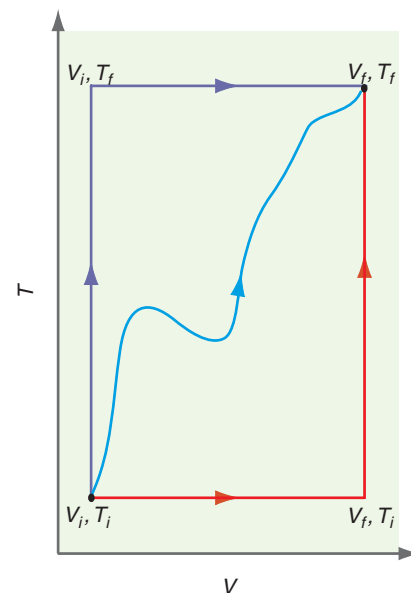


**FIGURE 3.2**
Because $U$ is a state function, all paths connecting $V_i T_i$ and $V_f T_f$ are equally valid in calculating $\Delta U$. Therefore, a specification of the path is irrelevant.

# 3.3 Does the Internal Energy Depend More Strongly on *V* or *T*?

Chapter 2 demonstrated that *U* is a function of *T* alone for an ideal gas. However, this statement is not true for real gases, liquids, and solids for which the change in *U* with *V* must be considered. In this section, we ask if the temperature or the volume dependence of *U* is most important in determining $\Delta U$ for a process of interest. To answer this question, systems consisting of an ideal gas, a real gas, a liquid, and a solid are considered separately. Example Problem 3.3 shows that Equation (3.19) leads to a simple result for a system consisting of an ideal gas.

## EXAMPLE PROBLEM 3.3

Evaluate $(\partial U/\partial V)_T$ for an ideal gas and modify Equation (3.20) accordingly for the specific case of an ideal gas.

**Solution**

$$\left(\frac{\partial U}{\partial V}\right)_T = T\left(\frac{\partial P}{\partial T}\right)_V - P = T\left(\frac{\partial[nRT/V]}{\partial T}\right)_V - P = \frac{nRT}{V} - P = 0$$

Therefore, $dU = C_V dT$, showing that for an ideal gas, *U* is a function of *T* only.

Example Problem 3.3 shows that *U* is only a function of *T* for an ideal gas. Specifically, *U* is not a function of *V*. This result is understandable in terms of the potential function of Figure 1.10. Because ideal gas molecules do not attract or repel one another, no energy is required to change their average distance of separation (increase or decrease *V*):

$$\Delta U = \int_{T_i}^{T_f} C_V(T)\, dT \tag{3.21}$$

Recall that because *U* is only a function of *T*, Equation (3.21) holds for an ideal gas even if *V* is not constant.

Next consider the variation of *U* with *T* and *V* for a real gas. The experimental determination of $(\partial U/\partial V)_T$ was carried out by James Joule using an apparatus consisting of two glass flasks separated by a stopcock, all of which were immersed in a water bath. An idealized view of the experiment is shown in Figure 3.3. As a valve between the volumes is opened, a gas initially in volume A expands to completely fill the volume A + B. In interpreting the results of this experiment, it is important to understand where the boundary between the system and surroundings lies. Here, the decision was made to place the system boundary so that it includes all the gas. Initially, the boundary lies totally within $V_A$, but it moves during the expansion so that it continues to include all gas molecules. With this choice, the volume of the system changes from $V_A$ before the expansion to $V_A + V_B$ after the expansion has taken place.

The first law of thermodynamics [Equation (3.13)] states that

$$đq - P_{external}\, dV = \left(\frac{\partial U}{\partial T}\right)_V dT + \left(\frac{\partial U}{\partial V}\right)_T dV$$

However, all the gas is contained in the system; therefore, $P_{external} = 0$ because a vacuum cannot exert a pressure. Therefore Equation (3.13) becomes

$$đq = \left(\frac{\partial U}{\partial T}\right)_V dT + \left(\frac{\partial U}{\partial V}\right)_T dV \tag{3.22}$$
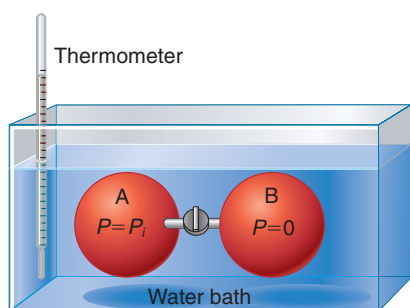


**FIGURE 3.3**
Schematic depiction of the Joule experiment to determine $(\partial U/\partial V)_T$. Two spherical vessels, A and B, are separated by a valve. Both vessels are immersed in a water bath, the temperature of which is monitored. The initial pressure in each vessel is indicated.

To within experimental accuracy, Joule found that $dT_{surroundings} = 0$. Because the water bath and the system are in thermal equilibrium, $dT = dT_{surroundings} = 0$. With this observation, Joule concluded that $dq = 0$. Therefore, Equation (3.22) becomes

$$\left(\frac{\partial U}{\partial V}\right)_T dV = 0 \qquad (3.23)$$

Because $dV \neq 0$, Joule concluded that $(\partial U/\partial V)_T = 0$. Joule's experiment was not definitive because the experimental sensitivity was limited, as shown in Example Problem 3.4.

## EXAMPLE PROBLEM 3.4

In Joule's experiment to determine $(\partial U/\partial V)_T$, the heat capacities of the gas and the water bath surroundings were related by $C_{surroundings}/C_{system} \approx 1000$. If the precision with which the temperature of the surroundings could be measured is $\pm 0.006°C$, what is the minimum detectable change in the temperature of the gas?

### Solution

View the experimental apparatus as two interacting systems in a rigid adiabatic enclosure. The first is the volume within vessels A and B, and the second is the water bath and the vessels. Because the two interacting systems are isolated from the rest of the universe,

$$q = C_{water\ bath}\Delta T_{water\ bath} + C_{gas}\Delta T_{gas} = 0$$

$$\Delta T_{gas} = -\frac{C_{water\ bath}}{C_{gas}}\Delta T_{water\ bath} = -1000 \times (\pm 0.006°C) = \mp 6°C$$

In this calculation, $\Delta T_{gas}$ is the temperature change that the expanded gas undergoes to reach thermal equilibrium with the water bath, which is the negative of the temperature change during the expansion.

Because the minimum detectable value of $\Delta T_{gas}$ is rather large, this apparatus is clearly not suited for measuring small changes in the temperature of the gas in an expansion.

More sensitive experiments were carried out by Joule in collaboration with William Thomson (Lord Kelvin). These experiments, which are discussed in Section 3.8, demonstrate that $(\partial U/\partial V)_T$ is small, but nonzero for real gases.

Example Problem 3.3 has shown that $(\partial U/\partial V)_T = 0$ for an ideal gas. We next calculate $(\partial U/\partial V)_T$ and $\Delta U_T = \int_{V_{m,i}}^{V_{m,f}}(\partial U/\partial V)_T dV_m$ for a real gas, in which the van der Waals equation of state is used to describe the gas, as illustrated in Example Problem 3.5.

## EXAMPLE PROBLEM 3.5

For a gas described by the van der Waals equation of state,
$P = nRT/(V - nb) - an^2/V^2$. Use this equation to complete these tasks:

**a.** Calculate $(\partial U/\partial V)_T$ using $(\partial U/\partial V)_T = T(\partial P/\partial T)_V - P$

**b.** Derive an expression for the change in internal energy, $\Delta U_T = \int_{V_i}^{V_f}(\partial U/\partial V)_T dV$, in compressing a van der Waals gas from an initial molar volume $V_i$ to a final molar volume $V_f$ at constant temperature.

### Solution

**a.** $T\left(\frac{\partial P}{\partial T}\right)_V - P = T\left(\frac{\partial\left[\dfrac{nRT}{V - nb} - \dfrac{n^2a}{V^2}\right]}{\partial T}\right)_V - P = \frac{nRT}{V - nb} - P$

$$= \frac{nRT}{V - nb} - \frac{nRT}{V - nb} + \frac{n^2a}{V^2} = \frac{n^2a}{V^2}$$

**b.** $\Delta U_T = \int_{V_i}^{V_f} \left(\frac{\partial U}{\partial V}\right)_T dV = \int_{V_i}^{V_f} \frac{n^2 a}{V^2} dV = n^2 a\left(\frac{1}{V_i} - \frac{1}{V_f}\right)$

Note that $\Delta U_T$ is zero if the attractive part of the intermolecular potential is zero.

Example Problem 3.5 demonstrates that in general $(\partial U/\partial V)_T \neq 0$, and that $\Delta U_T$ can be calculated if the equation of state of the real gas is known. This allows the relative importance of $\Delta U_T = \int_{V_i}^{V_f} (\partial U/\partial V)_T dV$ and $\Delta U_V = \int_{T_i}^{T_f} C_V dT$ to be determined in a process in which both $T$ and $V$ change, as shown in Example Problem 3.6.

---

**EXAMPLE PROBLEM 3.6**

One mole of $N_2$ gas undergoes a change from an initial state described by $T = 200.$ K and $P_i = 5.00$ bar to a final state described by $T = 400.$ K and $P_f = 20.0$ bar. Treat $N_2$ as a van der Waals gas with the parameters $a = 0.137$ Pa $m^6$ $mol^{-2}$ and $b = 3.87 \times 10^{-5}$ $m^3$ $mol^{-1}$. We use the path $N_2$ $(g, T = 200.$ K$, P = 5.00$ bar$) \rightarrow$ $N_2(g, T = 200.$ K$, P = 20.0$ bar$) \rightarrow N_2(g, T = 400.$ K$, P = 20.0$ bar$)$, keeping in mind that all paths will give the same answer for $\Delta U$ of the overall process.

**a.** Calculate $\Delta U_T = \int_{V_i}^{V_f} (\partial U/\partial V)_T dV$ using the result of Example Problem 3.5. Note that $V_i = 3.28 \times 10^{-3}$ $m^3$ and $V_f = 7.88 \times 10^{-4}$ $m^3$ at 200. K, as calculated using the van der Waals equation of state.

**b.** Calculate $\Delta U_V = n\int_{T_i}^{T_f} C_{V,m} dT$ using the following relationship for $C_{V,m}$ in this temperature range:

$$\frac{C_{V,m}}{J\,K^{-1}\,mol^{-1}} = 22.50 - 1.187 \times 10^{-2}\frac{T}{K} + 2.3968 \times 10^{-5}\frac{T^2}{K^2} - 1.0176 \times 10^{-8}\frac{T^3}{K^3}$$

The ratios $T^n/K^n$ ensure that $C_{V,m}$ has the correct units.

**c.** Compare the two contributions to $\Delta U$. Can $\Delta U_T$ be neglected relative to $\Delta U_V$?

**Solution**

**a.** Using the result of Example Problem 3.5,

$$\Delta U_T = n^2 a\left(\frac{1}{V_{m,i}} - \frac{1}{V_{m,f}}\right) = 0.137 \text{ Pa } m^6$$

$$\times \left(\frac{1}{3.28 \times 10^{-3} \text{ m}^3} - \frac{1}{7.88 \times 10^{-4} \text{ m}^3}\right) = -132 \text{ J}$$

**b.** $\Delta U_V = n\int_{T_i}^{T_f} C_{V,m} dT$

$$= \int_{200.}^{400.} \left(\begin{array}{l} 22.50 - 1.187 \times 10^{-2}\dfrac{T}{K} + 2.3968 \times 10^{-5}\dfrac{T^2}{K^2} \\ -1.0176 \times 10^{-8}\dfrac{T^3}{K^3} \end{array}\right) d\left(\frac{T}{K}\right) \text{ J}$$

$$= (4.50 - 0.712 + 0.447 - 0.0610)kJ = 4.17 \text{ kJ}$$

**c.** $\Delta U_T$ is 3.2% of $\Delta U_V$ for this case. In this example, and for most processes, $\Delta U_T$ can be neglected relative to $\Delta U_V$ for real gases.

---

The calculations in Example Problems 3.5 and 3.6 show that to a good approximation $\Delta U_T = \int_{V_i}^{V_f} (\partial U/\partial V)_T dV \approx 0$ for real gases under most conditions. Therefore, it

is sufficiently accurate to consider $U$ as a function of $T$ only $[U = U(T)]$ for real gases in processes that do not involve unusually high gas densities.

Having discussed ideal and real gases, what can be said about the relative magnitude of $\Delta U_T = \int_{V_i}^{V_f} (\partial U/\partial V)_T dV$ and $\Delta U_V = \int_{T_i}^{T_f} C_V dT$ for processes involving liquids and solids? From experiments, it is known that the density of liquids and solids varies only slightly with the external pressure over the range in which these two forms of matter are stable. This conclusion is not valid for extremely high pressure conditions such as those in the interior of planets and stars. However, it is safe to say that $dV$ for a solid or liquid is very small in most processes. Therefore,

$$\Delta U_T^{solid, liq} = \int_{V_1}^{V_2} \left(\frac{\partial U}{\partial V}\right)_T dV \approx \left(\frac{\partial U}{\partial V}\right)_T \Delta V \approx 0 \tag{3.24}$$

because $\Delta V \approx 0$. This result is valid even if $(\partial U/\partial V)_T$ is large.

The conclusion that can be drawn from this section is as follows. Under most conditions encountered by chemists in the laboratory, $U$ can be regarded as a function of $T$ alone for all substances. The following equations give a good approximation even if $V$ is not constant in the process under consideration:

$$U(T_f, V_f) - U(T_i, V_i) = \Delta U = \int_{T_i}^{T_f} C_V dT = n \int_{T_i}^{T_f} C_{V,m} dT \tag{3.25}$$

Note that Equation (3.25) is only applicable to a process in which there is no change in the phase of the system, such as vaporization or fusion, and in which there are no chemical reactions. Changes in $U$ that arise from these processes will be discussed in Chapters 4 and 8.

## 3.4 The Variation of Enthalpy with Temperature at Constant Pressure

As for $U$, $H$ can be defined as a function of any two of the three variables $P$, $V$, and $T$. It was convenient to choose $U$ to be a function of $T$ and $V$ because this choice led to the identity $\Delta U = q_V$. Using a similar reasoning, we choose $H$ to be a function of $T$ and $P$. How does $H$ vary with $P$ and $T$? The variation of $H$ with $T$ at constant $P$ is discussed next, and a discussion of the variation of $H$ with $P$ at constant $T$ is deferred to Section 3.6.

Consider the constant pressure process shown schematically in Figure 3.4. For this process defined by $P = P_{external}$,

$$dU = đq_P - P\,dV \tag{3.26}$$

Although the integral of $đq$ is in general path dependent, it has a unique value in this case because the path is specified, namely, $P = P_{external} =$ constant. Integrating both sides of Equation (3.26),

$$\int_i^f dU = \int_i^f đq_P - \int_i^f P\,dV \quad \text{or} \quad U_f - U_i = q_P - P(V_f - V_i) \tag{3.27}$$

Because $P = P_f = P_i$, this equation can be rewritten as

$$(U_f + P_f V_f) - (U_i + P_i V_i) = q_P \quad \text{or} \quad \Delta H = q_P \tag{3.28}$$

The preceding equation shows that the value of $\Delta H$ can be determined for an arbitrary process at constant $P$ in a closed system in which only $P$–$V$ work occurs by simply measuring $q_P$, the heat transferred between the system and surroundings in a constant pressure

$P_{external} = P$



Initial state        Final state
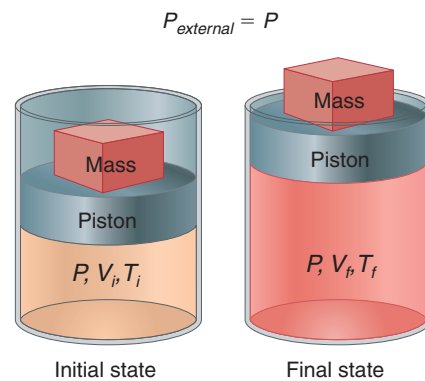
**FIGURE 3.4**

The initial and final states are shown for an undefined process that takes place at constant pressure.

process. Note the similarity between Equations (3.28) and (3.18). For an arbitrary process in a closed system in which there is no work other than $P$–$V$ work, $\Delta U = q_V$ if the process takes place at constant $V$, and $\Delta H = q_P$ if the process takes place at constant $P$. These two equations are the basis for the fundamental experimental techniques of bomb calorimetry and constant pressure calorimetry discussed in Chapter 4.

A useful application of Equation (3.28) is in experimentally determining $\Delta H$ and $\Delta U$ of fusion and vaporization for a given substance. Fusion (solid $\rightarrow$ liquid) and vaporization (liquid $\rightarrow$ gas) occur at a constant temperature if the system is held at a constant pressure and heat flows across the system–surroundings boundary. In both of these phase transitions, attractive interactions between the molecules of the system must be overcome. Therefore, $q > 0$ in both cases and $C_P \rightarrow \infty$. Because $\Delta H = q_P$, $\Delta H_{fusion}$ and $\Delta H_{vaporization}$ can be determined by measuring the heat needed to effect the transition at constant pressure. Because $\Delta H = \Delta U + \Delta(PV)$, at constant $P$,

$$\Delta H_{vaporization} - \Delta U_{vaporization} = P\Delta V_{vaporization} > 0 \qquad (3.29)$$

The change in volume upon vaporization is $\Delta V_{vaporization} = V_{gas} - V_{liquid} \gg 0$; therefore, $\Delta U_{vaporization} < \Delta H_{vaporization}$. An analogous expression to Equation (3.29) can be written relating $\Delta U_{fusion}$ and $\Delta H_{fusion}$. Note that $\Delta V_{fusion}$ is much smaller than $\Delta V_{vaporization}$ and can be either positive or negative. Therefore, $\Delta U_{fusion} \approx \Delta H_{fusion}$. The thermodynamics of fusion and vaporization will be discussed in more detail in Chapter 8.

Because $H$ is a state function, $dH$ is an exact differential, allowing us to link $(\partial H/\partial T)_P$ to a measurable quantity. In analogy to the preceding discussion for $dU$, $dH$ is written in the form

$$dH = \left(\frac{\partial H}{\partial T}\right)_P dT + \left(\frac{\partial H}{\partial P}\right)_T dP \qquad (3.30)$$

Because $dP = 0$ at constant $P$, and $dH = đq_P$ from Equation (3.28), Equation (3.30) becomes

$$đq_P = \left(\frac{\partial H}{\partial T}\right)_P dT \qquad (3.31)$$

Equation (3.31) allows the **heat capacity at constant pressure** $C_P$ to be defined in a fashion analogous to $C_V$ in Equation (3.15):

$$C_P = \frac{đq_P}{dT} = \left(\frac{\partial H}{\partial T}\right)_P \qquad (3.32)$$

Although this equation looks abstract, $C_P$ is a readily measurable quantity. To measure it, one need only measure the heat flow to or from the surroundings for a constant pressure process together with the resulting temperature change in the limit in which $dT$ and $đq$ approach zero and form the ratio $\lim_{dT \to 0} (đq/dT)_P$.

As was the case for $C_V$, $C_P$ is an extensive property of the system and varies from substance to substance. The temperature dependence of $C_P$ must be known in order to calculate the change in $H$ with $T$. For a constant pressure process in which there is no change in the phase of the system and no chemical reactions,

$$\Delta H_P = \int_{T_i}^{T_f} C_P(T)dT = n \int_{T_i}^{T_f} C_{P,m}(T)dT \qquad (3.33)$$

If the temperature interval is small enough, it can usually be assumed that $C_P$ is constant. In that case,

$$\Delta H_P = C_P \Delta T = nC_{P,m}\Delta T \qquad (3.34)$$

The calculation of $\Delta H$ for chemical reactions and changes in phase will be discussed in Chapters 4 and 8.

## EXAMPLE PROBLEM 3.7

A 143.0 g sample of C(s) in the form of graphite is heated from 300. to 600. K at a constant pressure. Over this temperature range, $C_{P,\,m}$ has been determined to be

$$\frac{C_{P,m}}{J\,K^{-1}mol^{-1}} = -12.19 + 0.1126\,\frac{T}{K} - 1.947 \times 10^{-4}\,\frac{T^2}{K^2} + 1.919 \times 10^{-7}\,\frac{T^3}{K^3}$$

$$-7.800 \times 10^{-11}\,\frac{T^4}{K^4}$$

Calculate $\Delta H$ and $q_P$. How large is the relative error in $\Delta H$ if we neglect the temperature-dependent terms in $C_{P,\,m}$ and assume that $C_{P,\,m}$ maintains its value at 300. K throughout the temperature interval?

### Solution

$$\Delta H = \frac{m}{M} \int_{T_i}^{T_f} C_{P,m}(T)\,dT$$

$$= \frac{143.0\ g}{12.00\ g\ mol^{-1}}\,\frac{J}{mol} \int_{300.}^{600.} \left(\begin{array}{l} -12.19 + 0.1126\,\dfrac{T}{K} - 1.947 \times 10^{-4}\,\dfrac{T^2}{K^2} + 1.919 \\[2mm] \times 10^{-7}\,\dfrac{T^3}{K^3} - 7.800 \times 10^{-11}\,\dfrac{T^4}{K^4} \end{array}\right)\,d\,\frac{T}{K}$$

$$= \frac{143.0}{12.00} \times \left[\begin{array}{l} -12.19\,\dfrac{T}{K} + 0.0563\,\dfrac{T^2}{K^2} - 6.49 \times 10^{-5}\,\dfrac{T^3}{K^3} + 4.798 \\[2mm] \times 10^{-8}\dfrac{T^4}{K^4} - 1.56 \times 10^{-11}\,\dfrac{T^5}{K^5} \end{array}\right]_{300.}^{600.}\ J = 46.9\ kJ$$

From Equation (3.28), $\Delta H = q_P$.

If we had assumed $C_{P,\,m} = 8.617\ J\ mol^{-1}\ K^{-1}$, which is the calculated value at 300. K, $\Delta H = 143.0\ g/12.00\ g\ mol^{-1} \times 8.617\ JK^{-1}\ mol^{-1} \times [600.\ K - 300.\ K] = 30.8\ kJ$. The relative error is $100 \times (30.8\ kJ - 46.9\ kJ)/46.9\ kJ = -34.3\%$. In this case, it is not reasonable to assume that $C_{P,\,m}$ is independent of temperature.

# 3.5 How Are $C_P$ and $C_V$ Related?

To this point, two separate heat capacities, $C_P$ and $C_V$, have been defined. How are these quantities related? To answer this question, the differential form of the first law is written as

$$đq = C_V\,dT + \left(\frac{\partial U}{\partial V}\right)_T dV + P_{external}\,dV \tag{3.35}$$

Consider a process that proceeds at constant pressure for which $P = P_{external}$. In this case, Equation (3.35) becomes

$$đq_P = C_V\,dT + \left(\frac{\partial U}{\partial V}\right)_T dV + P\,dV \tag{3.36}$$

Because $đq_P = C_P dT$,

$$C_P = C_V + \left(\frac{\partial U}{\partial V}\right)_T \left(\frac{\partial V}{\partial T}\right)_P + P\left(\frac{\partial V}{\partial T}\right)_P = C_V + \left[\left(\frac{\partial U}{\partial V}\right)_T + P\right]\left(\frac{\partial V}{\partial T}\right)_P$$

$$= C_V + T\left(\frac{\partial P}{\partial T}\right)_V \left(\frac{\partial V}{\partial T}\right)_P \tag{3.37}$$

To obtain Equation (3.37), both sides of Equation (3.36) have been divided by $dT$, and the ratio $dV/dT$ has been converted to a partial derivative at constant $P$. Equation (3.19) has been used in the last step. Using Equation (3.9) and the cyclic rule, one can simplify Equation (3.37) to

$$C_P = C_V + T\left(\frac{\partial P}{\partial T}\right)_V \left(\frac{\partial V}{\partial T}\right)_P = C_V - T\frac{\left(\frac{\partial V}{\partial T}\right)_P^2}{\left(\frac{\partial V}{\partial P}\right)_T}$$

$$C_P = C_V + TV\frac{\beta^2}{\kappa} \quad \text{or} \quad C_{P,m} = C_{V,m} + TV_m\frac{\beta^2}{\kappa} \tag{3.38}$$

Equation (3.38) provides another example of the usefulness of the formal theory of thermodynamics in linking seemingly abstract partial derivatives with experimentally available data. The difference between $C_{P,m}$ and $C_{V,m}$ can be determined at a given temperature knowing only the molar volume, the isobaric volumetric thermal expansion coefficient, and the isothermal compressibility.

Equation (3.38) is next applied to ideal and real gases, as well as liquids and solids, in the absence of phase changes and chemical reactions. Because $\beta$ and $\kappa$ are always positive for real and ideal gases, $C_P - C_V > 0$ for these substances. First, $C_P - C_V$ is calculated for an ideal gas, and then it is calculated for liquids and solids. For an ideal gas, $(\partial U/\partial V)_T = 0$ as shown in Example Problem 3.3, and

$$T\left(\frac{\partial P}{\partial T}\right)_V \left(\frac{\partial V}{\partial T}\right)_P = T\left(\frac{nR}{V}\right)\left(\frac{nR}{P}\right) = nR \text{ so that Equation (3.37) becomes}$$

$$C_P - C_V = nR \tag{3.39}$$

This result was stated without derivation in Section 2.4. The partial derivative $(\partial V/\partial T)_P = V\beta$ is much smaller for liquids and solids than for gases. Therefore, generally

$$C_V \gg \left[\left(\frac{\partial U}{\partial V}\right)_T + P\right]\left(\frac{\partial V}{\partial T}\right)_P \tag{3.40}$$

so that $C_P \approx C_V$ for a liquid or a solid. As shown earlier in Example Problem 3.2, it is not feasible to carry out heating experiments for liquids and solids at constant volume because of the large pressure increase that occurs. Therefore, tabulated heat capacities for liquids and solids list $C_{P,m}$ rather than $C_{V,m}$.

## 3.6 The Variation of Enthalpy with Pressure at Constant Temperature

In the previous section, we learned how $H$ changes with $T$ at constant $P$. To calculate how $H$ changes as both $P$ and $T$ change, $(\partial H/\partial P)_T$ must be calculated. The partial derivative $(\partial H/\partial P)_T$ is less straightforward to determine in an experiment than $(\partial H/\partial T)_P$. As will be seen, for many processes involving changes in both $P$ and $T$, $(\partial H/\partial T)_P\, dT \gg (\partial H/\partial P)_T\, dP$ and the pressure dependence of $H$ can be neglected relative to its temperature dependence. However, the knowledge that $(\partial H/\partial P)_T$ is not zero is essential for understanding the operation of a refrigerator and the liquefaction of gases. The following discussion is applicable to gases, liquids, and solids.

Given the definition $H = U + PV$, we begin by writing $dH$ as

$$dH = dU + P\, dV + V\, dP \tag{3.41}$$

Substituting the differential forms of $dU$ and $dH$,

$$C_P dT + \left(\frac{\partial H}{\partial P}\right)_T dP = C_V\, dT + \left(\frac{\partial U}{\partial V}\right)_T dV + P\, dV + V\, dP$$

$$= C_V\, dT + \left[\left(\frac{\partial U}{\partial V}\right)_T + P\right]dV + V\, dP \tag{3.42}$$

For isothermal processes, $dT = 0$, and Equation (3.42) can be rearranged to

$$\left(\frac{\partial H}{\partial P}\right)_T = \left[\left(\frac{\partial U}{\partial V}\right)_T + P\right]\left(\frac{\partial V}{\partial P}\right)_T + V \qquad (3.43)$$

Using Equation (3.19) for $(\partial U/\partial V)_T$,

$$\left(\frac{\partial H}{\partial P}\right)_T = T\left(\frac{\partial P}{\partial T}\right)_V\left(\frac{\partial V}{\partial P}\right)_T + V$$

$$= V - T\left(\frac{\partial V}{\partial T}\right)_P = V(1 - T\beta) \qquad (3.44)$$

The second formulation of Equation (3.44) is obtained through application of the cyclic rule [Equation (3.7)]. This equation is applicable to all systems containing pure substances or mixtures at a fixed composition, provided that no phase changes or chemical reactions take place. The quantity $(\partial H/\partial P)_T$ is evaluated for an ideal gas in Example Problem 3.8.

## EXAMPLE PROBLEM 3.8

Evaluate $(\partial H/\partial P)_T$ for an ideal gas.

### Solution

$(\partial P/\partial T)_V = (\partial[nRT/V]/\partial T)_V = nR/V$ and $(\partial V/\partial P)_T = (d[nRT/P]/dP)_T = -nRT/P^2$ for an ideal gas. Therefore,

$$\left(\frac{\partial H}{\partial P}\right)_T = T\left(\frac{\partial P}{\partial T}\right)_V\left(\frac{\partial V}{\partial P}\right)_T + V = T\frac{nR}{V}\left(-\frac{nRT}{P^2}\right) + V = -\frac{nRT}{P}\frac{nRT}{nRT} + V = 0$$

This result could have been derived directly from the definition $H = U + PV$. For an ideal gas, $U = U(T)$ only and $PV = nRT$. Therefore, $H = H(T)$ for an ideal gas and $(\partial H/\partial P)_T = 0$.

Because Example Problem 3.8 shows that $H$ is only a function of $T$ for an ideal gas,

$$\Delta H = \int_{T_i}^{T_f} C_P(T)\,dT = n\int_{T_i}^{T_f} C_{P,m}(T)\,dT \qquad (3.45)$$

for an ideal gas. Because $H$ is only a function of $T$, Equation (3.45) holds for an ideal gas even if $P$ is not constant. This result is also understandable in terms of the potential function of Figure 1.10. Because ideal gas molecules do not attract or repel one another, no energy is required to change their average distance of separation (increase or decrease $P$).

Equation (3.44) is next applied to several types of systems. We have seen that $(\partial H/\partial P)_T = 0$ for an ideal gas. For liquids and solids, $1 \gg T\beta$ for $T < 1000$ K as can be seen from the data in Table 3.1. Therefore, for liquids and solids, $(\partial H/\partial P)_T \approx V$ to a good approximation, and $dH$ can be written as

$$dH \approx C_P\,dT + V\,dP \qquad (3.46)$$

for systems that consist only of liquids or solids.

## EXAMPLE PROBLEM 3.9

Calculate the change in enthalpy when 124 g of liquid methanol initially at 1.00 bar and 298 K undergoes a change of state to 2.50 bar and 425 K. The density of liquid methanol under these conditions is 0.791 g cm$^{-3}$, and $C_{P,m}$ for liquid methanol is 81.1 J K$^{-1}$ mol$^{-1}$.

**Solution**

Because $H$ is a state function, any path between the initial and final states will give the same $\Delta H$. We choose the path methanol ($l$, 1.00 bar, 298 K) $\rightarrow$ methanol ($l$, 1.00 bar, 425 K) $\rightarrow$ methanol ($l$, 2.50 bar, 425 K). The first step is isothermal, and the second step is isobaric. The total change in $H$ is

$$\Delta H = n \int_{T_i}^{T_f} C_{P,m} dT + \int_{P_i}^{P_f} V dP \approx nC_{P,m}(T_f - T_i) + V(P_f - P_i)$$

$$= 81.1 \text{ J K}^{-1} \text{ mol}^{-1} \times \frac{124 \text{ g}}{32.04 \text{ g mol}^{-1}} \times (425 \text{ K} - 298 \text{ K})$$

$$+ \frac{124 \text{ g}}{0.791 \text{ g cm}^{-3}} \times \frac{10^{-6} \text{ m}^3}{\text{cm}^3} \times (2.50 \text{ bar} - 1.00 \text{ bar}) \times \frac{10^5 \text{ Pa}}{\text{bar}}$$

$$= 39.9 \times 10^3 \text{ J} + 23.5 \text{ J} \approx 39.9 \text{ kJ}$$

Note that the contribution to $\Delta H$ from the change in $T$ is far greater than that from the change in $P$.

Example Problem 3.9 shows that because molar volumes of liquids and solids are small, $H$ changes much more rapidly with $T$ than with $P$. Under most conditions, $H$ can be assumed to be a function of $T$ only for solids and liquids. Exceptions to this rule are encountered in geophysical or astrophysical applications, for which extremely large pressure changes can occur.

The following conclusion can be drawn from this section: under most conditions encountered by chemists in the laboratory, $H$ can be regarded as a function of $T$ alone for liquids and solids. It is a good approximation to write

$$H(T_f, P_f) - H(T_i, P_i) = \Delta H = \int_{T_1}^{T_2} C_P dT = n \int_{T_1}^{T_2} C_{P,m} dT \quad \textbf{(3.47)}$$

even if $P$ is not constant in the process under consideration. The dependence of $H$ on $P$ for real gases is discussed in Section 3.8 and Section 3.9 in the context of the Joule-Thomson experiment.

Note that Equation (3.47) is only applicable to a process in which there is no change in the phase of the system, such as vaporization or fusion, and in which there are no chemical reactions. Changes in $H$ that arise from chemical reactions and changes in phase will be discussed in Chapters 4 and 8.

Having dealt with solids, liquids, and ideal gases, we are left with real gases. For real gases, $(\partial H/\partial P)_T$ and $(\partial U/\partial V)_T$ are small, but still have a considerable effect on the properties of the gases upon expansion or compression. Conventional technology for the liquefaction of gases and for the operation of refrigerators is based on the fact that $(\partial H/\partial P)_T$ and $(\partial U/\partial V)_T$ are not zero for real gases. To derive a useful formula for calculating $(\partial H/\partial P)_T$ for a real gas, the Joule-Thomson experiment is discussed first in the next section.

# 3.7 The Joule-Thomson Experiment

If the valve on a cylinder of compressed $N_2$ at 298 K is opened fully, it will become covered with frost, demonstrating that the temperature of the valve is lowered below the freezing point of $H_2O$. A similar experiment with a cylinder of $H_2$ leads to a considerable increase in temperature and, potentially, an explosion. How can these effects be understood? To explain them, we discuss the **Joule-Thomson experiment.**
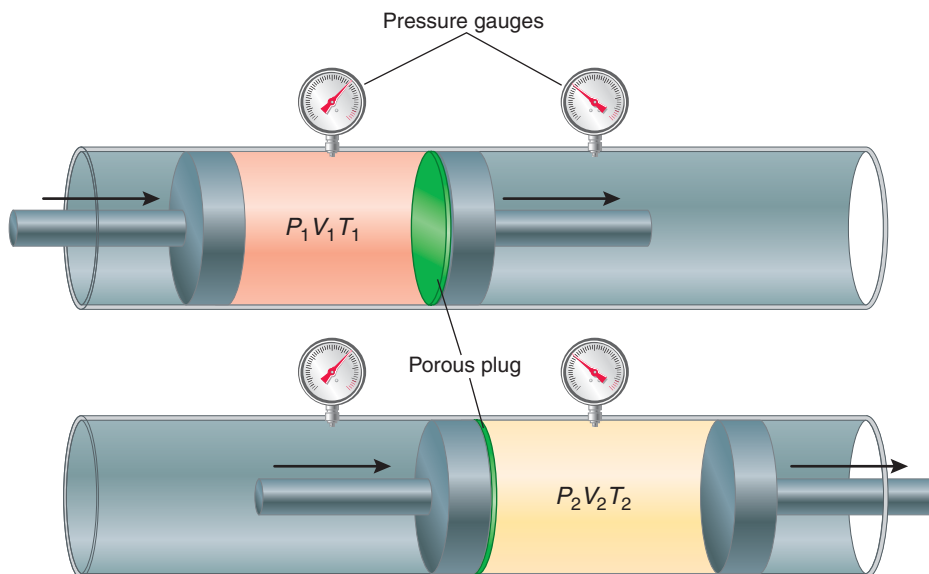
Pressure gauges



$P_1 V_1 T_1$

Porous plug

$P_2 V_2 T_2$

The Joule-Thomson experiment shown in Figure 3.5 can be viewed as an improved version of the Joule experiment because it allows $(\partial U/\partial V)_T$ to be measured with a much higher sensitivity than in the Joule experiment. In this experiment, gas flows from the high-pressure cylinder on the left to the low-pressure cylinder on the right through a porous plug in an insulated pipe. The pistons move to keep the pressure unchanged in each region until all the gas has been transferred to the region to the right of the porous plug. If $N_2$ is used in the expansion process $(P_1 > P_2)$, it is found that $T_2 < T_1$; in other words, the gas is cooled as it expands. What is the origin of this effect? Consider an amount of gas equal to the initial volume $V_1$ as it passes through the apparatus from left to right. The total work in this expansion process is the sum of the work performed on each side of the plug separately by the moving pistons:

$$w = w_{left} + w_{right} = -\int_{V_1}^{0} P_1 \, dV - \int_{0}^{V_2} P_2 \, dV = P_1 V_1 - P_2 V_2 \qquad (3.48)$$

Because the pipe is insulated, $q = 0$, and

$$\Delta U = U_2 - U_1 = w = P_1 V_1 - P_2 V_2 \qquad (3.49)$$

This equation can be rearranged to

$$U_2 + P_2 V_2 = U_1 + P_1 V_1 \quad \text{or} \quad H_2 = H_1 \qquad (3.50)$$

Note that the enthalpy is constant in the expansion; the expansion is **isenthalpic.** For the conditions of the experiment using $N_2$, both $dT$ and $dP$ are negative, so $(\partial T/\partial P)_H > 0$. The experimentally determined limiting ratio of $\Delta T$ to $\Delta P$ at constant enthalpy is known as the **Joule-Thomson coefficient:**

$$\mu_{J-T} = \lim_{\Delta P \to 0} \left( \frac{\Delta T}{\Delta P} \right)_H = \left( \frac{\partial T}{\partial P} \right)_H \qquad (3.51)$$

If $\mu_{J-T}$ is positive, the conditions are such that the attractive part of the potential dominates, and if $\mu_{J-T}$ is negative, the repulsive part of the potential dominates. Using experimentally determined values of $\mu_{J-T}$, $(\partial H/\partial P)_T$ can be calculated. For an isenthalpic process,

$$dH = C_P \, dT + \left( \frac{\partial H}{\partial P} \right)_T dP = 0 \qquad (3.52)$$

**TABLE 3.3 Joule-Thomson Coefficients for Selected Substances at 273 K and 1 atm**

| Gas | $\mu_{J-T}$ (K/MPa) |
|---|---|
| Ar | 3.66 |
| $C_6H_{14}$ | –0.39 |
| $CH_4$ | 4.38 |
| $CO_2$ | 10.9 |
| $H_2$ | –0.34 |
| He | –0.62 |
| $N_2$ | 2.15 |
| Ne | –0.30 |
| $NH_3$ | 28.2 |
| $O_2$ | 2.69 |

*Source:* Linstrom, P. J., and Mallard, W. G., eds. *NIST Chemistry Webbook: NIST Standard Reference Database Number 69.* Gaithersburg, MD: National Institute of Standards and Technology. Retrieved from *http://webbook.nist.gov*.

Dividing through by $dP$ and making the condition $dH = 0$ explicit,

$$C_P \left( \frac{\partial T}{\partial P} \right)_H + \left( \frac{\partial H}{\partial P} \right)_T = 0$$

$$\text{giving} \quad \left( \frac{\partial H}{\partial P} \right)_T = -C_P \mu_{J-T} \tag{3.53}$$

Equation (3.53) states that $(\partial H/\partial P)_T$ can be calculated using the measurement of material-dependent properties $C_P$ and $\mu_{J-T}$. Because $\mu_{J-T}$ is not zero for a real gas, the pressure dependence of $H$ for an expansion or compression process for which the pressure change is large cannot be neglected. Note that $(\partial H/\partial P)_T$ can be positive or negative, depending on the value of $\mu_{J-T}$ at the $P$ and $T$ of interest.

If $\mu_{J-T}$ is known from experiment, $(\partial U/\partial V)_T$ can be calculated as shown in Example Problem 3.10. This has the advantage that a calculation of $(\partial U/\partial V)_T$ based on measurements of $C_P$, $\mu_{J-T}$ and the isothermal compressibility $\kappa$ is much more accurate than a measurement based on the Joule experiment. Values of $\mu_{J-T}$ are shown for selected gases in Table 3.3. Keep in mind that $\mu_{J-T}$ is a function of $P$ and $\Delta P$, so the values listed in the table are only valid for a small pressure decrease originating at 1 atm pressure.

**EXAMPLE PROBLEM 3.10**

Using Equation (3.43), $(\partial H/\partial P)_T = [(\partial U/\partial V)_T + P](\partial V/\partial P)_T + V$, derive an expression giving $(\partial U/\partial V)_T$ entirely in terms of measurable quantities for a gas.

**Solution**

$$\left( \frac{\partial H}{\partial P} \right)_T = \left[ \left( \frac{\partial U}{\partial V} \right)_T + P \right] \left( \frac{\partial V}{\partial P} \right)_T + V$$

$$\left( \frac{\partial U}{\partial V} \right)_T = \frac{\left( \dfrac{\partial H}{\partial P} \right)_T - V}{\left( \dfrac{\partial V}{\partial P} \right)_T} - P$$

$$= \frac{C_P \mu_{J-T} + V}{\kappa V} - P$$

In this equation, $\kappa$ is the isothermal compressibility defined in Equation (3.9).

**EXAMPLE PROBLEM 3.11**

Using Equation (3.43),

$$\left( \frac{\partial H}{\partial P} \right)_T = \left[ \left( \frac{\partial U}{\partial V} \right)_T + P \right] \left( \frac{\partial V}{\partial P} \right)_T + V$$

show that $\mu_{J-T} = 0$ for an ideal gas.

**Solution**

$$\mu_{J-T} = -\frac{1}{C_P} \left( \frac{\partial H}{\partial P} \right)_T = -\frac{1}{C_P} \left[ \left( \frac{\partial U}{\partial V} \right)_T \left( \frac{\partial V}{\partial P} \right)_T + P \left( \frac{\partial V}{\partial P} \right)_T + V \right]$$

$$= -\frac{1}{C_P} \left[ 0 + P \left( \frac{\partial V}{\partial P} \right)_T + V \right]$$

$$= -\frac{1}{C_P} \left[ P \left( \frac{\partial [nRT/P]}{\partial P} \right)_T + V \right] = -\frac{1}{C_P} \left[ -\frac{nRT}{P} + V \right] = 0$$

In this calculation, we have used the result that $(\partial U/\partial V)_T = 0$ for an ideal gas.

Example Problem 3.11 shows that for an ideal gas, $\mu_{J-T}$ is zero. It can be shown that for a van der Waals gas in the limit of zero pressure

$$\mu_{J-T} = \frac{1}{C_{P,m}}\left(\frac{2a}{RT} - b\right) \qquad (3.54)$$

# 3.8 Liquefying Gases Using an Isenthalpic Expansion

For real gases, the Joule-Thomson coefficient $\mu_{J-T}$ can take on either negative or positive values in different regions of $P$–$T$ space. If $\mu_{J-T}$ is positive, a decrease in pressure leads to a cooling of the gas; if it is negative, the expansion of the gas leads to a heating. Figure 3.6 shows the variation of $\mu_{J-T}$ with $T$ and $P$ for $N_2$ and $H_2$. All along the solid curve, $\mu_{J-T} = 0$. To the left of each curve, $\mu_{J-T}$ is positive, and to the right, it is negative. The temperature for which $\mu_{J-T} = 0$ is referred to as the inversion temperature. If the expansion conditions are kept in the region in which $\mu_{J-T}$ is positive, $\Delta T$ can be made sufficiently large as $\Delta P$ decreases in the expansion to liquefy the gas. Note that Equation (3.54) predicts that the inversion temperature for a van der Waals gas is independent of $P$, which is not in agreement with experiment.

The results in Figure 3.6 are in accord with the observation that a high-pressure $(100 < P < 500 \text{ atm})$ expansion of $N_2$ at 300 K leads to cooling and that similar conditions for $H_2$ lead to heating. To cool $H_2$ in an expansion, it must first be precooled below 200 K, and the pressure must be less than 160 atm. He and $H_2$ are heated in an isenthalpic expansion at 300 K for $P < 200$ atm.

The Joule-Thomson effect can be used to liquefy gases such as $N_2$, as shown in Figure 3.7. The gas at atmospheric pressure is first compressed to a value of 50 atm to 200 atm, which leads to a substantial increase in its temperature. It is cooled and subsequently passed through a heat exchanger in which the gas temperature decreases to a value within ~50 K of the boiling point. At the exit of the heat exchanger, the gas expands through a nozzle to a final pressure of 1 atm in an isenthalpic expansion. The cooling that occurs because $\mu_{J-T} > 0$ results in liquefaction. The gas that boils away passes back through the heat exchanger in the opposite direction than the gas to be liquefied is passing. The two gas streams are separated, but in good thermal contact. In this process, the gas to be liquefied is effectively precooled, enabling a single-stage expansion to achieve liquefaction.
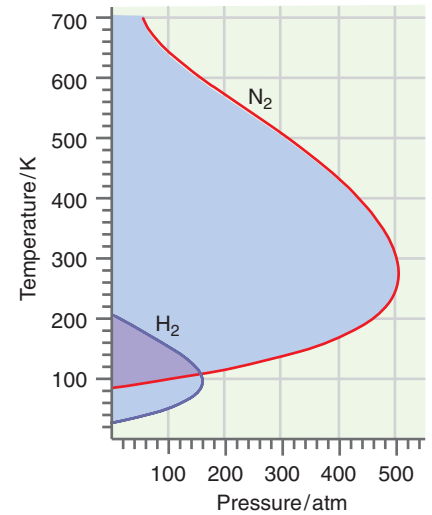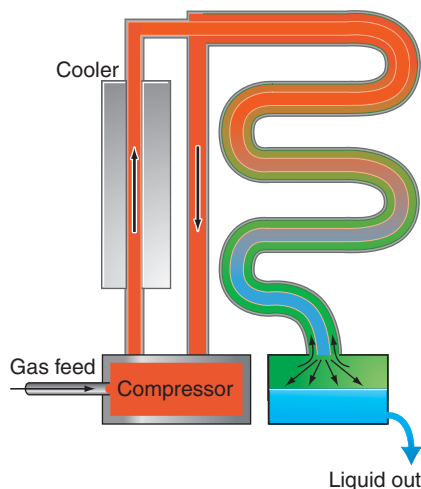


**FIGURE 3.6**
All along the curves in the figure, $\mu_{J-T} = 0$, and $\mu_{J-T}$ is positive to the left of the curves and negative to the right. To experience cooling upon expansion at 100. atm, $T$ must lie between 50. K and 150. K for $H_2$. The corresponding temperatures for $N_2$ are 100. K and 650. K.



**FIGURE 3.7**
Schematic depiction of the liquefaction of a gas using an isenthalpic Joule-Thomson expansion. Heat is extracted from the gas exiting from the compressor. It is further cooled in the countercurrent heat exchanger before expanding through a nozzle. Because its temperature is sufficiently low at the exit to the countercurrent heat exchanger, liquefaction occurs.

# Vocabulary

| | | |
|---|---|---|
| cyclic rule | internal pressure | isothermal compressibility |
| exact differential | isenthalpic | Joule-Thomson coefficient |
| heat capacity at constant pressure | isobaric volumetric thermal expansion coefficient | Joule-Thomson experiment |
| heat capacity at constant volume | | partial derivatives |

# Concept Problems

**Q3.1**    The heat capacity $C_{P, m}$ is less than $C_{V, m}$ for $H_2O(l)$ near 4°C. Explain this result.

**Q3.2**    What is the physical basis for the experimental result that $U$ is a function of $V$ at constant $T$ for a real gas? Under what conditions will $U$ decrease as $V$ increases?

**Q3.3**    Why didn't Joule change his experiment to make $C_{surroundings}/C_{system} \approx 0.001$ to increase the sensitivity of the apparatus?

**Q3.4**    Why does the relation $C_P > C_V$ always hold for a gas? Can $C_P < C_V$ be valid for a liquid?

**Q3.5**    Why can $q_V$ be equated with a state function if $q$ is not a state function?

**Q3.6**    Explain without using equations why $(\partial H/\partial P)_T$ is generally small for a real gas.

**Q3.7**    Why is it reasonable to write $dH \approx C_P dT + V dP$ for a liquid or solid sample?

**Q3.8**    Refer to Figure 1.10 and explain why $(\partial U/\partial V)_T$ is generally small for a real gas.

**Q3.9**    Can a gas be liquefied through an isenthalpic expansion if $\mu_{J-T} = 0$?

**Q3.10**    Why is $q_v = \Delta U$ only for a constant volume process? Is this formula valid if work other than $P$–$V$ work is possible?

**Q3.11**    Classify the following variables and functions as intensive or extensive: $T, P, V, q, w, U, H$.

**Q3.12**    Why are $q$ and $w$ not state functions?

**Q3.13**    Why is the equation $\Delta H = \int_{T_i}^{T_f} C_P(T)\, dT = n \int_{T_i}^{T_f} C_{P,m}(T)\, dT$ valid for an ideal gas even if $P$ is not constant in the process? Is this equation also valid for a real gas? Why or why not?

**Q3.14**    What is the relationship between a state function and an exact differential?

**Q3.15**    Is the following statement always, never, or sometimes valid? Explain your reasoning: $\Delta H$ is only defined for a constant pressure process.

**Q3.16**    Is the following statement always, never, or sometimes valid? Explain your reasoning: a thermodynamic process is completely defined by the initial and final states of the system.

**Q3.17**    Is the following statement always, never, or sometimes valid? Explain your reasoning: $q = 0$ for a cyclic process.

**Q3.18**    The molar volume of $H_2O(l)$ decreases with increasing temperature near 4°C. Can you explain this behavior using a molecular level model?

**Q3.19**    Why was the following qualification made in Section 3.7? Note that Equation (3.47) is only applicable to a process in which there is no change in the phase of the system, such as vaporization or fusion, and in which there are no chemical reactions.

**Q3.20**    Is the expression $\Delta U_V = \int_{T_1}^{T_2} C_V dT = n \int_{T_1}^{T_2} C_{V, m} dT$ only valid for an ideal gas if $V$ is constant?

# Numerical Problems

Problem numbers in **red** indicate that the solution to the problem is given in the *Student's Solutions Manual*.

**P3.1**    Obtain an expression for the isothermal compressibility $\kappa = -1/V\, (\partial V/\partial P)_T$ for a van der Waals gas.

**P3.2**    Use the result of Problem P3.10 to show that $(\partial C_V/\partial V)_T$ for the van der Waals gas is zero.

**P3.3**    The molar heat capacity $C_{P, m}$ of $SO_2(g)$ is described by the following equation over the range $300\ K < T < 1700\ K$:

$$\frac{C_{P,m}}{R} = 3.093 + 6.967 \times 10^{-3}\frac{T}{K} - 45.81 \times 10^{-7}\frac{T^2}{K^2}$$
$$+ 1.035 \times 10^{-9}\frac{T^3}{K^3}$$

In this equation, $T$ is the absolute temperature in kelvin. The ratios $T^n/K^n$ ensure that $C_{P, m}$ has the correct dimension. Assuming ideal gas behavior, calculate $q, w, \Delta U$, and $\Delta H$ if 1.50 moles of $SO_2(g)$ is heated from 22.5°C to 1140.°C at a constant pressure of 1 bar. Explain the sign of $w$.

**P3.4**    Use the relation $(\partial U/\partial V)_T = T(\partial P/\partial T)_V - P$ and the cyclic rule to obtain an expression for the internal pressure, $(\partial U/\partial V)_T$, in terms of $P, \beta, T$, and $\kappa$.

**P3.5**    A mass of 34.05 g of $H_2O(s)$ at 273 K is dropped into 185 g of $H_2O(l)$ at 310. K in an insulated container at 1 bar of pressure. Calculate the temperature of the system once equilibrium has been reached. Assume that $C_{P, m}$ for $H_2O(l)$ is constant at its values for 298 K throughout the temperature range of interest.

**P3.6** A vessel is filled completely with liquid water and sealed at 13.56°C and a pressure of 1.00 bar. What is the pressure if the temperature of the system is raised to 82.0°C? Under these conditions, $\beta_{water} = 2.04 \times 10^{-4} \text{ K}^{-1}$, $\beta_{vessel} = 1.42 \times 10^{-4} \text{ K}^{-1}$, and $\kappa_{water} = 4.59 \times 10^{-5} \text{ bar}^{-1}$.

**P3.7** Integrate the expression $\beta = 1/V (\partial V/\partial T)_P$ assuming that $\beta$ is independent of temperature. By doing so, obtain an expression for $V$ as a function of $T$ and $\beta$ at constant $P$.

**P3.8** A mass of 32.0 g of $H_2O(g)$ at 373 K is flowed into 295 g of $H_2O(l)$ at 310. K and 1 atm. Calculate the final temperature of the system once equilibrium has been reached. Assume that $C_{P\,m}$ for $H_2O(l)$ is constant at its values for 298 K throughout the temperature range of interest. Describe the state of the system.

**P3.9** Because $(\partial H/\partial P)_T = -C_P\mu_{J-T}$, the change in enthalpy of a gas expanded at constant temperature can be calculated. To do so, the functional dependence of $\mu_{J-T}$ on $P$ must be known. Treating Ar as a van der Waals gas, calculate $\Delta H$ when 1 mole of Ar is expanded from 325 bar to 1.75 bar at 375 K. Assume that $\mu_{J-T}$ is independent of pressure and is given by $\mu_{J-T} = [(2a/RT) - b]/C_{P,m}$, and $C_{P,m} = 5R/2$ for Ar. What value would $\Delta H$ have if the gas exhibited ideal gas behavior?

**P3.10** Derive the following expression for calculating the isothermal change in the constant volume heat capacity: $(\partial C_V/\partial V)_T = T(\partial^2 P/\partial T^2)_V$.

**P3.11** A 75.0 g piece of gold at 650. K is dropped into 180. g of $H_2O(l)$ at 310. K in an insulated container at 1 bar pressure. Calculate the temperature of the system once equilibrium has been reached. Assume that $C_{P,\,m}$ for $Au(s)$ and $H_2O(l)$ is constant at their values for 298 K throughout the temperature range of interest.

**P3.12** Calculate $w$, $q$, $\Delta H$, and $\Delta U$ for the process in which 1.75 moles of water undergoes the transition $H_2O(l, 373 \text{ K}) \rightarrow H_2O(g, 610. \text{ K})$ at 1 bar of pressure. The volume of liquid water at 373 K is $1.89 \times 10^{-5} \text{ m}^3 \text{ mol}^{-1}$ and the molar volume of steam at 373 K and 610. K is 3.03 and $5.06 \times 10^{-2} \text{ m}^3 \text{ mol}^{-1}$, respectively. For steam, $C_{P,\,m}$ can be considered constant over the temperature interval of interest at 33.58 J mol$^{-1}$ K$^{-1}$.

**P3.13** Equation (3.38), $C_P = C_V + TV(\beta^2/\kappa)$, links $C_P$ and $C_V$ with $\beta$ and $\kappa$. Use this equation to evaluate $C_P - C_V$ for an ideal gas.

**P3.14** Use the result of Problem P3.10 to derive a formula for $(\partial C_V/\partial V)_T$ for a gas that obeys the Redlich-Kwong equation of state,

$$P = \frac{RT}{V_m - b} - \frac{a}{\sqrt{T}} \frac{1}{V_m(V_m + b)}$$

**P3.15** The function $f(x, y)$ is given by $f(x, y) = xy \sin 5x + x^2 \sqrt{y} \ln y + 3e^{-2x^2} \cos y$. Determine

$$\left(\frac{\partial f}{\partial x}\right)_y, \left(\frac{\partial f}{\partial y}\right)_x, \left(\frac{\partial^2 f}{\partial x^2}\right)_y, \left(\frac{\partial^2 f}{\partial y^2}\right)_x, \left(\frac{\partial}{\partial y}\left(\frac{\partial f}{\partial x}\right)_y\right)_x$$

and $\left(\frac{\partial}{\partial x}\left(\frac{\partial f}{\partial y}\right)_x\right)_y$. Is $\left(\frac{\partial}{\partial y}\left(\frac{\partial f}{\partial x}\right)_y\right)_x = \left(\frac{\partial}{\partial x}\left(\frac{\partial f}{\partial y}\right)_x\right)_y$?

Obtain an expression for the total differential $df$.

**P3.16** The Joule coefficient is defined by $(\partial T/\partial V)_U = (1/C_V)[P - T(\partial P/\partial T)_V]$. Calculate the Joule coefficient for an ideal gas and for a van der Waals gas.

**P3.17** Using the result of Equation (3.8), $(\partial P/\partial T)_V = \beta/\kappa$, express $\beta$ as a function of $\kappa$ and $V_m$ for an ideal gas, and $\beta$ as a function of $b$, $\kappa$, and $V_m$ for a van der Waals gas.

**P3.18** Show that the expression $(\partial U/\partial V)_T = T(\partial P/\partial T)_V - P$ can be written in the form

$$\left(\frac{\partial U}{\partial V}\right)_T = T^2\left(\partial\left[\frac{P}{T}\right]\Big/\partial T\right)_V = -\left(\partial\left[\frac{P}{T}\right]\Big/\partial\left[\frac{1}{T}\right]\right)_V$$

**P3.19** Derive an expression for the internal pressure of a gas that obeys the Bethelot equation of state,

$$P = \frac{RT}{V_m - b} - \frac{a}{TV_m^2}$$

**P3.20** Because $U$ is a state function, $(\partial/\partial V (\partial U/\partial T)_V)_T = (\partial/\partial T (\partial U/\partial V)_T)_V$. Using this relationship, show that $(\partial C_V/\partial V)_T = 0$ for an ideal gas.

**P3.21** Starting with the van der Waals equation of state, find an expression for the total differential $dP$ in terms of $dV$ and $dT$. By calculating the mixed partial derivatives $(\partial(\partial P/\partial V)_T/\partial T)_V$ and $(\partial(\partial P/\partial T)_V/\partial V)_T$, determine if $dP$ is an exact differential.

**P3.22** Use $(\partial U/\partial V)_T = (\beta T - \kappa P)/\kappa$ to calculate $(\partial U/\partial V)_T$ for an ideal gas.

**P3.23** Derive the following relation,

$$\left(\frac{\partial U}{\partial V_m}\right)_T = \frac{3a}{2\sqrt{T}V_m(V_m + b)}$$

for the internal pressure of a gas that obeys the Redlich-Kwong equation of state,

$$P = \frac{RT}{V_m - b} - \frac{a}{\sqrt{T}} \frac{1}{V_m(V_m + b)}$$

**P3.24** A differential $dz = f(x, y)dx + g(x, y)dy$ is exact if the integral $\int f(x, y)dx + \int g(x, y)dy$ is independent of the path. Demonstrate that the differential $dz = 2xydx + x^2dy$ is exact by integrating $dz$ along the paths $(1,1) \rightarrow (1,8) \rightarrow (6,8)$ and $(1,1) \rightarrow (1,3) \rightarrow (4,3) \rightarrow (4,8) \rightarrow (6,8)$. The first number in each set of parentheses is the $x$ coordinate, and the second number is the $y$ coordinate.

**P3.25** Show that $d\rho/\rho = -\beta dT + \kappa dP$ where $\rho$ is the density $\rho = m/V$. Assume that the mass $m$ is constant.

**P3.26** For a gas that obeys the equation of state

$$V_m = \frac{RT}{P} + B(T)$$

derive the result

$$\left(\frac{\partial H}{\partial P}\right)_T = B(T) - T\frac{dB(T)}{dT}$$

**P3.27** Because $V$ is a state function, $(\partial(\partial V/\partial T)_P/\partial P)_T = (\partial(\partial V/\partial P)_T/\partial T)_P$. Using this relationship, show that the isothermal compressibility and isobaric expansion coefficient are related by $(\partial\beta/\partial P)_T = -(\partial\kappa/\partial T)_P$.

**P3.28** Use the relation

$$C_{P,m} - C_{V,m} = T\left(\frac{\partial V_m}{\partial T}\right)_P \left(\frac{\partial P}{\partial T}\right)_V$$

the cyclic rule, and the van der Waals equation of state to derive an equation for $C_{P,m} - C_{V,m}$ in terms of $V_m$, $T$, and the gas constants $R$, $a$, and $b$.

**P3.29** For the equation of state $V_m = RT/P + B(T)$, show that

$$\left(\frac{\partial C_{P,m}}{\partial P}\right)_T = -T\frac{d^2B(T)}{dT^2}$$

[*Hint:* Use Equation (3.44) and the property of state functions with respect to the order of differentiation in mixed second derivatives.]

**P3.30** Starting with $\beta = (1/V)(\partial V/\partial T)_P$, show that $\beta = -(1/\rho)(\partial \rho/\partial T)_P$, where $\rho$ is the density.

**P3.31** This problem will give you practice in using the cyclic rule. Use the ideal gas law to obtain the three functions $P = f(V,T)$, $V = g(P,T)$, and $T = h(P,V)$. Show that the cyclic rule $(\partial P/\partial V)_T (\partial V/\partial T)_P (\partial T/\partial P)_V = -1$ is obeyed.

**P3.32** Regard the enthalpy as a function of $T$ and $P$. Use the cyclic rule to obtain the expression

$$C_P = -\left(\frac{\partial H}{\partial P}\right)_T \bigg/ \left(\frac{\partial T}{\partial P}\right)_H$$

**P3.33** Using the chain rule for differentiation, show that the isobaric expansion coefficient expressed in terms of density is given by $\beta = -1/\rho(\partial\rho/\partial T)_P$.

**P3.34** Derive the equation $(\partial P/\partial V)_T = -1/(\kappa V)$ from basic equations and definitions.

**P3.35** Derive the equation $(\partial H/\partial T)_V = C_V + V\beta/\kappa$ from basic equations and definitions.

**P3.36** For an ideal gas, $\left(\frac{\partial U}{\partial V}\right)_T$ and $\left(\frac{\partial H}{\partial P}\right)_T = 0$. Prove that $C_V$ and $C_P$ are independent of volume and pressure.

**P3.37** Prove that $C_V = -\left(\frac{\partial U}{\partial V}\right)_T \left(\frac{\partial V}{\partial T}\right)_U$

**P3.38** Show that $\left(\frac{\partial C_V}{\partial V}\right)_T = T\left(\frac{\partial^2 P}{\partial T^2}\right)_V$

**P3.39** Show that $\left(\frac{\partial C_V}{\partial V}\right)_T = 0$ for an ideal and for a van der Waals gas.

# Thermochemistry

Thermochemistry is the branch of thermodynamics that investigates the heat flow into or out of a reaction system and deduces the energy stored in chemical bonds. As reactants are converted into products, energy can either be taken up by the system or released to the surroundings. For a reaction that takes place at constant volume, the heat that flows to or out of the system is equal to $\Delta U$ for the reaction. For a reaction that takes place at constant pressure, the heat that flows to or out of the system is equal to $\Delta H$ for the reaction. The enthalpy of formation is defined as the heat flow into or out of the system in a reaction between pure elements that leads to the formation of 1 mol of product. Because $H$ is a state function, the reaction enthalpy can be written as the enthalpies of formation of the products minus those of the reactants. This property allows $\Delta H$ and $\Delta U$ for a reaction to be calculated for many reactions without carrying out an experiment.

## 4.1 Energy Stored in Chemical Bonds Is Released or Taken Up in Chemical Reactions

A significant amount of the internal energy or enthalpy of a molecule is stored in the form of chemical bonds. As reactants are transformed to products in a chemical reaction, energy can be released or taken up as bonds are made or broken, respectively. For example, consider a reaction in which $N_2(g)$ and $H_2(g)$ dissociate into atoms, and the atoms recombine to form $NH_3(g)$. The enthalpy changes associated with individual steps and with the overall reaction $1/2\ N_2(g) + 3/2\ H_2(g) \longrightarrow NH_3(g)$ are shown in Figure 4.1. Note that large enthalpy changes are associated with the individual steps but the enthalpy change in the overall reaction is much smaller.

The change in enthalpy or internal energy resulting from chemical reactions appears in the surroundings in the form of a temperature increase or decrease resulting from heat flow and/or in the form of expansion or nonexpansion work. For example, the combustion of gasoline in an automobile engine can be used to do expansion work on the surroundings. Nonexpansion electrical work is possible if the chemical

reaction is carried out in an electrochemical cell. In Chapters 6 and 11, the extraction
of nonexpansion work from chemical reactions will be discussed. In this chapter, the
focus is on using measurements of heat flow to determine changes in $U$ and $H$ due to
chemical reactions.

## 4.2 Internal Energy and Enthalpy Changes Associated with Chemical Reactions

In the previous chapters, we discussed how $\Delta U$ and $\Delta H$ are calculated from work and
heat flow between the system and the surroundings for processes that do not involve
phase changes or chemical reactions. In this section, this discussion is extended to
reaction systems.

Imagine that a reaction involving a stoichiometric mixture of reactants (the system)
is carried out in a constant pressure reaction vessel with diathermal walls immersed in a
water bath (the surroundings). If the temperature of the water bath increases, heat has
flowed from the system (the contents of the reaction vessel) to the surroundings (the
water bath and the vessel). In this case, we say that the reaction is **exothermic.** If the
temperature of the water bath decreases, the heat has flowed from the surroundings to
the system, and we say that the reaction is **endothermic.**

Consider the reaction in Equation (4.1):

$$Fe_3O_4(s)\ +\ 4\ H_2(g)\ \longrightarrow\ 3\ Fe(s)\ +\ 4\ H_2O(l) \qquad \textbf{(4.1)}$$
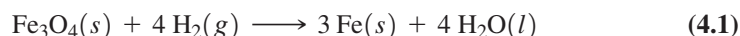
Note that the phase (solid, liquid, or gas) for each reactant and product has been speci-
fied because $U$ and $H$ are different for each phase. This reaction will only proceed at a
measurable rate at elevated temperatures. However, as we show later, it is useful to tab-
ulate values for $\Delta H$ for reactions at a pressure of 1 bar and a specified temperature,
generally 298.15 K. The pressure value of 1 bar defines a **standard state,** and changes
in $H$ and $U$ at the standard pressure of 1 bar are indicated by a superscript ° as in
$\Delta H°$ and $\Delta U°$. The standard state for gases is a hypothetical state in which the gas
behaves ideally at a pressure of 1 bar. For most gases, deviations from ideal behavior

are very small. The **enthalpy of reaction, $\Delta H_R$**, at specific values of $T$ and $P$ is defined as the heat exchanged between the system and the surroundings as the reactants are transformed into products at conditions of constant $T$ and $P$. By convention, heat flowing into the system is given a positive sign. $\Delta H_R$ is, therefore, a negative quantity for an exothermic reaction and a positive quantity for an endothermic reaction. The **standard enthalpy of reaction, $\Delta H_R^{\circ}$**, refers to one mole of the specified reaction at a pressure of 1 bar, and unless indicated otherwise, to $T = 298.15$ K.

How can the reaction enthalpy and internal energy be determined? We proceed in the following way. The reaction is carried out at 1 bar pressure, and the temperature change $\Delta T$ that occurs in a finite size water bath, initially at 298.15 K, is measured. The water bath is large enough that $\Delta T$ is small. If $\Delta T$ is negative as a result of the reaction, the bath is heated to return it, the reaction vessel, and the system to 298.15 K using an electrical heater. By doing so, we ensure that the initial and final states are the same and therefore the measured $\Delta H$ is equal to $\Delta H_R^{\circ}$. The electrical work done on the heater that restores the temperature of the water bath and the system to 298.15 K is equal to $\Delta H_R^{\circ}$. If the temperature of the water bath increases as a result of the reaction, the electrical work done on a heater in the water bath at 298.15 K that increases its temperature and that of the system by $\Delta T$ in a separate experiment is measured. In this case, $\Delta H_R^{\circ}$ is equal to the negative of the electrical work done on the heater.
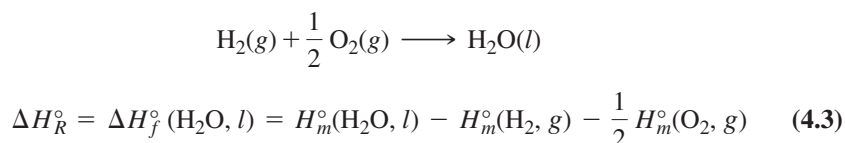
Although an experimental method for determining $\Delta H_R^{\circ}$ has been described, to tabulate the reaction enthalpies for all possible chemical reactions would be a monumental undertaking. Fortunately, $\Delta H_R^{\circ}$ can be calculated from tabulated enthalpy values for individual reactants and products. This is advantageous because there are far fewer reactants and products than there are reactions among them. Consider $\Delta H_R^{\circ}$ for the reaction of Equation (4.1) at $T = 298.15$ K and $P = 1$ bar. These values for $P$ and $T$ are chosen because thermodynamic values are tabulated for these values. However, $\Delta H_R$ at other values of $P$ and $T$ can be calculated as discussed in Chapters 2 and 3. In principle, we could express $\Delta H_R^{\circ}$ in terms of the individual enthalpies of reactants and products:

$$\Delta H_R^{\circ} = H_{products}^{\circ} - H_{reactants}^{\circ}$$
$$= 3H_m^{\circ}(\text{Fe},s) + 4H_m^{\circ}(\text{H}_2\text{O},l) - H_m^{\circ}(\text{Fe}_3\text{O}_4,s) - 4H_m^{\circ}(\text{H}_2,g) \qquad \textbf{(4.2)}$$

The $m$ subscripts refer to molar quantities. Although Equation (4.2) is correct, it does not provide a useful way to calculate $\Delta H_R^{\circ}$. There is no experimental way to determine the absolute enthalpy for any element or compound because there is no unique reference zero against which individual enthalpies can be measured. Only $\Delta H$ and $\Delta U$, as opposed to $H$ and $U$, can be determined in an experiment.

Equation (4.2) can be transformed into a more useful form by introducing the enthalpy of formation. The **standard enthalpy of formation, $\Delta H_f^{\circ}$**, is defined as the enthalpy change of the reaction in which the only reaction product is 1 mol of the species of interest, and only pure elements in their most stable state of aggregation under the standard state conditions appear as reactants. We refer to these species as being in their **standard reference state.** For example, the standard reference state of water and carbon at 298.15 K are $\text{H}_2\text{O}(l)$ and solid carbon in the form of graphite. Note that with this definition, $\Delta H_f^{\circ} = 0$ for an element in its standard reference state because the reactants and products are identical.

We next illustrate how reaction enthalpies can be expressed in terms of formation enthalpies. The only compounds that are produced or consumed in the reaction $\text{Fe}_3\text{O}_4(s) + 4\,\text{H}_2(g) \longrightarrow 3\,\text{Fe}(s) + 4\,\text{H}_2\text{O}(l)$ are $\text{Fe}_3\text{O}_4(s)$ and $\text{H}_2\text{O}(l)$. All elements that appear in the reaction are in their standard reference states. The formation reactions for the compounds at 298.15 K and 1 bar are

$$\text{H}_2(g) + \frac{1}{2}\,\text{O}_2(g) \longrightarrow \text{H}_2\text{O}(l)$$

$$\Delta H_R^{\circ} = \Delta H_f^{\circ}\,(\text{H}_2\text{O},\, l) = H_m^{\circ}(\text{H}_2\text{O},\, l) - H_m^{\circ}(\text{H}_2,\, g) - \frac{1}{2}\,H_m^{\circ}(\text{O}_2,\, g) \qquad \textbf{(4.3)}$$

$$3\,\text{Fe}(s) + 2\,\text{O}_2(g) \longrightarrow \text{Fe}_3\text{O}_4(s)$$
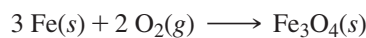
$$\Delta H_R^\circ = \Delta H_f^\circ(\text{Fe}_3\text{O}_4, s) = H_m^\circ(\text{Fe}_3\text{O}_4, s) - 3H_m^\circ(\text{Fe}, s) - 2H_m^\circ(\text{O}_2, g) \quad \text{(4.4)}$$

If Equation (4.2) is rewritten in terms of the enthalpies of formation, a simple equation for the reaction enthalpy is obtained:

$$\Delta H_R^\circ = 4\Delta H_f^\circ(\text{H}_2\text{O}, l) - \Delta H_f^\circ(\text{Fe}_3\text{O}_4, s) \quad \text{(4.5)}$$

Note that elements in their standard reference state do not appear in this equation because $\Delta H_f^\circ = 0$ for these species. This result can be generalized to any chemical transformation

$$\nu_\text{A}\text{A} + \nu_\text{B}\text{B} + \ldots \longrightarrow \nu_\text{X}\text{X} + \nu_\text{Y}\text{Y} + \ldots \quad \text{(4.6)}$$
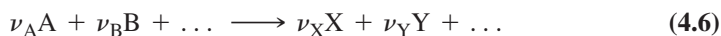
which we write in the form

$$0 = \sum_i \nu_i X_i \quad \text{(4.7)}$$

The $X_i$ refer to all species that appear in the overall equation. The unitless stoichiometric coefficients $\nu_i$ are positive for products and negative for reactants. The enthalpy change associated with this reaction is

$$\Delta H_R^\circ = \sum_i \nu_i \Delta H_{f,i}^\circ \quad \text{(4.8)}$$

The rationale behind Equation (4.8) can also be depicted as shown in Figure 4.2. Two paths are considered between the reactants A and B and the products C and D in the reaction $\nu_\text{A}\text{A} + \nu_\text{B}\text{B} \longrightarrow \nu_\text{C}\text{C} + \nu_\text{D}\text{D}$. The first of these is a direct path for which $\Delta H^\circ = \Delta H_R^\circ$. In the second path, A and B are first broken down into their elements, each in its standard reference state. Subsequently, the elements are combined to form C and D. The enthalpy change for the second route is $\Delta H_R^\circ = \sum_i \nu_i \Delta H_{f,products}^\circ - \sum_i |\nu_i| \Delta H_{f,reactants}^\circ = \sum_i \nu_i \Delta H_{f,i}^\circ$. Because $H$ is a state function, the enthalpy change is the same for both paths. This is stated in mathematical form in Equation (4.8).

Writing $\Delta H_R^\circ$ in terms of formation enthalpies is a great simplification over compiling measured values of reaction enthalpies. Standard formation enthalpies for atoms and inorganic compounds at 298.15 K are listed in Table 4.1, and standard formation enthalpies for organic compounds are listed in Table 4.2 (Appendix A, Data Tables).

Another thermochemical convention is introduced at this point in order to calculate enthalpy changes involving electrolyte solutions. The solution reaction that occurs when a salt such as NaCl is dissolved in water is

$$\text{NaCl}(s) \longrightarrow \text{Na}^+(aq) + \text{Cl}^-(aq)$$
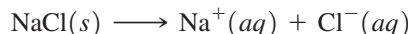
Because it is not possible to form only positive or negative ions in solution, the measured enthalpy of solution of an electrolyte is the sum of the enthalpies of all anions and cations formed. To be able to tabulate values for enthalpies of formation of individual ions, the enthalpy for the following reaction is set equal to zero at $P = 1$ bar for all temperatures:

$$1/2\,\text{H}_2(g) \longrightarrow \text{H}^+(aq) + e^-(\text{metal electrode})$$
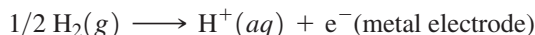
In other words, solution enthalpies of formation of ions are measured relative to that for $\text{H}^+(aq)$. The thermodynamics of electrolyte solutions will be discussed in detail in Chapter 10.

As the previous discussion shows, only the $\Delta H_f^\circ$ of each reactant and product is needed to calculate $\Delta H_R^\circ$. Each $\Delta H_f^\circ$ is a *difference* in enthalpy between the compound and its constituent elements, rather than an absolute enthalpy. However, there is a convention that allows absolute enthalpies to be specified using the experimentally determined values of the $\Delta H_f^\circ$ of compounds. In this convention, the absolute enthalpy of each pure element in its standard reference state is set equal to zero. With this convention, the absolute molar enthalpy of any chemical species in its standard reference state $H_m^\circ$ is equal to $\Delta H_f^\circ$ for that species. To demonstrate this convention, the reaction in Equation (4.4) is considered:

$$\Delta H_R^\circ = \Delta H_f^\circ(\text{Fe}_3\text{O}_4, s) = H_m^\circ(\text{Fe}_3\text{O}_4, s) - 3H_m^\circ(\text{Fe}, s) - 2H_m^\circ(\text{O}_2, g) \quad \text{(4.4)}$$
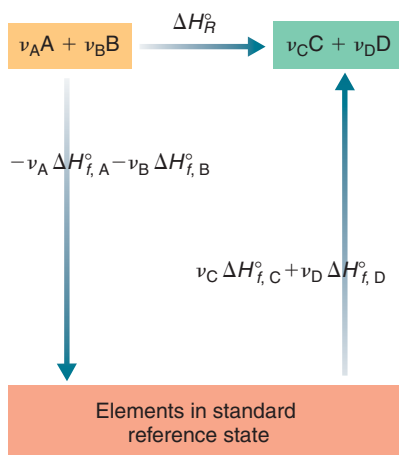


**FIGURE 4.2**
Equation (4.8) follows from the fact that $\Delta H$ for both paths is the same because they connect the same initial and final states.

Setting $H_m^{\circ} = 0$ for each element in its standard reference state,

$$\Delta H_f^{\circ}(Fe_3O_4,s) = H_m^{\circ}(Fe_3O_4,s) - 3 \times 0 - 2 \times 0 = H_m^{\circ}(Fe_3O_4,s) \qquad \textbf{(4.9)}$$

The value of $\Delta H_R^{\circ}$ for any reaction involving compounds and elements is unchanged by this convention. In fact, one could choose a different number for the absolute enthalpy of each pure element in its standard reference state, and it would still not change the value of $\Delta H_R^{\circ}$. However, it is much more convenient (and easier to remember) if one sets $H_m^{\circ} = 0$ for all elements in their standard reference state. This convention will be used again in Chapter 6 when the chemical potential is discussed.
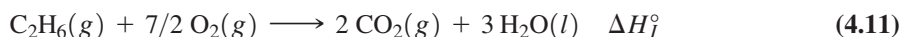
# 4.3 Hess's Law Is Based on Enthalpy Being a State Function

As discussed in the previous section, it is extremely useful to have tabulated values of $\Delta H_f^{\circ}$ for chemical compounds at one fixed combination of $P$ and $T$. Tables 4.1 and 4.2 list this data for 1 bar and 298.15 K. With access to these values of $\Delta H_f^{\circ}$, $\Delta H_R^{\circ}$ can be calculated for all reactions among these elements and compounds at 1 bar and 298.15 K.

But how is $\Delta H_f^{\circ}$ determined? Consider the formation reaction for $C_2H_6(g)$:

$$2\,C(graphite) + 3\,H_2(g) \longrightarrow C_2H_6(g) \qquad \textbf{(4.10)}$$
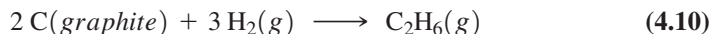
Graphite is the standard reference state for carbon at 298.15 K and 1 bar because it is slightly more stable than diamond under these conditions. However, it is unlikely that one would obtain only ethane if the reaction were carried out as written. Given this experimental hindrance, how can $\Delta H_f^{\circ}$ for ethane be determined? To determine $\Delta H_f^{\circ}$ for ethane, we take advantage of the fact that $\Delta H$ is path independent. In this context, path independence means that the enthalpy change for any sequence of reactions that sum to the same overall reaction is identical. This statement is known as **Hess's law.** Therefore, one is free to choose any sequence of reactions that leads to the desired outcome. Combustion reactions are well suited for these purposes because in general they proceed rapidly, go to completion, and produce only a few products. To determine $\Delta H_f^{\circ}$ for ethane, one can carry out the following combustion reactions:

$$C_2H_6(g) + 7/2\,O_2(g) \longrightarrow 2\,CO_2(g) + 3\,H_2O(l) \quad \Delta H_I^{\circ} \qquad \textbf{(4.11)}$$

$$C(graphite) + O_2(g) \longrightarrow CO_2(g) \qquad\qquad \Delta H_{II}^{\circ} \qquad \textbf{(4.12)}$$

$$H_2(g) + 1/2\,O_2(g) \longrightarrow H_2O(l) \qquad\qquad \Delta H_{III}^{\circ} \qquad \textbf{(4.13)}$$

These reactions are combined in the following way to obtain the desired reaction:

$$2 \times [C(graphite) + O_2(g) \longrightarrow CO_2(g)] \qquad 2\Delta H_{II}^{\circ} \qquad \textbf{(4.14)}$$

$$2\,CO_2(g) + 3\,H_2O(l) \longrightarrow C_2H_6(g) + 7/2\,O_2(g) \quad -\Delta H_I^{\circ} \qquad \textbf{(4.15)}$$

$$3 \times [H_2(g) + 1/2\,O_2(g) \longrightarrow H_2O(l)] \qquad 3\Delta H_{III}^{\circ} \qquad \textbf{(4.16)}$$

$$\overline{2\,C(graphite) + 3\,H_2(g) \longrightarrow C_2H_6(g) \qquad 2\Delta H_{II}^{\circ} - \Delta H_I^{\circ} + 3\Delta H_{III}^{\circ}}$$
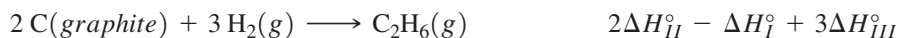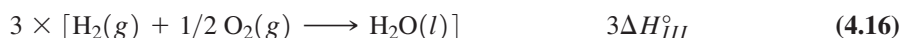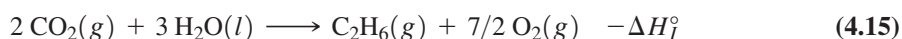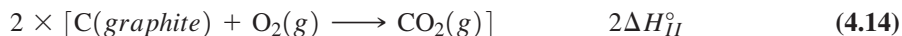
We emphasize again that it is not necessary for these reactions to be carried out at 298.15 K. The reaction vessel is immersed in a water bath at 298.15 K and the combustion reaction is initiated. If the temperature in the vessel rises during the course of the reaction, the heat flow that restores the system and surroundings to 298.15 K after completion of the reaction is measured, allowing $\Delta H_R^{\circ}$ to be determined at 298.15 K.

Several points should be made about enthalpy changes in relation to balanced overall equations describing chemical reactions. First, because $H$ is an extensive function, multiplying all stoichiometric coefficients with any number changes $\Delta H_R^{\circ}$ by the same factor. Therefore, it is important to know which set of stoichiometric coefficients has

been assumed if a numerical value of $\Delta H_R^\circ$ is given. Second, because the units of $\Delta H_f^\circ$ for all compounds in the reaction are kJ mol$^{-1}$, the units of the reaction enthalpy $\Delta H_R^\circ$ are also kJ mol$^{-1}$. One might pose the question "per mole of what?" given that all the stoichiometric coefficients may differ from each other and from one. The answer to this question is *per mole of the reaction as written*. Doubling all the stoichiometric coefficients doubles $\Delta H_R^\circ$.
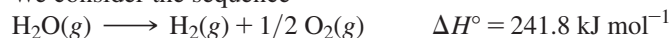
### EXAMPLE PROBLEM 4.1

The average **bond enthalpy** of the O—H bond in water is defined as one-half of the enthalpy change for the reaction $H_2O(g) \longrightarrow 2\,H(g) + O(g)$. The formation enthalpies, $\Delta H_f^\circ$, for H(g) and O(g) are 218.0 and 249.2 kJ mol$^{-1}$, respectively, at 298.15 K, and $\Delta H_f^\circ$ for $H_2O(g)$ is –241.8 kJ mol$^{-1}$ at the same temperature.

  **a.** Use this information to determine the average bond enthalpy of the O—H bond in water at 298.15 K.

  **b.** Determine the average **bond energy** $\Delta U$ of the O—H bond in water at 298.15 K. Assume ideal gas behavior.

#### Solution

**a.** We consider the sequence

$$H_2O(g) \longrightarrow H_2(g) + 1/2\,O_2(g) \qquad \Delta H^\circ = 241.8\ \text{kJ mol}^{-1}$$

$$H_2(g) \longrightarrow 2\,H(g) \qquad \Delta H^\circ = 2 \times 218.0\ \text{kJ mol}^{-1}$$

$$1/2\,O_2(g) \longrightarrow O(g) \qquad \Delta H^\circ = 249.2\ \text{kJ mol}^{-1}$$

$$\overline{H_2O(g) \longrightarrow 2\,H(g) + O(g) \qquad \Delta H^\circ = 927.0\ \text{kJ mol}^{-1}}$$

This is the enthalpy change associated with breaking both O—H bonds under standard conditions. We conclude that the average bond enthalpy of the O—H bond in water is $\frac{1}{2} \times 927.0\,\text{kJ mol}^{-1} = 463.5\,\text{kJ mol}^{-1}$. We emphasize that this is the average value because the values of $\Delta H$ for the transformations $H_2O(g) \longrightarrow H(g) + OH(g)$ and $OH(g) \longrightarrow O(g) + H(g)$ differ.

**b.** $\Delta U^\circ = \Delta H^\circ - \Delta(PV) = \Delta H^\circ - \Delta nRT$

$$= 927.0\ \text{kJ mol}^{-1} - 2 \times 8.314\ \text{J mol}^{-1}\text{K}^{-1} \times 298.15\ \text{K}$$

$$= 922.0\ \text{kJ mol}^{-1}$$

The average value for $\Delta U^\circ$ for the O—H bond in water is $\frac{1}{2} \times 922.0\ \text{kJ mol}^{-1} = 461.0\ \text{kJ mol}^{-1}$. The bond energy and the bond enthalpy are nearly identical.

Example Problem 4.1 shows how bond energies can be calculated from reaction enthalpies. The value of a bond energy is of particular importance for chemists in estimating the thermal stability of a compound as well as its stability with respect to reactions with other molecules. Values of bond energies tabulated in the format of the periodic table together with the electronegativities are shown in Table 4.3 [Kildahl, N. K. "Bond Energy Data Summarized." *Journal of Chemical Education*. 72 (1995): 423]. The value of the single bond energy, $\Delta U_{A-B}$, for a combination A–B not listed in the table can be estimated using the empirical relationship due to Linus Pauling in Equation (4.17):

$$\Delta U_{A-B} = \sqrt{\Delta U_{A-A} \times \Delta U_{B-B}} + 96.48(\chi_A - \chi_B)^2 \qquad (4.17)$$

where $\chi_A$ and $\chi_B$ are the electronegativities of atoms A and B.

**TABLE 4.3  Mean Bond Energies**

| 1 | 2 | Selected Bond Energies (kJ/mol) | 13 | 14 | 15 | 16 | 17 | 18 |
|---|---|---|---|---|---|---|---|---|
| **H**,2.20<br>432<br>---<br>432<br>459<br>565 | | | | | | | | **He** |
| **Li**,0.98<br>105<br>---<br>243<br>---<br>573 | **Be**,1.57<br>208<br>---<br>---<br>---,444<br>632 | | **B**,2.04<br>293<br>---<br>389<br>536,636<br>613 | **C**,2.55<br>346<br>602,835<br>411<br>358,799<br>485 | **N**,3.04<br>167<br>418,942<br>386<br>201,607<br>283 | **O**,3.44<br>142<br>494<br>459<br>142,494<br>190 | **F**,3.98<br>155<br>---<br>565<br>---<br>155 | **Ne** |
| **Na**,0.93<br>72<br>---<br>197<br>---<br>477 | **Mg**,1.31<br>129<br>---<br>---<br>---,377<br>513 | | **Al**,1.61<br>--<br>---<br>272<br>---<br>583 | **Si**,1.90<br>222<br>318<br>318<br>452,640<br>565 | **P**,2.19<br>≈220<br>---,481<br>322<br>335,544<br>490 | **S**,2.58<br>240<br>425<br>363<br>---,523<br>284 | **Cl**,3.16<br>240<br>---<br>428<br>218<br>249 | **Ar** |
| **K**,0.82<br>49<br>---<br>180<br>---<br>490 | **Sr**,1.00<br>105<br>---<br>---<br>---,460<br>550 | | **Ga**,1.81<br>113<br>---<br>---<br>---<br>≈469 | **Ge**,2.01<br>188<br>272<br>---<br>---<br>≈470 | **As**,2.18<br>146<br>---,380<br>247<br>301,389<br>≈440 | **Se**,2.55<br>172<br>272<br>276<br>---<br>≈351 | **Br**,2.96<br>190<br>---<br>362<br>201<br>250 | **Kr**<br>50 |
| **Rb**,0.82<br>45<br>---<br>163<br>---<br>490 | **Sr**,0.95<br>84<br>---<br>---<br>---,347<br>553 | | **In**,1.78<br>100<br>---<br>---<br>---<br>≈523 | **Sn**,1.80<br>146<br>---<br>---<br>---<br>≈450 | **Sb**,2.05<br>121<br>---,295<br>---<br>----<br>≈420 | **Te**,2.10<br>126<br>218<br>238<br>----<br>≈393 | **I**,2.66<br>149<br>--<br>295<br>201<br>278 | **Xe**<br>84<br>≈131 |
| **Cs**,0.79<br>44<br>---<br>176<br>---<br>502 | **Ba**,0.89<br>44<br>---<br>---<br>467,561<br>578 | | **Tl**,2.04<br>---<br>---<br>---<br>---<br>439 | **Pb**,2.33<br>---<br>---<br>---<br>---<br>≈360 | **Bi**,2.02<br>---<br>---,192<br>---<br>≈350 | **Po**,2.00<br>116 | **At**,2.20 | **Rn** |

KEY

Element symbol — **C**,2.55 — Electronegativity
C—C — 346 — Single bond with self
C=C,  C≡C — 602,835 — Double, triple bond with self
H—C — 411 — Bond with H
O—C,  O=C — 358,799 — Single, double bond with O
C—F — 485 — Bond with F

# 4.4 The Temperature Dependence of Reaction Enthalpies

Suppose that we plan to carry out a reaction that is mildly exothermic at 298.15 K at another temperature. Is the reaction endothermic or exothermic at the second temperature? To answer this question, it is necessary to determine $\Delta H_R^\circ$ at the second temperature. We assume that no phase changes occur in the temperature interval of interest. The enthalpy for each reactant and product at temperature $T$ is related to the value at 298.15 K by Equation (4.18), which accounts for the energy supplied in order to heat the substance to the new temperature at constant pressure:

$$H_T^\circ = H_{298.15\,\text{K}}^\circ + \int_{298.15\,\text{K}}^{T} C_P(T')dT' \tag{4.18}$$

The prime in the integral indicates a "dummy variable" that is otherwise identical to the temperature. This notation is needed because $T$ appears in the upper limit of the integral. In Equation (4.18), $H^\circ_{298.15\,K}$ is the absolute enthalpy at 1 bar and 298.15 K. However, because there are no unique values for absolute enthalpies, it is useful to combine similar equations for all reactants and products with the appropriate stoichiometic coefficients to obtain the following equation for the reaction enthalpy at temperature $T$:

$$\Delta H^\circ_{R,T} = \Delta H^\circ_{R,298.15\,K} + \int_{298.15\,K}^{T} \Delta C_P(T')dT' \qquad (4.19)$$

where

$$\Delta C_P(T') = \sum_i \nu_i C_{P,i}(T') \qquad (4.20)$$

Recall that in our notation, $\Delta H^\circ_R$ or $\Delta H^\circ_f$ without an explicit temperature value implies that $T = 298.15$ K. In Equation (4.20), the sum is over all reactants and products, *including both elements and compounds*. A calculation of $\Delta H^\circ_R$ at an elevated temperature is shown in Example Problem 4.2.

---

**EXAMPLE PROBLEM 4.2**

Calculate $\Delta H^\circ_{R,\,1450\,K}$ for the reaction $1/2\,H_2(g) + 1/2\,Cl_2(g) \longrightarrow HCl(g)$ and 1 bar pressure given that $\Delta H^\circ_f(HCl,g) = -92.3$ kJ mol$^{-1}$ at 298.15 K and that

$$C_{P,m}(H_2,g) = \left(29.064 - 0.8363 \times 10^{-3}\frac{T}{K} + 20.111 \times 10^{-7}\frac{T^2}{K^2}\right) J\,K^{-1}mol^{-1}$$

$$C_{P,m}(Cl_2,g) = \left(31.695 + 10.143 \times 10^{-3}\frac{T}{K} - 40.373 \times 10^{-7}\frac{T^2}{K^2}\right) J\,K^{-1}mol^{-1}$$

$$C_{P,m}(HCl,g) = \left(28.165 + 1.809 \times 10^{-3}\frac{T}{K} + 15.464 \times 10^{-7}\frac{T^2}{K^2}\right) J\,K^{-1}mol^{-1}$$

over this temperature range. The ratios $T/K$ and $T^2/K^2$ appear in these equations in order to have the right units for the heat capacity.

**Solution**

$$\Delta H^\circ_{R,1450K} = \Delta H^\circ_{R,298.15K} + \int_{298.15}^{1450} \Delta C_P(T)\,dT$$

$$\Delta C_P(T) = \left[28.165 + 1.809 \times 10^{-3}\frac{T}{K} + 15.464 \times 10^{-7}\frac{T^2}{K^2}\right.$$

$$-\frac{1}{2}\left(29.064 - 0.8363 \times 10^{-3}\frac{T}{K} + 20.111 \times 10^{-7}\frac{T^2}{K^2}\right)$$

$$\left.-\frac{1}{2}\left(31.695 + 10.143 \times 10^{-3}\frac{T}{K} - 40.373 \times 10^{-7}\frac{T^2}{K^2}\right)\right] J\,K^{-1}mol^{-1}$$

$$= \left(-2.215 - 2.844 \times 10^{-3}\frac{T}{K} + 25.595 \times 10^{-7}\frac{T^2}{K^2}\right) J\,K^{-1}mol^{-1}$$

$$\Delta H^\circ_{R,1450K} = -92.3\,kJ\,mol^{-1}$$

$$+ \int_{298.15}^{1450} \left(-2.215 - 2.844 \times 10^{-3}\frac{T}{K} + 25.595 \times 10^{-7}\frac{T^2}{K^2}\right) \times d\frac{T}{K} J\,mol^{-1}$$

$$= -92.3\,kJ\,mol^{-1} - 2.836\,kJ\,mol^{-1} = -95.1\,kJ\,mol^{-1}$$

In this particular case, the change in the reaction enthalpy with $T$ is not large. This is the case because $\Delta C_P(T)$ is small and not because an individual $C_{P,i}(T)$ is small.

# 4.5 The Experimental Determination of $\Delta U$ and $\Delta H$ for Chemical Reactions

For chemical reactions, $\Delta U$ and $\Delta H$ are generally determined through experiment. In this section, we discuss how these experiments are carried out. If some or all of the reactants or products are volatile, it is necessary to contain the reaction mixture for which $\Delta U$ and $\Delta H$ are being measured. Such an experiment can be carried out in a **bomb calorimeter,** shown schematically in Figure 4.3. In a bomb calorimeter, the reaction is carried out at constant volume. The motivation for doing so is that if $dV = 0$, $\Delta U = q_V$. Therefore, a measurement of the heat flow normalized to 1 mole of the specified reaction provides a direct measurement of $\Delta U_R$. Bomb calorimetry is restricted to reaction mixtures containing gases because it is impractical to carry out chemical reactions at constant volume for systems consisting solely of liquids and solids, as shown in Example Problem 3.2. In the following, we describe how $\Delta U_R$ and $\Delta H_R$ are determined for an experiment in which a single liquid or solid reactant undergoes combustion in an excess of $O_2(g)$.

The bomb calorimeter is a good illustration of how one can define the system and surroundings to simplify the analysis of an experiment. The system is defined as the contents of a stainless steel thick-walled pressure vessel, the pressure vessel itself, and the inner water bath. Given this definition of the system, the surroundings consist of the container holding the inner water bath, the outer water bath, and the rest of the universe. The outer water bath encloses the inner bath and, through a heating coil, its temperature is always held at the temperature of the inner bath. Therefore, no heat flow will occur between the system and surroundings, and $q = 0$. Because the combustion experiment takes place at constant volume, $w = 0$. Therefore, $\Delta U = 0$. These conditions describe an isolated system of finite size that is not coupled to the rest of the universe. We are only interested in one part of this system, namely, the reaction mixture.

What are the individual components that make up $\Delta U$? Consider the system as consisting of three subsystems: the reactants in the calorimeter, the calorimeter vessel, and the inner water bath. These three subsystems are separated by rigid diathermal walls and are in thermal equilibrium. Energy is redistributed among the subsystems as reactants are converted to products, the temperature of the inner water bath changes, and the temperature of the calorimeter changes.

$$\Delta U = \frac{m_s}{M_s}\Delta U_{combustion} + \frac{m_{H_2O}}{M_{H_2O}} \times C_{P,m}(H_2O) \times \Delta T + C_{calorimeter} \times \Delta T = 0 \quad \textbf{(4.21)}$$

In Equation (4.21), $\Delta T$ is the change in the temperature of the three subsystems. The mass of water in the inner bath, $m_{H_2O}$; its molecular weight, $M_{H_2O}$; its heat capacity, $C_{P,m}(H_2O)$; the mass of the sample, $m_s$; and its molecular weight, $M_s$, are known. $\Delta U_{combustion}$ is defined per mole of the combustion reaction, but because the reaction includes exactly 1 mole of reactant, the factor $m_s/M_s$ in Equation (4.21) is appropriate. We wish to measure $\Delta U_{combustion}$. However, to determine $\Delta U_{combustion}$, the heat capacity of the calorimeter, $C_{calorimeter}$, must first be determined by carrying out a reaction for which $\Delta U_R$ is already known, as illustrated in Example Problem 4.3. To be more specific, we consider a combustion reaction between a compound and an excess of $O_2$.
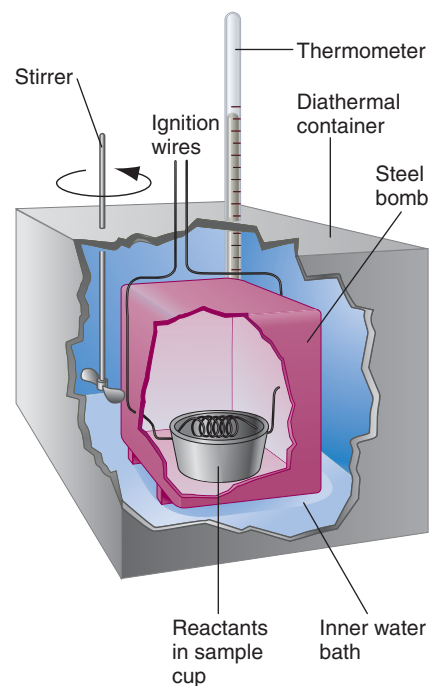


**FIGURE 4.3**
Schematic diagram of a bomb calorimeter. The liquid or solid reactant is placed in a cup suspended in the thick-walled steel bomb, which is filled with $O_2$ gas. The vessel is immersed in an inner water bath, and its temperature is monitored. The diathermal container is immersed in an outer water bath (not shown) whose temperature is maintained at the same value as the inner bath through a heating coil. By doing so, there is no heat exchange between the inner water bath and the rest of the universe.

## EXAMPLE PROBLEM 4.3

When 0.972 g of cyclohexane undergoes complete combustion in a bomb calorimeter, $\Delta T$ of the inner water bath is 2.98°C. For cyclohexane, $\Delta U_{combustion}$ is −3913 kJ mol$^{-1}$. Given this result, what is the value for $\Delta U_{combustion}$ for the combustion of benzene if $\Delta T$ is 2.36°C when 0.857 g of benzene undergoes complete combustion in the same calorimeter? The mass of the water in the inner bath is $1.812 \times 10^3$ g, and the $C_{P,m}$ of water is 75.3 J K$^{-1}$ mol$^{-1}$.

## Solution

To calculate the calorimeter constant through the combustion of cyclohexane, we write Equation (4.21) in the following form:

$$C_{calorimeter} = \dfrac{-\dfrac{m_s}{M_s}\Delta U_{combustion} - \dfrac{m_{H_2O}}{M_{H_2O}}C_{P,m}(H_2O)\Delta T}{\Delta T}$$

$$= \dfrac{\dfrac{0.972\,\text{g}}{84.16\,\text{g mol}^{-1}}\times 3913\times 10^3\,\text{J mol}^{-1} - \dfrac{1.812\times 10^3\,\text{g}}{18.02\,\text{g mol}^{-1}}\times 75.3\,\text{J mol}^{-1}\,\text{K}^{-1}\times 2.98°\text{C}}{2.98°\text{C}}$$

$$= 7.59 \times 10^3\,\text{J (°C)}^{-1}$$

In calculating $\Delta U_{combustion}$ for benzene, we use the value for $C_{calorimeter}$:

$$\Delta U_{combustion} = -\dfrac{M_s}{m_s}\left(\dfrac{m_{H_2O}}{M_{H_2O}}C_{P,m}(H_2O)\Delta T + C_{calorimeter}\Delta T\right)$$

$$= -\dfrac{78.12\,\text{g mol}^{-1}}{0.857\,\text{g}}\times\left(\begin{array}{l}\dfrac{1.812\times 10^3\,\text{g}}{18.02\,\text{g mol}^{-1}}\times 75.3\,\text{J mol}^{-1}\,\text{K}^{-1}\times 2.36°\text{C} \\ + 7.59\times 10^3\,\text{J(°C)}^{-1}\times 2.36°\text{C}\end{array}\right)$$

$$= -3.26 \times 10^6\,\text{J mol}^{-1}$$

Once $\Delta U_{combustion}$ has been determined, $\Delta H_{combustion}$ can be determined using the following equation:

$$\Delta H_{combustion} = \Delta U_{combustion} + \Delta(PV) \tag{4.22}$$

For reactions involving only solids and liquids, $\Delta U \gg \Delta(PV)$ and $\Delta H \approx \Delta U$. If some of the reactants or products are gases, the small change in the temperature that is measured in a calorimetric experiment can generally be ignored and $\Delta(PV) = \Delta(nRT) = \Delta nRT$

$$\Delta H_{combustion} = \Delta U_{combustion} + \Delta nRT \tag{4.23}$$

where $\Delta n$ is the change in the number of moles of gas in the overall reaction. For the first reaction of Example Problem 4.3,

$$C_6H_{12}(l) + 9\,O_2(g) \longrightarrow 6\,CO_2(g) + 6\,H_2O(l) \tag{4.24}$$
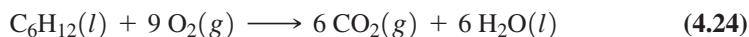
and $\Delta n = -3$. Note that at $T = 298.15$ K, the most stable form of cyclohexane and water is a liquid.

$$\Delta H_{combustion} = \Delta U_{combustion} - 3RT = -3913 \times 10^3\,\text{kJ mol}^{-1}$$

$$-3 \times 8.314\,\text{J K}^{-1}\text{mol}^{-1} \times 298.15\,\text{K}$$

$$= -3920 \times 10^3\,\text{J mol}^{-1} \tag{4.25}$$

For this reaction, $\Delta H_{combustion}$ and $\Delta U_{combustion}$ differ by only 0.2%. Note that because the contents of the bomb calorimeter are not at 1 bar pressure, $\Delta U_{combustion}$ rather than $\Delta U_{combustion}°$ is measured. The difference is small, but it can be calculated.

If the reaction under study does not involve gases or highly volatile liquids, there is no need to operate under constant volume conditions. It is preferable to carry out the reaction at constant $P$ using a **constant pressure calorimeter.** $\Delta H$ is directly determined because $\Delta H = q_P$. A vacuum-insulated vessel with a loosely fitting stopper as shown in Figure 4.4 is adequate for many purposes and can be treated as an isolated composite system. Equation (4.21) takes the following form for constant pressure calorimetry involving the solution of a salt in water:

$$\Delta H° = \dfrac{m_{salt}}{M_{salt}}\Delta H°_{solution} + \dfrac{m_{H_2O}}{M_{H_2O}}C_{P,m}(H_2O)\Delta T + C_{calorimeter}\Delta T = 0 \tag{4.26}$$
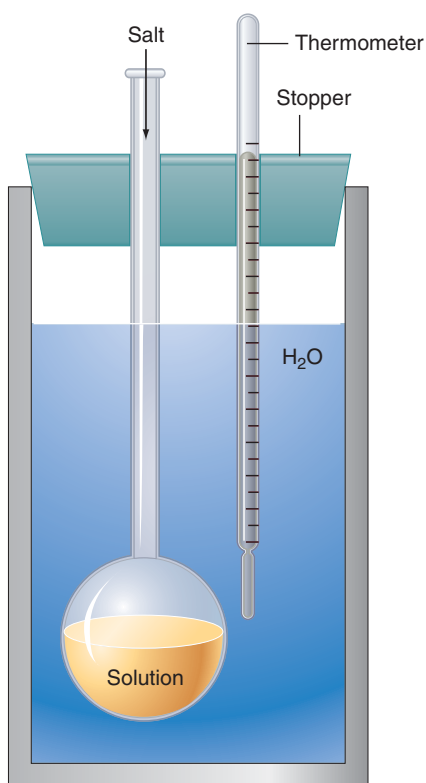


**FIGURE 4.4**

Schematic diagram of a constant pressure calorimeter suitable for measuring the enthalpy of solution of a salt in water.

Salt — Thermometer

Stopper

H₂O

Solution

$\Delta H^{\circ}_{solution}$ is defined per mole of the solution reaction, but because the reaction includes exactly 1 mole of reactant, the factor $m_{salt}/M_{salt}$ in Equation (4.21) is appropriate. Because $\Delta(PV)$ is negligibly small for the solution of a salt in a solvent, $\Delta U^{\circ}_{solution} = \Delta H^{\circ}_{solution}$. The solution must be stirred to ensure that equilibrium is attained before $\Delta T$ is measured.

---

### EXAMPLE PROBLEM 4.4

The enthalpy of solution for the reaction

$$Na_2SO_4(s) \xrightarrow{H_2O(l)} 2\,Na^+(aq) + SO_4^{2-}(aq)$$

is determined in a constant pressure calorimeter. The calorimeter constant was determined to be 342.5 J K$^{-1}$. When 1.423 g of Na$_2$SO$_4$ is dissolved in 100.34 g of H$_2$O($l$), $\Delta T = 0.031$ K. Calculate $\Delta H^{\circ}_{solution}$ for Na$_2$SO$_4$ from these data. Compare your result with that calculated using the standard enthalpies of formation in Table 4.1 (Appendix A, Data Tables) and in Chapter 10 in Table 10.1.

#### Solution

$$\Delta H^{\circ}_{solution} = -\frac{M_{salt}}{m_{salt}}\left(\frac{m_{H_2O}}{M_{H_2O}}C_{P,m}(H_2O)\Delta T + C_{calorimeter}\Delta T\right)$$

$$= -\frac{142.04\ \text{g mol}^{-1}}{1.423\ \text{g}} \times \left(\begin{array}{c}\dfrac{100.34\ \text{g}}{18.02\ \text{g mol}^{-1}} \times 75.3\ \text{J K}^{-1}\,\text{mol}^{-1} \times 0.031\ \text{K} \\ + \ 342.5\ \text{J K}^{-1} \times 0.031\ \text{K}\end{array}\right)$$

$$= -2.4 \times 10^3\ \text{J mol}^{-1}$$

We next calculate $\Delta H^{\circ}_{solution}$ using the data tables.

$$\begin{aligned}\Delta H^{\circ}_{solution} &= 2\Delta H^{\circ}_f(Na^+,aq) + \Delta H^{\circ}_f(SO_4^{2-},aq) - \Delta H^{\circ}_f(Na_2SO_4,s)\\ &= 2 \times (-240.1\ \text{kJ mol}^{-1}) - 909.3\ \text{kJ mol}^{-1} + 1387.1\ \text{kJ mol}^{-1}\\ &= -2.4\ \text{kJ mol}^{-1}\end{aligned}$$

The agreement between the calculated and experimental results is good.

---

SUPPLEMENTAL

# 4.6 Differential Scanning Calorimetry

**Differential scanning calorimetry (DSC)** is a form of constant pressure calorimetry that is well suited to routine laboratory tests in pharmaceutical and material sciences. It is also used to study chemical changes such as polymer cross-linking, melting, and unfolding of protein molecules in which heat is absorbed or released in the transition. The experimental apparatus for such an experiment is shown schematically in Figure 4.5. The word *differential* appears in the name of the technique because the uptake of heat is measured relative to that for a reference material, and *scanning* refers to the fact that the temperature of the sample is varied, usually linearly with time.

The temperature of the enclosure $T_E$ is increased linearly with time using a power supply. Heat flows from the enclosure through the disk to the sample because of the temperature gradient generated by the heater. Because the sample and reference are equidistant from the enclosure, the heat flow to each sample is the same. The reference material is chosen such that its melting point is not in the range of that of the samples.

We consider a simplified one-dimensional model of the heat flow in the DSC in Figure 4.6 following the treatment of Höhne, Hemminger, and Flammersheim in *Differential Scanning Calorimetry*, 2nd Edition, Berlin: Springer, 2003. The electrical current through the resistive heater increases the temperature of the calorimeter enclosure $T_E$ to a value greater than that of the sample and reference, $T_S$, and $T_R$. The
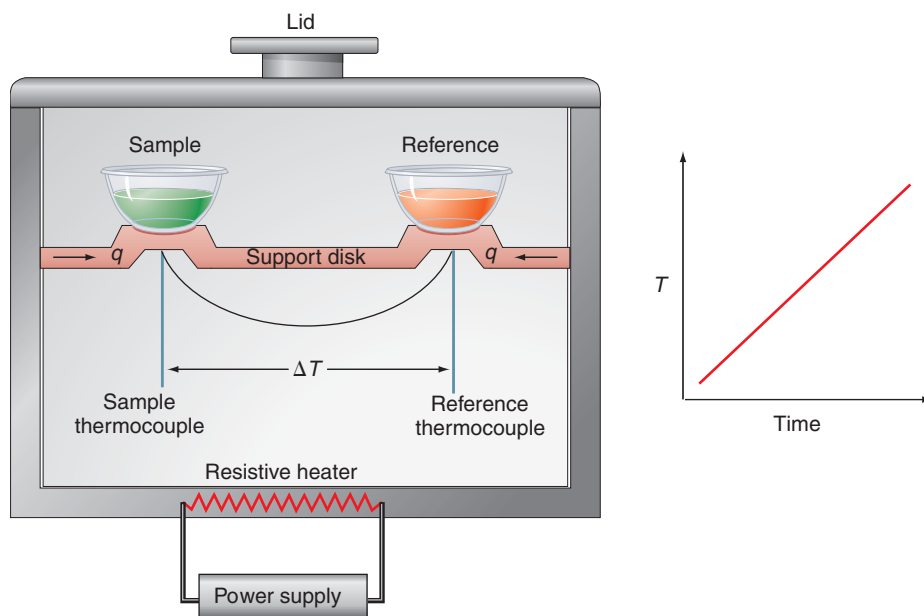
heat flow per unit time from the enclosure to the sample and reference are designated
by $\Phi_{ES}$ and $\Phi_{ER}$, respectively, which typically have the units of J g$^{-1}$ s$^{-1}$.

Assume that a process such as melting occurs in the sample and not in the refer-
ence. The heat flow per unit time associated with the process is given by $\Phi(t)$. It is
time dependent because, using melting as an example, heat flow associated with the
phase change begins at the onset of melting and ceases when the sample is completely
in the liquid state. This additional heat flow changes the sample temperature by $dT_S$ and
consequently both $T_E - T_S$ and the heat flow rate to the sample $\Phi_{ES}$ change. In the
experiment $\Delta T(t) = T_S(t) - T_R(t)$ is measured. The change in the heat flow to the
sample resulting from the process is

$$C_S \frac{dT_S(t)}{dt} = \Phi_{ES}(t) - \Phi(t) \tag{4.27}$$

where $C_S$ is the constant pressure heat capacity of the sample. Equation (4.27) relates
the sample temperature to the heat flow generated by the process of interest. If the
process is exothermic, $\Phi(t) < 0$ and if it is endothermic, $\Phi(t) > 0$. We rewrite
Equation (4.27) to explicitly contain the experimentally accessible function $\Delta T(t)$.

$$C_S \frac{dT_R(t)}{dt} + C_S \frac{d\Delta T(t)}{dt} = \Phi_{ES}(t) - \Phi(t) \tag{4.28}$$

The corresponding equation for the reference in which only heating occurs is

$$C_R \frac{dT_R(t)}{dt} = \Phi_{ER}(t) \tag{4.29}$$

The essence of DSC is that a difference between the heat flux to the sample and reference is measured. We therefore subtract Equation (4.29) from Equation (4.28) and obtain

$$\Phi_{ES}(t) - \Phi_{ER}(t) = (C_S - C_R)\frac{dT_R(t)}{dt} + C_S\frac{d\Delta T(t)}{dt} + \Phi(t) \tag{4.30}$$

The quantities $\Phi_{ES}$ and $\Phi_{ER}$ are directly proportional to the temperature differences $T_E - T_S$ and $T_E - T_R$ and are inversely proportional to the thermal resistance $R_{thermal}$ between the heated enclosure and the sample and reference. The latter are equal because of the symmetry of the calorimeter. The thermal resistance $R_{thermal}$ is an intrinsic property of the calorimeter and can be obtained through calibration of the instrument.

$$\Phi_{ES} = \frac{T_E - T_S}{R_{thermal}} \text{ and } \Phi_{ER} = \frac{T_E - T_R}{R_{thermal}} \tag{4.31}$$

Therefore,

$$\Phi(t) = -\frac{\Delta T(t)}{R_{thermal}} - (C_S - C_R)\frac{dT_R(t)}{dt} - C_S\frac{d\Delta T(t)}{dt} \tag{4.32}$$

Equation (4.32) links the heat flow per unit mass generated by the process of interest, $\Phi(t)$, to the measured quantity $\Delta T(t)$. Typically $T_R$ is increased linearly with time,

$$T_R(t) = T_0 + \alpha t$$

and Equation (4.32) simplifies to

$$\Phi(t) = -\frac{\Delta T(t)}{R_{thermal}} - \alpha(C_S - C_R) - C_S\frac{d\Delta T(t)}{dt} \tag{4.33}$$

We see that $\Delta T(t)$ is not simply related to $\Phi(t)$, which is to be determined in the experiment. The second term in Equation (4.33) arises because the heat capacities of the sample and reference are not equal. Additionally, the heat capacity of the sample changes as it undergoes a phase change.

The third term in Equation (4.33) is proportional to $d\Delta T(t)/dt$ and has the effect of broadening $\Delta T(t)$ relative to $\Phi(t)$ and shifting it to longer times. A schematic picture of a DSC scan in this model is shown in Figure 4.6.

Because $C_R\alpha = \Phi_{ER}(t)$ from Equation (4.29) and $\Delta T$ are proportional as shown in Equation (4.31), a graph of $C_R$ versus time has the same shape as shown in Figure 4.6. An analogous equation can be written for the sample, so that

$$\Phi_{ES} - \Phi_{ER} = \alpha(C_S - C_R)$$

Therefore, a graph of $(C_S - C_R)$ versus time also has the same shape as Figure 4.6.

The goal of the experiment is to determine the heat absorbed or evolved in the process per unit mass, which is given by

$$q_P = \Delta H = \int_{t_1}^{t_2} \Phi(t)dt$$

$$= -\frac{1}{R_{thermal}}\int_{t_1}^{t_2}\Delta T(t)dt - \frac{1}{R_{thermal}}\int_{t_1}^{t_2}\left(-\alpha\left(C_S - C_R\right)\right)dt \tag{4.34}$$

In Equation (4.34), the baseline contribution to the integral has been subtracted as it has no relevance for the process of interest.

Interpreting DSC curves in terms of heat capacities must be done with caution as illustrated for a melting transition in Figure 4.7. At the melting temperature, the enthalpy rises abruptly as discussed in Chapter 8 and as shown in Figure 4.7a. The heat capacity is the derivative of the enthalpy with respect to temperature and has the form shown in Figure 4.7b. As discussed in Section 2.5, the heat capacity of the liquid is higher than that of the solid. However, a measured DSC curve has the shape shown in Figure 4.7d rather than in Figure 4.7b.

There are two reasons for this discrepancy. Heat is taken up by the sample during the melting transition, but the sample temperature does not change. However, the
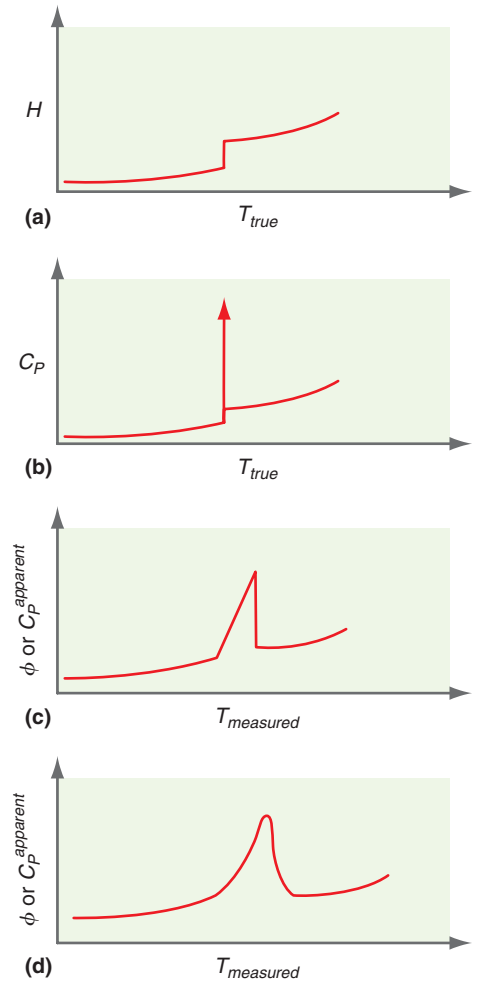


**FIGURE 4.7**
(a) $\Delta H$ is shown as a function of the true temperature for a melting process. (b) The heat capacity becomes infinite at the transition temperature because the temperature remains constant as heat flows into the sample. (c) The heat capacity curve in (b) is distorted because the measured temperature increases while the sample temperature remains constant during the melting transition. (d) Further distortions to the hypothetical scan (c) and a shift of the peak to higher temperature occur because of the thermal inertia of the calorimeter.
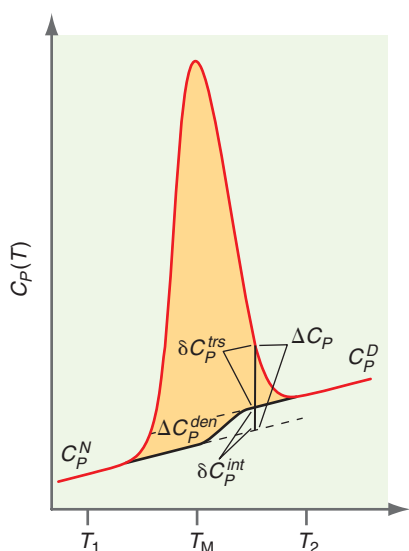
**FIGURE 4.8**

The apparent heat capacity of a protein undergoing a reversible, thermal denaturation within the temperature interval $T_1$–$T_2$ is shown. The temperature at the heat capacity maximum is to a good approximation the melting temperature $T_m$, defined as the temperature at which half the total protein has been denatured. The excess heat capacity $\Delta C_P = C_P(T) - C_P^N(T)$ is composed of two parts; the intrinsic excess heat capacity $\delta C_P^{int}$ and the transition excess heat capacity $\delta C_P^{trs}$. See the text.

sample crucible temperature continues to increase as heat flows to the sample. Therefore the apparent heat capacity would have the shape shown in Figure 4.7c if there were no resistances to heat flow in the calorimeter. The thermal resistances present in the calorimeter smear out the curve shown in Figure 4.7c and shift it to higher temperatures as shown in Figure 4.7d. Clearly, the temperature dependence of the apparent heat capacity obtained directly from a DSC scan is significantly different from the temperature dependence of the true heat capacity. Deconvolution procedures must be undertaken to obtain accurate heat capacities. Because the heat absorbed or evolved in the process per unit mass is proportional to the area under the DSC scan, it is less affected by the instrument distortions than the heat capacity.

DSC is the most direct method for determining the energetics of biological macromolecules undergoing conformational transitions, which is important in understanding their biological activity. In particular, DSC has been used to determine the temperature range over which proteins undergo the conformational changes associated with reversible **denaturation,** a process in which a protein unfolds. The considerations for a melting process discussed earlier apply as well as for denaturation, although melting enthalpies are generally much larger than denaturation enthalpies. From the preceding discussion, when a protein solution is heated at a constant rate and at constant pressure, DSC reports the apparent heat capacity of the protein solution. Protein structures are stabilized by the cooperation of numerous weak forces. Assume that a protein solution is heated from a temperature $T_1$ to a temperature $T_2$. If the protein denatures within this temperature interval reversibly and cooperatively, the $C_P(T)$ versus $T$ curve has the form shown in Figure 4.8.

The heat capacity of denaturation is defined as

$$\Delta C_P^{den} = C_P^D(T) - C_P^N(T) \tag{4.35}$$

which is the difference between the heat capacity of the denatured protein, $C_P^D(T)$, and the heat capacity of the native (i.e., structured) protein, $C_P^N(T)$. The value of $\Delta C_P^{den}$ can be determined as shown in Figure 4.8. The value of $\Delta C_P^{den}$ is a positive quantity and for many globular proteins varies from 0.3 to 0.7 J $K^{-1}$ $g^{-1}$. The higher heat capacity of the protein in the denatured state can be understood in the following way. In the structured state, internal motions of the protein are characterized by coupled bending and rotations of several bonds that occur at frequencies on the order of $k_B T/h$, where $k_B$ is Boltzmann's constant and $h$ is Planck's constant. When the protein denatures, these "soft" vibrations are shifted to lower frequencies, higher frequency bond vibrations are excited, and the heat capacity increases. In addition to increased contributions from vibrational motions, when a protein structure is disrupted, nonpolar amino acid residues formerly isolated from solvent within the interior of the protein are exposed to water. Water molecules now order about these nonpolar amino acids, further increasing the heat capacity.

The **excess heat capacity** is defined as

$$\Delta C_P = C_P(T) - C_P^N(T) \tag{4.36}$$

where $\Delta C_P$ is obtained at a given temperature from the difference between the point on the heat capacity curve $C_P(T)$ and the linearly extrapolated value for the heat capacity of the native state $C_P^N(T)$; see Figure 4.8. The excess heat capacity is in turn composed of two parts:

$$\Delta C_P(T) = \delta C_P^{int} + \delta C_P^{trs} \tag{4.37}$$

Within the interval $T_1$–$T_2$ the protein structure does not unfold suddenly. There occurs instead a gradual unfolding of the protein such that at any given temperature a fraction of the structured protein remains, and an ensemble of unfolded species is produced. The heat capacity and enthalpy change observed arise from this ensemble of physical forms of the partially unfolded protein, and as such these properties are averages over possible configurations of the protein. The component of the heat capacity that accounts for the sum of molecular species produced in the course of making a transition from the folded to the unfolded state is the **intrinsic excess heat capacity** or $\delta C_P^{int}$. The second component of the heat capacity is called the **transition excess heat capacity** $\delta C_P^{trs}$. The transition excess heat capacity results from fluctuations of the system as the protein changes from different states in the course of denaturation.

The intrinsic and transition excess heat capacities are determined by first extrapolating the functions $C_P^N(T)$ and $C_P^D(T)$ into the transition zone between $T_1$ and $T_2$. This is indicated in Figure 4.8 by the solid line connecting the heat capacity baselines above and below $T_m$. Once this baseline extrapolation is accomplished, $\delta C_P^{int}$ is the difference at a given temperature between the extrapolated baseline curve and $C_P^N(T)$. The value of $\delta C_P^{trs}$ is obtained from the difference between $C_P(T)$ and the extrapolated baseline curve. The excess enthalpy of thermal denaturation is finally given by $\Delta H_{den} = \int_{T_1}^{T_2} \delta C_P^{trs} dT$. In other words the excess enthalpy of thermal denaturation is the area under the peak in Figure 4.8 above the extrapolated baseline curve.

# Vocabulary

| | | |
|---|---|---|
| bomb calorimeter | endothermic | intrinsic excess heat capacity |
| bond energy | enthalpy of fusion | standard enthalpy of formation |
| bond enthalpy | enthalpy of reaction | standard enthalpy of reaction |
| constant pressure calorimeter | excess heat capacity | standard reference state |
| denaturation | exothermic | standard state |
| differential scanning calorimetry | Hess's law | transition excess heat capacity |

# Conceptual Problems

**Q4.1**  In calculating $\Delta H_R^\circ$ at 285.15 K, only the $\Delta H_f^\circ$ of the compounds that take part in the reactions listed in Tables 4.1 and 4.2 (Appendix A, Data Tables) are needed. Is this statement also true if you want to calculate $\Delta H_R^\circ$ at 500. K?

**Q4.2**  What is the point of having an outer water bath in a bomb calorimeter (see Figure 4.3), especially if its temperature is always equal to that of the inner water bath?

**Q4.3**  Is the following statement correct? If not rewrite it so that it is correct. The standard state of water is $H_2O(g)$.

**Q4.4**  Does the enthalpy of formation of $H_2O(l)$ change if the absolute enthalpies of $H_2(g)$ and $O_2(g)$ are set equal to 100. kJ mol$^{-1}$ rather than to zero? Answer the same question for $CO_2(g)$. Will $\Delta H_R^\circ$ for the reaction $H_2O(l) + CO_2(g) \longrightarrow H_2CO_3(l)$ change as a result of this change in the enthalpy of formation of the elements?

**Q4.5**  Why are elements included in the sum in Equation (4.20) when they are not included in calculating $\Delta H_R^\circ$ at 298 K?

**Q4.6**  Why are heat capacities of reactants and products required for calculations of $\Delta H_R^\circ$ at elevated temperatures?

**Q4.7**  Is the following statement correct? If not rewrite it so that it is correct. The superscript zero in $\Delta H_f^\circ$ means that the reactions conditions are 298.15 K.

**Q4.8**  Why is it valid to add the enthalpies of any sequence of reactions to obtain the enthalpy of the reaction that is the sum of the individual reactions?

**Q4.9**  In a calorimetric study, the temperature of the system rises to 325 K before returning to its initial temperature of 298 K. Why does this temperature rise not affect your measurement of $\Delta H_R^\circ$ at 298 K?

**Q4.10**  Is the following statement correct? If not rewrite it so that it is correct. Because the reaction $H_2(g) + O_2(g) \longrightarrow H_2O(l)$ is exothermic, the products are at a higher temperature than the reactants.

**Q4.11**  The reactants in the reaction $2NO(g) + O_2(g) \longrightarrow 2NO_2(g)$ are initially at 298 K. Why is the reaction enthalpy the same if (a) the reaction is constantly kept at 298 K or (b) if the reaction temperature is not controlled and the heat flow to the surroundings is measured only after the temperature of the products is returned to 298 K?

**Q4.12**  What is the advantage of a differential scanning calorimeter over a bomb calorimeter in determining the enthalpy of fusion of a series of samples?

**Q4.13**  You wish to measure the heat of solution of NaCl in water. Would the calorimetric technique of choice be at constant pressure or constant volume? Why?

**Q4.14**  Is the following statement correct? If not rewrite it so that it is correct. Because the enthalpy of formation of elements is zero, $\Delta H_f^\circ (O(g)) = 0$.

**Q4.15**  If the $\Delta H_f^\circ$ for the chemical compounds involved in a reaction is available at a given temperature, how can $\Delta H_R^\circ$ be calculated at another temperature?

**Q4.16**  Is the following statement correct? If not rewrite it so that it is correct. If $\Delta H_R^\circ$ for a chemical reaction does not change appreciably with temperature, the heat capacities for reactants and products must be small.

**Q4.17** Under what conditions are $\Delta H$ and $\Delta U$ for a reaction involving gases and/or liquids or solids identical?

**Q4.18** Dogs cool off in hot weather by panting. Write a chemical equation to describe this process and calculate $\Delta H_R^\circ$.

**Q4.19** Is $\Delta H$ for breaking the first C—H bond in methane equal to the average C—H bond enthalpy in this molecule? Explain your answer.

**Q4.20** Humans cool off through perspiration. How does the effectiveness of this process depend on the relative humidity?

# Numerical Problems

Problem numbers in **red** indicate that the solution to the problem is given in the *Student's Solutions Manual*.

**P4.1** Given the data in Table 4.1 (Appendix A, Data Tables) and the following information, calculate the single bond enthalpies and energies for Si–F, Si–Cl, C–F, N–F, O–F, H–F:

| Substance | $SiF_4(g)$ | $SiCl_4(g)$ | $CF_4(g)$ | $NF_3(g)$ | $OF_2(g)$ | $HF(g)$ |
|---|---|---|---|---|---|---|
| $\Delta H_f^\circ$ (kJ mol$^{-1}$) | −1614.9 | −657.0 | −925 | −125 | −22 | −271 |

**P4.2** At 1000. K, $\Delta H_R^\circ = -123.77$ kJ mol$^{-1}$ for the reaction $N_2(g) + 3 H_2(g) \longrightarrow 2 NH_3(g)$, with $C_{P,m} = 3.502R$, 3.466R, and 4.217R for $N_2(g)$, $H_2(g)$, and $NH_3(g)$, respectively. Calculate $\Delta H_f^\circ$ of $NH_3(g)$ at 450. K from this information. Assume that the heat capacities are independent of temperature.

**P4.3** A sample of K(s) of mass 2.740 g undergoes combustion in a constant volume calorimeter at 298.15 K. The calorimeter constant is 1849 J K$^{-1}$, and the measured temperature rise in the inner water bath containing 1450. g of water is 1.60 K. Calculate $\Delta U_f^\circ$ and $\Delta H_f^\circ$ for $K_2O$.

**P4.4** Calculate $\Delta H_f^\circ$ for NO(g) at 975 K, assuming that the heat capacities of reactants and products are constant over the temperature interval at their values at 298.15 K.

**P4.5** The total surface area of the earth covered by ocean is $3.35 \times 10^8$ km$^2$. Carbon is fixed in the oceans via photosynthesis performed by marine plants according to the reaction $6 CO_2(g) + 6 H_2O(l) \longrightarrow C_6H_{12}O_6(s) + 6 O_2(g)$. A lower range estimate of the mass of carbon fixed in the oceans is 44.5 metric tons/km$^2$. Calculate the annual enthalpy change resulting from photosynthetic carbon fixation in the ocean given earlier. Assume $P = 1$ bar and $T = 298$ K.

**P4.6** Derive a formula for $\Delta H_R^\circ(T)$ for the reaction CO(g) + $1/2 O_2(g) \longrightarrow CO_2(g)$ assuming that the heat capacities of reactants and products do not change with temperature.

**P4.7** Given the data in Table 4.3 and the data tables, calculate the bond enthalpy and energy of the following:

**a.** The C—H bond in $CH_4$

**b.** The C—C single bond in $C_2H_6$

**c.** The C═C double bond in $C_2H_4$

Use your result from part (a) to solve parts (b) and (c).

**P4.8** Use the following data at 298.15 K to complete this problem:

| | $\Delta H_R^\circ$ (kJ mol$^{-1}$) |
|---|---|
| $1/2 H_2(g) + 1/2 O_2(g) \longrightarrow OH(g)$ | 38.95 |
| $H_2(g) + 1/2 O_2(g) \longrightarrow H_2O(g)$ | −241.814 |
| $H_2(g) \longrightarrow 2 H(g)$ | 435.994 |
| $O_2(g) \longrightarrow 2 O(g)$ | 498.34 |

Calculate $\Delta H_R^\circ$ for

**a.** $OH(g) \longrightarrow H(g) + O(g)$

**b.** $H_2O(g) \longrightarrow 2 H(g) + O(g)$

**c.** $H_2O(g) \longrightarrow H(g) + OH(g)$

Assuming ideal gas behavior, calculate $\Delta H_R^\circ$ and $\Delta U_R^\circ$ for all three reactions.

**P4.9** Calculate the standard enthalpy of formation of $FeS_2(s)$ at 600.°C from the following data at 298.15 K. Assume that the heat capacities are independent of temperature.

| Substance | Fe(s) | $FeS_2(s)$ | $Fe_2O_3(s)$ | S(*rhombic*) | $SO_2(g)$ |
|---|---|---|---|---|---|
| $\Delta H_f^\circ$ (kJ mol$^{-1}$) | | −824.2 | | | −296.81 |
| $C_{P,m}/R$ | 3.02 | 7.48 | | 2.72 | |

You are also given that for the reaction $2 FeS_2(s) + 11/2 O_2(g) \longrightarrow Fe_2O_3(s) + 4 SO_2(g)$, $\Delta H_R^\circ = -1655$ kJ mol$^{-1}$.

**P4.10** The following data are a DSC scan of a solution of a T4 lysozyme mutant. From the data determine $T_m$. Determine also the excess heat capacity $\Delta C_P$ at $T = 308$ K. Determine also the intrinsic $\delta C_P^{int}$ and transition $\delta C_P^{trs}$ excess heat capacities at $T = 308$ K. In your calculations use the extrapolated curves, shown as dashed lines in the DSC scan.
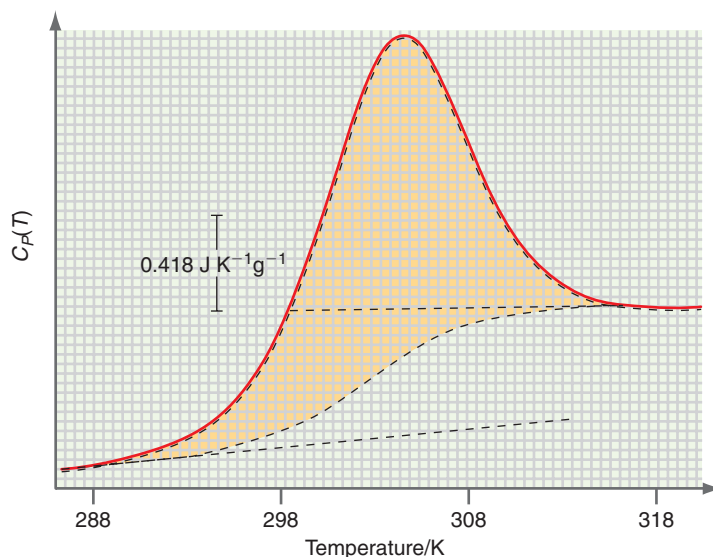


**P4.11** At 298 K, $\Delta H_R^\circ = 131.28$ kJ mol$^{-1}$ for the reaction C(*graphite*) + $H_2O(g) \longrightarrow CO(g) + H_2(g)$, with $C_{P,m} = 8.53$, 33.58, 29.12, and 28.82 J K$^{-1}$ mol$^{-1}$ for graphite, $H_2O(g)$, CO(g), and $H_2(g)$, respectively. Calculate $\Delta H_R^\circ$ at 240°C from this information. Assume that the heat capacities are independent of temperature.

**P4.12** Consider the reaction $TiO_2(s) + 2\,C(graphite) + 2\,Cl_2(g) \longrightarrow 2\,CO(g) + TiCl_4(l)$ for which $\Delta H^\circ_{R,298K} = -80.\ kJ\,mol^{-1}$. Given the following data at 25°C, (a) calculate $\Delta H^\circ_R$ at 135.8°C, the boiling point of $TiCl_4$, and (b) calculate $\Delta H^\circ_f$ for $TiCl_4(l)$ at 25°C:

| Substance | $TiO_2(s)$ | $Cl_2(g)$ | $C(graphite)$ | $CO(g)$ | $TiCl_4(l)$ |
|---|---|---|---|---|---|
| $\Delta H^\circ_f$ (kJ mol$^{-1}$) | –945 | | | –110.5 | |
| $C_{P,m}$ (J K$^{-1}$ mol$^{-1}$) | 55.06 | 33.91 | 8.53 | 29.12 | 145.2 |

Assume that the heat capacities are independent of temperature.

**P4.13** Calculate $\Delta H^\circ_R$ and $\Delta U^\circ_R$ for the oxidation of benzene. Also calculate

$$\frac{\Delta H^\circ_R - \Delta U^\circ_R}{\Delta H^\circ_R}$$

**P4.14** Several reactions and their standard reaction enthalpies at 298.15 K are given here:

| | $\Delta H^\circ_R$ (kJ mol$^{-1}$) |
|---|---|
| $CaC_2(s) + 2\,H_2O(l) \longrightarrow Ca(OH)_2(s) + C_2H_2(g)$ | −127.9 |
| $Ca(s) + 1/2\,O_2(g) \longrightarrow CaO(s)$ | −635.1 |
| $CaO(s) + H_2O(l) \longrightarrow Ca(OH)_2(s)$ | –65.2 |

The standard enthalpies of combustion of graphite and $C_2H_2(g)$ are –393.51 and –1299.58 kJ mol$^{-1}$, respectively. Calculate the standard enthalpy of formation of $CaC_2(s)$ at 25°C.

**P4.15** Benzoic acid, 1.35 g, is reacted with oxygen in a constant volume calorimeter to form $H_2O(l)$ and $CO_2(g)$ at 298 K. The mass of the water in the inner bath is $1.55 \times 10^3$ g. The temperature of the calorimeter and its contents rises 2.76 K as a result of this reaction. Calculate the calorimeter constant.

**P4.16** The total surface area of Asia consisting of forest, cultivated land, grass land, and desert is $4.46 \times 10^7$ km$^2$. Every year, the mass of carbon fixed by photosynthesis by vegetation covering this land surface according to the reaction $6\,CO_2(g) + 6\,H_2O(l) \longrightarrow C_6H_{12}O_6(s) + 6\,O_2(g)$ is about $455.\times 10^3$ kg km$^{-2}$. Calculate the annual enthalpy change resulting from photosynthetic carbon fixation over the land surface given earlier. Assume $P = 1$ bar and $T = 298$ K.

**P4.17** Calculate $\Delta H^\circ_R$ and $\Delta U^\circ_R$ at 298.15 K for the following reactions:

a. $4\,NH_3(g) + 6\,NO(g) \longrightarrow 5\,N_2(g) + 6\,H_2O(g)$

b. $2\,NO(g) + O_2(g) \longrightarrow 2\,NO_2(g)$

c. $TiCl_4(l) + 2\,H_2O(l) \longrightarrow TiO_2(s) + 4\,HCl(g)$

d. $2\,NaOH(aq) + H_2SO_4(aq) \longrightarrow Na_2SO_4(aq) + 2\,H_2O(l)$
   Assume complete dissociation of NaOH, $H_2SO_4$, and $Na_2SO_4$

e. $CH_4(g) + H_2O(g) \longrightarrow CO(g) + 3\,H_2(g)$

f. $CH_3OH(g) + CO(g) \longrightarrow CH_3COOH(l)$

**P4.18** A sample of $Na_2SO_4(s)$ is dissolved in 225 g of water at 298 K such that the solution is 0.325 molar in $Na_2SO_4$. A temperature rise of 0.146°C is observed. The calorimeter

constant is 330. J K$^{-1}$. Calculate the enthalpy of solution of $Na_2SO_4$ in water at this concentration. Compare your result with that calculated using the data in Table 4.1 (Appendix A, Data Tables).

**P4.19** Nitrogen is a vital component of proteins and nucleic acids, and thus is necessary for life. The atmosphere is composed of roughly 80% $N_2$, but most organisms cannot directly utilize $N_2$ for biosynthesis. Bacteria capable of "fixing" nitrogen (i.e., converting $N_2$ to a chemical form, such as $NH_3$, which can be utilized in the biosynthesis of proteins and nucleic acids) are called diazotrophs. The ability of some plants like legumes to fix nitrogen is due to a symbiotic relationship between the plant and nitrogen-fixing bacteria that live in the plant's roots. Assume that the hypothetical reaction for fixing nitrogen biologically is

$$N_2(g) + 3\,H_2O(l) \longrightarrow 2\,NH_3(aq) + \tfrac{3}{2}O_2(g)$$
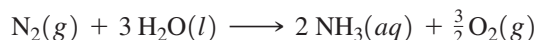
a. Calculate the standard enthalpy change for the biosynthetic fixation of nitrogen at $T = 298$ K. For $NH_3(aq)$, ammonia dissolved in aqueous solution, $\Delta H^\circ_f = -80.3$ kJ mol$^{-1}$.

b. In some bacteria, glycine is produced from ammonia by the reaction

$$NH_3(g) + 2\,CH_4(g) + \tfrac{5}{2}O_2(g)$$
$$\longrightarrow NH_2CH_2COOH(s) + H_2O(l)$$
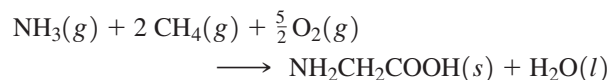
Calculate the standard enthalpy change for the synthesis of glycine from ammonia. For glycine, $\Delta H^\circ_f = -537.2$ kJ mol$^{-1}$. Assume $T = 298$ K.

c. Calculate the standard enthalpy change for the synthesis of glycine from nitrogen, oxygen, and methane.

**P4.20** If 3.365 g of ethanol $C_2H_5OH(l)$ is burned completely in a bomb calorimeter at 298.15 K, the heat produced is 99.472 kJ.

a. Calculate $\Delta H^\circ_{combustion}$ for ethanol at 298.15 K.

b. Calculate $\Delta H^\circ_f$ of ethanol at 298.15 K.

**P4.21** From the following data, calculate $\Delta H^\circ_{R,391.4\ K}$ for the reaction $CH_3COOH(g) + 2\,O_2(g) \longrightarrow 2\,H_2O(g) + 2\,CO_2(g)$:

| | $\Delta H^\circ_R$ (kJ mol$^{-1}$) |
|---|---|
| $CH_3COOH(l) + 2\,O_2(g) \longrightarrow 2\,H_2O(l) + 2\,CO_2(g)$ | –871.5 |
| $H_2O(l) \longrightarrow H_2O(g)$ | 40.656 |
| $CH_3COOH(l) \longrightarrow CH_3COOH(g)$ | 24.4 |

Values for $\Delta H^\circ_R$ for the first two reactions are at 298.15 K, and for the third reaction at 391.4 K.

| Substance | $CH_3COOH(l)$ | $O_2(g)$ | $CO_2(g)$ | $H_2O(l)$ | $H_2O(g)$ |
|---|---|---|---|---|---|
| $C_{P,m}/R$ | 14.9 | 3.53 | 4.46 | 9.055 | 4.038 |

**P4.22** A 0.1429 g sample of sucrose $C_{12}H_{22}O_{11}$ is burned in a bomb calorimeter. In order to produce the same temperature rise in the calorimeter as the reaction, 2353 J must be expended.

a. Calculate $\Delta U$ and $\Delta H$ for the combustion of 1 mole of sucrose.

**b.** Using the data tables and your answer to (a), calculate $\Delta H_f^{\circ}$ for sucrose.

**c.** The rise in temperature of the calorimeter and its contents as a result of the reaction is 1.743 K. Calculate the heat capacity of the calorimeter and its contents.

**P4.23**    Calculate $\Delta H_R^{\circ}$ at 675 K for the reaction $4\,NH_3(g) + 6\,NO(g) \longrightarrow 5\,N_2(g) + 6\,H_2O(g)$ using the temperature dependence of the heat capacities from the data tables. Compare your result with $\Delta H_R^{\circ}$ at 298.15. Is the difference large or small? Why?

**P4.24**    From the following data at 298.15 K as well as data in Table 4.1 (Appendix A, Data Tables), calculate the standard enthalpy of formation of $H_2S(g)$ and of $FeS_2(s)$:

|  | $\Delta H_R^{\circ}$ (kJ mol$^{-1}$) |
|---|---|
| $Fe(s) + 2\,H_2S(g) \longrightarrow FeS_2(s) + 2\,H_2(g)$ | $-137.0$ |
| $H_2S(g) + 3/2\,O_2(g) \longrightarrow H_2O(l) + SO_2(g)$ | $-562.0$ |

**P4.25**    Using the protein DSC data in Problem P4.10, calculate the enthalpy change between $T = 288$ K and $T = 318$ K. Give your answer in units of kJ per mole. Assume the molecular weight of the protein is 14,000. grams. [*Hint: You can perform the integration of the heat capacity by estimating the area under the DSC curve and above the dotted baseline in Problem P4.10. This can be done by dividing the area up into small rectangles and summing the areas of the rectangles. Comment on the accuracy of this method.*]

**P4.26**    Given the following heat capacity data at 298 K, calculate $\Delta H_f^{\circ}$ of $CO_2(g)$ at 525 K. Assume that the heat capacities are independent of temperature.

| Substance | C(*graphite*) | O$_2$(g) | CO$_2$(g) |
|---|---|---|---|
| $C_{P,m}$/J mol$^{-1}$K$^{-1}$ | 8.52 | 28.8 | 37.1 |

**P4.27**    Calculate $\Delta H$ for the process in which $Cl_2(g)$ initially at 298.15 K at 1 bar is heated to 690. K at 1 bar. Use the temperature-dependent heat capacities in the data tables. How large is the relative error if the molar heat capacity is assumed to be constant at its value of 298.15 K over the temperature interval?

**P4.28**    From the following data at 298.15 K C, calculate the standard enthalpy of formation of $FeO(s)$ and of $Fe_2O_3(s)$:

|  | $\Delta H_R^{\circ}$ (kJ mol$^{-1}$) |
|---|---|
| $Fe_2O_3(s) + 3\,C(graphite) \longrightarrow 2\,Fe(s) + 3\,CO(g)$ | 492.6 |
| $FeO(s) + C(graphite) \longrightarrow Fe(s) + CO(g)$ | 155.8 |
| $C(graphite) + O_2(g) \longrightarrow CO_2(g)$ | $-393.51$ |
| $CO(g) + 1/2\,O_2(g) \longrightarrow CO_2(g)$ | $-282.98$ |

**P4.29**    Calculate the average C—H bond enthalpy in methane using the data tables. Calculate the percent error in equating the average C—H bond energy in Table 4.3 with the bond enthalpy.

**P4.30**    Use the average bond energies in Table 4.3 to estimate $\Delta U$ for the reaction $C_2H_4(g) + H_2(g) \longrightarrow C_2H_6(g)$. Also calculate $\Delta U_R^{\circ}$ from the tabulated values of $\Delta H_f^{\circ}$ for reactant and products (Appendix A, Data Tables). Calculate the percent error in estimating $\Delta U_R^{\circ}$ from the average bond energies for this reaction.

**P4.31**    Use the tabulated values of the enthalpy of combustion of benzene and the enthalpies of formation of $CO_2(g)$ and $H_2O(l)$ to determine $\Delta H_f^{\circ}$ for benzene.

**P4.32**    Compare the heat evolved at constant pressure per mole of oxygen in the combustion of sucrose ($C_{12}H_{22}O_{11}$) and palmitic acid ($C_{16}H_{32}O_2$) with the combustion of a typical protein, for which the empirical formula is $C_{4.3}H_{6.6}NO$. Assume for the protein that the combustion yields $N_2(g)$, $CO_2(g)$, and $H_2O(l)$. Assume that the enthalpies for combustion of sucrose, palmitic acid, and a typical protein are 5647 kJ mol$^{-1}$, 10,035 kJ mol$^{-1}$, and 22.0 kJ g$^{-1}$, respectively. Based on these calculations, determine the average heat evolved per mole of oxygen consumed, assuming combustion of equal moles of sucrose, palmitic acid, and protein.

**P4.33**    A camper stranded in snowy weather loses heat by wind convection. The camper is packing emergency rations consisting of 58% sucrose, 31% fat, and 11% protein by weight. Using the data provided in Problem P4.32 and assuming the fat content of the rations can be treated with palmitic acid data and the protein content similarly by the protein data in Problem P4.32, how much emergency rations must the camper consume in order to compensate for a reduction in body temperature of 3.5 K? Assume the heat capacity of the body equals that of water. Assume the camper weighs 67 kg. State any additional assumptions.

**P4.34**    In order to get in shape for mountain climbing, an avid hiker with a mass of 60. kg ascends the stairs in the world's tallest structure, the 828 m tall Burj Khalifa in Dubai, United Arab Emirates. Assume that she eats energy bars on the way up and that her body is 25% efficient in converting the energy content of the bars into the work of climbing. How many energy bars does she have to eat if a single bar produces $1.08 \times 10^3$ kJ of energy upon metabolizing?

**P4.35**    We return to the 60. kg hiker of P4.34, who is climbing the 828 m tall Burj Khalifa in Dubai. If the efficiency of converting the energy content of the bars into the work of climbing is 25%, the remaining 75% of the energy released through metabolism is heat released to her body. She eats two energy bars and a single bar produces $1.08 \times 10^3$ kJ of energy upon metabolizing. Assume that the heat capacity of her body is equal to that for water. Calculate the increase in her temperature at the top of the structure. Is your result reasonable? Can you think of a mechanism by which her body might release energy to avoid a temperature increase?

# Entropy and the Second and Third Laws of Thermodynamics

Real-world processes have a natural direction of change. Heat flows from hotter bodies to colder bodies, and gases mix rather than separate. Entropy, designated by $S$, is the state function that predicts the direction of natural, or spontaneous, change and entropy increases for a spontaneous change in an isolated system. For a spontaneous change in a system interacting with its environment, the sum of the entropy of the system and that of the surroundings increases. In this chapter, we introduce entropy, derive the conditions for spontaneity, and show how $S$ varies with the macroscopic variables $P$, $V$, and $T$.

## 5.1 The Universe Has a Natural Direction of Change

To this point, we have discussed $q$ and $w$, as well as $U$ and $H$. The first law of thermodynamics states that in any process, the total energy of the universe remains constant. However, it does not predict which of several possible energy conserving processes will occur. Consider the following two examples. A metal rod initially at a uniform temperature could, in principle, undergo a spontaneous transformation in which one end becomes hot and the other end becomes cold without being in conflict with the first law, as long as the total energy of the rod remains constant. However, experience demonstrates that this does not occur. Similarly, an ideal gas that is uniformly distributed in a rigid adiabatic container could undergo a spontaneous transformation such that all of the gas moves to one-half of the container, leaving a vacuum in the other half. For an ideal gas, $(\partial U/\partial V)_T = 0$, therefore the energy of the initial and final states is the same. Neither of these transformations violates the first law of thermodynamics—and yet neither occurs.

Experience tells us that there is a natural direction of change in these two processes. A metal rod with a temperature gradient reaches a uniform temperature at some time after it has been isolated from a heat source. A gas confined to one-half of a container with a vacuum in the other half distributes itself uniformly throughout the container if a valve separating the two parts is opened. The transformations described in the previous paragraph are **unnatural transformations.** The word *unnatural* is

used to indicate that such an energy-conserving process can occur but is extremely unlikely. By contrast, the reverse processes, in which the temperature gradient along the rod disappears and the gas becomes distributed uniformly throughout the container, are **natural transformations,** also called **spontaneous processes,** which are extremely likely. Spontaneous does not mean that the process occurs immediately, but rather that it will occur with high probability if any barrier to the change is overcome. For example, the transformation of a piece of wood to $CO_2$ and $H_2O$ in the presence of oxygen is spontaneous, but it only occurs at elevated temperatures because an activation energy barrier must be overcome for the reaction to proceed.

Our experience is sufficient to predict the direction of spontaneous change for the two examples cited, but can the direction of spontaneous change be predicted in less obvious cases? In this chapter, we show that there is a thermodynamic function called entropy that allows us to predict the direction of spontaneous change for a system in a given initial state. For example, assume that a reaction vessel contains a given number of moles of $N_2$, $H_2$, and $NH_3$ at 600 K and at a total pressure of 280 bar. An iron catalyst is introduced that allows the mixture of gases to equilibrate according to $1/2 \, N_2 + 3/2 \, H_2 \rightleftharpoons NH_3$. What is the direction of spontaneous change, and what are the partial pressures of the three gases at equilibrium? The answer to this question is obtained by calculating the entropy change in the system and the surroundings.

Most students are initially uncomfortable when working with entropy because entropy is further removed from direct experience than energy, work, or heat. Historically, entropy was introduced by Clausius in 1850, several decades before entropy was understood at a microscopic level by Boltzmann. Boltzmann's explanation of entropy will be presented in Chapter 15, and we briefly state his conclusions here. At the microscopic level, matter consists of atoms or molecules that have energetic degrees of freedom (i.e., translational, rotational, vibrational, and electronic), each of which is associated with discrete energy levels that can be calculated using quantum mechanics. Quantum mechanics also characterizes a molecule by a state associated with a set of quantum numbers and a molecular energy. Entropy is a measure of the number of quantum states accessible to a macroscopic system at a given energy. Quantitatively, $S = k \ln W$, where $W$ is the number of states accessible to the system, and $k = R/N_A$. As demonstrated later in this chapter, the entropy of an isolated system is maximized at equilibrium. Therefore, the approach to equilibrium can be envisioned as a process in which the system achieves the distribution of energy among molecules that corresponds to a maximum value of $W$ and, correspondingly, to a maximum in $S$.

# 5.2 Heat Engines and the Second Law of Thermodynamics

The development of entropy presented here follows the historical route by which this state function was first introduced. The concept of entropy arose as 19th-century scientists attempted to maximize the work output of engines. An automobile engine operates in a cyclical process of fuel intake, compression, ignition and expansion, and exhaust, which occurs several thousand times per minute and is used to perform work on the surroundings. Because the work produced by such an engine is a result of the heat released in a combustion process, it is referred to as a **heat engine.** An idealized version of a heat engine is depicted in Figure 5.1. The system consists of a working substance (in this case an ideal gas) confined in a piston and cylinder assembly with diathermal walls. This assembly can be brought into contact with a hot reservoir at $T_{hot}$ or a cold reservoir at $T_{cold}$. The expansion or contraction of the gas caused by changes in its temperature drives the piston in or out of the cylinder. This linear motion is converted to circular motion as shown in Figure 5.1, and the rotary motion is used to do work in the surroundings.

The efficiency of a heat engine is of particular interest in practical applications. Experience shows that work can be converted to heat with 100% efficiency. Consider an example from calorimetry discussed in Chapter 4, in which electrical work is done on a resistive heater immersed in a water bath. We observe that all of the electrical work done on the heater has been converted to heat, resulting in an increase in the temperature
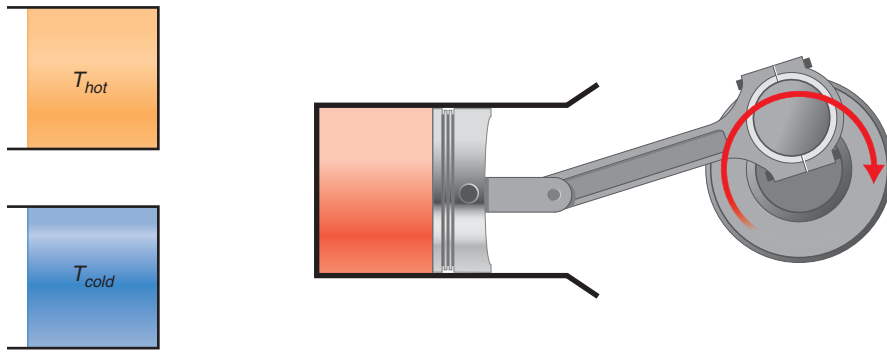
of the water and the heater. What is the maximum theoretical efficiency of the reverse process, the conversion of heat to work? As shown later, it is less than 100%. *There is a natural asymmetry in the efficiency of converting work to heat and converting heat to work. Thermodynamics provides an explanation for this asymmetry.*

As discussed in Section 2.7, the maximum work output in an isothermal expansion occurs in a reversible process. For this reason, we next calculate the efficiency of a reversible heat engine, because the efficiency of a reversible engine is an upper bound to the efficiency of a real engine. This reversible engine converts heat into work by exploiting the spontaneous tendency of heat to flow from a hot reservoir to a cold reservoir. It does work on the surroundings by operating in a cycle of reversible expansions and compressions of an ideal gas in a piston and cylinder assembly. We discuss automotive engines in Section 5.11.

The cycle for a reversible heat engine is shown in Figure 5.2 in a *P–V* diagram. The expansion and compression steps are designed so that the engine returns to its initial state after four steps. Recall from Section 2.7 that the area within the cycle equals the work done by the engine. As discussed later, four separate isothermal and adiabatic steps are needed to make the enclosed area in the cycle greater than zero. Beginning at point *a*, the first segment is a reversible isothermal expansion in which the gas absorbs heat from the reservoir at $T_{hot}$, and does work on the surroundings. In the second segment, the gas expands further, this time adiabatically. Work is also done on the surroundings in this step. At the end of the second segment, the gas has cooled to the temperature $T_{cold}$. The third segment is an isothermal compression in which the surroundings do work on the system and heat is absorbed by the cold reservoir. In the final segment, the gas is compressed to its initial volume, this time adiabatically. Work is done on the system in this segment, and the temperature returns to its initial value, $T_{hot}$. In summary, heat is taken up by the engine in the first segment at $T_{hot}$, and released to the surroundings in the third segment at $T_{cold}$. Work is done on the
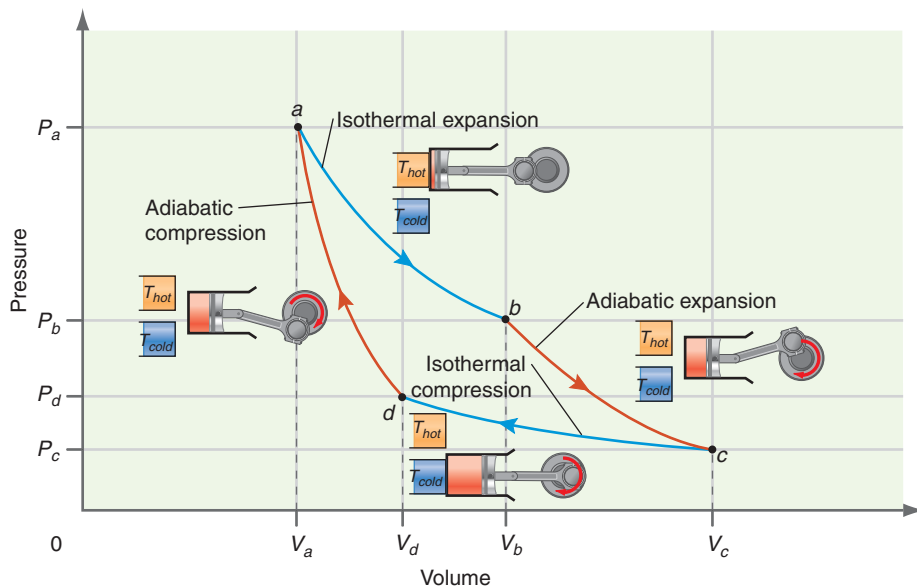
surroundings in the first two segments and on the system in the last two segments. An engine is only useful if net work is done on the surroundings, that is, if the magnitude of the work done in the first two steps is greater than the magnitude of the work done in the last two steps. The efficiency of the engine can be calculated by comparing the net work per cycle with the heat taken up by the engine from the hot reservoir.

Before carrying out this calculation, we discuss the rationale for the design of this reversible cycle in more detail. To avoid losing heat to the surroundings at temperatures between $T_{hot}$ and $T_{cold}$, adiabatic segments 2 ($b \rightarrow c$) and 4 ($d \rightarrow a$) are used to move the gas between these temperatures. To absorb heat only at $T_{hot}$ and release heat only at $T_{cold}$, segments 1 ($a \rightarrow b$) and 3 ($c \rightarrow d$) must be isothermal. The reason for using alternating isothermal and adiabatic segments is that no two isotherms at different temperatures intersect, and no two adiabats starting from two different temperatures intersect. Therefore, it is impossible to create a closed cycle of nonzero area in an indicator diagram out of isothermal or adiabatic segments alone. However, net work can be done using alternating adiabatic and isothermal segments. The reversible cycle depicted in Figure 5.2 is called a **Carnot cycle,** after the French engineer who first studied such cycles.

The efficiency of the Carnot cycle can be determined by calculating $q$, $w$, and $\Delta U$ for each segment of the cycle, assuming that the working substance is an ideal gas. The results are shown first in a qualitative fashion in Table 5.1. The appropriate signs for $q$ and $w$ are indicated. If $\Delta V > 0$, $w < 0$ for the segment, and the corresponding entry for work has a negative sign. For the isothermal segments, $q$ and $w$ have opposite signs because $\Delta U = q + w = 0$. From Table 5.1, it is seen that

$$w_{cycle} = w_{cd} + w_{da} + w_{ab} + w_{bc} \quad \text{and} \quad q_{cycle} = q_{ab} + q_{cd} \quad \text{(5.1)}$$

Because $\Delta U_{cycle} = 0$,

$$w_{cycle} = -(q_{cd} + q_{ab}) \quad \text{(5.2)}$$

By comparing the areas under the two expansion segments with those under the two compression segments in the indicator diagram in Figure 5.2, we can see that the total work as seen from the system is negative, meaning that work is done on the surroundings in each cycle. Using this result, we arrive at an important conclusion that relates the heat flow in the two isothermal segments

$$w_{cycle} < 0, \text{ therefore } |q_{ab}| > |q_{cd}| \quad \text{(5.3)}$$

More heat is withdrawn from the hot reservoir than is deposited in the cold reservoir as is also seen by rearranging Equation (5.2) to the form $q_{ab} + w_{cycle} = -q_{cd}$. It is useful to make a model of this heat engine that indicates the relative magnitude and direction of the heat and work flow, as shown in Figure 5.3a. The figure makes it clear that not all of the heat withdrawn from the higher temperature reservoir is converted to work done by the system (the engine) on the surroundings.

The efficiency, $\varepsilon$, of the reversible Carnot engine is defined as the ratio of the work output to the heat withdrawn from the hot reservoir. Referring to Table 5.1,

$$\varepsilon = -\frac{w_{cycle}}{q_{ab}} = \frac{q_{ab} + q_{cd}}{q_{ab}}$$

$$= 1 - \frac{|q_{cd}|}{|q_{ab}|} < 1 \text{ because } |q_{ab}| > |q_{cd}|, q_{ab} > 0, \text{ and } q_{cd} < 0 \quad \text{(5.4)}$$

**TABLE 5.1** Heat, Work, and $\Delta U$ for the Reversible Carnot Cycle

| Segment | Initial State | Final State | $q$ | $w$ | $\Delta U$ |
|---|---|---|---|---|---|
| $a \rightarrow b$ | $P_a, V_a, T_{hot}$ | $P_b, V_b, T_{hot}$ | $q_{ab}$ (+) | $w_{ab}$ (−) | $\Delta U_{ab} = 0$ |
| $b \rightarrow c$ | $P_b, V_b, T_{hot}$ | $P_c, V_c, T_{cold}$ | 0 | $w_{bc}$ (−) | $\Delta U_{bc} = w_{bc}$ (−) |
| $c \rightarrow d$ | $P_c, V_c, T_{cold}$ | $P_d, V_d, T_{cold}$ | $q_{cd}$ (−) | $w_{cd}$ (+) | $\Delta U_{cd} = 0$ |
| $d \rightarrow a$ | $P_d, V_d, T_{cold}$ | $P_a, V_a, T_{hot}$ | 0 | $w_{da}$ (+) | $\Delta U_{da} = w_{da}$ (+) |
| Cycle | $P_a, V_a, T_{hot}$ | $P_a, V_a, T_{hot}$ | $q_{ab} + q_{cd}$ (+) | $w_{ab} + w_{bc} + w_{cd} + w_{da}$ (−) | $\Delta U_{cycle} = 0$ |

Both $q_{ab}$ and $q_{cd}$ are nonzero because the corresponding processes are isothermal. Equation (5.4) shows that the efficiency of a heat engine operating in a reversible Carnot cycle is always less than one. Equivalently, not all of the heat withdrawn from the hot reservoir can be converted to work. This conclusion is valid for all engines and illustrates the asymmetry in converting heat to work and work to heat.

These considerations on the efficiency of reversible heat engines led to the Kelvin–Planck formulation of the **second law of thermodynamics:**

> It is impossible for a system to undergo a cyclic process whose sole effects are the flow of heat into the system from a heat reservoir and the performance of an equal amount of work by the system on the surroundings.

The second law asserts that the heat engine depicted in Figure 5.3b cannot be constructed. Any heat engine must eject heat into the cold reservoir as shown in Figure 5.3a. The second law has been put to the test many times by inventors who have claimed that they have invented an engine that has an efficiency of 100%. No such claim has ever been validated. To test the assertion made in this statement of the second law, imagine that such an engine has been invented. We mount it on a boat in Seattle and set off on a journey across the Pacific Ocean. Heat is extracted from the ocean, which is the single heat reservoir, and is converted entirely to work in the form of a rapidly rotating propeller. Because the ocean is huge, the decrease in its temperature as a result of withdrawing heat is negligible. By the time we arrive in Japan, not a gram of diesel fuel has been used, because all the heat needed to power the boat has been extracted from the ocean. The money that was saved on fuel is used to set up an office and begin marketing this wonder engine. Does this scenario sound too good to be true? It is. Such an impossible engine is called a **perpetual motion machine of the second kind** because it violates the second law of thermodynamics. A **perpetual motion machine of the first kind** violates the first law.

The first statement of the second law can be understood using an indicator diagram. For an engine to produce work, the area of the cycle in a $P$–$V$ diagram must be greater than zero. However, this is impossible in a simple cycle using a single heat reservoir. If $T_{hot} = T_{cold}$ in Figure 5.2, the cycle $a \rightarrow b \rightarrow c \rightarrow d \rightarrow a$ collapses to a line, and the area of the cycle is zero. An arbitrary reversible cycle can be constructed that does not consist of individual adiabatic and isothermal segments. However, as shown in Figure 5.4, any reversible cycle can be approximated by a succession of adiabatic and isothermal segments, an approximation that becomes exact as the length of each segment approaches zero. It can be shown that the efficiency of such a cycle is also given by Equation (5.9) so that the efficiency of all heat engines operating in any reversible cycle between the same two temperatures, $T_{hot}$ and $T_{cold}$, is identical.

A more useful form than Equation (5.4) for the efficiency of a reversible heat engine can be derived by assuming that the working substance in the engine is an ideal gas. Calculating the work flow in each of the four segments of the Carnot cycle using the results of Sections 2.7 and 2.9,

$$w_{ab} = -nRT_{hot} \ln \frac{V_b}{V_a} \qquad w_{ab} < 0 \text{ because } V_b > V_a$$

$$w_{bc} = nC_{V,m}(T_{cold} - T_{hot}) \quad w_{bc} < 0 \text{ because } T_{cold} < T_{hot} \tag{5.5}$$

$$w_{cd} = -nRT_{cold} \ln \frac{V_d}{V_c} \qquad w_{cd} > 0 \text{ because } V_d < V_c$$

$$w_{da} = nC_{V,m}(T_{hot} - T_{cold}) \quad w_{da} > 0 \text{ because } T_{hot} > T_{cold}$$

As derived in Section 2.10, the volume and temperature in the reversible adiabatic segments are related by

$$T_{hot}V_b^{\gamma-1} = T_{cold}V_c^{\gamma-1} \quad \text{and} \quad T_{cold}V_d^{\gamma-1} = T_{hot}V_a^{\gamma-1} \tag{5.6}$$



(a)

(b)
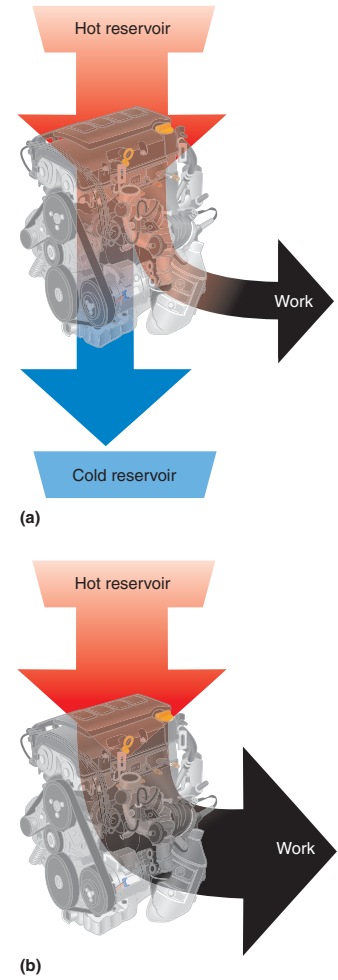
**FIGURE 5.3**
(a) A schematic model of the heat engine operating in a reversible Carnot cycle. The relative widths of the two paths leaving the hot reservoir show the partitioning between work and heat injected into the cold reservoir. (b) The second law of thermodynamics asserts that it is impossible to construct a heat engine that operates using a single heat reservoir and converts the heat withdrawn from the reservoir into work with 100% efficiency as shown.
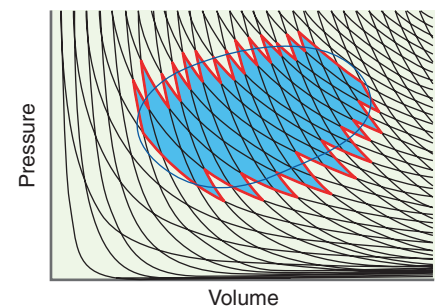


**FIGURE 5.4**
An arbitrary reversible cycle, indicated by the ellipse, can be approximated to any desired accuracy by a sequence of alternating adiabatic and isothermal segments.

You will show in the end-of-chapter problems that $V_c$ and $V_d$ can be eliminated from the set of Equations (5.5) to yield

$$w_{cycle} = -nR(T_{hot} - T_{cold}) \ln \frac{V_b}{V_a} < 0 \tag{5.7}$$

Because $\Delta U_{a \to b} = 0$, the heat withdrawn from the hot reservoir is

$$q_{ab} = -w_{ab} = nRT_{hot} \ln \frac{V_b}{V_a} \tag{5.8}$$

and the efficiency of the reversible Carnot heat engine with an ideal gas as the working substance can be expressed solely in terms of the reservoir temperatures.

$$\varepsilon = \frac{|w_{cycle}|}{q_{ab}} = \frac{T_{hot} - T_{cold}}{T_{hot}} = 1 - \frac{T_{cold}}{T_{hot}} < 1 \tag{5.9}$$

The efficiency of this reversible heat engine can approach one only as $T_{hot} \to \infty$ or $T_{cold} \to 0$, neither of which can be accomplished in practice. Therefore, heat can never be totally converted to work in a reversible cyclic process. Because $w_{cycle}$ for an engine operating in an irreversible cycle is less than the work attainable in a reversible cycle, $\varepsilon_{irreversible} < \varepsilon_{reversible} < 1$.

---

**EXAMPLE PROBLEM 5.1**

Calculate the maximum work that can be done by a reversible heat engine operating between 500. and 200. K if 1000. J is absorbed at 500. K.

**Solution**

The fraction of the heat that can be converted to work is the same as the fractional fall in the absolute temperature. This is a convenient way to link the efficiency of an engine with the properties of the absolute temperature.

$$\varepsilon = 1 - \frac{T_{cold}}{T_{hot}} = 1 - \frac{200. \text{ K}}{500. \text{ K}} = 0.600$$

$$w = \varepsilon q_{ab} = 0.600 \times 1000. \text{ J} = 600. \text{ J}$$

---

In this section, only the most important features of heat engines have been discussed. It can also be shown that the efficiency of a reversible heat engine is independent of the working substance. For a more in-depth discussion of heat engines, the interested reader is referred to *Heat and Thermodynamics,* seventh edition, by M. W. Zemansky and R. H. Dittman (McGraw-Hill, 1997). We will return to a discussion of the efficiency of engines when we discuss refrigerators, heat pumps, and real engines in Section 5.11.

# 5.3 Introducing Entropy

Equating the two formulas for the efficiency of the reversible heat engine given in Equations (5.4) and (5.9),

$$\frac{T_{hot} - T_{cold}}{T_{hot}} = \frac{q_{ab} + q_{cd}}{q_{ab}} \quad \text{or} \quad \frac{q_{ab}}{T_{hot}} + \frac{q_{cd}}{T_{cold}} = 0 \tag{5.10}$$

The last expression in Equation (5.10) is the sum of the quantity $q_{reversible}/T$ around the Carnot cycle. This result can be generalized to any reversible cycle made up of any number of segments to give the important result stated in Equation (5.11):

$$\oint \frac{dq_{reversible}}{T} = 0 \tag{5.11}$$

This equation can be regarded as the mathematical statement of the second law. What conclusions can be drawn from Equation (5.11)? Because the cyclic integral of $đq_{reversible}/T$ is zero, this quantity must be the exact differential of a state function. This state function is called the **entropy,** and given the symbol $S$

$$dS \equiv \frac{đq_{reversible}}{T} \tag{5.12}$$

For a macroscopic change,

$$\Delta S = \int \frac{đq_{reversible}}{T} \tag{5.13}$$

Note that whereas $đq_{reversible}$ is not an exact differential, multiplying this quantity by $1/T$ makes the differential exact.

---

**EXAMPLE PROBLEM 5.2**

**a.** Show that the following differential expression is not an exact differential:

$$\frac{RT}{P}dP + RdT$$

**b.** Show that $RTdP + PRdT$, obtained by multiplying the function in part (a) by $P$, is an exact differential.

**Solution**

**a.** For the expression $f(P,T)dP + g(P,T)dT$ to be an exact differential, the condition $(\partial f(P,T)/\partial T)_P = (\partial g(P,T)/\partial P)_T$ must be satisfied as discussed in Section 3.1. Because

$$\left(\frac{\partial \left(\dfrac{RT}{P}\right)}{\partial T}\right)_P = \frac{R}{P} \quad \text{and} \quad \frac{\partial R}{\partial P} = 0$$

the condition is not fulfilled.
**b.** Because $(\partial(RT)/\partial T)_P = R$ and $(\partial(RP)/\partial P)_T = R$, $RTdP + RPdT$ is an exact differential.

---

Keep in mind that it has only been shown that S is a state function. It has not yet been demonstrated that $S$ is a suitable function for measuring the natural direction of change in a process that the system may undergo. We will do so in Section 5.5.

# 5.4 Calculating Changes in Entropy

The most important thing to remember in doing entropy calculations using Equation (5.13) is that $\Delta S$ *must be calculated along a reversible path*. In considering an **irreversible process,** $\Delta S$ must be calculated for a reversible process that proceeds between the same initial and final states corresponding to the irreversible process. Because $S$ is a state function, $\Delta S$ is necessarily path independent, *provided that the transformation is between the same initial and final states in both processes.*

We first consider two cases that require no calculation. For any reversible adiabatic process, $q_{reversible} = 0$, so that $\Delta S = \int(đq_{reversible}/T) = 0$. For any cyclic process, $\Delta S = \oint(đq_{reversible}/T) = 0$, because the change in any state function for a cyclic process is zero.

Next consider $\Delta S$ for the reversible isothermal expansion or compression of an ideal gas, described by $V_i, T_i \rightarrow V_f, T_i$. Because $\Delta U = 0$ for this case,

$$q_{reversible} = -w_{reversible} = nRT \ln \frac{V_f}{V_i} \quad \text{and} \tag{5.14}$$

$$\Delta S = \int \frac{dq_{reversible}}{T} = \frac{1}{T} \times q_{reversible} = nR \ln \frac{V_f}{V_i} \tag{5.15}$$

Note that $\Delta S > 0$ for an expansion ($V_f > V_i$) and $\Delta S < 0$ for a compression ($V_f < V_i$). Although the preceding calculation is for a reversible process, $\Delta S$ has exactly the same value for any reversible or irreversible isothermal path that goes between the same initial and final volumes and satisfies the condition $T_f = T_i$. This is the case because $S$ is a state function.

Why does the entropy increase with increasing $V$ at constant $T$ if the system is viewed at a microscopic level? As discussed in Section 4.2 in *Quantum Chemistry and Spectroscopy*, the translational energy levels for atoms and molecules are all shifted to lower energies as the volume of the system increases. Therefore, more states of the system can be accessed at constant $T$ as $V$ increases. This is a qualitative argument that does not give the functional form shown in Equation (5.15). The logarithmic dependence arises because $S$ is proportional to the logarithm of the number of states accessible to the system rather than to the number of states.

Consider next $\Delta S$ for an ideal gas that undergoes a reversible change in $T$ at constant $V$ or $P$. For a reversible process described by $V_i, T_i \rightarrow V_i, T_f$, $dq_{reversible} = C_V dT$, and

$$\Delta S = \int \frac{dq_{reversible}}{T} = \int \frac{nC_{V,m} \, dT}{T} \approx nC_{V,m} \ln \frac{T_f}{T_i} \tag{5.16}$$

For a constant pressure process described by $P_i, T_i \rightarrow P_i, T_f$, $dq_{reversible} = C_P dT$, and

$$\Delta S = \int \frac{dq_{reversible}}{T} = \int \frac{nC_{P,m} \, dT}{T} \approx nC_{P,m} \ln \frac{T_f}{T_i} \tag{5.17}$$

The last expressions in Equations (5.16) and (5.17) are valid if the temperature interval is small enough that the temperature dependence of $C_{V,m}$ and $C_{P,m}$ can be neglected. Again, although $\Delta S$ has been calculated for a reversible process, Equations (5.16) and (5.17) hold for any reversible or irreversible process between the same initial and final states for an ideal gas.

We again ask what a microscopic model would predict for the dependence of $S$ on $T$. As discussed in Chapter 13, the probability of a molecule accessing a state with energy $E_i$ is proportional to $\exp(-E_i/k_B T)$. This quantity increases exponentially as $T$ increases, so that more states become accessible to the system as $T$ increases. Because $S$ is a measure of the number of states the system can access, it increases with increasing $T$. Again, the logarithmic dependence arises because $S$ is proportional to the logarithm of the number of states accessible to the system rather than to the number of states.

The results of the last two calculations can be combined in the following way. Because the macroscopic variables $V,T$ or $P,T$ completely define the state of an ideal gas, any change $V_i, T_i \rightarrow V_f, T_f$ can be separated into two segments, $V_i, T_i \rightarrow V_f, T_i$ and $V_f, T_i \rightarrow V_f, T_f$. A similar statement can be made about $P$ and $T$. Because $S$ is a state function, $\Delta S$ is independent of the path. Therefore, any reversible or irreversible process for an ideal gas described by $V_i, T_i \rightarrow V_f, T_f$ can be treated as consisting of two segments, one of which occurs at constant volume and the other of which occurs at constant temperature. For this two-step process, $\Delta S$ is given by

$$\Delta S = nR \ln \frac{V_f}{V_i} + nC_{V,m} \ln \frac{T_f}{T_i} \tag{5.18}$$

Similarly, for any reversible or irreversible process for an ideal gas described by $P_i, T_i \rightarrow P_f, T_f$

$$\Delta S = -nR \ln \frac{P_f}{P_i} + nC_{P,m} \ln \frac{T_f}{T_i} \tag{5.19}$$

In writing Equations (5.18) and (5.19), it has been assumed that the temperature dependence of $C_{V,m}$ and $C_{P,m}$ can be neglected over the temperature range of interest.

---

## EXAMPLE PROBLEM 5.3

Using the equation of state and the relationship between $C_{P,m}$ and $C_{V,m}$ for an ideal gas, show that Equation (5.18) can be transformed into Equation (5.19).

### Solution

$$\Delta S = nR \ln \frac{V_f}{V_i} + nC_{V,m} \ln \frac{T_f}{T_i} = nR \ln \frac{T_f P_i}{T_i P_f} + nC_{V,m} \ln \frac{T_f}{T_i}$$

$$= -nR \ln \frac{P_f}{P_i} + n(C_{V,m} + R) \ln \frac{T_f}{T_i} = -nR \ln \frac{P_f}{P_i} + nC_{P,m} \ln \frac{T_f}{T_i}$$

Next consider $\Delta S$ for phase changes. Experience shows that a liquid is converted to a gas at a constant boiling temperature through heat input if the process is carried out at constant pressure. Because $q_P = \Delta H$, $\Delta S$ for the reversible process is given by

$$\Delta S_{vaporization} = \int \frac{d q_{reversible}}{T} = \frac{q_{reversible}}{T_{vaporization}} = \frac{\Delta H_{vaporization}}{T_{vaporization}} \tag{5.20}$$

Similarly, for the phase change solid $\rightarrow$ liquid,

$$\Delta S_{fusion} = \int \frac{d q_{reversible}}{T} = \frac{q_{reversible}}{T_{fusion}} = \frac{\Delta H_{fusion}}{T_{fusion}} \tag{5.21}$$

Finally, consider $\Delta S$ for an arbitrary process involving real gases, solids, and liquids for which the isobaric volumetric thermal expansion coefficient $\beta$ and the isothermal compressibility $\kappa$, but not the equation of state, are known. The calculation of $\Delta S$ for such processes is described in Supplemental Sections 5.12 and 5.13, in which the properties of $S$ as a state function are fully exploited. The results are stated here. For the system undergoing the change $V_i, T_i \rightarrow V_f, T_f$,

$$\Delta S = \int_{T_i}^{T_f} \frac{C_V}{T} dT + \int_{V_i}^{V_f} \frac{\beta}{\kappa} dV = C_V \ln \frac{T_f}{T_i} + \frac{\beta}{\kappa}(V_f - V_i) \tag{5.22}$$

In deriving the last result, it has been assumed that $\kappa$ and $\beta$ are constant over the temperature and volume intervals of interest. For the system undergoing a change $P_i, T_i \rightarrow P_f, T_f$,

$$\Delta S = \int_{T_i}^{T_f} \frac{C_P}{T} dT - \int_{P_i}^{P_f} V\beta \, dP \tag{5.23}$$

For a solid or liquid, the last equation can be simplified to

$$\Delta S = C_P \ln \frac{T_f}{T_i} - V\beta(P_f - P_i) \tag{5.24}$$

if $C_P$, $V$, and $\beta$ are assumed constant over the temperature and pressure intervals of interest. The integral forms of Equations (5.22) and (5.23) are valid for ideal and real gases, liquids, and solids. Examples of calculations using these equations are given in Example Problems 5.4 through 5.6.

### EXAMPLE PROBLEM 5.4

One mole of CO gas is transformed from an initial state characterized by $T_i = 320.$ K and $V_i = 80.0$ L to a final state characterized by $T_f = 650.$ K and $V_f = 120.0$ L. Using Equation (5.22), calculate $\Delta S$ for this process. Use the ideal gas values for $\beta$ and $\kappa$. For CO,

$$\frac{C_{V,m}}{\text{J mol}^{-1}\text{K}^{-1}} = 31.08 - 0.01452\frac{T}{K} + 3.1415 \times 10^{-5}\frac{T^2}{K^2} - 1.4973 \times 10^{-8}\frac{T^3}{K^3}$$

#### Solution

For an ideal gas,

$$\beta = \frac{1}{V}\left(\frac{\partial V}{\partial T}\right)_P = \frac{1}{V}\left(\frac{\partial[nRT/P]}{\partial T}\right)_P = \frac{1}{T} \quad \text{and}$$

$$\kappa = -\frac{1}{V}\left(\frac{\partial V}{\partial P}\right)_T = -\frac{1}{V}\left(\frac{\partial[nRT/P]}{\partial P}\right)_T = \frac{1}{P}$$

Consider the following reversible process in order to calculate $\Delta S$. The gas is first heated reversibly from 320. to 650. K at a constant volume of 80.0 L. Subsequently, the gas is reversibly expanded at a constant temperature of 650. K from a volume of 80.0 L to a volume of 120.0 L. The entropy change for this process is obtained using the integral form of Equation (5.22) with the values of $\beta$ and $\kappa$ cited earlier. The result is

$$\Delta S = \int_{T_i}^{T_f}\frac{C_V}{T}dT + nR\ln\frac{V_f}{V_i}$$

$\Delta S =$

$$1\text{ mol} \times \int_{320.}^{650.}\frac{\left(31.08 - 0.01452\frac{T}{K} + 3.1415 \times 10^{-5}\frac{T^2}{K^2} - 1.4973 \times 10^{-8}\frac{T^3}{K^3}\right)}{\frac{T}{K}}d\frac{T}{K}$$

$$+ 1\text{ mol} \times 8.314\text{ J K}^{-1}\text{mol}^{-1} \times \ln\frac{120.0\text{ L}}{80.0\text{ L}}$$

$$= 22.025\text{ J K}^{-1} - 4.792\text{ J K}^{-1} + 5.028\text{ J K}^{-1}$$

$$- 1.207\text{ J K}^{-1} + 3.371\text{ J K}^{-1}$$

$$= 24.4\text{ J K}^{-1}$$

### EXAMPLE PROBLEM 5.5

In this problem, 2.50 mol of $CO_2$ gas is transformed from an initial state characterized by $T_i = 450.$ K and $P_i = 1.35$ bar to a final state characterized by $T_f = 800.$ K and $P_f = 3.45$ bar. Using Equation (5.23), calculate $\Delta S$ for this process. Assume ideal gas behavior and use the ideal gas value for $\beta$. For $CO_2$,

$$\frac{C_{P,m}}{\text{J mol}^{-1}\text{K}^{-1}} = 18.86 + 7.937 \times 10^{-2}\frac{T}{K} - 6.7834 \times 10^{-5}\frac{T^2}{K^2} + 2.4426 \times 10^{-8}\frac{T^3}{K^3}$$

#### Solution

Consider the following reversible process in order to calculate $\Delta S$. The gas is first heated reversibly from 450. to 800. K at a constant pressure of 1.35 bar. Subsequently, the gas is reversibly compressed at a constant temperature of 800. K from a pressure of

1.35 bar to a pressure of 3.45 bar. The entropy change for this process is obtained using Equation (5.23) with the value of $\beta = 1/T$ from Example Problem 5.4.

$$\Delta S = \int_{T_i}^{T_f}\frac{C_P}{T}dT - \int_{P_i}^{P_f}V\beta\,dP = \int_{T_i}^{T_f}\frac{C_P}{T}dT - nR\int_{P_i}^{P_f}\frac{dP}{P} = \int_{T_i}^{T_f}\frac{C_P}{T}dT - nR\ln\frac{P_f}{P_i}$$

$$= 2.50 \times \int_{450.}^{800.}\frac{\left(18.86 + 7.937\times10^{-2}\frac{T}{K} - 6.7834\times10^{-5}\frac{T^2}{K^2} + 2.4426\times10^{-8}\frac{T^3}{K^3}\right)}{\frac{T}{K}}d\frac{T}{K}$$

$$-2.50\,\text{mol} \times 8.314 \ \text{J K}^{-1}\text{mol}^{-1} \times \ln\frac{3.45\ \text{bar}}{1.35\ \text{bar}}$$

$$= \ 27.13 \ \text{J K}^{-1} + 69.45 \ \text{J K}^{-1} - 37.10 \ \text{J K}^{-1} + 8.57 \ \text{J K}^{-1}$$

$$-19.50 \ \text{J K}^{-1}$$

$$= \ 48.6 \ \text{J K}^{-1}$$

---

## EXAMPLE PROBLEM 5.6

In this problem, 3.00 mol of liquid mercury is transformed from an initial state characterized by $T_i = 300.$ K and $P_i = 1.00$ bar to a final state characterized by $T_f = 600.$ K and $P_f = 3.00$ bar.

**a.** Calculate $\Delta S$ for this process; $\beta = 1.81 \times 10^{-4} \ \text{K}^{-1}$, $\rho = 13.54 \ \text{g cm}^{-3}$, and $C_{P,m}$ for Hg(l) = 27.98 J mol$^{-1}$K$^{-1}$.

**b.** What is the ratio of the pressure-dependent term to the temperature-dependent term in $\Delta S$? Explain your result.

### Solution

**a.** Because the volume changes only slightly with temperature and pressure over the range indicated,

$$\Delta S = \int_{T_i}^{T_f}\frac{C_P}{T}dT - \int_{P_i}^{P_f}V\beta\,dP \approx nC_{P,m}\ln\frac{T_f}{T_i} - nV_{m,i}\beta(P_f - P_i)$$

$$= 3.00\,\text{mol} \times 27.98 \ \text{J mol}^{-1}\text{K}^{-1} \times \ln\frac{600.\ \text{K}}{300.\ \text{K}}$$

$$-3.00\,\text{mol} \times \frac{200.59 \ \text{g mol}^{-1}}{13.54 \ \text{g cm}^{-3} \times \frac{10^6\,\text{cm}^3}{\text{m}^3}} \times 1.81 \times 10^{-4}\text{K}^{-1} \times 2.00 \ \text{bar}$$

$$\times 10^5 \ \text{Pa bar}^{-1}$$

$$= \ 58.2 \ \text{J K}^{-1} - 1.61 \times 10^{-3} \ \text{J K}^{-1} = 58.2 \ \text{J K}^{-1}$$

**b.** The ratio of the pressure-dependent to the temperature-dependent term is $-3 \times 10^{-5}$. Because the volume change with pressure is very small, the contribution of the pressure-dependent term is negligible in comparison with the temperature-dependent term.

As Example Problem 5.6 shows, $\Delta S$ for a liquid or solid as both $P$ and $T$ change is dominated by the temperature dependence of $S$. *Unless the change in pressure is very large, $\Delta S$ for liquids and solids can be considered to be a function of temperature only.*
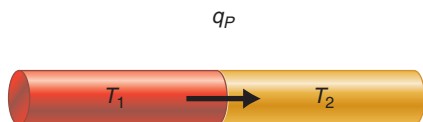
$q_P$



**FIGURE 5.5**
Two systems at constant $P$, each consisting of a metal rod, are placed in thermal contact. The temperatures of the two rods differ by $\Delta T$. The composite system is contained in a rigid adiabatic enclosure (not shown) and is, therefore, an isolated system.

## 5.5 Using Entropy to Calculate the Natural Direction of a Process in an Isolated System

To show that $\Delta S$ is useful in predicting the direction of spontaneous change, we now return to the two processes introduced in Section 5.1. The first process concerns the natural direction of change in a metal rod with a temperature gradient. Will the gradient become larger or smaller as the system approaches its equilibrium state? To model this process, consider the *isolated* composite system shown in Figure 5.5. Two systems, in the form of metal rods with uniform, but different, temperatures $T_1 > T_2$, are brought into thermal contact.

In the following discussion, heat is withdrawn from the left rod. (The same reasoning would hold if the direction of heat flow were reversed.) To calculate $\Delta S$ for this irreversible process using the heat flow, one must imagine a reversible process in which the initial and final states are the same as for the irreversible process. In the imaginary reversible process, the rod is coupled to a reservoir whose temperature is lowered very slowly. The temperatures of the rod and the reservoir differ only infinitesimally throughout the process in which an amount of heat, $q_P$, is withdrawn from the rod. The total change in temperature of the rod, $\Delta T$, is related to $q_P$ by

$$d q_P = C_P dT \quad \text{or} \quad \Delta T = \frac{1}{C_P} \int d q_P = \frac{q_P}{C_P} \tag{5.25}$$

It has been assumed that $\Delta T = T_2 - T_1$ is small enough that $C_P$ is constant over the interval.

Because the path is defined (constant pressure), $\int d q_P$ is independent of how rapidly the heat is withdrawn (the path); it depends only on $C_P$ and $\Delta T$. More formally, because $q_P = \Delta H$ and because $H$ is a state function, $q_P$ is independent of the path between the initial and final states. Therefore, $q_P = q_{reversible}$ if the temperature increment $\Delta T$ is identical for the reversible and irreversible processes.

Using this result, the entropy change for this irreversible process in which heat flows from one rod to the other is calculated. Because the composite system is isolated, $q_1 + q_2 = 0$, and $q_1 = -q_2 = q_P$. The entropy change of the composite system is the sum of the entropy changes in each rod

$$\Delta S = \frac{q_{reversible,1}}{T_1} + \frac{q_{reversible,2}}{T_2} = \frac{q_1}{T_1} + \frac{q_2}{T_2} = q_P \left( \frac{1}{T_1} - \frac{1}{T_2} \right) \tag{5.26}$$

Because $T_1 > T_2$, the quantity in parentheses is negative. This process has two possible directions:

- If heat flows from the hotter to the colder rod, the temperature gradient will become smaller. In this case, $q_P < 0$ and $\Delta S > 0$.
- If heat flows from the colder to the hotter rod, the temperature gradient will become larger. In this case, $q_P > 0$ and $\Delta S < 0$.

Note that $\Delta S$ has the same magnitude, but a different sign, for the two directions of change. $\Delta S$ appears to be a useful function for measuring the direction of natural change in an isolated system. Experience tells us that the temperature gradient will become less with time. *It can be concluded that the process in which S increases is the direction of natural change in an isolated system.*

Next, consider the second process introduced in Section 5.1 in which an ideal gas spontaneously collapses to half its initial volume without a force acting on it. This process and its reversible analog are shown in Figure 5.6. Recall that $U$ is independent of $V$ for an ideal gas. Because $U$ does not change as $V$ increases, and $U$ is a function of $T$ only for an ideal gas, the temperature remains constant in the irreversible process. Therefore, the spontaneous irreversible process shown in Figure 5.6a is both adiabatic and isothermal and is described by $V_i, T_i \rightarrow 1/2 V_i, T_i$. The imaginary reversible process that we use to carry out the calculation of $\Delta S$ is shown in



Initial state      Final state
Irreversible process
**(a)**



Initial state      Final state
Reversible process
**(b)**
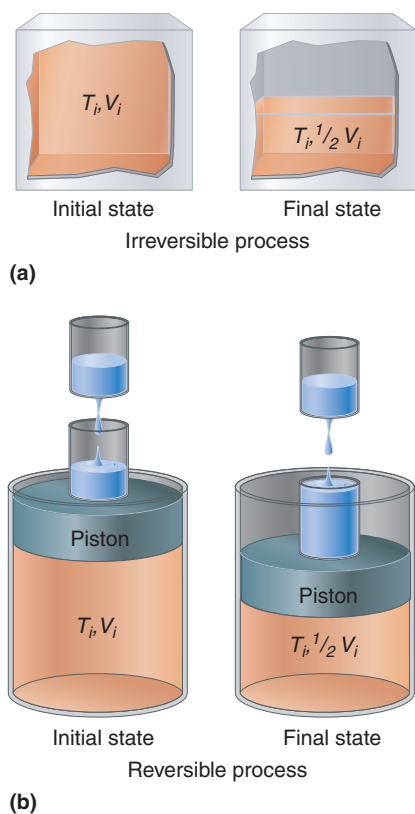
**FIGURE 5.6**
**(a)** An irreversible process is shown in which an ideal gas confined in a container with rigid adiabatic walls is spontaneously reduced to half its initial volume. **(b)** A reversible isothermal compression is shown between the same initial and final states as for the irreversible process. Reversibility is achieved by adjusting the rate at which the beaker on top of the piston is filled with water relative to the evaporation rate.

Figure 5.6b. In this process, which must have the same initial and final states as the irreversible process, water is slowly and continuously added to the beaker on the piston to ensure that $P = P_{external}$. The ideal gas undergoes a reversible isothermal transformation described by $V_i, T_i \rightarrow 1/2V_i, T_i$. Because $\Delta U = 0$, $q = -w$. We calculate $\Delta S$ for this process:

$$\Delta S = \int \frac{dq_{reversible}}{T} = \frac{q_{reversible}}{T_i} = -\frac{w_{reversible}}{T_i} = nR \ln \frac{\frac{1}{2}V_i}{V_i} = -nR \ln 2 < 0 \; \textbf{(5.27)}$$

For the opposite process, in which the gas spontaneously expands so that it occupies twice the volume, the reversible model process is an isothermal expansion for which

$$\Delta S = nR \ln \frac{2V_i}{V_i} = nR \ln 2 > 0 \tag{5.28}$$

*Again, the process with $\Delta S > 0$ is the direction of natural change in this isolated system. The reverse process for which $\Delta S < 0$ is the unnatural direction of change.*
The results obtained for isolated systems are generalized in the following statement:

> For any irreversible process in an isolated system, there is a unique direction of spontaneous change: $\Delta S > 0$ for the spontaneous process, $\Delta S < 0$ for the opposite or nonspontaneous direction of change, and $\Delta S = 0$ only for a reversible process. In a quasi-static reversible process, there is no direction of spontaneous change because the system is proceeding along a path, each step of which corresponds to an equilibrium state.

We cannot emphasize too strongly that $\Delta S > 0$ is a criterion for spontaneous change *only* if the system does not exchange energy in the form of heat or work with its surroundings. Note that if any process occurs in the isolated system, it is by definition spontaneous and the entropy increases. Whereas $U$ can neither be created nor destroyed, $S$ for an isolated system can be created ($\Delta S > 0$), but not destroyed ($\Delta S < 0$).

# 5.6 The Clausius Inequality

In the previous section, it was shown using two examples that $\Delta S > 0$ provides a criterion to predict the natural direction of change in an isolated system. This result can also be obtained without considering a specific process. Consider the differential form of the first law for a process in which only $P$–$V$ work is possible

$$dU = dq - P_{external} \, dV \tag{5.29}$$

Equation (5.29) is valid for both reversible and irreversible processes. If the process is reversible, we can write Equation (5.29) in the following form:

$$dU = dq_{reversible} - P \, dV = T \, dS - P \, dV \tag{5.30}$$

Because $U$ is a state function, $dU$ is independent of the path, and Equation (5.30) holds for both reversible and irreversible processes, as long as there are no phase transitions or chemical reactions, and only $P$–$V$ work occurs.
To derive the Clausius inequality, we equate the expressions for $dU$ in Equations (5.29) and (5.30):

$$dq_{reversible} - dq = (P - P_{external}) \, dV \tag{5.31}$$

If $P - P_{external} > 0$, the system will spontaneously expand, and $dV > 0$. If $P - P_{external} < 0$, the system will spontaneously contract, and $dV < 0$. In both possible cases, $(P - P_{external}) \, dV > 0$. Therefore, we conclude that

$$dq_{reversible} - dq = T \, dS - dq \geq 0 \text{ or } T \, dS \geq dq \tag{5.32}$$

The equality holds only for a reversible process. We rewrite the **Clausius inequality** in Equation (5.32) for an irreversible process in the form

$$dS > \frac{\not{d}q}{T} \tag{5.33}$$

For an irreversible process in an isolated system, $\not{d}q = 0$. *Therefore, we have again proved that for any irreversible process in an isolated system, $\Delta S > 0$.*

How can the result from Equations (5.29) and (5.30) that $dU = \not{d}q - P_{external}dV = TdS - PdV$ be reconciled with the fact that work and heat are path functions? The answer is that $\not{d}w \geq -PdV$ and $\not{d}q \leq TdS$, where the equalities hold only for a reversible process. The result $\not{d}q + \not{d}w = TdS - PdV$ states that the amount by which the work is greater than $-PdV$ and the amount by which the heat is less than $TdS$ in an irreversible process involving only $PV$ work are exactly equal. *Therefore, the differential expression for dU in Equation (5.30) is obeyed for both reversible and irreversible processes.* In Chapter 6, the Clausius inequality is used to generate two new state functions, the Gibbs energy and the Helmholtz energy. These functions allow predictions to be made about the direction of change in processes for which the system interacts with its environment.

The Clausius inequality is next used to evaluate the cyclic integral $\oint \not{d}q/T$ for an arbitrary process. Because $dS = \not{d}q_{reversible}/T$, the value of the cyclic integral is zero for a reversible process. Consider a process in which the transformation from state 1 to state 2 is reversible, but the transition from state 2 back to state 1 is irreversible:

$$\oint \frac{\not{d}q}{T} = \int_1^2 \frac{\not{d}q_{reversible}}{T} + \int_2^1 \frac{\not{d}q_{irreversible}}{T} \tag{5.34}$$

The limits of integration on the first integral can be interchanged to obtain

$$\oint \frac{\not{d}q}{T} = -\int_2^1 \frac{\not{d}q_{reversible}}{T} + \int_2^1 \frac{\not{d}q_{irreversible}}{T} \tag{5.35}$$

Exchanging the limits as written is only valid for a state function. Because $\not{d}q_{reversible} > \not{d}q_{irreversible}$

$$\oint \frac{\not{d}q}{T} \leq 0 \tag{5.36}$$

where the equality only holds for a reversible process. Note that the cyclic integral of an exact differential is always zero, but the integrand in Equation (5.36) is only an exact differential for a reversible cycle.

# 5.7 The Change of Entropy in the Surroundings and $\Delta S_{total} = \Delta S + \Delta S_{surroundings}$

As shown in Section 5.6, the entropy of an isolated system increases in a spontaneous process. Is it always true that a process is spontaneous if $\Delta S$ for the system is positive? As shown later, this statement is only true for an isolated system. In this section, a criterion for spontaneity is developed that takes into account the entropy change in both the system and the surroundings.

In general, a system interacts only with the part of the universe that is very close. Therefore, one can think of the system and the interacting part of the surroundings as forming an interacting composite system that is isolated from the rest of the universe. The part of the surroundings that is relevant for entropy calculations is a thermal reservoir at a fixed temperature, $T$. The mass of the reservoir is sufficiently large that its temperature is only changed by an infinitesimal amount $dT$ when heat is transferred

between the system and the surroundings. Therefore, the surroundings always remain in internal equilibrium during heat transfer.

Next consider the entropy change of the surroundings, whereby the surroundings are at either constant $V$ or constant $P$. We assume that the system and surroundings are at the same temperature. If this were not the case, heat would flow across the boundary until $T$ is the same for system and surroundings, unless the system is surrounded by adiabatic walls, in which case $q_{surroundings} = 0$. The amount of heat absorbed by the surroundings, $q_{surroundings}$, depends on the process occurring in the system. If the surroundings are at constant $V$, $q_{surroundings} = \Delta U_{surroundings}$, and if the surroundings are at constant $P$, $q_{surroundings} = \Delta H_{surroundings}$. Because $H$ and $U$ are state functions, the amount of heat entering the surroundings is independent of the path; $q$ is the same whether the transfer occurs reversibly or irreversibly. Therefore,

$$dS_{surroundings} = \frac{\text{đ}q_{surroundings}}{T} \text{ or for a macroscopic change,}$$

$$\Delta S_{surroundings} = \frac{q_{surroundings}}{T} \tag{5.37}$$

Note that the heat that appears in Equation (5.37) is the *actual* heat transferred because the heat transferred to the surroundings is independent of the path as discussed earlier. By contrast, in calculating $\Delta S$ for the system, $\text{đ}q_{reversible}$ for a *reversible* process that connects the initial and final states of the system must be used, *not* the actual $\text{đ}q$ for the process. *It is essential to understand this reasoning in order to carry out calculations for $\Delta S$ and $\Delta S_{surroundings}$.*

This important difference is discussed in calculating the entropy change of the system as opposed to the surroundings with the aid of Figure 5.7. A gas (the system) is enclosed in a piston and cylinder assembly with diathermal walls. The gas is reversibly compressed by the external pressure generated by droplets of water slowly filling the beaker on top of the piston. The piston and cylinder assembly is in contact with a water bath thermal reservoir that keeps the temperature of the gas fixed at the value $T$. In Example Problem 5.7, $\Delta S$ and $\Delta S_{surroundings}$ are calculated for this reversible compression.



### EXAMPLE PROBLEM 5.7

One mole of an ideal gas at 300. K is reversibly and isothermally compressed from a volume of 25.0 L to a volume of 10.0 L. Because the water bath thermal reservoir in the surroundings is very large, $T$ remains essentially constant at 300. K during the process. Calculate $\Delta S$, $\Delta S_{surroundings}$, and $\Delta S_{total}$.
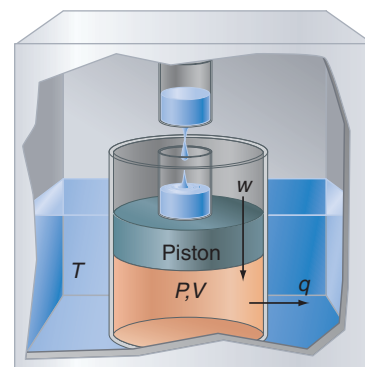
**FIGURE 5.7**
A sample of an ideal gas (the system) is confined in a piston and cylinder assembly with diathermal walls. The assembly is in contact with a thermal reservoir that holds the temperature at a value of 300 K. Water dripping into the beaker on the piston increases the external pressure slowly enough to ensure a reversible compression. The value of the pressure is determined by the relative rates of water filling and evaporation from the beaker. The directions of work and heat flow are indicated.

#### Solution

Because this is an isothermal process, $\Delta U = 0$, and $q_{reversible} = -w$. From Section 2.7,

$$q_{reversible} = -w = nRT \int_{V_i}^{V_f} \frac{dV}{V} = nRT \ln \frac{V_f}{V_i}$$

$$= 1.00 \text{ mol} \times 8.314 \text{ J mol}^{-1}\text{K}^{-1} \times 300. \text{ K} \times \ln \frac{10.0 \text{ L}}{25.0 \text{ L}} = -2.285 \times 10^3 \text{ J}$$

The entropy change of the system is given by

$$\Delta S = \int \frac{\text{đ}q_{reversible}}{T} = \frac{q_{reversible}}{T} = \frac{-2.285 \times 10^3 \text{ J}}{300. \text{ K}} = -7.62 \text{ J K}^{-1}$$

The entropy change of the surroundings is given by

$$\Delta S_{surroundings} = \frac{q_{surroundings}}{T} = -\frac{q_{system}}{T} = \frac{2.285 \times 10^3 \text{ J}}{300. \text{ K}} = 7.62 \text{ J K}^{-1}$$

The total change in the entropy is given by

$$\Delta S_{total} = \Delta S + \Delta S_{surroundings} = -7.62 \text{ J K}^{-1} + 7.62 \text{ J K}^{-1} = 0$$

Because the process in Example Problem 5.7 is reversible, there is no direction of spontaneous change and, therefore, $\Delta S_{total} = 0$. In Example Problem 5.8, this calculation is repeated for an irreversible process that goes between the same initial and final states of the system.

### EXAMPLE PROBLEM 5.8

One mole of an ideal gas at 300. K is isothermally compressed by a constant external pressure equal to the final pressure in Example Problem 5.7. At the end of the process, $P = P_{external}$. Because $P \neq P_{external}$ at all but the final state, this process is irreversible. The initial volume is 25.0 L and the final volume is 10.0 L. The temperature of the surroundings is 300. K. Calculate $\Delta S$, $\Delta S_{surroundings}$, and $\Delta S_{total}$.

#### Solution

We first calculate the external pressure and the initial pressure in the system

$$P_{external} = \frac{nRT}{V} = \frac{1 \text{ mol} \times 8.314 \text{ J mol}^{-1}\text{K}^{-1} \times 300. \text{ K}}{10.0 \text{ L} \times \dfrac{1 \text{ m}^3}{10^3 \text{ L}}} = 2.494 \times 10^5 \text{ Pa}$$

$$P_i = \frac{nRT}{V} = \frac{1 \text{ mol} \times 8.314 \text{ J mol}^{-1}\text{K}^{-1} \times 300. \text{ K}}{25.0 \text{ L} \times \dfrac{1 \text{ m}^3}{10^3 \text{ L}}} = 9.977 \times 10^4 \text{ Pa}$$

Because $P_{external} > P_i$, we expect that the direction of spontaneous change will be the compression of the gas to a smaller volume. Because $\Delta U = 0$,

$$q = -w = P_{external}(V_f - V_i) = 2.494 \times 10^5 \text{ Pa}$$
$$\times \left(10.0 \times 10^{-3} \text{ m}^3 - 25.0 \times 10^{-3} \text{ m}^3\right) = -3.741 \times 10^3 \text{ J}$$

The entropy change of the surroundings is given by:

$$\Delta S_{surroundings} = \frac{q_{surroundings}}{T} = -\frac{q}{T} = \frac{3.741 \times 10^3 \text{ J}}{300. \text{ K}} = 12.47 \text{ J K}^{-1}$$

The entropy change of the system must be calculated on a reversible path and has the value obtained in Example Problem 5.7

$$\Delta S = \int \frac{d q_{reversible}}{T} = \frac{q_{reversible}}{T} = \frac{-2.285 \times 10^3 \text{ J}}{300. \text{ K}} = -7.62 \text{ J K}^{-1}$$

It is seen that $\Delta S < 0$, and $\Delta S_{surroundings} > 0$. The total change in the entropy is given by

$$\Delta S_{total} = \Delta S + \Delta S_{surroundings} = -7.62 \text{ J K}^{-1} + 12.47 \text{ J K}^{-1} = 4.85 \text{ J K}^{-1}$$

The previous calculations lead to the following conclusion: *if the system and the part of the surroundings with which it interacts are viewed as an isolated composite system, the criterion for spontaneous change is* $\Delta S_{total} = \Delta S + \Delta S_{surroundings} > 0$. A decrease in the entropy of the universe will never be observed, because $\Delta S_{total} \geq 0$ for any change that actually occurs. *Any process* that occurs in the universe is by definition spontaneous and leads to an increase of $S_{total}$. Therefore, $\Delta S_{total} > 0$ as time increases, which defines a unique direction of time. Consider the following example to illustrate the connection between entropy and time: we view a movie in which two ideal gases are mixed, and then run the movie backward, separation of the gases occurs. We cannot decide which direction corresponds to real time (the spontaneous process) on the basis of the first law. However, using the criterion $\Delta S_{total} \geq 0$, the direction of real time can be

established. The English astrophysicist Eddington coined the phrase "entropy is time's arrow" to emphasize this relationship between entropy and time.

Note that a spontaneous process in a system that interacts with its surroundings is not characterized by $\Delta S > 0$, but by $\Delta S_{total} > 0$. The entropy of the system can decrease in a spontaneous process, as long as the entropy of the surroundings increases by a greater amount. In Chapter 6, the spontaneity criterion $\Delta S_{total} = \Delta S + \Delta S_{surroundings} > 0$ will be used to generate two state functions, the Gibbs energy and the Helmholtz energy. These functions allow one to predict the direction of change in systems that interact with their environment using *only* the changes in system state functions.

# 5.8 Absolute Entropies and the Third Law of Thermodynamics

All elements and many compounds exist in three different states of aggregation. One or more solid phases are the most stable forms at low temperature, and when the temperature is increased to the melting point, a constant temperature transition to the liquid phase is observed. After the temperature is increased further, a constant temperature phase transition to a gas is observed at the boiling point. At temperatures higher than the boiling point, the gas is the stable form.

The entropy of an element or a compound is experimentally determined using heat capacity data through the relationship $đq_{reversible,P} = C_P dT$. Just as for the thermochemical data discussed in Chapter 4, entropy values are generally tabulated for a standard temperature of 298.15 K and a standard pressure of 1 bar. We describe such a determination for the entropy of $O_2$ at 298.15 K, first in a qualitative fashion, and then quantitatively in Example Problem 5.9.

The experimentally determined heat capacity of $O_2$ is shown in Figure 5.8 as a function of temperature for a pressure of 1 bar. $O_2$ has three solid phases, and transitions between them are observed at 23.66 and 43.76 K. The solid form that is stable above 43.76 K melts to form a liquid at 54.39 K. The liquid vaporizes to form a gas at 90.20 K. These phase transitions are indicated in Figure 5.8. Experimental measurements of $C_{P,m}$ are available above 12.97 K. Below this temperature, the data are extrapolated to zero kelvin by assuming that in this very low temperature range $C_{P,m}$ varies with temperature as $T^3$. This extrapolation is based on a model of the vibrational spectrum of a crystalline solid that will be discussed in Chapter 15. The explanation for the dependence of $C_{P,m}$ on $T$ is the same as that presented for $Cl_2$ in Section 2.4.

Under constant pressure conditions, the molar entropy of the gas can be expressed in terms of the molar heat capacities of the solid, liquid, and gaseous forms and the enthalpies of fusion and vaporization as



$$S_m(T) = S_m(0\,K) + \int_0^{T_f} \frac{C_{P,m}^{solid} dT'}{T'} + \frac{\Delta H_{fusion}}{T_f} + \int_{T_f}^{T_b} \frac{C_{P,m}^{liquid} dT'}{T'}$$

$$+ \frac{\Delta H_{vaporization}}{T_b} + \int_{T_b}^{T} \frac{C_{P,m}^{gas} dT'}{T'} \tag{5.38}$$

If the substance has more than one solid phase, each will give rise to a separate integral. Note that the entropy change associated with the phase transitions solid $\rightarrow$ liquid and liquid $\rightarrow$ gas discussed in Section 5.4 must be included in the calculation. To obtain a numerical value for $S_m(T)$, the heat capacity must be known down to zero kelvin, and $S_m(0\,K)$ must also be known.

We first address the issue of the entropy of a solid at zero kelvin. The **third law of thermodynamics** can be stated in the following form, due to Max Planck:

> The entropy of a pure, perfectly crystalline substance (element or compound) is zero at zero kelvin.
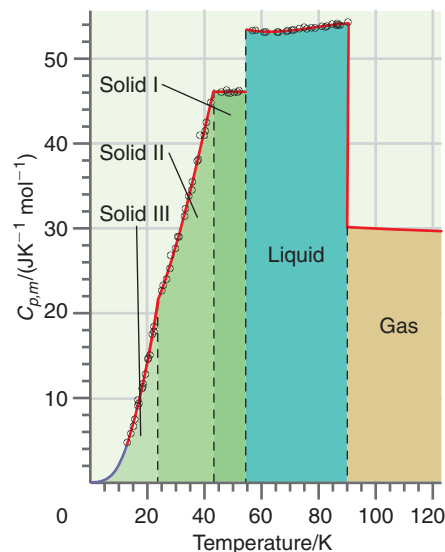
**FIGURE 5.8**
The experimentally determined heat capacity for $O_2$ is shown as a function of temperature below 125 K. The dots are data from Giauque and Johnston [*J. American Chemical Society* 51 (1929), 2300]. The red solid lines below 90 K are polynomial fits to these data. The red line above 90 K is a fit to data from the *NIST Chemistry Webbook*. The blue line is an extrapolation from 12.97 to 0 K as described in the text. The vertical dashed lines indicate constant temperature-phase transitions, and the most stable phase at a given temperature is indicated in the figure.

**FIGURE 5.9**

$C_P/T$ as a function of temperature for $O_2$. The vertical dashed lines indicate constant temperature-phase transitions, and the most stable phase at a given temperature is indicated in the figure.
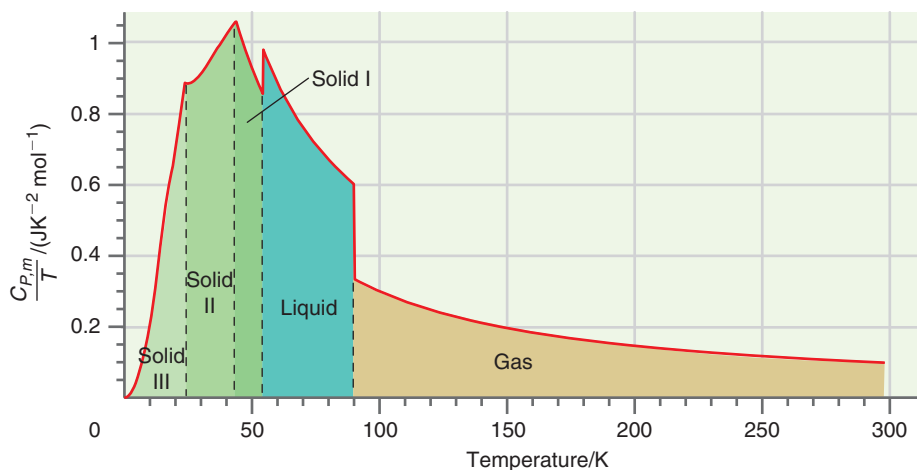


A more detailed discussion of the third law using a microscopic model will be presented in Chapter 15. Recall that in a perfectly crystalline atomic (or molecular) solid, the position of each atom is known. Because the individual atoms are indistinguishable, exchanging the positions of two atoms does not lead to a new state. Therefore, a perfect crystalline solid has only one state at zero kelvin and $S = k \ln W = k \ln 1 = 0$. The importance of the third law is that it allows calculations of the *absolute* entropies of elements and compounds to be carried out for any value of $T$. To calculate $S$ at a temperature $T$ using Equation (5.38), the $C_{P,m}$ data of Figure 5.8 are graphed in the form $C_{P,m}/T$ as shown in Figure 5.9.

The entropy can be obtained as a function of temperature by numerically integrating the area under the curve in Figure 5.9 and adding the entropy changes associated with phase changes at the transition temperatures. Calculations of $S_m^\circ$ for $O_2$ at 298.15 K are carried out in Example Problem 5.9 and $S_m^\circ(T)$ is shown in Figure 5.10.

One can also make the following general remarks about the relative magnitudes of the entropy of different substances and different phases of the same substance. These remarks will be justified on the basis of a microscopic model in Chapter 15.

- Because $C_P/T$ in a single phase region and $\Delta S$ for melting and vaporization are always positive, $S_m$ for a given substance is greatest for the gas-phase species. The molar entropies follow the order $S_m^{gas} >> S_m^{liquid} > S_m^{solid}$.

- The molar entropy increases with the size of a molecule because the number of degrees of freedom increases with the number of atoms. A non-linear gas-phase molecule has three translational degrees of freedom, three rotational degrees of freedom, and $3n - 6$ vibrational degrees of freedom. A linear molecule has three translational, two rotational, and $3n - 5$ vibrational degrees of freedom. For a molecule in a liquid, the three translational degrees of freedom are converted to local vibrational modes because of the attractive interaction between neighboring molecules.

**FIGURE 5.10**

The molar entropy for $O_2$ is shown as a function of temperature. The vertical dashed lines indicate constant temperature-phase transitions, and the most stable phase at a given temperature is indicated in the figure.
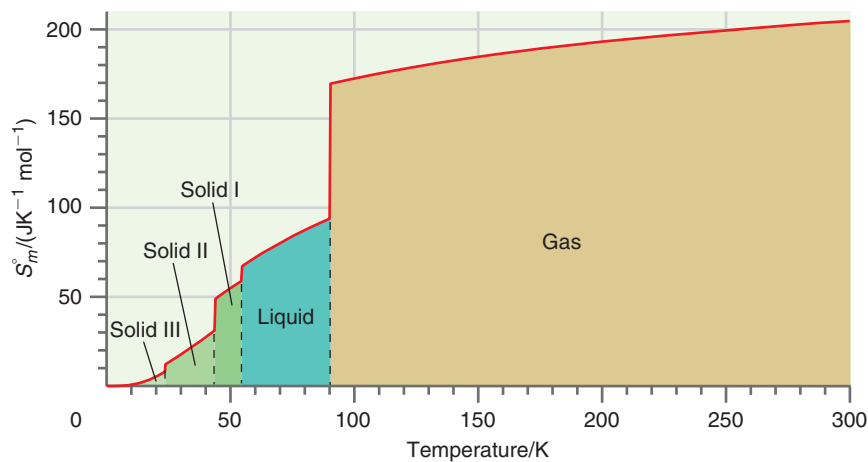
- A solid has only vibrational modes. It can be modeled as a three-dimensional array of coupled harmonic oscillators as shown in Figure 5.11. This solid has a wide spectrum of vibrational frequencies, and solids with a large binding energy have higher frequencies than more weakly bound solids. Because modes with high frequencies are not activated at low temperatures, $S_m^{solid}$ is larger for weakly bound solids than for strongly bound solids at low and moderate temperatures.

- The entropy of all substances is a monotonically increasing function of temperature.
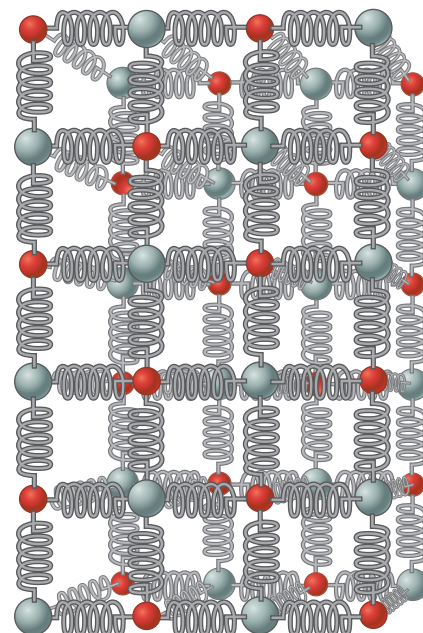
## EXAMPLE PROBLEM 5.9

The heat capacity of $O_2$ has been measured at 1 atm pressure over the interval 12.97 K $< T <$ 298.15 K. The data have been fit to the following polynomial series in $T/K$, in order to have a unitless variable:

0 K $< T <$ 12.97 K:

$$\frac{C_{P,m}(T)}{J\,mol^{-1}K^{-1}} = 2.11 \times 10^{-3}\frac{T^3}{K^3}$$

12.97 K $< T <$ 23.66 K:

$$\frac{C_{P,m}(T)}{J\,mol^{-1}K^{-1}} = -5.666 + 0.6927\frac{T}{K} - 5.191 \times 10^{-3}\frac{T^2}{K^2} + 9.943 \times 10^{-4}\frac{T^3}{K^3}$$

23.66 K $< T <$ 43.76 K:

$$\frac{C_{P,m}(T)}{J\,mol^{-1}K^{-1}} = 31.70 - 2.038\frac{T}{K} + 0.08384\frac{T^2}{K^2} - 6.685 \times 10^{-4}\frac{T^3}{K^3}$$

43.76 K $< T <$ 54.39 K:

$$\frac{C_{P,m}(T)}{J\,mol^{-1}K^{-1}} = 46.094$$

54.39 K $< T <$ 90.20 K:

$$\frac{C_{P,m}(T)}{J\,mol^{-1}K^{-1}} = 81.268 - 1.1467\frac{T}{K} + 0.01516\frac{T^2}{K^2} - 6.407 \times 10^{-5}\frac{T^3}{K^3}$$

90.20 K $< T <$ 298.15 K:

$$\frac{C_{P,m}(T)}{J\,mol^{-1}K^{-1}} = 32.71 - 0.04093\frac{T}{K} + 1.545 \times 10^{-4}\frac{T^2}{K^2} - 1.819 \times 10^{-7}\frac{T^3}{K^3}$$

The transition temperatures and the enthalpies for the transitions indicated in Figure 5.8 are as follows:

| | | |
|---|---|---|
| Solid III → solid II | 23.66 K | 93.8 J mol$^{-1}$ |
| Solid II → solid I | 43.76 K | 743 J mol$^{-1}$ |
| Solid I → liquid | 54.39 K | 445.0 J mol$^{-1}$ |
| Liquid → gas | 90.20 K | 6815 J mol$^{-1}$ |

**a.** Using these data, calculate $S_m^{\circ}$ for $O_2$ at 298.15 K.
**b.** What are the three largest contributions to $S_m^{\circ}$?



**FIGURE 5.11**
A useful model of a solid is a three-dimensional array of coupled harmonic oscillators. In solids with a high binding energy, the atoms are coupled by stiff springs.

**Solution**

**a.** $S_m^{\circ}(298.15\,\text{K}) = \displaystyle\int_0^{23.66} \frac{C_{P,m}^{solid,III}dT}{T} + \frac{93.80\,\text{J}}{23.66\,\text{K}} + \int_{23.66}^{43.76} \frac{C_{P,m}^{solid,II}dT}{T} + \frac{743\,\text{J}}{43.76\,\text{K}}$

$\qquad + \displaystyle\int_{43.76}^{54.39} \frac{C_{P,m}^{solid,I}dT}{T} + \frac{445.0\,\text{J}}{54.39\,\text{K}} + \int_{54.39}^{90.20} \frac{C_{P,m}^{liquid}dT}{T} + \frac{6815\,\text{J}}{90.20\,\text{K}}$

$\qquad + \displaystyle\int_{90.20}^{298.15} \frac{C_{P,m}^{gas}dT}{T}$

$\qquad = 8.182\,\text{J K}^{-1} + 3.964\,\text{J K}^{-1} + 19.61\,\text{J K}^{-1} + 16.98\,\text{J K}^{-1}$

$\qquad\quad + 10.13\,\text{J K}^{-1} + 8.181\,\text{J K}^{-1} + 27.06\,\text{J K}^{-1} + 75.59\,\text{J K}^{-1}$

$\qquad\quad + 35.27\,\text{J K}^{-1}$

$\qquad = 204.9\,\text{J mol}^{-1}\text{K}^{-1}$

There is an additional small correction for nonideality of the gas at 1 bar. The currently accepted value is $S_m^{\circ}(298.15\,\text{K}) = 205.152\,\text{J mol}^{-1}\text{K}^{-1}$ (Linstrom, P. J., and Mallard, W. G., eds. *NIST Chemistry Webbook: NIST Standard Reference Database Number 69.* Gaithersburg, MD: National Institute of Standards and Technology. Retrieved from http://webbook.nist.gov.)

**b.** The three largest contributions to $S_m^{\circ}$ are $\Delta S$ for the vaporization transition, $\Delta S$ for the heating of the gas from the boiling temperature to 298.15 K, and $\Delta S$ for heating of the liquid from the melting temperature to the boiling point.

The preceding discussion and Example Problem 5.9 show how numerical values of the entropy for a specific substance can be determined at a standard pressure of 1 bar for different values of the temperature. These numerical values can then be used to calculate entropy changes in chemical reactions, as will be shown in Section 5.10.
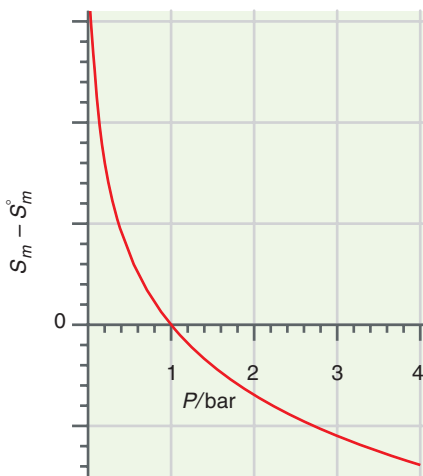
# 5.9 Standard States in Entropy Calculations

As discussed in Chapter 4, changes in $U$ and $H$ are calculated using the result that $\Delta H_f$ values for pure elements in their standard state at a pressure of 1 bar and a temperature of 298.15 K are zero. For $S$, the third law provides a natural definition of zero, namely, the crystalline state at zero kelvin. Therefore, the absolute entropy of a compound as a given temperature can be experimentally determined from heat capacity measurements as described in the previous section. The entropy is a also a function of pressure, and tabulated values of entropies refer to a standard pressure of 1 bar. The value of $S$ varies most strongly with $P$ for a gas. From Equation (5.19), for an ideal gas at constant $T$,

$$\Delta S_m = R\,\ln\frac{V_f}{V_i} = -R\,\ln\frac{P_f}{P_i} \qquad (5.39)$$

Choosing $P_i = P^{\circ} = 1$ bar,

$$S_m(P) = S_m^{\circ} - R\,\ln\frac{P(\text{bar})}{P^{\circ}} \qquad (5.40)$$

Figure 5.12 shows a plot of the molar entropy of an ideal gas as a function of pressure. It is seen that as $P \to 0$, $S_m \to \infty$. This is a consequence of the fact that as $P \to 0$, $V \to \infty$. As Equation (5.18) shows, the entropy becomes infinite in this limit.



**FIGURE 5.12**
The molar entropy of an ideal gas is shown as a function of the gas pressure. By definition, at 1 bar, $S_m = S_m^{\circ}$, the standard state molar entropy.

Equation (5.40) provides a way to calculate the entropy of a gas at any pressure. For solids and liquids, $S$ varies so slowly with $P$, as shown in Section 5.4 and Example Problem 5.6, that the pressure dependence of $S$ can usually be neglected.

# 5.10 Entropy Changes in Chemical Reactions

The entropy change in a chemical reaction is a major factor in determining the equilibrium concentration in a reaction mixture. In an analogous fashion to calculating $\Delta H_R^\circ$ and $\Delta U_R^\circ$ for chemical reactions, $\Delta S_R^\circ$ is equal to the difference in the entropies of products and reactants, which can be written as

$$\Delta S_R^\circ = \sum_i v_i S_i^\circ \qquad (5.41)$$

In Equation (5.41), the stoichiometric coefficients $v_i$ are positive for products and negative for reactants. For example, in the reaction

$$Fe_3O_4(s) + 4 H_2(g) \rightarrow 3 Fe(s) + 4 H_2O(l) \qquad (5.42)$$
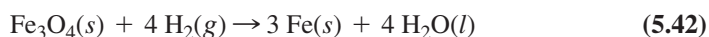
the entropy change under standard state conditions of 1 bar and 298.15 K is given by

$$\Delta S_{R,298.15}^\circ = 3S_{298.15}^\circ(Fe, s) + 4S_{298.15\,K}^\circ(H_2O, l) - S_{298.15}^\circ(Fe_3O_4, s) - 4S_{298.15}^\circ(H_2, g)$$

$$= 3 \times 27.28 \text{ J K}^{-1}\text{mol}^{-1} + 4 \times 69.61 \text{ J K}^{-1}\text{mol}^{-1} - 146.4 \text{ J K}^{-1}\text{mol}^{-1}$$

$$- 4 \times 130.684 \text{ J K}^{-1}\text{mol}^{-1}$$

$$= -308.9 \text{ J K}^{-1}\text{mol}^{-1}$$

For this reaction, $\Delta S_R^\circ$ is large and negative, primarily because gaseous species are consumed in the reaction, and none are generated. $\Delta S_R^\circ$ is generally positive for $\Delta n > 0$, and negative for $\Delta n < 0$ where $\Delta n$ is the change in the number of moles of gas in the overall reaction.

Tabulated values of $S_m^\circ$ are generally available at the standard temperature of 298.15 K, and values for selected elements and compounds are listed in Tables 4.1 and 4.2 (see Appendix A, Data Tables). However, it is often necessary to calculate $\Delta S^\circ$ at other temperatures. Such calculations are carried out using the temperature dependence of $S$ discussed in Section 5.4:

$$\Delta S_{R,T}^\circ = \Delta S_{R,298.15}^\circ + \int_{298.15}^{T} \frac{\Delta C_P^\circ}{T'} dT' \qquad (5.43)$$

This equation is only valid if no phase changes occur in the temperature interval between 298.15 K and $T$. If phase changes occur, the associated entropy changes must be included as they were in Equation (5.38).

## EXAMPLE PROBLEM 5.10

The standard entropies of CO, $CO_2$, and $O_2$ at 298.15 K are

$$S_{298.15}^\circ(CO, g) = 197.67 \text{ J K}^{-1}\text{mol}^{-1}$$

$$S_{298.15}^\circ(CO_2, g) = 213.74 \text{ J K}^{-1}\text{mol}^{-1}$$

$$S_{298.15}^\circ(O_2, g) = 205.138 \text{ J K}^{-1}\text{mol}^{-1}$$

The temperature dependence of constant pressure heat capacity for CO, $CO_2$, and $O_2$ is given by

$$\frac{C_{P,m}(CO, g)}{\text{J K}^{-1}\text{mol}^{-1}} = 31.08 - 1.452 \times 10^{-2}\frac{T}{K} + 3.1415 \times 10^{-5}\frac{T^2}{K^2} - 1.4973 \times 10^{-8}\frac{T^3}{K^3}$$

$$\frac{C_{P,m}(CO_2, g)}{J\,K^{-1}\,mol^{-1}} = 18.86 + 7.937 \times 10^{-2}\frac{T}{K} - 6.7834 \times 10^{-5}\frac{T^2}{K^2} + 2.4426 \times 10^{-8}\frac{T^3}{K^3}$$

$$\frac{C_{P,m}(O_2, g)}{J\,K^{-1}\,mol^{-1}} = 30.81 - 1.187 \times 10^{-2}\frac{T}{K} + 2.3968 \times 10^{-5}\frac{T^2}{K^2}$$

Calculate $\Delta S_R^\circ$ for the reaction $CO(g) + 1/2\,O_2(g) \rightarrow CO_2(g)$ at 475.0 K.

**Solution**

$$\frac{\Delta C_{P,m}}{J\,K^{-1}\,mol^{-1}} = \left(18.86 - 31.08 - \frac{1}{2} \times 30.81\right)$$

$$+ \left(7.937 + 1.452 + \frac{1}{2} \times 1.187\right) \times 10^{-2}\frac{T}{K}$$

$$- \left(6.7834 + 3.1415 + \frac{1}{2} \times 2.3968\right) \times 10^{-5}\frac{T^2}{K^2}$$

$$+ (2.4426 + 1.4973) \times 10^{-8}\frac{T^3}{K^3}$$

$$= -27.625 + 9.9825 \times 10^{-2}\frac{T}{K} - 1.1123 \times 10^{-4}\frac{T^2}{K^2} + 3.9399 \times 10^{-8}\frac{T^3}{K^3}$$

$$\Delta S_R^\circ = S_{R\,298.15}^\circ(CO_2, g) - S_{298.15}^\circ(CO, g) - \frac{1}{2} \times S_{298.15}^\circ(O_2, g)$$

$$= 213.74\,J\,K^{-1}\,mol^{-1} - 197.67\,J\,K^{-1}\,mol^{-1} - \frac{1}{2} \times 205.138\,J\,K^{-1}\,mol^{-1}$$

$$= -86.50\,J\,K^{-1}\,mol^{-1}$$

$$\Delta S_{R,T}^\circ = \Delta S_{R\,298.15}^\circ + \int_{298.15}^{T} \frac{\Delta C_P}{T'}\,dT'$$

$$= -86.50\,J\,K^{-1}\,mol^{-1}$$

$$+ \int_{298.15}^{475} \frac{\left(-27.63 + 9.983 \times 10^{-2}\frac{T}{K} - 1.112 \times 10^{-4}\frac{T^2}{K^2} + 3.940 \times 10^{-8}\frac{T^3}{K^3}\right)}{\frac{T}{K}}\,d\frac{T}{K}\,J\,K^{-1}\,mol^{-1}$$

$$= -86.50\,J\,K^{-1}\,mol^{-1} + (-12.866 + 17.654 - 7.604 + 1.0594)\,J\,K^{-1}\,mol^{-1}$$

$$= -86.50\,J\,K^{-1}\,mol^{-1} - 1.757\,J\,K^{-1}\,mol^{-1} = -88.26\,J\,K^{-1}\,mol^{-1}$$

The value of $\Delta S_R^\circ$ is negative at both temperatures because the number of moles of gaseous species is reduced in the reaction.

SUPPLEMENTAL

# 5.11 Energy Efficiency: Heat Pumps, Refrigerators, and Real Engines

Thermodynamics provides the tools to study the release of energy through chemical reactions or physical processes such as light harvesting to do work or generate heat. As Earth's population continues to increase in the coming decades and per capita energy consumption also rises, the need for energy in various forms will rise rapidly. Electricity is a major component of this energy demand and fossil fuels are expected to be the major source for electricity production for the foreseeable future. The increased
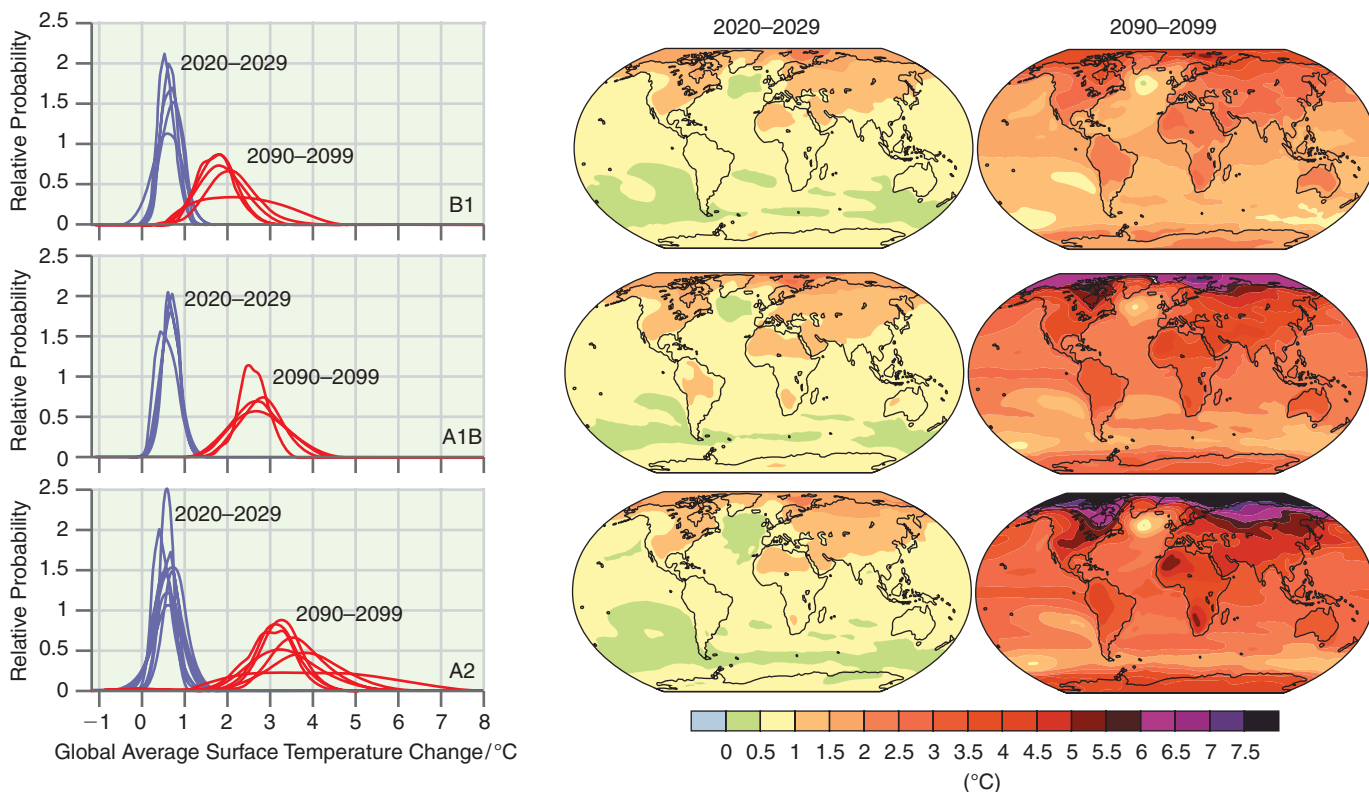
**FIGURE 5.13**

Projected surface temperature increase (right panel) for different scenarios of greenhouse emissions (left panel). Each curve in the left panel represents a different scenario. The uncertainty in the predicted temperature increase is represented by the width of a curve. Note that the most probable temperature increase is similar for nearly all scenarios.

*Source:* Climate Change 2007: The Physical Science Basis. Working Group I Contribution to the Fourth Assessment Report of the Intergovernmental Panel on Climate Change, Figure SPM.6. Cambridge University Press.

combustion of fossil fuels will continue the rapid increase in the $CO_2$ concentration in the atmosphere that began with the Industrial Revolution.

The increase in the atmospheric $CO_2$ concentration is expected to lead to a significant increase in the global average surface temperature as shown for different scenarios of the rate of atmospheric $CO_2$ increase in Figure 5.13. For details on the scenarios and the possible consequences of this temperature increase, which include flooding of land areas near sea level, acidification of the oceans leading to coral reef disappearance, and more severe droughts and storms, see the Intergovernmental Panel on Climate Change website at www.ipcc.ch/.

In order to slow or to reverse the buildup of greenhouse gases in the atmosphere, we must move to energy sources that do not generate greenhouse gases, and develop ways to capture greenhouses gases produced in the combustion of fossil fuels. We must also find ways to do more with less energy input. Table 5.2 shows that the per capita energy use in the United States is substantially higher than in other regions and nations with similar climates and living standards.

**TABLE 5.2   Per Capita Energy Use 2005**

| Nation or region | Per capita energy use/(mega BTU) 1 J = 1054 BTU | Ratio to U.S. per capita use |
|---|---|---|
| United States | 340 | 1 |
| Eurasia | 160 | 0.429 |
| Europe | 146 | 0.471 |
| Africa | 16.1 | 0.0473 |
| World | 71.8 | 0.211 |
| France | 181 | 0.532 |
| Germany | 176 | 0.518 |

*Source:* U.S. Energy Information Administration

The energy flow in the United States for 2002 through various sectors of the economy is shown in Figure 5.14. The parallel pathway for $CO_2$ emissions into the atmosphere is shown in Figure 5.15. By comparing the useful and lost energy, it is seen that 62% of the energy is lost in the form of heat including friction in engines and turbines, resistive losses in the distribution of electricity, and heat loss from poorly insulated buildings. Our study of heat engines such as coal or natural gas fired electricity generation plants shows that the conversion of heat to work cannot be achieved with an efficiency of 100% even if dissipative processes such as friction are neglected. Therefore, significant losses are inevitable, but substantial increases in energy efficiency are possible, as will be discussed later. Electricity generation by wind turbines, photovoltaic panels, hydroelectric plants, and fuel cells (See Section 11.13) is of particular importance because it involves the conversion of one form of work to another. The efficiency for these methods is not subject to the limitations imposed on the conversion of heat to work by the second law.

What can we learn from thermodynamics to use less energy and achieve the same goals? To address this question, consider how energy is used in the residential sector as shown in Figure 5.16. Space and water heating account for 47% of residential energy usage, and electrical energy is often used for these purposes. Both space and water heating can be provided with significantly less energy input using an electrically powered heat pump.
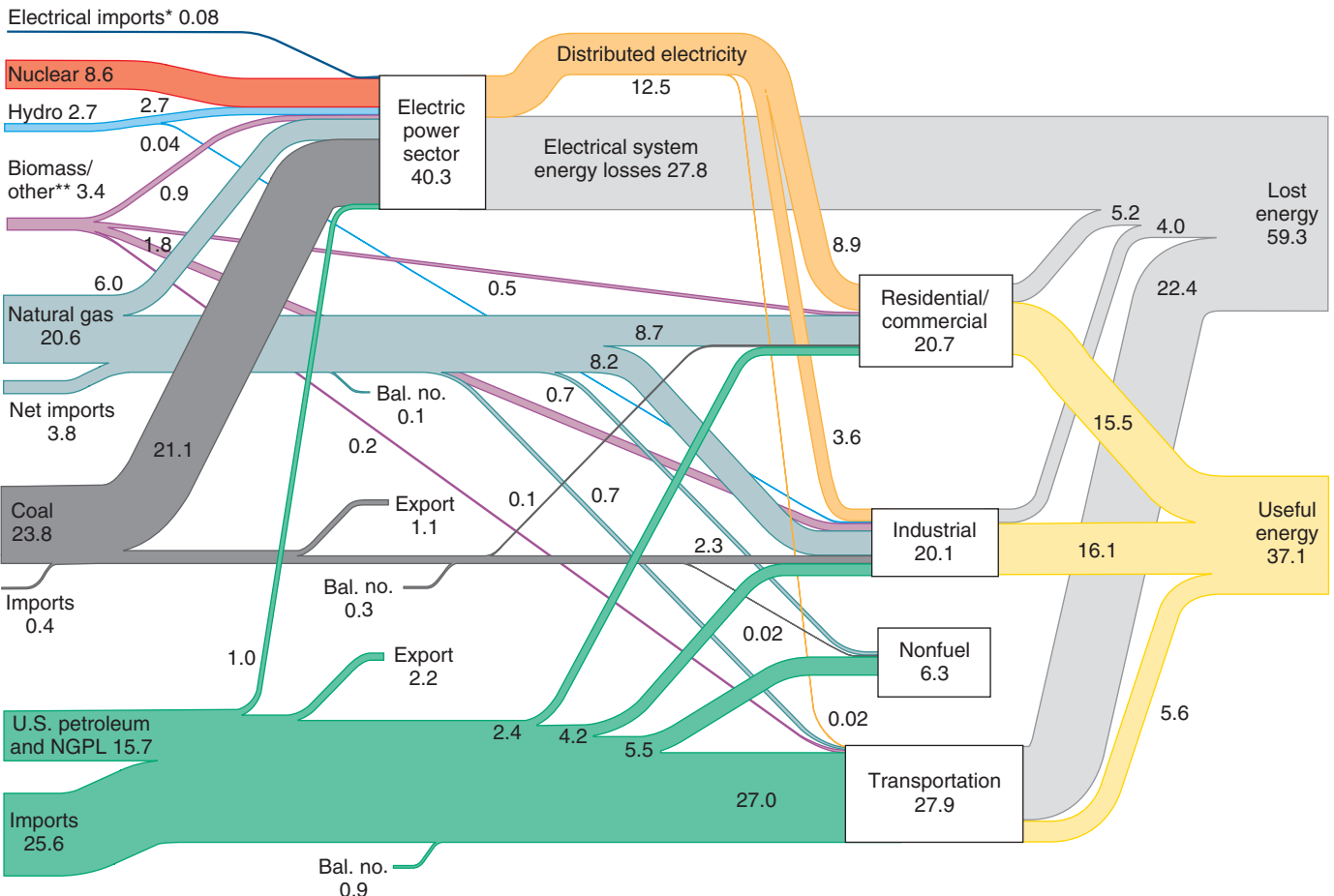
In an idealized reversible **heat pump,** the Carnot cycle in Figure 5.2 is traversed in the opposite direction. The signs of $w$ and $q$ in the individual segments and the signs of the overall $w$ and $q$ are changed. Heat is now withdrawn from the cold reservoir (the surroundings) and deposited in the home, which is the hot reservoir. Because this is not

**FIGURE 5.14**

U.S. energy flow trends for 2002. The energy contributions from different sources to each economic sector such as electrical power are shown together with net useful and lost energy for each sector. Note that 62% of the total consumed energy in all sectors is lost.

*Source:* Lawrence Livermore National Laboratory, U.S. Department of Energy

U.S. Energy Flow Trends – 2002
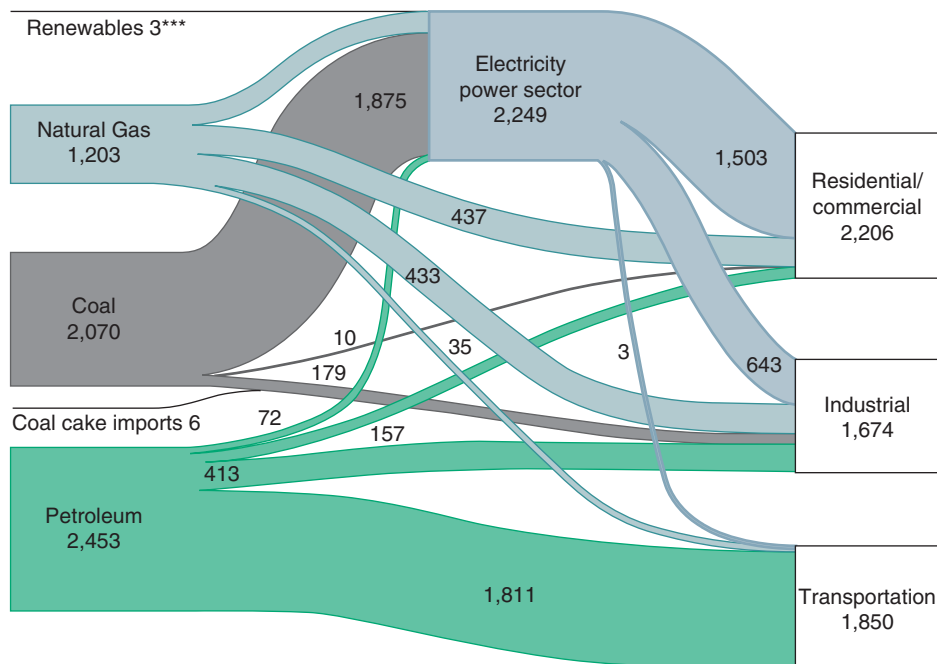Net Primary Resource Consumption ~103 Exajoules

U.S. 2002 Carbon Dioxide Emissions from Energy
Consumption – 5,682* Million Metric Tons of CO$_2$**



Source: Energy Information Administration. *Emissions of Greenhouse Gases in the United States 2002.* Tables 4–10.
*Includes adjustments of 42.9 million metric tons of carbon dioxide from U.S. territories, less 90.2 MtCO$_2$ from international and military bunker fuels.
**Previous versions of this chart showed emissions in metric tons of carbon, not of CO$_2$.
***Municipal solid waste and geothermal energy.
Note: Numbers may not equal sum of components because of independent rounding.

**FIGURE 5.15**
U.S. carbon dioxide emissions from energy consumption for 2002. The pathways of CO$_2$ generation in three economic sectors are shown together with a breakdown in the three fossil fuel sources of natural gas, coal, and petroleum.
*Source:* Lawrence Livermore National Laboratory, U.S. Department of Energy

a spontaneous process, work must be done on the system to effect this direction of heat flow. The heat and work flow for a heat pump is shown in Figure 5.17b.

A heat pump is used to heat a building by extracting heat from a colder thermal reservoir such as a lake, the ground, or the ambient air. The **coefficient of performance** of a heat pump, $\eta_{hp}$, is defined as the ratio of the heat pumped into the hot reservoir to the work input to the heat pump:

$$\eta_{hp} = \frac{q_{hot}}{w} = \frac{q_{hot}}{q_{hot} + q_{cold}} = \frac{T_{hot}}{T_{hot} - T_{cold}} \quad (5.44)$$

Assume that $T_{hot}$ = 294 K and $T_{cold}$ = 278 K, typical for a mild winter day. The maximum $\eta_{hp}$ value is calculated to be 18. Such high values cannot be attained for real heat pumps operating in an irreversible cycle with dissipative losses. Typical values for commercially available heat pumps lie in the range of 3 to 4. This means that for every joule of electrical work supplied to the heat pump, 3 to 4 J of heat are made available for space heating.

Heat pumps become less effective as $T_{cold}$ decreases, as shown by Equation (5.44). Therefore, geothermal heat pumps, which use ~55°F soil 6–10 feet below Earth's surface rather than ambient air as the cold reservoir, are much more efficient in cold climates than air source heat pumps. Note that a coefficient of performance of 3.5 for a heat pump means that a house can be heated using 29% of the electrical power consumption that would be required to heat the same house using electrical baseboard heaters. This is a significant argument for using heat pumps for residential heating. Heat pumps can also be used to heat water. Assuming a heat pump coefficient of performance of 3.5, the energy usage of a typical household can be reduced by 35% simply by replacing electrical water heaters and electrical baseboard heaters by heat pumps, which pay for the increased initial cost by lower monthly electricity bills within a few years. The flow of CO$_2$ into the atmosphere is reduced by the same
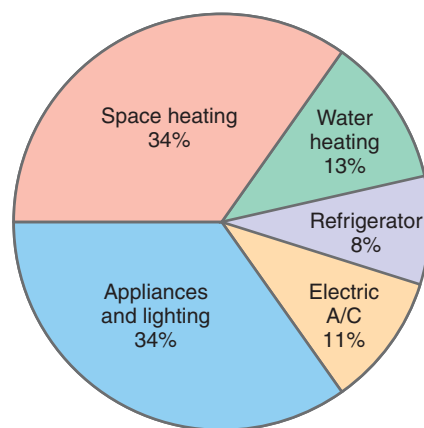


**FIGURE 5.16**
Distribution of U.S. residential energy use among household needs.
*Source:* U.S. Energy Information Agency

**FIGURE 5.17**
Reverse heat engines can be used to induce heat flow from a cold reservoir to a hot reservoir with the input of work. **(a)** Refrigerator: the cold reservoir is the interior of a refrigerator, and the hot reservoir is the room in which the refrigerator is located. **(b)** Heat pump: the cold reservoir is water-filled pipes buried in the ground, and the hot reservoir is the interior of the house to be heated. The relative widths of the two paths entering the hot reservoir show that a small amount of work input can move a larger amount of heat from the cold to the hot reservoir. In both cases, the engine is a compressor.



Hot reservoir

Work

Cold reservoir

**(a)**



Hot reservoir

Work

Cold reservoir

**(b)**
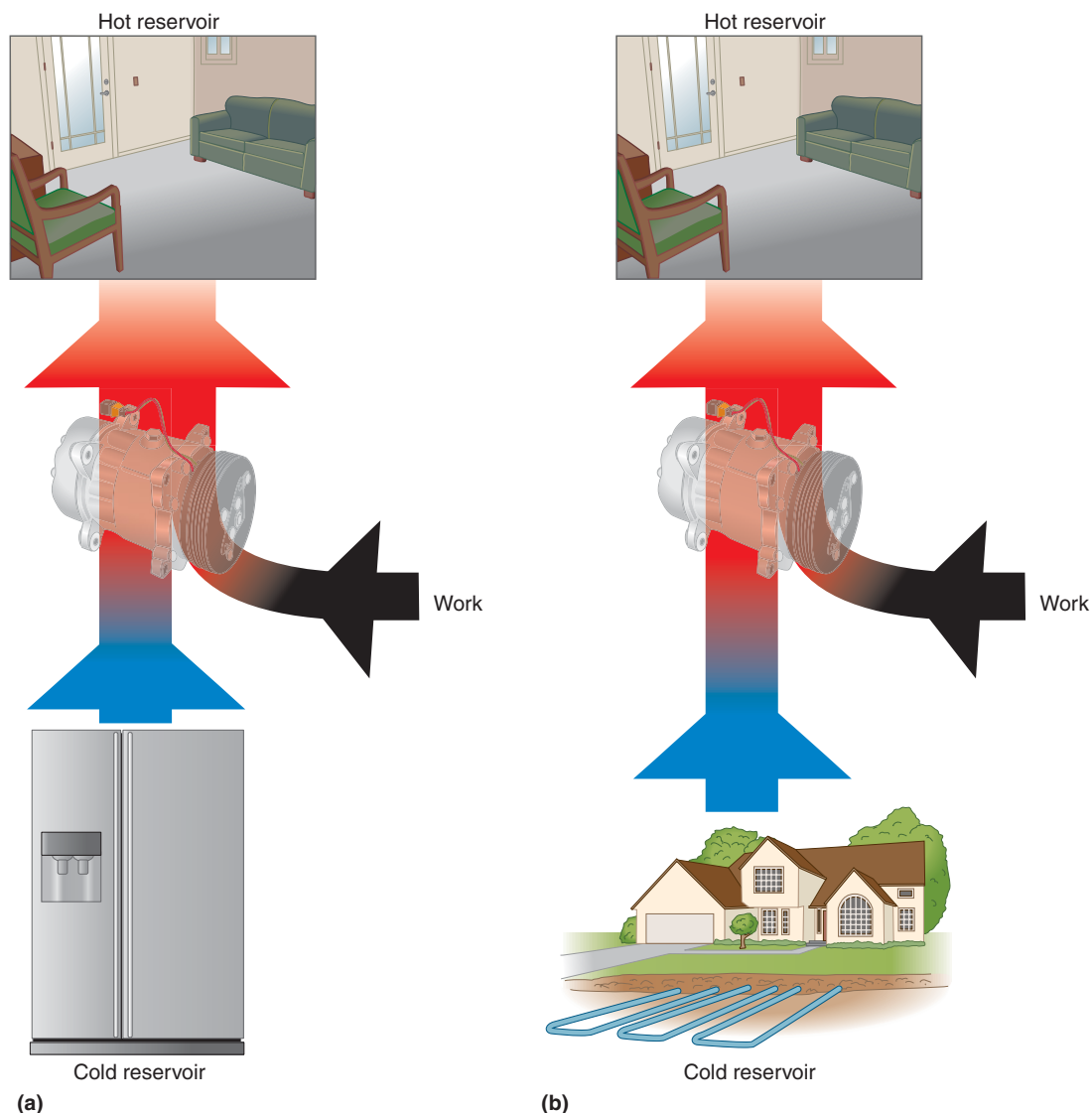
amount. Houses can be designed to significantly reduce total energy use. The "Passive House" uses a small fraction of the energy needed to operate a typical house. More than 15,000 of these houses have been built in Europe and as of 2010, only 13 have been built in the United States. For more information on the Passive House concept, see http://www.passivehouse.us/passiveHouse/PHIUSHome.html.

A **refrigerator** is also a heat engine operated in reverse. (Figure 5.17a). The interior of the refrigerator is the system, and the room in which the refrigerator is situated is the hot reservoir. Because more heat is deposited in the room than is withdrawn from the interior of the refrigerator, the overall effect of such a device is to increase the temperature of the room. However, the usefulness of the device is that it provides a cold volume for food storage. The coefficient of performance, $\eta_r$, of a reversible Carnot refrigerator is defined as the ratio of the heat withdrawn from the cold reservoir to the work supplied to the device:

$$\eta_r = \frac{q_{cold}}{w} = \frac{q_{cold}}{q_{hot} + q_{cold}} = \frac{T_{cold}}{T_{hot} - T_{cold}} \tag{5.45}$$

This formula shows that as $T_{cold}$ decreases from $0.9 \, T_{hot}$ to $0.1 \, T_{hot}$, $\eta_r$ decreases from 9 to 0.1. Equation (5.44) states that if the refrigerator is required to provide a lower temperature, more work is required to extract a given amount of heat.

A household refrigerator typically operates at 255 K in the freezing compartment, and 277 K in the refrigerator section. Using the lower of these temperatures for the cold

reservoir and 294 K as the temperature of the hot reservoir (the room), the maximum $\eta_r$ value is 6.5. This means that for every joule of work done on the system, 6.5 J of heat can be extracted from the contents of the refrigerator. This is the maximum coefficient of performance, and it is only applicable to a refrigerator operating in a reversible Carnot cycle with no dissipative losses. Taking losses into account, it is difficult to achieve $\eta_r$ values greater than ~1.5 in household refrigerators. This shows the significant loss of efficiency in an irreversible dissipative cycle.

It is also instructive to consider refrigerators and heat pumps from an entropic point of view. Transferring an amount of heat, $q$, from a cold reservoir to a hot reservoir is not a spontaneous process in an isolated system, because

$$\Delta S = q\left(\frac{1}{T_{hot}} - \frac{1}{T_{cold}}\right) < 0 \qquad (5.46)$$

However, work can be converted to heat with 100% efficiency. Therefore, the coefficient of performance, $\eta_r$, can be calculated by determining the minimum amount of work input required to make $\Delta S$ for the withdrawal of $q$ from the cold reservoir, together with the deposition of $q + w$ in the hot reservoir, a spontaneous process.

We have seen that a heat engine cannot convert heat into electricity with 100% efficiency because some of the heat is injected into the cold reservoir. The cold reservoir in electrical generation plants is generally the atmosphere. Generally, heat and electricity are produced separately as shown in Figure 5.18a. However, it is possible to increase the efficiency of the overall process by collecting the waste heat from electricity production and using it to heat buildings as shown in Figure 5.18b in a process called cogeneration. An example of cogeneration is to burn a fuel such as coal to generate steam that is used to drive a turbine that generates electricity. The steam exiting the turbine is still at a high temperature and can be used to heat buildings. In New York City, many buildings are heated using steam generated to produce electricity. Because of losses in piping heat over long distances, cogeneration is most suitable for urban areas. The U.S. Department of Energy has set a goal of having 20% of the electricity produced by cogeneration by the year 2030.

Further possible increases in energy efficiency in the household sector include cooking and lighting. Traditional electric cooktops use either natural gas or electricity to create heat, which is transferred to the cooking pot and its contents by conduction and convection. About 45% of the energy produced by the combustion of natural gas
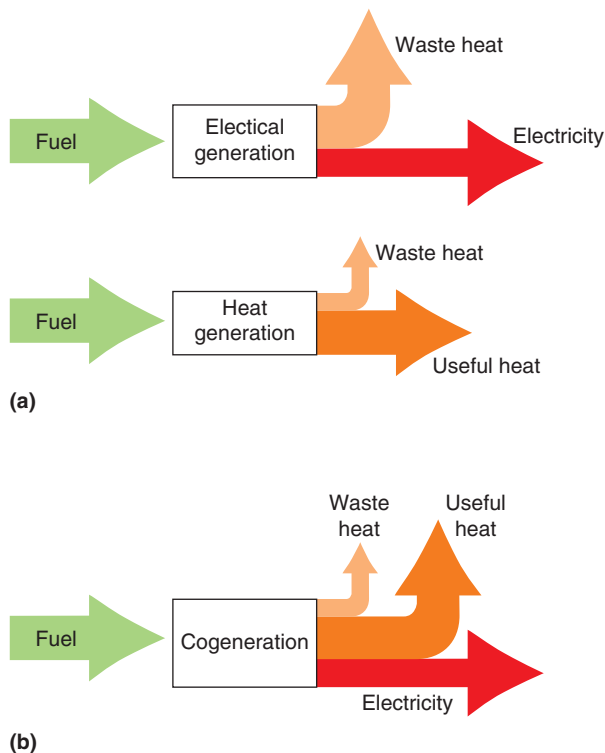


(a)

(b)

**FIGURE 5.18**
(a) Conventionally, electricity and heat for buildings are produced separately. Waste heat is produced in each process. (b) Using cogeneration, most of the waste heat generated in electricity production is used to heat buildings.

and 35% of the electrical energy is lost because the air rather than the pot is heated. The most efficient method for cooking is induction cooking, in which an induction coil generates a magnetic field that induces heating in metal cookware placed on top of it. Although the efficiency of this method is 90%, the initial investment is significantly greater than for a gas or electric range. Traditional lighting technology is very inefficient, with incandescent lights converting only 2% of the electrical work required to heat the tungsten filament to visible light. The remaining 98% of the radiated energy appears as heat. Fluorescent lights, which are much more efficient, contain a small amount of Hg vapor that emits UV light from an excited state created by an electrical discharge. The UV light is absorbed by a fluorescent coating on the surface of the bulb, which radiates the light in the visible spectrum. The fraction of the emitted light in the visible spectrum is much larger than in incandescent lighting. For this reason, fluorescent lighting is a factor of 5 to 6 more efficient. Australia has plans to ban the use of incandescent lighting in favor of fluorescent lighting because of its low efficiency. LED lighting (light emitting diodes) is a rapidly growing sector of lighting. LED lights have an efficiency similar to fluorescent lighting, but are more compact and can be highly directed or diffuse sources of light.

Because the transportation sector is a major user of energy, we next discuss real engines, using the Otto engine, typically used in automobiles, and the diesel engine as examples. The **Otto engine** is the most widely used engine in automobiles. The engine cycle consists of four strokes as shown in Figure 5.19. The intake valve opens as the piston is moving downward, drawing a fuel–air mixture into the cylinder. The intake valve is closed, and the mixture is compressed as the piston moves upward. Just after the piston has reached its highest point, the fuel–air mixture is ignited by a spark plug, and the rapid heating resulting from the combustion process causes the gas to expand and the pressure to increase. This drives the piston down in a power stroke. Finally, the combustion products are forced out of the cylinder by the upward-moving piston as the exhaust valve is opened. To arrive at a maximum theoretical efficiency for the Otto engine, the reversible Otto cycle shown in Figure 5.20a is analyzed, assuming reversibility.

The reversible Otto cycle begins with the intake stroke $e \rightarrow c$, which is assumed to take place at constant pressure. At this point, the intake valve is closed, and the piston compresses the fuel–air mixture along the adiabatic path $c \rightarrow d$ in the second step. This path can be assumed to be adiabatic because the compression occurs too rapidly to allow much heat to be transferred out of the cylinder. Ignition of the fuel–air mixture takes place at $d$. The rapid increase in pressure takes place at constant volume. In this reversible cycle, the combustion is modeled as a quasi-static heat transfer from a series of reservoirs at temperatures ranging from $T_d$ to $T_a$. The power stroke is modeled as the adiabatic expansion $a \rightarrow b$. At this point, the exhaust valve opens and the gas is expelled. This step is modeled as the constant volume pressure decrease $b \rightarrow c$. The upward movement of the piston expels the remainder of the gas along the line $c \rightarrow e$, after which the cycle begins again.
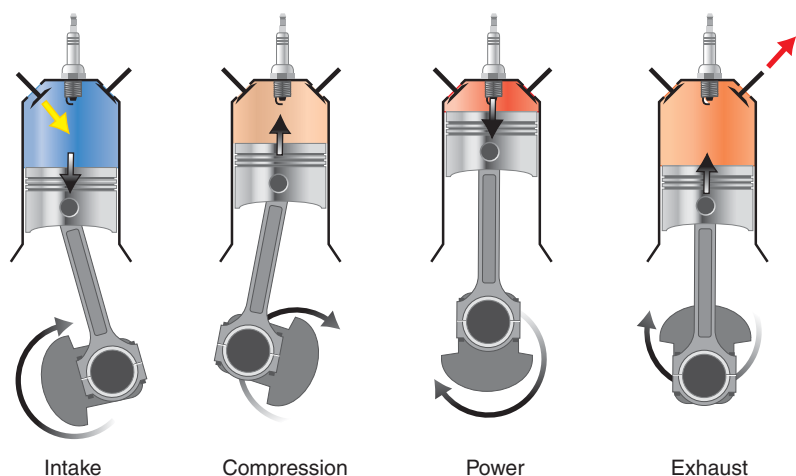


**FIGURE 5.19**
Illustration of the four-stroke cycle of an Otto engine, as explained in the text. The left valve is the intake valve, and the right valve is the exhaust valve.

Intake          Compression          Power          Exhaust

The efficiency of this reversible cyclic engine can be calculated as follows. Assuming $C_V$ to be constant along the segments $d \rightarrow a$ and $b \rightarrow c$, we write

$$q_{hot} = C_V(T_a - T_d) \quad \text{and} \quad q_{cold} = C_V(T_b - T_c) \tag{5.47}$$

The efficiency is given by

$$\varepsilon = \frac{q_{hot} + q_{cold}}{q_{hot}} = 1 - \frac{q_{cold}}{q_{hot}} = 1 - \left(\frac{T_b - T_c}{T_a - T_d}\right) \tag{5.48}$$

The temperatures and volumes along the reversible adiabatic segments are related by

$$T_c V_c^{\gamma-1} = T_d V_d^{\gamma-1} \quad \text{and} \quad T_b V_c^{\gamma-1} = T_a V_d^{\gamma-1} \tag{5.49}$$

because $V_b = V_c$ and $V_d = V_e$. Recall that $\gamma = C_P/C_V$. $T_a$ and $T_b$ can be eliminated from Equation (5.48) to give

$$\varepsilon = 1 - \frac{T_c}{T_d} \tag{5.50}$$

where $T_c$ and $T_d$ are the temperatures at the beginning and end of the compression stroke $c \rightarrow d$. Temperature $T_c$ is fixed at ~300 K, and the efficiency can be increased only by increasing $T_d$. This is done by increasing the compression ratio, $V_c/V_d$. However, if the compression ratio is too high, $T_d$ will be sufficiently high that the fuel ignites before the end of the compression stroke. A reasonable upper limit for $T_d$ is 600 K, and for $T_c = 300$ K, $\varepsilon = 0.50$. This value is an upper limit, because a real engine does not operate in a reversible cycle, and because heat is lost along the $c \rightarrow d$ segment. Achievable efficiencies in Otto engines used in passenger cars lie in the range of 0.20 to 0.30. However, additional losses occur in the drive chain, in tire deformation and in displacing air as the vehicle moves. As shown in Figure 5.14, the overall efficiency of the transportation sector is only 20%.

In the **diesel engine** depicted in Figure 5.20b, higher compression ratios are possible because only air is let into the cylinder in the intake stroke. The fuel is injected into the cylinder at the end of the compression stroke, thus avoiding spontaneous ignition of the fuel–air mixture during the compression stroke $d \rightarrow a$. Because $T \sim 950$ K for the compressed air, combustion occurs spontaneously without a spark plug along the constant pressure segment $a \rightarrow b$ after fuel injection. Because the fuel is injected over a time period in which the piston is moving out of the cylinder, this step can be modeled as a constant-pressure heat intake. In this segment, it is assumed that heat is absorbed from a series of reservoirs at temperatures between $T_a$ and $T_b$ in a quasi-static process. In the other segments, the same processes occur as described for the reversible Otto cycle.

The heat intake along the segment $a \rightarrow b$ is given by

$$q_{hot} = C_p(T_b - T_a) \tag{5.51}$$

and $q_{cold}$ is given by Equation (5.47). Therefore, the efficiency is given by

$$\varepsilon = 1 - \frac{1}{\gamma}\left(\frac{T_c - T_d}{T_b - T_a}\right) \tag{5.52}$$

Similarly to the treatment of the Otto engine, $T_b$ and $T_c$ can be eliminated from Equation (5.52), and the expression

$$\varepsilon = 1 - \frac{1}{\gamma}\frac{\left(\dfrac{V_b}{V_d}\right)^\gamma - \left(\dfrac{V_a}{V_d}\right)^\gamma}{\left(\dfrac{V_b}{V_d}\right) - \left(\dfrac{V_a}{V_d}\right)} \tag{5.53}$$

can be derived. For typical values $V_b/V_d = 0.2, V_a/V_d = 1/15$, $\gamma = 1.5$, and $\varepsilon = 0.64$. The higher efficiency achievable with the diesel cycle in comparison with the Otto cycle is a result of the higher temperature attained in the compression cycle. Real diesel engines used in trucks and passenger cars have efficiencies in the range of 0.30 to 0.35.
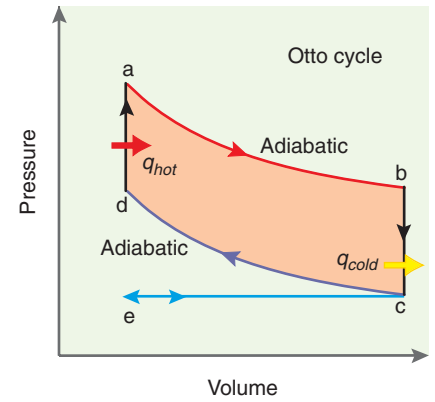
(a)
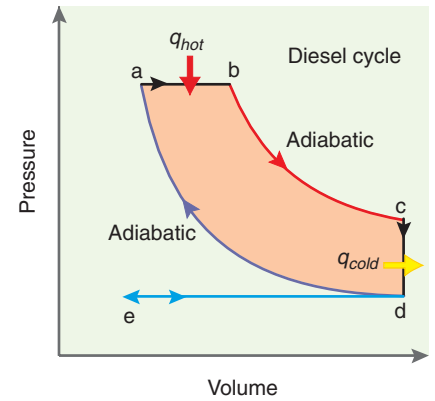
(b)

**FIGURE 5.20**
Idealized reversible cycles of the (a) Otto and (b) diesel engines.

Just as for space heating, the energy usage in the U.S. transportation sector can be drastically reduced. The U.S. personal vehicle fleet currently averages 27.5 miles per gallon of gasoline. The corresponding figure for the European Union, where gasoline prices are more than twice as high as in the United States, is 43 miles per gallon, corresponding to 130 g $CO_2$ emission per kilometer. Hybrid gasoline–electric vehicles (Figure 5.21b) that use electrical motors to power the vehicle at low speeds, switch automatically to an Otto engine at higher speeds, and use regenerative braking to capture the energy used to slow the vehicle are currently the most efficient vehicles, averaging more than 50 miles per gallon. Purely electric vehicles (Figure 5.21a) and plug-in hybrids, which will allow the batteries that power the electrical operation mode to be recharged at the owner's residence are expected to be available in 2011. Advances in battery technology are likely to make the use of electrical vehicles more widespread in the near future.

Automobiles that use fuel cells (See Section 11.13) as a power source are of particular interest for future development because the work arising from a chemical reaction can be converted to work with 100% efficiency (ignoring dissipative losses), rather than first capturing the heat from the reaction and subsequently (partially) converting the heat to work.

Reversing global climate change requires that energy be generated without also producing $CO_2$. Hydrogen meets this need and can be used in internal combustion engines without substantial modifications. Currently, 96% of the $H_2$ consumed worldwide is produced using fossil fuels, primarily through steam reforming of methane. Reversing global climate change would require that $H_2$ be produced using water electrolysis and electricity from renewable resources such as wind, solar, hydroelectric, or nuclear power. At present, such processes are not cost competitive, but rising oil prices and the falling cost of renewable energy may change this balance. A further unsolved problem for vehicular use is $H_2$ storage. The volumetric energy density of liquid $H_2$ (boiling temperature 20 K) is a factor of 4 below that of gasoline, and solid hydrides from which $H_2$ can be released at ambient temperature have a much lower energy density.

A possible alternative to the current fossil fuel economy is a methanol economy (see G. A. Olah et al., *Beyond Oil and Gas: The Methanol Economy*, Wiley-VCH, 2006). Methanol is a suitable fuel for internal combustion engines and has half the volumetric energy density of gasoline. It is also a good source for producing synthetic hydrocarbons, which could replace petroleum feedstocks widely used in the chemical industry. As shown in Figure 5.22, methanol could be synthesized by recycling $CO_2$ if hydrogen generated using renewable energy were available in sufficient quantities. An initial source of $CO_2$ could be coal-fired electrical plants, and it is conceivable that in the future $CO_2$ could be extracted from the atmosphere (See the previous reference for details.). These pathways would slow or reverse global climate change.

**FIGURE 5.21**

The Nissan Leaf **(a)** is a purely electric vehicle with an estimated range between 47 and 138 miles between recharging cycles, depending on driving conditions. The Chevrolet Volt **(b)** is an electric vehicle that has a small gasoline motor that can recharge the batteries used to power the vehicle. The U.S. Environmental Protection Agency has given the Leaf and Volt energy consumption ratings of 99 and 60 miles per gallon, respectively, using 33.7 kW-hrs as being equivalent in energy to one gallon of gasoline.



**(a) Nissan Leaf**



**(b) Chevrolet Volt**
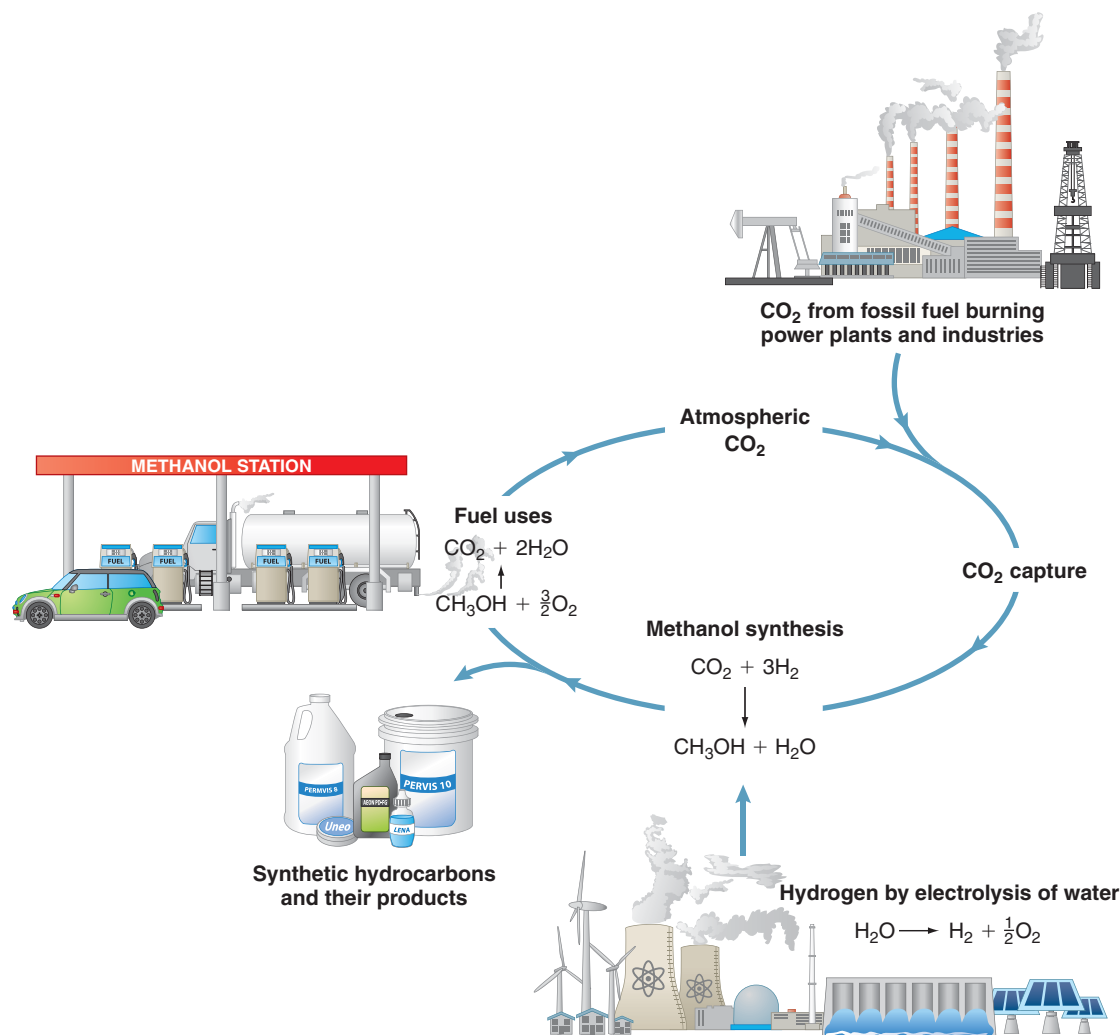
**SUPPLEMENTAL**

## 5.12 Using the Fact that *S* Is a State Function to Determine the Dependence of *S* on *V* and *T*

Section 5.4 showed how the entropy varies with *P*, *V*, and *T* for an ideal gas. In this section, we derive general equations for the dependence of *S* on *V* and *T* that can be applied to solids, liquids, and real gases. We do so by using the property that *dS* is an exact differential. A similar analysis of *S* as a function of *P* and *T* is carried out in Section 5.13. Consider Equation (5.30), rewritten in the form

$$dS = \frac{1}{T}dU + \frac{P}{T}dV \tag{5.54}$$

Because $1/T$ and $P/T$ are greater than zero, the entropy of a system increases with the internal energy at constant volume, and increases with the volume at constant internal energy. However, because internal energy is not generally a variable under experimental control, it is more useful to obtain equations for the dependence of *dS* on *V* and *T*.

We first write the total differential *dS* in terms of the partial derivatives with respect to *V* and *T*:

$$dS = \left(\frac{\partial S}{\partial T}\right)_V dT + \left(\frac{\partial S}{\partial V}\right)_T dV \tag{5.55}$$

To evaluate $(\partial S/\partial T)_V$ and $(\partial S/\partial V)_T$, Equation (5.54) for $dS$ is rewritten in the form

$$dS = \frac{1}{T}\left[C_V dT + \left(\frac{\partial U}{\partial V}\right)_T dV\right] + \frac{P}{T}dV = \frac{C_V}{T}dT + \frac{1}{T}\left[P + \left(\frac{\partial U}{\partial V}\right)_T\right]dV \quad (5.56)$$

Equating the coefficients of $dT$ and $dV$ in Equations (5.55) and (5.56),

$$\left(\frac{\partial S}{\partial T}\right)_V = \frac{C_V}{T} \text{ and } \left(\frac{\partial S}{\partial V}\right)_T = \frac{1}{T}\left[P + \left(\frac{\partial U}{\partial V}\right)_T\right] \quad (5.57)$$

The temperature dependence of entropy at constant volume can be calculated straight-forwardly using the first equality in Equation (5.57):

$$dS = \frac{C_V}{T}dT, \text{ constant } V \quad (5.58)$$

The expression for $(\partial S/\partial V)_T$ in Equation (5.57) is not in a form that allows for a direct comparison with experiment to be made. A more useful relation follows from the fact that $dS$ is an exact differential (see Section 3.1):

$$\left(\frac{\partial}{\partial T}\left(\frac{\partial S}{\partial V}\right)_T\right)_V = \left(\frac{\partial}{\partial V}\left(\frac{\partial S}{\partial T}\right)_V\right)_T \quad (5.59)$$

Taking the mixed second derivatives of the expressions in Equation (5.57),

$$\left(\frac{\partial}{\partial V}\left(\frac{\partial S}{\partial T}\right)_V\right)_T = \frac{1}{T}\left(\frac{\partial}{\partial V}\left(\frac{\partial U}{\partial T}\right)_V\right)_T$$

$$\left(\frac{\partial}{\partial T}\left(\frac{\partial S}{\partial V}\right)_T\right)_V = \frac{1}{T}\left[\left(\frac{\partial P}{\partial T}\right)_V + \left(\frac{\partial}{\partial T}\left(\frac{\partial U}{\partial V}\right)_T\right)_V\right] - \frac{1}{T^2}\left[P + \left(\frac{\partial U}{\partial V}\right)_T\right] \quad (5.60)$$

Substituting the expressions for the mixed second derivatives in Equation (5.60) into Equation (5.59), canceling the double mixed derivative of $U$ that appears on both sides of the equation, and simplifying the result, the following equation is obtained:

$$P + \left(\frac{\partial U}{\partial V}\right)_T = T\left(\frac{\partial P}{\partial T}\right)_V \quad (5.61)$$

This equation provides the expression for $(\partial U/\partial V)_T$ that was used without a derivation in Section 3.2. It provides a way to calculate the internal pressure of the system if the equation of state for the substance is known.

Comparing the result in Equation (5.61) with the second equality in Equation (5.57), a practical equation is obtained for the dependence of entropy on volume under constant temperature conditions:

$$\left(\frac{\partial S}{\partial V}\right)_T = \left(\frac{\partial P}{\partial T}\right)_V = -\frac{(\partial V/\partial T)_P}{(\partial V/\partial P)_T} = \frac{\beta}{\kappa} \quad (5.62)$$

where $\beta$ is the coefficient for thermal expansion at constant pressure, and $\kappa$ is the isothermal compressibility coefficient. Both of these quantities are readily obtained from experiments. In simplifying this expression, the cyclic rule for partial derivatives, Equation (3.7) has been used.

The result of these considerations is that $dS$ can be expressed in terms of $dT$ and $dV$ as

$$dS = \frac{C_V}{T}dT + \frac{\beta}{\kappa}dV \quad (5.63)$$

Integrating both sides of this equation along a reversible path yields

$$\Delta S = \int_{T_i}^{T_f}\frac{C_V}{T}dT + \int_{V_i}^{V_f}\frac{\beta}{\kappa}dV \quad (5.64)$$

This result applies to a single-phase system of a liquid, solid, or gas that undergoes a transformation from the initial result $T_i$, $V_i$ to $T_f$, $V_f$, provided that no phase changes or chemical reactions occur in the system.

# 5.13 The Dependence of *S* on *T* and *P*

Because chemical transformations are normally carried out at constant pressure rather than constant volume, we need to know how $S$ varies with $T$ and $P$. The total differential $dS$ is written in the form

$$dS = \left(\frac{\partial S}{\partial T}\right)_P dT + \left(\frac{\partial S}{\partial P}\right)_T dP \tag{5.65}$$

Starting from the relation $U = H - PV$, we write the total differential $dU$ as

$$dU = T\,dS - P\,dV = dH - P\,dV - V\,dP \tag{5.66}$$

This equation can be rearranged to give an expression for $dS$:

$$dS = \frac{1}{T}\,dH - \frac{V}{T}\,dP \tag{5.67}$$

The previous equation is analogous to Equation (5.54), but contains the variable $P$ rather than $V$.

$$dH = \left(\frac{\partial H}{\partial T}\right)_P dT + \left(\frac{\partial H}{\partial P}\right)_T dP = C_P dT + \left(\frac{\partial H}{\partial P}\right)_T dP \tag{5.68}$$

Substituting this expression for $dH$ into Equation (5.67),

$$dS = \frac{C_P}{T}dT + \frac{1}{T}\left[\left(\frac{\partial H}{\partial P}\right)_T - V\right]dP = \left(\frac{\partial S}{\partial T}\right)_P dT + \left(\frac{\partial S}{\partial P}\right)_T dP \tag{5.69}$$

Because the coefficients of $dT$ and $dP$ must be the same on both sides of Equation (5.69),

$$\left(\frac{\partial S}{\partial T}\right)_P = \frac{C_P}{T} \quad \text{and} \quad \left(\frac{\partial S}{\partial P}\right)_T = \frac{1}{T}\left[\left(\frac{\partial H}{\partial P}\right)_T - V\right] \tag{5.70}$$

The ratio $C_P/T$ is positive for all substances, allowing us to conclude that $S$ is a monotonically increasing function of the temperature.

Just as for $(\partial S/\partial V)_T$ in Section 5.12, the expression for $(\partial S/\partial P)_T$ is not in a form that allows a direct comparison with experimental measurements to be made. Just as in our evaluation of $(\partial S/\partial V)_T$, we equate the mixed second partial derivatives of $(\partial S/\partial T)_P$ and $(\partial S/\partial P)_T$:

$$\left(\frac{\partial}{\partial T}\left(\frac{\partial S}{\partial P}\right)_T\right)_P = \left(\frac{\partial}{\partial P}\left(\frac{\partial S}{\partial T}\right)_P\right)_T \tag{5.71}$$

These mixed partial derivatives can be evaluated using Equation (5.70):

$$\left(\frac{\partial}{\partial P}\left(\frac{\partial S}{\partial T}\right)_P\right)_T = \frac{1}{T}\left(\frac{\partial C_P}{\partial P}\right)_T = \frac{1}{T}\left(\frac{\partial}{\partial P}\left(\frac{\partial H}{\partial T}\right)_P\right)_T \tag{5.72}$$

$$\left(\frac{\partial}{\partial T}\left(\frac{\partial S}{\partial P}\right)_T\right)_P = \frac{1}{T}\left[\left(\frac{\partial}{\partial T}\left(\frac{\partial H}{\partial P}\right)_T\right)_P - \left(\frac{\partial V}{\partial T}\right)_P\right] - \frac{1}{T^2}\left[\left(\frac{\partial H}{\partial P}\right)_T - V\right] \tag{5.73}$$

Equating Equations (5.72) and (5.73) yields

$$\frac{1}{T}\left(\frac{\partial}{\partial T}\left(\frac{\partial H}{\partial P}\right)_T\right)_P = \frac{1}{T}\left[\left(\frac{\partial}{\partial T}\left(\frac{\partial H}{\partial P}\right)_T\right)_P - \left(\frac{\partial V}{\partial T}\right)_P\right] - \frac{1}{T^2}\left[\left(\frac{\partial H}{\partial P}\right)_T - V\right] \tag{5.74}$$

Simplifying this equation results in

$$\left(\frac{\partial H}{\partial P}\right)_T - V = -T\left(\frac{\partial V}{\partial T}\right)_P \tag{5.75}$$

Using this result and Equation (5.70), the pressure dependence of the entropy at constant temperature can be written in a form that easily allows an experimental determination of this quantity to be made:

$$\left(\frac{\partial S}{\partial P}\right)_T = -\left(\frac{\partial V}{\partial T}\right)_P = -V\beta \tag{5.76}$$

Using these results, the total differential $dS$ can be written in terms of experimentally accessible parameters as

$$dS = \frac{C_P}{T}dT - V\beta\,dP \tag{5.77}$$

Integrating both sides of this equation along a reversible path yields

$$\Delta S = \int_{T_i}^{T_f}\frac{C_P}{T}dT - \int_{P_i}^{P_f}V\beta\,dP \tag{5.78}$$

This result applies to a single-phase system of a pure liquid, solid, or gas that undergoes a transformation from the initial result $T_i, P_i$ to $T_f, P_f$, provided that no phase changes or chemical reactions occur in the system.

**SUPPLEMENTAL**

# 5.14 The Thermodynamic Temperature Scale

The reversible Carnot cycle provides a basis for the **thermodynamic temperature scale,** a scale that is independent of the choice of a particular thermometric substance. This is the case because all reversible Carnot engines have the same efficiency, regardless of the working substance. The basis for the thermodynamic temperature scale is the fact that the heat withdrawn from a reservoir is a thermometric property. Both on experimental and theoretical grounds, it can be shown that

$$q = a\theta \tag{5.79}$$

where $\theta$ is the thermodynamic temperature, and $a$ is an arbitrary scale constant that sets numerical values for the thermodynamic temperature. Using Equations (5.9) and (5.10) for the efficiency of the reversible Carnot engine,

$$\varepsilon = \frac{q_{hot} + q_{cold}}{q_{hot}} = \frac{\theta_{hot} + \theta_{cold}}{\theta_{hot}} \tag{5.80}$$

This equation is the fundamental equation establishing an absolute temperature scale. To this point, we have no numerical values for this scale. Note, however, that $q \to 0$ as $\theta \to 0$, so that there is a natural zero for this temperature scale. Additionally, if we choose one value of $\theta$ to be positive, all other values of $\theta$ must be greater than zero. Otherwise, we could find conditions under which the heats $q_{hot}$ and $q_{cold}$ have the same sign. This would lead to a perpetual motion machine. Both of these characteristics fit the requirements of an absolute temperature scale.

A numerical scale for the thermodynamic temperature scale can be obtained by assigning the value 273.16 to the $\theta$ value corresponding to the triple point of water, and by making the size of a degree equal to the size of a degree on the Celsius scale. With this choice, the thermodynamic temperature scale becomes numerically equal to the absolute temperature scale based on the ideal gas law. However, the thermodynamic temperature scale is the primary scale because it is independent of the nature of the working substance.

# Vocabulary

Carnot cycle

Clausius inequality

coefficient of performance

diesel engine

entropy

heat engine

heat pump

irreversible process

natural transformations

Otto engine

perpetual motion machine of the
   first kind

perpetual motion machine of the
   second kind

refrigerator

second law of thermodynamics

spontaneous process

thermodynamic temperature scale

third law of thermodynamics

unnatural transformations

# Conceptual Problems

**Q5.1**   Under what conditions is $\Delta S < 0$ for a spontaneous process?

**Q5.2**   Why are $\Delta S_{fusion}$ and $\Delta S_{vaporization}$ always positive?

**Q5.3**   An ideal gas in thermal contact with the surroundings is cooled in an irreversible process at constant pressure. Are $\Delta S$, $\Delta S_{surroundings}$, and $\Delta S_{total}$ positive, negative, or zero? Explain your reasoning.

**Q5.4**   The amplitude of a pendulum consisting of a mass on a long wire is initially adjusted to have a very small value. The amplitude is found to decrease slowly with time. Is this process reversible? Would the process be reversible if the amplitude did not decrease with time?

**Q5.5**   A process involving an ideal gas and in which the temperature changes at constant volume is carried out. For a fixed value of $\Delta T$, the mass of the gas is doubled. The process is repeated with the same initial mass and $\Delta T$ is doubled. For which of these processes is $\Delta S$ greater? Why?

**Q5.6**   You are told that $\Delta S = 0$ for a process in which the system is coupled to its surroundings. Can you conclude that the process is reversible? Justify your answer.

**Q5.7**   Under what conditions does the equality $\Delta S = \Delta H/T$ hold?

**Q5.8**   Is the following statement true or false? If it is false, rephrase it so that it is true. The entropy of a system cannot increase in an adiabatic process.

**Q5.9**   Which of the following processes is spontaneous?

**a.** The reversible isothermal expansion of an ideal gas.

**b.** The vaporization of superheated water at 102°C and 1 bar.

**c.** The constant pressure melting of ice at its normal freezing point by the addition of an infinitesimal quantity of heat.

**d.** The adiabatic expansion of a gas into a vacuum.

**Q5.10**   One Joule of work is done on a system, raising its temperature by one degree centigrade. Can this increase in temperature be harnessed to do one Joule of work? Explain.

**Q5.11**   Your roommate decides to cool the kitchen by opening the refrigerator. Will this strategy work? Explain your reasoning.

**Q5.12**   An ideal gas undergoes an adiabatic expansion into a vacuum. Are $\Delta S$, $\Delta S_{surroundings}$, and $\Delta S_{total}$ positive, negative, or zero? Explain your reasoning.

**Q5.13**   When a saturated solution of a salt is cooled, a precipitate crystallizes out. Is the entropy of the crystalline precipitate greater or less than the dissolved solute? Explain why this process is spontaneous.

**Q5.14**   A system undergoes a change from one state to another along two different pathways, one of which is reversible and the other of which is irreversible. What can you say about the relative magnitudes of $q_{reversible}$ and $q_{irreversible}$?

**Q5.15**   An ideal gas in a piston and cylinder assembly with adiabatic walls undergoes an expansion against a constant external pressure. Are $\Delta S$, $\Delta S_{surroundings}$, and $\Delta S_{total}$ positive, negative, or zero? Explain your reasoning.

**Q5.16**   Is the equation

$$\Delta S = \int_{T_i}^{T_f} \frac{C_V}{T} dT + \int_{V_i}^{V_f} \frac{\beta}{\kappa} dV = C_V \ln\frac{T_f}{T_i} + \frac{\beta}{\kappa}(V_f - V_i)$$

valid for an ideal gas?

**Q5.17**   Why is the efficiency of a Carnot heat engine the upper bound to the efficiency of an internal combustion engine?

**Q5.18**   Two vessels of equal volume, pressure and temperature both containing Ar are connected by a valve. What is the change in entropy when the valve is opened, allowing mixing of the two volumes? Is $\Delta S$ the same if one of the volumes contained Ar, and the other contained Ne?

**Q5.19**   Without using equations, explain why $\Delta S$ for a liquid or solid is dominated by the temperature dependence of $S$ as both $P$ and $T$ change.

**Q5.20**   Solid methanol in thermal contact with the surroundings is reversibly melted at the normal melting point at a pressure of 1 atm. Are $\Delta S$, $\Delta S_{surroundings}$, and $\Delta S_{total}$ positive, negative, or zero? Explain your reasoning.

**Q5.21**   Can incandescent lighting be regarded as an example of cogeneration during the heating season? In a season where air conditioning is required?

# Numerical Problems

Problem numbers in red indicate that the solution to the problem is given in the *Student's Solutions Manual*.

**P5.1** Consider the formation of glucose from carbon dioxide and water (i.e., the reaction of the photosynthetic process): $6CO_2(g) + 6H_2O(l) \rightarrow C_6H_{12}O_6(s) + 6O_2(g)$.

The following table of information will be useful in working this problem:

| $T = 298K$ | $CO_2$ (g) | $H_2O$ (l) | $C_6H_{12}O_6(s)$ | $O_2(g)$ |
|---|---|---|---|---|
| $\Delta H_f^\circ$ kJ mol$^{-1}$ | −393.5 | −285.8 | −1273.1 | 0.0 |
| $S^\circ$ J mol$^{-1}$K$^{-1}$ | 213.8 | 70.0 | 209.2 | 205.2 |
| $C_{P,m}^\circ$ J mol$^{-1}$K$^{-1}$ | 37.1 | 75.3 | 219.2 | 29.4 |

Calculate the entropy and enthalpy changes for this chemical system at $T = 298$ K and $T = 310$. K. Calculate also the entropy change of the surroundings and the universe at both temperatures, assuming that the system and surroundings are at the same temperature.

**P5.2** The Chalk Point, Maryland, generating station supplies electrical power to the Washington, D.C., area. Units 1 and 2 have a gross generating capacity of 710. MW (megawatt). The steam pressure is $25 \times 10^6$ Pa, and the superheater outlet temperature ($T_h$) is 540.°C. The condensate temperature ($T_c$) is 30.0°C.

**a.** What is the efficiency of a reversible Carnot engine operating under these conditions?

**b.** If the efficiency of the boiler is 91.2%, the overall efficiency of the turbine, which includes the Carnot efficiency and its mechanical efficiency, is 46.7%, and the efficiency of the generator is 98.4%, what is the efficiency of the total generating unit? (Another 5.0% needs to be subtracted for other plant losses.)

**c.** One of the coal-burning units produces 355 MW. How many metric tons (1 metric ton = $1 \times 10^6$ g) of coal per hour are required to operate this unit at its peak output if the enthalpy of combustion of coal is $29.0 \times 10^3$ kJ kg$^{-1}$?

**P5.3** An electrical motor is used to operate a Carnot refrigerator with an interior temperature of 0.00°C. Liquid water at 0.00°C is placed into the refrigerator and transformed to ice at 0.00°C. If the room temperature is 300. K, what mass of ice can be produced in one day by a 0.50-hp motor that is running continuously? Assume that the refrigerator is perfectly insulated and operates at the maximum theoretical efficiency.

**P5.4** An air conditioner is a refrigerator with the inside of the house acting as the cold reservoir and the outside atmosphere acting as the hot reservoir. Assume that an air conditioner consumes $1.70 \times 10^3$ W of electrical power, and that it can be idealized as a reversible Carnot refrigerator. If the coefficient of performance of this device is 3.30, how much heat can be extracted from the house in a day?

**P5.5** One mole of $H_2O(l)$ is compressed from a state described by $P = 1.00$ bar and $T = 350$. K to a state described by $P = 590$. bar and $T = 750$. K. In addition, $\beta = 2.07 \times 10^{-4}$ K$^{-1}$ and the density can be assumed to be constant at the value 997 kg m$^{-3}$. Calculate $\Delta S$ for this transformation, assuming that $\kappa = 0$.

**P5.6** 2.25 moles of an ideal gas with $C_{V,m} = 3R/2$ undergoes the transformations described in the following list from an initial state described by $T = 310$. K and $P = 1.00$ bar. Calculate $q$, $w$, $\Delta U$, $\Delta H$, and $\Delta S$ for each process.

**a.** The gas is heated to 675 K at a constant external pressure of 1.00 bar.

**b.** The gas is heated to 675 K at a constant volume corresponding to the initial volume.

**c.** The gas undergoes a reversible isothermal expansion at 310. K until the pressure is one third of its initial value.

**P5.7** Consider the reversible Carnot cycle shown in Figure 5.2 with 1.25 mol of an ideal gas with $C_V = 5R/2$ as the working substance. The initial isothermal expansion occurs at the hot reservoir temperature of $T_{hot} = 740$. K from an initial volume of 3.75 L ($V_a$) to a volume of 12.8 L ($V_b$). The system then undergoes an adiabatic expansion until the temperature falls to $T_{cold} = 310$. K. The system then undergoes an isothermal compression and a subsequent adiabatic compression until the initial state described by $T_a = 740$. K and $V_a = 3.75$ L is reached.

**a.** Calculate $V_c$ and $V_d$.

**b.** Calculate $w$ for each step in the cycle and for the total cycle.

**c.** Calculate $\varepsilon$ and the amount of heat that is extracted from the hot reservoir to do 1.00 kJ of work in the surroundings.

**P5.8** The average heat evolved by the oxidation of foodstuffs in an average adult per hour per kilogram of body weight is 7.20 kJ kg$^{-1}$ hr$^{-1}$. Assume the weight of an average adult is 62.0 kg. Suppose the total heat evolved by this oxidation is transferred into the surroundings over a period lasting one week. Calculate the entropy change of the surroundings associated with this heat transfer. Assume the surroundings are at $T = 293$ K.

**P5.9** Calculate $\Delta S$, $\Delta S_{total}$, and $\Delta S_{surroundings}$ when the volume of 150. g of CO initially at 273 K and 1.00 bar increases by a factor of two in (a) an adiabatic reversible expansion, (b) an expansion against $P_{external} = 0$, and (c) an isothermal reversible expansion. Take $C_{P,m}$ to be constant at the value 29.14 J mol$^{-1}$K$^{-1}$ and assume ideal gas behavior. State whether each process is spontaneous. The temperature of the surroundings is 273 K.

**P5.10** The maximum theoretical efficiency of an internal combustion engine is achieved in a reversible Carnot cycle. Assume that the engine is operating in the Otto cycle and that $C_{V,m} = 5R/2$ for the fuel–air mixture initially at 273 K (the temperature of the cold reservoir). The mixture is compressed by a factor of 6.9 in the adiabatic compression step. What is the maximum theoretical efficiency of this engine? How much would the efficiency increase if the compression

ratio could be increased to 15? Do you see a problem in doing so?

**P5.11** 2.25 moles of an ideal gas with $C_{V,m} = 5R/2$ are transformed from an initial state $T = 680.$ K and $P = 1.15$ bar to a final state $T = 298$ K and $P = 4.75$ bar. Calculate $\Delta U$, $\Delta H$, and $\Delta S$ for this process.

**P5.12** 1.10 moles of $N_2$ at 20.5°C and 6.20 bar undergoes a transformation to the state described by 215°C and 1.75 bar. Calculate $\Delta S$ if

$$\frac{C_{P,m}}{\mathrm{J\,mol^{-1}K^{-1}}} = 30.81 - 11.87 \times 10^{-3}\frac{T}{K} + 2.3968 \times 10^{-5}\frac{T^2}{K^2}$$
$$-1.0176 \times 10^{-8}\frac{T^3}{K^3}$$

**P5.13** Calculate $\Delta S$ for the isothermal compression of 1.75 mole of Cu(s) from 2.15 bar to 1250. bar at 298 K. $\beta = 0.492 \times 10^{-4}$ K$^{-1}$, $\kappa = 0.78 \times 10^{-6}$ bar$^{-1}$, and the density is 8.92g cm$^{-3}$. Repeat the calculation assuming that $\kappa = 0$.

**P5.14** Calculate $\Delta S°$ for the reaction $3H_2(g) + N_2(g) \rightarrow 2NH_3(g)$ at 725 K. Omit terms in the temperature-dependent heat capacities higher than $T^2/K^2$.

**P5.15** Using the expression $dS = \dfrac{C_P}{T}dT - V\beta dP$, calculate the decrease in temperature that occurs if 2.25 moles of water at 310. K and 1650. bar is brought to a final pressure of 1.30 bar in a reversible adiabatic process. Assume that $\kappa = 0$.

**P5.16** 3.75 moles of an ideal gas with $C_{V,m} = 3/2R$ undergoes the transformations described in the following list from an initial state described by $T = 298$ K and $P = 4.50$ bar. Calculate $q$, $w$, $\Delta U$, $\Delta H$, and $\Delta S$ for each process.

a. The gas undergoes a reversible adiabatic expansion until the final pressure is one third its initial value.

b. The gas undergoes an adiabatic expansion against a constant external pressure of 1.50 bar until the final pressure is one third its initial value.

c. The gas undergoes an expansion against a constant external pressure of zero bar until the final pressure is equal to one third of its initial value.

**P5.17** The interior of a refrigerator is typically held at 36°F and the interior of a freezer is typically held at 0.00°F. If the room temperature is 65°F, by what factor is it more expensive to extract the same amount of heat from the freezer than from the refrigerator? Assume that the theoretical limit for the performance of a reversible refrigerator is valid in this case.

**P5.18** Using your results from Problem P5.7, calculate $q$, $\Delta U$, and $\Delta H$ for each step in the cycle and for the total cycle described in Figure 5.2.

**P5.19** At the transition temperature of 95.4°C, the enthalpy of transition from rhombic to monoclinic sulfur is 0.38 kJ mol$^{-1}$.

a. Calculate the entropy of transition under these conditions.

b. At its melting point, 119°C, the enthalpy of fusion of monoclinic sulfur is 1.23 kJ mol$^{-1}$. Calculate the entropy of fusion.

c. The values given in parts (a) and (b) are for 1 mol of sulfur; however, in crystalline and liquid sulfur, the molecule is present as $S_8$. Convert the values of the enthalpy and entropy of fusion in parts (a) and (b) to those appropriate for $S_8$.

**P5.20** One mole of a van der Waals gas at 25.0°C is expanded isothermally and reversibly from an initial volume of 0.010 m$^3$ to a final volume of 0.095 m$^3$. For the van der Waals gas, $(\partial U/\partial V)_T = a/V_m^2$. Assume that $a = 0.556$ Pa m$^6$ mol$^{-2}$, and that $b = 64.0 \times 10^{-6}$ m$^3$ mol$^{-1}$. Calculate $q$, $w$, $\Delta U$, $\Delta H$, and $\Delta S$ for the process.

**P5.21** From the following data, derive the absolute entropy of crystalline glycine at $T = 300.$ K.

You can perform the integration numerically using either a spreadsheet program or a curve-fitting routine and a graphing calculator (see Example Problem 5.9).

| $T$ (K) | $C_{P,m}$ (J K$^{-1}$ mol$^{-1}$) |
|---|---|
| 10. | 0.30 |
| 20. | 2.4 |
| 30. | 7.0 |
| 40. | 13.0 |
| 60. | 25.1 |
| 80. | 35.2 |
| 100. | 43.2 |
| 120. | 50.0 |
| 140. | 56.0 |
| 160. | 61.6 |
| 180. | 67.0 |
| 200. | 72.2 |
| 220. | 77.4 |
| 240. | 82.8 |
| 260. | 88.4 |
| 280. | 94.0 |
| 300. | 99.7 |

**P5.22** Calculate $\Delta H$ and $\Delta S$ if the temperature of 1.75 moles of Hg(l) is increased from 0.00°C to 75.0°C at 1 bar. Over this temperature range, $C_{P,m}$(J K$^{-1}$ mol$^{-1}$) = $30.093 - 4.944 \times 10^{-3}T/K$.

**P5.23** Calculate $\Delta S$ if the temperature of 2.50 mol of an ideal gas with $C_V = 5/2R$ is increased from 160. to 675 K under conditions of (a) constant pressure and (b) constant volume.

**P5.24** Beginning with Equation (5.5), use Equation (5.6) to eliminate $V_c$ and $V_d$ to arrive at the result $w_{cycle} = nR(T_{hot} - T_{cold}) \ln V_b/V_a$.

**P5.25** Calculate $\Delta S_R°$ for the reaction $H_2(g) + Cl_2(g) \rightarrow 2HCl(g)$ at 870. K. Omit terms in the temperature-dependent heat capacities higher than $T^2/K^2$.

**P5.26** A 22.0 g mass of ice at 273 K is added to 136 g of $H_2O(l)$ at 310. K at constant pressure. Is the final state of the system ice or liquid water? Calculate $\Delta S$ for the process. Is the process spontaneous?

**P5.27** Under anaerobic conditions, glucose is broken down in muscle tissue to form lactic acid according to the reaction $C_6H_{12}O_6(s) \rightarrow 2CH_3CHOHCOOH(s)$. Thermodynamic data at $T = 298$ K for glucose and lactic acid are given in the following table:

| | $\Delta H_f^\circ(\text{kJ mol}^{-1})$ | $C_{P,m}(\text{J K}^{-1}\text{mol}^{-1})$ | $S_m^\circ(\text{J K}^{-1}\text{mol}^{-1})$ |
|---|---|---|---|
| Glucose | −1273.1 | 219.2 | 209.2 |
| Lactic Acid | −673.6 | 127.6 | 192.1 |

Calculate, $\Delta S$ for the system, the surroundings, and the universe at $T = 325$ K. Assume the heat capacities are constant between $T = 298$ K and $T = 330$. K.

**P5.28** The amino acid glycine dimerizes to form the dipeptide glycylglycine according to the reaction

$$2\text{Glycine}(s) \rightarrow \text{Glycylglycine}(s) + H_2O(l)$$

Calculate $\Delta S$, $\Delta S_{surr}$, and $\Delta S_{universe}$ at $T = 298$ K. Useful thermodynamic data follow:

| | Glycine | Glycylglycine | Water |
|---|---|---|---|
| $\Delta H_f^\circ(\text{kJ mol}^{-1})$ | −537.2 | −746.0 | −285.8 |
| $S_m^\circ(\text{J K}^{-1}\text{mol}^{-1})$ | 103.5 | 190.0 | 70.0 |

**P5.29** One mole of $H_2O(l)$ is supercooled to −3.75°C at 1 bar pressure. The freezing temperature of water at this pressure is 0.00°C. The transformation $H_2O(l) \rightarrow H_2O(s)$ is suddenly observed to occur. By calculating $\Delta S$, $\Delta S_{surroundings}$, and $\Delta S_{total}$, verify that this transformation is spontaneous at −3.75°C. The heat capacities are given by $C_{P,m}(H_2O(l)) = 75.3$ J K$^{-1}$ mol$^{-1}$ and $C_{P,m}(H_2O(s)) = 37.7$ J K$^{-1}$ mol$^{-1}$, and $\Delta H_{fusion} = 6.008$ kJ mol$^{-1}$ at 0.00°C. Assume that the surroundings are at −3.75°C. [*Hint:* Consider the two pathways at 1 bar: (a) $H_2O(l, -3.75°C) \rightarrow H_2O(s, -3.75°C)$ and (b) $H_2O(l, -3.75°C) \rightarrow H_2O(l, 0.00°C) \rightarrow H_2O(s, 0.00°C) \rightarrow H_2O(s, -3.75°C)$. Because $S$ is a state function, $\Delta S$ must be the same for both pathways.]

**P5.30** Calculate $\Delta S$, $\Delta S_{surr}$, and $\Delta S_{universe}$ per day for the air-conditioned house described in Problem 5.4. Assume that the interior temperature is 65°F and the exterior temperature is 99°F.

**P5.31** The following heat capacity data have been reported for L-alanine:

| $T(\text{K})$ | 10. | 20. | 40. | 60. | 80. | 100. | 140. | 180. | 220. | 260. | 300. |
|---|---|---|---|---|---|---|---|---|---|---|---|
| $C_{P,m}(\text{J K}^{-1}\text{mol}^{-1})$ | 0.49 | 3.85 | 17.45 | 30.99 | 42.59 | 52.50 | 68.93 | 83.14 | 96.14 | 109.6 | 122.7 |

By a graphical treatment, obtain the molar entropy of L-alanine at $T = 300$. K. You can perform the integration numerically using either a spreadsheet program or a curve-fitting routine and a graphing calculator (see Example Problem 5.9).

**P5.32** Calculate $\Delta S_{surroundings}$ and $\Delta S_{total}$ for the processes described in parts (a) and (b) of Problem P5.16. Which of the processes is a spontaneous process? The state of the surroundings for each part is 298 K, 1.50 bar.

**P5.33** A refrigerator is operated by a 0.25-hp (1 hp = 746 watts) motor. If the interior is to be maintained at 4.50°C and the room temperature on a hot day is 38°C, what is the maximum heat leak (in watts) that can be tolerated? Assume that the coefficient of performance is 50.% of the maximum theoretical value. What happens if the leak is greater than your calculated maximum value?

**P5.34** Using your results from Problems P5.18 and P5.7, calculate $\Delta S$, $\Delta S_{surroundings}$, and $\Delta S_{total}$ for each step in the cycle and for the total Carnot cycle described in Figure 5.2.

**P5.35** Between 0°C and 100°C, the heat capacity of $Hg(l)$ is given by

$$\frac{C_{P,m}(\text{Hg},l)}{\text{J K}^{-1}\text{mol}^{-1}} = 30.093 - 4.944 \times 10^{-3}\frac{T}{K}$$

Calculate $\Delta H$ and $\Delta S$ if 2.25 moles of $Hg(l)$ are raised in temperature from 0.00° to 88.0°C at constant $P$.

**P5.36** Calculate $\Delta S_{surroundings}$ and $\Delta S_{total}$ for part (c) of Problem P5.6. Is the process spontaneous? The state of the surroundings is $T = 310$. K, $P = 0.333$ bar.

**P5.37** Calculate the entropy of one mole of water vapor at 175°C and 0.625 bar using the information in the data tables.

**P5.38** The heat capacity of $\alpha$-quartz is given by

$$\frac{C_{P,m}(\alpha\text{-quartz},s)}{\text{J K}^{-1}\text{mol}^{-1}} = 46.94 + 34.31 \times 10^{-3}\frac{T}{K}$$

$$- 11.30 \times 10^{-5}\frac{T^2}{K^2}$$

The coefficient of thermal expansion is given by $\beta = 0.3530 \times 10^{-4}$ K$^{-1}$ and $V_m = 22.6$ cm$^3$ mol$^{-1}$. Calculate $\Delta S_m$ for the transformation $\alpha$-quartz (15.0°C, 1 atm) $\rightarrow \alpha$-quartz (420. °C, 925 atm).

**P5.39**

a. Calculate $\Delta S$ if 1.00 mol of liquid water is heated from 0.00° to 10.0°C under constant pressure and if $C_{P,m} = 75.3$ J K$^{-1}$ mol$^{-1}$.

b. The melting point of water at the pressure of interest is 0.00°C and the enthalpy of fusion is 6.010 kJ mol$^{-1}$. The boiling point is 100.°C and the enthalpy of vaporization is 40.65 kJ mol$^{-1}$. Calculate $\Delta S$ for the transformation $H_2O(s, 0°C) \rightarrow H_2O(g, 100.°C)$.

**P5.40** 21.05 g of steam at 373 K is added to 415 g of $H_2O(l)$ at 298 K at a constant pressure of 1 bar. Is the final state of the system steam or liquid water? Calculate $\Delta S$ for the process.

**P5.41** Using your result from fitting the data in Problem 5.31, extrapolate the absolute entropy of L-alanine to physiological conditions, $T = 310.$ K.

**P5.42** The mean solar flux at Earth's surface is ~2.00 J $cm^{-2}$ $min^{-1}$. In a nonfocusing solar collector, the temperature reaches a value of 79.5°C. A heat engine is operated using the collector as the hot reservoir and a cold reservoir at 298 K. Calculate the area of the collector needed to produce 1000. W. Assume that the engine operates at the maximum Carnot efficiency.

**P5.43** An ideal gas sample containing 1.75 moles for which $C_{V,m} = 5R/2$ undergoes the following reversible cyclical process from an initial state characterized by $T = 275$ K and $P = 1.00$ bar:

**a.** It is expanded reversibly and adiabatically until the volume triples.

**b.** It is reversibly heated at constant volume until $T$ increases to 275 K.

**c.** The pressure is increased in an isothermal reversible compression until $P = 1.00$ bar.

Calculate $q$, $w$, $\Delta U$, $\Delta H$, and $\Delta S$ for each step in the cycle, and for the total cycle.

**P5.44** For protein denaturation, the excess entropy of

denaturation is defined as $\Delta S_{den} = \int_{T_1}^{T_2} \dfrac{\delta C_P^{trs}}{T} dT$, where $\delta C_P^{trs}$

is the transition excess heat capacity. The way in which $\delta C_P^{trs}$ can be extracted from differential scanning calorimetry (DSC) data is discussed in Section 4.6 and shown in Figure 4.7. The following DSC data are for a protein mutant that denatures between $T_1 = 288$ K and $T_2 = 318$ K. Using the equation for $\Delta S_{den}$ given previously, calculate the excess entropy of denaturation. In your calculations, use the dashed curve below the yellow area as the heat capacity base line that defines $\delta C_P^{trs}$ as shown in Figure 4.8. Assume the molecular weight of the protein is 14,000. grams.
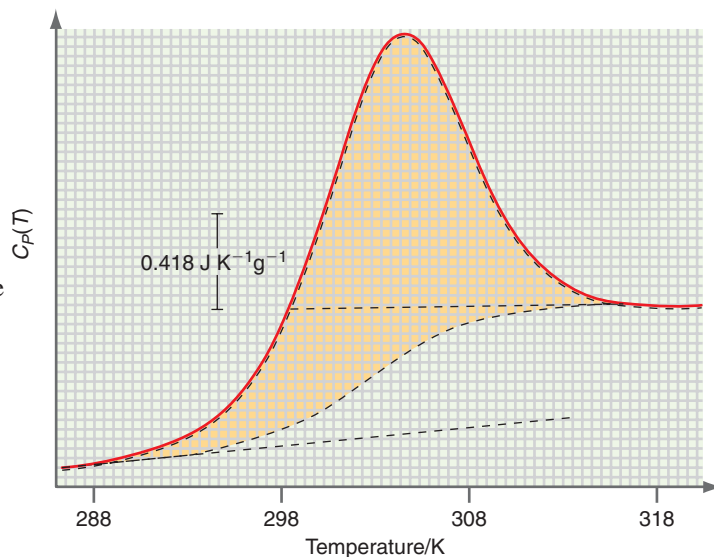


You can perform the integration numerically by counting squares.

**P5.45** The standard entropy of Pb(s) at 298.15 K is 64.80 J $K^{-1}$ $mol^{-1}$. Assume that the heat capacity of Pb(s) is given by

$$\frac{C_{P,m}(Pb,s)}{J\ mol^{-1}\ K^{-1}} = 22.13 + 0.01172\frac{T}{K} + 1.00 \times 10^{-5}\frac{T^2}{K^2}$$

The melting point is 327.4°C and the heat of fusion under these conditions is 4770. J $mol^{-1}$. Assume that the heat capacity of Pb(l) is given by

$$\frac{C_{P,m}(Pb,l)}{J\ K^{-1}\ mol^{-1}} = 32.51 - 0.00301\frac{T}{K}$$

**a.** Calculate the standard entropy of Pb(l) at 725°C.

**b.** Calculate $\Delta H$ for the transformation Pb(s, 25.0°C) → Pb(l, 725°C).

# Web-Based Simulations, Animations, and Problems

**W5.1** The reversible Carnot cycle is simulated with adjustable values of $T_{hot}$ and $T_{cold}$, and $\Delta U$, $q$, and $w$ are determined for each segment and for the cycle. The efficiency is also determined for the cycle.

*This page intentionally left blank*

# Chemical Equilibrium

In the previous chapter, criteria for the spontaneity of arbitrary processes were developed. In this chapter, spontaneity is discussed in the context of the approach to equilibrium of a reactive mixture of gases. Two new state functions are introduced that express spontaneity in terms of the properties of the system only, so that the surroundings do not have to be considered explicitly. The Helmholtz energy provides a criterion for determining if a reaction mixture will evolve toward reactants or products if the system is at constant $V$ and $T$. The Gibbs energy is the criterion for determining if a reaction mixture will evolve toward reactants or products if the system is at constant $P$ and $T$. Using the Gibbs energy, a thermodynamic equilibrium constant $K_P$ is derived that predicts the equilibrium concentrations of reactants and products in a mixture of reactive ideal gases.

## 6.1 The Gibbs Energy and the Helmholtz Energy

In Chapter 5, it was shown that the direction of spontaneous change for an arbitrary process is predicted by $\Delta S + \Delta S_{surroundings} > 0$. In this section, this spontaneity criterion is used to derive two new state functions, the Gibbs and Helmholtz energies. These new state functions provide the basis for all further discussions of spontaneity. Formulating spontaneity in terms of the Gibbs and Helmholtz energies rather than $\Delta S + \Delta S_{surroundings} > 0$ has the important advantage that spontaneity and equilibrium can be defined using only properties of the system rather than of the system and surroundings. We will also show that the Gibbs and Helmholtz energies allow us to calculate the maximum work that can be extracted from a chemical reaction.

The fundamental expression governing spontaneity is the Clausius inequality [Equation (5.33)], written in the form

$$T dS \geq đq \qquad (6.1)$$

The equality is satisfied only for a reversible process. Because $đq = dU - đw$,

$$T dS \geq dU - đw \text{ or, equivalently, } -dU + đw + T dS \geq 0 \qquad (6.2)$$

As discussed in Section 2.2, a system can do different types of work on the surroundings. It is particularly useful to distinguish between expansion work, in which the work arises from a volume change in the system, and nonexpansion work (for example, electrical work). We rewrite Equation (6.2) in the form

$$-dU - P_{external}\, dV + đw_{nonexpansion} + T dS \geq 0 \qquad (6.3)$$

Equation 6.3 expresses the condition of spontaneity for an arbitrary process in terms of the changes in the state functions $U$, $V$, $S$, and $T$ as well as the path-dependent functions $P_{external}\, dV$ and $đw_{nonexpansion}$.

To make a connection with the discussion of spontaneity in Chapter 5, consider a special case of Equation (6.3). For an isolated system, $w = 0$ and $dU = 0$. Therefore, Equation (6.3) reduces to the familiar result derived in Section 5.5:

$$dS \geq 0 \qquad (6.4)$$

Because chemists are interested in systems that interact with their environment, we define equilibrium and spontaneity for such systems. As was done in Chapters 1 through 5, it is useful to consider transformations at constant temperature and either constant volume or constant pressure. *Note that constant T and P (or V) does not imply that these variables are constant throughout the process*, *but rather that they are the same for the initial and final states of the process.*

For isothermal processes, $T dS = d(TS)$, and Equation (6.3) can be written in the following form:

$$-dU + T dS \geq -đw_{expansion} - đw_{nonexpansion} \text{ or, equivalently,}$$

$$d(U - TS) \leq đw_{expansion} + đw_{nonexpansion} \qquad (6.5)$$

The combination of state functions $U - TS$, which has the units of energy, defines a new state function that we call the **Helmholtz energy,** abbreviated $A$. Using this definition, the general condition of spontaneity for isothermal processes becomes

$$dA - đw_{expansion} - đw_{nonexpansion} \leq 0 \qquad (6.6)$$

Because the equality applies for a reversible transformation, Equation (6.6) provides a way to calculate the maximum work that a system can do on the surroundings in an isothermal process.

$$đw_{total} = đw_{expansion} + đw_{nonexpansion} \geq dA \qquad (6.7)$$

The equality holds for a reversible process. Example Problem 6.1 illustrates the usefulness of $A$ for calculating the maximum work available through carrying out a chemical reaction.
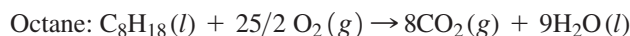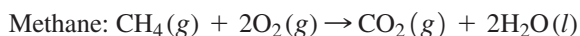
## EXAMPLE PROBLEM 6.1

You wish to construct a fuel cell based on the oxidation of a hydrocarbon fuel. The two choices for a fuel are methane and octane. Calculate the maximum work available through the combustion of these two hydrocarbons, on a per mole and a per gram basis at 298.15 K and 1 bar pressure. The standard enthalpies of combustion are $\Delta H^{\circ}_{combustion}(CH_4, g) = -891$ kJ mol$^{-1}$, $\Delta H^{\circ}_{combustion}(C_8H_{18}, l) = -5471$ kJ mol$^{-1}$, and $S^{\circ}_m (C_8H_{18}, l) = 361.1$ J mol$^{-1}$ k$^{-1}$. Use tabulated values of $S^{\circ}_m$ in Appendix A for these calculations. Are there any other factors that should be taken into account in making a decision between these two fuels?

### Solution

At constant $T$, $\Delta A$ and $\Delta H$ are related by $\Delta A = \Delta U - T\Delta S = \Delta H - \Delta(PV) - T\Delta S = \Delta H - \Delta nRT - T\Delta S$

The combustion reactions are

$$\text{Methane: } CH_4(g) + 2O_2(g) \rightarrow CO_2(g) + 2H_2O(l)$$

$$\text{Octane: } C_8H_{18}(l) + 25/2\, O_2(g) \rightarrow 8CO_2(g) + 9H_2O(l)$$

$$\Delta A^{\circ}_{combustion}(CH_4, g) = \Delta U^{\circ}_{combustion}(CH_4, g) - T\left(\begin{array}{c}S^{\circ}_m(CO_2, g) + 2S^{\circ}_m(H_2O, l)\\ -S^{\circ}_m(CH_4, g) - 2S^{\circ}_m(O_2, g)\end{array}\right)$$

$$= \Delta H^{\circ}_{combustion}(CH_4, g) - \Delta nRT$$

$$-T(S^{\circ}_m(CO_2, g) + 2S^{\circ}_m(H_2O, l) - S^{\circ}_m(CH_4, g)$$

$$- 2S^{\circ}_m(O_2, g))$$

$$= -891 \times 10^3\,\mathrm{J\,mol^{-1}} + 2 \times 8.314\,\mathrm{J\,mol^{-1}\,K^{-1}} \times 298.15\,\mathrm{K}$$

$$-298.15\,\mathrm{K} \times \left(\begin{array}{c}213.8\,\mathrm{J\,mol^{-1}\,K^{-1}} + 2 \times 70.0\,\mathrm{J\,mol^{-1}\,K^{-1}}\\ -186.3\,\mathrm{J\,mol^{-1}\,K^{-1}} - 2 \times 205.2\,\mathrm{J\,mol^{-1}\,K^{-1}}\end{array}\right)$$

$$\Delta A^{\circ}_{combustion}(CH_4, g) = -814\,\mathrm{kJ\,mol^{-1}}$$

$$\Delta A^{\circ}_{combustion}(C_8H_{18}, l) = \Delta U^{\circ}_{combustion}(C_8H_{18}, l)$$

$$-T\left(8S^{\circ}_m(CO_2, g) + 9S^{\circ}_m(H_2O, l) - S^{\circ}_m(C_8H_{18}, l)\right.$$

$$\left.- \frac{25}{2}S^{\circ}_m(O_2, g)\right)$$

$$= \Delta H^{\circ}_{combustion}(C_8H_{18}, l) - \Delta nRT$$

$$-T\left(8S^{\circ}_m(CO_2, g) + 9S^{\circ}_m(H_2O, l) - S^{\circ}_m(C_8H_{18}, l)\right.$$

$$\left.- \frac{25}{2}S^{\circ}_m(O_2, g)\right)$$

$$= -5471 \times 10^3\,\mathrm{J\,mol^{-1}} + \frac{9}{2} \times 8.314\,\mathrm{J\,mol^{-1}\,K^{-1}} \times 298.15\,\mathrm{K}$$

$$-298.15\,\mathrm{K} \times \left(\begin{array}{c}8 \times 213.8\,\mathrm{J\,mol^{-1}\,K^{-1}} + 9 \times 70.0\,\mathrm{J\,mol^{-1}\,K^{-1}}\\ - 361.1\,\mathrm{J\,mol^{-1}\,K^{-1}} - \frac{25}{2} \times 205.2\,\mathrm{J\,mol^{-1}\,K^{-1}}\end{array}\right)$$

$$\Delta A^{\circ}_{combustion}(C_8H_{18}, l) = -5285\,\mathrm{kJ\,mol^{-1}}$$

On a per mol basis, octane (molecular weight 114.25 g mol$^{-1}$) is capable of producing a factor of 6.5 more work than methane (molecular weight 16.04 g mol$^{-1}$). However, on a per gram basis, methane and octane are nearly equal in their ability to produce work (–50.6 kJ g$^{-1}$ versus –46.3 kJ g$^{-1}$). You might want to choose octane because it can be stored as a liquid at atmospheric pressure. By contrast, a pressurized tank is needed to store methane as a liquid at 298.15 K.

In discussing the Helmholtz energy, $dT = 0$ was the only constraint applied. We now apply the additional constraint for a constant volume process, $dV = 0$. This condition implies $đw_{expansion} = 0$, because $dV = 0$. If nonexpansion work also is not possible in the transformation $đw_{nonexpansion} = đw_{expansion} = 0$, the condition that defines spontaneity and equilibrium becomes

$$dA \le 0 \qquad\qquad (6.8)$$

Chemical reactions are more commonly studied under constant pressure than constant volume conditions. Therefore, the condition for spontaneity is considered next for an isothermal constant pressure process. At constant $P$ and $T$, $PdV = d(PV)$ and $TdS = d(TS)$. In this case, using the relation $H = U + PV$, Equation (6.3) can be written in the form

$$d(U + PV - TS) = d(H - TS) \le đw_{nonexpansion} \qquad\qquad (6.9)$$

The combination of state functions $H - TS$, which has the units of energy, defines a new state function called the **Gibbs energy,** abbreviated $G$. Using the Gibbs energy, the condition for spontaneity and equilibrium for an isothermal process at constant pressure becomes

$$dG - đw_{nonexpansion} \leq 0 \tag{6.10}$$

For a reversible process, the equality holds, and the change in the Gibbs energy is a measure of the maximum nonexpansion work that can be produced in the transformation.

We next consider a transformation at constant $P$ and $T$ for which nonexpansion work is not possible, for example, the burning of fuel in an internal combustion engine. In this case, Equation 6.10 becomes

$$dG \leq 0 \tag{6.11}$$

What is the advantage of using the state functions $G$ and $A$ as criteria for spontaneity rather than entropy? We answer this question by considering the Clausius inequality, which can be written in the form

$$dS - \frac{đq}{T} \geq 0 \tag{6.12}$$

As was shown in Section 5.8, $dS_{surroundings} = -đq/T$. Therefore, the Clausius inequality is equivalent to the spontaneity condition:

$$dS + dS_{surroundings} \geq 0 \tag{6.13}$$

By introducing $G$ and $A$, the fundamental conditions for spontaneity have not been changed. However, $G$ and $A$ are expressed only in terms of the macroscopic state variables of the system. By introducing $G$ and $A$, it is no longer necessary to consider the surroundings explicitly. Knowledge of $\Delta G$ and $\Delta A$ for the system alone is sufficient to predict the direction of natural change.

Apart from defining the condition of spontaneity, Equation (6.10) is very useful because it allows one to calculate the **maximum nonexpansion work** that can be produced by a chemical transformation. A particularly important application of this equation is to calculate the electrical work produced by a reaction in an electrochemical cell or fuel cell as shown in Example Problem 6.2. This topic will be discussed in detail in Chapter 11. The redox current that flows between the two half cells is used to do work. By contrast, only expansion work is possible in a conventional combustion process such as that in an automobile engine.

### EXAMPLE PROBLEM 6.2

Calculate the maximum nonexpansion work that can be produced by the fuel cell oxidation reactions in Example Problem 6.1.

#### Solution

$$\Delta G^\circ_{combustion}(CH_4, g) = \Delta H^\circ_{combustion}(CH_4, g)$$

$$- T\left( \begin{array}{c} S^\circ_m(CO_2, g) + 2S^\circ_m(H_2O, l) \\ -S^\circ_m(CH_4, g) - 2S^\circ_m(O_2, g) \end{array} \right)$$

$$= -890. \times 10^3 \text{ J mol}^{-1}$$

$$- 298.15K \times \left( \begin{array}{c} 213.8 \text{ J mol}^{-1}K^{-1} + 2 \times 70.0 \text{ J mol}^{-1}K^{-1} \\ - 186.3 \text{ J mol}^{-1}K^{-1} - 2 \times 205.2 \text{ J mol}^{-1}K^{-1} \end{array} \right)$$

$$\Delta G^\circ_{combustion}(CH_4, g) = -818 \text{ kJ mol}^{-1}$$

$$\Delta G^\circ_{combustion}(C_8H_{18}, l) = \Delta H^\circ_{combustion}(C_8H_{18}, l)$$

$$-T\Big( 8S^\circ_m(CO_2, g) + 9S^\circ_m(H_2O, l) - S^\circ_m(C_8H_{18}, l)$$

$$-\frac{25}{2} S^\circ_m(O_2, g)\Big)$$

$$= -5471 \times 10^3 \, J \, mol^{-1}$$

$$-298.15K \times \begin{pmatrix} 8 \times 213.8 \, J \, mol^{-1} \, K^{-1} + 9 \times 70.0 \, J \, mol^{-1} K^{-1} \\ - 361.1 \, J \, mol^{-1} K^{-1} - \dfrac{25}{2} \times 205.2 \, J \, mol^{-1} \, K^{-1} \end{pmatrix}$$

$$\Delta G^\circ_{combustion}(C_8H_{18}, l) = -5296 \, kJ \, mol^{-1}$$

Compare this result with that of Example Problem 6.1. What can you conclude about the relative amounts of expansion and nonexpansion work available in these reactions?

It is useful to compare the available work that can be done by a reversible heat engine with the electrical work done by an electrochemical fuel cell using the same chemical reaction. In the reversible heat engine, the maximum available work is the product of the heat withdrawn from the hot reservoir and the efficiency of the heat engine. Consider a heat engine with $T_{hot} = 600. \, K$ and $T_{cold} = 300. \, K$, which has an efficiency of 0.50, and set $q_{hot} = \Delta H^\circ_{combustion}$. For these values, the maximum work available from the heat engine is 54% of that available in the electrochemical fuel cell for the combustion of methane. The corresponding value for octane is 52%. Why are these values less than 100%? If the oxidation reactions of Example Problem 6.1 can be carried out as redox reactions using two physically separated half cells, electrical work can be harnessed directly and converted to mechanical work. All forms of work can theoretically (but not practically) be converted to other forms of work with 100% efficiency. However, if chemical energy is converted to heat by burning the hydrocarbon fuel, and the heat is subsequently converted to work using a heat engine, the theoretical efficiency is less than 100% as discussed in Section 5.2. It is clear from this comparison why considerable research and development effort is currently being spent on fuel cells.

After this discussion of the usefulness of $G$ in calculating the maximum nonexpansion work available through a chemical reaction, our focus turns to the use of $G$ to determine the direction of spontaneous change in a reaction mixture. For macroscopic changes at constant $P$ and $T$ in which no nonexpansion work is possible, the condition for spontaneity is $\Delta G_R < 0$ where

$$\Delta G_R = \Delta H_R - T\Delta S_R \qquad \textbf{(6.14)}$$

The subscript $R$ is a reminder that the process of interest is a chemical reaction. Note that there are two contributions to $\Delta G_R$ that determine if an isothermal chemical transformation is spontaneous. They are the energetic contribution $\Delta H_R$ and the entropic contribution $T\Delta S_R$.

The following conclusions can be drawn based on Equation (6.14):

- The entropic contribution to $\Delta G_R$ is greater for higher temperatures.
- A chemical transformation is always spontaneous if $\Delta H_R < 0$ (an exothermic reaction) and $\Delta S_R > 0$.
- A chemical transformation is never spontaneous if $\Delta H_R > 0$ (an endothermic reaction) and $\Delta S_R < 0$.
- For all other cases, the relative magnitudes of $\Delta H_R$ and $T\Delta S_R$ determine if the chemical transformation is spontaneous.
- If the chemical reaction, for example $CH_4(g) + 2O_2(g) \rightarrow CO_2(g) + 2H_2O(l)$ is not spontaneous, then the reverse process $CO_2(g) + 2H_2O(l) \rightarrow CH_4(g) + 2O_2(g)$ is spontaneous.
- If $\Delta G_R = 0$, the reaction mixture is at equilibrium, and neither direction of change is spontaneous.

$\Delta G_R$ depends on the concentrations of reactants and products in the reaction vessel, and a reaction mixture will evolve until $\Delta G_R = 0$ when equilibrium is achieved unless the reaction rate is zero. At this point, we have not developed a framework to calculate the concentrations of a reaction mixture at equilibrium. As we will see in Section 6.8, the function $exp\left(-\Delta G_R^\circ/RT\right)$ will allow us to do so.

For macroscopic changes at constant $V$ and $T$ in which no nonexpansion work is possible, the condition for spontaneity is $\Delta A_R < 0$, where

$$\Delta A_R = \Delta U_R - T\Delta S_R \tag{6.15}$$

Again, two contributions determine if an isothermal chemical transformation is spontaneous: $\Delta U_R$ is an energetic contribution, and $T\Delta S_R$ is an entropic contribution to $\Delta A_R$. The same conclusions can be drawn from this equation as for those listed for $\Delta G_R$, with $U$ substituted for $H$.

# 6.2 The Differential Forms of *U*, *H*, *A*, and *G*

To this point, the state functions $U$, $H$, $A$, and $G$, all of which have the units of energy have been defined. The functions $U$ and $H$ are used to calculate changes in energy for processes, and $A$ and $G$ are used to calculate the direction in which processes evolve and the maximum work the reactions can produce. In this section, we discuss how these state functions depend on the macroscopic system variables. To do so, the differential forms $dU$, $dH$, $dA$, and $dG$ are developed. As we will see, these differential forms are essential in calculating how $U$, $H$, $A$, and $G$ vary with state variables such as $P$ and $T$. Starting from the definitions

$$H = U + PV$$

$$A = U - TS$$

$$G = H - TS = U + PV - TS \tag{6.16}$$

the following total differentials can be formed:

$$dU = TdS - PdV \tag{6.17}$$

$$dH = TdS - PdV + PdV + VdP = TdS + VdP \tag{6.18}$$

$$dA = TdS - PdV - TdS - SdT = -SdT - PdV \tag{6.19}$$

$$dG = TdS + VdP - TdS - SdT = -SdT + VdP \tag{6.20}$$

These differential forms express the internal energy as $U(S,V)$, the enthalpy as $H(S,P)$, the Helmholtz energy as $A(T,V)$, and the Gibbs energy as $G(T,P)$. Although other combinations of variables can be used, these **natural variables** are used because the differential expressions are compact.

What information can be obtained from the differential expressions in Equations (6.17) through (6.20)? Because $U$, $H$, $A$, and $G$ are state functions, two different equivalent expressions such as those written for $dU$ here can be formulated:

$$dU = TdS - PdV = \left(\frac{\partial U}{\partial S}\right)_V dS + \left(\frac{\partial U}{\partial V}\right)_S dV \tag{6.21}$$

For Equation (6.21) to be valid, the coefficients of $dS$ and $dV$ on both sides of the equation must be equal. Applying this reasoning to Equations (6.17) through (6.20), the following expressions are obtained:

$$\left(\frac{\partial U}{\partial S}\right)_V = T \text{ and } \left(\frac{\partial U}{\partial V}\right)_S = -P \tag{6.22}$$

$$\left(\frac{\partial H}{\partial S}\right)_P = T \text{ and } \left(\frac{\partial H}{\partial P}\right)_S = V \tag{6.23}$$

$$\left(\frac{\partial A}{\partial T}\right)_V = -S \text{ and } \left(\frac{\partial A}{\partial V}\right)_T = -P \qquad \textbf{(6.24)}$$

$$\left(\frac{\partial G}{\partial T}\right)_P = -S \text{ and } \left(\frac{\partial G}{\partial P}\right)_T = V \qquad \textbf{(6.25)}$$

These expressions state how $U$, $H$, $A$, and $G$ vary with their natural variables. For example, because $T$ and $V$ always have positive values, Equation (6.23) states that $H$ increases if either the entropy or the pressure of the system increases. We discuss how to use these relations for macroscopic changes in the system variables in Section 6.4.

There is also a second way in which the differential expressions in Equations (6.17) through (6.20) can be used. From Section 3.1, we know that because $dU$ is an exact differential:

$$\left(\frac{\partial}{\partial V}\left(\frac{\partial U\,(S,V)}{\partial S}\right)_V\right)_S = \left(\frac{\partial}{\partial S}\left(\frac{\partial U\,(S,V)}{\partial V}\right)_S\right)_V$$

Equating the mixed second partial derivative derived from Equations (6.17) through (6.20), we obtain the following four **Maxwell relations:**

$$\left(\frac{\partial T}{\partial V}\right)_S = -\left(\frac{\partial P}{\partial S}\right)_V \qquad \textbf{(6.26)}$$

$$\left(\frac{\partial T}{\partial P}\right)_S = \left(\frac{\partial V}{\partial S}\right)_P \qquad \textbf{(6.27)}$$

$$\left(\frac{\partial S}{\partial V}\right)_T = \left(\frac{\partial P}{\partial T}\right)_V = \frac{\beta}{\kappa} \qquad \textbf{(6.28)}$$

$$-\left(\frac{\partial S}{\partial P}\right)_T = \left(\frac{\partial V}{\partial T}\right)_P = V\beta \qquad \textbf{(6.29)}$$

Equations (6.26) and (6.27) refer to a partial derivative at constant $S$. What conditions must a transformation at constant entropy satisfy? Because $dS = dq_{reversible}/T$, a transformation at constant entropy refers to a reversible adiabatic process.

---

**EXAMPLE PROBLEM 6.3**

Show that $\left(\dfrac{\partial T}{\partial V}\right)_S = -\left(\dfrac{\partial P}{\partial S}\right)_V$

**Solution**

Because $U$ is a state function, $\left(\dfrac{\partial}{\partial V}\left(\dfrac{\partial U\,(S,V)}{\partial S}\right)_V\right)_S = \left(\dfrac{\partial}{\partial S}\left(\dfrac{\partial U\,(S,V)}{\partial V}\right)_S\right)_V$.

Substituting $dU = TdS - PdV$ in the previous expression,

$$\left(\frac{\partial}{\partial V}\left(\frac{\partial[TdS - PdV]}{\partial S}\right)_V\right)_S = \left(\frac{\partial}{\partial S}\left(\frac{\partial[TdS - PdV]}{\partial V}\right)_S\right)_V$$

$$\left(\frac{\partial T}{\partial V}\right)_S = -\left(\frac{\partial P}{\partial S}\right)_V$$

---

The Maxwell relations have been derived using only the property that $U$, $H$, $A$, and $G$ are state functions. These four relations are extremely useful in transforming seemingly obscure partial derivatives in other partial derivatives that can be directly measured. For example, these relations will be used to express $U$, $H$, and heat capacities solely in terms of measurable quantities such as $\kappa$, $\beta$ and the state variables $P$, $V$, and $T$ in Supplemental Section 6.15.

## 6.3 The Dependence of the Gibbs and Helmholtz Energies on *P*, *V*, and *T*

The state functions $A$ and $G$ are particularly important for chemists because of their roles in determining the direction of spontaneous change in a reaction mixture. For this reason, we need to know how $A$ changes with $T$ and $V$, and how $G$ changes with $T$ and $P$.

We begin by asking how $A$ changes with $T$ and $V$. From Section 6.2,

$$\left(\frac{\partial A}{\partial T}\right)_V = -S \text{ and } \left(\frac{\partial A}{\partial V}\right)_T = -P \qquad (6.30)$$

where $S$ and $P$ always take on positive values. Therefore, the general statement can be made that the Helmholtz energy of a pure substance decreases as either the temperature or the volume increases.

Because most reactions of interest to chemists are carried out under constant pressure rather than constant volume conditions, we will devote more attention to the properties of $G$ than to those of $A$. From Section 6.2,

$$\left(\frac{\partial G}{\partial T}\right)_P = -S \text{ and } \left(\frac{\partial G}{\partial P}\right)_T = V \qquad (6.25)$$

Whereas the Gibbs energy decreases with increasing temperature, it increases with increasing pressure.

How can Equation (6.25) be used to calculate changes in $G$ with macroscopic changes in the variables $T$ and $P$? In doing so, each of the variables is considered separately. The total change in $G$ as both $T$ and $P$ are varied is the sum of the separate contributions, because $G$ is a state function. We first discuss the change in $G$ with $P$.

For a macroscopic change in $P$ at constant $T$, the second expression in Equation (6.25) is integrated at constant $T$:

$$\int_{P^\circ}^{P} dG = G(T, P) - G^\circ(T, P^\circ) = \int_{P^\circ}^{P} V dP' \qquad (6.31)$$

where we have chosen the initial pressure to be the standard state pressure $P^\circ = 1$ bar. This equation takes on different forms for liquids and solids and for gases. For liquids and solids, the volume is, to a good approximation, independent of $P$ over a limited range in $P$ and

$$G(T, P) = G^\circ(T, P^\circ) + \int_{P^\circ}^{P} V dP' \approx G^\circ(T, P^\circ) + V(P - P^\circ) \qquad (6.32)$$

By contrast, the volume of a gaseous system changes appreciably with pressure. In calculating the change of $G_m$ with $P$ at constant $T$, any path connecting the same initial and final states gives the same result. Choosing the reversible path and assuming ideal gas behavior,

$$G(T, P) = G^\circ(T) + \int_{P^\circ}^{P} V dP' = G^\circ(T) + \int_{P^\circ}^{P} \frac{nRT}{P'} dP' = G^\circ(T) + nRT \ln \frac{P}{P^\circ}$$

$$(6.33)$$

The functional dependence of the molar Gibbs energy $G_m$ on $P$ for an ideal gas is shown in Figure 6.1, where $G_m$ approaches minus infinity as the pressure approaches zero. This is a result of the volume dependence of $S$ that was discussed in Section 5.5, $\Delta S = nR \ln(V_f/V_i)$ at constant $T$. As $P \to 0$, $V \to \infty$. Because the volume available to a gas molecule is maximized as $V \to \infty$, $S \to \infty$ as $P \to 0$. Therefore, $G = H - TS \to -\infty$ in this limit.
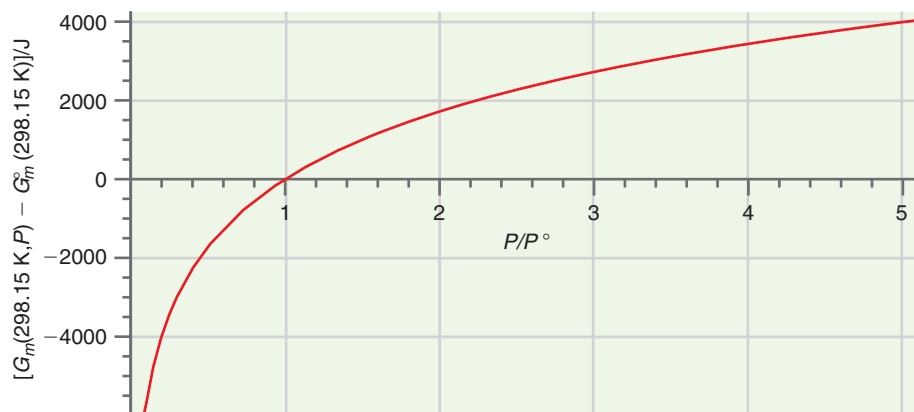
**FIGURE 6.1**
The molar Gibbs energy of an ideal gas relative to its standard state value is shown as a function of the pressure at 298.15 K.

We next investigate the dependence of $G$ on $T$. As we see in the next section, the thermodynamic equilibrium constant $K$ is related to $G/T$. Therefore, it is more useful to obtain an expression for the temperature dependence of $G/T$ than for the temperature dependence of $G$. Using the chain rule, this dependence is given by

$$\left(\frac{\partial[G/T]}{\partial T}\right)_P = \frac{1}{T}\left(\frac{\partial G}{\partial T}\right)_P + G\frac{d[1/T]}{dT}$$

$$= \frac{1}{T}\left(\frac{\partial G}{\partial T}\right)_P - \frac{G}{T^2} = -\frac{S}{T} - \frac{G}{T^2} = -\frac{G+TS}{T^2} = -\frac{H}{T^2} \qquad (6.34)$$

In the second line of Equation (6.34), we have used Equation (6.25), $(\partial G/\partial T)_P = -S$, and the definition $G = H - TS$. Equation (6.34) is known as the **Gibbs–Helmholtz equation.** Because

$$\frac{d(1/T)}{dT} = -\frac{1}{T^2}$$

the Gibbs–Helmholtz equation can also be written in the form

$$\left(\frac{\partial[G/T]}{\partial[1/T]}\right)_P = \left(\frac{\partial[G/T]}{\partial T}\right)_P \left(\frac{dT}{d[1/T]}\right) = -\frac{H}{T^2}(-T^2) = H \qquad (6.35)$$

The preceding equation also applies to the change in $G$ and $H$ associated with a process such as a chemical reaction. Replacing $G$ by $\Delta G$ and integrating Equation (6.35) at constant $P$,

$$\int_{T_1}^{T_2} d\left(\frac{\Delta G}{T}\right) = \int_{T_1}^{T_2} \Delta H d\left(\frac{1}{T}\right)$$

$$\frac{\Delta G(T_2)}{T_2} = \frac{\Delta G(T_1)}{T_1} + \Delta H(T_1)\left(\frac{1}{T_2} - \frac{1}{T_1}\right) \qquad (6.36)$$

It has been assumed in the second equation that $\Delta H$ is independent of $T$ over the temperature interval of interest. If this is not the case, the integral must be evaluated numerically, using tabulated values of $\Delta H_f^\circ$ and temperature-dependent expressions of $C_{P,m}$ for reactants and products.

### EXAMPLE PROBLEM 6.4

The value of $\Delta G_f^\circ$ for Fe(g) is 370.7 kJ mol$^{-1}$ at 298.15 K, and $\Delta H_f^\circ$ for Fe(g) is 416.3 kJ mol$^{-1}$ at the same temperature. Assuming that $\Delta H_f^\circ$ is constant in the interval 250–400 K, calculate $\Delta G_f^\circ$ for Fe(g) at 400. K.

**Solution**

$$\Delta G_f^\circ(T_2) = T_2 \left[ \frac{\Delta G_f^\circ(T_1)}{T_1} + \Delta H_f^\circ(T_1) \times \left( \frac{1}{T_2} - \frac{1}{T_1} \right) \right]$$

$$= 400.\,\text{K} \times \left[ \begin{array}{l} \dfrac{370.7 \times 10^3 \text{ J mol}^{-1}}{298.15 \text{ K}} + 416.3 \times 10^3 \text{ J mol}^{-1} \\[2mm] \times \left( \dfrac{1}{400.\,\text{K}} - \dfrac{1}{298.15 \text{ K}} \right) \end{array} \right]$$

$$\Delta G_f^\circ(400.\,\text{K}) = 355.1 \text{ kJ mol}^{-1}$$

Analogies to Equations (6.31) and (6.36) for the dependence of $A$ on $V$ and $T$ are left to the end-of-chapter problems.

# 6.4 The Gibbs Energy of a Reaction Mixture

To this point, the discussion has been limited to systems at a fixed composition. Our focus in the rest of the chapter is in using the Gibbs energy to understand equilibrium in a reaction mixture under constant pressure conditions that correspond to typical laboratory experiments. Because reactants are consumed and products are generated in chemical reactions, the expressions derived for state functions such as $U$, $H$, $S$, $A$, and $G$ must be revised to include changes in composition. We focus on $G$ in the following discussion.

For a reaction mixture containing species 1, 2, 3, ..., $G$ is no longer a function of the variables $T$ and $P$ only. Because it depends on the number of moles of each species, $G$ is written in the form $G = G(T, P, n_1, n_2, n_3, \ldots)$. The total differential $dG$ is

$$dG = \left( \frac{\partial G}{\partial T} \right)_{P,n_1,n_2\ldots} dT + \left( \frac{\partial G}{\partial P} \right)_{T,n_1,n_2\ldots} dP + \left( \frac{\partial G}{\partial n_1} \right)_{T,P,n_2\ldots} dn_1$$

$$+ \left( \frac{\partial G}{\partial n_2} \right)_{T,P,n_1\ldots} dn_2 + \ldots \quad (6.37)$$

Note that if the concentrations do not change, all of the $dn_i = 0$, and Equation (6.37) reduces to $dG = \left( \dfrac{\partial G}{\partial T} \right)_P dT + \left( \dfrac{\partial G}{\partial P} \right)_T dP$.

Equation (6.37) can be simplified by defining the **chemical potential** $\mu_i$ as

$$\mu_i = \left( \frac{\partial G}{\partial n_i} \right)_{P,T,n_j \neq n_i} \quad (6.38)$$

It is important to realize that although $\mu_i$ is defined mathematically in terms of an infinitesimal change in the amount $dn_i$ of species $i$, the chemical potential $\mu_i$ is the change in the Gibbs energy per mole of substance $i$ added *at constant concentration*. These two requirements are not contradictory. To keep the concentration constant, one adds a mole of substance $i$ to a huge vat containing many moles of the various species. In this case, the slope of a plot of $G$ versus $n_i$ is the same if the differential $(\partial G / \partial n_i)_{P,T,n_j \neq n_i}$ is formed, where $dn_i \to 0$, or the ratio $(\Delta G / \Delta n_i)_{P,T,n_j \neq n_i}$ is formed, where $\Delta n_i$ is 1 mol. Using the notation of Equation (6.38), Equation (6.37) can be written as follows:

$$dG = \left( \frac{\partial G}{\partial T} \right)_{P,n_1,n_2\ldots} dT + \left( \frac{\partial G}{\partial P} \right)_{T,n_1 n_2\ldots} dP + \sum_i \mu_i dn_i \quad (6.39)$$

Now imagine integrating Equation (6.39) at constant composition and at constant $T$ and $P$ from an infinitesimal size of the system where $n_i \to 0$ and therefore $G \to 0$ to a macroscopic size where the Gibbs energy has the value $G$. Because $T$ and $P$ are constant,

the first two terms in Equation (6.39) do not contribute to the integral. Because the composition is constant, $\mu_i$ is constant:

$$\int_0^G dG' = \sum_i \mu_i \int_0^{n_i} dn_i'$$

$$G = \sum_i n_i \mu_i \qquad (6.40)$$

Note that because $\mu_i$ depends on the number of moles of each species present, it is a function of concentration. If the system consists of a single pure substance A, $G = n_A G_{m,A}$ because $G$ is an extensive quantity. Applying Equation (6.38),

$$\mu_A = \left(\frac{\partial G}{\partial n_A}\right)_{P,T} = \left(\frac{\partial [n_A G_{m,A}]}{\partial n_A}\right)_{P,T} = G_{m,A}$$

showing that $\mu_A$ is an intensive quantity equal to the molar Gibbs energy of A *for a pure substance.* As shown later, this statement is not true for mixtures.

Why is $\mu_i$ called the chemical potential of species $i$? This can be understood by assuming that the chemical potential for species $i$ has the values $\mu_i^I$ in region I, and $\mu_i^{II}$ in region II of a given mixture with $\mu_i^I > \mu_i^{II}$. If $dn_i$ moles of species $i$ are transported from region I to region II at constant $T$ and $P$, the change in $G$ is given by

$$dG = -\mu_i^I \, dn_i + \mu_i^{II} \, dn_i = (\mu_i^{II} - \mu_i^I) dn_i < 0 \qquad (6.41)$$

Because $dG < 0$, this process is spontaneous. *For a given species, transport will occur spontaneously from a region of high chemical potential to one of low chemical potential. The flow of material will continue until the chemical potential has the same value in all regions of the mixture.* Note the analogy between this process and the flow of mass in a gravitational potential or the flow of charge in an electrostatic potential. Therefore, the term *chemical potential* is appropriate. In this discussion, we have defined a new criterion for equilibrium in a multicomponent mixture: *at equilibrium*, the chemical potential of each species is the same throughout a mixture.

# 6.5 The Gibbs Energy of a Gas in a Mixture

In the next three sections, the conditions for equilibrium in a reactive mixture of ideal gases are derived in terms of the $\mu_i$ of the chemical constituents. Imagine that we have a reaction vessel in which all reactants are initially confined to separate volumes through barriers that are suddenly removed to let the reaction proceed. Two important processes occur, namely (i) the mixing of reactants and (ii) the conversion of reactants to products. In both processes, the concentration of individual species and their chemical potentials change. In this section, we describe how the chemical potential of a reactant or product species changes as its concentration in the reaction mixture changes. In the next section, we describe how the chemical potential of a reactant or product species changes through mixing with other species. Using these results, we show in Section 6.7 that the partial pressures of all constituents of a gaseous reaction mixture are related by the thermodynamic equilibrium constant $K_P$.

Consider first the simple system consisting of two volumes separated by a semipermeable membrane, as shown in Figure 6.2. On the left side, the gas consists solely of pure $H_2$. On the right side, $H_2$ is present as one constituent of a mixture. The membrane allows only $H_2$ to pass in both directions.

Once equilibrium has been reached with respect to the concentration of $H_2$ throughout the system, the hydrogen pressure (but not the total pressure) is the same on both sides of the membrane and therefore

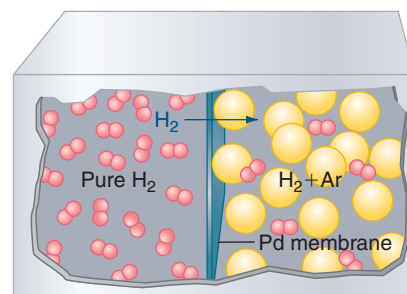$$\mu_{H_2}^{pure} = \mu_{H_2}^{mixture} \qquad (6.42)$$



**FIGURE 6.2**
An isolated system consists of two subsystems. Pure $H_2$ gas is present on the left of a palladium membrane that is permeable to $H_2$, but not to argon. The $H_2$ is contained in a mixture with Ar in the subsystem to the right of the membrane.

Recall from Section 6.3 that the molar Gibbs energy of a pure ideal gas depends on its pressure as $G(T, P) = G^\circ(T) + nRT \ln(P/P^\circ)$. Therefore, Equation (6.42) can be written in the form

$$\mu_{H_2}^{pure}(T, P_{H_2}) = \mu_{H_2}^{mixture}(T, P_{H_2}) = \mu_{H_2}^\circ(T) + RT \ln\frac{P_{H_2}}{P^\circ} \qquad \textbf{(6.43)}$$

The chemical potential of a gas in a mixture depends logarithmically on its partial pressure. Equation (6.43) applies to any mixture, not just to those for which an appropriate semipermeable membrane exists. We therefore generalize the discussion by referring to a component of the mixture as A. The partial pressure of species A in the gas mixture $P_A$ can be expressed in terms of $x_A$, its mole fraction in the mixture, and the total pressure $P$:

$$P_A = x_A P \qquad \textbf{(6.44)}$$

Using this relationship, Equation (6.43) becomes

$$\mu_A^{mixture}(T, P) = \mu_A^\circ(T) + RT \ln\frac{P}{P^\circ} + RT \ln x_A$$

$$= \left(\mu_A^\circ(T) + RT \ln\frac{P}{P^\circ}\right) + RT \ln x_A \text{ or}$$

$$\mu_A^{mixture}(T, P) = \mu_A^{pure}(T, P) + RT \ln x_A \qquad \textbf{(6.45)}$$

Because $x_A < 0$, we find that the chemical potential of a gas in a mixture is less than that of the pure gas if the total pressure $P$ is the same for the pure sample and the mixture. Because $\mu_A^{mixture}(T, P) < \mu_A^{pure}(T, P)$, diffusion of $H_2$ from the left side to the right side of the system in Figure 6.2 will continue until the partial pressures of $H_2$ on both sides of the membrane are equal. There is a further important conclusion that can be drawn from Equation (6.45): mixing of the two subsystems in Figure 6.2 would be spontaneous if they were not separated by the membrane.

# 6.6 Calculating the Gibbs Energy of Mixing for Ideal Gases

In the previous section, we showed how the chemical potential of a species in a mixture is related to the chemical potential of the pure species and the mole fraction of the species in the mixture. We also demonstrated that the mixing of gases is a spontaneous process, so that $\Delta G_{mixing}$ must be negative. We now obtain a quantitative relationship between $\Delta G_{mixing}$ and the mole fractions of the individual constituents of the mixture. Consider the system shown in Figure 6.3. The four compartments contain the gases He, Ne, Ar, and Xe at the same temperature and pressure. The volumes of the four compartments differ. To calculate $\Delta G_{mixing}$, we must compare $G$ for the initial state shown in Figure 6.3 and the final state in which all gases are uniformly distributed in the container. For the initial state, in which we have four pure separated substances,

$$G_i = G_{He} + G_{Ne} + G_{Ar} + G_{Xe} = n_{He}G_{m,He} + n_{Ne}G_{m,Ne} + n_{Ar}G_{m,Ar} + n_{Xe}G_{m,Xe} \qquad \textbf{(6.46)}$$

For the final state in which all four components are dispersed in the mixture, from Equation (6.45),

$$G_f = n_{He}(G_{m,He} + RT \ln x_{He}) + n_{Ne}(G_{m,Ne} + RT \ln x_{Ne})$$
$$+ n_{Ar}(G_{m,Ar} + RT \ln x_{Ar}) + n_{Xe}(G_{m,Xe} + RT \ln x_{Xe}) \qquad \textbf{(6.47)}$$

The Gibbs energy of mixing is $G_f - G_i$ or

$$\Delta G_{mixing} = RT n_{He} \ln x_{He} + RT n_{Ne} \ln x_{Ne} + RT n_{Ar} \ln x_{Ar} + RT n_{Xe} \ln x_{Xe}$$

$$= RT \sum_i n_i \ln x_i = nRT \sum_i x_i \ln x_i \qquad \textbf{(6.48)}$$

Note that because all the $x_i < 1$, each term in the last expression of Equation (6.48) is negative, so that $\Delta G_{mixing} < 0$, showing that mixing is a spontaneous process.



**FIGURE 6.3**
An isolated system consists of four separate subsystems containing He, Ne, Ar, and Xe, each at a pressure of 1 bar. The barriers separating these subsystems can be removed, leading to mixing.

Equation (6.48) allows us to calculate $\Delta G_{mixing}$ for any given set of the mole fractions $x_i$. It is easiest to graphically visualize the results for a binary mixture of species A and B. To simplify the notation, we set $x_A = x$, so that $x_B = 1 - x$. It follows that

$$\Delta G_{mixing} = nRT\left[x \ln x + (1 - x)\ln(1 - x)\right] \qquad \textbf{(6.49)}$$

A plot of $\Delta G_{mixing}$ versus $x$ is shown in Figure 6.4 for a binary mixture. Note that $\Delta G_{mixing}$ is zero for $x_A = 0$ and $x_A = 1$ because only pure substances are present in these limits. Also, $\Delta G_{mixing}$ has a minimum for $x_A = 0.5$, because the largest decrease in $G$ arises from mixing when A and B are present in equal amounts.

The entropy of mixing can be calculated from Equation (6.48):

$$\Delta S_{mixing} = -\left(\frac{\partial \Delta G_{mixing}}{\partial T}\right)_P = -nR\sum_i x_i \ln x_i \qquad \textbf{(6.50)}$$

As shown in Figure 6.5, the entropy of mixing increases in the range $x_A = 0$ to $x_A = 0.5$ and is greatest for $x_A = 0.5$. What is the cause of the initial increase in entropy? Each of the components of the mixture expands from its initial volume to a larger final volume. Therefore, $\Delta S_{mixing}$ arises from the dependence of $S$ on $V$ at constant $T$. We verify this assertion using the expression derived in Section 5.4 for the change of $S$ with $V$, and obtain Equation (6.50).

$$\Delta S = R\left(n_A \ln\frac{V_f}{V_{iA}} + n_B \ln\frac{V_f}{V_{iB}}\right) = R\left(nx_A \ln\frac{1}{x_A} + nx_B \ln\frac{1}{x_B}\right)$$

$$= -nR(x_A \ln x_A + x_B \ln x_B)$$

if both components and the mixture are at the same pressure and temperature. The maximum at $x_A = 0.5$ occurs because at that value, each component contributes equally to $\Delta S$.
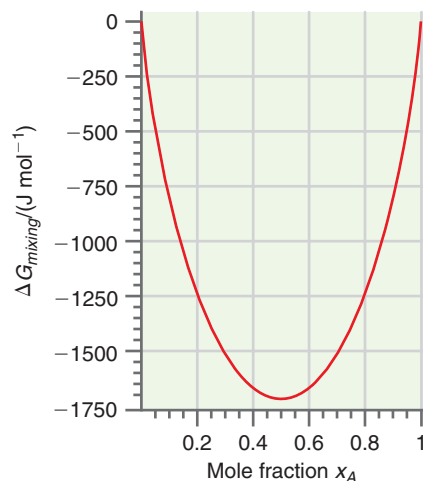


**FIGURE 6.4**
The Gibbs energy of mixing of the ideal gases A and B as a function of $x_A$, with $n_A + n_B = 1$ mole and $T = 298.15$ K.
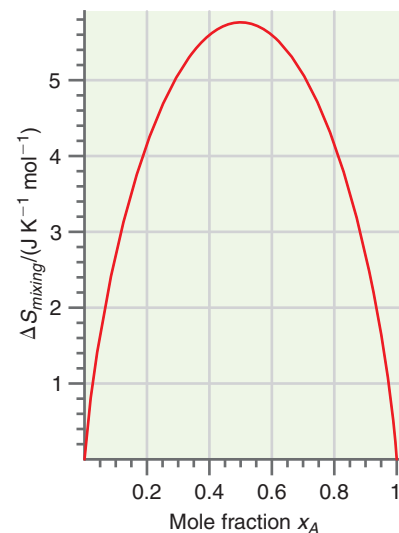


**FIGURE 6.5**
The entropy of mixing of the ideal gases A and B is shown as a function of the mole fraction of component A at 298.15 K, with $n_A + n_B = 1$.

---

**EXAMPLE PROBLEM 6.5**

Consider the system shown in Figure 6.3. Assume that the separate compartments contain 1.0 mol of He, 3.0 mol of Ne, 2.0 mol of Ar, and 2.5 mol of Xe at 298.15 K. The pressure in each compartment is 1 bar.

**a.** Calculate $\Delta G_{mixing}$.

**b.** Calculate $\Delta S_{mixing}$.

**Solution**

**a.** $\Delta G_{mixing} = RTn_{He} \ln x_{He} + RTn_{Ne} \ln x_{Ne} + RTn_{Ar} \ln x_{Ar} + RTn_{Xe} \ln x_{Xe}$

$$= RT\sum_i n_i \ln x_i = nRT\sum_i x_i \ln x_i$$

$$= 8.5 \text{ mol} \times 8.314 \text{ J K}^{-1} \text{ mol}^{-1} \times 298.15 \text{ K}$$

$$\times \left(\frac{1.0}{8.5}\ln\frac{1.0}{8.5} + \frac{3.0}{8.5}\ln\frac{3.0}{8.5} + \frac{2.0}{8.5}\ln\frac{2.0}{8.5} + \frac{2.5}{8.5}\ln\frac{2.5}{8.5}\right)$$

$$= -2.8 \times 10^4 \text{ J}$$

**b.** $\Delta S_{mixing} = -nR\sum_i x_i \ln x_i$

$$= -8.5 \text{ mol} \times 8.314 \text{ J K}^{-1} \text{ mol}^{-1}$$

$$\times \left(\frac{1.0}{8.5}\ln\frac{1.0}{8.5} + \frac{3.0}{8.5}\ln\frac{3.0}{8.5} + \frac{2.0}{8.5}\ln\frac{2.0}{8.5} + \frac{2.5}{8.5}\ln\frac{2.5}{8.5}\right)$$

$$= 93 \text{ J K}^{-1}$$

What is the driving force for the mixing of gases? We saw in Section 6.1 that there are two contributions to $\Delta G$, an enthalpic contribution $\Delta H$ and an entropic contribution $T\Delta S$. By calculating $\Delta H_{mixing}$ from $\Delta H_{mixing} = \Delta G_{mixing} + T\Delta S_{mixing}$ using Equations (6.49) and (6.50), you will see that for the mixing of ideal gases,

$\Delta H_{mixing} = 0$. Because the molecules in an ideal gas do not interact, there is no enthalpy change associated with mixing. We conclude that the mixing of ideal gases is driven entirely by $\Delta S_{mixing}$ as shown earlier.

Although the mixing of gases is always spontaneous, the same is not true of liquids. Liquids can be either miscible or immiscible. How can this fact be explained? For gases or liquids, $\Delta S_{mixing} > 0$. Therefore, if two liquids are immiscible, $\Delta G_{mixing} > 0$ and $\Delta H_{mixing} = \Delta G_{mixing} + T\Delta S_{mixing} > 0$, showing that there are repulsive interactions between the components to be mixed. If two liquids mix, $\Delta G_{mixing} < 0$ so that $\Delta H_{mixing} < T\Delta S_{mixing}$. In this case, there can be a weak repulsive interaction between the components if it is outweighed by the entropic contribution to $\Delta G_{mixing}$.

# 6.7 Calculating $\Delta G_R^\circ$ for a Chemical Reaction

Given a set of initial number of moles of all pure separated gaseous components in a reaction mixture, there is only one set of partial pressures $P_i$ that corresponds to equilibrium. In this section, we combine the results of the two previous sections to identify the equilibrium position in a reaction mixture.

Consider the balanced chemical reaction

$$\alpha A + \beta B + \chi C + ... \rightarrow \delta M + \varepsilon N + \gamma O + ... \qquad (6.51)$$
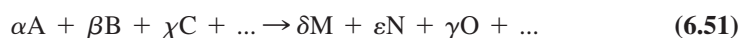
in which Greek letters represent stoichiometric coefficients and uppercase Roman letters represent reactants and products. We can write an abbreviated expression for this reaction in the form

$$0 = \sum_i v_i X_i \qquad (6.52)$$

where $v_i$ represents the stoichiometric coefficients and $X_i$ represents the reactants and products. In Equation (6.52), the $v_i$ of the products are positive, and those of the reactants are negative.

What determines the equilibrium partial pressures of the reactants and products? Imagine that the reaction proceeds in the direction indicated in Equation (6.51) by an infinitesimal amount. The change in the Gibbs energy is given by

$$dG = \sum_i \mu_i dn_i \qquad (6.53)$$

In this equation, the individual $dn_i$ are not independent, because they are linked by the stoichiometric equation.

The direction of spontaneous change is determined by $\Delta G_R$. How can $\Delta G_R$ be calculated for a reaction mixture? We distinguish between calculating $\Delta G_R^\circ$ for the standard state in which $P_i = P^\circ = 1$ bar for all species and calculating $\Delta G_R$ for the set of $P_i$ corresponding to equilibrium. Tabulated values of $\Delta G_f^\circ$ for compounds are used to calculate $\Delta G_R^\circ$ at $P^\circ = 1$ bar and $T = 298.15$ K as shown in Example Problem 6.6. Just as for enthalpy, $\Delta G_f^\circ$ for a pure element in its standard reference state is equal to zero because the reactants and products in the formation reaction are identical.

$$\Delta G_R^\circ = \sum_i v_i \Delta G_{f,i}^\circ \qquad (6.54)$$

---

**EXAMPLE PROBLEM 6.6**

Calculate $\Delta G_R^\circ$ for the reaction $2NO_2(g) \rightarrow N_2O_4(g)$ at 298.15 K. Is the reaction spontaneous if the pressure of $NO(g)$ is 1 bar at this temperature?

**Solution**

$$\Delta G_R^\circ = \Delta G_f^\circ(N_2O_4, g) - 2\Delta G_f^\circ(NO_2, g)$$
$$= 99.8 \text{ kJ mol}^{-1} - 2 \times 51.3 \text{ kJ mol}^{-1}$$
$$= -2.80 \text{ kJ mol}^{-1}$$

Because $\Delta G_R^\circ < 0$, the reaction is spontaneous at 298.15 K.

At other temperatures, $\Delta G_R^\circ$ is calculated as shown in Example Problem 6.7.

### EXAMPLE PROBLEM 6.7

Calculate $\Delta G_R^\circ$ for the reaction in Example Problem 6.6 at 325 K. Is the reaction spontaneous at this temperature?

**Solution**

To calculate $\Delta G_R^\circ$ at the elevated temperature, we use Equation (6.36) assuming that $\Delta H_R^\circ$ is independent of $T$:

$$\Delta G_R^\circ (T_2) = T_2 \left[ \frac{\Delta G_R^\circ (298.15 \text{ K})}{298.15 \text{ K}} + \Delta H_R^\circ (298.15 \text{ K}) \left( \frac{1}{T_2} - \frac{1}{298.15 \text{ K}} \right) \right]$$

$$\Delta H_R^\circ (298.15 \text{ K}) = \Delta H_f^\circ (N_2O_4, g) - 2\Delta H_f^\circ (NO_2, g)$$

$$= 11.1 \text{ kJ mol}^{-1} - 2 \times 33.2 \text{ kJ mol}^{-1} = -55.3 \text{ kJ mol}^{-1}$$

$$\Delta G_R^\circ (325 \text{ K}) = 325 \text{ K} \times \left[ \begin{array}{c} \dfrac{-2.80 \times 10^3 \text{J mol}^{-1}}{298.15 \text{ K}} \\[2mm] -55.3 \times 10^3 \text{J mol}^{-1} \left( \dfrac{1}{325 \text{ K}} - \dfrac{1}{298.15 \text{ K}} \right) \end{array} \right]$$

$$\Delta G_R^\circ (325 \text{ K}) = 1.92 \text{ kJ mol}^{-1}$$

Because $\Delta G_R^\circ > 0$, the reaction is not spontaneous at 325 K.

# 6.8 Introducing the Equilibrium Constant for a Mixture of Ideal Gases

Spontaneity for a reaction does not imply that the reaction goes to completion, but rather that the equilibrium reaction mixture contains more products than reactants. In this and the next section, we establish a framework for calculating the partial pressures of reactants and products in a chemical reaction at equilibrium.

In a reaction mixture with a total pressure of 1 bar, the partial pressures of each species $P_i$ is less than the standard state pressure of 1 bar. In this section, we introduce the pressure dependence of $\mu_i$ in order to calculate $\Delta G_R$ for a typical reaction mixture. Consider the following reaction that takes place between ideal gas species A, B, C, and D:

$$\alpha A(g) + \beta B(g) \rightleftharpoons \gamma C(g) + \delta D(g) \tag{6.55}$$
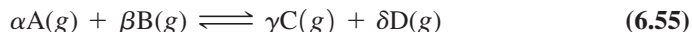
Because all four species are present in the reaction mixture, the reaction Gibbs energy for the arbitrary set of partial pressures $P_A$, $P_B$, $P_C$, and $P_D$, is given by

$$\Delta G_R = \sum_i v_i \Delta G_{f,i} = \gamma \mu_C^\circ + \gamma RT \ln \frac{P_C}{P^\circ} + \delta \mu_D^\circ + \delta RT \ln \frac{P_D}{P^\circ}$$

$$-\alpha \mu_A^\circ - \alpha RT \ln \frac{P_A}{P^\circ} - \beta \mu_B^\circ - \beta RT \ln \frac{P_B}{P^\circ} \tag{6.56}$$

The terms in the previous equation can be separated into those at the standard condition of $P^\circ = 1$ bar and the remaining terms:

$$\Delta G_R = \Delta G_R^\circ + \gamma RT \ln \frac{P_C}{P^\circ} + \delta RT \ln \frac{P_D}{P^\circ} - \alpha RT \ln \frac{P_A}{P^\circ} - \beta RT \ln \frac{P_B}{P^\circ}$$

$$= \Delta G_R^\circ + RT \ln \frac{\left( \dfrac{P_C}{P^\circ} \right)^\gamma \left( \dfrac{P_D}{P^\circ} \right)^\delta}{\left( \dfrac{P_A}{P^\circ} \right)^\alpha \left( \dfrac{P_B}{P^\circ} \right)^\beta} \tag{6.57}$$

where

$$\Delta G_R^\circ = \gamma \mu_C^\circ (T) + \delta \mu_D^\circ (T) - \alpha \mu_A^\circ (T) - \beta \mu_B^\circ (T) = \sum_i v_i \Delta G_{f,i}^\circ \tag{6.58}$$

Recall from Example Problem 6.6 that standard Gibbs energies of formation rather than chemical potentials are used to calculate $\Delta G_R^\circ$.

The combination of the partial pressures of reactants and products in Equation (6.57) is called the **reaction quotient of pressures,** which is abbreviated $Q_P$ and defined as follows:

$$Q_P = \frac{\left(\dfrac{P_C}{P^\circ}\right)^\gamma \left(\dfrac{P_D}{P^\circ}\right)^\delta}{\left(\dfrac{P_A}{P^\circ}\right)^\alpha \left(\dfrac{P_B}{P^\circ}\right)^\beta} \tag{6.59}$$

With these definitions of $\Delta G_R^\circ$ and $Q_P$, Equation (6.56) becomes

$$\Delta G_R = \Delta G_R^\circ + RT \ln Q_P \tag{6.60}$$

*Note this important result that $\Delta G_R$ can be separated into two terms, only one of which depends on the partial pressures of reactants and products.*

We next show how Equation (6.60) can be used to predict the direction of spontaneous change for a given set of partial pressures of the reactants and products. If the partial pressures of the reactants A and B are large, and those of the products C and D are small compared to their values at equilibrium, $Q_P$ will be small. As a result, $RT \ln Q_P$ will be large and negative. In this case, $\Delta G_R = \Delta G_R^\circ + RT \ln Q_P < 0$ and the reaction will be spontaneous as written from left to right, as some of the reactants combine to form products.

Next, consider the opposite extreme. If the partial pressures of the products C and D are large, and those of the reactants A and B are small compared to their values at equilibrium, $Q_P$ will be large. As a result, $RT \ln Q_P$ will be large and positive, and $\Delta G_R = \Delta G_R^\circ + RT \ln Q_P > 0$. In this case, the reaction as written in Equation (6.55) from left to right is not spontaneous, but the reverse of the reaction is spontaneous.

## EXAMPLE PROBLEM 6.8

$NO_2(g)$ and $N_2O_4(g)$ are in a reaction vessel with partial pressures of 0.350 and 0.650 bar, respectively, at 298 K. Is this system at equilibrium? If not, will the system move toward reactants or products to reach equilibrium?

### Solution

The reaction of interest is $2\,NO_2(g) \rightleftharpoons N_2O_4(g)$. We calculate $\Delta G_R$ using $\Delta G_R = \Delta G_R^\circ + RT \ln Q_P$

$$\Delta G_R = 99.8 \text{ kJ mol}^{-1} - 2 \times 51.3 \text{ kJ mol}^{-1} + 8.314 \text{ J mol}^{-1} \text{ K}^{-1}$$

$$\times\ 298 \text{ K} \ln\frac{0.650 \text{ bar}/1 \text{ bar}}{(0.350 \text{ bar}/1 \text{ bar})^2}$$

$$= -2.80 \times 10^3 \text{ J mol}^{-1} + 4.13 \times 10^3 \text{ J mol}^{-1}$$

$$= 1.33 \times 10^3 \text{ J mol}^{-1}$$

Since $\Delta G_R \neq 0$, the system is not at equilibrium, and because $\Delta G_R > 0$, the system moves toward reactants.

Whereas the two cases that we have considered lead to a change in the partial pressures of the reactants and products, the most interesting case is equilibrium, for which $\Delta G_R = 0$. At equilibrium, $\Delta G_R^\circ = -RT \ln Q_P$. We denote this special system configuration by adding a superscript $eq$ to each partial pressure and renaming $Q_P$ as $K_P$. The quantity $K_P$ is called the **thermodynamic equilibrium constant:**

$$0 = \Delta G_R^\circ + RT \ln \frac{\left(\dfrac{P_C^{eq}}{P^\circ}\right)^\gamma \left(\dfrac{P_D^{eq}}{P^\circ}\right)^\delta}{\left(\dfrac{P_A^{eq}}{P^\circ}\right)^\alpha \left(\dfrac{P_B^{eq}}{P^\circ}\right)^\beta} \quad \text{or, equivalently,} \quad \Delta G_R^\circ = -RT \ln K_P$$

or

$$\ln K_P = -\frac{\Delta G_R^\circ}{RT} \tag{6.61}$$

Because $\Delta G_R^\circ$ is a function of $T$ only, $K_P$ is also a function of $T$ only. *The thermodynamic equilibrium constant $K_P$ does not depend on the total pressure or the partial pressure of reactants or products.* Note also that $K_P$ is a dimensionless number because each partial pressure is divided by $P^\circ$.

It is important to understand that the equilibrium condition of Equation (6.61) links the partial pressures of all reactants and products. Imagine that a quantity of species D is added to the system initially at equilibrium. The system will reach a new equilibrium state in which $P_A^{eq}$, $P_B^{eq}$, $P_C^{eq}$ and $P_D^{eq}$ all have new values because the value of

$$K_P = \left(\frac{P_C^{eq}}{P^\circ}\right)^\gamma \left(\frac{P_D^{eq}}{P^\circ}\right)^\delta \bigg/ \left(\frac{P_A^{eq}}{P^\circ}\right)^\alpha \left(\frac{P_B^{eq}}{P^\circ}\right)^\beta \quad \text{has not changed.}$$

### EXAMPLE PROBLEM 6.9

a. Using data from Table 4.1 (see Appendix A, Data Tables), calculate $K_P$ at 298.15 K for the reaction $CO(g) + H_2O(l) \rightarrow CO_2(g) + H_2(g)$.

b. Based on the value that you obtained for part (a), do you expect the mixture to consist mainly of $CO_2(g)$ and $H_2(g)$ or mainly of $CO(g) + H_2O(l)$ at equilibrium?

#### Solution

a. $\ln K_P = -\dfrac{1}{RT} \Delta G_R^\circ$

$= -\dfrac{1}{RT}\left(\begin{array}{l} \Delta G_f^\circ(CO_2, g) + \Delta G_f^\circ(H_2, g) - \Delta G_f^\circ(H_2O, l) \\ -\Delta G_f^\circ(CO, g) \end{array}\right)$

$= -\dfrac{1}{8.314 \text{ J mol}^{-1} \text{ K}^{-1} \times 298.15 \text{ K}}$

$\times \left(\begin{array}{l} -394.4 \times 10^3 \text{ J mol}^{-1} + 0 + 237.1 \\ \times 10^3 \text{ J mol}^{-1} + 137.2 \times 10^3 \text{ J mol}^{-1} \end{array}\right)$

$= 8.1087$

$K_P = 3.32 \times 10^3$

b. Because $K_P \gg 1$, the mixture will consist mainly of the products $CO_2(g) + H_2(g)$ at equilibrium.

## 6.9 Calculating the Equilibrium Partial Pressures in a Mixture of Ideal Gases

As shown in the previous section, the partial pressures of the reactants and products in a mixture of gases at equilibrium cannot take on arbitrary values, because they are related through $K_P$. In this section, we show how the equilibrium partial pressures can be calculated for ideal gases. Similar calculations for real gases will be discussed in the next chapter. In Example Problem 6.10, we consider the dissociation of chlorine:

$$Cl_2(g) \rightleftharpoons 2Cl(g) \tag{6.62}$$

It is useful to set up the calculation in a tabular form as shown in the following example problem.

### EXAMPLE PROBLEM 6.10

In this example, $n_0$ moles of chlorine gas are placed in a reaction vessel whose temperature can be varied over a wide range, so that molecular chlorine can partially dissociate to atomic chlorine.

**a.** Define the degree of dissociation as $\alpha = \delta_{eq}/n_0$, where $2\delta_{eq}$ is the number of moles of $Cl(g)$ present at equilibrium, and $n_0$ represents the number of moles of $Cl_2(g)$ that would be present in the system if no dissociation occurred. Derive an expression for $K_P$ in terms of $n_0$, $\delta_{eq}$, and $P$.

**b.** Derive an expression for $\alpha$ as a function of $K_P$ and $P$.

#### Solution

**a.** We set up the following table:

|  | $Cl_2(g)$ | $\rightleftharpoons$ | $2Cl(g)$ |
|---|---|---|---|
| Initial number of moles | $n_0$ |  | $0$ |
| Moles present at equilibrium | $n_0 - \delta_{eq}$ |  | $2\delta_{eq}$ |
| Mole fraction present at equilibrium, $x_i$ | $\dfrac{n_0 - \delta_{eq}}{n_0 + \delta_{eq}}$ |  | $\dfrac{2\delta_{eq}}{n_0 + \delta_{eq}}$ |
| Partial pressure at equilibrium, $P_i = x_iP$ | $\left(\dfrac{n_0 - \delta_{eq}}{n_0 + \delta_{eq}}\right)P$ |  | $\left(\dfrac{2\delta_{eq}}{n_0 + \delta_{eq}}\right)P$ |

We next express $K_P$ in terms of $n_0$, $\delta_{eq}$, and $P$:

$$K_P(T) = \frac{\left(\dfrac{P_{Cl}^{eq}}{P^\circ}\right)^2}{\left(\dfrac{P_{Cl_2}^{eq}}{P^\circ}\right)} = \frac{\left[\left(\dfrac{2\delta_{eq}}{n_0 + \delta_{eq}}\right)\dfrac{P}{P^\circ}\right]^2}{\left(\dfrac{n_0 - \delta_{eq}}{n_0 + \delta_{eq}}\right)\dfrac{P}{P^\circ}}$$

$$= \frac{4\delta_{eq}^2}{\left(n_0 + \delta_{eq}\right)\left(n_0 - \delta_{eq}\right)}\frac{P}{P^\circ} = \frac{4\delta_{eq}^2}{(n_0)^2 - \delta_{eq}^2}\frac{P}{P^\circ}$$

This expression is converted into one in terms of $\alpha$:

$$K_P(T) = \frac{4\delta_{eq}^2}{(n_0)^2 - \delta_{eq}^2}\frac{P}{P^\circ} = \frac{4\alpha^2}{1 - \alpha^2}\frac{P}{P^\circ}$$

**b.** $\left(K_P(T) + 4\dfrac{P}{P^\circ}\right)\alpha^2 = K_P(T)$

$$\alpha = \sqrt{\frac{K_P(T)}{K_P(T) + 4\dfrac{P}{P^\circ}}}$$

Because $K_P(T)$ depends strongly on temperature, $\alpha$ will also be a strong function of temperature. Note that $\alpha$ also depends on both $K_P$ and $P$ for this reaction.

Whereas $K_P(T)$ is independent of $P$, $\alpha$ as calculated in Example Problem 6.10 does depend on $P$. In the particular case considered, $\alpha$ decreases as $P$ increases for constant $T$. As will be shown in Section 6.12, $\alpha$ depends on $P$ whenever $\Delta v \neq 0$ for a reaction.

# 6.10 The Variation of $K_P$ with Temperature

In Section 6.8, we showed that $K_P$ and $\Delta G_R^\circ$ are related by $\ln K_P = -\Delta G_R^\circ/RT = -\Delta H_R^\circ/RT + \Delta S_R^\circ$. We illustrate how these individual functions vary with temperature for two reactions of industrial importance, beginning with
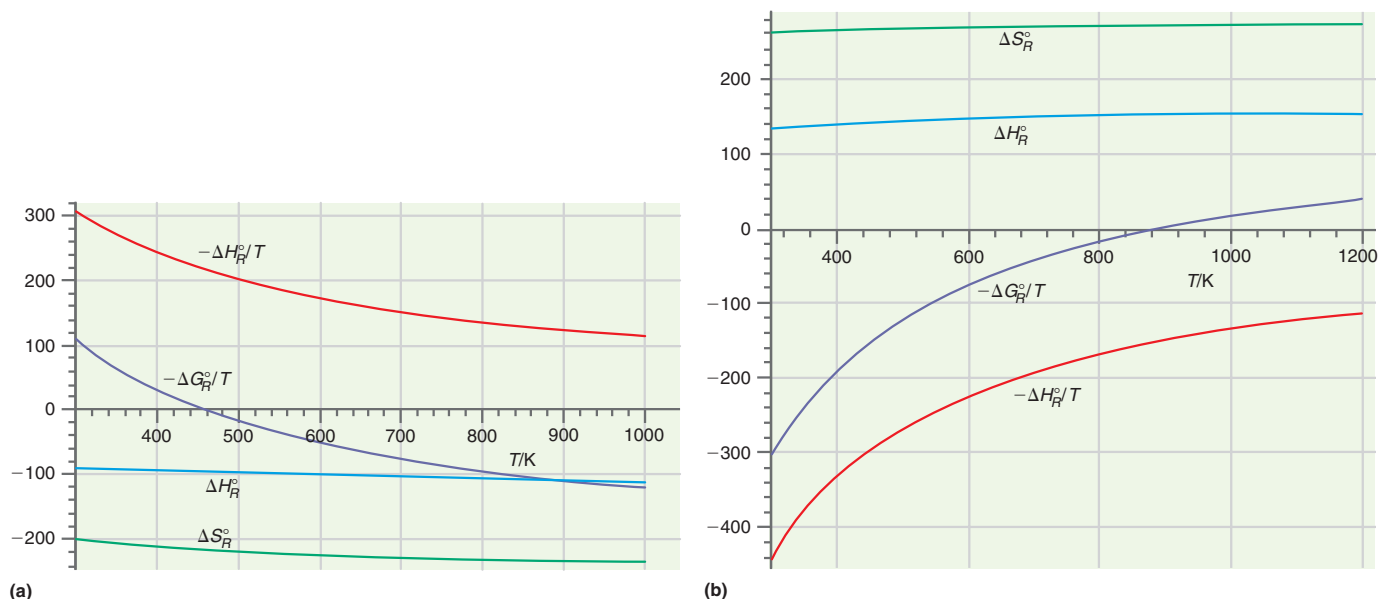
(a)



(b)

ammonia synthesis. This reaction is used to produce almost all of the fertilizer used in growing foodcrops and will be discussed in detail in Section 6.14. The overall reaction is
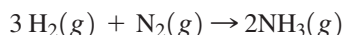
$$3\,H_2(g)\,+\,N_2(g)\rightarrow 2NH_3(g)$$

Figure 6.6a shows that $\Delta H_R^{\circ}$ is large, negative, and weakly dependent on temperature. Because the number of moles of gaseous species decreases as the reaction proceeds, $\Delta S_R^{\circ}$ is negative and is weakly dependent on temperature. The temperature dependence of $\ln K_P = -\Delta G_R^{\circ}/RT$ is determined by $-\Delta H_R^{\circ}/RT$. Because $\Delta H_R^{\circ}$ is negative, $K_P$ decreases as $T$ increases. We see that $K_P > 1$ for $T < 450$ K, and it decreases with increasing $T$ throughout the temperature range shown.

Figure 6.6b shows analogous results for the coal gasification reaction

$$H_2O(g)\,+\,C(s)\rightarrow CO(g)\,+\,H_2(g)$$
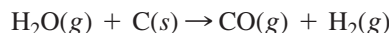
This reaction produces a mixture of $CO(g)$ and $H_2(g)$, which is known as syngas. It can be used to produce diesel engine fuel in the form of alkanes through the Fischer-Tropsch process in the reaction $(2n\,+\,1)H_2(g)\,+\,nCO(g)\rightarrow C_nH_{(2n+2)}(l)\,+\,nH_2O(l)$. For the coal gasification reaction, the number of moles of gaseous species increases as the reaction proceeds so that $\Delta S_R^{\circ}$ is positive. $\Delta H_R^{\circ}$ is large, positive, and not strongly dependent on temperature. Again, the temperature dependence of $K_P$ is determined by $-\Delta H_R^{\circ}/RT$. Because $\Delta H_R^{\circ}$ is positive, $K_P$ increases as $T$ increases.

The following conclusions can be drawn from Figure 6.6:

- The temperature dependence of $K_P$ is determined by $\Delta H_R^{\circ}$.
- If $\Delta H_R^{\circ} > 0$, $K_P$ increases with increasing $T$; if $\Delta H_R^{\circ} < 0$, $K_P$ decreases with increasing $T$.
- $\Delta S_R^{\circ}$ has essentially no effect on the dependence of $K_P$ on $T$.
- If $\Delta S_R^{\circ} > 0$, $\ln K_P$ is increased by the same amount relative to $-\Delta H_R^{\circ}/RT$ at all temperatures. If $\Delta S_R^{\circ} < 0$, $\ln K_P$ is decreased by the same amount relative to $-\Delta H_R^{\circ}/RT$ at all temperatures.

We can also derive an expression for the dependence of $\ln K_P$ on $T$. Starting with Equation (6.61), we write

$$\frac{d\ln K_P}{dT} = -\frac{d\left(\Delta G_R^{\circ}/RT\right)}{dT} = -\frac{1}{R}\frac{d\left(\Delta G_R^{\circ}/T\right)}{dT} \qquad \textbf{(6.63)}$$

Using the Gibbs–Helmholtz equation [Equation (6.34)], the preceding equation reduces to

$$\frac{d\ln K_P}{dT} = -\frac{1}{R}\frac{d(\Delta G_R^{\circ}/T)}{dT} = \frac{\Delta H_R^{\circ}}{RT^2} \qquad \textbf{(6.64)}$$

Because tabulated values of $\Delta G_f^\circ$ are available at 298.15 K, we can calculate $\Delta G_R^\circ$ and $K_P$ at this temperature; $K_P$ can be calculated at the temperature $T_f$ by integrating Equation (6.64) between the appropriate limits:

$$\int_{K_P(298.15\,K)}^{K_P(T_f)} d\ln K_P = \frac{1}{R}\int_{298.15\,K}^{T_f} \frac{\Delta H_R^\circ}{T^2}\,dT \tag{6.65}$$

If the temperature $T_f$ is not much different from 298.15 K, it can be assumed that $\Delta H_R^\circ$ is constant over the temperature interval. This assumption is better than it might appear at first glance as was shown in Figures 6.5 and 6.6. Although $H$ is strongly dependent on temperature, the temperature dependence of $\Delta H_R^\circ$ is governed by the difference in heat capacities $\Delta C_P$ between reactants and products (see Section 3.4). If the heat capacities of reactants and products are nearly the same, $\Delta H_R^\circ$ is nearly independent of temperature. With the assumption that $\Delta H_R^\circ$ is independent of temperature, Equation (6.65) becomes

$$\ln K_P(T_f) = \ln K_P(298.15\,K) - \frac{\Delta H_R^\circ}{R}\left(\frac{1}{T_f} - \frac{1}{298.15\,K}\right) \tag{6.66}$$

### EXAMPLE PROBLEM 6.11

Using the result of Example Problem 6.10 and the data tables, consider the dissociation equilibrium $Cl_2(g) \rightleftharpoons 2Cl(g)$.

a.  Calculate $K_P$ at 800. K, 1500. K, and 2000. K for $P = 0.010$ bar.

b.  Calculate the degree of dissociation $\alpha$ at 300. K, 1500. K, and 2000. K.

#### Solution

a.  $\Delta G_R^\circ = 2\Delta G_f^\circ(Cl, g) - \Delta G_f^\circ(Cl_2, g) = 2 \times 105.7 \times 10^3\,J\,mol^{-1} - 0$

$\qquad = 211.4\,kJ\,mol^{-1}$

$\Delta H_R^\circ = 2\Delta H_f^\circ(Cl, g) - \Delta H_f^\circ(Cl_2, g) = 2 \times 121.3 \times 10^3\,J\,mol^{-1} - 0$

$\qquad = 242.6\,kJ\,mol^{-1}$

$$\ln K_P(T_f) = -\frac{\Delta G_R^\circ}{RT} - \frac{\Delta H_R^\circ}{R}\left(\frac{1}{T_f} - \frac{1}{298.15\,K}\right)$$

$$= -\frac{211.4 \times 10^3\,J\,mol^{-1}}{8.314\,J\,K^{-1}\,mol^{-1} \times 298.15\,K} - \frac{242.6 \times 10^3\,J\,mol^{-1}}{8.314\,J\,K^{-1}\,mol^{-1}}$$

$$\times \left(\frac{1}{T_f} - \frac{1}{298.15\,K}\right)$$

$\ln K_P(800.\,K)$

$$= -\frac{211.4 \times 10^3\,J\,mol^{-1}}{8.314\,J\,K^{-1}\,mol^{-1} \times 298.15\,K} - \frac{242.6 \times 10^3\,J\,mol^{-1}}{8.314\,J\,K^{-1}\,mol^{-1}}$$

$$\times \left(\frac{1}{800.\,K} - \frac{1}{298.15\,K}\right) = -23.888$$

$K_P(800.\,K) = 4.22 \times 10^{-11}$

The values for $K_P$ at 1500. and 2000. K are $1.03 \times 10^{-3}$ and 0.134, respectively.

b.  The value of $\alpha$ at 2000. K is given by

$$\alpha = \sqrt{\frac{K_P(T)}{K_P(T) + 4\dfrac{P}{P^\circ}}} = \sqrt{\frac{0.134}{0.134 + 4 \times 0.01}} = 0.878$$

The values of $\alpha$ at 1500. and 800. K are 0.159 and $3.23 \times 10^{-5}$, respectively.

The degree of dissociation of $Cl_2$ increases with temperature as shown in Example Problem 6.11. This is always the case for an endothermic reaction.

# 6.11 Equilibria Involving Ideal Gases and Solid or Liquid Phases

In the preceding sections, we discussed chemical equilibrium in a homogeneous system of ideal gases. However, many chemical reactions involve a gas phase in equilibrium with a solid or liquid phase. An example is the thermal decomposition of $CaCO_3(s)$:

$$CaCO_3(s) \rightleftharpoons CaO(s) + CO_2(g) \tag{6.67}$$

In this case, a pure gas is in equilibrium with two solid phases at the pressure $P$. At equilibrium,

$$\Delta G_R = \sum_i n_i \mu_i = 0$$

$$0 = \mu_{eq}(CaO, s, P) + \mu_{eq}(CO_2, g, P) - \mu_{eq}(CaCO_3, s, P) \tag{6.68}$$

Because the equilibrium pressure is $P \neq P°$, the pressure dependence of $\mu$ for each species must be taken into account. From Section 6.3, we know that the pressure dependence of $G$ for a solid or liquid is very small:

$$\mu_{eq}(CaO, s, P) \approx \mu°(CaO, s) \text{ and } \mu_{eq}(CaCO_3, s, P) \approx \mu°(CaCO_3, s) \tag{6.69}$$

You will verify the validity of Equation (6.69) in the end-of-chapter problems. Using the dependence of $\mu$ on $P$ for an ideal gas, Equation (6.68) becomes

$$0 = \mu°(CaO, s) + \mu°(CO_2, g) - \mu°(CaCO_3, s) + RT \ln \frac{P_{CO_2}}{P°} \text{ or}$$

$$\Delta G_R° = \mu°(CaO, s) + \mu°(CO_2, g) - \mu°(CaCO_3, s) = -RT \ln \frac{P_{CO_2}}{P°} \tag{6.70}$$

Rewriting this equation in terms of $K_P$, we obtain

$$\ln K_P = \ln \frac{P_{CO_2}}{P°} = -\frac{\Delta G_R°}{RT} \tag{6.71}$$

We generalize this result as follows. *$K_P$ for an equilibrium involving gases with liquids and/or solids contains only contributions from the gaseous species. However, $\Delta G_R°$ is calculated taking all species into account.*

## EXAMPLE PROBLEM 6.12

Using the preceding discussion and the tabulated values of $\Delta G_f°$ and $\Delta H_f°$ in Appendix A, calculate the $CO_2(g)$ pressure in equilibrium with a mixture of $CaCO_3(s)$ and $CaO(s)$ at 1000., 1100., and 1200. K.

### Solution

For the reaction $CaCO_3(s) \rightleftharpoons CaO(s) + O_2(g)$, $\Delta G_R° = 131.1 \text{ kJ mol}^{-1}$ and $\Delta H_R° = 178.5 \text{ kJ mol}^{-1}$ at 298.15 K. We use Equation (6.71) to calculate $K_P(298.15 \text{ K})$ and Equation (6.66) to calculate $K_P$ at elevated temperatures.

$$\ln \frac{P_{CO_2}}{P°}(1000. \text{ K}) = \ln K_P(1000. \text{ K})$$

$$= \ln K_P(298.15 \text{ K}) - \frac{\Delta H_{R,298.15K}°}{R}\left(\frac{1}{1000. \text{ K}} - \frac{1}{298.15 \text{ K}}\right)$$

$$= \frac{-131.1 \times 10^3 \text{ J mol}^{-1}}{8.314 \text{ J K}^{-1} \text{ mol}^{-1} \times 298.15 \text{ K}} - \frac{178.5 \times 10^3 \text{ J mol}^{-1}}{8.314 \text{ J K}^{-1} \text{ mol}^{-1}}$$

$$\times \left( \frac{1}{1000. \text{ K}} - \frac{1}{298.15 \text{ K}} \right)$$

$$= -2.348; \quad P_{CO_2}(1000. \text{ K}) = 0.0956 \text{ bar}$$

The values for $P_{CO_2}$ at 1100. K and 1200. K are 0.673 bar and 1.23 bar.

If the reaction involves only liquids or solids, the pressure dependence of the chemical potential is generally small and can be neglected. However, it cannot be neglected if $P \gg 1$ bar as shown in Example Problem 6.13.

**EXAMPLE PROBLEM 6.13**

At 298.15 K, $\Delta G_f^\circ(\text{C}, graphite) = 0$, and $\Delta G_f^\circ(\text{C}, diamond) = 2.90 \text{ kJ mol}^{-1}$. Therefore, graphite is the more stable solid phase at this temperature at $P = P^\circ = 1$ bar. Given that the densities of graphite and diamond are 2.25 and 3.52 kg/L, respectively, at what pressure will graphite and diamond be in equilibrium at 298.15 K?

**Solution**

At equilibrium $\Delta G = G(\text{C}, graphite) - G(\text{C}, diamond) = 0$. Using the pressure dependence of $G$, $(\partial G_m/\partial P)_T = V_m$, we establish the condition for equilibrium:

$$\Delta G = \Delta G_f^\circ(\text{C}, graphite) - \Delta G_f^\circ(\text{C}, diamond)$$
$$+ (V_m^{graphite} - V_m^{diamond})(\Delta P) = 0$$
$$0 = 0 - 2.90 \times 10^3 + (V_m^{graphite} - V_m^{diamond})(P - 1 \text{ bar})$$
$$P = 1 \text{ bar} + \frac{2.90 \times 10^3}{M_C \left( \dfrac{1}{\rho_{graphite}} - \dfrac{1}{\rho_{diamond}} \right)}$$

$$= 1 \text{ bar} + \frac{2.90 \times 10^3}{12.00 \times 10^{-3} \text{ kg mol}^{-1} \times \left( \dfrac{1}{2.25 \times 10^3 \text{ kg m}^{-3}} - \dfrac{1}{3.52 \times 10^3 \text{ kg m}^{-3}} \right)}$$

$$= 10^5 \text{ Pa} + 1.51 \times 10^9 \text{ Pa} = 1.51 \times 10^4 \text{ bar}$$

Fortunately for all those with diamond rings, although the conversion of diamond to graphite at 1 bar and 298 K is spontaneous, the rate of conversion is vanishingly small.

## 6.12 Expressing the Equilibrium Constant in Terms of Mole Fraction or Molarity

Chemists often find it useful to express the concentrations of reactants and products in units other than partial pressures. Two examples of other units that we will consider in this section are mole fraction and molarity. Note, however, that this discussion is still limited to a mixture of ideal gases. The extension of chemical equilibrium to include neutral and ionic species in aqueous solutions will be made in Chapter 10, after the concept of activity has been introduced.

We first express the equilibrium constant in terms of mole fractions. The mole fraction $x_i$ and the partial pressure $P_i$ are related by $P_i = x_i P$. Therefore,

$$
K_P = \frac{\left(\dfrac{P_C^{eq}}{P^\circ}\right)^\gamma \left(\dfrac{P_D^{eq}}{P^\circ}\right)^\delta}{\left(\dfrac{P_A^{eq}}{P^\circ}\right)^\alpha \left(\dfrac{P_B^{eq}}{P^\circ}\right)^\beta} = \frac{\left(\dfrac{x_C^{eq} P}{P^\circ}\right)^\gamma \left(\dfrac{x_D^{eq} P}{P^\circ}\right)^\delta}{\left(\dfrac{x_A^{eq} P}{P^\circ}\right)^\alpha \left(\dfrac{x_B^{eq} P}{P^\circ}\right)^\beta} = \frac{\left(x_C^{eq}\right)^\gamma \left(x_D^{eq}\right)^\delta}{\left(x_A^{eq}\right)^\alpha \left(x_B^{eq}\right)^\beta} \left(\frac{P}{P^\circ}\right)^{\gamma+\delta-\alpha-\beta}
$$

$$
= K_x \left(\frac{P}{P^\circ}\right)^{\Delta v}
$$

$$
K_x = K_P \left(\frac{P}{P^\circ}\right)^{-\Delta v} \tag{6.72}
$$

Recall that $\Delta v$ is the difference in the stoichiometric coefficients of products and reactants. Note that just as for $K_P$, $K_x$ is a dimensionless number.

Because the molarity $c_i$ is defined as $c_i = n_i/V = P_i/RT$, we can write $P_i/P^\circ = (RT/P^\circ)c_i$. To work with dimensionless quantities, we introduce the ratio $c_i/c^\circ$, which is related to $P_i/P^\circ$ by

$$
\frac{P_i}{P^\circ} = \frac{c^\circ RT}{P^\circ} \frac{c_i}{c^\circ} \tag{6.73}
$$

Using this notation, we can express $K_c$ in terms of $K_P$:

$$
K_P = \frac{\left(\dfrac{P_C^{eq}}{P^\circ}\right)^\gamma \left(\dfrac{P_D^{eq}}{P^\circ}\right)^\delta}{\left(\dfrac{P_A^{eq}}{P^\circ}\right)^\alpha \left(\dfrac{P_B^{eq}}{P^\circ}\right)^\beta} = \frac{\left(\dfrac{c_C^{eq}}{c^\circ}\right)^\gamma \left(\dfrac{c_D^{eq}}{c^\circ}\right)^\delta}{\left(\dfrac{c_A^{eq}}{c^\circ}\right)^\alpha \left(\dfrac{c_B^{eq}}{c^\circ}\right)^\beta} \left(\frac{c^\circ RT}{P^\circ}\right)^{\gamma+\delta-\alpha-\beta} = K_c \left(\frac{c^\circ RT}{P^\circ}\right)^{\Delta v}
$$

$$
K_c = K_P \left(\frac{c^\circ RT}{P^\circ}\right)^{-\Delta v} \tag{6.74}
$$

Equations (6.72) and (6.74) show that $K_x$ and $K_c$ are in general different from $K_P$. They are only equal in the special case that $\Delta v = 0$.

# 6.13 The Dependence of the Extent of Reaction on *T* and *P*

In previous sections, we have discussed how $K_P$ varies with $T$ and how $K_x$ varies with $P$. In this section, we consider how the extent of reaction varies with $T$ and $P$ in a more general framework that encompasses the previous discussions. It is useful at this point to introduce a parameter, $\xi$, called the **extent of reaction** in discussing the shift in the position of equilibrium of a chemical reaction if $T$ and/or $P$ change. If the reaction advances by $\xi$ moles, the number of moles of each species $i$ changes according to

$$
n_i = n_i^{initial} + v_i \xi \tag{6.75}
$$

Differentiating this equation leads to $dn_i = v_i d\xi$. By inserting this result in Equation (6.53), we can write $dG$ in terms of $\xi$. At constant $T$ and $P$,

$$
dG = \left(\sum_i v_i \mu_i\right) d\xi = \Delta G_R d\xi \tag{6.76}
$$

An advancing reaction can be described in terms of the partial derivative of $G$ with $\xi$:

$$
\left(\frac{\partial G}{\partial \xi}\right)_{T,P} = \sum_i v_i \mu_i = \Delta G_R \tag{6.77}
$$

The direction of spontaneous change is that in which $\Delta G_R$ is negative. This direction corresponds to $(\partial G/\partial \xi)_{T,P} < 0$. At a given composition of the reaction mixture, the partial pressures of the reactants and products can be determined, and the $\mu_i$ can be calculated. Because $\mu_i = \mu_i(T, P, n_A, n_B,...)$, $\sum_i v_i\mu_i = \Delta G_R$ must be evaluated at specific values of $T$, $P$, $n_A$, $n_B$,.... Based on the value of $\Delta G_R$ obtained, the following conclusions can be drawn:

- If $\Delta G_R = (\partial G/\partial \xi)_{T,P} < 0$, the reaction proceeds spontaneously as written.
- If $\Delta G_R = (\partial G/\partial \xi)_{T,P} > 0$, the reaction proceeds spontaneously in the opposite direction.
- If $\Delta G_R = (\partial G/\partial \xi)_{T,P} = 0$, the reaction system is at equilibrium, and there is no direction of spontaneous change.

Suppose that we have a mixture of reactive gases at equilibrium. Does the equilibrium shift toward reactants or products as $T$ or $P$ is changed? Because $\xi_{eq}$ increases if $K_P$ or $K_x$ increases, and decreases if $K_P$ or $K_x$ decreases, we need only consider the dependence of $K_P$ on $T$ or $K_x$ on $T$ and $P$. We first consider the dependence of $K_P$ on $T$. We know from Equation (6.64) that

$$\frac{d \ln K_P}{dT} = \frac{\Delta H_R^\circ}{RT^2} \tag{6.78}$$

so that $K_P$ will change differently with temperature for an exothermic reaction than for an endothermic reaction. For an exothermic reaction, $d \ln K_P/dT < 0$, and $\xi_{eq}$ will shift toward the reactants as $T$ increases. For an endothermic reaction, $d \ln K_P/dT > 0$, and $\xi_{eq}$ will shift toward the products as $T$ increases.

The dependence of $\xi_{eq}$ on pressure can be determined from the relationship between $K_x$ and $P$:

$$K_x = K_P \left(\frac{P}{P^\circ}\right)^{-\Delta v} \tag{6.79}$$

Because $K_P$ is independent of pressure, the pressure dependence of $K_x$ arises solely from $(P/P^\circ)^{-\Delta v}$. If $\Delta v > 0$, the number of moles of gaseous products increases as the reaction proceeds. In this case, $K_x$ decreases as $P$ increases, and $\xi_{eq}$ shifts back toward the reactants. If the number of moles of gaseous products decreases as the reaction proceeds, $K_x$ increases as $P$ increases, and $\xi_{eq}$ shifts forward toward the products. If $\Delta v = 0$, $\xi_{eq}$ is independent of pressure.

A combined change in $T$ and $P$ leads to a superposition of the effects just discussed. According to the French chemist Le Chatelier, reaction systems at chemical equilibrium respond to an outside stress, such as a change in $T$ or $P$, by countering the stress. Consider the $Cl_2(g) \rightleftharpoons 2Cl(g)$ reaction discussed in Example Problems 6.9 and 6.10 for which $\Delta H_R > 0$. There, $\xi_{eq}$ responds to an increase in $T$ in such a way that heat is taken up by the system; in other words, more $Cl_2(g)$ dissociates. This counters the stress imposed on the system by an increase in $T$. Similarly, $\xi_{eq}$ responds to an increase in $P$ in such a way that the volume of the system decreases. Specifically, $\xi_{eq}$ changes in the direction that $\Delta v < 0$, and for the reaction under consideration, $Cl(g)$ is converted to $Cl_2(g)$. This shift in the position of equilibrium counters the stress brought about by an increase in $P$.

**SUPPLEMENTAL**

## 6.14 A Case Study: The Synthesis of Ammonia

In this section, we discuss a specific reaction and show both the power and the limitations of thermodynamics in developing a strategy to maximize the rate of a desired reaction. Ammonia synthesis is the primary route to the manufacture of fertilizers in agriculture. The commercial process used today is essentially the same as that invented by the German chemists Robert Bosch and Fritz Haber in 1908. In terms of its impact

on human life, the Haber-Bosch synthesis may be the most important chemical process ever invented, because the increased food production possible with fertilizers based on $NH_3$ has allowed the large increase in Earth's population in the 20th century to occur. In 2000, more than 2 million tons of ammonia were produced per week using the Haber-Bosch process, and more than 98% of the inorganic nitrogen input to soils used in agriculture worldwide as fertilizer is generated using the Haber-Bosch process.

What useful information can be obtained about the ammonia synthesis reaction from thermodynamics? The overall reaction is

$$1/2\ N_2(g) + 3/2\ H_2(g) \rightleftharpoons NH_3(g) \tag{6.80}$$

Because the reactants are pure elements in their standard states at 298.15 K,

$$\Delta H_R^\circ = \Delta H_f^\circ(NH_3, g) = -45.9 \times 10^3\ \text{J mol}^{-1}\ \text{at 298.15 K} \tag{6.81}$$

$$\Delta G_R^\circ = \Delta G_f^\circ(NH_3, g) = -16.5 \times 10^3\ \text{J mol}^{-1}\ \text{at 298.15 K} \tag{6.82}$$

Assuming ideal gas behavior, the equilibrium constant $K_p$ is given by

$$K_P = \frac{\left(\dfrac{P_{NH_3}}{P^\circ}\right)}{\left(\dfrac{P_{N_2}}{P^\circ}\right)^{\frac{1}{2}}\left(\dfrac{P_{H_2}}{P^\circ}\right)^{\frac{3}{2}}} = \frac{(x_{NH_3})}{(x_{N_2})^{\frac{1}{2}}(x_{H_2})^{\frac{3}{2}}}\left(\frac{P}{P^\circ}\right)^{-1} \tag{6.83}$$

We will revisit this equilibrium and include deviations from ideal behavior in Chapter 7. Because the goal is to maximize $x_{NH_3}$, Equation (6.83) is written in the form

$$x_{NH_3} = (x_{N_2})^{\frac{1}{2}}(x_{H_2})^{\frac{3}{2}}\left(\frac{P}{P^\circ}\right)K_P \tag{6.84}$$

What conditions of temperature and pressure are most appropriate to maximizing the yield of ammonia? Because

$$\frac{d\ln K_P}{dT} = \frac{\Delta H_R^\circ}{RT^2} < 0 \tag{6.85}$$

$K_P$ and, therefore, $x_{NH_3}$ decrease as $T$ increases. Because $\Delta v = -1$, $x_{NH_3}$ increases with $P$. We conclude that the best conditions to carry out the reaction are high $P$ and low $T$. In fact, industrial production is carried out for $P > 100$ atm and $T \sim 700$ K.

Our discussion has focused on reaching equilibrium because this is the topic of inquiry in thermodynamics. However, note that many synthetic processes are deliberately carried out far from equilibrium in order to selectively generate a desired product. For example, ethylene oxide, which is produced by the partial oxidation of ethylene, is an industrially important chemical used to manufacture antifreeze, surfactants, and fungicides. Although the complete oxidation of ethylene to $CO_2$ and $H_2O$ has a more negative value of $\Delta G_R^\circ$ than the partial oxidation, it is undesirable because it does not produce useful products.

These predictions provide information about the equilibrium state of the system but lack one important component. How long will it take to reach equilibrium? Unfortunately, thermodynamics gives us no information about the rate at which equilibrium is attained. Consider the following example. Using values of $\Delta G_f^\circ$ from the data tables, convince yourself that the oxidation of potassium and coal (essentially carbon) are both spontaneous processes. For this reason, potassium has to be stored in an environment free of oxygen. However, coal is stable in air indefinitely. Thermodynamics tells us that both processes are spontaneous at 298.15 K, but experience shows us that only one proceeds at a measurable rate. However, by heating coal to an elevated temperature, the oxidation reaction becomes rapid. This result implies that there is an energetic **activation barrier** to the reaction that can be overcome with the aid of thermal energy. As we will see, the same is true of the ammonia synthesis reaction. Although Equations (6.84) and (6.85) predict that $x_{NH_3}$ is maximized as $T$ approaches 0 K, the reaction rate is vanishingly small unless $T > 500$ K.

To this point, we have only considered the reaction system using state functions. However, a chemical reaction consists of a number of individual steps, called a **reaction mechanism.** How might the ammonia synthesis reaction proceed? One possibility is the gas-phase reaction sequence:

$$N_2(g) \rightarrow 2N(g) \qquad \qquad \textbf{(6.86)}$$

$$H_2(g) \rightarrow 2H(g) \qquad \qquad \textbf{(6.87)}$$

$$N(g) + H(g) \rightarrow NH(g) \qquad \qquad \textbf{(6.88)}$$

$$NH(g) + H(g) \rightarrow NH_2(g) \qquad \qquad \textbf{(6.89)}$$

$$NH_2(g) + H(g) \rightarrow NH_3(g) \qquad \qquad \textbf{(6.90)}$$
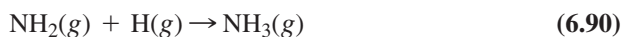
In each of the recombination reactions, other species that are not involved in the reaction can facilitate energy transfer. The enthalpy changes associated with each of the individual steps are known and are indicated in Figure 6.7. This diagram is useful because it gives much more information than the single-value $\Delta H_R^\circ$. Although the overall process is slightly exothermic, the initial step, which is the dissociation of $N_2(g)$ and $H_2(g)$, is highly endothermic. Heating a mixture of $N_2(g)$ and $H_2(g)$ to high enough temperatures to dissociate a sizable fraction of the $N_2(g)$ would require such a high temperature that all the $NH_3(g)$ formed would dissociate into reactants. This can be shown by carrying out a calculation such as that in Example Problem 6.11. The conclusion is that the gas phase reaction between $N_2(g)$ and $H_2(g)$ is not a practical route to ammonia synthesis.

The way around this difficulty is to find another reaction sequence for which the enthalpy changes of the individual steps are not prohibitively large. For the ammonia synthesis reaction, such a route is a heterogeneous catalytic reaction, using iron as a catalyst. The mechanism for this path between reactants and products is

$$N_2(g) + \square \rightarrow N_2(a) \qquad \qquad \textbf{(6.91)}$$

$$N_2(a) + \square \rightarrow 2N(a) \qquad \qquad \textbf{(6.92)}$$

$$H_2(g) + 2\square \rightarrow 2H(a) \qquad \qquad \textbf{(6.93)}$$

$$N(a) + H(a) \rightarrow NH(a) + \square \qquad \qquad \textbf{(6.94)}$$

$$NH(a) + H(a) \rightarrow NH_2(a) + \square \qquad \qquad \textbf{(6.95)}$$

$$NH_2(a) + H(a) \rightarrow NH_3(a) + \square \qquad \qquad \textbf{(6.96)}$$

$$NH_3(a) \rightarrow NH_3(g) + \square \qquad \qquad \textbf{(6.97)}$$
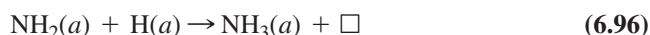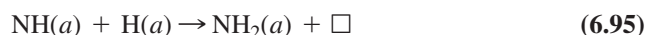
The symbol $\square$ denotes an ensemble of neighboring Fe atoms, also called surface sites, which are capable of forming a chemical bond with the indicated entities. The designation (*a*) indicates that the chemical species is adsorbed (chemically bonded) to a surface site.
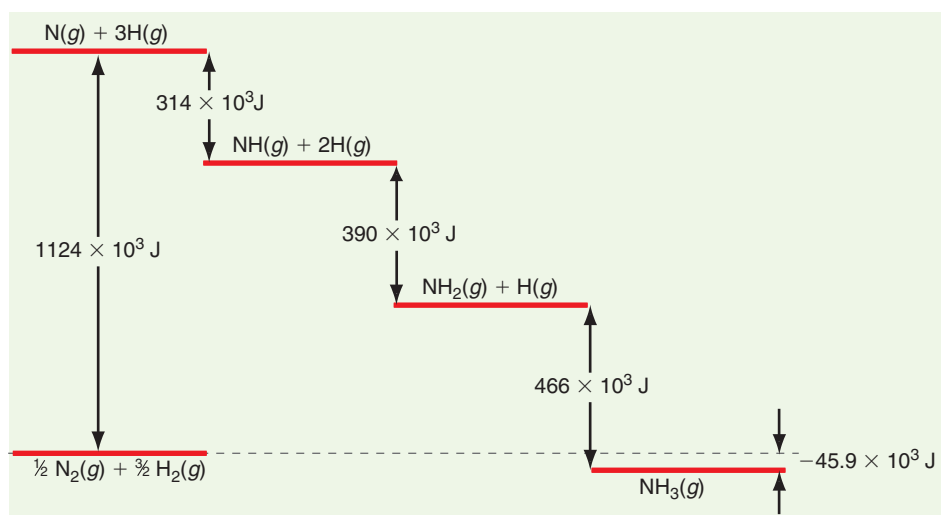
**FIGURE 6.7**
An enthalpy diagram is shown for the reaction mechanism in Equations (6.86) through (6.90). The successive steps in the reaction proceed from left to right in the diagram.

The enthalpy change for the overall reaction $N_2(g) + 3/2\ H_2(g) \rightarrow NH_3(g)$ is the same for the mechanisms in Equations (6.86) through (6.90) and (6.91) through (6.97) because $H$ is a state function. This is a characteristic of a catalytic reaction. A catalyst can affect the *rate* of the forward and backward reaction but not the *position of equilibrium* in a reaction system. The enthalpy diagram in Figure 6.8 shows that the enthalpies of the individual steps in the gas phase and surface catalyzed reactions are very different. These enthalpy changes have been determined in experiments but are not generally listed in thermodynamic tables.

In the catalytic mechanism, the enthalpy for the dissociation of the gas-phase $N_2$ and $H_2$ molecules is greatly reduced by the stabilization of the atoms through their bond to the surface sites. However, a small activation barrier to the dissociation of adsorbed $N_2$ remains. This barrier is the rate-limiting step in the overall reaction. As a result of this barrier, only one in a million gas-phase $N_2$ molecules incident on the catalyst surface per unit time dissociates and is converted into ammonia. Such a small reaction probability is not uncommon for industrial processes based on heterogeneous catalytic reactions. In industrial reactors, on the order of $\sim 10^7$ collisions of the reactants with the catalyst occur in the residence time of the reactants in the reactor. Therefore, even reactions with a reaction probability per collision of $10^{-6}$ can be carried out with a high yield.

How was Fe chosen as the catalyst for ammonia synthesis? Even today, catalysts are usually optimized using a trial-and-error approach. Haber and Bosch tested hundreds of catalyst materials, and more than 2500 substances have been tried since. On the basis of this extensive screening, it was concluded that a successful catalyst must fulfill two different requirements: it must bind $N_2$ strongly enough that the molecule can dissociate into N atoms. However, it must not bind N atoms too strongly. If that were the case, the N atoms could not react with H atoms to produce gas-phase $NH_3$. As was known by Haber and Bosch, both osmium and ruthenium are better catalysts than iron for $NH_3$ synthesis, but these elements are far too expensive for commercial production. Why are these catalysts better than Fe? Quantum mechanical calculations by Jacobsen *et al.* [*J. American Chemical Society* 123(2001), 8404–8405] were able to explain the "volcano plot" of the activity versus the $N_2$ binding energy shown in Figure 6.9.

Jacobsen et al. concluded that molybdenum is a poor catalyst because N is bound too strongly, whereas $N_2$ is bound too weakly. Nickel is a poor catalyst for the opposite reason: N is bound too weakly and $N_2$ is bound too strongly. Osmium and ruthenium are the best elemental catalysts because they fulfill both requirements well. Jacobsen et al. suggested that a catalyst that combined the favorable properties of Mo and Co to create Co-Mo surface sites would be a good catalyst, and they concluded that the ternary compound $Co_3Mo_3N$ best satisfied these requirements. On the basis of
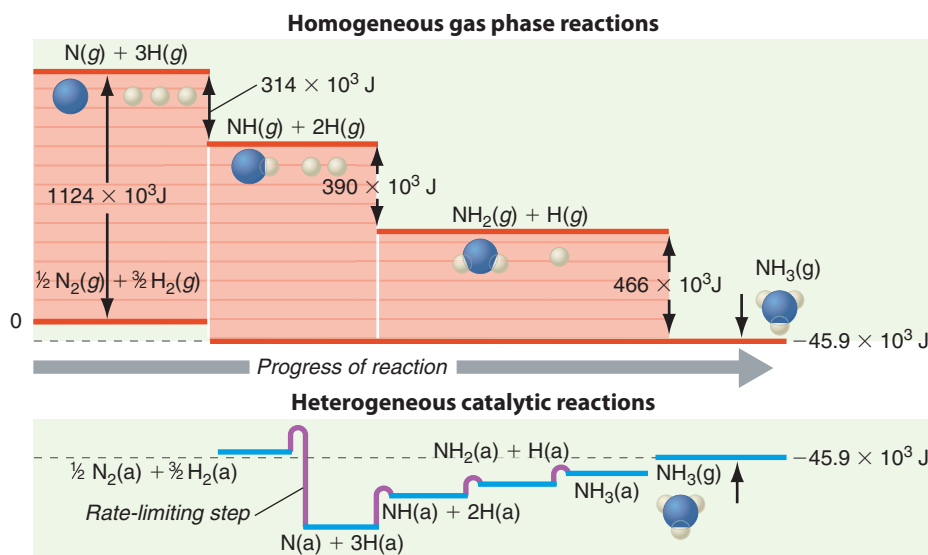


**FIGURE 6.8**
Enthalpy diagram that compares the homogeneous gas phase and heterogeneous catalytic reactions for the ammonia synthesis reaction. The activation barriers for the individual steps in the surface reaction are shown. The successive steps in the reaction proceed from left to right in the diagram.

*Source*: Ertl, G. "Surface Science and Catalysis—Studies on the Mechanism of Ammonia *Synthesis*: The P.H. Emmett Award Address." *Catalysis Reviews—Science and Engineering* 21, no.2 (1980): 201–223.

**FIGURE 6.9**

The calculated turnover frequency (TOF) for $NH_3$ production (molecules of $NH_3$ per surface site per second) as a function of the calculated binding energy of $N_2$ on the surface, relative to that on ruthenium. The reaction conditions are 400°C, 50 bar total pressure, and gas composition $H_2:N_2 = 3:1$ containing 5% $NH_3$.

*Source*: Jacobsen, C. J. H., Dahl, S., Clausen, B. S., Bahn, S., Logadottir, A., and Norskov, J. K. "Catalyst Design by Interpolation in the Periodic Table: Bimetallic Ammonia Synthesis Catalysts." *Journal of the American Chemical Society* 123, no. 34 (2001): 8404–8405.
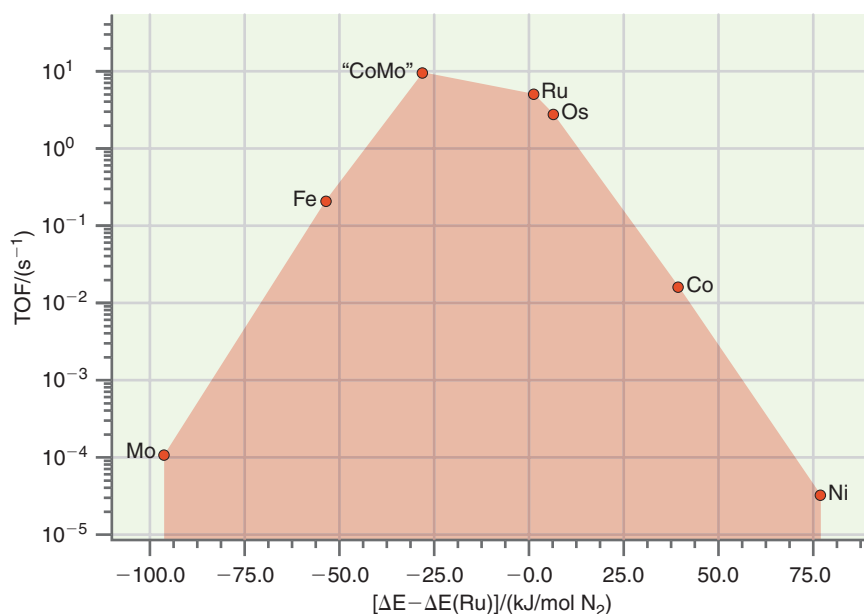


these calculations, the catalyst was synthesized with the results shown in Figure 6.10. The experiments show that $Co_3Mo_3N$ is far more active than Fe, and more active than Ru over most of the concentration range. These experiments also show that the turnover frequency for $Co_3Mo_3N$ lies at the point shown on the volcano plot of Figure 6.8. This catalyst is one of the few that have been developed on the basis of theoretical calculations as opposed to the trial and error method.

An unresolved issue is the nature of the surface sites indicated by □ in Equations (6.91) through (6.97). Are all adsorption sites on an $NH_3$ synthesis catalyst surface equally reactive? To answer this question, it is important to know that metal surfaces at equilibrium consist of large flat terraces separated by monatomic steps. It was long suspected that the steps rather than the terraces play an important role in ammonia synthesis. This was convincingly shown by Dahl et al. [*Physical Review Letters* 83(1999), 1814–1817] in an elegant experiment. They evaporated a small amount of gold on a Ru crystal. As had been demonstrated by Hwang et al. [*Physical Review Letters* 67(1991), 3279], the inert Au atoms migrate to the step sites on Ru and thereby block these sites, rendering them inactive in $NH_3$ synthesis.

**FIGURE 6.10**

Experimental data for the TOF for $NH_3$ production as a function of the $NH_3$ concentration in the mixture. The $Co_3Mo_3N$ catalyst is superior to both Fe and Ru as predicted by the calculations. The reaction conditions are those for Figure 6.9. The number of active surface sites is assumed to be 1% of the total number of surface sites.

*Source*: Jacobsen, C. J. H., Dahl, S., Clausen, B. S., Bahn, S., Logadottir, A., and Norskov, J. K. "Catalyst Design by Interpolation in the Periodic Table: Bimetallic Ammonia Synthesis Catalysts." *Journal of the American Chemical Society* 123, no. 34 (2001): 8404–8405.
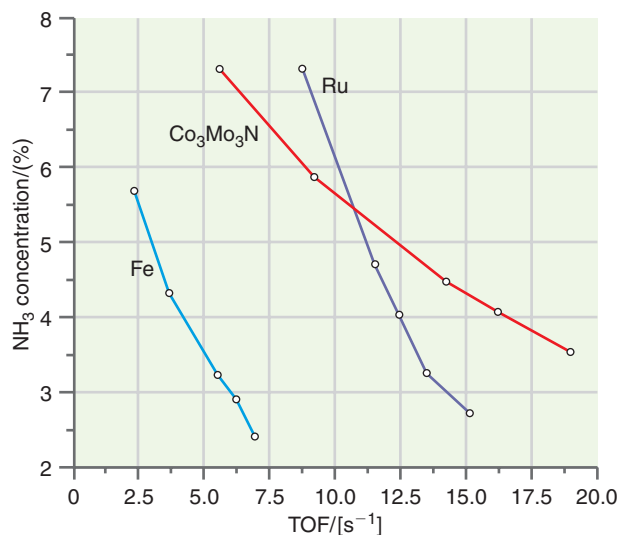
This site blocking is demonstrated using scanning tunneling microscopy as shown in Figure 6.11.

Dahl et al. showed that the rate of ammonia synthesis was lowered by a factor of $10^9$ after the step sites, which make up only 1% to 2% of all surface sites, were blocked by Au atoms! This result clearly shows that in this reaction only step sites are active. They are more active because they have fewer nearest neighbors than terrace sites. This enables the step sites to bind $N_2$ more strongly, promoting dissociation into N atoms that react rapidly with H atoms to form $NH_3$.

This discussion has shown the predictive power of thermodynamics in analyzing chemical reactions. Calculating $\Delta G_R^\circ$ allowed us to predict that the reaction of $N_2$ and $H_2$ to form $NH_3$ is a spontaneous process at 298.15 K. Calculating $\Delta H_R^\circ$ allowed us to predict that the yield of ammonia increases with increasing pressure and decreases with increasing temperature. However, thermodynamics cannot be used to determine how rapidly equilibrium is reached in a reaction mixture. If thermodynamic tables of species such as $N_2(a)$, $N(a)$, $NH(a)$, $NH_2(a)$, and $NH_3(a)$ were available, it would be easier for chemists to develop synthetic strategies that are likely to proceed at an appreciable rate. However, whether an activation barrier exists in the conversion of one species to another—and how large the barrier is—are not predictable within thermodynamics. Therefore, synthetic strategies must rely on chemical intuition, experiments, and quantum mechanical calculations to develop strategies that reach thermodynamic equilibrium at a reasonable rate.
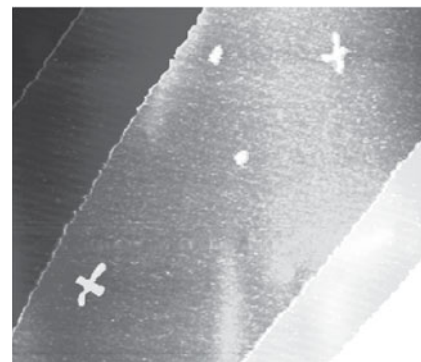


**FIGURE 6.11**
This scanning tunneling microscope image of a Ru surface shows wide, flat terraces separated by monatomic steps. The bright "ribbon" at the step edge is due to Au atoms, which are also seen in the form of four islands on the middle terrace.
*Source:* T. Diemant, T. Hager, H. E. Hoster, H. Rauscher, and R. J. Behm, *Surf. Sci* 141(2003) 137, fig. 1a.

**SUPPLEMENTAL**

# 6.15 Expressing *U* and *H* and Heat Capacities Solely in Terms of Measurable Quantities

In this section, we use the Maxwell relations derived in Section 6.2 to express $U$, $H$, and heat capacities solely in terms of measurable quantities such as $\kappa$, $\beta$ and the state variables $P$, $V$, and $T$. Often, it is not possible to determine an equation of state for a substance over a wide range of the macroscopic variables. This is the case for most solids and liquids. However, material constants such as heat capacities, the thermal expansion coefficient, and the isothermal compressibility may be known over a limited range of their variables. If this is the case, the enthalpy and internal energy can be expressed in terms of the material constants and the variables $V$ and $T$ or $P$ and $T$, as shown later. The Maxwell relations play a central role in deriving these formulas.

We begin with the following differential expression for $dU$ that holds for solids, liquids, and gases provided that no nonexpansion work, phase transitions, or chemical reactions occur in the system:

$$dU = TdS - PdV \tag{6.98}$$

Invoking a transformation at constant temperature and dividing both sides of the equation by $dV$,

$$\left(\frac{\partial U}{\partial V}\right)_T = T\left(\frac{\partial S}{\partial V}\right)_T - P = T\left(\frac{\partial P}{\partial T}\right)_V - P \tag{6.99}$$

To arrive at the second expression in Equation (6.99), we have used the third Maxwell relation Equation (6.28). We next express $(\partial P/\partial T)_V$ in terms of $\beta$ and $\kappa$, where $\beta$ is the isobaric volumetric thermal expansion coefficient at constant pressure, and $\kappa$ is the isothermal compressibility:

$$\left(\frac{\partial P}{\partial T}\right)_V = -\frac{(\partial V/\partial T)_P}{(\partial V/\partial P)_T} = \frac{\beta}{\kappa} \tag{6.100}$$

Equation (6.100) allows us to write Equation (6.99) in the form

$$\left(\frac{\partial U}{\partial V}\right)_T = \frac{\beta T - \kappa P}{\kappa} \tag{6.101}$$

Through this equation, we have linked $(\partial U/\partial V)_T$, which is called the internal pressure, to easily measured material properties. This allows us to calculate the internal pressure of a liquid or a gas as shown in Example Problem 6.14.

### EXAMPLE PROBLEM 6.14

At 298 K, the thermal expansion coefficient and the isothermal compressibility of liquid water are $\beta = 2.04 \times 10^{-4} \text{ K}^{-1}$ and $\kappa = 45.9 \times 10^{-6} \text{ bar}^{-1}$.

a. Calculate $(\partial U/\partial V)_T$ for water at 320. K and $P = 1.00$ bar.

b. If an external pressure equal to $(\partial U/\partial V)_T$ were applied to 1.00 m³ of liquid water at 320. K, how much would its volume change? What is the relative change in volume?

c. As shown in Example Problem 3.5, $(\partial U/\partial V_m)_T = a/V_m^2$ for a van der Waals gas. Calculate $(\partial U/\partial V_m)_T$ for $N_2(g)$ at 320 K and $P = 1.00$ atm given that $a = 1.35 \text{ atm L}^2 \text{ mol}^{-2}$. Compare the value that you obtain with that of part (a) and discuss the difference.

#### Solution

a. $\left(\dfrac{\partial U}{\partial V}\right)_T = \dfrac{\beta T - \kappa P}{\kappa}$

$= \dfrac{2.04 \times 10^{-4} \text{ K}^{-1} \times 320. \text{ K} - 45.9 \times 10^{-6} \text{ bar}^{-1} \times 1.00 \text{ bar}}{45.9 \times 10^{-6} \text{ bar}^{-1}}$

$= 1.4 \times 10^{3} \text{ bar}$

b. $\kappa = -\dfrac{1}{V}\left(\dfrac{\partial V}{\partial P}\right)_T$

$\Delta V_T = -\displaystyle\int_{P_i}^{P_f} V(T)\kappa dP \approx -V(T)\kappa(P_f - P_i)$

$= -1.00 \text{ m}^3 \times 45.9 \times 10^{-6} \text{ bar} \times (1.4 \times 10^3 \text{ bar} - 1 \text{ bar})$

$= -6.4 \times 10^{-2} \text{ m}^3$

$\dfrac{\Delta V_T}{V} = -\dfrac{6.4 \times 10^{-2} \text{ m}^3}{1 \text{ m}^3} = -6.4\%$

c. At atmospheric pressure, we can calculate $V_m$ using the ideal gas law and

$\left(\dfrac{\partial U}{\partial V_m}\right)_T = \dfrac{a}{V_m^2} = \dfrac{aP^2}{R^2 T^2} = \dfrac{1.35 \text{ atm L}^2 \text{ mol}^{-2} \times (1.00 \text{ atm})^2}{(8.206 \times 10^{-2} \text{ atm L mol}^{-1} \text{ K}^{-1} \times 320. \text{ K})^2}$

$= 1.96 \times 10^{-3} \text{ atm}$

The internal pressure is much smaller for $N_2$ gas than for $H_2O$ liquid. This is the case because $H_2O$ molecules in a liquid are relatively strongly attracted to one another, whereas the interaction between gas phase $N_2$ molecules is very weak. Gases, which have a small internal pressure, are more easily compressed by an external pressure than liquids or solids, which have a high internal pressure.

Using the result in Equation (6.101) for the internal pressure, we can write $dU$ in the form

$$dU = \left(\frac{\partial U}{\partial T}\right)_V dT + \left(\frac{\partial U}{\partial V}\right)_T dV = C_V dT + \frac{\beta T - \kappa P}{\kappa} dV \qquad \textbf{(6.102)}$$

The usefulness of Equation (6.102) arises from the fact that it contains only the material constants $C_V$, $\beta$, $\kappa$, and the macroscopic variables $T$ and $V$. In Example Problems 6.14

and 6.15 we show that $\Delta U$, $\Delta H$ and $C_P - C_V$ can be calculated even if the equation of state for the material of interest is not known, as long as the thermal expansion coefficient and the isothermal compressibility are known.

## EXAMPLE PROBLEM 6.15

A 1000. g sample of liquid Hg undergoes a reversible transformation from an initial state $P_i = 1.00$ bar, $T_i = 300.$ K to a final state $P_f = 300.$ bar, $T_f = 600.$ K. The density of Hg is 13,534 kg m$^{-3}$, $\beta = 1.81 \times 10^{-4}$ K$^{-1}$, $C_P = 27.98$ J mol$^{-1}$ K$^{-1}$, and $\kappa = 3.91 \times 10^{-6}$ bar$^{-1}$, in the range of the variables in this problem. Recall from Section 3.5 that $C_P - C_V = (TV \beta^2/\kappa)$, and that $C_P \approx C_V$ for liquids and solids.

**a.** Calculate $\Delta U$ and $\Delta H$ for the transformation. Describe the path assumed for the calculation.

**b.** Compare the relative contributions to $\Delta U$ and $\Delta H$ from the change in pressure and the change in temperature. Can the contribution from the change in pressure be neglected?

### Solution

Because $U$ is a state function, $\Delta U$ is independent of the path. We choose the reversible path $P_i = 1.00$ bar, $T_i = 300.$ K $\rightarrow P_i = 1.00$ bar, $T_f = 600.$ K $\rightarrow P_f = 300.$ bar, $T_f = 600.$ K. Note that because we have assumed that all the material constants are independent of $P$ and $T$ in the range of interest, the numerical values calculated will depend slightly on the path chosen. However, if the $P$ and $T$ dependence of the material constant were properly accounted for, all paths would give the same value of $\Delta U$.

$$\Delta U = \int_{T_i}^{T_f} C_P dT + \int_{V_i}^{V_f} \frac{\beta T - \kappa P}{\kappa} dV$$

Using the definition $\kappa = -1/V(\partial V/\partial P)_T$, $\ln V_f/V_i = -\kappa(P_f - P_i)$, and $V(P) = V_i e^{-\kappa(P - P_i)}$. We can also express $P(V)$ as $P(V) = P_i - (1/\kappa)\ln(V/V_i)$

$$\Delta U = \int_{T_i}^{T_f} C_P dT + \int_{V_i}^{V_f} \left[ \frac{\beta T}{\kappa} - \left( P_i - \frac{1}{\kappa} \ln \frac{V}{V_i} \right) \right] dV$$

$$= \int_{T_i}^{T_f} C_P dT + \left( \frac{\beta T}{\kappa} - P_i \right) \int_{V_i}^{V_f} dV + \frac{1}{\kappa} \int_{V_i}^{V_f} \ln \frac{V}{V_i} dV$$

Using the standard integral $\int \ln (x/a) dx = -x + x \ln (x/a)$

$$\Delta U = \int_{T_i}^{T_f} C_P dT + \left( \frac{\beta T}{\kappa} - P_i \right)(V_f - V_i) + \frac{1}{\kappa} \left[ -V + V \ln \frac{V}{V_i} \right]_{V_i}^{V_f}$$

$$= C_P(T_f - T_i) + \left( \frac{\beta T}{\kappa} - P_i \right)(V_f - V_i) + \frac{1}{\kappa} \left( V_i - V_f + V_f \ln \frac{V_f}{V_i} \right)$$

$$V_i = \frac{m}{\rho} = \frac{1.000 \, \text{kg}}{13534 \, \text{kg m}^{-3}} = 7.389 \times 10^{-5} \, \text{m}^3$$

$$V_f = V_i e^{-\kappa(P_f - P_i)} = 7.389 \times 10^{-5} \, \text{m}^3 \exp(-3.91 \times 10^{-6} \, \text{bar}^{-1} \times 299 \, \text{bar})$$

$$= 7.380 \times 10^{-5} \, \text{m}^3$$

$$V_f - V_i = -9 \times 10^{-8} \, \text{m}^3$$

$$\Delta U = \frac{1000.\text{ g}}{200.59 \text{ g mol}^{-1}} \times 27.98 \text{ J mol}^{-1}\text{ K}^{-1} \times (600.\text{ K} - 300.\text{ K})$$

$$-\left(\frac{1.81 \times 10^{-4}\text{ K}^{-1} \times 300.\text{ K}}{3.91 \times 10^{-6}\text{ bar}^{-1}} - 1.00\text{ bar}\right) \times \frac{10^5\text{ Pa}}{1\text{ bar}} \times 9 \times 10^{-8}\text{ m}^3$$

$$+ \frac{1}{3.91 \times 10^{-6}\text{ bar}^{-1}} \times \frac{10^5\text{ Pa}}{1\text{ bar}} \times \left(\begin{array}{c} 9 \times 10^{-8}\text{ m}^3 + 7.380 \times 10^{-5}\text{m}^3 \\ \times \ln\dfrac{7.380 \times 10^{-5}\text{ m}^3}{7.389 \times 10^{-5}\text{ m}^3} \end{array}\right)$$

$$= 41.8 \times 10^3\text{ J} - 100\text{ J} + 1\text{ J} \approx 41.7 \times 10^3\text{ J}$$

As shown in Section 3.1,

$$V(P, 600.\text{ K}) = [1 + \beta(600.\text{ K} - 300.\text{ K})]V(P_i, 300.\text{ K})e^{-\kappa(P-P_i)} = V'\,e^{-\kappa(P-P_i)}$$

$$\Delta H = \int_{T_i}^{T_f} C_P dT + \int_{P_i}^{P_f} V dP = \int_{T_i}^{T_f} C_P dT + V'e^{\kappa P_i}\int_{P_i}^{P_f} e^{-\kappa P}\,dP$$

$$= nC_{P,m}(T_f - T_i) + \frac{V_i'e^{\kappa P_i}}{\kappa}(e^{-\kappa P_i} - e^{-\kappa P_f})$$

$$= \frac{1000.\text{ g}}{200.59 \text{ g mol}^{-1}} \times 27.98 \text{ J mol}^{-1}\text{K}^{-1} \times (600.\text{ K} - 300.\text{ K})$$

$$+ 7.389 \times 10^{-5}\text{ m}^3 \times (1 + 300.\text{ K} \times 1.81 \times 10^{-4}\text{ K}^{-1})$$

$$\times \frac{\exp(3.91 \times 10^{-6}\text{bar}^{-1} \times 1\text{ bar})}{3.91 \times 10^{-6}\text{ bar}^{-1} \times (1\text{ bar}/10^5\text{ Pa})}$$

$$\times \left[\exp(-3.91 \times 10^{-6}\text{ bar}^{-1} \times 1\text{ bar})\right.$$

$$\left. - \exp(-3.91 \times 10^{-6}\text{ bar}^{-1} \times 300.\text{ bar})\right]$$

$$\Delta H = 41.8 \times 10^3\text{ J} + 2.29 \times 10^3\text{ J} = 44.1 \times 10^3\text{ J}$$

The temperature dependent contribution to $\Delta U$ is 98% of the total change in $U$, and the corresponding value for $\Delta H$ is $\sim$ 95%. The contribution from the change in pressure to $\Delta U$ and to $\Delta H$ is small.

### EXAMPLE PROBLEM 6.16

In the previous Example Problem, it was assumed that $C_P = C_V$.

a. Use equation 3.38, $C_{P,m} = C_{V,m} + TV_m\dfrac{\beta^2}{\kappa}$, and the experimentally determined value $C_{P,m} = 27.98$ J mol$^{-1}$ K$^{-1}$ to obtain a value for $C_{V,m}$ for Hg($l$) at 300. K.

b. Did the assumption that $C_{P,m} \approx C_{V,m}$ in Example Problem 6.15 introduce an appreciable error in your calculation of $\Delta U$ and $\Delta H$?

#### Solution

a. $C_{P,m} - C_{V,m} = \dfrac{TV_m\beta^2}{\kappa}$

$$= \frac{300.\text{ K} \times \dfrac{0.20059\text{ kg mol}^{-1}}{13534\text{ kgm}^3} \times (1.81 \times 10^{-4}\text{ K}^{-1})^2}{3.91 \times 10^{-6}\text{ bar}^{-1} \times (1\text{ bar}/10^5\text{ Pa})}$$

$$= 3.73\text{ J K}^{-1}\text{ mol}^{-1}$$

$$C_{V,m} = C_{P,m} - \frac{TV_m\beta^2}{\kappa}$$

$$= 27.98 \text{ J K}^{-1} \text{ mol}^{-1} - 3.73 \text{ J K}^{-1} \text{ mol}^{-1} = 24.25 \text{ J K}^{-1} \text{ mol}^{-1}$$

**b.** $\Delta U$ is in error by ~ 15% and $\Delta H$ is unaffected by assuming that $C_{P,m} \approx C_{V,m}$. It is a reasonable approximation to set $C_P = C_V$ for a liquid or solid.

**SUPPLEMENTAL**

# 6.16 Measuring ΔG for the Unfolding of Single RNA Molecules

In general, $\Delta G$, $\Delta H$, and $\Delta U$ are measured using thermochemical methods as discussed in Chapter 4. However, many biochemical systems are irreversibly changed upon heating so that calorimetric methods are less suitable for such systems. With the advent of atomic scale manipulation of molecules, which began with the invention of scanning probe microscopies (see Chapter 5 in Engel, *Quantum Chemistry & Spectroscopy*), it has become possible to measure $\Delta G$ for a change using an individual molecule. An interesting illustration is the measurement of $\Delta G$ for the unfolding of single RNA molecules. RNA molecules must fold into very specific shapes in order to carry out their function as catalysts for biochemical reactions. It is not well understood how the molecule achieves its equilibrium shape, and the energetics of the folding is a key parameter in modeling the folding process.

Liphardt et al. [*Science* 292, (2001), 733] have obtained $\Delta G$ for this process by unzipping a single RNA molecule. The measurement relies on Equation (6.9), which states that Gibbs energy is a measure of the maximum nonexpansion work that can be produced in a transformation. Figure 6.12 shows how the force associated with the unfolding of RNA into two strands can be measured. Each of the two strands that make up the RNA is attached to a chemical "handle" that allows the individual strands to be firmly linked to 2-$\mu$m-diameter polystyrene beads. Using techniques based on scanning probe microscopies, the distance between the beads is increased, and the force needed to do so is measured.

The force versus distance plot for the P5abcΔA RNA is shown in Figure 6.13 for two different rates at which the force was increased with time. For a rate of 10 pN s$^{-1}$ (right panel), the folding and unfolding curves have different forms, showing that the process is not reversible. However, for a rate of 1 pN s$^{-1}$ (left panel), the red and black curves are superimposable, showing that the process is essentially reversible. (No process that occurs at a finite rate is truly reversible.) We next discuss the form of the force versus distance curve.



**(a)**

**(b)** Biotin    Digoxigenin
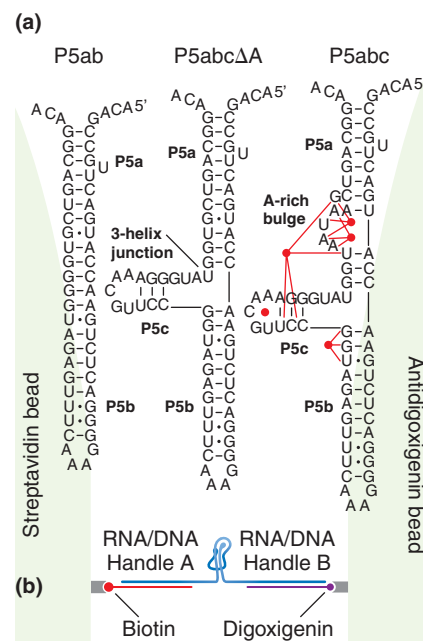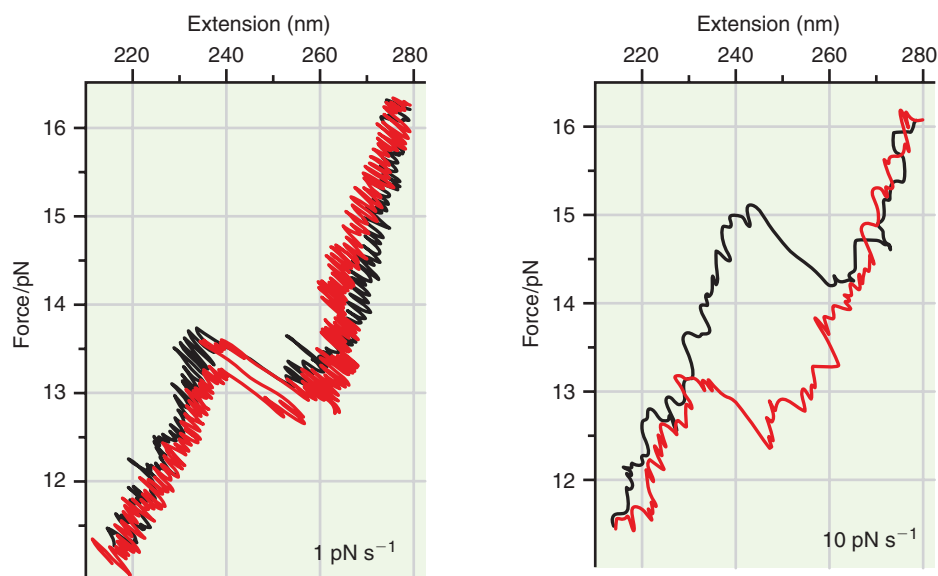
**FIGURE 6.12**
The three types of RNA studied by Liphardt et al. are shown. The letters G, C, A, and U refer to the bases guanine, cytosine, adenine, and uracil. The strands are held together by hydrogen bonding between the complementary base pairs A and U, and G and C. The pronounced bulge at the center of P5abcΔA is a hairpin loop. Such loops are believed to play a special role in the folding of RNA. (b) An individual RNA molecule is linked by handles attached to the end of each strand to functionalized polystyrene spheres that are moved relative to one another to induce unfolding of the RNA mechanically.
*Source:* Figures 1 and 2 from "Reversible Unfolding of Single RNA Molecules by Mechanical Force" by Jan Liphardt, et al., in *Science* 27, Vol. 292 No. 5517: 733-737, April 2001. Copyright © 2001, The American Association for the Advancement of Science. Reprinted with permission from AAAS.

**FIGURE 6.13**
The measured force versus distance curve is shown for the P5abcΔA form of RNA. The black trace represents the stretching of the molecule, and the red curve represents the refolding of the molecule as the beads are brought back to their original separation. The left panel shows data for an increase in force of 1 pN s$^{-1}$, and the right panel shows the corresponding results for 10 pN s$^{-1}$.
*Source:* Figures 1 and 2 from "Reversible Unfolding of Single RNA Molecules by Mechanical Force" by Jan Liphardt, et al., in *Science* 27, Vol. 292 No. 5517: 733–737, April 2001. Copyright © 2001, The American Association for the Advancement of Science. Reprinted with permission from AAAS.

The initial increase in distance between ~210 and ~225 nm nm is due to the stretching of the handles. However, a marked change in the shape of the curve is observed for $F \approx 13$ pN, for which the distance increases abruptly. This behavior is the signature of the unfolding of the two strands. The negative slope of the curve between 230 and 260 nm is determined by the experimental technique used to stretch the RNA. In a "perfect" experiment, this portion of the curve would be a horizontal line, corresponding to an increase in length at constant force. The observed length increase is identical to the length of the molecule, showing that the molecule unfolds all at once in a process in which all bonds between the complementary base pairs are broken. The analysis of the results to obtain $\Delta G$ from the force curves is complex and will not be discussed here. The experimentally obtained value for $\Delta G$ is 193 kJ/mol, showing that a change in the thermodynamic state function $G$ can be determined by a measurement of work on a single molecule. The unfolding can also be carried out by increasing the temperature of the solution containing the RNA to ~80°C, in which case the process is referred to as melting. In the biochemical environment, the unfolding is achieved through molecular forces exerted by enzymes called DNA polymerases, which act as molecular motors.

SUPPLEMENTAL

# 6.17 The Role of Mixing in Determining Equilibrium in a Chemical Reaction

Three factors determine the equilibrium partial pressures of gases in a reaction system: the Gibbs energies of the reactants, the Gibbs energies of the products, and the Gibbs energy of mixing of reactants. In this section, we examine the role of each of these factors.

It is generally not necessary to assign values to the molar Gibbs energies $G_m^\circ$, because only differences in the Gibbs energy rather than absolute values can be obtained from experiments. However, in order to make this discussion quantitative, we introduce a convention that allows an assignment of numerical values to $G_m^\circ$. With the convention from Section 4.2 that $H_m^\circ = 0$ for an element in its standard state,

$$G_m^\circ = H_m^\circ - TS_m^\circ = -TS_m^\circ \tag{6.103}$$

for a pure *element* in its standard state at 1 bar. To obtain an expression for $G_m^\circ$ for a pure *compound* in its standard state, consider $\Delta G^\circ$ for the formation reaction. Recall that 1 mol of the product appears on the right side in the formation reaction, and only elements in their standard states appear on the left side:

$$\Delta G_f^\circ = G_{m, \, product}^\circ + \sum_i v_i G_{m, \, reactant \, i}^\circ$$

$$G_{m, \, product}^\circ = \Delta G_f^\circ + \sum_i^{elements \, only} v_i T S_{m,i}^\circ \tag{6.104}$$

where the $v_i$ are the stoichiometric coefficients of the elemental reactants in the balanced formation reaction, all of which have negative values. Note that this result differs from the corresponding value for the enthalpy, $H_m^\circ = \Delta H_f^\circ$. The values for $G_m^\circ$ obtained in this way are called the **conventional molar Gibbs energies.** This formalism is illustrated in Example Problem 6.17. We note that this convention is not unique. An alternative is to set $H_m^\circ = G_m^\circ = 0$ for all elements in their standard states at 298.15 K. With this convention, $G_m^\circ = \Delta G_f^\circ$ for a compound in its standard state.

**EXAMPLE PROBLEM 6.17**

Calculate the conventional molar Gibbs energy of (a) Ar(g) and (b) $H_2O(l)$ at 1 bar and 298.15 K.

**Solution**

a. Because Ar(g) is an element in its standard state for these conditions, $H_m^\circ = 0$ and $G_m^\circ = H_m^\circ - TS_m^\circ = -TS_m^\circ = -298.15$ K $\times$ 154.8 J K$^{-1}$mol$^{-1}$ = $-4.617$ kJ mol$^{-1}$.

**b.** The formation reaction for $H_2O(l)$ is $H_2(g) + 1/2\,O_2(g) \rightarrow H_2O(l)$

$$G^\circ_{m,\,product} = \Delta G^\circ_f\,(product) + \overset{elements\ only}{\underset{i}{\sum}} v_i TS^\circ_{m,i}$$

$$G^\circ_m\,(H_2O,\,l) = \Delta G^\circ_f\,(H_2O,\,l) - \left[TS^\circ_m\,(H_2,\,g) + \frac{1}{2}TS^\circ_m\,(O_2,\,g)\right]$$

$$= -237.1 \text{ kJ mol}^{-1} - 298.15 \text{ K} \times \begin{bmatrix} 130.7 \text{ J K}^{-1} \text{ mol}^{-1} + \frac{1}{2} \times \\ 205.2 \text{ J K}^{-1} \text{ mol}^{-1} \end{bmatrix}$$

$$= -306.6 \text{ kJ mol}^{-1}$$

These calculations give $G^\circ_m$ at 298.15 K. To calculate the conventional molar Gibbs energy at another temperature, use the Gibbs–Helmholtz equation as discussed next.

Now that we have a way to assign numerical values to molar Gibbs energies, we consider the reaction system $2\,NO_2(g) \rightleftharpoons N_2O_4(g)$, with $(2 - 2\xi)$ moles of $NO_2(g)$ and $\xi$ moles of $N_2O_4(g)$ present in a vessel at a constant pressure of 1 bar and 298 K. The parameter $\xi$ could in principle take on any value between zero and one, corresponding to pure $NO_2(g)$ and pure $N_2O_4(g)$, respectively. The Gibbs energy of the pure unmixed reagents and products $G_{pure}$ is given by

$$G_{pure} = (2 - 2\xi)G^\circ_m\,(NO_2,\,g) + \xi G^\circ_m\,(N_2O_4,\,g) \tag{6.105}$$

where $G^\circ_m$ is the conventional molar Gibbs energy defined by Equation (6.104). Note that $G_{pure}$ varies linearly with $\xi$, as shown in Figure 6.14. Because the reactants and products are mixed throughout the range accessible to $\xi$, $G_{pure}$ is not equal to $G_{mixture}$, which is given by

$$G_{mixture} = G_{pure} + \Delta G_{mixing} \tag{6.106}$$

Recall that $G_{mixture}$ is minimized at equilibrium. Equation (6.106) shows that if $G_{pure}$ alone determined $\xi_{eq}$, either $\xi_{eq} = 0$ or $\xi_{eq} = 1$ mole, depending on whether $G_{pure}$ were lower for reagents or products. For the reaction under consideration, $\Delta G^\circ_f\,(N_2O_4,\,g) < \Delta G^\circ_f\,(NO_2,\,g)$ so that $\xi_{eq} = 1$ mole if $G_{pure}$ alone determined $\xi_{eq}$. More generally, if $G_{pure}$ alone determined $\xi_{eq}$, every chemical reaction would go to completion, or the reverse reaction would go to completion. The value of $\Delta G_{mixing}$ can be calculated using Equation (6.48). You will show in the end-of-chapter problems that $\Delta G_{mixing}$ for this reaction system has a minimum at $\xi_{eq} = 0.55$ moles.

If $G_{pure}$ alone determined $\xi_{eq}$, then $\xi_{eq} = 1$ mole, and if $\Delta G_{mixing}$ alone determined $\xi_{eq}$, then $\xi_{eq} = 0.55$ mole. However, the minimum in $\Delta G_R$ is determined by the minimum in $G_{pure} + \Delta G_{mixing}$ rather than in the minimum of the individual components. For our specific case, $\xi_{eq} = 0.72$ moles at 298 K. We see that $\Delta G_{mixing}$ plays a critical role in determining the position of equilibrium in this chemical reaction. How sensitive is $\xi_{eq}$ to the values of the Gibbs energies of reactants and products? Figure 6.15 shows the same calculation carried out earlier for the reaction $2A \rightleftharpoons B$ setting $G^\circ_B = 100.$ kJ mol$^{-1}$ for different values of $G^\circ_A$.

For $2G^\circ_A \approx G^\circ_B$ as is the case for $G^\circ_A = 50.5$ kJ mol$^{-1}$, $\xi_{eq}$ is largely determined by $\Delta G_{mixing}$. However, as $2G^\circ_A$ becomes much larger than $G^\circ_B$, $\xi_{eq}$ approaches one. However, because of the contribution of $\Delta G_{mixing}$ to $G_{mixture}$, which is entirely entropic in origin, $\xi_{eq}$ is always less than one and only approaches one in the limit that $G^\circ_{reactants} - G^\circ_{products} \rightarrow \infty$.

We summarize the roles of $G_{pure}$ and $\Delta G_{mixing}$ in determining $\xi_{eq}$. For reactions in which $G^{reactants}_{pure}$ and $G^{products}_{pure}$ are very similar, $\xi_{eq}$ will be largely determined by $\Delta G_{mixing}$. For reactions in which $G^{reactants}_{pure}$ and $G^{products}_{pure}$ are very different, $\xi_{eq}$ will not be greatly influenced by $\Delta G_{mixing}$, and the equilibrium mixture approaches but never reaches one of the two extremes of pure reactants or pure products.
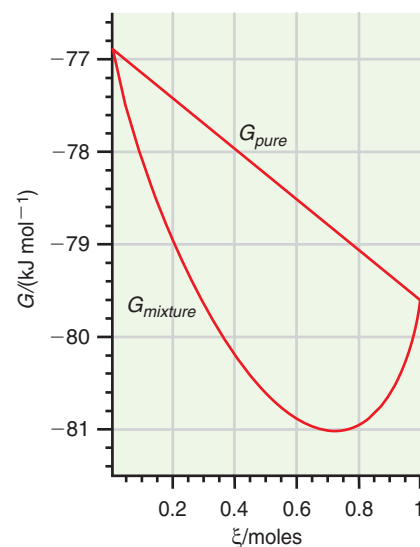


**FIGURE 6.14**

$G_{mixture}$ and $G_{pure}$ are depicted for the $2\,NO_2(g) \rightleftharpoons N_2O_4(g)$ equilibrium. For this reaction system, the equilibrium position would correspond to $\xi = 1$ mole in the absence of mixing. The mixing contribution to $G_{mixture}$ shifts $\xi_{eq}$ to values smaller than one. Note the correspondence between the three bulleted relations for $(\partial G/\partial \xi)_{T,P}$ following Equation (6.77) and the slope of $G_{mixture}$ vs $\xi$ curve.

(a)



(b)



(c)
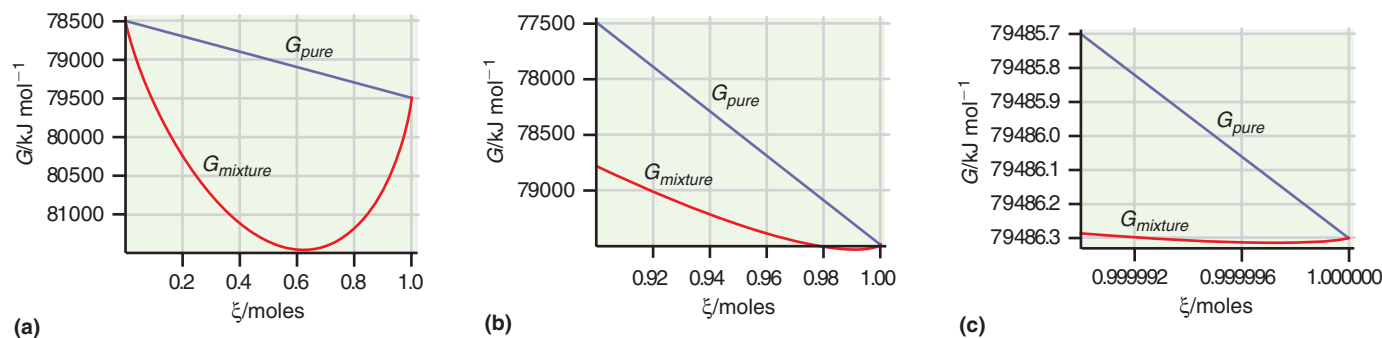
**FIGURE 6.15**
The corresponding graph to Figure 6.14 is shown for $G_B^\circ = 100.$ kJ mol$^{-1}$ and $G_A^\circ$ values of (a) 50.5 kJ mol$^{-1}$, (b) 60.0 kJ mol$^{-1}$, and (c) 80.0 kJ mol$^{-1}$. Only the portion of the graph for $\xi$ values near one is shown for (b) and (c) so that the minimum in $G_{mixture}$ can be seen. Note that $\xi_{eq}$ approaches one as $G_A^\circ$ increases.

# Vocabulary

| | | |
|---|---|---|
| activation barrier | Gibbs–Helmholtz equation | natural variables |
| chemical potential | Helmholtz energy | reaction mechanism |
| conventional molar Gibbs energies | maximum nonexpansion work | reaction quotient of pressures |
| extent of reaction | Maxwell relations | thermodynamic equilibrium constant |
| Gibbs energy | | |

# Conceptual Problems

**Q6.1** $K_P$ is independent of $T$ for a particular chemical reaction. What does this tell you about the reaction?

**Q6.2** The reaction A + B $\rightleftharpoons$ C + D is at equilibrium for $\xi = 0.1$. What does this tell you about the variation of $G_{pure}$ with $\xi$?

**Q6.3** Under what condition is $K_P = K_x$?

**Q6.4** What is the relationship between the $K_P$ for the two reactions $3/2\,H_2 + 1/2\,N_2 \rightleftharpoons NH_3$ and $3H_2 + N_2 \rightleftharpoons 2NH_3$?

**Q6.5** Under what conditions is $dA \leq 0$ a condition that defines the spontaneity of a process?

**Q6.6** By invoking the pressure dependence of the chemical potential, show that if a valve separating a vessel of pure A from a vessel containing a mixture of A and B is opened, mixing will occur. Both A and B are ideal gases, and the initial pressure in both vessels is 1 bar.

**Q6.7** Under what conditions is $dG \leq 0$ a condition that defines the spontaneity of a process?

**Q6.8** Can equilibrium with respect to the concentration of Ar and H$_2$ be attained in the system shown in Figure 6.2? If so, what can you say about the partial pressure in each part of the system?

**Q6.9** Is the equation $(\partial U/\partial V)_T = (\beta T - \kappa P)/\kappa$ valid for liquids, solids, and gases?

**Q6.10** Why is it reasonable to set the chemical potential of a pure liquid or solid substance equal to its standard state chemical potential at that temperature independent of the pressure in considering chemical equilibrium?

**Q6.11** The reaction A + B $\rightleftharpoons$ C + D is at equilibrium for $\xi = 0.5$. What does this tell you about the variation of $G_{pure}$ with $\xi$?

**Q6.12** Which thermodynamic state function gives a measure of the maximum electric work that can be carried out in a fuel cell?

**Questions 6.13–6.18 refer to the reaction system CO(g) + 1/2 O$_2$(g) $\rightleftharpoons$ CO$_2$(g) at equilibrium for which $\Delta H_R^\circ = -283.0$ kJ mol$^{-1}$.**

**Q6.13** Predict the change in the partial pressure of CO$_2$ as the temperature is increased at constant total pressure.

**Q6.14** Predict the change in the partial pressure of CO$_2$ as the pressure is increased at constant temperature.

**Q6.15** Predict the change in the partial pressure of CO$_2$ as Xe gas is introduced into the reaction vessel at constant pressure and temperature.

**Q6.16** Predict the change in the partial pressure of CO$_2$ as Xe gas is introduced into the reaction vessel at constant volume and temperature.

**Q6.17** Predict the change in the partial pressure of CO$_2$ as a platinum catalyst is introduced into the reaction vessel at constant volume and temperature.

**Q6.18** Predict the change in the partial pressure of CO$_2$ as O$_2$ is removed from the reaction vessel at constant pressure and temperature.

**Q6.19** Calculate the maximum expansion work that is available in carrying out the combustion reactions in

Example Problems 6.1 and 6.2. Explain both the magnitude and the sign of the work.

**Q6.20** Is the equation $\Delta G = \Delta H - T\Delta S$ applicable to all processes?

**Q6.21** Is the equation $\Delta A = \Delta U - T\Delta S$ applicable to all processes?

**Q6.22** Under what conditions is $K_x > K_P$?

**Q6.23** Under what conditions is the distribution of products in an ideal gas reactions system at equilibrium unaffected by an increase in the pressure?

**Q6.24** If $K_P$ is independent of pressure, why does the degree of dissociation in the reaction $Cl_2(g) \rightleftharpoons 2Cl(g)$ depend on presure?

**Questions 6.25–6.28 refer to the reaction system $H_2(g) + Cl_2(g) \rightleftharpoons 2HCl(g)$ at equilibrium. Assume ideal gas behavior.**

**Q6.25** How does the total number of moles in the reaction system change as $T$ increases?

**Q6.26** If the reaction is carried out at constant $V$, how does the total pressure change if $T$ increases?

**Q6.27** Is the partial pressure of $H_2(g)$ dependent on $T$? If so, how will it change as $T$ decreases?

**Q6.28** If the total pressure is increased at constant $T$, how will the relative amounts of of $H_2(g)$ and $HCl(g)$ change?

**Q6.29** If additional $Cl_2(g)$ is added to the reaction system at constant total pressure and temperature, how will the partial pressures of $H_2(g)$ and $HCl(g)$ change?

**Q6.30** If additional $Cl_2(g)$ is added to the reaction system at constant $V$ and $T$, how will the degree of dissociation of $HCl(g)$ change?

**Q6.31** If $T$ is increased at constant total pressure, how will the degree of dissociation of $HCl(g)$ change?

# Numerical Problems

Problem numbers in **red** indicate that the solution to the problem is given in the *Student's Solutions Manual*.

**P6.1** Calculate $\Delta A_R^{\circ}$ and $\Delta G_R^{\circ}$ for the reaction $C_6H_6(l) + 15/2\, O_2(g) \rightarrow 6CO_2(g) + 3H_2O(l)$ at 298 K from the combustion enthalpy of benzene and the entropies of the reactants and products.

**P6.2** Calculate $K_P$ at 298 and 490. K for the reaction $NO(g) + 1/2\, O_2(g) \rightarrow NO_2(g)$ assuming that $\Delta H_R^{\circ}$ is constant over the interval 298–600. K. Do you expect $K_P$ to increase or decrease as the temperature is increased to 600. K?

**P6.3** A sample containing 2.75 moles of $N_2$ and 6.25 mol of $H_2$ is placed in a reaction vessel and brought to equilibrium at 52.0 bar and 690. K in the reaction $1/2\, N_2(g) + 3/2\, H_2(g) \rightleftharpoons NH_3(g)$.
a. Calculate $K_P$ at this temperature.
b. Set up an equation relating $K_P$ and the extent of reaction as in Example Problem 6.10.
c. Using numerical equation solving software, calculate the number of moles of each species present at equilibrium.

**P6.4** Consider the equilibrium $NO_2(g) \rightleftharpoons NO(g) + 1/2\, O_2(g)$. One mole of $NO_2(g)$ is placed in a vessel and allowed to come to equilibrium at a total pressure of 1 bar. An analysis of the contents of the vessel gives the following results:

| $T$ | 700. K | 800. K |
|---|---|---|
| $P_{NO}/P_{NO_2}$ | 0.872 | 2.50 |

a. Calculate $K_P$ at 700. and 800. K.
b. Calculate $\Delta G_R^{\circ}$ and $\Delta H_R^{\circ}$ for this reaction at 298.15 K, using only the data in the problem. Assume that $\Delta H_R^{\circ}$ is independent of temperature.
c. Calculate $\Delta G_R^{\circ}$ and $\Delta H_R^{\circ}$ using the data tables and compare your answer with that obtained in part (b).

**P6.5** The shells of marine organisms contain calcium carbonate, $CaCO_3$, largely in a crystalline form known as calcite.

There is a second crystalline form of calcium carbonate known as aragonite. Physical and thermodynamic properties of calcite and aragonite are given in the following table.

| Properties ($T = 298$ K, $P = 1$ bar) | Calcite | Aragonite |
|---|---|---|
| $\Delta H_f^{\circ}$ (kJ mol$^{-1}$) | −1206.9 | −1207.0 |
| $\Delta G_f^{\circ}$ (kJ mol$^{-1}$) | −1128.8 | −1127.7 |
| $S^{\circ}$ (J K$^{-1}$ mol$^{-1}$) | 92.9 | 88.7 |
| $C_{P,m}^{\circ}$ (J K$^{-1}$ mol$^{-1}$) | 81.9 | 81.3 |
| Density (g mL$^{-1}$) | 2.710 | 2.930 |

a. Based on the thermodynamic data given, would you expect an isolated sample of calcite at $T = 298$ K and $P = 1$ bar to convert to aragonite, given sufficient time? Explain.
b. Suppose the pressure applied to an isolated sample of calcite is increased. Can the pressure be increased to the point that isolated calcite will be converted to aragonite? Explain.
c. What pressure must be achieved to induce the conversion of calcite to aragonite at $T = 298$ K. Assume both calcite and aragonite are incompressible at $T = 298$ K.
d. Can calcite be converted to aragonite at $P = 1$ bar if the temperature is increased? Explain.

**P6.6** Consider the equilibrium $C_2H_6(g) \rightleftharpoons C_2H_4(g) + H_2(g)$. At 1000. K and a constant total pressure of 1.00 bar, $C_2H_6(g)$ is introduced into a reaction vessel. The total pressure is held constant at 1 bar and at equilibrium the composition of the mixture in mole percent is $H_2(g)$: 26.0% $C_2H_4(g)$: 26.0% and $C_2H_6(g)$: 48.0%.
a. Calculate $K_P$ at 1000. K.
b. If $\Delta H_R^{\circ} = 137.0$ kJ mol$^{-1}$, calculate the value of $K_P$ at 298.15K.
c. Calculate $\Delta G_R^{\circ}$ for this reaction at 298.15 K.

**P6.7**   The pressure dependence of $G$ is quite different for gases and condensed phases. Calculate $\Delta G_m$ for the processes (C, *solid*, *graphite*, 1 bar, 298.15 K) → (C, *solid*, *graphite*, 325 bar, 298.15 K) and (He, $g$, 1 bar, 298.15 K) → (He, $g$, 325 bar, 298.15 K). By what factor is $\Delta G_m$ greater for He than for graphite?

**P6.8**   Many biological macromolecules undergo a transition called denaturation. Denaturation is a process whereby a structured, biological active molecule, called the native form, unfolds or becomes unstructured and biologically inactive. The equilibrium is

$$\text{native (folded)} \rightleftharpoons \text{denatured (unfolded)}$$
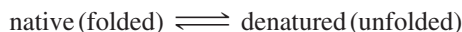
For a protein at pH $= 2$ the enthalpy change at 298 K associated with denaturation is $\Delta H° = 418.0$ kJ mol$^{-1}$ and the entropy change at 298 K is $\Delta S° = 1.30$ kJ K$^{-1}$ mol$^{-1}$.

**a.** Calculate the Gibbs energy change for the denaturation of the protein at pH $= 2$ and $T = 310.$ K. Assume the enthalpy and entropy are temperature-independent between 298 K and 303 K.

**b.** Calculate the equilibrium constant for the denaturation of the protein at pH 2 and $T = 310.$ K.

**c.** Based on your answer for parts (a) and (b), is the protein structurally stable at pH 2 and $T = 310.$ K?

**P6.9**   Assume that a sealed vessel at constant pressure of 1 bar initially contains 2.00 mol of $NO_2(g)$. The system is allowed to equilibrate with respect to the reaction $2\,NO_2(g) \rightleftharpoons N_2O_4(g)$. The number of moles of $NO_2(g)$ and $N_2O_4(g)$ at equilibrium is $2.00 - 2\xi$ and $\xi$, respectively, where $\xi$ is the extent of reaction.

**a.** Derive an expression for the entropy of mixing as a function of $\xi$.

**b.** Graphically determine the value of $\xi$ for which $\Delta S_{mixing}$ has its maximum value.

**c.** Write an expression for $G_{pure}$ as a function of $\xi$. Use Equation 6.104 to obtain values of $G_m°$ for $NO_2$ and $N_2O_4$.

**d.** Plot $G_{mixture} = G_{pure} + \Delta G_{mixing}$ as a function of $\xi$ for $T = 298$ K and graphically determine the value of $\xi$ for which $G_{mixture}$ has its minimum value. Is this value the same as for part (b)?

**P6.10**   Calculate $K_P$ at 600. K for the reaction $N_2O_4(l) \rightleftharpoons 2NO_2(g)$ assuming that $\Delta H_R°$ is constant over the interval 298–725 K.

**P6.11**   Consider the equilibrium $CO(g) + H_2O(g) \rightleftharpoons CO_2(g) + H_2(g)$. At 1150. K, the composition of the reaction mixture is

| Substance | $CO_2(g)$ | $H_2(g)$ | $CO(g)$ | $H_2O(g)$ |
|---|---|---|---|---|
| Mole % | 20.3 | 20.3 | 29.7 | 29.7 |

**a.** Calculate $K_P$ and $\Delta G_R°$ at 1150. K.

**b.** Given the answer to part (a), use the $\Delta H_f°$ of the reaction species to calculate $\Delta G_R°$ at 298.15 K. Assume that $\Delta H_R°$ is independent of temperature.

**P6.12**   For the reaction $C(graphite) + H_2O(g) \rightleftharpoons CO(g) + H_2(g)$, $\Delta H_R° = 131.28$ kJ mol$^{-1}$ at 298.15 K. Use the values of $C_{P,m}°$ at 298.15 K in the data tables to calculate $\Delta H_R°$ at 125.0°C.

**P6.13**   $Ca(HCO_3)_2(s)$ decomposes at elevated temperatures according to the stoichiometric equation $Ca(HCO_3)_2(s) \rightleftharpoons CaCO_3(s) + H_2O(g) + CO_2(g)$.

**a.** If pure $Ca(HCO_3)_2(s)$ is put into a sealed vessel, the air is pumped out, and the vessel and its contents are heated, the total pressure is 0.290 bar. Determine $K_P$ under these conditions.

**b.** If the vessel also contains 0.120 bar $H_2O(g)$ at the final temperature, what is the partial pressure of $CO_2(g)$ at equilibrium?

**P6.14**   Calculate $\Delta A$ for the isothermal compression of 2.95 mol of an ideal gas at 325 K from an initial volume of 60.0 L to a final volume of 20.5 L. Does it matter whether the path is reversible or irreversible?

**P6.15**   Nitrogen is a vital element for all living systems, but except for a few types of bacteria, blue-green algae, and some soil fungi, most organisms cannot utilize $N_2$ from the atmosphere. The formation of "fixed" nitrogen is therefore necessary to sustain life and the simplest form of fixed nitrogen is ammonia $NH_3$.

A possible pathway for ammonia synthesis by a living system is

$$\tfrac{1}{2}N_2(g) + \tfrac{3}{2}H_2O(l) \rightleftharpoons NH_3(aq) + \tfrac{3}{4}O_2(g)$$
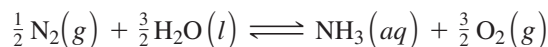
where $(aq)$ means the ammonia is dissolved in water and $\Delta G_f°(NH_3, aq) = -80.3$ kJ mol$^{-1}$.

**a.** Calculate $\Delta G°$ for the biological synthesis of ammonia at 298 K.

**b.** Calculate the equilibrium constant for the biological synthesis of ammonia at 298 K.

**c.** Based on your answer to part (b), is the pathway a spontaneous reaction?

**P6.16**   Collagen is the most abundant protein in the mammalian body. It is a fibrous protein that serves to strengthen and support tissues. Suppose a collagen fiber can be stretched reversibly with a force constant of $k = 10.0$ N m$^{-1}$ and that the force $\mathbf{F}$ (see Table 2.1) is given by $\mathbf{F} = k \cdot \mathbf{l}$. When a collagen fiber is contracted reversibly, it absorbs heat $q_{rev} = 0.050$ J. Calculate the change in the Helmholtz energy $\Delta A$ as the fiber contracts isothermally from $l = 0.20$ to 0.10 m. Calculate also the reversible work performed $w_{rev}$, $\Delta S$, and $\Delta U$. Assume that the temperature is constant at $T = 310.$ K.

**P6.17**   Calculate $\mu_{O_2}^{mixture}$ (298.15 K, 1 bar) for oxygen in air, assuming that the mole fraction of $O_2$ in air is 0.210. Use the conventional molar Gibbs energy defined in Section 6.17.

**P6.18**   Calculate the maximum nonexpansion work that can be gained from the combustion of benzene($l$) and of $H_2(g)$ on a per gram and a per mole basis under standard conditions. Is it apparent from this calculation why fuel cells based on $H_2$ oxidation are under development for mobile applications?

**P6.19**   You wish to design an effusion source for Br atoms from $Br_2(g)$. If the source is to operate at a total pressure of

7.5 Torr, what temperature is required to produce a degree of dissociation of 0.20? What value of the pressure would increase the degree of dissociation to 0.65 at this temperature?

**P6.20** Calculate $\Delta G$ for the isothermal expansion of 2.25 mol of an ideal gas at 325 K from an initial pressure of 12.0 bar to a final pressure of 2.5 bar.

**P6.21** You place 3.00 mol of $NOCl(g)$ in a reaction vessel. Equilibrium is established with respect to the decomposition reaction $NOCl(g) \rightleftharpoons NO(g) + 1/2\ Cl_2(g)$.

a. Derive an expression for $K_P$ in terms of the extent of reaction $\xi$.

b. Simplify your expression for part (a) in the limit that $\xi$ is very small.

c. Calculate $\xi$ and the degree of dissociation of NOCl in the limit that $\xi$ is very small at 375 K and a pressure of 2.00 bar.

d. Solve the expression derived in part (a) using a numerical equation solver for the conditions stated in the previous part. What is the relative error in $\xi$ made using the approximation of part (b)?

**P6.22** A sample containing 2.50 moles of He (1 bar, 350. K) is mixed with 1.75 mol of Ne (1 bar, 350. K) and 1.50 mol of Ar (1 bar, 350. K). Calculate $\Delta G_{mixing}$ and $\Delta S_{mixing}$.

**P6.23** A hard-working horse can lift a 350. lb. weight 100. ft. in one minute. Assuming the horse generates energy to accomplish this work by metabolizing glucose:

$$C_6H_{12}O_6(s) + 6O_2(g) \rightarrow 6CO_2(g) + 6H_2O(l)$$
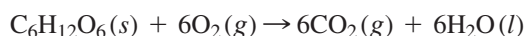
Calculate how much glucose a horse must metabolize to sustain this rate of work for one hour at 298 K.

**P6.24** Consider the reaction $FeO(s) + CO(g) \rightleftharpoons Fe(s) + CO_2(g)$ for which $K_P$ is found to have the following values:

| $T$ | 700.°C | 1200.°C |
|-----|--------|---------|
| $K_P$ | 0.688 | 0.310 |

a. Using this data, calculate $\Delta G_R^\circ$, $\Delta S_R^\circ$, and $\Delta H_R^\circ$ for this reaction at 700.°C. Assume that $\Delta H_R^\circ$ is independent of temperature.

b. Calculate the mole fraction of $CO_2(g)$ present in the gas phase at 700.°C.

**P6.25** Derive an expression for $A(V,T)$ analagous to that for $G(T,P)$ in Equation (6.33).

**P6.26** Show that

$$\left[\frac{\partial(A/T)}{\partial(1/T)}\right]_V = U$$

Write an expression analogous to Equation (6.36) that would allow you to relate $\Delta A$ at two temperatures.

**P6.27** A gas mixture with 4.50 mol of Ar, $x$ moles of Ne, and $y$ moles of Xe is prepared at a pressure of 1 bar and a temperature of 298 K. The total number of moles in the mixture is five times that of Ar. Write an expression for $\Delta G_{mixing}$ in terms of $x$. At what value of $x$ does the magnitude of $\Delta G_{mixing}$ have its minimum value? Answer this part graphically or by using an equation solver. Calculate $\Delta G_{mixing}$ for this value of $x$.

**P6.28** In Example Problem 6.9, $K_P$ for the reaction $CO(g) + H_2O(l) \rightleftharpoons CO_2(g) + H_2(g)$ was calculated to be $3.32 \times 10^3$ at 298.15 K. At what temperature is $K_P = 5.50 \times 10^3$? What is the highest value that $K_P$ can have by changing the temperature? Assume that $\Delta H_R^\circ$ is independent of temperature.

**P6.29** Assuming that $\Delta H_f^\circ$ is constant in the interval 275 K – 600. K, calculate $\Delta G^\circ$ for the process $(H_2O, g, 298\ K) \rightarrow (H_2O, g, 600.\ K)$. Calculate the relative change in the Gibbs energy.

**P6.30** Calculate the degree of dissociation of $N_2O_4$ in the reaction $N_2O_4(g) \rightleftharpoons 2NO_2(g)$ at 300. K and a total pressure of 1.50 bar. Do you expect the degree of dissociation to increase or decrease as the temperature is increased to 550. K? Assume that $\Delta H_R^\circ$ is independent of temperature.

**P6.31** Oxygen reacts with solid glycylglycine $C_4H_8N_2O_3$ to form urea $CH_4N_2O$, carbon dioxide, and water:

$$3O_2(g) + C_4H_8N_2O_3(s) \rightleftharpoons$$
$$CH_4N_2O(s) + 3CO_2(g) + 2H_2O(l)$$
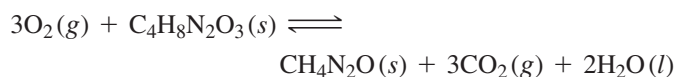
At $T = 298$ K and 1.00 atm solid glycylglycine has the following thermodynamic properties:

$$\Delta G_f^\circ = -491.5\ kJ\ mol^{-1},\ \Delta H_f^\circ = -746.0\ kJ\ mol^{-1},$$
$$S^\circ = 190.0J\ K^{-1}\ mol^{-1}$$

Calculate $\Delta G_R^\circ$ at $T = 298.15$ K and at $T = 310.0$ K. State any assumptions that you make.

**P6.32** Calculate $\Delta G_R^\circ$ for the reaction $CO(g) + 1/2\ O_2(g) \rightarrow CO_2(g)$ at 298.15 K. Calculate $\Delta G_R^\circ$ at 600. K assuming that $\Delta H_R^\circ$ is constant in the temperature interval of interest.

**P6.33** A sample containing 2.50 mol of an ideal gas at 325 K is expanded from an initial volume of 10.5 L to a final volume of 60.0 L. Calculate the final pressure. Calculate $\Delta G$ and $\Delta A$ for this process for (a) an isothermal reversible path and (b) an isothermal expansion against a constant external pressure equal to the final pressure. Explain why $\Delta G$ and $\Delta A$ do or do not differ from one another.

**P6.34** You have containers of pure $O_2$ and $N_2$ at 298 K and 1 atm pressure. Calculate $\Delta G_{mixing}$ relative to the unmixed gases of

a. a mixture of 10. mol of $O_2$ and 10. mol of $N_2$

b. a mixture of 10. mol of $O_2$ and 20. mol of $N_2$

c. Calculate $\Delta G_{mixing}$ if 10. mol of pure $N_2$ is added to the mixture of 10. mol of $O_2$ and 10. mol of $N_2$.

**P6.35** In this problem, you calculate the error in assuming that $\Delta H_R^\circ$ is independent of $T$ for the reaction $2CuO(s) \rightleftharpoons 2Cu(s) + O_2(g)$.

The following data are given at 25° C:

| Compound | CuO(s) | Cu(s) | $O_2(g)$ |
|----------|--------|-------|----------|
| $\Delta H_f^\circ$ (kJ mol$^{-1}$) | −157 | | |
| $\Delta G_f^\circ$ (kJ mol$^{-1}$) | −130. | | |
| $C_{P,m}$ (J K$^{-1}$ mol$^{-1}$) | 42.3 | 24.4 | 29.4 |

**a.** From Equation (6.65),

$$\int_{K_P(T_0)}^{K_P(T_f)} d\ln K_P = \frac{1}{R}\int_{T_0}^{T_f}\frac{\Delta H_R^\circ}{T^2}dT$$

To a good approximation, we can assume that the heat capacities are independent of temperature over a limited range in temperature, giving $\Delta H_R^\circ(T) = \Delta H_R^\circ(T_0) + \Delta C_P(T - T_0)$ where $\Delta C_P = \Sigma_i \nu_i C_{P,m}(i)$. By integrating Equation (6.65), show that

$$\ln K_P(T) = \ln K_P(T_0) - \frac{\Delta H_R^\circ(T_0)}{R}\left(\frac{1}{T} - \frac{1}{T_0}\right)$$
$$+ \frac{T_0 \times \Delta C_P}{R}\left(\frac{1}{T} - \frac{1}{T_0}\right)$$
$$+ \frac{\Delta C_P}{R}\ln\frac{T}{T_0}$$

**b.** Using the result from part (a), calculate the equilibrium pressure of oxygen over copper and $CuO(s)$ at 1275 K. How is this value related to $K_P$ for the reaction $2CuO(s) \rightleftharpoons 2Cu(s) + O_2(g)$?

**c.** What value of the equilibrium pressure would you obtain if you assumed that $\Delta H_R^\circ$ were constant at its value for 298.15 K up to 1275 K?

**P6.36** Consider the equilibrium in the reaction $3O_2(g) \rightleftharpoons 2O_3(g)$. Assume that $\Delta H_R^\circ$ is independent of temperature.

**a.** Without doing a calculation, predict whether the equilibrium position will shift toward reactants or products as the pressure is increased.

**b.** Using only the data tables, predict whether the equilibrium position will shift toward reactants or products as the temperature is increased.

**c.** Calculate $K_P$ at 600. and 700. K. Compare your results with your answer to part (b).

**d.** Calculate $K_x$ at 600. K and pressures of 1.00 and 2.25 bar. Compare your results with your answer to part (a).

**P6.37** $N_2O_3$ dissociates according to the equilibrium $N_2O_3(g) \rightleftharpoons NO_2(g) + NO(g)$. At 298 K and one bar pressure, the degree of dissociation defined as the ratio of moles of $NO_2(g)$ or $NO(g)$ to the moles of the reactant assuming no dissociation occurs is $3.5 \times 10^{-3}$. Calculate $\Delta G_R^\circ$ for this reaction.

**P6.38** If the reaction $Fe_2N(s) + 3/2\,H_2(g) \rightleftharpoons 2Fe(s) + NH_3(g)$ comes to equilibrium at a total pressure of 1 bar, analysis of the gas shows that at 700. and 800. K, $P_{NH_3}/P_{H_2} = 2.165$ and 1.083, respectively, if only $H_2(g)$ was initially present in the gas phase and $Fe_2N(s)$ was in excess.

**a.** Calculate $K_P$ at 700. and 800. K.

**b.** Calculate $\Delta S_R^\circ$ at 700. K and 800. K and $\Delta H_R^\circ$ assuming that it is independent of temperature.

**c.** Calculate $\Delta G_R^\circ$ for this reaction at 298.15 K.

**P6.39** Assume the internal energy of an elastic fiber under tension (see Problem P6.16) is given by $dU = T\,dS - P\,dV - F\,d\ell$. Obtain an expression for $(\partial G/\partial\ell)_{P,T}$ and calculate the maximum nonexpansion work obtainable when a collagen fiber contracts from $\ell = 20.0$ to 10.0 cm at constant $P$ and $T$. Assume other properties as described in Problem P6.16.

**P6.40** Under anaerobic conditions, glucose is broken down in muscle tissue to form lactic acid according to the reaction: $C_6H_{12}O_6(s) \rightleftharpoons 2CH_3CHOHCOOH(aq)$. Thermodynamic data at $T = 298$ K for glucose and lactic acid are given in the following table.

| | $\Delta H_f^\circ$ (kJ mol$^{-1}$) | $C_{Pm}$ (J K$^{-1}$ mol$^{-1}$) | $S_m^\circ$ (J K$^{-1}$ mol$^{-1}$) |
|---|---|---|---|
| Glucose | −1273.1 | 219.2 | 209.2 |
| Lactic Acid | −673.6 | 127.6 | 192.1 |

Calculate $\Delta G_R^\circ$ at $T = 298$ K. and $T = 310$. K. In your calculation at 310. K, assume (a) that $\Delta H_R^\circ$ and $\Delta S_R^\circ$ are constant in this temperature interval and (b) calculate $\Delta H_R^\circ$ and $\Delta S_R^\circ$ at 310. K using the data in the previous table. Assume all heat capacities are constant in this temperature interval.

**P6.41** Consider the equilibrium $3O_2(g) \rightleftharpoons 2O_3(g)$.

**a.** Using the data tables, calculate $K_P$ at 298 K.

**b.** Assuming that the extent of reaction at equilibrium is much less than one, show that the degree of reaction defined as half the number of moles of $O_3(g)$ divided by the initial number moles of $O_2(g)$ present before dissociation is given by $\xi_{eq} = (1/2)\sqrt{K_P \times P/P^\circ}$.

**c.** Calculate the degree of reaction at 298 K and a pressure of 5.00 bar.

**d.** Calculate $K_x$ at 298 K and a pressure of 5.00 bar.

**P6.42** Use the equation $C_{P,m} - C_{V,m} = TV_m\beta^2/\kappa$ and the data tables to determine $C_{V,m}$ for $H_2O(l)$ at 298 K. Calculate $(C_{P,m} - C_{V,m})/C_{P,m}$.

**P6.43** As shown in Example Problem 3.5, $(\partial U_m/\partial V)_T = a/V_m^2$ for a van der Waals gas. In this problem, you will compare the change in energy with temperature and volume for $N_2$, treating it as a van der Waals gas.

**a.** Calculate $\Delta U$ per mole of $N_2(g)$ at 1 bar pressure and 298 K if the volume is increased by 1.00% at constant $T$. Approximate the molar volume as the ideal gas value.

**b.** Calculate $\Delta U$ per mole of $N_2(g)$ at 1 bar pressure and 298 K if the temperature is increased by 1.00% at constant $V$.

**c.** Calculate the ratio of your results in part (a) to the result in part (b). What can you conclude about the relative importance of changes in temperature and volume on $\Delta U$?

# Web-Based Simulations, Animations, and Problems

**W6.1** The equilibrium $A \rightleftharpoons B$ is simulated. The variables $\Delta G_{reactants}^\circ$ and $\Delta H_{products}^\circ$ and T can be varied independently using sliders. The position of the equilibrium as well as the time required to reach equilibrium is investigated as a function of these variables.

# The Properties of Real Gases

Τhe ideal gas law is only accurate for gases at low values of the density. To design production plants that use real gases at high pressures, equations of state valid for gases at higher densities are needed. Such equations must take the finite volume of a molecule and the intermolecular potential into account. They accurately describe the *P–V* relationship of a given gas at a fixed value of *T* within their range of validity using parameters that are specific to a given gas. An important consequence of nonideality is that the chemical potential of a real gas must be expressed in terms of its fugacity rather than its partial pressure. Fugacities rather than pressures must also be used in calculating the thermodynamic equilibrium constant $K_P$ for a real gas.

## 7.1 Real Gases and Ideal Gases

To this point, the ideal gas equation of state has been assumed to be sufficiently accurate to describe the *P–V–T* relationship for a real gas. This assumption has allowed calculations of expansion work and of the equilibrium constant $K_P$ in terms of partial pressures using the ideal gas law. In fact, the ideal gas law provides an accurate description of the *P–V–T* relationship for many gases, such as He, for a wide range of *P*, *V*, and *T* values. However, it describes the *P–V* relationship for water for a wide range of *P* and *V* values within ±10% only for *T* > 1300 K, as shown in Section 7.4. What is the explanation for this different behavior of He and $H_2O$? Is it possible to derive a "universal" equation of state that can be used to describe the *P–V* relationship for gases as different as He and $H_2O$?

In Section 1.5, the two main deficiencies in the microscopic model on which the ideal gas law is based were discussed. The first assumption is that gas molecules are point masses. However, molecules occupy a finite volume; therefore, a real gas cannot be compressed to a volume that is less than the total molecular volume. The second assumption is that the molecules in the gas do not interact, but molecules in a real gas do interact with one another through a potential as depicted in Figure 1.10. Because the potential has a short range, its effect is negligible at low densities, which correspond to large distances between molecules. Additionally, at low densities, the molecular volume is negligible compared with the volume that the gas occupies. Therefore, the *P–V–T* relationship of a real gas is the same as that for an ideal gas at sufficiently low densities and high temperatures. At higher densities and low temperatures, molecular interactions cannot be neglected. Because of these interactions, the pressure of a real

**165**

gas can be higher or lower than that for an ideal gas at the same density and temperature. What determines which of these two cases applies? The questions raised in this section are the major themes of this chapter.

## 7.2 Equations of State for Real Gases and Their Range of Applicability

In this section, several equations of state for real gases and the range of the variables $P$, $V$, and $T$ over which they accurately describe a real gas are discussed. Such equations of state must exhibit a limiting $P$–$V$–$T$ behavior identical to that for an ideal gas at low density. They must also correctly model the deviations for ideal gas behavior that real gases exhibit at moderate and high densities. The first two equations of state considered here include two parameters, $a$ and $b$, that must be experimentally determined for a given gas. The parameter $a$ is a measure of the strength of the attractive part of the intermolecular potential, and $b$ is a measure of the minimum volume that a mole of molecules can occupy. Real gas equations of state are best viewed as empirical equations whose functional form has been chosen to fit experimentally determined $P$–$V$–$T$ data.

The most widely used is the **van der Waals equation of state**:

$$P = \frac{RT}{V_m - b} - \frac{a}{V_m^2} = \frac{nRT}{V - nb} - \frac{n^2a}{V^2} \tag{7.1}$$

A second useful equation of state is the **Redlich-Kwong equation of state**:

$$P = \frac{RT}{V_m - b} - \frac{a}{\sqrt{T}}\frac{1}{V_m(V_m + b)} = \frac{nRT}{V - nb} - \frac{n^2a}{\sqrt{T}}\frac{1}{V(V + nb)} \tag{7.2}$$

Although the same symbols are used for parameters $a$ and $b$ in both equations of state, they have different values for a given gas.

Figure 7.1 shows that the degree to which the ideal gas, van der Waals, and Redlich-Kwong equations of state correctly predict the $P$–$V$ behavior of $CO_2$ depends on $P$, $V$, and $T$. At 426 K, all three equations of state reproduce the correct $P$–$V$ behavior reasonably well over the range shown, with the ideal gas law having the largest error. By contrast, the three equations of state give significantly different results at 310. K. The ideal gas law gives unacceptably large errors, and the Redlich-Kwong equation of state is more accurate than is the van der Waals equation. We will have more to say about the range over which the ideal gas law is reasonably accurate when discussing the compression factor in Section 7.3.

A third widely used equation of state for real gases is the **Beattie-Bridgeman equation of state.** This equation uses five experimentally determined parameters to fit $P$–$V$–$T$ data. Because of its complexity, it will not be discussed further.

$$P = \frac{RT}{V_m^2}\left(1 - \frac{c}{V_m T^3}\right)(V_m + B) - \frac{A}{V_m^2} \quad \text{with}$$

$$A = A_0\left(1 - \frac{a}{V_m}\right) \quad \text{and} \quad B = B_0\left(1 - \frac{b}{V_m}\right) \tag{7.3}$$

A further important equation of state for real gases has a different form than any of the previous equations. The **virial equation of state** is written in the form of a power series in $1/V_m$

$$P = RT\left[\frac{1}{V_m} + \frac{B(T)}{V_m^2} + ...\right] \tag{7.4}$$

The power series does not converge at high pressures where $V_m$ becomes small. The $B(T)$, $C(T)$, and so on are called the second, third, and so on virial coefficients. This equation is more firmly grounded in theory than the previously discussed three equations because a series expansion is always valid in its convergence range. In practical use, the series is usually terminated after the second virial coefficient because values for the higher coefficients
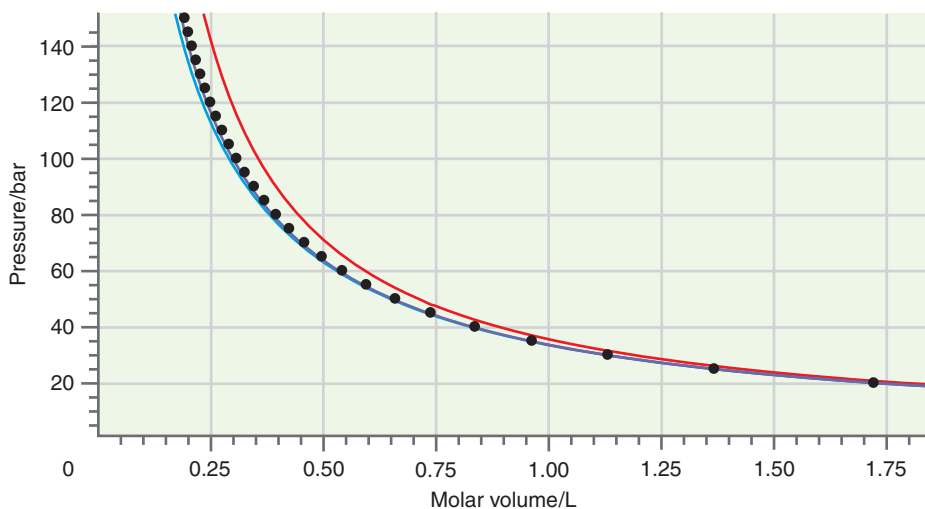
**FIGURE 7.1**
Isotherms for $CO_2$ are shown at (a) 426 K and (b) 310 K using the van der Waals equation of state (purple curve), the Redlich-Kwong equation of state (blue curve), and the ideal gas equation of state (red curve). The black dots are accurate values taken from the *NIST Chemistry Webbook.*
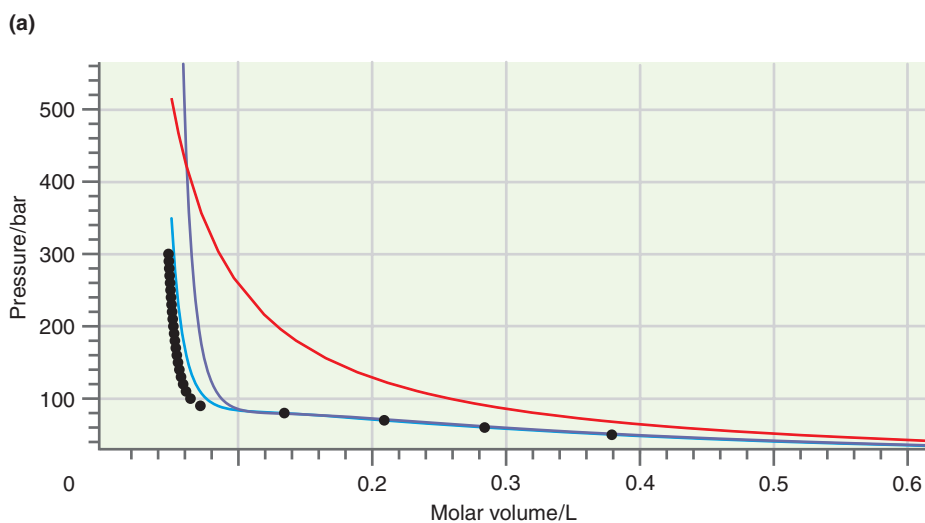
are not easily obtained from experiments. Table 7.1 (see Appendix A, Data Tables) lists values for the second virial coefficient for selected gases for different temperatures. If $B(T)$ is negative (positive), the attractive (repulsive) part of the potential dominates at that value of $T$. Statistical thermodynamics can be used to relate the virial coefficients with the intermolecular potential function. As you will show in the end-of-chapter problems, $B(T)$ for a van der Waals gas is given by $B(T) = b - (a/RT)$.

The principal limitation of the ideal gas law is that it does not predict that a gas can be liquefied under appropriate conditions. Consider the approximate $P$–$V$ diagram for $CO_2$ shown in Figure 7.2. (It is approximate because it is based on the van der Waals equation of state, rather than experimental data.) Each of the curves is an isotherm corresponding to a fixed temperature. The behavior predicted by the ideal gas law is shown for $T = 334$ K. Consider the isotherm for $T = 258$ K. Starting at large values of $V$, the pressure rises as $V$ decreases and then becomes constant over a range of values of $V$. The value of $V$ at which $P$ becomes constant depends on $T$. As the volume of the system is decreased further, the pressure suddenly increases rapidly as $V$ decreases.

The reason for this unusual dependence of $P$ on $V_m$ becomes clear when the $CO_2$ compression experiment is carried out in the piston and transparent cylinder assembly shown in Figure 7.3. The system consists of either a single phase or two phases separated by a sharp interface, depending on the values of $T$ and $V_m$. For points a, b, c, and d on the 258 K isotherm of Figure 7.2, the system has the following composition: at point a, the system consists entirely of $CO_2(g)$. However, at points b and c, a sharp interface separates $CO_2(g)$ and $CO_2(l)$. Along the line linking points b and c, the system contains $CO_2(g)$ and $CO_2(l)$ in equilibrium with one another. The proportion of liquid to gas changes, but the pressure remains constant. The temperature-dependent

equilibrium pressure is called the **vapor pressure** of the liquid. As the volume is decreased further, the system becomes a single-phase system again, consisting of $CO_2(l)$ only. The pressure changes slowly with increasing $V$ if $V_m > 0.33$ L because $CO_2(g)$ is quite compressible. However, the pressure changes rapidly with decreasing $V$ if $V_m < 0.06$ L because $CO_2(l)$ is nearly incompressible. The single-phase regions and the two-phase gas–liquid coexistence region are shown in Figure 7.2.

If the same experiment is carried out at successively higher temperatures, it is found that the range of $V_m$ in which two phases are present becomes smaller, as seen in the 243, 258, and 274 K isotherms of Figure 7.2. The temperature at which the range of $V_m$ has shrunk to a single value is called the **critical temperature,** $T_c$. For $CO_2$, $T_c = 304.12$ K. At $T = T_c$, the isotherm exhibits an inflection point so that

$$\left(\frac{\partial P}{\partial V_m}\right)_{T=T_c} = 0 \quad \text{and} \quad \left(\frac{\partial^2 P}{\partial V_m^2}\right)_{T=T_c} = 0 \tag{7.5}$$

What is the significance of the critical temperature? Critical behavior will be discussed in Chapter 8. At this point, it is sufficient to know that as the critical point is approached, the density of $CO_2(l)$ decreases and the density of $CO_2(g)$ increases, and at $T = T_c$ the densities are equal. Above $T_c$, no interface is observed in the experiment depicted in Figure 7.3, and liquid and gas phases can no longer be distinguished. The term *supercritical fluid* is used instead. As will be discussed in Chapter 8, $T_c$ and the corresponding values $P_c$ and $V_c$, which together are called the **critical constants**, take on particular significance in describing the phase diagram of a pure substance. The critical constants for a number of different substances are listed in Table 7.2 (see Appendix A, Data Tables).
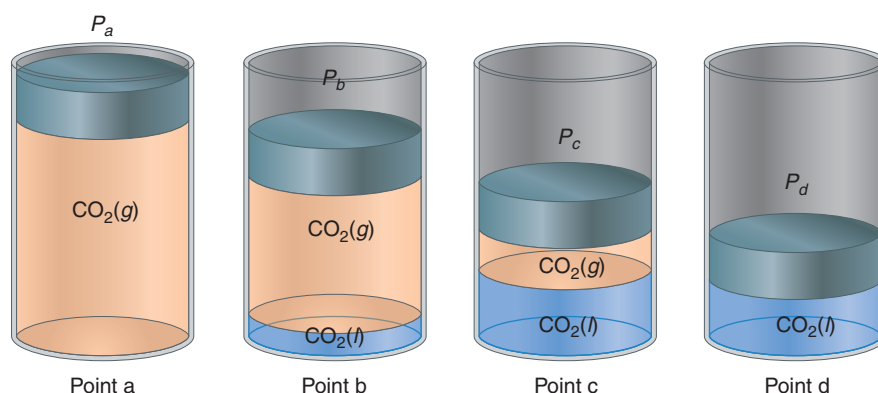


**FIGURE 7.3**
The volume and the composition of a system containing $CO_2$ at 258 K is shown at points a, b, c, and d indicated in Figure 7.2. The liquid and gas volumes are not shown to scale.

The parameters $a$ and $b$ for the van der Waals and Redlich-Kwong equations of state are chosen so that the equation of state best represents real gas data. This can be done by using the values of $P$, $V$, and $T$ at the critical point $T_c$, $P_c$, and $V_c$ as shown in Example Problem 7.1. Parameters $a$ and $b$ calculated from critical constants in this way are listed in Table 7.4 (see Appendix A, Data Tables).

## EXAMPLE PROBLEM 7.1

At $T = T_c$, $(\partial P/\partial V_m)_{T=T_c} = 0$ and $(\partial^2 P/\partial V_m^2)_{T=T_c} = 0$. Use this information to determine $a$ and $b$ in the van der Waals equation of state in terms of the experimentally determined values $T_c$ and $P_c$.

**Solution**

$$\left(\frac{\partial\left[\frac{RT}{V_m - b} - \frac{a}{V_m^2}\right]}{\partial V_m}\right)_{T=T_c} = -\frac{RT_c}{(V_{mc} - b)^2} + \frac{2a}{V_{mc}^3} = 0$$

$$\left(\frac{\partial^2\left[\frac{RT}{V_m - b} - \frac{a}{V_m^2}\right]}{\partial V_m^2}\right)_{T=T_c} = \left(\frac{\partial\left[-\frac{RT}{(V_m - b)^2} + \frac{2a}{V_m^3}\right]}{\partial V_m}\right)_{T=T_c}$$

$$= \frac{2RT_c}{(V_{mc} - b)^3} - \frac{6a}{V_{mc}^4} = 0$$

Equating $RT_C$ from these two equations gives

$$RT_c = \frac{2a}{V_{mc}^3}(V_{mc} - b)^2 = \frac{3a}{V_{mc}^4}(V_{mc} - b)^3, \text{ which simplifies to}$$

$$\frac{3}{2V_{mc}}(V_{mc} - b) = 1$$

The solution to this equation is $V_{mc} = 3b$. Substituting this result into $(\partial P/\partial V_m)_{T=T_c} = 0$ gives

$$-\frac{RT_c}{(V_{mc} - b)^2} + \frac{2a}{V_{mc}^3} = -\frac{RT_c}{(2b)^2} + \frac{2a}{(3b)^3} = 0 \quad \text{or} \quad T_c = \frac{2a}{(3b)^3}\frac{(2b)^2}{R} = \frac{8a}{27Rb}$$

Substituting these results for $T_c$ and $V_{mc}$ in terms of $a$ and $b$ into the van der Waals equation gives the result $P_c = a/27b^2$. We only need two of the critical constants $T_c$, $P_c$, and $V_{mc}$ to determine $a$ and $b$. Because the measurements for $P_c$ and $T_c$ are more accurate than for $V_{mc}$, we use these constants to obtain expressions for $a$ and $b$. These results for $P_c$ and $T_c$ can be used to express $a$ and $b$ in terms of $P_c$ and $T_c$. The results are

$$b = \frac{RT_c}{8P_c} \quad \text{and} \quad a = \frac{27R^2T_c^2}{64P_c}$$

A similar analysis for the Redlich-Kwong equation gives

$$a = \frac{R^2 T_c^{5/2}}{9P_c(2^{1/3} - 1)} \quad \text{and} \quad b = \frac{(2^{1/3} - 1)RT_c}{3P_c}$$

What is the range of validity of the van der Waals and Redlich-Kwong equations? No two-parameter equation of state is able to reproduce the isotherms shown in Figure 7.2 for $T < T_c$ because it cannot reproduce either the range in which $P$ is constant or the discontinuity in $(\partial P/\partial V)_T$ at the ends of this range. This failure is illustrated in Figure 7.4, in which isotherms calculated using the van der Waals equation of state are plotted for some of the values of $T$ as in Figure 7.2. Below $T_c$, all calculated isotherms have an oscillating region that is unphysical because $V$ increases as $P$ increases. In the **Maxwell construction,** the oscillating region is replaced by the horizontal line for which the areas above and below the line are equal, as indicated in Figure 7.4. The Maxwell construction is used in generating the isotherms shown in Figure 7.2.
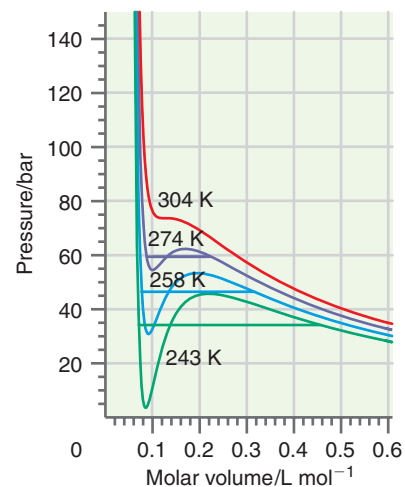


**FIGURE 7.4**

Van der Waals isotherms show the relationship between pressure and molar volume for $CO_2$ at the indicated temperatures. The Maxwell construction is shown. No oscillations in the calculated isotherms occur for $T \geq T_c$.

The Maxwell construction can be justified on theoretical grounds, but the equilibrium vapor pressure determined in this way for a given value of $T$ is only in qualitative agreement with experiment. The van der Waals and Redlich-Kwong equations of state do a good job of reproducing $P$–$V$ isotherms for real gases only in the single-phase gas region $T > T_c$ and for densities well below the critical density, $\rho_c = M/V_{mc}$, where $V_{mc}$ is the molar volume at the critical point. The Beattie-Bridgeman equation, which has three more adjustable parameters, is accurate above $T_c$ for higher densities.

# 7.3 The Compression Factor

How large is the error in $P$–$V$ curves if the ideal gas law is used rather than the van der Waals or Redlich-Kwong equations of state? To address this question, it is useful to introduce the **compression factor**, $z$, defined by

$$z = \frac{V_m}{V_m^{ideal}} = \frac{PV_m}{RT} \tag{7.6}$$

For the ideal gas, $z = 1$ for all values of $P$ and $V_m$. If $z > 1$, the real gas exerts a greater pressure than the ideal gas, and if $z < 1$, the real gas exerts a smaller pressure than the ideal gas for the same values of $T$ and $V_m$.

The compression factor for a given gas is a function of temperature, as shown in Figure 7.5. In this figure, $z$ has been calculated for $N_2$ at two values of $T$ using the van der Waals and Redlich-Kwong equations of state. The dots are calculated from accurate values of $V_m$ taken from the *NIST Chemistry Workbook*. Although the results calculated using these equations of state are not in quantitative agreement with accurate results for all $P$ and $T$, the trends in the functional dependence of $z$ on $P$ for different $T$ values are correct. Because it is inconvenient to rely on tabulated data for individual gases, we focus on $z(P)$ curves calculated from real gas equations of state. Both the van der Waals and Redlich-Kwong equations predict that for $T = 200$ K, $z$ initially decreases with pressure. The compression factor only becomes greater than the ideal gas value of one for pressures in excess of 200 bar. For $T = 400$. K, $z$ increases linearly with $T$. This functional dependence is also predicted by the Redlich-Kwong equation. The van der Waals equation predicts that the initial slope is zero, and $z$ increases slowly with $P$. For both temperatures, $z \rightarrow 1$ as $P \rightarrow 0$. This result shows that the ideal gas law is obeyed if $P$ is sufficiently small.

To understand why the low pressure value of the compression factor varies with temperature for a given gas, we use the van der Waals equation of state. Consider the variation of the compression factor with $P$ at constant $T$,

$$\left(\frac{\partial z}{\partial P}\right)_T = \left(\frac{\partial z}{\partial[RT/V_m]}\right)_T = \frac{1}{RT}\left(\frac{\partial z}{\partial[1/V_m]}\right)_T$$

**FIGURE 7.5**
The calculated compression factor for $N_2$ is shown as a function of pressure for $T = 200$. and 400. K and compared with accurate values. The purple and red curves have been calculated using the van der Waals and Redlich-Kwong equations of state, respectively. The Redlich-Kwong equation does not give physically meaningful solutions above $P = 175$ bar for 200. K, where $\rho = 2.5\rho_c$. The dots are calculated from accurate values for $V_m$ taken from the *NIST Chemistry Webbook*.

for a van der Waals gas in the ideal gas limit as $1/V_m \to 0$. As shown in Example Problem 7.2, the result $(\partial z/\partial P)_T = b/RT - a/(RT)^2$ is obtained.

## EXAMPLE PROBLEM 7.2

Show that the slope of $z$ as a function of $P$ as $P \to 0$ is related to the van der Waals parameters by

$$\lim_{p \to 0} \left( \frac{\partial z}{\partial P} \right)_T = \frac{1}{RT} \left( b - \frac{a}{RT} \right)$$

### Solution

Rather than differentiating $z$ with respect to $P$, we transform the partial derivative to one involving $V_m$:

$$z = \frac{V_m}{V_m^{ideal}} = \frac{PV_m}{RT} = \frac{\left( \dfrac{RT}{V_m - b} - \dfrac{a}{V_m^2} \right) V_m}{RT} = \frac{V_m}{V_m - b} - \frac{a}{RTV_m}$$

$$\left( \frac{\partial z}{\partial P} \right)_T = \left( \frac{\dfrac{\partial z}{\partial V_m}}{\dfrac{\partial P}{\partial V_m}} \right)_T = \left( \frac{\dfrac{\partial}{\partial V_m}\left[ \dfrac{V_m}{V_m - b} - \dfrac{a}{RTV_m} \right]}{\dfrac{\partial}{\partial V_m}\left( \dfrac{RT}{V_m - b} - \dfrac{a}{V_m^2} \right)} \right)_T$$

$$= \left( \frac{\dfrac{1}{V_m - b} - \dfrac{V_m}{(V_m - b)^2} + \dfrac{a}{RTV_m^2}}{-\dfrac{RT}{(V_m - b)^2} + 2\dfrac{a}{V_m^3}} \right)$$

$$= \left( \frac{\dfrac{V_m - b}{(V_m - b)^2} - \dfrac{V_m}{(V_m - b)^2} + \dfrac{a}{RTV_m^2}}{-\dfrac{RT}{(V_m - b)^2} + 2\dfrac{a}{V_m^3}} \right)$$

$$= \left( \frac{\dfrac{-b}{(V_m - b)^2} + \dfrac{a}{RTV_m^2}}{-\dfrac{RT}{(V_m - b)^2} + 2\dfrac{a}{V_m^3}} \right) \to \left( \frac{\dfrac{-b}{V_m^2} + \dfrac{a}{RTV_m^2}}{-\dfrac{RT}{V_m^2}} \right) \to$$

$$\to \frac{1}{RT} \left( b - \frac{a}{RT} \right) \text{ as } V_m \to \infty$$

In the second to last line, $-\dfrac{RT}{(V_m - b)^2} + 2\dfrac{a}{V_m^3} \to -\dfrac{RT}{V_m^2}$ as $V_m \to \infty$

because the second term approaches zero more rapidly than the first term and $V_m \gg b$.

From Example Problem 7.2, the van der Waals equation predicts that the initial slope of the $z$ versus $P$ curve is zero if $b = a/RT$. The corresponding temperature is known as the **Boyle temperature** $T_B$

$$T_B = \frac{a}{Rb} \tag{7.7}$$

Values for the Boyle temperature of several gases are shown in Table 7.3.

Because the parameters $a$ and $b$ are substance dependent, $T_B$ is different for each gas. Using the van der Waals parameters for $N_2$, $T_B = 425$ K, whereas the experimentally

**TABLE 7.3  Boyle Temperatures of Selected Gases**

| Gas | $T_B$ (K) | Gas | $T_B$ (K) |
|-----|-----------|-----|-----------|
| He  | 23        | $O_2$ | 400. |
| $H_2$ | 110.    | $CH_4$ | 510. |
| Ne  | 122       | Kr  | 575 |
| $N_2$ | 327     | Ethene | 735 |
| CO  | 352       | $H_2O$ | 1250 |

*Source:* Calculated from data in Lide, D. R., ed. *CRC Handbook of Thermophysical and Thermochemical Data.* Boca Raton, FL: CRC Press, 1994.

determined value is 327 K. The agreement is qualitative rather than quantitative. At the Boyle temperature both $z \to 1$, and $(\partial z / \partial P)_T \to 0$ as $P \to 0$, which is the behavior exhibited by an ideal gas. It is only at $T = T_B$ that a real gas exhibits ideal behavior as $P \to 0$ with respect to $\lim_{P \to 0} (\partial z / \partial P)_T$. Above the Boyle temperature, $(\partial z / \partial P)_T > 0$ as $P \to 0$, and below the Boyle temperature, $(\partial z / \partial P)_T < 0$ as $P \to 0$. These inequalities provide a criterion to predict whether $z$ increases or decreases with pressure at low pressures for a given value of $T$.

Note that the initial slope of a $z$ versus $P$ plot is determined by the relative magnitudes of $b$ and $a/RT$. Recall that the repulsive interaction is represented through $b$, and the attractive part of the potential is represented through $a$. From the previous discussion, $\lim_{P \to 0} (\partial z / \partial P)_T$ is always positive at high temperatures, because $b - (a/RT) \to b > 0$ as $T \to \infty$. This means that molecules primarily feel the repulsive part of the potential for $T \gg T_B$. Conversely, for $T \ll T_B$, $\lim_{P \to 0} (\partial z / \partial P)_T$ will always be negative because the molecules primarily feel the attractive part of the potential. For high enough values of $P$, $z > 1$ for all gases, showing that the repulsive part of the potential dominates at high gas densities, regardless of the value of $T$.

Next consider the functional dependence of $z$ on $P$ for different gases at a single temperature. Calculated values for oxygen, hydrogen, and ethene obtained using the van der Waals equation at $T = 400$ K are shown in Figure 7.6 together with accurate results for these gases. It is seen that $\lim_{P \to 0} (\partial z / \partial P)_T$ at 400 K is positive for $H_2$, negative for ethane, and approximately zero for $O_2$. These trends are correctly predicted by the van der Waals equation. How can this behavior be explained? It is useful to compare the shape of the curves for $H_2$ and ethene curves with those in Figure 7.5 for $N_2$ at different temperatures. This comparison suggests that at 400. K the gas temperature is well above $T_B$ for $H_2$ so that the repulsive part of the potential dominates. By contrast, it suggests that 400. K is well below $T_B$ for ethene, and the attractive part of the potential dominates. Because the initial slope is nearly zero, the data in Figure 7.6 suggests that 400. K is near $T_B$ for oxygen. As is seen in Table 7.3, $T_B = 735$ K for ethene, 400. K for $O_2$, and 110. K for $H_2$. These values are consistent with the previous explanation.

The results shown in Figure 7.6 can be generalized as follows. If $\lim_{P \to 0} (\partial z / \partial P)_T < 0$ for a particular gas, $T < T_B$, and the attractive part of the potential dominates. If $\lim_{P \to 0} (\partial z / \partial P)_T > 0$ for a particular gas, $T > T_B$, and the repulsive part of the potential dominates.
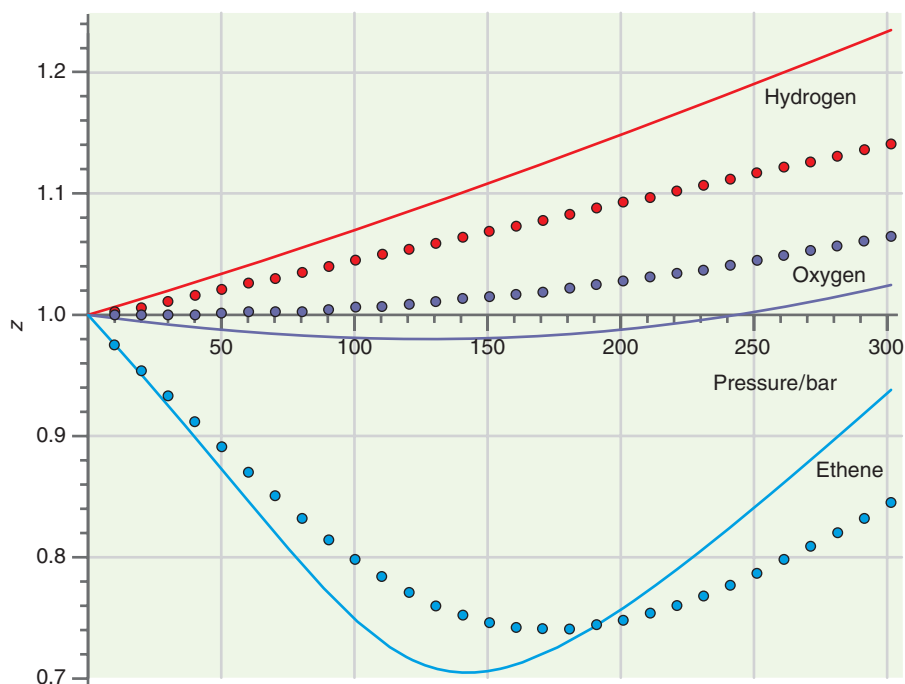


**FIGURE 7.6**

The compression factor is shown as a function of pressure for $T = 400$. K for three different gases. The solid lines have been calculated using the van der Waals equation of state. The dots are calculated from accurate values for $V_m$ taken from the *NIST Chemistry Webbook*.

# 7.4 The Law of Corresponding States

As shown in Section 7.3, the compression factor is a convenient way to quantify deviations from the ideal gas law. In calculating $z$ using the van der Waals and Redlich-Kwong equations of state, different parameters must be used for each gas. Is it possible to find an equation of state for real gases that does not explicitly contain material-dependent parameters? Real gases differ from one another primarily in the value of the molecular volume and in the depth of the attractive potential. Because molecules that have a stronger attractive interaction exist as liquids to higher temperatures, one might think that the critical temperature is a measure of the depth of the attractive potential. Similarly, one might think that the critical volume is a measure of the molecular volume. If this is the case, different gases should behave similarly if $T$, $V$, and $P$ are measured relative to their critical values.

These considerations suggest the following hypothesis. Different gases have the same equation of state if each gas is described by the dimensionless reduced variables $T_r = T/T_c$, $P_r = P/P_c$, and $V_{mr} = V_m/V_{mc}$, rather than by $T$, $P$, and $V_m$. The preceding statement is known as the **law of corresponding states.** If two gases have the same values of $T_r$, $P_r$, and $V_{mr}$, they are in corresponding states. The values of $P$, $V$, and $T$ can be very different for two gases that are in corresponding states. For example, $H_2$ at 12.93 bar and 32.98 K in a volume of $64.2 \times 10^{-3}$ L and $Br_2$ at 103 bar and 588 K in a volume of $127 \times 10^{-3}$ L are in the same corresponding state.

Next we justify the law of corresponding states and show that it is obeyed by many gases. The parameters $a$ and $b$ can be eliminated from the van der Waals equation of state by expressing the equation in terms of the reduced variables $T_r$, $P_r$, and $V_{mr}$. This can be seen by writing the van der Waals equation in the form

$$P_r P_c = \frac{RT_r T_c}{V_{mr}V_{mc} - b} - \frac{a}{V_{mr}^2 V_{mc}^2} \tag{7.8}$$

Next replace $T_c$, $V_{mc}$, and $P_c$ by the relations derived in Example Problem 7.1:

$$P_c = \frac{a}{27b^2}, \quad V_{mc} = 3b, \quad \text{and} \quad T_c = \frac{8a}{27Rb} \tag{7.9}$$

Equation (7.8) becomes

$$\frac{aP_r}{27b^2} = \frac{8aT_r}{27b\,(3bV_{mr} - b)} - \frac{a}{9b^2 V_{mr}^2} \quad \text{or}$$

$$P_r = \frac{8T_r}{3V_{mr} - 1} - \frac{3}{V_{mr}^2} \tag{7.10}$$

Equation (7.10) relates $T_r$, $P_r$, and $V_{mr}$ without reference to the parameters $a$ and $b$. Therefore, it has the character of a universal equation, like the ideal gas equation of state. To a good approximation, the law of corresponding states is obeyed for a large number of different gases as shown in Figure 7.7, as long as $T_r > 1$. However, Equation (7.10) is not really universal because the material-dependent quantities enter through values of $P_c$, $T_c$, and $V_c$ rather than through $a$ and $b$.

The law of corresponding states implicitly assumes that two parameters are sufficient to describe an intermolecular potential. This assumption is best for molecules that are nearly spherical, because for such molecules the potential is independent of the molecular orientation. It is not nearly as good for dipolar molecules such as HF, for which the potential is orientation dependent.

The results shown in Figure 7.7 demonstrate the validity of the law of corresponding states. How can this law be applied to a specific gas? The goal is to calculate $z$ for specific values of $P_r$ and $T_r$, and to use these $z$ values to estimate the error in using the ideal gas law. A convenient way to display these results is in the form of a graph. Calculated results for $z$ using the van der Waals equation of state as a function of $P_r$ for different values of $T_r$ are shown in Figure 7.8. For a given gas and specific $P$ and
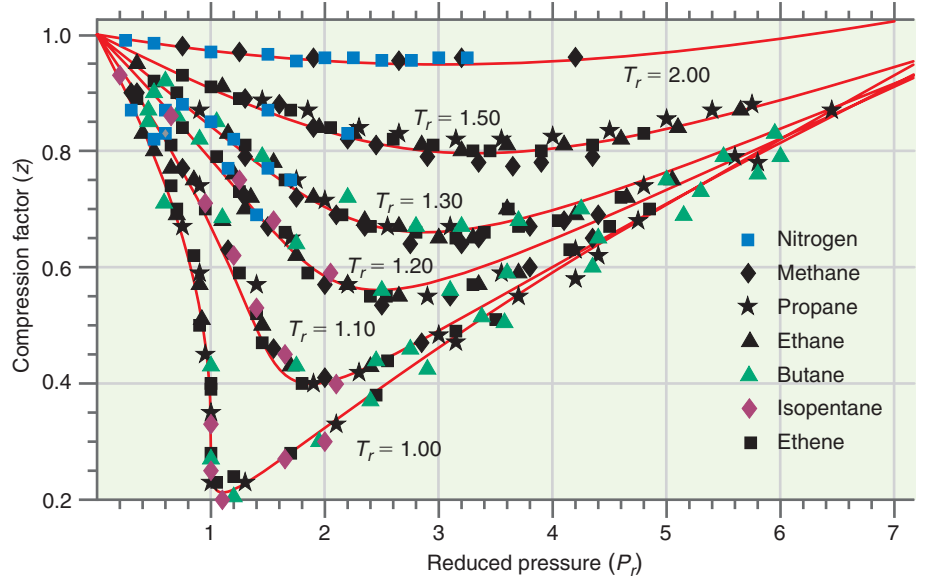
$T$ values, $P_r$ and $T_r$ can be calculated. A value of $z$ can then be read from the curves in Figure 7.8.

From Figure 7.8, we see that for $P_r < 5.5$, $z < 1$ as long as $T_r < 2$. This means that the real gas exerts a smaller pressure than an ideal gas in this range of $T_r$ and $P_r$. We con- clude that for these values of $T_r$ and $P_r$, the molecules are more influenced by the attractive part of the potential than the repulsive part that arises from the finite molecular volume. However, $z > 1$ for $P_r > 7$ for all values of $T_r$ as well as for all values of $P_r$ if $T_r > 4$. Under these conditions, the real gas exerts a larger pressure than an ideal gas. The mole- cules are more influenced by the repulsive part of the potential than the attractive part.

Using the compression factor, the error in assuming that the pressure can be calcu- lated using the ideal gas law can be defined by

$$\text{Error} = 100\% \frac{z - 1}{z} \tag{7.11}$$

Figure 7.8 shows that the ideal gas law is in error by less than 30% in the range of $T_r$ and $P_r$ where the repulsive part of the potential dominates if $P_r < 8$. However, the error can be as great as –300% in the range of $T_r$ and $P_r$ where the attractive part of the potential dominates. The error is greatest near $T_r = 1$ because at this value of the reduced temperature, the liquid and gaseous phases can coexist. At or slightly above
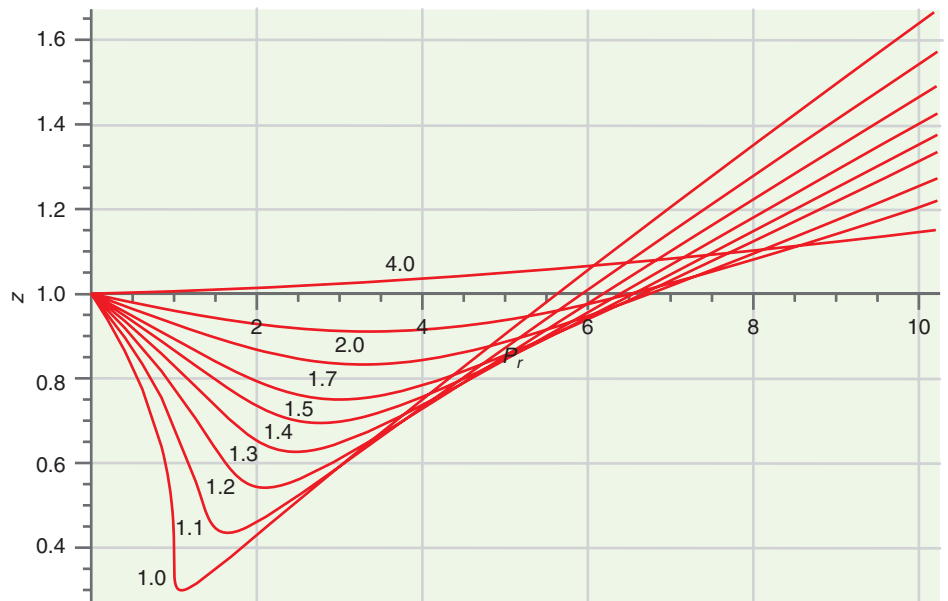


**FIGURE 7.8**
Compression factor $z$ as a function of $P_r$
for the $T_r$ values indicated. The curves
were calculated using the van der Waals
equation of state.

the critical temperature, a real gas is much more compressible than an ideal gas. These curves can be used to estimate the temperature range over which the molar volume for $H_2O(g)$ predicted by the ideal gas law is within 10% of the result predicted by the van der Waals equation of state over a wide range of pressure. From Figure 7.8, this is true only if $T_r > 2.0$, or if $T > 1300$ K.

## EXAMPLE PROBLEM 7.3

Using Figure 7.8 and the data in Table 7.2 (see Appendix A, Data Tables), calculate the volume occupied by 1.000 kg of $CH_4$ gas at $T = 230.$ K and $P = 68.0$ bar. Calculate $V - V_{ideal}$ and the relative error in $V$ if $V$ were calculated from the ideal gas equation of state.

### Solution

From Table 7.2, $T_r$ and $P_r$ can be calculated:

$$T_r = \frac{230.\ \text{K}}{190.56\ \text{K}} = 1.21 \text{ and } P_r = \frac{68.0\ \text{bar}}{45.99\ \text{bar}} = 1.48$$

From Figure 7.8, $z = 0.63$.

$$V = \frac{znRT}{P} = \frac{0.63 \times \dfrac{1000.\ \text{g}}{16.04\ \text{g mol}^{-1}} \times 0.08314\ \text{L bar K}^{-1}\text{mol}^{-1} \times 230.\ \text{K}}{68.0\ \text{bar}} = 11.0\ \text{L}$$

$$V - V_{ideal} = 11.0\ \text{L} - \frac{11.0\ \text{L}}{0.63} = -6.5\ \text{L}$$

$$\frac{V - V_{ideal}}{V} = -\frac{6.5\ \text{L}}{11.0\ \text{L}} = -58\%$$

Because the critical variables can be expressed in terms of the parameters $a$ and $b$ as shown in Example Problem 7.1, the compression factor at the critical point can also be calculated. For the van der Waals equation of state,

$$z_c = \frac{P_c V_c}{RT_c} = \frac{1}{R} \times \frac{a}{27b^2} \times 3b \times \frac{27Rb}{8a} = \frac{3}{8} \tag{7.12}$$

Equation (7.12) predicts that the critical compressibility is independent of the parameters $a$ and $b$ and should, therefore, have the same value for all gases. A comparison of this prediction with the experimentally determined value of $z_c$ in Table 7.2 shows qualitative but not quantitative agreement. A similar analysis using the critical parameters obtained from the Redlich-Kwong equation also predicts that the critical compression factor should be independent of $a$ and $b$. In this case, $z_c = 0.333$. This value is in better agreement with the values listed in Table 7.2 than that calculated using the van der Waals equation.

## 7.5 Fugacity and the Equilibrium Constant for Real Gases

As shown in the previous section, the pressure exerted by a real gas can be greater or less than that for an ideal gas. We next discuss how this result affects the value of the equilibrium constant for a mixture of reactive gases. For a pure ideal gas, the chemical potential as a function of the pressure has the form (see Section 6.3)

$$\mu(T, P) = \mu^{\circ}(T) + RT \ln \frac{P}{P^{\circ}} \tag{7.13}$$

To construct an analogous expression for a real gas, we write

$$\mu(T, P) = \mu^{\circ}(T) + RT \ln \frac{f}{f^{\circ}} \tag{7.14}$$
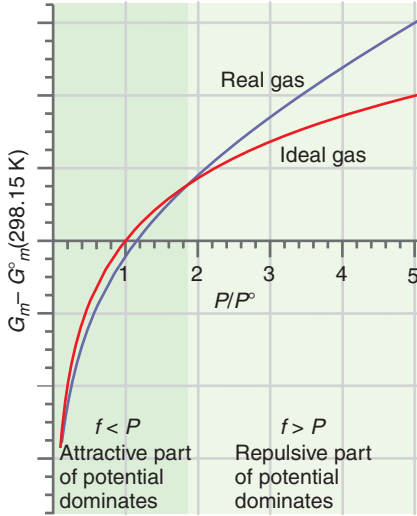
**FIGURE 7.9**
For densities corresponding to the attractive range of the potential, $P < P_{ideal}$. Therefore, $G_m^{real} < G_m^{ideal}$ and $f < P$. The inequalities are reversed for densities corresponding to the repulsive range of the potential.

where the quantity $f$ is called the **fugacity** of the gas. The fugacity can be viewed as the effective pressure that a real gas exerts. For densities corresponding to the attractive range of the intermolecular potential, $G_m^{real} < G_m^{ideal}$ and $f < P$. For densities corresponding to the repulsive range of the intermolecular potential, $G_m^{real} > G_m^{ideal}$ and $f > P$. These relationships are depicted in Figure 7.9.

The fugacity has the limiting behavior that $f \rightarrow P$ as $P \rightarrow 0$. The standard state of fugacity, denoted $f°$, is defined as the value that the fugacity would have if the gas behaved ideally at 1 bar pressure. This is equivalent to saying that $f° = P°$. This standard state is a hypothetical standard state, because a real gas will not exhibit ideal behavior at a pressure of one bar. However, the standard state defined in this way makes Equation (7.14) become identical to Equation (7.13) in the ideal gas limit $f \rightarrow P$ as $P \rightarrow 0$.

The preceding discussion provides a method to calculate the fugacity for a given gas. How are the fugacity and the pressure related? For any gas, real or ideal, at constant $T$,

$$dG_m = V_m dP \tag{7.15}$$

Therefore,

$$d\mu_{ideal} = V_m^{ideal} dP$$
$$d\mu_{real} = V_m^{real} dP \tag{7.16}$$

Equation (7.16) shows that because $V_m^{ideal} \neq V_m^{real}$, the chemical potential of a real gas will change differently with pressure than the chemical potential of an ideal gas. We form the difference

$$d\mu_{real} - d\mu_{ideal} = (V_m^{real} - V_m^{ideal})dP \tag{7.17}$$

and integrate Equation (7.17) from an initial pressure $P_i$ to a final pressure $P$:

$$\int_{P_i}^{P} (d\mu_{real} - d\mu_{ideal}) = [\mu_{real}(P) - \mu_{real}(P_i)] - [\mu_{ideal}(P) - \mu_{ideal}(P_i)]$$

$$= \int_{P_i}^{P} (V_m^{real} - V_m^{ideal})dP' \tag{7.18}$$

The previous equations allow us to calculate the difference in chemical potential between a real and an ideal gas at pressure $P$. Now let $P_i \rightarrow 0$. In this limit, $\mu_{real}(P_i) = \mu_{ideal}(P_i)$ because all real gases approach ideal gas behavior at a sufficiently low pressure. Equation (7.18) becomes

$$\mu_{real}(P) - \mu_{ideal}(P) = \int_{0}^{P} (V_m^{real} - V_m^{ideal})dP' \tag{7.19}$$

Equation (7.19) provides a way to calculate the fugacity of a real gas. Using Equations (7.13) and (7.14) for $\mu_{real}(P)$ and $\mu_{ideal}(P)$, $P$ and $f$ are related at the final pressure by

$$\ln f = \ln P + \frac{1}{RT}\int_{0}^{P} (V_m^{real} - V_m^{ideal})dP' \tag{7.20}$$

Because tabulated values of the compression factor $z$ of real gases are widely available, it is useful to rewrite Equation (7.20) in terms of $z$ by substituting $z = V_m^{real}/V_m^{ideal}$. The result is

$$\ln f = \ln P + \int_{0}^{P} \frac{z-1}{P'}dP' \text{ or } f = P \exp\left[\int_{0}^{P}\left(\frac{z-1}{P'}\right)dP'\right] \text{ or } f = \gamma(P,T)P \tag{7.21}$$

Equation (7.21) provides a way to calculate the fugacity if $z$ is known as a function of pressure. It is seen that $f$ and $P$ are related by the proportionality factor $\gamma$, which is called the **fugacity coefficient.** However, $\gamma$ is not a constant; it depends on both $P$ and $T$.

## EXAMPLE PROBLEM 7.4

For $T > T_B$, the equation of state $P(V_m - b) = RT$ is an improvement over the ideal gas law because it takes the finite volume of the molecules into account. Derive an expression for the fugacity coefficient for a gas that obeys this equation of state.

### Solution

Because $z = PV_m/RT = 1 + Pb/RT$, the fugacity coefficient is given by

$$\ln \gamma = \ln \frac{f}{P} = \int_0^P \frac{z-1}{P'} dP' = \int_0^P \frac{b}{RT} dP' = \frac{bP}{RT}$$

Equivalently, $\gamma = e^{bP/RT}$. Note that $\gamma > 1$ for all values of $P$ and $T$ because the equation of state does not take the attractive part of the intermolecular potential into account.

Calculated values for $\gamma (P,T)$ for $H_2$, $N_2$, and $NH_3$ are shown in Figure 7.10 for $T = 700.$ K. It can be seen that $\gamma \to 1$ as $P \to 0$. This must be the case because the fugacity and pressure are equal in the ideal gas limit. The following general statements can be made about the relationship between $\gamma$ and $z$: $\gamma (P,T) > 1$ if the integrand of Equation (7.21) satisfies the condition $(z - 1)/P > 0$ for all pressures up to $P$. Similarly, $\gamma (P,T) < 1$ if $(z - 1)/P < 0$ for all pressures up to $P$.

These predictions can be related to the Boyle temperature. If $T > T_B$, then $\gamma (P,T) > 1$ for all pressures, the fugacity is greater than the pressure, and $\gamma > 1$. However, if $T < T_B$, then $\gamma (P,T) < 1$, and the fugacity is smaller than the pressure. The last statement does not hold for very high values of $P_r$, because as shown in Figure 7.8, $z > 1$ for all values of $T$ at such high relative pressures. Are these conclusions in accord with the curves in Figure 7.10? The Boyle temperatures for $H_2$, $N_2$, and $NH_3$ are 110, 327, and 995 K, respectively. Because at 700. K, $T > T_B$ for $H_2$ and $N_2$, but $T < T_B$ for $NH_3$, we conclude that $\gamma > 1$ at all pressures for $H_2$ and $N_2$, and $\gamma < 1$ at all but very high pressures for $NH_3$. These conclusions are consistent with the results shown in Figure 7.10.

The fugacity coefficient can also be graphed as a function of $T_r$ and $P_r$. This is convenient because it allows $\gamma$ for any gas to be estimated once $T$ and $P$ have been expressed as reduced variables. Graphs of $\gamma$ as functions of $P_r$ and $T_r$ are shown in Figure 7.11. The curves have been calculated using Beattie-Bridgeman parameters for $N_2$, and are known to be accurate for $N_2$ over the indicated range of reduced temperature and pressure. Their applicability to other gases assumes that the law of corresponding states holds. As Figure 7.7 shows, this is generally a good assumption.

What are the consequences of the fact that except in the dilute gas limit $f \neq P$? Because the chemical potential of a gas in a reaction mixture is given by Equation (7.14), the thermodynamic equilibrium constant for a real gas $K_f$ must be expressed in terms of the fugacities. Therefore $K_f$ for the reaction $3/2\ H_2 + 1/2\ N_2 \to NH_3$ is given by

$$K_f = \frac{\left(\dfrac{f_{NH_3}}{f^\circ}\right)}{\left(\dfrac{f_{N_2}}{f^\circ}\right)^{1/2}\left(\dfrac{f_{H_2}}{f^\circ}\right)^{3/2}} = \frac{\left(\dfrac{\gamma_{NH_3}P_{NH_3}}{P^\circ}\right)}{\left(\dfrac{\gamma_{N_2}P_{N_2}}{P^\circ}\right)^{1/2}\left(\dfrac{\gamma_{H_2}P_{H_2}}{P^\circ}\right)^{3/2}}$$

$$= K_P \frac{\gamma_{NH_3}}{(\gamma_{N_2})^{1/2}(\gamma_{H_2})^{3/2}} \tag{7.22}$$

We next calculate the error in using $K_P$ rather than $K_f$ to calculate an equilibrium constant, using the ammonia synthesis reaction at 700. K and a total pressure of 400. bar as an example. In the industrial synthesis of ammonia, the partial pressures of $H_2$, $N_2$, and $NH_3$ are typically 270, 90, and 40 bar, respectively. The calculated fugacity coefficients under these conditions are $\gamma_{H_2} = 1.11$, $\gamma_{N_2} = 1.04$, and $\gamma_{NH_3} = 0.968$ using the Beattie-Bridgeman equation of state. Therefore,

$$K_f = K_P \frac{(0.968)}{(1.04)^{1/2}(1.11)^{3/2}} = 0.917\ K_P \tag{7.23}$$
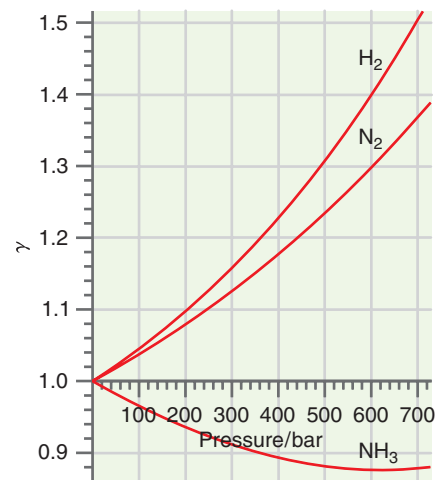


### FIGURE 7.10

The fugacity coefficients for $H_2$, $N_2$, and $NH_3$ are plotted as a function of the partial pressure of the gases for $T = 700.$ K. The calculations were carried out using the Beattie-Bridgeman equation of state.

**FIGURE 7.11**
The fugacity coefficient is plotted as a function of the reduced pressure for the indicated values of the reduced temperature.



(a)

(b)
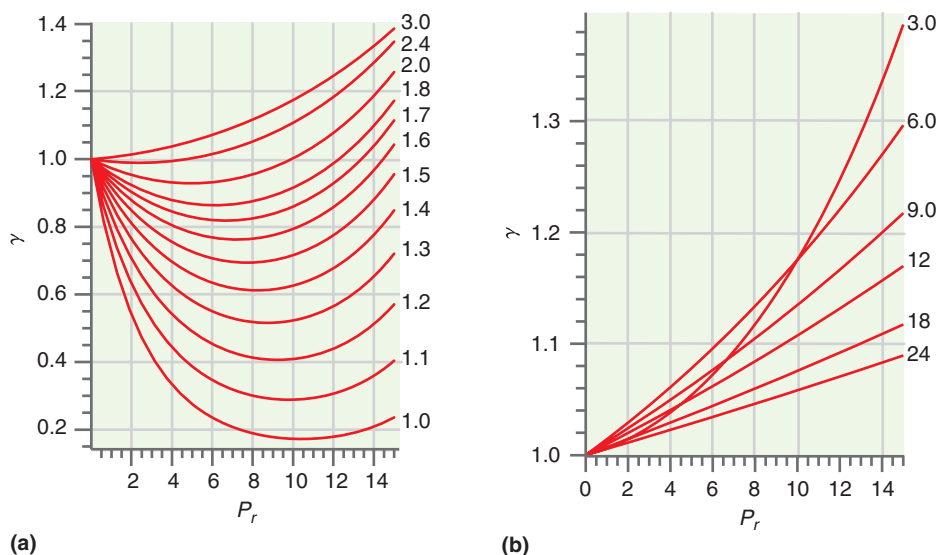
Note that $K_f$ is smaller than $K_p$ for the conditions of interest. The $NH_3$ concentration at equilibrium is proportional to the equilibrium constant, as shown in Section 6.14.

$$x_{NH_3} = (x_{N_2})^{1/2}(x_{H_2})^{3/2}\left(\frac{P}{P^\circ}\right)K_f \qquad (7.24)$$

What conclusions can be drawn from this calculation? If $K_P$ were used rather than $K_f$, the calculated mole fraction of ammonia would be in error by $-9\%$, which is a significant error in calculating the economic viability of a production plant. However, for pressures near 1 bar, activity coefficients for most gases are very close to unity as can be seen in Figure 7.11. Therefore, under typical laboratory conditions, the fugacity of a gas can be set equal to its partial pressure if $P$, $V$, and $T$ are not close to their critical values.

# Vocabulary

| | | |
|---|---|---|
| Beattie-Bridgeman equation of state | fugacity | Redlich-Kwong equation of state |
| Boyle temperature | fugacity coefficient | van der Waals equation of state |
| compression factor | law of corresponding states | vapor pressure |
| critical constants | Maxwell construction | virial equation of state |
| critical temperature | | |

# Conceptual Problems

**Q7.1**   Using the concept of the intermolecular potential, explain why two gases in corresponding states can be expected to have the same value for $z$.

**Q7.2**   Consider the comparison made between accurate results and those based on calculations using the van der Waals and Redlich-Kwong equations of state in Figures 7.1 and 7.5. Is it clear that one of these equations of state is better than the other under all conditions?

**Q7.3**   Why is the standard state of fugacity, $f^\circ$, equal to the standard state of pressure, $P^\circ$?

**Q7.4**   Explain the significance of the Boyle temperature.

**Q7.5**   A van der Waals gas undergoes an isothermal reversible expansion under conditions such that $z > 1$. Is the work done more or less than if the gas followed the ideal gas law?

**Q7.6**   For a given set of conditions, the fugacity of a gas is greater than the pressure. What does this tell you about the interaction between the molecules of the gas?

**Q7.7**   What can you conclude about the ratio of fugacity to pressure for $N_2$, $H_2$, and $NH_3$ at 500. bar using the data in Figure 7.10?

**Q7.8**   Is the ratio of fugacity to pressure greater to or less than 1 if the attractive part of the interaction potential between gas molecules dominates?

**Q7.9**   A gas is slightly above its Boyle temperature. Do you expect $z$ to increase or decrease as $P$ increases?

**Q7.10**   Explain why the oscillations in the two-phase coexistence region using the Redlich-Kwong and van der Waals equations of state (see Figure 7.4) do not correspond to reality.

**Q7.11**  A van der Waals gas undergoes an isothermal reversible expansion under conditions such that $z < 1$. Is the work done more or less than if the gas followed the ideal gas law?

**Q7.12**  The value of the Boyle temperature increases with the strength of the attractive interactions between molecules. Arrange the Boyle temperatures of the gases Ar, $CH_4$, and $C_6H_6$ in increasing order.

**Q7.13**  A system containing argon gas is at pressure $P_1$ and temperature $T_1$. How would you go about estimating the fugacity coefficient of the gas?

**Q7.14**  By looking at the $a$ and $b$ values for the van der Waals equation of state, decide whether 1 mole of $O_2$ or $H_2O$ has the higher pressure at the same value of $T$ and $V$.

**Q7.15**  Will the fugacity coefficient of a gas above the Boyle temperature be less than 1 at low pressures?

**Q7.16**  Show that the van der Waals and Redlich-Kwong equations of state reduce to the ideal gas law in the limit of low gas density.

**Q7.17**  Which of Ne or Ar has the larger van der Waals parameter $a$? Explain your reasoning.

**Q7.18**  Which of Ne or Ar has the larger van der Waals parameter $b$? Explain your reasoning.

**Q7.19**  You have calculated the pressure exerted by ethane using the ideal gas law and the Redlich-Kwong equations of state. How do you decide if the repulsive or attractive part of the molecular potential dominates under the given conditions?

**Q7.20**  Equation (1.19) states that the total pressure in a mixture of gases is equal to the sum of the partial pressures. Is this equation valid for real gases? If so, under what conditions?

# Numerical Problems

Problem numbers in **red** indicate that the solution to the problem is given in the *Student's Solutions Manual*.

**P7.1**  A van der Waals gas has a value of $z = 1.00061$ at 410. K and 1 bar and the Boyle temperature of the gas is 195 K. Because the density is low, you can calculate $V_m$ from the ideal gas law. Use this information and the result of Problem P7.28, $z \approx 1 + (b - a/RT)(1/V_m)$, to estimate $a$ and $b$.

**P7.2**

**a.**  Using the relationships derived in Example Problem 7.1 and the values of the critical constants for water from Table 7.2, calculate values for the van der Waals parameters $a$, $b$, and $R$ from $z_c$, $T_c$, $P_c$, and $V_c$. Do your results agree with those in Tables 1.2 and 7.4?

**b.**  Calculate the van der Waals parameters $a$ and $b$ using the critical constants for water and the correct value for $R$. Do these results agree with those in Tables 1.2 and 7.4?

**P7.3**  Assume that the equation of state for a gas can be written in the form $P(V_m - b(T)) = RT$. Derive an expression for $\beta = 1/V\ (\partial V/\partial T)_P$ and $\kappa = -1/V\ (\partial V/\partial P)_T$ for such a gas in terms of $b(T)$, $db(T)/dT$, $P$, and $V_m$.

**P7.4**  One mole of Ar initially at 310. K undergoes an adiabatic expansion against a pressure $P_{external} = 0$ from a volume of 8.5 L to a volume of 82.0 L. Calculate the final temperature using the ideal gas and van der Waals equations of state. Assume $C_{V,m} = 3R/2$.

**P7.5**  Calculate the $P$ and $T$ values for which $Br_2(g)$ is in a corresponding state to $Xe(g)$ at 330. K and 72.0 bar.

**P7.6**  For values of $z$ near 1, it is a good approximation to write $z(P) = 1 + (\partial z/\partial P)_T P$. If $z = 1.00104$ at 298 K and 1 bar, and the Boyle temperature of the gas is 155 K, calculate the values of $a$, $b$, and $V_m$ for the van der Waals gas.

**P7.7**  For a gas at a given temperature, the compression factor is described by the empirical equation

$$z = 1 - 8.50 \times 10^{-3} \frac{P}{P°} + 3.50 \times 10^{-5} \left(\frac{P}{P°}\right)^2$$

where $P° = 1$ bar. Calculate the fugacity coefficient for $P = 150., 250., 350., 450.,$ and 550. bar. For which of these values is the fugacity coefficient greater than 1?

**P7.8**  The experimentally determined density of $O_2$ at 140. bar and 298 K is 192 g $L^{-1}$. Calculate $z$ and $V_m$ from this information. Compare this result with what you would have estimated from Figure 7.8. What is the relative error in using Figure 7.8 for this case?

**P7.9**  At 725 K and 280. bar, the experimentally determined density of $N_2$ is 4.13 mol $L^{-1}$. Compare this with values calculated from the ideal and Redlich-Kwong equations of state. Use a numerical equation solver to solve the Redlich-Kwong equation for $V_m$ or use an iterative approach starting with $V_m$ equal to the ideal gas result. Discuss your results.

**P7.10**  A 1.75 mole sample of Ar undergoes an isothermal reversible expansion from an initial volume of 2.00 L to a final volume of 85.0 L at 310. K. Calculate the work done in this process using the ideal gas and van der Waals equations of state. What percentage of the work done by the van der Waals gas arises from the attractive potential?

**P7.11**  Show that the second virial coefficient for a van der Waals gas is given by

$$B(T) = \frac{1}{RT}\left(\frac{\partial z}{\partial \frac{1}{V_m}}\right)_T = b - \frac{a}{RT}$$

**P7.12**  The volume of a spherical molecule can be estimated as $V = b/(4N_A)$ where $b$ is the van der Waals parameter and $N_A$ is Avogadro's number. Justify this relationship by considering a spherical molecule of radius $r$, with volume $V = (4/3)\pi r^3$. What is the volume centered at the molecule that is excluded for the center of mass of a second molecule in terms of $V$? Multiply this volume by $N_A$ and set it equal to $b$. Apportion this volume equally among the molecules to arrive at $V = b/(4N_A)$. Calculate the radius of a methane molecule from the value of its van der Waals parameter $b$.

**P7.13**   Show that the van der Waals and Redlich-Kwong equations of state reduce to the ideal gas equation of state in the limit of low density.

**P7.14**   Use the law of corresponding states and Figure 7.8 to estimate the molar volume of propane at $T = 500.$ K and $P = 75.0$ bar. The experimentally determined value is $0.438$ mol $L^{-1}$. What is the relative error of your estimate?

**P7.15**   Another equation of state is the Berthelot equation, $V_m = (RT/P) + b - a/(RT^2)$. Derive expressions for $\beta = 1/V\,(\partial V/\partial T)_P$ and $\kappa = -1/V\,(\partial V/\partial P)_T$ from the Berthelot equation in terms of $V$, $T$, and $P$.

**P7.16**   Show that $P\kappa = 1 - P\left(\dfrac{\partial \ln z}{\partial P}\right)_T$ for a real gas where $\kappa$ is the isothermal compressibility.

**P7.17**   Calculate the van der Waals parameters of carbon dioxide from the values of the critical constants and compare your results with the values for $a$ and $b$ in Table 7.4.

**P7.18**   Calculate the Redlich-Kwong parameters of fluorine from the values of the critical constants and compare your results with the values for $a$ and $b$ in Table 7.4.

**P7.19**   Calculate the critical volume for ethane using the data for $T_c$ and $P_c$ in Table 7.2 (see Appendix A, Data Tables) assuming (a) the ideal gas equation of state and (b) the van der Waals equation of state. Use an iterative approach to obtain $V_c$ from the van der Waals equation, starting with the ideal gas result. How well do the calculations agree with the tabulated values for $V_c$?

**P7.20**   Show that $T\beta = 1 + T\left(\dfrac{\partial \ln z}{\partial T}\right)_P$ for a real gas where $\beta$ is the volumetric thermal expansion coefficient.

**P7.21**   At what temperature does the slope of the $z$ versus $P$ curve as $P \to 0$ have its maximum value for a van der Waals gas? What is the value of the maximum slope?

**P7.22**   Calculate the density of $O_2(g)$ at 480. K and 280. bar using the ideal gas and the van der Waals equations of state. Use a numerical equation solver to solve the van der Waals equation for $V_m$ or use an iterative approach starting with $V_m$ equal to the ideal gas result. Based on your result, does the attractive or repulsive contribution to the interaction potential dominate under these conditions? The experimentally determined result is 208 g $L^{-1}$. What is the relative error of each of your two calculations?

**P7.23**   Show that $T\beta = 1 + T(\partial \ln z/\partial T)_P$ and that $P\kappa = 1 - P(\partial \ln z/\partial P)_T$.

**P7.24**   A sample containing 42.1 g of Ar is enclosed in a container of volume 0.0885 L at 375 K. Calculate $P$ using the ideal gas, van der Waals, and Redlich-Kwong equations of state. Based on your results, does the attractive or repulsive contribution to the interaction potential dominate under these conditions?

**P7.25**   The experimental critical constants of $CH_4$ are found in Table 7.2. Use the values of $P_c$ and $T_c$ to calculate $V_c$. Assume that $CH_4$ behaves as (a) an ideal gas, (b) a van der Waals gas, and (c) a Redlich-Kwong gas at the critical point. For parts (b) and (c), use the formulas for the critical compression factor. Compare your answers with the experimental value. Are any of your calculated results close to the experimental value in Table 7.2?

**P7.26**   The observed Boyle temperatures of $H_2$, $N_2$, and $CH_4$ are 110., 327, and 510. K, respectively. Compare these values with those calculated for a van der Waals gas with the appropriate parameters.

**P7.27**   For the Berthelot equation, $V_m = (RT/P) + b - (a/RT^2)$, find an expression for the Boyle temperature in terms of $a$, $b$, and $R$.

**P7.28**   For a van der Waals gas, $z = V_m/(V_m - b) - a/RTV_m$. Expand the first term of this expression in a Taylor series in the limit $V_m \gg b$ to obtain $z \approx 1 + (b - a/RT)(1/V_m)$.

# Web-Based Simulations, Animations, and Problems

**W7.1**   In this problem, the student gains facility in using the van der Waals equation of state. A set of isotherms will be generated by varying the temperature and initial volume using sliders for a given substance. Buttons allow a choice among more than 20 gases.

a. The student generates a number of P–V curves at and above the critical temperature for the particular gas, and explains trends in the ratio $P_{vdW}/P_{ideal}$ as a function of $V$ for a given $T$, and as a function of $T$ for a given $V$.

b. The compression factor $z$ is calculated for two gases at the same value of $T_r$ and is graphed versus $P$ and $P_r$. The degree to which the law of corresponding states is valid is assessed.

**W7.2**   A quantitative comparison is made between the ideal gas law and the van der Waals equation of state for 1 of more than 20 different gases. The temperature is varied using sliders, and $P_{ideal}$, $P_{vdW}$, the relative error $P_{vdW}/P_{vdW} - P_{ideal}$, and the density of gas relative to that at the critical point are

calculated. The student is asked to determine the range of pressures and temperatures in which the ideal gas law gives reasonably accurate results.

**W7.3**   The compression factor and molar volume are calculated for an ideal and a van der Waals gas as a function of pressure and temperature. These variables can be varied using sliders. Buttons allow a choice among more than 20 gases. The relative error $V_{vdW}/V_{vdW} - V_{ideal}$ and the density of gas relative to that at the critical point are calculated. The student is asked to determine the range of pressures and temperatures in which the ideal gas law gives reasonably accurate results for the molar volume.

**W7.4**   The fugacity and fugacity coefficient are determined as a function of pressure and temperature for a model gas. These variables can be varied using sliders. The student is asked to determine the Boyle temperature and also the pressure range in which the fugacity is either more or less than the ideal gas pressure for the temperature selected.

# Phase Diagrams and the Relative Stability of Solids, Liquids, and Gases

I t is our experience that the solid form of matter is most stable at low temperatures and that most substances can exist in liquid and gaseous phases at higher temperatures. In this chapter, criteria are developed that allow one to determine which of these phases is most stable at a given temperature and pressure. The conditions under which two or three phases of a pure substance can coexist in equilibrium are also discussed. *P–T*, *P–V*, and *P–V–T* phase diagrams summarize all of this information in a form that is very useful to chemists.

## 8.1 What Determines the Relative Stability of the Solid, Liquid, and Gas Phases?

Substances are found in solid, liquid, and gaseous phases. **Phase** refers to a form of matter that is uniform with respect to chemical composition and the state of aggregation on both microscopic and macroscopic length scales. For example, liquid water in a beaker is a single-phase system, but a mixture of ice and liquid water consists of two distinct phases, each of which is uniform on microscopic and macroscopic length scales. Although a substance may exist in several different solid phases, it can only exist in a single gaseous state. Most substances have a single liquid state, although there are exceptions such as helium, which can be a normal liquid or a superfluid. In this section, the conditions under which a pure substance spontaneously forms a solid, liquid, or gas are discussed.

Experience demonstrates that as *T* is lowered from 300. to 250. K at atmospheric pressure, liquid water is converted to a solid phase. Similarly, as liquid water is heated to 400. K at atmospheric pressure, it vaporizes to form a gas. Experience also shows that if a solid block of carbon dioxide is placed in an open container at 1 bar, it sublimes over time without passing through the liquid phase. Because of this property, solid $CO_2$ is known as dry ice. These observations can be generalized to state that the solid phase is the most stable state of a substance at sufficiently low temperatures, and that the gas phase is the most stable state of a substance at sufficiently high

temperatures. The liquid state is stable at intermediate temperatures if it exists at the pressure of interest. What determines which of the solid, liquid, or gas phases exists and which phase is most stable at a given temperature and pressure?

As discussed in Chapter 6, the criterion for stability at constant temperature and pressure is that the Gibbs energy, $G(T, P, n)$, be minimized. Because for a pure substance the chemical potential $\mu$ is defined as

$$\mu = \left(\frac{\partial G}{\partial n}\right)_{T,P} = \left(\frac{\partial [nG_m]}{\partial n}\right)_{T,P} = G_m$$

where $n$ designates the number of moles of substance in the system, $d\mu = dG_m$, and we can express the differential $d\mu$ as

$$d\mu = -S_m \, dT + V_m \, dP \tag{8.1}$$

From this equation, how $\mu$ varies with changes in $P$ and $T$ can be determined:

$$\left(\frac{\partial \mu}{\partial T}\right)_P = -S_m \quad \text{and} \quad \left(\frac{\partial \mu}{\partial P}\right)_T = V_m \tag{8.2}$$

Because $S_m$ and $V_m$ are always positive, $\mu$ decreases as the temperature increases, and it increases as the pressure increases. Section 5.4 demonstrated that $S$ varies slowly with $T$ (approximately as $\ln T$). Therefore, over a limited range in $T$, a plot of $\mu$ versus $T$ at constant $P$ is a curve with a slowly increasing negative slope, approximating a straight line.

It is also known from experience that heat is absorbed as a solid melts to form a liquid and as a liquid vaporizes to form a gas. Both processes are endothermic with $\Delta H > 0$. Because at the melting and boiling temperature the entropy increases in a stepwise fashion by $\Delta S = \Delta H_{transition}/T$, the entropy of the three phases follows this order:

$$S_m^{gas} > S_m^{liquid} > S_m^{solid} \tag{8.3}$$

The functional relation between $\mu$ and $T$ for the solid, liquid, and gas phases is graphed at a given value of $P$ in Figure 8.1. The molar entropy of a phase is the negative of the slope of the $\mu$ versus $T$ curve, and the relative entropies of the three phases are given by Equation (8.3). The stable state of the system at any given temperature is that phase that has the lowest $\mu$.

Assume that the initial state of the system is described by the dot in Figure 8.1. The most stable phase is the solid phase, because $\mu$ for the liquid and gas phases is much larger than that for the solid. As the temperature is increased, the chemical potential falls as $\mu$ remains on the solid curve. However, because the slope of the liquid and gas curves are greater than that of the solid, each of these $\mu$ versus $T$ curves will intersect the solid curve for some value of $T$. In Figure 8.1, the liquid curve intersects the solid curve at $T_m$, which is called the melting temperature. At this temperature, the solid and liquid phases coexist and are in thermodynamic equilibrium. However, if the temperature is raised by an infinitesimal amount $dT$, the solid will melt completely because the liquid phase has the lower chemical potential at $T_m + dT$. Similarly, the liquid and gas phases are in thermodynamic equilibrium at the boiling temperature $T_b$. For $T > T_b$, the system is entirely in the gas phase. Note that the progression of solid $\rightarrow$ liquid $\rightarrow$ gas as $T$ increases at this value of $P$ can be explained with no other information than that $(\partial \mu / \partial T)_P = -S_m$ and that $S_m^{gas} > S_m^{liquid} > S_m^{solid}$.

If the temperature is changed too quickly, the equilibrium state of the system may not be reached. For example, it is possible to form a superheated liquid in which the liquid phase is metastable above $T_b$. Superheated liquids are dangerous because of the large volume increase that occurs if the system suddenly converts to the stable vapor phase. Boiling chips are often used in chemical laboratories to avoid the formation of superheated liquids. Similarly, it is possible to form a supercooled liquid, in which case the liquid is metastable below $T_m$. Glasses are made by cooling a viscous liquid fast
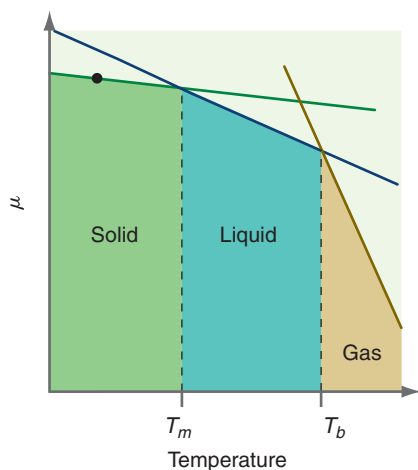


**FIGURE 8.1**

The chemical potential of a substance in the solid (green curve), liquid (blue curve), and gaseous (brown curve) states is plotted as a function of the temperature for a given value of pressure. The substance melts at the temperature $T_m$, corresponding to the intersection of the solid and liquid curves. It boils at the temperature $T_b$, corresponding to the intersection of the liquid and gas curves. The temperature ranges in which the different phases are the most stable are indicated by shaded areas. The three curves shown are actually curved slightly downward but have been approximated as straight lines.

enough to avoid crystallization. These disordered materials lack the periodicity of crystals but behave mechanically like solids. Seed crystals can be used to increase the rate of crystallization if the viscosity of the liquid is not too high and the cooling rate is sufficiently slow. Liquid crystals, which can be viewed as a state of matter intermediate between a solid and a liquid, are discussed in Section 8.10.

In Figure 8.1, we consider changes with $T$ at constant $P$. How is the relative stability of the three phases affected if $P$ is changed at constant $T$? From Equation (8.2), $(\partial \mu / \partial P)_T = V_m$ and $V_m^{gas} \gg V_m^{liquid}$. For most substances, $V_m^{liquid} > V_m^{solid}$. Therefore, the $\mu$ versus $T$ curve for the gas changes much more rapidly with pressure (by a factor of $\sim 1000$) than the liquid and solid curves. This behavior is illustrated in Figure 8.2, where it can be seen that the temperature at which the solid and the liquid curves intersect shifts as the pressure is increased. Because $V_m^{gas} \gg V_m^{liquid} > 0$, an increase in $P$ always leads to a **boiling point elevation.** An increase in $P$ leads to a **freezing point elevation** if $V_m^{liquid} > V_m^{solid}$ and to a **freezing point depression** if $V_m^{liquid} < V_m^{solid}$, as is the case for water. Few substances obey the relation $V_m^{liquid} < V_m^{solid}$; the consequences of this unusual behavior for water will be discussed in Section 8.2.

The $\mu$ versus $T$ curve for a gas shifts along the $T$ axis much more rapidly with $P$ than the liquid and solid curves. As a consequence, changes in $P$ can change the way in which a system progresses through the phases with increasing $T$ from the "normal" order solid $\rightarrow$ liquid $\rightarrow$ gas shown in Figure 8.1. For example, the sublimation of dry ice at 298 K and 1 bar can be explained using Figure 8.3a. For $CO_2$ at the given pressure, the $\mu$ versus $T$ curve for the gas intersects the corresponding curve for the solid at a lower temperature than the liquid curve. Therefore, the solid $\rightarrow$ liquid transition is



(a)



(b)

energetically unfavorable with respect to the solid $\rightarrow$ gas transition at this pressure. Under these conditions, the solid sublimes and the transition temperature $T_s$ is called the **sublimation temperature.** There is also a pressure at which the $\mu$ versus $T$ curves for all three phases intersect. The $P$, $V_m$, $T$ values for this point specify the **triple point,** so named because all three phases coexist in equilibrium at this point. This case is shown in Figure 8.3b. Triple point temperatures for a number of substances are listed in Table 8.1 (see Appendix A, Data Tables).

# 8.2 The Pressure–Temperature Phase Diagram

As shown in the previous section, at a given value of pressure and temperature a system containing a pure substance may consist of a single phase, two phases in equilibrium, or three phases in equilibrium. The usefulness of a **phase diagram** is that it displays this information graphically. Although any two of the macroscopic system variables $P$, $V$, and $T$ can be used to construct a phase diagram, the $P$–$T$ diagram is particularly useful. In this section, the features of a $P$–$T$ phase diagram that are common to pure substances are discussed. Phase diagrams must generally be determined experimentally because material-specific forces between atoms determine the temperatures and pressures at which different phases are stable. Increasingly, calculations have become sufficiently accurate that major features of phase diagrams can be obtained using microscopic theoretical models. However, as shown in Section 8.4, thermodynamics can say a great deal about the phase diagram without considering the microscopic properties of the system.

The **$P$–$T$ phase diagram,** a sample of which is shown in Figure 8.4, displays stability regions for a pure substance as a function of pressure and temperature. Most $P$, $T$ points correspond to a single solid, liquid, or gas phase. At the triple point, all three phases coexist. The triple point of water is 273.16 K and 611 Pa. All $P$, $T$ points for which the same two phases coexist at equilibrium fall on a curve. Such a curve is called a **coexistence curve.** Three separate coexistence curves are shown in Figure 8.4, corresponding to solid–gas, solid–liquid, and gas–solid coexistence. As shown in Section 8.5, the slopes of the solid-gas and liquid–gas curves are always positive. The slope of the solid–liquid curve can be either positive or negative.

The boiling point of a substance is defined as the temperature at which the vapor pressure of the substance is equal to the external pressure. The **standard boiling**

**FIGURE 8.4**
A $P$–$T$ phase diagram displays single-phase regions, coexistence curves for which two phases coexist at equilibrium, and a triple point. The processes corresponding to paths $a$, $b$, $c$, and the two processes labeled $d$ are described in the text. Two solid-liquid coexistence curves are shown. For most substances, the solid curve, which has a positive slope, is observed. For water or any other substance for which the volume increases in a transition from the liquid to the solid, the red dashed curve corresponding to a negative slope is observed.
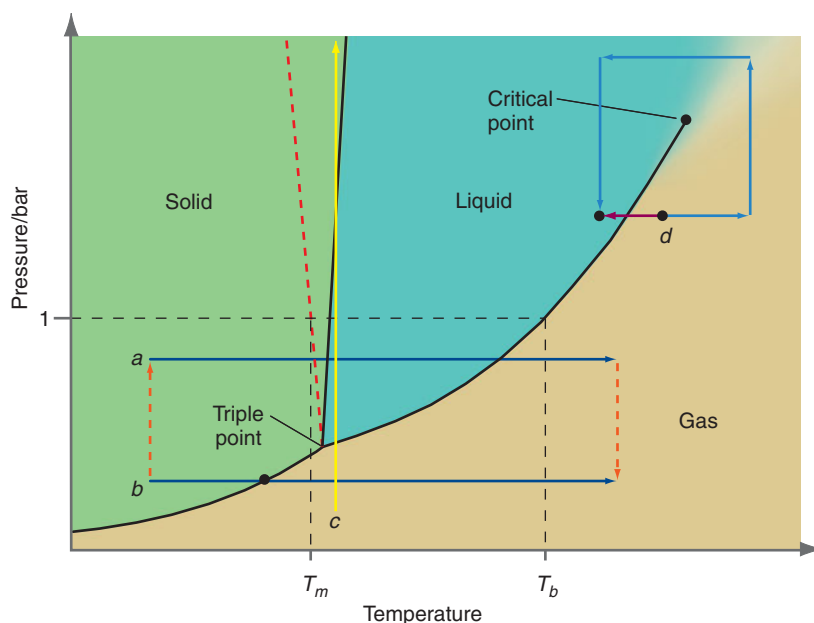
**temperature** is the temperature at which the vapor pressure of the substance is 1 bar. The **normal boiling temperature** is the temperature at which the vapor pressure of the substance is 1 atm. Values of the normal boiling and freezing temperatures for a number of substances are shown in Table 8.2. Because 1 bar is slightly less than 1 atm, the standard boiling temperature is slightly less than the normal boiling temperature. Along two-phase curves in which one of the coexisting phases is the gas, $P$ refers to the **vapor pressure** of the substance. In all regions, $P$ refers to the external pressure

| TABLE 8.2 | Melting and Boiling Temperatures and Enthalpies of Transition at 1 atm Pressure | | | | |
|---|---|---|---|---|---|
| Substance | Name | $T_m$ (K) | $\Delta H_{fusion}$ (kJ mol$^{-1}$) at $T_m$ | $T_b$ (K) | $\Delta H_{vaporization}$ (kJ mol$^{-1}$) at $T_b$ |
| Ar | Argon | 83.8 | 1.12 | 87.3 | 6.43 |
| $Cl_2$ | Chlorine | 171.6 | 6.41 | 239.18 | 20.41 |
| Fe | Iron | 1811 | 13.81 | 3023 | 349.5 |
| $H_2$ | Hydrogen | 13.81 | 0.12 | 20.4 | 0.90 |
| $H_2O$ | Water | 273.15 | 6.010 | 373.15 | 40.65 |
| He | Helium | 0.95 | 0.021 | 4.22 | 0.083 |
| $I_2$ | Iodine | 386.8 | 14.73 | 457.5 | 41.57 |
| $N_2$ | Nitrogen | 63.5 | 0.71 | 77.5 | 5.57 |
| Na | Sodium | 370.87 | 2.60 | 1156 | 98.0 |
| NO | Nitric oxide | 109.5 | 2.3 | 121.41 | 13.83 |
| $O_2$ | Oxygen | 54.36 | 0.44 | 90.7 | 6.82 |
| $SO_2$ | Sulfur dioxide | 197.6 | 7.40 | 263.1 | 24.94 |
| Si | Silicon | 1687 | 50.21 | 2628 | 359 |
| W | Tungsten | 3695 | 52.31 | 5933 | 422.6 |
| Xe | Xenon | 161.4 | 1.81 | 165.11 | 12.62 |
| $CCl_4$ | Carbon tetrachloride | 250 | 3.28 | 349.8 | 29.82 |
| $CH_4$ | Methane | 90.68 | 0.94 | 111.65 | 8.19 |
| $CH_3OH$ | Methanol | 175.47 | 3.18 | 337.7 | 35.21 |
| CO | Carbon monoxide | 68 | 0.83 | 81.6 | 6.04 |
| $C_2H_4$ | Ethene | 103.95 | 3.35 | 169.38 | 13.53 |
| $C_2H_6$ | Ethane | 90.3 | 2.86 | 184.5 | 14.69 |
| $C_2H_5OH$ | Ethanol | 159.0 | 5.02 | 351.44 | 38.56 |
| $C_3H_8$ | Propane | 85.46 | 3.53 | 231.08 | 19.04 |
| $C_5H_5N$ | Pyridine | 231.65 | 8.28 | 388.38 | 35.09 |
| $C_6H_6$ | Benzene | 278.68 | 9.95 | 353.24 | 30.72 |
| $C_6H_5OH$ | Phenol | 314.0 | 11.3 | 455.02 | 45.69 |
| $C_6H_5CH_3$ | Toluene | 178.16 | 6.85 | 383.78 | 33.18 |
| $C_{10}H_8$ | Naphthalene | 353.3 | 17.87 | 491.14 | 43.18 |

*Sources:* Data from Lide, D. R., ed. *Handbook of Chemistry and Physics*; 83rd ed. Boca Raton, FL: CRC Press, 2002; Lide, D. R., ed. *CRC Handbook of Thermophysical and Thermochemical Data*. Boca Raton, FL: CRC Press, 1994; and Blachnik, R., ed. *D'Ans Lax Taschenbuch für Chemiker und Physiker*, 4th ed. Berlin: Springer, 1998.
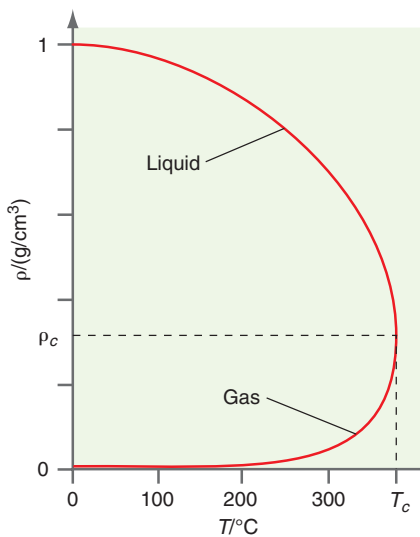
**FIGURE 8.5**

The density of the liquid and gaseous phases of water are shown as a function of temperature. At the critical point, the densities are equal.
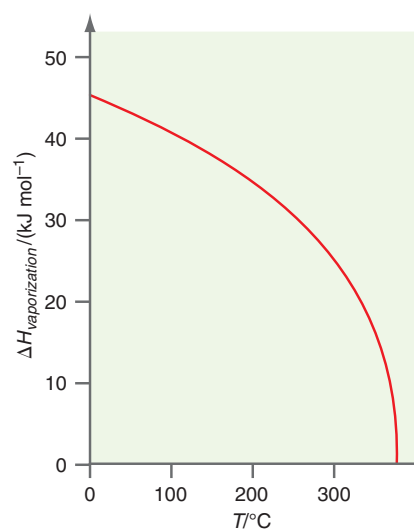


**FIGURE 8.6**

The enthalpy of vaporization for water is shown as a function of temperature. At the critical point, $\Delta H_{vaporization}$ approaches zero.

that would be exerted on the pure substance if it were confined in a piston and cylinder assembly.

The solid–liquid coexistence curve traces out the melting point as a function of pressure. The magnitude of the slope of this curve is large, as proven in Section 8.5. Therefore, $T_m$ is a weak function of the pressure. If the solid is more dense than the liquid, the slope of this curve is positive, and the melting temperature increases with pressure. This is the case for most substances. If the solid is less dense than the liquid, the slope is negative and the melting temperature decreases with pressure. Water is one of the few substances that exhibits this behavior. Imagine the fate of aquatic plants and animals in climate zones where the temperature routinely falls below 0°C in the winter if water behaved "normally." Lakes would begin to freeze over at the water–air interface, and the ice formed would fall to the bottom of the lake. This would lead to more ice formation until the whole lake was full of ice. In cool climate zones, it is likely that ice at the bottom of the lakes would remain throughout the summer. The aquatic life that we are familiar with would not survive under such a scenario.

The slope of the liquid–gas coexistence curve is much smaller than that of the solid–liquid coexistence curve, as proven in Section 8.5. Therefore, the boiling point is a much stronger function of the pressure than the freezing point. The boiling point always increases with pressure. This property is utilized in a pressure cooker, where increasing the pressure by 1 bar increases the boiling temperature of water by approximately 20°C. The rate of the chemical processes involved in cooking increase exponentially with $T$. Therefore, a pressure cooker operating at $P = 2$ bar can cook food in 20% to 40% of the time required for cooking at atmospheric pressure. By contrast, a mountain climber in the Himalayas would find that the boiling temperature of water is reduced by approximately 25°C relative to sea level. Cooking takes significantly longer under these conditions.

The solid–gas coexistence curve ends at the triple point. Whereas the liquid–solid coexistence curve extends indefinitely, the liquid–gas curve ends at the **critical point,** characterized by $T = T_c$ and $P = P_c$. For $T > T_c$ and $P > P_c$, the liquid and gas phases have the same density as shown in Figure 8.5, so it is not meaningful to refer to distinct phases. Because the liquid and gas phases are indistinguishable at the critical point, $\Delta H_{vaporization}$ approaches zero as the critical point is reached as shown in Figure 8.6.

Substances for which $T > T_c$ and $P > P_c$ are called **supercritical fluids.** As discussed in Section 8.9, supercritical fluids have unusual properties that make them useful in chemical technologies.

Each of the paths labeled $a$, $b$, $c$, and $d$ in Figure 8.4 corresponds to a process that demonstrates the usefulness of the $P-T$ phase diagram. In the following, each process is considered individually. Process $a$ follows a constant pressure (isobaric) path. An example of this path is heating one mole of ice. The system is initially in the solid single–phase region. Assume that heat is added to the system at a constant rate using current flow through a resistive heater. Because the pressure is constant, $q_P = \Delta H$. Furthermore, as discussed in Section 2.4, $\Delta H \approx C_P \Delta T$ in a single–phase region. Combining these equations, $\Delta T = q_P / C_P^{solid}$. Along path $a$, the temperature increases linearly with $q_P$ in the single–phase solid region as shown in Figure 8.7. At the melting temperature $T_m$, heat continues to be absorbed by the system as the solid is transformed into a liquid. This system now consists of two distinct phases, solid and liquid. As heat continues to flow into the system, the temperature will not increase until the system consists entirely of liquid. The heat taken up per mole of the system at the constant temperature $T_m$ is $\Delta H_{fusion}$.

The temperature again increases linearly with $q_P$ and $\Delta T = q_P / C_P^{liquid}$ until the boiling point is reached. At this temperature, the system consists of two phases, liquid and gas. The temperature remains constant until all the liquid has been converted into gas. The heat taken up per mol of the system at the constant temperature $T_b$ is $\Delta H_{vaporization}$. Finally, the system enters the single–phase gas region. Along path $b$, the pressure is less than the triple point pressure. Therefore, the liquid phase is not stable,
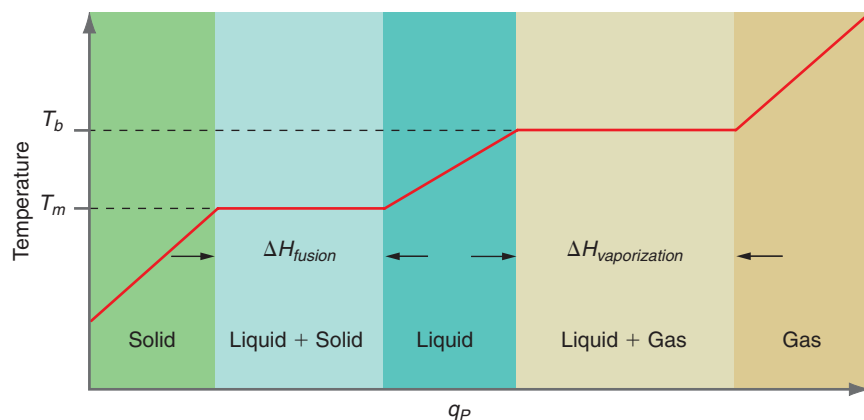
The trends in the temperature versus heat curve are shown schematically for the process corresponding to path a in Figure 8.4. The temperature rises linearly with $q_P$ in single-phase regions and remains constant along the two-phase curves as the relative amounts of the two phases in equilibrium change (not to scale).

and the solid is converted directly into the gaseous form. As Figure 8.4 shows, there is only one two-phase interval along this path. A diagram indicating the relationship between temperature and heat flow is shown in Figure 8.8.

Note that the initial and final states in process b can be reached by an alternative route described by the vertical dashed arrows in Figure 8.4. The pressure of the system in process b is increased to the value of the initial state of process a at constant temperature. The process follows that described for process a, after which the pressure is returned to the final pressure of process b. Invoking Hess's law, the enthalpy change for this pathway and for pathway b are equal. Now imagine that the constant pressures for processes a and b differ only by an infinitesimal amount, although that for a is higher than the triple point pressure, and that for b is lower than the triple point pressure. We can express this mathematically by setting the pressure for process a equal to $P_{tp} + dP$, and that for process b equal to $P_{tp} - dP$. We examine the limit $dP \rightarrow 0$. In this limit, $\Delta H \rightarrow 0$ for the two steps in the process indicated by the dashed arrows because $dP \rightarrow 0$ Therefore, $\Delta H$ for the transformation solid $\rightarrow$ liquid $\rightarrow$ gas in process a and for the transformation solid $\rightarrow$ gas in process b must be identical. We conclude that

$$\Delta H = \Delta H_{sublimation} = \Delta H_{fusion} + \Delta H_{vaporization} \qquad (8.4)$$

This statement is strictly true at the triple point. Far from the triple point, the temperature–dependent heat capacities of the different phases and the temperature dependence of the transition enthalpies must be taken into account.

Path c indicates an isothermal process in which the pressure is increased. The initial state of the system is the single–phase gas region. As the gas is compressed, it is liquefied as it crosses the gas–liquid coexistence curve. As the pressure is increased further, the sample freezes as it crosses the liquid–solid coexistence curve. Freezing is exothermic, and heat must flow to the surroundings as the liquid solidifies. If the process is reversed, heat must flow into the system to keep T constant as the solid melts.

If T is below the triple point temperature, the liquid exists at equilibrium only if the slope of the liquid–solid coexistence curve is negative, as is the case for water. Solid water below the triple point temperature can melt at constant T if the pressure is increased sufficiently to cross the liquid–solid coexistence curve. In an example of such a process, a thin wire to which a heavy weight is attached on each end is stretched over a block of ice. With time, it is observed that the wire lies within the ice block and eventually passes through the block. There is no visible evidence of the passage of the wire in the form of a narrow trench. What happens in this process? Because the wire is thin, the force on the wire results in a high pressure in the area of the ice block immediately below the wire. This high pressure causes local melting of the ice below the wire. Melting allows the wire to displace the liquid water, which flows to occupy the volume immediately above the wire. Because in this region water no longer experiences a high pressure, it freezes again and hides the passage of the wire.
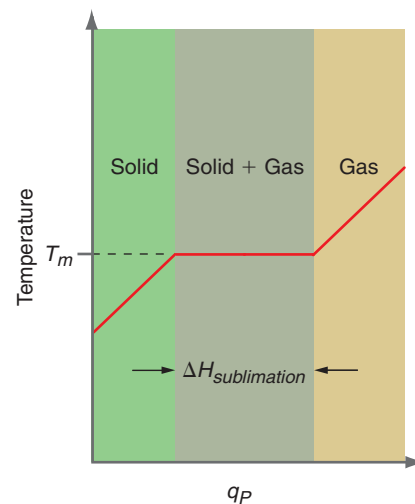
The temperature versus heat curve is shown for the process corresponding to path b in Figure 8.4. The temperature rises linearly with $q_P$ in single-phase regions and remains constant along the two-phase curves as the relative amounts of the two phases in equilibrium change (not to scale).

The consequences of having a critical point in the gas–liquid coexistence curve are illustrated in Figure 8.4. The gas–liquid coexistence curve is crossed in the constant pressure process starting at point $d$ and moving to lower temperatures. A clearly visible interface will be observed as the two-phase gas–liquid coexistence curve is crossed. However, the same overall process can be carried out in four steps indicated by the blue arrows. In this case, two–phase coexistence is not observed, because the gas–liquid coexistence curve ends at $P_{critical}$. The overall transition is the same along both paths, namely, gas is transformed into liquid. However, no interface will be observed if $P$ for the higher pressure constant pressure process is greater than $P_{critical}$.

## EXAMPLE PROBLEM 8.1

Draw a generic $P$–$T$ phase diagram like that shown in Figure 8.4. Draw pathways in the diagram that correspond to the processes described here:

**a.** You hang wash out to dry for a temperature below the triple point value. Initially, the water in the wet clothing is frozen. However, after a few hours in the sun, the clothing is warmer, dry, and soft.

**b.** A small amount of ethanol is contained in a thermos bottle. A test tube is inserted into the neck of the thermos bottle through a rubber stopper. A few minutes after filling the test tube with liquid nitrogen, the ethanol is no longer visible at the bottom of the bottle.

**c.** A transparent cylinder and piston assembly contains only a pure liquid in equilibrium with its vapor phase. An interface is clearly visible between the two phases. When you increase the temperature by a small amount, the interface disappears.

### Solution

The phase diagram with the paths is shown here:
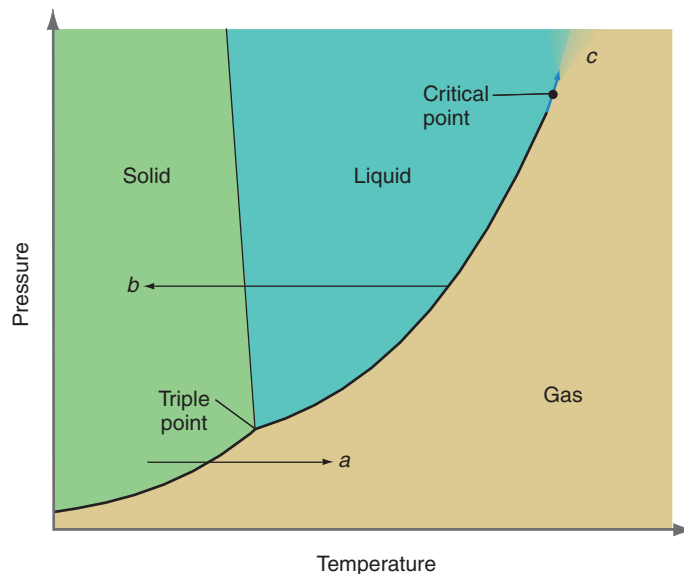


Paths $a$, $b$, and $c$ are not unique. Path $a$ must occur at a pressure lower than the triple point pressure. Process $b$ must occur at a pressure greater than the triple point pressure and originate on the liquid–gas coexistence line. Path $c$ will lie on the liquid–gas coexistence line up to the critical point, but it can deviate once $T > T_c$ and $P > P_c$.

A $P$–$T$ phase diagram for water at high $P$ values is shown in Figure 8.9. Because we plot $\ln P$ rather than $P$, the curvature of the solid–liquid and liquid–gas coexistence curves decreases with increasing temperature rather than increases as shown in Figure 8.4. Water has a number of solid phases that are stable in different pressure ranges because they have
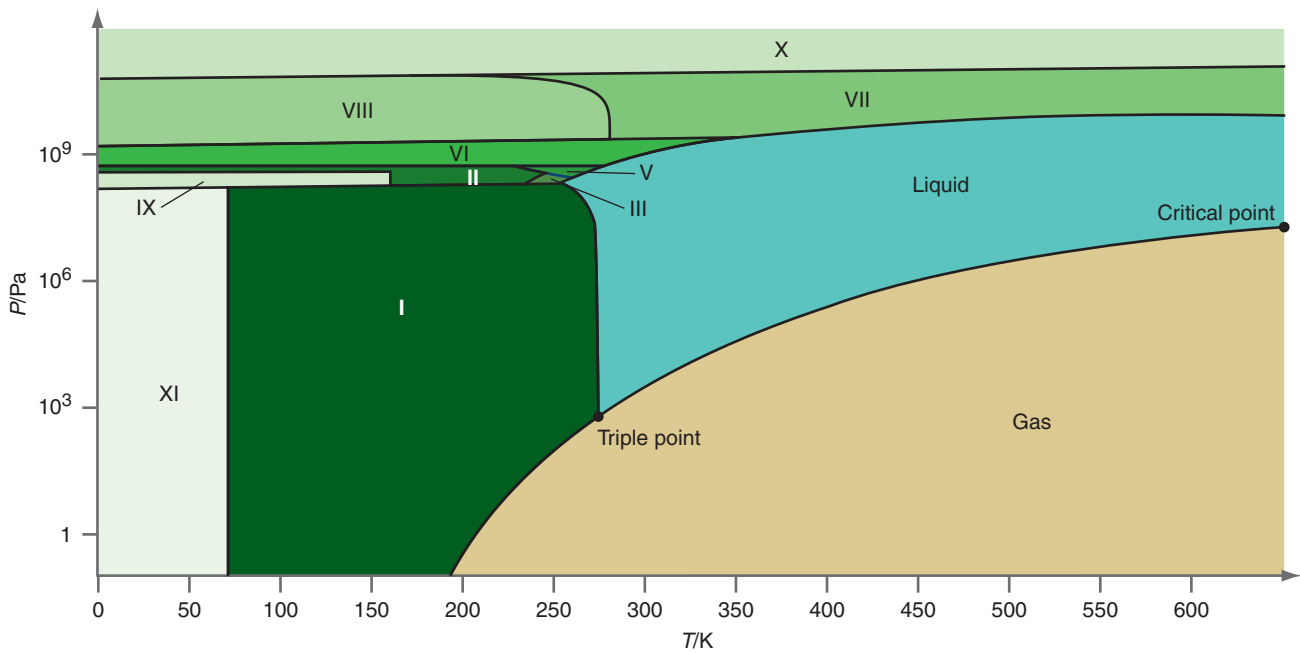
**FIGURE 8.9**

The $P$–$T$ phase diagram for $H_2O$ is shown for pressures up to $P = 10^{12}$ Pa and $T = T_c$.

*Source:* Adapted from "Water Structure and Science," http://www.lsbu.ac.uk/water/phase.html, courtesy of Martin Chaplin.

different densities. Eleven different crystalline forms of ice have been identified up to a pressure of $10^{12}$ Pa. Note for example in Figure 8.9 that ice VI does not melt until the temperature is raised to ~300 K for $P \approx$ 1000 MPa. For a comprehensive collection of material on the phase diagram of water, see http://www.lsbu.ac.uk/water/phase.html.

Hexagonal ice (ice I) is the normal form of ice and snow. The structure shown in Figure 8.10 may be thought of as consisting of a set of parallel sheets connected to one another through hydrogen bonding. Hexagonal ice has a fairly open structure with a density of 0.931 g cm$^{-3}$ near the triple point. Figure 8.10 also shows the crystal structure of ice VI. All water molecules in this structure are hydrogen bonded to four other molecules. Ice VII is much more closely packed than hexagonal ice and does not float on liquid water.

As shown in Figure 8.9, phase diagrams can be quite complex for simple substances because a number of solid phases can exist as $P$ and $T$ are varied. A further example is sulfur, which can also exist in several different solid phases. A portion of the phase diagram for sulfur is shown in Figure 8.11, and the solid phases are described by



**FIGURE 8.11**

The $P$–$T$ phase diagram for sulfur (not to scale).



**FIGURE 8.10**

Two different crystal structures are shown. Hexagonal ice (top) is the stable form of ice under atmospheric conditions. Ice VI (bottom) is only stable at elevated pressures as shown in the phase diagram of Figure 8.9. The dashed lines indicate hydrogen bonds.

**FIGURE 8.12**
The $P-T$ phase diagram for $CO_2$ (not to scale).
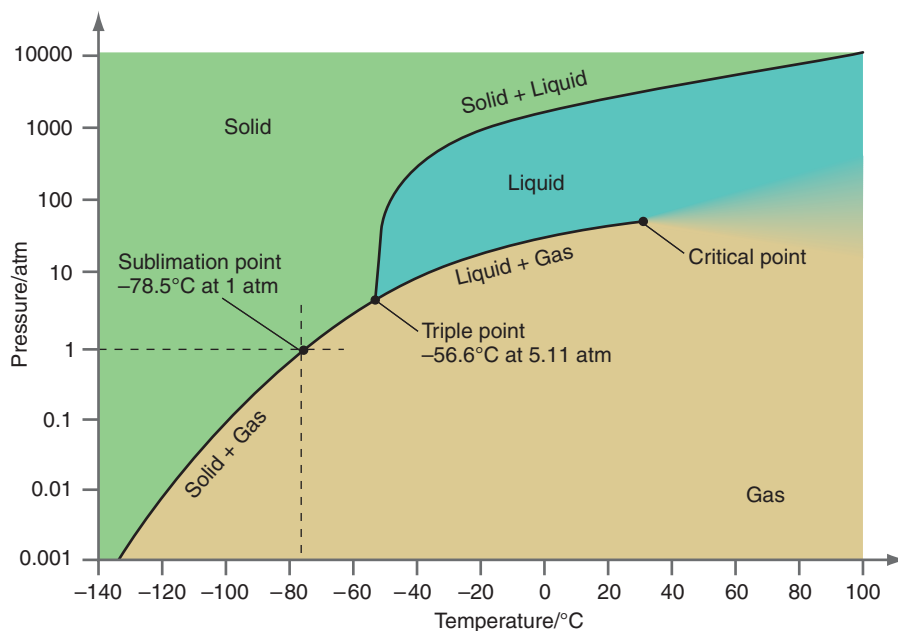


the symmetry of their unit cells. Note that several points correspond to three-phase equilibria. By contrast, the $CO_2$ phase diagram shown in Figure 8.12 is simpler. It is similar in structure to that of water, but the solid–liquid coexistence curve has a positive slope. Several of the end-of-chapter problems and questions refer to the phase diagrams in Figures 8.9, 8.11, and 8.12.

# 8.3 The Phase Rule

As we have seen in Section 8.1, the coexistence of two phases, $\alpha$ and $\beta$, of a substance requires that the chemical potentials are equal

$$\mu_\alpha(T, P) = \mu_\beta(T, P) \tag{8.5}$$

The state variables $T$ and $P$, which are independent in a single-phase region, are linked through Equation (8.5) for a two-phase coexistence region. Consequently, only one of $T$ and $P$ is needed to describe the system, and the other variable is determined by Equation (8.5). For this reason, the two-phase coexistence regions in Figures 8.4, 8.9, 8.11, and 8.12 are curves that have the functional form $P(T)$ or $T(P)$. If three phases, $\alpha$, $\beta$, and $\gamma$ coexist in equilibrium,

$$\mu_\alpha(T, P) = \mu_\beta(T, P) = \mu_\gamma(T, P) \tag{8.6}$$

which imposes another requirement on the variables $T$ and $P$. Now only one combination of $T$ and $P$ satisfies the requirement posed by Equation (8.6), and three-phase coexistence for a pure substance occurs only at a single point in the $P$, $T$ phase diagram called the triple point. These restrictions on the number of independent variables accessible to a system can be summarized as follows. Because $T$ and $P$ can be varied independently in a single-phase region, a system of a pure substance has two **degrees of freedom.** The system has one and zero degrees of freedom in a two-phase and three-phase coexistence region, respectively.

The American chemist J. W. Gibbs derived the **phase rule,** which links the number of degrees of freedom to the number of phases in a system at equilibrium. For a pure substance, the phase rule takes the form

$$F = 3 - p \tag{8.7}$$

where $F$ is the number of degrees of freedom, and $p$ is the number of phases. Gibbs proved that no more than three phases of a pure substance can be in equilibrium as $F$ cannot be a negative number. As we will see in Chapter 9, the number of degrees of freedom increases if a system contains several chemically independent species, for example in a system consisting of ethanol and water.

# 8.4 The Pressure–Volume and Pressure–Volume–Temperature Phase Diagrams

In Section 8.2, the regions of stability and equilibrium among the solid, liquid, and gas phases were described using a $P-T$ phase diagram. Any phase diagram that includes only two of the three state variables is limited because it does not contain information on the third variable. We first complement the information contained in the $P-T$ phase diagram with a **$P-V$ phase diagram,** and then combine these two representations into a $P-V-T$ phase diagram. Figure 8.13 shows a $P-V$ phase diagram for a substance for which $V_m^{liquid} > V_m^{solid}$.

Significant differences are seen in the way that two- and three-phase coexistence are represented in the two-phase diagrams. The two-phase coexistence curves of the $P-T$ phase diagram become two-phase regions in the $P-V$ phase diagram because the volume of a system in which two phases coexist varies with the relative amounts of the material in each phase. For pressures well below the critical point, the range in $V$ over which the gas and liquid coexist is large compared to the range in $V$ over which the solid and liquid coexist, because $V_m^{solid} < V_m^{liquid} \ll V_m^{gas}$. Therefore, the gas–liquid coexistence region is broader than the solid–liquid coexistence region. Note that the triple point in the $P-T$ phase diagram becomes a triple line in the $P-V$ diagram. Although $P$ and $T$ have unique values at the triple point, $V$ can range between a maximum value for which the system consists almost entirely of gas with traces of the liquid and solid phases and a minimum value for which the system consists almost entirely of solid with traces of the liquid and gas phases.

The usefulness of the $P-V$ diagram is illustrated by tracing several processes in Figure 8.13. In process $a$, a solid is converted to a gas by increasing the temperature in an isobaric process for which $P$ is greater than the triple point pressure. This same process was depicted in Figure 8.4. In the $P-V$ phase diagram, it is clear that this process involves large changes in volume in the two-phase coexistence region over which the temperature remains constant, which was not obvious in Figure 8.4. Process $b$ shows an isobaric transition from solid to gas for $P$ below the triple point pressure, for which the system has only one two-phase coexistence region. Process $c$ shows a constant volume transition from a system consisting of solid and vapor in equilibrium to a supercritical fluid. How does the temperature change along this path?

Process $b$ in Figure 8.13 is known as **freeze drying.** Assume that the food to be freeze dried is placed in a vessel at $-10°C$, and the system is allowed to equilibrate at this temperature. The partial pressure of $H_2O(g)$ in equilibrium with the ice crystals in the food under these conditions is 260 Pa. A vacuum pump is now started, and the gas phase is pumped away. The temperature reaches a steady-state value determined by heat conduction into the sample and heat loss through sublimation. The solid has an equilibrium vapor pressure determined by the steady-state temperature. As the pump removes water from the gas phase, ice spontaneously sublimes in order to keep the gas-phase water partial pressure at its equilibrium value. After the sublimation is complete, the food has been freeze dried. The advantage of freeze drying over boiling off water at 1 atm is that the food can be dehydrated at low temperatures at which the food is not cooked.

All the information on the values of $P$, $V$, and $T$ corresponding to single-phase regions, two-phase regions, and the triple point displayed in the $P-T$ and $P-V$ phase diagrams is best displayed in a three-dimensional **$P-V-T$ phase diagram.** Such a diagram is shown in
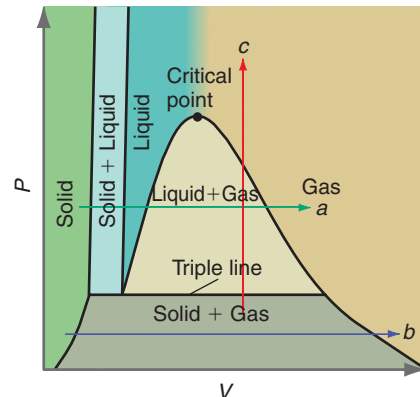


**FIGURE 8.13**

A $P-V$ phase diagram displays single- and two-phase coexistence regions, a critical point, and a triple line. The two-phase coexistence areas are colored.

**FIGURE 8.14**
A *P–V–T* diagram for an ideal gas.
Constant pressure, constant volume, and
constant temperature paths are shown as
gray, red, and blue curves, respectively.
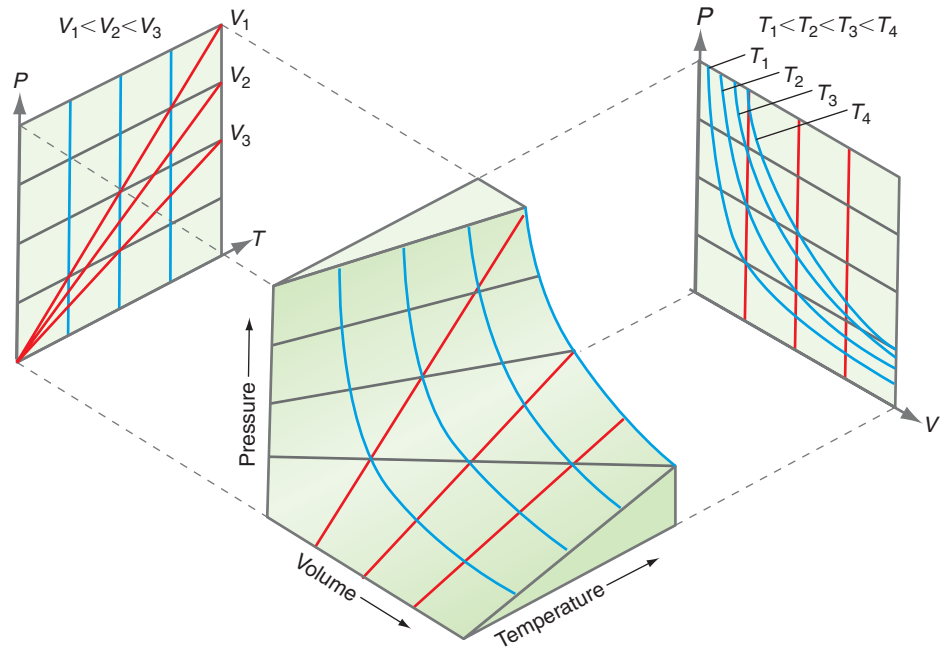


Figure 8.14 for an ideal gas, which does not exist in the form of condensed phases. It is
easy to obtain the *P–T* and *P–V* phase diagrams from the *P–V–T* phase diagram. The *P–T*
phase diagram is a projection of the three-dimensional surface on the *P–T* plane, and the
*P–V* phase diagram is a projection of the three-dimensional surface on the *P–V* plane.

Figure 8.15 shows a *P–V–T* diagram for a substance that expands upon melting. The
usefulness of the *P–V–T* phase diagram can be illustrated by revisiting the isobaric
conversion of a solid to a gas at a temperature above the triple point shown as process
*a* in Figure 8.4. This process is shown as the path $a \rightarrow b \rightarrow c \rightarrow d \rightarrow e \rightarrow f$ in
Figure 8.15. We can see now that the temperature increases along the segments
$a \rightarrow b, c \rightarrow d$, and $e \rightarrow f$, all of which lie within single-phase regions, and it remains
constant along the segments $b \rightarrow c$ and $d \rightarrow e$, which lie within two-phase regions.
Similarly, process *c* in Figure 8.4 is shown as the path $g \rightarrow h \rightarrow i \rightarrow k \rightarrow l \rightarrow m$
in Figure 8.15.
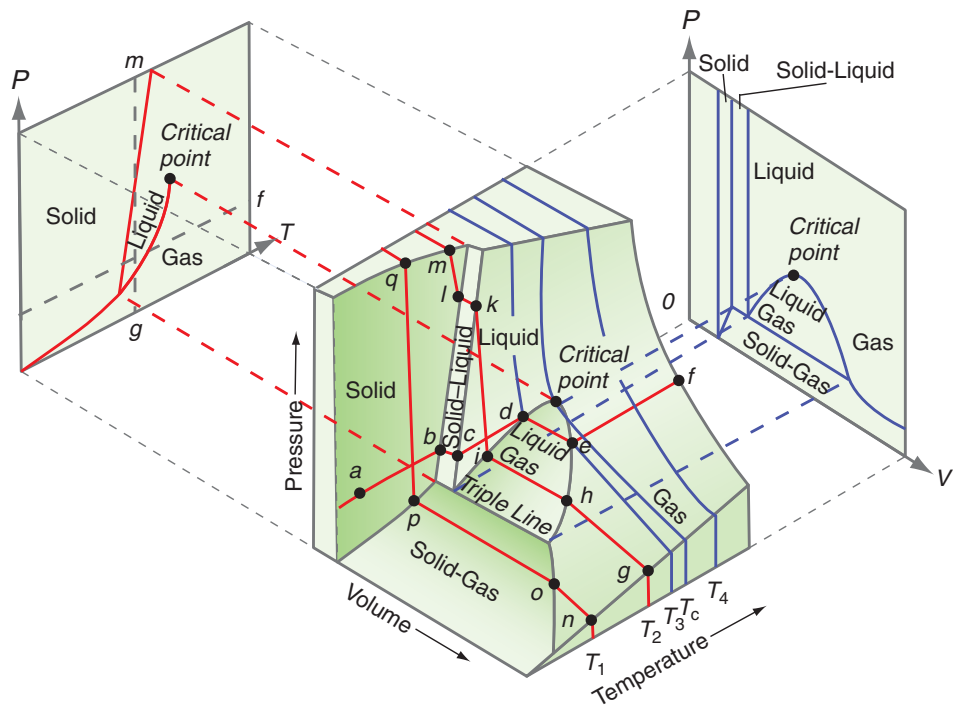


**FIGURE 8.15**
A *P–V–T* phase diagram is shown for a
substance that contracts on freezing.
The indicated processes are discussed in
the text.

# 8.5 Providing a Theoretical Basis for the *P–T* Phase Diagram

In this section, a theoretical basis is provided for the coexistence curves that separate different single-phase regions in the *P–T* phase diagram. Along the coexistence curves, two phases are in equilibrium. From Section 5.6, we know that if two phases, $\alpha$ and $\beta$, are in equilibrium at a pressure $P$ and temperature $T$, their chemical potentials must be equal:

$$\mu_\alpha(P, T) = \mu_\beta(P, T) \tag{8.8}$$

If the macroscopic variables are changed by a small amount, $P, T \rightarrow P + dP$, $T + dT$ such that the system pressure and temperature still lie on the coexistence curve, then

$$\mu_\alpha(P, T) + d\mu_\alpha = \mu_\beta(P, T) + d\mu_\beta \tag{8.9}$$

In order for the two phases to remain in equilibrium,

$$d\mu_\alpha = d\mu_\beta \tag{8.10}$$

Because $d\mu$ can be expressed in terms of $dT$ and $dP$,

$$d\mu_\alpha = -S_{m\alpha}\, dT + V_{m\alpha}\, dP \quad \text{and} \quad d\mu_\beta = -S_{m\beta}\, dT + V_{m\beta}\, dP \tag{8.11}$$

The expressions for $d\mu$ can be equated, giving

$$-S_{m\alpha}\, dT + V_{m\alpha}\, dP = -S_{m\beta}\, dT + V_{m\beta}\, dP \quad \text{or}$$

$$(S_{m\beta} - S_{m\alpha})\, dT = (V_{m\beta} - V_{m\alpha})\, dP \tag{8.12}$$

Assume that as $P, T \rightarrow P + dP, T + dT$ an incremental amount of phase $\alpha$ is transformed to phase $\beta$. In this case, $\Delta S_m = S_{m\beta} - S_{m\alpha}$ and $\Delta V_m = V_{m\beta} - V_{m\alpha}$. Rearranging Equation (8.12) gives the **Clapeyron equation:**

$$\frac{dP}{dT} = \frac{\Delta S_m}{\Delta V_m} \tag{8.13}$$

The Clapeyron equation allows us to calculate the slope of the coexistence curves in a *P–T* phase diagram if $\Delta S_m$ and $\Delta V_m$ for the transition are known. This information is necessary when constructing a phase diagram. We next use the Clapeyron equation to estimate the slope of the solid–liquid coexistence curve. At the melting temperature,

$$\Delta G_{fusion} = \Delta H_{fusion} - T\Delta S_{fusion} = 0 \tag{8.14}$$

Therefore, the $\Delta S_m$ values for the fusion transition can be calculated from the enthalpy of fusion and the fusion temperature. Values of the normal fusion and vaporization temperatures, as well as $\Delta H_m$ for fusion and vaporization, are shown in Table 8.2 for a number of different elements and compounds. Although there is a significant variation in these values, for our purposes it is sufficient to use the average value of $\Delta S_{fusion} = 22$ J mol$^{-1}$ K$^{-1}$ calculated from the data in Table 8.2 in order to estimate the slope of the solid–liquid coexistence curve.

For the fusion transition, $\Delta V$ is small because the densities of the solid and liquid states are quite similar. The average $\Delta V_{fusion}$ for Ag, AgCl, Ca, CaCl$_2$, K, KCl, Na, NaCl, and H$_2$O is $+4.0 \times 10^{-6}$ m$^3$ mol$^{-1}$. Of these substances, only H$_2$O has a negative value for $\Delta V_{fusion}$. We next use the average values of $\Delta S_{fusion}$ and $\Delta V_{fusion}$ to estimate the slope of the solid–liquid coexistence curve:

$$\left(\frac{dP}{dT}\right)_{fusion} = \frac{\Delta S_{fusion}}{\Delta V_{fusion}} \approx \frac{22\ \text{J mol}^{-1}\text{K}^{-1}}{\pm 4.0 \times 10^{-6}\,\text{m}^3\,\text{mol}^{-1}}$$

$$= \pm 5.5 \times 10^6\,\text{Pa K}^{-1} = \pm 55\ \text{bar K}^{-1} \tag{8.15}$$

Inverting this result, $(dT/dP)_{fusion} \approx \pm 0.018 \, \text{K bar}^{-1}$. An increase of $P$ by $\sim 50$ bar is required to change the melting temperature by one degree. This result explains the very steep solid–liquid coexistence curve shown in Figure 8.4.

The same analysis applies to the liquid–gas coexistence curve. Because $\Delta H_m^{vaporization}$ and $\Delta V_{vaporization} = V_m^{gas} - V_m^{liquid}$ are always positive, $(dP/dT)_{vaporization}$ is always positive. The average of $\Delta S_{vaporization}$ for the substances shown in Table 8.2 is $95 \, \text{J mol}^{-1} \, \text{K}^{-1}$. This value is in accord with **Trouton's rule,** which states that $\Delta S_{vaporization} \approx 90 \, \text{J mol}^{-1} \, \text{K}^{-1}$ for liquids. The rule fails for liquids in which there are strong interactions between molecules such as $-$OH or $-$NH$_2$ groups capable of forming hydrogen bonds. For these substances, $\Delta S_{vaporization} > 90 \, \text{J mol}^{-1} \, \text{K}^{-1}$.

The molar volume of an ideal gas is approximately $20. \, \text{L mol}^{-1}$ in the temperature range in which many liquids boil. Because $V_m^{gas} \gg V_m^{liquid}$, $\Delta V_{vaporization} \approx 20. \times 10^{-3} \, \text{m}^3 \text{mol}^{-1}$. The slope of the liquid–gas coexistence curve is given by

$$\left(\frac{dP}{dT}\right)_{vaporization} = \frac{\Delta S_{vaporization}}{\Delta V_{vaporization}} \approx \frac{95 \, \text{J mol}^{-1} \text{K}^{-1}}{2.0 \times 10^{-2} \, \text{m}^3 \text{mol}^{-1}} \approx 4.8 \times 10^3 \, \text{Pa K}^{-1}$$

$$= 4.8 \times 10^{-2} \, \text{bar K}^{-1} \tag{8.16}$$

This slope is a factor of $10^3$ smaller than the slope for the liquid–solid coexistence curve. Inverting this result, $(dT/dP)_{vaporization} \approx 21 \, \text{K bar}^{-1}$. This result shows that it takes only a modest increase in the pressure to increase the boiling point of a liquid by a significant amount. For this reason, a pressure cooker or automobile radiator does not need to be able to withstand high pressures. Note that the slope of the liquid–gas coexistence curve in Figure 8.4 is much less than that of the solid–liquid coexistence curve. The slope of both curves increases with $T$ because $\Delta S$ increases with increasing $T$ and $\Delta V$ decreases with increasing $P$.

The solid–gas coexistence curve can also be analyzed using the Clapeyron equation. Because entropy is a state function, the entropy change for the processes solid $(P, T) \rightarrow$ gas $(P, T)$ and solid $(P, T) \rightarrow$ liquid $(P, T) \rightarrow$ gas $(P, T)$ must be the same. Therefore, $\Delta S_{sublimation} = \Delta S_{fusion} + \Delta S_{vaporization} > \Delta S_{vaporization}$. However, because the molar volume of the gas is so much larger than that of the solid or liquid, $\Delta V_{sublimation} \approx \Delta V_{vaporization}$. We conclude that $(dP/dT)_{sublimation} > (dP/dT)_{vaporization}$. Therefore, the slope of the solid–gas coexistence curve will be greater than that of the liquid–gas coexistence curve. Because this comparison applies to a common value of the temperature, it is best made for temperatures just above and just below the triple point temperature. This difference in slope of these two coexistence curves is exaggerated in Figure 8.4.

## 8.6 Using the Clausius–Clapeyron Equation to Calculate Vapor Pressure as a Function of $T$

From watching a pot of water as it is heated on a stove, it is clear that the vapor pressure of a liquid increases rapidly with increasing temperature. The same conclusion holds for a solid below the triple point. To calculate the vapor pressure at different temperatures, the Clapeyron equation must be integrated. Consider the solid–liquid coexistence curve:

$$\int_{P_i}^{P_f} dP = \int_{T_i}^{T_f} \frac{\Delta S_{fusion}}{\Delta V_{fusion}} dT = \int_{T_i}^{T_f} \frac{\Delta H_{fusion}}{\Delta V_{fusion}} \frac{dT}{T} \approx \frac{\Delta H_{fusion}}{\Delta V_{fusion}} \int_{T_i}^{T_f} \frac{dT}{T} \tag{8.17}$$

where the integration is along the solid–liquid coexistence curve. In the last step, it has been assumed that $\Delta H_{fusion}$ and $\Delta V_{fusion}$ are independent of $T$ over the temperature range of interest. Assuming that $(T_f - T_i)/T_i$ is small, the previous equation can be simplified to give

$$P_f - P_i = \frac{\Delta H_{fusion}}{\Delta V_{fusion}} \ln \frac{T_f}{T_i} = \frac{\Delta H_{fusion}}{\Delta V_{fusion}} \ln \frac{T_i + \Delta T}{T_i} \approx \frac{\Delta H_{fusion}}{\Delta V_{fusion}} \frac{\Delta T}{T_i} \tag{8.18}$$

The last step uses the result $\ln(1 + x) \approx x$ for $x \ll 1$, obtained by expanding $\ln(1 + x)$ in a Taylor series about $x = 0$. We see that the vapor pressure of a solid varies linearly with $\Delta T$ in this limit. The value of the slope $dP/dT$ was discussed in the previous section.

For the liquid–gas coexistence curve, we have a different result because $\Delta V \approx V^{gas}$. Assuming that the ideal gas law holds, we obtain the **Clausius-Clapeyron equation,**

$$\frac{dP}{dT} = \frac{\Delta S_{vaporization}}{\Delta V_{vaporization}} \approx \frac{\Delta H_{vaporization}}{TV_m^{gas}} = \frac{P\Delta H_{vaporization}}{RT^2}$$

$$\frac{dP}{P} = \frac{\Delta H_{vaporization}}{R}\frac{dT}{T^2} \tag{8.19}$$

Assuming that $\Delta H_{vaporization}$ remains constant over the range of temperature of interest, the variation of the vapor pressure of the liquid with temperature is given by

$$\int_{P_i}^{P_f}\frac{dP}{P} = \frac{\Delta H_{vaporization}}{R} \times \int_{T_i}^{T_f}\frac{dT}{T^2}$$

$$\ln\frac{P_f}{P_i} = -\frac{\Delta H_{vaporization}}{R} \times \left(\frac{1}{T_f} - \frac{1}{T_i}\right) \tag{8.20}$$

We see that the vapor pressure of a liquid rises exponentially with temperature. The same procedure is followed for the solid–gas coexistence curve. The result is the same as Equation (8.20) with $\Delta H_{sublimation}$ substituted for $\Delta H_{vaporization}$. Equation (8.20) provides a way to determine the enthalpy of vaporization for a liquid by measuring its vapor pressure as a function of temperature, as shown in Example Problem 8.2. In this discussion, it has been assumed that $\Delta H_{vaporization}$ is independent of temperature. More accurate values of the vapor pressure as a function of temperature can be obtained by fitting experimental data. This leads to an expression for the vapor pressure as a function of temperature. These functions for selected liquids and solids are listed in Tables 8.3 and 8.4 (see Appendix A, Data Tables).

## EXAMPLE PROBLEM 8.2

The normal boiling temperature of benzene is 353.24 K, and the vapor pressure of liquid benzene is $1.19 \times 10^4$ Pa at 20.0°C. The enthalpy of fusion is 9.95 kJ mol$^{-1}$, and the vapor pressure of solid benzene is 137 Pa at −44.3°C. Calculate the following:

**a.** $\Delta H_{vaporization}$

**b.** $\Delta S_{vaporization}$

**c.** Triple point temperature and pressure

### Solution

**a.** We can calculate $\Delta H_{vaporization}$ using the Clausius-Clapeyron equation because we know the vapor pressure at two different temperatures:

$$\ln\frac{P_f}{P_i} = -\frac{\Delta H_{vaporization}}{R}\left(\frac{1}{T_f} - \frac{1}{T_i}\right)$$

$$\Delta H_{vaporization} = -\frac{R\ln\dfrac{P_f}{P_i}}{\left(\dfrac{1}{T_f} - \dfrac{1}{T_i}\right)} = -\frac{8.314\,\text{J mol}^{-1}\text{K}^{-1} \times \ln\dfrac{101,325\,\text{Pa}}{1.19 \times 10^4\,\text{Pa}}}{\left(\dfrac{1}{353.24\,\text{K}} - \dfrac{1}{273.15\,\text{K} + 20.0\,\text{K}}\right)}$$

$$= 30.7\,\text{kJ mol}^{-1}$$

**b.** $\Delta S_{vaporization} = \dfrac{\Delta H_{vaporization}}{T_b} = \dfrac{30.7 \times 10^3\,\text{J mol}^{-1}}{353.24\,\text{K}} = 86.9\,\text{J mol}^{-1}\text{K}^{-1}$

**c.** At the triple point, the vapor pressures of the solid and liquid are equal:

$$\ln \frac{P_{tp}^{liquid}}{P^\circ} = \ln \frac{P_i^{liquid}}{P^\circ} - \frac{\Delta H_{vaporization}}{R} \left( \frac{1}{T_{tp}} - \frac{1}{T_i^{liquid}} \right)$$

$$\ln \frac{P_{tp}^{solid}}{P^\circ} = \ln \frac{P_i^{solid}}{P^\circ} - \frac{\Delta H_{sublimation}}{R} \left( \frac{1}{T_{tp}} - \frac{1}{T_i^{solid}} \right)$$

$$\ln \frac{P_i^{liquid}}{P^\circ} - \ln \frac{P_i^{solid}}{P^\circ} - \frac{\Delta H_{sublimation}}{RT_i^{solid}} + \frac{\Delta H_{vaporization}}{RT_i^{liquid}}$$

$$= \frac{\Delta H_{vaporization} - \Delta H_{sublimation}}{RT_{tp}}$$

$$T_{tp} = \frac{\Delta H_{vaporization} - \Delta H_{sublimation}}{R \left( \ln \dfrac{P_i^{liquid}}{P^\circ} - \ln \dfrac{P_i^{solid}}{P^\circ} - \dfrac{\Delta H_{sublimation}}{RT_i^{solid}} + \dfrac{\Delta H_{vaporization}}{RT_i^{liquid}} \right)}$$

$$= \frac{-9.95 \times 10^3 \text{ J mol}^{-1}}{8.314 \text{ J K}^{-1}\text{mol}^{-1} \times \left( \begin{array}{c} \ln \dfrac{1.19 \times 10^4 \text{ Pa}}{10^5 \text{ Pa}} - \ln \dfrac{137 \text{ Pa}}{10^5 \text{ Pa}} - \dfrac{(30.7 \times 10^3 + 9.95 \times 10^3) \text{ J mol}^{-1}}{8.314 \text{ J K}^{-1}\text{mol}^{-1} \times 228.9 \text{ K}} \\ + \dfrac{30.7 \times 10^3 \text{mol}^{-1}}{8.314 \text{ J K}^{-1}\text{mol}^{-1} \times 293.15 \text{ K}} \end{array} \right)}$$

$$= 277 \text{ K}$$

We calculate the triple point pressure using the Clapeyron equation:

$$\ln \frac{P_f}{P_i} = -\frac{\Delta H_{vaporization}}{R} \left( \frac{1}{T_f} - \frac{1}{T_i} \right)$$

$$\ln \frac{P_{tp}}{101{,}325} = -\frac{30.7 \times 10^3 \text{ J mol}^{-1}}{8.314 \text{ J mol}^{-1}\text{K}^{-1}} \times \left( \frac{1}{278 \text{ K}} - \frac{1}{353.24 \text{ K}} \right)$$

$$\ln \frac{P_{tp}}{P^\circ} = 8.70483$$

$$P_{tp} = 6.03 \times 10^3 \text{ Pa}$$

## 8.7 The Vapor Pressure of a Pure Substance Depends on the Applied Pressure

Consider the piston and cylinder assembly containing water at 25°C shown in Figure 8.16. The equilibrium vapor pressure of water at this temperature is $P^* = 3.16 \times 10^3$ Pa, or 0.0316 bar. Therefore, if the weightless piston is loaded with a mass sufficient to generate a pressure of 1 bar, the system is in the single–phase liquid region of the phase diagram in Figure 8.4. This state of the system is shown in Figure 8.16a. The mass is reduced so that the pressure is exactly equal to the vapor pressure of water. The system now lies in the two-phase liquid–gas region of the phase diagram described by the liquid–gas coexistence curve. The piston can be pulled outward or pushed inward while maintaining this pressure. This action leads to a larger or smaller volume for the gas phase, but the pressure will remain constant at $3.16 \times 10^3$ Pa as long as the temperature of the system remains constant. This state of the system is shown in Figure 8.16b.

Keeping the temperature constant, enough argon gas is introduced into the cylinder such that the sum of the argon and $H_2O$ partial pressures is 1 bar. This state of the system is shown in Figure 8.16c. What is the vapor pressure of water in this case, and does it differ from that for the system shown in Figure 8.16b? The vapor pressure $P$ is used to denote the partial pressure of water in the gas phase, and **P** is used to denote the sum of the argon and water partial pressures.

To calculate the partial pressure of water in the argon-water mixture, the following equilibrium condition holds:

$$\mu_{liquid}(T, \mathbf{P}) = \mu_{gas}(T, P) \tag{8.21}$$

Differentiating this expression with respect to **P**, we obtain

$$\left(\frac{\partial \mu_{liquid}(T, \mathbf{P})}{\partial \mathbf{P}}\right)_T = \left(\frac{\partial \mu_{gas}(T, P)}{\partial P}\right)_T \left(\frac{\partial P}{\partial \mathbf{P}}\right)_T \tag{8.22}$$

Because $d\mu = -S_m\, dT + V_m\, dP$, $(d\mu/dP)_T = V_m$, and the previous equation becomes

$$V_m^{liquid} = V_m^{gas}\left(\frac{\partial P}{\partial \mathbf{P}}\right)_T \quad \text{or} \quad \left(\frac{\partial P}{\partial \mathbf{P}}\right)_T = \frac{V_m^{liquid}}{V_m^{gas}} \tag{8.23}$$

This equation shows that the vapor pressure $P$ increases if the total pressure **P** increases. However, the rate of increase is small because the ratio $V_m^{liquid}/V_m^{gas} \ll 1$. It is reasonable to replace $V_m^{gas}$ with the ideal gas value $RT/P$ in Equation (8.23). This leads to the equation

$$\frac{RT}{P}\, dP = V_m^{liquid}\, d\mathbf{P} \quad \text{or} \quad RT \int_{P^*}^{P} \frac{dP'}{P'} = V_m^{liquid} \int_{P^*}^{P} d\mathbf{P}' \tag{8.24}$$

Integrating Equation (8.24) gives

$$RT \ln\left(\frac{P}{P^*}\right) = V_m^{liquid}(\mathbf{P} - P^*) \tag{8.25}$$

For the specific case of water, $P^* = 0.0316$ bar, $\mathbf{P} = 1$ bar, and $V_m^{liquid} = 1.81 \times 10^{-5}\, m^3\, mol^{-1}$:

$$\ln\left(\frac{P}{P^*}\right) = \frac{V_m^{liquid}\left(\mathbf{P} - P^*\right)}{RT}$$

$$= \frac{1.81 \times 10^{-5}\, m^3\, mol^{-1} \times (1 - 0.0316) \times 10^5\, Pa}{8.314\, J\, mol^{-1}\, K^{-1} \times 298\, K} = 7.04 \times 10^{-4}$$

$$P = 1.0007\, P^* \approx 0.0316\, \text{bar}$$

For an external pressure of 1 bar, the effect is negligible. However, for $\mathbf{P} = 100.$ bar, $P = 0.0339$ bar, amounting to an increase in the vapor pressure of 7%.

# 8.8 Surface Tension

In discussing the liquid phase, the effect of the boundary surface on the properties of the liquid has been neglected. In the absence of a gravitational field, a liquid droplet will assume a spherical shape, because in this geometry the maximum number of molecules is surrounded by neighboring molecules. Because the interaction between molecules in a liquid is attractive, minimizing the surface-to-volume ratio minimizes the energy. How does the energy of the droplet depend on its surface area? Starting with the equilibrium spherical shape, assume that the droplet is distorted to create more

$P_{external} = 1.00$ bar

**(a)**

$P_{external} = 0.0316$ bar

**(b)**
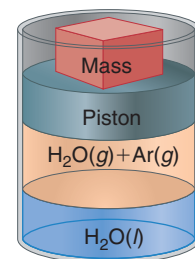
$P_{external} = 1.00$ bar

**(c)**

**FIGURE 8.16**
A piston and cylinder assembly at 298 K is shown with the contents being pure water **(a)** at a pressure greater than the vapor pressure, **(b)** at a pressure equal to the vapor pressure, and **(c)** at 1 bar for a mixture of argon and water.
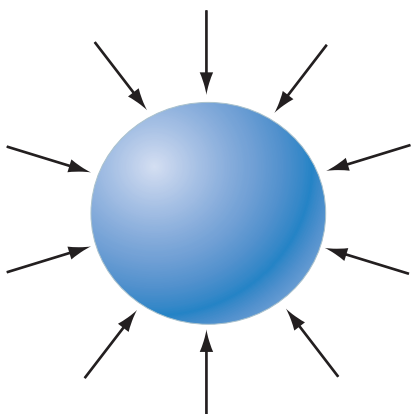
**FIGURE 8.17**
The forces acting on a spherical droplet that arise from surface tension.

area while keeping the volume constant. The work associated with the creation of additional surface area at constant $V$ and $T$ is

$$dA = \gamma d\sigma \tag{8.26}$$

where $A$ is the Helmholtz energy, $\gamma$ is the surface tension, and $\sigma$ is the unit element of area. The **surface tension** has the units of energy/area or $J\,m^{-2}$, which is equivalent to $N\,m^{-1}$ (Newtons per meter). Equation (8.26) predicts that a liquid, a bubble, or a liquid film suspended in a wire frame will tend to minimize its surface area because $dA < 0$ for a spontaneous process at constant $V$ and $T$.

Consider the spherical droplet depicted in Figure 8.17. There must be a force acting on the droplet in the radially inward direction for the liquid to assume a spherical shape. An expression for the force can be generated as follows. If the radius of the droplet is increased from $r$ to $r + dr$, the area increases by $d\sigma$.

$$\sigma = 4\pi r^2 \quad \text{so} \quad d\sigma = 8\pi r\, dr \tag{8.27}$$

From Equation (8.26), the work done in the expansion of the droplet is $8\pi\gamma r\, dr$. The force, which is normal to the surface of the droplet, is the work divided by the distance or

$$F = 8\pi\gamma r \tag{8.28}$$

The net effect of this force is to generate a pressure differential across the droplet surface. At equilibrium, there is a balance between the inward and outward acting forces. The inward acting force is the sum of the force exerted by the external pressure and the force arising from the surface tension, whereas the outward acting force arises solely from the pressure in the liquid:

$$4\pi r^2 P_{outer} + 8\pi\gamma r = 4\pi r^2 P_{inner} \quad \text{or}$$

$$P_{inner} = P_{outer} + \frac{2\gamma}{r} \tag{8.29}$$

Note that $P_{inner} - P_{outer} \to 0$ as $r \to \infty$. Therefore, the pressure differential exists only for a curved surface. From the geometry in Figure 8.17, it is apparent that the higher pressure is always on the concave side of the interface. Values for the surface tension for a number of liquids are listed in Table 8.5.

Equation (8.29) has interesting implications for the relative stabilities of bubbles with different curvatures $1/r$. Consider two air-filled bubbles of a liquid with the same surface tension $\gamma$, one with a large radius $R_1$, and one with a smaller radius $R_2$. Assume there is a uniform pressure outside both bubbles. From Equation (8.29) we obtain the difference between the pressures $P_1$ and $P_2$ within each bubble:

$$P_1 - P_2 = \frac{2\gamma}{R_1} - \frac{2\gamma}{R_2} = 2\gamma\left(\frac{1}{R_1} - \frac{1}{R_2}\right) \tag{8.30}$$

Now suppose the two bubbles come into contact as shown at the top of Figure 8.18. Because $R_1 > R_2$, from Equation (8.30) the pressure $P_2$ inside bubble 2 (with respect
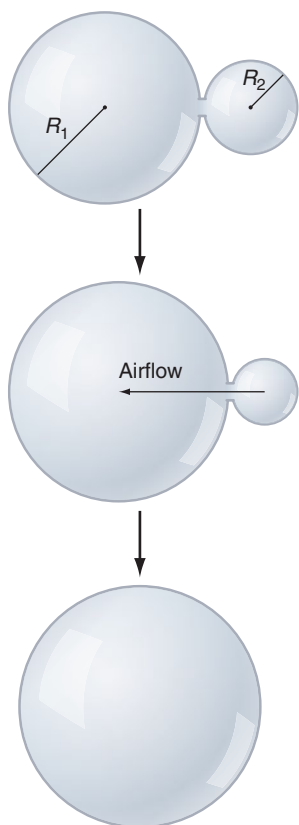


**FIGURE 8.18**
Two bubbles with unequal radii $R_1$ and $R_2$ make contact (top). Because the pressure within a bubble varies inversely with the bubble radius, air flows from the smaller into the larger bubble until a single large bubble remains (bottom).

**TABLE 8.5  Surface Tension of Selected Liquids at 298 K**

| Formula | Name | $\gamma$ (mN m⁻¹) | Formula | Name | (mN m⁻¹) |
|---|---|---|---|---|---|
| $Br_2$ | Bromine | 40.95 | $CS_2$ | Carbon disulfide | 31.58 |
| $H_2O$ | Water | 71.99 | $C_2H_5OH$ | Ethanol | 21.97 |
| Hg | Mercury | 485.5 | $C_6H_5N$ | Pyridine | 36.56 |
| $CCl_4$ | Carbon tetrachloride | 26.43 | $C_6H_6$ | Benzene | 28.22 |
| $CH_3OH$ | Methanol | 22.07 | $C_8H_{18}$ | Octane | 21.14 |

*Source:* Data from Lide, D. R., ed. *Handbook of Chemistry and Physics.* 83rd ed. Boca Raton, FL: CRC Press, 2002.

to some common exterior pressure) is greater than the pressure $P_1$ in bubble 1, so air will flow from bubble 2 to bubble 1 until the smaller bubble disappears entirely as shown at the bottom of Figure 8.18. In foams this process is called "coarsening" and in crystals it is called "Ostwald ripening."

A biologically relevant issue that follows from Equations (8.29) and (8.30) is the stability of lung tissue. Lung tissue is composed of small water-lined, air-filled chambers called alveoli. According to Equation (8.29), the pressure difference across the surface of a spherical air-filled cavity is proportional to the surface tension and inversely proportional to the radius of the cavity. Therefore, if two air-filled alveoli, approximated as spheres with radii $r$ and $R$ and for which $r < R$ are interconnected, the smaller alveolus will collapse and the larger alveolus will expand because the pressure within the smaller alveolus is greater than the pressure within the larger alveolus. In theory, due to the surface tension of water that lines the alveoli, these cavities will "coarsen" as smaller alveoli collapse, leaving an ever diminishing number of alveoli of increasing size. Coarsening of the alveoli according to Equations (8.29) will result eventually in the collapse of the lungs.

In the alveoli, a lipid surfactant called phosphatidylcholine lowers the surface tension of the water lining the alveoli, thus stabilizing the lungs. But in persons lacking sufficient surfactant in the lining of their lungs, such as prematurely born infants and heavy smokers, the surface tension of the water in the alveoli is not lowered, and as a consequence lung tissue is destabilized by coarsening.

Another consequence of the pressure differential across a curved surface is that the vapor pressure of a droplet depends on its radius. By substituting numbers in Equation (8.29) and using Equation (8.25) to calculate the vapor pressure, we find that the vapor pressure of a $10^{-7}$ m water droplet is increased by 1%, that of a $10^{-8}$ m droplet is increased by 11%, and that of a $10^{-9}$ m droplet is increased by 270%. [At such a small diameter, the application of Equation (8.29) is questionable because the size of an individual water molecule is comparable to the droplet diameter. Therefore, a microscopic theory is needed to describe the forces within the droplet.] This effect plays a role in the formation of liquid droplets in a condensing gas such as fog. Small droplets evaporate more rapidly than large droplets, and the vapor condenses on the larger droplets, allowing them to grow at the expense of small droplets.

**Capillary rise** and **capillary depression** are other consequences of the pressure differential across a curved surface. Assume that a capillary of radius $r$ is partially immersed in a liquid. When the liquid comes in contact with a solid surface, there is a natural tendency to minimize the energy of the system. If the surface tension of the liquid is lower than that of the solid, the liquid will wet the surface, as shown in Figure 8.19a. However, if the surface tension of the liquid is higher than that of the solid, the liquid will avoid the surface, as shown in Figure 8.19b. In either case, there is a pressure differential in the capillary across the gas–liquid interface because the interface is curved. If we assume that the liquid–gas interface is tangent to the interior wall of the capillary at the solid–liquid interface, the radius of curvature of the interface is equal to the capillary radius.

The difference in the pressure across the curved interface $2\gamma/r$ is balanced by the weight of the column in the gravitational field $\rho gh$. Therefore, $2\gamma/r = \rho gh$ and the capillary rise or depression is given by

$$h = \frac{2\gamma}{\rho g r} \tag{8.31}$$

In the preceding discussion, it was assumed that either (1) the liquid completely wets the interior surface of the capillary, in which case the liquid coats the capillary walls but does not fill the core, or (2) the liquid is completely nonwetting, in which case the liquid does not coat the capillary walls but fills the core. In a more realistic model, the interaction is intermediate between these two extremes. In this case, the liquid–surface is characterized by the **contact angle** $\theta$, as shown in Figure 8.20.
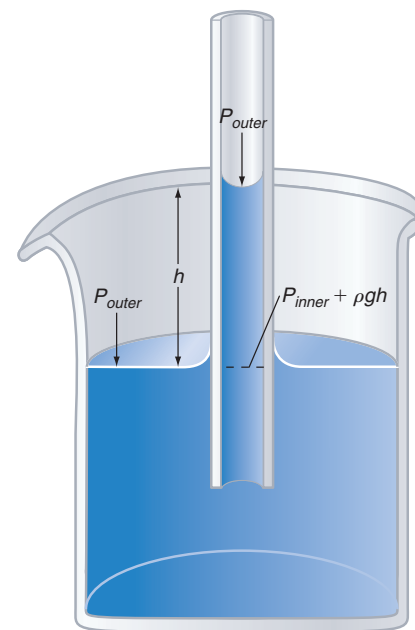
(a)
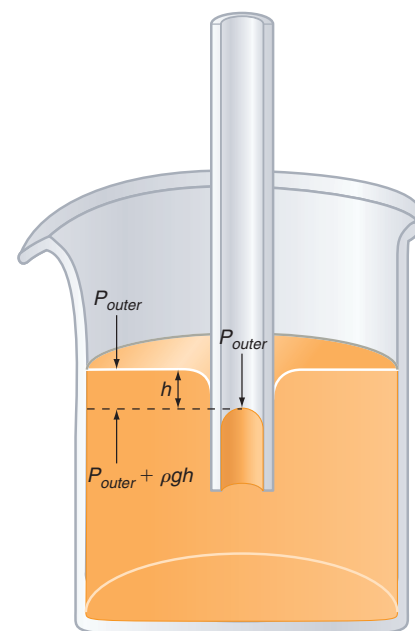
(b)

**FIGURE 8.19**
**(a)** If the liquid wets the interior wall of the capillary, a capillary rise is observed. The combination Pyrex–water exhibits this behavior. **(b)** If the liquid does not wet the capillary surface, a capillary depression is observed. The combination Pyrex–mercury exhibits this behavior.
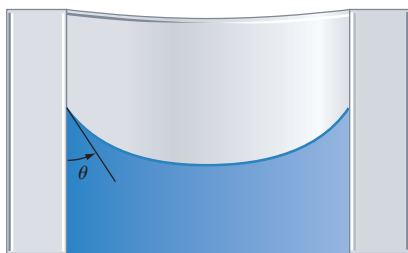
**FIGURE 8.20**
For cases intermediate between wetting and nonwetting, the contact angle $\theta$ lies in the range $0° < \theta < \; = 180°$.

Complete **wetting** corresponds to $\theta = 0°$, and complete **nonwetting** corresponds to $\theta = 180°$. For intermediate cases,

$$P_{inner} = P_{outer} + \frac{2\gamma \cos \theta}{r} \quad \text{and} \quad h = \frac{2\gamma \cos \theta}{\rho g r} \tag{8.32}$$

The measurement of the contact angle is one of the main experimental methods used to measure the difference in surface tension at the solid–liquid interface.

**EXAMPLE PROBLEM 8.3**

The six-legged water strider supports itself on the surface of a pond on four of its legs. Each of these legs causes a depression to be formed in the pond surface. Assume that each depression can be approximated as a hemisphere of radius $1.2 \times 10^{-4}$ m and that $\theta$ (as in Figure 8.20) is 0°. Calculate the force that one of the insect's legs exerts on the pond.

**Solution**

$$\Delta P = \frac{2\gamma \cos \theta}{r} = \frac{2 \times 71.99 \times 10^{-3} \text{N m}^{-1}}{1.2 \times 10^{-4} \text{m}} = 1.20 \times 10^3 \text{ Pa}$$

$$F = PA = P \times \pi r^2 = 1.20 \times 10^3 \text{Pa} \times \pi(1.2 \times 10^{-4}\text{m})^2 = 5.4 \times 10^{-5}\text{N}$$

**EXAMPLE PROBLEM 8.4**

Water is transported upward in trees through channels in the trunk called xylem. Although the diameter of the xylem channels varies from species to species, a typical value is $2.0 \times 10^{-5}$ m. Is capillary rise sufficient to transport water to the top of a redwood tree that is 100 m high? Assume complete wetting of the xylem channels.

**Solution**
From Equation (8.31),

$$h = \frac{2\gamma}{\rho g r \cos \theta} = \frac{2 \times 71.99 \times 10^{-3} \text{N m}^{-1}}{997 \text{ kg m}^{-3} \times 9.81 \text{ m s}^{-2} \times 2.0 \times 10^{-5}\text{m} \times 1} = 0.74 \text{ m}$$

No, capillary rise is not sufficient to account for water supply to the top of a redwood tree.

As Example Problem 8.4 shows, capillary rise is insufficient to account for water transport to the leaves in all but the smallest plants. The property of water that accounts for water supply to the top of a redwood is its high **tensile strength.** Imagine pulling on a piston and cylinder containing only liquid water to create a negative pressure. How hard can a person pull on the water without "breaking" the water column? The answer to this question depends on whether bubbles are nucleated in the liquid. This phenomenon is called cavitation. If cavitation occurs, the bubbles will grow rapidly as the piston is pulled outward. The bubble pressure is given by Equations (8.31), where $P_{external}$ is the vapor pressure of water. The height of the water column in this case is limited to about 9.7 m. However, bubble nucleation is a kinetic phenomenon initiated at certain sites at the wall surrounding the water, and under the conditions present in xylem tubes it is largely suppressed. In the absence of bubble nucleation, theoretical calculations predict that negative pressure in excess of 1000 atm can be generated. The pressure is negative because the water is under tension rather than compression. Experiments on water inclusions in very small cracks in natural rocks have verified these estimates. However, bubble nucleation occurs at much lower negative pressures in capillaries similar in diameter

to xylem tubes. Even in these capillaries, negative pressures of more than 50 atm have been observed.

How does the high tensile strength of water explain the transport of water to the top of a redwood? If one cuts into a tree near its base, the sap oozes rather than spurts out, showing that the pressure in the xylem tubes is $\sim 1$ atm at the base of a tree, whereas the pressure at the base of a tall water column would be much greater than 1 atm. Imagine the redwood in its infancy as a seedling. Capillary rise is sufficient to fill the xylem tubes to the top of the plant. As the tree grows higher, the water is pulled upward because of its high tensile strength. As the height of the tree increases, the pressure at the top becomes increasingly negative. As long as cavitation does not occur, the water column remains intact. As water evaporates from the leaves, it is resupplied from the roots through the pressure gradient in the xylem tubes that arises from the weight of the column. If the tree (and each xylem tube) grows to a height of $\sim 100$ m, and $P = 1$ atm at the base, the pressure at the top must be $\sim -9$ atm, from $\Delta P = \rho gh$. We again encounter a negative pressure because the water is under tension. If water did not have a sufficiently high tensile strength, gas bubbles would form in the xylem tubes. This would disrupt the flow of sap, and tall trees could not exist.

**SUPPLEMENTAL**

# 8.9 Chemistry in Supercritical Fluids

Chemical reactions can take place in the gas phase, in solution (homogeneous reactions) or on the surfaces of solids (heterogeneous reactions). Solvents with suitable properties can influence both the yield and the selectivity of reactions in solution. It has been found that the use of supercritical fluids as solvents increases the number of parameters that chemists have at their disposal to tune a reaction system to meet their needs.

Supercritical fluids (SCFs) near the critical point with reduced temperature and pressures in the range $T_r \sim 1.0-1.1$ and $P_r \sim 1-2$ have a density that is an appreciable fraction of the liquid–phase density. They are unique in that they exhibit favorable properties of liquids and gases. Because the density is high, the solubility of solid substances is quite high, but the diffusion of solutes in the fluid is higher than in the normal liquid. This is the case because the density of the SCF is lower than that in normal liquids. For similar reasons, the viscosity of SCFs is lower than that in normal liquids. As a result, mass transfer is faster, and the overall reaction rate can be increased. Because an SCF is more gas-like than a liquid, the solubility of gases can be much higher in the SCF. This property is of particular usefulness in enhancing the reactivity of reactions in which one of the reactants is a gas, such as oxidation or hydrogenation. For example, hydrogen generally has a low solubility in organic solvents but is quite soluble in organic SCFs.

Carbon dioxide and water exhibit the unusual properties of SCFs. Because the values for the critical pressure and temperature of $CO_2$ ($P_c = 73.74$ bar and $T_c = 304$ K) are easily attainable, it is possible to use chemically inert supercritical $CO_2$ to replace toxic organic solvents in the dry cleaning industry. Although supercritical $CO_2$ is a good solvent for nonpolar molecules, it must be mixed with other substances to achieve a required minimum solubility for polar substances. This can be done without increasing the toxicity of the process greatly. Supercritical $CO_2$ is also used in the decaffeination of coffee and tea.

The critical constants of $H_2O$ are considerably higher ($P_c = 220.64$ bar and $T_c = 647$ K), so the demands on the vessel used to contain the supercritical fluid are higher than for $CO_2$. However, as supercritical $H_2O$ is formed, many of the hydrogen bonds in the normal liquid are broken. As a result, the dielectric constant can be varied between the normal value for the liquid of 80 and 5. At the lower end of this range, supercritical water acts like a nonpolar solvent, and is effective in dissolving organic materials. Supercritical water has considerable potential for use at the high temperatures at which organic solvents begin to decompose. For example, it can be used to destroy toxic substances through oxidation in the decontamination of contaminated groundwater. One challenge in using supercritical water is that it is highly corrosive, placing demands on the materials used to construct a practical facility.
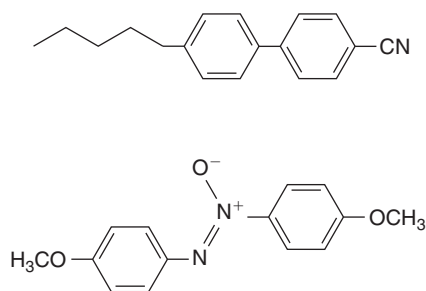
**FIGURE 8.21**

Liquid crystals are generally formed from polar organic molecules with a rod-like shape.

# 8.10 Liquid Crystal Displays

Liquid crystals are an exception to the general statement (superfluid He is another) that there are three equilibrium states of matter, namely solids, liquids, and gases. **Glasses** are liquids of such high viscosity that they cannot achieve equilibrium on the timescale of a human lifetime. Glasses are a commonly encountered nonequilibrium state of matter. An example is $SiO_2$ in the form of window glass. The properties of **liquid crystals** are intermediate between liquids and solids. Molecules that form liquid crystals typically contain rod-shaped structural elements. Several such molecules are shown in Figure 8.21.

How do liquid crystals differ from the other states of matter? The ordering in solid, liquid, and liquid crystal phases of such molecules is shown schematically in Figure 8.22. Whereas the crystalline solid phase is perfectly ordered and the liquid phase has no residual order, the liquid crystal phase retains some order. The axes of all molecules deviate only by a small amount from their value in the liquid crystal structure shown.

The **twisted nematic phase** shown in Figure 8.23 is of particular importance because liquid crystals with this structure are the basis of the multibillion-dollar liquid crystal display (LCD) industry and also the basis for sensor strips that change color with temperature. The twisted nematic phase consists of parallel planes in which the angle of the preferred orientation direction increases in a well-defined manner as the number of layers increases. If light is incident on such a crystal, it is partially reflected and partially transmitted from a number of layers. A maximum in the reflection occurs if the angle of incidence and the spacing between layers is such that constructive interference occurs in the light reflected from successive layers. Because this occurs only in a narrow range of wavelengths, the film appears colored, with the color determined by the wavelength. As the temperature increases or decreases, the layer spacing and, therefore, the color of the reflected light changes. For this reason, the color of the liquid crystal film changes with temperature.

The way in which an **LCD display** functions is illustrated in Figure 8.24. A twisted nematic liquid crystal film is sandwiched between two transparent conducting electrodes. The thickness of the film is such that the orientational direction rotates by a total of 90° from the bottom to the top of the film. Ambient light is incident on an upper polarizing filter that allows only one direction of polarization to pass. The rod-like molecules act as a waveguide and rotate the plane of polarization as the light passes through the liquid crystal film. Therefore, the light passes through the lower polarizer, which is rotated by 90° with respect to the first.

If an electric field is applied to the electrodes, the rotation of the orientational direction from plane to plane no longer occurs, because the polar molecules align along the
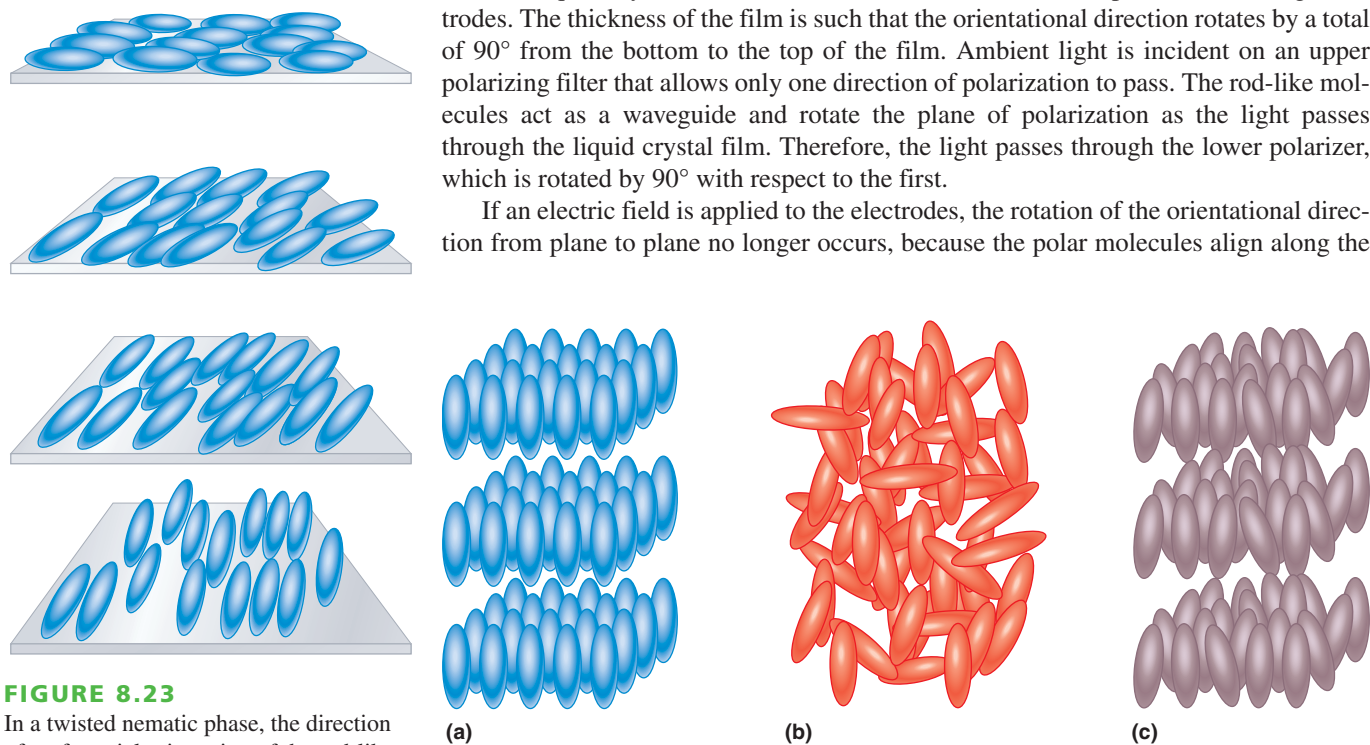


**FIGURE 8.23**

In a twisted nematic phase, the direction of preferential orientation of the rod-like molecules increases in a well-defined manner from one plane to the next.



(a)                              (b)                              (c)

**FIGURE 8.22**

Solid **(a)** liquid **(b)** and liquid crystal **(c)** phases are shown.
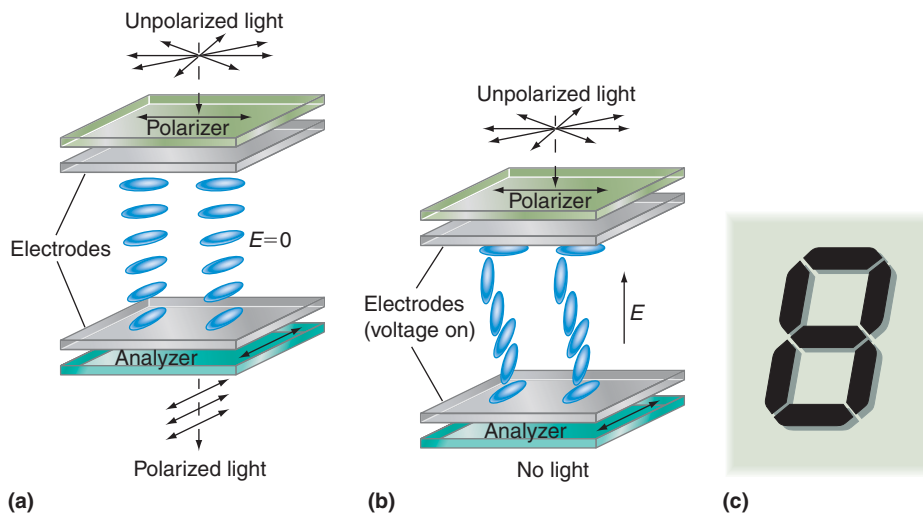
**FIGURE 8.24**
An LCD consists of a twisted nematic liquid film enclosed between parallel transparent conducting electrodes. Polarizers whose transmission direction is rotated 90° with respect to one another are mounted on the electrodes. **(a)** Light passing through the first polarizer is transmitted by the second polarizer because the plane of polarization of the light is rotated by the crystal. **(b)** The orientational ordering of the twisted nematic phase is destroyed by application of the electric field. No light is passed. **(c)** Arrangement of electrodes in an LCD alphanumeric display.

electric field. Therefore, the plane of polarization of the light transmitted by the upper polarizer is not rotated as it passes through the film. As a result, the light is not able to pass through the second polarizer. Now imagine the lower electrode to be in the form of a mirror. In the absence of the electric field (Figure 8.24a), the display will appear bright because the plane of polarization of the light reflected from the mirror is again rotated 90° as it passes back through the film. Consequently, it passes through the upper polarizer. By contrast, no light is reflected if the field is on (Figure 8.24b), and the display appears dark. Now imagine each of the electrodes to be patterned as shown in Figure 8.24c, and it will be clear why in a liquid crystal watch display dark numbers are observed on a light background.

# Vocabulary

| | | |
|---|---|---|
| boiling point elevation | freezing point elevation | $P–V–T$ phase diagram |
| capillary depression | glass | standard boiling temperature |
| capillary rise | LCD display | sublimation temperature |
| Clapeyron equation | liquid crystals | supercritical fluids |
| Clausius-Clapeyron equation | nonwetting | surface tension |
| coexistence curve | normal boiling temperature | tensile strength |
| contact angle | phase | triple point |
| critical point | phase diagram | Trouton's rule |
| degrees of freedom | phase rule | twisted nematic phase |
| freeze drying | $P–T$ phase diagram | vapor pressure |
| freezing point depression | $P–V$ phase diagram | wetting |

# Conceptual Problems

**Q8.1** Why is it reasonable to show the $\mu$ versus $T$ segments for the three phases as straight lines as is done in Figure 8.1? More realistic curves would have some curvature. Is the curvature upward or downward on a $\mu$ versus $T$ plot? Explain your answer.

**Q8.2** Why do the temperature versus heat curves in the solid, liquid, and gas regions of Figure 8.7 have different slopes?

**Q8.3** Figure 8.7 is not drawn to scale. What would be the relative lengths on the $q_P$ axis of the liquid + solid, liquid, and liquid + gas segments for water if the drawing were to scale and the system consisted of $H_2O$?

**Q8.4** Show the paths $n \rightarrow o \rightarrow p \rightarrow q$ and $a \rightarrow b \rightarrow c \rightarrow d \rightarrow e \rightarrow f$ of the $P–V–T$ phase diagram of Figure 8.15 in the $P–T$ phase diagram of Figure 8.4.

**Q8.5** At a given temperature, a liquid can coexist with its gas at a single value of the pressure. However, you can sense the presence of $H_2O(g)$ above the surface of a lake by the humidity, and it is still there if the barometric pressure rises or falls at constant temperature. How is this possible?

**Q8.6** Why are the triple point temperature and the normal freezing point very close in temperature for most substances?

**Q8.7** Give a molecular level explanation as to why the surface tension of $Hg(l)$ is not zero.

**Q8.8** A vessel containing a liquid is opened inside an evacuated chamber. Will you see a liquid–gas interface if the volume of the initially evacuated chamber is (a) less than the critical volume, (b) a factor of 10 larger than the critical volume, and (c) a factor of 1.05 larger than the critical volume?

**Q8.9** Why are there no points in the phase diagram for sulfur in Figure 8.11 that show rhombic and monoclinic solid phases in equilibrium with liquid and gaseous sulfur?

**Q8.10** What is the physical origin of the pressure difference across a curved liquid–gas interface?

**Q8.11** A triple point refers to a point in a phase diagram for which three phases are in equilibrium. Do all triple points correspond to a gas–liquid–solid equilibrium?

**Q8.12** Why does the liquid–gas coexistence curve in a $P-T$ phase diagram end at the critical point?

**Q8.13** How can you get a $P-T$ phase diagram from a $P-V-T$ phase diagram?

**Q8.14** Why does the triple point in a $P-T$ diagram become a triple line in a $P-V$ diagram?

**Q8.15** Why does water have several different solid phases but only one liquid and one gaseous phase?

**Q8.16** As the pressure is increased at $-45°C$, ice I is converted to ice II. Which of these phases has the lower density?

**Q8.17** Why is $\Delta H_{sublimation} = \Delta H_{fusion} + \Delta H_{vaporization}$?

**Q8.18** What can you say about the density of liquid and gaseous water as the pressure approaches the critical value from lower values? Assume that the temperature is constant at the critical value.

**Q8.19** What can you say about $\Delta H_{vaporization}$ of a liquid as the temperature approaches the critical temperature?

**Q8.20** Is the following statement correct? *Because dry ice sublimes at 298 K, carbon dioxide has no liquid phase.* Explain your answer.

**Q8.21** Redraw Figure 8.13 indicating the four-step process $d$ (blue arrows) in Figure 8.4.

# Numerical Problems

Problem numbers in **red** indicate that the solution to the problem is given in the *Student's Solutions Manual.*

**P8.1** Use the vapor pressures of tetrachloromethane given in the following table to calculate the enthalpy of vaporization using a graphical method or a least squares fitting routine.

| T (K) | P (Pa) | T (K) | P (Pa) |
|---|---|---|---|
| 280. | 6440. | 320. | 37130. |
| 290. | 10540. | 330. | 53250. |
| 300. | 16580. | 340. | 74520. |
| 310. | 25190. | | |

**P8.2** The vapor pressure of a liquid can be written in the empirical form known as the Antoine equation, where $A(1)$, $A(2)$, and $A(3)$ are constants determined from measurements:

$$\ln \frac{P(T)}{Pa} = A(1) - \frac{A(2)}{\frac{T}{K} + A(3)}$$

Starting with this equation, derive an equation giving $\Delta H_{vaporization}$ as a function of temperature.

**P8.3** In Section 8.8, it is stated that the maximum height of a water column in which cavitation does not occur is 9.7 m. Show that this is the case at 298 K.

**P8.4** Use the vapor pressures for tetrachloromethane given in the following table to estimate the temperature and pressure of the triple point and also the enthalpies of fusion, vaporization, and sublimation.

| Phase | T (K) | P (Pa) |
|---|---|---|
| Solid | 230. | 225.7 |
| Solid | 250. | 905 |
| Liquid | 280. | 6440. |
| Liquid | 340. | 62501 |

**P8.5** Within what range can you restrict the values of $P$ and $T$ if the following information is known about $CO_2$? Use Figure 8.12 to answer this question.

**a.** As the temperature is increased, the solid is first converted to the liquid and subsequently to the gaseous state.

**b.** An interface delineating liquid and gaseous phases is observed throughout the pressure range between 6 and 65 atm.

**c.** Solid, liquid, and gas phases coexist at equilibrium.

**d.** Only a liquid phase is observed in the pressure range from 10. to 50. atm.

**e.** An increase in temperature from $-80.°$ to $20.°C$ converts a solid to a gas with no intermediate liquid phase.

**P8.6**   A $P-T$ phase diagram for potassium is shown next.
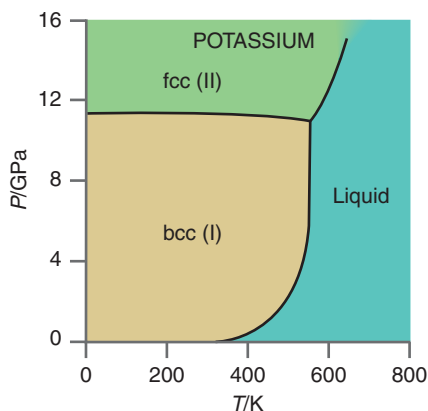


*Source: Phase Diagrams of the Elements* by David A. Young. © 1991 Regents of the University of California. Published by the University of California Press.

**a.** Which phase has the higher density, the fcc or the bcc phase? Explain your answer.

**b.** Indicate the range of $P$ and $T$ in the phase diagram for which fcc and liquid potassium are in equilibrium. Does fcc potassium float on or sink in liquid potassium? Explain your answer.

**c.** Redraw this diagram for a different pressure range and indicate where you expect to find the vapor phase. Explain how you chose the slope of your liquid–vapor coexistence line.

**P8.7**   A cell is roughly spherical with a radius of $20.0 \times 10^{-6}$ m. Calculate the work required to expand the cell surface against the surface tension of the surroundings if the radius increases by a factor of three. Assume the cell is surrounded by pure water and that $T = 298.15$ K.

**P8.8**   It has been suggested that the surface melting of ice plays a role in enabling speed skaters to achieve peak performance. Carry out the following calculation to test this hypothesis. At 1 atm pressure, ice melts at 273.15 K, $\Delta H_{fusion} = 6010.$ J mol$^{-1}$, the density of ice is 920. kg m$^{-3}$, and the density of liquid water is 997. kg m$^{-3}$.

**a.** What pressure is required to lower the melting temperature by 4.0°C?

**b.** Assume that the width of the skate in contact with the ice has been reduced by sharpening to $19 \times 10^{-3}$ cm, and that the length of the contact area is 18 cm. If a skater of mass 78 kg is balanced on one skate, what pressure is exerted at the interface of the skate and the ice?

**c.** What is the melting point of ice under this pressure?

**d.** If the temperature of the ice is $-4.0$°C, do you expect melting of the ice at the ice-skate interface to occur?

**P8.9**   Answer the following questions using the $P-T$ phase diagram for carbon shown next.
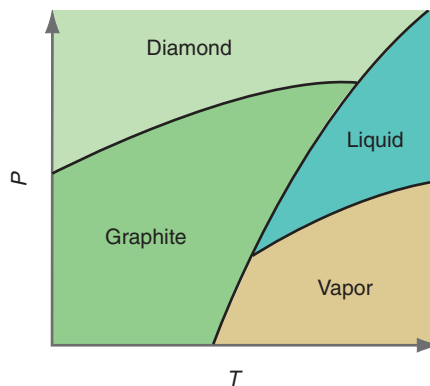


**a.** Which substance is more dense, graphite or diamond? Explain your answer.

**b.** Which phase is more dense, graphite or liquid carbon? Explain your answer.

**c.** Why does the phase diagram have two triple points? Explain your answer.

**P8.10**   You have a compound dissolved in chloroform and need to remove the solvent by distillation. Because the compound is heat sensitive, you hesitate to raise the temperature above 5.00°C and decide on vacuum distillation. What is the maximum pressure at which the distillation takes place?

**P8.11**   Use the vapor pressures for hexane given in the following table to estimate the temperature and pressure of the triple point and also the enthalpies of fusion, vaporization, and sublimation.

| Phase | $T$ (K) | $P$ (Pa) |
|---|---|---|
| Solid | 168 | 0.1296 |
| Solid | 178 | 1.111 |
| Liquid | 290. | $1.400 \times 10^4$ |
| Liquid | 320. | $4.822 \times 10^4$ |

**P8.12**   Are the following two $P-T$ phase diagrams likely to be observed for a pure substance? If not, explain all features of the diagram that will not be observed.
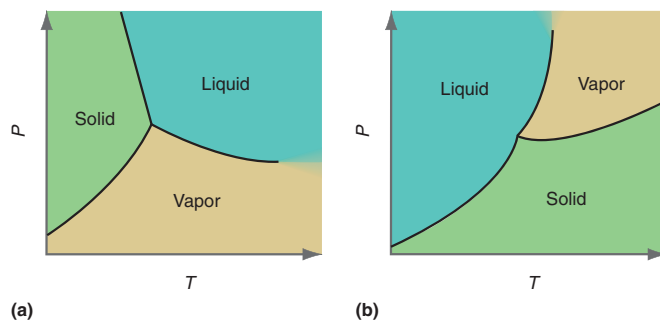


**P8.13**   Autoclaves that are used to sterilize surgical tools require a temperature of 120.°C to kill some bacteria. If water is used for this purpose, at what pressure must the autoclave operate?

**P8.14** You have collected a tissue specimen that you would like to preserve by freeze drying. To ensure the integrity of the specimen, the temperature should not exceed –5.00 °C. The vapor pressure of ice at 273.16 K is 624 Pa. What is the maximum pressure at which the freeze drying can be carried out?

**P8.15** The phase diagram of $NH_3$ can be characterized by the following information. The normal melting and boiling temperatures are 195.2 and 239.82 K, respectively, and the triple point pressure and temperature are 6077 Pa and 195.41 K, respectively. The critical point parameters are $112.8 \times 10^5$ Pa and 405.5 K. Make a sketch of the $P-T$ phase diagram (not necessarily to scale) for $NH_3$. Place a point in the phase diagram for the following conditions. State which and how many phases are present.

a. 195.41 K, 9506 Pa

b. 195.41 K, 6077 Pa

c. 245.45 K, 101,325 Pa

d. 415 K, $105 \times 10^5$ Pa

e. 185.5 K, 6077 Pa

**P8.16** Use the vapor pressures of ice given here to calculate the enthalpy of sublimation using a graphical method or a least squares fitting routine.

| T (K) | P (Torr) |
|-------|----------|
| 200.  | 0.1676   |
| 210.  | 0.7233   |
| 220.  | 2.732    |
| 230.  | 9.195    |
| 240.  | 27.97    |
| 250.  | 77.82    |
| 260.  | 200.2    |

**P8.17** Calculate the vapor pressure for a mist of spherical water droplets of radius (a) $1.95 \times 10^{-8}$ m and (b) $2.25 \times 10^{-6}$ m surrounded by water vapor at 298 K. The vapor pressure of water at this temperature is 25.2 Torr.

**P8.18** The vapor pressure of ethanol($l$) is given by

$$\ln\left(\frac{P}{Pa}\right) = 23.58 - \frac{3.6745 \times 10^3}{\frac{T}{K} - 46.702}$$

a. Calculate the standard boiling temperature.

b. Calculate $\Delta H_{vaporization}$ at 298 K and at the standard boiling temperature.

**P8.19** Use the following vapor pressures of propane given here to calculate the enthalpy of vaporization using a graphical method or a least squares fitting routine.

**P8.20** The vapor pressure of liquid benzene is 20170 Pa at 298.15 K, and $\Delta H_{vaporization} = 30.72$ kJ mol$^{-1}$ at 1 atm

| T (K) | P (Pa)                |
|-------|-----------------------|
| 100.  | 0.01114               |
| 120.  | 2.317                 |
| 140.  | 73.91                 |
| 160.  | 838.0                 |
| 180.  | 5054                  |
| 200.  | $2.016 \times 10^4$   |
| 220.  | $6.046 \times 10^4$   |

pressure. Calculate the normal and standard boiling points. Does your result for the normal boiling point agree with that in Table 8.3? If not, suggest a possible cause.

**P8.21** Benzene ($l$) has a vapor pressure of 0.1269 bar at 298.15 K and an enthalpy of vaporization of 30.72 kJ mol$^{-1}$. The $C_{P,m}$ of the vapor and liquid phases at that temperature are 82.4 and 136.0 J K$^{-1}$ mol$^{-1}$, respectively. Calculate the vapor pressure of $C_6H_6(l)$ at 340.0 K assuming

a. that the enthalpy of vaporization does not change with temperature.

b. that the enthalpy of vaporization at temperature $T$ can be calculated from the equation $\Delta H_{vaporization}(T) = \Delta H_{vaporization}(T_0) + \Delta C_P(T - T_0)$ assuming that $\Delta C_P$ does not change with temperature.

**P8.22** Use the values for $\Delta G_f^\circ$ ($CCl_4$, $l$) and $\Delta G_f^\circ$ ($CCl_4$, $g$) from Appendix A to calculate the vapor pressure of $CCl_4$ at 298.15 K.

**P8.23** Calculate the vapor pressure of water droplets of radius $1.00 \times 10^{-8}$ m at 360. K in equilibrium with water vapor. Use the tabulated value of the density and the surface tension at 298 K from Appendix A for this problem. (*Hint*: You need to calculate the vapor pressure of water at this temperature.)

**P8.24** The vapor pressure of an unknown solid is given by $\ln(P/Torr) = 22.413 - 2211(K/T)$, and the vapor pressure of the liquid phase of the same substance is approximately given by $\ln(P/Torr) = 18.352 - 1736(K/T)$.

a. Calculate $\Delta H_{vaporization}$ and $\Delta H_{sublimation}$.

b. Calculate $\Delta H_{fusion}$.

c. Calculate the triple point temperature and pressure.

**P8.25** For water, $\Delta H_{vaporization}$ is 40.656 kJ mol$^{-1}$, and the normal boiling point is 373.12 K. Calculate the boiling point for water on the top of Mt. Everest (elevation 8848 m), where the barometric pressure is 253 Torr.

**P8.26** Calculate the difference in pressure across the liquid–air interface for a (a) mercury and (b) methanol droplet of radius 125 nm.

**P8.27** Calculate the vapor pressure of $CH_3OH(l)$ at 298.15 K if He is added to the gas phase at a partial pressure

of 200. bar using the data tables. By what factor does the vapor pressure change?

**P8.28**    Use the vapor pressures of $SO_2(l)$ given in the following table to calculate the enthalpy of vaporization using a graphical method or a least squares fitting routine.

| $T$ (K) | $P$ (Pa) | $T$ (K) | $P$ (Pa) |
|---------|----------|---------|----------|
| 190.    | 824.1    | 240.    | $3.211 \times 10^4$ |
| 200.    | 2050     | 250.    | $5.440 \times 10^4$ |
| 210.    | 4591     | 260.    | $8.793 \times 10^4$ |
| 220.    | 9421     |         |          |
| 230.    | $1.795 \times 10^4$ |   |          |

**P8.29**    Prove that a substance for which the solid–liquid coexistence curve has a negative slope contracts upon melting.

**P8.30**    Are the following two $P-T$ phase diagrams likely to be observed for a pure substance? If not, explain all features of the diagram that will not be observed.



(a)

(b)
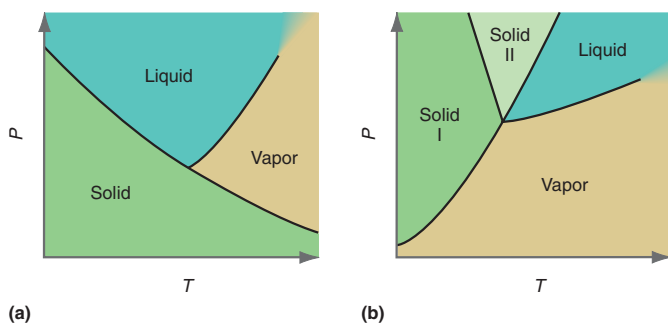
**P8.31**    The vapor pressure of methanol($l$) is $16.94 \times 10^3$ Pa at 298.15 K. Use this value to calculate $\Delta G_f^\circ$ ($CH_3OH$, $g$) $- \Delta G_f^\circ$ ($CH_3OH$, $l$). Compare your result with those in Table 4.1.

**P8.32**    Within what range can you restrict the values of $P$ and/or $T$ if the following information is known about sulfur? Use Figure 8.11 to answer this problem.

**a.** Only the rhombic solid phase is observed for $P = 1$ atm.

**b.** When the pressure on the vapor is increased, the monoclinic solid phase is formed.

**c.** Solid, liquid, and gas phases coexist at equilibrium.

**d.** As the temperature is increased, the rhombic solid phase is converted to the monoclinic solid phase.

**e.** As the temperature is increased at 1 atm, the rhombic solid phase is converted to the liquid directly.

**P8.33**    The normal melting point of $H_2O$ is 273.15 K, and $\Delta H_{fusion} = 6010.$ J $mol^{-1}$. Calculate the change in the normal freezing point at 100. and 500. bar compared to that at 1 bar assuming that the densities of the liquid and solid phases remains constant at 997 and 917 kg $m^{-3}$, respectively. Explain why your answer is positive (or negative).

**P8.34**    Carbon tetrachloride melts at 250. K. The vapor pressure of the liquid is 10,539 Pa at 290. K and 74,518 Pa at 340. K. The vapor pressure of the solid is 270. Pa at 232 K and 1092 Pa at 250. K.

**a.** Calculate $\Delta H_{vaporization}$ and $\Delta H_{sublimation}$.

**b.** Calculate $\Delta H_{fusion}$.

**c.** Calculate the normal boiling point and $\Delta S_{vaporization}$ at the boiling point.

**d.** Calculate the triple point pressure and temperature.

**P8.35**    In Equations (8.16), $(dP/dT)_{vaporization}$ was calculated by assuming that $V_m^{gas} \gg V_m^{liquid}$. In this problem, you will test the validity of this approximation. For water at its normal boiling point of 373.12 K, $\Delta H_{vaporization} = 40.656 \times 10^3$ J $mol^{-1}$, $\rho_{liquid} = 958.66$ kg $m^{-3}$, and $\rho_{gas} = 0.58958$ kg $m^{-3}$. Compare the calculated values for $(dP/dT)_{vaporization}$ with and without the approximation of Equation (8.16). What is the relative error in making the approximation?

**P8.36**    The densities of a given solid and liquid of molar mass 122.5 g $mol^{-1}$ at its normal melting temperature of 427.15 K are 1075 and 1012 kg $m^{-3}$, respectively. If the pressure is increased to 120. bar, the melting temperature increases to 429.35 K. Calculate $\Delta H_{fusion}^\circ$ and $\Delta S_{fusion}^\circ$ for this substance.

**P8.37**    The variation of the vapor pressure of the liquid and solid forms of a pure substance near the triple point are given by $\ln \dfrac{P_{solid}}{Pa} = -8750 \dfrac{K}{T} + 34.143$ and

$\ln \dfrac{P_{liquid}}{Pa} = -4053 \dfrac{K}{T} + 21.10$. Calculate the temperature and pressure at the triple point.

**P8.38**    Use the vapor pressures of $n$-butane given in the following table to calculate the enthalpy of vaporization using a graphical method or a least squares fitting routine.

| $T$ (°C) | $P$ (Pa) | $T$ (°C) | $P$ (Pa) |
|----------|----------|----------|----------|
| −134.3   | 1.000    | −49.10   | $1.000 \times 10^4$ |
| −121.0   | 10.00    | −0.800   | $1.000 \times 10^5$ |
| −103.9   | 100.0    |          |          |
| −81.10   | 1000.    |          |          |

**P8.39**    At 298.15 K, $\Delta G_f^\circ$ ($HCOOH$, $g$) $= -351.0$ kJ $mol^{-1}$ and $\Delta G_f^\circ$ ($HCOOH$, $l$) $= -361.4$ kJ $mol^{-1}$. Calculate the vapor pressure of formic acid at this temperature.

**P8.40**    In this problem, you will calculate the differences in the chemical potentials of ice and supercooled water and of steam and superheated water, all at 1 atm pressure shown schematically in Figure 8.1. For this problem,

$S^\circ_{H_2O,s} = 48.0$ J mol$^{-1}$ K$^{-1}$, $S^\circ_{H_2O,l} = 70.0$ J mol$^{-1}$ K$^{-1}$, and $S^\circ_{H_2O,g} = 188.8$ J mol$^{-1}$ K$^{-1}$.

a. By what amount does the chemical potential of water exceed that of ice at $-2.25°C$?

b. By what amount does the chemical potential of water exceed that of steam at $102.25°C$?

**P8.41** Calculate the vapor pressure of a droplet of benzene of radius $1.25 \times 10^{-8}$ m at $38.0°C$ in equilibrium with its vapor. Use the tabulated value of the density and the surface tension at 298 K from Appendix A for this problem. (*Hint*: You need to calculate the vapor pressure of benzene at this temperature.)

**P8.42** Solid iodine, $I_2(s)$, at $25.0°C$ has an enthalpy of sublimation of 56.30 kJ mol$^{-1}$. The $C_{P,m}$ of the vapor and solid phases at that temperature are 36.9 and 54.4 J K$^{-1}$ mol$^{-1}$, respectively. The sublimation pressure at $25.0°C$ is 0.30844 Torr. Calculate the sublimation pressure of the solid at the melting point ($113.6°C$) assuming

a. that the enthalpy of sublimation does not change with temperature.

b. that the enthalpy of sublimation at temperature $T$ can be calculated from the equation $\Delta H_{sublimation}(T) = \Delta H_{sublimation}(T_0) + \Delta C_P(T - T_0)$ and $\Delta C_P$ does not change with $T$.

**P8.43** Consider the transition between two forms of solid tin, $Sn(s, gray) \rightarrow Sn(s, white)$. The two phases are in equilibrium at 1 bar and $18°C$. The densities for gray and white tin are 5750 and 7280 kg m$^{-3}$, respectively, and the molar entropies for gray and white tin are 44.14 and 51.18 J K$^{-1}$ mol$^{-1}$, respectively. Calculate the temperature at which the two phases are in equilibrium at 350. bar.

**P8.44** A reasonable approximation to the vapor pressure of krypton is given by $\log_{10}(P/\text{Torr}) = b - 0.05223(a/T)$. For solid krypton, $a = 10,065$ and $b = 7.1770$. For liquid krypton, $a = 9377.0$ and $b = 6.92387$. Use these formulas to estimate the triple point temperature and pressure and also the enthalpies of vaporization, fusion, and sublimation of krypton.

**P8.45** 20.0 g of water is in a container of 20.0 L at 298.15 K. The vapor pressure of water at this temperature is 23.76 Torr.

a. What phases are present?

b. At what volume would only the gas phase be present?

c. At what volume would only the liquid phase be present?

# Ideal and Real Solutions

I n an ideal solution of A and B, the A–B interactions are the same as the A–A and B–B interactions. In this case, the relationship between the solution concentration and gas-phase partial pressure is described by Raoult's law for each component. In an ideal solution, the vapor over a solution is enriched in the most volatile component, allowing a separation into its components through fractional distillation. Nonvolatile solutes lead to a decrease of the vapor pressure above a solution. Such solutions exhibit a freezing point depression and a boiling point elevation. These properties depend only on the concentration and not on the identity of the non-volatile solutes for an ideal solution. Real solutions are described by a modification of the ideal dilute solution model. In an ideal dilute solution, the solvent obeys Raoult's law, and the solute obeys Henry's law. This model is limited in its applicability. To quantify deviations from the ideal dilute solution model, we introduce the concept of the *activity*. The activity of a component of the solution is defined with respect to a standard state. Knowledge of the activities of the various components of a reactive mixture is essential in modeling chemical equilibrium. The thermodynamic equilibrium constant for a reaction in solution is calculated by expressing the reaction quotient $Q$ in terms of activities rather than concentrations.

## 9.1 Defining the Ideal Solution

In an ideal gas, the atoms or molecules do not interact with one another. Clearly, this is not a good model for a liquid, because without attractive interactions, a gas will not condense. The attractive interaction in liquids varies greatly, as shown by the large variation in boiling points among the elements; for instance, helium has a normal boiling point of 4.2 K, whereas hafnium has a boiling point of 5400 K.

In developing a model for solutions, the vapor phase that is in equilibrium with the solution must be taken into account. Consider pure liquid benzene in a beaker placed in
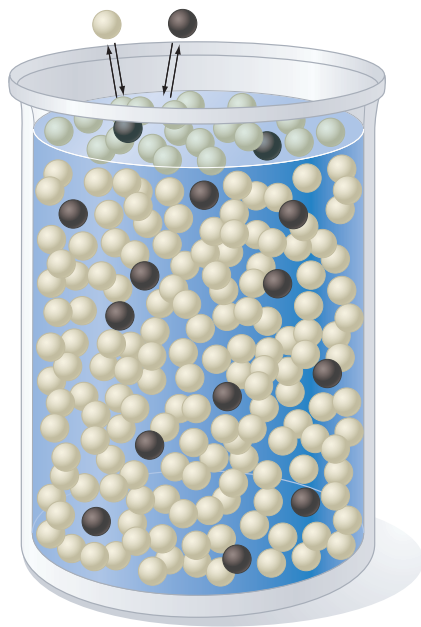
a closed room. Because the liquid is in equilibrium with the vapor phase above it, there is a nonzero partial pressure of benzene in the air surrounding the beaker. This pressure is called the vapor pressure of benzene at the temperature of the liquid. What happens when toluene is added to the beaker? It is observed that the partial pressure of benzene is reduced, and the vapor phase now contains both benzene and toluene. For this particular mixture, the partial pressure of each component ($i$) above the liquid is given by

$$P_i = x_i P_i^* \quad i = 1, 2 \tag{9.1}$$

where $x_i$ is the mole fraction of that component in the liquid. This equation states that the partial pressure of each of the two components is directly proportional to the vapor pressure of the corresponding pure substance $P_i^*$ and that the proportionality constant is $x_i$. Equation (9.1) is known as **Raoult's law** and is the definition of an **ideal solution.** Raoult's law holds for each substance in an ideal solution over the range from $0 \le x_i \le 1$. In binary solutions, one refers to the component that has the higher value of $x_i$ as the **solvent** and the component that has the lower value of $x_i$ as the **solute.**

Few solutions satisfy Raoult's law. However, it is useful to study the thermodynamics of ideal solutions and to introduce departures from ideal behavior later. Why is Raoult's law not generally obeyed over the whole concentration range of a binary solution consisting of molecules A and B? Equation (9.1) is only obeyed if the A–A, B–B, and A–B interactions are all equally strong. This criterion is satisfied for a mixture of benzene and toluene because the two molecules are very similar in size, shape, and chemical properties. However, it is not satisfied for arbitrary molecules. Raoult's law is an example of a **limiting law;** the solvent in a real solution obeys Raoult's law as the solution becomes highly dilute.

Raoult's law is derived in Example Problem 9.1 and can be rationalized using the model depicted in Figure 9.1. In the solution, molecules of solute are distributed in the solvent. The solution is in equilibrium with the gas phase, and the gas-phase composition is determined by a dynamic balance between evaporation from the solution and condensation from the gas phase, as indicated for one solvent and one solute molecule in Figure 9.1.



**FIGURE 9.1**

Schematic model of a solution. The white and black spheres represent solvent and solute molecules, respectively.

---

**EXAMPLE PROBLEM 9.1**

Assume that the rates of evaporation $R_{evap}$ and condensation $R_{cond}$ of the solvent from the surface of pure liquid solvent are given by the expressions

$$R_{evap} = A k_{evap}$$

$$R_{cond} = A k_{cond} P_{solvent}^*$$

where $A$ is the surface area of the liquid and $k_{evap}$ and $k_{cond}$ are the rate constants for evaporation and condensation, respectively. Derive a relationship between the vapor pressure of the solvent above a solution and above the pure solvent.

**Solution**

For the pure solvent, the equilibrium vapor pressure is found by setting the rates of evaporation and condensation equal:

$$R_{evap} = R_{cond}$$

$$A k_{evap} = A k_{cond} P_{solvent}^*$$

$$P_{solvent}^* = \frac{k_{evap}}{k_{cond}}$$

Next, consider the ideal solution. In this case, the rate of evaporation is reduced by the factor $x_{solvent}$ because only that fraction of the surface is available for evaporation of the solvent.

$$R_{evap} = A k_{evap} x_{solvent}$$

$$R_{cond} = A k_{cond} P_{solvent}$$

and at equilibrium

$$R_{evap} = R_{cond}$$

$$Ak_{evap}x_{solvent} = Ak_{cond}P_{solvent}$$

$$P_{solvent} = \frac{k_{evap}}{k_{cond}}x_{solvent} = P^*_{solvent}x_{solvent}$$

The derived relationship is Raoult's law.

# 9.2 The Chemical Potential of a Component in the Gas and Solution Phases

If the liquid and vapor phases are in equilibrium, the following equation holds for each component of the solution, where $\mu_i$ is the chemical potential of species $i$:

$$\mu_i^{solution} = \mu_i^{vapor} \tag{9.2}$$

Recall from Section 6.3 that the chemical potential of a substance in the gas phase is related to its partial pressure $P_i$ by

$$\mu_i^{vapor} = \mu_i^\circ + RT \ln \frac{P_i}{P^\circ} \tag{9.3}$$

where $\mu_i^\circ$ is the chemical potential of pure component $i$ in the gas phase at the standard state pressure $P^\circ = 1$ bar. Because at equilibrium $\mu_i^{solution} = \mu_i^{vapor}$, Equation (9.3) can be written in the form

$$\mu_i^{solution} = \mu_i^\circ + RT \ln \frac{P_i}{P^\circ} \tag{9.4}$$

For pure liquid $i$ in equilibrium with its vapor, $\mu_i^*(\text{liquid}) = \mu_i^*(\text{vapor}) = \mu_i^*$. Therefore, the chemical potential of the pure liquid is given by

$$\mu_i^* = \mu_i^\circ + RT \ln \frac{P_i^*}{P^\circ} \tag{9.5}$$

Subtracting Equation (9.5) from (9.4) gives

$$\mu_i^{solution} = \mu_i^* + RT \ln \frac{P_i}{P_i^*} \tag{9.6}$$

For an ideal solution, $P_i = x_i P_i^*$. Combining Equations (9.6) and (9.1), the central equation describing ideal solutions is obtained:

$$\mu_i^{solution} = \mu_i^* + RT \ln x_i \tag{9.7}$$

This equation relates the chemical potential of a component in an ideal solution to the chemical potential of the pure liquid form of component $i$ and the mole fraction of that component in the solution. This equation is most useful in describing the thermodynamics of solutions in which all components are volatile and miscible in all proportions.

Keeping in mind that $\mu_i = G_{i,m}$, the form of Equation (9.7) is identical to that derived for the Gibbs energy of a mixture of gases in Section 6.5. Therefore, one can derive relations for the thermodynamics of mixing to form ideal solutions as was done for ideal gases in Section 6.6. These relations are shown in Equation (9.8). Note in particular that $\Delta H_{mixing} = \Delta V_{mixing} = 0$ for an ideal solution:

$$\Delta G_{mixing} = nRT \sum_i x_i \ln x_i$$

$$\Delta S_{mixing} = -\left( \frac{\partial \Delta G_{mixing}}{\partial T} \right)_{P,n_1,n_2} = -nR \sum_i x_i \ln x_i$$

$$\Delta V_{mixing} = \left( \frac{\partial \Delta G_{mixing}}{\partial P} \right)_{T, n_1, n_2} = 0 \quad \text{and}$$

$$\Delta H_{mixing} = \Delta G_{mixing} + T \Delta S_{mixing}$$

$$= nRT \sum_i x_i \ln x_i - T \left( nR \sum_i x_i \ln x_i \right) = 0 \tag{9.8}$$

### EXAMPLE PROBLEM 9.2

An ideal solution is made from 5.00 mol of benzene and 3.25 mol of toluene. Calculate $\Delta G_{mixing}$ and $\Delta S_{mixing}$ at 298 K and 1 bar pressure. Is mixing a spontaneous process?

#### Solution

The mole fractions of the components in the solution are $x_{benzene} = 0.606$ and $x_{toluene} = 0.394$.

$$\Delta G_{mixing} = nRT \sum_i x_i \ln x_i$$

$$= 8.25 \text{ mol} \times 8.314 \text{ J mol}^{-1} \text{ K}^{-1}$$
$$\times 298 \text{ K} \times (0.606 \ln 0.606 + 0.394 \ln 0.394)$$

$$= -13.7 \times 10^3 \text{ J}$$

$$\Delta S_{mixing} = -nR \sum_i x_i \ln x_i$$

$$= -8.25 \text{ mol} \times 8.314 \text{ J mol}^{-1} \text{ K}^{-1} \times (0.606 \ln 0.606 + 0.394 \ln 0.394)$$

$$= 46.0 \text{ J K}^{-1}$$

Mixing is spontaneous because $\Delta G_{mixing} < 0$ for an ideal solution. If two liquids are miscible, it is always true that $\Delta G_{mixing} < 0$.

## 9.3 Applying the Ideal Solution Model to Binary Solutions

Although the ideal solution model can be applied to any number of components, to simplify the mathematics, the focus in this chapter is on binary solutions, which consist of only two components. Because Raoult's law holds for both components of the mixture, $P_1 = x_1 P_1^*$ and $P_2 = x_2 P_2^* = (1 - x_1) P_2^*$. The total pressure in the gas phase varies linearly with the mole fraction of each of its components in the liquid:

$$P_{total} = P_1 + P_2 = x_1 P_1^* + (1 - x_1) P_2^* = P_2^* + (P_1^* - P_2^*) x_1 \tag{9.9}$$

The individual partial pressures as well as $P_{total}$ above a benzene–1,2 dichloroethane ($C_2H_4Cl_2$) solution are shown in Figure 9.2. Small deviations from Raoult's law are seen. Such deviations are typical because few solutions obey Raoult's law exactly. Nonideal solutions, which generally exhibit large deviations from Raoult's law, are discussed in Section 9.9.

The concentration unit used in Equation (9.9) is the mole fraction of each component in the liquid phase. The mole fraction of each component in the gas phase can also be calculated. Using the definition of the partial pressure and the symbols $y_1$ and $y_2$ to denote the gas-phase mole fractions, we can write

$$y_1 = \frac{P_1}{P_{total}} = \frac{x_1 P_1^*}{P_2^* + (P_1^* - P_2^*) x_1} \tag{9.10}$$
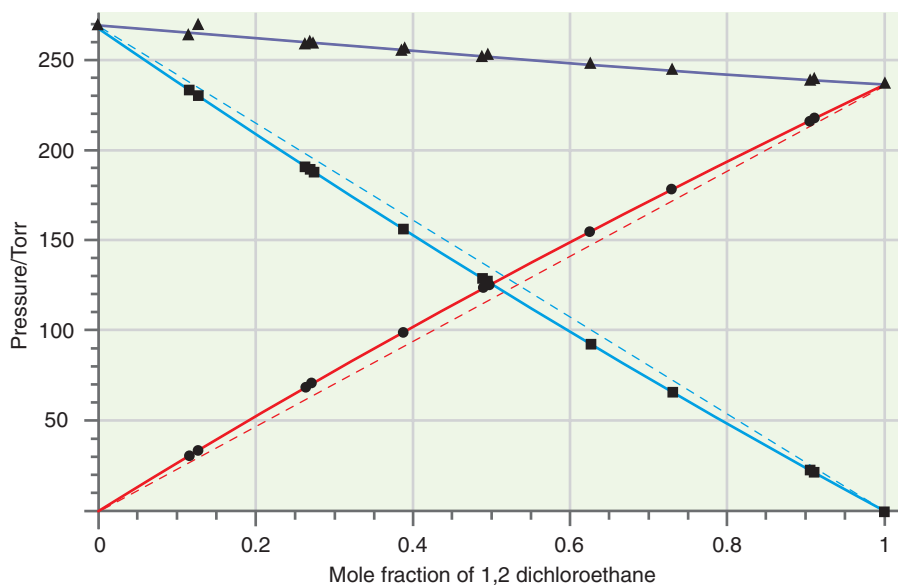
To obtain the pressure in the vapor phase as a function of $y_1$, we first solve Equation (9.10) for $x_1$:

$$x_1 = \frac{y_1 P_2^*}{P_1^* + (P_2^* - P_1^*)y_1} \tag{9.11}$$

and obtain $P_{total}$ from $P_{total} = P_2^* + (P_1^* - P_2^*)x_1$

$$P_{total} = \frac{P_1^* P_2^*}{P_1^* + (P_2^* - P_1^*)y_1} \tag{9.12}$$

Equation (9.12) can be rearranged to give an equation for $y_1$ in terms of the vapor pressures of the pure components and the total pressure:

$$y_1 = \frac{P_1^* P_{total} - P_1^* P_2^*}{P_{total}(P_1^* - P_2^*)} \tag{9.13}$$

The variation of the total pressure with $x_1$ and $y_1$ is not the same, as is seen in Figure 9.3. In Figure 9.3a, the system consists of a single-phase liquid for pressures above the curve and of a two-phase vapor–liquid mixture for points lying on the curve in the $P-x_1$ diagram. Only points lying above the curve are meaningful, because points lying below the curve do not correspond to equilibrium states at which liquid is present. In Figure 9.3b, the system consists of a single-phase vapor for pressures below the curve and of a two-phase vapor–liquid mixture for points lying on the curve in the $P-y_1$ diagram. Points lying above the curve do not correspond to equilibrium states at which vapor is present. The excess vapor would condense to form liquid.

Note that the pressure is plotted as a function of different variables in the two parts of Figure 9.3. To compare the gas phase and liquid composition at a given total pressure, both are graphed as a function of $Z_{benzene}$, which is called the **average composition** of benzene in the whole system in Figure 9.4. The average composition $Z$ is defined by

$$Z_{benzene} = \frac{n_{benzene}^{liquid} + n_{benzene}^{vapor}}{n_{toluene}^{liquid} + n_{toluene}^{vapor} + n_{benzene}^{liquid} + n_{benzene}^{vapor}} = \frac{n_{benzene}}{n_{total}}$$

In the region labeled "Liquid" in Figure 9.4, the system consists entirely of a liquid phase, and $Z_{benzene} = x_{benzene}$. In the region labeled "Vapor," the system consists entirely of a gaseous phase and $Z_{benzene} = y_{benzene}$. The area separating the single-phase liquid and vapor regions corresponds to the two-phase liquid–vapor coexistence region.

We next apply the phase rule to the benzene–toluene ideal solution for which there are two components (benzene and toluene) and three independent state variables,
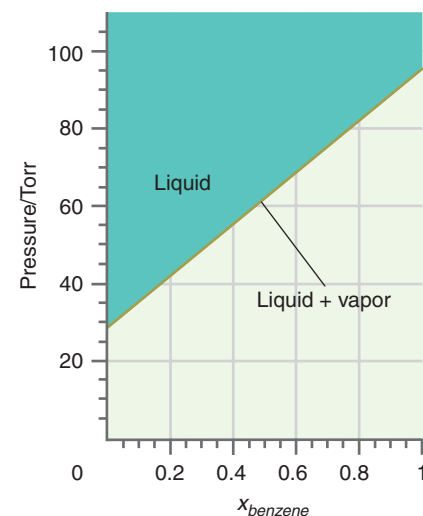


(a)
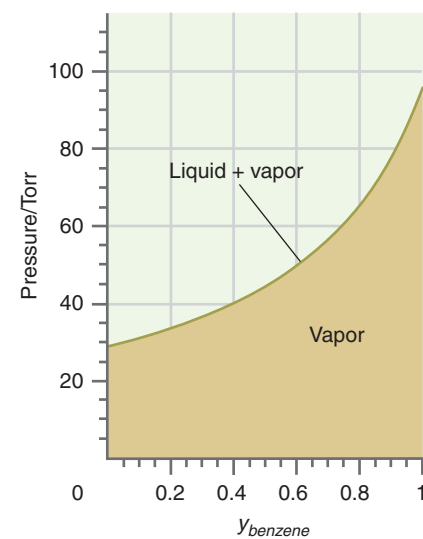


(b)

**FIGURE 9.3**
The total pressure above a benzene–toluene ideal solution is shown for different values of **(a)** the mole fraction of benzene in the solution and **(b)** the mole fraction of benzene in the vapor. Points on the curves correspond to vapor–liquid coexistence. Only the curves and the shaded areas are of physical significance as explained in text.

**FIGURE 9.4**
A $P$–$Z$ phase diagram is shown for a benzene-toluene ideal solution. The upper curve shows the vapor pressure as a function of $x_{benzene}$. The lower curve shows the vapor pressure as a function of $y_{benzene}$. Above the two curves, the system is totally in the liquid phase, and below the two curves, the system is totally in the vapor phase. The area intermediate between the two curves shows the liquid–vapor coexistence region. The horizontal lines connecting the curves are called tie lines.
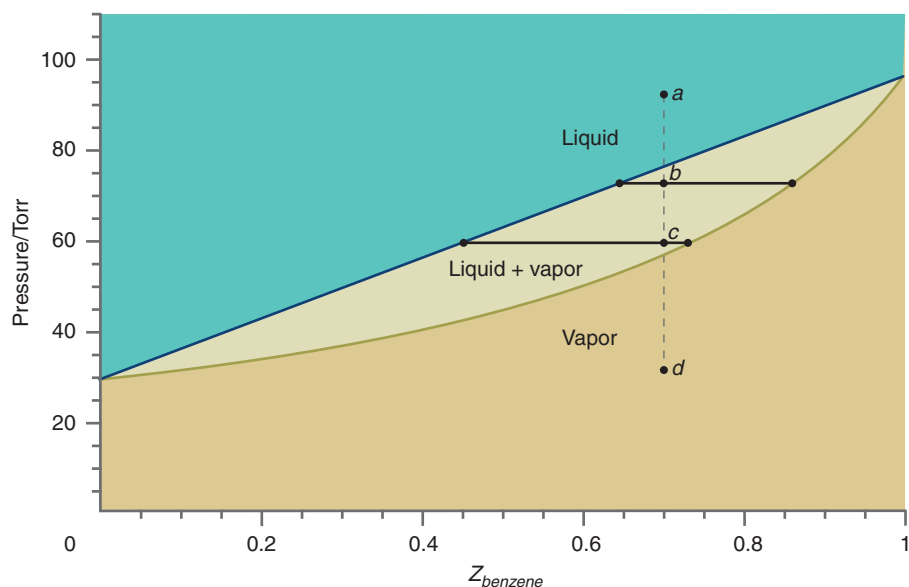


namely $P$, $T$, and $Z_{benzene}$ (or $Z_{toluene}$). Because $Z_{benzene} = 1 - Z_{toluene}$, these two variables are not independent. For a system containing $C$ components, the phase rule discussed in Section 8.3 takes the form

$$F = C - p + 2 \qquad (9.14)$$

For the benzene–toluene ideal solution, $C = 2$ and $F = 4 - p$. Therefore, in the single phase regions labeled liquid and vapor in Figure 9.4, the system has three degrees of freedom. One of these degrees of freedom is already fixed because the temperature is held constant in Figure 9.4. Therefore, the two remaining degrees of freedom are $P$ and $Z_{benzene}$. In the two-phase region labeled liquid + vapor, the system has only one degree of freedom. Once $P$ is fixed, the $Z$ values at the ends of the horizontal line fix $x_{benzene}$ and $y_{benzene}$ and therefore $Z_{benzene}$. We note that the number of components can be less than the number of chemical species. For example, a solution containing the three species $A$, $B$, and $C$ linked by the chemical equilibrium $A + B \rightleftharpoons C$ contains only two independent components because only two of the three concentrations are independent variables.

To demonstrate the usefulness of this **pressure–average composition ($P$–$Z$) diagram,** consider a constant temperature process in which the pressure of the system is decreased from the value corresponding to point $a$ in Figure 9.4. Because $P > P_{total}$, initially the system is entirely in the liquid phase. As the pressure is decreased at constant composition, the system remains entirely in the liquid phase until the constant composition line intersects the $P$ versus $x_{benzene}$ curve. At this point, the system enters the two-phase vapor–liquid coexistence region. As point $b$ is reached, what are the values for $x_{benzene}$ and $y_{benzene}$, the mole fractions of benzene in the liquid and vapor phases? These values can be determined by constructing a tie line in the two-phase coexistence region.

A **tie line** (see Figure 9.4) is a horizontal line at the pressure of interest that connects the $P$ versus $x_{benzene}$ and $P$ versus $y_{benzene}$ curves. Note that for all values of the pressure, $y_{benzene}$ is greater than $x_{benzene}$, showing that the vapor phase is always enriched in the more volatile or higher vapor pressure component in comparison with the liquid phase.

---

**EXAMPLE PROBLEM 9.3**

An ideal solution of 5.00 mol of benzene and 3.25 mol of toluene is placed in a piston and cylinder assembly. At 298 K, the vapor pressure of the pure substances are $P^*_{benzene} = 96.4$ Torr and $P^*_{toluene} = 28.9$ Torr.

**a.** The pressure above this solution is reduced from 760. Torr. At what pressure does the vapor phase first appear?

**b.** What is the composition of the vapor under these conditions?

### Solution

**a.** The mole fractions of the components in the solution are $x_{benzene} = 0.606$ and $x_{toluene} = 0.394$. The vapor pressure above this solution is

$$P_{total} = x_{benzene}P^*_{benzene} + x_{toluene}P^*_{toluene}$$

$$= 0.606 \times 96.4 \text{ Torr} + 0.394 \times 28.9 \text{ Torr}$$

$$= 69.8 \text{ Torr}$$

No vapor will be formed until the pressure has been reduced to this value.

**b.** The composition of the vapor at a total pressure of 69.8 Torr is given by

$$y_{benzene} = \frac{P^*_{benzene}P_{total} - P^*_{benzene}P^*_{toluene}}{P_{total}\left(P^*_{benzene} - P^*_{toluene}\right)}$$

$$= \frac{96.4 \text{ Torr} \times 69.8 \text{ Torr} - 96.4 \text{ Torr} \times 28.9 \text{ Torr}}{69.8 \text{ Torr} \times (96.4 \text{ Torr} - 28.9 \text{ Torr})} = 0.837$$

$$y_{toluene} = 1 - y_{benzene} = 0.163$$

Note that the vapor is enriched relative to the liquid in the more volatile component, which has the higher vapor pressure and lower boiling temperature.

To calculate the relative amount of material in each of the two phases in a coexistence region, we derive the lever rule for a binary solution of the components A and B. Figure 9.5 shows a magnified portion of Figure 9.4 centered at the tie line that passes through point $b$. We derive the lever rule using the following geometrical argument. The lengths of the line segments $lb$ and $bv$ are given by

$$lb = Z_B - x_B = \frac{n_B^{tot}}{n^{tot}} - \frac{n_B^{liq}}{n_{liq}^{tot}} \tag{9.15}$$

$$bv = y_B - Z_B = \frac{n_B^{vapor}}{n_{vapor}^{tot}} - \frac{n_B^{tot}}{n^{tot}} \tag{9.16}$$

The superscripts on $n$ indicate whether we are referring to the moles of component B in the vapor or liquid phases or the total number of moles of B in the system. If Equation (9.15) is multiplied by $n_{liq}^{tot}$, Equation (9.16) is multiplied by $n_{vapor}^{tot}$, and the two equations are subtracted, we find that

$$lb \, n_{liq}^{tot} - bv \, n_{vapor}^{tot} = \frac{n_B^{tot}}{n^{tot}}\left(n_{liq}^{tot} + n_{vapor}^{tot}\right) - \left(n_B^{liq} + n_B^{vapor}\right) = n_B^{tot} - n_B^{tot} = 0$$

We conclude that
$$\frac{n_{liq}^{tot}}{n_{vap}^{tot}} = \frac{bv}{lb} \tag{9.17}$$

It is convenient to restate this result as

$$n_{liq}^{tot}(Z_B - x_B) = n_{vapor}^{tot}(y_B - Z_B) \tag{9.18}$$

Equation (9.18) is called the **lever rule** by analogy with the torques acting on a lever of length $lb + bv$ with the fulcrum positioned at point $b$. For the specific case shown in Figure 9.5, $n_{liq}^{tot}/n_{vapor}^{tot} = 2.34$. Therefore, 70.1% of the total number of moles in the system is in the liquid phase, and 29.9% is in the vapor phase.
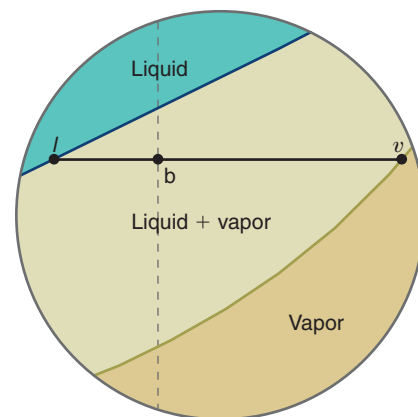


**FIGURE 9.5**
An enlarged region of the two-phase coexistence region of Figure 9.4 is shown. The vertical line through point $b$ indicates a transition at constant system composition. The lever rule (see text) is used to determine what fraction of the system is in the liquid and vapor phases.

### EXAMPLE PROBLEM 9.4

For the benzene–toluene solution of Example Problem 9.3, calculate

**a.** the total pressure

**b.** the liquid composition

**c.** the vapor composition

when 1.50 mol of the solution has been converted to vapor.

**Solution**

The lever rule relates the average composition, $Z_{benzene} = 0.606$, and the liquid and vapor compositions:

$$n_{vapor}^{tot}\left(y_{benzene} - Z_{benzene}\right) = n_{liq}^{tot}\left(Z_{benzene} - x_{benzene}\right)$$

Entering the parameters of the problem, this equation simplifies to

$$6.75x_{benzene} + 1.50y_{benzene} = 5.00$$

The total pressure is given by

$$P_{total} = x_{benzene}P_{benzene}^* + (1 - x_{benzene})P_{toluene}^*$$

$$= [96.4x_{benzene} + 28.9(1 - x_{benzene})]\text{Torr}$$

and the vapor composition is given by

$$y_{benzene} = \frac{P_{benzene}^* P_{total} - P_{benzene}^* P_{toluene}^*}{P_{total}(P_{benzene}^* - P_{toluene}^*)} = \left[\frac{96.4\dfrac{P_{total}}{\text{Torr}} - 2786}{67.5\dfrac{P_{total}}{\text{Torr}}}\right]$$

These three equations in three unknowns can be solved by using an equation solver or by eliminating the variables by combining equations. For example, the first equation can be used to express $y_{benzene}$ in terms of $x_{benzene}$. This result can be substituted into the second and third equations to give two equations in terms of $x_{benzene}$ and $P_{total}$. The solution for $x_{benzene}$ obtained from these two equations can be substituted in the first equation to give $y_{benzene}$. The relevant answers are $x_{benzene} = 0.561$, $y_{benzene} = 0.810$, and $P_{total} = 66.8$ Torr.

# 9.4 The Temperature–Composition Diagram and Fractional Distillation

The enrichment of the vapor phase above a solution in the more volatile component is the basis for fractional distillation, an important separation technique in chemistry and in the chemical industry. It is more convenient to discuss fractional distillation using a **temperature–composition diagram** than using the pressure–composition diagram discussed in the previous section. The temperature-composition diagram gives the temperature of the solution as a function of the average system composition for a predetermined total vapor pressure, $P_{total}$. It is convenient to use the value $P_{total} = 1$ atm so the vertical axis is the normal boiling point of the solution. Figure 9.6 shows a boiling temperature–composition diagram for a benzene–toluene solution. Neither the $T_b - x_{benzene}$ nor the $T_b - y_{benzene}$ curves are linear in a temperature–composition diagram. Note that because the more volatile component has the lower boiling point, the vapor and liquid regions are inverted when compared with the pressure–composition diagram.

The principle of **fractional distillation** can be illustrated using the sequence of lines labeled $a$ through $k$ in Figure 9.6. The vapor above the solution at point $a$ is enriched in benzene. If this vapor is separated from the original solution and condensed by lowering the temperature, the resulting liquid will have a higher mole fraction of benzene than the original solution. As for the original solution, the vapor above this separately collected liquid is enriched in benzene. As this process is repeated, the successively collected vapor samples become more enriched in benzene. In the limit of a very large number of steps, the last condensed samples are essentially pure benzene. The multistep procedure described earlier is very cumbersome because it requires the collection and evaporation of many different samples. In practice, the separation into pure benzene and toluene is accomplished using a distillation column, shown schematically in Figure 9.7.

Rather than have the whole system at a uniform temperature, a distillation column operates with a temperature gradient so that the top part of the column is at a lower temperature than the solution being boiled off. The horizontal segments $ab$, $cd$, $ef$, and so on in Figure 9.6 correspond to successively higher (cooler) portions of the column. Each of these segments corresponds to one of the distillation stages in Figure 9.7. Because the vapor is moving upward through the condensing liquid, heat and mass exchange facilitates equilibration between the two phases.

Distillation plays a major role in the separation of crude oil into its various components. The lowest boiling liquid is gasoline, followed by kerosene, diesel fuel and heating oil, and gas oil, which is further broken down into lower molecular weight components by catalytic cracking. It is important in distillation to keep the temperature of the boiling liquid as low as possible to avoid the occurrence of thermally induced reactions. A useful way to reduce the boiling temperature is to distill the liquid under a partial vacuum, which is done by pumping away the gas phase. The boiling point of a typical liquid mixture can be reduced by approximately 100°C if the pressure is reduced from 760 to 20 Torr.

Although the principle of fractional distillation is the same for real solutions, it is not possible to separate a binary solution into its pure components if the nonideality is strong enough. If the A–B interactions are more attractive than the A–A and B–B interactions, the boiling point of the solution will go through a maximum at a concentration intermediate between $x_A = 0$ and $x_A = 1$. An example of such a case is an acetone–chloroform mixture. The hydrogen on the chloroform forms a hydrogen bond with the oxygen in acetone as shown in Figure 9.8, leading to stronger A–B than A–A and B–B interactions.

A boiling point diagram for this case is shown in Figure 9.9a. At the maximum boiling temperature, the liquid and vapor composition lines are tangent to one another. Fractional distillation of such a solution beginning with an initial value of $x_A$ greater than that corresponding to the maximum boiling point is shown schematically in the figure. The component with the lowest boiling point will initially emerge at the top of the distillation column. In this case, it will be pure component A. However, the liquid left in the heated flask will not be pure component B, but rather the solution corresponding to the concentration at which the maximum boiling point is reached. Continued boiling of the solution at this composition will lead to evaporation at constant composition. Such a mixture is called an azeotrope, and because $T_{b,azeotrope} > T_{b,A}, T_{b,B}$, it is called a maximum boiling azeotrope. An example for a maximum boiling azeotrope is a mixture of $H_2O$ ($T_b = 100$°C) and HCOOH ($T_b = 100$°C) at $x_{H_2O} = 0.427$, which boils at 107.2°C. Other commonly occurring azeotropic mixtures are listed in Table 9.1.
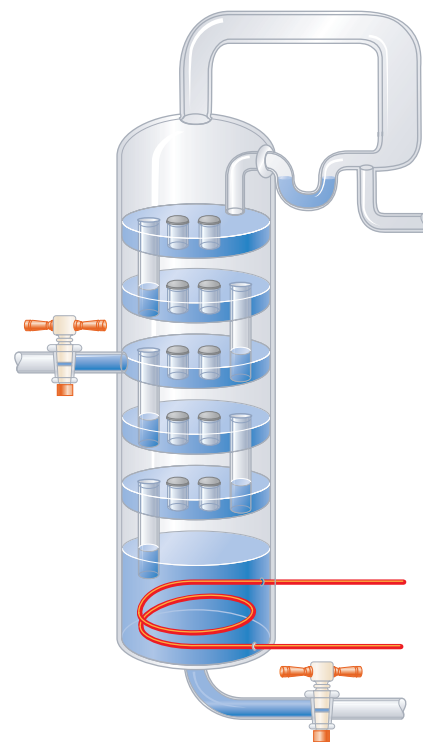
(a)



(b)
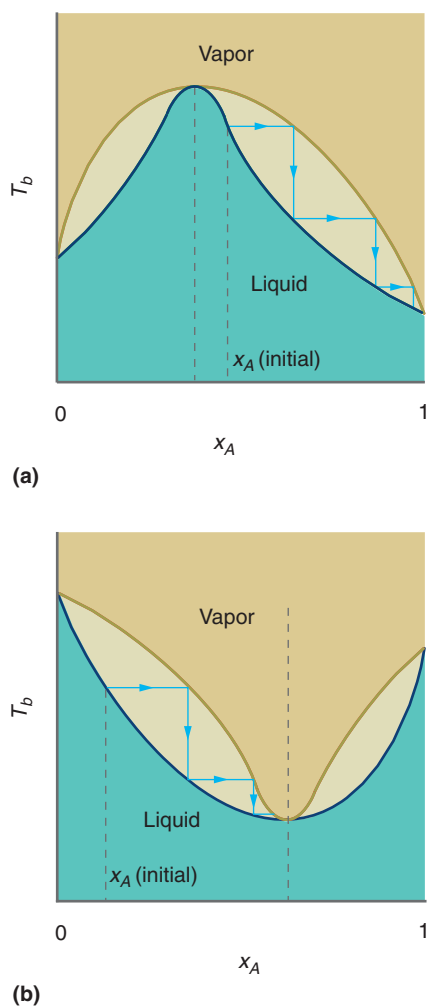
**FIGURE 9.9**
A boiling point diagram is shown for (a) maximum and (b) minimum boiling point azeotropes. The dashed lines indicate the initial composition of the solution and the composition of the azeotrope. The sequence of horizontal segments with arrows corresponds to successively higher (cooler) portions of the column.

**TABLE 9.1  Composition and Boiling Temperatures of Selected Azeotropes**

| Azeotropic Mixture | Boiling Temperature of Components (°C) | Mole Fraction of First Component | Azeotrope Boiling Point (°C) |
|---|---|---|---|
| Water–ethanol | 100./78.5 | 0.096 | 78.2 |
| Water–trichloromethane | 100./61.2 | 0.160 | 56.1 |
| Water–benzene | 100./80.2 | 0.295 | 69.3 |
| Water–toluene | 100./111 | 0.444 | 84.1 |
| Ethanol–hexane | 78.5/68.8 | 0.332 | 58.7 |
| Ethanol–benzene | 78.5/80.2 | 0.440 | 67.9 |
| Ethyl acetate–hexane | 78.5/68.8 | 0.394 | 65.2 |
| Carbon disulfide–acetone | 46.3/56.2 | 0.608 | 39.3 |
| Toluene-acetic acid | 111/118 | 0.625 | 100.7 |

*Source:* Lide, D. R., ed. *Handbook of Chemistry and Physics.* 83rd ed. Boca Raton, FL: CRC Press, 2002.

If the A–B interactions are less attractive than the A–A and B–B interactions, a minimum boiling azeotrope can be formed. A schematic boiling point diagram for such an azeotrope is also shown in Figure 9.9b. Fractional distillation of such a solution beginning with an initial value of $x_A$ less than that corresponding to the minimum boiling point leads to a liquid with the azeotropic composition initially emerging at the top of the distillation column. An example for a minimum boiling azeotrope is a mixture of $CS_2$ ($T_b = 46.3°C$) and acetone ($T_b = 56.2°C$) at $x_{CS_2} = 0.608$, which boils at 39.3°C.

It is still possible to collect one component of an azeotropic mixture using the property that the azeotropic composition is a function of the total pressure as shown in Figure 9.10. The mixture is first distilled at atmospheric pressure and the volatile distillate is collected. This vapor is condensed and subsequently distilled at a reduced pressure for which the azeotrope contains less A (more B). If this mixture is distilled, the azeotrope evaporates, leaving some pure B behind.

# 9.5 The Gibbs–Duhem Equation

In this section, we show that the chemical potentials of the two components in a binary solution are not independent. This is an important result, because it allows the chemical potential of a nonvolatile solute such as sucrose in a volatile solvent such as water to be determined. Such a solute has no measurable vapor pressure; therefore, its chemical potential cannot be measured directly. As shown later, its chemical potential can be determined knowing only the chemical potential of the solvent as a function of concentration.

From Chapter 6, the differential form of the Gibbs energy is given by

$$dG = -S \, dT + V \, dP + \sum_i \mu_i dn_i \tag{9.19}$$

For a binary solution at constant $T$ and $P$, this equation reduces to

$$dG = \mu_1 dn_1 + \mu_2 \, dn_2 \tag{9.20}$$

Imagine starting with an infinitesimally small amount of a solution at constant $T$ and $P$. The amount is gradually increased at constant composition. Because of this restriction, the chemical potentials are unchanged as the size of the system is changed. Therefore, the $\mu_i$ can be taken out of the integral:

$$\int_0^G dG' = \mu_1 \int_0^{n_1} dn'_1 + \mu_2 \int_0^{n_2} dn'_2 \quad \text{or}$$

$$G = \mu_1 n_1 + \mu_2 n_2 \tag{9.21}$$

The primes have been introduced to avoid using the same symbol for the integration variable and the upper limit. The total differential of the last equation is

$$dG = \mu_1 dn_1 + \mu_2 dn_2 + n_1 d\mu_1 + n_2 d\mu_2 \qquad \textbf{(9.22)}$$

The previous equation differs from Equation (9.20) because, in general, we have to take changes of the composition of the solution into account. Therefore, $\mu_1$ and $\mu_2$ must be regarded as variables. Equating the expressions for $dG$ in Equations (9.20) and (9.22), one obtains the **Gibbs–Duhem equation** for a binary solution, which can be written in either of two forms:

$$n_1 d\mu_1 + n_2 d\mu_2 = 0 \quad \text{or} \quad x_1 d\mu_1 + x_2 d\mu_2 = 0 \qquad \textbf{(9.23)}$$

This equation states that the chemical potentials of the components in a binary solution are not independent. If the change in the chemical potential of the first component is $d\mu_1$, the change of the chemical potential of the second component is given by

$$d\mu_2 = -\frac{n_1 d\mu_1}{n_2} \qquad \textbf{(9.24)}$$

The use of the Gibbs–Duhem equation is illustrated in Example Problem 9.5.

Because the azeotropic composition depends on the total pressure, pure B can be recovered from the A–B mixture by first distilling the mixture under atmospheric pressure and, subsequently, under a reduced pressure. Note that the boiling temperature is lowered as the pressure is reduced.

---

### EXAMPLE PROBLEM 9.5

One component in a solution follows Raoult's law, $\mu_1^{solution} = \mu_1^* + RT \ln x_1$ over the entire range $0 \le x_1 \le 1$. Using the Gibbs–Duhem equation, show that the second component must also follow Raoult's law.

#### Solution

From Equation (9.24),

$$d\mu_2 = -\frac{x_1 d\mu_1}{x_2} = -\frac{n_1}{n_2} d(\mu_1^* + RT \ln x_1) = -RT \frac{x_1}{x_2} \frac{dx_1}{x_1}$$

Because $x_1 + x_2 = 1$, then $dx_2 = -dx_1$ and $d\mu_2 = RT \, dx_2/x_2$. Integrating this equation, one obtains $\mu_2 = RT \ln x_2 + C$, where $C$ is a constant of integration. This constant can be evaluated by examining the limit $x_2 \to 1$. This limit corresponds to the pure substance 2 for which $\mu_2 = \mu_2^* = RT \ln 1 + C$. We conclude that $C = \mu_2^*$ and, therefore, $\mu_2^{solution} = \mu_2^* + RT \ln x_2$.

---

# 9.6 Colligative Properties

Many solutions consist of nonvolatile solutes that have limited solubility in a volatile solvent. Examples are solutions of sucrose or sodium chloride in water. Important properties of these solutions, including boiling point elevation, freezing point depression, and osmotic pressure are found to depend only on the solute concentration—not on the nature of the solute. These properties are called **colligative properties.** In this section, colligative properties are discussed using the model of the ideal solution. Corrections for nonideality are made in Section 9.13.

As discussed in Section 9.1, the vapor pressure above a solution containing a solute is lowered with respect to the pure solvent. Generally, the solute does not crystallize out with the solvent during freezing because the solute cannot be easily integrated into the solvent crystal structure. For this case, the change in the solvent chemical potential on dissolution of a nonvolatile solute can be understood using Figure 9.11a.

Only the liquid chemical potential is affected through formation of the solution. Although the gas pressure above the solution is lowered by the addition of the solute, the chemical potential of the gas is unaffected. This is the case because the comparison in Figure 9.11a is made at constant pressure. The chemical potential of the solid is
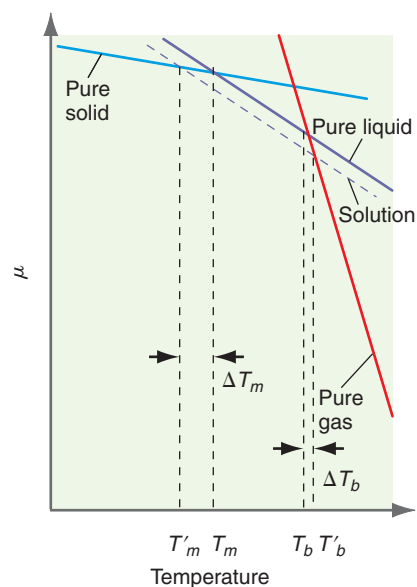
**(a)**
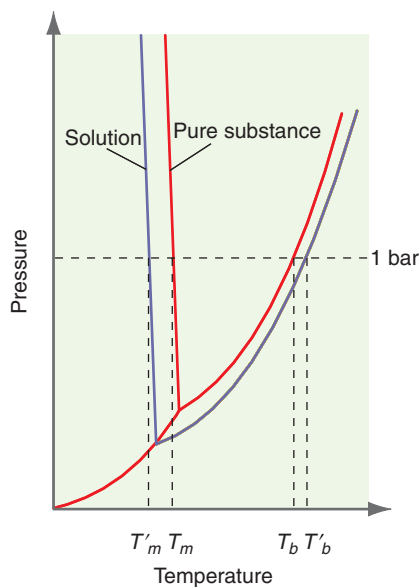


**(b)**

**FIGURE 9.11**
Illustration of the boiling point elevation
and freezing point depression in two dif-
ferent ways: **(a)** These effects arise
because the chemical potential of the solu-
tion is lowered through addition of the
nonvolatile solute, while the chemical
potential of the vapor and liquid is unaf-
fected at constant pressure. **(b)** The same
information from part (a) is shown using a
P–T phase diagram.

unaffected because of the assumption that the solute does not crystallize out with the
solvent. As shown in the figure, the melting temperature $T_m$, defined as the intersection
of the solid and liquid $\mu$ versus $T$ curves, is lowered. Similarly, the boiling temperature
$T_b$ is raised by dissolution of a nonvolatile solute in the solvent.

The same information is shown in a P–T phase diagram in Figure 9.11b. Because the
vapor pressure above the solution is lowered by the addition of the solute, the liquid–gas
coexistence curve intersects the solid–gas coexistence curve at a lower temperature than
for the pure solvent. This intersection defines the triple point, and it must also be the ori-
gin of the solid–liquid coexistence curve. Therefore, the solid–liquid coexistence curve
is shifted to lower temperatures through the dissolution of the nonvolatile solute. The
overall effect of the shifts in the solid–gas and solid–liquid coexistence curves is a
**freezing point depression** and a **boiling point elevation,** both of which arise because of
the lowering of the vapor pressure of the solvent. This effect depends only on the con-
centration, and not on the identity, of the nonvolatile solute. The preceding discussion is
qualitative in nature. In the next two sections, quantitative relationships are developed
between the colligative properties and the concentration of the nonvolatile solute.

# 9.7 The Freezing Point Depression and Boiling Point Elevation

If the solution is in equilibrium with the pure solid solvent, the following relation must
be satisfied:

$$\mu_{solution} = \mu_{solid}^* \tag{9.25}$$

Recall that $\mu_{solution}$ refers to the chemical potential of the solvent in the solution, and
$\mu_{solid}^*$ refers to the chemical potential of the pure solvent in solid form. From
Equation (9.7), we can express $\mu_{solution}$ in terms of the chemical potential of the pure
solvent and its concentration and rewrite Equation (9.25) in the form

$$\mu_{solvent}^* + RT \ln x_{solvent} = \mu_{solid}^* \tag{9.26}$$

This equation can be solved for $\ln x_{solvent}$:

$$\ln x_{solvent} = \frac{\mu_{solid}^* - \mu_{solvent}^*}{RT} \tag{9.27}$$

The difference in chemical potentials $\mu_{solid}^* - \mu_{solvent}^* = -\Delta G_{fusion}$ so that

$$\ln x_{solvent} = \frac{-\Delta G_{fusion}}{RT} \tag{9.28}$$

Because we are interested in how the freezing temperature is related to $x_{solvent}$ at con-
stant pressure, we need the partial derivative $(\partial T/\partial x_{solvent})_P$. This quantity can be
obtained by differentiating Equation (9.28) with respect to $x_{solvent}$:

$$\left(\frac{\partial \ln x_{solvent}}{\partial x_{solvent}}\right)_P = \frac{1}{x_{solvent}} = -\frac{1}{R}\left(\frac{\partial \frac{\Delta G_{fusion}}{T}}{\partial T}\right)_P \left(\frac{\partial T}{\partial x_{solvent}}\right)_P \tag{9.29}$$

The first partial derivative on the right side of Equation (9.29) can be simplified using
the Gibbs–Helmholtz equation (see Section 6.3), giving

$$\frac{1}{x_{solvent}} = \frac{\Delta H_{fusion}}{RT^2}\left(\frac{\partial T}{\partial x_{solvent}}\right)_P \quad \text{or}$$

$$\frac{dx_{solvent}}{x_{solvent}} = d \ln x_{solvent} = \frac{\Delta H_{fusion}}{R}\frac{dT}{T^2} \quad (\text{constant } P) \tag{9.30}$$

This equation can be integrated between the limits given by the pure solvent ($x_{solvent} = 1$) for which the fusion temperature is $T_{fusion}$, and an arbitrary small concentration of solute for which the fusion temperature is $T$:

$$\int_{1}^{x_{solvent}} \frac{dx}{x} = \int_{T_{fusion}}^{T} \frac{\Delta H_{fusion}}{R} \frac{dT'}{T'^2} \tag{9.31}$$

For $x_{solvent}$, not very different from 1, $\Delta H_{fusion}$ is assumed to be independent of $T$, and Equation (9.31) simplifies to

$$\frac{1}{T} = \frac{1}{T_{fusion}} - \frac{R \ln x_{solvent}}{\Delta H_{fusion}} \tag{9.32}$$

It is more convenient in discussing solutions to use the molality of the solute expressed in moles of solute per kg of solvent rather than the mole fraction of the solvent as the concentration unit. For dilute solutions $\ln x_{solvent} = \ln(n_{solvent}/(n_{solvent} + m_{solute} M_{solvent} n_{solvent})) = -\ln(1 + M_{solvent} m_{solute})$ and Equation (9.32) can be rewritten in terms of the molality ($m$) rather than the mole fraction. The result is

$$\Delta T_f = -\frac{RM_{solvent}T_{fusion}^2}{\Delta H_{fusion}} m_{solute} = -K_f m_{solute} \tag{9.33}$$

where $M_{solvent}$ is the molar mass of the solvent. In going from Equation 9.32 to Equation 9.33 we have made the approximation $\ln(1 + M_{solvent} m_{solute}) \approx M_{solvent} m_{solute}$ and $1/T - 1/T_{fusion} \approx -\Delta T_f/T_{fusion}^2$. Note that $K_f$ depends only on the properties of the solvent and is primarily determined by the molecular mass and the enthalpy of fusion. For most solvents, the magnitude of $K_f$ lies between 1.5 and 10 as shown in Table 9.2. However, $K_f$ can reach unusually high values, for example 30. (K kg)/mol for carbon tetrachloride and 40. (K kg)/mol for camphor.

The **boiling point elevation** can be calculated using the same argument with $\Delta G_{vaporization}$ and $\Delta H_{vaporization}$ substituted for $\Delta G_{fusion}$ and $\Delta H_{fusion}$. The result is

$$\left(\frac{\partial T}{\partial m_{solute}}\right)_{P, m\rightarrow 0} = \frac{RM_{solvent} T_{vaporization}^2}{\Delta H_{vaporization}} \tag{9.34}$$

**TABLE 9.2** Freezing Point Depression and Boiling Point Elevation Constants

| Substance | Standard Freezing Point (K) | $K_f$ (K kg mol$^{-1}$) | Standard Boiling Point (K) | $K_b$ (K kg mol$^{-1}$) |
|---|---|---|---|---|
| Acetic acid | 289.6 | 3.59 | 391.2 | 3.08 |
| Benzene | 278.6 | 5.12 | 353.3 | 2.53 |
| Camphor | 449 | 40. | 482.3 | 5.95 |
| Carbon disulfide | 161 | 3.8 | 319.2 | 2.40 |
| Carbon tetrachloride | 250.3 | 30. | 349.8 | 4.95 |
| Cyclohexane | 279.6 | 20.0 | 353.9 | 2.79 |
| Ethanol | 158.8 | 2.0 | 351.5 | 1.07 |
| Phenol | 314 | 7.27 | 455.0 | 3.04 |
| Water | 273.15 | 1.86 | 373.15 | 0.51 |

*Source:* Lide, D. R., ed. *Handbook of Chemistry and Physics.* 83rd ed. Boca Raton, FL: CRC Press, 2002.

and

$$\Delta T_b = \frac{RM_{solvent}T^2_{vaporization}}{\Delta H_{vaporization}}m_{solute} = K_b m_{solute} \tag{9.35}$$

Because $\Delta H_{vaporization} > \Delta H_{fusion}$, it follows that $K_f > K_b$. Typically, $K_b$ values range between 0.5 and 5.0 K/(mol kg$^{-1}$) as shown in Table 9.2. Note also that, by convention, both $K_f$ and $K_b$ are positive; hence the negative sign in Equation (9.33) is replaced by a positive sign in Equation (9.35).

## EXAMPLE PROBLEM 9.6

In this example, 4.50 g of a substance dissolved in 125 g of $CCl_4$ leads to an elevation of the boiling point of 0.650 K. Calculate the freezing point depression, the molar mass of the substance, and the factor by which the vapor pressure of $CCl_4$ is lowered.

### Solution

$$\Delta T_f = \left(\frac{K_f}{K_b}\right)\Delta T_b = -\frac{30. \text{ K/(mol kg}^{-1})}{4.95 \text{ K/(mol kg}^{-1})} \times 0.650 \text{ K} = -3.9 \text{ K}$$

To avoid confusion, we use the symbol $m$ for molality and $\mathbf{m}$ for mass. We solve for the molar mass $M_{solute}$ using Equation (9.35):

$$\Delta T_b = K_b m_{solute} = K_b \times \left(\frac{\mathbf{m}_{solute}/M_{solute}}{\mathbf{m}_{solvent}}\right)$$

$$M_{solute} = \frac{K_b \mathbf{m}_{solute}}{\mathbf{m}_{solvent}\Delta T_b}$$

$$M_{solute} = \frac{4.95 \text{ K kg mol}^{-1} \times 4.50 \text{ g}}{0.125 \text{ kg} \times 0.650 \text{ K}} = 274 \text{ g mol}^{-1}$$

We solve for the factor by which the vapor pressure of the solvent is reduced by using Raoult's law:

$$\frac{P_{solvent}}{P^*_{solvent}} = x_{solvent} = 1 - x_{solute} = 1 - \frac{n_{solute}}{n_{solute} + n_{solvent}}$$

$$= 1 - \frac{\dfrac{4.50 \text{ g}}{274 \text{ g mol}^{-1}}}{\left(\dfrac{4.50 \text{ g}}{274 \text{ g mol}^{-1}}\right) + \left(\dfrac{125 \text{ g}}{153.8 \text{ g mol}^{-1}}\right)} = 0.980$$

# 9.8 The Osmotic Pressure
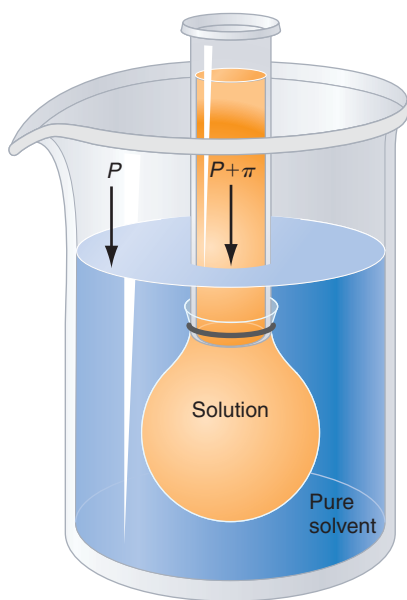


**FIGURE 9.12**
An osmotic pressure arises if a solution containing a solute that cannot pass through the membrane boundary is immersed in the pure solvent.

Some membranes allow the passage of small molecules like water, yet do not allow larger molecules like sucrose to pass through them. Such a **semipermeable membrane** is an essential component in medical technologies such as kidney dialysis, which is described later. If a sac of such a membrane containing a solute that cannot pass through the membrane is immersed in a beaker containing the pure solvent, then initially the solvent diffuses into the sac. Diffusion ceases when equilibrium is attained, and at equilibrium the pressure is higher in the sac than in the surrounding solvent. This result is shown schematically in Figure 9.12. The process in which the solvent diffuses through a membrane and dilutes a solution is known as **osmosis.** The amount by which the pressure in the solution is raised is known as the **osmotic pressure.**

To understand the origin of the osmotic pressure, denoted by $\pi$, the equilibrium condition is applied to the contents of the sac and the surrounding solvent:

$$\mu_{solvent}^{solution}(T, P + \pi, x_{solvent}) = \mu_{solvent}^{*}(T, P) \tag{9.36}$$

Using Raoult's law to express the concentration dependence of $\mu_{solvent}$,

$$\mu_{solvent}^{solution}(T, P + \pi, x_{solvent}) = \mu_{solvent}^{*}(T, P + \pi) + RT \ln x_{solvent} \tag{9.37}$$

Because $\mu$ for the solvent is lower in the solution than in the pure solvent, only an increased pressure in the solution can raise its $\mu$ sufficiently to achieve equilibrium with the pure solvent. The dependence of $\mu$ on pressure and temperature is given by $d\mu = dG_m = V_m dP - S_m dT$. At constant $T$ we can write

$$\mu_{solvent}^{*}(T, P + \pi, x_{solvent}) - \mu_{solvent}^{*}(T, P) = \int_{P}^{P+\pi} V_m^{*} dP' \tag{9.38}$$

where $V_m^{*}$ is the molar volume of the pure solvent and $P$ is the pressure in the solvent outside the sac. Because a liquid is nearly incompressible, it is reasonable to assume that $V_m^{*}$ is independent of $P$ to evaluate the integral in the previous equation. Therefore, $\mu_{solvent}^{*}(T, P + \pi, x_{solvent}) - \mu_{solvent}^{*}(T, P) = V_m^{*}\pi$, and Equation (9.37) reduces to

$$\pi V_m^{*} + RT \ln x_{solvent} = 0 \tag{9.39}$$

For a dilute solution, $n_{solvent} \gg n_{solute}$, and

$$\ln x_{solvent} = \ln(1 - x_{solute}) \approx -x_{solute} = -\frac{n_{solute}}{n_{solute} + n_{solvent}} \approx -\frac{n_{solute}}{n_{solvent}} \tag{9.40}$$

Equation (9.39) can be simplified further by recognizing that for a dilute solution, $V \approx n_{solvent}V_m^{*}$. With this substitution, Equation (9.39) becomes

$$\pi = \frac{n_{solute} RT}{V} \tag{9.41}$$

which is known as the **van't Hoff equation.** Note the similarity in form between this equation and the ideal gas law.

An important application of the selective diffusion of the components of a solution through a membrane is dialysis. In healthy individuals, the kidneys remove waste products from the bloodstream, whereas individuals with damaged kidneys use a dialysis machine for this purpose. Blood from the patient is shunted through tubes made of a selectively porous membrane surrounded by a flowing sterile solution made up of water, sugars, and other components. Blood cells and other vital components of blood are too large to fit through the pores in the membranes, but urea and salt flow out of the bloodstream through membranes into the sterile solution and are removed as waste.

### EXAMPLE PROBLEM 9.7

Calculate the osmotic pressure generated at 298 K if a cell with a total solute concentration of 0.500 mol $L^{-1}$ is immersed in pure water. The cell wall is permeable to water molecules, but not to the solute molecules.

#### Solution

$$\pi = \frac{n_{solute} RT}{V} = 0.500 \text{ mol L}^{-1} \times 8.206 \times 10^{-2} \text{ L atm K}^{-1} \text{ mol}^{-1} \times 298 \text{ K}$$

$$= 12.2 \text{ atm}$$

As this calculation shows, the osmotic pressure generated for moderate solute concentrations can be quite high. Hospital patients have died after pure water has accidentally been injected into their blood vessels, because the osmotic pressure is sufficient to burst the walls of blood cells.

Plants use osmotic pressure to achieve mechanical stability in the following way. A plant cell is bounded by a cellulose cell wall that is permeable to most components of the aqueous solutions that it encounters. A semipermeable cell membrane through which water, but not solute molecules, can pass is located just inside the cell wall. When the plant has sufficient water, the cell membrane expands, pushing against the cell wall, which gives the plant stalk a high rigidity. However, if there is a drought, the cell membrane is not totally filled with water and it moves away from the cell wall. As a result, only the cell wall contributes to the rigidity, and plants droop under these conditions.

Another important application involving osmotic pressure is the desalination of seawater using reverse osmosis. Seawater is typically 1.1 molar in NaCl. Equation (9.41) shows that an osmotic pressure of 27 bar is needed to separate the solvated $Na^+$ and $Cl^-$ ions from the water. If the seawater side of the membrane is subjected to a pressure greater than 27 bar, $H_2O$ from the seawater will flow through the membrane, resulting in a separation of pure water from the seawater. This process is called reverse osmosis. The challenge in carrying out reverse osmosis on the industrial scale needed to provide a coastal city with potable water is to produce robust membranes that accommodate the necessary flow rates without getting fouled by algae and also effectively separate the ions from the water. The mechanism that prevents passage of the ions through suitable membranes is not fully understood. It is not based on the size of pores within the membrane alone and involves charged surfaces within the hydrated pores. These membrane-anchored ions repel the mobile $Na^+$ and $Cl^-$ ions, while allowing the passage of the neutral water molecule.

# 9.9 Real Solutions Exhibit Deviations from Raoult's Law

In Sections 9.1 through 9.8, the discussion has been limited to ideal solutions. However, in general, if two volatile and miscible liquids are combined to form a solution, Raoult's law is not obeyed. This is the case because the A–A, B–B, and A–B interactions in a binary solution of A and B are in general not equal. If the A–B interactions are less (more) attractive than the A–A and B–B interactions, positive (negative) deviations from Raoult's law will be observed. An example of a binary solution with positive deviations from Raoult's law is $CS_2$–acetone. Experimental data for this system are shown in Table 9.3 and the data are plotted in Figure 9.13. How can a thermodynamic framework analogous to that presented for the ideal solution in Section 9.2 be developed for real solutions? This issue is addressed throughout the rest of this chapter.

Figure 9.13 shows that the partial and total pressures above a real solution can differ substantially from the behavior predicted by Raoult's law. Another way that ideal and real solutions differ is that the set of equations denoted in Equation (9.8), which describes the change in volume, entropy, enthalpy, and Gibbs energy that results from mixing, are not applicable to real solutions. For real solutions, these equations can only be written in a much less explicit form. Assuming that A and B are miscible,

$$\Delta G_{mixing} < 0$$
$$\Delta S_{mixing} > 0$$
$$\Delta V_{mixing} \neq 0$$
$$\Delta H_{mixing} \neq 0 \tag{9.42}$$

Whereas $\Delta G_{mixing} < 0$ and $\Delta S_{mixing} > 0$ always hold for miscible liquids, $\Delta V_{mixing}$ and $\Delta H_{mixing}$ can be positive or negative, depending on the nature of the A–B interaction in the solution.

**TABLE 9.3    Partial and Total Pressures above a CS₂–Acetone Solution**

| $x_{CS_2}$ | $P_{CS_2}$ (Torr) | $P_{acetone}$ (Torr) | $P_{total}$ (Torr) | $x_{CS_2}$ | $P_{CS_2}$ (Torr) | $P_{acetone}$ (Torr) | $P_{total}$ (Torr) |
|---|---|---|---|---|---|---|---|
| 0 | 0 | 343.8 | 343.8 | 0.4974 | 404.1 | 242.1 | 646.2 |
| 0.0624 | 110.7 | 331.0 | 441.7 | 0.5702 | 419.4 | 232.6 | 652.0 |
| 0.0670 | 119.7 | 327.8 | 447.5 | 0.5730 | 420.3 | 232.2 | 652.5 |
| 0.0711 | 123.1 | 328.8 | 451.9 | 0.6124 | 426.9 | 227.0 | 653.9 |
| 0.1212 | 191.7 | 313.5 | 505.2 | 0.6146 | 427.7 | 225.9 | 653.6 |
| 0.1330 | 206.5 | 308.3 | 514.8 | 0.6161 | 428.1 | 225.5 | 653.6 |
| 0.1857 | 258.4 | 295.4 | 553.8 | 0.6713 | 438.0 | 217.0 | 655.0 |
| 0.1991 | 271.9 | 290.6 | 562.5 | 0.6713 | 437.3 | 217.6 | 654.9 |
| 0.2085 | 283.9 | 283.4 | 567.3 | 0.7220 | 446.9 | 207.7 | 654.6 |
| 0.2761 | 323.3 | 275.2 | 598.5 | 0.7197 | 447.5 | 207.1 | 654.6 |
| 0.2869 | 328.7 | 274.2 | 602.9 | 0.8280 | 464.9 | 180.2 | 645.1 |
| 0.3502 | 358.3 | 263.9 | 622.2 | 0.9191 | 490.7 | 123.4 | 614.1 |
| 0.3551 | 361.3 | 262.1 | 623.4 | 0.9242 | 490.0 | 120.3 | 610.3 |
| 0.4058 | 379.6 | 254.5 | 634.1 | 0.9350 | 491.9 | 109.4 | 601.3 |
| 0.4141 | 382.1 | 253.0 | 635.1 | 0.9407 | 492.0 | 103.5 | 595.5 |
| 0.4474 | 390.4 | 250.2 | 640.6 | 0.9549 | 496.2 | 85.9 | 582.1 |
| 0.4530 | 394.2 | 247.6 | 641.8 | 0.9620 | 500.8 | 73.4 | 574.2 |
| 0.4933 | 403.2 | 242.8 | 646.0 | 0.9692 | 502.0 | 62.0 | 564.0 |
|  |  |  |  | 1 | 512.3 | 0 | 512.3 |

*Source:* Zawidski, J. v. *Zeitschrift für Physikalische Chemie* 35 (1900): 129.

As indicated in Equation (9.42), the volume change upon mixing is not generally 0. Therefore, the volume of a solution will not be given by

$$V_m^{ideal} = x_A V_{m,A}^* + (1 - x_A) V_{m,B}^* \tag{9.43}$$

as expected for 1 mol of an ideal solution, where $V_{m,A}^*$ and $V_{m,B}^*$ are the molar volumes of the pure substances A and B. Figure 9.14 shows $\Delta V_m = V_m^{real} - V_m^{ideal}$ for an acetone–chloroform solution as a function of $x_{chloroform}$. Note that $\Delta V_m$ can be positive or negative for this solution, depending on the value of $x_{chloroform}$. The deviations from ideality are small but are clearly evident.
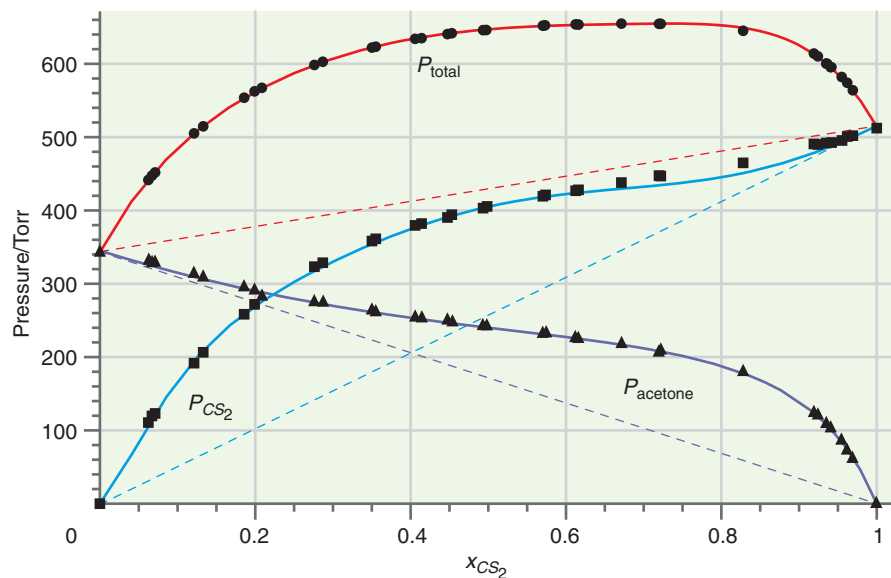


**FIGURE 9.13**
The data in Table 9.3 are plotted versus $x_{CS_2}$. The dashed lines show the expected behavior if Raoult's law were obeyed.
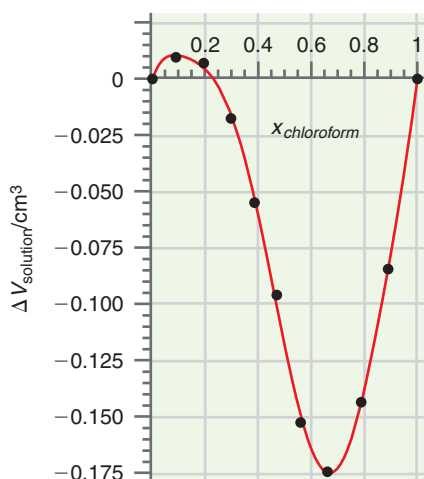
**FIGURE 9.14**
Deviations in the volume from the behavior expected for 1 mol of an ideal solution [Equation (9.43)] are shown for the acetone–chloroform system as a function of the mole fraction of chloroform.

The deviation of the volume from ideal behavior can best be understood by defining the concept of **partial molar quantities.** This concept is illustrated by discussing the **partial molar volume.** The volume of 1 mol of pure water at 25°C is 18.1 cm³. However, if 1 mol of water is added to a large volume of an ethanol–water solution with $x_{H_2O} = 0.75$, the volume of the solution increases by only 16 cm³. This is the case because the local structure around a water molecule in the solution is more compact than in pure water. The partial molar volume of a component in a solution is defined as the volume by which the solution changes if 1 mol of the component is added to such a large volume that the solution composition can be assumed constant. This statement is expressed mathematically in the following form:

$$\overline{V}_1(P, T, n_1, n_2) = \left(\frac{\partial V}{\partial n_1}\right)_{P, T, n_2} \tag{9.44}$$

With this definition, the volume of a binary solution is given

$$V = n_1 \overline{V}_1(P, T, n_1, n_2) + n_2 \overline{V}_2(P, T, n_1, n_2) \tag{9.45}$$

Note that because the partial molar volumes depend on the concentration of all components, the same is true of the total volume.

One can form partial molar quantities for any extensive property of a system (for example $U$, $H$, $G$, $A$, and $S$). Partial molar quantities (other than the chemical potential, which is the partial molar Gibbs energy) are usually denoted by the appropriate symbol topped by a horizontal bar. The partial molar volume is a function of $P$, $T$, $n_1$, and $n_2$, and $\overline{V}_i$ can be greater than or less than the molar volume of the pure component. Therefore, the volume of a solution of two miscible liquids can be greater than or less than the sum of the volumes of the pure components of the solution. Figure 9.15 shows data for the partial volumes of acetone and chloroform in an acetone–chloroform binary solution at 298 K. Note that the changes in the partial molar volumes with concentration are small, but not negligible.

In Figure 9.15, we can see that $\overline{V}_1$ increases if $\overline{V}_2$ decreases and vice versa. This is the case because partial molar volumes are related in the same way as the chemical potentials are related in the Gibbs–Duhem equation [Equation (9.23)]. In terms of the partial molar volumes, the Gibbs–Duhem equation takes the form

$$x_1 \, d\overline{V}_1 + x_2 \, d\overline{V}_2 = 0 \quad \text{or} \quad d\overline{V}_1 = -\frac{x_2}{x_1} d\overline{V}_2 \tag{9.46}$$

Therefore, as seen in Figure 9.15, if $\overline{V}_2$ changes by an amount $d\overline{V}_2$ over a small concentration interval, $\overline{V}_1$ will change in the opposite direction. The Gibbs–Duhem equation is applicable to both ideal and real solutions.
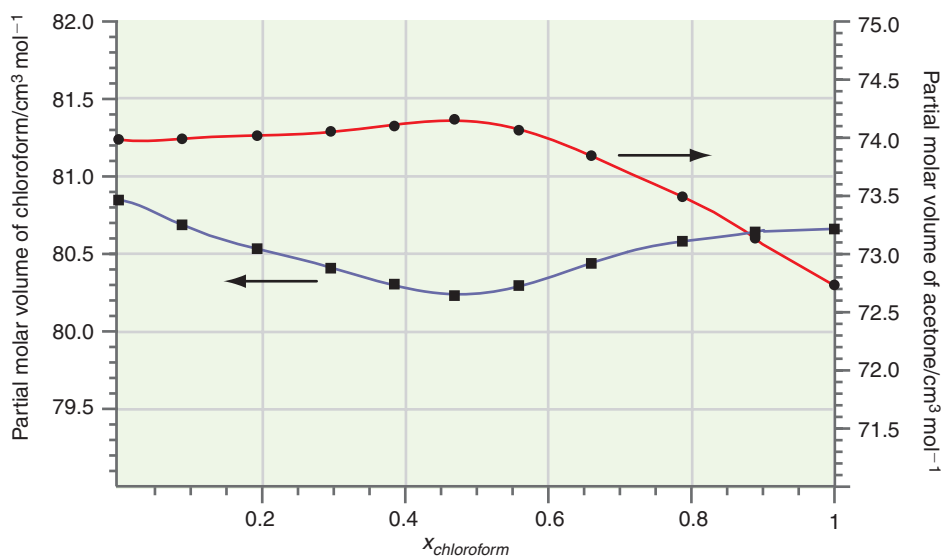


**FIGURE 9.15**
The partial molar volumes of chloroform (blue curve) and acetone (red curve) in a chloroform–acetone binary solution are shown as a function of $x_{chloroform}$.

# 9.10 The Ideal Dilute Solution

Although no simple model exists that describes all real solutions, there is a limiting law that merits further discussion. In this section, we describe the model of the ideal dilute solution, which provides a useful basis for describing the properties of real solutions if they are dilute. Just as for an ideal solution, at equilibrium the chemical potentials of a component in the gas and solution phase of a real solution are equal. As for an ideal solution, the chemical potential of a component in a real solution can be separated into two terms, a standard state chemical potential and a term that depends on the partial pressure.

$$\mu_i^{solution} = \mu_i^* + RT \ln \frac{P_i}{P_i^*} \tag{9.47}$$

Recall that for a pure substance $\mu_i^*(\text{vapor}) = \mu_i^*(\text{liquid}) = \mu_i^*$. Because the solution is not ideal, $P_i \neq x_i P_i^*$.

First consider only the solvent in a dilute binary solution. To arrive at an equation for $\mu_i^{solution}$ that is similar to Equation (9.7) for an ideal solution, we define the dimensionless **activity,** $a_{solvent,}$ of the solvent by

$$a_{solvent} = \frac{P_{solvent}}{P_{solvent}^*} \tag{9.48}$$

Note that $a_{solvent} = x_{solvent}$ for an ideal solution. For a nonideal solution, the activity and the mole fraction are related through the **activity coefficient** $\gamma_{solvent}$, defined by

$$\gamma_{solvent} = \frac{a_{solvent}}{x_{solvent}} \tag{9.49}$$

The activity coefficient quantifies the degree to which the solution is nonideal. The activity plays the same role for a component of a solution that the fugacity plays for a real gas in expressing deviations from ideal behavior. In both cases, ideal behavior is observed in the appropriate limit, namely, $P \rightarrow 0$ for the gas, and $x_{solute} \rightarrow 0$ for the solution. To the extent that there is no atomic-scale model that tells us how to calculate $\gamma$, it should be regarded as a correction factor that exposes the inadequacy of our model, rather than as a fundamental quantity. As will be discussed in Chapter 10, there is such an atomic-scale model for dilute electrolyte solutions.

How is the chemical potential of a component related to its activity? Combining Equations (9.47) and (9.48), one obtains a relation that holds for all components of a real solution:

$$\mu_i^{solution} = \mu_i^* + RT \ln a_i \tag{9.50}$$

Equation (9.50) is a central equation in describing real solutions. It is the starting point for the discussion in the rest of this chapter.

The preceding discussion focused on the solvent in a dilute solution. However, the ideal dilute solution is defined by the conditions $x_{solute} \rightarrow 0$ and $x_{solvent} \rightarrow 1$. Because the solvent and solute are considered in different limits, we use different expressions to relate the mole fraction of a component and the partial pressure of the component above the solution.

Consider the partial pressure of acetone as a function of $x_{CS_2}$ shown in Figure 9.16. Although Raoult's law is not obeyed over the whole concentration range, it is obeyed in the limit that $x_{acetone} \rightarrow 1$ and $x_{CS_2} \rightarrow 0$. In this limit, the average acetone molecule at the surface of the solution is surrounded by acetone molecules. Therefore, to a good approximation, $P_{acetone} = x_{acetone} P_{acetone}^*$ as $x_{acetone} \rightarrow 1$. Because the majority species is defined to be the solvent, we see that Raoult's law is obeyed for the solvent in a dilute solution. This limiting behavior is also observed for $CS_2$ *in the limit in which it is the solvent,* as seen in Figure 9.13.

Consider the opposite limit in which $x_{acetone} \rightarrow 0$. In this case, the average acetone molecule at the surface of the solution is surrounded by $CS_2$ molecules. Therefore, the

**FIGURE 9.16**
The partial pressure of acetone from
Table 9.3 is plotted as a function of $x_{CS_2}$.
Note that the $P_{acetone}$ follows Raoult's
law as $x_{CS_2} \to 0$, and Henry's law as
$x_{CS_2} \to 1$.
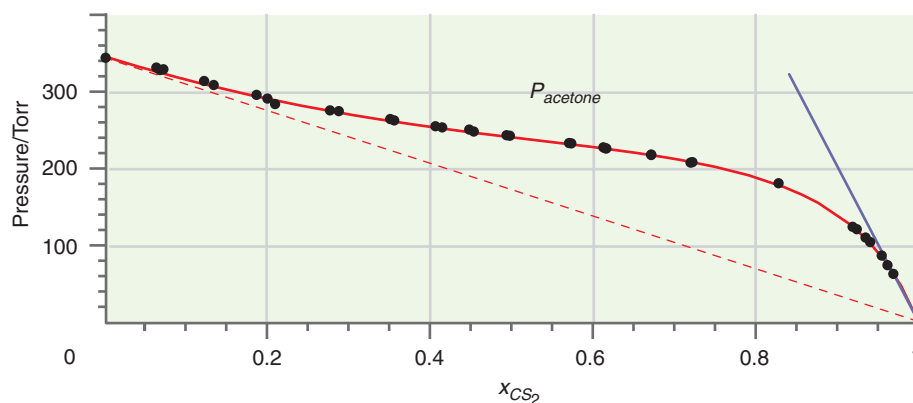


molecule experiences very different interactions with its neighbors than if it were
surrounded by acetone molecules. For this reason, $P_{acetone} \neq x_{acetone} P^*_{acetone}$ as
$x_{acetone} \to 0$. However, it is apparent from Figure 9.16 that $P_{acetone}$ also varies linearly
with $x_{acetone}$ in this limit. This behavior is described by the following equation:

$$P_{acetone} = x_{acetone}\, k_H^{acetone} \text{ as } x_{acetone} \to 0 \qquad (9.51)$$

This relationship is known as **Henry's law,** and the constant $k_H$ is known as the
**Henry's law constant.** The value of the constant depends on the nature of the solute
and solvent and quantifies the degree to which deviations from Raoult's law occur. As
the solution approaches ideal behavior, $k_H^i \to P_i^*$. For the data shown in Figure 9.13,
$k_H^{CS_2} = 1750$ Torr and $k_H^{acetone} = 1950$ Torr. Note that these values are substantially
greater than the vapor pressures of the pure substances, which are 512.3 and 343.8 Torr,
respectively. The Henry's law constants are less than the vapor pressures of the pure
substances if the system exhibits negative deviations from Raoult's law. Henry's law
constants for aqueous solutions are listed for a number of solutes in Table 9.4.

Based on these results, the **ideal dilute solution** is defined. *An ideal dilute
solution is a solution in which the solvent is described using Raoult's law and the
solute is described using Henry's law.* As shown by the data in Figure 9.13, the partial
pressures above the $CS_2$–acetone mixture are consistent with this model in either of
two limits, $x_{acetone} \to 1$ or $x_{CS_2} \to 1$. In the first of these limits, we consider acetone to
be the solvent and $CS_2$ to be the solute. Acetone is the solute and $CS_2$ is the solvent in
the second limit.

**TABLE 9.4   Henry's Law Constants for Aqueous Solutions Near 298 K**

| Substance | $k_H$ (Torr) | $k_H$ (bar) |
|---|---|---|
| Ar | $2.80 \times 10^7$ | $3.72 \times 10^4$ |
| $C_2H_6$ | $2.30 \times 10^7$ | $3.06 \times 10^4$ |
| $CH_4$ | $3.07 \times 10^7$ | $4.08 \times 10^4$ |
| CO | $4.40 \times 10^6$ | $5.84 \times 10^3$ |
| $CO_2$ | $1.24 \times 10^6$ | $1.65 \times 10^3$ |
| $H_2S$ | $4.27 \times 10^5$ | $5.68 \times 10^2$ |
| He | $1.12 \times 10^8$ | $1.49 \times 10^6$ |
| $N_2$ | $6.80 \times 10^7$ | $9.04 \times 10^4$ |
| $O_2$ | $3.27 \times 10^7$ | $4.95 \times 10^4$ |

*Source*: Alberty, R. A., and Silbey, R. S. *Physical Chemistry.* New York: John Wiley & Sons, 1992.

# 9.11 Activities Are Defined with Respect to Standard States

The ideal dilute solution model's predictions that Raoult's law is obeyed for the solvent and Henry's law is obeyed for the solute are not valid over a wide range of concentration. The concept of the activity coefficient introduced in Section 9.10 is used to quantify these deviations. In doing so, it is useful to define the activities in such a way that the solution approaches ideal behavior in the limit of interest, which is generally $x_A \to 0$, or $x_A \to 1$. With this choice, the activity approaches the concentration, and it is reasonable to set the activity coefficient equal to 1. Specifically, $a_i \to x_i$ as $x_i \to 1$ for the solvent, and $a_i \to x_i$ as $x_i \to 0$ for the solute. The reason for this choice is that numerical values for activity coefficients are generally not known. Choosing the standard state as described earlier ensures that the concentration (divided by the unit concentration to make it dimensionless), which is easily measured, is a good approximation to the activity.

In Section 9.10 the activity and activity coefficient for the solvent in a dilute solution ($x_{solvent} \to 1$) were defined by the relations

$$a_i = \frac{P_i}{P_i^*} \quad \text{and} \quad \gamma_i = \frac{a_i}{x_i} \tag{9.52}$$

As shown in Figure 9.13, the activity approaches unity as $x_{solvent} \to 1$. We refer to an activity calculated using Equation (9.52) as being based on a **Raoult's law standard state.** The standard state chemical potential based on Raoult's law is $\mu_{solvent}^*$, which is the chemical potential of the pure solvent.

However, this definition of the activity and choice of a standard state is not optimal for the solute at a low concentration, because the solute obeys Henry's law rather than Raoult's law and, therefore, the activity coefficient will differ appreciably from one. In this case,

$$\mu_{solute}^{solution} = \mu_{solute}^* + RT \ln\frac{k_H^{solute} x_{solute}}{P_{solute}^*} = \mu_{solute}^{*H} + RT \ln x_{solute} \text{ as } x_{solute} \to 0 \tag{9.53}$$

The standard state chemical potential is the value of the chemical potential when $x_i = 1$. We see that the Henry's law standard state chemical potential is given by

$$\mu_{solute}^{*H} = \mu_{solute}^* + RT \ln\frac{k_H^{solute}}{P_{solute}^*} \tag{9.54}$$

The activity and activity coefficient based on Henry's law are defined, respectively, by

$$a_i = \frac{P_i^H}{k_i^H} \text{ and } \gamma_i = \frac{a_i}{x_i} \tag{9.55}$$

We note that Henry's law is still obeyed for a solute that has such a small vapor pressure that we refer to it as a nonvolatile solute.

The **Henry's law standard state** is a state in which the pure solute has a vapor pressure $k_{H, solute}$ rather than its actual value $P_{solute}^*$. It is a hypothetical state that does not exist. Recall that the value $k_{H, solute}$ is obtained by extrapolation from the low coverage range in which Henry's law is obeyed. Although this definition may seem peculiar, only in this way can we ensure that $a_{solute} \to x_{solute}$ and $\gamma_{solute} \to 1$ as $x_{solute} \to 0$. We reiterate the reason for this choice. If the preceding conditions are satisfied, the concentration (divided by the unit concentration to make it dimensionless) is, to a good approximation, equal to the activity. Therefore, equilibrium constants for reactions in solution can be calculated without having numerical values for activity coefficients. We emphasize the difference in the Raoult's law and Henry's law standard states because it is the standard state chemical potentials $\mu_{solute}^*$ and $\mu_{solute}^{*H}$ that are used to

calculate $\Delta G°$ and the thermodynamic equilibrium constant $K$. Different choices for standard states will result in different numerical values for $K$. The standard chemical potential $\mu_{solute}^{*H}$ refers to the hypothetical standard state in which $x_{solute} = 1$, and each solute species is in an environment characteristic of the infinitely dilute solution.

We now consider a less well-defined situation. For solutions in which the components are miscible in all proportions, such as the $CS_2$−acetone system, either a Raoult's law or a Henry's law standard state can be defined, as we show with sample calculations in Example Problems 9.8 and 9.9. This is the case because there is no unique choice for the standard state over the entire concentration range in such a system. Numerical values for the activities and activity coefficients will differ, depending on whether the Raoult's law or the Henry's law standard state is used.

### EXAMPLE PROBLEM 9.8

Calculate the activity and activity coefficient for $CS_2$ at $x_{CS_2} = 0.3502$ using data from Table 9.3. Assume a Raoult's law standard state.

**Solution**

$$a_{CS_2}^R = \frac{P_{CS_2}}{P_{CS_2}^*} = \frac{358.3 \text{ Torr}}{512.3 \text{ Torr}} = 0.6994$$

$$\gamma_{CS_2}^R = \frac{a_{CS_2}^R}{x_{CS_2}} = \frac{0.6994}{0.3502} = 1.997$$

The activity and activity coefficients for $CS_2$ are concentration dependent. Results calculated as in Example Problem 9.8 using a Raoult's law standard state are shown in Figure 9.17 as a function of $x_{CS_2}$. For this solution, $\gamma_{CS_2}^R > 1$ for all values of the concentration for which $x_{CS_2} < 1$. Note that $\gamma_{CS_2}^R \to 1$ as $x_{CS_2} \to 1$ as the model requires. The activity and activity coefficients for $CS_2$ using a Henry's law standard state are shown in Figure 9.18 as a function of $x_{CS_2}$. For this solution, $\gamma_{CS_2}^H < 1$ for all values of the concentration for which $x_{CS_2} > 0$. Note that $\gamma_{CS_2}^H \to 1$ as $x_{CS_2} \to 0$ as the model requires. Which of these two possible standard states should be chosen? There is a good answer to this question only in the limits $x_{CS_2} \to 0$ or $x_{CS_2} \to 1$. For intermediate concentrations, either standard state can be used.

### EXAMPLE PROBLEM 9.9

Calculate the activity and activity coefficient for $CS_2$ at $x_{CS_2} = 0.3502$ using data from Table 9.3. Assume a Henry's law standard state.

**Solution**

$$a_{CS_2}^H = \frac{P_{CS_2}}{k_{H,CS_2}} = \frac{358.3 \text{ Torr}}{1750 \text{ Torr}} = 0.204$$

$$\gamma_{CS_2}^H = \frac{a_{CS_2}^H}{x_{CS_2}} = \frac{0.204}{0.3502} = 0.584$$

The Henry's law standard state just discussed is defined with respect to concentration measured in units of the mole fraction. This is not a particularly convenient scale, and either the molarity or molality concentration scales are generally used in laboratory experiments. The mole fraction of the solute can be converted to the molality scale by dividing the first expression in Equation (9.56) by $n_{solvent} M_{solvent}$:

$$x_{solute} = \frac{n_{solute}}{n_{solvent} + n_{solute}} = \frac{m_{solute}}{\dfrac{1}{M_{solvent}} + m_{solute}} \tag{9.56}$$



**FIGURE 9.17**

The activity and activity coefficient for $CS_2$ in a $CS_2$−acetone solution based on a Raoult's law standard state are shown as a function of $x_{CS_2}$.

where $m_{solute}$ is the molality of the solute, and $M_{solvent}$ is the molar mass of the solvent in kg mol$^{-1}$. We see that $m_{solute} \rightarrow x_{solute}/M_{solvent}$ as $x_{solute} \rightarrow 0$. Using molality as the concentration unit, the activity and activity coefficient of the solute are defined by

$$a_{solute}^{molality} = \frac{P_{solute}}{k_H^{molality}} \quad \text{with} \quad a_{solute}^{molality} \rightarrow m_{solute} \quad \text{as} \quad m_{solute} \rightarrow 0 \quad \text{and} \quad \textbf{(9.57)}$$

$$\gamma_{solute}^{molality} = \frac{a_{solute}^{molality}}{m_{solute}} \quad \text{with} \quad \gamma_{solute}^{molality} \rightarrow 1 \quad \text{as} \quad m_{solute} \rightarrow 0 \quad \textbf{(9.58)}$$

The Henry's law constants and activity coefficients determined on the mole fraction scale must be recalculated to describe a solution characterized by its molality or molarity. Example Problem 9.10 shows the conversion from mole fraction to molarity; similar conversions can be made if the concentration of the solution is expressed in terms of molality.

What is the standard state if concentrations rather than mole fractions are used? The standard state in this case is the hypothetical state in which Henry's law is obeyed by a solution that is 1.0 molar (or 1.0 molal) in the solute concentration. It is a hypothetical state because at this concentration, substantial deviations from Henry's law will be observed. Although this definition may seem peculiar at first reading, only in this way can we ensure that the activity becomes equal to the molarity (or molality), and the activity coefficient approaches 1, as the solute concentration approaches 0.

## EXAMPLE PROBLEM 9.10

a. Derive a general equation, valid for dilute solutions, relating the Henry's law constants for the solute on the mole fraction and molarity scales.

b. Determine the Henry's law constants for acetone on the molarity scale. Use the results for the Henry's law constants on the mole fraction scale cited in Section 9.10. The density of acetone is 789.9 g L$^{-1}$.

### Solution

a. We use the symbol $c_{solute}$ to designate the solute molarity, and $c°$ to indicate a 1 molar concentration.

$$\frac{dP}{d\left(\dfrac{c_{solute}}{c°}\right)} = \frac{dP}{dx_{solute}} \frac{dx_{solute}}{d\left(\dfrac{c_{solute}}{c°}\right)}$$

To evaluate this equation, we must determine

$$\frac{dx_{solute}}{d\left(\dfrac{c_{solute}}{c°}\right)}$$

$$x_{solute} = \frac{n_{solute}}{n_{solute} + n_{solvent}} \approx \frac{n_{solute}}{n_{solvent}} = \frac{n_{solute} M_{solvent}}{V_{solution} \rho_{solution}} = c_{solute} \frac{M_{solvent}}{\rho_{solution}}$$

Therefore,

$$\frac{dP}{d\left(\dfrac{c_{solute}}{c°}\right)} = \frac{c° M_{solvent}}{\rho_{solution}} \frac{dP}{dx_{solute}}$$

b. $$\frac{dP}{d\left(\dfrac{c_{solute}}{c°}\right)} = \frac{1 \text{ mol L}^{-1} \times 58.08 \text{ g mol}^{-1}}{789.9 \text{ g L}^{-1}} \times 1950 \text{ Torr} = 143.4 \text{ Torr}$$

The colligative properties discussed for an ideal solution in Sections 9.7 and 9.8 refer to the properties of the solvent in a dilute solution. The Raoult's law standard state
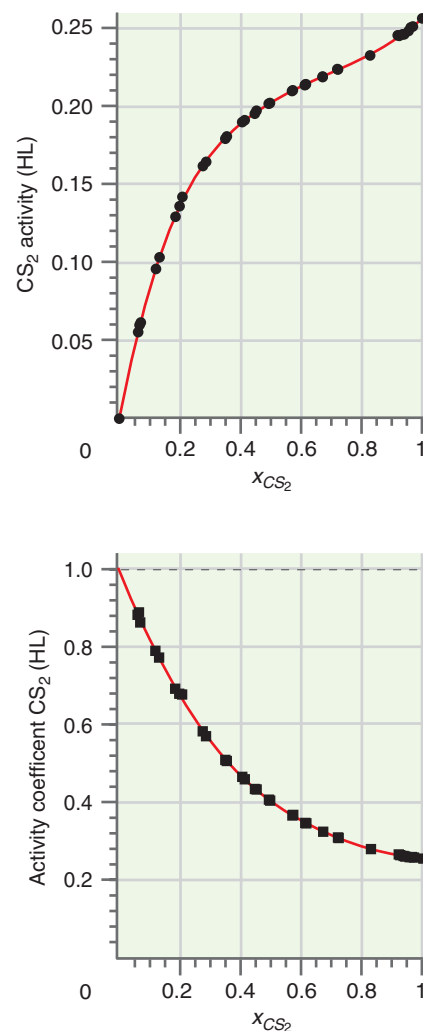


**FIGURE 9.18**
The activity and activity coefficient for $CS_2$ in a $CS_2-$acetone solution based on a Henry's law standard state are shown as a function of $x_{CS_2}$.

applies to this case and in an ideal dilute solution, Equations (9.33), (9.35) and (9.41) can be used with activities replacing concentrations:

$$\Delta T_f = -K_f \gamma m_{solute}$$

$$\Delta T_b = K_b \gamma m_{solute}$$

$$\pi = \gamma c_{solute} RT \tag{9.59}$$

The activity coefficients are defined with respect to molality for the boiling point elevation $\Delta T_b$ and freezing point depression $\Delta T_f$, and with respect to molarity for the osmotic pressure $\pi$. Equations (9.59) provide a useful way to determine activity coefficients as shown in Example Problem 9.11.

---

**EXAMPLE PROBLEM 9.11**

In 500. g of water, 24.0 g of a nonvolatile solute of molecular weight 241 g mol$^{-1}$ is dissolved. The observed freezing point depression is 0.359°C. Calculate the activity coefficient of the solute.

**Solution**

$$\Delta T_f = -K_f \gamma m_{solute}; \quad \gamma = -\frac{\Delta T_f}{K_f m_{solute}}$$

$$\gamma = \frac{0.359 \text{ K}}{1.86 \text{ K kg mol}^{-1} \times \dfrac{24.0}{241 \times 0.500} \text{ mol kg}^{-1}} = 0.969$$

---

# 9.12 Henry's Law and the Solubility of Gases in a Solvent

The ideal dilute solution model can be applied to the solubility of gases in liquid solvents. An example for this type of solution equilibrium is the amount of $N_2$ absorbed by water at sea level, which is considered in Example Problem 9.12. In this case, one of the components of the solution is a liquid and the other is a gas. The equilibrium of interest between the solution and the vapor phase is

$$N_2(\text{aqueous}) \rightleftharpoons N_2(\text{vapor}) \tag{9.60}$$
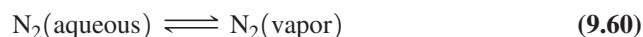
The chemical potential of the dissolved $N_2$ is given by

$$\mu_{N_2}^{solution} = \mu_{N_2}^{*H}(\text{vapor}) + RT \ln a_{solute} \tag{9.61}$$

In this case, a Henry's law standard state is the appropriate choice because the nitrogen is sparingly soluble in water. The mole fraction of $N_2$ in solution, $x_{N_2}$, is given by

$$x_{N_2} = \frac{n_{N_2}}{n_{N_2} + n_{H_2O}} \approx \frac{n_{N_2}}{n_{H_2O}} \tag{9.62}$$

The amount of dissolved gas is given by

$$n_{N_2} = n_{H_2O} x_{N_2} = n_{H_2O} \frac{P_{N_2}}{k_H^{N_2}} \tag{9.63}$$

Example Problem 9.12 shows how Equation (9.63) is used to model the dissolution of a gas in a liquid.

The average human with a body weight of 70. kg has a blood volume of 5.00 L. The Henry's law constant for the solubility of $N_2$ in $H_2O$ is $9.04 \times 10^4$ bar at 298 $K$. Assume that this is also the value of the Henry's law constant for blood and that the density of blood is 1.00 kg $L^{-1}$.

a. Calculate the number of moles of nitrogen absorbed in this amount of blood in air of composition 80.% $N_2$ at sea level, where the pressure is 1 bar, and at a pressure of 50. bar.

b. Assume that a diver accustomed to breathing compressed air at a pressure of 50. bar is suddenly brought to sea level. What volume of $N_2$ gas is released as bubbles in the diver's bloodstream?

**Solution**

$$n_{N_2} = n_{H_2O} \frac{P_{N_2}}{k_H^{N_2}}$$

a. $$= \frac{5.0 \times 10^3 g}{18.02 \text{ g mol}^{-1}} \times \frac{0.80 \text{ bar}}{9.04 \times 10^4 \text{ bar}}$$

$$= 2.5 \times 10^{-3} \text{ mol at 1 bar total pressure}$$

At 50. bar, $n_{N_2} = 50. \times 2.5 \times 10^{-3} \text{ mol} = 0.13 \text{ mol}$.

b. $$V = \frac{nRT}{P}$$

$$= \frac{(0.13 \text{ mol} - 2.5 \times 10^{-3} \text{ mol}) \times 8.314 \times 10^{-2} \text{ L bar mol}^{-1} \text{ K}^{-1} \times 300. \text{ K}}{1.00 \text{ bar}}$$

$$= 3.2 \text{ L}$$

The symptoms induced by the release of air into the bloodstream are known to divers as the bends. The volume of $N_2$ just calculated is far more than is needed to cause the formation of arterial blocks due to gas-bubble embolisms.

# 9.13 Chemical Equilibrium in Solutions

The concept of activity can be used to express the thermodynamic equilibrium constant in terms of activities for real solutions. Consider a reaction between solutes in a solution. At equilibrium, the following relation must hold:

$$\left( \sum_j \nu_j \mu_j (\text{solution}) \right)_{equilibrium} = 0 \qquad (9.64)$$

where the subscript states that the individual chemical potentials must be evaluated under equilibrium conditions. Each of the chemical potentials in Equation (9.64) can be expressed in terms of a standard state chemical potential and a concentration-dependent term. Assume a Henry's law standard state for each solute. Equation (9.64) then takes the form

$$\sum_j \nu_j \mu_j^{*H}(\text{solution}) + RT \sum_j \ln (a_i^{eq})^{\nu_j} = 0 \qquad (9.65)$$

Using the relation between the Gibbs energy and the chemical potential, the previous equation can be written in the form

$$\Delta G_{reaction}^\circ = -RT \sum_j \ln (a_i^{eq})^{\nu_j} = -RT \ln K \qquad (9.66)$$

The equilibrium constant in terms of activities is given by

$$K = \prod_i (a_i^{eq})^{\nu_j} = \prod_i (\gamma_i^{eq})^{\nu_j} \left(\frac{c_i^{eq}}{c^\circ}\right)^{\nu_j} \tag{9.67}$$

where the symbol $\prod$ indicates that the terms following the symbol are multiplied with one another. It can be viewed as a generalization of $K_P$, defined in Equation (6.60) and can be applied to equilibria involving gases, liquids, dissolved species, and solids. For gases, the fugacities divided by $f^\circ$ (see Section 7.5) are the activities.

To obtain a numerical value for $K$, the standard state Gibbs reaction energy $\Delta G_R^\circ$ must be known. As for gas-phase reactions, the $\Delta G_R^\circ$ must be determined experimentally. This can be done by measuring the individual activities of the species in solution and calculating $K$ from these results. After a series of $\Delta G_R^\circ$ for different reactions has been determined, they can be combined to calculate the $\Delta G_R^\circ$ for other reactions, as discussed for reaction enthalpies in Chapter 4. Because of the significant interactions between the solutes and the solvent, $K$ values depend on the nature of the solvent, and for electrolyte solutions to be discussed in Chapter 10, they additionally depend on the ionic strength.

An equilibrium constant in terms of molarities or molalities can also be defined starting from Equation (9.67) and setting all activity coefficients equal to 1. This is most appropriate for a dilute solution of a nonelectrolyte, using a Henry's law standard state:

$$K = \prod_i (\gamma_i^{eq})^{\nu_j} \left(\frac{c_i^{eq}}{c^\circ}\right)^{\nu_j} \approx \prod_i \left(\frac{c_i^{eq}}{c^\circ}\right)^{\nu_j} \tag{9.68}$$

### EXAMPLE PROBLEM 9.13

**a.** Write the equilibrium constant for the reaction $N_2(aq, m) \rightleftharpoons N_2(g, P)$ in terms of activities at 25°C, where $m$ is the molality of $N_2(aq)$.

**b.** By making suitable approximations, convert the equilibrium constant of part (a) into one in terms of pressure and molality only.

**Solution**

**a.** $K = \prod_i (a_i^{eq})^{\nu_j} = \prod_i (\gamma_i^{eq})^{\nu_j} \left(\frac{c_i^{eq}}{c^\circ}\right)^{\nu_j} = \dfrac{\left(\dfrac{\gamma_{N_2, g} \, P}{P^\circ}\right)}{\left(\dfrac{\gamma_{N_2, aq} \, m}{m^\circ}\right)}$

$= \dfrac{\gamma_{N_2, g}}{\gamma_{N_2, aq}} \dfrac{\left(\dfrac{P}{P^\circ}\right)}{\left(\dfrac{m}{m^\circ}\right)}$

**b.** Using a Henry's law standard state for dissolved $N_2$, $\gamma_{N_2, aq} \approx 1$, because the concentration is very low. Similarly, because $N_2$ behaves like an ideal gas up to quite high pressures at 25°C, $\gamma_{N_2, g} \approx 1$. Therefore,

$$K \approx \dfrac{\left(\dfrac{P}{P^\circ}\right)}{\left(\dfrac{m}{m^\circ}\right)}$$

Note that in this case, the equilibrium constant is simply the Henry's law constant in terms of molality.

The numerical values for the dimensionless thermodynamic equilibrium constant depend on the choice of the standard states for the components involved in the reaction. The same is true for $\Delta G_R^\circ$. Therefore, it is essential to know which standard state has

been assumed before an equilibrium constant is used. The activity coefficients of most neutral solutes are close to 1 with the appropriate choice of standard state. Therefore, example calculations of chemical equilibrium using activities will be deferred until electrolyte solutions are discussed in Chapter 10. For such solutions, $\gamma_{solute}$ differs substantially from 1, even for dilute solutions.

An important example of equilibrium processes in solution is the physical interaction of a molecule with a binding site. Such **binding equilibria** processes are ubiquitous in chemistry, being central to the function of oxygen transport proteins such as hemoglobin or myoglobin, the action of enzymes, and the adsorption of molecules to surfaces. All of these processes involve an equilibrium between the free molecule ($R$) and the molecule absorbed or "bound" to another species (protein, solid, etc.) containing a binding site ($M$). In the limit where there is a single binding site per species, the equilibrium can be written as

$$R + M \rightleftharpoons RM \qquad (9.69)$$

The equilibrium constant for this reaction in terms of the concentrations of the species of interest is

$$K = \frac{c_{RM}}{c_R \times c_M} \qquad (9.70)$$

(It is common in biochemistry that $K$ is expressed in terms of concentrations, and therefore has units.) Assuming that there is a single binding site for the molecule, then the average number of bound molecules per species ($\bar{\nu}$) is given by

$$\bar{\nu} = \frac{c_{RM}}{c_M + c_{RM}} \qquad (9.71)$$

Expressing this fraction in terms of the equilibrium constant yields

$$\bar{\nu} = \frac{c_{RM}}{c_M + c_{RM}} \left( \frac{1/(c_R c_M)}{1/(c_R c_M)} \right) = \frac{K}{1/c_R + K} = \frac{Kc_R}{1 + Kc_R} \qquad (9.72)$$

This expression demonstrates that $\bar{\nu}$ depends on both the molecular concentration and the value of the equilibrium constant. The variation of $\bar{\nu}$ with $c_R$ for different values of $K$ are presented in Figure 9.19. With an increase in $K$ (consistent with the bound form of the molecule being lower in Gibbs energy relative to the free form), the average number of bound molecules per species approaches unity (that is, the binding sites are completely occupied) even at low values of $c_R$.

The previous development was limited to the existence of a single molecular binding site; however, what species absorbing the molecules has more than one binding site? Two issues must be considered to address this case. First, binding to one site may have an effect on binding at other sites, and this effect is important in the binding of oxygen to hemoglobin. However, in this development we restrict ourselves to **independent site binding** where the binding at one site has no effect on binding to other sites. In this case the average number of molecules bound to a specific site ($i$) is

$$\bar{\nu}_i = \frac{K_i c_R}{1 + K_i c_R} \qquad (9.73)$$

If there are $N$ binding sites, then the average number of molecules adsorbed per species is simply the sum of the average values for each specific binding site:

$$\bar{\nu} = \sum_{i=1}^{N} \bar{\nu}_i = \sum_{i=1}^{N} \frac{K_i c_R}{1 + K_i c_R} \qquad (9.74)$$
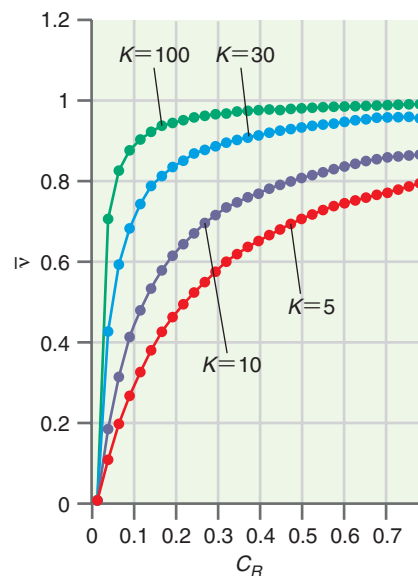


**FIGURE 9.19**

The average number of bound molecules per species $\bar{\nu}$ is plotted against the concentration of free species $c_R$ for $K$ values of 5, 10, 30, and 100.

**FIGURE 9.20**
Scatchard plot of independent binding for $K = 100$ and $N = 4$. Note that the $y$ intercept is $K \times N = 400$, the slope is $-K = -100$, and the $x$ intercept is 4.

The second issue to address is the equivalency of the binding sites. Assuming that all of the binding sites are equivalent $\bar{\nu}$ becomes

$$\bar{\nu} = \sum_{i=1}^{N} \frac{K_i c_R}{1 + K_i c_R} = \frac{NK c_R}{1 + K c_R} \tag{9.75}$$

This expression is almost identical to our previous expression for $\bar{\nu}$ for a single binding site, but with the addition of a factor of $N$. Therefore, at large values of $c_R$ the average number of bound molecules per species will approach $N$ instead of 1. To determine $K$ and $N$ for specific binding equilibrium, the expression for $\bar{\nu}$ is recast in a linear form referred to as the **Scatchard equation:**

$$\bar{\nu} = \frac{NK c_R}{1 + K c_R}$$

$$\frac{\bar{\nu}}{c_R} = -K\bar{\nu} + NK \tag{9.76}$$

The Scatchard equation demonstrates that a plot of $\bar{\nu}/c_R$ versus $\bar{\nu}$ should yield a straight line having a slope of $-K$ and a $y$-intercept of $NK$ from which $N$ can be readily determined. A **Scatchard plot** for $K = 100$ and $N = 4$ is presented in Figure 9.20. Deviations from linear behavior in a Scatchard plot can occur if the binding is not independent or if the binding sites are not equivalent.

---

### EXAMPLE PROBLEM 9.14

A variety of molecules physically bind to DNA by intercalation or insertion between the base pairs. The intercalation of chlorobenzylidine (CB) to calf thymus DNA was studied by circular dichroism spectroscopy [Zhong, W., Yu, J.-S., Liang, Y., Fan, K., and Lai, L., *Spectrochimica Acta*, Part A, 60A (2004): 2985]. Using the following representative binding data, determine the binding constant ($K$) and the number of binding sites per base ($N$).

| $c_{CB} (\times 10^6 \text{ M})$ | 1.0 | 2.0 | 3.0 | 5.0 | 10.0 |
|---|---|---|---|---|---|
| $\bar{\nu}$ | 0.006 | 0.012 | 0.018 | 0.028 | 0.052 |

#### Solution

A plot of $\bar{\nu}/c_{CB}$ versus $\bar{\nu}$. using binding data provided allows for a determination of $K$ and $N$. Using the data, the following Scatchard plot is constructed:
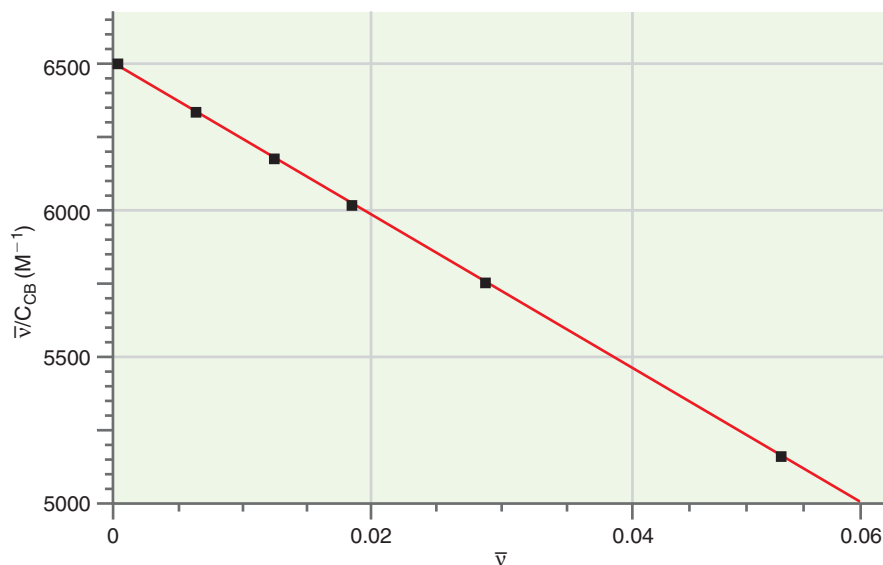
A best fit to a straight line results in a slope of $-26{,}000$ M$^{-1}$ and $y$-intercept of 6500. Comparison to the Scatchard equation reveals that the slope is equal to $-K$ so that $K = 26{,}000$ M$^{-1}$. In addition, the $y$-intercept is equal to the product of $N$ and $K$; therefore, $N = 0.25$. This value of $N$ is consistent with a binding site consisting of four bases, or two base pairs consistent with intercalation between base pairs.



**FIGURE 9.21**
A $T$–$x$ phase diagram is shown for the partially miscible liquids water and phenol. The pressure is held constant at 1 bar.

# 9.14 Solutions Formed from Partially Miscible Liquids

Two liquids need not be miscible in all proportions. Over a limited range of relative concentration, a homogeneous solution can be formed, and outside of this range, two liquid phases separated by a phase boundary can be observed. An example is the water-phenol system for which a $T$–$x$ phase diagram is shown in Figure 9.21. The pressure is assumed to be sufficiently high that no gas phase is present.

As the phenol concentration increases from 0 at the temperature $T_1$, a single liquid phase of variable composition is formed. However, at $x_1$, the appearance of a second liquid phase is observed, separated from the first phase by a horizontal boundary with the denser phase below the less dense phase. If we start with pure phenol and add water at $T_1$, separation into two phases is observed at $x_3$. In the phenol-water system, the solubility increases with temperature so that the extent in $x$ of the two-phase region decreases with increasing $T$, and phase separation is observed only at a single composition at the **upper consolate temperature** $T_{uc}$. For $T > T_{uc}$, phenol and water are completely miscible.

The composition of the two phases in equilibrium at a given temperature is given by the $x$ values at the ends of the tie line $l_1l_2$, and the relative amount of the two phases present is given by the lever rule:

$$\frac{\text{moles L}_1}{\text{moles L}_2} = \frac{al_2}{al_1} = \frac{x_3 - x_2}{x_2 - x_1} \qquad (9.77)$$

Although less common, liquid–liquid systems are known in which the solubility decreases as the temperature increases. In this case, a **lower consolate temperature** is observed below which the two liquids are completely miscible. An example is the triethylamine–water system shown in Figure 9.22. The water–nicotine system has both a lower and upper consolate temperature, and phase separation is only observed between 61°C and 210°C as shown in Figure 9.23.

We next consider solutions of partially miscible liquids at pressures for which a vapor phase is in equilibrium with one or more liquid phases. The composition of the vapor for a given value of the average composition of the liquid depends on the relative values of the upper consolate temperature and the minimum boiling temperature for the azeotrope. For the system shown in Figure 9.24a, the vapor phase is only present above the upper consolate temperature. In this case, the vapor and liquid composition is the same as that described in Section 9.4 for minimum boiling point azeotropes. However, if the upper consolate temperature lies above the boiling temperature of the minimum boiling azeotrope, the $T$–$x$ diagram shows new features as illustrated for the water–butanol system in Figure 9.24b.

First, consider the system at point $a$ in the phase diagram corresponding to a single liquid phase enriched in butanol. If the temperature is increased to $T_b$, the gas-phase composition is given by point $b$. If the vapor of this composition is removed from the system and cooled to the original temperature $T_a$, it is at point $c$ in the phase diagram, which corresponds to two liquid phases of composition $d$ and $e$ in equilibrium with the vapor phase. This system consists of two components and, therefore, $F = 4 - p$.

Next, consider heating the liquid described by point $f$ in the two-liquid-phase region in a piston and cylinder assembly at constant pressure. Vapor first appears when the temperature is increased to 94°C and has the composition given by point $i$,
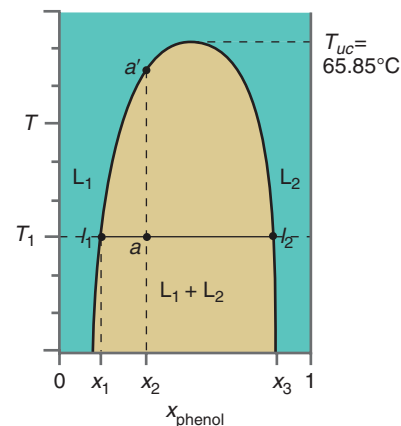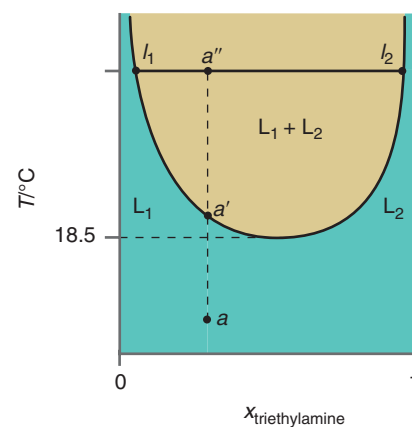


**FIGURE 9.22**
A $T$–$x$ phase diagram showing a lower consolate temperature is shown for the partially miscible liquids water and triethylamine. The pressure is held constant at 1 bar.
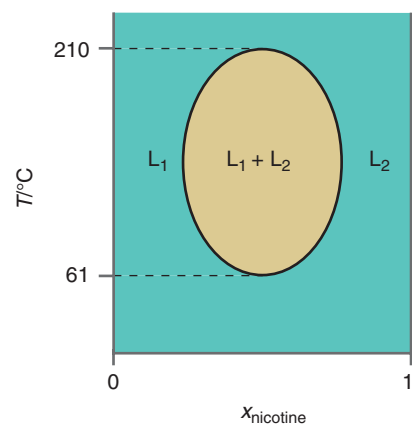


**FIGURE 9.23**
A $T$–$x$ phase diagram showing an upper and lower consolate temperature is shown for the partially miscible liquids water and nicotine. The pressure is held constant at 1 bar.

(a)



(b)
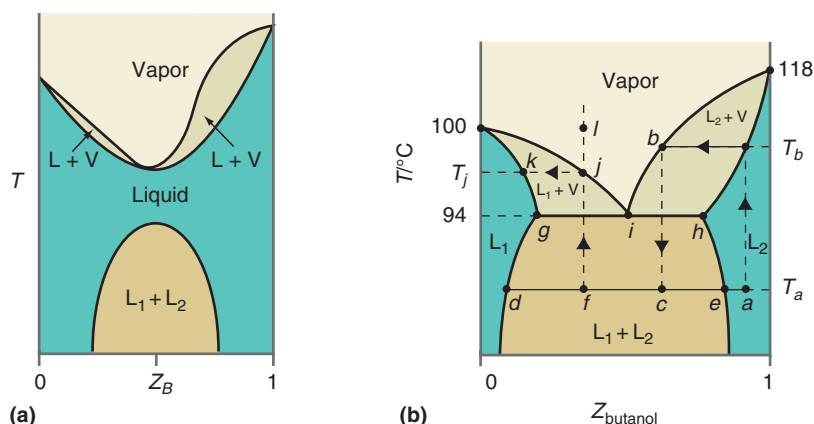
corresponding to a minimum boiling point azeotrope. The vapor is in equilibrium with two liquid phases that have the composition given by points *g* and *h*. Because the pressure is constant in Figure 9.24b and $p = 3$ at point *i*, the system has zero degrees of freedom. Distillation of the homogeneous solution results in two separate liquid phases of fixed composition *g* and *h*. As more heat is put into the system, liquid is converted to vapor, but the composition of the two liquid phases and the vapor phase remains constant as described by points *g*, *h*, and *i*. Because the vapor is enriched in butanol with respect to the liquid, the butanol-rich phase $L_2$ is converted to vapor before the water-rich phase $L_1$. At the point when the $L_2$ phase disappears, the temperature increases beyond 94°C and the vapor composition changes along the *i-j* curve. As the vapor approaches the composition corresponding to *j*, the entire system is converted to vapor and the last drop of $L_1$, which disappears at $T_j$, has the composition given by point *k*. Further heat input results in an increase in the temperature of the vapor with no change in its composition.

Summarizing these changes, heating increases the amount of material in the vapor phase. As long as the two phases of composition *g* and *h* are present, the temperature is constant and the amount of vapor increases, but its composition is fixed at *i*. After the last drop of $L_2$ of composition *h* boils off, the vapor composition continuously changes along the curve *i-j*. As the last drop of $L_1$ of composition *k* evaporates, the vapor composition approaches the average composition of the system given by *f*, *j*, and *l*.
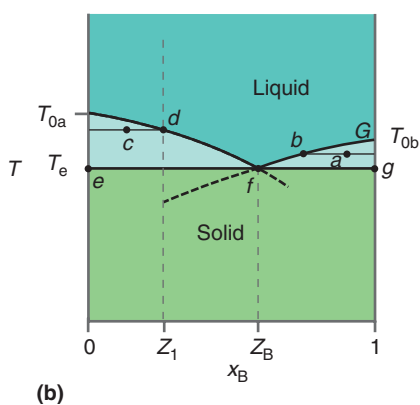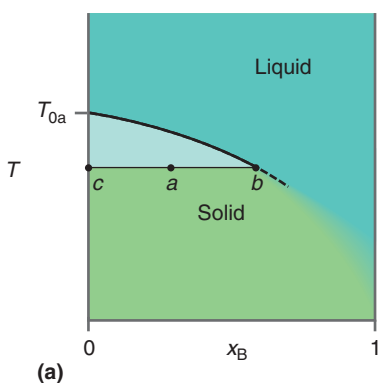


(a)



(b)

# 9.15 The Solid-Solution Equilibrium

If a dilute liquid solution of B in A is cooled sufficiently, pure solvent A will crystallize out in a solid phase as discussed in Section 9.7 in connection with the freezing point depression. Point *a* in Figure 9.25a represents a solution of composition *b* in equilibrium with pure solid A (point *c*). The relative number of moles of solution and solid can be found using the lever rule. The temperature *T* at which freezing occurs is given by

$$\frac{1}{T} = \frac{1}{T_{fusion}} - \frac{R \ln x_{solvent}}{\Delta H_{fusion}} \tag{9.78}$$

where $T_{fusion}$ and $\Delta H_{fusion}$ are the freezing temperature and enthalpy of fusion of the pure solvent. *T* is shown schematically as a function of $x_B$ in Figure 9.25a, and the dashed range indicates the region beyond which Equation (9.78) is unlikely to be valid.

The same argument holds for a dilute solution of A in B whereby we have interchanged the solvent and solute roles. Therefore, the appropriate phase diagram for all values of $Z_A$ and $Z_B$ is that shown in Figure 9.25b. We use the variables $Z_A$ and $Z_B$ rather than $x_A$ and $x_B$ because the solid is not homogeneous. In Figure 9.25b point *a* represents solid B in equilibrium with a solution of composition *b*, and point *c* represents pure solid A in equilibrium with the solution of composition *d*. Point *f* is a special point called the

eutectic point that is the minimum melting point observed in the A–B system. The temperature $T_e$ is called the **eutectic temperature** (from the Greek, easily melted).

Because the tie line at $T_e$ extends across the entire phase diagram, a solution at $T_e$ is in equilibrium with both pure A (point $e$) and pure B (point $g$). As more heat is put into the system, the volume of the solution phase increases but its composition remains constant at $Z_B$ until one of the pure solids is completely melted because $F = 0$.

Eutectic materials are widely used in making plumbing and electrical connections using a solder. Until the 1980s, copper plumbing components were connected using Pb–Sn solders but as even small amounts of lead present a health hazard, Pb–Sn solders have been replaced by lead-free solders which may contain tin, copper, silver, indium, zinc, antimony, or bismuth. Another important application of eutectic materials is making electrical connections to silicon chips in the microelectronics industry. Gold is deposited onto the Si surface using masks to establish an appropriate pattern. Subsequently, the chip is heated to near 400°C. As the temperature increases, gold atoms diffuse rapidly into the silicon, and a very thin liquid film forms at the interface once enough gold has diffused to reach the eutectic composition. As more heat is put into the chip, a larger volume of eutectic alloy is produced, which is ultimately the electrical connection. The Au–Si phase diagram is shown in Figure 9.26, and it is seen that the eutectic temperature is approximately 700°C and 950°C below the melting point of pure gold and Si, respectively.

The eutectic mixture is useful in bonding gold to silicon to form an electrical connection. Imagine that gold wire is placed in contact with a Si chip on which Au has been deposited. If the chip is heated, the eutectic liquid will form before the Si or the Au melts. Therefore, the eutectic will connect the gold wire to the chip without melting the Au or the Si.
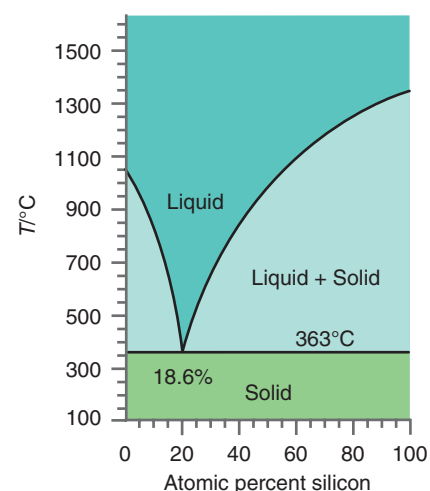


**FIGURE 9.26**

The $T–x$ phase diagram is shown for the gold–silicon system. Note that the eutectic melting point is much lower than the melting points of the pure substances Au and Si. The pressure is constant at 1 bar.

# Vocabulary

| | | |
|---|---|---|
| activity | Henry's law standard state | pressure–average composition diagram |
| activity coefficient | ideal dilute solution | Raoult's law |
| average composition | ideal solution | Raoult's law standard state |
| binding equilibria | independent site binding | Scatchard equation |
| boiling point elevation | lever rule | Scatchard plot |
| colligative properties | limiting law | semipermeable membrane |
| eutectic temperature | lower and upper consolate temperature | solute |
| fractional distillation | osmosis | solvent |
| freezing point depression | osmotic pressure | temperature–composition diagram |
| Gibbs–Duhem equation | partial molar quantities | tie line |
| Henry's law | partial molar volume | van't Hoff equation |
| Henry's law constant | | |

# Conceptual Problems

**Q9.1** Why is the magnitude of the boiling point elevation less than that of the freezing point depression?

**Q9.2** Fractional distillation of a particular binary liquid mixture leaves behind a liquid consisting of both components in which the composition does not change as the liquid is boiled off. Is this behavior characteristic of a maximum or a minimum boiling point azeotrope?

**Q9.3** In the description of Figure 9.24b, the following sentence appears: "At the point when the $L_2$ phase disappears,

the temperature increases beyond 94°C and the vapor composition changes along the $i$-$j$ curve." Why does the vapor composition change along the $i$-$j$ curve?

**Q9.4** Explain why chemists doing quantitative work using liquid solutions prefer to express concentration in terms of molality rather than molarity.

**Q9.5** Explain the usefulness of a tie line on a $P$–$Z$ phase diagram such as that of Figure 9.4.

**Q9.6** For a pure substance, the liquid and gaseous phases can only coexist for a single value of the pressure at a given temperature. Is this also the case for an ideal solution of two volatile liquids?

**Q9.7** Using the differential form of $G$, $dG = V\,dP - S\,dT$, show that if $\Delta G_{mixing} = nRT \sum_i x_i \ln x_i$, then
$\Delta H_{mixing} = \Delta V_{mixing} = 0$.

**Q9.8** What information can be obtained from a tie line in a $P–Z$ phase diagram?

**Q9.9** You boil an ethanol–benzene mixture with $x_{ethanol} = 0.35$. What is the composition of the vapor phase that first appears? What is the composition of the last liquid left in the vessel?

**Q9.10** What can you say about the composition of the solid below the eutectic temperature in Figure 9.26 on a microscopic scale?

**Q9.11** Is a whale likely to get the bends when it dives deep into the ocean and resurfaces? Answer this question by considering the likelihood of a scuba diver getting the bends if he or she dives and resurfaces on one lung full of air as opposed to breathing air for a long time at the deepest point of the dive.

**Q9.12** Why is the preferred standard state for the solvent in an ideal dilute solution the Raoult's law standard state? Why is the preferred standard state for the solute in an ideal dilute solution the Henry's law standard state? Is there a preferred standard state for the solution in which $x_{solvent} = x_{solute} = 0.5$?

**Q9.13** The entropy of two liquids is increased if they mix. How can immiscibility be explained in terms of thermodynamic state functions?

**Q9.14** Explain why colligative properties depend only on the concentration and not on the identity of the molecule.

**Q9.15** The statement "The boiling point of a typical liquid mixture can be reduced by approximately 100°C if the pressure is reduced from 760 to 20 Torr" is found in Section 9.4. What figure(s) in Chapter 9 can you identify to support this statement in a qualitative sense?

# Numerical Problems

Problem numbers in red indicate that the solution to the problem is given in the *Student's Solutions Manual*.

**P9.1** Ratcliffe and Chao [*Canadian Journal of Chemical Engineering* 47 (1969): 148] obtained the following tabulated results for the variation of the total pressure above a solution of isopropanol ($P_1^* = 1008$ Torr) and $n$-decane ($P_2^* = 48.3$ Torr) as a function of the mole fraction of the $n$-decane in the solution and vapor phases. Using these data, calculate the activity coefficients for both components using a Raoult's law standard state.

| $P$ (Torr) | $x_2$ | $y_2$ |
|---|---|---|
| 942.6 | 0.1312 | 0.0243 |
| 909.6 | 0.2040 | 0.0300 |
| 883.3 | 0.2714 | 0.0342 |
| 868.4 | 0.3360 | 0.0362 |
| 830.2 | 0.4425 | 0.0411 |
| 786.8 | 0.5578 | 0.0451 |
| 758.7 | 0.6036 | 0.0489 |

**P9.2** At a given temperature, a nonideal solution of the volatile components A and B has a vapor pressure of 795 Torr. For this solution, $y_A = 0.375$. In addition, $x_A = 0.310$, $P_A^* = 610$. Torr, and $P_B^* = 495$ Torr. Calculate the activity and activity coefficient of A and B.

**P9.3** Two liquids, A and B, are immiscible for $T < 75.0°C$ and for $T > 45.0°C$ and are completely miscible outside of this temperature range. Sketch the phase diagram, showing as much information as you can from these observations.

**P9.4** At 350. K, pure toluene and hexane have vapor pressures of $3.57 \times 10^4$ Pa and $1.30 \times 10^5$ Pa, respectively.

**a.** Calculate the mole fraction of hexane in the liquid mixture that boils at 350. K at a pressure of 1 atm.

**b.** Calculate the mole fraction of hexane in the vapor that is in equilibrium with the liquid of part (a).

**P9.5** The partial molar volumes of water and ethanol in a solution with $x_{H_2O} = 0.45$ at 25°C are 17.0 and 57.5 cm$^3$ mol$^{-1}$, respectively. Calculate the volume change upon mixing sufficient ethanol with 3.75 mol of water to give this concentration. The densities of water and ethanol are 0.997 and 0.7893 g cm$^{-3}$, respectively, at this temperature.

**P9.6** A solution is made up of 222.9 g of ethanol and 130.8 g of $H_2O$. If the volume of the solution is 403.4 cm$^3$ and the partial molar volume of $H_2O$ is 17.0 cm$^3$, what is the partial molar volume of ethanol under these conditions?

**P9.7** The osmotic pressure of an unknown substance is measured at 298 K. Determine the molecular weight if the concentration of this substance is 31.2 kg m$^{-3}$ and the osmotic pressure is $5.30 \times 10^4$ Pa. The density of the solution is 997 kg m$^{-3}$.

**P9.8** At 303. K, the vapor pressure of benzene is 120. Torr and that of hexane is 189 Torr. Calculate the vapor pressure of a solution for which $x_{benzene} = 0.28$ assuming ideal behavior.

**P9.9** The volatile liquids A and B, for which $P_A^* = 165$ Torr and $P_B^* = 85.1$ Torr are confined to a piston and cylinder assembly. Initially, only the liquid phase is present. As the pressure is reduced, the first vapor is observed at a total pressure of 110. Torr. Calculate $x_A$.

**P9.10** At high altitudes, mountain climbers are unable to absorb a sufficient amount of $O_2$ into their bloodstreams to maintain a high activity level. At a pressure of 1 bar, blood is

typically 95% saturated with $O_2$, but near 18,000 feet where the pressure is 0.50 bar, the corresponding degree of saturation is 71%. Assuming that the Henry's law constant for blood is the same as for water, calculate the amount of $O_2$ dissolved in 1.00 L of blood for pressures of 1 bar and 0.500 bar. Air contains 20.99% $O_2$ by volume. Assume that the density of blood is 998 kg m$^{-3}$.

**P9.11** At $-47.0°C$, the vapor pressure of ethyl bromide is 10.0 Torr and that of ethyl chloride is 40.0 Torr. Assume that the solution is ideal. Assume there is only a trace of liquid present and the mole fraction of ethyl chloride in the vapor is 0.80 and answer these questions:

a. What is the total pressure and the mole fraction of ethyl chloride in the liquid?

b. If there are 5.00 mol of liquid and 3.00 mol of vapor present at the same pressure as in part (a), what is the overall composition of the system?

**P9.12** A and B form an ideal solution at 298 K, with $x_A = 0.320$, $P_A^* = 84.3$ Torr, and $P_B^* = 41.2$ Torr.

a. Calculate the partial pressures of A and B in the gas phase.

b. A portion of the gas phase is removed and condensed in a separate container. Calculate the partial pressures of A and B in equilibrium with this liquid sample at 298 K.

**P9.13** Describe what you would observe if you heated the liquid mixture at the composition corresponding to point $i$ in Figure 9.24b from a temperature below $T_a$ to 118°C.

**P9.14** The heat of fusion of water is $6.008 \times 10^3$ J mol$^{-1}$ at its normal melting point of 273.15 K. Calculate the freezing point depression constant $K_f$.

**P9.15** At 39.9°C, a solution of ethanol ($x_1 = 0.9006$, $P_1^* = 130.4$ Torr) and isooctane ($P_2^* = 43.9$ Torr) forms a vapor phase with $y_1 = 0.6667$ at a total pressure of 185.9 Torr.

a. Calculate the activity and activity coefficient of each component.

b. Calculate the total pressure that the solution would have if it were ideal.

**P9.16** Calculate the solubility of $H_2S$ in 1 L of water if its pressure above the solution is 2.75 Pa. The density of water at this temperature is 997 kg m$^{-3}$.

**P9.17** The binding of NADH to human liver mitochondrial isozyme was studied [*Biochemistry* 28 (1989): 5367] and it was determined that only a single binding site is present with $K = 2.0 \times 10^7$ M$^{-1}$. What concentration of NADH is required to occupy 10% of the binding sites?

**P9.18** Given the vapor pressures of the pure liquids and the overall composition of the system, what are the upper and lower limits of pressure between which liquid and vapor coexist in an ideal solution?

**P9.19** A and B form an ideal solution. At a total pressure of 0.720 bar, $y_A = 0.510$ and $x_A = 0.420$. Using this information, calculate the vapor pressure of pure A and of pure B.

**P9.20** The partial pressures of $Br_2$ above a solution containing $CCl_4$ as the solvent at 25°C are found to have the values listed in the following table as a function of the mole fraction of $Br_2$ in

the solution [Lewis G. N., and Storch, H. *J. American Chemical Society* 39 (1917): 2544]. Use these data and a graphical method to determine the Henry's law constant for $Br_2$ in $CCl_4$ at 25°C.

| $x_{Br_2}$ | $P$ (Torr) | $x_{Br_2}$ | $P$ (Torr) |
|---|---|---|---|
| 0.00394 | 1.52 | 0.0130 | 5.43 |
| 0.00420 | 1.60 | 0.0236 | 9.57 |
| 0.00599 | 2.39 | 0.0238 | 9.83 |
| 0.0102 | 4.27 | 0.0250 | 10.27 |

**P9.21** The data from Problem P9.20 can be expressed in terms of the molality rather than the mole fraction of $Br_2$. Use the data from the following table and a graphical method to determine the Henry's law constant for $Br_2$ in $CCl_4$ at 25°C in terms of molality.

| $m_{Br_2}$ | $P$ (Torr) | $m_{Br_2}$ | $P$ (Torr) |
|---|---|---|---|
| 0.026 | 1.52 | 0.086 | 5.43 |
| 0.028 | 1.60 | 0.157 | 9.57 |
| 0.039 | 2.39 | 0.158 | 9.83 |
| 0.067 | 4.27 | 0.167 | 10.27 |

**P9.22** The densities of pure water and ethanol are 997 and 789 kg m$^{-3}$, respectively. For $x_{ethanol} = 0.35$, the partial molar volumes of ethanol and water are 55.2 and $17.8 \times 10^{-3}$ L mol$^{-1}$, respectively. Calculate the change in volume relative to the pure components when 2.50 L of a solution with $x_{ethanol} = 0.35$ is prepared.

**P9.23** Two liquids, A and B, are immiscible for $x_A = x_B = 0.5$, for $T < 75.0°C$ and completely miscible for $T > 75.0°C$. Sketch the phase diagram, showing as much information as you can from these observations.

**P9.24** An ideal solution is formed by mixing liquids A and B at 298 K. The vapor pressure of pure A is 151 Torr and that of pure B is 84.3 Torr. If the mole fraction of A in the vapor is 0.610, what is the mole fraction of A in the solution?

**P9.25** A solution is prepared by dissolving 45.2 g of a non-volatile solute in 119 g of water. The vapor pressure above the solution is 22.51 Torr and the vapor pressure of pure water is 23.76 Torr at this temperature. What is the molecular weight of the solute?

**P9.26** A sample of glucose ($C_6H_{12}O_6$) of mass 13.2 g is placed in a test tube of radius 1.25 cm. The bottom of the test tube is a membrane that is semipermeable to water. The tube is partially immersed in a beaker of water at 298 K so that the bottom of the test tube is only slightly below the level of the water in the beaker. The density of water at this temperature is 997 kg m$^{-3}$. After equilibrium is reached, how high is the level of the water in the tube above that in the beaker? What is the value of the osmotic pressure? You may find the approximation $\ln(1/(1 + x)) \approx -x$ useful.

**P9.27** A volume of 5.50 L of air is bubbled through liquid toluene at 298 K, thus reducing the mass of toluene in the beaker by 2.38 g. Assuming that the air emerging from the beaker is saturated with toluene, determine the vapor pressure of toluene at this temperature.

**P9.28** The vapor pressures of 1-bromobutane and 1-chlorobutane can be expressed in the form

$$\ln \frac{P_{bromo}}{\text{Pa}} = 17.076 - \frac{1584.8}{\dfrac{T}{K} - 111.88}$$

and

$$\ln \frac{P_{chloro}}{\text{Pa}} = 20.612 - \frac{2688.1}{\dfrac{T}{K} - 55.725}$$

Assuming ideal solution behavior, calculate $x_{bromo}$ and $y_{bromo}$ at 305 K and a total pressure of 9750. Pa.

**P9.29** In an ideal solution of A and B, 3.00 mol are in the liquid phase and 5.00 mol are in the gaseous phase. The overall composition of the system is $Z_A = 0.375$ and $x_A = 0.250$. Calculate $y_A$.

**P9.30** Assume that 1-bromobutane and 1-chlorobutane form an ideal solution. At 273 K, $P^*_{chloro} = 3790$ Pa and $P^*_{bromo} = 1394$ Pa. When only a trace of liquid is present at 273 K, $y_{chloro} = 0.750$.

**a.** Calculate the total pressure above the solution.

**b.** Calculate the mole fraction of 1-chlorobutane in the solution.

**c.** What value would $Z_{chloro}$ have in order for there to be 4.86 mol of liquid and 3.21 mol of gas at a total pressure equal to that in part (a)? [*Note:* This composition is different from that of part (a).]

**P9.31** DNA is capable of forming complex helical structures. An unusual triple-helix structure of poly(dA).2poly(dT) DNA was studied by P. V. Scaria and R. H. Shafer [*Journal of Biological Chemistry* 266 (1991): 5417] where the intercalation of ethidium bromide was studied using UV absorption and circular dichroism spectroscopy. The following representative data were obtained using the results of this study:

| $c_{Eth}$ 1($\mu$ M) | 0.63 | 1.7 | 5.0 | 10.0 | 14.7 |
|---|---|---|---|---|---|
| $\bar{\nu}$ | 0.00683 | 0.01675 | 0.0388 | 0.0590 | 0.0705 |

Using the data, determine $K$ and $N$ for the binding of ethidium bromide to the DNA triple-helical structure.

**P9.32** Calculate the activity and activity coefficient for $CS_2$ at $x_{CS_2} = 0.722$ using the data in Table 9.3 for both a Raoult's law and a Henry's law standard state.

**P9.33** The dissolution of 7.75 g of a substance in 825 g of benzene at 298 K raises the boiling point by 0.575°C. Note that $K_f = 5.12$ K kg mol$^{-1}$, $K_b = 2.53$ K kg mol$^{-1}$, and the density of benzene is 876.6 kg m$^{-3}$. Calculate the freezing point depression, the ratio of the vapor pressure above the solution to that of the pure solvent, the osmotic pressure, and the molecular weight of the solute. $P^*_{benzene} = 103$ Torr at 298 K.

**P9.34** Describe what you would observe if you heated the solid at the composition 40. atomic percent Si in Figure 9.26 from 300.°C to 1300.°C.

**P9.35** An ideal dilute solution is formed by dissolving the solute A in the solvent B. Write expressions equivalent to Equations (9.9) through (9.13) for this case.

**P9.36** Describe the changes you would observe as the temperature of a mixture of phenol and water at point $a$ in Figure 9.21 is increased until the system is at point $a'$. How does the relative amount of separate phases of phenol and water change along this path?

**P9.37** Describe the changes you would observe as the temperature of a mixture of triethylamine and water at point $a$ in Figure 9.22 is increased until the system is at point $a"$. How does the relative amount of separate phases of triethylamine and water change along this path?

**P9.38** Describe the changes in a beaker containing water and butanol that you would observe along the path $a \rightarrow b \rightarrow c$ in Figure 8.24b in *Quantum Chemistry & Spectroscopy*. How would you calculate the relative amounts of different phases present along the path?

**P9.39** Describe the changes in a beaker containing water and butanol that you would observe along the path $f \rightarrow j \rightarrow i$ in Figure 8.24b in *Quantum Chemistry & Spectroscopy*. How would you calculate the relative amounts of different phases present along the path?

**P9.40** Describe the changes in a beaker containing water and butanol that you would observe along the path $f \rightarrow j \rightarrow k$ in Figure 8.24b in *Quantum Chemistry & Spectroscopy*. How would you calculate the relative amounts of different phases present along the path?

**P9.41** Describe the system at points $a$ and $c$ in Figure 8.25b in *Quantum Chemistry & Spectroscopy*. How would you calculate the relative amounts of different phases present at these points?

# Electrolyte Solutions

Electrolyte solutions are quite different from the ideal and real solutions of neutral solutes discussed in Chapter 9. The fundamental reason for this difference is that solutes in electrolyte solutions exist as solvated positive and negative ions. In Chapter 4, the formation enthalpy and Gibbs energy of a pure element in its standard state at 1 bar of pressure were set equal to zero. These assumptions allow the formation enthalpies and Gibbs energies of compounds to be calculated using the results of thermochemical experiments. In electrolyte solutions, an additional assumption, $\Delta G_f^\circ(H^+, aq) = 0$, is made to allow the formation enthalpies, Gibbs energies, and entropies of individual ions to be determined. Why are electrolyte and nonelectrolyte solutions so different? The Coulomb interactions between ions in an electrolyte solution are of much longer range than the interactions between neutral solutes. For this reason, electrolyte solutions deviate from ideal behavior at much lower concentrations than do solutions of neutral solutes. Although a formula unit of an electrolyte dissociates into positive and negative ions, only the mean activity and activity coefficient of the ions produced is accessible through experiments. The Debye–Hückel limiting law provides a useful way to calculate activity coefficients for dilute electrolyte solutions.

## 10.1 The Enthalpy, Entropy, and Gibbs Energy of Ion Formation in Solutions

In this chapter, substances called **electrolytes,** which dissociate into positively and negatively charged mobile solvated ions when dissolved in an appropriate solvent, are discussed. Consider the following overall reaction in water:

$$1/2 \, H_2(g) + 1/2 \, Cl_2(g) \rightarrow H^+(aq) + Cl^-(aq) \qquad \textbf{(10.1)}$$
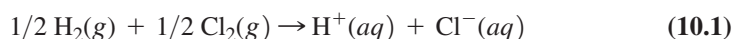
in which $H^+(aq)$ and $Cl^-(aq)$ represent mobile solvated ions. Although similar in structure, Equation (10.1) represents a reaction that is quite different than the gas-phase dissociation of an HCl molecule to give $H^+(g)$ and $Cl^-(g)$. For the reaction in solution, $\Delta H_R$ is $-167.2$ kJ mol$^{-1}$. The shorthand notation $H^+(aq)$ and $Cl^-(aq)$ refers to positive

and negative ions as well as their associated hydration shell. The **solvation shell** is essential in lowering the energy of the ions, thereby making the previous reaction spontaneous. Although energy flow into the system is required to dissociate and ionize hydrogen and chlorine, even more energy is gained in the reorientation of the dipolar water molecules around the ions in the solvation shell. Therefore, the reaction is exothermic.

The standard state enthalpy for this reaction can be written in terms of formation enthalpies:

$$\Delta H_R^\circ = \Delta H_f^\circ(H^+, aq) + \Delta H_f^\circ(Cl^-, aq) \tag{10.2}$$

There is no contribution of $H_2(g)$ and $Cl_2(g)$ to $\Delta H_R^\circ$ in Equation (10.2) because $\Delta H_f^\circ$ for a pure element in its standard state is zero.

Unfortunately, no direct calorimetric experiment can measure only the heat of formation of the solvated anion or cation. This is the case because the solution remains electrically neutral; any dissociation reaction of a neutral solute must produce both anions and cations. As we have seen in Chapter 4, tabulated values of formation enthalpies, entropies, and Gibbs energies for various chemical species are very useful. How can this information be obtained for individual solvated cations and anions?

The discussion in the rest of this chapter is restricted to aqueous solutions, for which water is the solvent, but can be generalized to other solvents. Values of thermodynamic functions for anions and cations in aqueous solutions can be obtained by making an appropriate choice for the zero of $\Delta H_f^\circ$, $\Delta G_f^\circ$, and $S_m^\circ$. By convention, the formation Gibbs energy for $H^+(aq)$ at unit activity is set equal to zero at all temperatures:

$$\Delta G_f^\circ(H^+, aq) = 0 \quad \text{for all } T \tag{10.3}$$

With this choice,

$$S_f^\circ(H^+, aq) = -\left(\frac{\partial \Delta G_f^\circ(H^+, aq)}{\partial T}\right)_P = 0 \quad \text{and}$$

$$\Delta H_f^\circ(H^+, aq) = \Delta G_f^\circ(H^+, aq) + TS_m^\circ(H^+, aq) = 0 \tag{10.4}$$

Using the convention of Equation (10.3), which has the consequences shown in Equation (10.4), the values of $\Delta H_f^\circ$, $\Delta G_f^\circ$, and $S_m^\circ$ for an individual ion can be assigned numerical values, as shown next.

As discussed earlier, $\Delta H_R^\circ$ for the reaction $1/2\, H_2(g) + 1/2\, Cl_2(g) \rightarrow H^+(aq) + Cl^-(aq)$ can be directly measured. The value of $\Delta G_R^\circ$ can be determined from $\Delta G_R^\circ = -RT \ln K$ by measuring the degree of dissociation in the reaction, using the solution conductivity, and $\Delta S_R^\circ$ can be determined from the relation

$$\Delta S_R^\circ = \frac{\Delta H_R^\circ - \Delta G_R^\circ}{T}$$

Using the conventions stated in Equations (10.3) and (10.4) together with the conventions regarding $\Delta H_f^\circ$ and $\Delta G_f^\circ$ for pure elements, $\Delta H_R^\circ = \Delta H_f^\circ(Cl^-, aq)$, $\Delta G_R^\circ = \Delta G_f^\circ(Cl^-, aq)$ and

$$\Delta S_R^\circ = S_m^\circ(Cl^-, aq) - \frac{1}{2} S_m^\circ(H_2, g) - \frac{1}{2} S_m^\circ(Cl_2, g)$$

for the reaction of Equation (10.1). In this way, the numerical values $\Delta H_f(Cl^-, aq) = -167.2$ kJ mol$^{-1}$, $S_m^\circ(Cl^-, aq) = 56.5$ J K$^{-1}$ mol$^{-1}$, and $\Delta G_f^\circ(Cl^-, aq) = -131.2$ kJ mol$^{-1}$ can be obtained.

These values can be used to determine the formation functions of other ions. To illustrate how this is done, consider the following reaction:

$$NaCl(s) \rightarrow Na^+(aq) + Cl^-(aq) \tag{10.5}$$
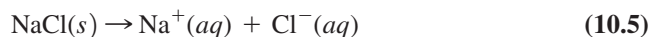
for which $\Delta H_R^\circ$ is found to be +3.90 kJ mol$^{-1}$. For this reaction,

$$\Delta H_R^\circ = \Delta H_f^\circ(Cl^-, aq) + \Delta H_f^\circ(Na^+, aq) - \Delta H_f^\circ(NaCl, s) \tag{10.6}$$

We use the tabulated value of $\Delta H_f^\circ(\text{NaCl}, s) = -411.2 \text{ kJ mol}^{-1}$ and the value for $\Delta H_f^\circ(\text{Cl}^-, aq)$ just determined to obtain a value for $\Delta H_f^\circ(\text{Na}^+, aq) = -240.1 \text{ kJ mol}^{-1}$. Proceeding to other reactions that involve either $\text{Na}^+(aq)$ or $\text{Cl}^-(aq)$, the enthalpies of formation of the counter ions can be determined. This procedure can be extended to include other ions. Values for $\Delta G_f^\circ$ and $S_m^\circ$ can be determined in a similar fashion. Values for $\Delta H_f^\circ$, $\Delta G_f^\circ$, and $S_m^\circ$ for aqueous ionic species are tabulated in Table 10.1. These thermodynamic quantities are called **conventional formation enthalpies, conventional Gibbs energies of formation,** and **conventional formation entropies** because of the convention described earlier.

Note that $\Delta H_f^\circ$, $\Delta G_f^\circ$, and $S_m^\circ$ for ions are defined relative to $\text{H}^+(aq)$. Negative values for $\Delta H_f^\circ$ indicate that the formation of the solvated ion is more exothermic than the formation of $\text{H}^+(aq)$. A similar statement can be made for $\Delta G_f^\circ$. Generally speaking, $\Delta H_f^\circ$ for multiply charged ions is more negative than that of singly charged ions, and $\Delta H_f^\circ$ for a given charge is more negative for smaller ions because of the stronger electrostatic attraction between the multiply charged or smaller ion and the water in the solvation shell.

Recall from Section 5.8 that the entropy of an atom or molecule was shown to be always positive. This is not the case for solvated ions because the entropy is measured relative to $\text{H}^+(aq)$. The entropy decreases as the hydration shell is formed because liquid water molecules are converted to relatively immobile molecules. Ions with a negative value for the conventional standard entropy such as $\text{Mg}^{2+}(aq)$, $\text{Zn}^{2+}(aq)$, and $\text{PO}_4^{3-}(aq)$ have a larger charge-to-size ratio than $\text{H}^+(aq)$. For this reason, the solvation shell is more tightly bound. Conversely, ions with a positive value for the standard entropy such as $\text{Na}^+(aq)$, $\text{Cs}^+(aq)$, and $\text{NO}_3^-(aq)$ have a smaller charge-to-size ratio than $\text{H}^+(aq)$ and a less tightly bound solvation shell.

**TABLE 10.1** Conventional Formation Enthalpies, Gibbs Energies, and Entropies of Selected Aqueous Anions and Cations

| Ion | $\Delta H_f^\circ$ (kJ mol$^{-1}$) | $\Delta G_f^\circ$ (kJ mol$^{-1}$) | $S_m^\circ$ (J K$^{-1}$ mol$^{-1}$) |
|---|---|---|---|
| $\text{Ag}^+(aq)$ | 105.6 | 77.1 | 72.7 |
| $\text{Br}^-(aq)$ | –121.6 | –104.0 | 82.4 |
| $\text{Ca}^{2+}(aq)$ | –542.8 | –553.6 | –53.1 |
| $\text{Cl}^-(aq)$ | –167.2 | –131.2 | 56.5 |
| $\text{Cs}^+(aq)$ | –258.3 | –292.0 | 133.1 |
| $\text{Cu}^+(aq)$ | 71.7 | 50.0 | 40.6 |
| $\text{Cu}^{2+}(aq)$ | 64.8 | 65.5 | –99.6 |
| $\text{F}^-(aq)$ | –332.6 | –278.8 | –13.8 |
| $\text{H}^+(aq)$ | 0 | 0 | 0 |
| $\text{I}^-(aq)$ | –55.2 | –51.6 | 111.3 |
| $\text{K}^+(aq)$ | –252.4 | –283.3 | 102.5 |
| $\text{Li}^+(aq)$ | –278.5 | –293.3 | 13.4 |
| $\text{Mg}^{2+}(aq)$ | –466.9 | –454.8 | –138.1 |
| $\text{NO}_3^-(aq)$ | –207.4 | –111.3 | 146.4 |
| $\text{Na}^+(aq)$ | –240.1 | –261.9 | 59.0 |
| $\text{OH}^-(aq)$ | –230.0 | –157.2 | –10.9 |
| $\text{PO}_4^{3-}(aq)$ | –1277.4 | –1018.7 | –220.5 |
| $\text{SO}_4^{2-}(aq)$ | –909.3 | –744.5 | 20.1 |
| $\text{Zn}^{2+}(aq)$ | –153.9 | –147.1 | –112.1 |

*Source:* Lide, D. R., ed. *Handbook of Chemistry and Physics.* 83rd ed. Boca Raton, FL: CRC Press 2002.

# 10.2 Understanding the Thermodynamics of Ion Formation and Solvation

As discussed in the preceding section, $\Delta H_f^\circ$, $\Delta G_f^\circ$, and $S_m^\circ$ can be determined for a formula unit but not for an individual ion in a calorimetric experiment. However, as seen next, values for thermodynamic functions associated with individual ions can be calculated with a reasonable level of confidence using a thermodynamic model. This result allows the conventional values of $\Delta H_f^\circ$, $\Delta G_f^\circ$, and $S_m^\circ$ to be converted to absolute values for individual ions. In the following discussion, the focus is on $\Delta G_f^\circ$.

We first discuss the individual contributions to $\Delta G_f^\circ$, and do so by analyzing the following sequence of steps that describe the formation of $H^+(aq)$ and $Cl^-(aq)$:

| | |
|---|---|
| $1/2\ H_2(g) \rightarrow H(g)$ | $\Delta G^\circ = 203.3\ \text{kJ mol}^{-1}$ |
| $1/2\ Cl_2(g) \rightarrow Cl(g)$ | $\Delta G^\circ = 105.7\ \text{kJ mol}^{-1}$ |
| $H(g) \rightarrow H^+(g) + e^-$ | $\Delta G^\circ = 1312\ \text{kJ mol}^{-1}$ |
| $Cl(g) + e^- \rightarrow Cl^-(g)$ | $\Delta G^\circ = -349\ \text{kJ mol}^{-1}$ |
| $Cl^-(g) \rightarrow Cl^-(aq)$ | $\Delta G^\circ = \Delta G_{solvation}^\circ(Cl^-, aq)$ |
| $H^+(g) \rightarrow H^+(aq)$ | $\Delta G^\circ = \Delta G_{solvation}^\circ(H^+, aq)$ |
| $1/2\ H_2(g) + 1/2\ Cl_2(g) \rightarrow H^+(aq) + Cl^-(aq)$ | $\Delta G_R^\circ = -131.2\ \text{kJ mol}^{-1}$ |
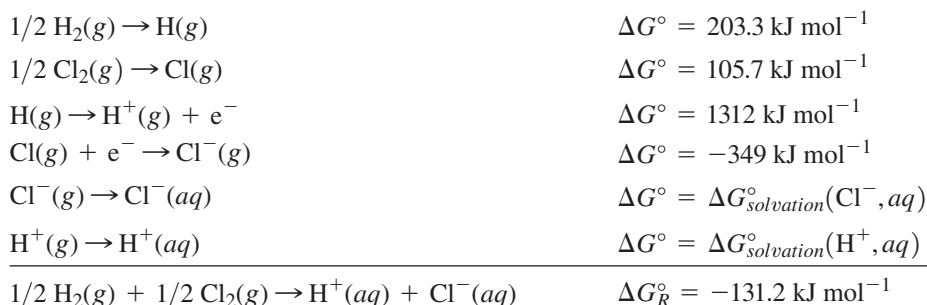
This pathway is shown pictorially in Figure 10.1. Because $G$ is a state function, both the black and red paths must have the same $\Delta G$ value. The first two reactions in this sequence are the dissociation of the molecules in the gas phase, and the second two reactions are the formation of gas phase ions from the neutral gas phase atoms. $\Delta G^\circ$ can be determined experimentally for these four reactions. Substituting the known values for $\Delta G^\circ$ for these four reactions in $\Delta G^\circ$ for the overall process,

$$\Delta G_R^\circ = \Delta G_{solvation}^\circ(Cl^-, aq) + \Delta G_{solvation}^\circ(H^+, aq) + 1272\ \text{kJ mol}^{-1} \quad \textbf{(10.7)}$$

Equation 10.7 allows us to relate the $\Delta G_{solvation}^\circ$ of the $H^+$ and $Cl^-$ ions with $\Delta G_R^\circ$ for the overall reaction.

As Equation (10.7) shows, $\Delta G_{solvation}^\circ$ plays a critical role in the determination of the Gibbs energies of ion formation. Although $\Delta G_{solvation}^\circ$ of an individual cation or anion cannot be determined experimentally, it can be estimated using a model developed by Max Born. In this model, the solvent is treated as a uniform fluid with the appropriate dielectric constant, and the ion is treated as a charged sphere. How can $\Delta G_{solvation}^\circ$ be calculated with these assumptions? At constant $T$ and $P$, the nonexpansion work for a reversible process equals $\Delta G$ for the process. Therefore, if the reversible work associated with solvation can be calculated, $\Delta G$ for the process is known. Imagine a process in which a neutral atom A gains the charge $Q$, first in a vacuum and secondly in a uniform dielectric medium. The value of $\Delta G_{solvation}^\circ$ of an ion with a charge $q$ is the reversible work for the process $(A(g) \rightarrow A^Q(aq))_{solvation}$ minus that for the reversible process $(A(g) \rightarrow A^Q(g))_{vacuum}$.
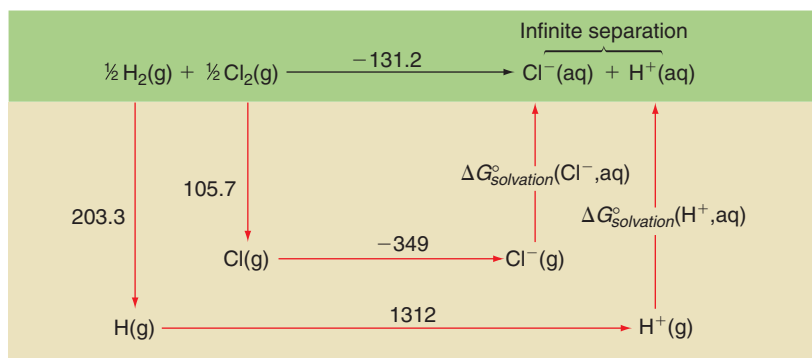
**FIGURE 10.1**
$\Delta G^\circ$ is shown pictorially for two different paths starting with $1/2\ H_2(g)$ and $1/2\ Cl_2(g)$ and ending with $H^+(aq) + Cl^-(aq)$. The units for the numbers are kJ mol$^{-1}$. Because $\Delta G$ is the same for both paths, $\Delta G_{solvation}^\circ(H^+, aq)$ can be expressed in terms of gas-phase dissociation and ionization energies.

The electrical potential around a sphere of radius $r$ with the charge $Q'$ is given by $\phi = Q'/4\pi\varepsilon r$. From electrostatics, the work in charging the sphere by the additional amount $dQ$ is $\phi\, dQ$. Therefore, the work in charging a neutral sphere in vacuum to the charge $Q$ is

$$w = \int_0^Q \frac{Q'\, dQ'}{4\pi\varepsilon_0 r} = \frac{1}{4\pi\varepsilon_0 r}\int_0^Q Q'\, dQ' = \frac{Q^2}{8\pi\varepsilon_0 r} \tag{10.8}$$

where $\varepsilon_0$ is the permittivity of free space. The work of the same process in a solvent is $Q^2/8\pi\varepsilon_0\varepsilon_r r$, where $\varepsilon_r$ is the relative permittivity (dielectric constant) of the solvent. Consequently, $\Delta G^\circ_{solvation}$ for an ion of charge $Q = ze$ is given by

$$\Delta G^\circ_{solvation} = \frac{z^2 e^2 N_A}{8\pi\varepsilon_0 r}\left(\frac{1}{\varepsilon_r} - 1\right) \tag{10.9}$$

Because $\varepsilon_r > 1$, $\Delta G^\circ_{solvation} < 0$, showing that solvation is a spontaneous process. Values for $\varepsilon_r$ for a number of solvents are listed in Table 10.2 (see Appendix A, Data Tables).

To test the Born model, we need to compare absolute values of $\Delta G^\circ_{solvation}$ for ions of different radii with the functional form proposed in Equation (10.9). However, this comparison requires knowledge of $\Delta G^\circ_{solvation}(H^+, aq)$ to convert experimentally determined values of $\Delta G^\circ_{solvation}$ referenced to $H^+(aq)$ to absolute values. It turns out that $\Delta G^\circ_{solvation}(H^+, aq)$, and $\Delta H^\circ_{solvation}(H^+, aq)$, and $S^\circ_{solvation}(H^+, aq)$ can be calculated. Because the calculation is involved, the results are simply stated here.

$$\Delta H^\circ_{solvation}(H^+, aq) \approx -1090\,\text{kJ mol}^{-1}$$

$$\Delta G^\circ_{solvation}(H^+, aq) \approx -1050\,\text{kJ mol}^{-1}$$

$$S^\circ_{solvation}(H^+, aq) \approx -130\,\text{J mol}^{-1}\text{K}^{-1} \tag{10.10}$$

The values listed in Equation (10.10) can be used to calculate absolute values of $\Delta H^\circ_{solvation}$, $\Delta G^\circ_{solvation}$, and $S^\circ_{solvation}$ for other ions from the conventional values referenced to $H^+(aq)$. These calculated absolute values can be used to test the validity of the Born model. If the model is valid, a plot of $\Delta G^\circ_{solvation}$ versus $z^2/r$ will give a straight line as shown by Equation (10.9), and the data points for individual ions should lie on the line. The results are shown in Figure 10.2, where $r$ is the ionic radius obtained from crystal structure determinations.

The first and second clusters of data points in Figure 10.2 are for singly and doubly charged ions, respectively. The data are compared with the result predicted by Equation (10.9) in Figure 10.2a. As can be seen from the figure, the trends are reproduced, but there is no quantitative agreement. The agreement can be considerably improved by using an effective radius for the solvated ion rather than the ionic radius from crystal structure determinations. The effective radius is defined as the distance from the center of the ion to the center of charge in the dipolar water molecule in the solvation shell. Latimer, Pitzer, and Slansky [*J. Chemical Physics*, 7 (1939) 109] found the best agreement with the Born equation by adding 0.085 nm to the crystal radius of positive ions, and 0.100 nm to the crystal radius for negative ions to account for the fact that the $H_2O$ molecule is not a point dipole. This difference is explained by the fact that the center of charge in the water molecule is closer to positive ions than to negative ions. Figure 10.2b shows that the agreement obtained between the predictions of Equation (10.9) and experimental values is very good if this correction to the ionic radii is made.

Figure 10.2 shows good agreement between the predictions of the Born model and calculated values for $\Delta G^\circ_{solvation}$, and justifies the approach used to calculate absolute enthalpies, Gibbs energies and entropies for solvated ions. However, because of uncertainties about the numerical values of the ionic radii and for the dielectric constant of the immobilized water in the solvation shell of an ion, the uncertainty is $\pm 50\,\text{kJ mol}^{-1}$ for the absolute solvation enthalpy and Gibbs energy and $\pm 10\,\text{J K}^{-1}\,\text{mol}^{-1}$ for the absolute solvation entropy. Because these uncertainties are large compared to the uncertainty of the thermodynamic functions using the convention described in Equations (10.3) and (10.4),

(a)

(b)
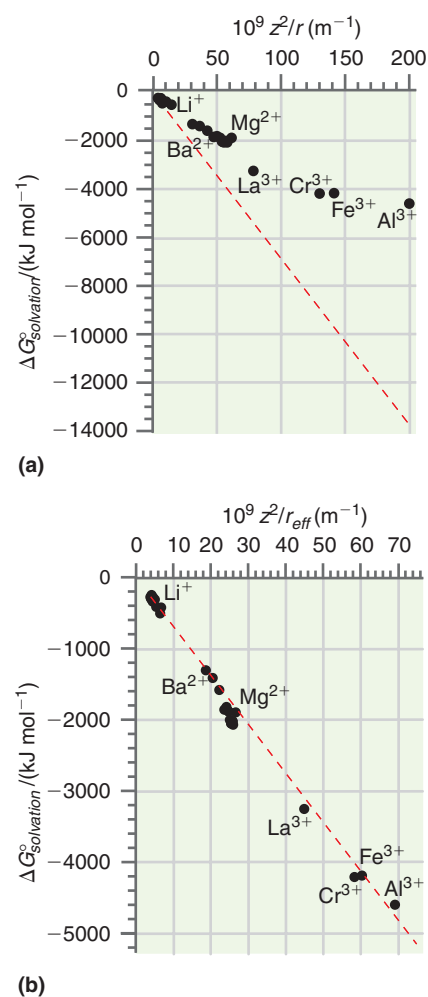
**FIGURE 10.2**
(a) The solvation energy calculated using the Born model is shown as a function of $z^2/r$. (b) The same results are shown as a function of $z^2/r_{eff}$. (See text.) The dashed line shows the behavior predicted by Equation (10.9).

conventional rather than absolute values of $\Delta H_f^\circ$, $\Delta G_f^\circ$, and $S_m^\circ$ for solvated ions in aqueous solutions are generally used by chemists.

## 10.3 Activities and Activity Coefficients for Electrolyte Solutions

The ideal dilute solution model presented for the activity and activity coefficient of components of real solutions in Chapter 9 is not valid for electrolyte solutions. This is the case because solute–solute interactions are dominated by the long-range electrostatic forces present between ions in electrolyte solutions. For example, the reaction that occurs when NaCl is dissolved in water is

$$\text{NaCl}(s) + \text{H}_2\text{O}(l) \rightarrow \text{Na}^+(aq) + \text{Cl}^-(aq) \tag{10.11}$$
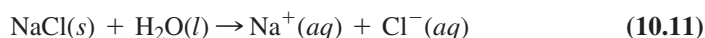
In dilute solutions, NaCl is completely dissociated. Therefore, all solute–solute interactions are electrostatic in nature.

Although the concepts of activity and activity coefficients introduced in Chapter 9 are applicable to electrolytes, these concepts must be formulated differently for electrolytes to include the Coulomb interactions among ions. We next discuss a model for electrolyte solutions that is stated in terms of the chemical potentials, activities, and activity coefficients of the individual ionic species. However, only mean activities and activity coefficients (to be defined later) can be determined through experiments.

Consider the Gibbs energy of the solution, which can be written as

$$G = n_{solvent}\,\mu_{solvent} + n_{solute}\,\mu_{solute} \tag{10.12}$$

For the general electrolyte $A_{\nu_+}B_{\nu_-}$ that dissociates completely, one can also write an equivalent expression for $G$:

$$G = n_{solvent}\,\mu_{solvent} + n_+\mu_+ + n_-\mu_- = n_{solvent}\,\mu_{solvent} + n_{solute}(\nu_+\mu_+ + \nu_-\mu_-) \tag{10.13}$$

where $\nu_+$ and $\nu_-$ are the stoichiometric coefficients of the cations and anions, respectively, produced upon dissociation of the electrolyte. In shorthand notation, an electrolyte is called a 1–1 electrolyte if $\nu_+ = 1$ and $\nu_- = 1$. Similarly, for a 2–3 electrolyte, $\nu_+ = 2$ and $\nu_- = 3$. Because Equations (10.12) and (10.13) describe the same solution, they are equivalent. Therefore,

$$\mu_{solute} = \nu_+\mu_+ + \nu_-\mu_- \tag{10.14}$$

Although this equation is formally correct for a strong electrolyte, one can never make a solution of either cations or anions alone, because any solution is electrically neutral. Therefore, it is useful to define a **mean ionic chemical potential** $\mu_\pm$ for the solute

$$\mu_\pm = \frac{\mu_{solute}}{\nu} = \frac{\nu_+\mu_+ + \nu_-\mu_-}{\nu} \tag{10.15}$$

where $\nu = \nu_+ + \nu_-$. The reason for doing so is that $\mu_\pm$ can be determined experimentally, whereas $\mu_+$ and $\mu_-$ are not accessible through experiments.

The next task is to relate the chemical potentials of the solute and its individual ions to the activities of these species. For the individual ions,

$$\mu_+ = \mu_+^\circ + RT\ln a_+ \quad \text{and} \quad \mu_- = \mu_-^\circ + RT\ln a_- \tag{10.16}$$

where the standard chemical potentials of the ions, $\mu_+^\circ$ and $\mu_-^\circ$, are based on a Henry's law standard state. Substituting Equation (10.16) in (10.15), an equation for the mean ionic chemical potential is obtained that is similar in structure to the expressions that we derived for the ideal dilute solution:

$$\mu_\pm = \mu_\pm^\circ + RT\ln a_\pm \tag{10.17}$$

The **mean ionic activity** $a_\pm$ is related to the individual ion activities by

$$a_\pm^\nu = a_+^{\nu_+}a_-^{\nu_-} \quad \text{or} \quad a_\pm = (a_+^{\nu_+}a_-^{\nu_-})^{1/\nu} \tag{10.18}$$

## EXAMPLE PROBLEM 10.1

Write the mean ionic activities of $NaCl$, $K_2SO_4$, and $H_3PO_4$ in terms of the ionic activities of the individual anions and cations. Assume complete dissociation.

### Solution

$$a_{NaCl}^2 = a_{Na^+} a_{Cl^-} \quad \text{or} \quad a_{NaCl} = \sqrt{a_{Na^+} a_{Cl^+}}$$

$$a_{K_2SO_4}^3 = a_{K^+}^2 a_{SO_4^{2-}} \quad \text{or} \quad a_{K_2SO_4} = (a_{K^+}^2 a_{SO_4^{2-}})^{1/3}$$

$$a_{H_3PO_4}^4 = a_{H^+}^3 a_{PO_4^{3-}} \quad \text{or} \quad a_{H_3PO_4} = (a_{H^+}^3 a_{PO_4^{3-}})^{1/4}$$

If the ionic activities are referenced to the concentration units of molality, then

$$a_+ = \frac{m_+}{m^\circ} \gamma_+ \quad \text{and} \quad a_- = \frac{m_-}{m^\circ} \gamma_- \tag{10.19}$$

where $m_+ = v_+ m$ and $m_- = v_- m$. Because the activity is unitless, the molality must be referenced to a standard state concentration chosen to be $m^\circ = 1\,\text{mol kg}^{-1}$. As in Chapter 9, a hypothetical standard state based on molality is defined. In this standard state, Henry's law, which is valid in the limit $m \to 0$, is obeyed up to a concentration of $m = 1$ molal. Substitution of Equation (10.19) in Equation (10.18) shows that

$$a_{\pm}^v = \left(\frac{m_+}{m^\circ}\right)^{v_+} \left(\frac{m_-}{m^\circ}\right)^{v_-} \gamma_+^{v_+} \gamma_-^{v_-} \tag{10.20}$$

To simplify this notation, we define the **mean ionic molality** $m_\pm$ and **mean ionic activity coefficient** $\gamma_\pm$ by

$$m_\pm^v = m_+^{v_+} m_-^{v_-}$$

$$m_\pm = (v_+^{v_+} v_-^{v_-})^{1/v} m \quad \text{and}$$

$$\gamma_\pm^v = \gamma_+^{v_+} \gamma_-^{v_-}$$

$$\gamma_\pm = (\gamma_+^{v_+} \gamma_-^{v_-})^{1/v} \tag{10.21}$$

With these definitions, the mean ionic activity is related to the mean ionic activity coefficient and mean ionic molality as follows:

$$a_{\pm}^v = \left(\frac{m_\pm}{m^\circ}\right)^v \gamma_\pm^v \quad \text{or} \quad a_\pm = \left(\frac{m_\pm}{m^\circ}\right) \gamma_\pm \tag{10.22}$$

Equations (10.19) through (10.22) relate the activities, activity coefficients, and molalities of the individual ionic species to mean ionic quantities and measurable properties of the system such as the molality and activity of the solute. With these definitions, Equation (10.17) defines the chemical potential of the electrolyte solute in terms of its activity:

$$\mu_{solute} = \mu_{solute}^\circ + RT \ln a_\pm^v \tag{10.23}$$

Equations (10.20) and (10.21) can be used to express the chemical potential of the solute in terms of measurable or easily accessible quantities:

$$\mu_{solute} = \mu_\pm = \left[ v\mu_\pm^\circ + RT \ln(v_+^{v_+} v_-^{v_-}) \right] + vRT \ln\left(\frac{m}{m^\circ}\right) + vRT \ln \gamma_\pm \tag{10.24}$$

The first term in the square bracket is defined by the "normal" standard state, which is usually taken to be a Henry's law standard state. The second term is obtained from the chemical formula for the solute. These two terms can be combined to create a new standard state $\mu_\pm^{\circ\circ}$ defined by the terms in the square brackets in Equation (10.24):

$$\mu_{solute} = \mu_\pm = \mu_\pm^{\circ\circ} + vRT \ln\left(\frac{m}{m^\circ}\right) + vRT \ln \gamma_\pm \tag{10.25}$$

The first two terms in Equation (10.25) correspond to the "ideal" ionic solution, which is associated with $\gamma_\pm = 1$.

The last term in Equation (10.25), which is the most important term in this discussion, contains the deviations from ideal behavior. The mean activity coefficient $\gamma_\pm$ can be obtained through experiment. For example, the activity coefficient of the solvent can be determined by measuring the boiling point elevation, the freezing point depression, or the lowering of the vapor pressure above the solution upon solution formation. The activity of the solute is obtained from that of the solvent using the Gibbs–Duhem equation. As shown in Section 11.8, $\gamma_\pm$ can also be determined through measurements on electrochemical cells. In addition, a very useful theoretical model allows $\gamma_\pm$ to be calculated for dilute electrolytic solutions. This model is discussed in the next section.

## 10.4 Calculating $\gamma_\pm$ Using the Debye–Hückel Theory

There is no model that adequately explains the deviations from ideality for the solutions of neutral solutes discussed in Sections 9.1 through 9.4. This is the case because the deviations arise through A–A, B–B, and A–B interactions that are specific to components A and B. This precludes a general model that holds for arbitrary A and B. However, the situation for solutions of electrolytes is different.

Deviations from ideal solution behavior occur at a much lower concentration for electrolytes than for nonelectrolytes, because the dominant interaction between the ions in an electrolyte is a long-range electrostatic Coulomb interaction rather than a short-range van der Waals or chemical interaction. Because of its long range, the Coulomb interaction among the ions cannot be neglected even for very dilute solutions of electrolytes. The Coulomb interaction allows a model of electrolyte solutions to be formulated independent of the identity of the solute for the following reason. The attractive or repulsive interaction of two ions depends only on their charge and separation, and not on their chemical identity. Therefore, the solute–solute interactions can be modeled knowing only the charge on the ions, and the model becomes independent of the identity of the solute species.

Measurements of activity coefficients in electrolyte solutions show that $\gamma_\pm \rightarrow 1$ for dilute solutions in the limit $m \rightarrow 0$. Because $\gamma_\pm < 1$, the chemical potential of the solute in a dilute solution is lower than that for a solution of uncharged solute species. Why is this the case? The lowering of $\mu_{solute}$ arises because the net electrostatic interaction among the ions surrounding an arbitrarily chosen central ion is attractive rather than repulsive. The model that describes the lowering of the energy of electrolytic solutions is due to Peter Debye and Erich Hückel. Rather than derive their results, we describe the essential features of their model next.

The solute ions in the solvent give rise to a spatially dependent electrostatic potential, $\phi$, which can be calculated if the spatial distribution of ions is known. In dilute electrolyte solutions, the energy increase or decrease experienced by an ion of charge $\pm ze$ if the potential $\phi$ could be turned on suddenly is small compared to the thermal energy. This condition can be expressed in the form

$$|\pm ze\phi| \ll k_B T \tag{10.26}$$

In Equation (10.26), $e$ is the charge on a proton, and $k$ is Boltzmann's constant. In this limit, the dependence of $\phi$ on the spatial coordinates and the spatial distribution of the ions around an arbitrary central ion can be calculated. In contrast to the potential around an isolated ion in a dielectric medium, which is described by

$$\phi_{isolated\ ion}(r) = \frac{\pm ze}{4\pi\varepsilon_r\varepsilon_0 r} \tag{10.27}$$

the potential in the dilute electrolyte solution has the form

$$\phi_{solution}(r) = \frac{\pm ze}{4\pi\varepsilon_r\varepsilon_0 r}\exp(-\kappa r) \tag{10.28}$$
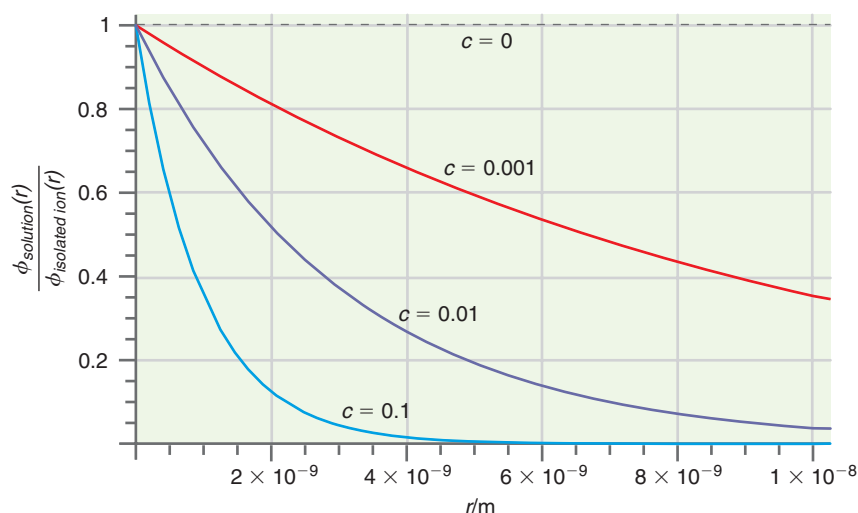
**FIGURE 10.3**
The ratio of the falloff in the electrostatic potential in the electrolyte solution to that for an iso-lated ion is shown as a function of the radial distance for three different molarities of a 1–1 elec-trolyte such as NaCl.

In Equations (10.27) and (10.28), $\varepsilon_0$ and $\varepsilon_r$ are the permittivity of free space and the relative permittivity (dielectric constant) of the dielectric medium or solvent, respec-tively. Because of the exponential term, $\phi_{solution}(r)$ falls off much more rapidly with $r$ than $\phi_{isolated\ ion}(r)$. We say that an individual ion experiences a **screened potential** from the other ions.

The Debye–Hückel theory shows that $\kappa$ is related to the individual charges on the ions and to the solute molality $m$ by

$$\kappa^2 = e^2 N_A \left(1000\ \text{L m}^{-3}\right) m \left(\frac{\nu_+ z_+^2 + \nu_- z_-^2}{\varepsilon_0 \varepsilon_r k_B T}\right) \rho_{solvent} \qquad (10.29)$$

From this formula, we can see that screening becomes more effective as the concentra-tion of the ionic species increases. Screening is also more effective for multiply charged ions and for larger values of $\nu_+$ and $\nu_-$.

The ratio

$$\frac{\phi_{solution}(r)}{\phi_{isolated\ ion}(r)} = e^{-\kappa r}$$

is plotted in Figure 10.3 for different values of $m$ for an aqueous solution of a 1–1 elec-trolyte. Note that the potential falls off much more rapidly with the radial distance $r$ in the electrolyte solution than in the uniform dielectric medium. Note also that the poten-tial falls off more rapidly with increasing concentration of the electrolyte. The origin of this effect is that ions of sign opposite to the central ion are more likely to be found close to the central ion. These surrounding ions form a diffuse ion cloud around the central ion, as shown pictorially in Figure 10.4. If a spherical surface is drawn centered at the central ion, the net charge within the surface can be calculated. The results show that the net charge has the same sign as the central charge, falls off rapidly with distance, and is close to zero for $\kappa r \sim 8$. For larger values of $\kappa r$, the central ion is completely screened by the diffuse ion cloud, meaning that the net charge in the sphere around the central ion is zero. The net effect of the diffuse ion cloud is to screen the central ion from the rest of the solution, and the quantity $1/\kappa$ is known as the **Debye–Hückel screening length.** Larger values of $\kappa$ correspond to a smaller diffuse cloud, and a more effective screening.

It is convenient to combine the concentration-dependent terms that contribute to $\kappa$ in the **ionic strength** $I$, which is defined by

$$I = \frac{m}{2} \sum_i \left(\nu_{i+} z_{i+}^2 + \nu_{i-} z_{i-}^2\right) = \frac{1}{2} \sum_i \left(m_{i+} z_{i+}^2 + m_{i-} z_{i-}^2\right) \qquad (10.30)$$
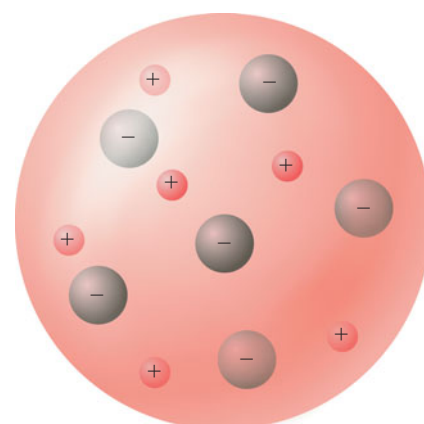


**FIGURE 10.4**
Pictorial rendering of the arrangement of ions about an arbitrary ion in an elec-trolyte solution. The central ion is more likely to have oppositely charged ions as neighbors. The large circle represents a sphere of radius $r \sim 8/\kappa$. From a point outside of this sphere, the charge on the central ion is essentially totally screened.

### EXAMPLE PROBLEM 10.2

Calculate $I$ for (a) a 0.050 molal solution of NaCl and for (b) a $Na_2SO_4$ solution of the same molality.

#### Solution

a. $I_{NaCl} = \dfrac{m}{2}(v_+z_+^2 + v_-z_-^2) = \dfrac{0.050\,mol\,kg^{-1}}{2} \times (1 + 1) = 0.050\,mol\,kg^{-1}$

b. $I_{Na_2SO_4} = \dfrac{m}{2}(v_+z_+^2 + v_-z_-^2) = \dfrac{0.050\,mol\,kg^{-1}}{2} \times (2 + 4) = 0.15\,mol\,kg^{-1}$

Using the definition of the ionic strength, Equation (10.29) can be written in the form

$$\kappa = \sqrt{\left(\frac{2e^2 N_A}{\varepsilon_0 k_B T}\right)(1000L\,m^{-3})}\sqrt{\left(\frac{I}{\varepsilon_r}\right)\rho_{solvent}}$$

$$= 2.91 \times 10^8 \sqrt{\frac{I/mol\,kg^{-1}}{\varepsilon_r}\frac{\rho_{solvent}}{kg\,L^{-1}}}\,m^{-1} \quad \text{at 298 K} \tag{10.31}$$

The first factor in this equation contains only fundamental constants that are independent of the solvent and solute as well as the temperature. The second factor contains the ionic strength of the solution and the unitless relative permittivity of the solvent. For the more conventional units of mol $L^{-1}$, and for water, for which $\varepsilon_r = 78.5$, $\kappa = 3.29 \times 10^9 \sqrt{I}\ m^{-1}$ at 298 K.

By calculating the charge distribution of the ions around the central ion and the work needed to charge these ions up to their charges $z_+$ and $z_-$ from an initially neutral state, Debye and Hückel were able to obtain an expression for the mean ionic activity coefficient. It is given by

$$\ln \gamma_\pm = -|z_+z_-|\frac{e^2\kappa}{8\pi\varepsilon_0\varepsilon_r k_B T} \tag{10.32}$$

This equation is known as the **Debye–Hückel limiting law.** It is called a limiting law because Equation (10.32) is only obeyed for small values of the ionic strength. Note that because of the negative sign in Equation (10.32), $\gamma_\pm < 1$. From the concentration dependence of $\kappa$ shown in Equation (10.31), the model predicts that $\ln \gamma_\pm$ decreases with the ionic strength as $\sqrt{I}$. This dependence is shown in Figure 10.5. Although all three solutions have the same solute concentration, they have different values for $z^+$ and $z^-$. For this reason, the three lines have a different slope.

Equation (10.32) can be simplified for a particular choice of solvent and temperature. For aqueous solutions at 298.15 K, the result is

$$\log \gamma_\pm = -0.5092|z_+z_-|\sqrt{I} \quad \text{or} \quad \ln\gamma_\pm = -1.173|z_+z_-|\sqrt{I} \tag{10.33}$$

How well does the Debye–Hückel limiting law agree with experimental data? Figure 10.6 shows a comparison of the model with data for aqueous solutions of $AgNO_3$ and $CaCl_2$. In each case, $\ln \gamma_\pm$ is plotted versus $\sqrt{I}$. The Debye–Hückel limiting law predicts that the data will fall on the line indicated in each figure. The data points deviate from the predicted behavior above $\sqrt{I} = 0.1$ for $AgNO_3$ ($m = 0.01$), and above $\sqrt{I} = 0.006$ for $CaCl_2$ ($m = 0.004$). In the limit that $I \rightarrow 0$, the limiting law is obeyed. However, the deviations are significant at a concentration for which a neutral solute would exhibit ideal behavior.

The deviations continue to increase with increasing ionic strength. Figure 10.7 shows experimental data for $ZnBr_2$ out to $\sqrt{I} = 5.5$, corresponding to $m = 10$. Note that, although the Debye–Hückel limiting law is obeyed as $I \rightarrow 0$, $\ln \gamma_\pm$ goes through a minimum and begins to increase with increasing ionic strength. At the highest value of the ionic strength, $\gamma_\pm = 2.32$, which is significantly greater than one. Although the deviations from ideal behavior are less pronounced in Figure 10.6, the trend is the same for all the solutes. The mean ionic activity coefficient $\gamma_\pm$ falls off more slowly with the ionic strength than predicted by the Debye–Hückel limiting law. The behavior shown in Figure 10.7 is typical for most electrolytes; after passing through a minimum, $\gamma_\pm$ rises
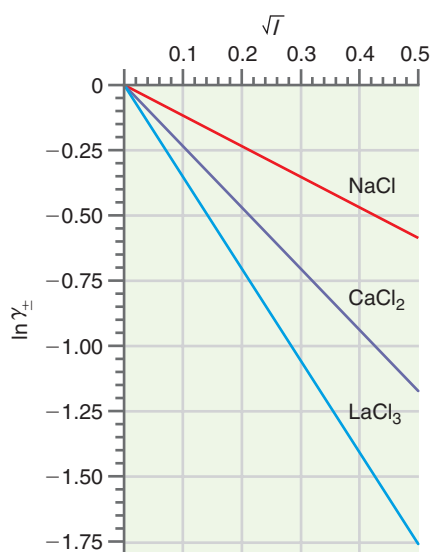


#### FIGURE 10.5

The decrease in the Debye–Hückel mean activity coefficient with the square root of the ionic strength is shown for a 1–1, a 1–2, and a 1–3 electrolyte, all of the same molality in the solute.

with increasing ionic strength, and for high values of $I$, $\gamma_\pm > 1$. Experimental values for $\gamma_\pm$ for a number of solutes at different concentrations in aqueous solution are listed in Table 10.3 (see Appendix A, Data Tables).

There are a number of reasons why the experimental values of $\gamma_\pm$ differ at high ionic strength from those calculated from the Debye–Hückel limiting law. They mainly involve the assumptions made in the model. It has been assumed that the ions can be treated as point charges with zero volume, whereas ions and their associated solvation shells occupy a finite volume. As a result, there is an increase in the repulsive interaction among ions in an electrolyte over that predicted for point charges, which becomes more important as the concentration increases. Repulsive interactions raise the energy of the solution and, therefore, increase $\gamma_\pm$. The Debye–Hückel model also assumes that the solvent can be treated as a structureless dielectric medium. However, the ion is surrounded by a relatively ordered primary solvation shell, as well as by more loosely bound water molecules. The atomic level structure of the solvation shell is not adequately represented by using the dielectric strength of bulk solvent. Another factor that has not been taken into account is that as the concentration increases, some ion pairing occurs such that the concentration of ionic species is less than would be calculated assuming complete dissociation.

Additionally, consider the fact that the water molecules in the solvation shell have effectively been removed from the solvent. For example, in an aqueous solution of $H_2SO_4$, approximately nine $H_2O$ molecules are tightly bound per dissolved $H_2SO_4$ formula unit. Therefore, the number of moles of $H_2O$ as solvent in 1 L of a one molar $H_2SO_4$ solution is reduced from 55 for pure $H_2O$ to 46 in the solution. Consequently, the actual solute molarity is larger than that calculated by assuming that all the $H_2O$ is in the form of solvent. Because the activity increases linearly with the actual molarity, $\gamma_\pm$ increases as the solute concentration increases. If there were no change in the enthalpy of solvation with concentration, all the $H_2O$ molecules would be removed from the solvent at a concentration of six molar $H_2SO_4$. Clearly, this assumption is unreasonable. What actually happens is that solvation becomes energetically less favorable as the $H_2SO_4$ concentration increases. This corresponds to a less negative value of $\ln \gamma_\pm$, or equivalently to an increase in $\gamma_\pm$. Summing up, many factors explain why the Debye–Hückel limiting law is only valid for small concentrations. Because of the complexity of these different factors, there is no simple formula based on theory that can replace the Debye–Hückel limiting law. However, the main trends exhibited in Figures 10.6 and 10.7 are reproduced in more sophisticated theories of electrolyte solutions.

Because none of the usual models are valid at high concentrations, empirical models that "improve" on the Debye–Hückel model by predicting an increase in $\gamma_\pm$ for high concentrations are in widespread use. An empirical modification of the Debye–Hückel limiting law that has the form

$$\log_{10} \gamma_\pm = -0.51|z_+ z_-| \left[ \frac{\left(\dfrac{I}{m^\circ}\right)^{1/2}}{1 + \left(\dfrac{I}{m^\circ}\right)^{1/2}} - 0.30 \left(\frac{I}{m^\circ}\right) \right] \qquad \textbf{(10.34)}$$
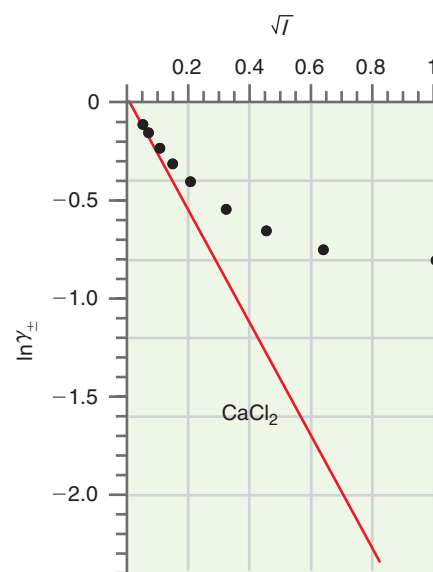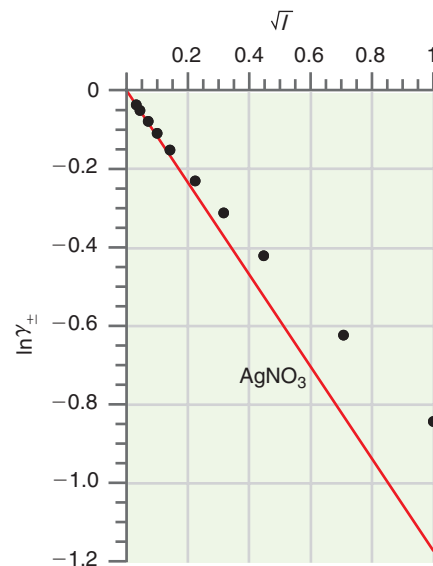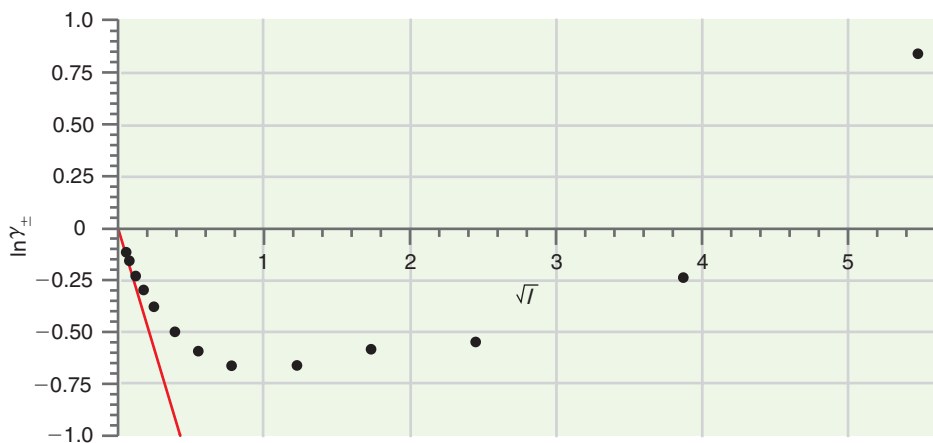


**FIGURE 10.6**
The experimentally determined activity coefficients for $AgNO_3$ and $CaCl_2$ are shown as a function of the square root of the ionic strength. The solid lines are the prediction of the Debye–Hückel theory.



**FIGURE 10.7**
Experimentally determined values for the mean activity coefficient for $ZnBr_2$ are shown as a function of the square root of the ionic strength. The solid line is the prediction of the Debye–Hückel theory.
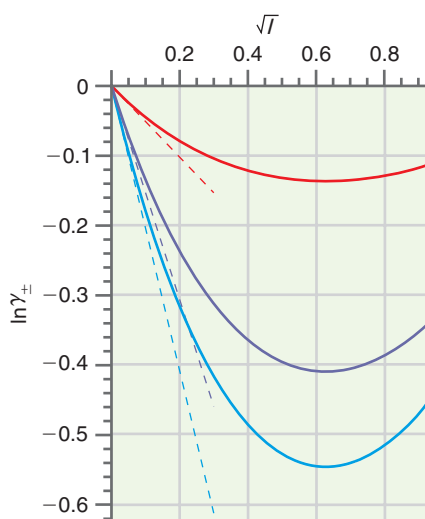
**FIGURE 10.8**
Comparison between the predictions of the Debye–Hückel limiting law (dashed lines) and the Davies equation (solid curves) for 1–1 (red), 1–2 (purple), and 1–3 (blue) electrolytes.

is known as the **Davies equation.** As seen in Figure 10.8, this equation for $\gamma_\pm$ shows the correct limiting behavior for low $I$ values, and the trend at higher values of $I$ is in better agreement with the experimental results shown in Figures 10.6 and 10.7. However, unlike the Debye–Hückel limiting law, there is no theoretical basis for the Davies equation.

# 10.5 Chemical Equilibrium in Electrolyte Solutions

As discussed in Section 9.13, the equilibrium constant in terms of activities is given by Equation (9.66):

$$K = \prod_i (a_i^{eq})^{\nu_j} \tag{10.35}$$

It is convenient to define the activity of a species relative to its molarity. In this case,

$$a_i = \gamma_i \frac{c_i}{c^\circ} \tag{10.36}$$

where $\gamma_i$ is the activity coefficient of species $i$. We next specifically consider chemical equilibrium in electrolyte solutions, illustrating that activities rather than concentrations must be taken into account to accurately model equilibrium concentrations. We first restrict our considerations to the range of ionic strengths for which the Debye–Hückel limiting law is valid. As an example, we calculate the degree of dissociation of $MgF_2$ in water. The equilibrium constant in terms of molarities for ionic salts is usually given the symbol $K_{sp}$, where the subscript refers to the solubility product. The equilibrium constant $K_{sp}$ is unitless and has the value of $6.4 \times 10^{-9}$ for the reaction shown in Equation (10.37). Values for $K_{sp}$ are generally tabulated for reduced concentration units of molarity $(c/c^\circ)$ rather than molality $(m/m^\circ)$, and values for selected substances are listed in Table 10.4. Because the mass of 1 L of water is 0.998 kg, the numerical value of the concentration is the same on both scales for dilute solutions.

We next consider dissociation of $MgF_2$ in an aqueous solution:

$$MgF_2(s) \rightarrow Mg^{2+}(aq) + 2F^-(aq) \tag{10.37}$$
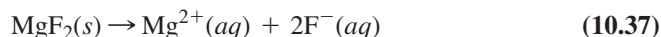
Because the activity of the pure solid can be set equal to one,

$$K_{sp} = a_{Mg^{2+}} a_{F^-}^2 = \left(\frac{c_{Mg^{2+}}}{c^\circ}\right)\left(\frac{c_{F^-}}{c^\circ}\right)^2 \gamma_\pm^3 = 6.4 \times 10^{-9} \tag{10.38}$$

From the stoichiometry of the overall equation, we know that $c_{F^-} = 2c_{Mg^{2+}}$, but Equation (10.38) still contains two unknowns, $\gamma_\pm$ and $c_{F^-}$, that we solve for iteratively as shown in Example Problem 10.3.

| **TABLE 10.4** | Solubility Product Constants (Molarity Based) for Selected Salts | | |
|---|---|---|---|
| Salt | $K_{sp}$ | Salt | $K_{sp}$ |
| AgBr | $4.9 \times 10^{-13}$ | CaSO$_4$ | $4.9 \times 10^{-6}$ |
| AgCl | $1.8 \times 10^{-10}$ | Mg(OH)$_2$ | $5.6 \times 10^{-11}$ |
| AgI | $8.5 \times 10^{-17}$ | Mn(OH)$_2$ | $1.9 \times 10^{-13}$ |
| Ba(OH)$_2$ | $5.0 \times 10^{-3}$ | PbCl$_2$ | $1.6 \times 10^{-5}$ |
| BaSO$_4$ | $1.1 \times 10^{-10}$ | Pb SO$_4$ | $1.8 \times 10^{-8}$ |
| CaCO$_3$ | $3.4 \times 10^{-9}$ | ZnS | $1.6 \times 10^{-23}$ |

*Source:* Lide, D. R., ed. *Handbook of Chemistry and Physics.* 83rd ed. Boca Raton, FL: CRC Press 2002.

## EXAMPLE PROBLEM 10.3

Calculate the solubility of $MgF_2$ in an aqueous solution. Use the Debye–Hückel limiting law to obtain $\gamma_\pm$. $K_{sp} = 6.4 \times 10^{-9}$.

### Solution

The equilibrium expression is stated in Equation 10.38.

$$K_{sp} = a_{Mg^{2+}}a_{F^-}^2 = \left(\frac{c_{Mg^{2+}}}{c^\circ}\right)\left(\frac{c_{F^-}}{c^\circ}\right)^2 \gamma_\pm^3 = 6.4 \times 10^{-9}$$

First assume that $\gamma_\pm = 1$, and solve Equation (10.38) for $c_{Mg^{2+}}$.

$$K_{sp} = a_{Mg^{2+}}a_{F^-}^2 = \left(\frac{c_{Mg^{2+}}}{c^\circ}\right)\left(\frac{c_{F^-}}{c^\circ}\right)^2 = 6.4 \times 10^{-9}$$

$$4x^3 = 6.4 \times 10^{-9};\ x = \frac{c_{Mg^{2+}}}{c^\circ} = 1.17 \times 10^{-3}\,\text{mol L}^{-1} = 1.17 \times 10^{-3}\,\text{mol kg}^{-1}$$

We next calculate the ionic strength of the solution using the concentrations just obtained.

$$I_{MgF_2} = \frac{m}{2}(v_+z_+^2 + v_-z_-^2) = \frac{1.17 \times 10^{-3}\,\text{mol kg}^{-1}}{2} \times (2^2 + 2)$$

$$= 3.51 \times 10^{-3}\,\text{mol kg}^{-1}$$

We next calculate $\gamma_\pm$ from the Debye–Hückel limiting law of Equation (10.33).

$$\ln \gamma_\pm = -1.173|z_+z_-|\sqrt{I}$$

$$\ln \gamma_\pm = -1.173 \times 2 \times \sqrt{3.51 \times 10^{-3}} = -0.1390$$

$$\gamma_\pm = 0.870$$

We use this value of $\gamma_\pm$ in the equilibrium expression and recalculate the solubility.

$$K_{sp} = a_{Mg^{2+}}a_{F^-}^2 = \left(\frac{c_{Mg^{2+}}}{c^\circ}\right)\left(\frac{c_{F^-}}{c^\circ}\right)^2 \gamma_\pm^3 = 6.4 \times 10^{-9}$$

$$4x^3 = \frac{6.4 \times 10^{-9}}{(0.870)^3};\ x = \frac{c_{Mg^{2+}}}{c^\circ} = 1.34 \times 10^{-3}\,\text{mol L}^{-1} = 1.34 \times 10^{-3}\,\text{mol kg}^{-1}$$

A second iteration gives $\gamma_\pm = 0.862$ and $c_{Mg^{2+}} = 1.36 \times 10^{-3}$ mol $L^{-1}$, and a third iteration gives $\gamma_\pm = 0.861$ and $c_{Mg^{2+}} = 1.36 \times 10^{-3}$ mol $L^{-1}$, showing that the iteration has converged. These results show that assuming that $\gamma_\pm = 1$ leads to an unacceptably large error of 14% in $c_{Mg^{2+}}$.

Another effect of the ionic strength on solubility is described by the terms *salting in* and *salting out*. The behavior shown in Figure 10.7, in which the activity coefficient first decreases and subsequently increases with concentration, affects the solubility of a salt in the following way. For a salt such as $MgF_2$, the product $\left[Mg^{2+}\right]\left[F^-\right]^2\gamma_\pm^3 = K_{sp}$ is constant as the concentration varies for constant $T$, because the thermodynamic equilibrium constant $K$ depends only on $T$. Therefore, the concentrations $\left[Mg^{2+}\right]$ and $\left[F^-\right]$ change in an opposite way to $\gamma_\pm$. At small values of the ionic strength, $\gamma_\pm < 1$, and the solubility increases as $\gamma_\pm$ decreases with concentration until the minimum in a plot of $\gamma_\pm$ versus $I$ is reached. This effect is known as **salting in.** For high values of the ionic strength, $\gamma_\pm > 1$ and the solubility is less than at low values of $I$. This effect is known as **salting out.** Salting out can be used to purify proteins by selective precipitation from solution. For example, the blood clotting protein fibrinogen is precipitated in a 0.8 molar ammonium sulfate solution, whereas a 2.4 molar concentration of ammonium sulfate is required to precipitate albumin.

We next consider equilibria in electrolyte solutions at concentrations where the Debye–Hückel limiting law is no longer valid. In this case, activity coefficients must

be estimated as there is no theoretical model for calculating them. The Davies [Equation (10.34)] can be used in such a case. An example is a buffer solution that consists of a weak acid and its conjugate base.

### EXAMPLE PROBLEM 10.4

Calculate the pH of a buffer solution that is 0.100 molar in $CH_3COOH$ and 0.100 molar in $CH_3COONa$. The molality based equilibrium constant $K$ for the dissociation of acetic acid is $1.75 \times 10^{-5}$. Compare your value with what you would have calculated assuming $\gamma_\pm = 1$.

#### Solution

We write the equilibrium constant in the form

$$K = \frac{\gamma_\pm m\left(H_3O^+\right)\gamma_\pm m\left(CH_3COO^-\right)}{m(CH_3COOH)}$$

$$1.75 \times 10^{-5} = \frac{(\gamma_\pm)^2 x \times (0.100 + x)}{(0.100 - x)} \approx (\gamma_\pm)^2 x$$

$$m\left(H_3O^+\right) = \frac{1.75 \times 10^{-5}}{(\gamma_\pm)^2}$$

$$pH = \log\left\{m\left(H_3O^+\right)\right\}$$

To calculate $\gamma_\pm$ from the Davies equation, we must first calculate the ionic strength of the solution. The small value of $K$ tells us that the degree of ionization of the acetic acid is small so that the ionic strength can be calculated from the concentration of $CH_3COONa$ alone.

$$I = \frac{m}{2}\left(v_+ z_+^2 + v_- z_-^2\right) = \frac{0.100\,\text{mol kg}^{-1}}{2} \times (1 + 1) = 0.100\,\text{mol kg}^{-1}$$

Using the Davies equation

$$\log_{10}\gamma_\pm = -0.51\left|z_+ z_-\right|\left[\frac{\left(\dfrac{I}{m°}\right)^{1/2}}{1 + \left(\dfrac{I}{m°}\right)^{1/2}} - 0.30\left(\dfrac{I}{m°}\right)\right]$$

$$= -0.51\left[\frac{(0.100)^{1/2}}{1 + (0.100)^{1/2}} - 0.30 \times 0.100\right] = -0.1270$$

$$\gamma_\pm = 0.746$$

$$m\left(H_3O^+\right) = \frac{1.75 \times 10^{-5}}{(0.746)^2} = 3.14 \times 10^{-5}\,\text{mol kg}^{-1}$$

$$pH = -\log\left\{3.14 \times 10^{-5}\right\} = 4.50$$

If we had assumed $\gamma_\pm = 1$

$$m\left(H_3O^+\right) = \frac{1.75 \times 10^{-5}}{(\gamma_\pm)^2} = 1.75 \times 10^{-5}$$

This value for $m\left(H_3O^+\right)$ gives a pH value of 4.76, which is significantly different from the value calculated earlier.

# Vocabulary

conventional formation enthalpies

conventional formation entropies

conventional Gibbs energies of formation

Davies equation

Debye–Hückel limiting law

Debye–Hückel screening length

electrolyte

ionic strength

mean ionic activity

mean ionic activity coefficient

mean ionic chemical potential

mean ionic molality

salting in

salting out

screened potential

solvation shell

# Conceptual Problems

**Q10.1** Discuss how the Debye–Hückel screening length changes as the (a) temperature, (b) dielectric constant, and (c) ionic strength of an electrolyte solution are increased.

**Q10.2** Why is it not possible to measure the Gibbs energy of solvation of $Cl^-$ directly?

**Q10.3** Why are activity coefficients calculated using the Debye–Hückel limiting law always less than one?

**Q10.4** How is the mean ionic chemical potential of a solute related to the chemical potentials of the anion and cation produced when the solute is dissolved in water?

**Q10.5** How is the chemical potential of a solute related to its activity?

**Q10.6** Tabulated values of standard entropies of some aqueous ionic species are negative. Why is this statement not inconsistent with the third law of thermodynamics?

**Q10.7** Why is it not possible to measure the activity coefficient of $Na^+(aq)$?

**Q10.8** Why is it possible to formulate a general theory for the activity coefficient for electrolyte solutions, but not for nonelectrolyte solutions?

**Q10.9** Why does an increase in the ionic strength in the range where the Debye–Hückel law is valid lead to an increase in the solubility of a weakly soluble salt?

**Q10.10** What is the correct order of the following inert electrolytes in their ability to increase the degree of dissociation of acetic acid?

**a.** 0.001 $m$ NaCl

**b.** 0.001 $m$ KBr

**c.** 0.10 $m$ $CuCl_2$

**Q10.11** How does salting in affect solubility?

**Q10.12** Why is it not appropriate to use ionic radii from crystal structures to calculate $\Delta G^\circ_{solvation}$ of ions using the Born model?

**Q10.13** Why do deviations from ideal behavior occur at lower concentrations for electrolyte solutions than for solutions in which the solute species are uncharged?

**Q10.14** Why is the value for the dielectric constant for water in the solvation shell around ions less than that for bulk water?

**Q10.15** What can you conclude about the interaction between ions in an electrolyte solution if the mean ionic activity coefficient is greater than one?

**Q10.16** Why is the inequality $\gamma_\pm < 1$ always satisfied in dilute electrolyte solutions?

**Q10.17** Under what conditions does $\gamma_\pm \rightarrow 1$ for electrolyte solutions?

**Q10.18** How do you expect $S^\circ_m$ for an ion in solution to change as the ionic radius increases at constant charge?

**Q10.19** How do you expect $S^\circ_m$ for an ion in solution to change as the charge increases at constant ionic radius?

**Q10.20** It takes considerable energy to dissociate NaCl in the gas phase. Why does this process occur spontaneously in an aqueous solution? Why does it not occur spontaneously in $CCl_4$?

# Numerical Problems

Problem numbers in **red** indicate that the solution to the problem is given in the *Student's Solutions Manual*.

**P10.1** Calculate $\Delta S^\circ_{reaction}$ for the reaction
$Ba(NO_3)_2(aq) + 2KCl(aq) \rightarrow BaCl_2(s) + 2KNO_3(aq)$.

**P10.2** Calculate $\Delta S^\circ_{reaction}$ for the reaction
$AgNO_3(aq) + KCl(aq) \rightarrow AgCl(s) + KNO_3(aq)$.

**P10.3** Using the Debye–Hückel limiting law, calculate the value of $\gamma_\pm$ in (a) a $7.2 \times 10^{-3}$ $m$ solution of NaBr, (b) a

$7.50 \times 10^{-4}$ $m$ solution of $SrCl_2$, and (c) a $2.25 \times 10^{-3}$ $m$ solution of $CaHPO_4$. Assume complete dissociation.

**P10.4** Calculate the mean ionic molality $m_\pm$ in 0.0750 $m$ solutions of (a) $Ca(NO_3)_2$, (b) NaOH, (c) $MgSO_4$, and (d) $AlCl_3$.

**P10.5** A weak acid has a dissociation constant of $K_a = 2.50 \times 10^{-2}$. (a) Calculate the degree of dissociation for a 0.093 $m$ solution of this acid using the Debye-Hückel

limiting law. (b) Calculate the degree of dissociation for a 0.093 $m$ solution of this acid that is also 0.200 $m$ in KCl from the Debye–Hückel limiting law using an iterative calculation until the answer is constant in the second decimal place. (c) Repeat the calculation in (b) using the mean activity coefficient for KCl in Table 10.3. Is the use of the Debye–Hückel limiting law advisable at the given KCl concentration? Do you need to repeat the iterative calculation of (a) to solve (b) and (c)?

**P10.6**   Calculate the mean ionic activity of a 0.0350 $m$ $Na_3PO_4$ solution for which the mean activity coefficient is 0.685.

**P10.7**   At 25°C, the equilibrium constant for the dissociation of acetic acid $K_a$ is $1.75 \times 10^{-5}$. Using the Debye–Hückel limiting law, calculate the degree of dissociation in 0.150 $m$ and 1.50 $m$ solutions using an iterative calculation until the answer is constant to within $\pm 2$ in the second decimal place. Compare these values with what you would obtain if the ionic interactions had been ignored. Compare your results with the degree of dissociation of the acid assuming $\gamma_\pm = 1$.

**P10.8**   From the data in Table 10.3 (see Appendix B, Data Tables), calculate the activity of the electrolyte in 0.200 $m$ solutions assuming complete dissociation of

a. KCl

b. $Na_2SO_4$

c. $MgCl_2$

**P10.9**   Estimate the degree of dissociation of a 0.200 $m$ solution of nitrous acid ($K_a = 4.00 \times 10^{-4}$) that is also 0.500 $m$ in the strong electrolyte given in parts (a) through (c). Use the data tables to obtain $\gamma_\pm$, as the electrolyte concentration is too high to use the Debye–Hückel limiting law.

a. $Ba(Cl)_2$

b. KOH

c. $AgNO_3$

Compare your results with the degree of dissociation of the acid in the absence of other electrolytes.

**P10.10**   Calculate $\Delta H_R^\circ$ and $\Delta G_R^\circ$ for the reaction $Ba(NO_3)_2(aq) + 2\,KCl(aq) \rightarrow BaCl_2(s) + 2KNO_3(aq)$.

**P10.11**   Express $a_\pm$ in terms of $a_+$ and $a_-$ for (a) $Li_2CO_3$, (b) $CaCl_2$, (c) $Na_3PO_4$, and (d) $K_4Fe(CN)_6$. Assume complete dissociation.

**P10.12**   Calculate $\Delta G_{solvation}^\circ$ in an aqueous solution for $Rb^+(aq)$ using the Born model. The radius of the $Rb^+$ ion is 161 pm.

**P10.13**   Calculate the ionic strength in a solution that is 0.0750 $m$ in $K_2SO_4$, 0.0085 $m$ in $Na_3PO_4$, and 0.0150 $m$ in $MgCl_2$.

**P10.14**   Calculate $I$, $\gamma_\pm$, and $a_\pm$ for a 0.0120 $m$ solution of $Na_3PO_4$ at 298 K. Assume complete dissociation.

**P10.15**   Express $\mu_\pm$ in terms of $\mu_+$ and $\mu_-$ for (a) NaCl, (b) $MgBr_2$, (c) $Li_3PO_4$, and (d) $Ca(NO_3)_2$. Assume complete dissociation.

**P10.16**   In the Debye–Hückel theory, the counter charge in a spherical shell of radius $r$ and thickness $dr$ around the central ion of charge $+Q$ is given by $-Q\kappa^2 re^{-\kappa r}dr$. Calculate the radius at which the counter charge has its maximum value

$r_{max}$, from this expression. Evaluate $r_{max}$ for a 0.090 $m$ solution of $Na_3PO_4$ at 298 K.

**P10.17**   Calculate the solubility of $CaCO_3$ ($K_{sp} = 3.4 \times 10^{-9}$) (a) in pure $H_2O$ and (b) in an aqueous solution with $I = 0.0250$ mol kg$^{-1}$. For part (a), do an iterative calculation of $\gamma_\pm$ and the solubility until the answer is constant in the second decimal place. Do you need to repeat this procedure in part (b)?

**P10.18**   Calculate the probability of finding an ion at a distance greater than $1/\kappa$ from the central ion.

**P10.19**   Express $\gamma_\pm$ in terms of $\gamma_+$ and $\gamma_-$ for (a) $SrSO_4$, (b) $MgBr_2$, (c) $K_3PO_4$, and (d) $Ca(NO_3)_2$. Assume complete dissociation.

**P10.20**   Calculate the mean ionic molality and mean ionic activity of a 0.105 $m$ $K_3PO_4$ solution for which the mean ionic activity coefficient is 0.225.

**P10.21**   The base dissociation constant of dimethylamine,

$$(CH_3)_2NH(aq) + H_2O(aq) \rightarrow CH_3NH_3{}^+(aq) + OH^-(aq)$$

is $5.12 \times 10^{-4}$. Calculate the extent of hydrolysis for (a) a 0.210 $m$ solution of $(CH_3)_2NH$ in water using an iterative calculation until the answer is constant to within $\pm 2$ in the second decimal place. (b) Repeat the calculation for a solution that is also 0.500 $m$ in $NaNO_3$. Do you need to use an iterative calculation in this case?

**P10.22**   Dichloroacetic acid has a dissociation constant of $K_a = 3.32 \times 10^{-2}$. Calculate the degree of dissociation for a 0.105 $m$ solution of this acid (a) from the Debye–Hückel limiting law using an iterative calculation until the answer is constant to within $\pm 2$ in the second decimal place. (b) Repeat the calculation assuming that the mean ionic activity coefficient is one.

**P10.23**   Calculate the Debye–Hückel screening length $1/\kappa$ at 298 K in a 0.0075 $m$ solution of $K_3PO_4$.

**P10.24**   Calculate $I$, $\gamma_\pm$, and $a_\pm$ for a 0.0215 $m$ solution of $K_2SO_4$ at 298 K. How confident are you that your calculated results will agree with experimental results?

**P10.25**   Calculate $I$, $\gamma_\pm$, and $a_\pm$ for a 0.0175 $m$ solution of $Na_3PO_4$ at 298 K. Assume complete dissociation. How confident are you that your calculated results will agree with experimental results?

**P10.26**   Calculate the ionic strength of each of the solutions in Problem P10.4.

**P10.27**   Calculate the value of $m_\pm$ in $5.5 \times 10^{-3}$ molal solutions of (a) KCl, (b) $Ca(NO_3)_2$, and (c) $ZnSO_4$. Assume complete dissociation.

**P10.28**   Calculate $\Delta H_R^\circ$ and $\Delta G_R^\circ$ for the reaction $AgNO_3(aq) + KCl(aq) \rightarrow AgCl(s) + KNO_3(aq)$.

**P10.29**   Calculate the pH of a buffer solution that is 0.200 molal in $CH_3COOH$ and 0.15 molal in $CH_3COONa$ using the Davies equation to calculate $\gamma_\pm$. What pH value would you have calculated if you had assumed that $\gamma_\pm = 1$?

**P10.30**   Use the Davies equation to calculate $\gamma_\pm$ for a 1.00 molar solution of KOH. Compare your answer with the value in Table 10.3.

# Electrochemical Cells, Batteries, and Fuel Cells

I f a metal electrode is immersed in an aqueous solution containing cations of that metal, an equilibrium that leads to negative charge formation on the electrode is established. This configuration of electrode and solution is called a half-cell. Two half-cells can be combined to form an electrochemical cell. The equilibrium condition in an electrochemical cell is that the electrochemical potential, rather than the chemical potential, of a species is the same in all parts of the cell. The electrochemical potential can be changed through the application of an electrical potential external to the cell. This allows the direction of spontaneous change in the cell reaction to be reversed. Electrochemical cells can be used to determine the equilibrium constant for the cell reaction and to determine the mean activity coefficient of a solute. Electrochemical cells can also be used to provide power, in which case they are called batteries. Electrochemical cells in which the reactants can be supplied continuously are called fuel cells.

## 11.1 The Effect of an Electrical Potential on the Chemical Potential of Charged Species

If a Zn electrode is partially immersed in an aqueous solution of $ZnSO_4$, an equilibrium is established between $Zn(s)$ and $Zn^{2+}(aq)$ as a small amount of the Zn goes into solution as $Zn^{2+}(aq)$ ions as depicted in Figure 11.1. However, the electrons remain on the Zn electrode. Therefore, a negative charge builds up on the Zn electrode, and a corresponding positive charge builds up in the surrounding solution. This charging leads to a difference in the electrical potential $\phi$ between the electrode and the solution, which we call the half-cell potential. As we will see in Section 11.2, two half-cells are combined to form an electrochemical cell. The charge separation in the system arises through the dissociation equilibrium

$$Zn(s) \rightleftharpoons Zn^{2+}(aq) + 2e^- \qquad (11.1)$$

**FIGURE 11.1**

When a Zn electrode is immersed in an aqueous solution containing $Zn^{2+}(aq)$ ions, a very small amount of the Zn goes into solution as $Zn^{2+}(aq)$, leaving two electrons behind on the Zn electrode per ion formed.

The equilibrium position in this reaction lies far toward Zn(s). At equilibrium, fewer than $10^{-14}$ mol of the Zn(s) dissolves in 1 liter of solution to form $Zn^{2+}(aq)$. However, this minuscule amount of charge transfer between the electrode and the solution is sufficient to create a difference of approximately 1 V in the electrical potential between the Zn electrode and the electrolyte solution. A similar dissociation equilibrium is established for other metal electrodes. Because the value of the equilibrium constant depends on $\Delta G_f^\circ$ of the solvated metal ion, the equilibrium constant for the dissociation reaction and $\phi$ depends on the identity of the metal.

Can $\phi$ be measured directly? Let us assume that we can carry out the measurement using two chemically inert Pt wires as probes. One Pt wire is placed on the Zn electrode, and the second Pt wire is placed in the $ZnSO_4$ solution. However, the measured voltage is the difference in electrical potential between a Pt wire connected to a Zn electrode in a $ZnSO_4$ solution and a Pt electrode in a $ZnSO_4$ solution, which is not what we want. A difference in electrical potential can only be measured between one phase and a second phase *of identical composition*. For example, the difference in electrical potential across a resistor is measured by contacting the metal wire at each end of the resistor with two metal probes of identical composition connected to the terminals of a voltmeter. Although we can not measure the half-cell potential $\phi$ directly, half-cell potentials can be determined relative to a reference half-cell as will be shown in Section 11.2.

How are chemical species affected by the electrical potential $\phi$? To a very good approximation, the chemical potential of a **neutral** atom or molecule is not affected if a small electrical potential is applied to the environment containing the species. However, this is not the case for a **charged** species such as an $Na^+$ ion in an electrolyte solution. The work required to transfer $dn$ moles of charge reversibly from a chemically uniform phase at an electrical potential $\phi_1$ to a second, otherwise identical phase at an electrical potential $\phi_2$ is equal to the product of the charge and the difference in the electrical potential between the two locations:

$$d w_{rev} = (\phi_2 - \phi_1)\, dQ \qquad (11.2)$$

In this equation, $dQ = -zF\, dn$ is the charge transferred through the potential, $z$ is the charge in units of the electron charge $(+1, -1, +2, -2, \ldots)$, and the **Faraday constant** $F$ is the absolute magnitude of the charge associated with 1 mol of a singly charged species. The Faraday constant has the numerical value $F = 96,485$ Coulombs mole$^{-1}$ $(C\ mol^{-1})$.

Because the work being carried out in this reversible process is nonexpansion work, $d w_{rev} = dG$, which is the difference in the **electrochemical potential** $\tilde{\mu}$ of the charged particle in the two phases:

$$dG = \tilde{\mu}_2\, dn - \tilde{\mu}_1\, dn \qquad (11.3)$$

The electrochemical potential is a generalization of the chemical potential to include the effect of an electrical potential on a charged particle. It is the sum of the normal chemical potential $\mu$ and a term that results from the nonzero value of the electrical potential:

$$\tilde{\mu} = \mu + z\phi F \qquad (11.4)$$

Note that with this definition $\tilde{\mu} \to \mu$ as $\phi \to 0$.

Combining Equations (11.2) and (11.4) gives

$$\tilde{\mu}_2 - \tilde{\mu}_1 = + z(\phi_2 - \phi_1)F \quad \text{or} \quad \tilde{\mu}_2 = \tilde{\mu}_1 + z(\phi_2 - \phi_1)F \qquad (11.5)$$

Because only the difference in the electrical potential between two points can be measured, one can set $\phi_1 = 0$ in Equation (11.5) to obtain the result

$$\tilde{\mu}_2 = \tilde{\mu}_1 + z\phi F \qquad (11.6)$$

This result shows that charged particles in two otherwise identical phases have different values for the electrochemical potential if the phases are at different electrical

potentials. Because the particles will flow in a direction that decreases their electrochemical potential, the flow of negatively charged particles in a conducting phase is toward a region of more positive electric potential. The opposite is true for positively charged particles.

Equation (11.6) is the basis for understanding all electrochemical reactions. In an electrochemical environment, the equilibrium condition is

$$\Delta G_R = \sum_i \nu_i \widetilde{\mu}_i = 0, \text{ rather than } \Delta G_R = \sum_i \nu_i \mu_i = 0 \qquad \textbf{(11.7)}$$

Chemists have a limited ability to change $\Delta G_R$ by varying $P$, $T$, and concentration. However, because the electrochemical potential can be varied through the application of an electrical potential, $\Delta G_R$ can be changed easily because $z_i \phi F$ can be larger in magnitude than $\sum_i \nu_i \mu_i$ and can have either the same or the opposite sign. Because a change in the electrical potential can lead to a change in the sign of $\Delta G_R$, the direction of spontaneous change in an electrochemical reaction system can be changed simply by applying suitable electrical potentials within the system. A practical example of changing the sign of $\Delta G_R$ is the recharging of a battery by the application of an external potential.

# 11.2 Conventions and Standard States in Electrochemistry

How can we assign value to $\widetilde{\mu}$ for the individual species in the equilibrium $Zn(s) \rightleftharpoons Zn^{2+}(aq) + 2e^-$? Because $Zn(s)$ is in its standard reference state and is uncharged, $\widetilde{\mu}(Zn(s)) = \mu(Zn(s)) = \Delta G_f(Zn(s)) = 0$. We next consider $Zn^{2+}(aq)$. We consider only the case that the overall chemical reaction in an electrochemical cell takes place in a single phase, and therefore $\phi$ has the same value for all solvated ionic reactants and products. In this case the equilibrium condition becomes

$$\Delta G_R = \sum_i \nu_i \widetilde{\mu}_i = \sum_i \nu_i \mu_i + F\varphi \sum_i \nu_i z_i = \sum_i \nu_i \mu_i = 0 \qquad \textbf{(11.7a)}$$

because $\sum_i \nu_i z_i = 0$. We see that the value of $\phi$ does not influence the equilibrium if the overall reaction takes place in a single phase. Therefore we can set $\phi = 0$ and adopt the convention

$$\widetilde{\mu}_i = \mu_i \text{ (ions in solution)} \qquad \textbf{(11.8)}$$

Adopting this standard state simplifies calculations because $\mu_i$ can be calculated from the solute concentration at low concentrations using the Debye–Hückel limiting law discussed in Section 10.4 or at higher concentrations if the activity coefficients are known.

Next, consider the appropriate standard state for an electron in a metal electrode. We cannot set $\phi = 0$ as we did for the ions in solution because there is a potential difference between the solution and the electrode. As shown in Equation (11.6), the electrochemical potential consists of two parts, a chemical component and a component that depends on the electrical potential. For an electron in a metal, there is no way to determine the relative magnitude of the two components. Therefore, it is convenient to choose the standard state $\mu_i$ (electrons in electrode) $= 0$ so that

$$\widetilde{\mu}_{e^-} = -\phi F \text{ (electrons in metal electrode)} \qquad \textbf{(11.9)}$$

As we discussed earlier, half-cell potentials cannot be measured directly. They are measured relative to one another rather than absolutely. To understand how this is done, it is useful to consider an **electrochemical cell,** which consists of two half-cells, such as the one shown in Figure 11.2 This particular cell is known as the **Daniell cell,** after its inventor. On the left, a Zn electrode is immersed in a solution of $ZnSO_4$. The solute is completely dissociated to form $Zn^{2+}(aq)$ and $SO_4^{2-}(aq)$. On the right, a Cu electrode

Schematic diagram of the Daniell cell. $Zn^{2+}/Zn$ and $Cu^{2+}/Cu$ half-cells are connected through a salt bridge in the internal circuit. A voltmeter is shown in the external circuit. The inset shows the atomic level processes that occur at each electrode.
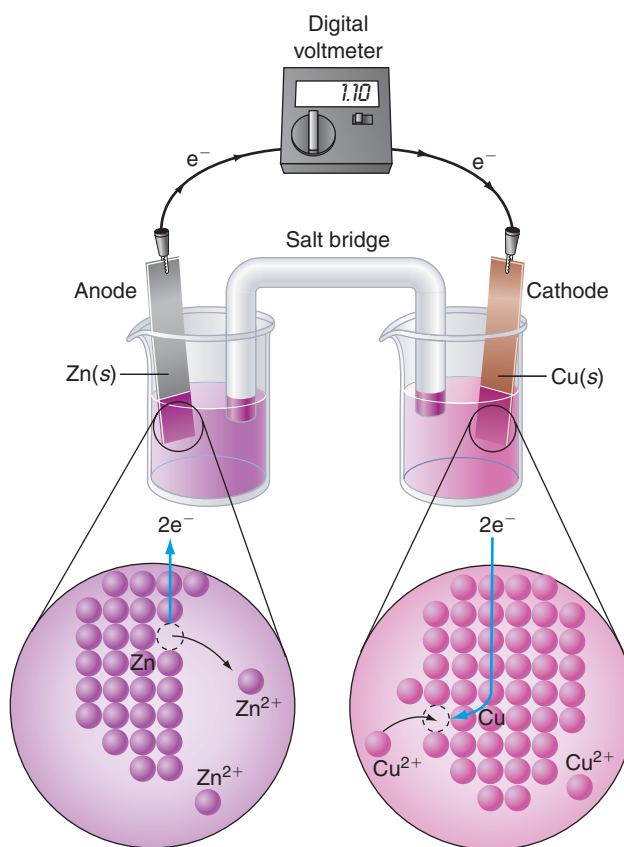


is immersed in a solution of $CuSO_4$, which is completely dissociated to form $Cu^{2+}(aq)$ and $SO_4^{2-}(aq)$. The two half-cells are connected by an ionic conductor known as a salt bridge. The **salt bridge** consists of an electrolyte such as KCl suspended in a gel. A salt bridge allows current to flow between the half-cells while preventing the mixing of the solutions. A metal wire fastened to each electrode allows the electron current to flow through the external part of the circuit. Note that because the wire is connected on one end to a Cu electrode and on the other end to a Zn electrode, the two phases between which we are measuring the electrical potential are not identical.

Using the experimental setup of Figure 11.2, the electrical potential difference between two half-cells can be measured, rather than the absolute electrical potential of each half-cell. However, we need potentials of individual half-cells. Therefore, it is convenient to choose one half-cell as a reference and arbitrarily assign an electrical potential of zero to this half-cell. Once this is done, the electrical potential associated with any other half-cell can be determined by combining it with the reference half-cell. The measured potential difference across the cell is associated with the half-cell of interest. It is next shown that the standard hydrogen electrode fulfills the role of a reference half-cell of zero potential. The measurement of electrical potentials is discussed using this cell. The reaction in the standard hydrogen electrode is
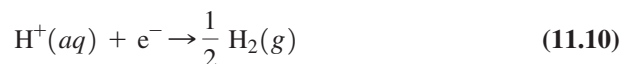
$$H^+(aq) + e^- \rightarrow \frac{1}{2} H_2(g) \tag{11.10}$$

and the equilibrium in the half-cell is described by

$$\mu_{H^+}(aq) + \tilde{\mu}_{e^-} = \frac{1}{2}\mu_{H_2(g)} \tag{11.11}$$

Half-cell reactions such as Equation (11.10) are generally written as reduction reactions by convention as is done in Tables 11.1 and 11.2 (see Appendix A, Data Tables) even though equilibrium is established in the half-cell. It is useful to separate $\mu_{H_2(g)}$ and $\mu_{H^+}(aq)$ into a standard state portion and a portion that depends on the

activity and use Equation (11.9) for the electrochemical potential of the electron. The preceding equation then takes the form

$$\mu_{H^+}^{\circ} + RT \ln a_{H^+} - F\phi_{H^+/H_2} = \frac{1}{2}\mu_{H_2}^{\circ} + \frac{1}{2}RT \ln f_{H_2} \qquad (11.12)$$

where $f_{H_2}$ is the fugacity of the hydrogen gas. Solving Equation (11.12) for $\phi_{H^+/H_2}$

$$\phi_{H^+/H_2} = \frac{\mu_{H^+}^{\circ} - \frac{1}{2}\mu_{H_2}^{\circ}}{F} - \frac{RT}{F}\ln\frac{f_{H_2}^{1/2}}{a_{H^+}} \qquad (11.13)$$

For unit activities of all species, the cell has its standard state potential, designated $\phi_{H^+/H_2}^{\circ}$. Because $\mu_{H_2}^{\circ} = \Delta G_f^{\circ}(H_2, g) = 0$,

$$\phi_{H^+/H_2}^{\circ} = \frac{\mu_{H^+}^{\circ}}{F} \qquad (11.14)$$

In Section 10.1 the convention that $\Delta G_f^{\circ}(H^+, aq) = \mu_{H^+}^{\circ} = 0$ was introduced. Therefore, we find that

$$\phi_{H^+/H_2}^{\circ} = 0 \qquad (11.15)$$

We have shown that the standard hydrogen electrode is a convenient **reference electrode** with zero potential against which the potentials of all other half-cells can be measured. A schematic drawing of this electrode is shown in Figure 11.3. To achieve equilibrium on a short timescale, this reaction $H^+(aq) + e^- \rightleftharpoons 1/2\ H_2(g)$ is carried out over a Pt catalyst electrode. It is also necessary to establish a standard state for the activity of $H^+(aq)$. It is customary to use a Henry's law standard state based on molarity. Therefore, $a_i \to c_i$ and $\gamma_i \to 1$ as $c_i \to 0$. The standard state is a (hypothetical) aqueous solution of $H^+(aq)$ that shows ideal solution behavior at a concentration of $c^{\circ} = 1\ \text{mol L}^{-1}$.

The usefulness of the result $\phi_{H^+/H_2}^{\circ} = 0$ is that values for the electrical potential can be assigned to individual half-cells by measuring their potential relative to the $H^+/H_2$ half-cell. For example, the cell potential of the electrochemical cell in Figure 11.4 is assigned to the $Zn/Zn^{2+}$ half-cell if the $H^+(aq)$ and $H_2(g)$ activities both have the value 1. Although not directly measurable, absolute values for half-cell potentials can be determined. In Supplemental Section 11.16 it is shown that the absolute potential of the standard hydrogen electrode is $-4.44 \pm 0.02$ V. Because only changes in energy rather than absolute energies can be measured, chemists generally use half-cell potentials relative to the standard hydrogen electrode assuming that $\phi_{H^+/H_2}^{\circ} = 0$.
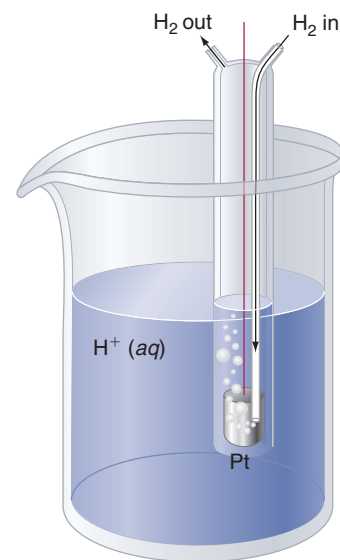


**FIGURE 11.3**
The standard hydrogen electrode consists of a solution of an acid such as HCl, $H_2$ gas, and a Pt catalyst electrode that allows the equilibrium in the half-cell reaction to be established rapidly. The activities of $H_2$ and $H^+$ are equal to one.
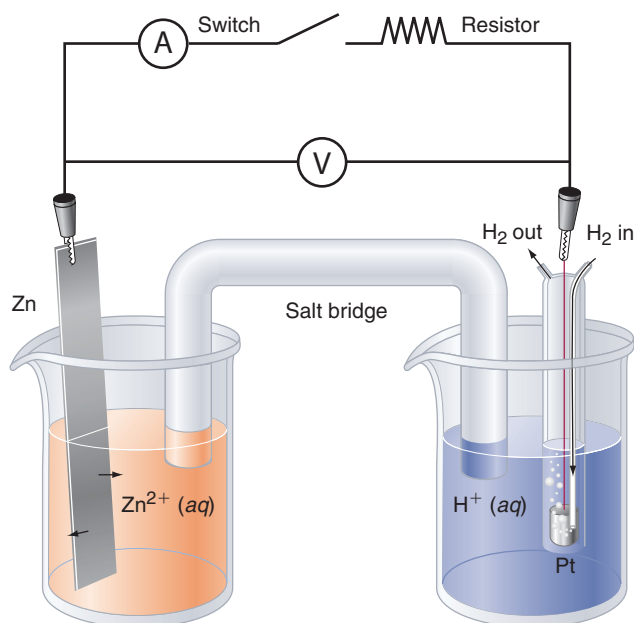


**FIGURE 11.4**
In a cell consisting of a half-cell and the standard hydrogen electrode, the entire cell voltage is assigned to the half-cell.

dc source
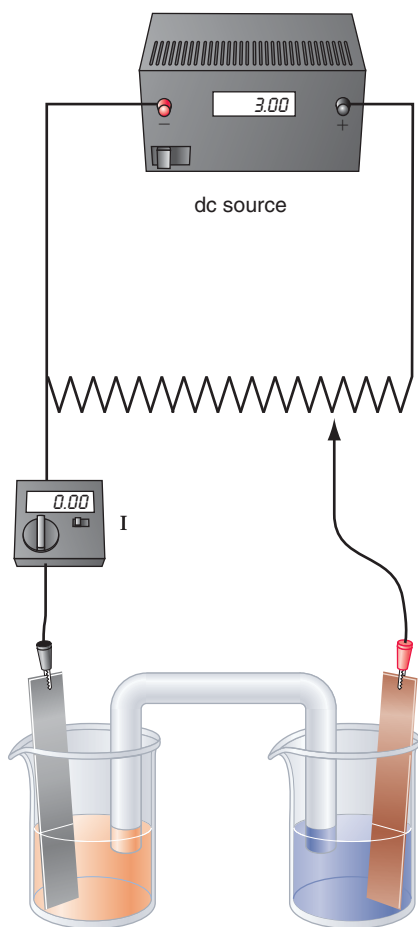
**FIGURE 11.5**
Schematic diagram showing how the reversible cell potential is measured.

## 11.3 Measurement of the Reversible Cell Potential

The cell potential measured under reversible conditions is directly related to the state functions *G, H,* and *S.* The reversible cell potential, also called **electromotive force (emf),** is determined in an experiment depicted in Figure 11.5. The dc source provides a voltage to a potentiometer circuit with a sliding contact. The sliding contact is attached to the positive cell terminal as shown, and the slider is adjusted until the current-sensing device labeled *I* shows a null current. At this position of the potentiometer, the voltage applied through the potentiometer exactly opposes the cell potential. The voltage measured in this way is the reversible cell potential. If the sliding contact is moved to a position slightly to the left of this position, the electron current will flow through the external circuit in one direction. However, if the sliding contact is moved to a position slightly to the right of this position, the electron current will flow through the external circuit in the opposite direction, showing that the direction of the cell reaction has been reversed. Because a small variation of the applied voltage can reverse the direction of spontaneous change, the criterion for reversibility is established. This discussion also demonstrates that the direction of spontaneous change in the cell can be reversed by changing the electrochemical potential of the electrons in one of the electrodes relative to that in the other electrode using an external voltage source.

## 11.4 Chemical Reactions in Electrochemical Cells and the Nernst Equation

What reactions occur in the Daniell cell shown in Figure 11.2? If the half-cells are connected through the external circuit, Zn atoms leave the Zn electrode to form $Zn^{2+}$ in solution, and $Cu^{2+}$ ions are deposited as Cu atoms on the Cu electrode. In the external circuit, it is observed that electrons flow through the wires and the resistor in the direction from the Zn electrode to the Cu electrode. These observations are consistent with the following electrochemical reactions:

$$\text{Left half-cell: } Zn(s) \rightarrow Zn^{2+}(aq) + 2e^- \tag{11.16}$$

$$\text{Right half-cell: } Cu^{2+}(aq) + 2e^- \rightarrow Cu(s) \tag{11.17}$$

$$\text{Overall: } Zn(s) + Cu^{2+}(aq) \rightleftharpoons Zn^{2+}(aq) + Cu(s) \tag{11.18}$$
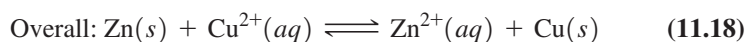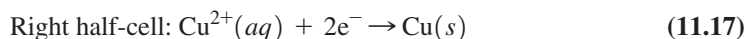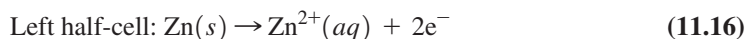
In the left half-cell, Zn is being oxidized to $Zn^{2+}$, and in the right half-cell, $Cu^{2+}$ is being reduced to Cu. By convention, the electrode at which oxidation occurs is called the **anode,** and the electrode at which reduction occurs is called the **cathode.** Each half-cell in an electrochemical cell must contain a species that can exist in an oxidized and a reduced form. For a general redox reaction, the reactions at the anode and cathode and the overall reaction can be written as follows:

$$\text{Anode: } Red_1 \rightarrow Ox_1^{n_1^+} + n_1 e^- \tag{11.19}$$

$$\text{Cathode: } Ox_2 + n_2 e^- \rightarrow Red_2^{n_2^-} \tag{11.20}$$

$$\text{Overall: } n_2 Red_1 + n_1 Ox_2 \rightleftharpoons n_2 Ox_1^{n_1^+} + n_1 Red_2^{n_2^-} \tag{11.21}$$
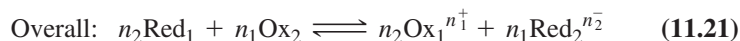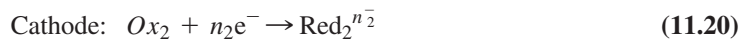
Note that electrons do not appear in the overall reaction because the electrons produced at the anode are consumed at the cathode.

How are the cell voltage and $\Delta G_R$ for the overall reaction related? This important relationship can be determined from the electrochemical potentials of the species involved in the overall reaction of the Daniell cell:

$$\Delta G_R = \tilde{\mu}_{Zn^{2+}} + \tilde{\mu}_{Cu} - \tilde{\mu}_{Cu^{2+}} - \tilde{\mu}_{Zn} = \mu^{\circ}_{Zn^{2+}} - \mu^{\circ}_{Cu^{2+}} + RT \ln\frac{a_{Zn^{2+}}}{a_{Cu^{2+}}}$$

$$= \Delta G_R^{\circ} + RT \ln\frac{a_{Zn^{2+}}}{a_{Cu^{2+}}} \tag{11.22}$$

If this reaction is carried out reversibly, the electrical work done is equal to the product of the charge and the potential difference through which the charge is moved. However, the reversible work at constant pressure is also equal to $\Delta G$. Therefore, we can write the following equation:

$$\Delta G_R = -nF\Delta\phi \tag{11.23}$$

In Equation (11.23), $\Delta\phi$ is the measured potential difference generated by the spontaneous chemical reaction for particular values of $a_{Zn^{2+}}$ and $a_{Cu^{2+}}$, and $n$ is the number of moles of electrons involved in the redox reaction. The measured cell voltage is directly proportional to $\Delta G$. For a reversible reaction, the symbol $E$ is used in place of $\Delta\phi$, and $E$ is referred to as the **electromotive force (emf).** Using this definition, we rewrite Equation (11.23) as follows:

$$-2FE = \Delta G_R^\circ + RT \ln\frac{a_{Zn^{2+}}}{a_{Cu^{2+}}} \tag{11.24}$$

For standard state conditions, $a_{Zn^{2+}} = a_{Cu^{2+}} = 1$, and Equation (11.24) takes the form $\Delta G_R^\circ = -2FE^\circ$. This definition of $E^\circ$ allows Equation (11.24) to be rewritten as

$$E = E^\circ - \frac{RT}{2F}\ln\frac{a_{Zn^{2+}}}{a_{Cu^{2+}}} \tag{11.25}$$

For a general overall electrochemical reaction involving the transfer of $n$ moles of electrons,

$$E = E^\circ - \frac{RT}{nF}\ln Q \tag{11.26}$$

where $Q$ is the familiar reaction quotient. The preceding equation is known as the **Nernst equation.** At 298.15 K, the Nernst equation can be written in the form

$$E = E^\circ - \frac{0.05916\text{ V}}{n}\log_{10}Q \tag{11.27}$$

This function is graphed in Figure 11.6. The Nernst equation allows the emf for an electrochemical cell to be calculated if the activity is known for each species and if $E^\circ$ is known.

The Nernst equation has been derived on the basis of the overall cell reaction. For a half-cell, an equation of a similar form can be derived. The equilibrium condition for the half-cell reaction

$$Ox^{n+} + ne^- \rightleftharpoons Red \tag{11.28}$$

is given by

$$\mu_{Ox^{n+}} + n\tilde{\mu}_{e-} = \mu_{Red} \tag{11.29}$$

Using the convention for the electrochemical potential of an electron in a metal electrode [Equation (11.9)], Equation (11.29) can be written in the form

$$\mu_{Ox^{n+}}^\circ + RT\ln a_{Ox^{n+}} - nF\phi_{Ox/Red} = \mu_{Red}^\circ + RT\ln a_{Red}$$

$$\phi_{Ox/Red} = -\frac{\mu_{Red}^\circ - \mu_{Ox^{n+}}^\circ}{nF} - \frac{RT}{nF}\ln\frac{a_{Red}}{a_{Ox^{n+}}}$$

$$E_{Ox/Red} = E_{Ox/Red}^\circ - \frac{RT}{nF}\ln\frac{a_{Red}}{a_{Ox^{n+}}} \tag{11.30}$$

The last line in Equation (11.30) has the same form as the Nernst equation, but the activity of the electrons does not appear in $Q$. An example of the application of Equation (11.30) to a half-cell reaction is shown in Example Problem 11.1.
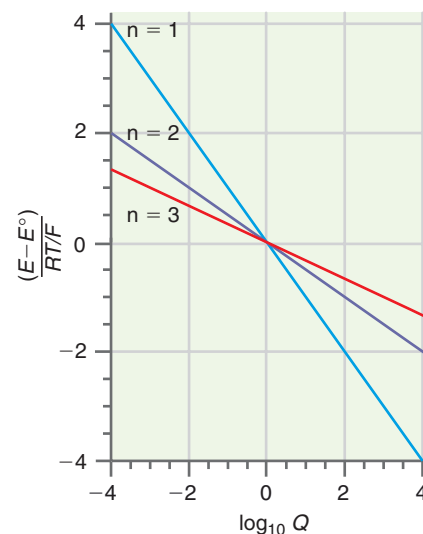


**FIGURE 11.6**
The cell potential $E$ varies linearly with log $Q$. The slope of a plot of $(E - E^\circ)/(RT/F)$ is inversely proportional to the number of electrons transferred in the redox reaction.

### EXAMPLE PROBLEM 11.1

Calculate the potential of the $H^+/H_2$ half-cell when $a_{H^+} = 0.770$ and $f_{H_2} = 1.13$.

**Solution**

$$E = E^\circ - \frac{0.05916\text{ V}}{n}\log_{10}\frac{a_{H^+}}{\sqrt{f_{H_2}}} = 0 - \frac{0.05916\text{ V}}{1}\log_{10}\frac{0.770}{\sqrt{1.13}} = 0.0083\text{ V}$$

# 11.5 Combining Standard Electrode Potentials to Determine the Cell Potential

A representative set of standard potentials is listed in Tables 11.1 and 11.2 (see Appendix A, Data Tables). By convention, half-cell emfs are always tabulated as reduction potentials. However, whether the reduction or the oxidation reaction is spontaneous in a half-cell is determined by the relative emfs of the two half-cells that make up the electrochemical cell. Because $\Delta G_R^\circ = -nFE^\circ$, and $\Delta G_R^\circ$ for the oxidation and reduction reactions are equal in magnitude and opposite in sign,

$$E_{reduction}^\circ = -E_{oxidation}^\circ \tag{11.31}$$

How is the cell potential related to the potentials of the half-cells? The standard potential of a half-cell is given by $E^\circ = -\Delta G_R^\circ/nF$ and is an intensive property because although both $\Delta G_R^\circ$ and $n$ are extensive quantities, the ratio $\Delta G_R^\circ/n$ is an intensive quantity. In particular, $E^\circ$ is not changed if all the stoichiometric coefficients are multiplied by any integer, because both $\Delta G_R^\circ$ and $n$ are changed by the same factor. Therefore,

$$E_{cell}^\circ = E_{reduction}^\circ + E_{oxidation}^\circ \tag{11.32}$$

even if the balanced reaction for the overall cell is multiplied by an arbitrary number. In Equation (11.32), the standard potentials on the right refer to the half-cells.

## EXAMPLE PROBLEM 11.2

An electrochemical cell is constructed using a half-cell for which the reduction reaction is given by

$$Fe(OH)_2(s) + 2e^- \rightarrow Fe(s) + 2\,OH^-(aq) \qquad E^\circ = -0.877\ V$$
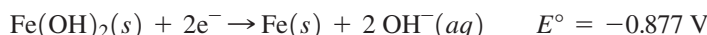
It is combined with a half-cell for which the reduction reaction is given by

a. $Al^{3+}(aq) + 3e^- \rightarrow Al(s)$ $\qquad\qquad\qquad E^\circ = -1.66\ V$

b. $AgBr(s) + e^- \rightarrow Ag(s) + Br^-(aq)$ $\qquad E^\circ = +0.071\ V$

The activity of all species is one for both reactions. Write the overall reaction for the cells in the direction of spontaneous change. Is the Fe reduced or oxidized in the spontaneous reaction?

### Solution

The emf for the cell is the sum of the emfs for the half-cells, one of which is written as an oxidation reaction, and the other of which is written as a reduction reaction. For the direction of spontaneous change, $E^\circ = E_{reduction}^\circ + E_{oxidation}^\circ > 0$. Note that the two half-cell reactions are combined with the appropriate stoichiometry so that electrons do not appear in the overall equation. Recall that the half-cell emfs are not changed in multiplying the overall reactions by the integers necessary to eliminate the electrons in the overall equation, because $E^\circ$ is an intensive quantity.

a. $3\,Fe(OH)_2(s) + 2\,Al(s) \rightleftharpoons 3\,Fe(s) + 6\,OH^-(aq) + 2\,Al^{3+}(aq)$

$E^\circ = -0.877\ V + 1.66\ V = +0.783\ V$
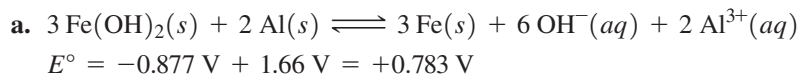
In this cell, Fe is reduced.

b. $Fe(s) + 2\,OH^-(aq) + 2\,AgBr(s) \rightleftharpoons Fe(OH)_2(s) + 2\,Ag(s) + 2\,Br^-(aq)$

$E^\circ = 0.071\ V + 0.877\ V = +0.95\ V$
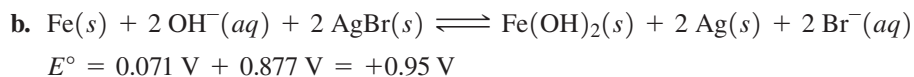
In this cell, Fe is oxidized.

Because $\Delta G$ is a state function, the cell potential for a third half-cell can be obtained from the cell potentials of two half-cells if they have an oxidation or reduction

reaction in common. The procedure is analogous to the use of Hess's law in Chapter 4 and is illustrated in Example Problem 11.3.

## EXAMPLE PROBLEM 11.3

You are given the following reduction reactions and $E°$ values:

$$Fe^{3+}(aq) + e^- \rightarrow Fe^{2+}(aq) \qquad E° = +0.771 \text{ V}$$

$$Fe^{2+}(aq) + 2e^- \rightarrow Fe(s) \qquad E° = -0.447 \text{ V}$$
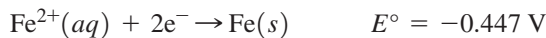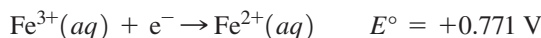
Calculate $E°$ for the half-cell reaction $Fe^{3+}(aq) + 3e^- \rightarrow Fe(s)$.

### Solution

We calculate the desired value of $E°$ by converting the given $E°$ values to $\Delta G°$ values, and combining these reduction reactions to obtain the desired equation.

$$Fe^{3+}(aq) + e^- \rightarrow Fe^{2+}(aq)$$
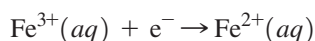
$$\Delta G° = -nFE° = -1 \times 96485 \text{C mol}^{-1} \times 0.771 \text{ V} = -74.39 \text{ kJ mol}^{-1}$$

$$Fe^{2+}(aq) + 2e^- \rightarrow Fe(s)$$
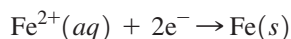
$$\Delta G° = -nFE° = -2 \times 96485 \text{ C mol}^{-1} \times (-0.447 \text{ V}) = 86.26 \text{kJ mol}^{-1}$$

We next add the two equations as well as their $\Delta G°$ to obtain

$$Fe^{3+}(aq) + 3e^- \rightarrow Fe(s)$$
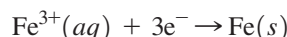
$$\Delta G° = -74.39 \text{kJ mol}^{-1} + 86.26 \text{kJ mol}^{-1} = 11.87 \text{kJ mol}^{-1}$$

$$E°_{Fe^{3+}/Fe} = -\frac{\Delta G°}{nF} = \frac{-11.87 \times 10^3 \text{J mol}^{-1}}{3 \times 96485 \text{ C mol}^{-1}} = -0.041 \text{ V}$$

The $E°$ values cannot be combined directly, because they are intensive rather than extensive quantities.

The preceding calculation can be generalized as follows. Assume that $n_1$ electrons are transferred in the reaction with the potential $E°_{A/B}$, and $n_2$ electrons are transferred in the reaction with the potential $E°_{B/C}$. If $n_3$ electrons are transferred in the reaction with the potential $E°_{A/C}$, then $n_3 E°_{A/C} = n_1 E°_{A/B} + n_2 E°_{B/C}$.

# 11.6 Obtaining Reaction Gibbs Energies and Reaction Entropies from Cell Potentials

In Section 11.4, we demonstrated that $\Delta G_R = -nF\Delta\phi$. Therefore, if the cell potential is measured under standard conditions,

$$\Delta G_R° = -nFE° \tag{11.33}$$

If $E°$ is known, $\Delta G_R°$ can be determined using Equation (11.33). For example, $E°$ for the Daniell cell is $+1.10$ V. Therefore, $\Delta G_R°$ for the reaction $Zn(s) + Cu^{2+}(aq) \rightleftharpoons Zn^{2+}(aq) + Cu(s)$ is

$$\Delta G_R° = -nFE° = -2 \times 96{,}485 \text{ C mol}^{-1} \times 1.10 \text{ V} = -212 \text{ kJ mol}^{-1} \tag{11.34}$$

The reaction entropy is related to $\Delta G_R°$ by

$$\Delta S_R° = -\left(\frac{\partial \Delta G_R°}{\partial T}\right)_P = nF\left(\frac{\partial E°}{\partial T}\right)_P \tag{11.35}$$

Therefore, a measurement of the temperature dependence of $E°$ can be used to determine $\Delta S_R°$, as shown in Example Problem 11.4.

**EXAMPLE PROBLEM 11.4**

The standard potential of the cell formed by combining the $Cl_2(g)/Cl^-(aq)$ half-cell with the standard hydrogen electrode is $+1.36$ V, and $(\partial E°/\partial T)_P = -1.20 \times 10^{-3}$ V $K^{-1}$. Calculate $\Delta S_R°$ for the reaction $H_2(g) + Cl_2(g) \rightleftharpoons 2\,H^+(aq) + 2\,Cl^-(aq)$. Compare your result with the value that you obtain by using the values of $\Delta S°$ in the data tables from Appendix A.

**Solution**

From Equation (11.35),

$$\Delta S_R° = -\left(\frac{\partial \Delta G_R°}{\partial T}\right)_P = nF\left(\frac{\partial E°}{\partial T}\right)_P$$

$$= 2 \times 96480\,C\,mol^{-1} \times (-1.2 \times 10^{-3}\,V\,K^{-1})$$

$$= -2.3 \times 10^2\,J\,K^{-1}\,mol^{-1}$$

From Table 10.1 (see Appendix A, Data Tables),

$$\Delta S_R° = 2S_m°(H^+, aq) + 2S_m°(Cl^-, aq) - S_m°(H_2, g) - S_m°(Cl_2, g)$$

$$= 2 \times 0 + 2 \times 56.5\,J\,K^{-1}mol^{-1} - 130.7\,J\,K^{-1}mol^{-1} - 223.1\,J\,K^{-1}mol^{-1}$$

$$= -2.408 \times 10^2\,J\,K^{-1}mol^{-1}$$

The limited precision of the temperature dependence of $E°$ limits the precision in the determination of $\Delta S_R°$.

## 11.7 The Relationship between the Cell EMF and the Equilibrium Constant

If the redox reaction is allowed to proceed until equilibrium is reached, $\Delta G = 0$, so that $E = 0$. For the equilibrium state, the reaction quotient $Q = K$. Therefore,

$$E° = \frac{RT}{nF}\ln K \tag{11.36}$$

Equation (11.36) shows that a measurement of the standard state cell potential, for which $a_i = 1$ for all species in the redox reaction, allows $K$ for the overall reaction to be determined. Although this statement is true, it is not practical to adjust all activities to the value 1. The experimental determination of $E°$ is discussed in the next section.

Tabulated half-cell potentials provide a powerful way to determine the equilibrium constant in an electrochemical cell using Equation (11.36). To determine $K$, the overall reaction must be separated into the oxidation and reduction half-reactions, and the number of electrons transferred must be determined. For example, consider the reaction

$$2\,MnO_4^-(aq) + 6\,H^+(aq) + 5\,HOOCCOOH(aq) \rightleftharpoons$$
$$2\,Mn^{2+}(aq) + 8\,H_2O(l) + 10\,CO_2(g) \tag{11.37}$$
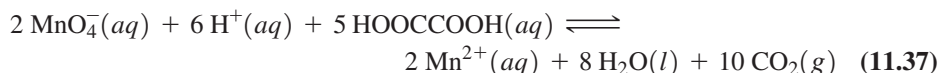
The reduction and oxidation half-reactions are

$$MnO_4^-(aq) + 8\,H^+(aq) + 5e^- \rightarrow Mn^{2+}(aq) + 4\,H_2O(l) \quad E° = +1.51\,V \tag{11.38}$$

$$HOOCCOOH(aq) \rightarrow 2\,H^+(aq) + 2\,CO_2(g) + 2e^- \quad E° = +0.49\,V \tag{11.39}$$
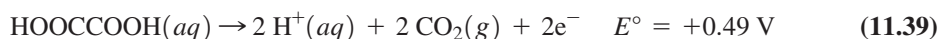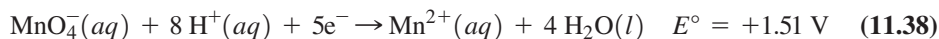
To eliminate the electrons in the overall equation, the first equation must be multiplied by 2, and the second equation must be multiplied by 5; $E°$ is unchanged by doing so. However, $n$ is affected by the multipliers. In this case $n = 10$. Therefore,

$$\Delta G° = -nFE° = -10 \times 96485\,C\,mol^{-1} \times (1.51\,V + 0.49\,V)$$

$$= -1.93 \times 10^2\,kJ\,mol^{-1}$$

$$\ln K = -\frac{\Delta G°}{RT} = \frac{1.93 \times 10^2\,kJ\,mol^{-1}}{8.314\,J\,K^{-1}\,mol^{-1} \times 298.15\,K} = 778 \tag{11.40}$$

As this result shows, the equilibrium corresponds to essentially complete conversion of reactants to products. Example Problem 11.5 shows the same calculation for the Daniell cell.

### EXAMPLE PROBLEM 11.5

For the Daniell cell $E° = 1.10$ V. Calculate $K$ for the reaction at 298.15 K
$Zn(s) + Cu^{2+}(aq) \rightleftharpoons Zn^{2+}(aq) + Cu(s)$.
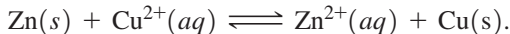
**Solution**

$$\ln K = \frac{nF}{RT}E° = \frac{2 \times 96485 \text{ C mol}^{-1} \times 1.10 \text{ V}}{8.314 \text{ J K}^{-1} \text{mol}^{-1} \times 298.15 \text{ K}}$$

$$= 85.63$$

$$K = 1.55 \times 10^{37}$$

Note that the equilibrium constant calculated in Example Problem 11.5 is so large that it could not have been measured by determining the activities of $a_{Zn^{2+}}$ and $a_{Cu^{2+}}$ by spectroscopic methods. This would require a measurement technique that is accurate over more than 30 orders of magnitude in the activity. By contrast, the equilibrium constant in an electrochemical cell can be determined with high accuracy using only a voltmeter.

A further example of the use of electrochemical measurements to determine equilibrium constants is the solubility constant for a weakly soluble salt. If the overall reaction corresponding to dissolution can be generated by combining half-cell potentials, then the solubility constant can be calculated from the potentials. For example, the following half-cell reactions can be combined to calculate the solubility product of AgBr.

$$AgBr(s) + e^- \rightarrow Ag(s) + Br^-(aq) \qquad E° = 0.07133 \text{ V} \quad \text{and}$$

$$\underline{Ag(s) \rightarrow Ag^+(aq) + e^- \hspace{5.5cm} E° = -0.7996 \text{ V}}$$

$$AgBr(s) \rightleftharpoons Ag^+(aq) + Br^-(aq) \qquad E° = -0.7283 \text{ V}$$

$$\ln K_{sp} = \frac{nF}{RT}E° = \frac{1 \times 96485 \text{ C mol}^{-1} \times (-0.7283 \text{ V})}{8.314 \text{ J K}^{-1}\text{mol}^{-1} \times 298.15 \text{ K}} = -28.35$$
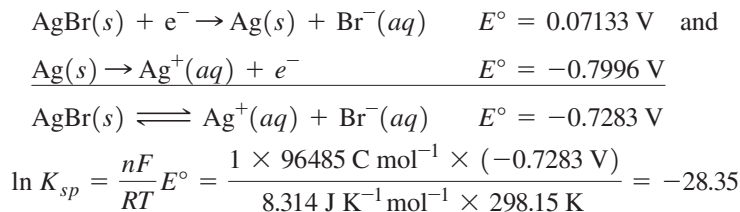
The value of the solubility constant is $K_{sp} = 4.88 \times 10^{-13}$.

### EXAMPLE PROBLEM 11.6

A concentration cell consists of two half-cells that are identical except for the activities of the redox components. Consider two half-cells based on the $Ag^+(aq) + e^- \rightarrow Ag(s)$ reaction. The left half-cell contains $AgNO_3$ at unit activity, and the right half-cell initially had the same concentration of $AgNO_3$, but just enough $NaCl(aq)$ has been added to precipitate the $Ag^+(aq)$ as AgCl. Write an equation for the overall cell reaction. If the emf of this cell is 0.29 V, what is $K_{sp}$ for AgCl?

**Solution**

The overall reaction is $Ag^+(aq, a = 1) \rightleftharpoons Ag^+(aq, a)$ with a concurrent transport of $Cl^-$ in the opposite direction through the salt bridge between the half-cells. In the right half-cell we have the equilibrium $AgCl(s) \rightleftharpoons Ag^+(aq, a_\pm) + Cl^-(aq, a_\pm)$, so that $a_{Ag^+}a_{Cl^-} = a_\pm^2 = K_{sp}$.

Because the half-cell reactions are the same, $E° = 0$ and

$$E = -\frac{0.05916 \text{ V}}{n} \log_{10}\frac{a_\pm}{1} = -\frac{0.05916}{1} \log_{10}\sqrt{K_{sp}}$$

$$= -\frac{0.05916 \text{ V}}{2} \log_{10} K_{sp}$$

$$\log_{10} K_{sp} = -\frac{2E}{0.05916} = -\frac{2 \times (0.29 \text{ V})}{0.05916 \text{ V}} = -9.804$$

$$K_{sp} = 1.57 \times 10^{-10}$$
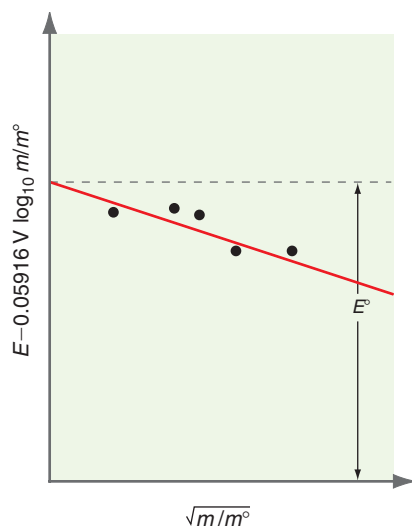
**FIGURE 11.7**
The value of $E°$ and the activity coefficient can be measured by plotting the left-hand side of Equation (11.42) against the square root of the molality.

# 11.8 Determination of $E°$ and Activity Coefficients Using an Electrochemical Cell

The main problem in determining standard potentials lies in knowing the value of the activity coefficient $\gamma_\pm$ for a given solute concentration. The best strategy is to carry out measurements of the cell potential at low concentrations, where $\gamma_\pm \rightarrow 1$, rather than near unit activity, where $\gamma_\pm$ differs appreciably from 1. Consider an electrochemical cell consisting of the $Ag^+/Ag$ and standard hydrogen electrode half-cells at 298 K. The cell reaction is $Ag^+(aq) + 1/2\,H_2(g) \rightleftharpoons Ag(s) + H^+(aq)$ and $Q = (a_{Ag+})^{-1}$. Because the activities of $H_2(g)$ and $H^+(aq)$ are 1, they do not appear in $Q$. Assume that the $Ag^+$ arises from the dissociation of $AgNO_3$. Recall that the activity of an individual ion cannot be measured directly. It must be calculated from the measured activity $a_\pm$ and the definition $a_\pm^\nu = a_+^{\nu+} a_-^{\nu-}$. In this case, $a_\pm^2 = a_{Ag+}a_{NO_3^-}$ and $a_\pm = a_{Ag+} = a_{NO_3^-}$. Similarly, $\gamma_\pm = \gamma_{Ag+} = \gamma_{NO_3^-}$ and $m_{Ag+} = m_{NO_3^-} = m_\pm = m$, and $E$ is given by

$$E = E°_{Ag^+/Ag} + \frac{RT}{F}\ln a_{Ag+} = E°_{Ag^+/Ag} + \frac{RT}{F}\ln(m/m°) + \frac{RT}{F}\ln\gamma_\pm \quad \text{(11.41)}$$

At low enough concentrations, the Debye–Hückel limiting law is valid and $\log\gamma_\pm = -0.5092\sqrt{m_\pm/m°}$ at 298 K as discussed in Section 10.4. Using this relation, Equation (11.41) can be rewritten in the form

$$E - 0.05916\log_{10}(m/m°) = E°_{Ag^+/Ag} - 0.05916 \times 0.5090\sqrt{(m/m°)}$$
$$= E°_{Ag^+/Ag} - 0.03011\sqrt{(m/m°)} \quad \text{(11.42)}$$

The left-hand side of this equation can be calculated from measurements and plotted as a function of $\sqrt{(m/m°)}$. The results will resemble the graph shown in Figure 11.7. An extrapolation of the line that best fits the data to $m = 0$ gives $E°$ as the intercept with the vertical axis. Once $E°$ has been determined, Equation (11.41) can be used to calculate $\gamma_\pm$.

Electrochemical cells provide a powerful method of determining activity coefficients because cell potentials can be measured more accurately and more easily than colligative properties such as freezing point depression or boiling point elevation. Note that although the Debye–Hückel limiting law was used to determine $E°$, it is not necessary to use the limiting law to calculate activity coefficients once $E°$ is known.

# 11.9 Cell Nomenclature and Types of Electrochemical Cells

It is useful to use an abbreviated notation to describe an electrochemical cell. This notation includes all species involved in the cell reaction and phase boundaries within the cell, which are represented by a vertical line. As will be seen later in this section, the metal electrodes appear at the ends of this notation, the half-cell in which oxidation occurs is written on the left, and the electrode is called the anode. The half-cell in which reduction occurs is written on the right, and the electrode is called the cathode.

We briefly discuss an additional small contribution to the cell potential that arises from the differing diffusion rates of large and small ions in an electrical field. As an electrochemical reaction proceeds, ions that diffuse rapidly across a liquid–liquid junction, such as $H^+$, will travel farther than ions that diffuse slowly, such as $Cl^-$, in a given time. At steady state, a dipole layer is built up across this junction, and the rates of ion transfer through this dipole layer become equal. This kinetic effect will give rise to a small **junction potential** between two liquids of different composition or concentration. Such a junction potential is largely eliminated by a salt bridge. An interface for which the junction potential has been eliminated is indicated by a pair of vertical lines.The separation of different phases that are in contact and allow electron transfer is shown by a solid vertical line. A single dashed line is used to indicate a liquid–liquid interface across which charge transfer can occur.

For example, the abbreviated notation for the Daniell cell containing a salt bridge is

$$Zn(s)|ZnSO_4(aq)\|CuSO_4(aq)|Cu(s) \tag{11.43}$$
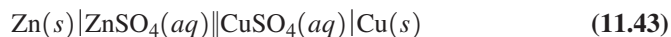
and a cell made up of the $Zn/Zn^{2+}$ half-cell and the standard hydrogen electrode is described by

$$Zn(s)|ZnSO_4(aq)\|H^+(aq)|H_2(g)|Pt(s) \tag{11.44}$$
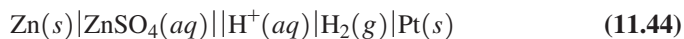
The overall reaction in this cell is $Zn(s) + 2 H^+(aq) \rightleftharpoons Zn^{2+}(aq) + H_2(g)$. In general, in such a cell the solutions are physically separated by a porous membrane to prevent mixing of the solutions. In this case, the junction potential has not been eliminated.

The half-cell and overall reactions can be determined from the abbreviated notation in the following way. An electron is transferred from the electrode at the far left of the abbreviated notation to the electrode on the far right through the external circuit. The number of electrons is then adjusted to fit the half-cell reaction. This procedure is illustrated in Example Problem 11.7.

### EXAMPLE PROBLEM 11.7

Determine the half-cell reactions and the overall reaction for the cell designated

$$Ag(s)|AgCl(s)|Cl^-(aq, a_\pm = 0.0010)\|Fe^{2+}(aq, a_\pm = 0.50)$$
$$Fe^{3+}(aq, a_\pm = 0.10)|Pt(s)$$
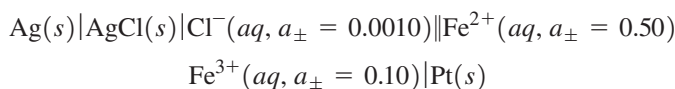
#### Solution

The anode and cathode reactions are

$$Ag(s) + Cl^-(aq) \rightarrow AgCl(s) + e^-$$
$$Fe^{3+}(aq) + e^- \rightarrow Fe^{2+}(aq)$$

The overall reaction is

$$Ag(s) + Cl^-(aq) + Fe^{3+}(aq) \rightleftharpoons AgCl(s) + Fe^{2+}(aq)$$
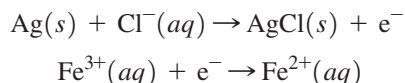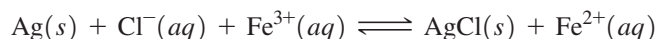
Only after the cell potential is calculated is it clear whether the reaction or the reverse reaction is spontaneous.

We have already discussed several specific half-cells and next discuss different types of half-cells. The standard hydrogen electrode involves the equilibrium between a gas and a dissolved species. A second such electrode is the $Cl_2/Cl^-$ electrode, for which the reduction reaction is

$$Cl_2(g) + 2e^- \rightarrow 2 Cl^-(aq) \quad E° = +1.36 \text{ V} \tag{11.45}$$
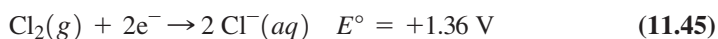
Another type of half-cell that is frequently encountered involves a metal and a metal ion in solution. Both half-cells in the Daniell cell fall into this category.

$$Zn^{2+}(aq) + 2e^- \rightarrow Zn(s) \quad E° = -0.76 \text{ V} \tag{11.46}$$
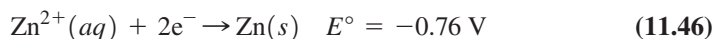
A number of half-cells consist of a metal, an insoluble salt containing the metal, and an aqueous solution containing the anion of the salt. Two examples of this type of half-cell are the Ag–AgCl half-cell for which the reduction reaction is

$$AgCl(s) + e^- \rightarrow Ag(s) + Cl^-(aq) \quad E° = +0.22 \text{ V} \tag{11.47}$$
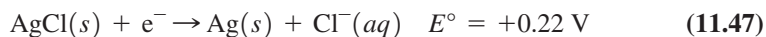
and the calomel (mercurous chloride) electrode, which is frequently used as a reference electrode in electrochemical cells:

$$Hg_2Cl_2(s) + 2e^- \rightarrow 2 Hg(l) + 2 Cl^-(aq) \quad E° = +0.27 \text{ V} \tag{11.48}$$

In a further type of half-cell, both species are present in solution, and the electrode is an inert conductor such as Pt, which allows an electrical connection to be made to the solution. For example, in the $Fe^{3+}/Fe^{2+}$ half-cell, the reduction reaction is

$$Fe^{3+}(aq) + e^- \rightarrow Fe^{2+}(aq) \quad E° = 0.771 \text{ V} \tag{11.49}$$

  
| **TABLE 11.3** |
|---|
| **The Electrochemical Series** |
| **Most Strongly Reducing (The metal is least easily oxidized.)** |
| Gold (most positive reduction potential) |
| Platinum |
| Palladium |
| Silver |
| Rhodium |
| Copper |
| Mercury (Hydrogen; zero reduction potential by convention) |
| Lead |
| Tin |
| Nickel |
| Iron |
| Zinc |
| Chromium |
| Vanadium |
| Manganese |
| Magnesium |
| Sodium |
| Calcium |
| Potassium |
| Rubidium |
| Cesium |
| Lithium (most negative reduction potential) |
| **Least Strongly Reducing (The metal is most easily oxidized.)** |

# 11.10 The Electrochemical Series

Tables 11.1 and 11.2 (see Appendix A, Data Tables) list the reduction potentials of commonly encountered half-cells. The emf of a cell constructed from two of these half-cells with standard reduction potentials $E_1^\circ$ and $E_2^\circ$ is given by

$$E_{cell}^\circ = E_1^\circ - E_2^\circ \qquad (11.50)$$

The potential $E_{cell}^\circ$ will be positive and, therefore, $\Delta G < 0$, if the reduction potential for reaction 1 is more positive than that of reaction 2. Therefore, the relative strength of a species as an oxidizing agent follows the order of the numerical value of its reduction potential in Table 11.2. The **electrochemical series** shown in Table 11.3 is obtained if the oxidation of neutral metals to their most common oxidation state is considered. For example, the entry for gold in Table 11.3 refers to the reduction reaction

$$Au^{3+}(aq) + 3e^- \rightarrow Au(s) \quad E^\circ = 1.498 \text{ V}$$
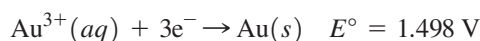
In a redox couple formed from two entries in the list shown in Table 11.3, the species lying higher in the list will be reduced, and the species lying lower in the list will be oxidized in the spontaneous reaction. For example, the table predicts that the spontaneous reaction in the copper–zinc couple is $Zn(s) + Cu^{2+}(aq) \rightarrow Zn^{2+}(aq) + Cu(s)$ and not the reverse reaction.

## EXAMPLE PROBLEM 11.8

For the reduction of the permanganate ion $MnO_4^-$ to $Mn^{2+}$ in an acidic solution, $E^\circ = +1.51 \text{ V}$. The reduction reactions and standard potentials for $Zn^{2+}$, $Ag^+$, and $Au^+$ are given here:

$$Zn^{2+}(aq) + 2e^- \rightarrow Zn(s) \qquad E^\circ = -0.7618 \text{ V}$$

$$Ag^+(aq) + e^- \rightarrow Ag(s) \qquad E^\circ = 0.7996 \text{ V}$$

$$Au^+(aq) + e^- \rightarrow Au(s) \qquad E^\circ = 1.692 \text{ V}$$
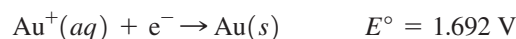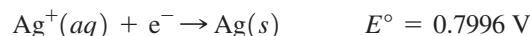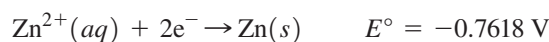
Which of these metals will be oxidized by the $MnO_4^-$ ion?

### Solution

The cell potentials assuming the reduction of the permanganate ion and oxidation of the metal are

$$Zn: \quad 1.51 \text{ V} + 0.761 \text{ V} = 2.27 \text{ V} > 0$$

$$Ag: \quad 1.51 \text{ V} - 0.7996 \text{ V} = 0.710 \text{ V} > 0$$

$$Au: \quad 1.51 \text{ V} - 1.692 \text{ V} = -0.18 \text{ V} < 0$$

If $E^\circ > 0$, $\Delta G < 0$. On the basis of the sign of the cell potential, we conclude that only Zn and Ag will be oxidized by the $MnO_4^-$ ion.

# 11.11 Thermodynamics of Batteries and Fuel Cells

Batteries and fuel cells are electrochemical cells that are designed to maximize the ratio of output power to the cell weight or volume. **Batteries** contain the reactants needed to support the overall electrochemical reaction, whereas **fuel cells** are designed to accept a continuous flow of reactants from the surroundings. Batteries that cannot be recharged are called primary batteries, whereas rechargeable batteries are called secondary batteries.

It is useful to compare the relative amount of work that can be produced through an electrochemical reaction with the work that a heat engine could produce using the same overall reaction. The maximum electrical work is given by

$$w_{electrical} = -\Delta G = -\Delta H \left( 1 - \frac{T\Delta S}{\Delta H} \right) \tag{11.51}$$

whereas the maximum work available through a reversible heat engine operating between $T_h$ and $T_c$ is

$$w_{thermal} = q_{hot} \, \varepsilon = -\Delta H \left( \frac{T_h - T_c}{T_h} \right) \tag{11.52}$$

where $\varepsilon$ is the efficiency of a reversible heat engine (see Section 5.2). To compare the maximum thermal and electrical work, we use the overall reaction for the familiar lead-acid battery used in cars. For this reaction, $\Delta G_R^\circ = -376.97 \, \text{kJ mol}^{-1}$, $\Delta H_R^\circ = -227.58 \, \text{kJ mol}^{-1}$, and $\Delta S_R^\circ = 501.1 \, \text{J K}^{-1} \, \text{mol}^{-1}$. Assuming $T_h = 600. \, \text{K}$ and $T_c = 300. \, \text{K}$ and that the battery operates at 300. K, then

$$\frac{w_{electrical}}{w_{thermal}} = 3.31 \tag{11.53}$$

This calculation shows that much more work can be produced in the electrochemical reaction than in the thermal reaction. This comparison does not even take into account that the lead-acid battery can be recharged, whereas the thermal reaction can only be run once.

# 11.12 The Electrochemistry of Commonly Used Batteries

The lead-acid battery was invented in 1859 and is still widely used in automobiles. Because the power required to start an automobile engine is on the order of a kilowatt, the current capacity of such a battery must be on the order of a hundred amperes. Additionally, such a battery must be capable of 500 to 1500 recharging cycles from a deep discharge. In recharging batteries, the reaction product in the form of a solid must be converted back to the reactant, also in the form of a solid. Because the solids in general have a different crystal structure and density, the conversion induces mechanical stress in the anode and cathode, which ultimately leads to a partial disintegration of these electrodes. This is the main factor that limits the number of charge–discharge cycles that a battery can tolerate.

The electrodes in the lead-acid battery consist of Pb powder and finely divided PbO and $PbSO_4$ supported on a Pb frame. The electrodes are supported in a container containing concentrated $H_2SO_4$. In use, a battery is discharged. Some batteries, including the lead-acid battery, can be recharged by applying an external voltage to convert products back to reactants. In that case, the role of anode and cathode are reversed. To avoid confusion, we write half cell and overall reactions for the discharge mode. In the lead-acid battery, the cell reactions at the cathode and anode are

$$PbO_2(s) + 4 \, H^+(aq) + SO_4^{2-}(aq) + 2e^- \rightarrow PbSO_4(s) + 2 \, H_2O(l)$$

$$E^\circ = 1.685 \, \text{V} \tag{11.54}$$

$$Pb(s) + SO_4^{2-}(aq) \rightarrow PbSO_4(s) + 2e^- \quad E^\circ = -0.356 \, \text{V} \tag{11.55}$$
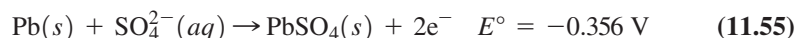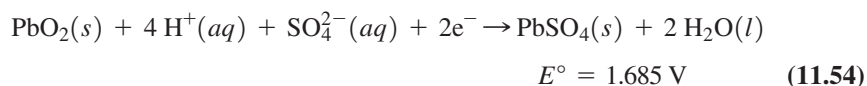
respectively, and the overall reaction is

$$PbO_2(s) + Pb(s) + 2 \, H_2SO_4(aq) \rightleftharpoons 2 \, PbSO_4(s) + 2 \, H_2O(l) \quad E^\circ = 2.04 \, \text{V} \tag{11.56}$$

The arrows would point in the opposite direction and the sign of the emfs would be reversed for the charging mode.

Six such cells connected in series are required for a battery that provides a nominal potential of 12 V. The lead-acid battery is very efficient in that more than 90% of the electrical charge used to charge the battery is available in the discharge part of the cycle.

**FIGURE 11.8**

A number of different batteries are classi-fied with their specific energy density per unit volume and per unit mass.
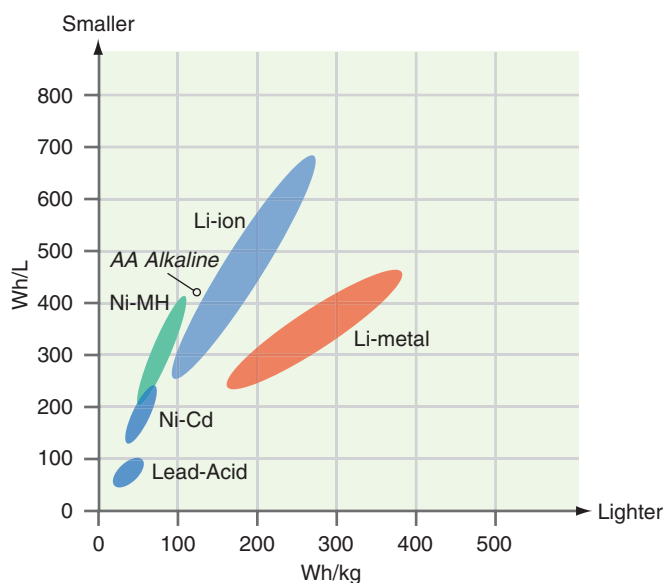


This means that side reactions such as the electrolysis of water play a minimal role in charging the battery. However, only about 50% of the lead in the battery is converted between $PbO_2$ and $PbSO_4$. Because Pb has a large atomic mass, this limited convertibil-ity decreases the power per unit mass figure of merit for the battery. Parasitic side reac-tions also lead to a self-discharge of the cell without current flowing in the external circuit. For the lead-acid battery, the capacity is diminished by approximately 0.5% per day through self-discharge.

As batteries have become more common in portable devices such as cell phones and laptop computers, energy density is a major criterion in choosing the most suitable battery chemistry for a specific application. Figure 11.8 shows a comparison of differ-ent battery types. The lead-acid battery has the lowest specific energy either in terms of volume or mass. Next we discuss the chemistry of three commonly used rechargeable batteries: the alkaline, nickel metal hydride, and lithium ion batteries.

The individual elements of the alkaline cell are shown in Figure 11.9. The anode in this cell is powdered zinc, and the cathode is in the form of a $MnO_2$ paste mixed with
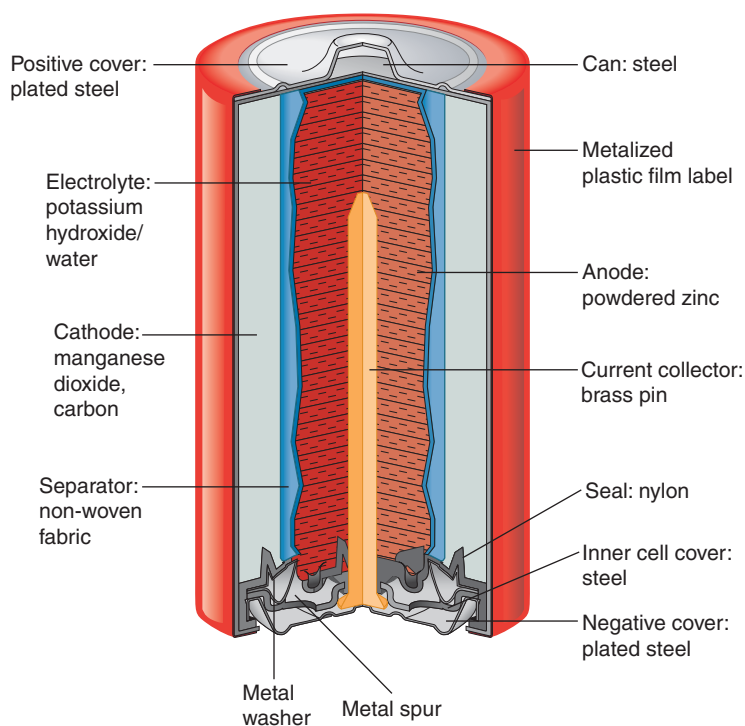


**FIGURE 11.9**

Schematic diagram of an alkaline cell.

powdered carbon to impart conductivity. KOH is used as the electrolyte. The anode and cathode reactions are

Anode: $Zn(s) + 2\,OH^-(aq) \rightarrow ZnO(s) + H_2O(l) + 2e^-$    $E° = 1.1$ V    **(11.57)**

Cathode: $2\,MnO_2(s) + H_2O(l) + 2e^- \rightarrow Mn_2O_3(s) + 2\,OH^-(aq)$ $E° = -0.76$ V

**(11.58)**
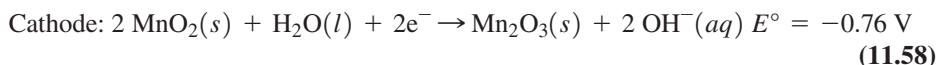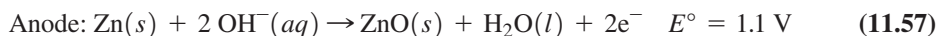
Nickel metal hydride batteries are currently used in hybrid vehicles that rely on dc motors to drive the vehicle in city traffic and use a gasoline engine for higher speed driving. The Toyota Prius uses 28 modules of 6 cells, each with a nominal voltage of 1.2 V and a total voltage of 201.6 V to power the vehicle. The capacity of the battery pack is ~1100 Wh. The anode and cathode reactions are

Anode: $MH(s) + OH^-(aq) \rightarrow M + H_2O(l) + e^-$   $E° = 0.83$ V   **(11.59)**

Cathode: $NiOOH(s) + H_2O(l) + 2e^- \rightarrow Ni(OH)_2(s) + OH^-(aq)$

$E° = 0.52$ V    **(11.60)**
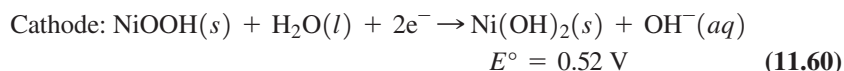
The electrolyte is $KOH(aq)$, and the overall reaction is

$$MH(s) + NiOOH(s) \rightleftharpoons M + Ni(OH)_2(s)\quad E° = 1.35 \text{ V}\qquad \textbf{(11.61)}$$
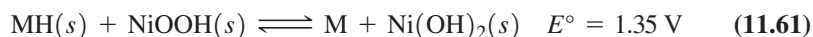
where M designates an alloy that can contain V, Ti, Zr, Ni, Cr, Co, and Fe.

Lithium ion batteries find applications as diverse as cell phones, where a high energy density per unit volume is required, and electric vehicles, where a high energy density per unit mass is required. The electrodes in lithium ion batteries contain $Li^+$ ions, and the cell voltage reflects the difference in the binding strength of $Li^+$ in the two materials. The structure of a cylindrical lithium ion battery is shown schematically in Figure 11.10. The two electrodes are separated by an electrolyte–saturated polymer membrane through which the $Li^+$ ions move in the internal circuit. The electrolyte is a lithium salt dissolved in an organic solvent, for example, 1M $LiPF_6$ in a mixture of ethylene carbonate and diethyl carbonate. Aqueous electrolytes would limit the cell voltage to 1.2 V because at larger potentials, water is reduced or oxidized. Figure 11.11 shows a number of materials that can be used as electrodes. Materials that fall outside of the band gap of the electrolyte are unsuitable because their use initiates reduction or oxidation of the solvent. It would appear that carbon is unsuitable, but the formation of a thin solid/electrolyte interface layer stabilizes carbon with respect to solvent reactions, and it is the
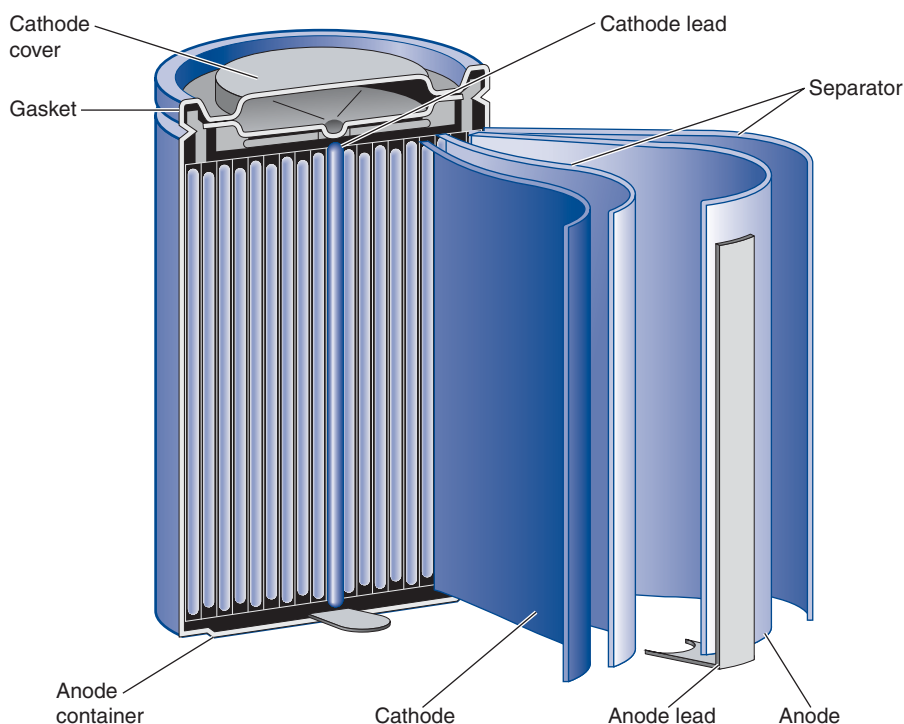


**FIGURE 11.10**
Schematic structure of a cylindrical lithium ion battery. The anode and cathode material are formed of thin sheets to optimize the transport kinetics of $Li^+$ ions.

**FIGURE 11.11**

The cell potential of a lithium ion battery versus the energy density per unit mass for a number of electrode materials is shown. The dashed lines indicate the voltage range in which 1M LiPF$_6$ in a 1:1 mixture of ethylene carbonate and diethyl carbonate is stable with respect to reduction or oxidation.

*Source:* Goodenough J. B. and Kim Y. *Chemistry of Materials* 22 (2010), 587.
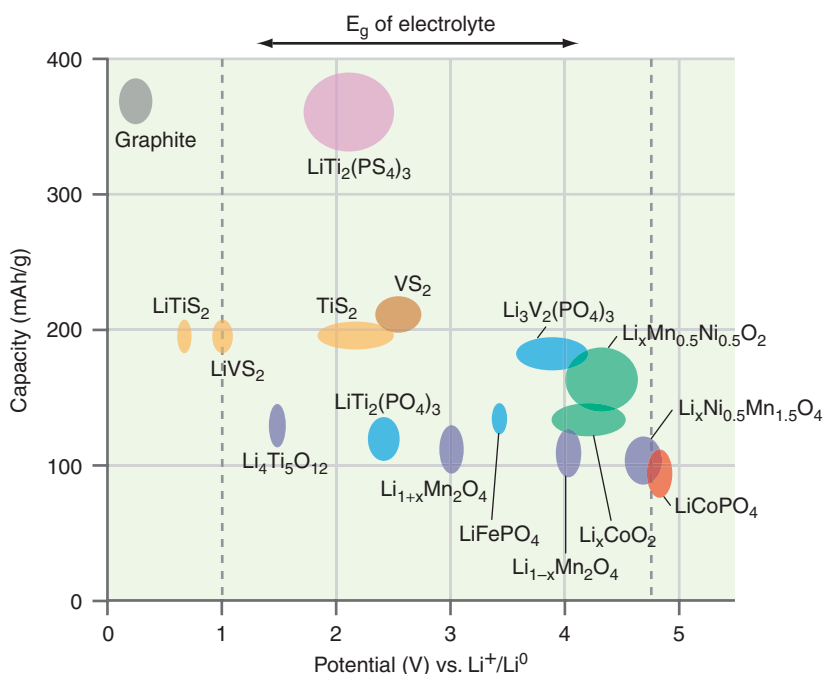


most widely used anode electrode. Using a carbon anode and LiCoO$_2$(s) as the cathode allows a cell potential of 3.7 V to be achieved. As Figure 11.11 shows, higher potentials are possible, but batteries with long life cycles using materials other than LiCoO$_2$(s) have not yet been developed.

Rechargeable lithium batteries have the following half-cell reactions while discharging the battery:

positive electrode:   $Li_{1-x}CoO_2(s) + xLi^+(solution) + xe^- \rightarrow LiCoO_2(s)$

$$(11.62)$$

negative electrode:   $CLi_x \rightarrow C(s) + xLi^+(solution) + xe^-$    $(11.63)$
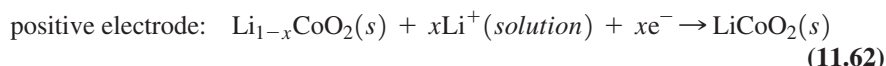
The right arrows indicate the discharge directions. In these equations, $x$ is a small positive number. The overall cell reaction is

$$Li_{1-x}CoO_2(s) + CLi_x \rightleftharpoons LiCoO_2(s) + C(graphite)   E° \sim 3.7 \text{ V}    (11.64)$$
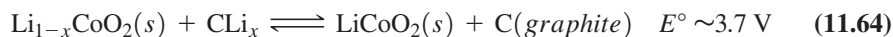
and the fully charged battery has a cell potential of ~3.7 V. The structures of LiCoO$_2$(s) and CLi$_x$ are shown schematically in Figure 11.12. CLi$_x$ designates Li atoms intercalated between sheets of graphite; it is not a stoichiometric compound. In a lithium-ion battery the lithium ions are transported to and from the cathode or anode, with the transition metal, cobalt (Co), in Li$_x$CoO$_2$ being oxidized from Co$^{3+}$ to Co$^{4+}$ during charging, and reduced from Co$^{4+}$ to Co$^{3+}$ during discharge.
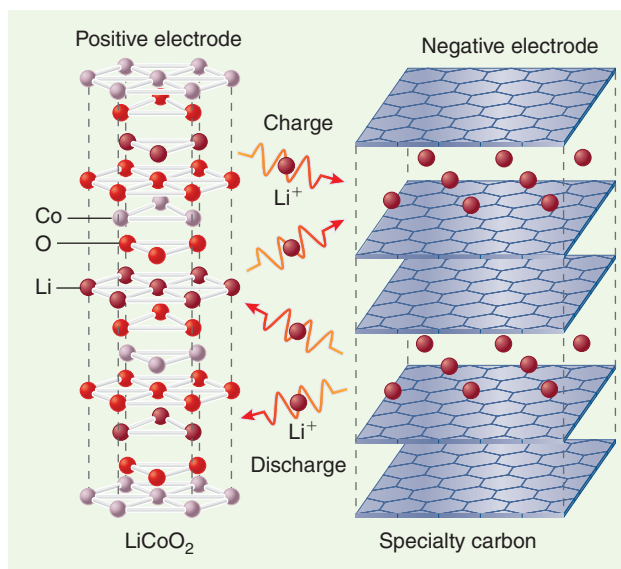


**FIGURE 11.12**

The cell voltage in a lithium battery is generated by moving the lithium between a lattice site in LiCoO$_2$ and an intercalation position between sheets of graphite.

# 11.13 Fuel Cells

The primary advantage of fuel cells over batteries is that they can be continually refueled and do not require a downtime for recharging. A number of different technologies are used in fuel cells. Most are still in the research and development stage, and only phosphoric acid fuel cells are available as off-the-shelf technology. Figure 11.13 shows a number of different types of fuel cells. All use $O_2$ or air as the oxidant, and the fuel can be either pure $H_2$ or $H_2$ produced on board by reforming hydrocarbons, methanol, or glucose. The different operating temperature and available power for the types of fuel cells shown in Figure 11.13 are shown in Figure 11.14.

The following discussion is restricted to the most widely understood technology, the **proton exchange membrane fuel cell (PEMFC)** using $H_2(g)$ as a fuel.

Proton exchange membrane fuel cells using $H_2$ and $O_2$ as the reactants were originally used in the NASA *Gemini* space flights of the 1960s. The principles underlying this technology have not changed in the intervening years. However, advances in technology have significantly increased the power generated per unit weight as well as the power generated per unit area of the electrodes. A schematic drawing of a single PEMFC and the relevant half-cell reactions is shown in Figure 11.15. The anode and cathode have channels that transport $H_2$ and $O_2$ to the catalyst and membrane. An intermediate diffusion layer ensures uniform delivery of reactants and separation of gases from the water formed in the reaction. The membrane is coated with a catalyst (usually Pt or Pt alloys) that facilitates the $H^+$ formation and the reaction between $O_2$ and $H^+$. Individual units can be arranged back to back to form a stack so that the potential across the stack is a multiple of the individual cell potential.

The heart of this fuel cell is the proton exchange membrane, which functions as a solid electrolyte. This membrane facilitates the passage of $H^+$ from the anode to the cathode in the internal circuit, and it also prevents electrons and negative ions from moving in the opposite direction. The membrane must be thin ($\sim 10-100 \ \mu m$) to allow rapid charge transport at reasonably high current densities and must be unreactive under the potentials present in the cell. The most widely used membranes are polymeric forms of perfluorosulfonic acids. These membranes are quite conductive if fully hydrated. The membrane structure consists of spherical cavities, or inverted micelles ~4 nm in diameter, connected by cylindrical channels ~1 nm in diameter. The interior of the cavities and channels is lined with $SO_3^-$ groups. The $-CF_2-$ backbone of the polymer provides rigidity, makes the membrane unreactive, and increases the

**FIGURE 11.13**
Working principles of some fuel cells: EFC, enzymatic fuel cell; AFC, alkaline fuel cell; DMFC, direct methanol fuel cell; PEFC, polymer electrolyte fuel cell; PAFC, phosphoric acid fuel cell; MCFC, molten carbonate fuel cell; and SOFC, solid oxide fuel cell. (Legend of components: A, anode; E, electrolyte; PEM proton exchange membrane and C, cathode (YSZ) yttria-stabilized zirconia.)
*Source:* Sundmacher, K. Fuel Cell Engineering: Toward the Design of Efficient Electrochemical Power Plants. *Industrial Engineering Chemical Research 49* (2010): 10159–10182, fig 4.

**Types of fuel cells**



Direct methanol fuel cell

Polymer electrolyte fuel cell

Proton exchange membrane fuel cells (PEMFC)

Enzymatic fuel cell

Alkaline fuel cell

Phosphoric acid fuel cell

Molten carbonate fuel cell

Solid oxide fuel cell

Legend of components:
A = anode
E = electrolyte
C = cathode
PEM = proton exchange membrane
YSZ = yttria-stabilized zirconia

| Typical operating temperature (°C) | EFC | AFC | DMFC | PEFC | PAFC | MCFC | SOFC |
|---|---|---|---|---|---|---|---|
| | 35 | 60 | 80 | <160 | 200 | 620 | <1000 |

**FIGURE 11.14**

The optimal temperature of operation and the application potential of the different types of fuels cells is shown.

*Source:* Fuel Cell Engineering: Toward the Design of Efficient Electrochemical Power Plants. Sundermacher, K., *Industrial Engineering Chemical Research*, *49* (2010): 10159–10182, fig 5.

acidity of the terminal $SO_3^-$ groups. The positively charged $H^+$ can migrate through this network under the influence of the electrical potential gradient across the membrane that arises through the half-cell reactions. By contrast, negatively charged species in a cavity cannot migrate through the network, because they are repelled by the negatively charged $SO_3^-$ groups that are covalently bonded to long polymer chains in the narrow channels that connect adjacent cavities.

The electrochemistry of the two half-cell reactions shown in Figure 11.15 is well understood. The main challenges in manufacturing a fuel cell based on the overall reaction $H_2 + 1/2\,O_2 \rightarrow H_2O$ lie in maintaining a high cell potential at the necessary current output. A number of strategies have been pursued to improve the performance of proton exchange membrane fuel cells. Optimizing the interface between the gas diffusion element and the membrane has been the most important area of progress. The use of porous and finely divided materials allows the electrode surface area to be maximized per unit volume of the fuel cell. Careful integration of the catalyst and membrane surface also allows the amount of the expensive Pt-based catalysts to be minimized. A future goal is to develop operating conditions that do not require highly pure $H_2$. Currently, high purity is required because trace amounts (~50 ppm) of CO poison the Pt catalyst surface and render it inactive for $H_2$ dissociation. Fuel cells that operate at temperatures above 100°C are much
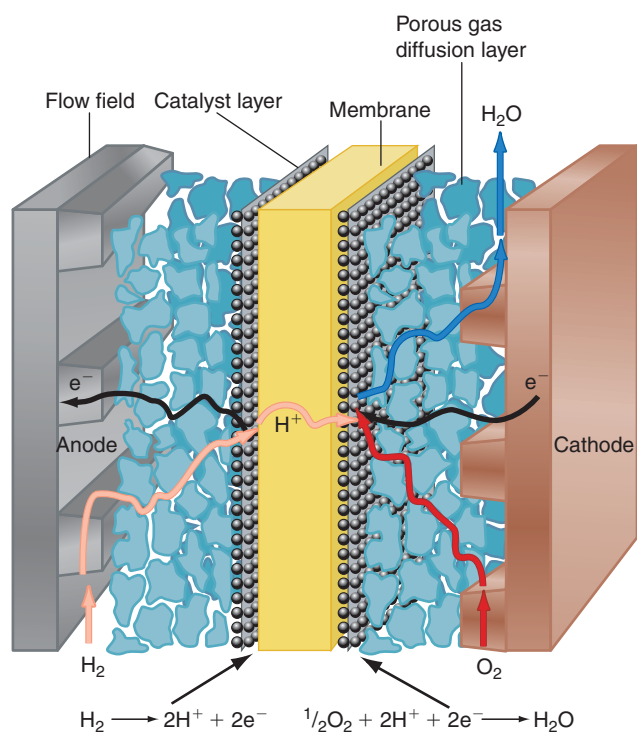
less sensitive to poisoning by CO. However, operation at these temperatures requires proton exchange membranes that use ionic liquids other than water to maintain a high conductivity.

The goals of much current research on fuel cells are to develop inexpensive catalysts not based on noble metals and using fuels other than pure hydrogen. Because gaseous $H_2$ has a low energy density per unit volume, it is not an economically useful fuel unless it is produced at the site of the fuel cell using renewable techniques. Reforming fuels such as methane to produce hydrogen or direct methanol oxidation are the most promising avenues to pursue. A recent review of the many types of fuel cells is Sundmacher, K. Fuel Cell Engineering: Toward the Design of Efficient Electrochemical Power Plants. *Industrial Engineering Chemical Research 49* (2010): 10159–10182.

SUPPLEMENTAL

# 11.14 Electrochemistry at the Atomic Scale

The half-cell reaction $Cu^{2+}(aq) + 2e^- \rightarrow Cu(s)$ only describes an overall process. What is known about this reaction at an atomic scale? In addressing this question, we draw extensively on a review article by Dieter Kolb [*Surface Science* 500 (2002), 722–740].

We first describe the structure of the interface between the solution and a metal electrode in an electrochemical cell, which is known as the electrical double layer. To a good approximation, the interface can be modeled as a parallel plate capacitor as depicted in Figure 11.16a. In this figure, the positively charged plate of the capacitor is the metal electrode, and the negative plate is made of negative ions that are surrounded by their solvation shells. The two types of negative ions at the interface are distinguished by the forces that hold them in this region. Specifically bound ions are those that form a chemical bond with one or more of the metal atoms at the surface of the electrode. Examples of specifically bound ions are

**FIGURE 11.16**

(a) The electrical double layer, showing specifically and nonspecifically adsorbed ions and water molecules, and the inner and outer Helmholtz planes. (b) Variation of the electrical potential in the electrical double layer, which has a thickness ~3 nm. The red solid line passes through the center of a nonspecifically adsorbed ion, and the dashed line passes through the center of a specifically adsorbed ion. (c) The electrochemical cell. The region that is shown greatly magnified in parts (a) and (b) is indicated.

[Kolb, D.M. "An Atomistic View of Electrochemistry." *Surface Science* 500 (2002): 722–740, Figure 1.]
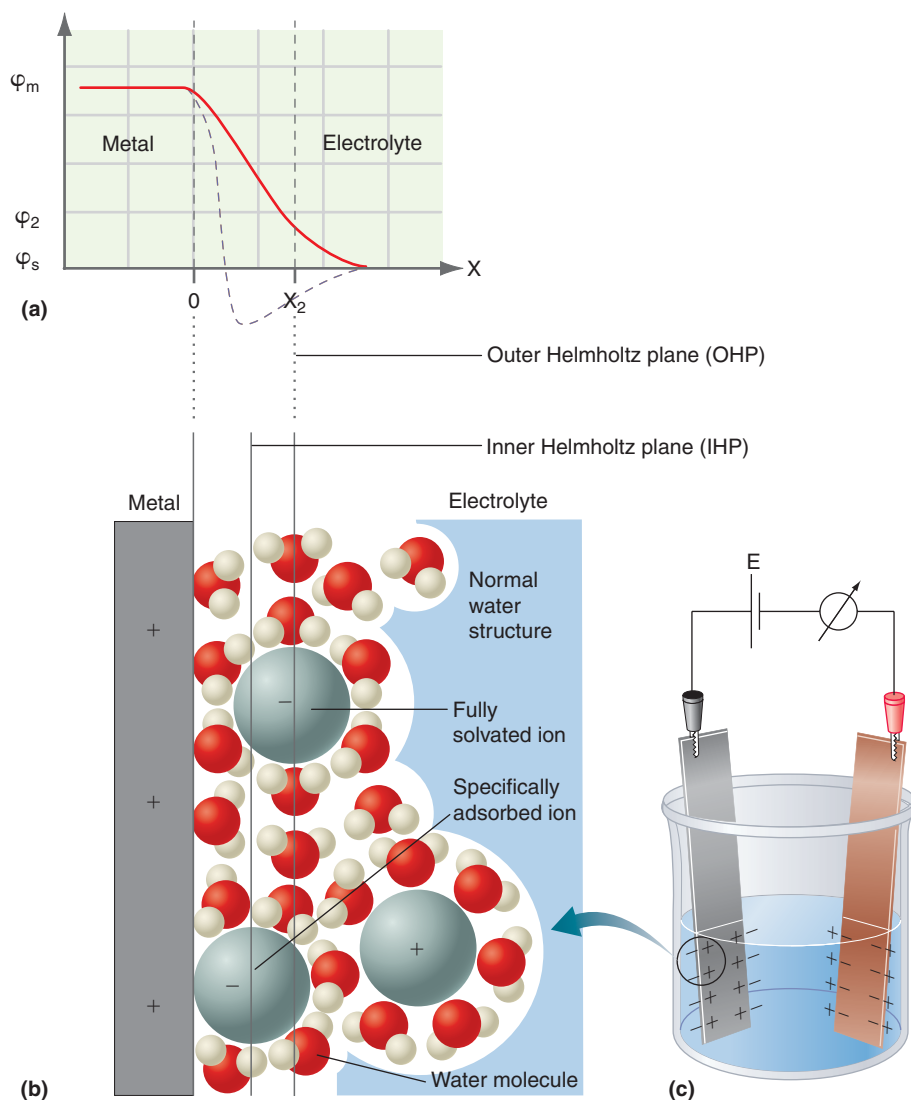


Cl⁻ and Br⁻. It is advantageous for these ions to form bonds with the surface, because the water molecules in their solvation shell are not as strongly bound as in positive ions such as $Na^+$ and $K^+$. The part of the solvation shell directed toward the electrode atoms to which the ion is bonded is missing. The plane that goes through the center of the specifically adsorbed ions is known as the inner Helmholtz plane. The second type of ion that is found close to the positively charged electrode consists of fully solvated ions, which are called nonspecifically adsorbed ions. The plane that goes through the center of the nonspecifically adsorbed ions is known as the outer Helmholtz plane. Fully solvated positive ions are found outside the electrical double layer.

As shown in Figure 11.16b, the falloff in the electrical potential between the metal electrode and the electrolyte solution occurs in a very small distance of approximately 3 nm, resulting in an electrical field in the electrical double layer as large as $3 \times 10^7 \, V \, cm^{-1}$. Because the charge that can be accommodated at the surface of the electrode by the specifically and nonspecifically adsorbed ions is on the order of 0.1–0.2 electron per atom of metal at the surface, the electrical double layer has a very large capacitance of 20–50 $\mu C \, cm^{-2}$. This property makes the metal-electrolyte interface useful in supercapacitors, which can provide energy storage at a very high energy density. For a typical difference in potential between the electrode and the solution of ~1 V, the energy stored in the interfacial capacitance can be as large as 150 kJ $kg^{-1}$. Because this density is so high, electrochemical capacitors can be used to provide backup electrical energy in the event of a power failure in electronic devices. Note in Figure 11.16b that the electrical potential has fallen to the value in the middle of the solution at a distance

of approximately 5 nm. All important aspects of an electrochemical reaction occur in this region immediately adjacent to the electrode surface.

Having described the structure of the solution adjacent to the electrode surface, what can be said about the structure of the electrode surface at an atomic scale? Much of what is known about the structure of the electrode surface at an atomic scale has been obtained using the scanning tunneling microscope (STM) discussed in Chapter 5 in Engel, *Quantum Chemistry & Spectroscopy*, and the reader is encouraged to review this material before proceeding. In an STM, a metal tip is positioned within 0.5–2 nm of a conducting surface, and at these distances, electrons can tunnel between the tip and surface. The tunneling current falls off exponentially with the tip–surface distance. Using piezoelectric elements, the tip height is varied as the tip is scanned over the surface to keep the tunneling current at a constant value, typically 1 nA. The voltage applied to the piezoelectric element normal to the surface is a direct measure of the height of the surface at a point parallel to the surface. These voltage values are used to construct a topographical map of the surface. A schematic picture of the essential elements of an STM is shown in Figure 11.17.

In an electrochemical STM, the tip is coated with an insulating material except in the immediate vicinity of the tunneling region, as illustrated in Figure 11.18, to avoid current passing from the tip to the surface through the conducting electrolyte solution.

The structure of an electrode surface in an electrochemical environment depends on the possible reactions that the electrode can undergo in the solution and the applied potential. For a material such as platinum, which is not easily oxidized, it is possible

by careful preparation to obtain an electrode that is virtually identical to what is expected from terminating the crystal structure of the electrode material. An example of this ideal case is shown in Figure 11.19a for a platinum electrode surface. The great majority of Pt atoms are in their ideal lattice positions. A much smaller number are located at the steps that form the edges of large terraces that make up the long-range structure of the surface. A detail showing the arrangement of the Pt atoms at the edge of a terrace is shown in Figure 11.19b. Although the step atoms are a small minority of the total number of surface atoms, they play a significant role in electrochemical processes, as shown later.

For the case of the platinum electrode, the surface corresponds to the most densely packed plane of the face-centered cubic lattice, which has the lowest surface energy. What is the atomic level structure of an electrode surface if the surface plane is not that of lowest surface energy? An example for this case is shown in Figure 11.20. The gold surface consists of a square array of Au atoms rather than the lowest energy close-packed layer, which has hexagonal symmetry. To minimize its energy, the topmost surface layer undergoes a reconstruction to a close-packed layer with the same structure as shown in Figure 11.19b. Because the hexagonal surface layer and the underlying square lattice do not have the same symmetry, the topmost layer of the electrode is periodically buckled.

The process in which the surface of the electrode undergoes the reconstruction described earlier can be imaged with the electrochemical STM, as shown in Figure 11.21. The light areas in this image are gold islands, around which the reconstruction must detour. Because of the square symmetry of the underlying layers, the reconstruction proceeds in two domains along two directions oriented at 90° with respect to one another. Note the defects in the reconstructed layer that arise from a meandering of a reconstructed part of a domain, defects that arise through the intersection of two domains of different orientation, as well as defects due to the Au islands present on the surface.

We now return to the influence of surface defects in electrochemical reactions. If an Au electrode is immersed in a $CuSO_4$ solution, and the potential is adjusted appropriately, Cu will be deposited on the electrode, as described by the reaction $Cu^{2+}(aq) + 2e^- \rightarrow Cu(s)$. How does the Cu layer grow on the Au surface? The answer is provided by the STM image shown in Figure 11.22. The initial stage of the Cu film is the formation of small Cu islands that are exclusively located at step edges of the underlying Au surface. This result can be understood by realizing that

10 nm × 10 nm



$E_{SCE}$ = –0.2 V
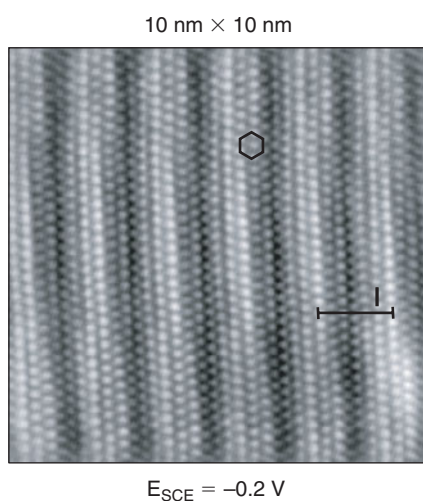
**FIGURE 11.20**

A 10-nm × 10-nm image of a well-prepared gold electrode. Each dot corresponds to an individual Au atom. The topmost layer undergoes a reconstruction to form a close-packed layer of hexagonal symmetry as indicated by the hexagon. Because this hexagonal layer is not in registry with the underlying square lattice, the surface plane is buckled with the repeat unit labeled $l$. At the bottom, $E_{SCE}$ indicates that the potential is measured relative to a standard calomel electrode, for which the half-cell reaction is
$Hg_2Cl_2(s) + 2e^- \rightarrow$
$$2 Hg(l) + 2 Cl^-(aq).$$
[Kolb, D.M. "An Atomistic View of Electrochemistry." *Surface Science* 500 (2002): 722–740, Figure 6.]
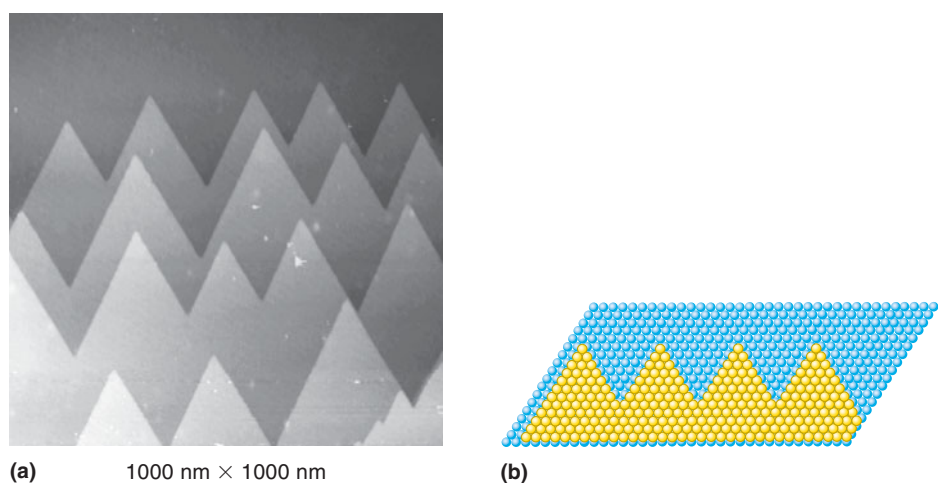


**(a)**    1000 nm × 1000 nm    **(b)**

**FIGURE 11.19**

(a) A 1000-nm × 1000-nm STM image of a well-prepared platinum electrode exposing a close-packed layer of Pt atoms in the surface. The image shows several stacked terraces, which differ in height by one atomic layer. (b) Ball model showing the atomic layer structure underlying the image of part (a). Only step edges in which the step edge of a terrace consists of a close-packed row of atoms is observed in part (a). Note the lateral offset in successively higher terraces, which are characteristic of the stacking in planes of a face-centered cubic lattice.

[Part (a) Kolb, D.M. "An Atomistic View of Electrochemistry." *Surface Science* 500 (2002): 722–740, Figure 3.]

80 nm × 80 nm

14 nm × 14 nm



$E_{SCE} = -250$ mV
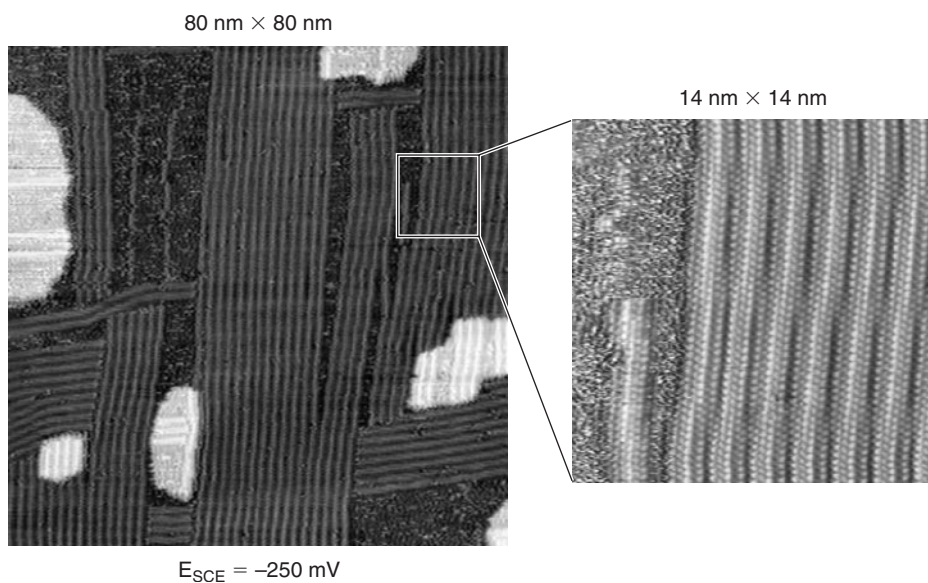
**FIGURE 11.21**

STM images of a gold electrode in which the reconstruction of the topmost layer is not complete. The light areas are higher-lying Au islands. Note that the reconstruction proceeds along two perpendicular directions. This occurs because the underlying lattice structure has square symmetry. [Kolb, D.M. "An Atomistic View of Electrochemistry." *Surface Science* 500 (2002): 722–740, Figure 7.]

the coordination number of a Cu atom at a gold site at the step edge is larger than on a flat portion of the surface. As more copper is deposited, the initially formed islands grow laterally and eventually merge to form a uniform layer.

Several important conclusions can be made concerning the growth of an electrochemically deposited metal film from these studies. The fact that island growth is observed rather than random deposition of Cu atoms indicates that the initially adsorbed Cu atoms have a high mobility parallel to the surface. They diffuse across a limited region of the surface until they encounter the edge of an island. Because these edge sites have a higher coordination number than a site on the terrace, they are strongly bound and diffuse no further. The other conclusion that can be drawn is that the metal film grows one layer at a time. A second layer is not nucleated until the underlying layer is nearly completed. Layer-by-layer growth ensures that a compact and crystalline film is formed.

As the deposition of Cu on a gold electrode shows, step edges play a central role in determining the formation of electrochemically deposited layers. Although small in number, surface defects such as step edges or vacancies play a major role in the chemistry of a wide range of chemical processes including catalytic cracking of crude oil and the corrosion of metals.

Electrochemical scanning tunneling microscopy has also provided new insight into the atomic level processes underlying the electrochemical dissolution of a metal electrode. To carry out these studies, an STM was constructed that allowed 25 images to be obtained per second. A comparison of images obtained at closely spaced times allows researchers to follow the ongoing processes [Magnussen O. et al. *Electrochimica Acta* 46 (2001):3725–3733]. A mode of growth was observed in which individual atoms were added to a single row at the edge of a terrace as shown in Figure 11.23.



← Scan direction

170 nm × 170 nm
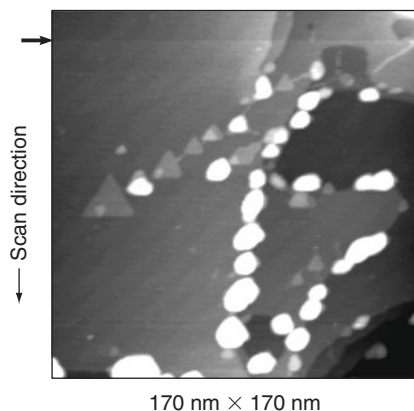
**FIGURE 11.22**

Image of a gold electrode in which a small amount of copper has been electrochemically deposited. Note that the Cu is deposited in the form of small islands that are anchored at step edges of the underlying gold electrode. The onset of the deposition is initiated by the horizontal arrow in the figure. At that point, the electrode potential was increased to a value that allows the reaction $Cu^{2+}(aq) + 2e^- \rightarrow Cu(s)$ to proceed. [Kolb, D.M. Engelmann, G.E., Ziegler, J.C. "On the Unusual Electochemical Stability of Nanofabricated Copper Clusters." *Angewandte Chemie International Edition* 39 (2000): 1123–1125.]

**FIGURE 11.23**

A series of images taken at the indicated time intervals is shown as Cu is deposited electrochemically on a copper electrode. Note that an individual row at the edge of the upper terrace grows from the top to the bottom of the image.

[Photo courtesy of R. J. Behm, University of Ulm. Magnussen et al., "In-Situ Atomic-Scale Studies of the Mechanisms and Dynamics of Metal STM." *Electrochemica Acta* 46 (2001): 3725–3733, Figure 1.]
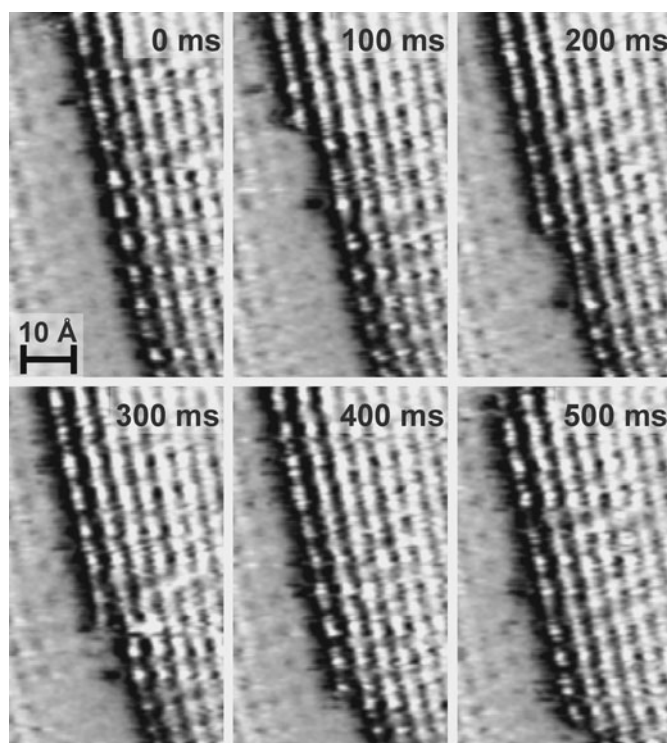


**FIGURE 11.24**

The arrows indicate examples of a concerted removal of whole or multiple steps for a copper electrode: (a) dissolution and (b) growth. The times at which the images were acquired relative to the first image are shown.

[Photo courtesy of R. J. Behm, University of Ulm. Magnussen et al., "In-Situ Atomic-Scale Studies of the Mechanisms and Dynamics of Metal STM." *Electrochemica Acta* 46 (2001); 3725–3733, Figure 2.]



(a)    (b)
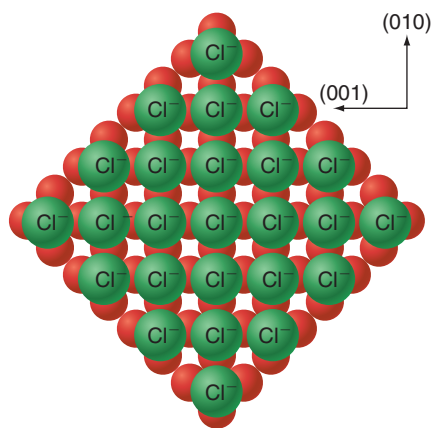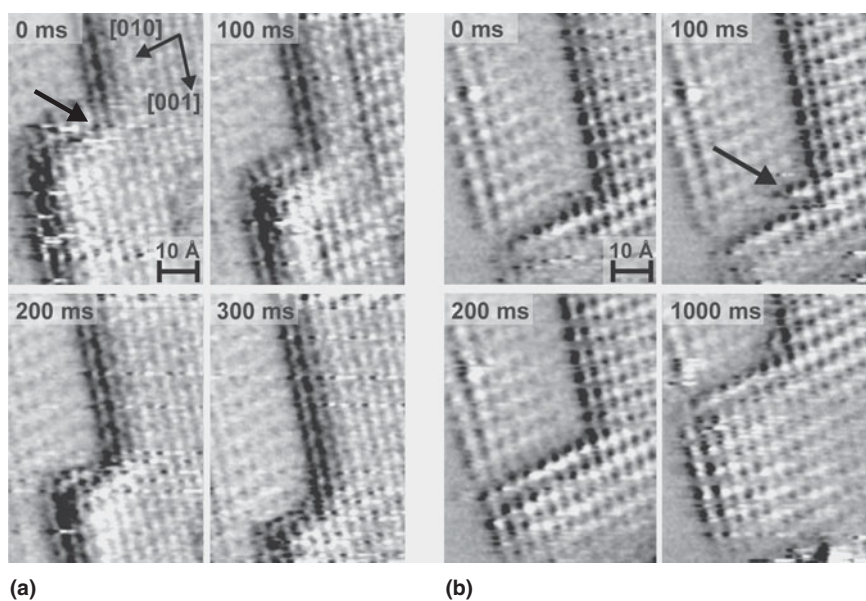


**FIGURE 11.25**

Because they are larger, the $Cl^-$ ions cannot form the same structure as the underlying Cu surface. Instead, they form a square lattice that is rotated by 45° with respect to the copper unit cell.

However, a second mode of growth and dissolution is observed in which entire segments of a row can grow or dissolve collectively. By adjusting the electrode potential slightly, either Cu growth or dissolution can be initiated. Figure 11.24a shows a sequence of images for electrode dissolution, and Figure 11.24b shows a sequence for Cu deposition on the electrode. In both cases, entire rows or row segments are deposited at once rather than in the atom-by-atom fashion depicted in Figure 11.23.

The Cu electrode has a square symmetry in this case, and one might assume that growth and dissolution occur with equal probability in either of two directions oriented 90° to one another. However, the images in Figure 11.24 indicate that this is not the case. Growth or dissolution occurs only in the crystallographic direction labeled (001) and not along the direction labeled (010). This behavior is a consequence of the atomic level structure of the $Cl^-$ specifically adsorbed ions of the HCl electrolyte. This structure is shown in Figure 11.25, and consists of a square lattice that has a larger unit cell length than the underlying Cu lattice and is rotated 45° with respect to the Cu lattice.

The adsorbed $Cl^-$ layer removes the equivalence of the (010) and (001) directions as is shown in Figure 11.26. The kinks formed along step edges along these two directions have a different structure. Therefore, they are expected to have a different reactivity in the dissolution/process. As these experiments show, specifically adsorbed ions play a central role in an electrochemical reaction.

The ability to verify that an electrode is both crystalline and has a low defect density using STM has made the interpretation of experimental results obtained through classical electrochemical techniques significantly easier. An example is cyclic voltammetry, in which the electrode potential is varied linearly with time and then the potential is changed in the opposite direction and returned to the initial value. As the potential is varied, the electrode current is measured. Because the area in a plot of current versus time is the electrical charge, cyclic voltammetry provides a way to identify regions of potential in which significant amounts of charge are transferred to or from the electrode. These are the regions in which electrochemical reactions proceed. An example of a cyclic voltammogram for the deposition of less than one monolayer of Cu on a gold electrode is shown in Figure 11.27.

STM studies show that Cu can form a low-density ordered structure on the surface that has a saturated coverage of 0.67 monolayer, and a monolayer structure that has the same structure as the underlying Au electrode. Metal deposition begins to occur at a potential of 0.4 V and the surface is fully covered as the potential is lowered to 0 V. Deposition corresponds to a positive current in Figure 11.27 (the scan direction is from right to left in the figure), and dissolution corresponds to a negative current (left to right in the figure). Two well-defined peaks are observed in both the growth and dissolution directions. The emf associated with these peaks can be used to calculate the $\Delta G_f^\circ$ associated with the formation of a chemically bonded Cu atom at the site on the Au surface characteristic of the different geometries of the two ordered Cu phases. Both of these peaks occur at a potential less than that needed to deposit copper on a copper electrode, because Cu atoms are more strongly bound to surface sites on the Au surface than on the copper surface. One refers to underpotential deposition to emphasize that the potential is less than that expected for a material deposited on its own lattice. The combination of a structural determination at the atomic level provided by STM with the *I–V* relation provided by cyclic voltammetry is well suited to understanding electrochemical processes at surfaces.



Growth or dissolution occurs only in this direction

(010)
(001)
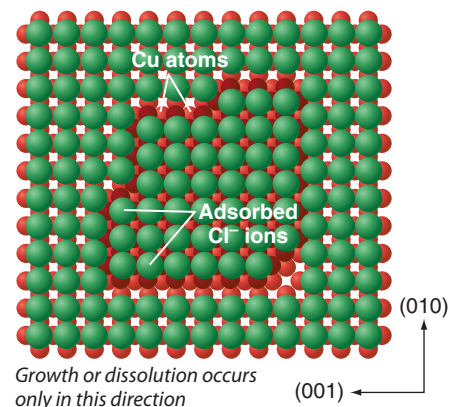
**FIGURE 11.26**

The kinks formed in step edges along the (010) and (001) directions have a different structure. This explains the different reactivity observed along these directions as shown in Figure 11.24. The small light and dark red spheres denote Cu atoms, and the large green spheres denote specifically adsorbed $Cl^-$ ions.

*Source:* Reprinted from O.M. Magnussen et al., "In-Situ Atomic-Scale Studies of the Mechanisms and Dynamics of Metal STM," *Electrochimica Acta* 46: 3725–3733 (2001). Copyright 2001, with permission from Elsevier.
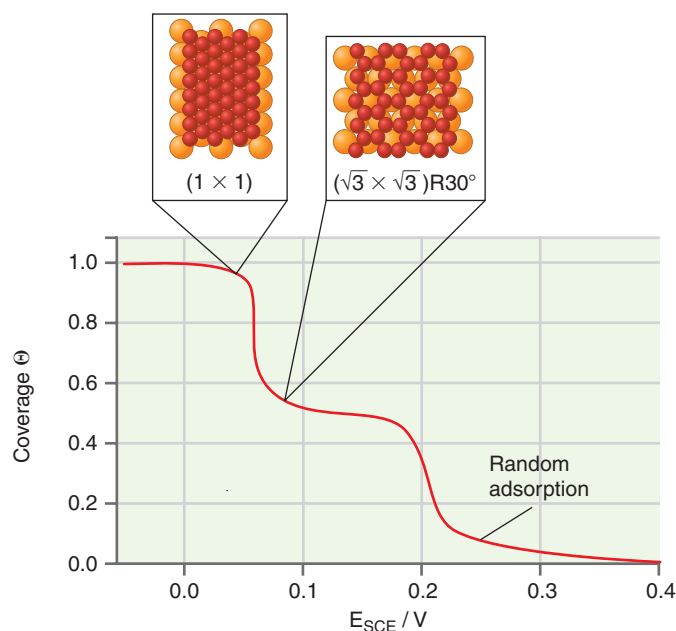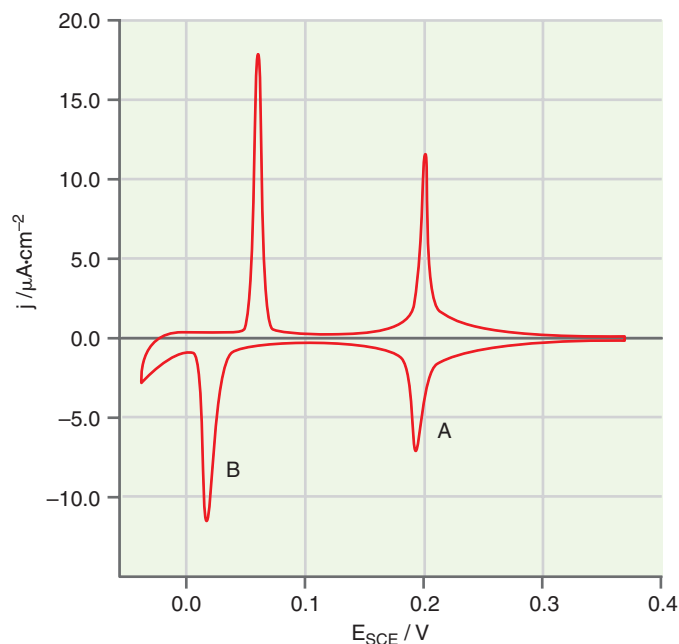


**FIGURE 11.27**

(a) A cyclic voltammogram is shown for the deposition/dissolution of Cu on a well-ordered single-crystal gold electrode. By measuring the area under the peaks, the total amount of Cu deposited or dissolved can be determined. This result is plotted in part (b). The amount by which peaks A and B are displaced in voltage in the dissolution process from their values in the deposition process is a measure of the rate of electron transfer in the processes. Cu and Au atoms are colored red and orange, respectively.

[Kolb, D.M. "An Atomistic View of Electrochemistry." *Surface Science* 500 (2002): 722–740, Figure 11.]

# 11.15 Using Electrochemistry for Nanoscale Machining

Many current technologies require fabrication of miniature devices with dimensional control in the micron to nanometer scale. For example, lithographic methods are used to make the masks employed in the fabrication of integrated circuits. Until recently, electrochemical machining techniques have not been able to provide dimensional control better than 10 $\mu$m for a reason related to the capacitance of the electrical double layer. If the external voltage is changed in an electrochemical cell, how long does it take for the cell to reach equilibrium with respect to the potential distribution? As discussed in the previous section, the electrical double region can be modeled as a large capacitor that must be charged up to the value of the new potential as the external voltage is changed. The current must flow through the electrolyte solution, which has an ohmic resistance, and the cell can be modeled as a series $R$-$C$ circuit with $R$ equal to the electrical resistance of the solution, and $C$ equal to the capacitance of the electrical double layer.

If a metal tool is placed very close to an electrode, the resistance associated with a current path between the tool and the electrode depends on the path, as shown in Figure 11.28. Those paths immediately below the tool correspond to those of smallest electrical resistance. It can be shown that the time-dependent voltage across the capacitor in an $R$-$C$ series circuit is given by

$$V(t) = V_0\left(1 - e^{-t/RC}\right) \qquad \textbf{(11.65)}$$

The rate at which $V/V_0$ increases for a point on the surface directly below the tool and a point well to one side of the tool is shown in Figure 11.29. Below the tool, the potential is built up to its full value at much shorter times than outside of this region. Until the potential is built up to the value required for an electrochemical reaction of interest, the reaction will not proceed. Rolf Schuster and coworkers [*Electrochimica Acta* 48 (2003), 20] have used this fact to supply the external voltage in the form of a short pulse, rather than as a dc voltage. As a consequence, the reaction of interest occurs directly under the tool, and only to a negligible extent outside of this region. For example, if the dissolution reaction in which material is
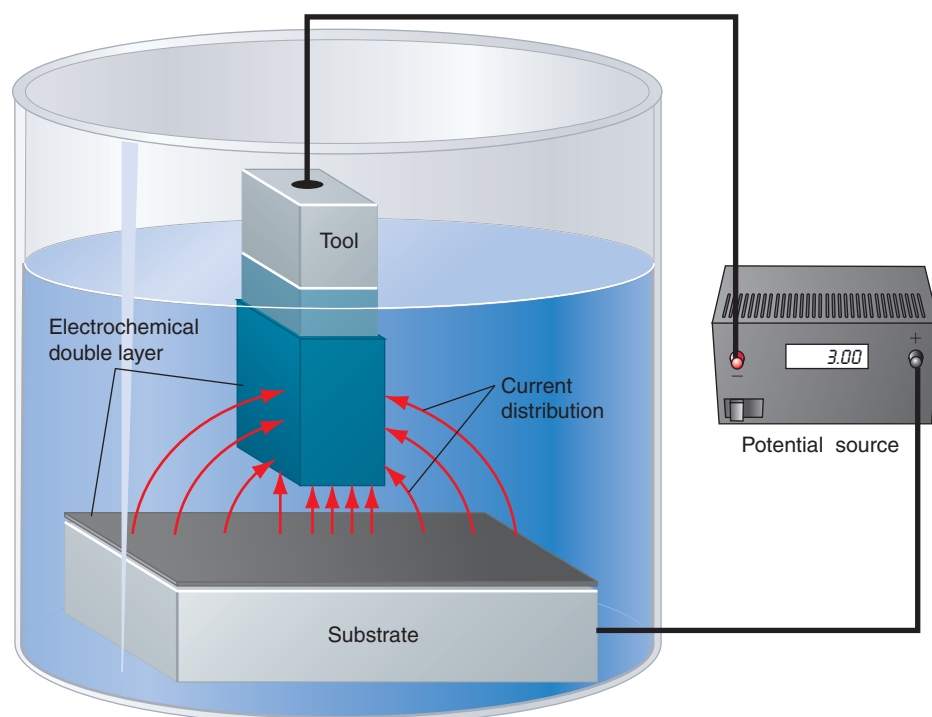
**FIGURE 11.28**

Possible current paths between a tool and an electrode immersed in an electrolyte solution. Before a reaction can proceed, the capacitance of the electrical double layer must be built up to its full value.

*Source:* Reprinted with permission from A.L. Trimmer et al., "Single-Step Electochemical Machining of Complex Nanostructures with Ultrashort Voltage Pulses," *Applied Physics Letters* 82 (19): 3327 (2003). Copyright 2003 American Institute of Physics.

removed from the work piece only takes place at potentials higher than that indicated by the horizontal bar in Figure 11.29, it will only take place under the tool for a short enough pulse. Note that if a dc potential is applied instead of a pulse, the reaction will not be localized.

Examples of the patterns that have been generated in this way by metal dissolution are shown in Figure 11.30. A resolution of ~20 nm has been obtained by using pulses of 200-ps duration.

**SUPPLEMENTAL**

# 11.16 Absolute Half-Cell Potentials

The cell potentials listed in Tables 11.1 and 11.2 (see Appendix A, Data Tables) are all measured relative to the standard hydrogen electrode. Because an electrochemical cell consists of two half-cells, any common reference for the half-cell potentials cancels when calculating the cell potential. For this reason, equilibrium constants, activity coefficients, and the direction of spontaneous change can all be determined without absolute half-cell potentials. However, there is no reason why a half-cell potential cannot be determined in principle. The difficulty is in devising an appropriate experiment to measure this quantity. Recall that putting one lead of a voltmeter on the electrode and the second lead in the solution will not give the half-cell potential as discussed in Section 11.1. Although not necessary for discussing electrochemical reactions, absolute half-cell potentials are useful in formulating a microscopic model of electrochemical processes. For example, absolute values for half-cell potentials allow the solvation Gibbs energy of the ion involved in the redox reaction to be calculated directly, rather than to rely on a calculation as outlined in Section 10.2. We next describe a method for the determination of half-cell potentials that was formulated by R. Gomer and G. Tryson [*J. Chem. Phys.* 66 (1977), 4413–4424]. The following discussion assumes familiarity with the particle in a box model of the conduction electrons in a metal (see Chapters 4 and 5 in Engel, *Quantum Chemistry & Spectroscopy*).

Consider the electrochemical cell shown schematically in Figure 11.31. The conduction electrons in each metal electrode are described using the particle in a box model, and all energy levels up to the highest occupied level, called the Fermi level, are filled. The vertical distance corresponds to energy for a negative test charge, and the horizontal axis corresponds to distance. The double layer acts as a capacitor and shifts the potential
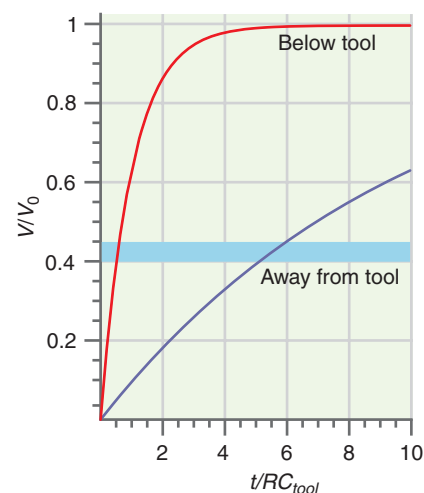


**FIGURE 11.29**
The ratio $V/V_0$ is shown as a function of $t/RC_{tool}$ for a point immediately below the tool, and away from the tool at a point where the resistance along the path is higher by a factor of 10.
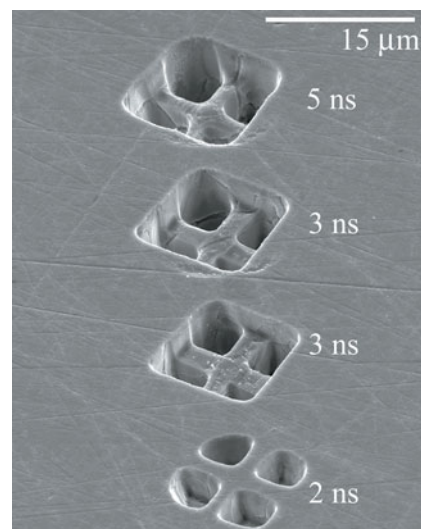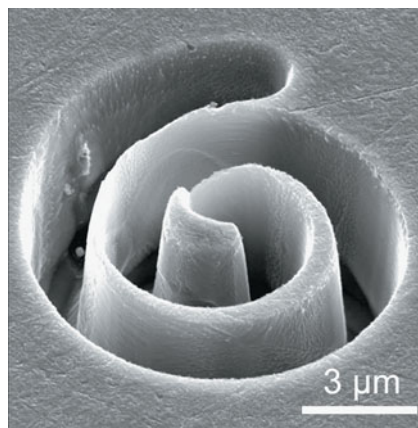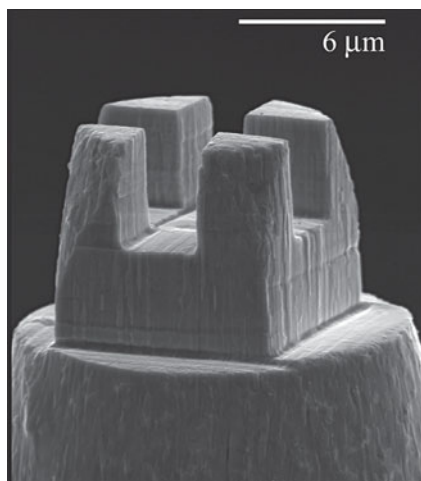


**FIGURE 11.30**
Results obtained using electrochemical machining of nickel in an HCl solution using the tool shown in the left image. Note the dependence of the resolution on pulse length in the middle image.
[Left and middle images reprinted with permission from Trimmer A.L. et al. *Applied Physics Letters* 82 (2003):3327–3329; right image reprinted with permission from Kock, M. et al. *Electrochemica Acta 4*8, 20–22, 2003:3213–3219.]

**FIGURE 11.31**
An energy diagram for a cell. The energies associated with differences in electrical potential are shown as a product of the test charge (negative in this case) and the potential difference. The vertical bar in the center indicates a salt bridge junction. The decrease in energy on the solution side of each electrode is due to the electrical double layer.
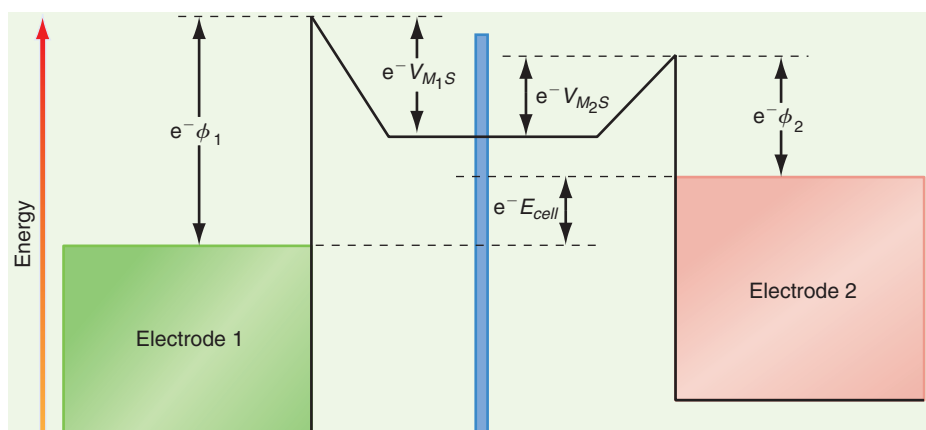


in the solution relative to the Fermi level by the amount $e^-V_{M_1S}$ or $e^-V_{M_2S}$ as shown in Figure 11.31. The change in potential within the double layer is depicted as being linear rather than as shown correctly in Figure 11.14. To remove an electron from the metal, it is necessary to give an electron at the Fermi level an amount of energy equal to the work function $\phi$. The **work function** of a metal is analogous to the ionization energy of an atom, and different metals have different values of the work function. Because of the presence of the double layer at each electrode, a negatively charged ion or an electron has a lower energy in the bulk of the solution than at the surface of an electrode.

How do the two half-cells line up in an energy diagram? This question can be answered by recognizing that the electrochemical potential of an electron in a metal is the Fermi energy. If two metals are placed in contact, electrons flow from one metal to the other until the electrochemical potential of an electron is the same in each metal. This is equivalent to saying that the Fermi levels of the two electrodes lie at the same energy. The equilibrium

$$M^{n+}(aq) + ne^- \rightarrow M(s) \tag{11.66}$$

that is established separately in each half-cell determines the drop in electrical potential across the double layer and thereby shifts the Fermi level of each metal electrode relative to the energy of the bulk solution. Therefore, the Fermi levels of the two electrodes are exactly offset by the Gibbs energy:

$$\Delta G = -e^- E_{cell} \tag{11.67}$$

How can an absolute half-cell potential be defined that is consistent with the energy diagram in Figure 11.31? To answer this question, the reversible work and, therefore, the Gibbs energy associated with the half-cell reaction $M^{n+}(aq) + ne^- \rightarrow M(s)$ is calculated. For simplicity, it is assumed that $n = 1$. Because $G$ is a state function, any convenient path between the initial states of the metal atom in the solid and the final state of the ion in the bulk solution and the electron at the Fermi level of the electrode can be chosen. Breaking this overall process down into the individual steps shown in the following equations simplifies the analysis. The $\Delta G$ associated with each step is indicated.

$$M_1(s) \rightarrow M_1(g) \qquad\qquad \Delta G = \Delta G_{vaporization} \tag{11.68}$$

$$M_1(g) \rightarrow M_1^+(g) + e^-(M_1) \qquad\qquad \Delta G = e^-(I_1 - \phi_1) \tag{11.69}$$

$$M_1^+(g) \rightarrow M_1^+ (aq, \text{ at } M_1) \qquad\qquad \Delta G = \Delta G_{solvation} \tag{11.70}$$

$$M_1^+(aq, \text{ at } M_1) \rightarrow M_1^+(aq, \text{ bulk solution}) \qquad \Delta G = e^-V_{M_1S} \tag{11.71}$$
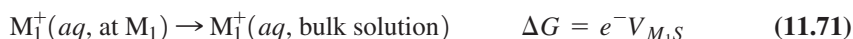
Note that in the final step, the solvated ion at the electrode is transferred through the double layer into the solution. The overall process is

$M_1(s) \rightarrow M_1^+(aq, \text{ bulk solution}) + e^-(M_1)$, and the $\Delta G$ for the overall process is

$$\Delta G_1 = \Delta G_{vaporization, 1} + e^-(I_1 - \phi_1) + \Delta G_{solvation, 1} + e^-V_{M_1S} \tag{11.72}$$
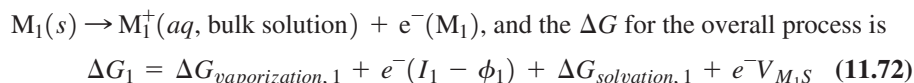
The analogous equation for electrode 2 is

$$\Delta G_2 = \Delta G_{vaporization, 2} + e^-(I_2 - \phi_2) + \Delta G_{solvation, 2} + e^-V_{M_2S} \tag{11.73}$$

If the two half-cells are in equilibrium, $\Delta G_1 = \Delta G_2$ and

$$(\Delta G_{vaporization,1} - \Delta G_{vaporization,2}) + (\Delta G_{solvation,1} - \Delta G_{solvation,2}) + e^-(I_1 - I_2)$$
$$= e^-(V_{M_2S} - \phi_2) - e^-(V_{M_1S} - \phi_1) = e^- E_{cell} \qquad (11.74)$$

Equating $e^-(V_{M_1S} - \phi_1) - e^-(V_{M_2S} - \phi_2)$ with $e^- E_{cell}$ follows from the energy diagram shown in Figure 11.31.

Equation (11.74) shows that a plausible definition of each of the half-cell potentials in terms of the physical parameters of the problem is given by

$$E_1 = V_{M_1S} - \phi_1 \quad \text{and} \quad E_2 = V_{M_2S} - \phi_2 \qquad (11.75)$$

Note that the half-cell potential is not the difference in the electrical potential between the electrode and the bulk solution. Only if the potential is defined in this way will $E = E_1 + E_2$, as can be seen in Figure 11.31.

Although Equation (11.75) defines an absolute half-cell potential, numerical values for the half-cell can only be determined if $V_{MS}$ and $\phi$ are known. Note that the work function in Equation (11.75) is not the work function in air or in vacuum, but the work function in solution. The value of $\phi$ will vary for these different environments because of molecular layers absorbed on the metal surface. As discussed in Section 11.2, $V_{MS}$ cannot be measured directly using a voltmeter and a probe inserted in the solution. However, $V_{MS}$ can be measured without contacting the solution using the experimental setup shown schematically in Figure 11.32.

The electrode of interest is immersed in the electrolyte solution. A reference electrode (in this case gold) in the form of a flat plate is oriented parallel to the surface of the electrolyte solution. Gold is chosen because the work function in air is known. The Au and metal electrodes are connected by a metal wire, and a variable dc voltage source is inserted in the wire. The gold electrode is mounted in such a way that its distance to the electrolyte surface can be varied in a periodic fashion. The energy diagram shown in Figure 11.33 is used to understand how the experimental setup can be used to measure $V_{MS}$. By connecting the electrode in the solution with the gold electrode in air, their Fermi levels are equalized as shown in Figure 11.33a. Note that there is no double-layer potential on the electrode in air. The difference in the electrical potential of the gold electrode and the surface of the electrolyte surface is designated as $V_{M_2Au}$.

Because of the connecting wire shown in Figure 11.32, the Au electrode and the electrochemical double layer of the immersed electrode form a capacitor that charges up because of the potential difference between the two plates that arises through equalizations of the Fermi levels in the electrodes. First consider the case in which the adjustable voltage in Figure 11.32 is set equal to zero. The potential difference between the surface of the electrolyte and the parallel gold electrode is shown in Figure 11.33a. As the Au plate is vibrated, the capacitance changes and, therefore, an alternating current flows in the external circuit as the capacitor is alternately charged and discharged. Next carefully adjust the variable voltage in the wire as the Au electrode vibrates until no current can be detected in the external circuit. If no current flows, the voltage difference between the Au electrode and the electrolyte surface must be equal to zero. This case corresponds to the energy diagram of Figure 11.33b. The null current must correspond to the condition

$$\Delta V = V_{M_2Au} \qquad (11.76)$$

Note that in this experiment, $V_{M_2Au}$ can be determined experimentally without inserting a probe into the liquid. Because $\phi_{Au}$ is known, $E_2 = V_{M_2Au} - \phi_{Au}$ can be calculated, and therefore the absolute half-cell potential can be determined.

Using this method, Gomer and Tryson first determined the absolute half-cell potential of the standard hydrogen electrode. More recent measurements use the more reliable value of the work function of the Hg surface of 4.50 eV to obtain the value $E_{SHE}^\circ = -4.44 \pm 0.02$ V [S. Trassatti, Pure & Applied Chemistry, 58 (1986) 955]. The absolute half-cell potentials of all other half-cell potentials can be determined by adding $-4.44$ to the values in Tables 11.1 and 11.2 (see Appendix A, Data Tables).
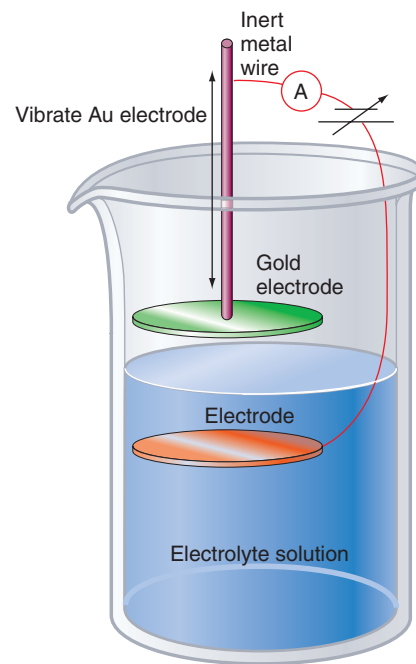


**FIGURE 11.32**
Apparatus used to determine absolute half-cell potentials.
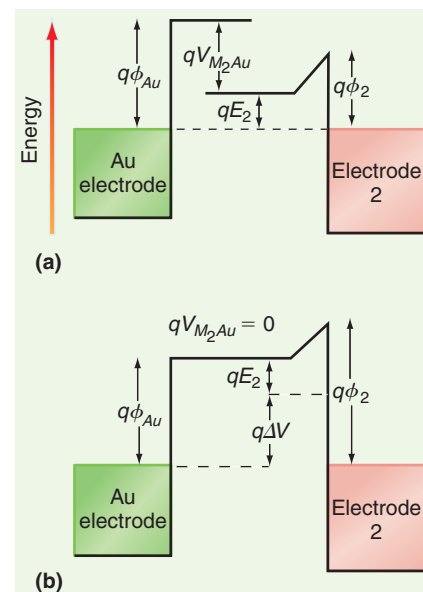


**FIGURE 11.33**
These energy diagrams are used to explain how the absolute half-cell potential can be determined using the experiment illustrated in Figure 11.32. (a) The variable voltage in series with the wire is set equal to zero. (b) The variable voltage is adjusted so that the current flow in the external circuit is equal to zero.

Once the absolute half-cell potential is known, the important (and otherwise experimentally inaccessible) quantity $\Delta G_{solvation}$ can be calculated. From Equations (11.68) through (11.71), the relation between the half-cell potential and the energetic parameters in these equations is

$$E_{half\text{-}cell} = -\frac{1}{e^-}(\Delta G_{vaporization} + \Delta G_{solvation} + Ie^-) \qquad \textbf{(11.77)}$$

This equation allows $\Delta G_{solvation}$ of an individual ion to be determined from the appropriate half-cell potential. The solvation Gibbs energy calculated in this way is in good agreement with the values calculated from the Born model if the ionic radii obtained from crystal structures are corrected for the water of solvation as discussed in Section 10.2.

# Vocabulary

| | | |
|---|---|---|
| anode | electrochemical series | proton exchange membrane fuel cell |
| battery | electromotive force (emf) | (PEMFC) |
| cathode | Faraday constant | reference electrode |
| charged | fuel cell | salt bridge |
| Daniell cell | junction potential | work function |
| electrochemical cell | Nernst equation | |
| electrochemical potential | neutral | |

# Conceptual Problems

**Q11.1**  To determine standard cell potentials, measurements are carried out in very dilute solutions rather than at unit activity. Why is this the case?

**Q11.2**  Show that if $\Delta G_f^\circ(H^+, aq) = 0$ for all $T$, the potential of the standard hydrogen electrode is zero.

**Q11.3**  How is it possible to deposit Cu on an Au electrode at a potential lower than that corresponding to the reaction $Cu^{2+}(aq) + 2e^- \rightarrow Cu(s)$?

**Q11.4**  Explain why the magnitude of the maximum work available from a battery can be greater than the magnitude of the reaction enthalpy of the overall cell reaction.

**Q11.5**  How can one conclude from Figure 11.22 that Cu atoms can diffuse rapidly over a well-ordered Au electrode in an electrochemical cell?

**Q11.6**  The temperature dependence of the potential of a cell is vanishingly small. What does this tell you about the thermodynamics of the cell reaction?

**Q11.7**  Why is the capacitance of an electrolytic capacitor so high compared with conventional capacitors of similar size?

**Q11.8**  What is the difference in the chemical potential and the electrochemical potential for an ion and for a neutral species in solution? Under what conditions is the electrochemical potential equal to the chemical potential for an ion?

**Q11.9**  Why is it possible to achieve high-resolution electrochemical machining by applying a voltage pulse rather than a dc voltage to the electrode being machined?

**Q11.10**  Can specifically adsorbed ions in the electrochemical double layer influence electrode reactions?

**Q11.11**  Why is it not necessary to know absolute half-cell potentials to determine the emf of an electrochemical cell?

**Q11.12**  What is the voltage between the terminals of a battery in which the contents are in chemical equilibrium?

**Q11.13**  By convention, the anode of a battery is where oxidation takes place. Is this true when the battery is charged, discharged, or both?

**Q11.14**  You wish to maximize the emf of an electrochemical cell. To do so, should the concentrations of the products in the overall reaction be high or low relative to those of the reactants? Explain your answer.

**Q11.15**  If you double all the coefficients in the overall chemical reaction in an electrochemical cell, the equilibrium constant changes. Does the emf change? Explain your answer.

**Q11.16**  Why can batteries only be recharged a limited number of times?

**Q11.17**  Why can more work be extracted from a fuel cell than a combustion engine for the same overall reaction?

**Q11.18**  What is the function of a salt bridge in an electrochemical cell?

**Q11.19**  How does the emf of an electrochemical cell change if you increase the temperature?

**Q11.20**  What thermodynamic quantity that cannot be measured directly can be calculated from absolute half-cell potentials?

# Numerical Problems

Problem numbers in **red** indicate that the solution to the problem is given in the *Student's Solutions Manual*.

**P11.1**   You are given the following half-cell reactions:

$$Pd^{2+}(aq) + 2e^- \rightarrow Pd(s) \qquad\qquad E^° = 0.83 \text{ V}$$

$$PdCl_4^{2-}(aq) + 2e^- \rightarrow Pd(s) + 4\,Cl^-(aq) \qquad E^° = 0.64 \text{ V}$$

**a.** Calculate the equilibrium constant for the reaction

$$Pd^{2+}(aq) + 4\,Cl^-(aq) \rightleftharpoons PdCl_4^{2-}(aq)$$
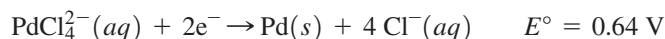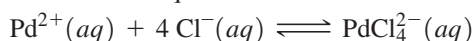
**b.** Calculate $\Delta G^°$ for this reaction.

**P11.2**   For the half-cell reaction $AgBr(s) + e^- \rightarrow Ag(s) + Br^-(aq)$, $E^° = +0.0713$ V. Using this result and $\Delta G_f^°(AgBr, s) = -96.9$ kJ mol$^{-1}$, determine $\Delta G_f^°$ (Br$^-$, aq).

**P11.3**   For the half-cell reaction $Hg_2Cl_2(s) + 2e^- \rightarrow 2Hg(l) + 2Cl^-(aq)$, $E^° = +0.26808$ V. Using this result and $\Delta G_f^°(Hg_2Cl_2, s) = -210.7$ kJ mol$^{-1}$, determine $\Delta G_f^°$ (Cl$^-$, aq ).

**P11.4**   Determine the half-cell reactions and the overall cell reaction, calculate the cell potential, and determine the equilibrium constant at 298.15 K for the cell

$$Cd^{2+}(aq, a_{Cd^{2+}} = 0.150)|Cd(s)$$
$$|Cl^-(aq, a_{Cl^-} = 0.0100)|Ag(s)|AgCl(s)$$
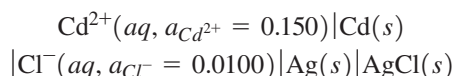
Is the cell reaction spontaneous as written?

**P11.5**   The standard half-cell potential for the reaction $O_2(g) + 4\,H^+(aq) + 4e^- \rightarrow 2\,H_2O(l)$ is $+1.229$ V at 298.15 K. Calculate $E$ for a 0.300-molal solution of $H_2SO_4$ for $a_{O_2} = 1.00$ (a) assuming that the $a_{H^+}$ is equal to the molality and (b) using the measured mean ionic activity coefficient for this concentration from the data tables. How large is the relative error if the concentrations, rather than the activities, are used?

**P11.6**   Determine the half-cell reactions and the overall cell reaction, calculate the cell potential, and determine the equilibrium constant at 298.15 K for the cell

$$H_2(g)|Pt(s)\ |H^+(aq, a_{H^+} = 0.250)|Cu^{2+}$$
$$(aq, a_{Cu^{2+}} = 0.100)|Cu(s)$$
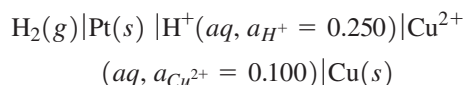
Is the cell reaction spontaneous as written?

**P11.7**   Consider the Daniell cell for the indicated molalities: $Zn(s)|ZnSO_4(aq, 0.200\ m)||CuSO_4\ (aq, 0.400\ m)|Cu(s)$. The activity coefficient $\gamma_\pm$ for the indicated concentrations can be found in the data tables. Calculate $E$ by a) setting the activity equal to the molality and b) by using the correct values for $\gamma_\pm$. How large is the relative error if the concentrations, rather than the activities, are used?

**P11.8**   Determine the half-cell reactions and the overall cell reaction, calculate the cell potential, and determine the equilibrium constant at 298.15 K for the cell

$$Zn(s)|Zn^{2+}(aq, a_\pm = 0.0120)|$$
$$|Mn^{3+}(aq, a_\pm = 0.200), Mn^{2+}(aq, a_\pm = 0.0250)\ |Pt(s)$$
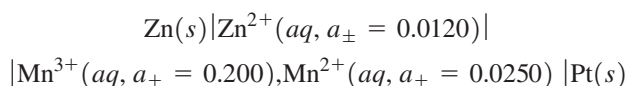
Is the cell reaction spontaneous as written?

**P11.9**   Consider the half-cell reaction $AgCl(s) + e^- \rightarrow Ag(s) + Cl^-(aq)$. If $\mu^°(AgCl, s) = -109.71$ kJ mol$^{-1}$, and if $E^° = +0.222$ V for this half-cell, calculate the standard Gibbs energy of formation of $Cl^-(aq)$.

**P11.10**   For a given overall cell reaction, $\Delta S_R^° = 16.5$ J mol$^{-1}$K$^{-1}$ and $\Delta H_R^° = -270.0$ kJ mol$^{-1}$. Calculate $E^°$ and $(\partial E^°/\partial T)_P$. Assume that $n = 2$.

**P11.11**   Consider the cell $Fe(s)|FeSO_4(aq, a_\pm = 0.0250)$ $|Hg_2SO_4(s)|Hg(l)$.

**a.** Write the cell reaction.

**b.** Calculate the cell potential, the equilibrium constant for the cell reaction, and $\Delta G_R^°$ at 25°C.

**P11.12**   Between 0° and 90°C, the potential of the cell $Pt(s)|H_2(g, f = 1.00\ \text{atm})|HCl(aq, m = 0.100)|AgCl(s)|$ $Ag(s)$ is described by the equation $E(V) = 0.35510 - 0.3422 \times 10^{-4}\, t - 3.2347 \times 10^{-6}\, t^2 + 6.314 \times 10^{-9}\, t^3$, where $t$ is the temperature on the Celsius scale. Write the cell reaction and calculate $\Delta G_R$, $\Delta H_R$, and $\Delta S_R$ for the cell reaction at 50.°C.

**P11.13**

**a.** Calculate $\Delta G_R^°$ and the equilibrium constant $K$ at 298.15 K for the reaction $2\,Hg(l) + Cl_2(g) \rightleftharpoons Hg_2Cl_2(s)$.

**b.** Calculate $K$ using Table 4.1. What value of $\Delta G_R$ would make the value of $K$ the same as calculated from the half-cell potentials?

**P11.14**   Consider the couple $Ox + e^- \rightarrow Red$ with the oxidized and reduced species at unit activity. What must be the value of $E^°$ for this half-cell if the reductant Red is to liberate hydrogen at 1.00 atm from

**a.** an acidic solution with $a_{H^+} = 2.50$ and $a_{H_2} = 1.00$?

**b.** a basic solution with pH = 9.00?

**c.** Is hydrogen a better reducing agent in acid or basic solution? Explain your answer.

**P11.15**   By finding appropriate half-cell reactions, calculate the equilibrium constant at 298.15 K for the following reactions:

**a.** $4\,NiOOH(s) + 2\,H_2O(l) \rightleftharpoons 4\,Ni(OH)_2(s) + O_2(g)$

**b.** $4\,NO_3^-(aq) + 4\,H^+(aq) \rightleftharpoons$ $4\,NO(g) + 2\,H_2O(l) + 3\,O_2(g)$
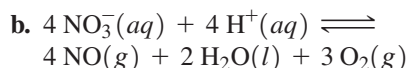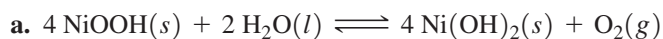
**P11.16**   The cell potential $E$ for the cell $Pt(s)|$ $|H_2(g, a_{H_2} = 1.00)|H^+(aq, a_{H^+} = 1.00)||NaCl(aq, m = 0.300)|AgCl(s)|\ Ag(s)$ is $+ 0.260$ V. Determine $\gamma_{Cl^-}$ assuming that $\gamma_\pm = \gamma_{Na^+} = \gamma_{Cl^-}$.

**P11.17**   The Edison storage cell is described by

$$Fe(s)|FeO(s)|KOH(aq, a_{KOH})|Ni_2O_3(s)|NiO(s)|Ni(s)$$

and the half-cell reactions are as follows:

$$Ni_2O_3(s) + H_2O(l) + 2e^- \rightarrow 2\,NiO(s) + 2\,OH^-(aq)$$
$$E^° = 0.40 \text{ V}$$

$$FeO(s) + H_2O(l) + 2e^- \rightarrow Fe(s) + 2\,OH^-(aq)$$
$$E^° = -0.87 \text{ V}$$
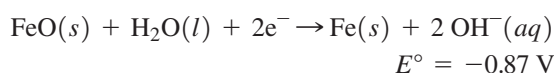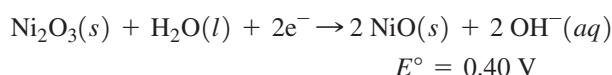
**a.** What is the overall cell reaction?

**b.** How does the cell potential depend on the activity of the KOH?

**c.** How much electrical work can be obtained per kilogram of the active materials in the cell?

**P11.18** Consider the Daniell cell, for which the overall cell reaction is $Zn(s) + Cu^{2+}(aq) \rightleftharpoons Zn^{2+}(aq) + Cu(s)$. The concentrations of $CuSO_4$ and $ZnSO_4$ are $2.50 \times 10^{-3}$ m and $1.10 \times 10^{-3}$ m, respectively.

**a.** Calculate $E$ setting the activities of the ionic species equal to their molalities.

**b.** Calculate $\gamma_{\pm}$ for each of the half-cell solutions using the Debye–Hückel limiting law.

**c.** Calculate $E$ using the mean ionic activity coefficients determined in part (b).

**P11.19** The standard potential $E°$ for a given cell is 1.135 V at 298.15 K and $(\partial E°/\partial T)_P = -4.10 \times 10^{-5}\,\text{V K}^{-1}$. Calculate $\Delta G_R°$, $\Delta S_R°$, and $\Delta H_R°$. Assume that $n = 2$.

**P11.20** Determine $E°$ for the reaction $Cr^{2+}(aq) + 2e^- \rightarrow Cr(s)$ from the one-electron reduction potential for $Cr^{3+}(aq)$ and the three-electron reduction potential for $Cr^{3+}(aq)$ given in Table 11.1 (see Appendix A).

**P11.21** Harnet and Hamer [*J. American Chemical Society* 57 (1935): 33] report values for the potential of the cell $Pt(s)|PbSO_4(s)|H_2SO_4(aq, a)|PbSO_4(s)|PbO_2(s)|Pt(s)$ over a wide range of temperature and $H_2SO_4$ concentrations. In 1.00 m $H_2SO_4$, their results were described by $E(V) = 1.91737 + 56.1 \times 10^{-6}\,t + 108 \times 10^{-8}\,t^2$, where $t$ is the temperature on the Celsius scale. Calculate $\Delta G_R°$, $\Delta H_R°$, and $\Delta S_R°$ for the cell reaction at 11° and 35°C.

**P11.22** Consider the reaction $Sn(s) + Sn^{4+}(aq) \rightleftharpoons 2Sn^{2+}(aq)$. If metallic tin is in equilibrium with a solution of $Sn^{2+}(aq)$ in which $a_{Sn^{2+}} = 0.250$, what is the activity of $Sn^{4+}(aq)$ at equilibrium at 298.15 K?

**P11.23** Consider the half-cell reaction $O_2(g) + 4\,H^+(aq) + 4e^- \rightarrow 2\,H_2O(l)$. By what factor are $n$, $Q$, $E$, and $E°$ changed if all the stoichiometric coefficients are multiplied by the factor two? Justify your answers.

**P11.24** Calculate $\Delta G_R°$ and the equilibrium constant at 298.15 K for the reaction $Cr_2O_7^{2-}(aq) + 3\,H_2(g) + 8\,H^+(aq) \rightarrow 2\,Cr^{3+}(aq) + 7\,H_2O(l)$.

**P11.25** The half-cell potential for the reaction $O_2(g) + 4\,H^+(aq) + 4e^- \rightarrow 2\,H_2O(l)$ is +1.03 V at 298.15 K when $a_{O_2} = 1.00$. Determine $a_{H^+}$.

**P11.26** Using half-cell potentials, calculate the equilibrium constant at 298.15 K for the reaction $2\,H_2O(l) \rightleftharpoons 2\,H_2(g) + O_2(g)$. Compare your answer with that calculated using $\Delta G_j°$ values from Table 4.1 (see Appendix A). What is the value of $E°$ for the overall reaction that makes the two methods agree exactly?

**P11.27** The data in the following table have been obtained for the potential of the cell $Pt(s)|H_2(g, f = 1.00\,\text{atm})|HCl(aq,m)|AgCl(s)|Ag(s)$ as a function of $m$ at 25°C.

| $m/\text{mol kg}^{-1}$ | $E/V$ | $m/\text{mol kg}^{-1}$ | $E/V$ | $m/\text{mol kg}^{-1}$ | $E/V$ |
|---|---|---|---|---|---|
| 0.00100 | 0.57915 | 0.0200 | 0.43024 | 0.500 | 0.27231 |
| 0.00200 | 0.54425 | 0.0500 | 0.38588 | 1.000 | 0.23328 |
| 0.00500 | 0.49846 | 0.100 | 0.35241 | 1.500 | 0.20719 |
| 0.0100 | 0.46417 | 0.200 | 0.31874 | 2.000 | 0.18631 |

**a.** Determine $E°$ using a graphical method.

**b.** Calculate $\gamma_{\pm}$ for HCl at $m = 0.00100$, 0.0100, and 0.100 mol kg$^{-1}$.

**P11.28** Consider the cell $Pt(s)|H_2(g, 1\,\text{atm})|H^+(aq, a = 1.00)\,|Fe^{3+}(aq), Fe^{2+}(aq)|Pt(s)$ given that $Fe^{3+} + e^- \rightarrow Fe^{2+}$ and $E° = 0.771$ V.

**a.** If the cell potential is 0.712 V, what is the ratio of $Fe^{2+}(aq)$ to $Fe^{3+}(aq)$?

**b.** What is the ratio of these concentrations if the cell potential is 0.830 V?

**c.** Calculate the fraction of the total iron present as $Fe^{3+}(aq)$ at cell potentials of 0.650, 0.700, 0.750, 0.771, 0.800, and 0.900 V. Graph the result as a function of the cell potential.

**P11.29** Determine $K_{sp}$ for AgBr at 298.15 K using the electrochemical cell described by

$$Ag(s)|Ag^+(aq, a_{Ag^+})\|Br^-(aq, a_{Br^-})|AgBr(s)|Ag(s)$$
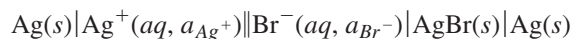
**P11.30** By finding appropriate half-cell reactions, calculate the equilibrium constant at 298.15 K for the following reactions:

**a.** $2\,Cd(s) + O_2(g) + 2\,H_2O(l) \rightleftharpoons 2\,Cd(OH)_2(s)$

**b.** $2\,MnO_2(s) + 4\,OH^-(aq) + O_2(g)$
$$\rightleftharpoons 2\,MnO_4^{2-}(aq) + 2\,H_2O(l)$$

# Probability

The concept of probability is central to many areas of chemistry. The characterization of large assemblies of atoms and molecules, from experimental observations to theoretical descriptions, relies on the concepts from statistics and probability. Given the utility of these concepts in chemistry, the central ideas of probability theory are presented in this chapter, including permutations, configurations, probability distribution functions, and the use of these functions to determine benchmark values that characterize the probability distribution.

## 12.1 Why Probability?

Physical chemistry can be partitioned into two perspectives of matter. One perspective is the microscopic viewpoint utilized by quantum mechanics, in which matter is described through a detailed analysis of its atomic and molecular components. This approach is elegant in its detail and was triumphant in describing many experimental observations that escaped classical descriptions of matter. For example, the observation of discrete emission from the hydrogen atom can only be explained using quantum theory. So successful is this approach that it stands as one of the greatest human accomplishments of the 20th century, and the ramifications of the quantum perspective continue to be explored.

Given the success of quantum theory in describing aspects of nature that are beyond the reach of classical mechanics, some might be tempted to dismiss classical, macroscopic descriptions of matter as irrelevant. However, this macroscopic perspective utilized by thermodynamics is extremely powerful in its ability to predict the outcome of chemical events. Thermodynamics involves the numerous relationships between macroscopic observables and relates experimental measurements of macroscopic properties to predictions of chemical behavior. Perhaps the most impressive aspect of thermodynamics is its ability to predict reaction spontaneity. By simply considering the Gibbs or Helmholtz energy difference between reactants and products, it is possible to state with certainty if a reaction will occur spontaneously. Even though it has impressive predictive utility, thermodynamics is of limited help if we want to know why a reaction occurs in the first place. What are the molecular details that give rise to Gibbs energy, and why should this quantity vary from one species to the next? Unfortunately, answers to these questions are beyond the descriptive bounds of thermodynamics. Can the detailed molecular descriptions available from quantum mechanics be used to formulate an answer to these questions? This type of approach demands that the quantum

perspective converge with that of thermodynamics. The link between these perspectives is developed in the following four chapters.

Statistical mechanics allows for the translation between the microscopic properties of matter and its macroscopic behavior. In this approach, a thermodynamic system is described as a collection of smaller units, a reduction in scale that can be taken to the atomic or molecular level. Starting from the microscopic perspective, statistical mechanics allows one to take detailed quantum descriptions of atoms and molecules and determine the corresponding thermodynamic properties. For example, consider a system consisting of 1 mol of gaseous HCl. We can take our knowledge of the quantum energetics of HCl and use this information in combination with statistical mechanics to determine thermodynamic properties of the system such as internal energy, heat capacity, entropy, and other properties described earlier in this book.

However, the question remains as to how this statistical bridge will be built. The task at hand is to consider a single atom or molecule and scale this perspective up to assemblies on the order of $10^{23}$! Such an approach necessitates a quantitative description of chemistry as a collection of events or observables, a task that is readily met by probability theory. Therefore, the mathematical tools of probability theory are required before proceeding with a statistical development. Probability is a concept of central utility in discussing chemical systems; the mathematical tools developed in this section will find wide application in subsequent chapters.

# 12.2 Basic Probability Theory

Probability theory was initially developed in the late 1600s as a mathematical formalism for describing games of chance. Consistent with these origins, the majority of illustrative examples employed in this chapter involve games of chance. Central to probability theory are random **variables,** or quantities that can change in value throughout the course of an experiment or series of events. A simple example of a variable is the outcome of a coin toss, with the variable being the side of the coin observed after tossing the coin. The variable can assume one of two values—heads or tails—and the value the variable assumes may change from one coin toss to the next. Variables can be partitioned into two categories: discrete variables and continuous variables.

**Discrete variables** assume only a number of specific values. The outcome of a coin toss is an excellent example of a discrete variable in that the outcome can be only one of two values: heads or tails. For another example, imagine a classroom with 100 desks in it, each of which is numbered. If we define the variable *chair number* as being the number on the chair, then this variable can assume values ranging from 1 to 100 in integer values. The possible values a variable can assume are collectively called the **sample space** of the variable. In the chair example, the sample space is equal to the collection of integers from 1 to 100, that is, $\{1, 2, 3, \ldots, 100\}$.

**Continuous variables** can assume any value within a set of limits, for example, the variable $X$ that can have any value in the range of $1 \leq X \leq 100$. Thermodynamics provides another well-known example of a continuous variable: temperature. The absolute temperature scale ranges from 0 K to infinity, with the variable, temperature, able to assume any value between these two limits. For continuous variables, the sample space is defined by the limiting values of the variable.

The treatment of probability differs depending on whether the variable of interest is discrete or continuous. Probability for discrete variables is mathematically simpler to describe; therefore, we focus on the discrete case first and then generalize to the continuous case later in Section 12.5.

Once a variable and its corresponding sample space have been defined, the question becomes "To what extent will the variable assume any individual value from the sample space?" In other words, we are interested in the **probability** that the variable will assume a certain value. Imagine a lottery where balls numbered 1 to 50 are mixed

inside a machine, and a single ball is selected. What is the probability that the ball chosen will have the value one (①)? Since the value chosen is random, the probability of selecting ① is simply 1/50. Does this mean that we will select ① only once every 50 selections? Consider each ball selection as an individual experiment, and after each experiment the selected ball is thrown back into the machine and another experiment is performed. The probability of selecting ① in any experiment is 1/50, but if the outcome of each experiment is independent of other outcomes, then it is not inconceivable that ① will not be selected after 50 trials, *or* that ① will be retrieved more than once. However, if the experiment is performed many times, the end result will be the retrieval of ① a proportion of times that approaches 1/50th of the total number of trials. This simple example illustrates a very important point: probabilities dictate the likelihood that the variable will assume a given value as determined from an infinite number of experiments. As scientists, we are not able to perform an infinite number of experiments; therefore, the extension of probabilities to situations involving a limited number of experiments is done with the understanding that the probabilities provide an approximate expectation of an experimental outcome.

In the lottery example, the probability of selecting any single ball is 1/50. Because there are 50 balls total, the sum of the probabilities for selecting each individual ball must be equal to 1. Consider a variable $X$ for which the sample space consists of $M$ values denoted as $\{x_1, x_2, \ldots, x_M\}$. The probability that the variable $X$ will assume one of these values ($p_i$) is

$$0 \le p_i \le 1 \tag{12.1}$$

where the subscript indicates one of the values contained in the set space ($i = 1, 2, \ldots, M$). Furthermore, $X$ must assume some value from the sample set in a given experiment dictating that the sum of all probabilities will equal unity:

$$p_1 + p_2 + \cdots + p_M = \sum_{i=1}^{M} p_i = 1 \tag{12.2}$$

In Equation (12.2), the sum of probabilities has been indicated by the summation sign, with the limits of summation indicating that the sum is taken over the entire sample space, from $i = 1$ to $M$. The combination of the sample space, $S = \{x_1, x_2, \ldots, x_M\}$, and corresponding probabilities, $P = \{p_1, p_2, \ldots, p_M\}$, is known as the **probability model** for the experiment.

## EXAMPLE PROBLEM 12.1

What is the probability model for the lottery experiment described in the preceding text?

### Solution

The value of the ball that is retrieved in an individual experiment is the variable of interest, and it can take on integer values from 1 to 50. Therefore, the sample space is

$$S = \{1, 2, 3, \ldots, 50\}.$$

If the probability of retrieving any individual ball is equal, and there are 50 balls total, then the probabilities are given by

$$P = \{p_1, p_2, \ldots, p_{50}\} \text{ with all } p_i = 1/50$$

Finally, we note that the sum of all probabilities is equal to 1:

$$p_{total} = \sum_{i=1}^{50} p_i = \left(\frac{1}{50}\right)_1 + \left(\frac{1}{50}\right)_2 + \cdots + \left(\frac{1}{50}\right)_{50} = 1$$

The preceding discussion described the probability associated with a single experiment; however, there are times when one is more interested in the probability associated with a given outcome for a series of experiments, that is, the **event probability.**

**FIGURE 12.1**
Potential outcomes after tossing a coin four times. Red signifies heads and blue signifies tails.
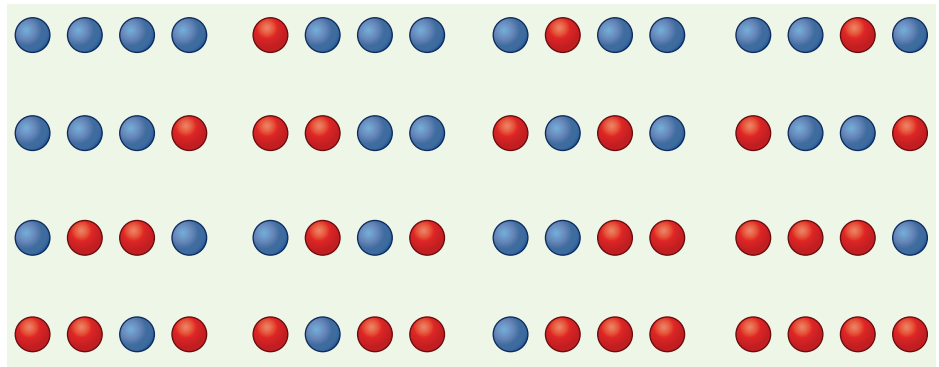


For example, imagine tossing a coin four times. What is the probability that at least two heads are observed after four tosses? All of the potential outcomes for this series of experiments are given in Figure 12.1. Of the 16 potential outcomes, 11 have at least two heads. Therefore, the probability of obtaining at least two heads after tossing a coin four times is 11/16, or the number of outcomes of interest divided by the total number of outcomes.

Let the sample space associated with a particular variable be $S$ where $S = \{s_1, s_2, \ldots, s_N\}$, and let the probability that the outcome or event of interest $E$ occurs be equal to $P_E$. Finally, there are $j$ values in $S$ corresponding to the outcome of interest. If the probability of observing an individual value is equivalent, then $P_E$ is given by

$$P_E = \left(\frac{1}{N}\right)_1 + \left(\frac{1}{N}\right)_2 + \cdots + \left(\frac{1}{N}\right)_j = \frac{j}{N} \qquad (12.3)$$

This expression states that the probability of the event outcome of interest occurring is equal to the sum of the probabilities for each individual value in sample space corresponding to the desired outcome. Alternatively, if there are $N$ values in sample space, and $N_E$ of these values correspond to the event of interest, then $P_E$ simply becomes

$$P_E = \frac{N_E}{N} \qquad (12.4)$$

**EXAMPLE PROBLEM 12.2**

What is the probability of selecting a heart from a standard deck of 52 cards?

**Solution**

In a standard deck of cards, each suit has 13 cards and there are 4 suits total (hearts, spades, clubs, and diamonds). The sample space consists of the 52 cards, of which 13 correspond to the event of interest (selecting a heart). Therefore,

$$P_E = \frac{N_E}{N} = \frac{13}{52} = \frac{1}{4}$$

### 12.2.1 The Fundamental Counting Principle

In the preceding examples, the number of ways a given event could be accomplished was determined by counting. This "brute force" approach can be used when dealing with just a few experiments, but what if we toss a coin 50 times and are interested in the probability of the coin landing heads 20 times out of the 50 tosses? Clearly, writing down every possible outcome and counting would be a long and tedious process. A more efficient method for determining the number of arrangements is illustrated by the following example. Imagine that the instructor of a class consisting of 30 students needs to assemble these students into a line. How many arrangements of students are possible? There are

30 possibilities for the selection of the first student in line, 29 possibilities for the second, and so on until the last student is placed in line. If the probabilities for picking any given student are equal, then the total number of ways to arrange the students ($W$) is

$$W = (30)(29)(28)\ldots(2)(1) = 30! = 2.65 \times 10^{32}$$

The exclamation point symbol (!) in this expression is referred to as **factorial,** with $n!$ indicating the product of all values from 1 to $n$, and $0! = 1$. The preceding result in its most general form is known as the **fundamental counting principle.**

---

**FUNDAMENTAL COUNTING PRINCIPLE:** For a series of manipulations $\{M_1, M_2 \ldots, M_j\}$ having $n_i$ ways to accomplish $M_i$, the total number of ways to perform the entire series of manipulations ($Total_M$) is the product of the number of ways to perform each manipulation under the assumption that the ways are independent:

$$Total_M = (n_1)(n_2)\ldots(n_j) \tag{12.5}$$

---

### EXAMPLE PROBLEM 12.3

How many 5-card arrangements are possible from a standard deck of 52 cards?

#### Solution

Employing the fundamental counting principle, each manipulation is receiving a card in your hand; therefore, five manipulations are required. There are 52 possible cards we could receive as our first card, or 52 ways to accomplish the first manipulation ($n_1 = 52$). Next, there are 51 possible cards we could receive as the second card in our hand, or 51 ways to accomplish the second manipulation ($n_2 = 51$). Following this logic

$$\begin{aligned} Total_M &= (n_1)(n_2)(n_3)(n_4)(n_5) \\ &= (52)(51)(50)(49)(48) = 311{,}875{,}200 \end{aligned}$$

### EXAMPLE PROBLEM 12.4

The electron configuration for the first excited state of He is $1s^12s^1$. Using the fundamental counting principle, how many possible spin states are expected for this excited-state electron configuration?

#### Solution

Because the electrons are in different orbitals, they do not have to be spin paired. Therefore, there are two choices for the spin state of the first electron, and two choices for the spin state of the second electron such that

$$Total_M = (n_1)(n_2) = (2)(2) = 4$$

### 12.2.2 Permutations

In the example of a classroom with 30 students, we found that there are 30! unique ways of arranging the students into a line, or 30! **permutations.** The total number of objects that are arranged is known as the order of the permutation, denoted as $n$, such that there are $n!$ total permutations of $n$ objects. Thus far we have assumed that the entire set of $n$ objects is used, but how many permutations are possible if only a subset of objects is employed in constructing the permutation? Let $P(n, j)$ represent the number of permutations possible using a subset of $j$ objects from the total group of $n$; $P(n, j)$ is equal to

$$P(n, j) = n(n - 1)(n - 2)\ldots(n - j + 1) \tag{12.6}$$

Equation (12.6) can be rewritten by noting that

$$n(n-1)\ldots(n-j+1) = \frac{n(n-1)\ldots(1)}{(n-j)(n-j-1)\ldots(1)} = \frac{n!}{(n-j)!} \quad \textbf{(12.7)}$$

Therefore, $P(n, j)$ is given by the following relationship:

$$P(n, j) = \frac{n!}{(n-j)!} \quad \textbf{(12.8)}$$

### EXAMPLE PROBLEM 12.5

The coach of a basketball team has 12 players on the roster but can only play 5 players at one time. How many 5-player arrangements are possible using the 12-player roster?

#### Solution

For this problem the permutation order ($n$) is 12, and the subset ($j$) is 5 such that

$$P(n, j) = P(12,5) = \frac{12!}{(12-5)!} = 95{,}040$$

### 12.2.3 Configurations

The previous section discussed the number of ordered arrangements or permutations possible using a given number of objects. However, many times one is instead interested in the number of *unordered* arrangements that are possible. The basketball team example of Example Problem 12.5 is an excellent illustration of this point. In a basketball game, the coach is generally more concerned with which five players are in the game at any one time rather than the order in which they entered the game. An unordered arrangement of objects is referred to as a **configuration.** Similar to permutations, configurations can also be constructed using all objects in the set being manipulated ($n$), or just a subset of objects with size $j$. We will refer to configurations using the nomenclature $C(n, j)$.

For a conceptual example of configurations, consider the four colored balls shown in Figure 12.2. How many three-ball configurations and associated permutations can be
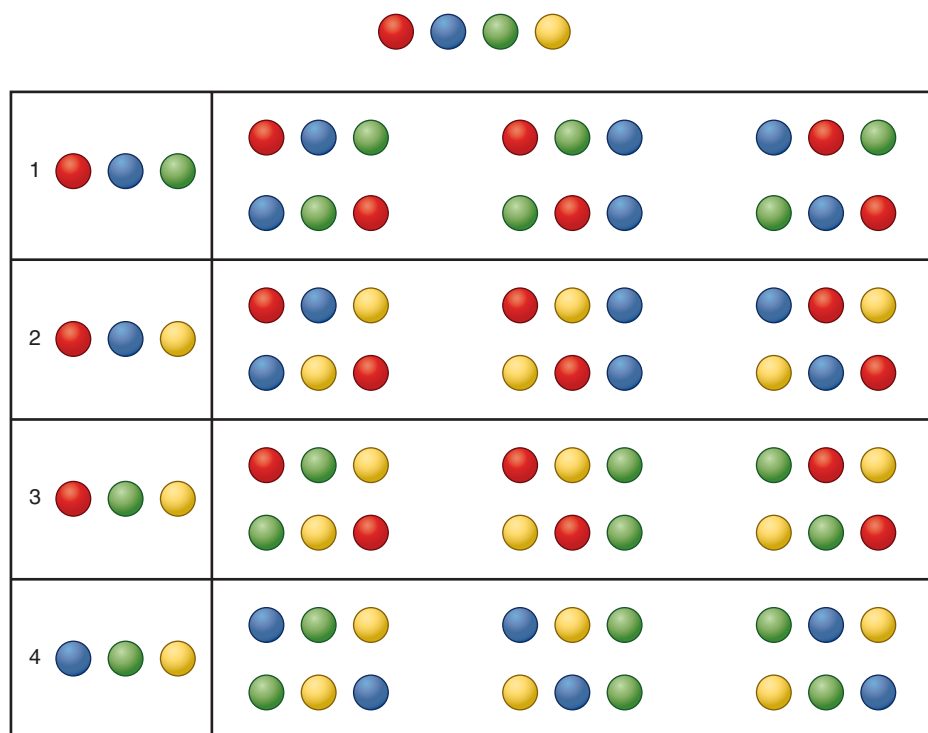


**FIGURE 12.2**

Illustration of configurations and permutations using four colored balls. The left-hand column presents the four possible three-color configurations, and the right-hand column presents the six permutations corresponding to each configuration.

made using these balls? The possibilities are illustrated in the figure. Notice that a configuration is simply a collection of three colored balls, and that a permutation corresponds to an ordered arrangement of these same balls such that there are four possible configurations with each configuration having six associated permutations. This observation can be used to develop the following mathematical relationship between configurations and permutations:

$$C(n, j) = \frac{P(n, j)}{j!}$$

$C(n, j)$ is the number of configurations that are possible using a subset of $j$ objects from a total number of $n$ objects. Substituting the definition of $P(n, j)$ from Equation (12.8) into the preceding expression results in the following relationship:

$$C(n, j) = \frac{P(n, j)}{j!} = \frac{n!}{j!(n - j)!} \tag{12.9}$$

### EXAMPLE PROBLEM 12.6

If you are playing cards with a standard 52-card deck, how many possible 5-card combinations or "hands" are there?

#### Solution

Each 5-card hand is a configuration or subset taken from the 52-card deck. Therefore, $n = 52$, $j = 5$, and

$$C(n, j) = C(52, 5) = \frac{52!}{5!(52 - 5)!} = \frac{52!}{(5!)(47!)} = 2,598,960$$

This result should be contrasted with the 311,875,200 permutations obtained in Example Problem 12.3. Generally, card players are more interested in the five cards in their possession at any time and not on the order in which those cards arrived.

## 12.2.4 A Counting Example: Bosons and Fermions (Advanced)

The concepts of permutation and configuration will be exceedingly important in the next chapter, but we can introduce a simple counting problem here to demonstrate the connection between probability theory and chemistry. Consider the following question: how many ways can a set of $n$ indistinguishable particles be arranged into $x$ equally accessible states, with each state capable of holding any number of particles? This counting problem is encountered when describing particles known as **bosons,** in which multiple particles can occupy the same state. Photons and particles of integer spin such as $^4$He are bosons, and these particles follow **Bose–Einstein statistics.** To describe the arrangement of such particles over a collection of states, we first consider a manageable example consisting of four particles and three states, as illustrated in Figure 12.3. In the figure, each particle is shown as a red circle, and the three states are shown by rectangles. The four possible configurations have a collection of associated permutations given by the numerals on the right side of each configuration. For example, the second configuration with three particles in one state, one in a second state, and no particles in the third state has six associated permutations. The total number of possible arrangements is equal to the total number of permutations, or 15 in this example.

Another way to envision the possible configurations in this example is shown in Figure 12.4. Here, the particles are confined to a single box with two movable walls allowing for three separate partitions. The figure demonstrates that there are again four possible configurations, identical to the result shown in Figure 12.3. The advantage of this depiction is that we can envision this problem as counting the number of permutations associated with a collection of six indistinguishable objects: four particles and two
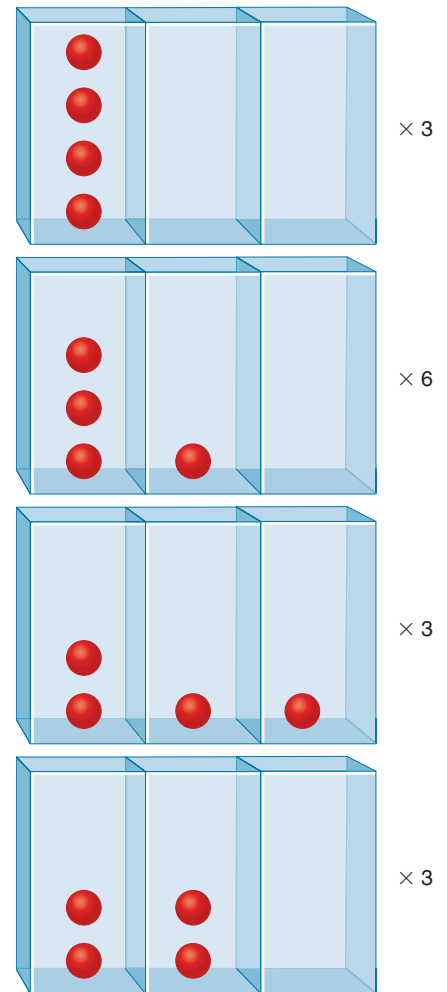


**FIGURE 12.3**
Configurations associated with arranging four identical particles (red balls) in three states (rectangles). The number of permutations associated with each configuration is given by the numerals to the right of each configuration.
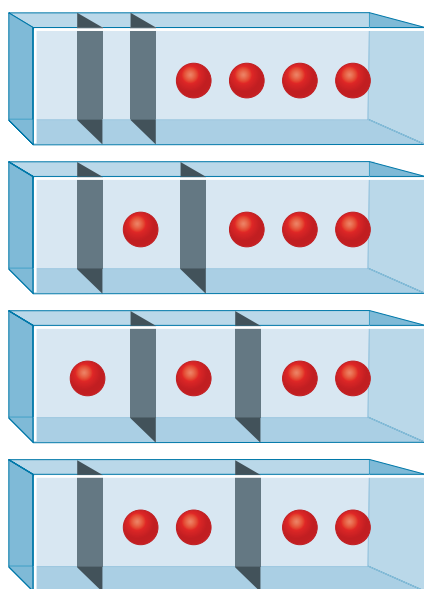
**FIGURE 12.4**
Second model for the four-particle/three-state arrangement depicted in Figure 12.3. In this model, states correspond to regions inside a single rectangle created by movable walls (black rectangles).

movable walls. For a given number of states $x$ there will be $x - 1$ movable walls. Combining the walls with the $n$ particles, the total number of permutations is

$$P_{BE} = \frac{(n + x - 1)!}{n!(x - 1)!} \tag{12.10}$$

The subscript $BE$ refers to Bose–Einstein, reflecting the fact that we are discussing bosons. Employing Equation (12.10) to our illustrative example with $n = 4$ and $x = 3$, we find that $P_{BE} = 15$ consistent with our earlier result from counting. This result can be understood using the probability concepts introduced to this point. Specifically, the total number of objects being manipulated is $n + x - 1$ corresponding to $(n + x - 1)!$ permutations if the particles and walls were distinguishable. To account for the fact that the particles and walls are indistinguishable, we divided by $n!$ and $(x - 1)!$ resulting in the final expression for $P_{BE}$.

The second type of particles are **fermions,** which are species of noninteger spin such as electrons or $^3$He. In a collection of fermions, each particle has a unique set of quantum numbers such that no two particles will occupy the same state. Fermions follow **Fermi-Dirac statistics.** Suppose we have $n$ fermions to distribute over $x$ states. How many possible arrangement permutations are there? There will be $x$ choices for placement of the first particle, $x - 1$ choices for the second, and so forth so that the total number of state arrangements is given by

$$x(x - 1)(x - 2)\ldots(x - n + 1) = \frac{x!}{(x - n)!}$$

However, as in the boson example, the particles are indistinguishable, requiring that we divide the above expression by $n!$ resulting in

$$P_{FD} = \frac{x!}{n!(x - n)!} \tag{12.11}$$

---

**EXAMPLE PROBLEM 12.7**

How many quantum states are possible for a carbon atom with the configuration $1s^2 2s^2 2p^2$?

**Solution**

Since this problem involves the arrangement of electrons, Fermi-Dirac statistics apply. Since only the two electrons in the $p$ orbitals contribute to defining the number of states (recall, electrons in the $s$ orbitals must be spin paired) we have $n = 2$. Next, there are three $p$ orbitals and two possible spin orientations in each orbital such that $x = 6$. Therefore, the total number of quantum states, or arrangement permutations, is

$$P_{FD} = \frac{x!}{n!(x - n)!} = \frac{6!}{2!(4!)} = 15$$

---

### 12.2.5 Binomial Probabilities

The probability of an event E occurring out of a total number of possible outcomes was denoted as $P_E$ in Equation (12.4). We can also define the **complement** of $P_E$ as the probability of an outcome other than that associated with the event of interest and denote this quantity as $P_{EC}$. With this definition, the sum of $P_E$ and $P_{EC}$ are related as follows:

$$P_E + P_{EC} = 1 \tag{12.12}$$

Equation (12.12) states that the probability of the event of interest occurring combined with the event not occurring must be equal to unity and provides a definition for experiments known as **Bernoulli trials.** In such a trial, the outcome of a given experiment will be a success (i.e., the outcome of interest) or a failure (i.e., not the outcome of interest). The tossing of a coin is one example of a Bernoulli trial where the outcome "heads" can

be considered a success and "tails" a failure (or vice versa). A collection of Bernoulli trials is known as a **binomial experiment,** and these simple experiments provide a framework in which to explore probability distributions. It is critical to note that the outcome of each trial is independent of the outcome of any other trial in the experiment. That is, previous or the subsequent outcomes have no effect on the outcome of the current trial. Consider a binomial experiment in which a coin is tossed four times and this question is asked: "What is the probability of observing heads (or a successful outcome) every time?" Because the probability of success for each trial is $1/2$, the total probability is the product of the success probabilities for each trial:

$$P_E = \left(\frac{1}{2}\right)\left(\frac{1}{2}\right)\left(\frac{1}{2}\right)\left(\frac{1}{2}\right) = \frac{1}{16}$$

Note that this is the answer one would reach by considering all of the possible permutations encountered when flipping a coin four times as illustrated in Figure 12.1.

For a series of Bernoulli trials in which the probability of success for a single trial is $P_E$, the probability of obtaining $j$ successes in a trial consisting of $n$ trials is given by

$$P(j) = C(n, j)(P_E)^j(1 - P_E)^{n-j} \tag{12.13}$$

The $(P_E)^j$ term in the preceding expression is the product of probabilities for the $j$ successful trials. Because $n$ total trials were performed, $(n - j)$ trials must have failed, and the probability of these trials occurring is given by $(1 - P_E)^{n-j}$. But why does the total number of configurations appear in Equation (12.13)? The answer to this question lies in the difference between permutations and configurations. Again, consider a series of four coin tosses where the outcome of interest is the exact permutation {H, T, T, H}. If H is a successful trial occurring with probability $P_E$, then the probability of observing this permutation is

$$P = (P_E)(1 - P_E)(1 - P_E)(P_E) = (P_E)^2(1 - P_E)^2 = \left(\frac{1}{2}\right)^2\left(\frac{1}{2}\right)^2 = \frac{1}{16} \tag{12.14}$$

but this is also the probability for observing {H, H, H, H}. That is, the probability of observing a specific order of trial outcomes, or a single permutation, is equivalent. If the outcome of interest is two successful trials that can occur in any order, then the probabilities for all possible permutations corresponding to two successful trials must be added, and this is accomplished by the inclusion of $C(n, j)$ in Equation (12.13).

---

#### EXAMPLE PROBLEM 12.8

Imagine tossing a coin 50 times. What are the probabilities of observing heads 25 times (i.e., 25 successful experiments) and just 10 times?

#### Solution

The trial of interest consists of 50 separate experiments; therefore, $n = 50$. Considering the case of 25 successful experiments where $j = 25$. The probability $(P_{25})$ is

$$\begin{aligned}
P_{25} &= C(n, j)(P_E)^j(1 - P_E)^{n-j} \\
&= C(50, 25)(P_E)^{25}(1 - P_E)^{25} \\
&= \left(\frac{50!}{(25!)(25!)}\right)\left(\frac{1}{2}\right)^{25}\left(\frac{1}{2}\right)^{25} = (1.26 \times 10^{14})(8.88 \times 10^{-16}) = 0.11
\end{aligned}$$

For the case of 10 successful experiments, $j = 10$ such that

$$\begin{aligned}
P_{10} &= C(n, j)(P_E)^j(1 - P_E)^{n-j} \\
&= C(50, 10)(P_E)^{10}(1 - P_E)^{40} \\
&= \left(\frac{50!}{(10!)(40!)}\right)\left(\frac{1}{2}\right)^{10}\left(\frac{1}{2}\right)^{40} = (1.03 \times 10^{10})(8.88 \times 10^{-16}) = 9.1 \times 10^{-6}
\end{aligned}$$

# 12.3 Stirling's Approximation

When calculating $P(n, j)$ and $C(n, j)$, it is necessary to evaluate factorial quantities. In the examples encountered so far, $n$ and $j$ were sufficiently small such that these quantities could be evaluated on a calculator. However, this approach to evaluating factorial quantities is limited to relatively small numbers. For example, 100! is equal to $9.3 \times 10^{157}$, which is an extremely large number and beyond the range of many calculators. Furthermore, we are interested in extending the probability concepts we have developed up to chemical systems for which $n \approx 10^{23}$! The factorial of such a large number is simply beyond the computational ability of most calculators.

Fortunately, approximation methods are available that will allow us to calculate the factorial of large numbers. The most famous of these methods is known as **Stirling's approximation,** which provides a simple method by which to calculate the natural log of $N!$. A simplified version of this approximation is

$$\ln N! = N \ln N - N \tag{12.15}$$

Equation (12.15) is readily derived as follows:

$$\ln(N!) = \ln \left[ (N)(N-1)(N-2)\ldots(2)(1) \right]$$

$$= \ln(N) + \ln(N-1) + \ln(N-2) + \cdots + \ln(2) + \ln(1)$$

$$= \sum_{n=1}^{N} \ln(n) \approx \int_{1}^{N} \ln(n) \, dn$$

$$= N \ln N - N - (1 \ln 1 - 1) \approx N \ln N - N \tag{12.16}$$

The replacement of the summation by an integral is appropriate when $N$ is large. The final result is obtained by evaluating the integral over the limits indicated. Note that the main assumption inherent in this approximation is that $N$ is a large number. The central concern in applying Stirling's approximation is whether $N$ is sufficiently large to justify its application. Example Problem 12.9 illustrates this point.

---

### EXAMPLE PROBLEM 12.9

Evaluate $\ln(N!)$ for $N = 10$, 50, and 100 using a calculator, and compare the result to that obtained using Stirling's approximation.

#### Solution

For $N = 10$, using a calculator we can determine that $N! = 3.63 \times 10^6$ and $\ln(N!) = 15.1$ Using Stirling's approximation

$$\ln(N!) = N \ln N - N = 10 \ln(10) - 10 = 13.0$$

This value represents a 13.9% error relative to the exact result, a substantial difference. The same procedure for $N = 50$ and 100 results in the following:

| $N$ | $\ln(N!)$ Calculated | $\ln(N!)$ Stirling | Error (%) |
|-----|---------------------|--------------------|-----------|
| 50  | 148.5               | 145.6              | 2.0       |
| 100 | 363.7               | 360.5              | 0.9       |

This problem demonstrates that there are significant differences between the exact and approximate results even for $N = 100$ but that the magnitude of this error decreases as $N$ increases. For the chemical systems encountered in subsequent chapters, $N$ will be $\sim 10^{23}$, many orders of magnitude larger than the values studied in this example. Therefore, for our purposes Stirling's approximation represents an elegant and sufficiently accurate method by which to evaluate the factorial of large quantities.

# 12.4 Probability Distribution Functions

Returning to the coin-tossing experiment, we now ask what is the probability of obtaining a given outcome (for example, the number of heads) after tossing a coin 50 times. Using Equation (12.13), a table of probability as a function of the number of heads can be constructed with $n = 50$ (total number of tosses) and $j = $ the number of heads (i.e., the number of successful tosses):

| Number of Heads | Probability | Number of Heads | Probability |
|---|---|---|---|
| 0 | $8.88 \times 10^{-16}$ | 30 | 0.042 |
| 1 | $4.44 \times 10^{-14}$ | 35 | $2.00 \times 10^{-3}$ |
| 2 | $1.09 \times 10^{-12}$ | 40 | $9.12 \times 10^{-6}$ |
| 5 | $1.88 \times 10^{-9}$ | 45 | $1.88 \times 10^{-9}$ |
| 10 | $9.12 \times 10^{-6}$ | 48 | $1.09 \times 10^{-12}$ |
| 15 | $2.00 \times 10^{-3}$ | 49 | $4.44 \times 10^{-14}$ |
| 20 | 0.042 | 50 | $8.88 \times 10^{-16}$ |
| 25 | 0.112 | | |

Rather than reading all of the probability values from a table, this same information can be presented graphically by plotting the probability as a function of outcome. This plot for the case where $P_E = 0.5$ (i.e., the coin landing heads or tails is equally likely) is shown as the red line in Figure 12.5. Notice that the maximum probability is predicted to be 25 heads corresponding to the most probable outcome (as intuition suggests). A second feature of this distribution of probabilities is that the actual value of the probability corresponding to 25 successful trials is not unity, but 0.112. However, summing all of the outcome probabilities reveals that

$$P_0 + P_1 + \cdots + P_{50} = \sum_{j=0}^{50} P_j = 1 \qquad \textbf{(12.17)}$$
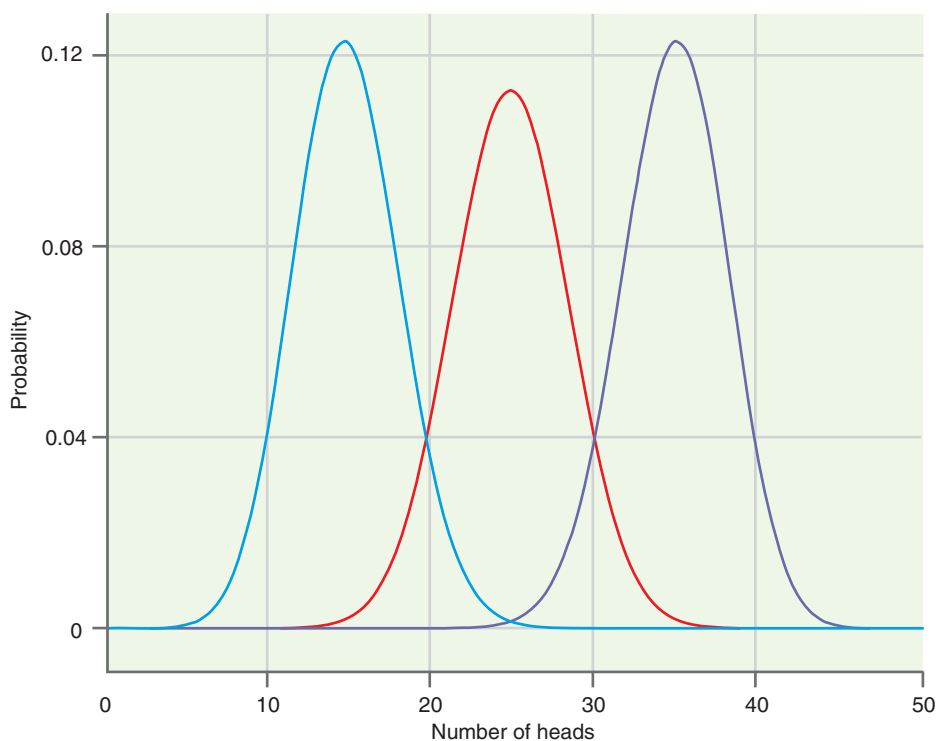


**FIGURE 12.5**
Plot of the probability of the number of heads being observed after flipping a coin 50 times. The red curve represents the distribution of probabilities for $P_E = 0.5$, the blue curve for $P_E = 0.3$, and the purple curve for $P_E = 0.7$.

Figure 12.5 presents the variation in probability of event outcome as a function of the number of heads observed after flipping a coin 50 times. This plot also demonstrates that the probability formula for Bernoulli trials can be used to describe the variation or distribution of probability versus event outcome. Therefore, the probability expression we have employed can also be thought of as the distribution function for a binomial experiment. From Equation (12.13), the probability of observing $j$ successful trials following $n$ total trials is given by

$$P(j) = \frac{n!}{j!(n-j)!}(P_E)^j(1 - P_E)^{n-j} \quad \text{for} \quad j = 0, 1, 2, \ldots, n \qquad \textbf{(12.18)}$$

Equation (12.18) is valid when $0 \leq P_E \leq 1$. In the coin-flipping experiment just discussed, the assumption was made that the coin can land either heads or tails with equal probability such that $P_E = 0.5$. What would happen if a coin were used where the probability of observing heads is 0.7? First, we would expect the probability distribution of trial outcomes to vary with respect to the case where $P_E = 0.5$. For the experiment in which $P_E = 0.7$ and $(1 - P_E) = 0.3$, the distribution function $P(j)$ can be calculated and compared to the previous case, as illustrated in Figure 12.5. Comparison of the probability distributions demonstrates that the most probable outcome has shifted to a greater number of heads, H $= 35$ in the case of $P_E = 0.7$. The outcome H $= 15$ is most probable when $P_E = 0.3$. A final aspect to note is that in addition to the maximum probability changing from H $= 25$ as $P_E$ is changed from 0.5 to some other value, the probability for the most likely outcome also increases. For example, for $P_E = 0.5$, the maximum probability is 0.112 for H $= 25$. If $P_E = 0.7$, the maximum probability now becomes 0.128 for H $= 35$. That is, not only does the most probable outcome depend on $P_E$, but the probability of observing the most probable outcome also changes with $P_E$.

The coin-tossing experiment provides an excellent example of a probability distribution function and motivates a more formal definition of such functions. A **probability distribution function** represents the probability of a variable ($X$) having a given value, with the probability described by a function

$$P(X_i) \propto f_i \qquad \textbf{(12.19)}$$

In Equation (12.19), $P(X_i)$ is the probability that the variable $X$ will have some value $X_i$ in the sample space. This equation states that the set of probabilities $\{P(X_1), P(X_2), \ldots, P(X_M)\}$ will be proportional to the value of the distribution function evaluated for the corresponding value of the variable given by $\{f_1, f_2, \ldots, f_M\}$. In the coin toss example, the variable *number of heads* could assume a value between 0 and 50, and Equation (12.13) was employed to determine the corresponding probability $P(X_i)$ for each possible value of the variable. For a binomial experiment, Equation (12.13) represents the function $f$ in Equation (12.19). We can express Equation (12.19) as an equality by introducing a proportionality constant ($C$), and

$$P(X_i) = Cf_i \qquad \textbf{(12.20)}$$

Imposing the requirement that the total probability be equal to unity results in

$$\sum_{i=1}^{M} P(X_i) = 1 \qquad \textbf{(12.21)}$$

Equation (12.21) is readily evaluated to yield the proportionality constant:

$$1 = \sum_{i=1}^{M} Cf_i = Cf_1 + Cf_2 + \cdots + Cf_M$$

$$1 = C(f_1 + f_2 + \cdots + f_M) = C\sum_{i=1}^{M} f_i$$

$$C = \frac{1}{\sum_{i=1}^{M} f_i} \qquad \textbf{(12.22)}$$

Substitution into our original expression for probability provides the final result of interest:

$$P(X_i) = \frac{f_i}{\sum\limits_{i=1}^{M} f_i} \tag{12.23}$$

Equation (12.23) states that the probability of a variable having a given value from the sample space is given by the value of the probability function for this outcome divided by the sum of the probabilities for all possible outcomes. Equation (12.23) is a general expression for probability, and we will use this construct in the upcoming chapter when defining the Boltzmann distribution, one of the central results of statistical thermodynamics.

### EXAMPLE PROBLEM 12.10

What is the probability of receiving any 1 card from a standard deck of 52 cards?

#### Solution

The variable of interest is the card received, which can be any one of 52 cards (that is, the sample space for the variable consists of the 52 cards in the deck). The probability of receiving any card is equal so that $f_i = 1$ for $i = 1$ to 52. With these definitions, the probability becomes

$$P(X_i) = \frac{f_i}{\sum\limits_{i=1}^{52} f_i} = \frac{1}{\sum\limits_{i=1}^{52} f_i} = \frac{1}{52}$$

## 12.5 Probability Distributions Involving Discrete and Continuous Variables

To this point we have assumed that the variable of interest is discrete. As such, probability distributions can be constructed by calculating the corresponding probability when $X$ assumes each value from the sample set. However, what if the variable $X$ is continuous? In this case the probability must be determined for the variable having a value within a portion of the domain of $X$, denoted as $dX$. In this case we employ the **probability density** $P(X)$, and $P(X)\,dX$ is the probability that the variable $X$ has a value in the range of $dX$. By analogy with the development for discrete variables, the probability is then given by

$$P(X)\,dX = Cf(X)\,dX \tag{12.24}$$

which states that the probability $P(X)\,dX$ is proportional to some function $f(X)\,dX$ as yet undefined. Applying the normalization condition to ensure that the total probability is unity over the domain of the variable ($X_1 \leq X \leq X_2$):

$$\int_{X_1}^{X_2} P(X)\,dX = C \int_{X_1}^{X_2} f(X)\,dX = 1 \tag{12.25}$$

The second equality in Equation (12.25) dictates that

$$C = \frac{1}{\displaystyle\int_{X_1}^{X_2} f(X)\,dX} \tag{12.26}$$

Equation (12.26) is identical to the discrete variable result [Equation (12.22)] except that summation has been replaced by integration since we are now interested in continuous

variables. With the preceding definition of the proportionality constant, the probability is defined as

$$P(X) \, dX = \frac{f(X) \, dX}{\displaystyle\int_{X_1}^{X_2} f(X) \, dX} \tag{12.27}$$

The similarity of this expression to the corresponding expression for discrete variables [Equation (12.23)] illustrates an important point. When working with probability distributions for continuous variables, integration over the domain of the variable is performed. In contrast, summation is performed when the variable is discrete. Although the mathematics changes slightly between discrete and continuous variables, it is important to realize that the conceptual description of probability is unchanged. Continuous probability distributions are common in quantum mechanics. For example, the normalization condition is applied to the spatial domain of the wave function through the following relationship:

$$\int \psi^*(x, t)\psi(x, t) \, dx = 1$$

The product of the wave function with its complex conjugate represents the probability density for the spatial location of the particle, and it is equivalent to $P(X)$ in Equation (12.24). By integrating this product over all space, all possible locations of the particle are included such that the probability of the particle being somewhere must be one.

For another example of probability distribution functions involving continuous variables, consider the following probability distribution function associated with the translational kinetic energy of ideal gas particles $(E)$, a topic that will be discussed in detail in Chapter 16:

$$P(E) \, dE = 2\pi \left(\frac{1}{\pi RT}\right)^{3/2} E^{1/2} e^{-E/RT} \, dE \tag{12.28}$$

In Equation (12.28), $T$ is temperature and $R$ is the ideal gas constant. The variable of interest $E$ is continuous in the domain from 0 to infinity. Figure 12.6 presents an illustration of this distribution function for three temperatures: 300., 400., and 500. K.
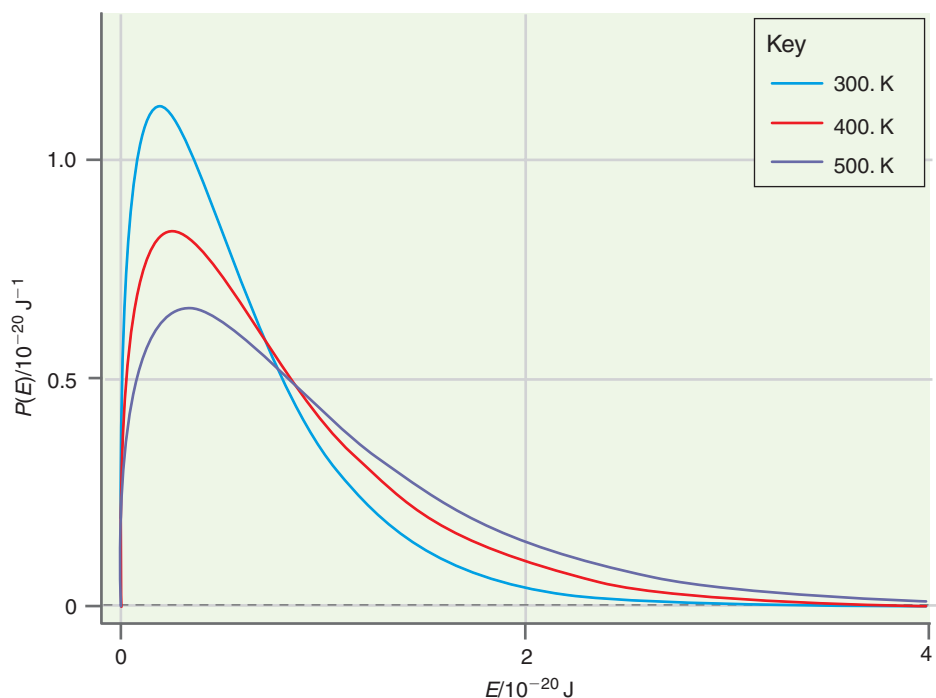


**FIGURE 12.6**
Probability distributions for the translational kinetic energy of an ideal gas.

Notice that energy corresponding to maximum probability changes as a function of temperature and that the probability of finding a particle at larger kinetic energies also increases with temperature. This example demonstrates that a substantial amount of information regarding the behavior of a chemical system can be succinctly presented using probability distributions.

## 12.5.1 Continuous Representation of Discrete Variables

We have seen that it is possible to evaluate probabilities involving discrete variables by summation; however, we will encounter situations in later chapters where summation involves a prohibitively large number of terms. In such cases, treating a discrete variable as continuous can simplify matters greatly. However, one concern with this approach is the error introduced by including values for the discrete variable that are not contained in the sample set. Under what conditions are such errors acceptable? Consider the following unnormalized probability distribution function:

$$P(X) = e^{-0.3X} \tag{12.29}$$

We are interested in normalizing this distribution by determining the total probability $P_{total}$. First, $X$ is treated as a discrete variable with the sample space consisting of integer values ranging from 0 to 100, and $P_{total}$ is

$$P_{total} = \sum_{X=0}^{100} e^{-0.3X} = 3.86 \tag{12.30}$$

Next, $X$ is treated as continuous with the domain of the sample set equal to $0 \le X \le 100$. The corresponding expression for the total probability is

$$P_{total} = \int_{0}^{100} e^{-0.3X} \, dX = 3.33 \tag{12.31}$$

The only difference between these last two equations is that the summation over discrete values of the variable $X$ has been replaced by integration over the range of the variable. The preceding comparison demonstrates that the continuous approximation is close to the exact result given by summation. In general, if the differences between values the function can assume are small relative to the domain of interest, then treating a discrete variable as continuous is appropriate. This issue will become critical when the various energy levels of an atom or molecule are discussed. Specifically, the approximation of Equation (12.31) will be used to treat translational and rotational states from a continuous perspective where direct summation is impractical. In the remainder of this text, situations in which the continuous approximation is not valid will be carefully noted.

### EXAMPLE PROBLEM 12.11

Using the following distribution function

$$P(X) = e^{-0.05X}$$

Determine the total probability if the variable $X$ is discrete with the sample space consisting of integer values ranging from 0 to 100. Compare this result to that if $X$ is a continuous variable with a range of $0 \le X \le 100$.

#### Solution

This is the same analysis performed in the previous experiment, but now the differences between values are smaller in comparison to the previous distribution. Therefore, we would expect the discrete and continuous results to be closer in value. First, treating $X$ as a discrete variable, we get

$$P_{total} = \sum_{X=0}^{100} e^{-0.05X} = 20.4$$

Next, treating $X$ as continuous

$$P_{total} = \int_0^{100} e^{-0.05X}\, dX = 19.9$$

Comparison of these results demonstrates that the difference between the discrete and continuous treatments is smaller for this more "fine-grain" distribution.

# 12.6 Characterizing Distribution Functions

Distribution functions provide all the probability information available for a given system; however, there will be times when a full description of the distribution function is not required. For example, imagine a series of experiments in which only certain aspects of a molecular distribution are studied, and the aspects of the distribution function of interest are those addressed by experiment. Consider the translational kinetic energy distribution depicted in Figure 12.6. What if all we were interested in was the kinetic energy where the probability distribution function was at a maximum? In this case, full knowledge of the probability distribution is not needed. Instead, a single quantity for comparison to experiment, or a "benchmark" value, is all that is needed. In this section, benchmark values of substantial utility when characterizing distribution functions are presented.

## 12.6.1 Average Values

The **average value** of a quantity is perhaps the most useful way to characterize a distribution function. Consider a function $g(X)$ whose value is dependent on variable $X$. The average value of this function is dependent on the probability distribution associated with the variable $X$. If the probability distribution describing the likelihood of $X$ assuming some value is known, this distribution can be employed to determine the average value for the function as follows:

$$\langle g(X) \rangle = \sum_{i=1}^{M} g(X_i) P(X_i) = \frac{\displaystyle\sum_{i=1}^{M} g(X_i) f_i}{\displaystyle\sum_{i=1}^{M} f_i} \tag{12.32}$$

Equation (12.32) states that in order to determine the average value of the function $g(X)$, one simply sums the values of this function determined for each value of the sample set, $\{X_1, X_2, \ldots, X_M\}$, multiplied by the probability of the variable assuming this value. The summation in the denominator provides for normalization of the probability distribution. The angle brackets around $g(X)$ denotes the average value of the function, a quantity that is also referred to as an **expectation value.**

---

### EXAMPLE PROBLEM 12.12

Imagine that you are at a carnival and observe a dart game in which you throw a single dart at the following target:
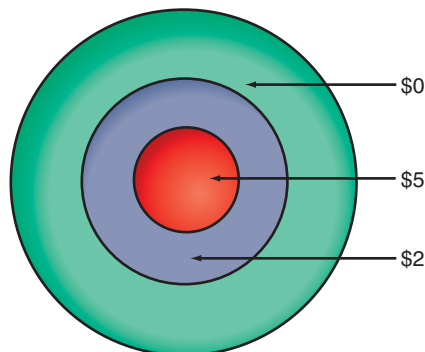
The dollar amounts in the figure indicate the amount of money you will win if you hit the corresponding part of the target with your dart. The geometry of the target is such that the radii of the circles increase linearly between successive areas. Finally, you are a sufficiently accomplished dart thrower that you will not miss the target altogether. If it costs you $1.50 each time you throw a dart, is this carnival game something you should play?

### Solution

We will assume that the probability of hitting each section of the target is directly proportional to the area. If the radius of the inner circle is $r$, then the radii of the second and third circles are $2r$ and $3r$, respectively. The area of the inner curve $A_1$ is $\pi r^2$ and the areas of the outer two circles are

$$A_2 = \pi(2r)^2 - \pi r^2 = 3A_1$$

$$A_3 = \pi(3r)^2 - \pi(2r)^2 = 5A_1$$

Finally, total area is given by the sum of the individual areas, or $9A_1$, such that the probability of hitting each part of the target is

$$f_1 = \frac{A_1}{A_1 + A_2 + A_3} = \frac{A_1}{9A_1} = \frac{1}{9}$$

$$f_2 = \frac{A_2}{A_1 + A_2 + A_3} = \frac{3A_1}{9A_1} = \frac{3}{9}$$

$$f_3 = \frac{A_3}{A_1 + A_2 + A_3} = \frac{5A_1}{9A_1} = \frac{5}{9}$$

The sum of probabilities equals 1 so that the probability distribution is normalized. The quantity of interest is the average payout, or $\langle n_\$ \rangle$, given by

$$\langle n_\$ \rangle = \frac{\sum_{i=1}^{3} n_{\$,i} f_i}{\sum_{i=1}^{3} f_i} = \frac{(\$5)\dfrac{1}{9} + (\$2)\dfrac{3}{9} + (\$0)\dfrac{5}{9}}{1} = \$1.22$$

Comparison of the average payout to the amount you pay to throw a dart ($1.50) suggests that this game is a money-losing activity (from the dart-thrower's perspective). Notice in this example that the "experimental" quantities you are comparing are the amount of money you have to pay and the amount of money you can expect to receive on average, which is the benchmark of the distribution of primary interest when you make a decision to play.

## 12.6.2  Distribution Moments

Some of the most widely used benchmark values for distributions involve functions of the form $\langle x^n \rangle$ where $n$ is an integer. If $n = 1$, the corresponding function $\langle x \rangle$ is referred to as the **first moment** of the distribution function, and it is equal to the average value of the distribution as discussed earlier. If $n = 2$, $\langle x^2 \rangle$ is referred to as the **second moment** of the distribution. Finally, the square root of $\langle x^2 \rangle$ is referred to as the root-mean-squared or "rms" value. The first and second moments, as well as the rms value, are extremely useful quantities for characterizing distribution functions of atomic and molecular properties. For example, in the upcoming discussion of molecular motion in Chapter 16 we will find that a collection of molecules will have a distribution of speeds. Rather than discussing the entire speed distribution, the moments of the distribution are instead used to describe the system of interest. **Distribution moments** are readily calculated for both discrete and continuous distributions as Example Problem 12.13 illustrates.

**EXAMPLE PROBLEM 12.13**

Consider the following distribution function:

$$P(x) = Cx^2 e^{-ax^2}$$

Probability distributions of this form are encountered when describing speed distributions of ideal gas particles. In this probability distribution function, $C$ is a normalization constant that ensures the total probability is equal to one, and $a$ is also a constant that depends on atomic or molecular properties and temperature. The domain of interest is given by $\{0 \leq x \leq \infty\}$. Are the mean and rms values for this distribution the same?

**Solution**

First, the normalization condition is applied to the probability:

$$1 = \int_0^\infty Cx^2 e^{-ax^2}\,dx = C\int_0^\infty x^2 e^{-ax^2}\,dx$$

The integral is easily evaluated using the integral tables provided in Appendix B, Math Supplement:

$$\int_0^\infty x^2 e^{-ax^2}\,dx = \frac{1}{4a}\sqrt{\frac{\pi}{a}}$$

resulting in the following definition for the normalization constant:

$$C = \frac{1}{\frac{1}{4a}\sqrt{\frac{\pi}{a}}} = \frac{4a^{3/2}}{\sqrt{\pi}}$$

With this normalization constant, the mean and rms values of the distribution function can be determined. The mean is equal to $\langle x \rangle$, which is determined as follows:

$$\langle x \rangle = \int_0^\infty xP(x)\,dx = \int_0^\infty x\left(\frac{4a^{3/2}}{\sqrt{\pi}}x^2 e^{-ax^2}\right)dx$$

$$= \frac{2}{\sqrt{\pi a}}$$

Proceeding in a similar fashion for the second moment ($\langle x^2 \rangle$),

$$\langle x^2 \rangle = \int_0^\infty x^2 P(x)\,dx = \int_0^\infty x^2\left(\frac{4a^{3/2}}{\sqrt{\pi}}x^2 e^{-ax^2}\right)dx$$

$$= \frac{3}{2a}$$

The resulting rms value is:

$$\text{rms} = \sqrt{\langle x^2 \rangle} = \sqrt{\frac{3}{2a}}$$

The mean and rms values for the distribution are not equivalent. The normalized distribution and the location of the mean and rms values for the case where $a = 0.3$ are shown here:
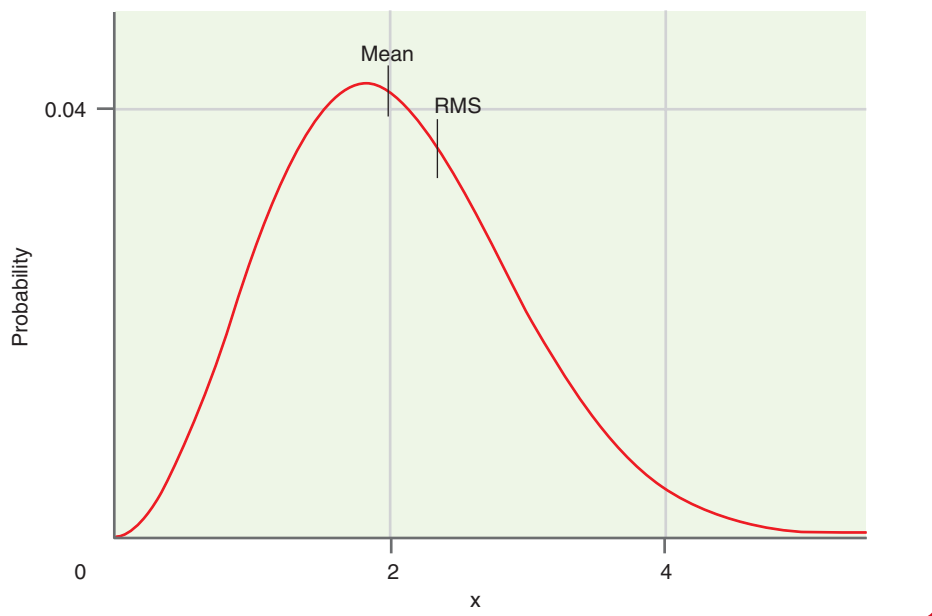


### 12.6.3 Variance

The **variance** (denoted as $\sigma^2$) provides a measure of the width of a distribution. The variance is defined as the average deviation squared from the mean of the distribution:

$$\sigma^2 = \langle (x - \langle x \rangle)^2 \rangle = \langle x^2 - 2x\langle x \rangle + \langle x \rangle^2 \rangle \qquad (12.33)$$

It is important to remember that the value for the mean (or first moment $\langle x \rangle$) is a constant and should not be confused with the variable $x$. Equation (12.33) can be simplified by using the following two general properties for the averages involving two functions, $b(x)$ and $d(x)$:

$$\langle b(x) + d(x) \rangle = \langle b(x) \rangle + \langle d(x) \rangle \qquad (12.34)$$

$$\langle cb(x) \rangle = c\langle b(x) \rangle \qquad (12.35)$$

In the second property, $c$ is simply a constant. Using these properties the expression for variance becomes:

$$\sigma^2 = \langle x^2 - 2x\langle x \rangle + \langle x \rangle^2 \rangle = \langle x^2 \rangle - \langle 2x\langle x \rangle \rangle + \langle x \rangle^2$$

$$= \langle x^2 \rangle - 2\langle x \rangle \langle x \rangle + \langle x \rangle^2$$

$$\sigma^2 = \langle x^2 \rangle - \langle x \rangle^2 \qquad (12.36)$$

In other words, the variance of a distribution is equal to the difference between the second moment and the square of the first moment.

To illustrate the use of variance as a benchmark, consider the following distribution function, which is referred to as a **Gaussian distribution:**

$$P(X)\, dX = \frac{1}{(2\pi\sigma^2)^{1/2}} e^{-(X-\delta)^2/2\sigma^2} \qquad (12.37)$$

The Gaussian distribution is the "bell-shaped curve" of renown in the social sciences, employed widely through chemistry and physics and well known to any college students concerned about their course grade. It is the primary distribution function utilized to describe error in experimental measurements. The variable $X$ is continuous in the domain

**FIGURE 12.7**
The influence of variance on Gaussian probability distribution functions. The figure presents the evolution in probability $P(X)$ as a function of the variable $X$. The distributions for two values of the variance of the distribution $\sigma^2$ are presented: 2.0 (red line) and 0.4 (purple line). Notice that an increase in the variance corresponds to an increase in the width of the distribution.
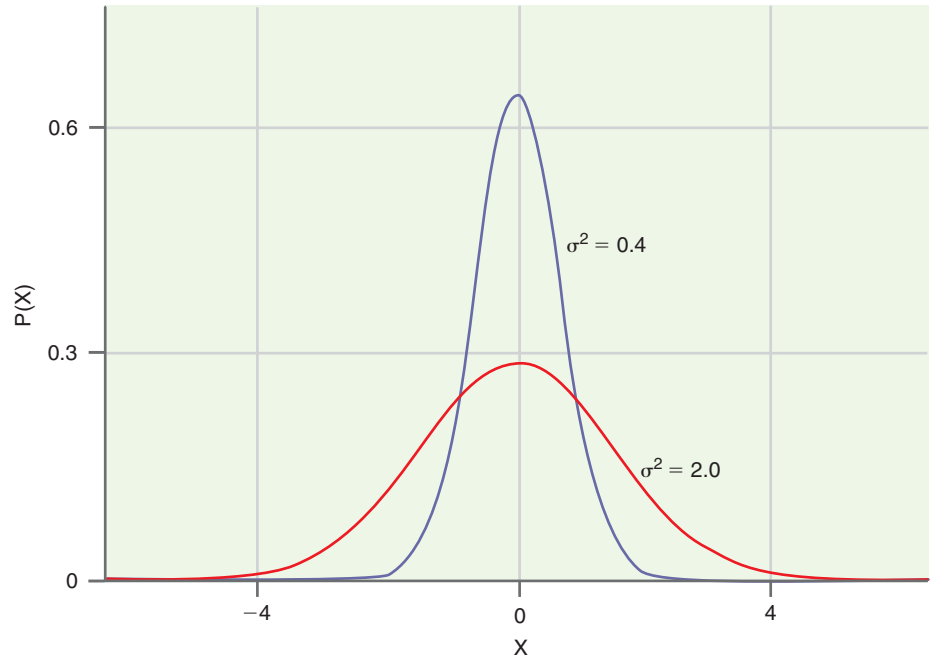


from negative infinity to infinity, $\{-\infty \leq X \leq \infty\}$. The Gaussian probability distribution has a maximum at $X = \delta$. The width of the distribution is determined by the variance $\sigma^2$ with an increase in the variance corresponding to increased width. The dependence of the Gaussian distribution on variance is illustrated in Figure 12.7 using Equation (12.37) with $\delta = 0$. As the variance of the distribution increases from $\sigma^2 = 0.4$ to 2.0, the width of the probability distribution increases.

---

**EXAMPLE PROBLEM 12.14**

Determine the variance for the distribution function $P(x) = Cx^2 e^{-ax^2}$.

**Solution**

This is the distribution function employed in Example Problem 12.13, and we have for the first and second moments

$$\langle x \rangle = \frac{2}{\sqrt{\pi a}}$$

$$\langle x^2 \rangle = \frac{3}{2a}$$

Using these values in the expression for variance, we find

$$\sigma^2 = \langle x^2 \rangle - \langle x \rangle^2 = \frac{3}{2a} - \left(\frac{2}{\sqrt{\pi a}}\right)^2$$

$$= \frac{3}{2a} - \frac{4}{\pi a} = \frac{0.23}{a}$$

---

# Vocabulary

| | | |
|---|---|---|
| average values | bosons | discrete variable |
| Bernoulli trial | complement | distribution moments |
| binomial experiment | configuration | event probability |
| Bose–Einstein statistics | continuous variable | expectation value |

| factorial | permutation | sample space |
|---|---|---|
| Fermi–Dirac statistics | Poisson distribution | second moment |
| fermions | probability | Stirling's approximation |
| first moment | probability density | variable |
| fundamental counting principle | probability distribution function | variance |
| Gaussian distribution | probability model | |

# Conceptual Problems

**Q12.1**   What is the difference between a configuration and a permutation?

**Q12.2**   What are the elements of a probability model, and how do they differ for continuous and discrete variables?

**Q12.3**   How does Figure 12.2 change if one is concerned with two versus three colored-ball configurations and permutations?

**Q12.4**   What is Stirliing's Approximation? Why is it useful? When is it applicable?

**Q12.5**   What is a Bernoulli Trial?

**Q12.6**   What must the outcome of a binomial experiment be if $P_E = 1$?

**Q12.7**   Why is normalization of a probability distribution important? What would one have to consider when working with a probability distribution that was not normalized?

**Q12.8**   When can one make the approximation of treating a probability distribution involving discrete variables as continuous?

**Q12.9**   What properties of atomic and molecular systems could you imagine describing using probability distributions?

**Q12.10**   What is the difference between average and root-mean-squared?

**Q12.11**   When is the higher moment of a probability distribution more useful as a benchmark value as opposed to simply using the mean of the distribution?

# Numerical Problems

Problem numbers in **red** indicate that the solution to the problem is given in the *Student's Solutions Manual.*

**P12.1**   Suppose that you draw a card from a standard deck of 52 cards. What is the probability of drawing

**a.** an ace of any suit?

**b.** the ace of spades?

**c.** How would your answers to parts (a) and (b) change if you were allowed to draw three times, replacing the card drawn back into the deck after each draw?

**P12.2**   You are dealt a hand consisting of 5 cards from a standard deck of 52 cards. Determine the probability of obtaining the following hands:

**a.** flush (five cards of the same suit)

**b.** a king, queen, jack, ten, and ace of the same suit (a "royal flush")

**P12.3**   A pair of standard dice are rolled. What is the probability of observing the following:

**a.** The sum of the dice is equal to 7.

**b.** The sum of the dice is equal to 9.

**c.** The sum of the dice is less than or equal to 7.

**P12.4**   Answer Problem P12.3 assuming that "shaved" dice are used so that the number 6 appears twice as often as any other number.

**P12.5**   **a.**  Consider assigning phone numbers to an area where each number consists of seven digits, each of which can be between 0 and 9. How many phone numbers can be assigned to the area?

**b.** To serve multiple areas, you decide to introduce an area code that serves as an identifier. In the United States, area codes were initially three-digit numbers in which the first digit ranged from 2 to 9, the second digit was either 0 or 1, and the third digit ranged from 1 to 9. How many areas could be specified using this system?

**c.** Using area codes with individual phone numbers, how many unique phones could this system support?

**P12.6**   Proteins are made up of individual molecular units of unique structure known as amino acids. The order or "sequence" of amino acids is an important factor in determining protein structure and function. There are 20 naturally occurring amino acids.

**a.** How many unique proteins consisting of 8 amino acids are possible?

**b.** How does your answer change if a specific amino acid can only appear once in the protein?

**P12.7**   Atomic chlorine has two naturally occurring isotopes, $^{35}Cl$ and $^{37}Cl$. If the molar abundance of these isotopes are 75.4% and 24.6%, respectively, what fraction of a mole of molecular chlorine ($Cl_2$) will have one of each isotope? What fraction will contain just the $^{35}Cl$ isotope?

**P12.8**   The natural molar abundance of $^{13}C$ is roughly 1%. What is the probability of having a single $^{13}C$ isotope in

benzene ($C_6H_6$)? What is the probability that two $^{13}C$ isotopes will be adjacent to each other in benzene?

**P12.9**   Evaluate the following:

**a.** the number of permutations employing all objects in a six-object set

**b.** the number of permutations employing four objects from a six-object set

**c.** the number of permutations employing no objects from a six-object set

**d.** $P(50,10)$

**P12.10**   Determine the number of permutations of size 3 that can be made from the set $\{1, 2, 3, 4, 5, 6\}$. Write down all of the permutations.

**P12.11**   Determine the numerical values for the following:

**a.** the number of configurations employing all objects in a six-object set

**b.** the number of configurations employing four objects from a six-object set

**c.** the number of configurations employing no objects from a six-object set

**d.** $C(50,10)$

**P12.12**   Radio station call letters consist of four letters (for example, KUOW).

**a.** How many different station call letters are possible using the 26 letters in the English alphabet?

**b.** Stations west of the Mississippi River must use the letter K as the first call letter. Given this requirement, how many different station call letters are possible if repetition is allowed for any of the remaining letters?

**c.** How many different station call letters are possible if repetition is not allowed for any of the letters?

**P12.13**   Four bases (A, C, T, and G) appear in DNA. Assume that the appearance of each base in a DNA sequence is random.

**a.** What is the probability of observing the sequence AAGACATGCA?

**b.** What is the probability of finding the sequence GGGGGAAAAA?

**c.** How do your answers to parts (a) and (b) change if the probability of observing A is twice that of the probabilities used in parts (a) and (b) of this question when the preceding base is G?

**P12.14**   The natural abundance of $^{13}C$ is roughly 1%, and the abundance of deuterium ($^2H$ or D) is 0.015%. Determine the probability of finding the following in a mole of acetylene:

**a.** H-$^{13}C$-$^{13}C$-H

**b.** D-$^{12}C$-$^{12}C$-D

**c.** H-$^{13}C$-$^{12}C$-D

**P12.15**   In the neck of the flask depicted in the following figure, five red balls rest on five blue balls. Suppose the balls are tipped back into the flask, shaken, and the flask is reinverted. What is the probability that the order depicted in the figure will be seen?
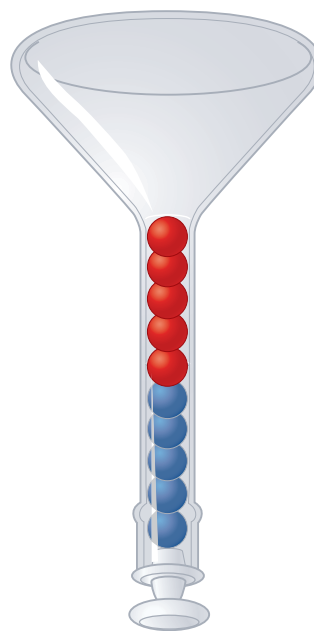


**P12.16**   The Washington State Lottery consists of drawing five balls numbered 1 to 43 and a single ball numbered 1 to 23 from a separate machine.

**a.** What is the probability of hitting the jackpot in which the values for all six balls are correctly predicted?

**b.** What is the probability of predicting just the first five balls correctly?

**c.** What is the probability of predicting the first five balls in the exact order they are picked?

**P12.17**   Fermions and bosons demonstrate different distribution statistics over a set of quantum states. However, in Chapter 13 we will encounter the Boltzmann distribution, in which we essentially ignore the differentiation between fermions and bosons. This is appropriate only in the "dilute limit" in which the number of available states far outnumbers the number of particles. To illustrate this convergence

**a.** determine the number of arrangement permutations possible for 3 bosons and 10 states, and repeat this calculation for fermions.

**b.** repeat the calculations from part (a) for 3 particles, but now 100 states. What do you notice about the difference between the two results?

**P12.18**   Consider the 25 players on a professional baseball team. At any point, 9 players are on the field.

**a.** How many 9-player batting orders are possible given that the order of batting is important?

**b.** How many 9-player batting orders are possible given that the all-star designated hitter must be batting in the fourth spot in the order?

**c.** How many 9-player fielding teams are possible under the assumption that the location of the players on the field is not important?

**P12.19**   Imagine an experiment in which you flip a coin 4 times. Furthermore, the coin is balanced fairly such that the probability of landing heads or tails is equivalent. After

tossing the coin 10 times, what is the probability of observing the following specific outcomes:

**a.** no heads

**b.** two heads

**c.** five heads

**d.** eight heads

**P12.20**  Imagine performing the coin-flip experiment of Problem P12.19, but instead of using a fair coin, a weighted coin is employed for which the probability of landing heads is two-fold greater than landing tails. After tossing the coin 10 times, what is the probability of observing the following specific outcomes:

**a.** no heads

**b.** two heads

**c.** five heads

**d.** eight heads

**P12.21**  In Chapter 17 we will model particle diffusion as a random walk in one dimension. In such processes, the probability of moving an individual step in the $+x$ or $-x$ direction is equal to $1/2$. Imagine starting at $x = 0$ and performing a random walk in which 20 steps are taken.

**a.** What is the farthest distance the particle can possibly move in the $+x$ direction? What is the probability of this occurring?

**b.** What is the probability the particle will not move at all?

**c.** What is the probability of the particle moving half the maximum distance in the $+x$ direction?

**d.** Plot the probability of the particle moving a given distance versus distance. What does the probability distribution look like? Is the probability normalized?

**P12.22**  Simplify the following expressions:

**a.** $\dfrac{n!}{(n-2)!}$

**b.** $\dfrac{n!}{\left(\dfrac{n}{2}!\right)^2}$ (for even $n$)

**P12.23**  Another form of Stirling's approximation is

$$N! = \sqrt{2\pi N}\left(\frac{N}{e}\right)^N$$

Use this approximation for $N = 10, 50, 100$ and compare your results to those given in Example Problem 2.9 in *Quantum Chemistry & Spectroscopy*.

**P12.24**  You are at a carnival and are considering playing the dart game described in Example Problem 12.12; however, you are confident of your dart-throwing skills such that the probability of hitting the center area of the target is three times greater than the probability determined by area. Assuming the confidence in your skills is warranted, is it a good idea to play?

**P12.25**  Radioactive decay can be thought of as an exercise in probability theory. Imagine that you have a collection of radioactive nuclei at some initial time ($N_0$) and are interested in how many nuclei will still remain at a later time ($N$). For first-order radioactive decay, $N/N_0 = e^{-kt}$. In this expression, $k$ is known as the decay constant and $t$ is time.

**a.** What is the variable of interest in describing the probability distribution?

**b.** At what time will the probability of nuclei undergoing radioactive decay be 0.50?

**P12.26**  First order decay processes as described in the previous problem can also be applied to a variety of atomic and molecular processes. For example, in aqueous solution the decay of singlet molecular oxygen ($O_2(^1\Delta_g)$) to the ground-state triplet configuration proceeds according to

$$\frac{[O_2(^1\Delta_g)]}{[O_2(^1\Delta_g)]_0} = e^{-(2.4\times 10^5\,\mathrm{s}^{-1})t}$$

In this expression, $[O_2(^1\Delta_g)]$ is the concentration of singlet oxygen at a given time, and the subscript "0" indicates that this is the concentration of singlet oxygen present at the beginning of the decay process corresponding to $t = 0$.

**a.** How long does one have to wait until 90% of the singlet oxygen has decayed?

**b.** How much singlet oxygen remains after $t = (2.4 \times 10^5\,\mathrm{s}^{-1})^{-1}$?

**P12.27**  In a subsequent chapter we will encounter the energy distribution $P(\varepsilon) = Ae^{-\varepsilon/kT}$, where $P(\varepsilon)$ is the probability of a molecule occupying a given energy state, $\varepsilon$ is the energy of the state, $k$ is a constant equal to $1.38 \times 10^{-23}\,\mathrm{J\,K^{-1}}$, and $T$ is temperature. Imagine that there are three energy states at 0, 100., and 500. J mol$^{-1}$.

**a.** Determine the normalization constant for this distribution.

**b.** What is the probability of occupying the highest energy state at 298 K?

**c.** What is the average energy at 298 K?

**d.** Which state makes the largest contribution to the average energy?

**P12.28**  Assume that the probability of occupying a given energy state is given by the relationship provided in Problem P12.27.

**a.** Consider a collection of three total states with the first state located at $\varepsilon = 0$ and others at $kT$ and $2kT$, respectively, relative to this first state. What is the normalization constant for the probability distribution?

**b.** How would your answer change if there are five states with $\varepsilon = kT$ in addition to the single states at $\varepsilon = 0$ and $\varepsilon = 2kT$?

**c.** Determine the probability of occupying the energy level $\varepsilon = kT$ for the cases in which one and five states exist at this energy.

**P12.29**  Consider the following probability distribution corresponding to a particle located between point $x = 0$ and $x = a$:

$$P(x)\,dx = C\sin^2\left[\frac{\pi x}{a}\right]dx$$

**a.** Determine the normalization constant $C$.

**b.** Determine $\langle x \rangle$.

**c.** Determine $\langle x^2 \rangle$.

**d.** Determine the variance.

**P12.30** Consider the probability distribution for molecular velocities in one dimension ($v_x$) given by
$P(v_x)\,dv_x = Ce^{-mv^2_x/2kT}dv_x$.

**a.** Determine the normalization constant $C$.

**b.** Determine $\langle v_x \rangle$.

**c.** Determine $\langle v_x^2 \rangle$.

**d.** Determine the variance.

**P12.31** One classic problem in quantum mechanics is the "harmonic oscillator." In this problem a particle is subjected to a one-dimensional potential (taken to be along $x$) of the form $V(x) \propto x^2$ where $-\infty \le x \le \infty$. The probability distribution function for the particle in the lowest-energy state is

$$P(x) = Ce^{-ax^2/2}$$

Determine the expectation value for the particle along $x$ (that is, $\langle x \rangle$). Can you rationalize your answer by considering the functional form of the potential energy?

**P12.32** A crude model for the molecular distribution of atmospheric gases above Earth's surface (denoted by height $h$) can be obtained by considering the potential energy due to gravity:

$$P(h) = e^{-mgh/kT}$$

In this expression $m$ is the per-particle mass of the gas, $g$ is the acceleration due to gravity, $k$ is a constant equal to $1.38 \times 10^{-23}$ J K$^{-1}$, and $T$ is temperature. Determine $\langle h \rangle$ for methane ($CH_4$) using this distribution function.

**P12.33** Another use of distribution functions is determining the most probable value, which is done by realizing that at the distribution maximum the derivative of the distribution function with respect to the variable of interest is zero. Using this concept, determine the most probable value of $x$ ($0 \le x \le \infty$) for the following function:

$$P(x) = Cx^2e^{-ax^2}$$

Compare your result to $\langle x \rangle$ and $x_{rms}$ when $a = 0.3$ (see Example Problem 12.13).

**P12.34** In nonlinear optical switching devices based on dye-doped polymer systems, the spatial orientation of the dye molecules in the polymer is an important parameter. These devices are generally constructed by orienting dye molecules with a large dipole moment using an electric field. Imagine placing a vector along the molecular dipole moment such that the molecular orientation can be described by the orientation of this vector in space relative to the applied field ($z$ direction) as illustrated here:
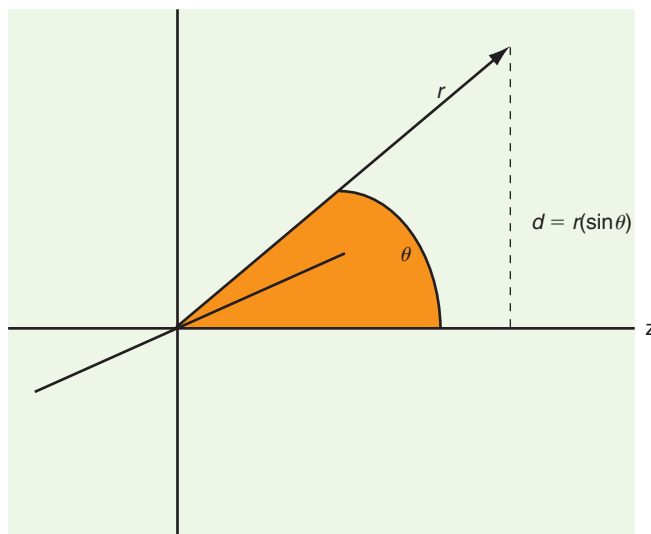


For random molecular orientation about the $z$ axis, the probability distribution describing molecular orientation along the $z$ axis is given by $P(\theta) = \sin\theta\,d\theta / \int_0^\pi \sin\theta\,d\theta$. Orientation is quantified using moments of $\cos\theta$.

**a.** Determine $\langle \cos\theta \rangle$ for this probability distribution.

**b.** Determine $\langle \cos^2\theta \rangle$ for this probability distribution.

**P12.35** The **Poisson distribution** is a widely used discrete probability distribution in science:

$$P(x) = \frac{e^{-\lambda}\lambda^x}{x!}$$

This distribution describes the number of events ($x$) occurring in a fixed period of time. The events occur with a known average rate corresponding to $\lambda$, and event occurrence does not depend on when other events occur. This distribution can be applied to describe the statistics of photon arrival at a detector as illustrated by the following:

**a.** Assume that you are measuring a light source with an average output of 5 photons per second. What is the probability of measuring 5 photons in any 1-second interval?

**b.** For this same source, what is the probability of observing 8 photons in any 1-second interval?

**c.** Assume a brighter photon source is employed with an average output of 50 photons per second. What is the probability of observing 50 photons in any 1-second interval?

# For Further Reading

Bevington, P., and D. Robinson. *Reduction and Error Analysis for the Physical Sciences*. New York: McGraw-Hill, 1992.

Dill, K., and S. Bromberg. *Molecular Driving Forces*. New York: Garland Science, 2003.

McQuarrie, D. *Mathematical Methods for Scientists and Engineers*. Sausalito, CA: University Science Books, 2003.

Nash, L. K. *Elements of Statistical Thermodynamics*. San Francisco: Addison-Wesley, 1972.

Ross, S. *A First Course in Probability Theory*, 3rd ed. New York: Macmillan, 1988.

Taylor, J. R. *An Introduction to Error Analysis*. Mill Valley, CA: University Science Books, 1982.

# 13

# The Boltzmann Distribution

Employing statistical concepts, one can determine the most probable distribution of energy in a chemical system. This distribution, referred to as the Boltzmann distribution, represents the most probable configuration of energy for a chemical system at equilibrium and also gives rise to the thermodynamic properties of the system. In this chapter, the Boltzmann distribution is derived starting with the probability concepts introduced in the previous chapter. This distribution is then applied to some elementary examples to demonstrate how the distribution of energy in a chemical system depends on both the available energy and the energy-level spacings that characterize the system. The concepts outlined here provide the conceptual framework required to apply statistical mechanics to atomic and molecular systems.

## 13.1 Microstates and Configurations

We begin by extending the concepts of probability theory introduced in the previous chapter to chemical systems. Although such an extension of probability theory may appear difficult, the sheer size of chemical systems makes the application of these statistical concepts straightforward. Recall the discussion of permutations and configurations illustrated by tossing a coin four times. The possible outcomes for this experiment are presented in Figure 13.1.

Figure 13.1 illustrates that there are five possible outcomes for the trial: from no heads to all heads. Which of these trial outcomes is most likely? Using probability theory, we found that the most probable outcome will be the one with the most possible ways to achieve that outcome. In the coin toss example, the configuration "2 Head" has the greatest number of ways to achieve this configuration; therefore, the "2 Head" configuration represents the most likely outcome. In the language of probability theory, the configuration with the largest number of corresponding permutations will be the most likely trial outcome. As discussed in the previous chapter, the probability $P_E$ of this configuration representing the trial outcome is given by

$$P_E = \frac{E}{N} \tag{13.1}$$

**317**
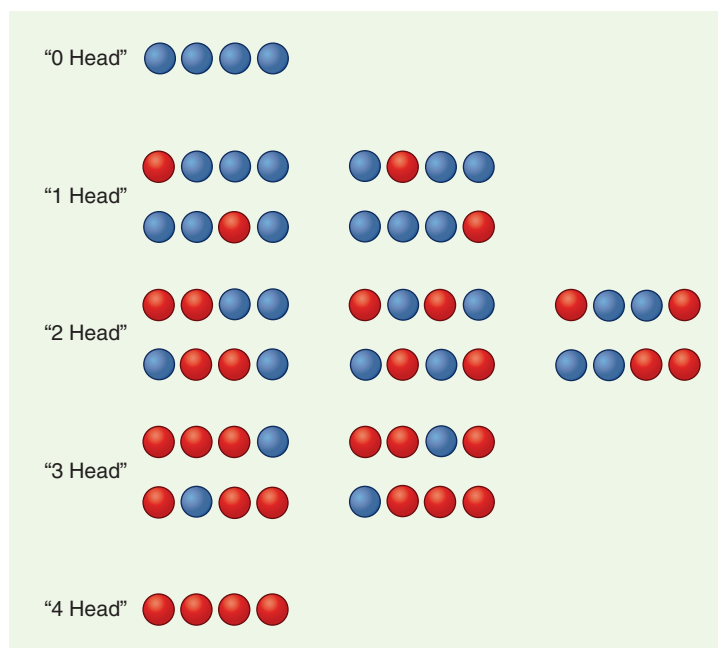
where $E$ is the number of permutations associated with the event of interest, and $N$ is the total number of possible permutations. This relatively simple equation provides the key idea for this entire chapter: *the most likely configurational outcome for a trial is the configuration with the greatest number of associated permutations*. The application of this idea to macroscopic chemical systems is aided by the fact that for systems containing a large number of units, one configuration will have vastly more associated permutations than any other configuration. As such, this configuration will be the only one that is observed to an appreciable extent.

The application of probability theory to chemical systems is achieved by considering system energy. Specifically, we are interested in developing a formalism that is capable of identifying the most likely configuration or distribution of energy in a chemical system. To begin, consider a simple "molecular" system consisting of three quantum harmonic oscillators that share a total of three quanta of energy. The energy levels for the oscillators are given by

$$E_n = h\nu\left(n + \frac{1}{2}\right) \quad \text{for } n = 0, 1, 2, \ldots, \infty \qquad \textbf{(13.2)}$$

In this equation, $h$ is Planck's constant, $\nu$ is the oscillator frequency, and $n$ is the quantum number associated with a given energy level of the oscillator. This quantum number can assume integer values starting at 0 and increasing to infinity; therefore, the energy levels of the quantum harmonic oscillator consist of a ladder or "manifold" of equally spaced levels. The lowest level ($n = 0$) has an energy of $h\nu/2$ referred to as the zero point energy. Employed here is a modified version of the harmonic oscillator in which the ground-state energy ($n = 0$) is zero so that the level energies are given by

$$E_n = h\nu n \quad \text{for } n = 0, 1, 2, \ldots, \infty \qquad \textbf{(13.3)}$$

When considering atomic and molecular systems in the upcoming chapters, the relative difference in energy levels will prove to be the relevant quantity of interest, and a similar modification will be employed. The final important point to note is that the oscillators are distinguishable. That is, each oscillator in the three-oscillator collection can be readily identified. This assumption must be relaxed when describing molecular systems such as an ideal gas because atomic or molecular motion prohibits identification of each gaseous particle. The extension of this approach to indistinguishable particles is readily accomplished; therefore, starting with the distinguishable case will not prove problematic.

In this example system, the three oscillators are of equal frequency such that the energy levels for all three are identical. Three quanta of energy are placed into this system, and we ask the question "What is the most probable distribution of energy?" From the preceding discussion, probability theory dictates that the most likely distribution of energy corresponds to the configuration with the largest number of associated permutations. How can the concepts of configuration and permutations be connected to oscillators and energy? Two central definitions are introduced here that will prove useful in making this connection: a **configuration** is a general arrangement of total energy available to the system, and a **microstate** is a specific arrangement of energy that describes the energy contained by each individual oscillator. This definition of a configuration is equivalent to the definition of configuration from Chapter 12, and microstates are equivalent to permutations. To determine the most likely configuration of energy in the example system, we will simply count all of the possible microstates and arrange them with respect to their corresponding configurations.

In the first configuration depicted in Figure 13.2, each oscillator has one quantum of energy such that all oscillators populate the $n = 1$ energy level. Only one permutation is associated with this configuration. In terms of the nomenclature just introduced, there is one microstate corresponding to this energy configuration. In the next configuration illustrated in the figure, one oscillator contains two quanta of energy, a second contains one quantum of energy, and a third contains no energy. Six potential arrangements correspond to this general distribution of energy; that is, six microstates correspond to this configuration. The last configuration depicted is one in which all three quanta of energy reside on a single oscillator. Because there are three choices for which oscillator will have all three quanta of energy, there are three corresponding microstates for this configuration. It is important to note that the total energy of all of the arrangements just mentioned is the same and that the only difference is the distribution of the energy over the oscillators.

Which configuration of energy would we expect to observe? Just like the coin tossing example, we expect to see the energy configuration that has the largest number of microstates. In this example, that configuration is the second one discussed, or the "2, 1, 0" configuration. If all microstates depicted have an equal probability of being observed, the probability of observing the 2, 1, 0 configuration is simply the number of microstates associated with this configuration divided by the total number of microstates available, or

$$P_E = \frac{E}{N} = \frac{6}{6 + 3 + 1} = \frac{6}{10} = 0.6$$

Note that although this example involves a "molecular" system, the concepts encountered can be generalized to probability theory. Whether tossing a coin or distributing energy among distinguishable oscillators, the ideas are the same.

## 13.1.1 Counting Microstates and Weight

The three-oscillator example provides an approach for finding the most probable configuration of energy for a chemical system: determine all of the possible configurations of energy and corresponding microstates and identify the configuration with the greatest number of microstates. Clearly, this would be an extremely laborious task for a chemical system of interesting size. Fortunately, there are ways to obtain a quantitative count of all of the microstates associated with a given configuration without actually "counting" them. First, recall from Chapter 12 that the total number of possible permutations given $N$ objects is $N!$ For the most probable 2, 1, 0 configuration described earlier, there are three objects of interest (i.e., three oscillators) such that $N! = 3! = 6$. This is exactly the same number of microstates associated with this configuration. But what of the other configurations? Consider the 3, 0, 0 configuration in which one oscillator has all three quanta of energy. In assigning quanta of energy to this system to construct each microstate, there are three choices of where to place the three quanta of energy, and two remaining choices for zero quanta. However, this latter choice is redundant in that it does not matter which oscillator receives zero quanta first. The two
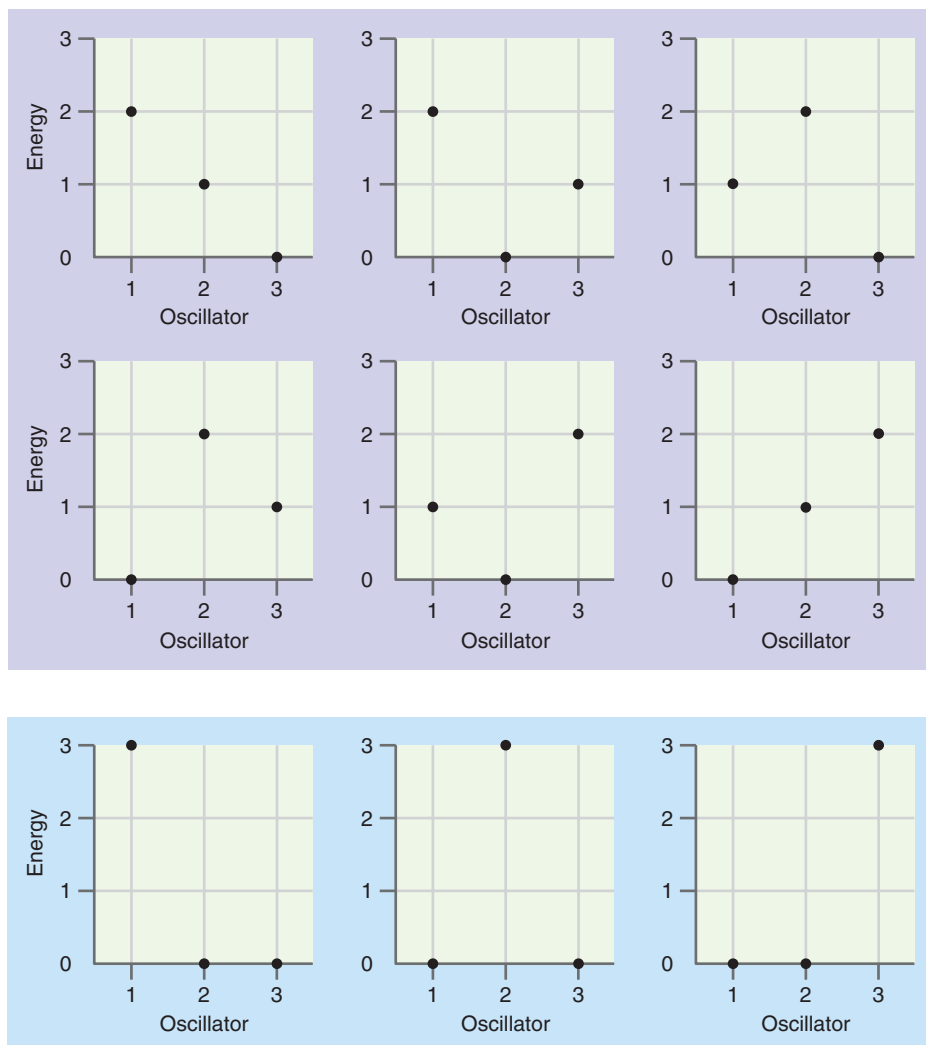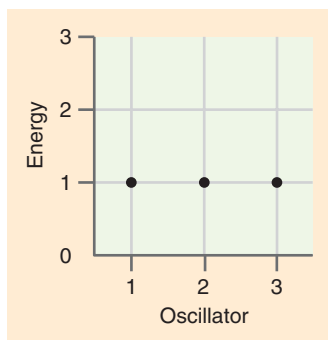
conceptually different arrangements correspond to exactly the same microstate and, thus, are indistinguishable. To determine the number of microstates associated with such distributions of energy, the total number of possible permutations is divided by a factor that corrects for overcounting, which for the '3, 0, 0' configuration is accomplished as follows:

$$\text{Number of microstates} = \frac{3!}{2!} = 3$$

This expression is simply the probability for the number of expression permutations available using a subgroup from an overall group of size $N$. Therefore, if no two oscillators reside in the same energy level, then the total number of microstates available is given by $N!$, where $N$ is the number of oscillators. However, if two or more oscillators

occupy the same energy state (including the zero-energy state), then we need to divide by a term that corrects for overcounting of identical permutations. The total number of microstates associated with a given configuration of energy is referred to as the **weight** of the configuration, $W$, which is given by

$$W = \frac{N!}{a_0! a_1! a_2! \dots a_n!} = \frac{N!}{\prod_j a_j!} \tag{13.4}$$

In Equation (13.4), $W$ is the weight of the configuration of interest, $N$ is the number of units over which energy is distributed, and the $a_n$ terms represent the number of units occupying the $n$th energy level. The $a_n$ quantities are referred to as **occupation numbers** because they describe how many units occupy a given energy level. For example, in the 3, 0, 0 configuration presented in Figure 13.2, $a_0 = 2$, $a_3 = 1$, and all other $a_n = 0$ (with $0! = 1$). The denominator in our expression for weight is evaluated by taking the product of the factorial of the occupation numbers ($a_n!$), with the product of these values denoted by the $\prod$ symbol (which is analogous to the $\Sigma$ symbol denoting summation). Equation (13.4) is not limited to our specific example but is a general relationship that applies to any collection of distinguishable units for which only one state is available at a given energy level. The situation in which multiple states exist at a given energy level is discussed later in this chapter.

### EXAMPLE PROBLEM 13.1

What is the weight associated with the configuration corresponding to observing 40 heads after flipping a coin 100 times? How does this weight compare to that of the most probable outcome?

#### Solution

Using the expression for weight in Equation (13.4), the coin flip can be envisioned as a system in which two states can be populated: heads or tails. In addition, the number of distinguishable units ($N$) is 100, the number of coin tosses. Using these definitions,

$$W = \frac{N!}{a_H! a_T!} = \frac{100!}{40! 60!} = 1.37 \times 10^{28}$$

The most probable outcome corresponds to the configuration where 50 heads are observed such that

$$W = \frac{N!}{a_H! a_T!} = \frac{100!}{50! 50!} = 1.01 \times 10^{29}$$

### 13.1.2 The Dominant Configuration

The three-oscillator example from the preceding section illustrates a few key ideas that will guide us toward our development of the Boltzmann distribution. Specifically, weight is the total number of permutations corresponding to a given configuration. The probability of observing a configuration is given by the weight of that configuration divided by the total weight:

$$P_i = \frac{W_i}{W_1 + W_2 + \dots + W_N} = \frac{W_i}{\sum_{j=1}^{N} W_j} \tag{13.5}$$

where $P_i$ is the probability of observing configuration $i$, $W_i$ is the weight associated with this configuration, and the denominator represents the sum of weights for all possible configurations. Equation (13.5) predicts that the configuration with the largest weight will have the greatest probability of being observed. The configuration with the largest weight is referred to as the **dominant configuration.**
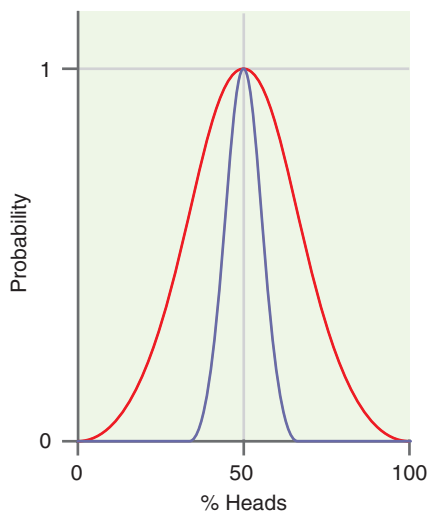
**FIGURE 13.3**
Comparison of relative probability (probability/maximum probability) for outcomes of a coin-flip trial in which the number of tosses is 10 (red line) and 100 (purple line). The x axis is the percentage of tosses that are heads. Notice that all trials have a maximum probability at 50% heads; however, as the number of tosses increases, the probability distribution becomes more centered about this value as evidenced by the decrease in distribution width.

Given the definition of the dominant configuration, the question arises as to how dominant this configuration is relative to other configurations. A conceptual answer to this question is provided by an experiment in which a coin is tossed 10 times. How probable is the outcome of four heads relative to five heads? Although the outcome of $n_H = 5$ has the largest weight, the weight of $n_H = 4$ is of comparable value. Therefore, observing the $n_H = 4$ configuration would not be at all surprising. But what if the coin were flipped 100 times? How likely would the outcome of $n_H = 40$ be relative to $n_H = 50$? This question was answered in Example Problem 13.1, and the weight of $n_H = 50$ was significantly greater than $n_H = 40$. As the number of tosses increases, the probability of observing heads 50% of the time becomes greater relative to any other outcome. In other words, the configuration associated with observing 50% heads should become the more dominant configuration as the number of coin tosses increases. An illustration of this expectation is presented in Figure 13.3 in which the relative weights associated with observing heads a certain percentage of the time after tossing a coin 10 and 100 times are presented. The figure demonstrates that after 10 tosses, the relative probability of observing something other than five heads is appreciable. However, as the number of coin tosses increases, the probability distribution narrows such that the final result of 50% heads becomes dominant. Taking this argument to sizes associated with molecular assemblies, imagine performing Avogadro's number of coin tosses! Given the trend illustrated in Figure 13.3, one would expect the probability to be sharply peaked at 50% heads. In other words, as the number of experiments in the trial increases, the 50% heads configuration will not only become the most probable, but also the weight associated with this configuration will become so large that the probability of observing another outcome is minuscule. Indeed, the most probable configuration evolves into the dominant configuration as the size of the system increases.

## EXAMPLE PROBLEM 13.2

Consider a collection of 10,000 particles with each particle capable of populating one of three energy levels having energies 0, $\varepsilon$, and $2\varepsilon$ with a total available energy of 5000 $\varepsilon$. Under the constraint that the total number of particles and total energy be constant, determine the dominant configuration.

### Solution

With constant total energy, only one of the energy-level populations is independent. Treating the number of particles in the highest energy level ($N_3$) as the independent variable, the number of particles in the intermediate ($N_2$) and lowest ($N_1$) energy levels is given by

$$N_2 = 5000 - 2N_3$$
$$N_1 = 10{,}000 - N_2 - N_3$$

Because the number of particles in a given energy level must be greater than or equal to 0, the preceding equations demonstrate that $N_3$ can range from 0 to 2500. Given the size of the state populations, it is more convenient to calculate the natural log of the weight associated with each configuration of energy as a function of $N_3$ by using Equation (13.4) in the following form:

$$\ln W = \ln \left( \frac{N!}{N_1! N_2! N_3!} \right) = \ln N! - \ln N_1! - \ln N_2! - \ln N_3!$$

Each term can be readily evaluated using Stirling's approximation, and results of this calculation are presented in Figure 13.4(a). This figure demonstrates that ln W has a maximum value at $N_3 \approx 1200$ (or 1162 to be precise). The dominance of this configuration is also illustrated in Figure 13.4(b), where the weight of the configurations corresponding to the allowed values of $N_3$ are compared with that of the dominant configuration. Even for this relatively simple system having only 10,000 particles, the weight is sharply peaked at the dominant configuration.

# 13.2 Derivation of the Boltzmann Distribution

As the size of the system increases, a single configurational outcome will have such a large relative weight that only this configuration will be observed. In this limit, it becomes pointless to define all possible configurations, and only the outcome associated with the dominant configuration is of interest. A method is needed by which to identify this configuration directly. Inspection of Figures 13.3 and 13.4 reveals that the dominant configuration can be determined as follows. Because the dominant configuration has the largest associated weight, any change in outcome corresponding to a different configuration will be reflected by a reduction in weight. Therefore, the dominant configuration can be identified by locating the peak of the curve corresponding to weight as a function of **configurational index,** denoted by $\chi$. Because $W$ will be large for molecular systems, it is more convenient to work with $\ln W$, and the search criterion for the dominant configuration becomes

$$\frac{d \ln W}{d\chi} = 0 \tag{13.6}$$

This expression is a mathematical definition of the dominant configuration, and it states that if a configuration space is searched by monitoring the change in $\ln W$ as a function of configurational index, a maximum will be observed that corresponds to the dominant configuration. A graphical description of the search criterion is presented in Figure 13.5.

The distribution of energy associated with the dominant configuration is known as the **Boltzmann distribution.** We begin our derivation of this distribution by taking the natural log of the weight using the expression for weight developed previously and applying Stirling's approximation:

$$\ln W = \ln N! - \ln \prod_n a_n!$$

$$= N \ln N - \sum_n a_n \ln a_n \tag{13.7}$$

In obtaining Equation 13.7 the following equality was employed:

$$N = \sum_n a_n \tag{13.8}$$

This equation makes intuitive sense. The objects in our collection must be in one of the available energy levels; therefore, summation over the occupation numbers is equivalent to counting all objects.

The criterion for the dominant configuration requires differentiation of $\ln W$ by some relevant configurational index, but what is this index? We are interested in the distribution of energy among a collection of molecules, or the number of molecules that resides in a given energy level. Because the number of molecules residing in a given energy level is the occupation number $a_n$, the occupation number provides a relevant configurational index. Recognizing this, differentiation of $\ln W$ with respect to $a_n$ yields the following:

$$\frac{d \ln W}{da_n} = \frac{dN}{da_n} \ln N + N\frac{d \ln N}{da_n} - \frac{d}{da_n}\sum_n (a_n \ln a_n) \tag{13.9}$$

The following mathematical relationship was employed in obtaining the previous relationship:

$$\frac{d \ln x}{dx} = \frac{1}{x}$$

such that

$$\frac{d \ln W}{da_n} = \ln N + N\left(\frac{1}{N}\right) - (\ln a_n + 1) = -\ln\left(\frac{a_n}{N}\right) \tag{13.10}$$

(a)

(b)
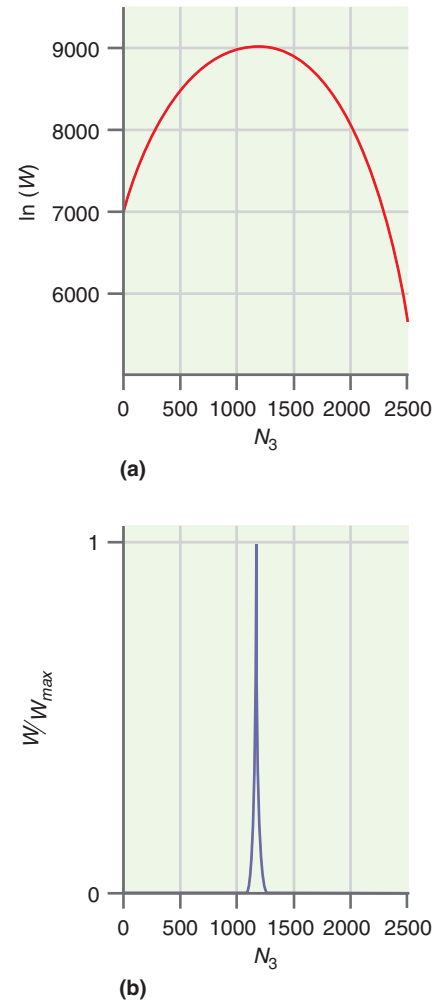
**FIGURE 13.4**
Illustration of the dominant configuration for a system consisting of 10,000 particles with each particle having three energy levels at energies of 0, $\varepsilon$, and $2\varepsilon$ as discussed in Example Problem 13.2. The number of particles populating the higher energy level is $N_3$, and the energy configurations are characterized by the population in this level. **(a)** Variation in the natural log of the weight $\ln W$ for energy configurations as a function of $N_3$, demonstrating that $\ln W$ has a maximum at $N_3 \approx 1200$. **(b)** Variation in the weight associated with a given configuration to that of the dominant configuration. The weight is sharply peaked around $N_3 \approx 1200$ corresponding to the dominant configuration of energy.
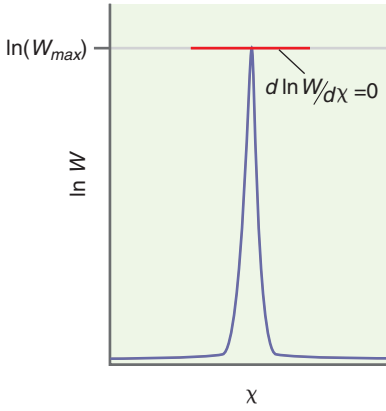
**FIGURE 13.5**
Mathematical definition of the dominant configuration. The change in the natural log of weight $\ln W$ as a function of configuration index $\chi$ is presented. If we determine the change in $\ln W$ as a function of configuration index, the change will equal zero at the maximum of the curve corresponding to the location of the dominant configuration.

Comparison of Equation (13.10) and the search criteria for the dominant configuration suggests that if $\ln(a_n/N) = 0$ our search is complete. However, this assumes that the occupation numbers are independent, yet the sum of the occupation numbers must equal $N$, dictating that reduction of one occupation number must be balanced by an increase in another. In other words, one object in the collection is free to gain or lose energy, but a corresponding amount of energy must be lost or gained elsewhere in the system. We can ensure that both the number of objects and total system energy are constant by requiring that

$$\sum_n da_n = 0 \quad \text{and} \quad \sum_n \varepsilon_n da_n = 0 \tag{13.11}$$

The $da_n$ terms denote change in occupation number $a_n$. In the expression on the right, $\varepsilon_n$ is the energy associated with the $n$th energy level. Because the conservation of $N$ and energy has not been required to this point, these conditions are now included by introducing Lagrange multipliers, $\alpha$ and $\beta$, as weights for the corresponding constraints into the differential as follows:

$$d \ln W = 0 = \sum_n - \ln\left(\frac{a_n}{N}\right) da_n + \alpha \sum_n da_n - \beta \sum_n \varepsilon_n da_n$$

$$= \sum_n \left(-\ln\left(\frac{a_n}{N}\right) + \alpha - \beta\varepsilon_n\right) da_n \tag{13.12}$$

The Lagrange method of undetermined multipliers is described in the Math Supplement. Formally, this technique allows for maximization of a function that is dependent on many variables that are constrained among themselves. The key step in this approach is to determine the identity of $\alpha$ and $\beta$ by noting that in Equation (13.12) the equality is only satisfied when the terms in parentheses are equal to zero:

$$0 = -\ln\left(\frac{a_n}{N}\right) + \alpha - \beta\varepsilon_n$$

$$\ln\left(\frac{a_n}{N}\right) = \alpha - \beta\varepsilon_n$$

$$\frac{a_n}{N} = e^\alpha e^{-\beta\varepsilon_n}$$

$$a_n = Ne^\alpha e^{-\beta\varepsilon_n} \tag{13.13}$$

At this juncture the Lagrange multipliers can be defined. First, $\alpha$ is defined by summing both sides of the preceding equality over all energy levels. Recognizing that $\sum a_n = N$,

$$N = \sum_n a_n = Ne^\alpha \sum_n e^{-\beta\varepsilon_n}$$

$$1 = e^\alpha \sum_n e^{-\beta\varepsilon_n}$$

$$e^\alpha = \frac{1}{\sum_n e^{-\beta\varepsilon_n}} \tag{13.14}$$

This last equality is a central result in statistical mechanics. The denominator in Equation (13.14) is referred to as the **partition function** $q$ and is defined as

$$q = \sum_n e^{-\beta\varepsilon_n} \tag{13.15}$$

The value of $\beta$ will be determined next. The partition function represents the sum over all terms that describes the probability associated with the variable of interest, in this case $\varepsilon_n$, or the energy of level $n$. Using the partition function with Equation (13.13), the probability of occupying a given energy level $p_n$ becomes

$$p_n = \frac{a_n}{N} = e^\alpha e^{-\beta\varepsilon_n} = \frac{e^{-\beta\varepsilon_n}}{q} \tag{13.16}$$
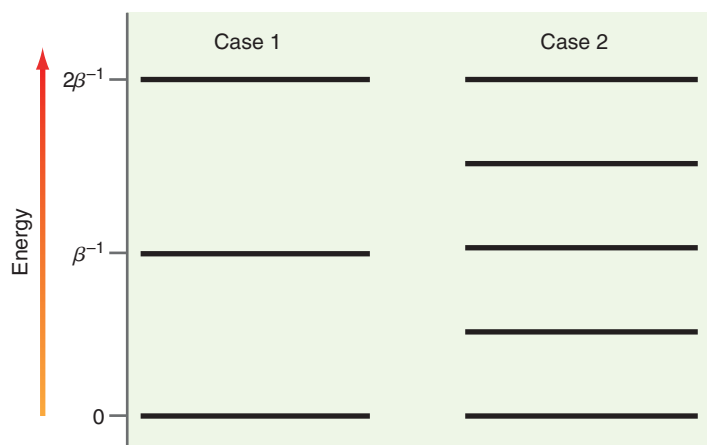
Equation (13.16) is the final result of interest. It quantitatively describes the probability of occupying a given energy for the dominant configuration of energy. This well-known and important result is referred to as the Boltzmann distribution. We can compare Equation (13.16) to the expression from Chapter 12 for probability involving discrete variables, where probability was defined as follows:

$$P(X_i) = \frac{f_i}{\sum\limits_{j=1}^{M} f_j} \tag{13.17}$$

This comparison demonstrates that the Boltzmann distribution is nothing more than a statement of probability, with the partition function serving to normalize the probability distribution.

Quantitative application of Equation (13.16) requires that we determine $\beta$, the second of our Lagrange multipliers. However, a conceptual discussion at this juncture can provide some insight into how this distribution describes molecular systems. Imagine a collection of harmonic oscillators as in the previous example, but instead of writing down all microstates and identifying the dominant configuration, the dominant configuration is instead given by the Boltzmann distribution law of Equation (13.16). This law establishes that the probability of observing an oscillator in a given energy level is dependent on level energy ($\varepsilon_n$) as $\exp(-\beta\varepsilon_n)$. Because the exponent must be unitless, $\beta$ must have units of inverse energy.[1] Recall that the energy levels of the harmonic oscillator (neglecting zero point energy) are $\varepsilon_n = nh\nu$ for $n = 0, 1, 2, \ldots, \infty$. Therefore, our conceptual example will employ oscillators where $h\nu = \beta^{-1}$ as illustrated in Figure 13.6.

Using this value for the energy spacings, the exponential terms in the Boltzmann distribution are easily evaluated:

$$e^{-\beta\varepsilon_n} = e^{-\beta(n/\beta)} = e^{-n} \tag{13.18}$$

The partition function is evaluated by performing the summation over the energy levels:

$$q = \sum_{n=0}^{\infty} e^{-n} = 1 + e^{-1} + e^{-2} + \ldots$$

$$= \frac{1}{1 - e^{-1}} = 1.58 \tag{13.19}$$

In the last step of this example, we have used the following series expression (where $|x| < 1$):

$$\frac{1}{1 - x} = 1 + x + x^2 + \ldots$$

---

[1]This simple unit analysis points to an important result: that $\beta$ is related to energy. As will be shown, $1/\beta$ provides a measure of the energy available to the system.

With the partition function, the probability of an oscillator occupying the first three levels ($n = 0$, $1$, and $2$) is

$$p_0 = \frac{e^{-\beta\varepsilon_0}}{q} = \frac{e^{-0}}{1.58} = \frac{1}{1.58} = 0.633$$

$$p_1 = \frac{e^{-\beta\varepsilon_1}}{q} = \frac{e^{-1}}{1.58} = 0.233$$

$$p_2 = \frac{e^{-\beta\varepsilon_2}}{q} = \frac{e^{-2}}{1.58} = 0.086 \qquad \textbf{(13.20)}$$

### EXAMPLE PROBLEM 13.3

For the example just discussed, what is the probability of finding an oscillator in energy levels $n \geq 3$?

### Solution

The Boltzmann distribution is a normalized probability distribution. As such, the sum of all probabilities equals unity:

$$p_{total} = 1 = \sum_{n=0}^{\infty} p_n$$

$$1 = p_0 + p_1 + p_2 + \sum_{n=3}^{\infty} p_n$$

$$1 - (p_0 + p_1 + p_2) = 0.048 = \sum_{n=3}^{\infty} p_n$$

In other words, only 4.8% of the oscillators in our collection will be found in levels $n \geq 3$.

We continue with our conceptual example by asking the following question: "How will the probability of occupying a given level vary with a change in energy separation between levels?" In the first example, the energy spacings were equal to $\beta^{-1}$. A reduction in energy-level spacings to half this value requires that $h\nu = \beta^{-1}/2$. It is important to note that $\beta$ has not changed relative to the previous example; only the separation in energy levels has changed. With this new energy separation, the exponential terms in the Boltzmann distribution become

$$e^{-\beta\varepsilon_n} = e^{-\beta(n/2\beta)} = e^{-n/2} \qquad \textbf{(13.21)}$$

Substituting this equation into the expression for the partition function,

$$q = \sum_{n=0}^{\infty} e^{-n/2} = 1 + e^{-1/2} + e^{-1} + \dots$$

$$= \frac{1}{1 - e^{-1/2}} = 2.54 \qquad \textbf{(13.22)}$$

Using this value for the partition function, the probability of occupying the first three levels ($n = 0$, $1$, and $2$) corresponding to this new spacing is

$$p_0 = \frac{e^{-\beta\varepsilon_0}}{q} = \frac{e^{-0}}{2.54} = \frac{1}{2.54} = 0.394$$

$$p_1 = \frac{e^{-\beta\varepsilon_1}}{q} = \frac{e^{-1/2}}{2.54} = 0.239$$

$$p_2 = \frac{e^{-\beta\varepsilon_2}}{q} = \frac{e^{-1}}{2.54} = 0.145 \qquad \textbf{(13.23)}$$

Comparison with the previous system probabilities in Equation (13.20) illustrates some interesting results. First, with a decrease in energy-level spacings, the probability of occupying the lowest energy level ($n = 0$) decreases, whereas the probability of occupying the other energy levels increases. Reflecting this change in probabilities, the value of the partition function has also increased. Since the partition function represents the sum of the probability terms over all energy levels, an increase in the magnitude of the partition function reflects an increase in the probability of occupying higher energy levels. That is, the partition function provides a measure of the number of energy levels that are occupied for a given value of $\beta$.

### EXAMPLE PROBLEM 13.4

For the preceding example with decreased energy-level spacings, what is the probability of finding an oscillator in energy states $n \geq 3$?

#### Solution

The calculation from the previous example is used to find that

$$\sum_{n=3}^{\infty} p_n = 1 - (p_0 + p_1 + p_2) = 0.222$$

Consistent with the discussion, the probability of occupying higher energy levels has increased substantially with a reduction in level spacings.

### 13.2.1 Degeneracy

To this point, the assumption has been that only one state is present at a given energy level; however, when discussing atomic and molecular systems, more than a single state may be present at a given energy. The presence of multiple states at a given energy level is referred to as **degeneracy,** and degeneracy is incorporated into the expression for the partition function as follows:

$$q = \sum_n g_n e^{-\beta \varepsilon_n} \tag{13.24}$$

Equation (13.24) is identical to the previous definition of $q$ from Equation (13.15) with the exception that the term $g_n$ has been included. This term represents the number of states present at a given energy level, or the degeneracy of the level. The corresponding expression for the probability of occupying energy level $\varepsilon_i$ is

$$p_i = \frac{g_i e^{-\beta \varepsilon_i}}{q} \tag{13.25}$$

In Equation (13.25), $g_i$ is the degeneracy of the level with energy-level $\varepsilon_i$, and $q$ is as defined in Equation (13.24).

How does degeneracy influence probability? Consider Figure 13.7 in which a system with single states at energy 0 and $\beta^{-1}$ is shown with a similar system in which two states are present at energy $\beta^{-1}$. The partition function for the first system is

$$q_{system1} = \sum_n g_n e^{-\beta \varepsilon_n} = 1 + e^{-1} = 1.37 \tag{13.26}$$

For the second system, $q$ is

$$q_{system2} = \sum_n g_n e^{-\beta \varepsilon_n} = 1 + 2e^{-1} = 1.74 \tag{13.27}$$

The corresponding probability of occupying a state at energy $\beta^{-1}$ for the two systems is given by

$$p_{system1} = \frac{g_i e^{-\beta \varepsilon_i}}{q} = \frac{e^{-1}}{1.37} = 0.27$$

$$p_{system2} = \frac{g_i e^{-\beta \varepsilon_i}}{q} = \frac{2e^{-1}}{1.74} = 0.42 \tag{13.28}$$
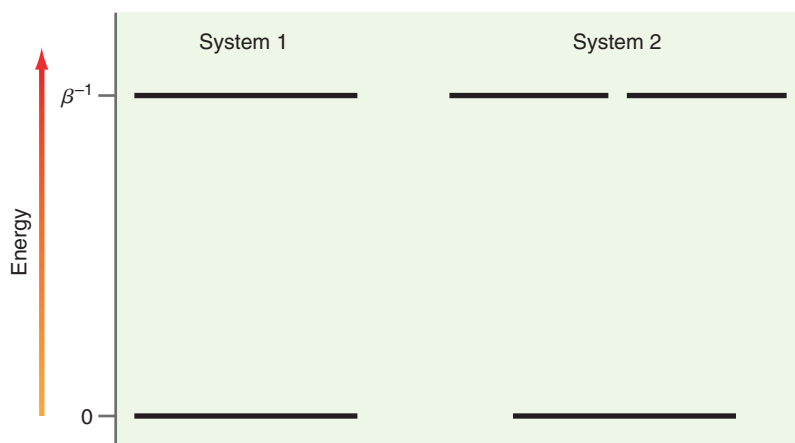
Notice that the probability of occupying a state at energy $\beta^{-1}$ is greater for system 2, the system with degeneracy. This increase reflects the fact that two states are now available for population at this energy. However, this increase is not simply twice that of the nondegenerate case (system 1) since the value of the partition function also changes due to degeneracy.

## 13.3 Dominance of the Boltzmann Distribution

The search criterion for the Boltzmann distribution as illustrated in Figure 13.5 dictates that there will be an energy distribution for which the number of corresponding microstates is greatest. However, the question remains as to just how dominant the Boltzmann distribution is. Another way to approach this question is to ask "What exactly is the width of the curve presented in Figure 13.5?" Is there sufficient breadth in this distribution that a slight change in configuration results in another energy distribution, different from that of the dominant configuration but with a reasonable probability of being observed?

Consider an isolated macroscopic assembly of distinguishable units.[2] The dominant configuration will be that having the largest number of microstates corresponding to weight – $W_{max}$. In addition, consider a slightly different configuration having weight – $W$, and $W < W_{max}$. Let $a_n$ be the fractional change in the number of units present in the $n$th energy state:

$$\alpha_n = \frac{a'_n - a_n}{a_n} = \frac{\delta_n}{a_n} \tag{13.29}$$

In this expression, $\delta_n$ is simply the change in occupation number $a_n$ to some new configuration (denoted as $a'_n$) relative to the occupation numbers corresponding to the dominant configuration. The system is isolated, dictating that both the number of particles and the total amount of energy are conserved, resulting in $\Delta N = 0$ and $\Delta E = 0$. With these definitions, the ratio of $W_{max}/W$ is given by the following equation:

$$\frac{W_{max}}{W} = \frac{\dfrac{N!}{\prod_n a_n!}}{\dfrac{N!}{\prod_n (a_n + \delta_n)!}} = \prod_n \left( a_n + \frac{\delta_n}{2} \right)^{\delta_n} \tag{13.30}$$

The term $(a_n + \delta_n)$ consists of $\delta$ factors from $(a + 1)$ to $(a + \delta)$. The last equality in Equation (13.30) is satisfied when $\delta$ is sufficiently small such that $|\delta_n| \ll a_n$. The ratio of weights provides a measure of the number of microstates associated with the

[2]A full presentation of the following derivation appears in L. K. Nash, "On the Boltzmann Distribution Law," *J. Chemical Education* 59 (1982): 824.

modified configuration versus the Boltzmann distribution. Because $W$ will be quite large for an assembly of molecules, the natural log of this ratio is used:

$$
\begin{aligned}
\ln\left(\frac{W_{max}}{W}\right) &= \sum_n \ln\left(a_n + \frac{\delta_n}{2}\right)^{\delta_n} \\
&= \sum_n \delta_n \ln\left(a_n + \frac{\delta_n}{2}\right) \\
&= \sum_n \delta_n \ln a_n\left(1 + \frac{\delta_n}{2a_n}\right) \\
&= \sum_n \delta_n \ln a_n + \sum_n \delta_n \ln\left(1 + \frac{\delta_n}{2a_n}\right) \qquad \textbf{(13.31)}
\end{aligned}
$$

The last equality in Equation (13.31) can be simplified by noting that $\ln(1 \pm z) = \pm z$ for small $z$. Because $\delta_n$ represents a fractional change in occupation number corresponding to the dominant configuration, $\delta_n/2a_n \ll 1$. Therefore,

$$
\ln\left(\frac{W_{max}}{W}\right) = \sum_n \delta_n \ln a_n + \sum_n \frac{\delta_n^2}{2a_n} \qquad \textbf{(13.32)}
$$

Recall the following definition, which related the fractional change in occupation number to the occupation numbers themselves:

$$
\alpha_n = \frac{\delta_n}{a_n} \qquad \textbf{(13.33)}
$$

Substitution of the preceding relationship for $\delta_n$ results in

$$
\begin{aligned}
\ln\left(\frac{W_{max}}{W}\right) &= \sum_n a_n\alpha_n \ln a_n + \sum_n \frac{a_n}{2}(\alpha_n^2) \\
&= \sum_n a_n\alpha_n(\ln a_0 - \beta\varepsilon_n) + \sum_n \frac{a_n}{2}(\alpha_n^2) \\
&= \sum_n a_n\alpha_n(\ln a_0) - \sum_n \beta\varepsilon_n a_n\alpha_n + \sum_n \frac{a_n}{2}(\alpha_n^2) \\
&= \ln a_0 \sum_n a_n\alpha_n - \beta\sum_n \varepsilon_n a_n\alpha_n + \sum_n \frac{a_n}{2}(\alpha_n^2) \\
&= \sum_n \frac{a_n}{2}(\alpha_n^2) \qquad \textbf{(13.34)}
\end{aligned}
$$

The last step in this derivation was performed by realizing that $\Delta N = 0$ (and the first summation is equal to zero) and $\Delta E = 0$ (so that the second summation is also equal to zero). The root-mean-squared deviation in occupation number relative to those of the dominant configuration is defined as follows:

$$
\alpha_{rms} = \left[\frac{\sum_n a_n\alpha_n^2}{N}\right]^{1/2} \qquad \textbf{(13.35)}
$$

Given this equation, the ratio of weights corresponding to the Boltzmann distribution $W_{max}$ and the slightly modified distribution $W$ reduces to

$$
\frac{W_{max}}{W} = e^{N\alpha_{rms}^2/2} \qquad \textbf{(13.36)}
$$

To apply this relationship to a chemical system, imagine that the system of interest is a mole of molecules such that $N = 6.022 \times 10^{23}$. In addition, the fractional change in occupation number will be exceedingly small corresponding to $\alpha_{rms} = 10^{-10}$ (that is, one part in $10^{10}$). Using these values,

$$
\frac{W_{max}}{W} = e^{\frac{(6.022 \times 10^{23}) \times (10^{-20})}{2}} \approx e^{3000} = 10^{1302}
$$

The ratio of weights is an extremely large number, and it demonstrates that a minute change in configuration will result in a significant reduction in weight. Clearly, the width of the curve illustrated in Figure 13.5 is extremely small in a system where $N$ is on the order of Avogadro's number, and the most probable distribution is virtually the only distribution that will be observed for a macroscopic assembly of units. Of the total number of microstates available to a large assembly of units, the vast majority of these microstates correspond to the dominant configuration and a subset of configurations that differ from the dominant configuration by exceedingly small amounts such that the macroscopic properties of the assembly will be identical to those of the dominant configuration. In short, the macroscopic properties of the assembly are defined by the dominant configuration.

# 13.4 Physical Meaning of the Boltzmann Distribution Law

How does one know other configurations exist if the dominant configuration is all one expects to see for a system at equilibrium? Furthermore, are the other nondominant configurations of the system of no importance? Modern experiments are capable of displacing systems from equilibrium and monitoring the system as it relaxes back toward equilibrium. Therefore, the capability exists to experimentally prepare a nondominant configuration so that these configurations can be studied. An illuminating, conceptual answer to this question is provided by the following logical arguments. First, consider the central postulate of statistical mechanics:

> Every possible microstate of an isolated assembly of units occurs with equal probability.

How does one know that this postulate is true? Imagine a collection of 100 oscillators having 100 quanta of energy. The total number of microstates available to this system is on the order of $10^{200}$, which is an extremely large number. Now, imagine performing an experiment in which the energy content of each oscillator is measured such that the corresponding microstate can be established. Also assume that a measurement can be performed every $10^{-9}$ s (1 nanosecond) such that microstates can be measured at a rate of $10^9$ microstates per second. Even with such a rapid determination of microstates, it would take us $10^{191}$ s to count every possible microstate, a period of time that is much larger than the age of the universe! In other words, the central postulate cannot be verified experimentally. However, we will operate under the assumption that the central postulate is true because statistical mechanical descriptions of chemical systems have provided successful and accurate descriptions of macroscopic systems.

Even if the validity of the central postulate is assumed, the question of its meaning remains. To gain insight into this question, consider a large or macroscopic collection of distinguishable and identical oscillators. Furthermore, the collection is isolated, resulting in both the total energy and the number of oscillators being constant. Finally, the oscillators are free to exchange energy such that any configuration of energy (and, therefore, any microstate) can be achieved. The system is set free to evolve, and the following features are observed:

1. All microstates are equally probable; however, one has the greatest probability of observing a microstate associated with the dominant configuration.

2. As demonstrated in the previous section, configurations having a significant number of microstates will be only infinitesimally different from the dominant configuration. The macroscopic properties of the system will be identical to that of the dominant configuration. Therefore, with overwhelming probability, one will observe a macroscopic state of the system characterized by the dominant configuration.

3. Continued monitoring of the system will result in the observation of macroscopic properties of the systems that appear unchanging, although energy is still being

exchanged between the oscillators in our assembly. This macroscopic state of the system is called the **equilibrium state.**

4. Given items 1 through 3, the equilibrium state of the system is characterized by the dominant configuration.

This logical progression brings us to an important conclusion: *the Boltzmann distribution law describes the energy distribution associated with a chemical system at equilibrium.* In terms of probability, the fact that all microstates have equal probability of being observed does not translate into an equal probability of observing all configurations. As illustrated in Section 13.3, the vast majority of microstates correspond to the Boltzmann distribution, thereby dictating that the most probable configuration that will be observed is the one characterized by the Boltzmann distribution.

# 13.5 The Definition of $\beta$

Use of the Boltzmann distribution requires an operative definition for $\beta$, preferably one in which this quantity is defined in terms of measurable system variables. Such a definition can be derived by considering the variation in weight $W$ as a function of total energy contained by an assembly of units $E$. To begin, imagine an assembly of 10 oscillators having only three quanta of total energy. In this situation, the majority of the oscillators occupy the lowest energy states, and the weight corresponding to the dominant configuration should be small. However, as energy is deposited into the system, the oscillators will occupy higher energy states and the denominator in Equation (13.4) will be reduced, resulting in an increase in $W$. Therefore, one would expect $E$ and $W$ to be correlated.

The relationship between $E$ and $W$ can be determined by taking the natural log of Equation (13.4):

$$\ln W = \ln N! - \ln \prod_n a_n!$$

$$= \ln N! - \sum_n \ln a_n! \tag{13.37}$$

Interest revolves around the change in $W$ with respect to $E$, a relationship that requires the total differential of $W$:

$$d \ln W = -\sum_n \ln a_n!$$

$$= -\sum_n \ln a_n \, da_n \tag{13.38}$$

The result provided by Equation (13.38) was derived using Stirling's approximation to evaluate $\ln(a_n!)$. Simplification of Equation (13.38) is accomplished using the Boltzmann relationship to define the ratio between the occupation number for an arbitrary energy level $\varepsilon_n$ versus the lowest or ground energy level ($\varepsilon_0 = 0$):

$$\frac{a_n}{a_0} = \frac{\dfrac{Ne^{-\beta\varepsilon_n}}{q}}{\dfrac{Ne^{-\beta\varepsilon_0}}{q}} = e^{-\beta\varepsilon_n} \tag{13.39}$$

$$\ln a_n = \ln a_0 - \beta\varepsilon_n \tag{13.40}$$

In the preceding steps, the partition function $q$ and $N$ simply cancel. Taking this expression for $\ln(a_n)$ and substituting into Equation (13.38) yields

$$d \ln W = -\sum_n (\ln a_0 - \beta\varepsilon_n) da_n$$

$$= -\ln a_0 \sum_n da_n + \beta \sum_n \varepsilon_n \, da_n \tag{13.41}$$

The first summation in Equation (13.41) represents the total change in occupation numbers, and it is equal to the change in the total number of oscillators in the system. Because the system is closed with respect to the number of oscillators, $dN = 0$ and the first summation is also equal to zero. The second term represents the change in total energy of the system ($dE$) accompanying the deposition of energy into the system:

$$\sum_n \varepsilon_n \, da_n = dE \tag{13.42}$$

With this last equality, the relationship between $\beta$, weight, and total energy is finally derived:

$$d \ln W = \beta dE \tag{13.43}$$

This last equality is quite remarkable and provides significant insight into the physical meaning of $\beta$. We began by recognizing that weight increases in proportion with the energy available to the system, and $\beta$ is simply the proportionality constant in this relationship. Unit analysis of Equation (13.43) also demonstrates that $\beta$ must have units of inverse energy as inferred previously.

Associating $\beta$ with measurable system variables is the last step in deriving a full definition for the Boltzmann distribution. This step can be accomplished through the following conceptual experiment. Imagine two separate systems of distinguishable units at equilibrium having associated weights $W_x$ and $W_y$. These assemblies are brought into thermal contact, and the composite system is allowed to evolve toward equilibrium, as illustrated in Figure 13.8. The composite system is then isolated from the surroundings such that the total energy available to the composite system is the sum of energy contained in the individual assemblies. The total weight of the combined system immediately after establishing thermal contact is the product of $W_x$ and $W_y$. If the two systems are initially at different equilibrium conditions, the instantaneous composite system weight will be less than the weight of the composite system at equilibrium. Since the composite weight will increase as equilibrium is approached

$$d(W_x \cdot W_y) \geq 0 \tag{13.44}$$

This inequality can be simplified as follows (see the Math Supplement):

$$W_y \, dW_x + W_x \, dW_y \geq 0$$

$$\frac{dW_x}{W_x} + \frac{dW_y}{W_y} \geq 0$$

$$d \ln W_x + d \ln W_y \geq 0 \tag{13.45}$$

Substitution of Equation (13.43) into the last expression of Equation (13.45) results in

$$\beta_x \, dE_x + \beta_y \, dE_y \geq 0 \tag{13.46}$$

where $\beta_x$ and $\beta_y$ are the corresponding $\beta$ values associated with the initial assemblies $x$ and $y$. Correspondingly, $dE_x$ and $dE_y$ refer to the change in total energy for the individual assemblies. Because the composite system is isolated from the surroundings, any change in energy for assembly $x$ must be offset by a corresponding change in assembly $y$:

$$dE_x + dE_y = 0$$

$$dE_x = -dE_y \tag{13.47}$$

Now, if $dE_x$ is positive, then by Equation (13.46),

$$\beta_x \geq \beta_y \tag{13.48}$$

Can the preceding result be interpreted in terms of system variables? This question can be answered by considering the following. If $dE_x$ is positive, energy flows into assembly $x$ from assembly $y$. Thermodynamics dictates that because temperature is a measure of internal kinetic energy, an increase in the energy will be accompanied by an increase in the temperature of assembly $x$. A corresponding decrease in the temperature of
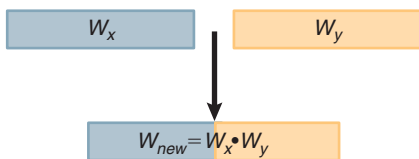


**FIGURE 13.8**
Two assemblies of distinguishable units, denoted $x$ and $y$, are brought into thermal contact.

assembly $y$ will also occur. Therefore, before equilibrium is established, thermody-namic considerations dictate that

$$T_y \geq T_x \tag{13.49}$$

In order for Equations (13.48) and Equations (13.49) to be true, $\beta$ must be inversely related to $T$. Furthermore, from unit analysis of Equation (13.43), we know that $\beta$ must have units of inverse energy. This requirement is met by including a proportionality constant in the relationship between $\beta$ and $T$, resulting in the final expression for $\beta$:

$$\beta = \frac{1}{kT} \tag{13.50}$$

The constant in Equation (13.50), $k$, is referred to as **Boltzmann's constant** and has a numerical value of $1.3806488 \times 10^{-23}$ J K$^{-1}$. The product of $k$ and Avogadro's number is equal to $R$, the ideal gas constant ($8.3144621$ J mol$^{-1}$ K$^{-1}$). Although the joule is the SI unit for energy, much of the information regarding molecular energy levels is derived from spectroscopic measurements. These spectroscopic quantities are generally expressed in units of wavenumbers (cm$^{-1}$). The **wavenumber** is simply the number of waves in an electromagnetic field per centimeter. Conversion from wavenumbers to joules is performed by multiplying the quantity in wavenumbers by Planck's constant $h$ and the speed of light $c$. In Example Problem 13.5, the vibrational energy levels for $I_2$ are given by the vibrational frequency of the oscillator $\tilde{\nu}$. Using this spectroscopic information, the vibrational level energies in joules are

$$E_n = nhc\tilde{\nu} = n(6.626 \times 10^{-34} \text{ J s}) (3.00 \times 10^{10} \text{ cm s}^{-1}) (208 \text{ cm}^{-1})$$
$$= n(4.13 \times 10^{-21} \text{J}) \tag{13.51}$$

At times the conversion from wavenumbers to joules will prove inconvenient. In such cases, Boltzmann's constant can be expressed in units of wavenumbers instead of joules where $k = 0.69503476$ cm$^{-1}$ K$^{-1}$. In this case, the spectroscopic quantities in wavenumbers can be used directly when evaluating partition functions and other statisti-cal-mechanical expressions.

### EXAMPLE PROBLEM 13.5

The vibrational frequency of $I_2$ is 208 cm$^{-1}$. What is the probability of $I_2$ populating the $n = 2$ vibrational level if the molecular temperature is 298 K?

#### Solution

Molecular vibrational energy levels can be modeled as harmonic oscillators; therefore, this problem can be solved by employing a strategy identical to the one just presented. To evaluate the partition function $q$, the "trick" used earlier was to write the partition function as a series and use the equivalent series expression:

$$q = \sum_n e^{-\beta\varepsilon_n} = 1 + e^{-\beta hc\tilde{\nu}} + e^{-2\beta hc\tilde{\nu}} + e^{-3\beta hc\tilde{\nu}} + \cdots$$

$$= \frac{1}{1 - e^{-\beta hc\tilde{\nu}}}$$

Since $\tilde{\nu} = 208$ cm$^{-1}$ and $T = 298$ K, the partition function is

$$q = \frac{1}{1 - e^{-\beta hc\tilde{\nu}}}$$

$$= \frac{1}{1 - e^{-hc\tilde{\nu}/kT}}$$

$$= \frac{1}{1 - \exp\left[-\left(\dfrac{(6.626 \times 10^{-34} \text{ Js})(3.00 \times 10^{10} \text{ cm s}^{-1})(208 \text{ cm}^{-1})}{(1.38 \times 10^{-23}\text{J K}^{-1})(298 \text{ K})}\right)\right]}$$

$$= \frac{1}{1 - e^{-1}} = 1.58$$

This result is then used to evaluate the probability of occupying the second vibrational state ($n = 2$) as follows:

$$p_2 = \frac{e^{-2\beta hc\tilde{\nu}}}{q}$$

$$= \frac{\exp\left[-2\left(\frac{(6.626 \times 10^{-34}\text{ J s}^{-1})(3.00 \times 10^{10}\text{ cm s}^{-1})(208\text{ cm}^{-1})}{(1.38 \times 10^{-23}\text{ J K}^{-1})(298\text{ K})}\right)\right]}{1.58}$$

$$= 0.086$$

The last result in Example Problem 13.5 should look familiar. An identical example was worked earlier in this chapter where the energy-level spacings were equal to $\beta^{-1}$ (case 1 in Figure 13.6) and the probability of populating states for which $n = 0, 1$, and 2 was determined. This previous example in combination with the molecular example just presented illustrates that the exponential term $\beta\varepsilon_n$ in the Boltzmann distribution and partition function can be thought of as a comparative term that describes the ratio of the energy needed to populate a given energy level versus the thermal energy available to the system, as quantified by $kT$. Energy levels that are significantly higher in energy than $kT$ are not likely to be populated, whereas the opposite is true for energy levels that are small relative to $kT$.

Example Problem 13.5 is reminiscent of the development presented in the discussion of vibrational and rotational spectroscopy in which the use of the Boltzmann distribution to predict the relative population in vibrational and rotational states and the effect of these populations on vibrational and rotational transition intensities was presented. In addition, the role of the Boltzmann distribution in nuclear magnetic resonance spectroscopy (NMR) is explored in the following example problem.

## EXAMPLE PROBLEM 13.6

In NMR spectroscopy, energy separation between spin states is created by placing nuclei in a magnetic field. Protons have two possible spin states: $+1/2$ and $-1/2$. The energy separation between these two states, $\Delta E$, is dependent on the strength of the magnetic field and is given by

$$\Delta E = g_N \beta_N B = (2.82 \times 10^{-26}\text{ J T}^{-1})B$$

where $B$ is the magnetic field strength in tesla (T). Also, $g_N$ and $\beta_N$ are the nuclear g-factor and nuclear magneton for a proton, respectively. Early NMR spectrometers employed magnetic field strengths of approximately 1.45 T. What is the ratio of the population between the two spin states given this magnetic field strength and $T = 298$ K?

### Solution

Using the Boltzmann distribution, the occupation number for energy levels is given by

$$a_n = \frac{Ne^{-\beta\varepsilon_n}}{q}$$

where $N$ is the number of particles, $\varepsilon_n$ is the energy associated with the level of interest, and $q$ is the partition function. Using the preceding equation, the ratio of occupation numbers is given by

$$\frac{a_{+1/2}}{a_{-1/2}} = \frac{\dfrac{Ne^{-\beta\varepsilon_{+1/2}}}{q}}{\dfrac{Ne^{-\beta\varepsilon_{-1/2}}}{q}} = e^{-\beta(\varepsilon_{+1/2}-\varepsilon_{-1/2})} = e^{-\beta\Delta E}$$

Substituting for $\Delta E$ and $\beta$ (and taking care that units cancel), the ratio of occupation numbers is given by

$$\frac{a_{+1/2}}{a_{-1/2}} = e^{-\beta \Delta E} = e - \Delta E/kt = \exp\left[\frac{-(2.82 \times 10^{-26} \text{ J T}^{-1})(1.45 \text{ T})}{(1.38 \times 10^{-23} \text{ J K}^{-1})(298 \text{ K})}\right]$$

$$= e^{-(9.94 \times 10^{-6})} = 0.999990$$

In other words, in this system the energy spacing is significantly smaller than the energy available ($kT$) such that the higher energy spin state is populated to a significant extent, and is nearly equal in population to that of the lower energy state.

# Vocabulary

Boltzmann distribution

Boltzmann's constant

configuration

configurational index

degeneracy

dominant configuration

equilibrium state

microstate

occupation number

partition function

wavenumber

weight

# Conceptual Problems

**Q13.1** What is the difference between a configuration and a microstate?

**Q13.2** What is meant by the "weight" of a configuration?

**Q13.3** How does one calculate the number of microstates associated with a given configuration?

**Q13.4** Describe what is meant by the phrase "the dominant configuration."

**Q13.5** What is an occupation number? How is this number used to describe energy distributions?

**Q13.6** What does a partition function represent? Can you describe this term using concepts from probability theory?

**Q13.7** Explain the significance of the Boltzmann distribution. What does this distribution describe?

**Q13.8** Why is the probability of observing a configuration of energy different from the Boltzmann distribution vanishingly small?

**Q13.9** What is degeneracy? Can you conceptually relate the expression for the partition function without degeneracy to that with degeneracy?

**Q13.10** How is $\beta$ related to temperature? What are the units of $kT$?

**Q13.11** How would you expect the partition function to vary with temperature? For example, what should the value of a partition function be at 0 K?

# Numerical Problems

Problem numbers in **red** indicate that the solution to the problem is given in the *Student's Solutions Manual*.

**P13.1**

**a.** What is the possible number of microstates associated with tossing a coin $N$ times and having it come up $H$ times heads and $T$ times tails?

**b.** For a series of 1000 tosses, what is the total number of microstates associated with 50% heads and 50% tails?

**c.** How much less probable is the outcome that the coin will land 40% heads and 60% tails?

**P13.2** In Example Problem 13.1, the weights associated with observing 40 heads and 50 heads after flipping a coin 100 times were determined. Perform a similar calculation to determine the weights associated with observing 400 and 500 heads after tossing a coin 1000 times. (Note: Stirling's approximation will be useful in performing these calculations).

**P13.3**

**a.** Realizing that the most probable outcome from a series of $N$ coin tosses is $N/2$ heads and $N/2$ tails, what is the expression for $W_{max}$ corresponding to this outcome?

**b.** Given your answer for part (a), derive the following relationship between the weight for an outcome other than the most probable, W, and $W_{max}$:

$$\log\left(\frac{W}{W_{max}}\right) = -H \log\left(\frac{H}{N/2}\right) - T \log\left(\frac{T}{N/2}\right)$$

**c.** We can define the deviation of a given outcome from the most probable outcome using a "deviation index," $\alpha = (H - T)/N$. Show that the number of heads or tails can be expressed as $H = (N/2)(1 + \alpha)$ and $T = (N/2)(1 - \alpha)$.

**d.** Finally, demonstrate that $W/W_{max} = e^{-N\alpha^2}$.

**P13.4** Consider the case of 10 oscillators and 8 quanta of energy. Determine the dominant configuration of energy for this system by identifying energy configurations and calculating the corresponding weights. What is the probability of observing the dominant configuration?

**P13.5** Determine the weight associated with the following card hands:

**a.** Having any five cards

**b.** Having five cards of the same suit (known as a "flush")

**P13.6** For a two-level system, the weight of a given energy distribution can be expressed in terms of the number of systems $N$ and the number of systems occupying the excited state $n_1$. What is the expression for weight in terms of these quantities?

**P13.7** The probability of occupying a given excited state $p_i$ is given by $p_i = n_i/N = e^{-\beta\varepsilon_i}/q$, where $n_i$ is the occupation number for the state of interest, $N$ is the number of particles, and $\varepsilon_i$ is the energy of the level of interest. Demonstrate that the preceding expression is independent of the definition of energy for the lowest state.

**P13.8** Barometric pressure can be understood using the Boltzmann distribution. The potential energy associated with being a given height above Earth's surface is $mgh$, where $m$ is the mass of the particle of interest, $g$ is the acceleration due to gravity, and $h$ is height. Using this definition of the potential energy, derive the following expression for pressure: $P = P_o e^{-mgh/kT}$. Assuming that the temperature remains at 298 K, what would you expect the relative pressures of $N_2$ and $O_2$ to be at the tropopause, the boundary between the troposphere and stratosphere roughly 11 km above Earth's surface? At Earth's surface, the composition of air is roughly 78% $N_2$, 21% $O_2$, and 1% other gases.

**P13.9** Consider the following energy-level diagrams:
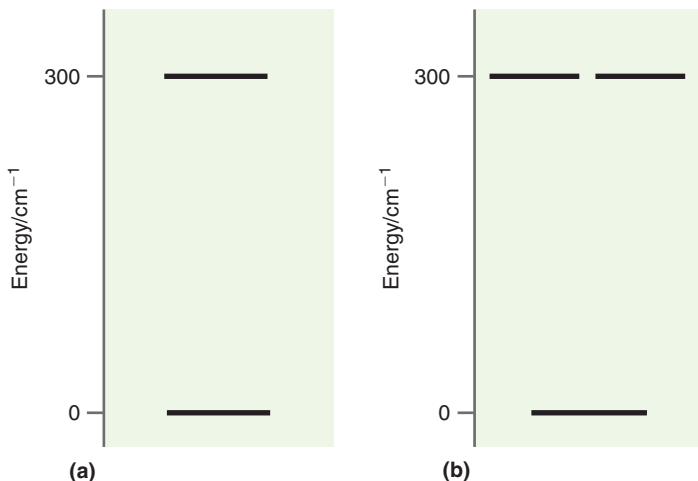


(a)  (b)

**a.** At what temperature will the probability of occupying the second energy level be 0.15 for the states depicted in part (a) of the figure?

**b.** Perform the corresponding calculation for the states depicted in part (b) of the figure. Before beginning the calculation, do you expect the temperature to be higher or lower than that determined in part (a) of this problem? Why?

**P13.10** Consider the following energy-level diagrams, modified from Problem P13.9 by the addition of another excited state with energy of 600. $cm^{-1}$:
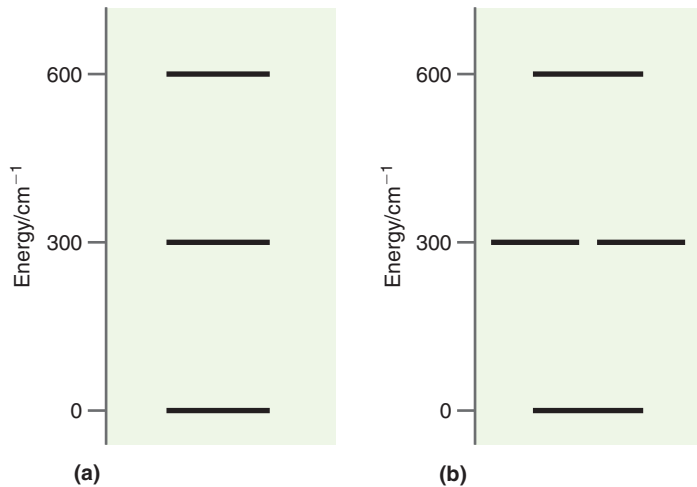


(a)  (b)

**a.** At what temperature will the probability of occupying the second energy level be 0.15 for the states depicted in part (a) of the figure?

**b.** Perform the corresponding calculation for the states depicted in part (b) of the figure.

(*Hint*: You may find this problem easier to solve numerically using a spreadsheet program such as Excel.)

**P13.11** Consider the following sets of populations for four equally spaced energy levels:

| $\varepsilon/\kappa$ (K) | Set A | Set B | Set C |
|---|---|---|---|
| 300. | 5 | 3 | 4 |
| 200. | 7 | 9 | 8 |
| 100. | 1 | 1 | 16 |
| 0 | 33 | 31 | 32 |

**a.** Demonstrate that the sets have the same energy.

**b.** Determine which of the sets is the most probable.

**c.** For the most probable set, is the distribution of energy consistent with a Boltzmann distribution?

**P13.12** A set of 13 particles occupies states with energies of 0, 100., and 200. $cm^{-1}$. Calculate the total energy and number of microstates for the following energy configurations:

**a.** $a_0 = 8$, $a_1 = 5$, and $a_2 = 0$

**b.** $a_0 = 9$, $a_1 = 3$, and $a_2 = 1$

**c.** $a_0 = 10$, $a_1 = 1$, and $a_2 = 2$

Do any of these configurations correspond to the Boltzmann distribution?

**P13.13**  For a set of nondegenerate levels with energy $\varepsilon/k = 0$, 100., and 200. K, calculate the probability of occupying each state when $T = 50.$, 500., and 5000. K. As the temperature continues to increase, the probabilities will reach a limiting value. What is this limiting value?

**P13.14**  For two nondegenerate energy levels separated by an amount of energy $\varepsilon/k = 500.$ K, at what temperature will the population in the higher-energy state be $1/2$ that of the lower-energy state? What temperature is required to make the populations equal?

**P13.15**  Consider a collection of molecules where each molecule has two nondegenerate energy levels that are separated by 6000. $cm^{-1}$. Measurement of the level populations demonstrates that there are exactly 8 times more molecules in the ground state than in the upper state. What is the temperature of the collection?

**P13.16**  Consider a molecule having three energy levels as follows:

| state | Energy ($cm^{-1}$) | degeneracy |
|-------|--------------------|------------|
| 1 | 0 | 1 |
| 2 | 500. | 3 |
| 3 | 1500. | 5 |

What is the value of the partition function when $T = 300.$ and 3000. K?

**P13.17**  Consider the molecule described in the previous problem. Imagine a collection of N molecules all at $T = 300.$ K in which one of these molecules is selected. What is the probability that this molecule will be in the lowest-energy state? What is the probability that it will be in the higher-energy state?

**P13.18**  The emission from C can be used for wavelength calibration of instruments in the ultraviolet. This is generally performed by electron-impact initiated decomposition of a precursor (for example, $CF_4$) resulting in the production of electronically excited C, which relaxes to the ground electronic state by emitting a photon at 193.09 nm. Suppose one wanted to take another approach where C is heated until 5% of the atoms occupy the electronically excited state. Considering only the lowest-energy ground state and the electronically excited state, what temperature is required to achieve this excited-state population?

**P13.19**  The $^{13}C$ nucleus is a spin $1/2$ particle as is a proton. However, the energy splitting for a given field strength is roughly $1/4$ of that for a proton. Using a 1.45 T magnet as in Example Problem 13.6, what is the ratio of populations in the excited and ground spin states for $^{13}C$ at 298 K?

**P13.20**  $^{14}N$ is a spin 1 particle such that the energy levels are at 0 and $\pm \gamma B \hbar$, where $\gamma$ is the magnetogyric ratio and $B$ is the strength of the magnetic field. In a 4.8 T field, the energy splitting between any two spin states expressed as the resonance frequency is 14.45 MHz. Determine the occupation numbers for the three spin states at 298 K.

**P13.21**  When determining the partition function for the harmonic oscillator, the zero-point energy of the oscillator was ignored. Show that the expression for the probability of occupying a specific energy level of the harmonic oscillator with the inclusion of zero-point energy is identical to that ignoring zero-point energy.

**P13.22**  The vibrational frequency of $I_2$ is 208 $cm^{-1}$. At what temperature will the population in the first excited state be half that of the ground state?

**P13.23**  The vibrational frequency of $Cl_2$ is 525 $cm^{-1}$. Will the temperature at which the population in the first excited vibrational state is half that of the ground state be higher or lower relative to $I_2$ (see Problem P13.22)? What is this temperature?

**P13.24**  Determine the partition function for the vibrational degrees of freedom of $Cl_2$ ($\widetilde{\nu} = 525 \ cm^{-1}$) and calculate the probability of occupying the first excited vibrational level at 300. and 1000. K. Determine the temperature at which identical probabilities will be observed for $F_2$ ($\widetilde{\nu} = 917 \ cm^{-1}$).

**P13.25**  Hydroxyl radicals are of interest in atmospheric processes due to their oxidative ability. Determine the partition function for the vibrational degrees of freedom for OH ($\widetilde{\nu} = 3735 \ cm^{-1}$) and calculate the probability of occupying the first excited vibrational level at 260. K. Would you expect the probability for occupying the first-excited vibrational level for OD ($\widetilde{\nu} = 2721 \ cm^{-1}$) to be greater or less than for OH?

**P13.26**  Calculate the partition function for the vibrational energetic degree of freedom for $^{1}H_2$ where $\widetilde{\nu} = 4401 \ cm^{-1}$. Perform this same calculation for $D_2$ (or $^{2}H_2$), assuming the force constant for the bond is the same as in $^{1}H_2$.

**P13.27**  A two-level system is characterized by an energy separation of $1.30 \times 10^{-18}$ J. At what temperature will the population of the ground state be 5 times greater than that of the excited state?

**P13.28**  Rhodopsin is the pigment in the retina rod cells responsible for vision, and it consists of a protein and the co-factor retinal. Retinal is a $\pi$-conjugated molecule which absorbs light in the blue-green region of the visible spectrum, where photon absorption represents the first step in the visual process. Absorption of a photon results in retinal undergoing a transition from the ground- or lowest-energy state of the molecule to the first electronic excited state. Therefore, the wavelength of light absorbed by rhodopsin provides a measure of the ground and excited-state energy gap.

**a.**  The absorption spectrum of rhodopsin is centered at roughly 500. nm. What is the difference in energy between the ground and excited state?

**b.**  At a physiological temperature of 37°C, what is the probability of rhodopsin populating the first excited state? How susceptible do you think rhodopsin is to thermal population of the excited state?

**P13.29** The lowest two electronic energy levels of the molecule NO are illustrated here:
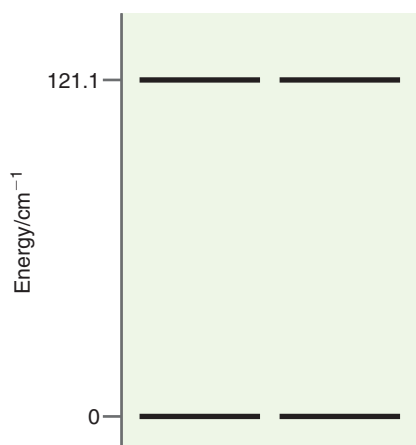


Determine the probability of occupying one of the higher energy states at 100., 500., and 2000. K.

**P13.30** Molecular oxygen populating the excited-singlet state ($^1\Delta_g$) can relax to the ground triplet state ($^3\Sigma_g$, which is the lowest energy state) by emitting a 1270 nm photon.

**a.** Construct the partition function involving the ground and excited-singlet state of molecular oxygen.

**b.** What temperature is required to have 10% population in the excited-singlet state?

**P13.31** The simplest polyatomic molecular ion is $H_3^+$, which can be thought of as molecular hydrogen with an additional proton. Infrared spectroscopic studies of interstellar space have identified this species in the atmosphere of Jupiter and other interstellar bodies. The rotational-vibrational spectrum of the $\nu_2$ band of $H_3^+$ was first measured in the laboratory by T. Oka in 1980 [*Phys. Rev. Lett*. 45 (1980): 531]. The spectrum consists of a series of transitions extending from 2450 to 2950 cm$^{-1}$. Employing an average value of 2700. cm$^{-1}$ for the energy of the first excited rotational-vibrational state of this molecule relative to the ground state, what temperature is required for 10% of the molecules to populate this excited state?

# Web-Based Simulations, Animations, and Problems

**W13.1** In this simulation the behavior of the partition function for a harmonic oscillator with temperature and oscillator frequency is explored. The variation in $q$ with temperature for an oscillator where $\widetilde{\nu} = 1000$ cm$^{-1}$ is studied, and variation in the individual level contributions to the partition function is studied. In addition, the change in level contributions as the oscillator frequency is varied is depicted. This simulation provides insight into the elements of the partition function and the variation of this function with temperature and energy-level spacings.

# For Further Reading

Chandler, D. *Introduction to Modern Statistical Mechanics*. New York: Oxford, 1987.

Hill, T. *Statistical Mechanics. Principles and Selected Applications*. New York: Dover, 1956.

McQuarrie, D. *Statistical Mechanics*. New York: Harper & Row, 1973.

Nash, L. K. "On the Boltzmann Distribution Law." *J. Chemical Education* 59 (1982): 824.

Nash, L. K. *Elements of Statistical Thermodynamics*. San Francisco: Addison-Wesley, 1972.

Noggle, J. H. *Physical Chemistry*. New York: HarperCollins, 1996.

# 14

# Ensemble and Molecular Partition Functions

The relationship between the microscopic description of individual molecules and the macroscopic properties of a collection of molecules is a central concept in statistical mechanics. In this chapter, the relationship between the partition function that describes a collection of noninteracting molecules and the partition function describing an individual molecule is developed. We demonstrate that the molecular partition function can be decomposed into the product of partition functions for each energetic degree of freedom and that the functional form of these partition functions is derived. The concepts outlined in this chapter provide the basic foundation on which statistical thermodynamics resides.

## 14.1 The Canonical Ensemble

An **ensemble** is defined as a large collection of identical units or replicas of a system. For example, a mole of water can be envisioned as an ensemble with Avogadro's number of identical units of water molecules. The ensemble provides a theoretical concept by which the microscopic properties of matter can be related to the corresponding thermodynamic system properties as expressed in the following postulate:

> The average value for a property of the ensemble corresponds to the time-averaged value for the corresponding macroscopic property of the system.

What does this postulate mean? Imagine the individual units of the ensemble sampling the available energy space; the energy content of each unit is measured at a single time, and the measured unit energies used to determine the average energy for the ensemble. According to the postulate, this energy will be equivalent to the average energy of the ensemble as measured over time. This idea, first formulated by
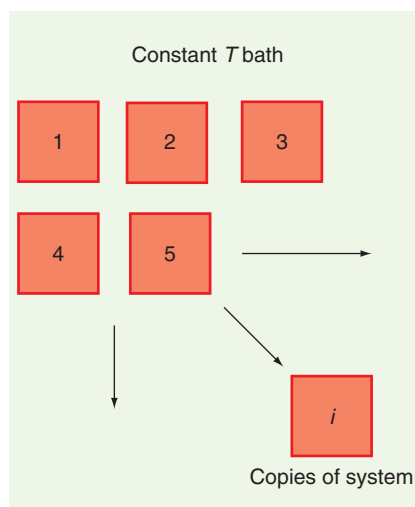
**FIGURE 14.1**
The canonical ensemble is comprised of a collection of identical systems having fixed temperature, volume, and number of particles. The units are embedded in a constant $T$ bath. The arrows indicate that an infinite number of copies of the system comprises the ensemble.

J. W. Gibbs in the late 1800s, lies at the heart of statistical thermodynamics and is explored in this chapter.

To connect ensemble average values and thermodynamic properties, we begin by imagining a collection of identical copies of the system as illustrated in Figure 14.1. These copies of the system are held fixed in space such that they are distinguishable. The volume $V$, temperature $T$, and number of particles in each system $N$ are constant. An ensemble in which $V$, $T$, and $N$ are constant is referred to as a **canonical ensemble.** The term *canonical* means "by common practice" because this is the ensemble employed unless the problem of interest dictates that other variables be kept constant. Note that other quantities can be constant to construct other types of ensembles. For example, if $N$, $V$, and energy are held fixed, the corresponding ensemble is referred to as *microcanonical.* However, for the purposes of this text, the canonical ensemble will prove sufficient.

In the canonical ensemble, each ensemble member is embedded in a temperature bath such that the total ensemble energy is constant. Furthermore, the walls that define the volume of the units can conduct heat, allowing for energy exchange with the surroundings. The challenge is to link the statistical development presented in the previous chapter to a similar statistical description for this ensemble. We begin by considering the total energy of the ensemble $E_c$ which is given by

$$E_c = \sum_i a_{(c)i} E_i \tag{14.1}$$

In Equation (14.1), the terms $a_{(c)i}$ are the occupation numbers corresponding to the number of ensemble members having energy $E_i$. Proceeding exactly as in the previous chapter, the weight $W_c$ associated with a specific configuration of energy among the $N_c$ members of the ensemble is given by

$$W_c = \frac{N_c!}{\prod_i a_{(c)i}!} \tag{14.2}$$

This relationship can be used to derive the probability of finding an ensemble unit at energy $E_i$:

$$p(E_i) = \frac{W_i e^{-\beta E_i}}{Q} \tag{14.3}$$

Equation (14.3) looks very similar to the probability expression derived previously. In this equation, $W_i$ can be thought of as the number of states present at a given energy $E_i$. The quantity $Q$ in Equation (14.3) is referred to as the **canonical partition function** and is defined as follows:

$$Q = \sum_n e^{-\beta E_n} \tag{14.4}$$

In Equation (14.4), the summation is over all energy levels. The probability defined in Equation (14.3) is dependent on two factors: $W_i$, or the number of states present at a given energy that will increase with energy, and a Boltzmann term $e^{-\beta E_i}/Q$ that describes the probability of an ensemble unit having energy $E_i$ that decreases exponentially with energy. The generic behavior of each term with energy is depicted in Figure 14.2. The product of these terms will reach a maximum corresponding to the average ensemble energy. The figure illustrates that an individual unit of the ensemble will have an energy that is equal to or extremely close to the average energy, and that units having energy far from this value will be exceedingly rare. We know this to be the case from experience. Imagine a swimming pool filled with water divided up into one-liter units. If the thermometer at the side of the pool indicates that the water temperature is 18°C, someone diving into the pool will not be worried that the liter of water immediately under his or her head will spontaneously freeze. That is, the temperature measured in one part of the pool is sufficient to characterize the temperature of the water in any part of the pool. Figure 14.2 provides an illustration of the statistical aspects underlying this expectation.
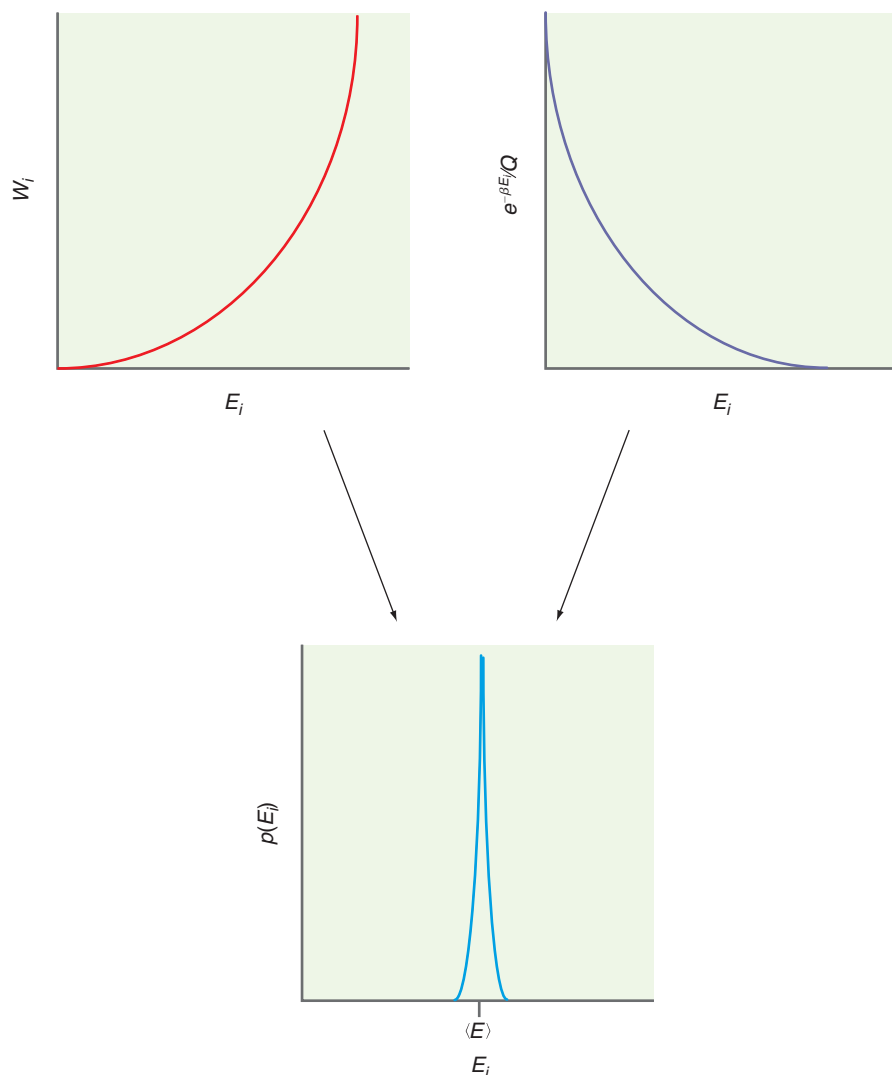
For the canonical ensemble, the probability of a member of the ensemble having a given energy is dependent on the product of $W_i$, the number of states present at a given energy, and the Boltzmann distribution function for the ensemble. The product of these two factors results in a probability distribution that is peaked about the average energy $\langle E \rangle$.

The vast majority of systems in the ensemble will have energy $\langle E \rangle$; therefore, the thermodynamic properties of the unit are representative of the thermodynamic properties of the ensemble, demonstrating the link between the microscopic unit and the macroscopic ensemble. To make this connection mathematically exact the canonical partition function $Q$ must be related to the partition function describing the individual members of the ensemble $q$.

# 14.2 Relating *Q* to *q* for an Ideal Gas

In relating the canonical partition function $Q$ to the partition function describing the members of the ensemble $q$ our discussion is limited to systems consisting of independent "ideal" particles in which the interactions between particles is negligible (for example, an ideal gas). The relationship between $Q$ and $q$ is derived by considering an ensemble made up of two distinguishable units, A and B, as illustrated in Figure 14.3. For this simple ensemble, the partition function is

$$Q = \sum_n e^{-\beta E_n} = \sum_n e^{-\beta(\varepsilon_{A_n} + \varepsilon_{B_n})} \tag{14.5}$$

In this expression, $\varepsilon_{A_n}$ and $\varepsilon_{B_n}$ refer to the energy levels associated with units A and B, respectively.
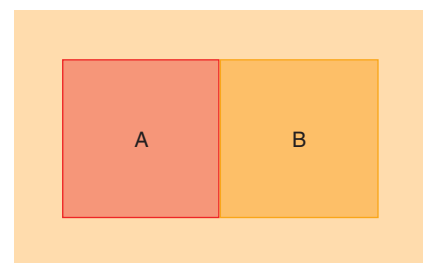
A two-unit ensemble. In this ensemble, the two units, A and B, are distinguishable.

Assuming that the energy levels are quantized such that they can be indexed $A_0$, $A_1$, $A_2$, etc. and $B_0$, $B_1$, $B_2$ and so forth, Equation (14.5) becomes

$$
\begin{aligned}
Q &= \sum_n e^{-\beta(\varepsilon_{A_n} + \varepsilon_{B_n})} = e^{-\beta(\varepsilon_{A_0} + \varepsilon_{B_0})} + e^{-\beta(\varepsilon_{A_0} + \varepsilon_{B_1})} + e^{-\beta(\varepsilon_{A_0} + \varepsilon_{B_2})} + \dots \\
&\quad + e^{-\beta(\varepsilon_{A_1} + \varepsilon_{B_0})} + e^{-\beta(\varepsilon_{A_1} + \varepsilon_{B_1})} + e^{-\beta(\varepsilon_{A_1} + \varepsilon_{B_2})} + \dots \\
&\quad + e^{-\beta(\varepsilon_{A_2} + \varepsilon_{B_0})} + e^{-\beta(\varepsilon_{A_2} + \varepsilon_{B_1})} + e^{-\beta(\varepsilon_{A_2} + \varepsilon_{B_2})} + \dots \\
&= (e^{-\beta\varepsilon_{A_0}} + e^{-\beta\varepsilon_{A_1}} + e^{-\beta\varepsilon_{A_2}} + \dots)(e^{-\beta\varepsilon_{B_0}} + e^{-\beta\varepsilon_{B_1}} + e^{-\beta\varepsilon_{B_2}} + \dots) \\
&= (q_A)(q_B) \\
&= q^2
\end{aligned}
$$

The last step in the derivation is accomplished by recognizing that the ensemble units are identical such that the partition functions are also identical. Extending the preceding result to a system with $N$ distinguishable units, the canonical partition function is found to be simply the product of unit partition functions

$$ Q = q^N \quad \text{for } N \text{ distinguishable units} \tag{14.6} $$

Thus far no mention has been made of the size of the identical systems comprising the ensemble. The systems can be as small as desired, including just a single molecule. Taking the single-molecule limit, a remarkable conclusion is reached: the canonical ensemble is nothing more than the product of the molecular partition functions. This is the direct connection between the microscopic and macroscopic perspectives that we have been searching for. The quantized energy levels of the molecular (or atomic) system are embedded in the **molecular partition function $q$,** and this partition function can be used to define the partition function for the ensemble $Q$. Finally, $Q$ can be directly related to the thermodynamic properties of the ensemble.

The preceding derivation assumed that the ensemble members were distinguishable. This might be the case for a collection of molecules coupled to a surface where they cannot move, but what happens to this derivation when the ensemble is in the gaseous state? Clearly, the translational motion of the gas molecules will make identification of each individual molecule impossible. Therefore, how does Equation (14.6) change if the units are indistinguishable? A simple counting example will help to answer this question. Consider three distinguishable oscillators (A, B, and C) with three total quanta of energy as described in the previous chapter. The dominant configuration of energy was with the oscillators in three separate energy states, denoted "2, 1, 0." The energy states relative to the oscillators can be arranged in six different ways:

| A | B | C |
|---|---|---|
| 2 | 1 | 0 |
| 2 | 0 | 1 |
| 1 | 2 | 0 |
| 0 | 2 | 1 |
| 1 | 0 | 2 |
| 0 | 1 | 2 |

However, if the three oscillators are indistinguishable, there is no difference among the arrangements listed. In effect, there is only one arrangement of energy that should be counted. This problem was encountered in the chapter on probability when discussing indistinguishable particles, and in such cases the total number of permutations was divided by $N!$ where $N$ was the number of units in the collection. Extending this logic to a molecular ensemble dictates that the canonical partition function for indistinguishable particles have the following form:

$$ Q = \frac{q^N}{N!} \quad \text{for } N \text{ indistinguishable units} \tag{14.7} $$

Equation (14.7) is correct in the limit for which the number of energy levels available is significantly greater than the number of particles. This discussion of statistical mechanics is limited to systems for which this is true, and the validity of this statement is demonstrated later in this chapter. It is also important to keep in mind that Equation (14.7) is limited to ideal systems of noninteracting particles such as an ideal gas.

# 14.3 Molecular Energy Levels

The relationship between the canonical and molecular partition functions provides the link between the microscopic and macroscopic descriptions of the system. The molecular partition function can be evaluated by considering molecular energy levels. For polyatomic molecules, there are four **energetic degrees of freedom** to consider in constructing the molecular partition function:

1. Translation
2. Rotation
3. Vibration
4. Electronic

Assuming the energetic degrees of freedom are not coupled, the total molecular partition function that includes all of these degrees of freedom can be decomposed into a product of partition functions corresponding to each degree of freedom. An equivalent approach is taken in quantum mechanics when separating the molecular Hamiltonian into translational, rotational, and vibrational components. Let $\varepsilon_{Total}$ represent the energy associated with a given molecular energy level. This energy will depend on the translational, rotational, vibrational, and electronic level energies as follows:

$$\varepsilon_{Total} = \varepsilon_T + \varepsilon_R + \varepsilon_V + \varepsilon_E \tag{14.8}$$

Recall that the molecular partition function is obtained by summing over molecular energy levels. Using the expression for the total energy and substituting into the expression for the partition function, the following expression is obtained:

$$
\begin{aligned}
q_{Total} &= \sum g_{Total} e^{-\beta \varepsilon_{Total}} \\
&= \sum (g_T g_R g_V g_E) e^{-\beta(\varepsilon_T + \varepsilon_T + \varepsilon_T + \varepsilon_E)} \\
&= \sum (g_T e^{-\beta \varepsilon_T})(g_R e^{-\beta \varepsilon_R})(g_V e^{-\beta \varepsilon_V})(g_E e^{-\beta \varepsilon_E}) \\
&= q_T q_R q_V q_E
\end{aligned}
\tag{14.9}
$$

This relationship demonstrates that the total molecular partition function is simply the product of partition functions for each molecular energetic degree of freedom. Using this definition for the molecular partition function, the final relationships of interest are

$$Q_{Total} = q_{Total}^N \text{ (distinguishable)} \tag{14.10}$$

$$Q_{Total} = \frac{1}{N!} q_{Total}^N \text{ (indistinguishable)} \tag{14.11}$$

All that remains to derive are partition functions for each energetic degree of freedom, a task that is accomplished in the remainder of this chapter.

# 14.4 Translational Partition Function

Translational energy levels correspond to the translational motion of atoms or molecules in a container of volume V. Rather than work directly in three dimensions, a one-dimensional model is first employed and then later extended to three dimensions. From quantum mechanics, the energy levels of a molecule confined to a box were described by the "particle-in-a-box" model as illustrated in Figure 14.4. In this figure, a particle with mass $m$ is free to move in the domain $0 \le x \le a$, where $a$ is the length of the box. Using the expression for the energy levels provided in Figure 14.4, the partition function for translational energy in one dimension becomes

$$q_{T,1D} = \sum_{n=1}^{\infty} e^{\frac{-\beta n^2 h^2}{8ma^2}} \tag{14.12}$$
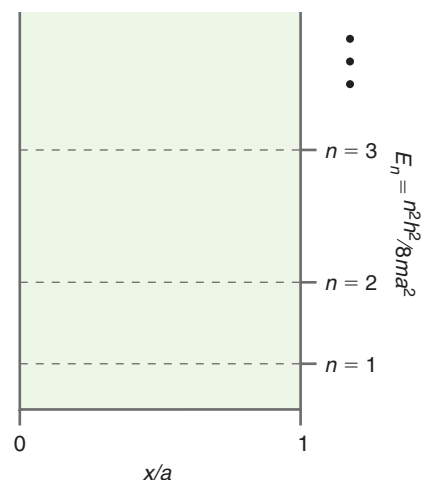


**FIGURE 14.4**
Particle-in-a-box model for translational energy levels.

Notice that the summation consists of an infinite number of terms. Furthermore, a closed-form expression for this series does not exist such that it appears one must evaluate the sum directly. However, a way around this apparently impossible task becomes evident when the spacing between energy translational energy states is considered, as illustrated in the following example.

### EXAMPLE PROBLEM 14.1

What is the difference in energy between the $n = 2$ and $n = 1$ states for molecular oxygen constrained by a one-dimensional box having a length of 1.00 cm?

### Solution

The energy difference is obtained by using the expression for the one-dimensional particle-in-a-box model as follows:

$$\Delta E = E_2 - E_1 = 3E_1 = \frac{3h^2}{8ma^2}$$

The mass of an $O_2$ molecule is $5.31 \times 10^{-26}$ kg such that

$$\Delta E = \frac{3(6.626 \times 10^{-34} \text{ J s})^2}{8(5.31 \times 10^{-26} \text{ kg})(0.01 \text{ m})^2}$$

$$= 3.10 \times 10^{-38} \text{ J}$$

Converting to units of $cm^{-1}$:

$$\Delta E = \frac{3.10 \times 10^{-38} \text{ J}}{hc} = 1.56 \times 10^{-15} cm^{-1}$$

At 298 K, the amount of thermal energy available as given by the product of Boltzmann's constant and temperature $kT$ is 207 $cm^{-1}$. Clearly, the spacings between translational energy levels are extremely small relative to $kT$ at room temperature.

Because numerous translational energy levels are accessible at room temperature, the summation in Equation (14.12) can be replaced by integration with negligible error:

$$q_T = \sum e^{-\beta\alpha n^2} \approx \int_0^\infty e^{-\beta\alpha n^2} dn \qquad (14.13)$$

In this expression, the following substitution was made to keep the collection of constant terms compact:

$$\alpha = \frac{h^2}{8ma^2} \qquad (14.14)$$

The integral in Equation (14.13) is readily evaluated (see Appendix B, Math Supplement):

$$q_T \approx \int_0^\infty e^{-\beta\alpha n^2} dn = \frac{1}{2}\sqrt{\frac{\pi}{\beta\alpha}} \qquad (14.15)$$

Substituting in for $\alpha$, the **translational partition function** in one dimension becomes

$$q_{T,1D} = \left(\frac{2\pi m}{h^2\beta}\right)^{1/2} a \qquad (14.16)$$

This expression can be simplified by defining the **thermal de Broglie wavelength,** or simply the **thermal wavelength,** as follows:

$$\Lambda = \left(\frac{h^2\beta}{2\pi m}\right)^{1/2} \qquad (14.17)$$

such that

$$q_{T,1D} = \frac{a}{\Lambda} = \left(\frac{2\pi m}{\beta}\right)^{1/2}\frac{a}{h} = (2\pi mkT)^{1/2}\frac{a}{h} \qquad (14.18)$$

Referring to $\Lambda$ as the thermal wavelength reflects the fact that the average momentum of a gas particle $p$ is equal to $(mkT)^{1/2}$. Therefore, $\Lambda$ is essentially $h/p$, or the de Broglie wavelength of the particle. The translational degrees of freedom are considered separable; therefore, the three-dimensional translational partition function is the product of one-dimensional partition functions for each dimension:

$$
\begin{aligned}
q_{T,3D} &= q_{T_x}q_{T_y}q_{T_z} \\
&= \left(\frac{a_x}{\Lambda}\right)\left(\frac{a_y}{\Lambda}\right)\left(\frac{a_z}{\Lambda}\right) \\
&= \left(\frac{1}{\Lambda}\right)^3 a_x a_y a_z \\
&= \left(\frac{1}{\Lambda}\right)^3 V
\end{aligned}
$$

$$q_{T,3D} = \frac{V}{\Lambda^3} = (2\pi mkT)^{3/2}\frac{V}{h^3} \qquad (14.19)$$

where $V$ is volume and $\Lambda$ is the thermal wavelength [Equation (14.17)]. Notice that the translational partition function depends on both $V$ and $T$. Recall the discussion from the previous chapter in which the partition function was described conceptually as providing a measure of the number of energy states available to the system at a given temperature. The increase in $q_T$ with volume reflects the fact that as volume is increased, the translational energy-level spacings decrease such that more states are available for population at a given $T$. Given the small energy spacings between translational energy levels relative to $kT$ at room temperature, we might expect that at room temperature a significant number of translational energy states are accessible. The following example provides a test of this expectation.

## EXAMPLE PROBLEM 14.2

What is the translational partition function for Ar confined to a volume of 1.00 L at 298 K?

### Solution

Evaluation of the translational partition function is dependent on determining the thermal wavelength [Equation (14.17)]:

$$\Lambda = \left(\frac{h^2\beta}{2\pi m}\right)^{1/2} = \frac{h}{(2\pi mkT)^{1/2}}$$

The mass of Ar is $6.63 \times 10^{-26}$ kg. Using this value for $m$, the thermal wavelength becomes

$$\Lambda = \frac{6.626 \times 10^{-34}\,\text{J s}}{\left(2\pi(6.63 \times 10^{-26}\,\text{kg})(1.38 \times 10^{-23}\,\text{JK}^{-1})(298\,\text{K})\right)^{1/2}}$$

$$= 1.60 \times 10^{-11}\,\text{m}$$

The units of volume must be such that the partition function is unitless. Therefore, conversion of volume to units of cubic meters ($\text{m}^3$) is performed as follows:

$$V = 1.00\,\text{L} = 1000\,\text{mL} = 1000\,\text{cm}^3\left(\frac{1\,\text{m}}{100\,\text{cm}}\right)^3 = 0.001\,\text{m}^3$$

The partition function is simply the volume divided by the thermal wavelength cubed:

$$q_{T,3D} = \frac{V}{\Lambda^3} = \frac{0.001\,\text{m}^3}{(1.60 \times 10^{-11}\,\text{m})^3} = 2.44 \times 10^{29}$$

The magnitude of the translational partition function determined in Example Problem 14.2 illustrates that a vast number of translation energy states are available at room temperature. In fact, the number of accessible states is roughly $10^6$ times larger than Avogadro's number, illustrating that the assumption that many more states are available relative to units in the ensemble (Section 14.2) is reasonable.

# 14.5 Rotational Partition Function: Diatomics
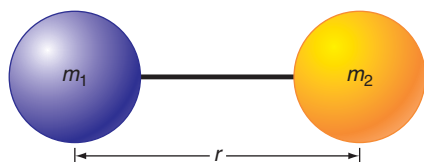
A **diatomic** molecule consists of two atoms joined by a chemical bond as illustrated in Figure 14.5. In treating rotational motion of diatomic molecules, the rigid rotor approximation is employed in which the bond length is assumed to remain constant during rotational motion and effects such as centrifugal distortion are neglected.

In deriving the rotational partition function, an approach similar to that used in deriving the translational partition function is employed. Within the rigid-rotor approximation, the quantum mechanical description of rotational energy levels for diatomic molecules dictates that the energy of a given rotational state $E_J$ is dependent on the rotational quantum number $J$:

$$E_J = hcBJ(J + 1) \quad \text{for } J = 0, 1, 2, \ldots \tag{14.20}$$

where $J$ is the quantum number corresponding to rotational energy level and can take on integer values beginning with zero. The quantity $B$ is the **rotational constant** and is given by

$$B = \frac{h}{8\pi^2 cI} \tag{14.21}$$

where $I$ is the moment of inertia, which is equal to

$$I = \mu r^2 \tag{14.22}$$

In the expression for the moment of inertia, $r$ is the distance separating the two atomic centers and $\mu$ is the reduced mass, which for a diatomic molecule consisting of atoms having masses $m_1$ and $m_2$ is equal to

$$\mu = \frac{m_1 m_2}{m_1 + m_2} \tag{14.23}$$

Because diatomic molecules differ depending on the masses of atoms in the molecule and the bond length, the value of the rotational constant is molecule dependent. Using the preceding expression for the rotational energy, the rotational partition function can be constructed by simply substituting into the general form of the molecular partition function:

$$q_R = \sum_J g_J e^{-\beta E_J} = \sum_J g_J e^{-\beta hcBJ(J+1)} \tag{14.24}$$

In this expression, the energies of the levels included in the summation are given by $hcBJ(J + 1)$. However, notice that the expression for the rotational partition function contains an addition term, $g_J$, that represents the number of rotational states present at a given energy level, or the degeneracy of the rotational energy level. To determine the degeneracy, consider a rigid rotor and the time-independent Schrödinger equation:

$$H\psi = E\psi \tag{14.25}$$

For the rigid rotor, the Hamiltonian ($H$) is proportional to the square of the total angular momentum given by the operator $\hat{l}^2$. The eigenstates of this operator are the spherical harmonics with the following eigenvalues:

$$\hat{l}^2\psi = \hat{l}^2 Y_{l,m}(\theta, \phi) = \hbar^2 l(l + 1)Y_{l,m}(\theta, \phi) \tag{14.26}$$

In this expression, $l$ is a quantum number corresponding to total angular momentum ranging from 0, 1, 2, ..., to infinity. The spherical harmonics are also eigenfunctions of



**FIGURE 14.5**
Schematic representation of a diatomic molecule, consisting of two masses ($m_1$ and $m_2$) joined by a chemical bond with the separation of atomic centers equal to the bond length $r$.

the $\hat{l}_z$ operator corresponding to the $z$ component of the angular momentum. The corresponding eigenvalues employing the $\hat{l}_z$ operator are given by

$$\hat{l}_z Y_{l,m}(\theta, \phi) = \hbar m Y_{l,m}(\theta, \phi) \qquad (14.27)$$

Possible values for the quantum number $m$ in Equation (14.27) are dictated by the quantum number $l$:

$$m = -l \ldots 0 \ldots l \quad \text{or} \quad (2l + 1) \qquad (14.28)$$

Thus, the degeneracy of the rotational energy levels originates from the quantum number $m$ because all values of $m$ corresponding to a given quantum number $l$ will have the same total angular momentum and, therefore, the same energy. Using the value of $(2l + 1)$ or $(2J + 1)$ for the degeneracy, the rotational partition function is

$$q_R = \sum_J (2J + 1)e^{-\beta hcBJ(J+1)} \qquad (14.29)$$

As written, evaluation of Equation (14.29) involves summation over all rotational states. A similar issue was encountered when the expression for the translational partition function was evaluated. The spacings between translational levels were very small relative to $kT$ such that the partition function could be evaluated by integration rather than discrete summation. Are the rotational energy-level spacings also small relative to $kT$ such that integration can be performed instead of summation?

   To answer this question, consider the energy-level spacings for the rigid rotor presented in Figure 14.6 The energy of a given rotational state (in units of the rotational constant $B$) are presented as a function of the rotational quantum number $J$. The energy-level spacings are multiples of $B$. The value of $B$ will vary depending on the molecule of interest, with representative values provided in Table 14.1. Inspection of the table reveals a few interesting trends. First, the rotational constant depends on the atomic mass, with an increase in atomic mass resulting in a reduction in the rotational constant. Second, the values for $B$ are quite different; therefore, any comparison of rotational state energies to $kT$ will depend on the diatomic of interest. For example, at 298 K, $kT = 207\ \text{cm}^{-1}$, which is roughly equal to the energy of the $J = 75$ level of $I_2$. For this species, the energy-level spacings are clearly much smaller than $kT$ and integration of the partition function is appropriate. However, for $H_2$ the $J = 2$ energy level is greater than $kT$ so that integration would be inappropriate, and evaluation of the partition function by direct summation must be performed. In the remainder of this chapter, we assume that integration of the rotational partition function is appropriate unless stated otherwise.

   With the assumption that the rotational energy-level spacings are small relative to $kT$, evaluation of the rotational partition function is performed with integration over the rotational states:

$$q_R = \int_0^\infty (2J + 1)e^{-\beta hcBJ(J+1)}\,dJ \qquad (14.30)$$

Evaluation of the preceding integral is simplified by recognizing the following:

$$\frac{d}{dJ}e^{-\beta hcBJ(J+1)} = -\beta hcB(2J + 1)e^{-\beta hcBJ(J+1)}$$
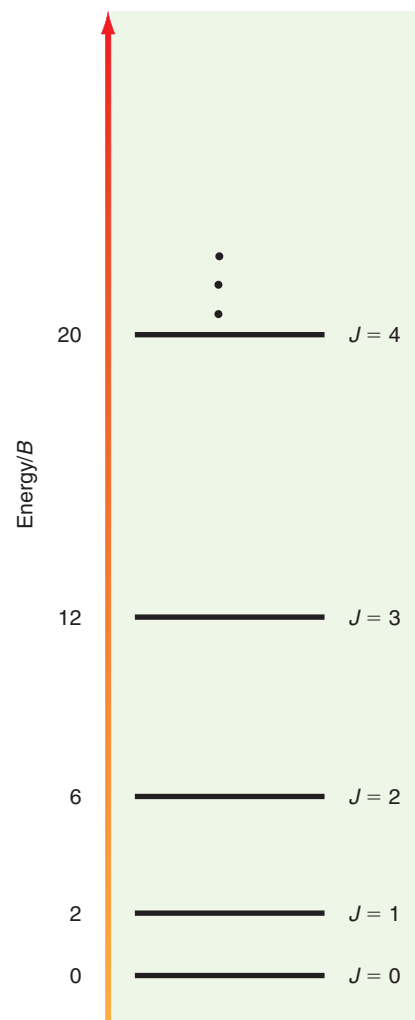


**FIGURE 14.6**
Rotational energy levels as a function of the rotational quantum number $J$. The energy of a given rotational state is equal to $BJ(J + 1)$.

| TABLE 14.1 | Rotational Constants for Some Representative Diatomic Molecules | | |
|---|---|---|---|
| Molecule | $B$ (cm$^{-1}$) | Molecule | $B$ (cm$^{-1}$) |
| $H^{35}Cl$ | 10.595 | $H_2$ | 60.853 |
| $H^{37}Cl$ | 10.578 | $^{14}N^{16}O$ | 1.7046 |
| $D^{35}Cl$ | 5.447 | $^{127}I^{127}I$ | 0.03735 |

*Source*: Herzberg, G., *Molecular Spectra and Molecular Structure, Volume 1: Spectra of Diatomic Molecules*. Melbourne, FL: Krieger Publishing, 1989.

Heterodiatomic
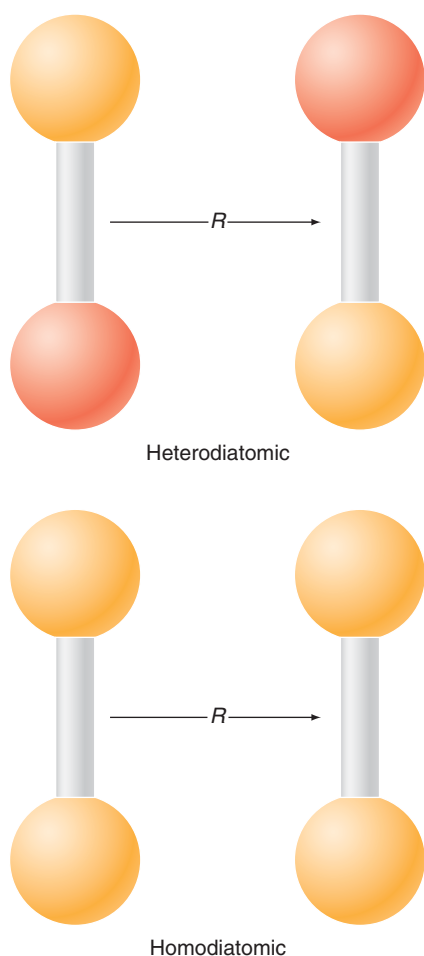


Homodiatomic

**FIGURE 14.7**
A 180° rotation of heterodiatomic and homodiatomic molecules.

Using this relationship, the expression for the **rotational partition function** can be rewritten and the result evaluated as follows:

$$q_R = \int_0^\infty (2J + 1)e^{-\beta hcBJ(J+1)}\, dJ = \int_0^\infty \frac{-1}{\beta hcB}\frac{d}{dJ}e^{-\beta hcBJ(J+1)}\, dJ$$

$$= \frac{-1}{\beta hcB}e^{-\beta hcBJ(J+1)}\Big|_0^\infty = \frac{1}{\beta hcB}$$

$$q_R = \frac{1}{\beta hcB} = \frac{kT}{hcB} \tag{14.31}$$

### 14.5.1 The Symmetry Number

The expression for the rotational partition function of a diatomic molecule provided in the previous section is correct for heterodiatomic species in which the two atoms comprising the diatomic are not equivalent. HCl is a heterodiatomic species because the two atoms in the diatomic, H and Cl, are not equivalent. However, the expression for the rotational partition function must be modified when applied to homodiatomic molecules such as $N_2$. A simple illustration of why such a modification is necessary is presented in Figure 14.7. In the figure, rotation of the heterodiatomic results in a species that is distinguishable from the molecule before rotation. However, the same 180° rotation applied to a homodiatomic results in a configuration that is equivalent to the prerotation form. This difference in behavior is similar to the differences between canonical partition functions for distinguishable and indistinguishable units. In the partition function case, the result for the distinguishable case was divided by $N!$ to take into account the "overcounting" of nonunique microstates encountered when the units are indistinguishable. In a similar spirit, for homodiatomic species the number of classical rotational states (i.e., distinguishable rotational configurations) is overcounted by a factor of 2.

To correct our rotational partition function for overcounting, we can simply divide the expression for the rotational partition function by the number of equivalent rotational configurations. This factor is known as the **symmetry number** $\sigma$ and is incorporated into the partition function as follows:

$$q_R = \frac{1}{\sigma\beta hcB} = \frac{kT}{\sigma hcB} \tag{14.32}$$

The concept of a symmetry number can be extended to molecules other than diatomics. For example, consider a trigonal pyramidal molecule such as $NH_3$ as illustrated in Figure 14.8.
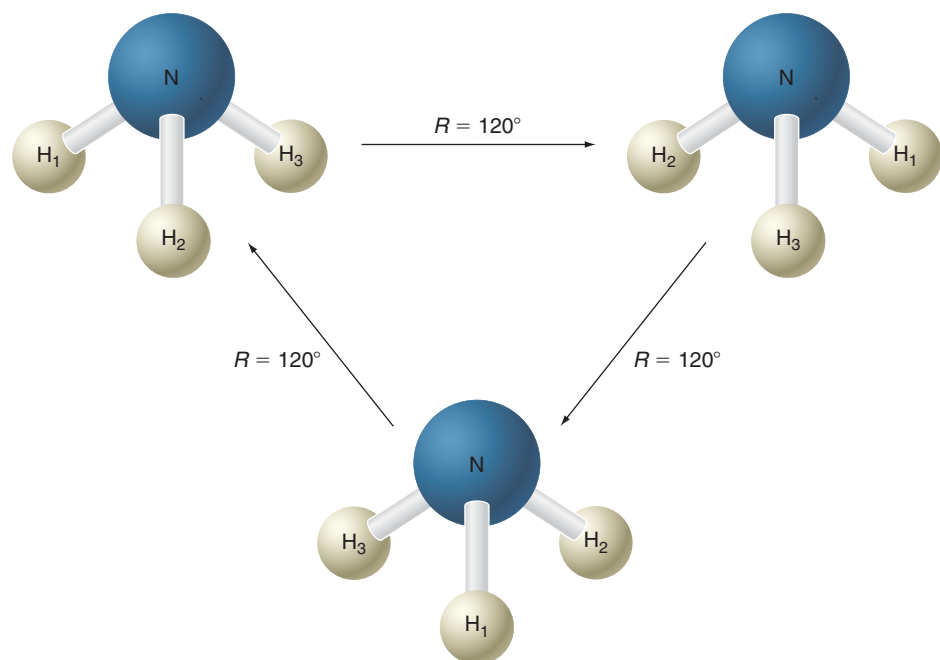


**FIGURE 14.8**
Rotational configurations for $NH_3$.

Imagine that performing a 120° rotation about an axis through the nitrogen atom and the center of the triangle made the three hydrogens. The resulting configuration would be exactly equivalent to the previous configuration before rotation. Furthermore, a second 120° rotation would produce a third configuration. A final 120° would result in the initial prerotation configuration. Therefore, $NH_3$ has three equivalent rotational configurations; therefore, $\sigma = 3$.

---

### EXAMPLE PROBLEM 14.3

What is the symmetry number for methane ($CH_4$)?

#### Solution

To determine the number of equivalent rotational configurations, we will proceed in a fashion similar to that employed for $NH_3$. The tetrahedral structure of methane is shown in the following figure:
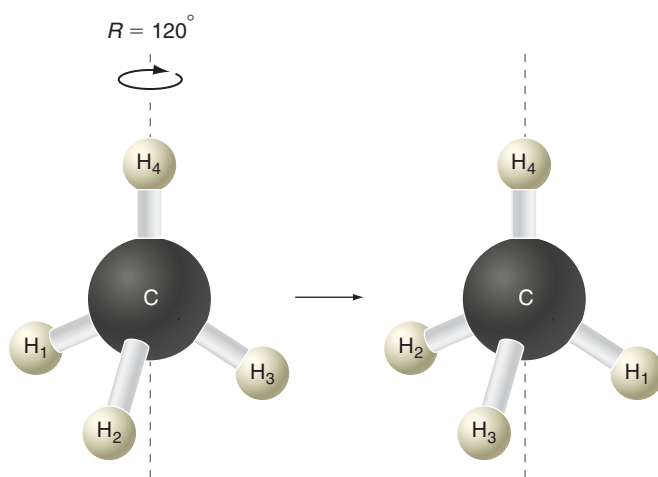


Similar to $NH_3$, three equivalent configurations can be generated by 120° rotation about the axis depicted by the dashed line in the figure. Furthermore, we can draw four such axes of rotation aligned with each of the four C—H bonds. Therefore, there are 12 total rotational configurations for $CH_4$ corresponding to $\sigma = 12$.

## 14.5.2 Rotational Level Populations and Spectroscopy

There is a direct relationship between the populations in various rotational energy levels and rotational-vibrational infrared absorption intensities. With the rotational partition function, we are in a position to explore this relationship in detail. The probability of occupying a given rotational energy level $p_J$ is given by

$$p_J = \frac{g_J e^{-\beta hcBJ(J+1)}}{q_R} = \frac{(2J+1)e^{-\beta hcBJ(J+1)}}{q_R} \tag{14.33}$$

Previously $H^{35}Cl$ where $B = 10.595 \text{ cm}^{-1}$ was employed to illustrate the relationship between $p_J$ and absorption intensity. At 300. K the rotational partition function for $H^{35}Cl$ is

$$q_R = \frac{1}{\sigma \beta hcB} = \frac{kT}{\sigma hcB} = \frac{(1.38 \times 10^{-23}\,\text{J}\,\text{K}^{-1})(300.\,\text{K})}{(1)(6.626 \times 10^{-34}\,\text{J}\,\text{s})(3.00 \times 10^{10}\,\text{cm}\,\text{s}^{-1})(10.595\,\text{cm}^{-1})}$$

$$= 19.7 \tag{14.34}$$

With $q_R$, the level probabilities can be readily determined using Equation (14.33), and the results of this calculation are presented in Figure 14.9. The intensity of the $P$ and $R$ branch transitions in a rotational-vibrational infrared absorption spectrum are proportional to the probability of occupying a given $J$ level. This dependence is reflected by the evolution in

Probability of occupying a rotational
energy level $p_J$ as a function of rotational
quantum number $J$ for $H^{35}Cl$ at 300. K.
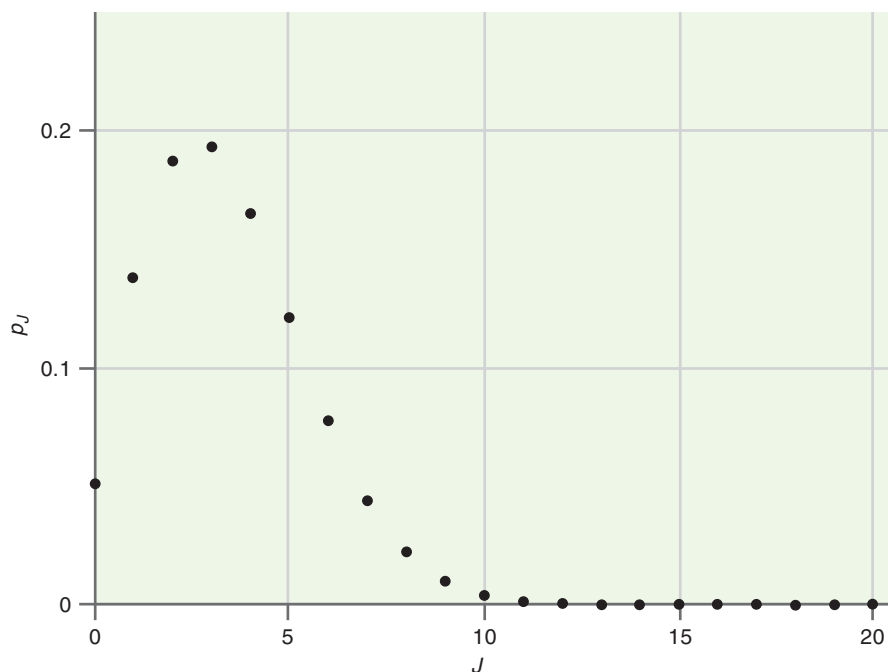


rotational-vibrational transition intensity as a function of $J$. The transition moment
demonstrates modest $J$ dependence as well such that the correspondence between transi-
tion intensity and rotational level population is not exact.

## EXAMPLE PROBLEM 14.4

In a rotational spectrum of HBr ($B = 8.46 \text{ cm}^{-1}$), the maximum intensity transition in
the R-branch corresponds to the $J = 4$ to 5 transition. At what temperature was the
spectrum obtained?

### Solution

The information provided for this problem dictates that the $J = 4$ rotational energy
level was the most populated at the temperature at which the spectrum was taken. To
determine the temperature, we first determine the change in occupation number for
the rotational energy level, $a_J$, versus $J$ as follows:

$$a_J = \frac{N(2J + 1)e^{-\beta hc BJ(J+1)}}{q_R} = \frac{N(2J + 1)e^{-\beta hc BJ(J+1)}}{\left(\dfrac{1}{\beta hc B}\right)}$$

$$= N\beta hc B(2J + 1)e^{-\beta hc BJ(J+1)}$$

Next, we take the derivative of $a_J$ with respect to $J$ and set the derivative equal to zero
to find the maximum of the function:

$$\frac{da_J}{dJ} = 0 = \frac{d}{dJ}N\beta hc B(2J + 1)e^{-\beta hc BJ(J+1)}$$

$$0 = \frac{d}{dJ}(2J + 1)e^{-\beta hc BJ(J+1)}$$

$$0 = 2e^{-\beta hc BJ(J+1)} - \beta hc B(2J + 1)^2 e^{-\beta hc BJ(J+1)}$$

$$0 = 2 - \beta hc B(2J + 1)^2$$

$$2 = \beta hc B(2J + 1)^2 = \frac{hc B}{kT}(2J + 1)^2$$

$$T = \frac{(2J + 1)^2 hc B}{2k}$$

Substitution of $J = 4$ into the preceding expression results in the following temperature at which the spectrum was obtained:

$$
\begin{aligned}
T &= \frac{(2J + 1)^2 hcB}{2k} \\
&= \frac{(2(4) + 1)^2 (6.626 \times 10^{-34}\,\text{J s})(3.00 \times 10^{10}\,\text{cm s}^{-1})(8.46\,\text{cm}^{-1})}{2(1.38 \times 10^{-23}\,\text{J K}^{-1})} \\
&= 4943\,\text{K}
\end{aligned}
$$

### 14.5.3 An Advanced Topic: The Rotational States of $H_2$

The rotational-level distribution of $H_2$ provides an elegant example of the influence of molecular symmetry on the partition function. Molecular hydrogen exists in two forms, one in which the nuclear spins are paired (***para*-hydrogen**) and one in which the spins are aligned (***ortho*-hydrogen**). Because the hydrogen nuclei are spin $1/2$ particles, they are fermions. The Pauli exclusion principle dictates that when two identical fermions interchange position, the overall wave function describing the system must be antisymmetric (or change sign) with interchange. The wave function in this case can be separated into a product of spin and rotational components. The spin component of the wave function is considered first. For *para*-hydrogen, rotation results in the interchange of two nuclei (A and B) having opposite spin ($\alpha$ and $\beta$) such that the spin component of the wave function should be antisymmetric with nuclei interchange due to rotation. This requirement is accomplished using the following linear combination of nuclear spin states:

$$ \psi_{spin,\,para} = \alpha(A)\beta(B) - \alpha(B)\beta(A) $$

Interchange of the nuclear labels A and B corresponding to rotation will result in the preceding wave function changing sign such that the spin component of the *para*-hydrogen wave function is antisymmetric with respect to interchange.

For *ortho*-hydrogen, rotation results in the interchange of two nuclei with the same spin; therefore, the spin wave function should be symmetric. Three combinations of nuclear spin states meet this requirement:

$$ \psi_{spin,\,ortho} = \{\alpha(A)\alpha(B), \beta(A)\beta(B), \alpha(A)\beta(B) + \beta(A)\alpha(B)\} $$

In summary, the spin component of the wave function is antisymmetric with respect to nuclei interchange for *para*-hydrogen, but symmetric for *ortho*-hydrogen.

Next, consider the symmetry of the rotational component of the wave function. It can be shown that the symmetry of rotational states is dependent on the rotational quantum number $J$. If $J$ is an even integer ($J = 0, 2, 4, 6, \ldots$) the corresponding rotational wave function is symmetric with respect to interchange, and if $J$ is odd ($J = 1, 3, 5, 7, \ldots$) the wave function is antisymmetric. Because the wave function is the product of spin and rotational components, this product must be antisymmetric. Therefore, the rotational wave function for *para*-hydrogen is restricted to even-$J$ levels, and for *ortho*-hydrogen is restricted to odd-$J$ levels. Finally, the nuclear-spin-state degeneracy for *ortho*- and *para*-hydrogen is three and one, respectively. Therefore, the rotational energy levels for *ortho*-hydrogen have an additional threefold degeneracy.

A collection of molecular hydrogen will contain both *ortho*- and *para*-hydrogen so that the rotational partition function is

$$ q_R = \frac{1}{4}\left[ 1 \sum_{J=0,2,4,6,\ldots} (2J + 1)e^{-\beta hcBJ(J+1)} + 3 \sum_{J=1,3,5,\ldots} (2J + 1)e^{-\beta hcBJ(J+1)} \right] \tag{14.35} $$

In Equation (14.35), the first term in brackets corresponds to *para*-hydrogen, and the second term corresponds to *ortho*-hydrogen. In essence, this expression for $q_R$ represents average $H_2$ consisting of one part *para*-hydrogen and three parts *ortho*-hydrogen. Notice that the symmetry number is omitted in Equation (14.35) because overcounting of the allowed rotational levels has already been taken into account by restricting the summations to even or odd $J$. At high temperatures, the value of $q_R$ determined using Equation (14.35) will, to good approximation, equal that obtained using Equation (14.32) with $\sigma = 2$, as the following example illustrates.

**EXAMPLE PROBLEM 14.5**

What is the rotational partition function for $H_2$ at 1000. K?

**Solution**

The rotational partition function for $H_2$, assuming that the high-temperature limit is valid, is given by

$$q_R = \frac{1}{\sigma\beta hcB} = \frac{1}{2\beta hcB}$$

With $B = 60.589$ cm$^{-1}$ (Table 14.1):

$$q_R = \frac{1}{2\beta hcB} = \frac{kT}{2hcB}$$

$$= \frac{(1.38 \times 10^{-23}\,\mathrm{J\,K^{-1}})(1000.\,\mathrm{K})}{2(6.626 \times 10^{-34}\,\mathrm{J\,s})(3.00 \times 10^{10}\,\mathrm{cm\,s^{-1}})(60.589\,\mathrm{cm^{-1}})} = 5.73$$

Evaluation of the rotational partition function by direct summation is performed as follows:

$$q_R = \frac{1}{4}\left[1 \sum_{J=0,2,4,6,\dots} (2J+1)e^{-\beta hcBJ(J+1)}\right.$$

$$\left. + 3\sum_{J=1,3,5,\dots} (2J+1)e^{-\beta hcBJ(J+1)}\right] = 5.91$$

Comparison of these two expressions demonstrates that the high-T expression for $q_R$ with $\sigma = 2$ provides a good estimate for the value of the rotational partition function of $H_2$.

## 14.5.4 The Rotational Temperature

Whether the rotational partition function should be evaluated by direct summation or integration is entirely dependent on the size of the rotational energy spacings relative to the amount of thermal energy available ($kT$). This comparison is facilitated through the introduction of the **rotational temperature** $\Theta_R$ defined as rotational constant divided by Boltzmann's constant:

$$\Theta_R = \frac{hcB}{k} \tag{14.36}$$

Unit analysis of Equation (14.36) dictates that $\Theta_R$ has units of temperature. We can rewrite the expression for the rotational partition function in terms of the rotational temperature as follows:

$$q_R = \frac{1}{\sigma\beta hcB} = \frac{kT}{\sigma hcB} = \frac{T}{\sigma\Theta_R}$$

A second application of the rotational temperature is as a comparative metric to the temperature at which the partition function is being evaluated. Figure 14.10 presents a comparison between $q_R$ for H$^{35}$Cl ($\Theta_R = 15.24$ K) determined by summation [Equation (14.29)] and using the integrated form of the partition function [Equation (14.36)]. At low temperatures, significant differences between the summation and integrated results are evident. At higher temperatures, the summation result remains larger than the integrated result; however, both results predict that $q_R$ will increase linearly with temperature. At high temperatures, the error in using the integrated result decreases such that for temperature where $T/\Theta_R \geq 10$, use of the integrated form of the rotational partition function is reasonable. The integrated form of the partition function is referred to as the **high-temperature or high-T limit** because it is applicable when $kT$ is significantly greater than the rotational energy spacings. The following example illustrates the use of the rotational temperature in deciding which functional form of the rotational partition function to use.
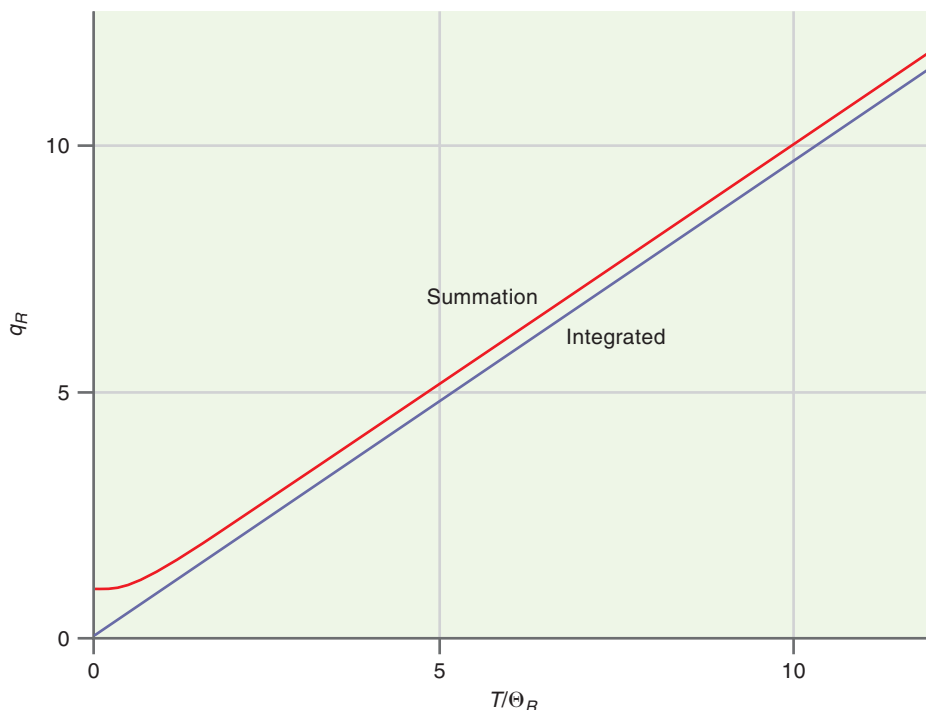
**FIGURE 14.10**
Comparison of $q_R$ for H$^{35}$Cl ($\Theta_R = 15.24$ K) determined by summation and by integration. Although the summation result remains greater than the integrated result at all temperatures, the fractional difference decreases with elevated temperatures such that the integrated form provides a sufficiently accurate measure of $q_R$ when $T/\Theta_R > 10$.

---

### EXAMPLE PROBLEM 14.6

Evaluate the rotational partition functions for $I_2$ at $T = 100.$ K.

#### Solution

Because $T = 100.$ K, it is important to ask how $kT$ compares to the rotational energy-level spacings. Using Table 14.1, $B(I_2) = 0.0374$ cm$^{-1}$ corresponding to rotational temperatures of

$$\Theta_R(I_2) = \frac{hcB}{k} = \frac{(6.626 \times 10^{-34} \,\text{J s})(3.00 \times 10^{10}\,\text{cm s}^{-1})(0.0374 \,\text{cm}^{-1})}{1.38 \times 10^{-23}\,\text{J K}^{-1}} = 0.0538 \,\text{K}$$

Comparison of these rotational temperatures to 100. K indicates that the high-temperature expression for the rotational partition function is valid for $I_2$:

$$q_R(I_2) = \frac{T}{\sigma \Theta_R} = \frac{100. \,\text{K}}{(2)(0.0539 \,\text{K})} = 929$$

---

# 14.6 Rotational Partition Function: Polyatomics

In the diatomic systems described in the preceding section, there are two nonvanishing moments of inertia as illustrated in Figure 14.11. For **polyatomic** molecules (more than two atoms) the situation can become more complex.

If the polyatomic system is linear, there are again only two nonvanishing moments of inertia such that a linear polyatomic molecule can be treated using the same formalism as diatomic molecules. However, if the polyatomic molecule is not linear, then there are three nonvanishing moments of inertia. Therefore, the partition function that describes the rotational energy levels must take into account rotation about all three axes. Derivation of this partition function is not trivial; therefore, the result without derivation is stated here:

$$q_R = \frac{\sqrt{\pi}}{\sigma} \left(\frac{1}{\beta hcB_A}\right)^{1/2} \left(\frac{1}{\beta hcB_B}\right)^{1/2} \left(\frac{1}{\beta hcB_C}\right)^{1/2} \tag{14.37}$$

The subscript on $B$ in Equation (14.37) indicates the corresponding moment of inertia as illustrated in Figure 14.11, and $\sigma$ is the symmetry number as discussed earlier. In addition,



$I_A = I_B \neq 0 \quad I_C = 0$



$I_A \neq 0, \ I_B \neq 0, \ I_C \neq 0$

**FIGURE 14.11**
Moments of inertia for diatomic and nonlinear polyatomic molecules. Note that in the case of the diatomic, $I_C = 0$ in the limit that the atomic masses are considered to be point masses that reside along the axis connecting the two atomic centers. Each moment of inertia will have a corresponding rotational constant.

the assumption is made that the polyatomic is "rigid" during rotational motion. The development of the rotational partition function for diatomic systems provides some intuition into the origin of this partition function. One can envision each moment of inertia contributing $(\beta hcB)^{-1/2}$ to the overall partition function. In the case of diatomics or linear polyatomics, the two nonvanishing moments of inertia are equivalent such that the product of the contribution from each moment results in the expression for the diatomic derived earlier. For the nonlinear polyatomic system, the partition function is the product of the contribution from each of the moments of inertia, which may or may not be equivalent as indicated by the subscripts on the corresponding rotational constants in the partition function presented earlier.

## EXAMPLE PROBLEM 14.7

Evaluate the rotational partition functions for the following species at 298 K. You can assume that the high-temperature expression is valid.

a. OCS ($B = 1.48$ cm$^{-1}$)

b. ONCl ($B_A = 2.84$ cm$^{-1}$, $B_B = 0.191$ cm$^{-1}$, $B_C = 0.179$ cm$^{-1}$)

c. CH$_2$O ($B_A = 9.40$ cm$^{-1}$, $B_B = 1.29$ cm$^{-1}$, $B_C = 1.13$ cm$^{-1}$)

### Solution

a. OCS is a linear molecule as indicated by the single rotational constant. In addition, the molecule is asymmetric such that $\sigma = 1$. Using the rotational constant, the rotational partition function is

$$q_R = \frac{1}{\sigma \beta hcB} = \frac{kT}{hcB}$$

$$= \frac{(1.38 \times 10^{-23}\,\text{J K}^{-1})(298\,\text{K})}{(6.626 \times 10^{-34}\,\text{J s})(3.00 \times 10^{10}\,\text{cm s}^{-1})(1.48\,\text{cm}^{-1})} = 140.$$

b. ONCl is a nonlinear polyatomic. It is asymmetric such that $\sigma = 1$, and the partition function becomes

$$q_R = \frac{\sqrt{\pi}}{\sigma}\left(\frac{1}{\beta hcB_A}\right)^{1/2}\left(\frac{1}{\beta hcB_B}\right)^{1/2}\left(\frac{1}{\beta hcB_C}\right)^{1/2}$$

$$= \sqrt{\pi}\left(\frac{kT}{hc}\right)^{3/2}\left(\frac{1}{B_A}\right)^{1/2}\left(\frac{1}{B_B}\right)^{1/2}\left(\frac{1}{B_C}\right)^{1/2}$$

$$= \sqrt{\pi}\left(\frac{(1.38 \times 10^{-23}\,\text{J K}^{-1})(298\,\text{K})}{(6.626 \times 10^{-34}\,\text{J s})(3.00 \times 10^{10}\,\text{cm s}^{-1})}\right)^{3/2}$$

$$\left(\frac{1}{2.84\,\text{cm}^{-1}}\right)^{1/2}\left(\frac{1}{0.191\,\text{cm}^{-1}}\right)^{1/2}\left(\frac{1}{0.179\,\text{cm}^{-1}}\right)^{1/2}$$

$$= 16,900$$

c. CH$_2$O is a nonlinear polyatomic. However, the symmetry of this molecule is such that $\sigma = 2$. With this value for the symmetry number, the rotational partition function becomes

$$q_R = \frac{\sqrt{\pi}}{\sigma}\left(\frac{1}{\beta hcB_A}\right)^{1/2}\left(\frac{1}{\beta hcB_B}\right)^{1/2}\left(\frac{1}{\beta hcB_C}\right)^{1/2}$$

$$= \frac{\sqrt{\pi}}{2}\left(\frac{kT}{hc}\right)^{3/2}\left(\frac{1}{B_A}\right)^{1/2}\left(\frac{1}{B_B}\right)^{1/2}\left(\frac{1}{B_C}\right)^{1/2}$$

$$= \frac{\sqrt{\pi}}{2}\left(\frac{(1.38 \times 10^{-23}\,\text{J K}^{-1})(298\,\text{K})}{(6.626 \times 10^{-34}\,\text{J s})(3.00 \times 10^{10}\,\text{cm s}^{-1})}\right)^{3/2}$$

$$\left(\frac{1}{9.40\,\text{cm}^{-1}}\right)^{1/2}\left(\frac{1}{1.29\,\text{cm}^{-1}}\right)^{1/2}\left(\frac{1}{1.13\,\text{cm}^{-1}}\right)^{1/2}$$

$$= 713$$

Note that the values for all three partition functions indicate that a substantial number of rotational states are populated at room temperature.

# 14.7 Vibrational Partition Function

The quantum mechanical model for vibrational degrees of freedom is the harmonic oscillator. In this model, each vibrational degree of freedom is characterized by a quadratic potential as illustrated in Figure 14.12. The energy levels of the harmonic oscillator are as follows:

$$E_n = hc\tilde{\nu}\left(n + \frac{1}{2}\right)$$ **(14.38)**

This equation demonstrates that the energy of a given level $E_n$ is dependent on the quantum number $n$, which can take on integer values beginning with zero ($n = 0, 1, 2, \dots$). The frequency of the oscillator, or vibrational frequency, is given by $\tilde{\nu}$ in units of $cm^{-1}$. Note that the energy of the $n = 0$ level is not zero, but $hc\tilde{\nu}/2$. This residual energy is known as the zero point energy and was discussed in detail during the quantum mechanical development of the harmonic oscillator. The expression for $E_n$ provided in Equation 14.38 can be used to construct the vibrational partition function as follows:

$$q_V = \sum_{n=0}^{\infty} e^{-\beta E_n}$$

$$= \sum_{n=0}^{\infty} e^{-\beta hc\tilde{\nu}\left(n + \frac{1}{2}\right)}$$

$$= e^{-\beta hc\tilde{\nu}/2} \sum_{n=0}^{\infty} e^{-\beta hc\tilde{\nu}n}$$ **(14.39)**

The sum can be rewritten using the series identity:

$$\frac{1}{1 - e^{-\alpha x}} = \sum_{n=0}^{\infty} e^{-n\alpha x}$$ **(14.40)**

With this substitution, we arrive at the following expression for the **vibrational partition function:**

$$q_V = \frac{e^{-\beta hc\tilde{\nu}/2}}{1 - e^{-\beta hc\tilde{\nu}}} \qquad \text{(with zero point energy)}$$ **(14.41)**

Although this expression is correct as written, at times it is advantageous to redefine the vibrational energy levels such that $E_0 = 0$ with all levels decreased by an amount equal to the zero point energy. Why would this be an advantageous thing to do? Consider the calculation of the probability of occupying a given vibrational energy level $p_n$ as follows:

$$p_n = \frac{e^{-\beta E_n}}{q_V} = \frac{e^{-\beta hc\tilde{\nu}\left(n+\frac{1}{2}\right)}}{\dfrac{e^{-\beta hc\tilde{\nu}/2}}{1 - e^{-\beta hc\tilde{\nu}}}} = \frac{e^{-\beta hc\tilde{\nu}/2}e^{-\beta hc\tilde{\nu}n}}{\dfrac{e^{-\beta hc\tilde{\nu}/2}}{1 - e^{-\beta hc\tilde{\nu}}}}$$

$$= e^{-\beta hc\tilde{\nu}n}(1 - e^{-\beta hc\tilde{\nu}})$$ **(14.42)**

Notice that in Equation (14.42) the zero point energy contributions for both the energy level and the partition function cancel. Therefore, the relevant energy for determining $p_n$ is not the absolute energy of a given level but the *relative* energy of the level. Given this, one can simply eliminate the zero point energy, resulting in the following expression for the vibrational partition function:

$$q_V = \frac{1}{1 - e^{-\beta hc\tilde{\nu}}} \qquad \text{(without zero point energy)}$$ **(14.43)**
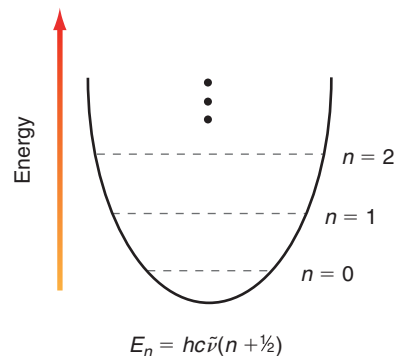


**FIGURE 14.12**
The harmonic oscillator model. Each vibrational degree of freedom is characterized by a quadratic potential. The energy levels corresponding to this potential are evenly spaced.

It is important to be consistent in including or not including zero point energy. For example, what if one were to perform the probability calculation presented earlier including zero point energy for the vibrational state of interest but not including zero point energy in the expression for the vibrational partition function? Proceeding as before, we arrive at the following *incorrect* result:

$$p_n = \frac{e^{-\beta E_n}}{q_V} = \frac{e^{-\beta hc\tilde{\nu}\left(n+\frac{1}{2}\right)}}{\dfrac{1}{1 - e^{-\beta hc\tilde{\nu}}}} = \frac{e^{-\beta hc\tilde{\nu}/2}e^{-\beta hc\tilde{\nu}n}}{\dfrac{1}{1 - e^{-\beta hc\tilde{\nu}}}}$$

$$= e^{-\beta hc\tilde{\nu}/2}\,e^{-\beta hc\tilde{\nu}n}\left(1 - e^{-\beta hc\tilde{\nu}}\right)$$

Note that the zero point energy terms did not cancel as in the previous case, reflecting the fact that the energy of state $n$ is defined differently relative to the expression for the partition function. In summary, once a decision has been made to include or ignore zero point energy, the approach taken must be consistently applied.

### EXAMPLE PROBLEM 14.8

At what temperature will the vibrational partition function for $I_2$ ($\tilde{\nu} = 208$ cm$^{-1}$) be greatest: 298 or 1000. K?

### Solution

Because the partition function is a measure of the number of states that are accessible given the amount of energy available ($kT$), we would expect the partition function to be greater for $T = 1000$ K relative to $T = 298$ K. We can confirm this expectation by numerically evaluating the vibrational partition function at these two temperatures:

$$(q_V)_{298\text{ K}} = \frac{1}{1 - e^{-\beta hc\tilde{\nu}}} = \frac{1}{1 - e^{-hc\tilde{\nu}/kT}}$$

$$= \frac{1}{1 - \exp\left[-\dfrac{(6.626 \times 10^{-34}\,\text{J s})(3.00 \times 10^{10}\,\text{cm s}^{-1})(208\,\text{cm}^{-1})}{(1.38 \times 10^{-23}\,\text{J K}^{-1})(298\,\text{K})}\right]} = 1.58$$

$$(q_V)_{1000\text{ K}} = \frac{1}{1 - e^{-\beta hc\tilde{\nu}}}$$

$$= \frac{1}{1 - \exp\left[-\dfrac{(6.626 \times 10^{-34}\,\text{J s})(3.00 \times 10^{10}\,\text{cm s}^{-1})(208\,\text{cm}^{-1})}{(1.38 \times 10^{-23}\,\text{J K}^{-1})(1000.\,\text{K})}\right]} = 3.86$$

Consistent with our expectation, the partition function increases with temperature, indicating that more states are accessible at elevated temperatures. The variation of $q_v$ with temperature for $I_2$ is shown here:
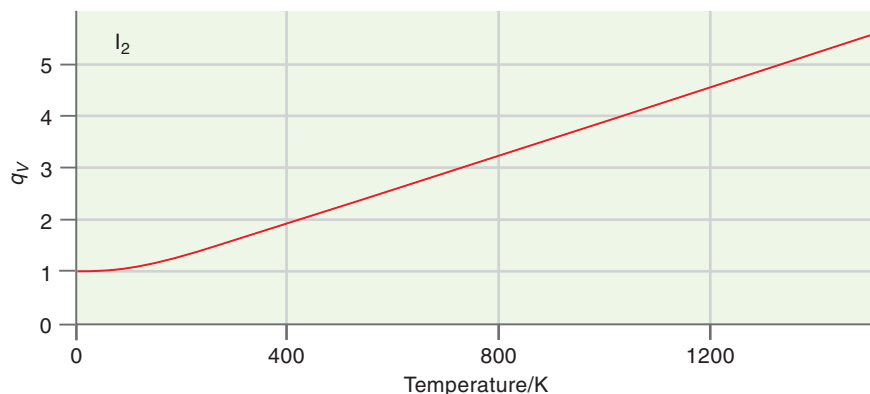
### 14.7.1 Beyond Diatomics: Multidimensional $q_V$

The expression for the vibrational partition function derived in the preceding subsection is for a single vibrational degree of freedom and is sufficient for diatomic molecules. However, triatomics and larger molecules (collectively referred to as polyatomics) require a different form for the partition function that takes into account all vibrational degrees of freedom. To define the vibrational partition function for polyatomics, we first need to know how many vibrational degrees of freedom there will be. A polyatomic molecule consisting of $N$ atoms has $3N$ total degrees of freedom corresponding to three cartesian degrees of freedom for each atom. The atoms are connected by chemical bonds; therefore, the atoms are not free to move independently of each other. First, the entire molecule can translate through space; therefore, three of the $3N$ total degrees of freedom correspond to translational motion of the entire molecule. Next, a rotational degree of freedom will exist for each nonvanishing moment of inertia. As discussed in the section on rotational motion, linear polyatomics have two rotational degrees of freedom because there are two nonvanishing moments of inertia, and nonlinear polyatomic molecules have three rotational degrees of freedom. The remaining degrees of freedom are vibrational such that the number of vibrational degrees of freedom are

$$\text{Linear polyatomics: } 3N - 5 \tag{14.44}$$

$$\text{Nonlinear polyatomics: } 3N - 6 \tag{14.45}$$

Note that a diatomic molecule can be viewed as linear polyatomic with $N = 2$, and the preceding expressions dictate that there is only one vibrational degree of freedom $[3(2) - 5 = 1]$ as stated earlier.

The final step in deriving the partition function for a polyatomic system is to recognize that within the harmonic approximation the vibrational degrees of freedom are separable and each vibration can be treated as a separate energetic degree of freedom. In Section 14.1, various forms of molecular energy were shown to be separable so that the total molecular partition function is simply the sum of the partition functions for each energetic degree of freedom. Similar logic applies to vibrational degrees of freedom where the total vibrational partition function is simply the product of vibrational partition functions for each vibrational degree of freedom:

$$(q_V)_{Total} = \prod_{i=1}^{3N-5 \text{ or } 3N-6} (q_V)_i \tag{14.46}$$

In Equation (14.46), the total vibrational partition function is equal to the product of vibrational partition functions for each vibrational mode (denoted by the subscript $i$). There will be $3N - 5$ or $3N - 6$ mode-specific partition functions depending on the geometry of the molecule.

### EXAMPLE PROBLEM 14.9

The triatomic chlorine dioxide (OClO) has three vibrational modes of frequency: 450, 945, and 1100 cm$^{-1}$. What is the value of the vibrational partition function for $T = 298$ K?

#### Solution

The total vibrational partition function is simply the product of the partition functions for each vibrational degree of freedom. Setting the zero point energy equal to zero, we find that

$$q_{450} = \frac{1}{1 - e^{-\beta hc(450 \text{ cm}^{-1})}}$$

$$= \frac{1}{1 - \exp\left[-\dfrac{(6.626 \times 10^{-34} \text{ J s})(3.00 \times 10^{10} \text{ cm s}^{-1})(450 \text{ cm}^{-1})}{(1.38 \times 10^{-23} \text{ J s})(298 \text{ K})}\right]}$$

$$= 1.13$$

$$q_{945} = \frac{1}{1 - e^{-\beta hc(945 \text{ cm}^{-1})}}$$

$$= \frac{1}{1 - \exp\left[-\dfrac{(6.626 \times 10^{-34} \text{ J s})(3.00 \times 10^{10} \text{ cm s}^{-1})(945 \text{ cm}^{-1})}{(1.38 \times 10^{-23} \text{ J s})(298 \text{ K})}\right]}$$

$$= 1.01$$

$$q_{1100} = \frac{1}{1 - e^{-\beta hc(1100 \text{ cm}^{-1})}}$$

$$= \frac{1}{1 - \exp\left[-\dfrac{(6.626 \times 10^{-34} \text{ J s})(3.00 \times 10^{10} \text{ cm s}^{-1})(1100 \text{ cm}^{-1})}{(1.38 \times 10^{-23} \text{ J s})(298 \text{ K})}\right]} = 1.00$$

$$(q_V)_{Total} = \prod_{i=1}^{3N-6} (q_V)_i = (q_{450})(q_{950})(q_{1100}) = (1.13)(1.01)(1.00) = 1.14$$

Note that the total vibrational partition function is close to unity. This is consistent with the fact that the vibrational energy spacings for all modes are significantly greater than $kT$ such that few states other than $n = 0$ are populated.

### 14.7.2 High Temperature Approximation to $q_V$

Similar to the development of rotations, the **vibrational temperature** ($\Theta_V$) is defined as the frequency of a given vibrational degree of freedom divided by $k$:

$$\Theta_V = \frac{hc\tilde{\nu}}{k} \tag{14.47}$$

Unit analysis of Equation (14.47) dictates that $\Theta_V$ will have units of temperature (K). We can incorporate this term into our expression for the vibrational partition function as follows:

$$q_V = \frac{1}{1 - e^{-\beta hc\tilde{\nu}}} = \frac{1}{1 - e^{-hc\tilde{\nu}/kT}} = \frac{1}{1 - e^{-\Theta_V/T}} \tag{14.48}$$

The utility of this form of the partition function is that the relationship between vibrational energy and temperature becomes transparent. Specifically, as $T$ becomes large relative to $\Theta_V$, the exponent becomes smaller and the exponential term approaches 1. The denominator in Equation (14.48) will decrease such that the vibrational partition function will increase. If the temperature becomes sufficiently large relative to $\Theta_V$, $q_V$ can be reduced to a simpler form. The Math Supplement (Appendix B) provides the following series expression for $\exp(-x)$:

$$e^{-x} = 1 - x + \frac{x^2}{2} - \dots$$

For the vibrational partition function in Equation (14.48), $x = -\Theta_V/T$. When $T \gg \Theta_V$, $x$ becomes sufficiently small that only the first two terms can be included in the series expression for $\exp(-x)$ since higher order terms are negligible. Substituting into the expression for the vibrational partition function:

$$q_V = \frac{1}{1 - e^{-\Theta_V/T}} = \frac{1}{1 - \left(1 - \dfrac{\Theta_V}{T}\right)} = \frac{T}{\Theta_V} \tag{14.49}$$

This result is the high-temperature (or high-T) limit for the vibrational partition function.

$$q_V = \frac{T}{\Theta_V} \quad \text{(high-T limit)} \tag{14.50}$$

When is Equation (14.50) appropriate for evaluating $q_V$ as opposed to the exact expression? The answer to this question depends on both the vibrational frequency of interest
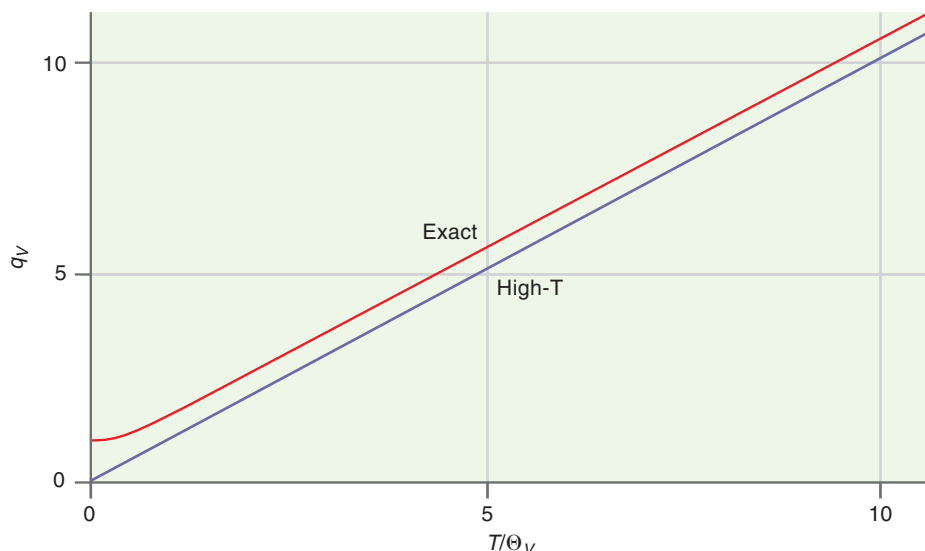
and the temperature. Figure 14.13 provides a comparison for $I_2$ ($\Theta_V = 299$ K) between
the exact expression without zero point energy [Equation (14.48)] and high-T expres-
sion [Equation (14.50)] for $q_V$. Similar to the case for rotations, the two results are sig-
nificantly different at low temperature, but predict the same linear dependence on $T$ at
elevated temperatures. When $T \geq 10\,\Theta_V$, the fractional difference between the high-T
and exact results is sufficiently small that the high-T result for $q_V$ can be used. For the
majority of molecules, this temperature will be extremely high as shown in Example
Problem 14.10.

---

**EXAMPLE PROBLEM 14.10**

At what temperature is the high-T limit for $q_V$ appropriate for $F_2$ ($\tilde{\nu} = 917$ cm$^{-1}$)?

**Solution**

The high-T limit is applicable when $T = 10\,\Theta_V$. The vibrational temperature for $F_2$ is

$$\Theta_V = \frac{hc\tilde{\nu}}{k} = \frac{(6.626 \times 10^{-34}\,\text{J s})(3.00 \times 10^{10}\,\text{cm s}^{-1})(917\,\text{cm}^{-1})}{1.38 \times 10^{-23}\,\text{J K}^{-1}} = 1320\,\text{K}$$

Therefore, the high-T limit is applicable when $T = \sim 13{,}000$ K. To make sure this is
indeed the case, we can compare the value for $q_V$ determined by both the full expres-
sion for the partition function and the high-T approximation:

$$q_V = \frac{1}{1 - e^{-\Theta_V/T}} = \frac{1}{1 - e^{-1319\,\text{K}/13{,}000\,\text{K}}} = 10.4$$

$$\approx \frac{T}{\Theta_V} = \frac{13{,}000\,\text{K}}{1319\,\text{K}} = 9.9$$

Comparison of the two methods for evaluating the partition function demonstrates
that the high-T limit expression provides a legitimate estimate of the partition func-
tion at this temperature. However, the temperature at which this is true is exceed-
ingly high.

---

### 14.7.3  Degeneracy and $q_V$

The total vibrational partition function for a polyatomic molecule is the product of the
partition functions for each vibrational degree of freedom. What if two or more of these
vibrational degrees of freedom have the same frequency such that the energy levels are
degenerate? It is important to keep in mind that there will always be $3N - 5$ or
$3N - 6$ vibrational degrees of freedom depending on geometry. In the case of degener-
acy, two or more of these degrees of freedom will have the same vibrational energy

spacings, or the same vibrational temperature. The total partition function is still the product of partition functions for each vibrational degree of freedom; however, the degenerate vibrational modes have identical partition functions. There are two ways to incorporate the effects of vibrational degeneracy into the expression for the vibrational partition function. First, one can simply use the existing form of the partition function and keep track of all degrees of freedom irrespective of frequency. A second method is to rewrite the total partition function as a product of partition functions corresponding to a given vibrational frequency and include degeneracy at a that frequency resulting in the corresponding partition function being raised to the power of the degeneracy:

$$(q_V)_{Total} = \prod_{i=1}^{n'} (q_V)_i^{g_i} \tag{14.51}$$

where $n'$ is the total number of unique vibrational frequencies indexed by $i$. It is important to note that $n'$ is *not* the number of vibrational degrees of freedom! Carbon dioxide serves as a classic example of vibrational degeneracy, as Example Problem 14.11 illustrates.

### EXAMPLE PROBLEM 14.11

$CO_2$ has the following vibrational degrees of freedom: 1388, 667.4 (doubly degenerate), and 2349 cm$^{-1}$. What is the total vibrational partition function for this molecule at 1000. K?

#### Solution

Evaluation of the partition function can be performed by calculating the individual vibrational partition functions for each unique frequency, then taking the product of these partition functions raised to the power of the degeneracy at a given frequency:

$$(q_V)_{1388} = \cfrac{1}{1-\exp\left[-\cfrac{(6.626 \times 10^{-34}\,\text{J s})(3.00 \times 10^{10}\,\text{cm s}^{-1})(1388\,\text{cm}^{-1})}{(1.38 \times 10^{-23}\,\text{J K}^{-1})(1000.\,\text{K})}\right]} = 1.16$$

$$(q_V)_{667.4} = \cfrac{1}{1-\exp\left[-\cfrac{(6.626 \times 10^{-34}\,\text{J s})(3.00 \times 10^{10}\,\text{cm s}^{-1})(667.4\,\text{cm}^{-1})}{(1.38 \times 10^{-23}\,\text{J K}^{-1})(1000.\,\text{K})}\right]} = 1.62$$

$$(q_V)_{2349} = \cfrac{1}{1-\exp\left[-\cfrac{(6.626 \times 10^{-34}\,\text{J s})(3.00 \times 10^{10}\,\text{cm s}^{-1})(2349\,\text{cm}^{-1})}{(1.38 \times 10^{-23}\,\text{J K}^{-1})(1000.\,\text{K})}\right]} = 1.04$$

$$(q_V)_{Total} = \prod_{i=1}^{n'} (q_V)_i^{g_i} = (q_V)_{1388}(q_V)_{667.4}^2(q_V)_{2349}$$

$$= (1.16)(1.62)^2(1.04) = 3.17$$

# 14.8 The Equipartition Theorem

In the previous sections regarding rotations and vibrations, equivalence of the high-T and exact expressions for $q_R$ and $q_V$, respectively, was observed when the temperature was sufficiently large that the thermal energy available to the system was significantly greater than the energy-level spacings. At these elevated temperatures, the quantum nature of the energy levels becomes unimportant, and a classical description of the energetics is all that is needed.

The definition of the partition function involves summation over quantized energy levels, and one might assume that there is a corresponding classical expression for the partition function in which a classical description of the system energetics is employed. Indeed there is such an expression; however, its derivation is beyond the scope of this

text, so we simply state the result here. The expression for the three-dimensional partition function for a molecule consisting of $N$ atoms is

$$q_{classical} = \frac{1}{h^{3N}} \int \cdots \int e^{-\beta H} dp^{3N} dx^{3N} \qquad (14.52)$$

In the expression for the partition function, the terms $p$ and $x$ represent the momentum and position coordinates for each particle, respectively, with three Cartesian dimensions available for each term. The integral is multiplied by $h^{-3N}$, which has units of $(\text{momentum} \times \text{distance})^{-3N}$ such that the partition function is unitless.

What does the term $e^{-\beta H}$ represent in $q_{classical}$? The $H$ represents the classical Hamiltonian and, like the quantum Hamiltonian, is the sum of a system's kinetic and potential energy. Therefore, $e^{-\beta H}$ is equivalent to $e^{-\beta \varepsilon}$ in our quantum expression for the molecular partition function. Consider the Hamiltonian for a classical one-dimensional harmonic oscillator with reduced mass $\mu$ and force constant $k$:

$$H = \frac{p^2}{2\mu} + \frac{1}{2}kx^2 \qquad (14.53)$$

Using this Hamiltonian, the corresponding classical partition function for the one-dimensional harmonic oscillator is

$$q_{classical} = \frac{1}{h} \int dp \int dx \, e^{-\beta\left(\frac{p^2}{2\mu} + \frac{1}{2}kx^2\right)} = \frac{T}{\Theta_V} \qquad (14.54)$$

This result is in agreement with the high-T approximation to $q_V$ derived using the quantum partition function of Equation (14.50). This example illustrates the applicability of classical statistical mechanics to molecular systems when the temperature is sufficiently high such that summation over the quantum states can be replaced by integration. Under these temperature conditions, knowledge of the quantum details of the system is not necessary because when evaluating Equation (14.54), nothing was implied regarding the quantization of the harmonic oscillator energy levels.

The applicability of classical statistical mechanics to molecular systems at high temperature finds application in an interesting theorem known as the **equipartition theorem.** This theorem states that any term in the classical Hamiltonian that is quadratic with respect to momentum or position (i.e., $p^2$ or $x^2$) will contribute $kT/2$ to the average energy. For example, the Hamiltonian for the one-dimensional harmonic oscillator [Equation (14.53)] has both a $p^2$ and $x^2$ term such that the average energy for the oscillator by equipartition should be $kT$ (or $NkT$ for a collection of $N$ harmonic oscillators). In the next chapter, the equipartition result will be directly compared to the average energy determined using quantum statistical mechanics. At present, it is important to recognize that the concept of equipartition is a consequence of classical mechanics because, for a given energetic degree of freedom, the change in energy associated with passing from one energy level to the other must be significantly less than $kT$. As discussed earlier, this is true for translational and rotational degrees of freedom but is not the case for vibrational degrees of freedom except at relatively high temperatures.

# 14.9 Electronic Partition Function

Electronic energy levels correspond to the various arrangements of electrons in an atom or molecule. The hydrogen atom provides an excellent example of an atomic system where the orbital energies are given by

$$E_n = \frac{-m_e e^4}{8\varepsilon_o^2 h^2 n^2} = -109{,}737 \, \text{cm}^{-1} \frac{1}{n^2} \quad (n = 1, 2, 3, \ldots) \qquad (14.55)$$

This expression demonstrates that the energy of a given orbital in the hydrogen atom is dependent on the quantum number $n$. In addition, each orbital has a degeneracy of $2n^2$. Using Equation (14.55), the energy levels for the electron in the hydrogen atom can be determined as illustrated in Figure 14.14.

**FIGURE 14.14**
Orbital energies for the hydrogen atom.
**(a)** The orbital energies as dictated by
solving the Schrödinger equation for the
hydrogen atom. **(b)** The energy levels
shifted by the addition of 109,737 cm$^{-1}$
of energy such that the lowest orbital
energy is 0.
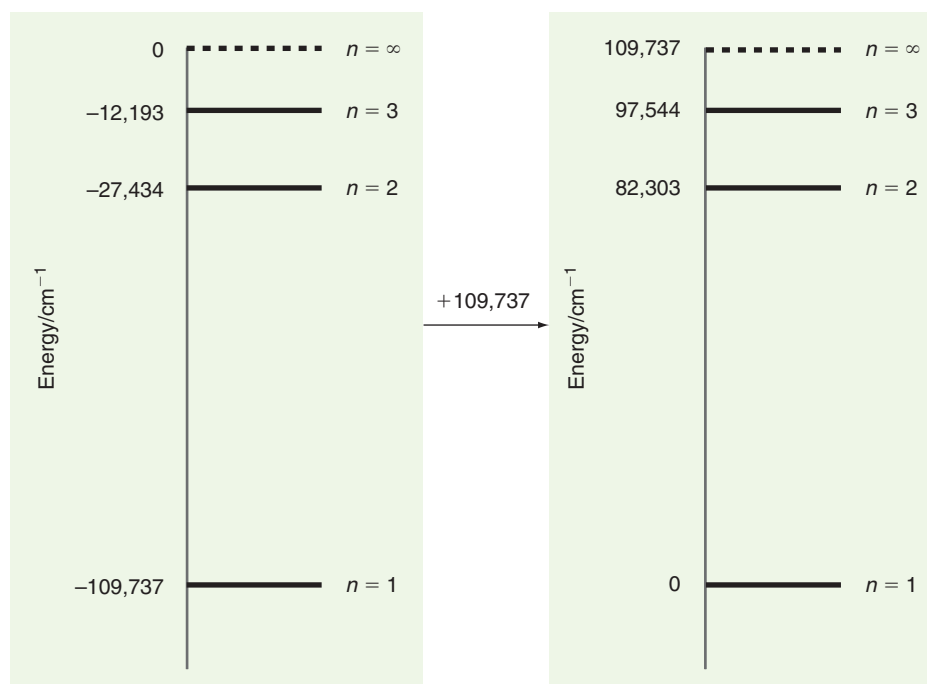
From the perspective of statistical mechanics, the energy levels of the hydrogen atom
represent the energy levels for the electronic energetic degree of freedom, with the corre-
sponding partition function derived by summing over the energy levels. However, rather
than use the absolute energies as determined in the quantum mechanical solution to the
hydrogen atom problem, we will adjust the energy levels such that the energy associated
with the $n = 1$ orbital is zero, similar to the adjustment of the ground-state energy of the
harmonic oscillator to zero by elimination of the zero point energy. With this redefinition
of the orbital energies, the electronic partition for the hydrogen atom becomes

$$q_E = \sum_{n=1}^{\infty} g_n e^{-\beta hc E_n} = 2e^{-\beta hc E_1} + 8e^{-\beta hc E_2} + 18e^{-\beta hc E_3} + \ldots$$

$$= 2e^{-\beta hc(0 \text{ cm}^{-1})} + 8e^{-\beta hc(82,303 \text{ cm}^{-1})} + 18e^{-\beta hc(97,544 \text{ cm}^{-1})} + \ldots$$

$$= 2 + 8e^{-\beta hc(82,303 \text{ cm}^{-1})} + 18e^{-\beta hc(97,544 \text{ cm}^{-1})} + \ldots \qquad (14.56)$$

The magnitude of the terms in the partition function corresponding to $n \geq 2$ will depend
on the temperature at which the partition function is being evaluated. However, note that
these energies are quite large. Consider defining the "electronic temperature," or $\Theta_E$, in
exactly the same way as the rotational and vibrational temperatures were defined:

$$\Theta_E = \frac{hc E_n}{k} = \frac{E_n}{0.695 \text{ cm}^{-1} \text{K}^{-1}} \qquad (14.57)$$

With the definition of $E_1 = 0$, the energy of the $n = 2$ orbital, $E_2$, is 82,303 cm$^{-1}$ corre-
sponding to $\Theta_E = 118,421$ K! This is an extremely high temperature, and this simple cal-
culation illustrates the primary difference between electronic energy levels and the other
energetic degrees of freedom discussed thus far. Electronic degrees of freedom are gener-
ally characterized by level spacings that are quite large relative to $kT$. Therefore, only the
ground electronic state is populated to a significant extent (although exceptions are known,
as presented in the problems at the end of this chapter). Applying this conceptual picture to
the hydrogen atom, the terms in the partition function corresponding to $n \geq 2$ should be
quite small at 298 K. For example, the term for the $n = 2$ state is as follows:

$$e^{-\beta hc E_2}$$

$$= \exp\left[\frac{-(6.626 \times 10^{-34} \text{ J s})(3.00 \times 10^{10} \text{ cm s}^{-1})(82,303 \text{ cm}^{-1})}{(1.38 \times 10^{-23} \text{ J K}^{-1})(298 \text{ K})}\right] = e^{-397.5} \approx 0$$

Terms corresponding to higher energy orbitals will also be extremely small such that the electronic partition function for the hydrogen atom is ~ 2 at 298 K. In general, the contribution of each state to the partition function must be considered, resulting in the following expression for the **electronic partition function:**

$$q_E = \sum_n g_n e^{-\beta hcE_n} \tag{14.58}$$

In the expression for the electronic partition function, the exponential term for each energy level is multiplied by the degeneracy of the level $g_n$. If the energy level spacings are very large compared to $kT$, then $q_E \approx g_o$, or the degeneracy of the ground state. However, certain atoms and molecules may have excited electronic states that are energetically accessible relative to $kT$, and the contribution of these states must be included in evaluating the partition function. The following problem provides an example of such a system.

## EXAMPLE PROBLEM 14.12

The lowest nine energy levels for gaseous vanadium (V) have the following energies and degeneracies:

| Level($n$) | Energy(cm$^{-1}$) | Degeneracy |
|:---:|:---:|:---:|
| 0 | 0 | 4 |
| 1 | 137.38 | 6 |
| 2 | 323.46 | 8 |
| 3 | 552.96 | 10 |
| 4 | 2112.28 | 2 |
| 5 | 2153.21 | 4 |
| 6 | 2220.11 | 6 |
| 7 | 2311.36 | 8 |
| 8 | 2424.78 | 10 |

What is the value of the electronic partition function for V at 298 K?

### Solution

Due to the presence of unpaired electrons in V, the electronic excited states are accessible relative to $kT$. Therefore, the partition function is not simply equal to the ground-state degeneracy and must instead be determined by writing out the summation explicitly, paying careful attention to the energy and degeneracy of each level:

$$q_E = \sum_n g_n e^{-\beta hcE_n} = g_o e^{-\beta hcE_0} + g_1 e^{-\beta hcE_1} + g_2 e^{-\beta hcE_2} + g_3 e^{-\beta hcE_0} + g_4 e^{-\beta hcE_0} + \ldots$$

$$= 4\exp\left[\frac{-0 \text{ cm}^{-1}}{(0.695 \text{ cm}^{-1}\text{K}^{-1})(298 \text{ K})}\right] + 6\exp\left[\frac{-137.38 \text{ cm}^{-1}}{(0.695 \text{ cm}^{-1}\text{K}^{-1})(298 \text{ K})}\right]$$

$$+ 8\exp\left[\frac{-323.46 \text{ cm}^{-1}}{(0.695 \text{ cm}^{-1}\text{K}^{-1})(298 \text{ K})}\right] + 10\exp\left[\frac{-552.96 \text{ cm}^{-1}}{(0.695 \text{ cm}^{-1}\text{K}^{-1})(298 \text{ K})}\right]$$

$$+ 2\exp\left[\frac{-2112.28 \text{ cm}^{-1}}{(0.695 \text{ cm}^{-1}\text{K}^{-1})(298 \text{ K})}\right] + \ldots$$

Notice in the preceding expression that the energy of state $n = 4$ (2112.28 cm$^{-1}$) is large with respect to $kT$ (208 cm$^{-1}$). The exponential term for this state is approximately $e^{-10}$, or $4.5 \times 10^{-5}$. Therefore, the contribution of state $n = 4$ and higher energy states to the partition function will be extremely modest, and these terms can be disregarded when evaluating the partition function. Focusing on the lower

energy states that make the dominant contribution to the partition function results in the following:

$$q_E \approx 4\exp\left[\frac{-0 \text{ cm}^{-1}}{(0.695 \text{ cm}^{-1}\text{K}^{-1})(298 \text{ K})}\right] + 6\exp\left[\frac{-137.38 \text{ cm}^{-1}}{(0.695 \text{ cm}^{-1}\text{K}^{-1})(298 \text{ K})}\right]$$

$$+ 8\ \exp\left[\frac{-323.46 \text{ cm}^{-1}}{(0.695 \text{ cm}^{-1}\text{K}^{-1})(298 \text{ K})}\right] + 10\ \exp\left[\frac{-552.96 \text{ cm}^{-1}}{(0.695 \text{ cm}^{-1}\text{K}^{-1})(298 \text{ K})}\right]$$

$$\approx 4 + 6(0.515) + 8(0.210) + 10(0.0693)$$

$$\approx 9.46$$

In summary, if the energy of an electronic excited state is sufficiently greater than $kT$, the contribution of the state to the electronic partition function will be minimal and the state can be disregarded in the numerical evaluation of the partition function.

Although the previous discussion focused on atomic systems, similar logic applies to molecules. Molecular electronic energy levels are described using molecular orbital (MO) theory. In MO theory, linear combinations of atomic orbitals are used to construct a new set of electronic orbitals known as molecular orbitals. The molecular orbitals differ in energy, and the electronic configuration of the molecule is determined by placing spin-paired electrons into the orbitals starting with the lowest energy orbital. The highest energy occupied molecular orbital is designated as the HOMO or highest occupied molecular orbital. The molecular orbital energy-level diagram for butadiene is presented in Figure 14.15.

Figure 14.15 presents both the lowest and next highest energy electronic energy states for butadiene, with the difference in energies corresponding to the promotion of an electron from the HOMO to the lowest unoccupied molecular orbital (LUMO). The separation in energy between these two states corresponds to the amount of energy it takes to excite the electron. The wavelength of the lowest energy electronic transition of butadiene is ~ 220 nm, demonstrating that the separation between the HOMO and LUMO is ~ 45,000 cm$^{-1}$, significantly greater than $kT$ at 298 K. As such, only the lowest energy electronic state contributes to the electronic partition function, and $q_E = 1$ for butadiene since the degeneracy of the lowest energy level is one. Typically, the first
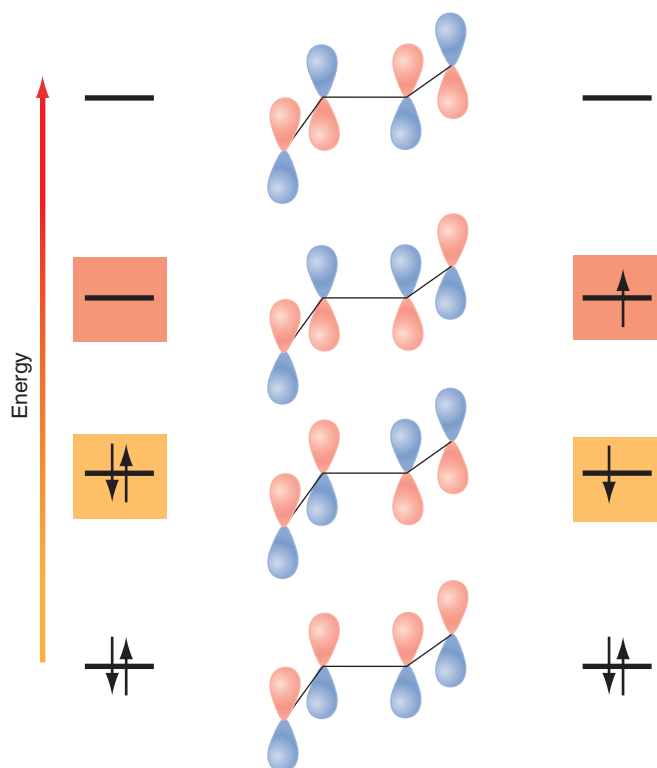
**FIGURE 14.15**

Depiction of the molecular orbitals for butadiene. The highest occupied molecular orbital (HOMO) is indicated by the orange rectangle, and the lowest unoccupied molecular orbital (LUMO) is indicated by the red rectangle. The lowest energy electron configuration is shown on the left, and the next highest energy configuration is shown on the right, corresponding to the promotion of an electron from the HOMO to the LUMO.

electronic excited level of molecules will reside 5000 to 50,000 $cm^{-1}$ higher in energy than the lowest level such that at room temperature only this lowest level is considered in evaluating the partition function

$$q_E = \sum_{n=0} g_n e^{-\beta E_n} \approx g_0 \qquad \textbf{(14.59)}$$

In the absence of degeneracy of the ground electronic state, the electronic partition function will equal one.

# 14.10 Review

Given the numerous derivations, equations, and examples provided in this chapter, it is important for the reader to focus on the primary concepts developed throughout. There are two primary goals of this chapter: to relate the canonical partition $Q$ to the molecular partition function $q$ and to express the molecular partition function in terms of the individual energetic degrees of freedom. The relationship between the molecular and canonical partition function depends on whether the individual units comprising the ensemble are distinguishable or indistinguishable such that

$$Q_{Total} = q_{Total}^N \ (\text{distinguishable})$$

$$Q_{Total} = \frac{1}{N!} q_{Total}^N \ (\text{indistinguishable})$$

Evaluation of the canonical partition function requires knowledge of the total molecular partition function, which is equal to the product of the partition functions for each energetic degree of freedom:

$$q_{Total} = q_T q_R q_V q_E$$

An example will help to illustrate the approach that was developed in this chapter. Imagine that we are interested in the canonical partition function for a mole of a diatomic molecule at an arbitrary temperature. First, gaseous molecules are indistinguishable such that

$$Q = \frac{1}{N_A!} q_{Total}^{N_A}$$

Next, the expression for the total molecular partition function is simply given by

$$q_{Total} = q_T q_R q_V q_E$$
$$= \left( \frac{V}{\Lambda^3} \right) \left( \frac{1}{\sigma \beta hcB} \right) \left( \frac{1}{1 - e^{-\beta hc\tilde{\nu}}} \right) (g_0)$$

Notice that we have used the appropriate expressions for the rotational and vibrational partition functions for a diatomic molecule. Numerical evaluation of the preceding equation requires knowledge of the specific molecular parameters, the volume of the gas, and the temperature of the ensemble. However, the conceptual approach is universal and illustrates the connection between the ensemble $Q$ and the microscopic properties of the individual units of the ensemble $q$. Using this approach, we can connect the microscopic description of molecules to the macroscopic behavior of molecular ensembles, an undertaking we explore in the next chapter.

# Vocabulary

| | | |
|---|---|---|
| canonical ensemble | electronic partition function | equipartition theorem |
| canonical partition function | energetic degrees of freedom | high-temperature (high-T) limit |
| diatomic | ensemble | molecular partition function |

| | | |
|---|---|---|
| *ortho*-hydrogen | rotational partition function | thermal wavelength |
| *para*-hydrogen | rotational temperature | translational partition function |
| polyatomic | symmetry number | vibrational partition function |
| rotational constant | thermal de Broglie wavelength | vibrational temperature |

# Conceptual Problems

**Q14.1** What is the canonical ensemble? What properties are held constant in this ensemble?

**Q14.2** What is the relationship between $Q$ and $q$? How does this relationship differ if the particles are distinguishable versus indistinguishable?

**Q14.3** List the atomic and/or molecular energetic degrees of freedom discussed in this chapter. For each energetic degree of freedom, briefly summarize the corresponding quantum mechanical model.

**Q14.4** For which energetic degrees of freedom are the energy-level spacings small relative to $kT$ at room temperature?

**Q14.5** For the translational and rotational degrees of freedom, evaluation of the partition function involved replacement of the summation by integration. Why could integration be performed? How does this relate back to the discussion of probability distributions of discrete variables treated as continuous?

**Q14.6** How many rotational degrees of freedom are there for linear and non-linear molecules?

**Q14.7** Assuming $^{19}F_2$ and $^{35}Cl_2$ have the same bond length, which molecule do you expect to have the largest rotational constant?

**Q14.8** Consider the rotational partition function for a non-linear polyatomic molecule. Can you describe the origin of each term in the partition function and why the partition function involves a product of terms?

**Q14.9** What is the high-T approximation for rotations and vibrations? For which of these two degrees of freedom do you expect this approximation to be generally valid at room temperature?

**Q14.10** In constructing the vibrational partition function, we found that the definition depended on whether zero-point energy was included in the description of the energy levels. However, the expression for the probability of occupying a specific vibrational energy level was independent of zero-point energy. Why?

**Q14.11** Although the vibrational degrees of freedom are generally not in the high-T limit, is the vibrational partition function evaluated by discrete summation?

**Q14.12** What is the form of the total vibrational partition function for a polyatomic molecule?

**Q14.13** How does the presence of degeneracy affect the form of the total vibrational partition function?

**Q14.14** What is the equipartition theorem? Why is this theorem inherently classical?

**Q14.15** Why is the electronic partition function generally equal to the degeneracy of the ground electronic state?

**Q14.16** What is $q_{Total}$, and how is it constructed using the partition functions for each energetic degree of freedom discussed in this chapter?

**Q14.17** Why is it possible to set the energy of the ground vibrational and electronic energy level to zero?

# Numerical Problems

Problem numbers in **red** indicate that the solution to the problem is given in the *Student's Solutions Manual*.

**P14.1** Evaluate the translational partition function for $H_2$ confined to a volume of 100. $cm^3$ at 298 K. Perform the same calculation for $N_2$ under identical conditions. (*Hint:* Do you need to reevaluate the full expression for $q_T$?)

**P14.2** Evaluate the translational partition function for $^{35}Cl_2$ confined to a volume of 1 L at 298 K. How does your answer change if the gas is $^{37}Cl_2$? (*Hint:* Can you reduce the ratio of translational partition functions to an expression involving mass only?)

**P14.3** He has a normal boiling point of 4.2 K. For a mole of gaseous He at 4.2 K and 1 atm, is the high-temperature limit for translational degrees of freedom applicable?

**P14.4** Evaluate the translational partition function for Ar confined to a volume of 1000. $cm^3$ at 298 K. At what temperature

will the translational partition function of Ne be identical to that of Ar at 298 K confined to the same volume?

**P14.5** At what temperature are there Avogadro's number of translational states available for $O_2$ confined to a volume of 1000. $cm^3$?

**P14.6** Imagine gaseous Ar at 298 K confined to move in a two-dimensional plane of area 1.00 $cm^2$. What is the value of the translational partition function?

**P14.7** Researchers at IBM have used scanning tunneling microscopy to place atoms in nanoscale arrangements that they refer to as "quantum corrals" (*Nature* 363 [1993]: 6429). Imagine constructing a square corral with 4.00 nm sides. If CO is confined to move in the two-dimensional space defined by this corral, what is the value of the translational partition function?

**P14.8** For $N_2$ at 77.3 K, 1.00 atm, in a 1.00-$cm^3$ container, calculate the translational partition function and ratio of this

partition function to the number of $N_2$ molecules present under these conditions.

**P14.9** What is the symmetry number for the following molecules?

a. $^{35}Cl^{37}Cl$

b. $^{35}Cl_2$

c. $^{16}O_2$

d. $C_6H_6$

e. $CH_2Cl_2$

**P14.10** Determine the symmetry number for the following halogenated methanes: $CCl_4$, $CFCl_3$, $CF_2Cl_2$, $CF_3Cl$.

**P14.11** Which species will have the largest rotational partition function at a given temperature: $H_2$, HD, or $D_2$? Which of these species will have the largest translational partition function assuming that volume and temperature are identical? When evaluating the rotational partition functions, you can assume that the high-temperature limit is valid.

**P14.12** Consider *para*-$H_2$ ($B = 60.853$ cm$^{-1}$) for which only even-$J$ levels are available. Evaluate the rotational partition function for this species at 50 K. Perform this same calculation for HD ($B = 45.655$ cm$^{-1}$).

**P14.13** Calculate the rotational partition function for the interhalogen compound $F^{35}Cl$ ($B = 0.516$ cm$^{-1}$) at 298 K.

**P14.14** Calculate the rotational partition function for $^{35}Cl_2$ (B $= 0.244$ cm$^{-1}$) at 298 K.

**P14.15** For which of the following diatomic molecules is the high-temperature expression for the rotational partition function valid at 40. K?

a. DBr ($B = 4.24$ cm$^{-1}$)

b. DI ($B = 3.25$ cm$^{-1}$)

c. CsI ($B = 0.0236$ cm$^{-1}$)

d. $F^{35}Cl$ ($B = 0.516$ cm$^{-1}$)

**P14.16** Calculate the rotational partition function for $SO_2$ at 298 K where $B_A = 2.03$ cm$^{-1}$, $B_B = 0.344$ cm$^{-1}$, and $B_C = 0.293$ cm$^{-1}$.

**P14.17** Calculate the rotational partition function for ClNO at 500. K where $B_A = 2.84$ cm$^{-1}$, $B_B = 0.187$ cm$^{-1}$, and $B_C = 0.175$ cm$^{-1}$.

**P14.18**

a. In the rotational spectrum of $H^{35}Cl$ ($I = 2.65 \times 10^{-47}$ kg m$^2$), the transition corresponding to the $J = 4$ to $J = 5$ transition is the most intense. At what temperature was the spectrum obtained?

b. At 1000. K, which rotational transition of $H^{35}Cl$ would you expect to demonstrate the greatest intensity?

c. Would you expect the answers for parts (a) and (b) to change if the spectrum were of $H^{37}Cl$?

**P14.19** What transition in the rotational spectrum of IF ($B = 0.280$ cm$^{-1}$) is expected to be the most intense at 298 K?

**P14.20** For a rotational-vibrational spectrum of $H^{81}Br$ ($B = 8.46$ cm$^{-1}$) taken at 500. K, which R-branch transition to you expect to be the most intense?

**P14.21** Calculate the rotational partition function for oxygen ($B = 1.44$ cm$^{-1}$) at its boiling point, 90.2 K, using the high-temperature approximation and by discrete summation. Why should only odd values of $J$ be included in this summation?

**P14.22** In microwave spectroscopy a traditional unit for the rotational constant is the Mc or "mega cycle" equal to $10^6$ s$^{-1}$. For $^{14}N^{14}N^{16}O$ the rotational constant is 12,561.66 Mc.

a. Convert the above value for the rotational constant from Mc to cm$^{-1}$.

b. Determine the value of the rotational partition function at 298 K.

**P14.23**

a. Calculate the population of the first 10 rotational energy levels for HBr ($B = 8.46$ cm$^{-1}$) at 298 K.

b. Repeat this calculation for HF assuming that the bond length of this molecule is identical to that of HBr.

**P14.24** In general, the high-temperature limit for the rotational partition function is appropriate for almost all molecules at temperatures above the boiling point. Hydrogen is an exception to this generality because the moment of inertia is small due to the small mass of H. Given this, other molecules with H may also represent exceptions to this general rule. For example, methane ($CH_4$) has relatively modest moments of inertia ($I_A = I_B = I_C = 5.31 \times 10^{-40}$ g cm$^2$) and has a relatively low boiling point of $T = 112$ K.

a. determine $B_A$, $B_B$, and $B_C$ for this molecule.

b. Use the answer from part (a) to determine the rotational partition function. Is the high-temperature limit valid?

**P14.25** When $^4He$ is cooled below 2.17 K it becomes a "superfluid" with unique properties such as a viscosity approaching zero. One way to learn about the superfluid environment is to measure the rotational-vibrational spectrum of molecules embedded in the fluid. For example, the spectrum of OCS in low-temperature $^4He$ droplet has been reported (*Journal of Chemical Physics* 112 [2000]: 4485). For $OC^{32}S$ the authors measured a rotational constant of 0.203 cm$^{-1}$ and found that the intensity of the J = 0 to 1 transition was roughly 1.35 times greater than that of the J = 1 to 2 transition. Using this information, provide a rough estimate of the temperature of the droplet.

**P14.26** Calculate the vibrational partition function for $H^{35}Cl$ ($\tilde{\nu} = 2990$ cm$^{-1}$) at 300. and 3000. K. What fraction of molecules will be in the ground vibrational state at these temperatures?

**P14.27** Determine the rotational partition function for $I^{35}Cl$ (B $= 0.114$ cm$^{-1}$) at 298 K.

**P14.28** For IF ($\tilde{\nu} = 610.$ cm$^{-1}$) calculate the vibrational partition function and populations in the first three vibrational energy levels for $T = 300.$ and 3000. K. Repeat this calculation for IBr ($\tilde{\nu} = 269$ cm$^{-1}$). Compare the probabilities for IF and IBr. Can you explain the differences between the probabilities of these molecules?

**P14.29** Evaluate the vibrational partition function for $H_2O$ at 2000. K where the vibrational frequencies are 1615, 3694, and 3802 cm$^{-1}$.

**P14.30** Evaluate the vibrational partition function for $SO_2$ at 298 K where the vibrational frequencies are 519, 1151, and 1361 $cm^{-1}$.

**P14.31** Evaluate the vibrational partition function for $NH_3$ at 1000. K where the vibrational frequencies are 950., 1627.5 (doubly degenerate), 3335, and 3414 $cm^{-1}$ (doubly degenerate). Are there any modes that you can disregard in this calculation? Why or why not?

**P14.32** Evaluate the vibrational partition function for $CFCl_3$ at 298 K where the vibrational frequencies are (with degeneracy in parenthesis) 1081, 847 (2), 535, 394 (2), 350., and 241(2) $cm^{-1}$.

**P14.33** Determine the populations in $n = 0$ and 1 for $H^{81}Br$ ($\tilde{\nu} = 2649$ $cm^{-1}$) at 298 K.

**P14.34** Isotopic substitution is employed to isolate features in a vibrational spectrum. For example, the C=O stretch of individual carbonyl groups in the backbone of a polypeptide can be studied by substituting $^{13}C^{18}O$ for $^{12}C^{16}O$.

a. From quantum mechanics the vibrational frequency of a diatomic molecules depends on the bond force constant ($\kappa$) and reduced mass ($\mu$) as follows:

$$\tilde{\nu} = \sqrt{\frac{\kappa}{\mu}}$$

If the vibrational frequency of $^{12}C^{16}O$ is 1680 $cm^{-1}$, what is the expected frequency for $^{13}C^{18}O$?

b. Using the vibrational frequencies for $^{12}C^{16}O$ and $^{13}C^{18}O$, determine the value of the corresponding vibrational partition functions at 298 K. Does this isotopic substitution have a dramatic effect on $q_V$?

**P14.35** In using statistical mechanics to describe the thermodynamic properties of molecules, high-frequency vibrations are generally not of importance under standard thermodynamic conditions since they are not populated to a significant extent. For example, for many hydrocarbons the C$-$H stretch vibrational degrees of freedom are neglected. Using cyclohexane as an example, the IR-absorption spectrum reveals that the C$-$H stretch transition are located at ~2850 $cm^{-1}$.

a. What is the value of the vibrational partition function for a mode of this frequency at 298 K?

b. At what temperature will this partition function reach a value of 1.1?

**P14.36** In deriving the vibrational partition function, a mathematical expression for the series expression for the partition function was employed. However, what if one performed integration instead of summation to evaluate the partition function? Evaluate the following expression for the vibrational partition function:

$$q_V = \sum_{n=0}^{\infty} e^{-\beta hcn\tilde{\nu}} \approx \int_0^{\infty} e^{-\beta hcn\tilde{\nu}} \, dn$$

Under what conditions would you expect the resulting expression for $q_V$ to be applicable?

**P14.37** You have in your possession the first vibrational spectrum of a new diatomic molecule $X_2$ obtained at 1000. K. From the spectrum you determine that the fraction of molecules occupying a given vibrational energy state $n$ is as follows:

| $n$ | 0 | 1 | 2 | 3 | >3 |
|---|---|---|---|---|---|
| **Fraction** | 0.352 | 0.184 | 0.0963 | 0.050. | 0.318 |

What are the vibrational energy spacings for $X_2$?

**P14.38**

a. In this chapter, the assumption was made that the harmonic oscillator model is valid such that anharmonicity can be neglected. However, anharmonicity can be included in the expression for vibrational energies. The energy levels for an anharmonic oscillator are given by

$$E_n = hc\tilde{\nu}\left(n + \frac{1}{2}\right) - hc\tilde{\chi}\tilde{\nu}\left(n + \frac{1}{2}\right)^2 + \dots$$

Neglecting zero point energy, the energy levels become $E_n = hc\tilde{\nu}n - hc\tilde{\chi}\tilde{\nu}n^2 + \dots$. Using the preceding expression, demonstrate that the vibrational partition function for the anharmonic oscillator is

$$q_{V, anharmonic} = q_{V, harm}[1 + \beta hc\tilde{\chi}\tilde{\nu}q_{V,harm}^2(e^{-2\beta\tilde{\nu}hc} + e^{-\beta\tilde{\nu}hc})]$$

In deriving the preceding result, the following series relationship will prove useful:

$$\sum_{n=0}^{\infty} n^2 x^n = \frac{x^2 + x}{(1-x)^3} \text{ for} |x| < 1$$

b. For $H_2$, $\tilde{\nu} = 4401.2$ $cm^{-1}$ and $\tilde{\chi}\tilde{\nu} = 121.3$ $cm^{-1}$. Use the result from part (a) to determine the percent error in $q_V$ if anharmonicity is ignored.

**P14.39** Consider a particle free to translate in one dimension. The classical Hamiltonian is $H = p^2/2m$.

a. Determine $q_{classical}$ for this system. To what quantum system should you compare it in order to determine the equivalence of the classical and quantum statistical mechanical treatments?

b. Derive $q_{classical}$ for a system with translational motion in three dimensions for which $H = (p_x^2 + p_y^2 + p_z^2)/2m$.

**P14.40** A general expression for the classical Hamiltonian is

$$H = \alpha p_i^2 + H'$$

where $p_i$ is the momentum along one dimension for particle $i$, $\alpha$ is a constant, and $H'$ are the remaining terms in the Hamiltonian. Substituting this into the equipartition theorem yields

$$q = \frac{1}{h^{3N}} \iint e^{-\beta(\alpha p^2_i + H')} dp^{3N} dx^{3N}$$

a. Starting with this expression, isolate the term involving $p_i$ and determine its contribution to $q$.

b. Given that the average energy $\langle \varepsilon \rangle$ is related to the partition function as follows,

$$\langle \varepsilon \rangle = \frac{-1}{q}\left(\frac{\delta q}{\delta \beta}\right)$$

evaluate the expression the contribution from $p_i$. Is your result consistent with the equipartiton theorem?

**P14.41**   Hydrogen isocyanide, HNC, is the tautomer of hydrogen cyanide (HCN). HNC is of interest as an intermediate species in a variety of chemical processes in interstellar space (T = 2.75 K).

**a.** For HCN the vibrational frequencies are 2041 cm$^{-1}$ (CN stretch), 712 cm$^{-1}$ (bend, doubly degenerate), and 3669 cm$^{-1}$ (CH stretch). The rotational constant is 1.477 cm$^{-1}$. Calculate the rotational and vibrational partition functions for HCN in interstellar space. Before calculating the vibrational partition function, is there an approximation you can make that will simplify this calculation?

**b.** Perform the same calculations for HNC which has vibrational frequencies of 2024 cm$^{-1}$ (NC stretch), 464 cm$^{-1}$ (bend, doubly degenerate), and 3653 cm$^{-1}$ v (NH stretch). The rotational constant is 1.512 cm$^{-1}$.

**c.** The presence of HNC in space was first established by Snyder and Buhl (*Bulletin of the American Astronomical Society* 3 [1971]: 388) through the microwave emission of the J = 1 to 0 transition of HNC at 90.665 MHz. Considering your values for the rotational partition functions, can you rationalize why this transition would be observed? Why not the J = 20-19 transition?

**P14.42**   Evaluate the electronic partition function for atomic Fe at 298 K given the following energy levels.

| Level ($n$) | Energy (cm$^{-1}$) | Degeneracy |
|---|---|---|
| 0 | 0 | 9 |
| 1 | 415.9 | 7 |
| 2 | 704.0 | 5 |
| 3 | 888.1 | 3 |
| 4 | 978.1 | 1 |

**P14.43**

**a.** Evaluate the electronic partition function for atomic Si at 298 K given the following energy levels:

| Level ($n$) | Energy(cm$^{-1}$) | Degeneracy |
|---|---|---|
| 0 | 0 | 1 |
| 1 | 77.1 | 3 |
| 2 | 223.2 | 5 |
| 3 | 6298 | 5 |

**b.** At what temperature will the $n = 3$ energy level contribute 0.100 to the electronic partition function?

**P14.44**   NO is a well-known example of a molecular system in which excited electronic energy levels are readily accessible at room temperature. Both the ground and excited electronic states are doubly degenerate and are separated by 121.1 cm$^{-1}$.

**a.** Evaluate the electronic partition function for this molecule at 298 K.

**b.** Determine the temperature at which $q_E = 3$.

**P14.45**   Rhodopsin is a biological pigment that serves as the primary photoreceptor in vision (*Science* 266 [1994]: 422). The chromophore in rhodopsin is retinal, and the absorption spectrum of this species is centered at roughly 500 nm. Using this information, determine the value of $q_E$ for retinal. Do you expect thermal excitation to result in a significant excited-state population of retinal?

**P14.46**   Determine the total molecular partition function for $I_2$, confined to a volume of 1000. cm$^3$ at 298 K. Other information you will find useful is that $B = 0.0374$ cm$^{-1}$, $(\tilde{\nu} = 208$ cm$^{-1})$, and the ground electronic state is nondegenerate.

**P14.47**   Determine the total molecular partition function for gaseous $H_2O$ at 1000. K confined to a volume of 1.00 cm$^3$. The rotational constants for water are $B_A = 27.8$ cm$^{-1}$, $B_B = 14.5$ cm$^{-1}$, and $B_C = 9.95$ cm$^{-1}$. The vibrational frequencies are 1615, 3694, and 3802 cm$^{-1}$. The ground electronic state is nondegenerate.

**P14.48**   The effect of symmetry on the rotational partition function for $H_2$ was evaluated by recognizing that each hydrogen is a spin 1/2 particle and is, therefore, a fermion. However, this development is not limited to fermions, but is also applicable to bosons. Consider $CO_2$ in which rotation by 180° results in the interchange of two spin 0 particles.

**a.** Because the overall wave function describing the interchange of two bosons must be symmetric with respect to exchange, to what $J$ levels is the summation limited in evaluating $q_R$ for $CO_2$?

**b.** The rotational constant for $CO_2$ is 0.390 cm$^{-1}$. Calculate $q_R$ at 298 K. Do you have to evaluate $q_R$ by summation of the allowed rotational energy levels? Why or why not?

# Web-Based Simulations, Animations, and Problems

**W14.1**   In this Web-based simulation, the variation in $q_T$, $q_R$, and $q_V$ with temperature is investigated for three diatomic molecules: HF, H$^{35}$Cl, and $^{35}$ClF. Comparisons of $q_T$ and $q_R$ are performed to illustrate the mass and temperature dependence of these partition functions. Also, the expected dependence of $q_T$, $q_R$, and $q_V$ on temperature in the high-temperature limit is investigated.

# Computational Problems

More detailed instructions on carrying out these calculations using Spartan Physical Chemistry are found on the book website at *www.masteringchemistry.com*.

**C14.1**   Using the Hartree-Fock 6-31G* basis set, determine the vibrational frequencies for $F_2O$ and $Br_2O$ and calculate the vibrational partition function for these species at 500. K.

**C14.2**   Halogenated methanes are of interest as greenhouse gases. Perform a Hartree-Fock 6-31G* calculation of $CFH_3$ including determination of the IR spectrum. Does this molecule possess any strong transitions in the infrared? Calculate the vibrational partition function for the vibrational degree of freedom with the strongest predicted IR-absorption intensity.

**C14.3**   Nitryl chloride ($ClNO_2$) is an important compound in atmospheric chemistry. It serves as a reservoir compound for Cl and is produced in the lower troposphere through the reaction of $N_2O_5$ with $Cl^-$ containing aerosols. Using the Hartree-Fock 3-21G basis set, determine the value of the vibrational partition function at 260. K. Does your answer change appreciably if you use the 6-31G* basis set?

**C14.4**   The rotational constant for 1,3-butadiyne ($C_4H_2$) is 4391.19 MHz. Performing a Hartree-Fock 6-31G* calculation, minimize the geometry of this species and compare the effective bond length determined using the rotational constant to the actual geometry of this species.

**C14.5**   Using Hartree-Fock with the 3-21G basis set, determine the value of the vibrational partition function for $CF_2Cl_2$ and $CCl_4$ at 298 K. What do you notice about the vibrational frequencies for the higher-symmetry species?

**C14.6**   The high-temperature limit was shown to be of limited applicability to vibrational degrees of freedom. As will be shown in the next chapter, this has a profound consequence when exploring the role of vibrations in statistical thermodynamics. For example, a coarse rule of thumb is that one usually does not need to worry about the contribution of CH, NH, and OH stretch vibrations. Perform a Hartree-Fock 6-31G* calculation on 1,3-cyclohexadiene, and calculate the IR intensities. Looking at the atomic displacements that make up the normal modes, identify those modes that are predominantly of C-H stretch character. In what frequency range are these modes located? Identify the lowest-energy C-H stretch and the lowest-frequency mode in general. Compare the value of the partition function for these two vibrational degrees of freedom at 298 K. How does this comparison support the "rule of thumb?"

**C14.7**   You are interested in designing a conducting polyene-based polymer. The design calls for maximizing the conjugation length, but as the conjugation length increases, the HOMO-LUMO energy gap corresponding to the lowest-energy electronic transition will decrease. If the gap becomes too small, then thermal excitation can result in population of the excited state. If thermal excitation is significant, it will degrade the performance of the polymer.

**a.** With a tolerance of 2% population in the first electronic excited state at 373 K, what is the smallest electronic energy gap that can be tolerated?

**b.** Using the Hartree-Fock 3-21G basis set, calculate the HOMO-LUMO energy gap for 1,3,5-hexatriene, 1,3,5,7-octatetraene, and 1,3,5,7,9-decapentaene. Using a plot of energy gap versus number of double bonds, determine the longest polyene structure that can be achieved while maintaining the 2% excited-state population tolerance, assuming that the energy gap varies linearly with conjugation length. (Note: This method provides a very rough estimate of the actual energy gap.)

**c.** (Advanced) In part (b) it was assumed that the HOMO-LUMO energy gap decreases linearly with an increase in conjugation length. Check this assumption by calculating this energy gap for the next two polyenes. Does the linear correlation continue?

# For Further Reading

Chandler, D. *Introduction to Modern Statistical Mechanics*. New York: Oxford, 1987.

Hill, T. *Statistical Mechanics. Principles and Selected Applications*. New York: Dover, 1956.

McQuarrie, D. *Statistical Mechanics*. New York: Harper & Row, 1973.

Nash, L. K. "On the Boltzmann Distribution Law." *J. Chemical Education* 59 (1982): 824.

Nash, L. K. *Elements of Statistical Thermodynamics*. San Francisco: Addison-Wesley, 1972.

Noggle, J. H. *Physical Chemistry*. New York: HarperCollins, 1996.

Townes, C. H., and A. L. Schallow. *Microwave Spectroscopy*. New York: Dover, 1975. (This book contains an excellent appendix of spectroscopic constants.)

Widom, B. *Statistical Mechanics*. Cambridge: Cambridge University Press, 2002.

# Statistical Thermodynamics

With the central concepts of statistical mechanics in hand, the relationship between statistical mechanics and classical thermodynamics can be explored. In this chapter, the microscopic viewpoint of matter is connected to fundamental thermodynamic quantities such as internal energy, entropy, and Gibbs free energy using statistical mechanics. As will be shown, the statistical perspective is not only capable of reproducing thermodynamic properties of matter, but it also provides critical insight into the microscopic details behind these properties. We will see that the insight into the behavior of chemical systems gained from the statistical perspective is remarkable.

## 15.1 Energy

We begin our discussion of statistical thermodynamics by returning to the canonical ensemble (Section 14.1) and considering the **average energy** content of an ensemble unit $\langle \varepsilon \rangle$, which is simply the **total energy** of the ensemble $E$ divided by the number of units in the ensemble $N$:

$$\langle \varepsilon \rangle = \frac{E}{N} = \frac{\sum_n \varepsilon_n a_n}{N} = \sum_n \varepsilon_n \frac{a_n}{N} \tag{15.1}$$

In this equation, $\varepsilon_n$ is the level energy and $a_n$ is the occupation number for the level. Consistent with our development in Chapter 14, the ensemble is partitioned such that there is one atom or molecule in each unit. The Boltzmann distribution for a series of nondegenerate energy levels is

$$\frac{a_n}{N} = \frac{e^{-\beta \varepsilon_n}}{q} \tag{15.2}$$

In this expression, $q$ is the molecular partition function and $\beta = (kT)^{-1}$. Substituting Equation (15.2) into Equation (15.1) yields

$$\langle \varepsilon \rangle = \sum_n \varepsilon_n \frac{a_n}{N} = \frac{1}{q} \sum_n \varepsilon_n e^{-\beta \varepsilon_n} \tag{15.3}$$

**371**

As a final step in deriving $\langle \varepsilon \rangle$, consider the derivative of the molecular partition function with respect to $\beta$, which is given by

$$\frac{-dq}{d\beta} = \sum_n \varepsilon_n e^{-\beta \varepsilon_n} \tag{15.4}$$

Using Equation (15.4), Equation (15.3) can be rewritten to obtain the following expressions for the average unit energy and total ensemble energy:

$$\langle \varepsilon \rangle = \frac{-1}{q}\left(\frac{dq}{d\beta}\right) = -\left(\frac{d \ln q}{d\beta}\right) \tag{15.5}$$

$$E = N\langle \varepsilon \rangle = \frac{-N}{q}\left(\frac{dq}{d\beta}\right) = -N\left(\frac{d \ln q}{d\beta}\right) \tag{15.6}$$

At times, Equation (15.5) and (15.6) are easier to evaluate by taking the derivative with respect to $T$ rather than $\beta$. Using the definition $\beta = (kT)^{-1}$,

$$\frac{d\beta}{dT} = \frac{d}{dT}(kT)^{-1} = -\frac{1}{kT^2} \tag{15.7}$$

Using Equation (15.7), the expressions for average and total energy can be written as follows:

$$\langle \varepsilon \rangle = kT^2\left(\frac{d \ln q}{dT}\right) \tag{15.8}$$

$$E = NkT^2\left(\frac{d \ln q}{dT}\right) \tag{15.9}$$

Equation (15.9) demonstrates that $E$ will change with temperature, a result we are familiar with from our study of thermodynamics. Example Problem 15.1 involves an ensemble comprised of particles with two energy levels, commonly referred to as a **two-level system** (see Figure 15.1), to illustrate the variation of $E$ with $T$. To derive the functional form of $E$ for this ensemble, $q$ must be constructed and used to derive an expression for $E$, as shown next.

### EXAMPLE PROBLEM 15.1

Determine the total energy of an ensemble consisting of $N$ particles that have only two energy levels separated by energy $h\nu$.

#### Solution

The energy levels for the particles are illustrated in Figure 15.1. As mentioned, systems with only two energy levels are commonly referred to as two-level systems. To determine the average energy, the partition function describing this system must be evaluated. The partition function consists of a sum of two terms as follows:

$$q = 1 + e^{-\beta h\nu}$$

The derivative of the partition function with respect to $\beta$ is

$$\frac{dq}{d\beta} = \frac{d}{d\beta}(1 + e^{-\beta h\nu})$$

$$= -h\nu e^{-\beta h\nu}$$

Using this result, the total energy is

$$E = \frac{-N}{q}\left(\frac{dq}{d\beta}\right) = \frac{-N}{(1 + e^{-\beta h\nu})}(-h\nu^{-\beta h\nu})$$

$$= \frac{Nh\nu e^{-\beta h\nu}}{1 + e^{-\beta h\nu}} = \frac{Nh\nu}{e^{\beta h\nu} + 1}$$

In the final step of this example, the expression for $E$ was multiplied by unity in the form of $\exp(\beta h\nu)/\exp(\beta h\nu)$ to facilitate numerical evaluation.
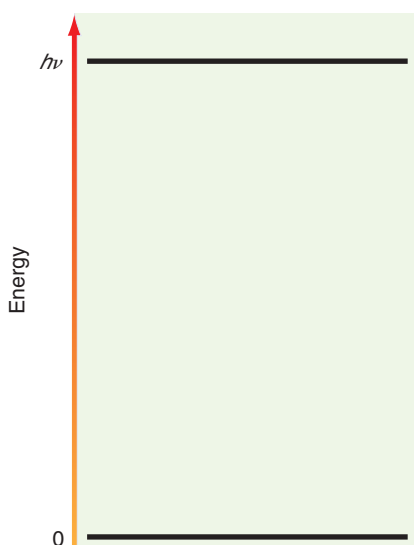
**FIGURE 15.1**
Depiction of the two-level system.

Figure 15.2 presents the evolution in $E$ with $T$ for the two-level system in Figure 15.1. The total energy as presented in the figure is divided by the number of particles in the ensemble $N$ and the energy-level spacing $h\nu$. In addition, temperature is expressed as $kT$ divided by the energy spacing between levels.

Two interesting trends are evident in Figure 15.2. First, at the lowest temperatures the total energy does not change appreciably as the temperature is increased until $kT/h\nu \approx 0.2$, at which point a significant increase in $E$ is observed. Second, the total energy reaches a limiting value at high temperature, and further increases in $T$ do not affect the total energy. Why does this occur? Recall that the change in energy of a system correlates with a change in occupation number, with higher energy levels being more readily populated as the temperature is increased. For the two-level system just presented, the probability of occupying the excited energy level from Equation (15.2) is

$$p_1 = \frac{a_1}{N} = \frac{e^{-\beta h\nu}}{q} = \frac{e^{-\beta h\nu}}{1 + e^{-\beta h\nu}} = \frac{1}{e^{\beta h\nu} + 1} \tag{15.10}$$

At $T = 0$, the exponential term in the denominator is infinite and $p_1 = 0$. The probability of occupying the excited state becomes finite when the amount of thermal energy available, $kT$, is comparable to the separation energy of the states, $h\nu$. At low temperatures $kT \ll h\nu$, and the probability of occupying the excited state is quite small such that the occupation number for the excited state $a_1$ is essentially zero. Inspection of Equation (15.10) demonstrates that $p_1$ will increase until $h\nu \ll kT$. At these elevated temperatures, the exponential term in the denominator approaches unity, and $p_1$ approaches its limiting value of 0.5. Because this is a two-level system, the probability of occupying the lower energy state must also be 0.5. When the probability of occupying all energy states is equal, the occupation numbers do not change. The exact result for the evolution of $p_1$ as a function of temperature is presented in Figure 15.3. Again, the evolution in temperature is described as $kT/h\nu$ such that $kT$ is measured with respect to the energy gap between the two states. Notice that the change in $p_1$ exactly mimics the behavior observed for the total energy depicted in Figure 15.2, demonstrating that changes in energy correspond to changes in occupation number.

## 15.1.1 Energy and the Canonical Partition Function

Equation (15.9) allows one to calculate the ensemble energy, but to what thermodynamic quantity is this energy related? Recall that we are interested in the canonical ensemble in which $N$, $V$, and $T$ are held constant. Because $V$ is constant, there can be no $P$–$V$-type work, and by the first law of thermodynamics any change in internal energy must occur by heat flow, $q_{Vol}$. Using the first law, the change in heat is related to the change in system **internal energy** at constant volume by

$$U - U_o = q_{Vol} \tag{15.11}$$

In Equation (15.11), $q_{Vol}$ is heat, not the molecular partition function. The energy as expressed by Equation (15.11) is the difference in internal energy at some finite temperature to that at 0 K. If there is residual, internal energy present at 0 K, it must be included to determine the overall energy of the system. However, by convention $U_o$ is
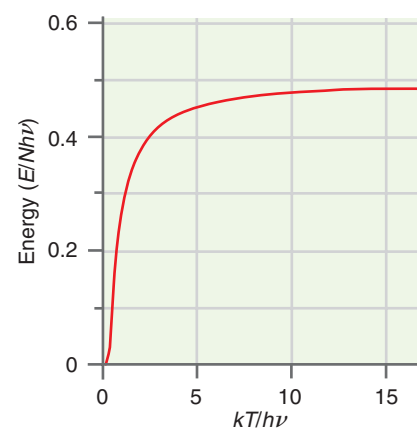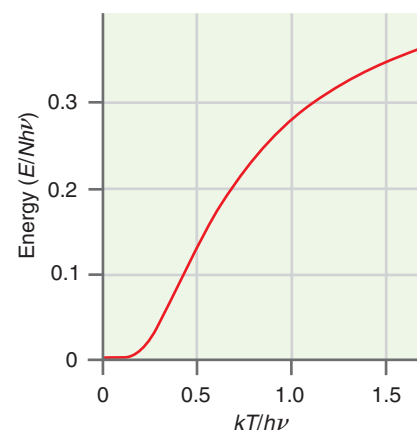


**FIGURE 15.2**
Total energy as a function of temperature is presented for an ensemble consisting of units that have two energy levels separated by an amount $h\nu$. Temperature is described relative to the energy gap through $kT/h\nu$. The plot on the top provides an expanded view of the low $kT/h\nu$ region plotted on the bottom.
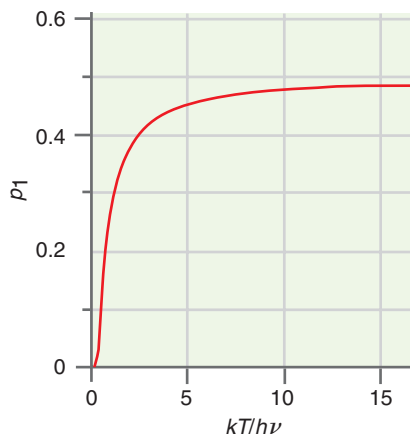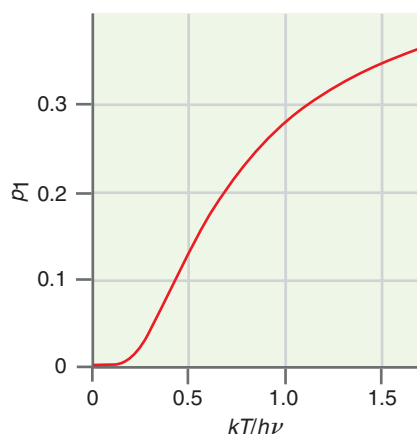


**FIGURE 15.3**
The probability of occupying the excited state in a two-level system is shown as a function of temperature. The evolution in temperature is plotted as $kT/h\nu$.

generally set to zero. For example, in the two-level example described earlier, the internal energy will be zero at 0 K since the energy of the ground state is defined as zero.

The second important relationship to establish is that between the internal energy and the canonical partition function. Fortunately, we have already encountered this relationship. For an ensemble of indistinguishable noninteracting particles, the canonical partition function is given by

$$Q = \frac{q^N}{N!} \tag{15.12}$$

In Equation (15.12), $q$ is the molecular partition function. Taking the natural log of Equation (15.12) yields

$$\ln Q = \ln\left(\frac{q^N}{N!}\right) = N \ln q - \ln N! \tag{15.13}$$

Finally, taking the derivative of Equation (15.13) with respect to $\beta$ and recognizing that $\ln(N!)$ is constant in the canonical ensemble,

$$\frac{d \ln Q}{d\beta} = \frac{d}{d\beta}(N \ln q) - \frac{d}{d\beta}(\ln N!)$$

$$= N\frac{d \ln q}{d\beta} \tag{15.14}$$

The last relationship is related to the total energy; therefore, the relationship between the canonical partition function and total internal energy $U$ is simply

$$U = -\left(\frac{\partial \ln Q}{\partial \beta}\right)_V \tag{15.15}$$

## EXAMPLE PROBLEM 15.2

For an ensemble consisting of 1.00 moles of particles having two energy levels separated by $h\nu = 1.00 \times 10^{-20}$ J, at what temperature will the internal energy of this system equal 1.00 kJ?

### Solution

Using the expression for total energy and recognizing that $N = nN_A$,

$$U = -\left(\frac{\partial \ln Q}{\partial \beta}\right)_V = -nN_A\left(\frac{\partial \ln q}{\partial \beta}\right)_V$$

Evaluating the preceding expression and paying particular attention to units, we get

$$U = -nN_A\left(\frac{\partial}{\partial \beta}\ln q\right)_V = -\frac{nN_A}{q}\left(\frac{\partial q}{\partial \beta}\right)_V$$

$$\frac{U}{nN_A} = \frac{-1}{(1 + e^{-\beta h\nu})}\left(\frac{\partial}{\partial \beta}(1 + e^{-\beta h\nu})\right)_V$$

$$= \frac{h\nu e^{-\beta h\nu}}{1 + e^{-\beta h\nu}} = \frac{h\nu}{e^{\beta h\nu} + 1}$$

$$\frac{nN_A h\nu}{U} - 1 = e^{\beta h\nu}$$

$$\ln\left(\frac{nN_A h\nu}{U} - 1\right) = \beta h\nu = \frac{h\nu}{kT}$$

$$T = \frac{h\nu}{k \ln\left(\frac{nN_A h\nu}{U} - 1\right)}$$

$$= \frac{1.00 \times 10^{-20} \text{ J}}{(1.38 \times 10^{-23} \text{ J K}^{-1}) \ln\left(\frac{(1.00 \text{ mol})(6.022 \times 10^{23} \text{ mol}^{-1})(1.00 \times 10^{-20} \text{ J})}{(1.00 \times 10^3 \text{ J})} - 1\right)}$$

$$= 449 \text{ K}$$

# 15.2 Energy and Molecular Energetic Degrees of Freedom

In the previous chapter, the relationship between the total molecular partition function ($q_{Total}$) and the partition functions corresponding to an individual energetic degree of freedom was derived under the assumption that the energetic degrees of freedom are not coupled:

$$q_{Total} = q_T q_R q_V q_E \tag{15.16}$$

In this expression, the subscripts $T$, $R$, $V$, and $E$ refer to translational, rotational, vibrational, and electronic energetic degrees of freedom, respectively. In a similar fashion, the internal energy can be decomposed into the contributions from each energetic degree of freedom:

$$
\begin{aligned}
U &= -\left(\frac{\partial \ln Q}{\partial \beta}\right)_V = -N\left(\frac{\partial \ln q}{\partial \beta}\right)_V \\
&= -N\left(\frac{\partial \ln (q_T q_R q_V q_E)}{\partial \beta}\right)_V \\
&= -N\left(\frac{\partial}{\partial \beta}(\ln q_T + \ln q_R + \ln q_V + \ln q_E)\right)_V \tag{15.17} \\
&= -N\left[\left(\frac{\partial \ln q_T}{\partial \beta}\right)_V + \left(\frac{\partial \ln q_R}{\partial \beta}\right)_V + \left(\frac{\partial \ln q_V}{\partial \beta}\right)_V + \left(\frac{\partial \ln q_E}{\partial \beta}\right)_V\right] \\
&= U_T + U_R + U_V + U_E
\end{aligned}
$$

The last line in this expression demonstrates a very intuitive and important result—that the total internal energy is simply the sum of contributions from each molecular energetic degree of freedom. This result also illustrates the connection between the macroscopic property of the ensemble (internal energy) and the microscopic details of the units themselves (molecular energy levels). To relate the total internal energy to the energetic degrees of freedom, expressions for the energy contribution from each energetic degree of freedom ($U_T$, $U_R$, and so on) are needed. The remainder of this section is dedicated to deriving these relationships.

## 15.2.1 Translations

The contribution to the system internal energy from translational motion is

$$U_T = \frac{-N}{q_T}\left(\frac{\partial q_T}{\partial \beta}\right)_V \tag{15.18}$$

In Equation (15.18), $q_T$ is the translational partition function, which in three dimensions is given by

$$q_T = \frac{V}{\Lambda^3} \text{ with } \Lambda^3 = \left(\frac{h^2\beta}{2\pi m}\right)^{3/2} \tag{15.19}$$

In Equation (15.19), $m$ is particle mass. With this partition function, the translational contribution to the internal energy becomes

$$
\begin{aligned}
U_T &= \frac{-N}{q_T}\left(\frac{\partial q_T}{\partial \beta}\right)_V = \frac{-N\Lambda^3}{V}\left(\frac{\partial}{\partial \beta}\frac{V}{\Lambda^3}\right)_V \\
&= -N\Lambda^3\left(\frac{\partial}{\partial \beta}\frac{1}{\Lambda^3}\right)_V \\
&= -N\Lambda^3\left(\frac{\partial}{\partial \beta}\left(\frac{2\pi m}{h^2\beta}\right)^{3/2}\right)_V \\
&= -N\Lambda^3\left(\frac{2\pi m}{h^2}\right)^{3/2}\left(\frac{\partial}{\partial \beta}\beta^{-3/2}\right)_V \\
&= -N\Lambda^3\left(\frac{2\pi m}{h^2}\right)^{3/2}\frac{-3}{2}\beta^{-5/2}
\end{aligned}
$$

$$= \frac{3}{2} N \Lambda^3 \left( \frac{2\pi m}{h^2 \beta} \right)^{3/2} \beta^{-1}$$

$$= \frac{3}{2} N \beta^{-1}$$

$$U_T = \frac{3}{2} NkT = \frac{3}{2} nRT \qquad (15.20)$$

Equation (15.20) should look familiar. Recall from Chapter 2 that the internal energy of an ideal monatomic gas is $nC_V \Delta T = 3/2(nRT)$ with $T_{initial} = 0$ K, identical to the result just obtained. The convergence between the thermodynamic and statistical mechanical descriptions of monatomic-gas systems is remarkable.

It is also interesting to note that the contribution of translational motion to the internal energy is equal to that predicted by the equipartition theorem (Section 14.8). The equipartition theorem states that any term in the classical Hamiltonian that is quadratic with respect to momentum or position will contribute $kT/2$ to the energy. The Hamiltonian corresponding to three-dimensional translational motion of an ideal monatomic gas is

$$H_{trans} = \frac{1}{2m} (p_x^2 + p_y^2 + p_z^2) \qquad (15.21)$$

Each $p^2$ term in Equation (15.21) will contribute $1/2 \, kT$ to the energy by equipartition such that the total contribution will be $3/2 \, kT$, or $3/2 \, RT$ for a mole of particles that is identical to the result derived using the quantum mechanical description of translational motion. This agreement is not surprising given the small energy gap between translational energy levels such that classical behavior is expected.

### 15.2.2 Rotations

Within the rigid rotor approximation, the rotational partition function for a diatomic molecule in the high-temperature limit is given by

$$q_R = \frac{1}{\sigma \beta hcB} \qquad (15.22)$$

With this partition function, the contribution to the internal energy from rotational motion is

$$U_R = \frac{-N}{q_R} \left( \frac{\partial q_R}{\partial \beta} \right)_V = -N\sigma \beta hcB \left( \frac{\partial}{\partial \beta} \frac{1}{\sigma \beta hcB} \right)_V$$

$$= -N\beta \left( \frac{\partial}{\partial \beta} \beta^{-1} \right)_V$$

$$= -N\beta(-\beta^{-2})$$

$$= N\beta^{-1}$$

$$U_R = NkT = nRT \qquad (15.23)$$

Recall from Chapter 14 that the rotational partition function employed in this derivation is for a diatomic in which the rotational temperature $\Theta_R$ is much less than $kT$. In this limit, a significant number of rotational states are accessible. If $\Theta_R$ is not small relative to $kT$, then full evaluation of the sum form of the rotational partition function is required to determine $U_R$.

In the high-temperature limit, the rotational energy can be thought of as containing contributions of $1/2 \, kT$ from each nonvanishing moment of inertia. This partitioning of energy is analogous to the case of translational energy discussed earlier within the context of the equipartition theorem. The concept of equipartition can be used to extend the result for $U_R$ obtained for a diatomic molecule to linear and nonlinear polyatomic molecules. Because each nonvanishing moment of inertia will provide $1/2 \, kT$ to the rotational energy equipartition, we can state that

$$U_R = nRT \quad \text{(linear polyatomic)} \qquad (15.24)$$

$$U_R = \frac{3}{2} nRT \quad \text{(nonlinear polyatomic)} \qquad (15.25)$$

The result for nonlinear polyatomic molecules can be confirmed by evaluating the expression for the average rotational energy employing the partition function for a nonlinear polyatomic that was presented in the previous chapter.

### 15.2.3 Vibrations

Unlike translational and rotational degrees of freedom, vibrational energy-level spacings are typically greater than $kT$ such that the equipartition theorem is usually not applicable to this energetic degree of freedom. Fortunately, within the harmonic oscillator model, the regular energy-level spacings provide for a relatively simple expression for the vibrational partition function neglecting zero-point energy:

$$q_V = (1 - e^{-\beta hc\tilde{\nu}})^{-1} \tag{15.26}$$

The term $\tilde{\nu}$ represents vibrational frequency in units of cm$^{-1}$. Using this partition function, the vibrational contribution to the average energy is

$$U_V = \frac{-N}{q_V}\left(\frac{\partial q_V}{\partial \beta}\right)_V = -N(1 - e^{-\beta hc\tilde{\nu}})\left(\frac{\partial}{\partial \beta}(1 - e^{-\beta hc\tilde{\nu}})^{-1}\right)_V$$

$$= -N\left(1 - e^{-\beta hc\tilde{\nu}}\right)\left(-hc\tilde{\nu}e^{-\beta hc\tilde{\nu}}\right)\left(1 - e^{-\beta hc\tilde{\nu}}\right)^{-2}$$

$$= \frac{Nhc\tilde{\nu}e^{-\beta hc\tilde{\nu}}}{\left(1 - e^{-\beta hc\tilde{\nu}}\right)}$$

$$U_V = \frac{Nhc\tilde{\nu}}{e^{\beta hc\tilde{\nu}} - 1} \tag{15.27}$$

The temperature dependence of $U_V/Nhc$ for a vibrational degree of freedom with $\tilde{\nu} = 1000$ cm$^{-1}$ is presented in Figure 15.4. First, note that at lowest temperatures $U_V$ is zero, which is reminiscent of the two-level example presented earlier in this chapter. At low temperatures, $kT \ll hc\tilde{\nu}$, such that there is insufficient thermal energy to populate the first excited vibrational state to an appreciable extent. However, for temperatures $\geq 1000$ K the average energy increases linearly with temperature, identical to the behavior observed for translational and rotational energy. This observation suggests that a high-temperature expression for $U_V$ also exists.

To derive the high-temperature limit expression for the vibrational energy, the exponential term in $q_V$ is written using the following series expression:

$$e^x = 1 + x + \frac{x^2}{2!} + \cdots$$

With $x = \beta hc\tilde{\nu} = hc\tilde{\nu}/kT$, and when $kT \gg hc\tilde{\nu}$, the series is approximately equal to $1 + x$ yielding

$$U_V = \frac{Nhc\tilde{\nu}}{e^{\beta hc\tilde{\nu}} - 1} = \frac{Nhc\tilde{\nu}}{(1 + \beta hc\tilde{\nu}) - 1}$$

$$= \frac{N}{\beta}$$

$$U_V = NkT = nRT \tag{15.28}$$

When the temperature is sufficiently high so that the high-temperature limit is applicable, the vibrational contribution to the internal energy is $nRT$, identical to the prediction of the equipartition theorem. Note that this is the contribution for a single vibrational degree of freedom and that the overall contribution will be the sum of contributions from all vibrational degrees of freedom. Furthermore, the applicability of the high-temperature approximation is dependent on the details of the vibrational energies for the system in question. In particular, the high-temperature approximation may be applicable for some low-energy vibrations but not applicable to higher energy vibrations.

The applicability of the high-temperature limit can be determined using the vibrational temperature defined previously:

$$\Theta_V = \frac{hc\tilde{\nu}}{k} \tag{15.29}$$
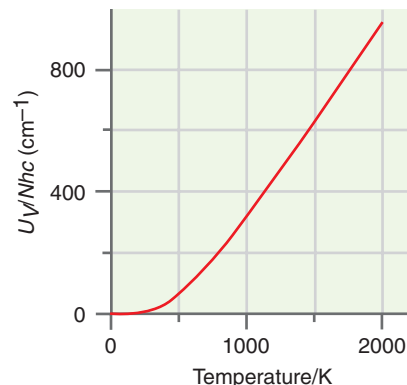


**FIGURE 15.4**
The variation in average vibrational energy as a function of temperature where $\tilde{\nu} = 1000$ cm$^{-1}$.

| TABLE 15.1 | Molecular Vibrational Temperatures | | |
|---|---|---|---|
| Molecule | $\Theta_V$ (K) | Molecule | $\Theta_V$ (K) |
| $I_2$ | 309 | $N_2$ | 3392 |
| $Br_2$ | 468 | CO | 3121 |
| $Cl_2$ | 807 | $O_2$ | 2274 |
| $F_2$ | 1329 | $H_2$ | 6338 |

It was stated that the high-temperature limit is applicable when $T \geq 10\Theta_V$. Some examples of $\Theta_V$ for diatomic molecules are provided in Table 15.1. Inspection of the table demonstrates that relatively elevated temperatures must be reached before the high-temperature limit is applicable to the vast majority of vibrational degrees of freedom. If the high-temperature limit is not applicable, then the vibrational energy must be determined using Eq. 15.27.

### 15.2.4  Electronic

Because electronic energy-level spacings are generally quite large compared to $kT$, the partition function is simply equal to the ground-state degeneracy. Since the degeneracy is a constant, the derivative of this quantity with respect to $\beta$ must be zero and

$$U_E = 0 \tag{15.30}$$

Exceptions to this result do exist. In particular, for systems in which electronic energy levels are comparable to $kT$, it is necessary to evaluate the full partition function.

---

**EXAMPLE PROBLEM 15.3**

The ground state of $O_2$ is $^3\Sigma_g^-$. When $O_2$ is electronically excited, emission from the excited state $(^1\Delta_g)$ to the ground state is observed at 1263 nm. Calculate $q_E$ and determine the electronic contribution to $U$ for a mole of $O_2$ at 500. K.

**Solution**

The first step to solving this problem is construction of the electronic partition function. The ground state is threefold degenerate, and the excited state is nondegenerate. The energy of the excited state relative to the ground state is detemined using the emission wavelength:

$$\varepsilon = \frac{hc}{\lambda} = \frac{(6.626 \times 10^{-34}\,\text{J s})(3.00 \times 10^8\,\text{m s}^{-1})}{1.263 \times 10^{-6}\,\text{m}} = 1.57 \times 10^{-19}\,\text{J}$$

Therefore, the electronic partition function is

$$q_E = g_0 + g_1 e^{-\beta\varepsilon} = 3 + e^{-\beta(1.57 \times 10^{-19}\,\text{J})}$$

With the electronic partition function, $U_E$ is readily determined:

$$U_E = \frac{-nN_A}{q_E}\left(\frac{\partial q_E}{\partial \beta}\right)_V = \frac{(1\,\text{mol})\,6.022 \times 10^{23}\,\text{mol}^{-1}(1.57 \times 10^{-19}\,\text{J})e^{-\beta(1.57 \times 10^{-19}\,\text{J})}}{3 + e^{-\beta(1.57 \times 10^{-19}\,\text{J})}}$$

$$= \frac{94.5\,\text{kJ}\exp\left[-\dfrac{1.57 \times 10^{-19}\,\text{J}}{(1.38 \times 10^{-23}\,\text{J K}^{-1})(500.\,\text{K})}\right]}{3 + \exp\left[-\dfrac{1.57 \times 10^{-19}\,\text{J}}{(1.38 \times 10^{-23}\,\text{J K}^{-1})(500.\,\text{K})}\right]}$$

$$= 4.14 \times 10^{-6}\,\text{J}$$

Notice that $U_E$ is quite small, reflecting the fact that even at 500. K the $^1\Delta_g$ excited state of $O_2$ is not readily populated. Therefore, the contribution to the internal energy from electronic degrees of freedom for $O_2$ at 500. K is negligible.

## 15.2.5 Review

At the beginning of this section, we established that the total average energy was simply the sum of average energies for each energetic degree of freedom. Applying this logic to a diatomic system, the total energy is given by

$$
\begin{aligned}
U_{Total} &= U_T + U_R + U_V + U_E \\
&= \frac{3}{2}NkT + NkT + \frac{Nhc\tilde{\nu}}{e^{\beta hc\tilde{\nu}} - 1} + 0 \\
&= \frac{5}{2}NkT + \frac{Nhc\tilde{\nu}}{e^{\beta hc\tilde{\nu}} - 1}
\end{aligned}
\tag{15.31}
$$

In arriving at Equation (15.31), the assumption has been made that the rotational degrees of freedom are in the high-temperature limit and that degeneracy of the ground electronic level makes the lone contribution to the electronic partition function. Although the internal energy is dependent on molecular details ($B$, $\tilde{\nu}$, and so on), it is important to realize that the total energy can be decomposed into contributions from each molecular degree of freedom.

# 15.3 Heat Capacity

As discussed in Chapter 2, the thermodynamic definition of the **heat capacity** at constant volume ($C_V$) is

$$
C_V = \left(\frac{\partial U}{\partial T}\right)_V = -k\beta^2\left(\frac{\partial U}{\partial \beta}\right)_V
\tag{15.32}
$$

Because the internal energy can be decomposed into contributions from each energetic degree of freedom, the heat capacity can also be similarly decomposed. In the previous section, the average internal energy contribution from each energetic degree of freedom was determined. Correspondingly, the heat capacity is given by the derivative of the internal energy with respect to temperature for a given energetic degree of freedom. In the remainder of this section, we use this approach to determine the translational, vibrational, rotational, and electronic contributions to the constant volume heat capacity.

### EXAMPLE PROBLEM 15.4

Determine the heat capacity for an ensemble consisting of units that have only two energy levels separated by an arbitrary amount of energy, $h\nu$.

#### Solution

This is the same system discussed in Example Problem 15.1 where the partition function was determined to be $q = 1 + e^{-\beta h\nu}$. The corresponding average energy calculated using this partition function is $U = Nh\nu/(e^{\beta h\nu} + 1)$. Given the functional form of the average energy, the heat capacity is most easily determined by taking the derivative with respect to $\beta$ as follows:

$$
\begin{aligned}
C_\nu &= -k\beta^2\left(\frac{\partial U}{\partial \beta}\right)_V = -Nk\beta^2\left(\frac{\partial}{\partial \beta}h\nu\left(e^{\beta h\nu} + 1\right)^{-1}\right)_V \\
&= \frac{Nk\beta^2(h\nu)^2 e^{\beta h\nu}}{(e^{\beta h\nu} + 1)^2}
\end{aligned}
$$

The functional form of the heat capacity is rather complex and is plotted in Figure 15.5. As observed previously, limiting behavior is observed at both low and high temperatures. At the lowest temperature, $C_V$ is zero and then increases to a maximum value after which further increases in temperature result in a decrease in the heat capacity. This behavior is reminiscent of the evolution in energy as a function of
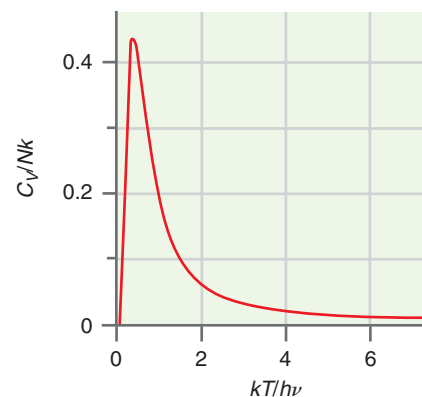


**FIGURE 15.5**

Constant volume heat capacity for a two-level system as a function of temperature. Note that the heat capacity has been divided by the product of Boltzmann's constant and the number of particles.

temperature (Figure 15.2) and can be traced back to the same origin, the evolution in state populations as a function of temperature. Heat capacity is a measure of the ability of a system to absorb energy from the surroundings. At the lowest temperatures, there is insufficient energy to access the excited state such that the two-level system is incapable of absorbing energy. As the available thermal energy is increased, the excited state becomes accessible and the heat capacity increases. Finally, at the highest temperatures the populations in the ground and excited states reach their limiting values of 0.5. Here, the system is again incapable of absorbing energy, and the heat capacity approaches zero.

### 15.3.1  Translational Heat Capacity

Translational energy-level spacings are extremely small such that the high-temperature approximation is valid. The contribution of translational motion to the average molecular energy for an ideal gas is

$$U_T = \frac{3}{2}NkT \qquad (15.33)$$

Therefore, the translational contribution to $C_V$ is readily determined by taking the derivative of the preceding expression with respect to temperature:

$$(C_V)_T = \left(\frac{\partial U_T}{\partial T}\right)_V = \frac{3}{2}Nk \qquad (15.34)$$

This result demonstrates that the contribution of translations to the overall constant volume heat capacity is simply a constant, with no temperature dependence. The constant value of the translational contribution to $C_V$ down to very low temperatures is a consequence of the dense manifold of closely spaced translational states.

### 15.3.2  Rotational Heat Capacity

Assuming that the rotational energy spacings are small relative to $kT$, the high-temperature expression for the rotational contribution to the average energy can be used to determine the rotational contribution to $C_V$. The internal energy is dependent on molecular geometry:

$$U_R = NkT \text{ (linear)} \qquad (15.35)$$

$$U_R = \frac{3}{2}NkT \text{ (nonlinear)} \qquad (15.36)$$

Using these two equations, the rotational contribution to $C_V$ becomes

$$(C_V)_R = Nk \text{ (linear)} \qquad (15.37)$$

$$(C_V)_R = \frac{3}{2}Nk \text{ (nonlinear)} \qquad (15.38)$$

Note that these expressions are correct in the high-temperature limit. What will occur at low temperature? At the lowest temperatures, there is insufficient thermal energy to provide for population of excited rotational energy levels. Therefore, the heat capacity approaches zero. As temperature is increased, the heat capacity increases until the high-temperature limit is reached. At these intermediate temperatures, the heat capacity must be determined by evaluating the summation form of $q_R$.

### 15.3.3  Vibrational Heat Capacity

In contrast to translations and rotations, the high-temperature limit is generally not applicable to the vibrational degrees of freedom. Therefore, the exact functional form of the energy must be evaluated to determine the vibrational contribution to $C_V$. The derivation is somewhat more involved, but still straightforward. First, recall that the vibrational contribution to $U$ is [Equation (15.27)]

$$U_V = \frac{Nhc\tilde{\nu}}{e^{\beta hc\tilde{\nu}} - 1} \qquad (15.39)$$

Given this equation, the vibrational contribution to the constant volume heat capacity is

$$(C_V)_{Vib} = \left(\frac{\partial U_V}{\partial T}\right)_V = -k\beta^2\left(\frac{\partial U_V}{\partial \beta}\right)_V$$

$$= -Nk\beta^2 hc\tilde{\nu}\left(\frac{\partial}{\partial \beta}(e^{\beta hc\tilde{\nu}} - 1)^{-1}\right)_V$$

$$= -Nk\beta^2 hc\tilde{\nu}(-hc\tilde{\nu}e^{\beta hc\tilde{\nu}}(e^{\beta hc\tilde{\nu}} - 1)^{-2})V$$

$$(C_V)_{Vib} = Nk\beta^2(hc\tilde{\nu})^2 \frac{e^{\beta hc\tilde{\nu}}}{(e^{\beta hc\tilde{\nu}} - 1)^2} \tag{15.40}$$

The heat capacity can also be cast in terms of the vibrational temperature $\Theta_V$ as follows

$$(C_V)_{Vib} = Nk\left(\frac{\Theta_V}{T}\right)^2 \frac{e^{\Theta_V/T}}{(e^{\Theta_V/T} - 1)^2} \tag{15.41}$$

As mentioned in Chapter 14, a polyatomic molecule has $3N - 6$ or $3N - 5$ vibrational degrees of freedom, respectively. Each vibrational degree of freedom contributes to the overall vibrational constant volume heat capacity such that

$$(C_V)_{Vib,Total} = \sum_{m=1}^{3N-6 \text{ or } 3N-5} (C_V)_{Vib,m} \tag{15.42}$$

How does the vibrational heat capacity change as a function of $T$? The contribution of a given vibrational degree of freedom depends on the spacing between vibrational levels relative to $kT$. Therefore, at lowest temperatures we expect the vibrational contribution to $C_V$ to be zero. As the temperature increases, the lowest energy vibrational modes have spacings comparable to $kT$ such that these modes will contribute to the heat capacity. Finally, the highest energy vibrational modes contribute only at high temperatures. In summary, we expect the vibrational contribution to $C_V$ to demonstrate a significant temperature dependence.

Figure 15.6 presents the vibrational contribution to $C_V$ as a function of temperature for a nonlinear triatomic molecule having three nondegenerate vibrational modes of frequency 100, 1000, and 3000 cm$^{-1}$. As expected, the lowest frequency mode contributes to the heat capacity at lowest temperatures, reaching a constant value of $Nk$ for temperatures greatly in excess of $\Theta_V$. As the temperature increases, each successively higher energy vibrational mode begins to contribute to the heat capacity and reaches the same limiting value of $Nk$ at highest temperatures. Finally, the total vibrational heat capacity, which is simply the sum of the contributions from the individual modes, approaches a limiting value of $3Nk$.

The behavior illustrated in Figure 15.6 demonstrates that for temperatures where $kT \gg hc\tilde{\nu}$, the heat capacity approaches a constant value, suggesting that, like translations and rotations, there is a high-temperature limit for the vibrational contribution to $C_V$. Recall that the high-temperature approximation for the average energy for an individual vibrational degree of freedom is

$$U_V = \frac{N}{\beta} = NkT \tag{15.43}$$

Differentiation of this expression with respect to temperature reveals that the vibrational contribution to the $C_V$ is indeed equal to $Nk$ per vibrational mode in the high-temperature limit as illustrated in Figure 15.6 and as expected from the equipartition theorem.



**FIGURE 15.6**
Evolution in the vibrational contribution to $C_V$ as a function of temperature. Calculations are for a molecule with three vibrational degrees of freedom as indicated in the top panel. Contribution for each vibrational mode (top) and the total vibrational contribution (bottom).

### 15.3.4 Electronic Heat Capacity

Because the partition function for the energetic degree of freedom is generally equal to the ground-state degeneracy, the resulting average energy is zero. Therefore, there is no contribution to the constant volume heat capacity from these degrees of freedom. However, for systems with electronic excited states that are comparable to $kT$, the contribution to $C_V$ from electronic degrees of freedom can be finite and must be determined using the summation form of the partition function.

## 15.3.5 Review

Similar to energy, the overall constant volume heat capacity is simply the sum of the contributions to the heat capacity from each individual degree of freedom. For example, for a diatomic molecule with translational and rotational degrees of freedom well described by the high-temperature approximation, we have

$$
\begin{aligned}
(C_V)_{Total} &= (C_V)_T + (C_V)_R + (C_V)_{Vib} \\
&= \frac{3}{2}Nk + Nk + Nk\beta^2(hc\tilde{\nu})^2 \frac{e^{\beta hc\tilde{\nu}}}{(e^{\beta hc\tilde{\nu}} - 1)^2} \\
&= \frac{5}{2}Nk + Nk\beta^2(hc\tilde{\nu})^2 \frac{e^{\beta hc\tilde{\nu}}}{(e^{\beta hc\tilde{\nu}} - 1)^2}
\end{aligned}
\tag{15.44}
$$

The theoretical prediction for the heat capacity for gaseous HCl as a function of temperature is presented in Figure 15.7. The figure illustrates that at the lowest temperatures the heat capacity is $3/2Nk$ due to the contribution of translational motion. As the temperature is increased, the rotational contribution to the heat capacity increases, reaching the high-temperature limit at ~150 K, which is approximately 10-fold greater than the rotational temperature of 15.2 K. The temperature dependence of the rotational contribution was determined by numerical evaluation, a tedious procedure that must be performed when the high-temperature limit is not applicable. Finally, the vibrational contribution to the heat capacity becomes significant at highest temperatures consistent with the high vibrational temperature of this molecule (~4000 K). The curve depicted in the figure is theoretical and does not take into account molecular dissociation or phase transitions.

## 15.3.6 The Einstein Solid

The **Einstein solid** model was developed to describe the thermodynamic properties of atomic crystalline systems. In this model, each atom is envisioned to occupy a lattice site where the restoring potential is described as a three-dimensional harmonic oscillator. All of the harmonic oscillators are assumed to be separable such that motion of the atom in one dimension does not affect the vibrational motion (i.e., energy) in orthogonal dimensions. Finally, the harmonic oscillators are assumed to be isoenergetic such that they are characterized by the same frequency. For a crystal containing $N$ atoms, there are $3N$ vibrational degrees of freedom, and the total heat capacity will simply be the sum of contributions from each vibrational degree of freedom. Therefore,

$$
(C_V)_{Total} = 3Nk\left(\frac{\Theta_V}{T}\right)^2 \frac{e^{\Theta_V/T}}{(e^{\Theta_V/T} - 1)^2}
\tag{15.45}
$$
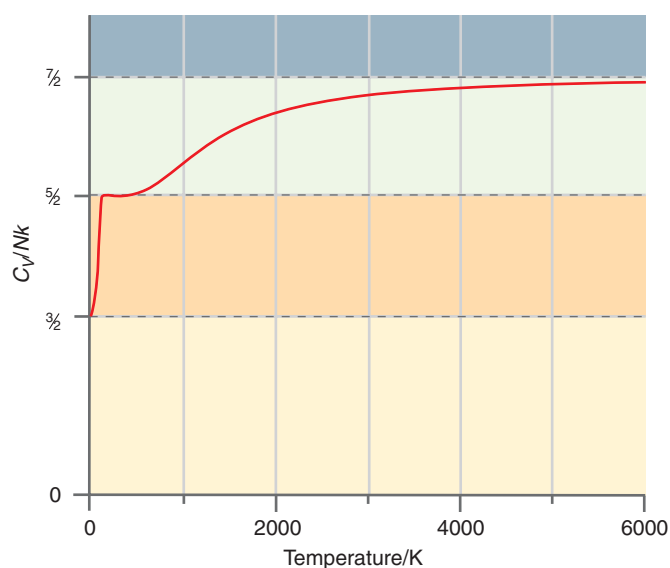


**FIGURE 15.7**

The constant volume heat capacity for gaseous HCl as a function of temperature. The contributions of translational (yellow), rotational (orange), and vibrational (light green) degrees of freedom to the heat capacity are shown.

This total heat capacity is identical to that of a collection of $3N$ harmonic oscillators. The important aspect to note about Equation (15.45) is that $C_V$ of the crystal at a given temperature is predicted to depend only on the vibrational frequency. This suggests that measurement of the constant volume heat capacity of an atomic crystal as a function of temperature allows for a determination of the characteristic vibrational temperature and corresponding vibrational frequency. This was one of the earliest quantum mechanical models used to describe a thermodynamic observable. For example, a comparison of the Einstein model and experiment for diamond ($\Theta_V = 1320$ K) is presented in Figure 15.8, and the agreement is remarkably good. Note that the model predicts that the heat capacity should reach a limiting value of 24.91 J mol$^{-1}$ K$^{-1}$, or $3R$, at high temperature. This limiting value is known as the **Dulong and Petit law,** and represents the high-temperature or classical prediction for the heat capacity of such systems. The elegance of the Einstein model is that it provides a reason for the failure of classical models at low temperatures where significant deviations from the Dulong and Petit law are observed. As has been seen, the quantum nature of vibrational degrees of freedom becomes exceedingly important when $\Theta_V > T$, and the Einstein model provided a critical view into the microscopic nature of matter manifesting itself in macroscopic behavior that classical mechanics cannot explain.

A second prediction of the Einstein model is that a plot of $C_V$ versus $T/\Theta_V$ can describe the variation in heat capacity for all solids. Figure 15.9 presents a comparison of this prediction to the experimental values for three atomic crystals. The agreement is nothing short of astonishing and suggests that one only need measure $C_V$ at a single temperature to determine the characteristic $\Theta_V$ for a given solid! Furthermore, with $\Theta_V$ in hand, the heat capacity at all other temperatures is defined! In short, starting with a quantum model for vibrations and the mathematics of probability theory, a unifying theory of heat capacity for atomic solids has been developed. This is quite an accomplishment.

The agreement between the Einstein model and experiment at high temperatures is excellent; however, discrepancies between this theory and experiment have been noted. First, the model is applicable only to atomic crystals, and it does not accurately reproduce the temperature dependence of $C_V$ for molecular solids. Second, the Einstein model predicts that the heat capacity should demonstrate exponential dependence at low temperature; however, experimentally the heat capacity demonstrates $T^3$ dependence. The discrepancy between the Einstein model and experiment lies in the fact that the normal frequencies of the crystal are not due to vibrations of single atoms but are due to concerted harmonic motion of all the atoms. These lattice vibrations are not all characterized by the same frequency. More advanced treatments of atomic crystals, such as the Debye model, are capable of quantitatively reproducing crystalline heat capacities.
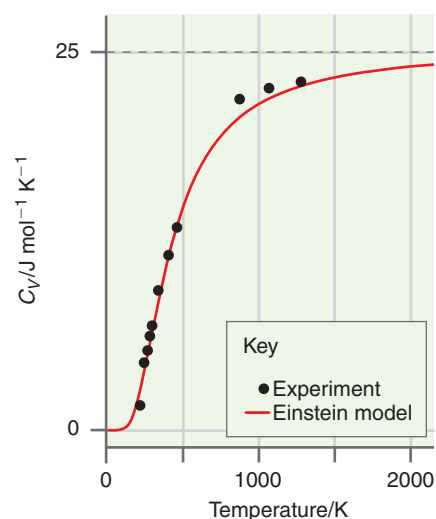


**FIGURE 15.8**
Comparison of $C_V$ for diamond to the theoretical prediction of the Einstein solid model. The classical limit of 24.91 J mol$^{-1}$ K$^{-1}$ is shown as the dashed line.
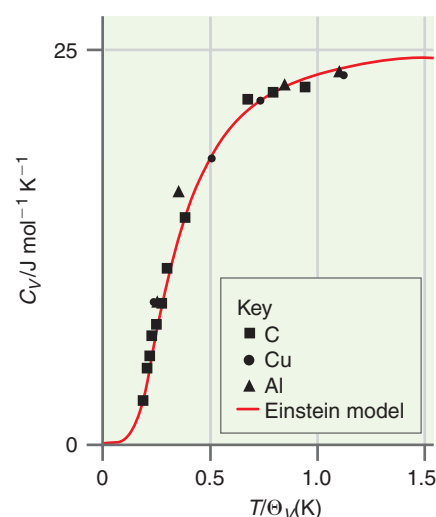


**FIGURE 15.9**
Comparison of $C_V$ versus $T > \Theta_V$ for C, Cu, and Al.

# 15.4 Entropy

Entropy is perhaps the most misunderstood thermodynamic property of matter. Introductory chemistry courses generally describe the entropic driving force for a reaction as an inherent desire for the system to increase its "randomness" or "disorder." With statistical mechanics, we will see that the tendency of an isolated system to evolve toward the state of maximum entropy is a direct consequence of statistics. To illustrate this point, recall from Chapter 13 that a system approaches equilibrium by achieving the configuration of energy with the maximum weight. In other words, the configuration of energy that will be observed at equilibrium corresponds to $W_{max}$. The tendency of a system to maximize $W$ and entropy $S$ suggests that the relationship exists between these quantities. Boltzmann expressed this relationship in the following equation, known as **Boltzmann's formula:**

$$S = k \ln W \qquad (15.46)$$

This relationship states that entropy is directly proportional to $\ln(W)$, with the Boltzmann constant serving as the proportionality constant. Equation (15.46) makes it

clear that a maximum in $W$ will correspond to a maximum in $S$. Although at first view the Boltzmann formula appears to be a rather ad hoc statement, this formula is in fact equivalent to the thermodynamic definition of entropy discussed in Chapter 5. To illustrate this equivalence, consider the energy of an ensemble of particles. This energy is equal to the sum of the product of level energies and the occupation numbers for these levels such that

$$E = \sum_n \varepsilon_n a_n \tag{15.47}$$

The total differential of $E$ is given by

$$dE = \sum_n \varepsilon_n \, da_n + \sum_n a_n \, d\varepsilon_n \tag{15.48}$$

Because volume is constant in the canonical ensemble, the level energies are also constant. Therefore, the second term in the preceding expression is zero, and the change in energy is related exclusively to changes in level occupation numbers:

$$dE = \sum_n \varepsilon_n \, da_n \tag{15.49}$$

The constraint of constant volume also dictates that there is no $P$–$V$-type work; therefore, by the first law of thermodynamics the change in energy must be due to heat flow:

$$dE = dq_{rev} = \sum_n \varepsilon_n \, da_n \tag{15.50}$$

where $dq_{rev}$ is the reversible heat exchanged between system and surroundings. The thermodynamic definition of entropy is

$$dS = \frac{dq_{rev}}{T} \tag{15.51}$$

Comparison of the last two equations provides for the following definition of entropy:

$$dS = \frac{1}{T} \sum_n \varepsilon_n \, da_n = k\beta \sum_n \varepsilon_n \, da_n \tag{15.52}$$

We have rewritten $T^{-1}$ as $k\beta$ anticipating our upcoming need for $\beta$. In the derivation of the Boltzmann distribution presented in Chapter 13, the following relationship was obtained:

$$\left( \frac{d \ln W}{da_n} \right) + \alpha - \beta\varepsilon_n = 0$$

$$\beta\varepsilon_n = \left( \frac{d \ln W}{da_n} \right) + \alpha \tag{15.53}$$

where $\alpha$ and $\beta$ are constants (i.e., the Lagrange multipliers in the derivation of the Boltzmann distribution). Employing Equation (15.53), our expression for entropy becomes

$$dS = k\beta \sum_n \varepsilon_n \, da_n = k \sum_n \left( \frac{d \ln W}{da_n} \right) da_n + k \sum_n \alpha \, da_n$$

$$= k \sum_n \left( \frac{d \ln W}{da_n} \right) da_n + k\alpha \sum_n da_n$$

$$= k \sum_n \left( \frac{d \ln W}{da_n} \right) da_n$$

$$= k(d \ln W) \tag{15.54}$$

The third line above was obtained by recognizing that when the change in occupation number is summed over all possible states, this sum must equal zero since the gain in occupation number for a given state must be accompanied by the loss in another state. Equation (15.54) is simply an alternative form of the Boltzmann formula of Equation (15.46). The definition of entropy provided by the Boltzmann formula provides insight into the underpinnings of entropy, but how does one calculate the entropy for a molecular system? The answer to this question requires a bit more work. Because the partition function provides a measure of energy state accessibility,

it can be assumed that a relationship between the partition function and entropy exists. This relationship can be derived by applying the Boltzmann formula as follows:

$$S = k \ln W = k \ln \left( \frac{N!}{\prod_n a_n!} \right) \tag{15.55}$$

which can be reduced as follows:

$$\begin{aligned} S &= k \ln \left( \frac{N!}{\prod_n a_n!} \right) \\ &= k \ln N! - k \ln \prod_n a_n! \\ &= k \ln N! - k \sum_n \ln a_n! \\ &= k(N \ln N - N) - k \sum_n (a_n \ln a_n - a_n) \\ &= k \left( N \ln N - \sum_n a_n \ln a_n \right) \end{aligned} \tag{15.56}$$

In the last step the following definition for $N$ was used:

$$N = \sum_n a_n \tag{15.57}$$

Using this definition again:

$$\begin{aligned} S &= k \left( N \ln N - \sum_n a_n \ln a_n \right) \\ &= k \left( \sum_n a_n \ln N - \sum_n a_n \ln a_n \right) \\ &= -k \sum_n a_n \ln \frac{a_n}{N} \\ &= -k \sum_n a_n \ln p_n \end{aligned} \tag{15.58}$$

In the last line of this equation, $p_n$ is the probability of occupying energy level $n$ as defined previously in Equation (15.10). The Boltzmann distribution law can be used to rewrite the probability term in Equation (15.58) as follows:

$$\ln p_n = \ln \left( \frac{e^{-\beta \varepsilon_n}}{q} \right) = -\beta \varepsilon_n - \ln q \tag{15.59}$$

The expression for entropy then becomes

$$\begin{aligned} S &= -k \sum_n a_n \ln p_n \\ &= -k \sum_n a_n (-\beta \varepsilon_n - \ln q) \\ &= k\beta \sum_n a_n \varepsilon_n + k \sum_n a_n \ln q \\ &= k\beta E + kN \ln q \\ &= \frac{E}{T} + k \ln q^N \end{aligned}$$

$$S = \frac{E}{T} + k \ln Q = \frac{U}{T} + k \ln Q \tag{15.60}$$

In this expression, $U$ is the internal energy of the system and $Q$ is the canonical partition function. In Equation (15.60), $E$ is replaced by $U$ consistent with the previous

discussion regarding internal energy. The internal energy is related to the canonical partition function by

$$U = -\left(\frac{\partial \ln Q}{\partial \beta}\right)_V = kT^2\left(\frac{\partial \ln Q}{\partial T}\right)_V \tag{15.61}$$

Using this relationship, we arrive at a very compact expression for entropy:

$$S = \frac{U}{T} + k \ln Q = kT\left(\frac{\partial \ln Q}{\partial T}\right)_V + k \ln Q$$

$$S = \left(\frac{\partial}{\partial T}(kT \ln Q)\right)_V \tag{15.62}$$

### 15.4.1 Entropy of an Ideal Monatomic Gas

What is the general expression for the molar entropy of an ideal monatomic gas? A monatomic gas is a collection of indistinguishable particles. Assuming that the electronic partition function is unity (i.e., the ground electronic energy level is nondegenerate), only translational degrees of freedom remain to be evaluated, resulting in

$$\begin{aligned} S &= \frac{U}{T} + k \ln Q \\ &= \frac{1}{T}\left(\frac{3}{2}NkT\right) + k \ln \frac{q_{trans}^N}{N!} \\ &= \frac{3}{2}Nk + Nk \ln q_{trans} - k(N \ln N - N) \\ &= \frac{5}{2}Nk + Nk \ln q_{trans} - Nk \ln N \\ &= \frac{5}{2}Nk + Nk \ln \frac{V}{\Lambda^3} - Nk \ln N \\ &= \frac{5}{2}Nk + Nk \ln V - Nk \ln \Lambda^3 - Nk \ln N \\ &= \frac{5}{2}Nk + Nk \ln V - Nk \ln\left(\frac{h^2}{2\pi mkT}\right)^{3/2} - Nk \ln N \\ &= \frac{5}{2}Nk + Nk \ln V + \frac{3}{2}Nk \ln T - Nk \ln\left(\frac{N^{2/3}h^2}{2\pi mk}\right)^{3/2} \\ &= \frac{5}{2}nR + nR \ln V + \frac{3}{2}nR \ln T - nR \ln\left(\frac{n^{2/3}N_A^{2/3}h^2}{2\pi mk}\right)^{3/2} \end{aligned} \tag{15.63}$$

The final line of Equation (15.63) is a version of the **Sackur–Tetrode equation,** which can be written in the more compact form:

$$S = nR \ln\left[\frac{e^{5/2}V}{\Lambda^3 N}\right] = nR \ln\left[\frac{RTe^{5/2}}{\Lambda^3 N_A P}\right] \quad \text{where } \Lambda^3 = \left(\frac{h^2}{2\pi mkT}\right)^{3/2} \tag{15.64}$$

The Sackur–Tetrode equation reproduces many of the classical thermodynamics properties of ideal monatomic gases encountered previously. For example, consider the isothermal expansion of an ideal monatomic gas from an initial volume $V_1$ to a final volume $V_2$. Inspection of the expanded form of the Sackur–Tetrode equation [Equation (15.63)] demonstrates that all of the terms in this expression are unchanged except for the second term involving volume such that

$$\Delta S = S_{final} - S_{initial} = nR \ln\frac{V_2}{V_1} \tag{15.65}$$

This is the same result obtained from classical thermodynamics. What if the entropy change were initiated by isochoric ($\Delta V = 0$) heating? Using the difference in temperature between initial ($T_1$) and final ($T_2$) states, Equation (15.63) yields

$$\Delta S = S_{final} - S_{initial} = \frac{3}{2}nR \ln\frac{T_2}{T_1} = nC_V \ln\frac{T_2}{T_1} \tag{15.66}$$

Recognizing that $C_V = 3/2\,R$ for an ideal monatomic gas, we again arrive at a result first encountered in thermodynamics.

Does the Sackur–Tetrode equation provide any information not available from thermodynamics? Indeed, note the first and fourth terms in Equation (15.63). These terms are simply constants, with the latter varying with the atomic mass. Classical thermodynamics is entirely incapable of explaining the origin of these terms, and only through empirical studies could the presence of these terms be determined. However, their contribution to entropy appears naturally (and elegantly) when using the statistical perspective.

## EXAMPLE PROBLEM 15.5

Determine the standard molar entropy of Ne and Kr under standard thermodynamic conditions.

### Solution

Beginning with the expression for entropy [see Equation (15.63)]:

$$S = \frac{5}{2}R + R\ln\left(\frac{V}{\Lambda^3}\right) - R\ln N_A$$
$$= \frac{5}{2}R + R\ln\left(\frac{V}{\Lambda^3}\right) - 54.75\,R$$
$$= R\ln\left(\frac{V}{\Lambda^3}\right) - 52.25\,R$$

The conventional standard state is defined by $T = 298$ K and $V_m = 24.4$ L ($0.0244$ m$^3$). The thermal wavelength for Ne is

$$\Lambda = \left(\frac{h^2}{2\pi mkT}\right)^{1/2}$$

$$= \left(\frac{(6.626 \times 10^{-34}\,\text{J s})^2}{2\pi\left(\dfrac{0.02018\,\text{kg mol}^{-1}}{N_A}\right)(1.38 \times 10^{-23}\,\text{J K}^{-1})(298\,\text{K})}\right)^{1/2}$$

$$= 2.25 \times 10^{-11}\,\text{m}$$

Using this value for the thermal wavelength, the entropy becomes

$$S = R\ln\left(\frac{0.0244\,\text{m}^3}{(2.25 \times 10^{-11}\,\text{m})^3}\right) - 52.25\,R$$
$$= 69.84\,R - 52.25\,R = 17.59\,R = 146\,\text{J mol}^{-1}\text{K}^{-1}$$

The experimental value is 146.48 J mol$^{-1}$ K$^{-1}$! Rather than determining the entropy of Kr directly, it is easier to determine the difference in entropy relative to Ne:

$$\Delta S = S_{Kr} - S_{Ne} = S = R\ln\left(\frac{V}{\Lambda_{Kr}^3}\right) - R\ln\left(\frac{V}{\Lambda_{Ne}^3}\right)$$
$$= R\ln\left(\frac{\Lambda_{Ne}}{\Lambda_{Kr}}\right)^3$$
$$= 3R\ln\left(\frac{\Lambda_{Ne}}{\Lambda_{Kr}}\right)$$
$$= 3R\ln\left(\frac{m_{Kr}}{m_{Ne}}\right)^{1/2}$$
$$= \frac{3}{2}R\ln\left(\frac{m_{Kr}}{m_{Ne}}\right) = \frac{3}{2}R\ln(4.15)$$
$$= 17.7\,\text{J mol}^{-1}\text{K}^{-1}$$

Using this difference, the standard molar entropy of Kr becomes

$$S_{Kr} = \Delta S + S_{Ne} = 164 \, \text{J mol}^{-1} \text{K}^{-1}$$

The experimental value is 163.89 J mol$^{-1}$ K$^{-1}$, and the calculated value is again in excellent agreement!

When calculating the entropy for an ideal gas consisting of diatomic or polyatomic molecules, it is best to start with the general expression for entropy [Equation (15.62)] and express the canonical partition function in terms of the product of molecular partition functions for each energetic degree of freedom. In addition to the translational entropy term derived earlier for an ideal monatomic gas, contributions from rotational, vibrational, and electronic degrees of freedom will also be included when calculating the entropy.

# 15.5 Residual Entropy

As illustrated in Example Problem 15.5, when the entropy calculated using statistical mechanics is compared to experiment, good agreement is observed for a variety of atomic and molecular systems. However, for many molecular systems, this agreement is less than ideal. A famous example of such a system is carbon monoxide where the calculated entropy at thermodynamic standard temperature and pressure is 197.9 J mol$^{-1}$ K$^{-1}$ and the experimental value is only 193.3 J mol$^{-1}$ K$^{-1}$. In this and other systems, the calculated entropy is always greater than that observed experimentally.

The reason for the systematic discrepancy between calculated and experimental entropies for such systems is **residual entropy,** or entropy associated with molecular orientation in the molecular crystal at low temperature. Using CO as an example, the weak electric dipole moment of the molecule dictates that dipole-dipole interactions do not play a dominant role in determining the orientation of one CO molecule relative to neighboring molecules in a crystal. Therefore, each CO can assume one of two orientations as illustrated in Figure 15.10. The solid corresponding to the possible orientations of CO will have an inherent randomness to it. Because each CO molecule can assume one of two possible orientations, the entropy associated with this orientational disorder is

$$S = k \ln W = k \ln 2^N = Nk \ln 2 = nR \ln 2 \tag{15.67}$$

In Equation (15.67), $W$ is the total number of CO arrangements possible, and it is equal to $2^N$ where $N$ is the number of CO molecules. For a system consisting of 1 mol of CO, the residual entropy is predicted to be $R \ln 2$ or 5.76 J mol$^{-1}$ K$^{-1}$, roughly equal to the difference between the experimental and calculated entropy values.

Finally, note that the concept of residual entropy sheds light on the origin of the third law of thermodynamics. As discussed in Chapter 5, the third law states that the entropy of a pure and crystalline substance is zero at 0 K. By "pure and crystalline," the third law means that the system must be pure with respect to both composition (i.e., a single component) and orientation in the solid at 0 K. For such a pure system, $W = 1$ and correspondingly $S = 0$ by Equation (15.67). Therefore, the definition of zero entropy provided by the third law is a natural consequence of the statistical nature of matter.

**FIGURE 15.10**

The origin of residual entropy for CO. Each CO molecule in the solid can have one of two possible orientations as illustrated by the central CO. Each CO will have two possible directions such that the total number of arrangements possible is $2^N$ where $N$ is the number of CO molecules.
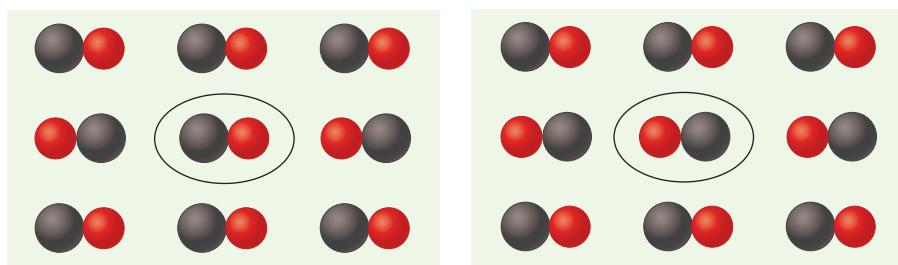
The van der Waals radii of H and F are similar such that steric effects on molecular ordering in the crystal are minimal. Do you expect the residual molar entropies for crystalline 1,2-difluorobenzene and 1,4-difluorobenzene to be the same?

**Solution**

The structures of 1,2-difluorobenzene and 1,4-difluorobenzene are shown here:



1,2-Difluorobenzene          1,4-Difluorobenzene
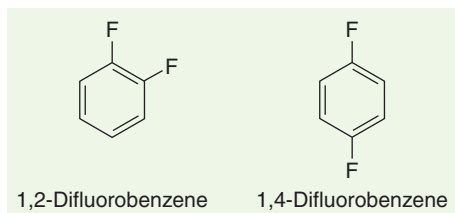
In crystalline 1,2-difluorobenzene, there will be six possible arrangements that can be visualized by rotation of the molecule. Therefore, $W = 6^N$ and

$$S = k \ln W = k \ln 6^{N_A} = N_A k \ln 6 = R \ln 6$$

Similarly, for 1,4-difluorobenzene, there are three possible arrangements such that $W = 3^N$ and $S = R \ln 3$. The residual molar entropies are expected to differ for molecular crystals involving these species.

# 15.6 Other Thermodynamic Functions

The discussion thus far illustrates the convergence of the statistical and thermodynamics perspectives, and the utility of the statistical perspective in illustrating the underlying contributions to macroscopic properties of matter is impressive. The relationship between the canonical partition function and other thermodynamic quantities can be derived using the following familiar thermodynamic relationships for enthalpy $H$, Helmholtz energy $A$, and Gibbs energy $G$:

$$H = U + PV \tag{15.68}$$

$$A = U - TS \tag{15.69}$$

$$G = H - TS \tag{15.70}$$

Using these expressions, relationships between the canonical partition function and the previous thermodynamic quantities can be derived.

## 15.6.1 Helmholtz Energy

Beginning with the thermodynamic definition of $A$ from Equation (15.69), the relationship of this quantity to the canonical partition function becomes

$$A = U - TS$$
$$= U - T\left(\frac{U}{T} + k \ln Q\right)$$
$$A = -kT \ln Q \tag{15.71}$$

The **Helmholtz energy** provides an interesting pathway to obtain a well-known relationship: the ideal gas law. From thermodynamics, pressure is related to the Helmholtz energy as described in Section 6.2 by

$$P = \left(\frac{-\partial A}{\partial V}\right)_T \tag{15.72}$$

Substituting the definition for $A$ provided in Equation (15.71) into the preceding equation,

$$P = \left( \frac{-\partial}{\partial V} (-kT \ln Q) \right)_T$$

$$= kT \left( \frac{\partial}{\partial V} \ln Q \right)_T \qquad (15.73)$$

The canonical partition function for an ideal gas is

$$Q = \frac{q^N}{N!}$$

Substituting this expression for the canonical partition function into the preceding equation,

$$P = kT \left( \frac{\partial}{\partial V} \ln \frac{q^N}{N!} \right)_T$$

$$= kT \left( \frac{\partial}{\partial V} \ln q^N - \frac{\partial}{\partial V} \ln N! \right)_T$$

$$= kT \left( \frac{\partial}{\partial V} \ln q^N \right)_T$$

$$= NkT \left( \frac{\partial}{\partial V} \ln q \right)_T \qquad (15.74)$$

For a monatomic gas,

$$q = \frac{V}{\Lambda^3} \qquad (15.75)$$

such that

$$P = NkT \left( \frac{\partial}{\partial V} \ln \frac{V}{\Lambda^3} \right)_T$$

$$= NkT \left( \frac{\partial}{\partial V} \ln V - \frac{\partial}{\partial V} \ln \Lambda^3 \right)_T$$

$$= NkT \left( \frac{\partial}{\partial V} \ln V \right)_T$$

$$= \frac{NkT}{V} = \frac{nRT}{V} \qquad (15.76)$$

This result is nothing short of remarkable. This relationship was first obtained by empirical measurements, expressed as the laws of Boyle, Charles, Avogadro, and Gay-Lussac. However, in deriving this relationship we have not employed these laws. Instead, starting with a quantum mechanical model for translational motion, we have derived the ideal gas law from a purely theoretical perspective. Once again, statistical mechanics has provided microscopic insight into a macroscopic property. This example illustrates one of the major contributions of statistical mechanics to physical chemistry: the ability to predict relationships that are largely derived from empirical observations and subsequently stated as thermodynamic laws. As a final point, an objection that may be raised is that the preceding derivation was performed for a monatomic gas. However, the skeptical reader is encouraged to demonstrate that this result also holds for poly-atomic systems, a task that is provided as a problem at the end of this chapter.

### 15.6.2 Enthalpy

Using the thermodynamic definition of enthalpy from Equation (15.68), this quantity can be expressed in terms of the canonical partition function as follows:

$$H = U + PV$$

$$= \left( \frac{-\partial}{\partial \beta} \ln Q \right)_V + V \left( \frac{-\partial A}{\partial V} \right)_T$$

$$= \left( \frac{-\partial}{\partial \beta} \ln Q \right)_V + V \left( \frac{-\partial}{\partial V} (-kT \ln Q) \right)_T$$

$$= kT^2 \left( \frac{\partial}{\partial T} \ln Q \right)_V + VkT \left( \frac{\partial}{\partial V} \ln Q \right)_T$$

$$H = T \left[ kT \left( \frac{\partial}{\partial T} \ln Q \right)_V + Vk \left( \frac{\partial}{\partial V} \ln Q \right)_T \right] \tag{15.77}$$

Although Equation (15.77) is correct, it clearly requires a bit of work to implement. Yet, the statistical perspective has shown that one can relate enthalpy to microscopic molecular details through the partition function. When calculating enthalpy, it is sometimes easier to use a combination of thermodynamic and statistical perspectives, as the following example demonstrates.

### EXAMPLE PROBLEM 15.7

What is the enthalpy of 1 mol of an ideal monatomic gas?

#### Solution

One approach to this problem is to start with the expression for the canonical partition function in terms of the molecular partition function for an ideal monatomic gas and evaluate the result. However, a more efficient approach is to begin with the thermodynamic definition of enthalpy:

$$H = U + PV$$

Recall that the translational contribution to $U$ is $3/2\ RT$, and this is the only degree of freedom operative for the monatomic gas. In addition, we can apply the ideal gas law (because we have now demonstrated its validity from a statistical perspective) such that the enthalpy is simply

$$H = U + PV$$
$$= \frac{3}{2} RT + RT$$
$$= \frac{5}{2} RT$$

The interested reader is encouraged to obtain this result through a full evaluation of the statistical expression for enthalpy.

### 15.6.3 Gibbs Energy

Perhaps the most important state function to emerge from thermodynamics is the **Gibbs energy.** Using this quantity, one can determine if a chemical reaction will occur spontaneously. The statistical expression for the Gibbs energy is also derived starting with the thermodynamic definition of this quantity [Equation (15.70)]:

$$G = A + PV$$
$$= -kT \ln Q + VkT \left( \frac{\partial}{\partial V} \ln Q \right)_T$$

$$G = -kT \left[ \ln Q - V \left( \frac{\partial \ln Q}{\partial V} \right)_T \right] \tag{15.78}$$

Previously derived expressions for the Helmholtz energy and pressure were employed in arriving at the result of Equation (15.78). A more intuitive result can be derived by applying the preceding relationship to an ideal gas such that $PV = nRT = NkT$. With this relationship

$$G = A + PV$$
$$= -kT \ln Q + NkT$$

$$= -kT \ln \left( \frac{q^N}{N!} \right) + NkT$$

$$= -kT \ln q^N + kT \ln N! + NkT$$

$$= -NkT \ln q + kT(N \ln N - N) + NkT$$

$$= -NkT \ln q + NkT \ln N$$

$$G = -NkT \ln\left(\frac{q}{N}\right) = -nRT \ln\left(\frac{q}{N}\right) \tag{15.79}$$

This relationship is extremely important because it provides insight into the origin of the Gibbs energy. At constant temperature the $nRT$ prefactor in the expression for $G$ is equivalent for all species; therefore, differences in the Gibbs energy between chemical species must be due to the partition function. Because the Gibbs energy is proportional to $-\ln(q)$, an increase in the value for the partition function will result in a lower Gibbs energy. The partition function quantifies the number of states that are accessible at a given temperature; therefore, the statistical perspective dictates that species with a comparatively greater number of accessible energy states will have a lower Gibbs energy. This relationship will have profound consequences when discussing chemical equilibria in the next section.

## EXAMPLE PROBLEM 15.8

Calculate the molar Gibbs energy of Ar at 298.15 K and $10^5$ Pa, assuming that the gas demonstrates ideal behavior.

### Solution

Argon is a monatomic gas; therefore, $q = q_{trans}$. Using Equation (15.79),

$$G° = -nRT \ln\left(\frac{q}{N}\right) = -nRT \ln\left(\frac{V}{N\Lambda^3}\right)$$

$$= -nRT \ln\left(\frac{kT}{P\Lambda^3}\right)$$

The superscript on $G$ indicates standard thermodynamic conditions. In the last step, the ideal gas law was used to express $V$ in terms of $P$, and the relationships $N = nN_A$ and $R = N_A k$ were employed. The units of pressure must be $Pa = J\,m^{-3}$. Solving for the thermal wavelength term $\Lambda^3$, we get

$$\Lambda^3 = \left(\frac{h^2}{2\pi mkT}\right)^{3/2}$$

$$= \left(\frac{(6.626 \times 10^{-34}\,J\,s)^2}{2\pi\left(\dfrac{0.040\,kg\,mol^{-1}}{6.022 \times 10^{23}\,mol^{-1}}\right)(1.38 \times 10^{-23}\,J\,K^{-1})(298\,K)}\right)^{3/2}$$

$$= 4.09 \times 10^{-33}\,m^3$$

With this result, $G°$ becomes

$$G° = -nRT \ln\left(\frac{kT}{P\Lambda^3}\right) = -(1\,mol)(8.314\,J\,mol^{-1}\,K^{-1})$$

$$\times (298\,K) \ln\left(\frac{(1.38 \times 10^{-23}\,J\,K^{-1})(298\,K)}{(10^5\,Pa)(4.09 \times 10^{-33}\,m^3)}\right)$$

$$= -3.99 \times 10^4\,J = -39.9\,kJ$$

# 15.7 Chemical Equilibrium

Consider the following generic reaction:

$$a\text{J} + b\text{K} \rightleftharpoons c\text{L} + d\text{M} \tag{15.80}$$

The change in Gibbs energy for this reaction is related to the Gibbs energy for the species involved in the reaction as follows:

$$\Delta G° = cG_L° + dG_M° - aG_J° - bG_K° \tag{15.81}$$

In this expression, the superscript indicates standard thermodynamic state. In addition, the equilibrium constant $K$ is given by

$$\Delta G° = -RT \ln K \tag{15.82}$$

In the previous section of this chapter, the Gibbs energy was related to the molecular partition function. Therefore, it should be possible to define $\Delta G°$ and $K$ in terms of partition functions for the various species involved. This development can be initiated by substituting into our expression for $\Delta G°$ from Equation (15.81) the definition for $G$ given in Equation (15.79) and considering molar quantities such that $N = N_A$:

$$\Delta G° = c\left(-RT \ln\left(\frac{q_L°}{N_A}\right)\right) + d\left(-RT \ln\left(\frac{q_M°}{N_A}\right)\right) - a\left(-RT \ln\left(\frac{q_J°}{N_A}\right)\right)$$

$$- b\left(-RT \ln\left(\frac{q_K°}{N_A}\right)\right)$$

$$= -RT \ln\left(\frac{\left(\frac{q_L°}{N_A}\right)^c\left(\frac{q_M°}{N_A}\right)^d}{\left(\frac{q_J°}{N_A}\right)^a\left(\frac{q_K°}{N_A}\right)^b}\right) \tag{15.83}$$

Comparison of the preceding relationship to the thermodynamics definition of $\Delta G°$ demonstrates that the equilibrium constant can be defined as follows:

$$K_P = \frac{\left(\frac{q_L°}{N_A}\right)^c\left(\frac{q_M°}{N_A}\right)^d}{\left(\frac{q_J°}{N_A}\right)^a\left(\frac{q_K°}{N_A}\right)^b} \tag{15.84}$$

Although Equation (15.84) is correct as written, there is one final detail to consider. Specifically, imagine taking the preceding relationship to $T = 0$ K such that only the lowest energy states along all energetic degrees of freedom are populated. The translational and rotational ground states for all species are equivalent; however, the vibrational and electronic ground states are not. Figure 15.11 illustrates the
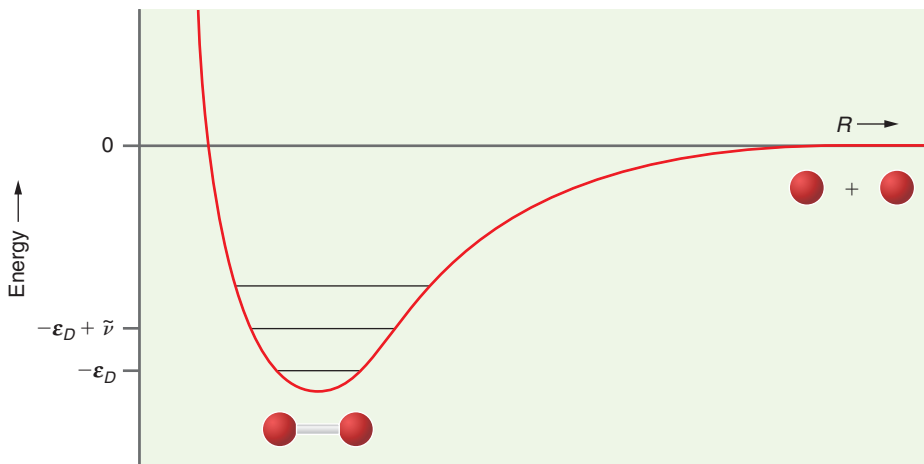


**FIGURE 15.11**
The ground-state potential energy curve for a diatomic molecule. The lowest three vibrational levels are indicated.

(a)



(b)
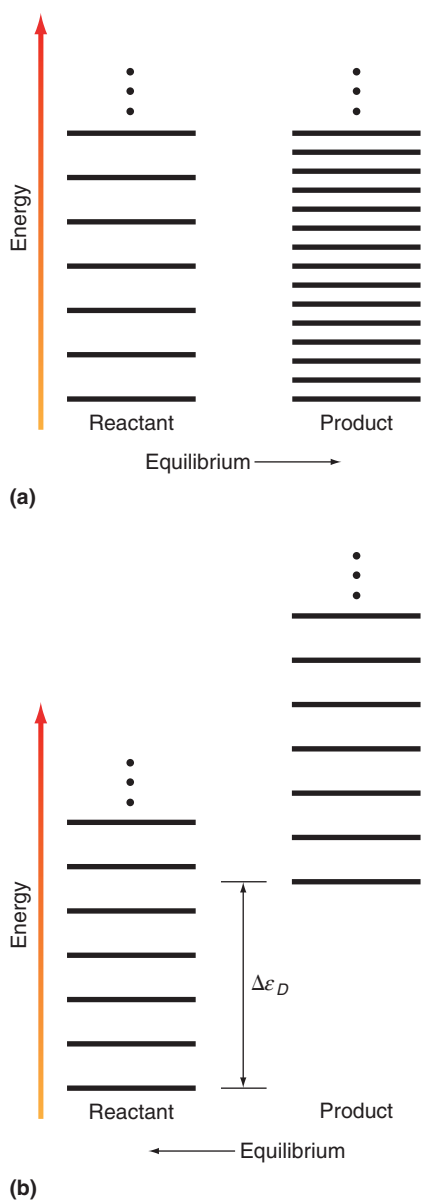
**FIGURE 15.12**
The statistical interpretation of equilibrium. **(a)** Reactant and product species having equal ground-state energies are depicted. However, the energy spacings of the product are less than the reactant such that more product states are available at a given temperature. Therefore, equilibrium will lie with the product. **(b)** Reactant and product species having equal state spacings are depicted. In this case, the product states are higher in energy than those of the reactant such that equilibrium lies with the reactant.

origin of this discrepancy. The figure illustrates the ground *vibronic* (vibrational and electronic) potential for a diatomic molecule. The presence of a bond between the two atoms in the molecule lowers the energy of the molecule relative to the separated atomic fragments. Because the energy of the atomic fragments is defined as zero, the ground vibrational state is lower than zero by an amount equal to the **dissociation energy** of the molecule $\varepsilon_D$. Furthermore, different molecules will have different values for the dissociation energy such that this offset from zero will be molecule specific.

Establishing a common reference state for vibrational and electronic degrees of freedom is accomplished as follows. First, differences in $\varepsilon_D$ can be incorporated into the vibrational part of the problem such that the electronic partition function remains identical to our earlier definition. Turning to the vibrational problem, the general expression for the vibrational partition function can be written incorporating $\varepsilon_D$ as follows:

$$q'_{vib} = \sum_n e^{-\beta\varepsilon_n} = e^{-\beta(-\varepsilon_D)} + e^{-\beta(-\varepsilon_D+\tilde{\nu})} + e^{-\beta(-\varepsilon_D+2\tilde{\nu})} + \cdots$$

$$= e^{\beta\varepsilon_D}(1 + e^{-\beta\tilde{\nu}} + e^{-2\beta\tilde{\nu}} + \cdots)$$

$$= e^{\beta\varepsilon_D}q_{vib} \tag{15.85}$$

In other words, the corrected form for the vibrational partition function is simply the product of our original $q_{vib}$ (without zero point energy) times a factor that corrects for the offset in energy due to dissociation. With this correction factor in place, the ground vibrational states are all set to zero. Therefore, the final expression for the equilibrium constant is

$$K_P = \frac{\left(\dfrac{q_L^\circ}{N_A}\right)^c\left(\dfrac{q_M^\circ}{N_A}\right)^d}{\left(\dfrac{q_J^\circ}{N_A}\right)^a\left(\dfrac{q_K^\circ}{N_A}\right)^b}e^{\beta(c\varepsilon_L+d\varepsilon_M-a\varepsilon_J-b\varepsilon_K)} \quad K_P = \frac{\left(\dfrac{q_L^\circ}{N_A}\right)^c\left(\dfrac{q_M^\circ}{N_A}\right)^d}{\left(\dfrac{q_J^\circ}{N_A}\right)^a\left(\dfrac{q_K^\circ}{N_A}\right)^b}e^{-\beta\Delta\varepsilon} \tag{15.86}$$

The dissociation energies needed to evaluate Equation (15.86) are readily obtained using spectroscopic techniques.

What insight does this expression for the equilibrium constant provide? Equation (15.86) can be viewed as consisting of two parts. The first part is the ratio of partition functions for products and reactants. Because the partition functions quantify the number of energy states available, this ratio dictates that equilibrium will favor those species with the greatest number of available energy states at a given temperature. The second half is the dissociation energy. This term dictates that equilibrium will favor those species with the lowest energy states. This behavior is illustrated in Figure 15.12. The upper part of the figure shows a reactant and product species having equal ground-state energies. The only difference between the two is that the product species has more accessible energy states at a given temperature than the reactant. Another way to envision this relationship is that the partition function describing the product will be greater than that for the reactant at the same temperature such that, at equilibrium, products will be favored ($K > 1$). On the lower part of the figure, the reactant and product energy spacings are equivalent; however, the product states lie higher in energy than those of the reactant. In this case, equilibrium will lie with the reactant ($K < 1$).

**EXAMPLE PROBLEM 15.9**

What is the general form of the equilibrium constant for the dissociation of a diatomic molecule?

**Solution**

The dissociation reaction is

$$X_2(g) \rightleftharpoons 2X(g)$$

We first need to derive the partition functions that describe the reactants and products. The products are monatomic species such that only translations and electronic degrees of freedom are relevant. The partition function is then

$$q_X^\circ = q_T^\circ q_E = \left(\frac{V^\circ}{\Lambda_X^3}\right) g_o$$

The superscripts indicate standard thermodynamic conditions. With these conditions, $V^\circ = RT/P^\circ$ (for 1 mol) such that

$$q_X^\circ = q_T^\circ q_E = \left(\frac{RT}{\Lambda_X^3 P^\circ}\right) g_o$$

For molar quantities

$$\frac{q_X^\circ}{N_A} = \frac{g_o RT}{N_A \Lambda_X^3 P^\circ}$$

The partition function for $X_2$ will be equivalent to that for $X$, with the addition of rotational and vibrational degrees of freedom:

$$\frac{q_{X_2}^\circ}{N_A} = \frac{g_o RT}{N_A \Lambda_{X_2}^3 P^\circ} q_R q_V$$

Using the preceding expressions, the equilibrium constant for the dissociation of a diatomic becomes

$$K_P = \frac{\left(\dfrac{q_X^\circ}{N_A}\right)^2}{\left(\dfrac{q_{X_2}^\circ}{N_A}\right)} e^{-\beta \varepsilon_D} = \frac{\left(\dfrac{g_{o,X} RT}{N_A \Lambda_X^3 P^\circ}\right)^2}{\left(\dfrac{g_{o,X_2} RT}{N_A \Lambda_{X_2}^3 P^\circ}\right) q_R q_V} e^{-\beta \varepsilon_D}$$

$$= \left(\frac{g_{o,X}^2}{g_{o,X_2}}\right)\left(\frac{RT}{N_A P^\circ}\right)\left(\frac{\Lambda_{X_2}^3}{\Lambda_X^6}\right)\frac{1}{q_R q_V} e^{-\beta \varepsilon_D}$$

For a specific example, we can use the preceding expression to predict $K_P$ for the dissociation of $I_2$ at 298 K given the following parameters:

$$g_{o,I} = 4 \quad \text{and} \quad g_{o,I_2} = 1$$

$$\Lambda_I = 8.98 \times 10^{-12} \text{ m} \quad \text{and} \quad \Lambda_{I_2} = 6.35 \times 10^{-12} \text{ m}$$

$$q_R = 2770$$

$$q_V = 1.58$$

$$\varepsilon_D = 12{,}461 \text{ cm}^{-1}$$

Evaluation of the thermal wavelengths, $q_R$, and $q_V$ was performed as described in Chapter 14. Given these values, $K_P$ becomes

$$K_P = \left(\frac{g_{o,I}^2}{g_{o,I_2}}\right)\left(\frac{RT}{N_A P^\circ}\right)\left(\frac{\Lambda_{I_2}^3}{\Lambda_I^6}\right)\frac{1}{q_R q_V} e^{-\beta \varepsilon_D}$$

$$= (16)(4.12 \times 10^{-26} \text{ m}^3)\left(\frac{(6.35 \times 10^{-12} \text{ m})^3}{(8.98 \times 10^{-12} \text{ m})^6}\right)\frac{1}{(2770)(1.58)}$$

$$\exp\left[\frac{-hc(12461 \text{ cm}^{-1})}{kT}\right]$$

$$= (7.81 \times 10^5) \exp\left[\frac{-(6.626 \times 10^{-34} \text{ J s})(3.00 \times 10^{10} \text{ cm s}^{-1})(12461 \text{ cm}^{-1})}{(1.38 \times 10^{-23} \text{ J K}^{-1})(298 \text{ K})}\right]$$

$$= 5.64 \times 10^{-22}$$

Using tabulated values for $\Delta G^\circ$ provided in the back of the text and the relationship $\Delta G^\circ = -RT \ln K$, a value of $K = 5.92 \times 10^{-22}$ is obtained for this reaction.

# Vocabulary

| | | |
|---|---|---|
| average energy | Gibbs energy | Sackur–Tetrode equation |
| Boltzmann's formula | heat capacity | total energy |
| dissociation energy | Helmholtz energy | translational heat capacity |
| Dulong and Petit law | internal energy | two-level system |
| Einstein solid | residual entropy | vibrational heat capacity |
| electronic heat capacity | rotational heat capacity | |

# Conceptual Problems

**Q15.1**   What is the relationship between ensemble energy and the thermodynamic concept of internal energy?

**Q15.2**   Why is the contribution of translational motion to the internal energy $3/2RT$ at 298 K?

**Q15.3**   List the energetic degrees of freedom expected to contribute to the internal energy of a diatomic molecule at 298 K. Given this list, what spectroscopic information do you need to numerically determine the internal energy?

**Q15.4**   List the energetic degrees of freedom for which the contribution to the internal energy determined by statistical mechanics is generally equal to the prediction of the equipartition theorem at 298 K.

**Q15.5**   Write down the contribution to the constant volume heat capacity from translations and rotations for an ideal monatomic, diatomic, and nonlinear polyatomic gas, assuming that the high-temperature limit is appropriate for the rotational degrees of freedom.

**Q15.6**   The constant volume heat capacity for all monatomic gases is 12.48 J mol$^{-1}$ K$^{-1}$. Why?

**Q15.7**   When are rotational degrees of freedom expected to contribute $R$ or $3/2R$ (linear and nonlinear, respectively) to the molar constant volume heat capacity? When will a vibrational degree of freedom contribute $R$ to the molar heat capacity?

**Q15.8**   The molar constant volume heat capacity of $N_2$ is 20.8 J mol$^{-1}$ K$^{-1}$. What is this value in terms of R? Can you make sense of this value?

**Q15.9**   Why do electronic degrees of freedom generally not contribute to the constant volume heat capacity?

**Q15.10**   Describe the model used to determine the heat capacity of atomic crystals.

**Q15.11**   What is the Boltzmann formula, and how can it be used to predict residual entropy?

**Q15.12**   How does the Boltzmann formula provide an understanding of the third law of thermodynamics?

**Q15.13**   For carbon monoxide, the calculated molar entropy was more negative than the experimental value. Why?

**Q15.14**   What thermodynamic property of what particular system does the Sackur–Tetrode equation describe?

**Q15.15**   Which thermodynamic quantity is used to derive the ideal gas law for a monatomic gas? What molecular partition function is employed in this derivation?

**Q15.16**   What is the definition of "zero" energy employed in constructing the statistical mechanical expression for the equilibrium constant? Why was this definition necessary?

**Q15.17**   Why should the equilibrium constant be dependent on the difference in Gibbs energy? How is this relationship described using statistical mechanics?

**Q15.18**   For the equilibrium involving the dissociation of a diatomic, what energetic degrees of freedom were considered for the diatomic, and for the atomic constituents?

**Q15.19**   The statistical mechanical expression for $Kp$ consisted of two general parts. What are these parts, and what energetic degrees of freedom do they refer to?

**Q15.20**   Assume you have an equilibrium expression that involves monatomic species only. What difference in energy between reactants and products would you use in the expression for $K_P$?

# Numerical Problems

Problem numbers in **red** indicate that the solution to the problem is given in the *Student's Solutions Manual*.

**P15.1**   In exploring the variation of internal energy with temperature for a two-level system with the ground and excited state separated by an energy of $hv$, the total energy was found to plateau at a value of $0.5Nhv$. Repeat this analysis for an ensemble consisting of $N$ particles having three energy levels corresponding to 0, $hv$, and $2hv$. What is the limiting value of the total energy for this system?

**P15.2**   For a two-level system where $v = 1.50 \times 10^{13}$ s$^{-1}$, determine the temperature at which the internal energy is equal to 0.25 $Nhv$, or 1/2 the limiting value of 0.50 $Nhv$.

**P15.3** Consider two separate molar ensembles of particles characterized by the following energy-level diagrams:



(a)    (b)
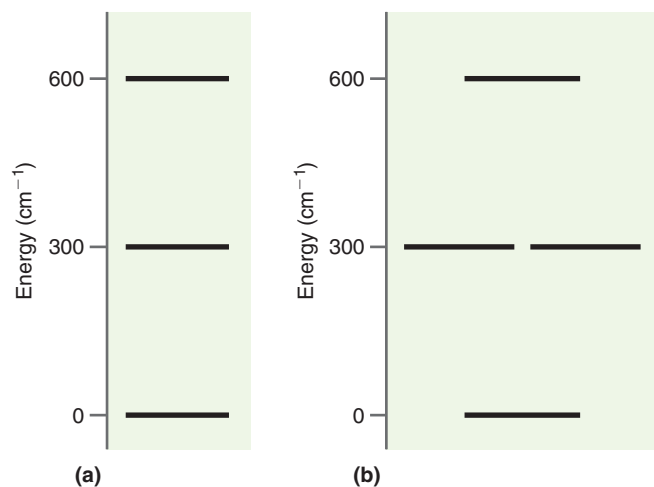
Derive expressions for the internal energy for each ensemble. At 298 K, which ensemble is expected to have the greatest internal energy?

**P15.4** For an ensemble consisting of a mole of particles having two energy levels separated by 1000. cm$^{-1}$, at what temperature will the internal energy equal 3.00 kJ?

**P15.5** What is the contribution to the internal energy from translations for an ideal monatomic gas confined to move on a surface? What is the expected contribution from the equipartition theorem?

**P15.6** For a system of energy levels, $\varepsilon_m = m^2\alpha$, where $\alpha$ is a constant with units of energy and $m = 0, 1, 2, \ldots, \infty$. What is the internal energy and heat capacity of this system in the high-temperature limit?

**P15.7** (Challenging) Building on the concept of equipartition, demonstrate that for any energy term of the form $\alpha x^2$ where $\alpha$ is a constant, the contribution to the internal energy is equal to $kT/2$ by evaluating the following expression:

$$\varepsilon = \frac{\displaystyle\int_{-\infty}^{\infty} \alpha x^2 e^{-\alpha x^2/kT}\, dx}{\displaystyle\int_{-\infty}^{\infty} e^{-\alpha x^2/kT}\, dx}$$

**P15.8** Consider the following table of diatomic molecules and associated rotational constants:

| Molecule | $B$ (cm$^{-1}$) | $\tilde{\nu}$ (cm$^{-1}$) |
|---|---|---|
| H$^{35}$Cl | 10.59 | 2886 |
| $^{12}$C$^{16}$O | 1.93 | 2170 |
| $^{39}$KI | 0.061 | 200. |
| CsI | 0.024 | 120. |

**a.** Calculate the rotational temperature for each molecule.

**b.** Assuming that these species remain gaseous at 100. K, for which species is the equipartition theorem prediction for the rotational contribution to the internal energy appropriate?

**c.** Calculate the vibrational temperature for each molecule.

**d.** If these species were to remain gaseous at 1000. K, for which species is the equipartition theorem prediction for the vibrational contribution to the internal energy appropriate?

**P15.9** The four energy levels for atomic vanadium (V) have the following energies and degeneracies:

| Level ($n$) | Energy (cm$^{-1}$) | Degeneracy |
|---|---|---|
| 0 | 0 | 4 |
| 1 | 137.38 | 6 |
| 2 | 323.46 | 8 |
| 3 | 552.96 | 10 |

What is the contribution to the average molar energy from electronic degrees of freedom for V when $T = 298$ K?

**P15.10** The three lowest energy levels for atomic carbon (C) have the following energies and degeneracies:

| Level ($n$) | Energy (cm$^{-1}$) | Degeneracy |
|---|---|---|
| 0 | 0 | 1 |
| 1 | 16.4 | 3 |
| 2 | 43.5 | 5 |

What is the contribution to the average molar energy from the electronic degrees of freedom for C when $T = 100$. K?

**P15.11** Consider an ensemble of units in which the first excited electronic state at energy $\varepsilon_1$ is $m_1$-fold degenerate, and the energy of the ground state is $m_o$-fold degenerate with energy $\varepsilon_0$.

**a.** Demonstrate that if $\varepsilon_0 = 0$, the expression for the electronic partition function is

$$q_E = m_o \left( 1 + \frac{m_1}{m_o} e^{-\varepsilon_1/kT} \right)$$

**b.** Determine the expression for the internal energy $U$ of an ensemble of $N$ such units. What is the limiting value of $U$ as the temperature approaches zero and infinity?

**P15.12** Calculate the internal energy of He, Ne, and Ar under standard thermodynamic conditions. Do you need to redo the entire calculation for each species?

**P15.13** Determine the molar internal energy of HCl $(B = 10.59$ cm$^{-1}$ and $\tilde{\nu} = 2886$ cm$^{-1})$ under standard thermodynamic conditions.

**P15.14** How would you expect the molar internal energy of $^{79}$BrF to compare to that of $^{79}$Br$^{35}$Cl at 298 K? Check your answer by using the following data:

| | $B$ (cm$^{-1}$) | $\tilde{\nu}$ (cm$^{-1}$) |
|---|---|---|
| $^{79}$BrF | 0.356 | 671 |
| $^{79}$Br$^{35}$Cl | 0.153 | 420. |

**P15.15**  Determine the vibrational contribution to $C_V$ for HCl ($\widetilde{\nu} = 2886$ cm$^{-1}$) over a temperature range from 500. to 5000. K in 500. K intervals and plot your result. At what temperature do you expect to reach the high-temperature limit for the vibrational contribution to $C_V$?

**P15.16**  Determine the vibrational contribution to $C_V$ for HCN where $\widetilde{\nu}_1 = 2041$ cm$^{-1}$, $\widetilde{\nu}_2 = 712$ cm$^{-1}$ (doubly degenerate), and $\widetilde{\nu}_3 = 3369$ cm$^{-1}$ at $T = 298, 500.,$ and 1000. K.

**P15.17**  Carbon dioxide has attracted much recent interest as a greenhouse gas. Determine the vibrational contribution to $C_V$ for $CO_2$ where $\widetilde{\nu}_1 = 2349$ cm$^{-1}$, $\widetilde{\nu}_2 = 667$ cm$^{-1}$ (doubly degenerate), and $\widetilde{\nu}_3 = 1333$ cm$^{-1}$ at $T = 260.$ K.

**P15.18**  The three lowest energy levels for atomic carbon (C) have the following energies and degeneracies:

| Level ($n$) | Energy (cm$^{-1}$) | Degeneracy |
|---|---|---|
| 0 | 0 | 1 |
| 1 | 16.4 | 3 |
| 2 | 43.5 | 5 |

Determine the electronic contribution to $C_V$ for atomic C at 100. K.

**P15.19**  Consider the following energy levels and associated degeneracies for atomic Fe:

| Level ($n$) | Energy (cm$^{-1}$) | Degeneracy |
|---|---|---|
| 0 | 0 | 9 |
| 1 | 415.9 | 7 |
| 2 | 704.0 | 5 |
| 3 | 888.1 | 3 |
| 4 | 978.1 | 1 |

a. Determine the electronic contribution to $C_V$ for atomic Fe at 150. K assuming that only the first two levels contribute to $C_V$.

b. How does your answer to part (a) change if the $n = 2$ level is included in the calculation of $C_V$? Do you need to include the other levels?

**P15.20**  The speed of sound is given by the relationship

$$c_{sound} = \left( \frac{C_p}{C_V} \frac{RT}{M} \right)^{1/2}$$

where $C_p$ is the constant pressure heat capacity (equal to $C_V + R$), $R$ is the ideal gas constant, $T$ is temperature, and $M$ is molar mass.

a. What is the expression for the speed of sound for an ideal monatomic gas?

b. What is the expression for the speed of sound of an ideal diatomic gas?

c. What is the speed of sound in air at 298 K, assuming that air is mostly made up of nitrogen ($B = 2.00$ cm$^{-1}$ and $\widetilde{\nu} = 2359$ cm$^{-1}$)?

**P15.21**  The measured molar heat capacities for crystalline KCl are as follows at the indicated temperatures:

| $T$(K) | $C_v$ (J/mol K) |
|---|---|
| 50. | 21.1 |
| 100. | 39.0 |
| 175 | 46.1 |
| 250. | 48.6 |

a. Explain why the high-temperature limit for $C_V$ is apparently twofold greater than that predicted by the Dulong–Petit law.

b. Determine if the Einstein model is applicable to ionic solids. To do this use the value for $C_V$ at 50.0 K to determine $\Theta_V$, and then use this temperature to determine $C_V$ at 175 K.

**P15.22**  The molar constant volume heat capacity for $I_2(g)$ is 28.6 J mol$^{-1}$ K$^{-1}$. What is the vibrational contribution to the heat capacity? You can assume that the contribution from the electronic degrees of freedom is negligible.

**P15.23**  Inspection of the thermodynamic tables in the back of the text reveals that many molecules have quite similar constant volume heat capacities.

a. The value of $C_{V, M}$ for $Ar(g)$ at standard temperature and pressure is 12.48 J mol$^{-1}$ K$^{-1}$, identical to gaseous $He(g)$. Using statistical mechanics, demonstrate why this equivalence is expected.

b. The value of $C_{V, M}$ for $N_2(g)$ is 20.8 J mol$^{-1}$ K$^{-1}$. Is this value expected given your answer to part (a)? For $N_2$, $\widetilde{\nu} = 2359$ cm$^{-1}$ and $B = 2.00$ cm$^{-1}$.

**P15.24**  Consider rotation about the C-C bond in ethane. A crude model for torsion about this bond is the "free rotor" model where rotation is considered unhindered. In this model the energy levels along the torsional degree of freedom are given by

$$E_j = \frac{\hbar^2 j^2}{2I} \quad \text{for } j = 0, \pm 1, \pm 2, ...$$

In this expression $I$ is the moment of inertia. Using these energies, the summation expression for the corresponding partition function is

$$Q = \frac{1}{\sigma} \sum_{j=-\infty}^{\infty} e^{-E_j/kT}$$

where $\sigma$ is the symmetry number.

a. Assuming that the torsional degree of freedom is in the high-temperature limit, evaluate the previous expression for $Q$.

b. Determine the contribution of the torsional degree of freedom to the molar constant-volume heat capacity.

c. The experimentally determined $C_v$ for the torsional degree of freedom is approximately equal to R at 340. K. Can you rationalize why the experimental value is greater that than predicted using the free rotor model?

**P15.25**  Determine the molar entropy for 1 mol of gaseous Ar at 200., 300., and 500. K and $V = 1000.$ cm$^3$ assuming that Ar can be treated as an ideal gas. How does the result of this calculation change if the gas is Kr instead of Ar?

**P15.26** The standard molar entropy of $O_2$ is 205.14 J mol$^{-1}$ K$^{-1}$ at $P = 1.00$ atm. Using this information, determine the bond length of $O_2$. For this molecule, $\tilde{\nu} = 1580.$ cm$^{-1}$, and the ground electronic state degeneracy is three.

**P15.27** Determine the standard molar entropy of $N_2O$, a linear triatomic molecule at $P = 1.00$ atm. For this molecule, $B = 0.419$ cm$^{-1}$ and $\tilde{\nu}_1 = 1285$ cm$^{-1}$, $\tilde{\nu}_2 = 589$ cm$^{-1}$ (doubly degenerate), and $\tilde{\nu}_3 = 2224$ cm$^{-1}$.

**P15.28** Determine the standard molar entropy of OClO, a nonlinear triatomic molecule where $B_A = 1.06$ cm$^{-1}$, $B_B = 0.31$ cm$^{-1}$, $B_C = 0.29$ cm$^{-1}$, $\tilde{\nu}_1 = 938$ cm$^{-1}$, $\tilde{\nu}_2 = 450.$ cm$^{-1}$, $\tilde{\nu}_3 = 1100.$ cm$^{-1}$, and $P = 1.00$ atm.

**P15.29** Determine the standard molar entropy for the hydroxyl radical, OH, for which $\tilde{\nu} = 3735$ cm$^{-1}$ and $B = 18.9$ cm$^{-1}$, the ground electronic state is doubly degenerate, and $P = 1.00$ atm.

**P15.30** Determine the standard molar entropy of $N_2$ ($\tilde{\nu} = 2359$ cm$^{-1}$, $B = 2.00$ cm$^{-1}$, $g_0 = 1$) and the molar entropy when $P = 1.00$ atm but $T = 2500.$ K.

**P15.31** Determine the standard molar entropy of $H^{35}Cl$ at 298 K where $B = 10.58$ cm$^{-1}$, $\tilde{\nu} = 2886$ cm$^{-1}$, the ground-state electronic level degeneracy is 1, and $P = 1.00$ atm.

**P15.32** Derive the expression for the standard molar entropy of a monatomic gas restricted to two-dimensional translational motion. (*Hint*: You are deriving the two-dimensional version of the Sackur–Tetrode equation.)

**P15.33** The standard molar entropy of CO is 197.7 J mol$^{-1}$ K$^{-1}$. How much of this value is due to rotational and vibrational motion of CO?

**P15.34** The standard molar entropy of the tropospheric pollutant $NO_2$ is 240.1 J mol$^{-1}$ K$^{-1}$. How much of this value is due to rotational motion? The vibrational frequencies of $NO_2$ are 1318, 750., and 1618 cm$^{-1}$, and the ground electronic state is doubly degenerate.

**P15.35** Determine the standard molar entropy of $CO_2$ where $B = 0.39$ cm$^{-1}$ and $P = 1.00$ atm. You can ignore the vibrational and electronic contributions to the standard molar entropy in this calculation.

**P15.36** Consider the molecule NNO, which has a rotational constant nearly identical to $CO_2$. Would you expect the standard molar entropy for NNO to be greater or less than $CO_2$? Can you provide a rough estimation of how much greater?

**P15.37** Entropy, heat, and temperature are related through the following expression:

$$\Delta S = \frac{\Delta q_{reversible}}{T}$$

This expression can be rearranged to provide an expression for $T$ in terms of heat and weight ($W$, the number of microstates for a given configuration of energy):

$$T = \frac{\Delta q_{reversible}}{\Delta S} = \frac{\Delta q_{reversible}}{k\Delta \ln W}$$

**a.** Substitute the expression for $W$ for a two-level system into the equation to define $T$ in terms of heat, Boltzmann's constant, the total number of two-state particles ($N$), and the number of particles in the excited state ($n$).

**b.** Determine the temperature for a two-level system where $N = 20$, the separation between energy levels is 100. cm$^{-1}$, and $q_{rev} = n(100.$ cm$^{-1})$. To perform this calculation, determine $q_{rev}$ and $\ln W$ for $n = 0$ to 20 for integer values of n. The temperature can then be determined by expressing $\Delta q_{rev}$ and $\Delta \ln W$ as

$$\Delta q_{reversible} = q_{rev,n+1} - q_{rev,n}$$
$$\Delta \ln W = \ln W_{n+1} - \ln W_n$$

**c.** Inspect the dependence of $T$ on $n$. Can you explain this dependence?

**P15.38** The molecule NO has a ground electronic level that is doubly degenerate, and a first excited level at 121.1 cm$^{-1}$ that is also twofold degenerate. Determine the contribution of electronic degrees of freedom to the standard molar entropy of NO. Compare your result to $R\ln(4)$. What is the significance of this comparison?

**P15.39** Determine the residual molar entropies for molecular crystals of the following:

**a.** $^{35}Cl^{37}Cl$          **b.** $CFCl_3$

**c.** $CF_2Cl_2$           **d.** $CO_2$

**P15.40** Using the Helmholtz energy, demonstrate that the pressure for an ideal polyatomic gas is identical to that derived for an ideal monatomic gas in the text.

**P15.41** Derive an expression for the standard molar enthalpy of an ideal monatomic gas by evaluation of the statistical mechanical expression for enthalpy as opposed to the thermodynamic argument provided in Example Problem 15.7.

**P15.42** Demonstrate that the molar enthalpy is equal to the molar energy for a collection of one-dimensional harmonic oscillators.

**P15.43** Calculate the standard Helmholtz energy for molar ensembles of Ne and Kr at 298 K.

**P15.44** What is the vibrational contribution to the Helmholtz and Gibbs energies from a molar ensemble of one-dimensional harmonic oscillators?

**P15.45** Determine the molar standard Gibbs energy for $^{35}Cl^{35}Cl$ where $\tilde{\nu} = 560.$ cm$^{-1}$, $B = 0.244$ cm$^{-1}$, and the ground electronic state is nondegenerate.

**P15.46** Determine the rotational and vibrational contributions to the molar standard Gibbs energy for $N_2O$ (NNO), a linear triatomic molecule where $B = 0.419$ cm$^{-1}$ and $\tilde{\nu}_1 = 1285$ cm$^{-1}$, $\tilde{\nu}_2 = 589$ cm$^{-1}$ (doubly degenerate), and $\tilde{\nu}_3 = 2224$ cm$^{-1}$.

**P15.47** Determine the equilibrium constant for the dissociation of sodium at 298 K: $Na_2(g) \rightleftharpoons 2\,Na(g)$. For $Na_2$, $B = 0.155$ cm$^{-1}$, $\tilde{\nu} = 159$ cm$^{-1}$, the dissociation energy is 70.4 kJ/mol, and the ground-state electronic degeneracy for Na is 2.

**P15.48** The isotope exchange reaction for $Cl_2$ is as follows: $^{35}Cl^{35}Cl + {}^{37}Cl^{37}Cl \rightleftharpoons 2\,{}^{37}Cl^{35}Cl$. The equilibrium constant for this reaction is ~4. Furthermore, the equilibrium

constant for similar isotope-exchange reactions is also close to this value. Demonstrate why this would be so.

**P15.49** Consider the following isotope exchange reaction:

$$DCl(g) + HBr(g) \rightleftharpoons DBr(g) + HCl(g)$$

The amount of each species at equilibrium can be measured using proton and deuterium NMR (see *Journal of Chemical Education* 73 [1996]:99). Using the following spectroscopic information, determine $K_p$ for this reaction at 298 K. For this reaction, $\Delta\varepsilon = 41$ cm$^{-1}$ equal to the difference in zero-point energies between products versus reactants, and the ground-state electronic degeneracy is zero for all species.

| | $M$ (g mol$^{-1}$) | $B$ (cm$^{-1}$) | $\widetilde{\nu}$ (cm$^{-1}$) |
|---|---|---|---|
| H$^{35}$Cl | 35.98 | 10.59 | 2991 |
| D$^{35}$Cl | 36.98 | 5.447 | 2145 |
| H$^{81}$Br | 81.92 | 8.465 | 2649 |
| D$^{81}$Br | 82.93 | 4.246 | 1885 |

**P15.50** The equilibrium between hydrogen cyanide (HCN) and its isomer hydrogen isocyanide (HNC) is important in interstellar chemistry:

$$HCN(g) \rightleftharpoons HNC(g)$$

A long-standing "puzzle" regarding this reaction is that in space (T = 2.75 K) surprisingly large amounts of HNC are observed. For example, HNC/HCN ratios approaching 20% have been observed in comets (*Advances in Space Research* 31 (2003):2577). Using the spectroscopic information provided in the following table and knowledge that the potential-energy surface minimum of HNC lies roughly 5200 cm$^{-1}$ higher in energy relative to HCN, calculate the theoretical value for $K_p$ for this reaction in interstellar space.

| | $M$ (g mol$^{-1}$) | $B$ (cm$^{-1}$) | $\widetilde{\nu}_1$ (cm$^{-1}$) | $\widetilde{\nu}_2$ (cm$^{-1}$) | $\widetilde{\nu}_3$ (cm$^{-1}$) |
|---|---|---|---|---|---|
| HCN | 27.03 | 1.477 | 2041 | 712 | 3669 |
| HNC | 27.03 | 1.512 | 2024 | 464 | 3653 |

**P15.51** In "Direct Measurement of the Size of the Helium Dimer" by F. Luo, C. F. Geise, and W. R. Gentry (*J. Chemical Physics* 104 [1996]: 1151), evidence for the helium dimer is presented. As one can imagine, the chemical bond in the dimer is extremely weak, with an estimated value of only 8.3 mJ mol$^{-1}$.

**a.** An estimate for the bond length of 65 Å is presented in the paper. Using this information, determine the rotational constant for He$_2$. Using this value for the rotational constant, determine the location of the first rotational state. If correct, you will determine that the first excited rotational level is well beyond the dissociation energy of He$_2$.

**b.** Consider the following equilibrium between He$_2$ and its atomic constituents: He$_2(g) \rightleftharpoons 2$He$(g)$. If there are no rotational or vibrational states to consider, the equilibrium is determined exclusively by the translational degrees of freedom and the dissociation energy of He$_2$. Using the dissociation energy provided earlier and $V = 1000.$ cm$^3$, determine $K_P$ assuming that $T = 10.$ K. The experiments were actually performed at 1 mK; why was such a low temperature employed?

# Computational Problems

More detailed instructions on carrying out these calculations using Spartan Physical Chemistry are found on the book website at *www.masteringchemistry.com*.

**C15.1** Perform a Hartree–Fock 6-31G* calculation on acetonitrile and determine the contribution of translations to the molar enthalpy and entropy under standard thermodynamic conditions. How does the calculation compare to the values determined by hand computation using the expressions for enthalpy and entropy presented in this chapter.

**C15.2** Perform a Hartree–Fock 3-21G calculation on cyclohexane and determine the frequency of the lowest-frequency mode consistent with the reaction coordinate corresponding to the "boat-to-boat" conformational change. Using the calculated frequency of this vibrational degree of freedom, determine how much this mode contributes to the vibrational heat capacity at 298 K.

**C15.3** In the treatment of $C_V$ presented in this chapter the contribution of electronic degrees of freedom was ignored. To further explore this issue, perform a Hartree–Fock 6-31G* calculation on anthracene and determine the HOMO–LUMO energy gap, which provides a measure of the energy difference between the ground and first excited electronic states.

Using this energy gap, determine the temperature where 2% of the anthracene molecules populate the excited electronic state, and using this temperature determine the contribution of electronic degrees of freedom to $C_V$. Reflecting on this result, why can we generally ignore electronic degrees of freedom when calculating standard thermodynamic properties?

**C15.4** In 2001 astronomers discovered the presence of vinyl alcohol (C$_2$H$_3$OH) in an interstellar cloud near the center of the Milky Way galaxy. This complex is a critical piece of the puzzle regarding the origin of complex organic molecules in space. The temperature of an interstellar cloud is ~20 K. Determine the vibrational frequencies of this compound using a Hartree–Fock 3-21G basis set, and determine if any of the vibrational modes of vinyl alcohol contribute more that $0.1R$ to $C_V$ at this temperature.

**C15.5** Nitrous acid (HONO) is of interest in atmospheric chemistry as a reservoir compound contributing to the NO$_x$ cycle. Perform a Hartree–Fock 6-31G* calculation on the cis conformer of this compound and determine the standard molar entropy of this compound. What are the contributions of vibrational and rotational degrees of freedom to the entropy? Using the techniques presented in this chapter and

treating HONO as an ideal gas, determine the translational contribution to the standard molar entropy and compare to the computational result.

**C15.6** For dibromine oxide (BrOBr), perform a Hartree–Fock 6-31G* calculation and determine the translational, rotational, and vibrational contribution to the standard molar entropy.

---

# Web-Based Simulations, Animations, and Problems

**W15.1** In this simulation, the temperature dependence of $C_V$ for vibrational degrees of freedom is investigated for diatomic and polyatomic molecules. Diatomic molecules are studied, as are polyatomics with and without mode degeneracy. Comparisons of exact values to those expected for the high-temperature limit are performed.

---

# For Further Reading

Chandler, D. *Introduction to Modern Statistical Mechanics*. New York, Oxford: 1987.

Hill, T. *Statistical Mechanics. Principles and Selected Applications*. New York, Dover: 1956.

Linstrom, P. J., and Mallard, W. G., Eds., *NIST Chemistry Webbook: NIST Standard Reference Database Number 69*. National Institute of Standards and Technology, Gaithersburg, MD, retrieved from http://webbook.nist.gov/chemistry. (This site contains a searchable database of thermodynamic and spectroscopic properties of numerous atomic and molecular species.)

McQuarrie, D. *Statistical Mechanics*. New York, Harper & Row: 1973.

Nash, L. K. "On the Boltzmann Distribution Law." *J. Chemical Education* 59 (1982): 824.

Nash, L. K. *Elements of Statistical Thermodynamics*. San Francisco, Addison-Wesley: 1972.

Noggle, J. H. *Physical Chemistry*. New York, HarperCollins: 1996.

Townes, C. H., and A. L. Schallow. *Microwave Spectroscopy*. New York, Dover: 1975. (This book contains an excellent appendix of spectroscopic constants.)

Widom, B. *Statistical Mechanics*. Cambridge, Cambridge University Press, 2002.

*This page intentionally left blank*

# Kinetic Theory of Gases

**G**as particle motion is of importance in many aspects of physical chemistry, from transport phenomena to chemical kinetics. In this chapter, the translational motion of gas particles is described. Gas particle motion is characterized by a distribution of velocities and speeds. These distributions, including the Maxwell speed distribution, are derived. Benchmark values for these distributions that provide insight into how the distributions change with temperature and particle mass are presented. Finally, molecular collisions are discussed, including the frequency of collisional events and the distance particles travel between collisions. The concepts presented in this chapter find wide application in the remainder of this text since they provide the first step in understanding gas-phase molecular dynamics.

## 16.1 Kinetic Theory of Gas Motion and Pressure

In this chapter, we expand on the microscopic viewpoint of matter by considering the translational motion of gas particles. **Gas kinetic theory** provides the starting point for this development and represents a central concept of physical chemistry. In this theory, gases are envisioned as a collection of atoms or molecules that we will refer to as *particles*. Gas kinetic theory is applicable when the particle density of the gas is such that the distance between particles is very large in comparison to their size. To illustrate this point, consider a mole of Ar at a temperature of 298 K and 1 atm pressure. Using the ideal gas law, the gas occupies a volume of 24.4 L or 0.0244 m³. Dividing this volume by Avogadro's number provides an average volume per Ar atom of $4.05 \times 10^{-26}$ m³, or 40.5 nm³. The diameter of Ar is ~0.29 nm corresponding to a particle volume of 0.013 nm³. Comparison of the particle volume to the average volume of an individual Ar atom demonstrates that on average only 0.03% of the available volume is occupied by the particle. Even for particles with diameters substantially greater than Ar, the difference between the average volume per particle and the volume of the particle itself will be such that the distance between particles in the gas phase is substantial.

Given the large distance between particles in a gas, each particle is envisioned as traveling through space as a separate, unperturbed entity until a collision occurs with another particle or with the walls of the container confining the gas. In gas kinetic theory, particle motion is described using Newton's laws of motion. Although in previous chapters we have seen that classical descriptions fail to capture many of the microscopic properties of atoms and molecules, recall from Chapter 14 that the energy spacings between translational energy states are very small relative to $kT$ such that a classical description of translational motion is appropriate.

One hallmark of kinetic theory is its ability to describe the pressure of an ideal gas as shown in Chapter 1. As opposed to the thermodynamic derivation of the ideal gas law, which relied on empirical relations between gas variables, the kinetic theory description of pressure relied on classical mechanics and a microscopic description of the system. The pressure exerted by a gas on the container confining the gas arose from collisions of gas particles with the container walls. By employing a classical description of a single molecular collision with the container wall and then scaling this result up to macroscopic proportions, one of the central results in the chemistry of gaseous systems was derived.

A second result derived from gas kinetic theory is the relationship between **root-mean-squared speed** and temperature. If the particle motion is random, the average velocities along all three Cartesian dimensions are equivalent. The average velocity along any dimension will be zero because there will be just as many particles traveling in both the positive and negative directions. In contrast, the root-mean-squared speed is given by the following using Equation (1.10):

$$\langle v^2 \rangle^{1/2} = \langle v_x^2 + v_y^2 + v_z^2 \rangle^{1/2}$$
$$= \langle 3v_x^2 \rangle^{1/2}$$
$$= \left( \frac{3kT}{m} \right)^{1/2} \tag{16.1}$$

Kinetic theory thus predicts that the root-mean-squared speed of the gas particles should increase as the square root of temperature and decrease as the square root of the particle mass.

The success of this approach is tempered by uncertainty regarding the assumptions made during the course of the derivation. For example, it has been assumed that the individual particle velocities can be characterized by some average value. Can we determine what this average value is given the distribution of molecular velocities that exist? Just what does the distribution of particle velocities or speed look like? In addition, the molecules collide with each other as well as the walls of the container. How frequent are such collisions? The frequency of molecular collisions will be important in subsequent chapters describing transport phenomena and the rates of chemical reactions. Therefore, a more critical look at atomic and molecular speed distributions and collisional dynamics is warranted.

## 16.2 Velocity Distribution in One Dimension

From the previous discussion of statistical thermodynamics, it is clear that a distribution of translational energies and, therefore, velocities will exist for a collection of gaseous particles. What does this distribution of velocities look like?

The variation in particle velocities is described by the **velocity distribution function.** In Chapter 12 the concept of a distribution function was presented. The velocity distribution function describes the probability of a gas particle having a velocity within a given range. In Section 14.4 we found that the translational energy-level spacings are sufficiently small that velocity can be treated as a continuous variable.

Therefore, the velocity distribution function describes the probability of a particle having a velocity in the range $v_x + dv_x$, $v_y + dv_y$, and $v_z + dv_z$.

To begin the derivation of the velocity distribution function, let $\Omega(v_x, v_y, v_z)$ represent the function that describes the distribution of velocity for an ensemble of gaseous particles. We assume that the distribution function can be decomposed into a product of distribution functions for each Cartesian dimension and the distribution of velocities in one dimension is independent of the distribution in the other two dimensions. With this assumption, $\Omega(v_x, v_y, v_z)$ is expressed as follows:

$$\Omega(v_x, v_y, v_z) = f(v_x)f(v_y)f(v_z) \tag{16.2}$$

In Equation (16.2), $f(v_x)$ is the velocity distribution for velocity in the $x$ direction, and so forth. We assume that the gas is confined to an isotropic space such that the direction in which the particle moves does not affect the properties of the gas. In this case, the distribution function $\Omega(v_x, v_y, v_z)$ only depends on the magnitude of the velocity, or speed ($v$). The natural log of Equation (16.2) yields

$$\ln \Omega(v) = \ln f(v_x) + \ln f(v_y) + \ln f(v_z)$$

To determine the velocity distribution along a single direction, the partial derivative of $\ln \Omega(v)$ is taken with respect to $v_x$ while keeping the velocity along the other two directions constant:

$$\left(\frac{\partial \ln \Omega(v)}{\partial v_x}\right)_{v_y, v_z} = \frac{d \ln f(v_x)}{dv_x} \tag{16.3}$$

Equation (16.3) can be rewritten using the chain rule for differentiation (see Appendix B, Math Supplement) allowing for the derivative of $\ln \Omega(v)$ with respect to $v_x$ to be written as

$$\left(\frac{d \ln \Omega(v)}{dv}\right)\left(\frac{\partial v}{\partial v_x}\right)_{v_y, v_z} = \frac{d \ln f(v_x)}{dv_x} \tag{16.4}$$

The second factor on the left-hand side of Equation (16.4) can be readily evaluated:

$$\left(\frac{\partial v}{\partial v_x}\right)_{v_y, v_z} = \left(\frac{\partial}{\partial v_x}(v_x^2 + v_y^2 + v_z^2)^{1/2}\right)_{v_y, v_z}$$

$$= \frac{1}{2}(2v_x)(v_x^2 + v_y^2 + v_z^2)^{-1/2}$$

$$= \frac{v_x}{v} \tag{16.5}$$

Substituting this result into Equation (16.4) and rearranging yields

$$\left(\frac{d \ln \Omega(v)}{dv}\right)\left(\frac{\partial v}{\partial v_x}\right)_{v_y, v_z} = \frac{d \ln f(v_x)}{dv_x}$$

$$\left(\frac{d \ln \Omega(v)}{dv}\right)\left(\frac{v_x}{v}\right) = \frac{d \ln f(v_x)}{dv_x}$$

$$\frac{d \ln \Omega(v)}{v \, dv} = \frac{d \ln f(v_x)}{v_x \, dv_x} \tag{16.6}$$

It is important to recall at this point that the velocity distributions along each direction are equivalent. Therefore, the preceding derivation could just as easily have been performed considering $v_y$ or $v_z$, resulting in the following expressions analogous to Equation (16.6):

$$\frac{d \ln \Omega(v)}{v \, dv} = \frac{d \ln f(v_y)}{v_y \, dv_y} \tag{16.7}$$

$$\frac{d \ln \Omega(v)}{v \, dv} = \frac{d \ln f(v_z)}{v_z \, dv_z} \tag{16.8}$$

Comparison of Equations (16.6), (16.7), and (16.8) suggests that the following equality exists:

$$\frac{d \ln f(v_x)}{v_x dv_x} = \frac{d \ln f(v_y)}{v_y dv_y} = \frac{d \ln f(v_z)}{v_z dv_z} \tag{16.9}$$

In order for Equation (16.9) to be correct, each of the terms in Equations (16.6), (16.7), and (16.8) must be equal to a constant, $\gamma$, such that

$$\frac{d \ln f(v_j)}{v_j dv_j} = \frac{df(v_j)}{v_j f(v_j) dv_j} = -\gamma \quad \text{for } j = x, y, z \tag{16.10}$$

In this equation, the negative of $\gamma$ has been employed, recognizing that $\gamma$ must be a positive quantity to ensure that $f(v_j)$ does not diverge as $v_j$ approaches infinity. Integration of Equation (16.10) results in the following expression for the velocity distribution along one direction:

$$\int \frac{df(v_j)}{f(v_j)} = -\int \gamma v_j \, dv_j$$

$$\ln f(v_j) = -\frac{1}{2} \gamma v_j^2$$

$$f(v_j) = Ae^{-\gamma v_j^2/2} \tag{16.11}$$

The last step remaining in the derivation is to determine the normalization constant $A$ and $\gamma$. To determine $A$, we refer back to Chapter 12 and the discussion of normalized distribution functions and require that the velocity distribution be normalized. Because a particle can be traveling in either the $+j$ or $-j$ direction, the range of the velocity distribution is $-\infty \le v_j \le \infty$. Applying the normalization condition and integrating over this range,

$$\int_{-\infty}^{\infty} f(v_j) \, dv_j = 1 = \int_{-\infty}^{\infty} Ae^{-\gamma v_j^2/2} dv_j$$

$$1 = 2A \int_{0}^{\infty} e^{-\gamma v_j^2/2} dv_j$$

$$1 = A\sqrt{\frac{2\pi}{\gamma}}$$

$$\sqrt{\frac{\gamma}{2\pi}} = A \tag{16.12}$$

In evaluating this integral, we use the property of even integrands, which says that the integral from $-\infty$ to $\infty$ is equal to twice the integral from 0 to $\infty$. With the normalization factor, the velocity distribution in one dimension becomes

$$f(v_j) = \left(\frac{\gamma}{2\pi}\right)^{1/2} e^{-\gamma v_j^2/2} \tag{16.13}$$

All that remains is to evaluate $\gamma$. Earlier we encountered the following definition for $\langle v_x^2 \rangle$:

$$\langle v_x^2 \rangle = \frac{kT}{m} \tag{16.14}$$

Recall that angle brackets around $v_x^2$ indicate that this quantity is an average over the ensemble of particles. Furthermore, this quantity is equal to the second moment of the velocity distribution; therefore, $\gamma$ can be determined as follows:

$$\langle v_x^2 \rangle = \frac{kT}{m} = \int_{-\infty}^{\infty} v_x^2 f(v_x) \, dv_x$$

$$= \int_{-\infty}^{\infty} v_x^2 \sqrt{\frac{\gamma}{2\pi}} e^{-\gamma v_x^2/2} dv_x$$

$$= \sqrt{\frac{\gamma}{2\pi}} \int_{-\infty}^{\infty} v_x^2 e^{-\gamma v_x^2/2} dv_x$$

$$= \sqrt{\frac{\gamma}{2\pi}} \left( \frac{1}{\gamma} \sqrt{\frac{2\pi}{\gamma}} \right)$$

$$= \frac{1}{\gamma}$$

$$\frac{m}{kT} = \gamma \tag{16.15}$$

The integration was performed using the integral tables provided in the Math Supplement, Appendix B. With the definition of $\gamma$, the **Maxwell–Boltzmann velocity distribution** in one dimension becomes

$$f(v_j) = \left( \frac{m}{2\pi kT} \right)^{1/2} e^{(-mv_j^2/2kT)} = \left( \frac{M}{2\pi RT} \right)^{1/2} e^{(-Mv_j^2/2RT)} \tag{16.16}$$

In Equation (16.16), $m$ is the particle mass in units of kilograms, and $M$ is the molar mass in units of kg mol$^{-1}$, obtained from the expression involving $m$ using the relationship $R = N_A k$. The velocity distribution is equal to the product of a preexponential factor that is independent of velocity, and an exponential factor that is velocity dependent, and this latter term is very reminiscent of the Boltzmann distribution. The one-dimensional velocity distribution in the $x$ direction for $CO_2$ at 298 K is presented in Figure 16.1. Notice that the distribution maximum is at 0 m s$^{-1}$.



**FIGURE 16.1**
One-dimensional velocity distribution for $CO_2$ at 298 K.

---

**EXAMPLE PROBLEM 16.1**

Compare $\langle v_x \rangle$ and $\langle v_x^2 \rangle$ for an ensemble of gaseous particles.

**Solution**

The average velocity is simply the first moment of the velocity distribution function:

$$\langle v_x \rangle = \int_{-\infty}^{\infty} v_x f(v_x) \, dv_x$$

$$= \int_{-\infty}^{\infty} v_x \left( \frac{m}{2\pi kT} \right)^{1/2} e^{-mv_x^2/2kT} \, dv_x$$

$$= \left( \frac{m}{2\pi kT} \right)^{1/2} \int_{-\infty}^{\infty} v_x e^{-mv_x^2/2kT} \, dv_x$$

$$= 0$$

The integral involves the product of odd ($v_x$) and even (exponential) factors so that the integral over the domain of $v_x$ equals zero (a further description of even and odd functions is provided in the Math Supplement). The fact that the average value of $v_x = 0$ reflects the vectorial character of velocity with particles equally likely to be moving in the $+x$ or $-x$ direction.

The quantity $\langle v_x^2 \rangle$ was determined earlier:

$$\langle v_x^2 \rangle = \int_{-\infty}^{\infty} v_x^2 f(v_x) \, dv_x = \frac{kT}{m}$$

Notice that the average value for the second moment is greater than zero, reflecting the fact that the square of the velocity must be a positive quantity.



**FIGURE 16.2**
One-dimensional velocity distributions for Ar at 298 K (red line) and 1000 K (purple line).

Figure 16.2 presents the one-dimensional velocity distribution functions for Ar at two different temperatures. Notice how the width of the distribution increases with temperature consistent with the increased probability of populating higher energy translational states with correspondingly greater velocities.
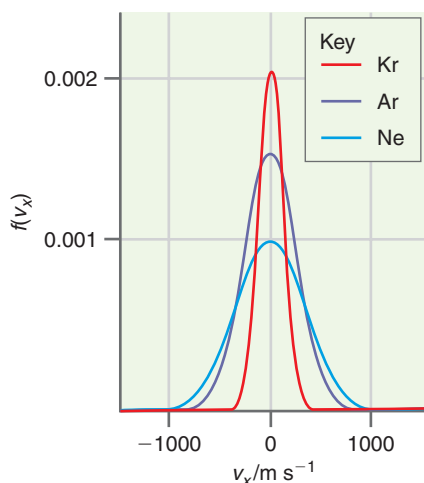
**FIGURE 16.3**

Velocity distributions for Kr (red line, molar mass = 83.8 g mol$^{-1}$), Ar (purple line, molar mass = 39.9 g mol$^{-1}$), and Ne (blue line, molar mass = 20.2 g mol$^{-1}$) at 298 K.

Figure 16.3 presents the distribution for Kr, Ar, and Ne at 298 K. The velocity distribution is narrowest for Kr and broadest for Ne reflecting the mass dependence of the distribution.

## 16.3 The Maxwell Distribution of Molecular Speeds

With one-dimensional velocity distributions in hand, the three-dimensional distribution of molecular speeds can be determined. First, it is important to recognize that speed is not a vector. The reason we concern ourselves with speed as opposed to velocity is that many physical properties of gases are dependent only on the speed of the gas particles and not on the direction of motion. Therefore, only the magnitude of the velocity, or speed, is generally of interest. As shown earlier, the **particle speed** $\nu$ is related to the one-dimensional velocity Cartesian components by the following:

$$\nu = (v_x^2 + v_y^2 + v_z^2)^{1/2} \tag{16.17}$$

We are interested in determining the particle speed distribution $F(\nu)$, but how can this distribution be derived using the velocity distributions derived in the previous section? We can connect these concepts using the geometric interpretation of velocity presented in Figure 16.4. The figure depicts **velocity space,** which can be understood in analogy to Cartesian space with linear distance $(x, y, z)$ replaced by the Cartesian components of velocity $(v_x, v_y, v_z)$. The figure demonstrates that the molecular velocity **v** is described by a vector with coordinates $v_x$, $v_y$, and $v_z$ in velocity space with length equal to the speed [Equation (16.17)].

Particle speed distribution $F(\nu)$ is defined in terms of one-dimensional velocity distributions along each direction [Equation (16.15)] as follows:

$$F(\nu)\, d\nu = f(v_x)f(v_y)f(v_z)\, dv_x\, dv_y\, dv_z$$

$$= \left[\left(\frac{m}{2\pi kT}\right)^{1/2} e^{-mv_x^2/2kT}\right]\left[\left(\frac{m}{2\pi kT}\right)^{1/2} e^{-mv_y^2/2kT}\right]$$

$$\times \left[\left(\frac{m}{2\pi kT}\right)^{1/2} e^{-mv_z^2/2kT}\right] dv_x\, dv_y\, dv_z$$

$$= \left(\frac{m}{2\pi kT}\right)^{3/2} e^{[-m(v_x^2 + v_y^2 + v_z^2)]/2kT} dv_x\, dv_y\, dv_z \tag{16.18}$$

Notice that in Equation (16.18), the speed distribution of interest is defined with respect to the Cartesian components of velocity; therefore, the factors involving velocity need to be expressed in terms of speed to obtain $F(\nu)\, d\nu$. This transformation is accomplished as follows. First, the factor $dv_x\, dv_y\, dv_z$ is an infinitesimal volume element in velocity space (Figure 16.4). Similar to the transformation from Cartesian coordinates to spherical coordinates (see the Math Supplement), the velocity volume element can be written as $4\pi\nu^2 d\nu$ after integration over angular dimensions leaving only a $\nu$ dependence. In addition, $v_x^2 + v_y^2 + v_z^2$ in the exponent of Equation (16.18) can be written as $\nu^2$ [Equation (16.17)] such that



**FIGURE 16.4**

Illustration of velocity space. The Cartesian components of the particle velocity **v** are given by $v_x$, $v_y$, and $v_z$. The spherical shell represents a differential volume element of velocity space having volume $4\pi\nu^2 d\nu$.

$$F(\nu)\, d\nu = 4\pi\left(\frac{m}{2\pi kT}\right)^{3/2} \nu^2 e^{-m\nu^2/2kT}\, d\nu \tag{16.19}$$

Equation (16.19) is written in terms of the mass of an individual gas particle. Because the molar mass $M$ is equal to $N_A \times m$, where $N_A$ is Avogadro's number and

$m$ is the particle mass, and $R = N_A \times k$, Equation (16.19) can be written in terms of $M$ as follows:

$$F(\nu)\, d\nu = 4\pi \left(\frac{M}{2\pi RT}\right)^{3/2} \nu^2 e^{-M\nu^2/2RT}\, d\nu \qquad \textbf{(16.20)}$$

The **Maxwell speed distribution** is given by Equation (16.19) or (16.20) and represents the probability distribution of a molecule having a speed between $\nu$ and $\nu + d\nu$. Comparison of this distribution to the one-dimensional velocity distribution of Equation (16.15) reveals many similarities, with the main difference being the $\nu^2$ dependence that now appears in the preexponential factor in Equation (16.19) or (16.20). A second difference is the range of the distribution. Unlike velocity where negative values are possible since the particle is always free to move in the negative direction with respect to a given coordinate, particle speeds must be greater than or equal to zero so that the range of the distribution is from zero to infinity.

Figure 16.5 presents the Maxwell speed distribution for Ar at 298 and 1000 K and illustrates the dependence of the speed distribution on temperature. Notice that unlike the velocity distribution of Equation (16.15), the speed distribution is not symmetric. This is because the initial increase in probability is due to the $\nu^2$ factor in Equation (16.19) or (16.20), but at higher speeds the probability decays exponentially. Also, as temperature increases two trends become evident. First, the maximum of the distribution shifts to higher speed as temperature increases. This is expected because an increase in temperature corresponds to an increase in kinetic energy and subsequently an increase in particle speed. Second, the entire distribution does not simply shift to higher velocity. Instead, the curvature of the distribution changes, with this behavior quite pronounced on the high-speed side of the distribution since an increase in $kT$ will increase the probability of occupying higher energy translational states. Finally, note that the area under both curves is identical and equal to one expected for a normalized distribution.

Figure 16.6 presents a comparison of the particle speed distributions for Ne, Ar, and Kr at 298 K. The speed distribution peaks at lower speeds for heavier particles. This behavior can be understood since the average kinetic energy is $3/2\, kT$, a quantity that is only dependent on temperature. Because kinetic energy is also equal to $1/2\, m\nu^2$, an increase in mass must be offset by a reduction in the root-mean-squared speed. This expectation is reflected by the distributions presented in Figure 16.6.

One of the first detailed experimental verifications of the Maxwell distribution law was provided in 1955 by Miller and Kusch [*Phys. Rev.* 99 (1955): 1314]. A schematic drawing of the apparatus employed in this study is presented in Figure 16.7. An oven was used to create a gas of known temperature, and a hole was placed in the side of the oven through which the gas could emerge. The stream of gas molecules escaping the oven was then directed through spatial apertures to create a beam of particles, which was then directed toward a velocity selector. By changing the rotational speed of the velocity selector, the required gas speed necessary to pass through the cylinder is varied. The number of gas particles passing through the cylinder as a function of rotational speed is then measured to determine the distribution of gas speeds.
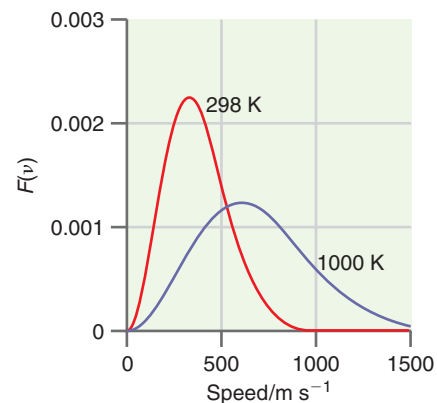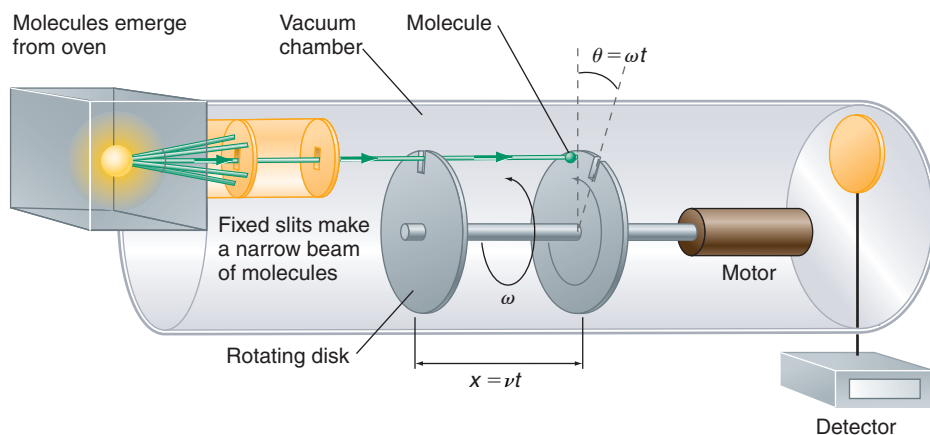


**FIGURE 16.5**
Speed distributions for Ar at 298 and 1000 K.
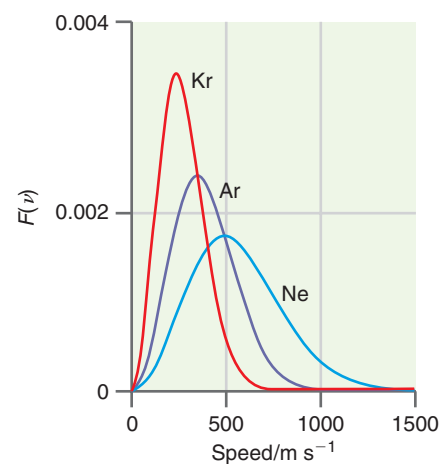


**FIGURE 16.6**
Speed distributions for Ne (blue line, molar mass $= 20.2$ g mol$^{-1}$), Ar (purple line, molar mass $= 39.9$ g mol$^{-1}$), and Kr (red line, molar mass $= 83.8$ g mol$^{-1}$) at 298 K.

**FIGURE 16.7**
Schematic of an experimental apparatus used to verify the Maxwell speed distribution. Molecules are emitted from the oven and pass through the slits to produce a beam of molecules. This beam reaches a velocity selector consisting of two rotating disks with slots in each disk. After passing through the first disk, the molecules will reach the second disk that will have rotated by angle $\theta$. Only molecules for which the velocity equals $\omega x/\theta$, where $\omega$ is the angular rotational velocity of the disks and $x$ is the separation between disks, will pass through the second disk and reach the detector.

**FIGURE 16.8**
Experimentally determined distribution
of particle speeds for gaseous potassium
at $466 \pm 2$ K (circles). The expected
Maxwellian distribution is presented as
the red line, and demonstrates excellent
agreement with experiment.
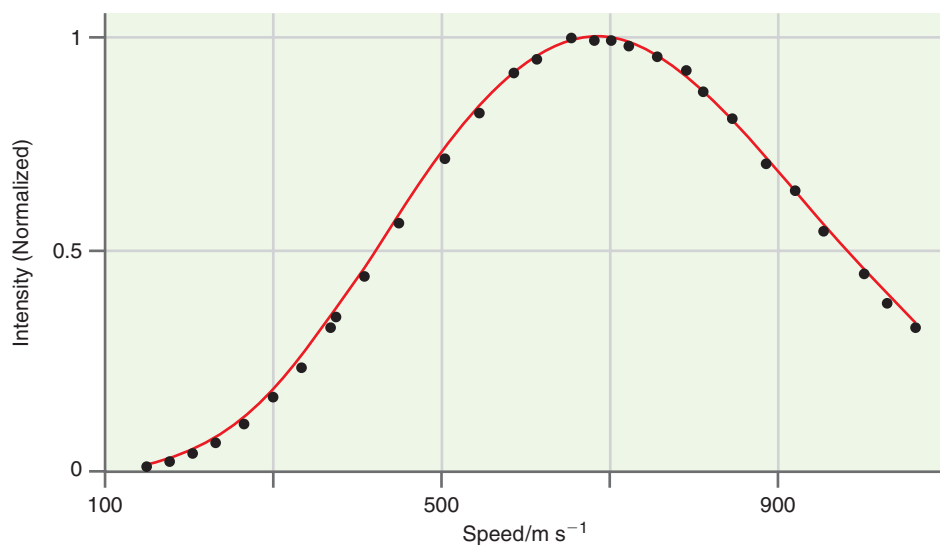


The results of this experiment for potassium at an oven temperature of $466 \pm 2$ K
are presented in Figure 16.8. The comparison between the experimentally measured
number of particles with a certain speed versus the theoretical prediction for a
Maxwellian distribution is excellent. The interested reader is encouraged to read the
Miller and Kusch manuscript for a fuller presentation of this elegant experiment.

## 16.4 Comparative Values for Speed Distributions: $\nu_{ave}$, $\nu_{mp}$, and $\nu_{rms}$

The Maxwell speed distribution describes the probability of observing a particle within
a given range of speeds; however, knowledge of the entire distribution is seldom
required when comparing the properties of gases. Instead, representative quantities of
this distribution that provide a metric as to how the distribution changes as a function of
mass or temperature are sometimes more useful. For example, in Figure 16.6 it is clear
that the speed distributions for Ne, Ar, and Kr are different, but can these differences be
described without depicting the entire distribution? It would be much more convenient
to compare only certain aspects of the distribution, such as the speed at which the
distribution is maximized, or the average speed.

The first comparative value we consider is the **most probable speed,** or $\nu_{mp}$, which
is equal to the speed at which $F(\nu)$ is at a maximum. This quantity is determined by
calculating the derivative of $F(\nu)$ with respect to speed:

$$\frac{dF(\nu)}{d\nu} = \frac{d}{d\nu}\left(4\pi\left(\frac{m}{2\pi kT}\right)^{3/2}\nu^2 e^{-m\nu^2/2kT}\right)$$

$$= 4\pi\left(\frac{m}{2\pi kT}\right)^{3/2}\frac{d}{d\nu}\left(\nu^2 e^{-m\nu^2/2kT}\right)$$

$$= 4\pi\left(\frac{m}{2\pi kT}\right)^{3/2}e^{-m\nu^2/2kT}\left[2\nu - \frac{m\nu^3}{kT}\right]$$

The most probable speed is the speed at which $dF(\nu)/d\nu$ is equal to zero, which
will be the case when the factor contained in the square brackets in the preceding equa-
tion is equal to zero. Recognizing this, $\nu_{mp}$ is given by

$$2\nu_{mp} - \frac{m\nu_{mp}^3}{kT} = 0$$

$$\nu_{mp} = \sqrt{\frac{2kT}{m}} = \sqrt{\frac{2RT}{M}} \qquad \textbf{(16.21)}$$

## EXAMPLE PROBLEM 16.2

What is the most probable speed for Ne and Kr at 298 K?

### Solution

First, $\nu_{mp}$ for Ne is readily determined using Equation (16.21):

$$\nu_{mp} = \sqrt{\frac{2RT}{M}} = \sqrt{\frac{2(8.314 \text{ J mol}^{-1} \text{ K}^{-1})298 \text{ K}}{0.020 \text{ kg mol}^{-1}}} = 498 \text{ m s}^{-1}$$

The corresponding $\nu_{mp}$ for Kr can be determined in the same manner, or with reference to Ne as follows:

$$\frac{(\nu_{mp})_{Kr}}{(\nu_{mp})_{Ne}} = \sqrt{\frac{M_{Ne}}{M_{Kr}}} = \sqrt{\frac{0.020 \text{ kg mol}^{-1}}{0.083 \text{ kg mol}^{-1}}} = 0.491$$

With this result, $\nu_{mp}$ for Kr is readily determined:

$$(\nu_{mp})_{kr} = 0.491(\nu_{mp})_{Ne} = 244 \text{ m s}^{-1}$$

For the sake of comparison, the speed of sound in dry air at 298 K is 346 m/s, and a typical commercial airliner travels at about 500 miles/hour or 224 m/s.

**Average speed** can be determined using the Maxwell speed distribution and the definition of average value provided in Chapter 12.

$$\nu_{ave} = \langle \nu \rangle = \int_0^\infty \nu F(\nu) \, d\nu$$

$$= \int_0^\infty \nu \left( 4\pi \left( \frac{m}{2\pi kT} \right)^{3/2} \nu^2 e^{-m\nu^2/2kT} \right) d\nu$$

$$= 4\pi \left( \frac{m}{2\pi kT} \right)^{3/2} \int_0^\infty \nu^3 e^{-m\nu^2/2kT} \, d\nu$$

$$= 4\pi \left( \frac{m}{2\pi kT} \right)^{3/2} \frac{1}{2} \left( \frac{2kT}{m} \right)^2$$

$$\nu_{ave} = \left( \frac{8kT}{\pi m} \right)^{1/2} = \left( \frac{8RT}{\pi M} \right)^{1/2} \quad \textbf{(16.22)}$$

A solution to the integral in Equation (16.22) is presented in the Math Supplement.

The final comparative quantity is the **root-mean-squared speed,** or $\nu_{rms}$. This quantity is equal to $[\langle \nu^2 \rangle]^{1/2}$, or simply the square root of the second moment of the distribution:

$$\nu_{rms} = \left[ \langle \nu^2 \rangle \right]^{1/2} = \left( \frac{3kT}{m} \right)^{1/2} = \left( \frac{3RT}{M} \right)^{1/2} \quad \textbf{(16.23)}$$



**FIGURE 16.9**
Comparison of $\nu_{mp}, \nu_{ave}$, and $\nu_{rms}$ for Ar at 298 K.

Notice that Equation (16.23) is equal to the prediction of kinetic theory of Equation (16.1). The locations of $\nu_{mp}, \nu_{ave}$, and $\nu_{rms}$ relative to the speed distribution for Ar at 298 K are presented in Figure 16.9. Comparison of Equation (16.21), (16.22), and (16.23) reveals that the only differences between the values are constants, which becomes evident when the ratios of these quantities are considered. Specifically, the ratio of $\nu_{rms}/\nu_{mp} = (3/2)^{1/2}$ and $\nu_{ave}/\nu_{mp} = (4/\pi)^{1/2}$ so that $\nu_{rms} > \nu_{ave} > \nu_{mp}$. Note also that all three **benchmark values** demonstrate the same dependence on T and particle mass: they increase as the square root of $T$ and decrease as the square root of $M$.
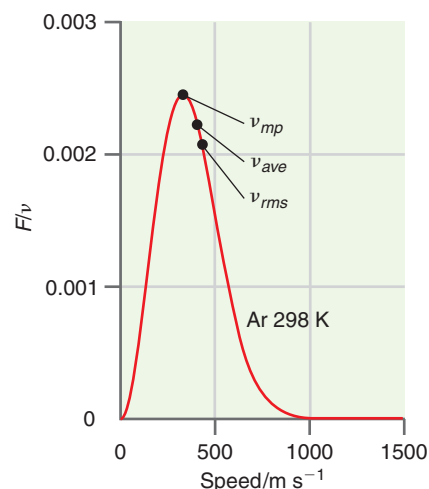
## EXAMPLE PROBLEM 16.3

Determine $\nu_{mp}, \nu_{ave}$, and $\nu_{rms}$ for Ar at 298 K.

**Solution**

Using Equations (16.21), (16.22), and (16.23), the benchmark speed values are as follows:

$$\nu_{mp} = \sqrt{\frac{2RT}{M}} = \sqrt{\frac{2(8.314 \text{ J mol}^{-1} \text{ K}^{-1})(298 \text{ K})}{0.040 \text{ kg mol}^{-1}}} = 352 \text{ m s}^{-1}$$

$$\nu_{ave} = \sqrt{\frac{8RT}{\pi M}} = \sqrt{\frac{8(8.314 \text{ J mol}^{-1} \text{ K}^{-1})(298 \text{ K})}{\pi(0.040 \text{ kg mol}^{-1})}} = 397 \text{ m s}^{-1}$$

$$\nu_{rms} = \sqrt{\frac{3RT}{M}} = \sqrt{\frac{3(8.314 \text{ J mol}^{-1} \text{ K}^{-1})(298 \text{ K})}{0.040 \text{ kg mol}^{-1}}} = 431 \text{ m s}^{-1}$$

# 16.5 Gas Effusion

As described earlier, the experiments that verified the accuracy of the Maxwell speed distribution were performed using a gas escaping through an aperture in the wall of the oven containing the gas (see Figure 16.7). In this technique, the gas confined to the box is at some finite pressure and is separated from a vacuum by a thin wall of the oven containing the aperture. The pressure of the gas and size of the aperture is such that molecules do not undergo collisions near or when passing through the aperture. The process by which a gas passes through an opening under these conditions is called **effusion** and is employed to produce a stream or "beam" of gas particles. For example, this technique is used to create atomic or molecular beams that can collide with beams of other molecules to study chemical reaction dynamics.

To derive the rate of gas effusion, we proceed in a fashion analogous to that used to derive pressure in Chapter 1. Let $dN_c$ be the number of particles that hit the wall of the container. The collisional rate, $dN_c/dt$, is the number of collisions with the wall per unit time. This quantity will be proportional to the area being struck, $A$. In addition, the collisional rate will depend on particle velocity, with increased velocity resulting in an increased collisional rate. Finally, the collisional rate should be directly proportional to the particle density $\widetilde{N}$ defined as the number of particles per unit volume. Taking these three ideas into account, we can write

$$\frac{dN_c}{dt} = \widetilde{N}A \int_0^\infty \text{v}_x f(\text{v}_x) \, d\text{v}_x \tag{16.24}$$

The integral in Equation (16.24) is simply the average particle velocity in the direction that will result in collision with the area of interest (taken as the positive $x$ direction with corresponding limits of integration from zero to positive infinity). Evaluating this integral yields the following expression for the collision rate:

$$\frac{dN_c}{dt} = \widetilde{N}A \int_0^\infty \text{v}_x \left(\frac{m}{2\pi kT}\right)^{1/2} e^{-m\text{v}_x^2/2kT} d\text{v}_x$$

$$= \widetilde{N}A \left(\frac{m}{2\pi kT}\right)^{1/2} \int_0^\infty \text{v}_x e^{-m\text{v}_x^2/2kT} d\text{v}_x$$

$$= \widetilde{N}A \left(\frac{m}{2\pi kT}\right)^{1/2} \left(\frac{kT}{m}\right)$$

$$= \widetilde{N}A \left(\frac{kT}{2\pi m}\right)^{1/2}$$

$$\frac{dN_c}{dt} = \widetilde{N}A \frac{1}{4}\nu_{ave} \tag{16.25}$$

In the final step, the definition of average speed $\nu_{ave}$ provided in Equation (16.22) has been used. The **collisional flux** $Z_c$ is defined as the number of collisions per unit time and per unit area. This quantity is equal to collisional rate divided by the area of interest $A$:

$$Z_c = \frac{dN_c/dt}{A} = \frac{1}{4}\tilde{N}\nu_{ave} \qquad (16.26)$$

It is sometimes more convenient to express the collisional flux in terms of gas pressure. This is accomplished by rewriting $\tilde{N}$ as follows:

$$\tilde{N} = \frac{N}{V} = \frac{nN_A}{V} = \frac{P}{kT} \qquad (16.27)$$

With this definition of $\tilde{N}$, $Z_c$ becomes

$$Z_c = \frac{P}{(2\pi m kT)^{1/2}} = \frac{PN_A}{(2\pi MRT)^{1/2}} \qquad (16.28)$$

where $m$ is the particle mass (in kilograms) and $M$ is molar mass (in kg mol$^{-1}$). Evaluating the preceding expression requires careful attention to units, as Example Problem 16.4 illustrates.

---

### EXAMPLE PROBLEM 16.4

How many collisions per second occur on a container wall with an area of 1 cm$^2$ for a collection of Ar particles at 1 atm and 298 K?

#### Solution

Using Equation (16.28):

$$Z_c = \frac{PN_A}{(2\pi MRT)^{1/2}} = \frac{(1.01325 \times 10^5\,\text{Pa})(6.022 \times 10^{23}\,\text{mol}^{-1})}{(2\pi(0.0400\,\text{kg mol}^{-1})(8.314\,\text{J mol}^{-1}\,\text{K}^{-1})(298\,\text{K}))^{1/2}}$$

$$= 2.45 \times 10^{27}\,\text{m}^{-2}\,\text{s}^{-1}$$

Notice that pressure is in units of Pa (kg m$^{-1}$ s$^{-2}$) resulting in the appropriate units for $Z_c$. Then, multiplying the collisional flux by the area of interest yields the collisional rate:

$$\frac{dN_c}{dt} = Z_cA = (2.45 \times 10^{27}\,\text{m}^{-2}\,\text{s}^{-1})(10^{-4}\,\text{m}^2) = 2.45 \times 10^{23}\,\text{s}^{-1}$$

This quantity represents the number of collisions per second with a section of the container wall having an area of 1 cm$^2$. This is a rather large quantity, and it demonstrates the substantial number of collisions that occur in a container for a gas under standard temperature and pressure conditions.

---

Effusion will result in a decrease in gas pressure as a function of time. The change in pressure is related to the change in the number of particles in the container, $N$, as follows:

$$\frac{dP}{dt} = \frac{d}{dt}\left(\frac{NkT}{V}\right) = \frac{kT}{V}\frac{dN}{dt} \qquad (16.29)$$

The quantity $dN/dt$ can be related to the collisional flux [Equation (16.28)] by recognizing the following. First, if the space outside of the container is at a significantly lower pressure than the container and a particle escapes the container, it will not return. Second, each collision corresponds to a particle striking the aperture area so that the number of collisions with the aperture area is equal to the number of molecules lost, resulting in $N_c = N$ in Equation (16.26) and

$$\frac{dN}{dt} = -Z_cA = \frac{-PA}{(2\pi m kT)^{1/2}} \qquad (16.30)$$

where the negative sign is consistent with the expectation that the number of particles in the container will decrease as effusion proceeds. Substituting the preceding result into Equation (16.29), the change in pressure as a function of time becomes

$$\frac{dP}{dt} = \frac{kT}{V}\left(\frac{-PA}{(2\pi m kT)^{1/2}}\right) \tag{16.31}$$

Integration of Equation (16.31) yields the following expression for container pressure as a function of time:

$$P = P_0 \exp\left[-\frac{At}{V}\left(\frac{kT}{2\pi m}\right)^{1/2}\right] \tag{16.32}$$

In Equation (16.32), $P_0$ is initial container pressure. This result demonstrates that effusion will result in an exponential decrease in container pressure as a function of time.

### EXAMPLE PROBLEM 16.5

A 1 L container filled with Ar at 298 K and at an initial pressure of $1.00 \times 10^{-2}$ atm is allowed to effuse through an aperture having an area of $0.01\ \mu m^2$. Will the pressure inside the container be significantly reduced after 1 hour of effusion?

### Solution

In evaluating Equation (16.32), it is easiest to first determine the exponential factor and then determine the pressure:

$$\frac{At}{V}\left(\frac{kT}{2\pi m}\right)^{1/2} = \frac{10^{-14}\,m^2(3600\,s)}{10^{-3}\,m^3}\left(\frac{1.38 \times 10^{-23}\,J\,K^{-1}(298\,K)}{2\pi\left(\dfrac{0.0400\,kg\,mol^{-1}}{N_A}\right)}\right)^{1/2}$$

$$= 3.60 \times 10^{-8}\,s\,m^{-1}(99.3\,m\,s^{-1}) = 3.57 \times 10^{-6}$$

The pressure after 1 hour of effusion, therefore, is

$$P = P_0\,e^{-3.57 \times 10^{-6}} = (1.00 \times 10^{-2}\,atm)e^{-3.57 \times 10^{-6}} \approx 1.00 \times 10^{-2}\,atm$$

Given the large volume of the container and the relatively small aperture through which effusion occurs, the pressure inside the container is essentially unchanged.

## 16.6 Molecular Collisions

Kinetic theory can also be used to determine the collisional frequency between gaseous particles. Recall that one of the primary ideas behind kinetic theory is that the distance between gaseous particles is on average much greater than the actual particle volume. However, the particles translate through space, and collisions between particles will occur. How does one think about these collisions with respect to the intermolecular interactions that occur between particles? At high gas pressures, intermolecular forces are substantial and particle interactions become important. Even during collisions at low pressures, the intermolecular forces must be relevant during the collisions. Modeling collisions including the subtleties of intermolecular interactions is beyond the scope of this text. Instead, we adopt a limiting viewpoint of collisions in which we treat the particles as hard spheres. Billiard balls are an excellent example of a hard-sphere particle. Collisions occur when two billiard balls attempt to occupy the same region of space, and this is the only time the particles interact. We will see in upcoming chapters that an understanding of the frequency of molecular collisions is important in describing a variety of chemical phenomena, including the rates of chemical reactions.

**FIGURE 16.10**
Schematic of the hard-sphere collisional process.
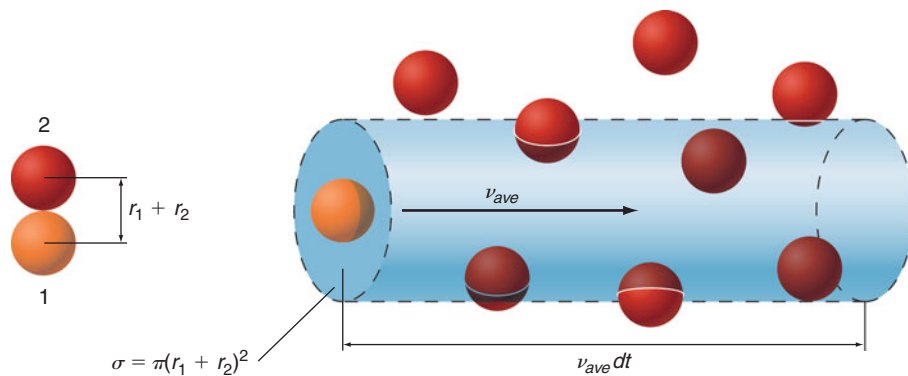


How frequent are molecular collisions? To answer this question, we assume that the particle of interest is moving and that all other molecules are stationary (we will relax this assumption shortly). In this picture, the particle of interest sweeps out a collisional cylinder, which determines the number of collisions the particle undergoes per unit time. A depiction of this cylinder is provided in Figure 16.10. Collisions occur between the particle of interest and other particles that are positioned within the cylinder. The area of the collisional cylinder base or **collisional cross section** $\sigma$ is dependent on the radii of the gas particles $r$ as follows:

$$\sigma = \pi(r_1 + r_2)^2 \tag{16.33}$$

The subscripts 1 and 2 in Equation (16.33) denote the two collisional partners, which may or may not be the same species. The length of the cylinder is given by the product of a given time interval ($dt$) and $v_{ave}$, the average speed of the molecule. Therefore, the total cylinder volume is equal to $\sigma v_{ave} dt$ as depicted in Figure 16.10.

This derivation of the cylinder volume is not exactly correct because the other molecules are not stationary. To incorporate the motion of other molecules in the derivation, we now introduce the concept of **effective speed.** To illustrate this concept, imagine two particles moving with some average speed as depicted in Figure 16.11. The effective speed at which two particles approach each other is dependent on the relative direction of particle motion. The first case depicted in the figure is of two particles traveling in the same direction where $\langle v_{12} \rangle = \langle v_1 \rangle - \langle v_2 \rangle$. If the particles were identical, the effective speed would be zero since the molecules would travel with constant separation and never collide. The opposite case is depicted in the middle of the figure, where the effective speed is $\langle v_1 \rangle + \langle v_2 \rangle$ when the particles are traveling directly at each other. Again, if the particles were identical then $\langle v_{12} \rangle = 2\langle v_1 \rangle$.

A full derivation of the effective speed is quite involved and results in the intuitive result depicted as the third case in Figure 16.11. In this third case, the average approach angle is 90° and, using the Pythagorean theorem, the effective speed is equal to

$$\langle v_{12} \rangle = (\langle v_1 \rangle^2 + \langle v_2 \rangle^2)^{1/2} = \left[ \left( \frac{8kT}{\pi m_1} \right) + \left( \frac{8kT}{\pi m_2} \right) \right]^{1/2}$$

$$= \left[ \frac{8kT}{\pi} \left( \frac{1}{m_1} + \frac{1}{m_2} \right) \right]^{1/2}$$

$$= \left( \frac{8kT}{\pi \mu} \right)^{1/2} \tag{16.34}$$

where

$$\mu = \frac{m_1 m_2}{m_1 + m_2}$$

With the effective speed as defined by Equation (16.34), the collisional-cylinder volume is now defined. The number of collisional partners in the collisional cylinder is equal to
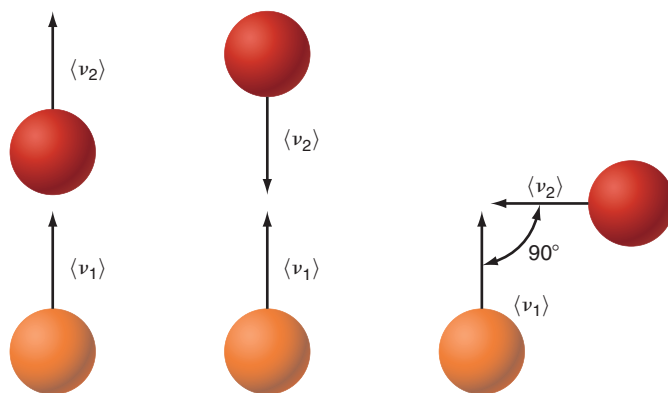
the product of the collisional-partner number density $(N_2/V)$ and the volume of the cylinder, $V_{cyl} = \sigma v_{ave} dt$ (Figure 16.10). We define the individual **particle collisional frequency** $z_{12}$ as the number of collisions an individual molecule (denoted by the subscript 1) undergoes with other collisional partners (denoted by the subscript 2) per unit time ($dt$). This quantity is equal to the number of collisional partners divided by $dt$:

$$z_{12} = \frac{N_2}{V}\left(\frac{V_{cyl}}{dt}\right) = \frac{N_2}{V}\left(\frac{\sigma v_{ave} dt}{dt}\right) = \frac{N_2}{V}\sigma\left(\frac{8kT}{\pi\mu}\right)^{1/2} \tag{16.35}$$

If the gas is comprised of one type of particle, $\mu = m_1/2$ and Equation (16.35) becomes

$$z_{11} = \frac{N_1}{V}\sigma\sqrt{2}\left(\frac{8kT}{\pi m_1}\right)^{1/2} = \frac{P_1 N_A}{RT}\sigma\sqrt{2}\left(\frac{8RT}{\pi M_1}\right)^{1/2} \tag{16.36}$$

The **total collisional frequency** is defined as the total number of collisions that occur for all gas particles. The total collisional frequency for a collection of two types of gas molecules $Z_{12}$ is given by $z_{12}$ times the number density of species 1:

$$Z_{12} = \frac{N_1}{V}z_{12} = \frac{N_1}{V}\frac{N_2}{V}\sigma\left(\frac{8kT}{\pi\mu}\right)^{1/2} = \left(\frac{P_1 N_A}{RT}\right)\left(\frac{P_2 N_A}{RT}\right)\sigma\left(\frac{8kT}{\pi\mu}\right)^{1/2} \tag{16.37}$$

The units of $Z_{12}$ are collisions per cubic meter, or the total number of collisions per unit volume. The corresponding collisional frequency for a gas consisting of only one type of particle is

$$Z_{11} = \frac{1}{2}\frac{N_1}{V}z_{11} = \frac{1}{\sqrt{2}}\left(\frac{N_1}{V}\right)^2\sigma\left(\frac{8kT}{\pi m_1}\right)^{1/2} = \frac{1}{\sqrt{2}}\left(\frac{P_1 N_A}{RT}\right)^2\sigma\left(\frac{8RT}{\pi M_1}\right)^{1/2} \tag{16.38}$$

The factor of $1/2$ appears in Equation (16.38) to ensure that each collision is only counted once. Evaluation of Equations (16.35) through (16.38) requires knowledge of the collisional cross sections that are in turn dependent on the effective hard-sphere radii. As we will see in the next chapter, these values can be determined by the measure of various gas properties. Table 16.1 provides the hard-sphere radii for a variety of

| TABLE 16.1 Collisional Parameters for Various Gases | | |
|---|---|---|
| **Species** | $r$ (nm) | $\sigma$ (nm$^2$) |
| He | 0.13 | 0.21 |
| Ne | 0.14 | 0.24 |
| Ar | 0.17 | 0.36 |
| Kr | 0.20 | 0.52 |
| $N_2$ | 0.19 | 0.43 |
| $O_2$ | 0.18 | 0.40 |
| $CO_2$ | 0.20 | 0.52 |

common gases determined from such measurements. Generally, for monatomic gases and small molecules the radius is on the order of 0.2 nm.

## EXAMPLE PROBLEM 16.6

What is $z_{11}$ for $CO_2$ at 298 K and 1 atm?

### Solution

The question asks for the single-particle collisional frequency of $CO_2$. Using Equation (16.36) and the collisional cross section provided in Table 16.1, we obtain

$$z_{CO_2} = \frac{P_{CO_2} N_A}{RT} \sigma \sqrt{2} \left( \frac{8RT}{\pi M_{CO_2}} \right)^{1/2}$$

$$= \frac{101,325 \text{ Pa } (6.022 \times 10^{23} \text{ mol}^{-1})}{8.314 \text{ J mol}^{-1} \text{ K}^{-1} (298 \text{ K})} (5.2 \times 10^{-19} \text{ m}^2) \sqrt{2}$$

$$\times \left( \frac{8(8.314 \text{ J mol}^{-1} \text{ K}^{-1})(298 \text{ K})}{\pi (0.044 \text{ kg mol}^{-1})} \right)^{1/2}$$

$$= 6.9 \times 10^9 \text{ s}^{-1}$$

This calculation demonstrates that a single $CO_2$ molecule undergoes roughly 7 billion collisions per second under standard temperature and pressure conditions! The inverse of the collisional frequency corresponds to the time between molecular collision or roughly 150 picoseconds (1 ps $= 10^{-12}$ s) between collisions.

## EXAMPLE PROBLEM 16.7

What is the total collisional frequency ($Z_{ArKr}$) at 298 K for a collection of Ar and Kr confined to a 1 cm$^3$ container with partial pressures of 360. Torr for Ar and 400. Torr for Kr?

### Solution

Evaluation of Equation (16.37) is best performed by evaluating each factor in the equation separately, then combining factors to calculate the total collisional frequency as follows:

$$\left( \frac{P_{Ar} N_A}{RT} \right) = \left( \frac{47,996 \text{ Pa } (6.022 \times 10^{23} \text{ mol}^{-1})}{8.314 \text{ J mol}^{-1} \text{ K}^{-1} (298 \text{ K})} \right) = 1.17 \times 10^{25} \text{ m}^{-3}$$

$$\left( \frac{P_{Kr} N_A}{RT} \right) = \left( \frac{53,328 \text{ Pa } (6.022 \times 10^{23} \text{ mol}^{-1})}{8.314 \text{ J mol}^{-1} \text{ K}^{-1} (298 \text{ K})} \right) = 1.30 \times 10^{25} \text{ m}^{-3}$$

$$\sigma = \pi (r_{Ar} + r_{Kr})^2 = \pi (0.17 \text{ nm} + 0.20 \text{ nm})^2 = 0.430 \text{ nm}^2 = 4.30 \times 10^{-19} \text{ m}^2$$

$$\mu = \frac{m_{Ar} m_{Kr}}{m_{Ar} + m_{Kr}} = \frac{(0.040 \text{ kg mol}^{-1})(0.084 \text{ kg mol}^{-1})}{(0.040 \text{ kg mol}^{-1}) + (0.084 \text{ kg mol}^{-1})} \times \frac{1}{N_A} = 4.50 \times 10^{-26} \text{ kg}$$

$$\left( \frac{8kT}{\pi \mu} \right)^{1/2} = \left( \frac{8(1.38 \times 10^{-23} \text{ J K}^{-1})(298 \text{ K})}{\pi (4.50 \times 10^{-26} \text{ kg})} \right)^{1/2} = 482 \text{ m s}^{-1}$$

$$Z_{ArKr} = \left( \frac{P_{Ar} N_A}{RT} \right) \left( \frac{P_{Kr} N_A}{RT} \right) \sigma \left( \frac{8kT}{\pi \mu} \right)^{1/2}$$

$$= (1.17 \times 10^{25} \text{ m}^{-3})(1.30 \times 10^{25} \text{ m}^{-3})(4.30 \times 10^{-19} \text{ m}^2)(482 \text{ m s}^{-1})$$

$$= 3.16 \times 10^{34} \text{ m}^{-3} \text{ s}^{-1} = 3.16 \times 10^{31} \text{ L}^{-1} \text{ s}^{-1}$$

Comparison of the last two example problems reveals that the total collisional frequency ($Z_{12}$) is generally much larger than the collisional frequency for an individual molecule ($z_{12}$). The total collisional frequency incorporates all collisions that occur for a collection

of gas particles (consistent with the units of inverse volume); therefore, the magnitude of this value relative to the collisional frequency for a single particle is not unexpected.

# 16.7 The Mean Free Path

The **mean free path** is defined as the average distance a gas particle travels between successive collisions. In a given time interval $dt$, the distance a particle will travel is equal to $\nu_{ave}\, dt$ where $\nu_{ave}$ is the average speed of the particle. In addition, the number of collisions the particle undergoes is given by $(z_{11} + z_{12})\, dt$, where the frequency of collisions with either type of collisional partner in the binary mixture is included. Given these quantities, the mean free path $\lambda$ is given by the average distance traveled divided by the number of collisions:

$$\lambda = \frac{\nu_{ave}\, dt}{(z_{11} + z_{12})\, dt} = \frac{\nu_{ave}}{(z_{11} + z_{12})} \tag{16.39}$$

If our discussion is limited to a gas with one type of particle, $N_2 = 0$ resulting in $z_{12} = 0$, and the mean free path becomes

$$\lambda = \frac{\nu_{ave}}{z_{11}} = \frac{\nu_{ave}}{\left(\dfrac{N_1}{V}\right)\sqrt{2}\sigma\nu_{ave}} = \left(\frac{RT}{P_1 N_A}\right)\frac{1}{\sqrt{2}\sigma} \tag{16.40}$$

Equation (16.40) demonstrates that the mean free path decreases if the pressure increases or if the collisional cross section of the particle increases. This behavior makes intuitive sense. As particle density increases (i.e., as pressure increases), we would expect the particle to travel a shorter distance between collisions. Also, as the particle size increases, we would expect the probability of collision to also increase, thereby reducing the mean free path.

   What does the mean free path tell us about the length scale of collisional events relative to molecular size? Recall that one of the assumptions of kinetic theory is that the distance between particles is large compared to their size. Is the mean free path consistent with this assumption? To answer this question, we return to the first example provided in this chapter, Ar at a pressure of 1 atm and temperature of 298 K, for which the mean free path is

$$\lambda_{Ar} = \left(\frac{RT}{P_{Ar} N_A}\right)\frac{1}{\sqrt{2}\sigma}$$

$$= \left(\frac{(8.314\ \text{J mol}^{-1}\,\text{K}^{-1})(298\ \text{K})}{(101{,}325\ \text{Pa})(6.022 \times 10^{23}\,\text{mol}^{-1})}\right)\frac{1}{\sqrt{2}(3.6 \times 10^{-19}\,\text{m}^2)}$$

$$= 7.98 \times 10^{-8}\,\text{m} \approx 80\ \text{nm}$$

Compared to the 0.29 nm diameter of Ar, the mean free path demonstrates that an Ar atom travels an average distance equal to $\sim 275$ times its diameter between collisions. This difference in length scales is consistent with the assumptions of kinetic theory. To provide further insight into the behavior of a collection of gaseous particles, as indicated in Example Problem 16.6, the collisional frequency can be used to determine the timescale between collisions as follows:

$$\frac{1}{z_{11}} = \frac{\lambda}{\nu_{ave}} = \frac{7.98 \times 10^{-8}\,\text{m}}{397\ \text{m s}^{-1}} = 2.01 \times 10^{-10}\,\text{s}$$

A picosecond is equal to $10^{-12}$ s; therefore, an individual Ar atom undergoes on average a collision every 200 ps. As will be discussed in the following chapters, properties such as collisional frequency and mean free path are important in describing transport properties of gases and chemical reaction dynamics involving collisional processes. The physical picture of gas particle motion outlined here will prove critical in understanding these important aspects of physical chemistry.

# Vocabulary

average speed

benchmark value

collisional cross section

collisional flux

effective speed

effusion

gas kinetic theory

Maxwell speed distribution

Maxwell–Boltzmann velocity
distribution

mean free path

most probable speed

particle collisional frequency

particle speed

root-mean-squared speed

total collisional frequency

velocity distribution function

velocity space

# Conceptual Problems

**Q16.1** Why is probability used to describe the velocity and speed of gas molecules?

**Q16.2** What is the most probable velocity for a one-dimensional gas velocity distribution? Why?

**Q16.3** Provide a physical explanation as to why the Maxwell speed distribution approaches zero at high speeds. Why is $f(\nu) = 0$ at $\nu = 0$?

**Q16.4** How would the Maxwell speed distributions for He versus Kr compare if the gases were at the same temperature?

**Q16.5** Imagine that you are performing an experiment using a molecular beam using Ar at a given temperature. If you switch the gas to Kr, will you have to increase or decrease the temperature of the gas to achieve a distribution of speeds identical to Ar?

**Q16.6** How does the average speed of a collection of gas particles vary with particle mass and temperature?

**Q16.7** Does the average kinetic energy of a particle depend on particle mass?

**Q16.8** Arrange $\nu_{mp}$, $\nu_{ave}$, and $\nu_{rms}$ in order from highest to lowest speed.

**Q16.9** Why does the mean free path depend on $\sigma$? Would an increase in $\widetilde{N}$ increase or decrease the mean free path?

**Q16.10** In effusion, how does the frequency of collisions with the opening scale with molecular mass?

**Q16.11** What is the typical length scale for a molecular diameter?

**Q16.12** What is the difference between $z_{11}$ and $z_{12}$?

**Q16.13** Define the mean free path. How does this quantity vary with number density, particle diameter, and average particle speed?

# Numerical Problems

Problem numbers in **red** indicate that the solution to the problem is given in the *Student's Solutions Manual*.

**P16.1** Consider a collection of gas particles confined to translate in two dimensions (for example, a gas molecule on a surface). Derive the Maxwell speed distribution for such a gas.

**P16.2** Determine $\nu_{mp}$, $\nu_{ave}$, and $\nu_{rms}$ for the following species at 298 K:

**a.** Ne **b.** Kr **c.** $CH_4$ **d.** $C_2H_6$ **e.** $C_{60}$

**P16.3** Compute $\nu_{mp}$, $\nu_{ave}$, and $\nu_{rms}$ for $O_2$ at 300. and 500. K. How would your answers change for $H_2$?

**P16.4** Compute $\nu_{ave}$ for $H_2O$, HOD, and $D_2O$ at 298 K. Do you need to perform the same calculation each time, or can you derive an expression that relates the ratio of average speeds for two gases to their respective masses?

**P16.5** Compare the average speed and average translational kinetic energy of $O_2$ with that of $CCl_4$ at 298 K.

**P16.6** How far, on average, does $O_2$ travel in 1 second at 298 K and 1 atm? How does this distance compare to that of Kr under identical conditions?

**P16.7**

**a.** What is the average time required for $H_2$ to travel 1.00 m at 298 K and 1 atm?

**b.** How much longer does it take $N_2$ to travel 1.00 m, on average, relative to $H_2$ under these same conditions?

**c.** (Challenging) What fraction of $N_2$ particles will require more than this average time to travel 1.00 m? Answering this question will require evaluating a definite integral of the speed distribution, which requires using numerical methods such as Simpson's rule.

**P16.8** As mentioned in Section 16.3, the only differences between the quantities $\nu_{mp}$, $\nu_{ave}$, and $\nu_{rms}$ involve constants.

a. Derive the expressions for $\nu_{ave}$ and $\nu_{rms}$ relative to $\nu_{mp}$ provided in the text.

b. Your result from part (a) will involve quantities that are independent of gas-specific quantities such as mass or temperature. Given this, it is possible to construct a "generic" speed distribution curve for speed in reduced units of $\nu/\nu_{mp}$. Transform the Maxwell distribution into a corresponding expression involving reduced speed.

**P16.9** At what temperature is the $\nu_{rms}$ of Ar equal to that of $SF_6$ at 298 K? Perform the same calculation for $\nu_{mp}$.

**P16.10** Determine the temperature at which $\nu_{ave}$ for Kr is equal to that of Ne at 298 K.

**P16.11** The probability that a particle will have a velocity in the $x$ direction in the range of $-v_{x0}$ and $v_{x0}$ is given by

$$f(-v_{x0} \le v_x \le v_{x0}) = \left(\frac{m}{2\pi kT}\right)^{1/2} \int_{v_{x_o}}^{v_{x_o}} e^{-mv_x^2/2kT} dv_x$$

$$= \left(\frac{2m}{\pi kT}\right)^{1/2} \int_0^{v_{x_o}} e^{-mv_x^2/2kT} dv_x$$

The preceding integral can be rewritten using the following substitution: $\xi^2 = mv_x^2/2kT$, resulting in $f(-v_{x0} \le v_x \le v_{x0}) = 2/\sqrt{\pi}\left(\int_0^{\xi_0} e^{-\xi^2} d\xi\right)$, which can be evaluated using the error function defined as $\mathrm{erf}(z) = 2/\sqrt{\pi}\left(\int_0^z e^{-x^2} dx\right)$.

The complementary error function is defined as $\mathrm{erfc}(z) = 1 - \mathrm{erf}(z)$. Finally, a plot of both $\mathrm{erf}(z)$ and $\mathrm{erfc}(z)$ as a function of $z$ is shown here:
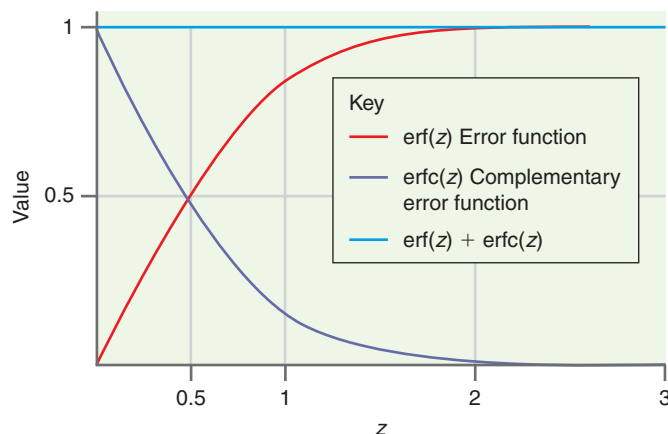


Using this graph of $\mathrm{erf}(z)$, determine the probability that $|v_x| \le (2kT/m)^{1/2}$. What is the probability that $|v_x| > (2kT/m)^{1/2}$?

**P16.12** The speed of sound is given by $\nu_{sound} = \sqrt{\gamma kT/m} = \sqrt{\gamma RT/M}$, where $\gamma = C_P/C_\nu$.

a. What is the speed of sound in Ne, Kr, and Ar at 1000. K?

b. At what temperature will the speed of sound in Kr equal the speed of sound in Ar at 1000. K?

**P16.13** For $O_2$ at 1 atm and 298 K, what fraction of molecules has a speed that is greater than $\nu_{rms}$?

**P16.14** The escape velocity from Earth's surface is given by $v_E = (2gR)^{1/2}$ where $g$ is the gravitational acceleration (9.807 m s$^{-2}$) and $R$ is the radius of Earth (6.37 × 10$^6$ m).

a. At what temperature will $\nu_{mp}$ for $N_2$ be equal to the escape velocity?

b. How does the answer for part (a) change if the gas of interest is He?

c. What is the largest molecular mass that is capable of escaping Earth's surface at 298 K?

**P16.15** For $N_2$ at 298 K, what fraction of molecules has a speed between 200. and 300. m/s? What is this fraction if the gas temperature is 500. K?

**P16.16** A molecular beam apparatus employs supersonic jets that allow gas molecules to expand from a gas reservoir held at a specific temperature and pressure into a vacuum through a small orifice. Expansion of the gas results for achieving internal temperatures of roughly 10 K. The expansion can be treated as adiabatic, with the change in gas enthalpy accompanying expansion being converted to kinetic energy associated with the flow of the gas:

$$\Delta H = C_P T_R = \frac{1}{2} M \nu^2$$

The temperature of the reservoir ($T_R$) is generally greater than the final temperature of the gas, allowing one to consider the entire enthalpy of the gas to be converted into translational motion.

a. For a monatomic gas $C_P = 5/2\, R$. Using this information, demonstrate that the final flow velocity of the molecular beam is related to the initial temperature of the reservoir ($T_R$) by

$$\nu = \sqrt{\frac{5RT_R}{M}}$$

b. Using this expression, what is the flow velocity of a molecular beam of Ar where $T_R = 298$ K? Notice that this is remarkably similar to the average speed of the gas. Therefore, the molecular beam resulting can be described as a gas that travels with velocity $\nu$ but with a very low internal energy. In other words, the distribution of molecular speeds around the flow velocity is significantly reduced in this process.

**P16.17** Demonstrate that the Maxwell–Boltzmann speed distribution is normalized.

**P16.18** (Challenging) Derive the Maxwell–Boltzmann distribution using the Boltzmann distribution introduced in statistical mechanics. Begin by developing the expression for the distribution in translational kinetic energy in one dimension and then extend it to three dimensions.

**P16.19** Starting with the Maxwell speed distribution, demonstrate that the probability distribution for translational kinetic energy for $\varepsilon_T \gg kT$ is given by

$$f(\varepsilon_T)\, d\varepsilon_T = 2\pi\left(\frac{1}{\pi kT}\right)^{3/2} e^{-\varepsilon_T/kT} \varepsilon_T^{1/2}\, d\varepsilon_T$$

**P16.20** Using the distribution of particle translational kinetic energy provided in Problem P16.19, derive expressions for the average and most probable translational kinetic energies for a collection of gaseous particles.

**P16.21** (Challenging) Using the distribution of particle translational kinetic energy provided in Problem P16.19, derive an expression for the fraction of molecules that have energy greater than some energy $\varepsilon^*$. The rate of many chemical reactions is dependent on the thermal energy available $kT$ versus some threshold energy. Your answer to this question will provide insight into why one might expect the rate of such chemical reactions to vary with temperature.

**P16.22** As discussed in Chapter 12 the $n$th moment of a distribution can be determined as follows: $\langle x^n \rangle = \int x^n f(x) dx$, where integration is over the entire domain of the distribution. Derive expressions for the $n$th moment of the gas speed distribution.

**P16.23** Imagine a cubic container with sides 1 cm in length that contains 1 atm of Ar at 298 K. How many gas–wall collisions are there per second?

**P16.24** The vapor pressure of various substances can be determined using effusion. In this process, the material of interest is placed in an oven (referred to as a Knudsen cell) and the mass of material lost through effusion is determined. The mass loss ($\Delta m$) is given by $\Delta m = Z_c A m \Delta t$, where $Z_c$ is the collisional flux, $A$ is the area of the aperture through which effusion occurs, $m$ is the mass of one atom, and $\Delta t$ is the time interval over which the mass loss occurs. This technique is quite useful for determining the vapor pressure of nonvolatile materials. A 1.00 g sample of $UF_6$ is placed in a Knudsen cell equipped with a 100.-$\mu$m-radius hole and heated to 18.2°C where the vapor pressure is 100. Torr.

**a.** The best scale in your lab has an accuracy of $\pm 0.01$ g. What is the minimum amount of time you must wait until the mass change of the cell can be determined by your balance?

**b.** How much $UF_6$ will remain in the Knudsen cell after 5.00 minutes of effusion?

**P16.25** Imagine designing an experiment in which the presence of a gas is determined by simply listening to the gas with your ear. The human ear can detect pressures as low as $2 \times 10^{-5}$ N m$^{-2}$. Assuming that the eardrum has an area of roughly 1 mm$^2$, what is the minimum collisional rate that can be detected by ear? Assume that the gas of interest is $N_2$ at 298 K.

**P16.26**

**a.** How many molecules strike a 1.00 cm$_2$ surface during 1 minute if the surface is exposed to $O_2$ at 1 atm and 298 K?

**b.** Ultrahigh vacuum studies typically employ pressures on the order of $10^{-10}$ Torr. How many collisions will occur at this pressure at 298 K?

**P16.27** You are a NASA engineer faced with the task of ensuring that the material on the hull of a spacecraft can withstand puncturing by space debris. The initial cabin air pressure in the craft of 1 atm can drop to 0.7 atm before the safety of the crew is jeopardized. The volume of the cabin is 100. m$^3$,

and the temperature in the cabin is 285 K. Assuming it takes the space shuttle about 8 hours from entry into orbit until landing, what is the largest circular aperture created by a hull puncture that can be safely tolerated assuming that the flow of gas out of the spaceship is effusive? Can the escaping gas from the spaceship be considered as an effusive process? (You can assume that the air is adequately represented by $N_2$.)

**P16.28** Many of the concepts developed in this chapter can be applied to understanding the atmosphere. Because atmospheric air is comprised primarily of $N_2$ (roughly 78% by volume), approximate the atmosphere as consisting only of $N_2$ in answering the following questions:

**a.** What is the single-particle collisional frequency at sea level, with $T = 298$ K and P $= 1.0$ atm? The corresponding single-particle collisional frequency is reported as $10^{10}$ s$^{-1}$ in the *CRC Handbook of Chemistry and Physics* (62nd ed., p. F-171).

**b.** At the tropopause (11 km), the collisional frequency decreases to $3.16 \times 10^9$ s$^{-1}$, primarily due to a reduction in temperature and barometric pressure (i.e., fewer particles). The temperature at the tropopause is ~220 K. What is the pressure of $N_2$ at this altitude?

**c.** At the tropopause, what is the mean free path for $N_2$?

**P16.29**

**a.** The stratosphere begins at 11 km above Earth's surface. At this altitude $P = 22.6$ kPa and $T = -56.5$°C. What is the mean free path of $N_2$ at this altitude assuming $N_2$ is the only component of the stratosphere?

**b.** The stratosphere extends to 50.0 km where $P = 0.085$ kPa and $T = 18.3$°C. What is the mean free path of $N_2$ at this altitude?

**P16.30**

**a.** Determine the total collisional frequency for $CO_2$ at 1 atm and 298 K.

**b.** At what temperature would the collisional frequency be 10.% of the value determined in part (a)?

**P16.31**

**a.** A standard rotary pump is capable of producing a vacuum on the order of $10^{-3}$ Torr. What is the single-particle collisional frequency and mean free path for $N_2$ at this pressure and 298 K?

**b.** A cryogenic pump can produce a vacuum on the order of $10^{-10}$ Torr. What is the collisional frequency and mean free path for $N_2$ at this pressure and 298 K?

**P16.32** Determine the mean free path for Ar at 298 K at the following pressures:

**a.** 0.5 atm

**b.** 0.005 atm

**c.** $5 \times 10^{-6}$ atm

**P16.33** Determine the mean free path at 500. K and 1 atm for the following:

**a.** Ne

**b.** Kr

**c.** $CH_4$

Rather than simply calculating the mean free path for each species separately, instead develop an expression for the ratio of mean free paths for two species and use the calculated value for one species to determine the other two.

**P16.34** Consider the following diagram of a molecular beam apparatus:
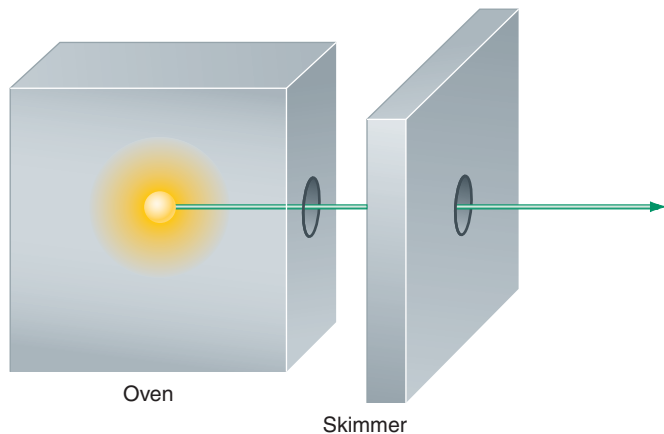


Oven

Skimmer

In the design of the apparatus, it is important to ensure that the molecular beam effusing from the oven does not collide with other particles until the beam is well past the skimmer, a device that selects molecules that are traveling in the appropriate direction, resulting in the creation of a molecular beam. The skimmer is located 10 cm in front of the oven so that a mean free path of 20. cm will ensure that the molecules are well past the skimmer before a collision can occur. If the molecular beam consists of $O_2$ at a temperature of 500. K, what must the pressure outside the oven be to ensure this mean free path?

**P16.35** A comparison of $\nu_{ave}, \nu_{mp}$, and $\nu_{rms}$ for the Maxwell speed distribution reveals that these three quantities are not equal. Is the same true for the one-dimensional velocity distributions?

**P16.36** At 30. km above Earth's surface (roughly in the middle of the stratosphere), the pressure is roughly 0.013 atm and the gas density is $3.74 \times 10^{23}$ molecules/m$^3$. Assuming $N_2$ is representative of the stratosphere, using the collisional diameter information provided in Table 16.1 determine

**a.** the number of collisions a single gas particle undergoes in this region of the stratosphere in 1.0 s.

**b.** the total number of particle collisions that occur in 1.0 s.

**c.** the mean free path of a gas particle in this region of the stratosphere.

# Web-Based Simulations, Animations, and Problems

**W16.1** In this simulation, the variations of gas particle velocity and speed distributions with particle mass and temperature are explored. Specifically, the variations in these distributions with mass are studied and compared to calculations performed by the student. Similar calculations are performed with respect to the distribution variation with temperature.

# For Further Reading

Castellan, G. W. *Physical Chemistry*, 3rd ed. Reading, MA: Addison Wesley, 1983.

Hirschfelder, J. O., C. F. Curtiss, and R. B. Bird. *The Molecular Theory of Gases and Liquids*. New York: Wiley, 1954.

Liboff, R. L. *Kinetic Theory: Classical, Quantum, and Relativistic Descriptions*. New York: Springer, 2003.

McQuarrie, D. *Statistical Mechanics*. New York: Harper & Row, 1973.

# Transport Phenomena

How will a system respond when it is not at equilibrium? The first steps toward answering this question are provided in this chapter. The study of system relaxation toward equilibrium is known as dynamics. In this chapter, transport phenomena involving the evolution of a system's physical properties such as mass or energy are described. All transport phenomena are connected by one central idea: the rate of change for a system's physical property is dependent on the spatial gradient of the property. In this chapter, this underlying idea is first described as a general concept, then applied to mass (diffusion), energy (thermal conduction), linear momentum (viscosity), and charge (ionic conductivity) transport. The timescale for mass transport is discussed and approached from both the macroscopic and microscopic perspective. It is important to note that although the various transport phenomena outlined here look different, the underlying concepts describing these phenomena have a common origin.

## 17.1 What Is Transport?

To this point we have been concerned with describing system properties at equilibrium. However, consider the application of an external perturbation to a system such that a property of the system is shifted away from equilibrium. Examples of such system properties are mass and energy. Once the external perturbation is removed, the system will evolve to reestablish the equilibrium distribution of the property. **Transport phenomena** involve the evolution of a system property in response to a nonequilibrium distribution of the property. The system properties of interest in this chapter are given in Table 17.1, and each property is listed with the corresponding transport process.

**TABLE 17.1 Transported Properties and the Corresponding Transport Process**

| Property Transported | Transport Process |
|---|---|
| Matter | Diffusion |
| Energy | Thermal conductivity |
| Linear momentum | Viscosity |
| Charge | Ionic conductivity |

In order for a system property to be transported, a spatial distribution of the property must be different from the distribution at equilibrium. Consider a collection of gas particles in which the equilibrium spatial distribution of the particles corresponds to the same particle number density throughout the container. What would happen if the particle number density were greater on one side of the container than the other? We would expect the gas particles to move in order to reestablish a homogeneous number density throughout the container. That is, the system evolves to reestablish a distribution of the system property that is consistent with equilibrium.

A central concept in transport phenomena is **flux,** defined as a quantity transferred through a given area in a given amount of time. Flux will occur when a spatial imbalance or gradient exists for a system property, and the flux will act in opposition to this gradient. In the example just discussed, imagine dividing the container into two parts with a partition and counting the number of particles that move from one side of the container to the other side, as illustrated in Figure 17.1. The flux in this case is equal to the number of particles that move through the partition per unit time. The theoretical underpinning of *all* of the transport processes listed in Table 17.1 involves flux and the fact that a spatial gradient in a system property will give rise to a corresponding flux. The most basic relationship between flux and the spatial gradient in transported property is as follows:

$$J_x = -\alpha \frac{d(\text{property})}{dx} \tag{17.1}$$

In Equation (17.1), $J_x$ is the flux expressed in units of property area$^{-1}$ time$^{-1}$. The derivative in Equation (17.1) represents the spatial gradient of the quantity of interest (mass, energy, etc.). The linear relationship between flux and the property spatial gradient is reasonable when the displacement away from equilibrium is modest. The limit of modest displacement of the system property away from equilibrium is assumed in the remainder of this chapter.

The negative sign in Equation (17.1) indicates that the flux occurs in the opposite direction of the gradient; therefore, flux will result in a reduction of the gradient if external action is not taken to maintain the gradient. If the gradient is externally maintained at a constant value, the flux will also remain constant. Again, consider Figure 17.1, which presents a graphical example of the relationship between gradient and flux. The gas density is greatest on the left-hand side of the container such that the particle density increases as one goes from the right side of the container to the left. According to Equation (17.1), particle flux occurs in opposition to the number density gradient in an attempt to make the particle density spatially homogeneous. The final quantity of interest in Equation (17.1) is the factor $\alpha$. Mathematically, this quantity serves as the proportionality constant between the gradient and flux and is referred to as the **transport coefficient.** In the following sections, we will determine the transport coefficients for the processes listed in Table 17.1 and derive the expressions for flux involving these various transport phenomena. Although the derivations for each transport property will look different, it is important to note that all originate from Equation (17.1). That is, the underlying principle behind all transport phenomena is the relationship between flux and gradient.
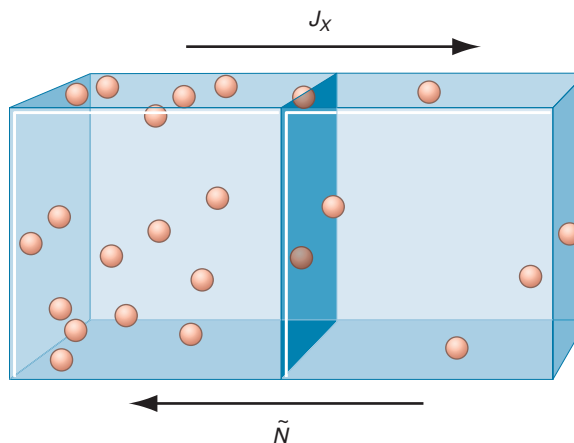


**FIGURE 17.1**
Illustration of flux. The flux $J_x$ of gas particles is in opposition to the gradient in particle number density $\tilde{N}$.

# 17.2 Mass Transport: Diffusion

**Diffusion** is the process by which particle density evolves in response to a spatial gradient in concentration. With respect to thermodynamics, this spatial gradient represents a gradient in chemical potential, and the system will relax toward equilibrium by eliminating this gradient. The first case to be considered is diffusion in an ideal gas. Diffusion in liquids will be treated later in this chapter.

Consider a gradient in gas particle number density, $\widetilde{N}$, as depicted in Figure 17.2. According to Equation (17.1), there will be a flux of gas particles in opposition to the gradient. The flux is determined by quantifying the flow of particles per unit time through an imaginary plane located at $x = 0$ with area $A$. We will refer to this plane as the *flux plane*. Two other planes are located one mean free path $\pm\lambda$ away on either side of the flux plane, and the net flux arises from particles traveling from either of these planes to the flux plane. The mean free path is the distance a particle travels on average between collisions as defined in Equation (16.39).

Figure 17.2 demonstrates that a gradient in particle number density exists in the $x$ direction such that

$$\frac{d\widetilde{N}}{dx} \neq 0$$

If the gradient in $\widetilde{N}$ were equal to zero, flux $J_x$ would also equal zero by Equation (17.1). However, this does not mean that particles are now stationary. Instead, $J_x = 0$ indicates that the flow of particles through the flux plane from left to right is exactly balanced by the flow of particles from right to left. Therefore, the flux expressed in Equation (17.1) represents the net flux, or sum of flux in each direction through the flux plane.

Equation (17.1) provides the relationship between the flux and the spatial gradient in $\widetilde{N}$. Solution of this **mass transport** problem involves determining the proportionality constant $\alpha$. This quantity is referred to as the diffusion coefficient for mass transport. To determine this constant, consider the particle number density at $\pm\lambda$:

$$\widetilde{N}(-\lambda) = \widetilde{N}(0) - \lambda\left(\frac{d\widetilde{N}}{dx}\right)_{x=0} \tag{17.2}$$

$$\widetilde{N}(\lambda) = \widetilde{N}(0) + \lambda\left(\frac{d\widetilde{N}}{dx}\right)_{x=0} \tag{17.3}$$
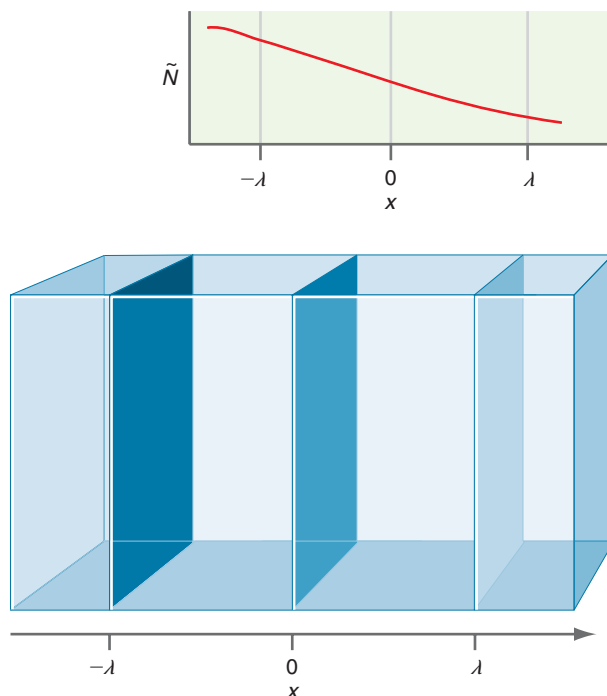


**FIGURE 17.2**
Model used to describe gas diffusion. The gradient in number density $\widetilde{N}$ results in particles diffusing from $-x$ to $+x$. The plane located at $x = 0$ is where the flux of particles in response to the gradient is calculated (the *flux plane*). Two planes, located one mean free path distance away ($\pm\lambda$) are considered with particles traveling from either of these planes to the flux plane. The total flux through the flux plane is equal to the difference in flux from the planes located at $\pm\lambda$.

These expressions state that the value of $\widetilde{N}$ away from $x = 0$ is equal to the value of $\widetilde{N}$ at $x = 0$ plus a second term representing the change in concentration as one moves toward the planes at $\pm\lambda$. Formally, Equation (17.2) and (17.3) are derived from a Taylor series expansion of the number density with respect to distance, and only the first two terms in the expansion are kept, consistent with $\lambda$ being sufficiently small such that higher order terms of the expansion can be neglected. The diffusion process can be viewed as an effusion of particles through a plane or aperture of area $A$. Effusion was described in detail in Section 16.5. Proceeding in a similar fashion to the derivation of effusion presented earlier, the number of particles, $N$, striking a given area per unit time is equal to

$$\frac{dN}{dt} = J_x \times A \tag{17.4}$$

Consider the flux of particles traveling from the plane at $-\lambda$ to the flux plane (Figure 17.2). We are interested in the number of particles striking the flux plane per unit time; therefore, we need to count only those particles traveling toward the flux plane. Again, this same problem was encountered in the section on gas effusion where the number of particles traveling toward the wall was equal to the product of number density and the average velocity in the $+x$ direction. Taking the identical approach, the flux in the $+x$ direction is given by

$$J_x = \widetilde{N} \int_0^\infty v_x f(v_x)\, dv_x$$

$$= \widetilde{N} \int_0^\infty v_x \left(\frac{m}{2\pi kT}\right)^{1/2} e^{-mv_x^2/2kT}\, dv_x$$

$$= \widetilde{N} \left(\frac{kT}{2\pi m}\right)^{1/2}$$

$$= \frac{\widetilde{N}}{4} v_{ave} \tag{17.5}$$

In this equation, we have employed the definition of $v_{ave}$ as defined in Equation (16.22). Substituting Equation (17.2) and (17.3) into the expression of Equation (17.5) for $J_x$, the flux from the planes located at $-\lambda$ and $\lambda$ is given by

$$J_{-\lambda,0} = \frac{1}{4} v_{ave} \widetilde{N}(-\lambda) = \frac{1}{4} v_{ave}\left[\widetilde{N}(0) - \lambda\left(\frac{d\widetilde{N}}{dx}\right)_{x=0}\right] \tag{17.6}$$

$$J_{\lambda,0} = \frac{1}{4} v_{ave} \widetilde{N}(\lambda) = \frac{1}{4} v_{ave}\left[\widetilde{N}(0) + \lambda\left(\frac{d\widetilde{N}}{dx}\right)_{x=0}\right] \tag{17.7}$$

The total flux through the flux plane is simply the difference in flux from the planes at $\pm\lambda$:

$$J_{Total} = J_{-\lambda,0} - J_{\lambda,0} = \frac{1}{4} v_{ave}\left(-2\lambda\left(\frac{d\widetilde{N}}{dx}\right)_{x=0}\right)$$

$$= -\frac{1}{2} v_{ave} \lambda \left(\frac{d\widetilde{N}}{dx}\right)_{x=0} \tag{17.8}$$

One correction remains before the derivation is complete. We have assumed that the particles move from the planes located at $\pm\lambda$ to the flux plane directly along the $x$ axis. However, Figure 17.3 illustrates that if the particle trajectory is not aligned with the $x$ axis, the particle will not reach the flux plane after traveling one mean free path. At this point, collisions with other particles can occur, resulting in postcollision particle trajectories away from the flux plane; therefore, these particles will not contribute to the flux. Inclusion of these trajectories requires one to take the orientational average of the mean



**FIGURE 17.3**
Particle trajectories aligned with the $x$ axis (dashed line) result in the particle traveling between planes without collision. However, trajectories not aligned with the $x$ axis (solid line) result in the particle not reaching the flux plane before a collision with another particle occurs. This collision may result in the particle being directed away from the flux plane.

free path, and this averaging results in a reduction in total flux as expressed by Equation (17.8) by a factor of 2/3. With this averaging, the total flux becomes

$$J_{total} = -\frac{1}{3}\nu_{ave}\lambda\left(\frac{d\widetilde{N}}{dx}\right)_{x=0} \qquad \textbf{(17.9)}$$

Equation (17.9) is identical to Equation (17.1), with the diffusion proportionality constant, or simply the **diffusion coefficient,** defined as follows:

$$D = \frac{1}{3}\nu_{ave}\lambda \qquad \textbf{(17.10)}$$

The diffusion coefficient has units of $m^2\,s^{-1}$ in SI units. With this definition of the diffusion coefficient, Equation (17.9) becomes

$$J_{Total} = -D\left(\frac{d\widetilde{N}}{dx}\right)_{x=0} \qquad \textbf{(17.11)}$$

Equation (17.11) is referred to as **Fick's first law** of diffusion. It is important to note that the diffusion coefficient is defined using parameters derived from gas kinetic theory first encountered in Chapter 16, namely, the average speed of the gas and the mean free path. Example Problem 17.1 illustrates the dependence of the diffusion coefficient on these parameters.

## EXAMPLE PROBLEM 17.1

Determine the diffusion coefficient for Ar at 298 K and a pressure of 1.00 atm.

### Solution

Using Equation (17.10) and the collisional cross section for Ar provided in Table 17.1,

$$D_{Ar} = \frac{1}{3}\nu_{ave,\,Ar}\lambda_{Ar}$$

$$= \frac{1}{3}\left(\frac{8RT}{\pi M_{Ar}}\right)^{1/2}\left(\frac{RT}{PN_A\sqrt{2}\sigma_{Ar}}\right)$$

$$= \frac{1}{3}\left(\frac{8(8.314\ \text{J mol}^{-1}\ \text{K}^{-1})298\ \text{K}}{\pi(0.040\ \text{kg mol}^{-1})}\right)^{1/2}\left(\left(\frac{(8.314\ \text{J mol}^{-1}\ \text{K}^{-1})298\ \text{K}}{(101{,}325\ \text{Pa})(6.022\times10^{23}\ \text{mol}^{-1})}\right)\times\frac{1}{\sqrt{2}(3.6\times10^{-19}\ \text{m}^2)}\right)$$

$$= \frac{1}{3}(397\ \text{m s}^{-1})(7.98\times10^{-8}\ \text{m})$$

$$= 1.1\times10^{-5}\ \text{m}^2\ \text{s}^{-1}$$

Transport properties of gases can be described using concepts derived from gas kinetic theory. For example, the diffusion coefficient is dependent on the mean free path, which is in turn dependent on the collisional cross section. One criticism of this approach is that parameters such as average velocity are derived using an equilibrium distribution, yet these concepts are now applied in a nonequilibrium context when discussing transport phenomena. The development presented here is performed under the assumption that the displacement of the system away from equilibrium is modest; therefore, equilibrium-based quantities remain relevant. That said, transport phenomena can be described using nonequilibrium distributions; however, the mathematical complexity of this approach is beyond the scope of this text.

With the expression for the diffusion coefficient in hand [Equation (17.10)], the relationship between this quantity and the details of the gas particles are clear. This relationship suggests that transport properties such as diffusion can be used to

determine particle parameters such as effective size as described by the collisional cross section. Example Problem 17.2 illustrates the connection between the diffusion coefficient and particle size.

---

### EXAMPLE PROBLEM 17.2

Under identical temperature and pressure conditions, the diffusion coefficient of He is roughly four times larger than that of Ar. Determine the ratio of the collisional cross sections.

### Solution

Using Equation (17.10), the ratio of diffusion coefficients (after canceling the 1/3 constant term) can be written in terms of the average speed and mean free path as follows:

$$\frac{D_{He}}{D_{Ar}} = 4 = \frac{\nu_{ave,He}\lambda_{He}}{\nu_{ave,Ar}\lambda_{Ar}}$$

$$= \frac{\left(\frac{8RT}{\pi M_{He}}\right)^{1/2}\left(\frac{RT}{P_{He}N_A\sqrt{2}\sigma_{He}}\right)}{\left(\frac{8RT}{\pi M_{Ar}}\right)^{1/2}\left(\frac{RT}{P_{Ar}N_A\sqrt{2}\sigma_{Ar}}\right)}$$

$$= \left(\frac{M_{Ar}}{M_{He}}\right)^{1/2}\left(\frac{\sigma_{Ar}}{\sigma_{He}}\right)$$

$$\left(\frac{\sigma_{He}}{\sigma_{Ar}}\right) = \frac{1}{4}\left(\frac{M_{Ar}}{M_{He}}\right)^{1/2} = \frac{1}{4}\left(\frac{39.9 \text{ g mol}^{-1}}{4.00 \text{ g mol}^{-1}}\right)^{1/2} = 0.79$$

---

Recall from Section 16.6 that the collisional cross section for a pure gas is equal to $\pi d^2$ where $d$ is the diameter of a gas particle. The ratio of collisional cross sections, determined using the diffusion coefficients, is consistent with a He diameter that is 0.89 smaller than that of Ar. However, the diameter of Ar as provided in tables of atomic radii is roughly 2.5 times greater than that of He. The origin of this discrepancy can be traced to the hard-sphere approximation for interparticle interactions.

---

## 17.3 The Time Evolution of a Concentration Gradient

As illustrated in the previous section, the existence of a concentration gradient results in particle diffusion. What is the timescale for diffusion, and how far can a particle diffuse in a given amount of time? These questions are addressed by the diffusion equation, which can be derived as follows. Beginning with Fick's first law, the particle flux is given by

$$J_x = -D\left(\frac{d\widetilde{N}(x)}{dx}\right) \tag{17.12}$$

The quantity $J_x$ in Equation (17.12) is the flux through a plane located at $x$ as illustrated in Figure 17.4. The flux at location $x + dx$ can also be written using Fick's first law:

$$J_{x+dx} = -D\left(\frac{d\widetilde{N}(x + dx)}{dx}\right) \tag{17.13}$$

The particle density at $(x + dx)$ is related to the corresponding value at $x$ as follows:

$$\widetilde{N}(x + dx) = \widetilde{N}(x) + dx\left(\frac{d\widetilde{N}(x)}{dx}\right) \tag{17.14}$$

This equation is derived by keeping the first two terms in the Taylor series expansion of number density with distance equivalent to the procedure described earlier for obtaining



$J_x$     $J_{x+dx}$

$x$     $x+dx$

**FIGURE 17.4**

Depiction of flux through two separate planes. If $J_x = J_{x+dx}$, then the concentration between the planes will not change. However, if the fluxes are unequal, then the concentration will change with time.

Equation (17.2) and (17.3). Substituting Equation (17.14) into Equation (17.13), the flux through the plane at $(x + dx)$ becomes

$$J_{x+dx} = -D\left(\frac{d\widetilde{N}(x)}{dx} + \left(\frac{d^2\widetilde{N}(x)}{dx^2}\right)dx\right) \qquad (17.15)$$

Consider the space between the two flux planes illustrated in Figure 17.4. The change in particle density in this region of space depends on the difference in flux through the two planes. If the fluxes are identical, the particle density will remain constant in time. However, a difference in flux will result in an evolution in particle number density as a function of time. The flux is equal to the number of particles that pass through a given area per unit time. If the area of the two flux planes is equivalent, then the difference in flux is directly proportional to the difference in number density. This relationship between the time dependence of the number density and the difference in flux is expressed as follows:

$$\frac{\partial\widetilde{N}(x,t)}{\partial t} = \frac{\partial(J_x - J_{x+dx})}{\partial x}$$

$$= \frac{\partial}{\partial x}\left[-D\left(\frac{\partial\widetilde{N}(x,t)}{\partial x}\right) - \left(-D\left(\left(\frac{\partial\widetilde{N}(x,t)}{\partial x}\right) + \left(\frac{\partial^2\widetilde{N}(x,t)}{\partial x^2}\right)\partial x\right)\right)\right]$$

$$\frac{\partial\widetilde{N}(x,t)}{\partial t} = D\frac{\partial^2\widetilde{N}(x,t)}{\partial x^2} \qquad (17.16)$$

Equation (17.16) is called the **diffusion equation,** and is also known as **Fick's second law of diffusion.** Notice that $\widetilde{N}$ depends on both position $x$ and time $t$. Equation (17.16) demonstrates that the time evolution of the concentration gradient is proportional to the second derivative of the spatial gradient in concentration. That is, the greater the "curvature" of the concentration gradient, the faster the relaxation will proceed. Equation (17.16) is a differential equation that can be solved using standard techniques and a set of initial conditions (see Crank entry in the Further Reading section at the end of the chapter) resulting in the following expression for $\widetilde{N}(x,t)$:

$$\widetilde{N}(x,t) = \frac{N_0}{2A(\pi Dt)^{1/2}}e^{-x^2/4Dt} \qquad (17.17)$$

In this expression, $N_0$ represents the initial number of molecules confined to a plane at $t = 0$, $A$ is the area of this plane, $x$ is distance away from the plane, and $D$ is the diffusion coefficient. Equation (17.17) can be viewed as a distribution function that describes the probability of finding a particle at time $t$ at a plane located a distance $x$ away from the initial plane at $t = 0$. An example of the spatial variation in $\widetilde{N}$ versus time is provided in Figure 17.5 for a species with $D = 10^{-5}$ m$^2$ s$^{-1}$, roughly equivalent to the diffusion coefficient of Ar at 298 K and 1 atm. The figure demonstrates that with an increase in time, $\widetilde{N}$ increases at distances farther away from the initial plane (located at 0 m in Figure 17.5).

Similar to other distribution functions encountered thus far, it is more convenient to use a metric or benchmark value that provides a measure of $\widetilde{N}(x,t)$ as opposed to describing the entire distribution. The primary metric employed to describe $\widetilde{N}(x,t)$ is the root-mean-square (rms) displacement, determined using what should by now be a familiar approach:

$$x_{rms} = \langle x^2 \rangle^{1/2} = \left[\frac{A}{N_0}\int_{-\infty}^{\infty} x^2\widetilde{N}(x,t)dx\right]^{1/2}$$

$$= \left[\frac{A}{N_0}\int_{-\infty}^{\infty} x^2\frac{N_0}{2A(\pi Dt)^{1/2}}e^{-x^2/4Dt}\,dx\right]^{1/2}$$

$$= \left[\frac{1}{2(\pi Dt)^{1/2}}\int_{-\infty}^{\infty} x^2 e^{-x^2/4Dt}\,dx\right]^{1/2}$$

$$x_{rms} = \sqrt{2Dt} \qquad (17.18)$$
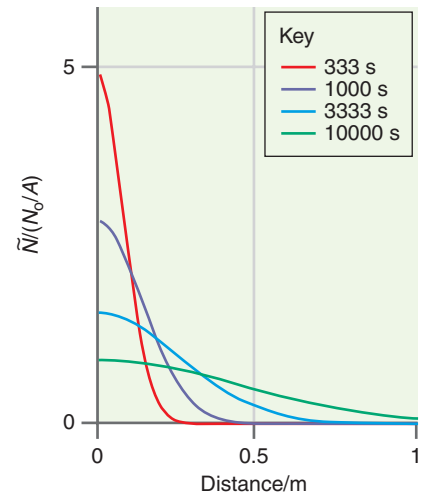


**FIGURE 17.5**
The spatial variation in particle number density $\widetilde{N}(x,t)$ as a function of time. The number density is defined with respect to $N_0/A$, the number of particles confined to a plane located at $x = 0$ of area $A$. In this example, $D = 10^{-5}$ m$^2$s$^{-1}$, a typical value for a gas at 1 atm and 298 K (see Example Problem 17.1). The corresponding diffusion time for a given concentration profile is indicated.

Notice that the rms displacement increases as the square root of both the diffusion coefficient and time. Equation (17.18) represents the rms displacement in a single dimension. For diffusion in three dimensions, the corresponding term $r_{rms}$ can be determined using the Pythagorean theorem under the assumption that diffusion is equivalent in all three dimensions:

$$r_{rms} = \sqrt{6Dt} \qquad (17.19)$$

The diffusion relationships derived in this section and the previous section involved gases and employed concepts from gas kinetic theory. However, these relationships are also applicable to diffusion in solution, as will be demonstrated later in this chapter.

### EXAMPLE PROBLEM 17.3

Determine $x_{rms}$ for a particle where $D = 1.00 \times 10^{-5}$ m$^2$ s$^{-1}$ for diffusion times of 1000. and 10,000. s.

### Solution

Employing Equation (17.18):

$$x_{rms,\ 1000\ s} = \sqrt{2\ Dt} = \sqrt{2(1.00 \times 10^{-5}\ \text{m}^2\ \text{s}^{-1})(1000\ \text{s})} = 0.141\ \text{m}$$

$$x_{rms,\ 10,000\ s} = \sqrt{2\ Dt} = \sqrt{2(1.00 \times 10^{-5}\ \text{m}^2\ \text{s}^{-1})(10,000\ \text{s})} = 0.447\ \text{m}$$

The diffusion coefficient employed in this example is equivalent to that used in Figure 17.5, and the rms displacements determined here can be compared to the spatial variation in $\widetilde{N}(x, t)$ depicted in the figure to provide a feeling for the $x_{rms}$ distance versus the overall distribution of particle diffusion distances versus time.

# 17.4 Statistical View of Diffusion

In deriving Fick's first law of diffusion, a gas particle was envisioned to move a distance equal to the mean free path before colliding with another particle. After this collision, memory of the initial direction of motion is lost and the particle is free to move in the same or a new direction until the next collision occurs. This conceptual picture of particle motion is mathematically described by the statistical approach to diffusion. In the statistical approach, illustrated in Figure 17.6a, particle diffusion is also modeled as a series of discrete displacements or steps, with the direction of one step being uncorrelated with that of the previous step. That is, once the particle has taken a step, the direction of the next step is random. A series of such steps is referred to as a **random walk.**

In the previous section we determined the probability of finding a particle at a distance $x$ away from the origin after a certain amount of time. The statistical model of diffusion can be connected directly to this idea using the random walk model. Consider a particle undergoing a random walk along a single dimension $x$ such that the particle moves one step in either the $+x$ or $-x$ direction (Figure 17.6b). After a certain number of steps, the particle will have taken $\Delta$ total steps with $\Delta_-$ steps in the $-x$ direction and $\Delta_+$ steps in the $+x$ direction. The probability that the particle will have traveled a distance $X$ from the origin is related to the weight associated with that distance, as given by the following expression:

$$W = \frac{\Delta!}{\Delta_+!\Delta_-!} = \frac{\Delta!}{\Delta_+!(\Delta - \Delta_+)!} \qquad (17.20)$$



(a)



$-x$      0      $+x$

(b)
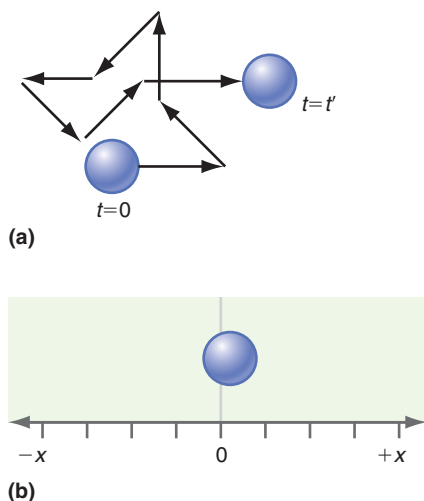
**FIGURE 17.6**
(a) Illustration of a random walk. Diffusion of the particle is modeled as a series of discrete steps (each arrow); the length of each step is the same, but the direction of the step is random. (b) Illustration of the one-dimensional random walk model.

Equation (17.20) is identical to the weight associated with observing a certain number of heads after tossing a coin $\Delta$ times, as discussed in Chapter 13. This similarity is not a coincidence—the one-dimensional random walk model is very much like tossing a coin. Each outcome of a coin toss is independent of the previous outcome, and only one of two outcomes is possible per toss. Evaluation of Equation (17.20) requires an expression for $\Delta_+$ in terms of $\Delta$. This relationship can be derived by recognizing that $X$ is equal to the difference in the number of steps in the $+x$ and $-x$ direction:

$$X = \Delta_+ - \Delta_- = \Delta_+ - (\Delta - \Delta_+) = 2\Delta_+ - \Delta$$

$$\frac{X + \Delta}{2} = \Delta_+$$

With this definition for $\Delta_+$, the expression for $W$ becomes

$$W = \frac{\Delta!}{\left(\dfrac{\Delta + X}{2}\right)!\left(\Delta - \dfrac{\Delta + X}{2}\right)!} = \frac{\Delta!}{\left(\dfrac{\Delta + X}{2}\right)!\left(\dfrac{\Delta - X}{2}\right)!} \qquad (17.21)$$

The probability of the particle being a distance $X$ away from the origin is given by the weight associated with this distance divided by the total weight, $2^\Delta$, such that

$$P = \frac{W}{W_{Total}} = \frac{W}{2^\Delta} \propto e^{-X^2/2\Delta} \qquad (17.22)$$

The final proportionality can be derived by evaluation of Equation (17.21) using Stirling's approximation. Recall from the solution to the diffusion equation in the previous section that the distance a particle diffuses away from the origin was also proportional to an exponential term:

$$\widetilde{N}(x, t) \propto e^{-x^2/4Dt} \qquad (17.23)$$

In Equation (17.23), $x$ is the actual diffusion distance, $D$ is the diffusion coefficient, and $t$ is time. For these two pictures of diffusion to converge on the same physical result, the exponents must be equivalent such that

$$\frac{x^2}{4Dt} = \frac{X^2}{2\Delta} \qquad (17.24)$$

At this point, the random walk parameters $X$ and $\Delta$ must be expressed in terms of the actual quantities of diffusion distance $x$ and total diffusion time $t$. The total number of random walk steps is expressed as the total diffusion $t$ time divided by the time per random walk step $\tau$:

$$\Delta = \frac{t}{\tau} \qquad (17.25)$$

In addition, $x$ can be related to the random walk displacement $X$ by using a proportionality constant $x_o$ that represents the average distance in physical space a particle traverses between collisions such that

$$x = Xx_o \qquad (17.26)$$

With these definitions for $\Delta$ and $X$, substitution into Equation (17.24) results in the following definition of $D$:

$$D = \frac{x_o^2}{2\tau} \qquad (17.27)$$

Equation (17.27) is the **Einstein–Smoluchowski equation.** The importance of this equation is that it relates a macroscopic quantity $D$ to microscopic aspects of the diffusion as described by the random walk model. For reactions in solution, $x_o$ is generally taken to be the particle diameter. Using this definition and the experimental value for $D$, the timescale associated with each random walk event can be determined.

The diffusion coefficient of liquid benzene is $2.2 \times 10^{-5}$ cm$^2$ s$^{-1}$. Given an estimated molecular diameter of 0.3 nm, what is the timescale for a random walk?

**Solution**

Rearranging Equation (17.27), the time per random walk step is

$$t = \frac{x_o^2}{2D} = \frac{(0.3 \times 10^{-9} \text{ m})^2}{2(2.2 \times 10^{-9} \text{ m}^2 \text{ s}^{-1})} = 2 \times 10^{-11} \text{ s}$$

This is an extremely short time, only 20 ps! This example illustrates that, on average, the diffusional motion of a benzene molecule in the liquid phase is characterized by short-range translational motion between frequent collisions with neighboring molecules.

The Einstein–Smoluchowski equation can also be related to gas diffusion described previously. If we equate $x_o$ with the mean free path $\lambda$ and define the time per step as the average time it takes a gas particle to translate one mean free path $\lambda/\nu_{ave}$, then the diffusion coefficient is given by

$$D = \frac{\lambda^2}{2\left(\dfrac{\lambda}{\nu_{ave}}\right)} = \frac{1}{2}\lambda\nu_{ave}$$

This is exactly the same expression for $D$ derived from gas kinetic theory in the absence of the 2/3 correction for particle trajectories as discussed earlier. That is, the statistical and kinetic theory viewpoints of diffusion provide equivalent descriptions of gas diffusion.

# 17.5 Thermal Conduction

**Thermal conduction** is the transport process in which energy migrates in response to a gradient in temperature. Figure 17.7 depicts a collection of identical gas particles for which a gradient in temperature exists. Note that the gradient is with respect to temperature only, and that the particle number density is the same throughout the box. Equilibrium is reached when the system has an identical temperature in all regions of the box. Because temperature and kinetic energy are related, relaxation toward equilibrium will involve the transport of kinetic energy from the high-temperature side of the box to the lower temperature side.

Thermal conduction occurs through a variety of mechanisms, depending on the phase of matter. In this derivation we assume that energy transfer occurs during particle collisions and that equilibrium with the energy gradient is established after each collision, thereby ensuring that the particles are at equilibrium with the gradient after each collision. This collisional picture of energy transfer is easy to envision for a gas; however, it can also be applied to liquids and solids. In these phases, molecules do not translate freely, yet the molecular energy can be transferred through collisions with nearby molecules, resulting in energy transfer. In addition to collisional energy transfer, energy can also be transferred through convection or radiative transfer. In convection, differences in density resulting from the temperature gradient can produce convection currents. Although energy is still transferred through collisional events when the particles in the currents collide with other particles, particle migration is not random such that transfer through convection is physically distinct from collisional transport as we have defined it. In radiative transfer, matter is treated as a blackbody that is capable of emitting and absorbing electromagnetic radiation. Radiation from higher temperature matter is absorbed by lower temperature matter, resulting in energy transfer. Both convection and radiative transfer are assumed to be negligible here.
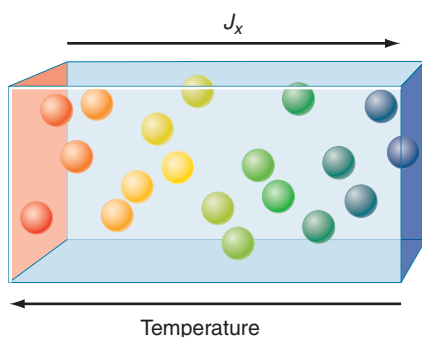


**FIGURE 17.7**

Temperature gradient in a collection of gas particles. Regions containing high kinetic energy particles are red and low kinetic energy regions are blue. The gradient in kinetic energy, and therefore temperature, is indicated, and the flux in energy in response to this gradient, $J_x$, is also shown.

The problem of thermal conduction is approached in exactly the same manner as for diffusion. The process begins by considering energy transfer for an ideal monatomic gas. Recall from statistical mechanics and thermodynamics that the average translational energy of a monatomic gas particle is $3/2 \, kT$. In addition to translational energy, diatomic and polyatomic molecules can carry more energy in rotational and vibrational energetic degrees of freedom, and our treatment will be extended to these more complex molecules shortly. Kinetic energy is transferred when the flux plane is struck by particles from one side of the plane. In this collision, energy is transmitted from one side of the flux plane to the other. It is important to note that the particle number density is equivalent throughout the box such that mass transfer does not occur. Energy transport and the relaxation toward thermal equilibrium are accomplished through molecular collisions, not diffusion.

Using techniques identical to those employed in Section 17.2 to describe diffusion, the energy at planes located $\pm\lambda$ away from the flux plane (Figure 17.8) is

$$\varepsilon(-\lambda) = \varepsilon(0) - \lambda\left(\frac{d\varepsilon}{dx}\right)_{x=0} \tag{17.28}$$

$$\varepsilon(\lambda) = \varepsilon(0) + \lambda\left(\frac{d\varepsilon}{dx}\right)_{x=0} \tag{17.29}$$

Proceeding in a manner identical to the derivation in Section 17.2 for diffusion, the flux is defined as

$$J_x = \widetilde{N}\varepsilon(x)\int_0^\infty v_x f(v_x)\,dv_x = \frac{1}{4}\widetilde{N}\varepsilon(x)v_{ave} \tag{17.30}$$

In Equation (17.30), $\widetilde{N}$ is the number density of gas particles, which is constant (recall that there is no spatial gradient in number density, only energy). Substituting Equation (17.28) and (17.29) into Equation (17.30) yields the following expression for the flux in energy from planes located $\pm\lambda$ from the flux plane:

$$J_{-\lambda,0} = \frac{1}{4}v_{ave}\widetilde{N}\varepsilon(-\lambda) \tag{17.31}$$

$$J_{\lambda,0} = \frac{1}{4}v_{ave}\widetilde{N}\varepsilon(\lambda) \tag{17.32}$$
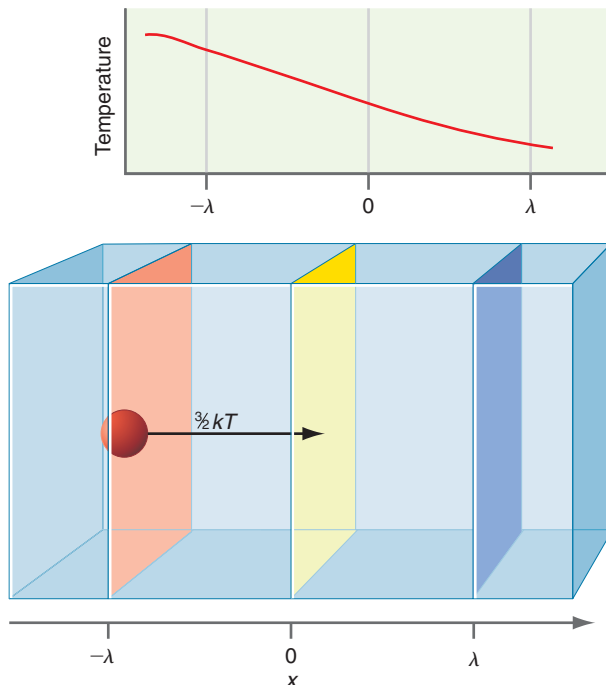


**FIGURE 17.8**
Model used to determine the thermal conductivity of a gas. The gradient in temperature will result in the transfer of kinetic energy from regions of high temperature (indicated by the red plane) to regions of lower temperature (indicated by the blue plane). The plane located at $x = 0$ is the location at which the flux of kinetic energy in response to the gradient is determined. Two planes, located one mean free path away ($\pm\lambda$) from the flux plane, are established, with particles traveling from one of these planes to the flux plane. Energy is transferred via collisional events at the flux plane.

The total energy flux is given by the difference between Equation (17.31) and (17.32):

$$
\begin{aligned}
J_{Total} &= J_{-\lambda,0} - J_{\lambda,0} \\
&= \frac{1}{4} v_{ave} \widetilde{N} (\varepsilon(-\lambda) - \varepsilon(\lambda)) \\
&= \frac{1}{4} v_{ave} \widetilde{N} \left( -2\lambda \left( \frac{d\varepsilon}{dx} \right)_{x=0} \right) \\
&= -\frac{1}{2} v_{ave} \widetilde{N} \lambda \left( \left( \frac{d\left( \frac{3}{2}kT \right)}{dx} \right)_{x=0} \right) \\
&= -\frac{3}{4} k v_{ave} \widetilde{N} \lambda \left( \frac{dT}{dx} \right)_{x=0}
\end{aligned}
\tag{17.33}
$$

After multiplying the total flux by 2/3 for orientational averaging of the particle trajectories, the expression for total flux through the flux plane becomes

$$
J_{Total} = -\frac{1}{2} k v_{ave} \widetilde{N} \lambda \left( \frac{dT}{dx} \right)_{x=0}
\tag{17.34}
$$

Equation (17.34) describes the total energy flux for an ideal monatomic gas, where the energy transferred per collision is $3/2\ kT$. The expression for total flux can be defined in terms of molar heat capacity, $C_{V,m}$, by recognizing that the constant volume molar heat capacity for a monatomic gas is $3/2\ R$; therefore,

$$
\frac{C_{V,m}}{N_A} = \frac{3}{2}k \text{ (for an ideal monatomic gas)}
$$

With this substitution, the flux can be expressed in terms of the $C_{V,m}$ for the species of interest and is not restricted to monatomic species. Employing this identity, the final expression for total energy flux is

$$
J_{Total} = -\frac{1}{3} \frac{C_{V,m}}{N_A} v_{ave} \widetilde{N} \lambda \left( \frac{dT}{dx} \right)_{x=0}
\tag{17.35}
$$

Comparison of Equation (17.35) to the general relationship between flux and gradient of Equation (17.1) dictates that the proportionality constant for energy transfer, referred to as the **thermal conductivity** $\kappa$ be given by

$$
\kappa = \frac{1}{3} \frac{C_{V,m}}{N_A} v_{ave} \widetilde{N} \lambda
\tag{17.36}
$$

Unit analysis of Equation (17.36) reveals that $\kappa$ has units of $J\ K^{-1}\ m^{-1}\ s^{-1}$. Every factor in the expression for thermal conductivity is known from thermodynamics or gas kinetic theory such that the evaluation of $\kappa$ is relatively straightforward for gases. For fluids, thermal conductivity still serves as the proportionality constant between the net flux in energy and the gradient in temperature; however, a simple expression similar to Equation (17.36) does not exist. The appearance of the mean free path in Equation (17.36) demonstrates that similar to the diffusion coefficient, the thermal conductivity can be used to estimate the hard-sphere radius of gases, as Example Problem 17.5 illustrates.

## EXAMPLE PROBLEM 17.5

The thermal conductivity of Ar at 300. K and 1 atm pressure is $0.0177\ J\ K^{-1}\ m^{-1}\ s^{-1}$. What is the collisional cross section of Ar assuming ideal gas behavior?

### Solution

The collisional cross section is contained in the mean free path. Rearranging Equation (17.36) to isolate the mean free path, we obtain

$$
\lambda = \frac{3\kappa}{\left( \dfrac{C_{V,m}}{N_A} \right) v_{ave} \widetilde{N}}
$$

The thermal conductivity is provided, and the other terms needed to calculate $\lambda$ are as follows:

$$\frac{C_{V,m}}{N_A} = \frac{\frac{3}{2}R}{N_A} = \frac{3}{2}k = 2.07 \times 10^{-23} \text{ J K}^{-1}$$

$$\nu_{ave} = \left(\frac{8RT}{\pi M}\right)^{1/2} = 398 \text{ m s}^{-1}$$

$$\widetilde{N} = \frac{N}{V} = \frac{N_A P}{RT} = 2.45 \times 10^{25} \text{m}^{-3}$$

With these quantities, the mean free path is

$$\lambda = \frac{3(0.0177 \text{ J K}^{-1} \text{ m}^{-1} \text{ s}^{-1})}{(2.07 \times 10^{-23}\text{J K}^{-1})(398 \text{ m s}^{-1})(2.45 \times 10^{25}\text{m}^{-3})} = 2.63 \times 10^{-7}\text{m}$$

Using the definition of the mean free path (Section 16.7), the collisional cross section is

$$\sigma = \frac{1}{\sqrt{2}\widetilde{N}\lambda} = \frac{1}{\sqrt{2}(2.45 \times 10^{25}\text{m}^{-3})(2.63 \times 10^{-7}\text{m})}$$

$$= 1.10 \times 10^{-19} \text{ m}^2$$

This value for the collisional cross section corresponds to a particle diameter of 187 pm (pm $= 10^{-12}$ m), which is remarkably close to the 194 pm value provided by the tabulated atomic radii of Ar.

The thermal conductivity of a material is dependent on $\nu_{ave}$, $\widetilde{N}$, and $\lambda$, quantities that are dependent on temperature and pressure. Therefore, $\kappa$ will also demonstrate temperature and pressure dependence. Predictions regarding the dependence of $\kappa$ on $T$ and $P$ can be made within the gas kinetic theory approach used to describe the gas particles. With respect to pressure, $\lambda$ is inversely proportional to $\widetilde{N}$ such that the mean free path will decrease with pressure:

$$\lambda = \left(\frac{RT}{PN_A}\right)\frac{1}{\sqrt{2}\sigma} = \left(\frac{V}{N}\right)\frac{1}{\sqrt{2}\sigma} = \frac{1}{\widetilde{N}\sqrt{2}\sigma}$$

The product of the mean free path and $\widetilde{N}$ results in the absence of $\widetilde{N}$ dependence in Equation (17.36), leading to the surprising result that $\kappa$ is predicted to be independent of pressure. Figure 17.9 illustrates the pressure dependence of $\kappa$ for $N_2$ and Ar at 300 K. The figure demonstrates that $\kappa$ is indeed essentially independent of pressure up to 50 atm! At elevated pressures, the intermolecular forces between gas molecules become appreciable, resulting in failure of the hard-sphere model, and the expressions derived using gas kinetic theory are not applicable. This region is indicated by the dramatic rise in $\kappa$ at high pressures. The pressure dependence of $\kappa$ is also observed at very low pressure, when the mean free path is greater than the dimensions of the container. In this case, the energy is transported from one side of the container to the other by wall–particle collisions such that $\kappa$ increases with pressure in this low-pressure regime.

With respect to the temperature dependence of $\kappa$, the cancellation of $\widetilde{N}$ with the mean free path results in only $\nu_{ave}$ and $C_{V, m}$ carrying temperature dependence. For a monatomic gas, $C_{V, m}$ is expected to demonstrate minimal temperature dependence. Therefore, the $\nu_{ave}$ term in Equation (17.36) predicts that $\kappa$ is proportional to $T^{1/2}$. Identical behavior is predicted for diatomic and polyatomic molecules in which the temperature dependence of $C_{V, m}$ is minimal. Figure 17.10 presents the variation in $\kappa$ with temperature for $N_2$ and Ar at 1 atm. Also presented is the predicted $T^{1/2}$ dependence of $\kappa$. The comparison between the experimental and predicted temperature dependence demonstrates that $\kappa$ increases more rapidly with temperature than the predicted $T^{1/2}$ dependence due to the presence of intermolecular interactions that are neglected in the hard-sphere approximation employed in gas kinetic theory. Notice that differences between the predicted and experimental $\kappa$ are evident at low temperature
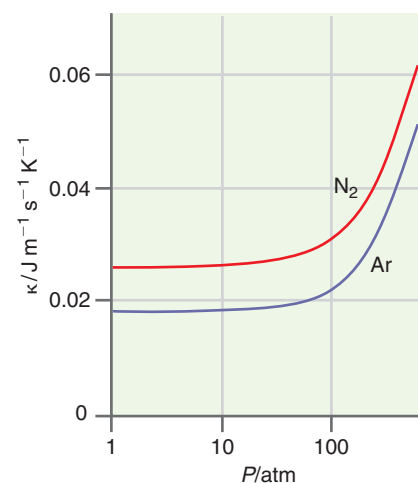
**FIGURE 17.9**
Thermal conductivity as a function of pressure for $N_2$ and Ar at 300 K. Note that the pressure scale is logarithmic. The figure demonstrates that $\kappa$ is roughly independent of pressure up to 50 atm.
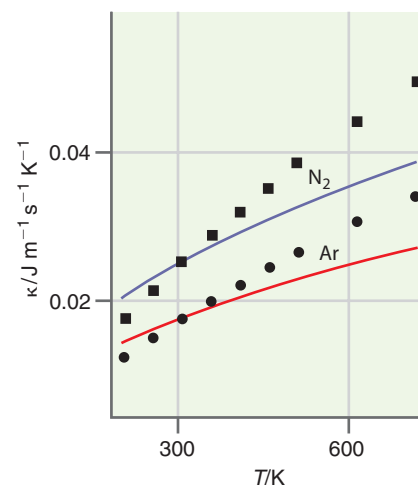
**FIGURE 17.10**
Variation of $\kappa$ with temperature for $N_2$ and Ar at 1 atm. Experimental data are indicated by the squares and circles, and the predicted $T^{1/2}$ dependence as the solid lines. The calculated $\kappa$ was set equal to the experimental value at 300 K, and then $T^{1/2}$ dependence was applied to generate the predicted variation in $\kappa$ with temperature.

as well, as opposed to the good agreement between the predicted and experimental behavior of $\kappa$ with pressure evident in Figure 17.9.

# 17.6 Viscosity of Gases
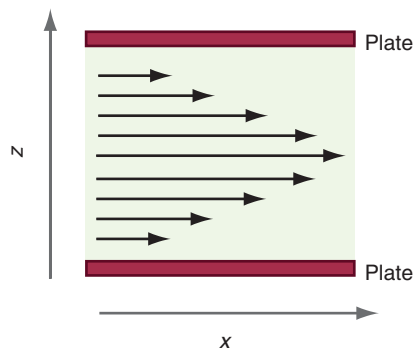


**FIGURE 17.11**
Cross section of a fluid flowing between two plates. The fluid is indicated by the green area between the plates, with arrow lengths representing the speed of the fluid.

The third transport phenomenon considered is that of linear momentum. Practical experience provides an intuitive guide with respect to this area of transport. Consider the flow of a gas through a pipe under pressure. Some gases will flow more easily than others, and the property that characterizes resistance of flow is **viscosity,** represented by the symbol $\eta$ (lowercase Greek eta). What does viscosity have to do with linear momentum? Figure 17.11 provides a cutaway view of a gas flowing between two plates. It can be shown experimentally that the velocity of the gas, $v_x$, is greatest midway between the plates and decreases as the gas approaches either plate with $v_x = 0$ at the fluid–plate boundary. Therefore, a gradient in $v_x$ exists along the coordinate orthogonal to the direction of flow ($z$ in Figure 17.11). Because the linear momentum in the $x$ direction is $mv_x$, a gradient in linear momentum must also exist.

We assume that the gas flow is **laminar flow,** meaning that the gas can be decomposed into layers of constant speed as illustrated in Figure 17.11. This regime will exist for most gases and some liquids provided the flow rate is not too high (see Problem P17.18 at the end of the chapter). At high flow rates, the **turbulent flow** regime is reached where the layers are intermixed such that a clear dissection of the gas in terms of layers of the same speed cannot be performed. The discussion presented here is limited to conditions of laminar flow.

The analysis of linear momentum transport proceeds in direct analogy to diffusion and thermal conductivity. As illustrated in Figure 17.11, a gradient in linear momentum exists in the $z$ direction; therefore, planes of similar linear momentum are defined parallel to the direction of fluid flow as illustrated in Figure 17.12. The transfer of linear momentum occurs by a particle from one momentum layer colliding with the flux plane and thereby transferring its momentum to the adjacent layer.

To derive the relationship between flux and the gradient in linear momentum, we proceed in a fashion analogous to that used to derive diffusion (Section 17.2) and thermal conductivity (Section 17.5). First, the linear momentum $p$ at $\pm\lambda$ is given by

$$p(-\lambda) = p(0) - \lambda\left(\frac{dp}{dz}\right)_{z=0} \tag{17.37}$$

$$p(\lambda) = p(0) + \lambda\left(\frac{dp}{dz}\right)_{z=0} \tag{17.38}$$
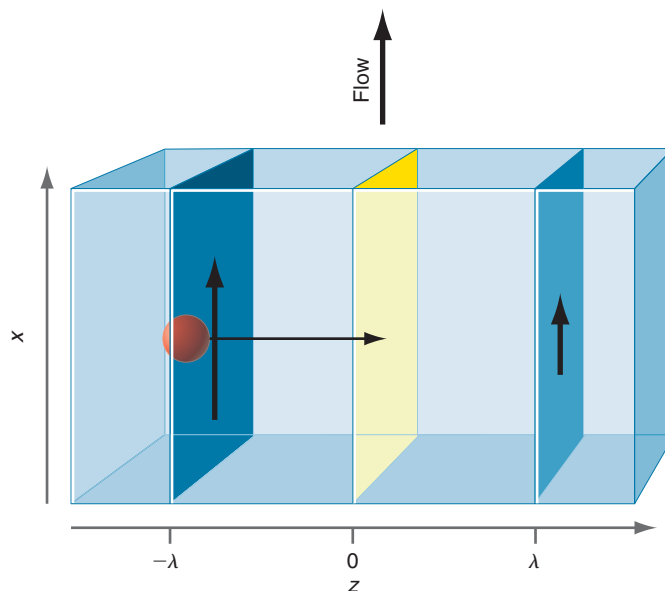
**FIGURE 17.12**
Parameterization of the box model used to derive viscosity. Planes of identical particle velocity ($v_x$) are given by the blue planes, with the magnitude of velocity given by the arrows. The gradient in linear momentum will result in momentum transfer from regions of high momentum (darker blue plane) to regions of lower momentum (indicated by the light blue plane). The plane located at $z = 0$ is the location at which the flux of linear momentum in response to the gradient is determined.

Proceeding just as before for diffusion and thermal conduction, the flux in linear momentum from each plane located at $\pm\lambda$ to the flux plane is

$$J_{-\lambda,0} = \frac{1}{4} \nu_{ave} \widetilde{N} p(-\lambda) \tag{17.39}$$

$$J_{\lambda,0} = \frac{1}{4} \nu_{ave} \widetilde{N} p(\lambda) \tag{17.40}$$

The total flux is the difference between Equations (17.39) and (17.40):

$$\begin{aligned}
J_{Total} &= \frac{1}{4} \nu_{ave} \widetilde{N} \left( -2\lambda \left( \frac{dp}{dz} \right)_{z=0} \right) \\
&= -\frac{1}{2} \nu_{ave} \widetilde{N} \lambda \left( \frac{d(m\nu_x)}{dz} \right)_{z=0} \\
&= -\frac{1}{2} \nu_{ave} \widetilde{N} \lambda m \left( \frac{d\nu_x}{dz} \right)_{z=0}
\end{aligned} \tag{17.41}$$

Finally, Equation (17.41) is multiplied by 2/3 as a result of orientational averaging of the particle trajectories, resulting in the final expression for the total flux in linear momentum:

$$J_{Total} = -\frac{1}{3} \nu_{ave} \widetilde{N} \lambda m \left( \frac{d\nu_x}{dz} \right)_0 \tag{17.42}$$

Comparison to Equation (17.1) indicates that the proportionality constant between flux and the gradient in velocity is defined as

$$\eta = \frac{1}{3} \nu_{ave} \widetilde{N} \lambda m \tag{17.43}$$

Equation (17.43) represents the viscosity of the gas $\eta$ given in terms of parameters derived from gas kinetic theory. The units of viscosity are the poise (P), or 0.1 kg m$^{-1}$ s$^{-1}$. Notice the quantity 0.1 in the conversion to SI units. Viscosities are generally reported in $\mu$P ($10^{-6}$ P) for gases and cP ($10^{-2}$ P) for liquids.

---

### EXAMPLE PROBLEM 17.6

The viscosity of Ar is 227 $\mu$P at 300. K and 1 atm. What is the collisional cross section of Ar assuming ideal gas behavior?

#### Solution

Because the collisional cross section is related to the mean free path, Equation (17.43) is first rearranged as follows:

$$\lambda = \frac{3\eta}{\nu_{ave} \widetilde{N} m}$$

Next, we evaluate each term separately, then use these terms to calculate the mean free path:

$$\nu_{ave} = \left( \frac{8RT}{\pi M} \right)^{1/2} = 398 \text{ m s}^{-1}$$

$$\widetilde{N} = \frac{PN_A}{RT} = 2.45 \times 10^{25} \text{m}^{-3}$$

$$m = \frac{M}{N_A} = \frac{0.040 \text{ kg mol}^{-1}}{6.022 \times 10^{23} \text{ mol}^{-1}} = 6.64 \times 10^{-26} \text{ kg}$$
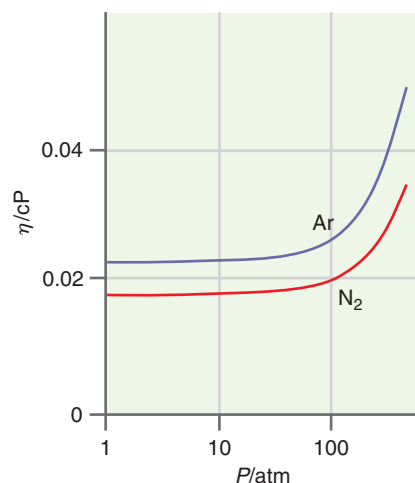
**FIGURE 17.13**
Pressure dependence of $\eta$ for gaseous $N_2$ and Ar at 300 K.
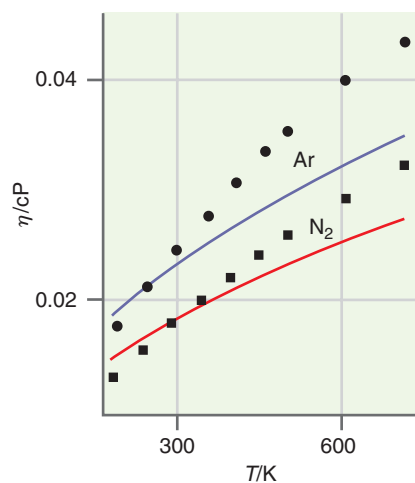


**FIGURE 17.14**
Temperature dependence of $\eta$ for $N_2$ and Ar at 1 atm. Experimental values are given by the squares and circles, and the predicted $T^{1/2}$ dependence is given as the solid line.

$$\lambda = \frac{3\eta}{\nu_{ave}\widetilde{N}m} = \frac{3(277 \times 10^{-6}\,\mathrm{P})}{(398\,\mathrm{m\,s^{-1}})(2.45 \times 10^{25}\,\mathrm{m^{-3}})(6.64 \times 10^{-26}\,\mathrm{kg})}$$

$$= \frac{3(227 \times 10^{-7}\,\mathrm{kg\,m^{-1}\,s^{-1}})}{(398\,\mathrm{m\,s^{-1}})(2.45 \times 10^{25}\,\mathrm{m^{-3}})(6.64 \times 10^{-26}\,\mathrm{kg})} = 1.28 \times 10^{-7}\,\mathrm{m}$$

Note the conversion of poise to SI units in the last step. Using the definition of the mean free path, the collisional cross section can be determined:

$$\sigma = \frac{1}{\sqrt{2}\widetilde{N}\lambda} = \frac{1}{\sqrt{2}(2.45 \times 10^{25}\,\mathrm{m^{-3}})(1.28 \times 10^{-7}\,\mathrm{m})} = 2.25 \times 10^{-19}\,\mathrm{m^2}$$

In Example Problem 17.5, the thermal conductivity of Ar provided an estimate for the collisional cross section that was roughly 1/2 this value. The discrepancy between collisional cross-section values determined using two different measured transport properties illustrates the approximate nature of the treatment presented here. Specifically, we have assumed that the intermolecular interactions are well modeled by the hard-sphere approximation. The difference in $\sigma$ suggests that attractive forces are also important in describing the interaction of particles during collisions.

Similar to thermal conductivity, viscosity is dependent on $\nu_{ave}$, $\widetilde{N}$, and $\lambda$, quantities that are both temperature and pressure dependent. Both $\widetilde{N}$ and $\lambda$ demonstrate pressure dependence, but the product of $\widetilde{N}$ and $\lambda$ contains no net $\widetilde{N}$ dependence; therefore, $\eta$ is predicted to be independent of pressure. Figure 17.13 presents the pressure dependence of $\eta$ for $N_2$ and Ar at 300 K. The behavior is almost identical to that observed for thermal conductivity (Figure 17.9), with $\eta$ demonstrating little pressure dependence until $P \sim 50$ atm. At elevated pressures, intermolecular interactions become important, and the increased interaction between particles gives rise to a substantial increase in $\eta$ for $P > 50$ atm, similar to the case for thermal conductivity.

With respect to the temperature dependence of $\eta$, the $\nu_{ave}$ term in Equation (17.43) dictates that $\eta$ should increase as $T^{1/2}$, identical to the temperature dependence of thermal conductivity (Figure 17.10). This result is perhaps a bit surprising since liquids demonstrate a decrease in $\eta$ with an increase in temperature. However, the predicted increase in $\eta$ with temperature for a gas is borne out by experiment, as illustrated in Figure 17.14 where the variation in $\eta$ with temperature for $N_2$ and Ar at 1 atm is presented. Also shown is the predicted $T^{1/2}$ dependence. The prediction of increased viscosity with temperature is a remarkable confirmation of gas kinetic theory. However, comparison of the experimental and predicted temperature dependence demonstrates that $\eta$ increases more rapidly than predicted due to the presence of intermolecular interactions that are neglected in the hard-sphere model, similar to the discussion of the temperature dependence of $\kappa$ provided earlier. The increase in $\eta$ with temperature for a gas is consistent with the increase in velocity accompanying a rise in temperature and corresponding increase in momentum flux.

# 17.7 Measuring Viscosity

Viscosity is a measure of a fluid's resistance to flow; therefore, it is not surprising that the viscosity of gases and liquids is measured using flow. Viscosity is typically measured by monitoring the flow of a fluid through a tube with the underlying idea that the greater the viscosity, the smaller the flow through the tube. The following equation was derived by Poiseuille to describe flow of a liquid through a round tube under conditions of laminar flow:

$$\frac{\Delta V}{\Delta t} = \frac{\pi r^4}{8\eta}\left(\frac{P_2 - P_1}{x_2 - x_1}\right) \tag{17.44}$$

This equation is referred to as **Poiseuille's law.** In Equation (17.44), $\Delta V/\Delta t$ represents the volume of fluid $\Delta V$ that passes through the tube in a specific amount of time $\Delta t$, $r$ is the radius of the tube through which the fluid flows, $\eta$ is the fluid viscosity, and the factor in parentheses represents the macroscopic pressure gradient over the tube length. Notice that the fluid flow rate is dependent on the radius of the tube and is also inversely proportional to fluid viscosity. As anticipated, the more viscous the fluid, the smaller the flow rate. The flow of an ideal gas through a tube is given by

$$\frac{\Delta V}{\Delta t} = \frac{\pi r^4}{16\eta L P_0}(P_2^2 - P_1^2) \tag{17.45}$$

where $L$ is the length of the tube, $P_2$ and $P_1$ are the pressures at the entrance and exit of the tube, respectively, and $P_0$ is the pressure at which the volume is measured (and is equal to $P_1$ if the volume is measured at the end of the tube).

## EXAMPLE PROBLEM 17.7

Gas cylinders of $CO_2$ are sold in terms of weight of $CO_2$. A cylinder contains 50 lb (22.7 kg) of $CO_2$. How long can this cylinder be used in an experiment that requires flowing $CO_2$ at 293 K ($\eta = 146\ \mu P$) through a 1.00-m-long tube (diameter $= 0.75$ mm) with an input pressure of 1.05 atm and output pressure of 1.00 atm? The flow is measured at the tube output.

### Solution

Using Equation (17.45), the gas flow rate $\Delta V/\Delta t$ is

$$\frac{\Delta V}{\Delta t} = \frac{\pi r^4}{16\eta L P_0}(P_2^2 - P_1^2)$$

$$= \frac{\pi(0.375 \times 10^{-3}\ \text{m})^4}{16(1.46 \times 10^{-5}\ \text{kg m}^{-1}\ \text{s}^{-1})(1.00\ \text{m})(101{,}325\ \text{Pa})}$$

$$\times ((106{,}391\ \text{Pa})^2 - (101{,}325\ \text{Pa})^2)$$

$$= 2.76 \times 10^{-6}\ \text{m}^3\ \text{s}^{-1}$$

Converting the $CO_2$ contained in the cylinder to the volume occupied at 298 K and 1 atm pressure, we get

$$n_{CO_2} = 22.7\ \text{kg}\left(\frac{1}{0.044\ \text{kg mol}^{-1}}\right) = 516\ \text{mol}$$

$$V = \frac{nRT}{P} = 1.24 \times 10^4\ \text{L}\left(\frac{10^{-3}\ \text{m}^3}{\text{L}}\right) = 12.4\ \text{m}^3$$

Given the effective volume of $CO_2$ contained in the cylinder, the duration over which the cylinder can be used is

$$\frac{12.4\ \text{m}^3}{2.76 \times 10^{-6}\ \text{m}^3\ \text{s}^{-1}} = 4.49 \times 10^6\ \text{s}$$

This time corresponds to roughly 52 days.

A convenient tool for measuring the viscosity of liquids is an **Ostwald viscometer** (Figure 17.15). To determine the viscosity, one measures the time it takes for the liquid level to fall from the "high" level mark to the "low" level mark, and the fluid flows through a thin capillary that ensures laminar flow. The pressure driving the liquid through the capillary is $\rho gh$, where $\rho$ is the fluid density, $g$ is the acceleration due to gravity, and $h$ is the difference in liquid levels in the two sections of the viscometer, as illustrated in the figure. Because the height difference will evolve as the fluid flows,



High

Low

$h$

Capillary
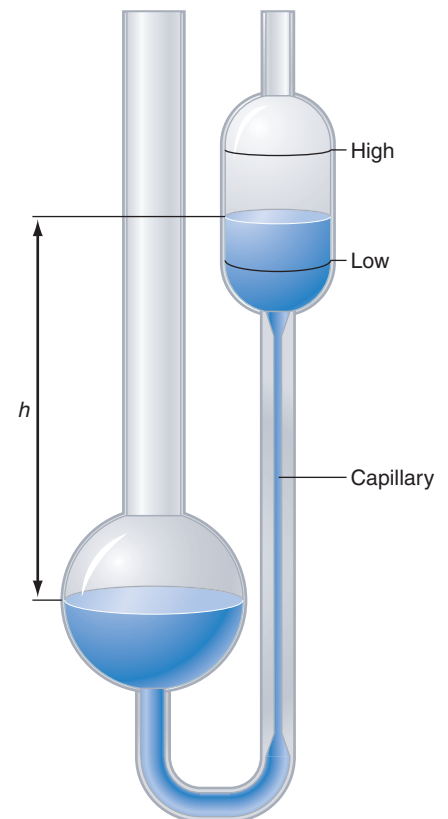
**FIGURE 17.15**
An Ostwald viscometer. The time for a volume of fluid ($\Delta V$) to flow from the "High" level mark to the "Low" level mark is measured and then used to determine the viscosity of the fluid by means of Equation (17.47).

*h* represents an average height. Because $\rho g h$ is the pressure generating flow, Equation (17.44) can be rewritten as follows:

$$\frac{\Delta V}{\Delta t} = \frac{\pi r^4}{8\eta} \frac{\rho g h}{(x_2 - x_1)} = \frac{\pi r^4}{8\eta} \frac{\rho g h}{l} \tag{17.46}$$

where *l* is the length of the capillary. This equation can be rearranged:

$$\eta = \left(\frac{\pi r^4}{8} \frac{gh}{\Delta V l}\right) \rho \Delta t = A \rho \Delta t \tag{17.47}$$

In Equation (17.47), *A* is known as the viscometer constant and is dependent on the geometry of the viscometer. All of the viscometer parameters can be determined through careful measurement of the viscometer dimensions; however, the viscometer constant is generally determined by calibration using a fluid of known density and viscosity.

# 17.8 Diffusion in Liquids and Viscosity of Liquids

The concept of random motion resulting in particle diffusion was evidenced in the famous microscopy experiments of Robert Brown performed in 1827. (An excellent account of this work can be found in *The Microscope* 40 [1992]: 235–241.) In these experiments, Brown took ~5 $\mu$m-diameter pollen grains suspended in water, and using a microscope he was able to see that the particles were "very evidently in motion." After performing experiments to show that the motion was not from convection or evaporation, Brown concluded that the motion was associated with the particle itself. This apparently random motion of the pollen grain is referred to as **Brownian motion,** and this motion is actually the diffusion of a large particle in solution.

Consider Figure 17.16 where a particle of mass *m* is embedded in a liquid having viscosity $\eta$. The motion of the particle is driven by collisions with liquid particles, which will provide a time-varying force, $F(t)$. We decompose $F(t)$ into its directional components and focus on the component in the *x* direction, $F_x(t)$. Motion of the particle in the *x* direction will result in a frictional force due to the liquid's viscosity:

$$F_{fr,x} = -f v_x = -f\left(\frac{dx}{dt}\right) \tag{17.48}$$

The negative sign in Equation (17.48) indicates that the frictional force is in opposition to the direction of motion. In Equation (17.48), *f* is referred to as the friction coefficient and is dependent on both the geometry of the particle and the viscosity of the fluid. The total force on the particle is simply the sum of the collisional and frictional forces:

$$F_{total,x} = F_x(t) + F_{fr,x}$$

$$m\left(\frac{d^2 x}{dt^2}\right) = F_x(t) - f\left(\frac{dx}{dt}\right) \tag{17.49}$$
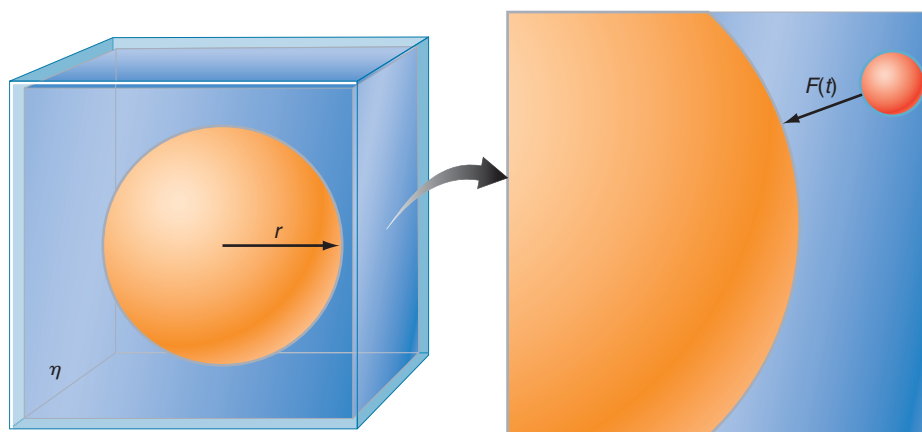


**FIGURE 17.16**
Illustration of Brownian motion. A spherical particle with radius *r* is embedded in a liquid of viscosity $\eta$. The particle undergoes collisions with solvent molecules (the red dot in the right-hand figure) resulting in a time-varying force, $F(t)$, that initiates particle motion. Particle motion is opposed by a frictional force that is dependent on the solvent viscosity.

This differential equation was studied in 1905 by Einstein, who demonstrated that when averaged over numerous fluid–particle collisions the average square displacement of the particle in a specific amount of time $t$ is given by

$$\langle x^2 \rangle = \frac{2kTt}{f} \qquad (17.50)$$

where $k$ is Boltzmann's constant and $T$ is temperature. If the particle undergoing diffusion is spherical, the frictional coefficient is given by

$$f = 6\pi\eta r \qquad (17.51)$$

such that

$$\langle x^2 \rangle = 2\left(\frac{kT}{6\pi\eta r}\right)t \qquad (17.52)$$

Comparison of this result to the value of $\langle x^2 \rangle$ determined by the diffusion equation [Equation (17.18)] dictates that the term in parentheses is the diffusion coefficient $D$ given by

$$D = \frac{kT}{6\pi\eta r} \qquad (17.53)$$

Equation (17.53) is the **Stokes–Einstein equation** for diffusion of a spherical particle. This equation states that the diffusion coefficient is dependent on the viscosity of the medium, the size of the particle, and the temperature. This form of the Stokes–Einstein equation is applicable to diffusion in solution when the radius of the diffusing particle is significantly greater than the radius of a liquid particle. For diffusion of a particle in a fluid of similar size, experimental data demonstrate that Equation (17.53) should be modified as follows:

$$D = \frac{kT}{4\pi\eta r} \qquad (17.54)$$

Equation (17.54) can also be used for **self-diffusion,** in which the diffusion of a single solvent molecule in the solvent itself occurs.

## EXAMPLE PROBLEM 17.8

Hemoglobin is a protein responsible for oxygen transport. The diffusion coefficient of human hemoglobin in water at 298 K ($\eta = 0.891$ cP) is $6.90 \times 10^{-11}$ m$^2$ s$^{-1}$. Assuming this protein can be approximated as spherical, what is the radius of hemoglobin?

### Solution

Rearranging Equation (17.53) and paying close attention to units, the radius is

$$r = \frac{kT}{6\pi\eta D} = \frac{(1.38 \times 10^{-23}\ \text{J K}^{-1})(298\ \text{K})}{6\pi(0.891 \times 10^{-3}\ \text{kg m}^{-1}\ \text{s}^{-1})(6.90 \times 10^{-11}\ \text{m}^2\ \text{s}^{-1})}$$

$$= 3.55\ \text{nm}$$

X-ray crystallographic studies of hemoglobin have shown that this globular protein can be approximated as a sphere having a radius of 2.75 nm. One reason for this discrepancy is that in aqueous solution, hemoglobin will have associated water, which is expected to increase the effective size of the particle relative to the crystallographic measurement.

Unlike gases, the dependence of fluid viscosity on temperature is difficult to explain theoretically. The primary reason for this is that, on average, the distance between particles in a liquid is small, and intermolecular interactions become important when describing particle interactions. As a general rule, the stronger the intermolecular interactions in a liquid, the greater the viscosity of the liquid. With respect to temperature, liquid viscosities increase as the temperature decreases. The reason for this behavior is that as the temperature

is reduced, the kinetic energy of the particles is also reduced, and the particles have less kinetic energy to overcome the potential energy arising from intermolecular interactions, resulting in the fluid being more resistant to flow.

# 17.9 Sedimentation and Centrifugation

An important application of transport phenomena in liquids is **sedimentation.** Sedimentation can be used with diffusion to determine the molecular weights of macromolecules. Figure 17.17 depicts a molecule with mass $m$ undergoing sedimentation in a liquid of density $\rho$ under the influence of Earth's gravitational field. Three distinct forces are acting on the particle:

1. The frictional force: $F_{fr} = -f\text{v}_x$
2. The gravitational force: $F_{gr} = mg$
3. The buoyant force: $F_b = -m\overline{V}\rho g$

In the expression for the buoyant force, $\overline{V}$ is the **specific volume** of the solute, equal to the change in solution volume per mass of solute in units of $cm^3 \ g^{-1}$.

Imagine placing the particle at the top of the solution and then letting it fall. Initially, the downward velocity $(\text{v}_x)$ is zero, but the particle will accelerate and the velocity will increase. Eventually, a particle velocity will be reached where the frictional and buoyant forces are balanced by the gravitational force. This velocity is known as the terminal velocity, and when this velocity is reached the particle acceleration is zero. Using Newton's second law,

$$F_{Total} = ma = F_{fr} + F_{gr} + F_b$$

$$0 = -f\text{v}_{x,ter} + mg - m\overline{V}\rho g$$

$$\text{v}_{x,ter} = \frac{mg(1 - \overline{V}\rho)}{f}$$

$$\overline{s} = \frac{\text{v}_{x,ter}}{g} = \frac{m(1 - \overline{V}\rho)}{f} \qquad (17.55)$$



**FIGURE 17.17**
Illustration of the forces involved in sedimentation of a particle; $F_{fr}$ is the frictional force, $F_{gr}$ is the gravitational force, and $F_b$ is the buoyant force.

The **sedimentation coefficient** $\overline{s}$ is defined as the terminal velocity divided by the acceleration due to gravity. Sedimentation coefficients are generally reported in the units of Svedbergs (S) with $1 \ S = 10^{-13}$ s; however, we will use units of seconds to avoid confusion with other units in upcoming sections of this chapter.

Sedimentation is generally not performed using acceleration due to Earth's gravity. Instead, acceleration of the particle is accomplished using a **centrifuge,** with ultracentrifuges capable of producing accelerations on the order of $10^5$ times the acceleration due to gravity. In centrifugal sedimentation, the acceleration is equal to $\varpi^2 x$ where $\varpi$ is the angular velocity (radians $s^{-1}$) and $x$ is the distance of the particle from the center of rotation. During centrifugal sedimentation, the particles will also reach a terminal velocity that depends on the acceleration due to centrifugation, and the sedimentation coefficient is expressed as

$$\overline{s} = \frac{\text{v}_{x,ter}}{\varpi^2 x} = \frac{m(1 - \overline{V}\rho)}{f} \qquad (17.56)$$

## EXAMPLE PROBLEM 17.9

The sedimentation coefficient of lysozyme ($M = 14{,}100 \ g \ mol^{-1}$) in water at 20°C is $1.91 \times 10^{-13}$ s and the specific volume is 0.703 $cm^3 \ g^{-1}$. The density of water at this temperature is 0.998 $g \ cm^{-3}$ and $\eta = 1.002$ cP. Assuming lysozyme is spherical, what is the radius of this protein?

### Solution

The frictional coefficient is dependent on molecular radius. Solving Equation (17.56) for $f$, we obtain

$$f = \frac{m(1 - \overline{V}\rho)}{\overline{s}} = \frac{\dfrac{(14{,}100 \text{ g mol}^{-1})}{(6.022 \times 10^{23} \text{ mol}^{-1})}\left(1 - (0.703 \text{ mL g}^{-1})(0.998 \text{ g mL}^{-1})\right)}{1.91 \times 10^{-13} \text{ s}}$$

$$= 3.66 \times 10^{-8} \text{ g s}^{-1}$$

The frictional coefficient is related to the radius for a spherical particle by Equation (17.51) such that

$$r = \frac{f}{6\pi\eta} = \frac{3.66 \times 10^{-8} \text{ g s}^{-1}}{6\pi(1.002 \text{ g m}^{-1} \text{ s}^{-1})} = 1.94 \times 10^{-9} \text{ m} = 1.94 \text{ nm}$$

One method for measurement of macromolecular sedimentation coefficients is by centrifugation, as illustrated in Figure 17.18. In this process, an initially homogeneous solution of macromolecules is placed in a centrifuge and spun. Sedimentation occurs, resulting in regions of the sample farther away from the axis of rotation experiencing an increase in macromolecule concentrations and a corresponding reduction in concentration for the sample regions closest to the axis of rotation. A boundary between these two concentration layers will be established, and this boundary will move away from the axis of rotation with time in the centrifuge. If we define the $x_b$ as the midpoint of the **boundary layer** (Figure 17.18), the following relationship exists between the location of the boundary layer and centrifugation time:

$$\overline{s} = \frac{v_{x,ter}}{\varpi^2 x} = \frac{\dfrac{dx_b}{dt}}{\varpi^2 x_b}$$

$$\varpi^2\overline{s}\int_0^t dt = \int_{x_{b,t=0}}^{x_{b,t}} \frac{dx_b}{x_b}$$

$$\varpi^2\overline{s}t = \ln\left(\frac{x_{b,t}}{x_{b,t=0}}\right) \tag{17.57}$$

Equation (17.57) suggests that a plot of $\ln(x_b/x_{b,t=0})$ versus time will yield a straight line with slope equal to $\varpi^2$ times the sedimentation coefficient. The determination of sedimentation coefficients by boundary centrifugation is illustrated in Example Problem 17.10.

---

### EXAMPLE PROBLEM 17.10

The sedimentation coefficient of lysozyme is determined by centrifugation at 55,000 rpm in water at 20°C. The following data were obtained regarding the location of the boundary layer as a function of time:

| Time (min) | $x_b$ (cm) |
|:----------:|:----------:|
| 0 | 6.00 |
| 30 | 6.07 |
| 60 | 6.14 |
| 90 | 6.21 |
| 120 | 6.28 |
| 150 | 6.35 |

Using these data, determine the sedimentation coefficient of lysozyme in water at 20°C.



(a)

(b)
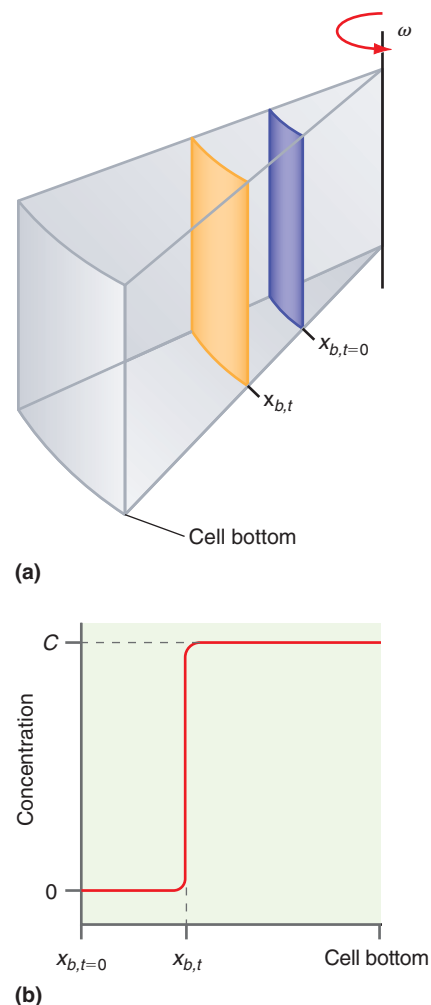
**FIGURE 17.18**
Determination of sedimentation coefficient by centrifugation. (**a**) Schematic drawing of the centrifuge cell, which is rotating with angular velocity $\varpi$. The blue plane at $x_{b,t=0}$ is the location of the solution meniscus before centrifugation. As the sample is centrifuged, a boundary between the solution with increased molecular concentration versus the solvent is produced. This boundary is represented by the yellow plane at $x_{b,t}$. (**b**) As centrifugation proceeds, the boundary layer will move toward the cell bottom. A plot of $\ln(x_{b,t}/x_{b,t=0})$ versus time will yield a straight line with slope equal to $\varpi^2$ times the sedimentation coefficient.

**Solution**

First, we transform the data to determine $\ln(x_b/x_{b,t=0})$ as a function of time:

| Time (min) | $x_b$ (cm) | $(x_b/x_{b,t=0})$ | $\ln(x_b/x_{b,t=0})$ |
|:---:|:---:|:---:|:---:|
| 0 | 6.00 | 1 | 0 |
| 30 | 6.07 | 1.01 | 0.00995 |
| 60 | 6.14 | 1.02 | 0.01980 |
| 90 | 6.21 | 1.03 | 0.02956 |
| 120 | 6.28 | 1.04 | 0.03922 |
| 150 | 6.35 | 1.05 | 0.04879 |

The plot of $\ln(x_b/x_{b,t=0})$ versus time is shown here:
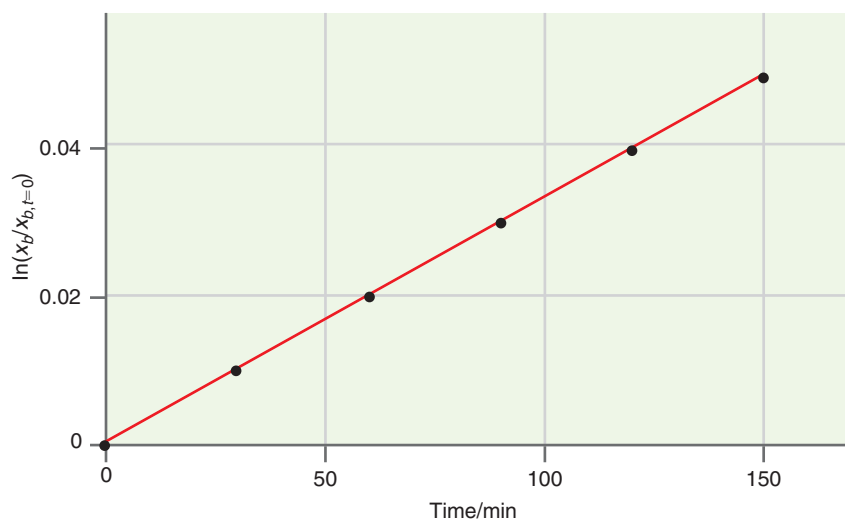


The slope of the line in the preceding plot is $3.75 \times 10^{-4}$ min$^{-1}$, which is equal to $\varpi^2$ times the sedimentation coefficient:

$$3.75 \times 10^{-4} \text{ min}^{-1} = 6.25 \times 10^{-6} \text{ s}^{-1} = \varpi^2 \bar{s}$$

$$\bar{s} = \frac{6.25 \times 10^{-6} \text{ s}^{-1}}{\varpi^2} = \frac{6.25 \times 10^{-6} \text{ s}^{-1}}{((55,000 \text{ rev min}^{-1})(2\pi \text{ rad rev}^{-1})(0.0167 \text{ min s}^{-1}))^2}$$

$$\bar{s} = 1.88 \times 10^{-13} \text{ s}$$

Finally with knowledge of the sedimentation coefficient and diffusion coefficient, the molecular weight of a macromolecule can be determined. Equation (17.56) can be rearranged to isolate the frictional coefficient:

$$f = \frac{m(1 - \overline{V}\rho)}{\bar{s}} \tag{17.58}$$

The frictional coefficient can also be expressed in terms of the diffusion coefficient [Equations (17.51) and (17.53)]:

$$f = \frac{kT}{D} \tag{17.59}$$

Setting Equations (17.58) and Equation (17.59) equal, the weight of the molecule is given by

$$m = \frac{kT\bar{s}}{D(1 - \overline{V}\rho)} \quad \text{or} \quad M = \frac{RT\bar{s}}{D(1 - \overline{V}\rho)} \tag{17.60}$$

Equation (17.60) dictates that with the sedimentation and diffusion coefficients, as well as the specific volume of the molecule, the molecular weight of a macromolecule can be determined.

# 17.10 Ionic Conduction

**Ionic conduction** is a transport phenomenon in which electrical charge in the form of electrons or ions migrates under the influence of an electrical potential. The amount of charge that migrates is equal to the electrical current $I$, which is defined as the amount of charge $Q$ migrating in a given time interval:

$$I = \frac{dQ}{dt} \tag{17.61}$$

The unit used for current is the ampere (A), which is equal to one coulomb of charge per second:

$$1\ A = 1\ C\ s^{-1} \tag{17.62}$$

Recall that the charge on an electron is $1.60 \times 10^{-19}$ C. Therefore, 1.00 A of current corresponds to the flow of $6.25 \times 10^{18}$ electrons in one second. Current can also be quantified by the current density $j$ defined as the amount of current that flows through a conductor of cross-sectional area $A$ (Figure 17.19):

$$j = \frac{I}{Area} \tag{17.63}$$

In the remainder of this section, the cross-sectional area will be written as $Area$ rather than $A$ to avoid confusion with amperes.

   The migration of charge is initiated by the presence of an electrical force, created by an electrical field. In Figure 17.19, the electric field across the conductor is generated using a battery. The current density is proportional to the magnitude of the electric field $E$, and the proportionality constant is known as the **electrical conductivity** $\kappa$:

$$j = \kappa E \tag{17.64}$$

Unfortunately, by convention thermal conductivity and electrical conductivity are both denoted by the symbol $\kappa$. Therefore, we will use the terms *thermal* or *electrical* when discussing conductivity to avoid confusion. Electrical conductivity has units of siemens per meter, or S m$^{-1}$, where 1 S equals $1\Omega^{-1}$ (ohm$^{-1}$). Finally, the **resistivity** $\rho$ of a material is the inverse of the electrical conductivity:

$$\rho = \frac{1}{\kappa} = \frac{E}{j} \tag{17.65}$$

Resistivity is expressed in units of $\Omega$ m. Consider Figure 17.19 in which an electric field $E$ is applied to a cylindrical conductor with a cross-sectional area and length $l$. If the cylinder is homogeneous in composition, the electric field and current density will be equivalent throughout the conductor, allowing us to write:

$$E = \frac{V}{l} \tag{17.66}$$

$$j = \frac{I}{Area} \tag{17.67}$$
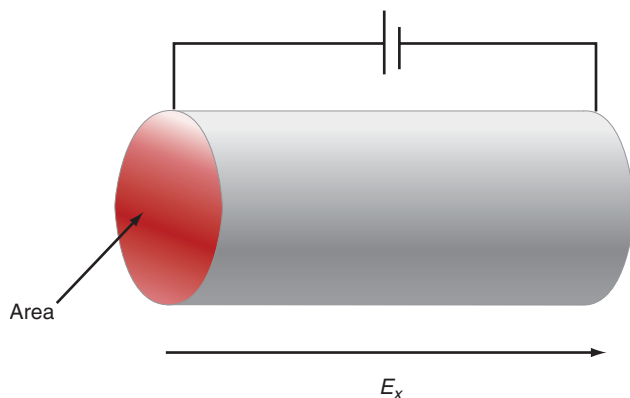


**FIGURE 17.19**
Cross section of a current-carrying conductor. The conductor cross-sectional area is indicated by the shaded area. The direction of the applied electric field $E_x$ created by the battery is also shown.

In Equation (17.66), $V$ is the magnitude of the electric potential difference between the ends of the conductor, commonly referred to as the voltage. Substituting Equation (17.66) and (17.67) into the expression for resistivity, Equation (17.65), yields the following:

$$\rho = \frac{1}{\kappa} = \left(\frac{V}{I}\right)\frac{Area}{l} = R\frac{Area}{l} \tag{17.68}$$

In Equation (17.68), Ohm's law was used to rewrite $V/I$ as $R$, the resistance. This equation demonstrates that the resistivity is proportional to the resistance of the material $R$ in units of $\Omega$ with a proportionality constant that is equal to the area $A$ of the conductor cross section divided by the conductor length $l$.

How is electrical conductivity related to transport? Again, consider the application of a battery to a conductor as shown in Figure 17.19. The battery will produce an electric field inside the conductor, and the direction of the electric field is taken to be the $x$ direction. The electric field is related to the gradient in the electrical potential as follows:

$$E_x = -\frac{d\phi}{dx} \tag{17.69}$$

Using this definition, Equation (17.64) becomes

$$\frac{1}{Area}\frac{dQ}{dt} = -\kappa\frac{d\phi}{dx} \tag{17.70}$$

The left-hand side of Equation (17.70) is simply the flux of charge through the conductor in response to the gradient in electrical potential. Comparison of Equation (17.70) to Equation (17.1) demonstrates that ionic conductivity is described exactly as other transport processes. The proportionality constant between the potential gradient and flux in charge is the electrical conductivity.

Insight into the nature of charge transport in solution can be obtained by measuring the conductivity of ion-containing solutions. Measurements are usually performed using a conductivity cell, which is simply a container in which two electrodes of well-defined area and spacing are placed, and into which a solution of electrolyte is added (Figure 17.20). The resistance of the conductivity cell is generally measured using alternating currents to limit the buildup of electrolysis products at the electrodes. The resistance of the cell is measured using a Wheatstone bridge as illustrated in Figure 17.20. The operating principle behind this circuit is that when the two "arms" of
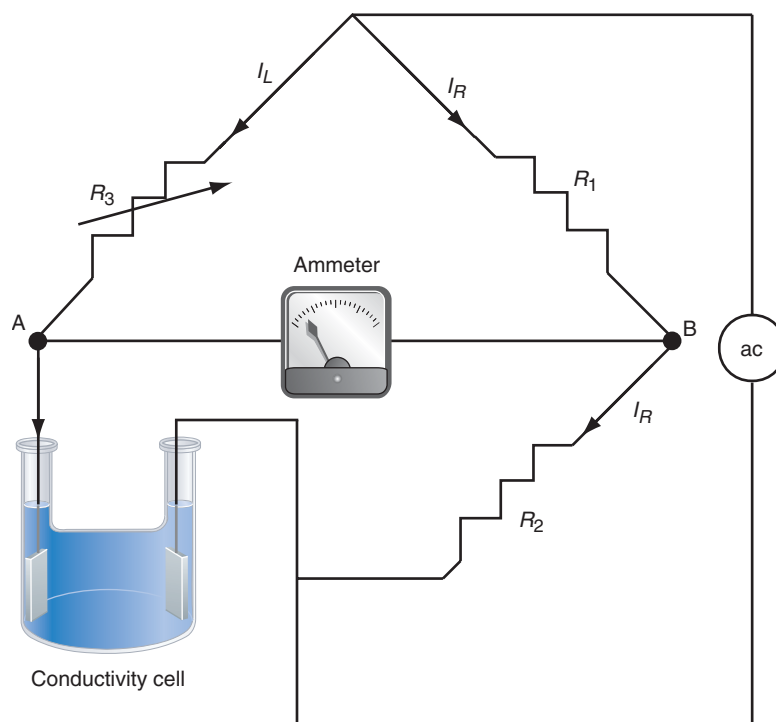


**FIGURE 17.20**
Schematic of the electrical circuit used to perform electrical conductivity measurements. The solution of interest is placed in the conductivity cell, which is placed in one arm of a Wheatstone bridge circuit, which includes $R_3$ and the cell. Resistor $R_3$ is adjusted until no current flows between points A and B. Under these conditions, the resistance of the cell can be determined.

the bridge have equal resistance, no current will flow between points A and B. In the experiment, the resistance of $R_3$ is varied until this occurs. Under these conditions, the resistance of the cell is given by

$$R_{cell} = \frac{R_2 R_3}{R_1} \qquad \textbf{(17.71)}$$

If the resistance of the cell is measured, the electrical conductivity of the solution can be determined using Equation (17.68).

The electrical conductivity of a solution depends on the number of ions present. The conductivity of ionic solutions is expressed as the **molar conductivity** $\Lambda_m$, which is defined as follows:

$$\Lambda_m = \frac{\kappa}{c} \qquad \textbf{(17.72)}$$

where $c$ is the molar concentration of electrolyte. The molar conductivity has units of $S \, m^2 \, mol^{-1}$. If $\kappa$ is linearly proportional to electrolyte concentration, then the molar conductivity will be independent of concentration. Figure 17.21 presents the measured molar conductivity for a variety of electrolytes as a function of concentration in water at 25°C. Two trends are immediately evident. First, none of the electrolytes demonstrates a concentration-independent molar conductivity. Second, the concentration dependence of the various species indicates that electrolytes can be divided into two categories. In the first category are **strong electrolytes,** which demonstrate a modest decrease in molar conductivity with an increase in concentration. In Figure 17.21, HCl, NaCl, KCl, and $CuSO_4$ are all strong electrolytes. In the second category are **weak electrolytes** represented by $CH_3COOH$ in Figure 17.21. The molar conductivity of a weak electrolyte is comparable to a strong electrolyte at low concentration but decreases rapidly with increased concentration. Note that a given species can behave as either a weak or strong electrolyte depending on the solvent employed. In the remainder of this section, we discuss the underlying physics behind the conductivity of strong and weak electrolytes.

## 17.10.1 Strong Electrolytes

The central difference between weak and strong electrolytes is the extent of ion formation in solution. Strong electrolytes, including ionic solids (e.g., KCl) and strong acids/bases (e.g., HCl), exist as ionic species in solution, and the electrolyte concentration is directly related to the concentration of ionic species in solution.
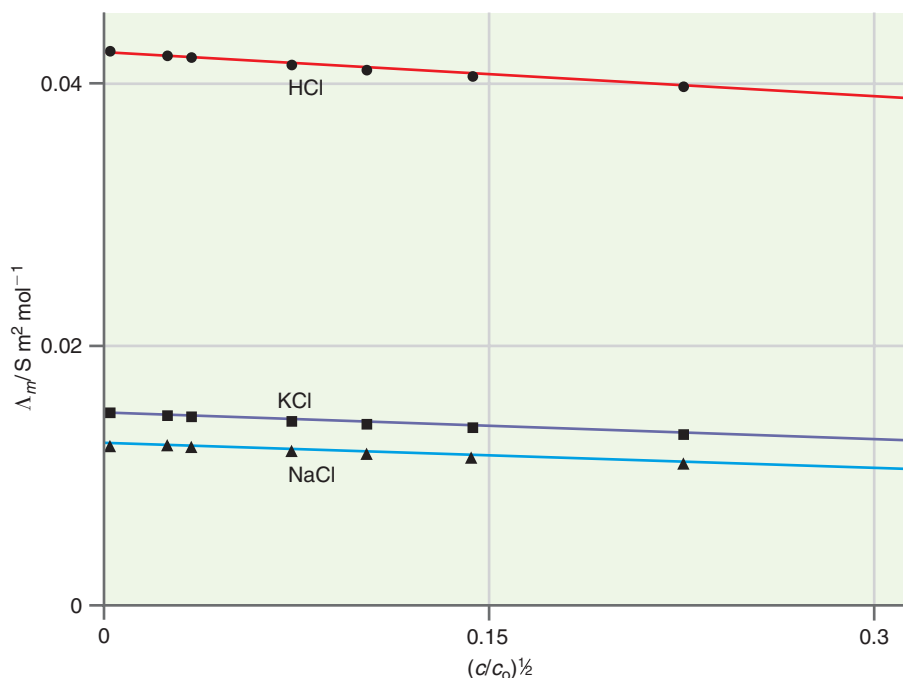
In 1900, Kohlrausch demonstrated that the concentration dependence of the molar conductivity for strong electrolytes is well described by the following equation:

$$\Lambda_m = \Lambda_m^0 - K\sqrt{\frac{c}{c_0}} \tag{17.73}$$

This equation, known as **Kohlrausch's law,** states that the molar conductivity for strong electrolytes decreases as the square root of concentration, with slope given by the quantity $K$. The slope is found to depend more on the stoichiometry of the electrolyte (AB, $AB_2$, etc.) than composition. In Equation (17.73), $\Lambda_m^0$ is the molar conductivity at infinite dilution and represents the expected molar conductivity if interionic interactions were entirely absent. Clearly, any measurement at "infinite" dilution is impossible to perform; however, Kohlrausch's law demonstrates that $\Lambda_m^0$ can be readily determined by plotting $\Lambda_m$ as a function of the square root of concentration (referenced to a standard concentration $c_0$, generally 1 M), and then extrapolating to $c = 0$. Figure 17.22 presents the molar conductivity of HCl, KCl, and NaCl originally presented in Figure 17.21, but now shown with $\Lambda_m$ plotted as a function of $(c/c_0)^{1/2}$. The solid line is a fit to the data using Kohlrausch's law, and it demonstrates the ability of this equation to reproduce the concentration dependence of $\Lambda_m$ for strong electrolytes.

Kohlrausch was also able to demonstrate that for strong electrolytes, the molar conductivity at infinite dilution can be described in terms of contributions from the individual ionic constituents as follows:

$$\Lambda_m^0 = \nu_+\lambda_+ + \nu_-\lambda_- \tag{17.74}$$

In Equation (17.74), $\nu_+$ and $\nu_-$ are the number of positively and negatively charged species, respectively, in the formula weight of the electrolyte. For example, $\nu_+ = \nu_- = 1$ for NaCl, corresponding to $Na^+$ and $Cl^-$. The **ionic equivalent conductance** of the cations and anions is denoted by $\lambda_+$ and $\lambda_-$, respectively, and represents the conductivity of an individual ionic constituent of the electrolyte. Equation (17.74) is known as the **law of independent migration of ions** and states that under dilute conditions the molecular conductivity of an electrolyte is equal to the sum of the conductivities of the ionic constituents. Table 17.2 provides the molar conductivities of various ions in aqueous solution.

**TABLE 17.2  Ionic Equivalent Conductance Values for Representative Ions**

| Ion | $\lambda$ (S m$^2$ mol$^{-1}$) | Ion | $\lambda$ (S m$^2$ mol$^{-1}$) |
|---|---|---|---|
| $H^+$ | 0.0350 | $OH^-$ | 0.0199 |
| $Na^+$ | 0.0050 | $Cl^-$ | 0.0076 |
| $K^+$ | 0.0074 | $Br^-$ | 0.0078 |
| $Mg^{2+}$ | 0.0106 | $F^-$ | 0.0054 |
| $Cu^{2+}$ | 0.0107 | $NO_3^-$ | 0.0071 |
| $Ca^{2+}$ | 0.0119 | $CO_3^{2-}$ | 0.0139 |

**EXAMPLE PROBLEM 17.11**

What is the expected molar conductivity at infinite dilution for $MgCl_2$?

**Solution**

Using Equation (17.74) and the data provided in Table 17.2,

$$\Lambda_m^0(MgCl_2) = 1\lambda(Mg^{2+}) + 2\lambda(Cl^-)$$
$$= (0.0106 \text{ S m}^2 \text{ mol}^{-1}) + 2(0.0076 \text{ S m}^2 \text{ mol}^{-1})$$
$$= 0.0258 \text{ S m}^2 \text{ mol}^{-1}$$

As determined by a plot of conductivity versus $(c/c_0)^{1/2}$, $\Lambda_m^0$ for $MgCl_2$ is equal to 0.0212 S m$^2$ mol$^{-1}$. Comparison of this value to the expected molar conductivity calculated earlier demonstrates that $MgCl_2$ behaves as a strong electrolyte in aqueous solution.

(a)

What is the origin of the $c^{1/2}$ dependence stated in Kohlrausch's law? In Chapter 10 it was shown that the activity of electrolytes demonstrates a similar concentration dependence, and this dependence was related to dielectric screening as expressed by the Debye–Hückel limiting law. This law states that the natural log of the ion activity is proportional to the square root of the solution ionic strength, or ion concentration. An ion in solution is characterized not only by the ion itself, but also by the ionic atmosphere surrounding the ion as discussed in Chapter 10, and depicted in Figure 17.23. In the figure, a negative ion is surrounded by a few close-lying positive ions comprising the ionic atmosphere. In the absence of an electric field, the ionic atmosphere will be spherically symmetric, and the centers of positive and negative charge will be identical. However, application of a field will result in ion motion, and this motion will create two effects. First, consider the situation where the negative ion in Figure 17.23 migrates and the atmosphere follows this migrating ion. The ionic atmosphere is not capable of responding to the motion of the negative ion instantaneously, and the lag in response will result in displacement of the centers of positive and negative charge. This displacement will give rise to a local electric field in opposition to the applied field. Correspondingly, the migration rate of the ion, and subsequently the conductivity, will be reduced. This effect is called the **relaxation effect,** and this term implies that a time dependence is associated with this phenomenon. In this case, it is the time it takes the ionic atmosphere to respond to the motion of the negative ion.

Information regarding the timescale for ionic atmosphere relaxation can be gained by varying the frequency of the ac electric field to study ionic conductivity. A second effect that reduces the migration rate of the ion is the **electrophoretic effect.** The negatively and positively charged ions will migrate in opposite directions such that the viscous drag the ion experiences will increase. The reduction in ion mobility accompanying the increase in viscous drag will decrease the conductivity.

(b)
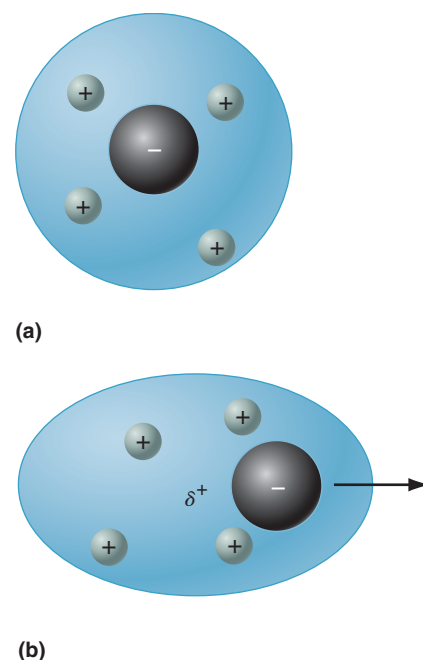
**FIGURE 17.23**
Negative ion in solution and associated ionic atmosphere. **(a)** In the absence of an electric field, the center of the positive and negative charge is identical. **(b)** However, when an electric field is present, the motion of the negative ion results in displacement of the center of the positive and negative charge. This local electric field is in opposition to the applied electric field such that the rate of ion migration is reduced.

## 17.10.2 Weak Electrolytes

Weak electrolytes undergo only fractional conversion into their ionic constituents in solution. Acetic acid, a weak acid, is a classic example of a weak electrolyte. Weak acids are characterized by incomplete conversion to $H_3O^+$ and the conjugate base. The dependence of $\Lambda_m$ on concentration for a weak electrolyte can be understood by considering the extent of ionization. For the case of a weak acid (HA) with dissociation in water to form $H_3O^+$ and the conjugate base ($A^-$), incomplete ionization can be factored into the ionic and electrolyte concentrations as follows:

$$[H_3O^+] = [A^-] = \alpha c \tag{17.75}$$

$$[HA] = (1 - \alpha)c \tag{17.76}$$

In Equations (17.75) and (17.76), $\alpha$ is the degree of ionization (ranging in value from 0 to 1), and $c$ is the initial concentration of electrolyte. Substituting Equations (17.75) and (17.76) into the expression for the equilibrium constant of a weak acid results in Equation (17.77):

$$K_a = \frac{\alpha^2 c}{(1 - \alpha)} \tag{17.77}$$

Solving Equation (17.77) for $\alpha$ yields

$$\alpha = \frac{K_a}{2c}\left(\left(1 + \frac{4c}{K_a}\right)^{1/2} - 1\right) \tag{17.78}$$

The molar conductivity of a weak electrolyte at a given electrolyte concentration $\Lambda_m$ will be related to the molar conductivity at infinite dilution $\Lambda_m^0$ by

$$\Lambda_m = \alpha \Lambda_m^0 \tag{17.79}$$

Using Equations (17.78) and (17.79), the concentration dependence of the molar conductivity can be determined and compared to experiment. The relationship between $\Lambda_m$ and $c$ for a weak electrolyte is described by the **Ostwald dilution law:**

$$\frac{1}{\Lambda_m} = \frac{1}{\Lambda_m^0} + \frac{c\Lambda_m}{K_a(\Lambda_m^0)^2} \tag{17.80}$$

The comparison of the predicted behavior given by Equation (17.80) to experiment for acetic acid ($K_a = 1.8 \times 10^{-5}$, $\Lambda_m^0 = 0.03957$ S m$^2$ mol$^{-1}$) is presented in Figure 17.24, and excellent agreement is observed. The Ostwald dilution law can be used to determine the molar conductivity at infinite dilution for a weak acid.
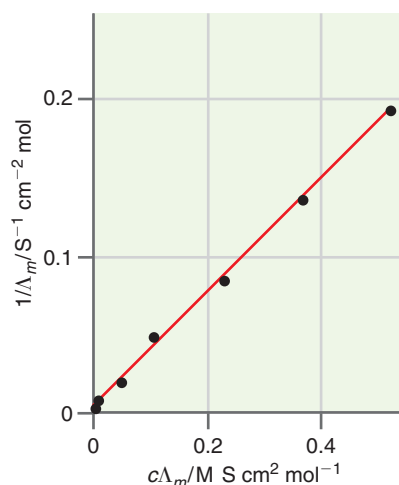


**FIGURE 17.24**
Comparison of experimental and predicted conductivity of acetic acid ($CH_3COOH$) as a function of concentration using the Ostwald dilution law of Equation (17.80). The $y$ intercept on the graph is equal to $1/\Lambda_m^0$.

# Vocabulary

boundary layer
Brownian motion
centrifuge
diffusion
diffusion coefficient
diffusion equation
Einstein–Smoluchowski equation
electrical conductivity
electrophoretic effect
Fick's first law
Fick's second law of diffusion
flux
ionic conduction

ionic equivalent conductance
Kohlrausch's law
laminar flow
law of independent migration of ions
mass transport
molar conductivity
Ostwald dilution law
Ostwald viscometer
Poiseuille's law
random walk
relaxation effect
resistivity
sedimentation

sedimentation coefficient
self-diffusion
specific volume
Stokes–Einstein equation
strong electrolytes
thermal conduction
thermal conductivity
transport coefficient
transport phenomena
turbulent flow
viscosity
weak electrolytes

# Conceptual Problems

**Q17.1** What is the general relationship between the spatial gradient in a system property and the flux of that property?

**Q17.2** What is the expression for the diffusion coefficient $D$ in terms of gas kinetic theory parameters? How is $D$ expected to vary with an increase in molecular mass or collisional cross section?

**Q17.3** Would you expect the diffusion coefficient of $H_2$ to be greater or less than that of $D_2$? By how much? Assume that $H_2$ and $D_2$ are the same size.

**Q17.4** Particles are confined to a plane and then allowed to diffuse. How does the number density vary with distance away from the initial plane?

**Q17.5** How does the root-mean-square diffusion distance vary with the diffusion coefficient? How does this quantity vary with time?

**Q17.6** What is the expression for thermal conductivity in terms of particle parameters derived from gas kinetic theory?

**Q17.7** Why is the thermal conductivity for an ideal gas expected to be independent of pressure? Why does the thermal conductivity for an ideal gas increase as $T^{1/2}$?

**Q17.8** In describing viscosity, what system quantity was transported? What is the expression for viscosity in terms of particle parameters derived from gas kinetic theory?

**Q17.9** What observable is used to measure the viscosity of a gas or liquid?

**Q17.10** How does the viscosity of a gas vary with pressure?

**Q17.11** What is Brownian motion?

**Q17.12** Based on the Stokes–Einstein equation, how does the diffusion coefficient for a particle depend on the size of the particle?

**Q17.13** Describe the random walk model of diffusion. How is this model related to Brownian motion?

**Q17.14** In the Stokes–Einstein equation that describes particle diffusion for a spherical particle, how does the diffusion coefficient depend on fluid viscosity and particle size?

**Q17.15** What forces are operative in particle sedimentation?

**Q17.16** What is the difference between a strong and weak electrolyte?

**Q17.17** According to Kohlrausch's law, how will the molar conductivity for a strong electrolyte change with concentration?

# Numerical Problems

Problem numbers in **red** indicate that the solution to the problem is given in the *Student's Solutions Manual*.

**P17.1** The diffusion coefficient for $CO_2$ at 273 K and 1 atm is $1.00 \times 10^{-5}$ m$^2$ s$^{-1}$. Estimate the collisional cross section of $CO_2$ given this diffusion coefficient.

**P17.2** The collisional cross section of $N_2$ is 0.43 nm$^2$. What is the diffusion coefficient of $N_2$ at a pressure of 1 atm and a temperature of 298 K?

**P17.3**

a. The diffusion coefficient for Xe at 273 K and 1.00 atm is $0.5 \times 10^{-5}$ m$^2$ s$^{-1}$. What is the collisional cross section of Xe?

b. The diffusion coefficient of $N_2$ is threefold greater than that of Xe under the same pressure and temperature conditions. What is the collisional cross section of $N_2$?

**P17.4**

a. The diffusion coefficient of sucrose in water at 298 K is $0.522 \times 10^{-9}$ m$^2$ s$^{-1}$. Determine the time it will take a sucrose molecule on average to diffuse an rms distance of 1 mm.

b. If the molecular diameter of sucrose is taken to be 0.8 nm, what is the time per random walk step?

**P17.5**

a. The diffusion coefficient of the protein lysozyme (MW = 14.1 kg/mol) is $0.104 \times 10^{-5}$ cm$^2$ s$^{-1}$. How long

will it take this protein to diffuse an rms distance of 1 $\mu$m? Model the diffusion as a three-dimensional process.

b. You are about to perform a microscopy experiment in which you will monitor the fluorescence from a single lysozyme molecule. The spatial resolution of the microscope is 1 $\mu$m. You intend to monitor the diffusion using a camera that is capable of one image every 60 s. Is the imaging rate of the camera sufficient to detect the diffusion of a single lysozyme protein over a length of 1 $\mu$m?

c. Assume that in the microscopy experiment of part (b) you use a thin layer of water such that diffusion is constrained to two dimensions. How long will it take a protein to diffuse an rms distance of 1 $\mu$m under these conditions?

**P17.6** A solution consisting of 1 g of sucrose in 10 mL of water is poured into a 1 L graduated cylinder with a radius of 2.5 cm. Then the cylinder is filled with pure water.

a. The diffusion of sucrose can be considered diffusion in one dimension. Derive an expression for the average distance of diffusion $x_{ave}$.

b. Determine $x_{ave}$ and $x_{rms}$ for sucrose for time periods of 1 s, 1 min, and 1 h.

**P17.7** A thermopane window consists of two sheets of glass separated by a volume filled with air (which we will model as $N_2$ where $\kappa = 0.0240$ J K$^{-1}$ m$^{-1}$ s$^{-1}$). For a thermopane

window that is 1 m$^2$ in area with a separation between glass sheets of 3 cm, what is the loss of energy when

**a.** the exterior of the window is at a temperature of 10°C and the interior of the window is at a temperature of 22°C?

**b.** the exterior of the window is at a temperature of −20°C and the interior of the window is at a temperature of 22°C?

**c.** the same temperature differential as in part (b) is used, but the window is filled with Ar ($\kappa = 0.0163$ J K$^{-1}$ m$^{-1}$ s$^{-1}$) rather than N$_2$?

**P17.8** An advertisement for a thermopane window company touts Kr-filled windows and states that these windows provide ten times better insulation than conventional windows filled with Ar. Do you agree with this statement? What should the ratio of thermal conductivities be for Kr ($\sigma = 0.52$ nm$^2$) versus Ar ($\sigma = 0.36$ nm$^2$)?

**P17.9** Two parallel metal plates separated by 1 cm are held at 300. and 298 K, respectively. The space between the plates is filled with N$_2$ ($\sigma = 0.430$ nm$^2$ and $C_{V,m} = 5/2\ R$). Determine the heat flux between the two plates in units of W cm$^{-2}$.

**P17.10** Determine the thermal conductivity of the following species at 273 K and 1.00 atm:

**a.** Ar ($\sigma = 0.36$ nm$^2$)

**b.** Cl$_2$ ($\sigma = 0.93$ nm$^2$)

**c.** SO$_2$ ($\sigma = 0.58$ nm$^2$, geometry: bent)

You will need to determine $C_{V,m}$ for the species listed. You can assume that the translational and rotational degrees of freedom are in the high-temperature limit and that the vibrational contribution to $C_{V,m}$ can be ignored at this temperature.

**P17.11** The thermal conductivity of Kr is 0.0087 J K$^{-1}$ m$^{-1}$ s$^{-1}$ at 273 K and 1 atm. Estimate the collisional cross section of Kr.

**P17.12** The thermal conductivity of N$_2$ at 298 K and 1 atm is 0.024 J K$^{-1}$ m$^{-1}$ s$^{-1}$. What is the collisional cross section of N$_2$ based on its thermal conductivity? For N$_2$ $C_{V,m} = 20.8$ J mol$^{-1}$ K$^{-1}$.

**P17.13** The thermal conductivity of Kr is roughly half that of Ar under identical pressure and temperature conditions. Both gases are monatomic such that $C_{V,m} = 3/2\ R$.

**a.** Why would one expect the thermal conductivity of Kr to be less than that of Ar?

**b.** Determine the ratio of collisional cross sections for Ar relative to Kr assuming identical pressure and temperature conditions.

**c.** For Kr at 273 K at 1 atm, $\kappa = 0.0087$ J K$^{-1}$ m$^{-1}$ s$^{-1}$. Determine the collisional cross section of Kr.

**P17.14**

**a.** Determine the ratio of thermal conductivity for N$_2$ ($\sigma = 0.43$ nm$^2$) at sea level ($T = 300.$ K, P $= 1.00$ atm) versus the lower stratosphere (T $= 230.$ K, P $= 0.25$ atm).

**b.** Determine the ratio of thermal conductivity for N$_2$ at sea level if $P = 1$ atm, but the temperature is 100. K. Which energetic degrees of freedom will be operative at the lower temperature, and how will this affect $C_{V,m}$?

**P17.15** The thermal conductivities of acetylene (C$_2$H$_2$) and N$_2$ at 273 K and 1 atm are 0.01866 and 0.0240 J K$^{-1}$ m$^{-1}$ s$^{-1}$, respectively. Based on these data, what is the ratio of the collisional cross section of acetylene relative to N$_2$?

**P17.16**

**a.** The viscosity of Cl$_2$ at 293 K and 1 atm is 132 $\mu$P. Determine the collisional cross section of this molecule based on the viscosity.

**b.** Given your answer in part (a), estimate the thermal conductivity of Cl$_2$ under the same pressure and temperature conditions.

**P17.17**

**a.** The viscosity of O$_2$ at 293 K and 1.00 atm is 204 $\mu$P. What is the expected flow rate through a tube having a radius of 2.00 mm, length of 10.0 cm, input pressure of 765 Torr, output pressure of 760. Torr, with the flow measured at the output end of the tube?

**b.** If Ar were used in the apparatus ($\eta = 223\ \mu$P) of part (a), what would be the expected flow rate? Can you determine the flow rate without evaluating Poiseuille's equation?

**P17.18** The Reynolds' number (Re) is defined as Re $= \rho\langle v_x\rangle d/\eta$, where $\rho$ and $\eta$ are the fluid density and viscosity, respectively; $d$ is the diameter of the tube through which the fluid is flowing; and $\langle v_x\rangle$ is the average velocity. Laminar flow occurs when Re $< 2000$, the limit in which the equations for gas viscosity were derived in this chapter. Turbulent flow occurs when Re $> 2000$. For the following species, determine the maximum value of $\langle v_x\rangle$ for which laminar flow will occur:

**a.** Ne at 293 K ($\eta = 313\ \mu$P, $\rho =$ that of an ideal gas) through a 2.00-mm-diameter pipe.

**b.** Liquid water at 293 K ($\eta = 0.891$ cP, $\rho = 0.998$ g mL$^{-1}$) through a 2.00-mm-diameter pipe.

**P17.19** The viscosity of H$_2$ at 273 K at 1 atm is 84 $\mu$P. Determine the viscosities of D$_2$ and HD.

**P17.20** An Ostwald viscometer is calibrated using water at 20°C ($\eta = 1.0015$ cP, $\rho = 0.998$ g mL$^{-1}$). It takes 15.0 s for the fluid to fall from the upper to the lower level of the viscometer. A second liquid is then placed in the viscometer, and it takes 37.0 s for the fluid to fall between the levels. Finally, 100. mL of the second liquid weighs 76.5 g. What is the viscosity of the liquid?

**P17.21** How long will it take to pass 200. mL of H$_2$ at 273 K through a 10. cm-long capillary tube of 0.25 mm if the gas input and output pressures are 1.05 and 1.00 atm, respectively?

**P17.22**

**a.** Derive the general relationship between the diffusion coefficient and viscosity for a gas.

**b.** Given that the viscosity of Ar is 223 $\mu$P at 293 K and 1 atm, what is the diffusion coefficient?

**P17.23**

**a.** Derive the general relationship between the thermal conductivity and viscosity.

**b.** Given that the viscosity of Ar is 223 $\mu$P at 293 K and 1.00 atm, what is the thermal conductivity?

**c.** What is the thermal conductivity of Ne under these same conditions (the collisional cross section of Ar is 1.5 times that of Ne)?

**P17.24** As mentioned in the text, the viscosity of liquids decreases with increasing temperature. The empirical equation $\eta(T) = Ae^{E/RT}$ provides the relationship between viscosity and temperature for a liquid. In this equation, $A$ and $E$ are constants, with $E$ being referred to as the activation energy for flow.

**a.** How can one use the equation provided to determine $A$ and $E$ given a series of viscosity versus temperature measurements?

**b.** Use your answer in part (a) to determine $A$ and $E$ for liquid benzene given the following data:

| T (°C) | $\eta$ (cP) |
|---|---|
| 5 | 0.826 |
| 40. | 0.492 |
| 80. | 0.318 |
| 120. | 0.219 |
| 160. | 0.156 |

**P17.25** Poiseuille's law can be used to describe the flow of blood through blood vessels. Using Poiseuille's law, determine the pressure drop accompanying the flow of blood through 5.00 cm of the aorta ($r = 1.00$ cm). The rate of blood flow through the body is 0.0800 L s$^{-1}$, and the viscosity of blood is approximately 4.00 cP at 310 K.

**P17.26** What is the flow of blood through a small vein (diameter $= 3.00$ mm) that is 1.00 cm long? The drop in blood pressure over this length is 40.0 Torr, and the viscosity of blood is approximately 4.00 cP at 310 K.

**P17.27** Myoglobin is a protein that participates in oxygen transport. For myoglobin in water at 20°C, $\bar{s} = 2.04 \times 10^{-13}$ s, $D = 1.13 \times 10^{-11}$ m$^2$ s$^{-1}$, and $\bar{V} = 0.740$ cm$^3$ g$^{-1}$. The density of water is 0.998 g cm$^{-3}$, and the viscosity is 1.002 cP at this temperature.

**a.** Using the information provided, estimate the size of myoglobin.

**b.** What is the molecular weight of myoglobin?

**P17.28** The molecular weight of bovine serum albumin (BSA) is 66,500 g mol$^{-1}$ and has a specific volume of 0.717 cm$^3$ g$^{-1}$. Velocity centrifugation demonstrates that $\bar{s} = 4.31 \times 10^{-13}$ s for this protein. Assuming a solution density of 1.00 g cm$^{-3}$ and viscosity of 1.00 cP, determine the friction coefficient and effective radius of BSA.

**P17.29** You are interested in purifying a sample containing the protein alcohol dehydrogenase obtained from horse liver; however, the sample also contains a second protein, catalase. These two proteins have the following transport properties at 298 K:

| | Catalase | Alcohol Dehydrogenase |
|---|---|---|
| $\bar{s}$ (s) | $11.3 \times 10^{-13}$ | $4.88 \times 10^{-13}$ |
| $D$(m$^2$ s$^{-1}$) | $4.1 \times 10^{-11}$ | $6.5 \times 10^{-11}$ |
| $\bar{V}$(cm$^3$ g$^{-1}$) | 0.715 | 0.751 |

**a.** Determine the molecular weight of catalase and alcohol dehydrogenase.

**b.** You have access to a centrifuge that can provide angular velocities up to 35,000 rpm. For the species you expect to travel the greatest distance in the centrifuge tube, determine the time it will take to centrifuge until a 3 cm displacement of the boundary layer occurs relative to the initial 5 cm location of the boundary layer relative to the centrifuge axis.

**c.** To separate the proteins, you need a separation of at least 1.5 cm between the boundary layers associated with each protein. Using your answer to part (b), will it be possible to separate the proteins by centrifugation?

**P17.30** Boundary centrifugation is performed at an angular velocity of 40,000 rpm to determine the sedimentation coefficient of cytochrome $c$ ($M = 13,400$ g mol$^{-1}$) in water at 20°C ($\rho = 0.998$ g cm$^{-3}$, $\eta = 1.002$ cP). The following data are obtained on the position of the boundary layer as a function of time:

| Time (h) | $x_b$ (cm) |
|---|---|
| 0 | 4.00 |
| 2.5 | 4.11 |
| 5.2 | 4.23 |
| 12.3 | 4.57 |
| 19.1 | 4.91 |

**a.** What is the sedimentation coefficient for cytochrome $c$ under these conditions?

**b.** The specific volume of cytochrome $c$ is 0.728 cm$^3$ g$^{-1}$. Estimate the size of cytochrome $c$.

**P17.31** T. Svedberg measured the molecular weight of carbonyl hemoglobin (specific volume $= 0.755$ mL g$^{-1}$, $D = 7.00 \times 10^{-11}$ m$^2$ s$^{-1}$) by velocity centrifugation. In this experiment, 0.96 g of protein were dissolved in 100. mL of water at 303 K ($\rho = 0.998$ g cm$^{-3}$), and the solution was spun at 39,300 rpm. After 30.0 min, the concentration boundary advanced by 0.074 cm from an initial position of 4.525 cm. Calculate the molecular weight of carbonyl hemoglobin.

**P17.32** A current of 2.00 A is applied to a metal wire for 30. s. How many electrons pass through a given point in the wire during this time?

**P17.33** Use the following data to determine the conductance at infinite dilution for NaNO$_3$:

$$\Lambda_m^0(KCl) = 0.0149 \text{ S m}^2 \text{ mol}^{-1}$$
$$\Lambda_m^0(NaCl) = 0.0127 \text{ S m}^2 \text{ mol}^{-1}$$
$$\Lambda_m^0(KNO_3) = 0.0145 \text{ S m}^2 \text{ mol}^{-1}$$

**P17.34** The following molar conductivity data are obtained for an electrolyte:

| Concentration (M) | $\Lambda_m$ (S m$^2$ mol$^{-1}$) |
|---|---|
| 0.0005 | 0.01245 |
| 0.001 | 0.01237 |
| 0.005 | 0.01207 |
| 0.01 | 0.01185 |
| 0.02 | 0.01158 |
| 0.05 | 0.01111 |
| 0.1 | 0.01067 |

Determine if the electrolyte is strong or weak, and determine the conductivity of the electrolyte at infinite dilution.

**P17.35** The molar conductivity of sodium acetate, $CH_3COONa$, is measured as a function of concentration in water at 298 K, and the following data are obtained:

| Concentration (M) | $\Lambda_m$ (S m$^2$ mol$^{-1}$) |
|---|---|
| 0.0005 | 0.00892 |
| 0.001 | 0.00885 |
| 0.005 | 0.00857 |
| 0.01 | 0.00838 |
| 0.02 | 0.00812 |
| 0.05 | 0.00769 |
| 0.1 | 0.00728 |

Is sodium acetate a weak or strong electrolyte? Determine $\Lambda_m^0$ using appropriate methodology depending on your answer.

**P17.36** Starting with Equations (17.47) and (17.48), derive the Ostwald dilution law.

**P17.37** For a one-dimensional random walk, determine the probability that the particle will have moved six steps in either the $+x$ or $-x$ direction after 10, 20, and 100 steps.

**P17.38** In the early 1990s, fusion involving hydrogen dissolved in palladium at room temperature, or *cold fusion,* was proposed as a new source of energy. This process relies on the diffusion of $H_2$ into palladium. The diffusion of hydrogen gas through a 0.005-cm-thick piece of palladium foil with a cross section of 0.750 cm$^2$ is measured. On one side of the foil, a volume of gas maintained at 298 K and 1 atm is applied, while a vacuum is applied to the other side of the foil. After 24 h, the volume of hydrogen has decreased by 15.2 cm$^3$. What is the diffusion coefficient of hydrogen gas in palladium?

**P17.39** In the determination of molar conductivities, it is convenient to define the cell constant as $K = 1/A$, where $l$ is the separation between the electrodes in the conductivity cell and $A$ is the area of the electrodes.

**a.** A standard solution of KCl (conductivity or $\kappa = 1.06296 \times 10^{-6}$ S m$^{-1}$ at 298 K) is employed to standardize the cell, and a resistance of 4.2156 $\Omega$ is measured. What is the cell constant?

**b.** The same cell is filled with a solution of HCl, and a resistance of 1.0326 $\Omega$ is measured. What is the conductivity of the HCl solution?

**P17.40** Conductivity measurements were one of the first methods used to determine the autoionization constant of water. The autoionization constant of water is given by the following equation:

$$K_w = a_{H^+} a_{OH^-} = \left(\frac{[H^+]}{1\,M}\right)\left(\frac{[OH^-]}{1\,M}\right)$$

where $a$ is the activity of the species, which is equal to the actual concentration of the species divided by the standard state concentration at infinite dilution. This substitution of concentrations for activities is a reasonable approximation given the small concentrations of $H^+$ and $OH^-$ that result from autoionization.

**a.** Using the expression provided, show that the conductivity of pure water can be written as

$$\Lambda_m(H_2O) = (1\,M)K_w^{1/2}(\lambda(H^+) + \lambda(OH^-))$$

**b.** Kohlrausch and Heydweiller measured the conductivity of water in 1894 and determined that $\Lambda_m$ ($H_2O$) $= 5.5 \times 10^{-6}$ S m$^{-1}$ at 298 K. Using the information in Table 17.2, determine $K_w$.

# Web-Based Simulations, Animations, and Problems

**W17.1** In this problem, concentration time dependence in one dimension is depicted as predicted using Fick's second law of diffusion. Specifically, variation of particle number density as a function of distance with time and diffusion constant $D$ is investigated. Comparisons of the full distribution to $x_{rms}$ are performed to illustrate the behavior of $x_{rms}$ with time and $D$.

# For Further Reading

Bird, R. B., W. E. Stewart, and E. N. Lightfoot. *Transport Phenomena*. New York: Wiley, 1960.

Cantor, C. R., and P. R. Schimmel. *Biophysical Chemistry. Part II: Techniques for the Study of Biological Structure and Function*. San Francisco: W. H. Freeman, 1980.

Castellan, G. W. *Physical Chemistry*. Reading, MA: Addison-Wesley, 1983.

Crank, J. *The Mathematics of Diffusion*. Oxford: Clarendon Press, 1975.

Hirschfelder, J. O., C. F. Curtiss, and R. B. Bird. *The Molecular Theory of Gases and Liquids*. New York: Wiley, 1954.

Reid, R. C., J. M. Prausnitz, and T. K. Sherwood. *The Properties of Gases and Liquids*. New York: McGraw-Hill, 1977.

Vargaftik, N. B. *Tables on the Thermophysical Properties of Liquids and Gases*. New York: Wiley, 1975.

Welty, J. R., C. E. Wicks, and R. E. Wilson. *Fundamentals of Momentum, Heat, and Mass Transfer*. New York: Wiley, 1969.

# Elementary Chemical Kinetics

In Chapters 18 and 19, the kinetics associated with chemical reactions are explored. The central question of interest in chemical kinetics is perhaps the first question one asks about any chemical reaction: Just how do the reactants become products? In chemical kinetics, this question is answered by determining the timescale and mechanism of a chemical reaction. In this chapter, the foundational tools of chemical kinetics are developed. These tools will be the central components of a kinetics "toolkit" to be used in describing complex reactions in Chapter 19. The importance of chemical kinetics is evidenced by its application in nearly every area of chemistry. Found in areas such as enzyme catalysis, materials processing, and atmospheric chemistry, chemical kinetics is clearly an important aspect of physical chemistry.

## 18.1 Introduction to Kinetics

In the previous chapter, transport processes involving the evolution of a system's physical properties toward equilibrium were discussed. In these processes, the system undergoes relaxation without a change in chemical composition. Transport phenomena are sometimes referred to as physical kinetics to indicate that the physical properties of the system are evolving, not the chemical composition. In this chapter and the next, we focus on chemical kinetics where the composition of the system evolves with time.

**Chemical kinetics** involves the study of the rates and mechanisms of chemical reactions. This area bridges an important gap in our discussion of chemical reactions to this point. Thermodynamic descriptions of chemical reactions involved the Gibbs or Helmholtz energy for a reaction and the corresponding equilibrium constant. These quantities are sufficient to predict the reactant and product concentrations at equilibrium but are of little use in determining the timescale over which the reaction occurs. That is, thermodynamics may dictate that a reaction is spontaneous, but it does not dictate the timescale over which the reaction will occur and reach equilibrium. Chemical kinetics provides information on the timescale of chemical reactions.

In the course of a chemical reaction, concentrations will change with time as "reactants" become "products." Figure 18.1 presents possibly the first chemical reaction

Concentration as a function of time
for the conversion of reactant A into
product B. The concentration of A at
$t = 0$ is $[A]_0$, and the concentration
of B is zero. As the reaction proceeds, the
loss of A results in the production of B.



A $\longrightarrow$ B
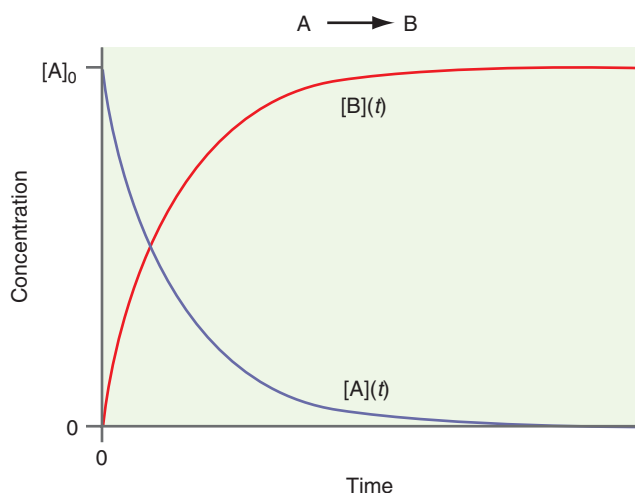
introduced in introductory chemistry: the conversion of reactant "A" into product "B."
The figure illustrates that, as the reaction proceeds, a decrease in reactant concentration
and a corresponding increase in product concentration are observed. One way to describe
this process is to define the rate of concentration change with time, a quantity that is
referred to as the reaction rate.

The central idea behind chemical kinetics is that by monitoring the rate at which
chemical reactions occur and determining the dependence of this rate on system
parameters such as temperature, concentration, and pressure, we can gain insight
into the mechanism of the reaction. Experimental chemical kinetics includes the
development of techniques that allow for the measurement and analysis of chemical
reaction dynamics. In addition to experiments, theoretical work has been performed
to understand reaction mechanisms and the underlying physics that govern the rates
of chemical reactions. The synergy between experimental and theoretical chemical
kinetics has provided for dramatic advances in this field.

# 18.2 Reaction Rates

Consider the following "generic" chemical reaction:

$$a A + b B + \ldots \rightarrow c C + d D + \ldots \tag{18.1}$$

In Equation (18.1), uppercase letters indicate a chemical species and lowercase letters
represent the stoichiometric coefficient for the species in the balanced reaction. The
number of moles of a species during any point of the reaction is given by

$$n_i = n_i^o + \nu_i \xi \tag{18.2}$$

where $n_i$ is the number of moles of species $i$ at any given time during the reaction, $n_i^o$ is
the number of moles of species $i$ present before initiation of the reaction, $\nu_i$ is related
to the stoichiometric coefficient of species $i$, and $\xi$ the extent or advancement of the
reaction equal to zero at the start of the reaction and one at completion. The advance-
ment variable allows us to quantify the rate of the reaction with respect to all species,
irrespective of stoichiometry (see the later discussion). For the reaction depicted in
Equation (18.1), reactants will be consumed and products formed during the reaction.
To ensure that this behavior is reflected in Equation (18.2), $\nu_i$ is set equal to $-1$ times
the stoichiometric coefficient for reactants and is set equal to the stoichiometric coeffi-
cient for products.

The time evolution of the reactant and product concentrations is quantified by
differentiating both sides of Equation (18.2) with respect to time:

$$\frac{dn_i}{dt} = \nu_i \frac{d\xi}{dt} \tag{18.3}$$

The **reaction rate** is defined as the change in the advancement of the reaction with time:

$$Rate = \frac{d\xi}{dt} \tag{18.4}$$

With this definition, the rate of reaction with respect to the change in the number of moles of a given species with time is

$$Rate = \frac{1}{\nu_i}\frac{dn_i}{dt} \tag{18.5}$$

As an example of how the rate of reaction is defined relative to the change in moles of reactant or product with time, consider the following reaction:

$$4\,NO_2(g) + O_2(g) \rightarrow 2\,N_2O_5(g) \tag{18.6}$$
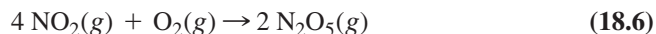
The rate of reaction can be expressed with respect to any species in Equation (18.6):

$$Rate = -\frac{1}{4}\frac{dn_{NO_2}}{dt} = -\frac{dn_{O_2}}{dt} = \frac{1}{2}\frac{dn_{N_2O_5}}{dt} \tag{18.7}$$

Notice the sign convention of the coefficient with respect to reactants and products: negative for reactants and positive for products. Since the number of moles of reactant decreases with time, the negative sign for the coefficient ensures that the *Rate* is positive. Also, notice that the rate of reaction can be defined with respect to both reactants and products. In our example, 4 mol of $NO_2$ react with 1 mol of $O_2$ to produce 2 mol of $N_2O_5$ product. Therefore, the **rate of conversion** of $NO_2$ will be four times greater than the rate of $O_2$ conversion. Although the conversion rates are different, the reaction rate defined with respect to either species will be the same.

In applying Equation (18.5) to define the reaction rate, a set of stoichiometric coefficients must be employed; however, these coefficients are not unique. For example, if we multiply both sides of Equation (18.6) by a factor of 2, the expression for the rate of conversion must also change. Generally, one decides on a given set of coefficients for a balanced reaction and uses these coefficients consistently throughout a given kinetics problem.

In our present definition, the rate of reaction as written is an extensive property; therefore, it will depend on the system size. The rate can be made intensive by dividing Equation (18.5) by the volume of the system:

$$R = \frac{Rate}{V} = \frac{1}{V}\left(\frac{1}{\nu_i}\frac{dn_i}{dt}\right) = \frac{1}{\nu_i}\frac{d[i]}{dt} \tag{18.8}$$

In Equation (18.8), $R$ is the intensive reaction rate. The last equality in Equation (18.8) is performed recognizing that moles of species $i$ per unit volume is simply the molarity of species $i$, or $[i]$. Equation (18.8) is the definition for the rate of reaction at constant volume. For species in solution, the application of Equation (18.8) in defining the rate of reaction is clear, but it can also be used for gases, as Example Problem 18.1 illustrates.

## EXAMPLE PROBLEM 18.1

The decomposition of acetaldehyde is given by the following balanced reaction:

$$CH_3COH(g) \rightarrow CH_4(g) + CO(g)$$
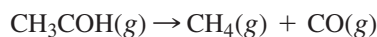
Define the rate of reaction with respect to the pressure of the reactant.

### Solution

Beginning with Equation (18.2) and focusing on the acetaldehyde reactant, we obtain

$$n_{CH_3COH} = n^o_{CH_3COH} - \xi$$

Using the ideal gas law, the pressure of acetaldehyde is expressed as

$$P_{CH_3COH} = \frac{n_{CH_3COH}}{V}RT = [CH_3COH]RT$$

Therefore, the pressure is related to the concentration by the quantity $RT$. Substituting this result into Equation (18.8) with $\nu_i = 1$ yields

$$R = \frac{Rate}{V} = -\frac{1}{\nu_{CH_3COH}} \frac{d[CH_3COH]}{dt}$$

$$= -\frac{1}{RT} \frac{dP_{CH_3COH}}{dt}$$

# 18.3 Rate Laws

We begin our discussion of rate laws with a few important definitions. The rate of a reaction will generally depend on the temperature, pressure, and concentrations of species involved in the reaction. In addition, the rate may depend on the phase or phases in which the reaction occurs. Homogeneous reactions occur in a single phase, whereas heterogeneous reactions involve more than one phase. For example, reactions that occur on surfaces are classic examples of heterogeneous reactions. We will limit our initial discussion to homogeneous reactions, with heterogeneous reactivity discussed in Chapter 19. For the majority of homogeneous reactions, an empirical relationship between reactant concentrations and the rate of a chemical reaction can be written. This relationship is known as a **rate law,** and for the reaction shown in Equation (18.1) it is written as

$$R = k[A]^\alpha[B]^\beta \ldots \tag{18.9}$$

where [A] is the concentration of reactant A, [B] is the concentration of reactant B, and so forth. The constant $\alpha$ is known as the **reaction order** with respect to species A, $\beta$ the reaction order with respect to species B, and so forth. The overall reaction order is equal to the sum of the individual reaction orders ($\alpha + \beta + \ldots$). Finally, the constant $k$ is referred to as the **rate constant** for the reaction. The rate constant is independent of concentration but dependent on pressure and temperature, as discussed later in Section 18.9.

The reaction order dictates the concentration dependence of the reaction rate. The reaction order may be an integer or a fraction. *It cannot be overemphasized that reaction orders have no relation to stoichiometric coefficients, and they are determined by experiment*. For example, reconsider the reaction of nitrogen dioxide with molecular oxygen [Equation (18.6)]:

$$4\,NO_2(g) + O_2(g) \rightarrow 2\,N_2O_5(g)$$
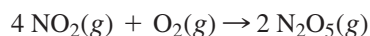
The experimentally determined rate law expression for this reaction is

$$R = k[NO_2]^2[O_2] \tag{18.10}$$

The reaction is second order with respect to $NO_2$, first order with respect to $O_2$, and third order overall. Notice that the reaction orders are not equal to the stoichiometric coefficients. *All rate laws must be determined experimentally with respect to each reactant,* and the order of the reaction is not determined by the stoichiometry of the reaction.

In the rate law expression of Equation (18.9), the rate constant serves as the proportionality constant between the concentrations of the various species and the reaction rate. Inspection of Equation (18.8) demonstrates that the reaction rate will *always* have units of concentration time$^{-1}$. Therefore, the units of $k$ must change with respect to the overall order of the reaction to ensure that the reaction rate has the correct units. The relationship between the rate law expression, order, and the units of $k$ is presented in Table 18.1.

## 18.3.1 Measuring Reaction Rates

With the definitions for the reaction rate and rate law provided by Equations (18.8) and (18.9), the question of how one measures the rate of reaction becomes important. To illustrate this point, consider the following reaction:

$$A \overset{k}{\rightarrow} B \tag{18.11}$$

**TABLE 18.1** Relationship between Rate Law, Order, and the Rate Constant $k^*$

| Rate Law | Order | Units of $k$ |
|---|---|---|
| $R = k$ | Zero | $M\,s^{-1}$ |
| $R = k[A]$ | First order with respect to A | $s^{-1}$ |
| | First order overall | |
| $R = k[A]^2$ | Second order with respect to A | $M^{-1}\,s^{-1}$ |
| | Second order overall | |
| $R = k[A][B]$ | First order with respect to A | $M^{-1}\,s^{-1}$ |
| | First order with respect to B | |
| | Second order overall | |
| $R = k[A][B][C]$ | First order with respect to A | $M^{-2}\,s^{-1}$ |
| | First order with respect to B | |
| | First order with respect to C | |
| | Third order overall | |

$^*$In the units of $k$, M represents mol L$^{-1}$ or moles per liter.

The rate of this reaction in terms of [A] is given by

$$R = -\frac{d[A]}{dt} \tag{18.12}$$

Furthermore, suppose experiments demonstrate that at a certain temperature and pressure the reaction is first order in A, first order overall, and $k = 40\ s^{-1}$ so that

$$R = k[A] = (40\ s^{-1})[A]$$

Equation (18.12) states that the rate of the reaction is equal to the negative of the time derivative of [A]. Imagine that we perform an experiment in which [A] is measured as a function of time as shown in Figure 18.2. The derivative in Equation (18.12) is simply the slope of the tangent for the concentration curve at a specific time. Therefore, the reaction rate will depend on the time at which the rate is determined. Figure 18.2 presents a measurement of the rate at two time points, $t = 0\ ms(1\ ms = 10^{-3}\ s)$ and $t = 30\ ms$. At $t = 0\ ms$, the reaction rate is given by the negative of the slope of the line corresponding to the change in [A] with time, per Equation (18.12):

$$R_{t=0} = -\frac{d[A]}{dt} = 40\ M\,s^{-1}$$

However, when measured at 30 ms the rate is

$$R_{t=30\,ms} = -\frac{d[A]}{dt} = 12\ M\,s^{-1}$$

Notice that the reaction rate is decreasing with time. This behavior is a direct consequence of the change of [A] as a function of time, as expected from the rate law of Equation (18.8). Specifically, at $t = 0$,

$$R_{t=0} = 40\ s^{-1}[A]_{t=0} = 40\ s^{-1}(1\ M) = 40\ M\,s^{-1}$$

However, by $t = 30\ ms$ the concentration of A has decreased to 0.3 M so that the rate is

$$R_{t=30\,ms} = 40\ s^{-1}[A]_{t=30\,ms} = 40\ s^{-1}(0.3\ M) = 12\ M\,s^{-1}$$

This difference in rates brings to the forefront an important issue in kinetics: how does one define a reaction rate if the rate changes with time? One convention is to define the rate before the reactant concentrations have undergone any substantial change from their initial values. The reaction rate obtained under such conditions is known as the **initial rate.** The initial rate in the previous example is that determined at $t = 0$. In the
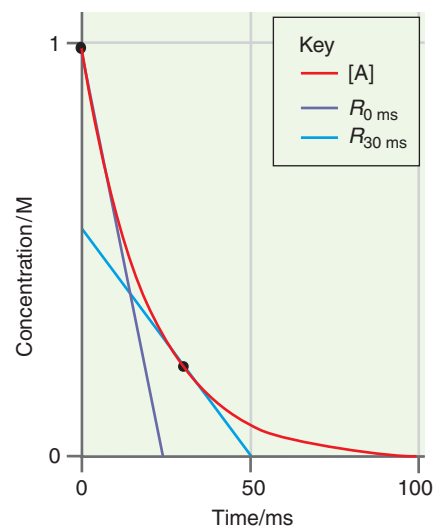


**FIGURE 18.2**
Measurement of the reaction rate. The concentration of reactant A as a function of time is presented. The rate $R$ is equal to the slope of the tangent of this curve. This slope depends on the time at which the tangent is determined. The tangent determined 30 ms into the reaction is presented as the blue line, and the tangent at $t = 0$ is presented as the purple line.

remainder of our discussion of kinetics, the rate of reaction is taken to be synonymous with initial rate. However, the rate constant is independent of concentration; therefore, if the rate constant, concentrations, and order dependence of the reaction rate are known, the reaction rate can be determined at any time.

### 18.3.2 Determining Reaction Orders

Consider the following reaction:

$$A + B \xrightarrow{k} C \qquad \qquad \textbf{(18.13)}$$
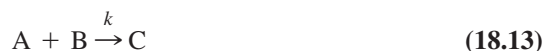
The rate law expression for this reaction is

$$R = k[A]^{\alpha}[B]^{\beta} \qquad \qquad \textbf{(18.14)}$$

How can one determine the order of the reaction with respect to A and B? First, note that the measurement of the rate under a single set of concentrations for A and B will not by itself provide a measure of $\alpha$ and $\beta$ because we have only one equation [Equation (18.14)], and two unknown quantities. Therefore, the determination of reaction order will involve the measurement of the reaction rate under various concentration conditions. The question then becomes "What set of concentrations should be used to determine the reaction rate?" One answer to this question is known as the **isolation method.** In this approach, the reaction is performed with all reactants but one in excess. Under these conditions, only the concentration of the reactant not in excess will vary to a significant extent during the reaction. For example, consider the A + B reaction shown in Equation (18.13). Imagine performing the experiment in which the initial concentration of A is 1.00 M and the concentration of B is 0.01 M. The rate of the reaction will be zero when all of reactant B has been used; however, the concentration of A will have been reduced to 0.99 M, only a slight reduction from the initial concentration. This simple example demonstrates that the concentration of species present in excess will be essentially constant with time. This time independence simplifies the reaction rate expression because the reaction rate will depend only on the concentration of the reactant not present in excess. In our example reaction where A is in excess, Equation (18.14) simplifies to

$$R = k'[B]^{\beta}, \text{ where } k' = k[A]^{\alpha} \qquad \qquad \textbf{(18.15)}$$

The quantity $k'$ is taken to be time-independent since $k$ is constant in time, and $[A]^{\alpha}$ will change only slightly with time since A is in excess. In this limit the reaction rate depends on [B] exclusively, and the reaction order with respect to B is determined by measuring the reaction rate as [B] is varied. Of course, the isolation method could just as easily be applied to determine $\alpha$ by performing measurements with B in excess and varying [A].

A second strategy employed to determine reaction rates is referred to as the **method of initial rates.** In this approach, the concentration of a single reactant is changed while holding all other concentrations constant, and the initial rate of the reaction is determined. The variation in the initial rate as a function of concentration is then analyzed to determine the order of the reaction with respect to the reactant that is varied. Consider the reaction depicted by Equation (18.13). To determine the order of the reaction for each reactant, the reaction rate is measured as [A] is varied and the concentration of B is held constant. The reaction rate at two different values of [A] is then analyzed to determine the order of the reaction with respect to [A] as follows:

$$\frac{R_1}{R_2} = \frac{k[A]_1^{\alpha}[B]_0^{\beta}}{k[A]_2^{\alpha}[B]_0^{\beta}} = \left(\frac{[A]_1}{[A]_2}\right)^{\alpha}$$

$$\ln\left(\frac{R_1}{R_2}\right) = \alpha \ln\left(\frac{[A]_1}{[A]_2}\right) \qquad \qquad \textbf{(18.16)}$$

Notice that [B] and $k$ are constant in each measurement; therefore, they cancel when one evaluates the ratio of the measured reaction rates. Using Equation (18.16), the order of the reaction with respect to A is readily determined. A similar experiment to determine $\beta$ is also performed where [A] is held constant and the dependence of the reaction rate on [B] is measured.

## EXAMPLE PROBLEM 18.2

Using the following data for the reaction illustrated in Equation (18.13), determine the order of the reaction with respect to A and B, and the rate constant for the reaction:

| [A] (M) | [B] (M) | Initial Rate $(M\,s^{-1})$ |
|---|---|---|
| $2.30 \times 10^{-4}$ | $3.10 \times 10^{-5}$ | $5.25 \times 10^{-4}$ |
| $4.60 \times 10^{-4}$ | $6.20 \times 10^{-5}$ | $4.20 \times 10^{-3}$ |
| $9.20 \times 10^{-4}$ | $6.20 \times 10^{-5}$ | $1.68 \times 10^{-2}$ |

### Solution

Using the last two entries in the table, the order of the reaction with respect to A is

$$\ln\left(\frac{R_2}{R_3}\right) = \alpha \ln\left(\frac{[A]_2}{[A]_3}\right)$$

$$\ln\left(\frac{4.20 \times 10^{-3}}{1.68 \times 10^{-2}}\right) = \alpha \ln\left(\frac{4.60 \times 10^{-4}}{9.20 \times 10^{-4}}\right)$$

$$-1.386 = \alpha(-0.693)$$

$$2 = \alpha$$

Using this result and the first two entries in the table, the order of the reaction with respect to B is given by

$$\frac{R_1}{R_2} = \frac{k[A]_1^2[B]_1^\beta}{k[A]_2^2[B]_2^\beta} = \frac{[A]_1^2[B]_1^\beta}{[A]_2^2[B]_2^\beta}$$

$$\left(\frac{5.25 \times 10^{-4}}{4.20 \times 10^{-3}}\right) = \left(\frac{2.30 \times 10^{-4}}{4.60 \times 10^{-4}}\right)^2\left(\frac{3.10 \times 10^{-5}}{6.20 \times 10^{-5}}\right)^\beta$$

$$0.500 = (0.500)^\beta$$

$$1 = \beta$$

Therefore, the reaction is second order in A, first order in B, and third order overall. Using any row from the table, the rate constant is readily determined:

$$R = k[A]^2[B]$$

$$5.2 \times 10^{-4}\,M\,s^{-1} = k(2.3 \times 10^{-4}\,M)^2(3.1 \times 10^{-5}\,M)$$

$$3.17 \times 10^8\,M^{-2}\,s^{-1} = k$$

Having determined $k$, the overall rate law is

$$R = (3.17 \times 10^8\,M^{-2}\,s^{-1})[A]^2[B]$$

 The remaining question to address is how one actually measures the rate of a chemical reaction. Measurement techniques are usually separated into one of two categories: chemical and physical. As the name implies, **chemical methods** in kinetics studies rely on chemical processing to determine the progress of a reaction with respect to time. In this method, a chemical reaction is initiated and samples are removed from the reaction and manipulated such that the reaction in the sample is terminated. Termination of the reaction is accomplished by rapidly cooling the sample or by adding a chemical species that depletes one of the reactants. After stopping the reaction, the sample contents are analyzed. By performing this analysis on a series of samples removed from the original reaction container as a function of time after initiation of the reaction, the kinetics of the reaction can be determined. Chemical methods are generally cumbersome to use and are limited to reactions that occur on slow timescales.

 The majority of modern kinetics experiments involve **physical methods.** In these methods, a physical property of the system is monitored as the reaction proceeds. For some reactions, the system pressure or volume provides a convenient physical property

for monitoring the progress of a reaction. For example, consider the thermal decomposition of $PCl_5$:

$$PCl_5(g) \rightarrow PCl_3(g) + Cl_2(g)$$

As the reaction proceeds, for every gaseous $PCl_5$ molecule that decays, two gaseous product molecules are formed. Therefore, the total system pressure will increase as the reaction proceeds in a container with fixed volume. Measurement of this pressure increase as a function of time provides information on the reaction kinetics.

More complex physical methods involve techniques that are capable of monitoring the concentration of an individual species as a function of time. Many of the spectroscopic techniques described in this text are extremely useful for such measurements. For example, electronic absorption measurements can be performed in which the concentration of a species is monitored using the electronic absorption of a molecule and the Beer–Lambert law. Vibrational spectroscopic measurements using infrared absorption and Raman scattering can be employed to monitor vibrational transitions of reactants or products providing information on their consumption or production. Finally, NMR spectroscopy is a useful technique for following the reaction kinetics of complex systems.

The challenge in chemical kinetics is to perform measurements with sufficient time resolution to monitor the chemistry of interest. If the reaction is slow (seconds or longer), then the chemical methods just described can be used to monitor the kinetics. However, many chemical reactions occur on timescales as short as picoseconds $(10^{-12}\,s)$ and femtoseconds $(10^{-15}\,s)$. Reactions occurring on these short timescales are most easily studied using physical methods.

For reactions that occur on timescales as short as 1 ms $(10^{-3}\,s)$, **stopped-flow techniques** provide a convenient method by which to measure solution phase reactions. These techniques are exceptionally popular for biochemical studies. A stopped-flow experiment is illustrated in Figure 18.3. Two reactants (A and B) are held in reservoirs connected to a syringe pump. The reaction is initiated by depressing the reactant syringes, and the reactants are mixed at the junction indicated in the figure. The reaction is monitored by observing the change in absorbance of the reaction mixture as a function of time. The temporal resolutions of stopped-flow techniques are generally limited by the time it takes for the reactants to mix.

Reactions that can be triggered by light are studied using **flash photolysis techniques.** In flash photolysis, the sample is exposed to a temporal pulse of light that initiates the reaction. Ultrafast light pulses as short as 10 femtoseconds $(10\,fs = 10^{-14}\,s)$ in the visible region of the electromagnetic spectrum are available such that reaction dynamics on this extremely short or ultrafast timescale can be studied. For reference, a 3000 $cm^{-1}$ vibrational mode has a period of roughly 10 fs; therefore, using short optical pulses reactions can be initiated on the same timescale as vibrational molecular motion, and this capability has opened up many exciting fields in chemical kinetics, referred to as **femtochemistry.** This capability has been used to determine the ultrafast chemical kinetics associated with vision, photosynthesis, atmospheric processes, and charge-carrier dynamics in semiconductors. Very recently, femtochemical techniques have been extended to the X-ray region of the spectrum, allowing for the direct interrogation of photoinitiated structural changes using time-resolved scattering techniques. Recent references to some of this work are included in the "For Further Reading" section at the end of this chapter.

**FIGURE 18.3**
Schematic of a stopped-flow experiment. Two reactants are rapidly introduced into the mixing chamber by syringes. After mixing, the reaction kinetics are monitored by observing the change in sample concentration versus time, in this example by measuring the absorption of light as a function of time after mixing.
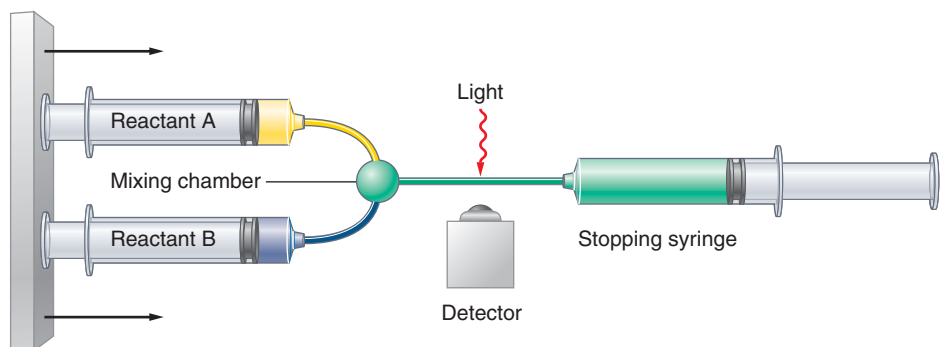
Short optical pulses can be used to perform vibrational spectroscopic measurements (infrared absorption or Raman) on the 100-fs timescale. Finally, NMR techniques, as well as optical absorption and vibrational spectroscopy, can be used to study reactions that occur on the microsecond $(10^{-6} \text{ s})$ and longer timescale.

Another approach to studying chemical kinetics is that of **perturbation-relaxation methods.** In this approach, a chemical system initially at equilibrium is perturbed such that the system is no longer at equilibrium. By following the relaxation of the system toward the new equilibrium state, the rate constants for the reaction can be determined. Any system variable that affects the position of the equilibrium such as pressure, pH, or temperature can be used in a perturbation-relaxation experiment. Temperature perturbation or $T$-jump experiments are the most common type of perturbation experiment and are described in detail later in this chapter.

In summary, the measurement technique chosen for reaction rate determination will depend on both the specifics of the reaction as well as the timescale over which the reaction occurs. In any event, the determination of reaction rates is an experimental exercise and must be accomplished through careful measurements involving well-designed experiments.

# 18.4 Reaction Mechanisms

As discussed previously, the order of a reaction is not determined by the stoichiometry of the reaction. The reason for the inequivalence of the stoichiometric coefficient and reaction order is that the balanced chemical reaction provides no information with respect to the mechanism of the chemical reaction. A **reaction mechanism** is defined as the collection of individual kinetic processes or elementary steps involved in the transformation of reactants into products. The rate law expression for a chemical reaction, including the order of the reaction, is entirely dependent on the reaction mechanism. In contrast, the Gibbs energy for a reaction is dependent on the equilibrium concentration of reactants and products. Just as the study of concentrations as a function of reaction conditions provides information on the thermodynamics of the reaction, the study of reaction rates as a function of reaction conditions provides information on the reaction mechanism.

All reaction mechanisms consist of a series of **elementary reaction steps,** or chemical processes that occur in a single step. The **molecularity** of a reaction step is the stoichiometric quantity of reactants involved in the reaction step. For example, unimolecular reactions involve a single reactant species. An example of a unimolecular reaction step is the decomposition of a diatomic molecule into its atomic fragments:

$$I_2 \xrightarrow{k_d} 2\,I \tag{18.17}$$

Although Equation (18.17) is referred to as a unimolecular reaction, enthalpy changes accompanying the reaction generally involve the transfer of this heat through collisions with other, neighboring molecules. The role of collisional energy exchange with surrounding molecules will figure prominently in the discussion of unimolecular dissociation reactions in the following chapter (Section (19.3), but these energy-exchange processes are suppressed here. Bimolecular reaction steps involve the interaction of two reactants. For example, the reaction of nitric oxide with ozone is a bimolecular reaction:

$$NO + O_3 \xrightarrow{k_r} NO_2 + O_2 \tag{18.18}$$

The importance of elementary reaction steps is that the corresponding rate law expression for the reaction can be written based on the molecularity of the reaction. For the unimolecular reaction, the rate law expression is that of a first-order reaction. For the unimolecular decomposition of $I_2$ presented in Equation (18.17), the rate law expression for this elementary step is

$$R = -\frac{d[I_2]}{dt} = k_d[I_2] \tag{18.19}$$

Likewise, the rate law expression for the bimolecular reaction of NO and $O_3$ is

$$R = -\frac{d[NO]}{dt} = k_r[NO][O_3] \tag{18.20}$$

Comparison of the rate law expressions with their corresponding reactions demonstrates that for elementary reactions the order of the reaction is equal to the stoichiometric coefficient. It is important to keep in mind that *the equivalence of order and molecularity is only true for elementary reaction steps*.

A common problem in kinetics is identifying which of a variety of proposed reaction mechanisms is the "correct" mechanism. The design of kinetic experiments to differentiate between proposed mechanisms is quite challenging. Due to the complexity of many reactions, it is often difficult to experimentally differentiate between several potential mechanisms. A general rule of kinetics is that although it may be possible to rule out a proposed mechanism, it is never possible to prove unequivocally that a given mechanism is correct. The following example illustrates the origins of this rule. Consider the following reaction:

$$A \rightarrow P \tag{18.21}$$

As written, the reaction is a simple first-order transformation of reactant A into product P, and it may occur through a single elementary step. However, what if the reaction were to occur through two elementary steps as follows:

$$A \xrightarrow{k_1} I$$
$$I \xrightarrow{k_2} P \tag{18.22}$$

In this mechanism, the decay of reactant A results in the formation of an intermediate species I that undergoes subsequent decay to produce the reaction product P. One way to validate this mechanism is to observe the formation of the intermediate species. However, if the rate of the second reaction step is fast compared to the rate of the first step, the concentration of [I] will be quite small such that detection of the intermediate may be difficult. As will be seen later, in this limit the product formation kinetics will be consistent with the single elementary step mechanism, and verification of the two-step mechanism is not possible. It is usually assumed that the simplest mechanism consistent with the experimentally determined order dependence is correct until proven otherwise. In this example, a simple single-step mechanism would be considered "correct" until a clever chemist discovered a set of reaction conditions that demonstrates that the reaction must occur by a sequential mechanism.

In order for a reaction mechanism to be valid, the order of the reaction predicted by the mechanism must be in agreement with the experimentally determined rate law. In evaluating a reaction mechanism, one must express the mechanism in terms of elementary reaction steps. The remainder of this chapter involves an investigation of various elementary reaction processes and derivations of the rate law expressions for these elementary reactions. The techniques developed in this chapter can be readily employed in the evaluation of complex kinetic problems, as illustrated in Chapter 19.

# 18.5 Integrated Rate Law Expressions

The rate law determination methods described in Section 18.3 assume that one has a substantial amount of control over the reaction. Specifically, application of the initial rates method requires that the reactant concentrations be controlled and mixed in any proportion desired. In addition, this method requires that the rate of reaction be measured immediately after initiation of the reaction. Unfortunately, many reactions cannot be studied by this technique due to the instability of the reactants involved, or the timescale of the reaction of interest. In this case, other approaches must be employed.

One approach is to assume that the reaction occurs with a given order dependence and then determine how the concentrations of reactants and products will vary as a

function of time. The predictions of the model are compared to experiment to determine if the model provides an appropriate description of the reaction kinetics. **Integrated rate law expressions** provide the predicted temporal evolution in reactant and product concentrations for reactions where the order is assumed. In this section these expressions are derived. For many elementary reactions, integrated rate law expressions can be derived, and some of those cases are considered in this section. However, more complex reactions may be difficult to approach using this technique, and one must resort to numerical methods to evaluate the kinetic behavior associated with a given reaction mechanism. Numerical techniques are discussed in Section 18.6.

### 18.5.1 First-Order Reactions

Consider the following elementary reaction step where reactant A decays, resulting in the formation of product P:

$$A \xrightarrow{k} P \tag{18.23}$$

If the reaction is first order with respect to [A], the corresponding rate law expression is

$$R = k[A] \tag{18.24}$$

where $k$ is the rate constant for the reaction. The reaction rate can also be written in terms of the time derivative of [A]:

$$R = -\frac{d[A]}{dt} \tag{18.25}$$

Because the reaction rates given by Equations (18.24) and (18.25) are the same, we can write

$$\frac{d[A]}{dt} = -k[A] \tag{18.26}$$

Equation (18.26) is known as a differential rate expression. It relates the time derivative of A to the rate constant and concentration dependence of the reaction. It is also a standard differential equation that can be integrated as follows:

$$\int_{[A]_0}^{[A]} \frac{d[A]}{[A]} = \int_0^t -k\,dt$$

$$\ln\left(\frac{[A]}{[A]_0}\right) = -kt$$

$$[A] = [A]_0 e^{-kt} \tag{18.27}$$

The limits of integration employed in obtaining Equation (18.27) correspond to the initial concentration of reactant when the reaction is initiated ($[A] = [A]_0$ at $t = 0$) and the concentration of reactant at a given time after the reaction has started. If only the reactant is present at $t = 0$, the sum of reactant and product concentrations at any time must be equal to $[A]_0$. Using this idea, the concentration of product with time for this **first-order reaction** is

$$[P] + [A] = [A]_0$$

$$[P] = [A]_0 - [A]$$

$$[P] = [A]_0(1 - e^{-kt}) \tag{18.28}$$

Equation (18.27) demonstrates that for a first-order reaction, the concentration of A will undergo exponential decay with time. A graphically convenient version of Equation (18.27) for comparison to experiment is obtained by taking the natural log of the equation:

$$\ln[A] = \ln[A]_0 - kt \tag{18.29}$$

**(a)**



**(b)**
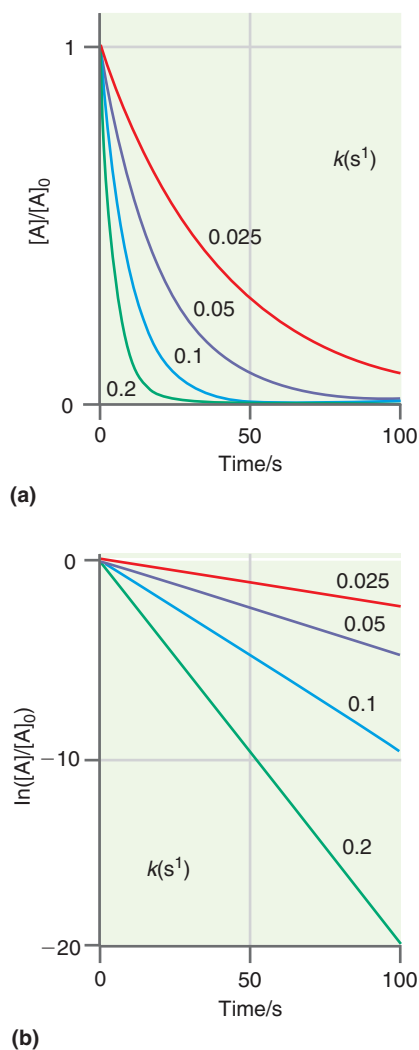
**FIGURE 18.4**
Reactant concentration as a function of time for a first-order chemical reaction as given by Equation (18.27). **(a)** Plots of [A] as a function of time for various rate constants $k$. The rate constant of a given curve is provided in the figure. **(b)** The natural log of reactant concentration as a function of time for a first-order chemical reaction as given by Equation (18.28).

Equation (18.29) predicts that for a first-order reaction, a plot of the natural log of the reactant concentration versus time will be a straight line of slope $-k$ and $y$ intercept equal to the natural log of the initial concentration. Figure 18.4 provides a comparison of the concentration dependences predicted by Equations (18.27) and (18.29) for first-order reactions. It is important to note that the comparison of experimental data to an integrated rate law expression requires that the variation in concentration with time be accurately known over a wide range of reaction times to determine if the reaction indeed follows a certain order dependence.

## 18.5.2 Half-Life and First-Order Reactions

The time it takes for the reactant concentration to decrease to one-half of its initial value is called the **half-life** of the reaction and is denoted as $t_{1/2}$. For a first-order reaction, substitution of the definition for $t_{1/2}$ into Equation (18.29) results in the following:

$$-kt_{1/2} = \ln\left(\frac{[A]_0/2}{[A]_0}\right) = -\ln 2$$

$$t_{1/2} = \frac{\ln 2}{k} \tag{18.30}$$

Notice that the half-life for a first-order reaction is independent of the initial concentration, and only the rate constant of the reaction influences $t_{1/2}$.

---

### EXAMPLE PROBLEM 18.3

The decomposition of $N_2O_5$ is an important process in tropospheric chemistry. The half-life for the first-order decomposition of this compound is $2.05 \times 10^4$ s. How long will it take for a sample of $N_2O_5$ to decay to 60% of its initial value?

### Solution

Using Equation (18.29), the rate constant for the decay reaction is determined using the half-life as follows:

$$k = \frac{\ln 2}{t_{1/2}} = \frac{\ln 2}{2.05 \times 10^4 \text{ s}} = 3.38 \times 10^{-5} \text{ s}^{-1}$$

The time at which the sample has decayed to 60% of its initial value is then determined using Equation (18.27):

$$[N_2O_5] = 0.6[N_2O_5]_0 = [N_2O_5]_0 e^{-(3.38 \times 10^{-5} \text{ s}^{-1})t}$$

$$0.6 = e^{-(3.38 \times 10^{-5} \text{ s}^{-1})t}$$

$$\frac{-\ln(0.6)}{3.38 \times 10^{-5} \text{ s}^{-1}} = t = 1.51 \times 10^4 \text{ s}$$

---

Radioactive decay of unstable nuclear isotopes is an important example of a first-order process. The decay rate is usually stated as the half-life. Example Problem 18.4 demonstrates the use of radioactive decay in determining the age of a carbon-containing material.

---

### EXAMPLE PROBLEM 18.4

Carbon-14 is a radioactive nucleus with a half-life of 5760 years. Living matter exchanges carbon with its surroundings (for example, through $CO_2$) so that a constant level of $^{14}C$ is maintained, corresponding to 15.3 decay events per minute. Once living matter has died, carbon contained in the matter is not exchanged with the surroundings, and the amount of $^{14}C$ that remains in the dead material decreases with time due to radioactive decay. Consider a piece of fossilized wood that demonstrates 2.4 $^{14}C$ decay events per minute. How old is the wood?

**Solution**

The ratio of decay events yields the amount of $^{14}C$ present currently versus the amount that was present when the tree died:

$$\frac{[^{14}C]}{[^{14}C]_0} = \frac{2.40 \text{ min}^{-1}}{15.3 \text{ min}^{-1}} = 0.157$$

The rate constant for isotope decay is related to the half-life as follows:

$$k = \frac{\ln 2}{t_{1/2}} = \frac{\ln 2}{5760 \text{ years}} = \frac{\ln 2}{1.82 \times 10^{11} \text{ s}} = 3.81 \times 10^{-12} \text{ s}^{-1}$$

With the rate constant and ratio of isotope concentrations, the age of the fossilized wood is readily determined:

$$\frac{[^{14}C]}{[^{14}C]_0} = e^{-kt}$$

$$\ln\left(\frac{[^{14}C]}{[^{14}C]_0}\right) = -kt$$

$$-\frac{1}{k}\ln\left(\frac{[^{14}C]}{[^{14}C]_0}\right) = -\frac{1}{3.81 \times 10^{-12} \text{ s}}\ln(0.157) = t$$

$$4.86 \times 10^{11} \text{ s} = t$$

This time corresponds to an age of roughly 15,400 years.

### 18.5.3  Second-Order Reaction (Type I)

Consider the following elementary reaction, which is second order with respect to the reactant A:

$$2 \text{ A} \xrightarrow{k} \text{P} \tag{18.31}$$

**Second-order reactions** involving a single reactant species are referred to as **type I.** Another reaction that is second order overall involves two reactants, A and B, with a rate law that is first order with respect to each reactant. Such reactions are referred to as **second-order reactions of type II.** We focus first on the type I case. For this reaction, the corresponding rate law expression is

$$R = k[\text{A}]^2 \tag{18.32}$$

The rate as expressed as the derivative of reactant concentration is

$$R = -\frac{1}{2}\frac{d[\text{A}]}{dt} \tag{18.33}$$

The rates in the preceding two expressions are equivalent such that

$$-\frac{d[\text{A}]}{dt} = 2k[\text{A}]^2 \tag{18.34}$$

Generally, the quantity $2k$ is written as an effective rate constant, denoted as $k_{eff}$. With this substitution, integration of Equation (18.34) yields

$$-\int_{[\text{A}]_0}^{[\text{A}]} \frac{d[\text{A}]}{[\text{A}]^2} = \int_0^t k_{eff}dt$$

$$\frac{1}{[\text{A}]} - \frac{1}{[\text{A}]_0} = k_{eff}t$$

$$\frac{1}{[\text{A}]} = \frac{1}{[\text{A}]_0} + k_{eff}t \tag{18.35}$$

**(a)**



**(b)**
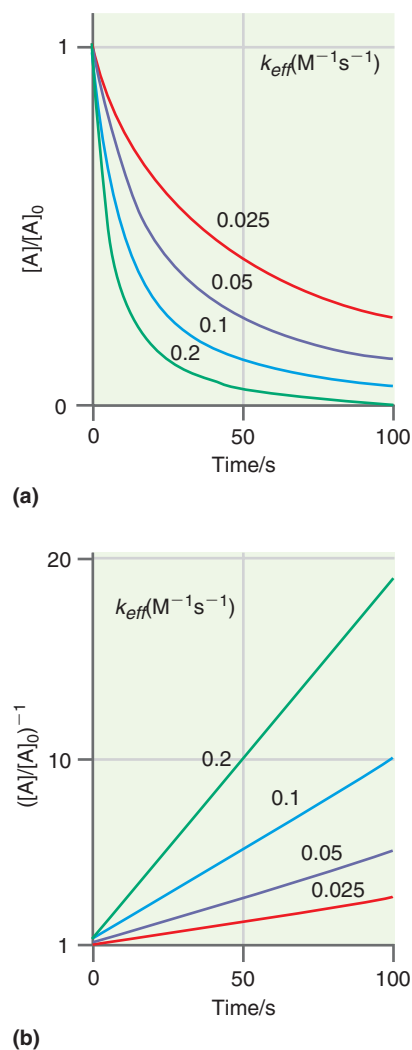
**FIGURE 18.5**
Reactant concentration as a function of time for a type I second-order chemical reaction. **(a)** Plots of [A] as a function of time for various rate constants. The rate constant of a given curve is provided in the figure. **(b)** The inverse of reactant concentration as a function of time as given by Equation (18.35).

Equation (18.35) demonstrates that for a second-order reaction, a plot of the inverse of reactant concentration versus time will result in a straight line having a slope of $k_{eff}$ and $y$ intercept of $1/[A]_0$. Figure 18.5 presents a comparison between [A] versus time for a second-order reaction and $1/[A]$ versus time. The linear behavior predicted by Equation (18.35) is evident.

### 18.5.4 Half-Life and Reactions of Second Order (Type I)

Recall that "half-life" refers to when the concentration of a reactant is half of its initial value. With this definition, the half-life for a type I second-order reaction is

$$t_{1/2} = \frac{1}{k_{eff}[A]_0} \tag{18.36}$$

In contrast to first-order reactions, the half-life for a second-order reaction is dependent on the initial concentration of reactant, with an increase in initial concentration resulting in a decrease in $t_{1/2}$. This behavior is consistent with a first-order reaction occurring through a unimolecular process, whereas the second-order reaction is a bimolecular process that involves the interaction of two species (for example, through collision). As such, the concentration dependence of the reaction rate is expected.

### 18.5.5 Second-Order Reaction (Type II)

Second-order reactions of type II involve two different reactants, A and B, as follows:

$$A + B \xrightarrow{k} P \tag{18.37}$$

Assuming that the reaction is first order in both A and B, the reaction rate is

$$R = k[A][B] \tag{18.38}$$

In addition, the rate with respect to the time derivative of the reactant concentrations is

$$R = -\frac{d[A]}{dt} = -\frac{d[B]}{dt} \tag{18.39}$$

The loss rate for the reactants is equal, so

$$[A]_0 - [A] = [B]_0 - [B]$$
$$[B]_0 - [A]_0 + [A] = [B]$$
$$\Delta + [A] = [B] \tag{18.40}$$

Equation (18.40) provides a definition for [B] in terms of [A] and the difference in initial concentration, $[B]_0 - [A]_0$, denoted as $\Delta$. Beginning with the case where $\Delta \neq 0$ (that is, the initial concentrations of A and B are not the same) setting Equations (18.38) and (18.39) equal results in the following expression:

$$\frac{d[A]}{dt} = -k[A][B] = -k[A](\Delta + [A])$$

$$\int_{[A]_0}^{[A]} \frac{d[A]}{[A](\Delta + [A])} = -\int_0^t k\, dt$$

Next, the solution to an integral of the previous form is given by

$$\int \frac{dx}{x(c + x)} = -\frac{1}{c} \ln\left(\frac{c + x}{x}\right)$$

Using this solution, the integrated rate law expression becomes

$$-\frac{1}{\Delta} \ln\left(\frac{\Delta + [A]}{[A]}\right)\Bigg|_{[A]_0}^{[A]} = -kt$$

$$\frac{1}{\Delta}\left[\ln\left(\frac{\Delta + [A]}{[A]}\right) - \ln\left(\frac{\Delta + [A]_0}{[A]_0}\right)\right] = kt$$

$$\frac{1}{\Delta}\left[\ln\left(\frac{[B]}{[A]}\right) - \ln\left(\frac{[B]_0}{[A]_0}\right)\right] = kt$$

$$\frac{1}{[B]_0 - [A]_0}\ln\left(\frac{[B]/[B]_0}{[A]/[A]_0}\right) = kt \qquad (18.41)$$

Equation (18.41) is applicable when $[B]_0 \neq [A]_0$. For the case where $[B]_0 = [A]_0$, the concentrations of [A] and [B] reduce to the expression for a second-order reaction of type I with $k_{eff} = k$. The time evolution in reactant concentrations depends on the amount of each reactant present. Finally, the concept of half-life does not apply to second-order reactions of type II. Unless the reactants are mixed in stoichiometric proportions (1:1 for the case discussed in this section), the concentrations of both species will not be 1/2 their initial concentrations at the identical time.

SUPPLEMENTAL

# 18.6 Numerical Approaches

For the simple reactions outlined in the preceding section, an integrated rate law expression can be readily determined. However, there is a wide variety of kinetic problems for which an integrated rate law expression cannot be obtained. How can one compare a kinetic model with experiment in the absence of an integrated rate law? In such cases, numerical methods provide another approach by which to determine the time evolution in concentrations predicted by a kinetic model. To illustrate this approach, consider the following first-order reaction:

$$A \xrightarrow{k} P \qquad (18.42)$$

The differential rate expression for this reaction is

$$\frac{d[A]}{dt} = -k[A] \qquad (18.43)$$

The time derivative corresponds to the change in [A] for a time duration that is infinitesimally small. Using this idea, we can state that for a finite time duration $\Delta t$, the change in [A] is given by

$$\frac{\Delta[A]}{\Delta t} = -k[A]$$

$$\Delta[A] = -\Delta t(k[A]) \qquad (18.44)$$

In Equation (18.44), [A] is the concentration of [A] at a specific time. Therefore, we can use this equation to determine the change in the concentration of A, or $\Delta[A]$, over a time period $\Delta t$ and then use this concentration change to determine the concentration at the end of the time period. This new concentration can be used to determine the subsequent change in [A] over the next time period, and this process is continued until the reaction is complete. Mathematically,

$$[A]_{t+\Delta t} = [A]_t + \Delta[A]$$
$$= [A]_t - k\Delta t[A]_t \qquad (18.45)$$

In Equation (18.45), $[A]_t$ is the concentration at the beginning of the time interval, and $[A]_{t+\Delta t}$ is the concentration at the end of the time interval. This process is illustrated in Figure 18.6. In the figure, the initial concentration is used to determine $\Delta[A]$ over the time interval $\Delta t$. The concentration at this next time point, $[A]_1$, is used to determine
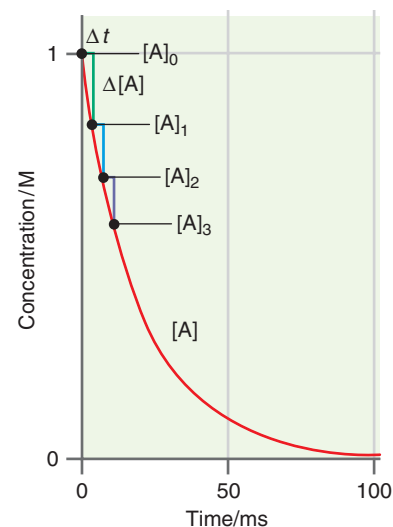


**FIGURE 18.6**
Schematic representation of the numerical evaluation of a rate law.
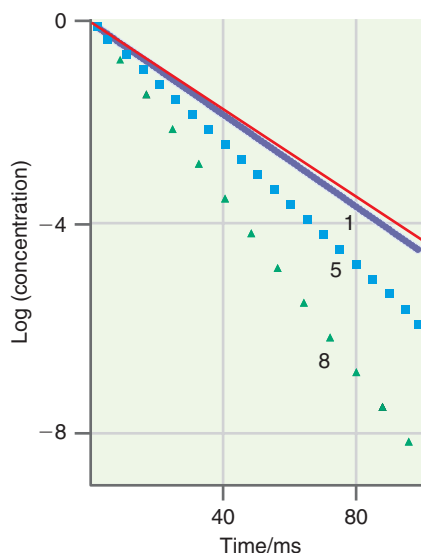
**FIGURE 18.7**
Comparison of the numerical approximation method to the integrated rate law expression for a first-order reaction. The rate constant for the reaction is $0.1 \text{ M s}^{-1}$. The time evolution in reactant concentration determined by the integrated rate law expression of Equation (18.27) is shown as the solid red line. Comparison to three numerical approximations is given, and the size of the time step (in ms) employed for each approximation is indicated. Notice the improvement in the numerical approximation as the time step is decreased.

$\Delta[A]$ over the next time interval, resulting in concentration $[A]_2$. This process is continued until the entire concentration profile is evaluated.

The specific example discussed here is representative of the general approach to numerically integrating differential equations, known as **Euler's method.** Application of Euler's method requires some knowledge of the timescale of interest, and then selection of a time interval $\Delta t$ that is sufficiently small to capture the evolution in concentration. Figure 18.7 presents a comparison of the reactant concentration determined using the integrated rate law expression for a first-order reaction to that determined numerically for three different choices for $\Delta t$. The figure illustrates that the accuracy of this method is highly dependent on an appropriate choice for $\Delta t$. In practice, convergence of the numerical model is demonstrated by reducing $\Delta t$ and observing that the predicted evolution in concentrations does not change.

The numerical method can be applied to any kinetic process for which differential rate expressions can be prescribed. Euler's method provides the most straightforward way by which to predict how reactant and product concentrations will vary for a specific kinetic scheme. However, this method is "brute force" in that a sufficiently small time step must be chosen to accurately capture the slope of the concentration, and the time steps may be quite small, requiring a large number of iterations in order to reproduce the full time course of the reaction. As such, Euler's method can be computationally demanding. More elegant approaches, such as the Runge–Kutta method, exist that allow for larger time steps to be performed in numerical evaluations, and the interested reader is encouraged to investigate these approaches.

# 18.7 Sequential First-Order Reactions

Many chemical reactions occur in a series of steps in which reactants are transformed into products through multiple sequential elementary reaction steps. For example, consider the following **sequential reaction** scheme:

$$A \overset{k_A}{\rightarrow} I \overset{k_I}{\rightarrow} P \tag{18.46}$$

In this scheme, the reactant A decays to form intermediate I, and this intermediate undergoes subsequent decay resulting in the formation of product P. Species I is known as an **intermediate.** The sequential reaction scheme illustrated in Equation (18.46) involves a series of elementary first-order reactions. Recognizing this, the differential rate expressions for each species can be written as follows:

$$\frac{d[A]}{dt} = -k_A[A] \tag{18.47}$$

$$\frac{d[I]}{dt} = k_A[A] - k_I[I] \tag{18.48}$$

$$\frac{d[P]}{dt} = k_I[I] \tag{18.49}$$

These expressions follow naturally from the elementary reaction steps in which a given species participates. For example, the decay of A occurs in the first step of the reaction. The decay is a first-order process, consistent with the differential rate expression in Equation (18.47). The formation of product P is also a first-order process per Equation (18.49). The expression of Equation (18.48) for intermediate I reflects the fact that I is involved in both elementary reaction steps, the decay of A ($k_A[A]$), and the formation of P ($-k_I[I]$). Correspondingly, the differential rate expression for [I] is the sum of the rates associated with these two reaction steps. To determine the concentrations of each species as a function of time, we begin with Equation (18.47), which can be readily integrated given a set of initial concentrations. Let only the reactant A be present at $t = 0$ such that

$$[A]_0 \neq 0; \ [I]_0 = 0; \ [P]_0 = 0 \tag{18.50}$$

With these initial conditions, the expression for [A] is exactly that derived previously:

$$[A] = [A]_0 e^{-k_A t} \tag{18.51}$$

The expression for [A] given by Equation (18.51) can be substituted into the differential rate expression for I resulting in

$$\frac{d[I]}{dt} = k_A[A] - k_I[I]$$

$$= k_A[A]_0 e^{-k_A t} - k_I[I] \tag{18.52}$$

Equation (18.52) is a differential equation that when solved yields the following expression for [I]:

$$[I] = \frac{k_A}{k_I - k_A}(e^{-k_A t} - e^{-k_I t})[A]_0 \tag{18.53}$$

Finally, the expression for [P] is readily determined using the initial conditions of the reaction, with the initial concentration of A, $[A]_0$, equal to the sum of all concentrations for $t > 0$:

$$[A]_0 = [A] + [I] + [P]$$

$$[P] = [A]_0 - [A] - [I] \tag{18.54}$$

Substituting Equations (18.51) and (18.53) into Equation (18.54) results in the following expression for [P]:

$$[P] = \left(\frac{k_A e^{-k_I t} - k_I e^{-k_A t}}{k_I - k_A} + 1\right)[A]_0 \tag{18.55}$$

Although the expressions for [I] and [P] look complicated, the temporal evolution in concentration predicted by these equations is intuitive as shown in Figure 18.8. Figure 18.8a presents the evolution in concentration when $k_A = 2k_I$. Notice that A undergoes exponential decay resulting in the production of I. The intermediate in turn undergoes subsequent decay to form the product. The temporal evolution of [I] is extremely dependent on the relative rate constants for the production $k_A$ and decay $k_I$. Figure 18.8b presents the case where $k_A > k_I$. Here, the maximum intermediate concentration is greater than in the first case. The opposite limit is illustrated in Figure 18.8c, where $k_A < k_I$ and the maximum in intermediate concentration is significantly reduced. This behavior is consistent with intuition: if the intermediate undergoes decay at a faster rate than the rate at which it is being formed, then the intermediate concentration will be small. Of course, the opposite logic holds as evidenced by the $k_A > k_I$ example presented in the Figure 18.8b.

**FIGURE 18.8**
Concentration profiles for a sequential reaction in which the reactant (A, blue line) forms an intermediate (I, purple line) that undergoes subsequent decay to form the product (P, red line) where (a) $k_A = 2k_I = 0.1$ s$^{-1}$ and (b) $k_A = 8k_I = 0.4$ s$^{-1}$. Notice that both the maximal amount of I in addition to the time for the maximum is changed relative to the first panel. (c) $k_A = 0.025k_I = 0.0125$ s$^{-1}$. In this case, very little intermediate is formed, and the maximum in [I] is delayed relative to the first two examples.



(a)



(b)



(c)
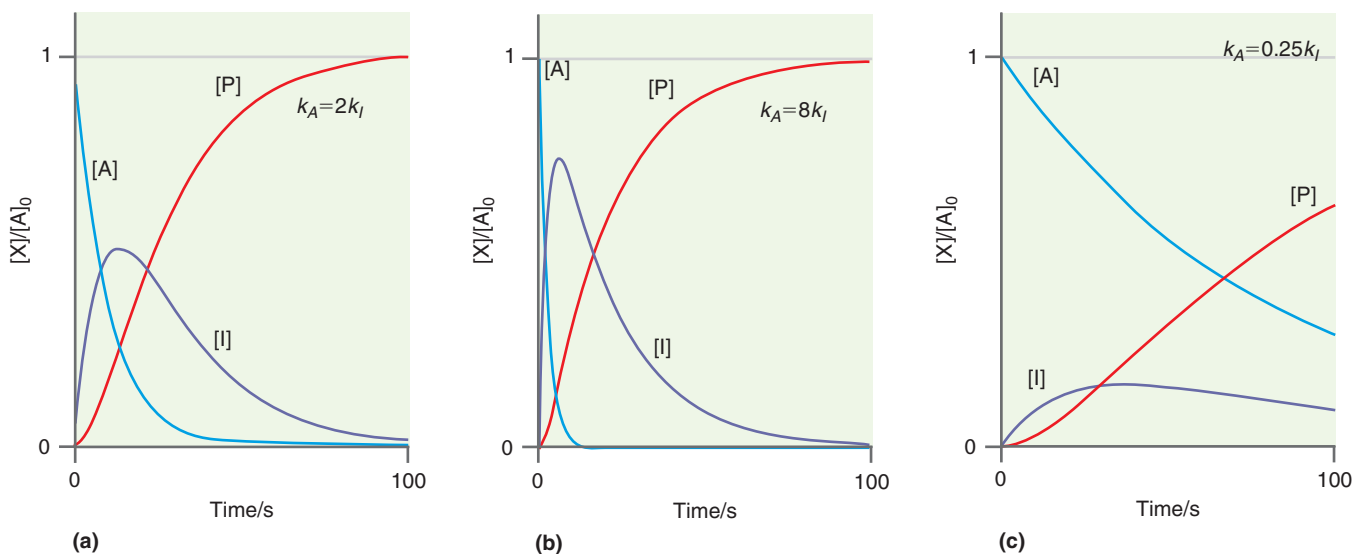
### 18.7.1 Maximum Intermediate Concentration

Inspection of Figure 18.8 demonstrates that the time at which the concentration of the intermediate species will be at a maximum depends on the rate constants for its production and decay. Can we predict when [I] will be at a maximum? The maximum intermediate concentration has been reached when the derivative of [I] with respect to time is equal to zero:

$$\left(\frac{d[\text{I}]}{dt}\right)_{t=t_{max}} = 0 \qquad (18.56)$$

Using the expression for [I] given in Equation (18.53) in the preceding equation, the time at which [I] is at a maximum, $t_{max}$, is

$$t_{max} = \frac{1}{k_A - k_I} \ln\left(\frac{k_A}{k_I}\right) \qquad (18.57)$$

---

**EXAMPLE PROBLEM 18.5**

Determine the time at which [I] is at a maximum for $k_A = 2k_I = 0.1 \text{ s}^{-1}$.

**Solution**

This is the first example illustrated in Figure 18.8 where $k_A = 0.1 \text{ s}^{-1}$ and $k_I = 0.05 \text{ s}^{-1}$. Using these rate constants and Equation (18.57), $t_{max}$ is determined as follows:

$$t_{max} = \frac{1}{k_A - k_I} \ln\left(\frac{k_A}{k_I}\right) = \frac{1}{0.1 \text{ s}^{-1} - 0.05 \text{ s}^{-1}} \ln\left(\frac{0.1 \text{ s}^{-1}}{0.05 \text{ s}^{-1}}\right) = 13.9 \text{ s}$$

---

### 18.7.2 Rate-Determining Steps

In the preceding subsection, the rate of product formation in a sequential reaction was found to depend on the timescale for production and decay of the intermediate species. Two limiting situations can be envisioned for a sequential reaction. The first limit is where the rate constant for intermediate decay is much greater than the rate constant for production, that is, where $k_I \gg k_A$ in Equation (18.46). In this limit, any intermediate formed will rapidly go on to product, and the rate of product formation depends on the rate of reactant decay. The opposite limit occurs when the rate constant for intermediate production is significantly greater than the intermediate decay rate constant, that is, where $k_A \gg k_I$ in Equation (18.46). In this limit, reactants quickly produce intermediate, but the rate of product formation depends on the rate of intermediate decay. These two limits give rise to one of the most important approximations made in the analysis of kinetic problems, that of the **rate-determining step** or the rate-limiting step. The central idea behind this approximation is as follows: if one step in the sequential reaction is much slower than any other step, the slow step will control the rate of product formation and is therefore the rate-determining step.

Consider the sequential reaction illustrated in Equation (18.46) when $k_A \gg k_I$. In this limit, the kinetic step corresponding to the decay of intermediate I is the rate limiting step. Because $k_A \gg k_I$, $e^{-k_A t} \ll e^{-k_I t}$ and the expression for [P] of Equation (18.55) becomes

$$\lim_{k_A \gg k_I} [\text{P}] = \lim_{k_A \gg k_I} \left(\left(\left(\frac{k_A e^{-k_I t} - k_I e^{-k_A t}}{k_I - k_A}\right) + 1\right)[\text{A}]_0\right) = (1 - e^{-k_I t})[\text{A}]_0 \quad (18.58)$$

The time dependence of [P] when $k_I$ is the rate-limiting step is identical to that predicted for first order decay of I resulting in product formation. The other limit occurs when $k_I \gg k_A$, where $e^{-k_I t} \ll e^{-k_A t}$, and the expression for [P] becomes

$$\lim_{k_I \gg k_A} [\text{P}] = \lim_{k_I \gg k_A} \left(\left(\frac{k_A e^{-k_I t} - k_I e^{-k_A t}}{k_I - k_A} + 1\right)[\text{A}]_0\right) = (1 - e^{-k_A t})[\text{A}]_0 \quad (18.59)$$

In this limit, the time dependence of [P] is identical to that predicted for the first-order decay of the reactant A, resulting in product formation.

When is the rate-determining step approximation appropriate? For the two-step reaction under consideration, 20-fold differences between rate constants are sufficient to ensure that the smaller rate constant will be rate determining. Figure 18.9 presents a comparison for [P] determined using the exact result from Equation (18.55) and the rate-limited prediction of Equations (18.58) and (18.59) for the case where $k_A = 20k_I = 1 \text{ s}^{-1}$ and where $k_A = 0.04k_I = 0.02 \text{ s}^{-1}$. In Figure 18.9a, decay of the intermediate is the rate-limiting step in product formation. Notice the rapid reactant decay, resulting in an appreciable intermediate concentration, with the subsequent decay of the intermediate reflected by a corresponding increase in [P]. The similarity of the exact and rate-limiting curves for [P] demonstrates the validity of the rate-limiting approximation for this ratio of rate constants. The opposite limit is presented in Figure 18.9b. In this case, decay of the reactant is the rate-limiting step in product formation. When reactant decay is the rate-limiting step, very little intermediate is produced. In this case, the loss of [A] is mirrored by an increase in [P]. Again, the agreement between the exact and rate-limiting descriptions of [P] demonstrates the validity of the rate-limiting approximation when a substantial difference in rate constants for intermediate production and decay exists.

### 18.7.3 The Steady-State Approximation

Consider the following sequential reaction scheme:

$$A \xrightarrow{k_A} I_1 \xrightarrow{k_1} I_2 \xrightarrow{k_2} P \qquad (18.60)$$

In this reaction, product formation results from the formation and decay of two intermediate species, $I_1$ and $I_2$. The differential rate expressions for this scheme are as follows:

$$\frac{d[A]}{dt} = -k_A[A] \qquad (18.61)$$

$$\frac{d[I_1]}{dt} = k_A[A] - k_1[I_1] \qquad (18.62)$$

$$\frac{d[I_2]}{dt} = k_1[I_1] - k_2[I_2] \qquad (18.63)$$

$$\frac{d[P]}{dt} = k_2[I_2] \qquad (18.64)$$

A determination of the time-dependent concentrations for the species involved in this reaction by integration of the differential rate expressions is not trivial; therefore, how can the concentrations be determined? One approach is to use Euler's method (Section 18.6) and numerically determine the concentrations as a function of time. The result of this approach for $k_A = 0.02 \text{ s}^{-1}$ and $k_1 = k_2 = 0.2 \text{ s}^{-1}$ is presented in Figure 18.10. Notice that the relative magnitude of the rate constants results in only modest intermediate concentrations.

Inspection of Figure 18.10 illustrates that [I$_1$] and [I$_2$] undergo little change with time. As such, the time derivative of these concentrations is approximately equal to zero:

$$\frac{d[I]}{dt} = 0 \qquad (18.65)$$

Equation (18.65) is known as the **steady-state approximation.** This approximation is used to evaluate the differential rate expressions by simply setting the time derivative of all intermediates to zero. This approximation is particularly good when the decay rate of the intermediate is greater than the rate of production so that the intermediates are present at very small concentrations during the reaction (as in the case illustrated in Figure 18.10). Applying the steady-state approximation to $I_1$ in our example reaction results in the following expression for [I$_1$]:

$$\frac{d[I_1]_{ss}}{dt} = 0 = k_A[A] - k_1[I_1]_{ss}$$

$$[I_1]_{ss} = \frac{k_A}{k_1}[A] = \frac{k_A}{k_1}[A]_0 e^{-k_A t} \qquad (18.66)$$
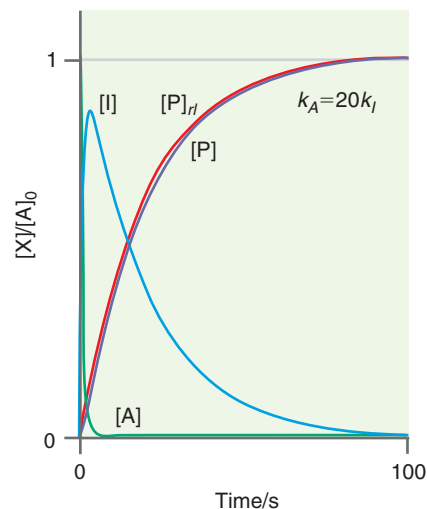
(a)
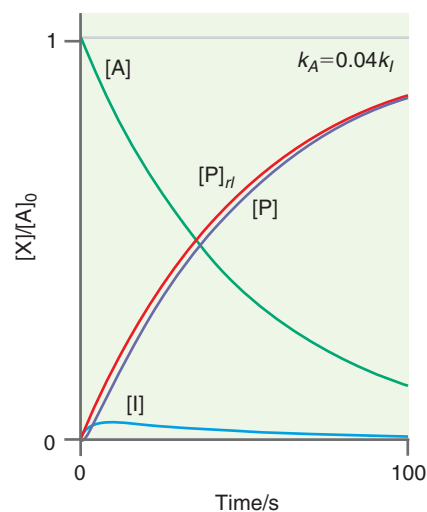
(b)

**FIGURE 18.9**
Rate-limiting step behavior in sequential reactions. **(a)** $k_A = 20k_I = 1 \text{ s}^{-1}$ such that the rate-limiting step is the decay of intermediate I. In this case, the reduction in [I] is reflected by the appearance of [P]. The time evolution of [P] predicted by the sequential mechanism is given by the purple line, and the corresponding evolution assuming rate-limiting step behavior, [P]$_{rl}$, is given by the red curve. **(b)** The opposite case from part (a) in which $k_A = 0.04k_I = 0.02 \text{ s}^{-1}$ such that the rate-limiting step is the decay of reactant A.

**FIGURE 18.10**
Concentrations determined by numerical evaluation of the sequential reaction scheme presented in Equation (18.60) where $k_A = 0.02 \text{ s}^{-1}$ and $k_1 = k_2 = 0.2 \text{ s}^{-1}$.
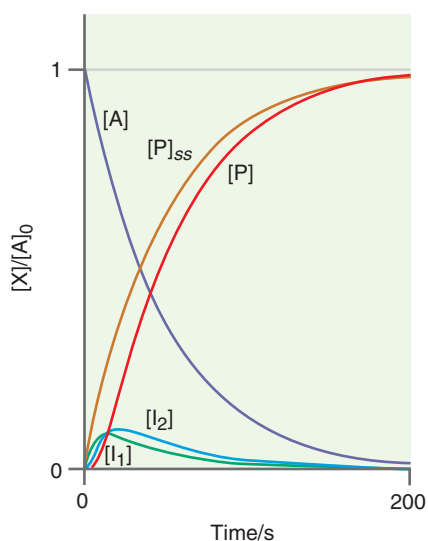
where the subscript *ss* indicates that the concentration is that predicted using the steady-state approximation. The final equality in Equation (18.66) results from integration of the differential rate expression for [A] with the initial conditions that $[A]_0 \neq 0$ and all other initial concentrations are zero. The corresponding expression for $[I_2]$ under the steady-state approximation is

$$\frac{d[I_2]_{ss}}{dt} = 0 = k_1[I_1]_{ss} - k_2[I_2]_{ss}$$

$$[I_2]_{ss} = \frac{k_1}{k_2}[I_1]_{ss} = \frac{k_A}{k_2}[A]_0 e^{-k_A t} \qquad (18.67)$$

Finally, the differential expression for *P* is

$$\frac{d[P]_{ss}}{dt} = k_2[I_2] = k_A[A]_0 e^{-k_A t} \qquad (18.68)$$

Integration of Equation (18.68) results in the now familiar expression for [P]:

$$[P]_{ss} = [A]_0 (1 - e^{-k_A t}) \qquad (18.69)$$

Equation (18.69) demonstrates that within the steady-state approximation, [P] is predicted to demonstrate appearance kinetics consistent with the first-order decay of A.

When is the steady-state approximation valid? The approximation requires that the concentration of intermediate be constant as a function of time. Consider the concentration of the first intermediate under the steady-state approximation. The time derivative of $[I_1]_{ss}$ is

$$\frac{d[I_1]_{ss}}{dt} = \frac{d}{dt}\left(\frac{k_A}{k_1}[A]_0 e^{-k_A t}\right) = -\frac{k_A^2}{k_1}[A]_0 e^{-k_A t} \qquad (18.70)$$

The steady-state approximation is valid when Equation (18.70) is equal to zero, which is true when $k_1 \gg k_A^2[A]_0$. In other words, $k_1$ must be sufficiently large such that $[I_1]$ is small at all times. Similar logic applies to $I_2$ for which the steady-state approximation is valid when $k_2 \gg k_A^2[A]_0$.

Figure 18.11 presents a comparison between the numerically determined concentrations and those predicted using the steady-state approximation for the two-intermediate sequential reaction where $k_A = 0.02 \text{ s}^{-1}$ and $k_1 = k_2 = 0.2 \text{ s}^{-1}$. Notice that even for these conditions where the steady-state approximation is expected to be valid, the discrepancy between [P] determined by numerical evaluation versus the steady-state approximation value, $[P]_{ss}$, is evident. For the examples presented here, the steady-state approximation is relatively easy to implement; however, for many reactions the approximation of constant intermediate concentration with time is not appropriate. In addition, the steady-state approximation is difficult to implement if the intermediate concentrations are not isolated to one or two of the differential rate expressions derived from the mechanism of interest.



**FIGURE 18.11**
Comparison of the numerical and steady-state concentration profiles for the sequential reaction scheme presented in Equation (18.44) where $k_A = 0.02 \text{ s}^{-1}$ and $k_1 = k_2 = 0.2 \text{ s}^{-1}$. Curves corresponding to the steady-state approximation are indicated by the subscript *ss*.

## EXAMPLE PROBLEM 18.6

Consider the following sequential reaction scheme:

$$A \xrightarrow{k_A} I \xrightarrow{k_I} P$$
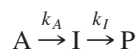
Assuming that only reactant A is present at $t = 0$, what is the expected time dependence of [P] using the steady-state approximation?

**Solution**

The differential rate expressions for this reaction were provided in Equations (18.47), (18.48), and (18.49):

$$\frac{d[A]}{dt} = -k_A[A]$$

$$\frac{d[I]}{dt} = k_A[A] - k_I[I]$$

$$\frac{d[P]}{dt} = k_I[I]$$

Applying the steady-state approximation to the differential rate expression for I and substituting in the integrated expression for [A] of Equation (18.51) yield

$$\frac{d[\text{I}]}{dt} = 0 = k_A[\text{A}] - k_I[\text{I}]$$

$$\frac{k_A}{k_I}[\text{A}] = \frac{k_A}{k_I}[\text{A}]_0\, e^{-k_A t} = [\text{I}]$$

Substituting the preceding expression for [I] into the differential rate expression for the product and integrating yield

$$\frac{d[\text{P}]}{dt} = k_I[\text{I}] = \frac{k_A}{k_I}\left(k_I[\text{A}]_0\, e^{-k_A t}\right)$$

$$\int_0^{[\text{P}]} d[\text{P}] = k_A[\text{A}]_0 \int_0^t e^{-k_A t}\, dt$$

$$[\text{P}] = k_A[\text{A}]_0\left[\frac{1}{k_A}\left(1 - e^{-k_A t}\right)\right]$$

$$[\text{P}] = [\text{A}]_0\left(1 - e^{-k_A t}\right)$$

This expression for [P] is identical to that derived when the decay of A is treated as the rate-limiting step in the sequential reaction [Equation (18.59)].

# 18.8 Parallel Reactions

In the reactions discussed thus far, reactant decay results in the production of only a single species. However, in many instances a single reactant can become a variety of products. Such reactions are referred to as **parallel reactions.** Consider the following reaction in which the reactant A can form one of two products, B or C:
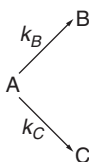


$$\text{(18.71)}$$

The differential rate expressions for the reactant and products are

$$\frac{d[\text{A}]}{dt} = -k_B[\text{A}] - k_C[\text{A}] = -(k_B + k_C)[\text{A}] \qquad \text{(18.72)}$$

$$\frac{d[\text{B}]}{dt} = k_B[\text{A}] \qquad \text{(18.73)}$$

$$\frac{d[\text{C}]}{dt} = k_C[\text{A}] \qquad \text{(18.74)}$$

Integration of the preceding expression involving [A] with the initial conditions $[\text{A}]_0 \neq 0$ and $[\text{B}] = [\text{C}] = 0$ yields

$$[\text{A}] = [\text{A}]_0\, e^{-(k_B + k_C)t} \qquad \text{(18.75)}$$

The product concentrations can be determined by substituting the expression for [A] into the differential rate expressions and integrating, which results in

$$[\text{B}] = \frac{k_B}{k_B + k_C}[\text{A}]_0\left(1 - e^{-(k_B + k_C)t}\right) \qquad \text{(18.76)}$$

$$[\text{C}] = \frac{k_C}{k_B + k_C}[\text{A}]_0\left(1 - e^{-(k_B + k_C)t}\right) \qquad \text{(18.77)}$$
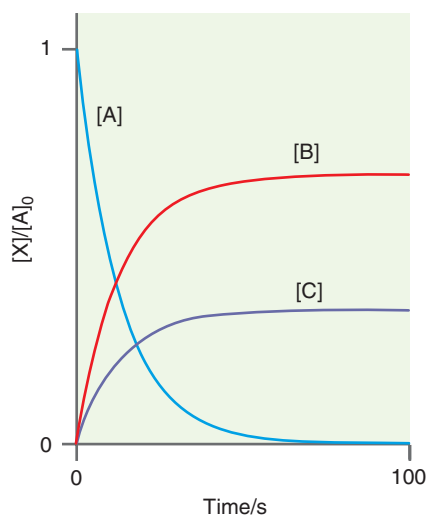
**FIGURE 18.12**
Concentrations for a parallel reaction where $k_B = 2k_C = 0.1 \text{ s}^{-1}$.

Figure 18.12 provides an illustration of the reactant and product concentrations for this branching reaction where $k_B = 2k_C = 0.1 \text{ s}^{-1}$. A few general trends demonstrated by branching reactions are evident in the figure. First, notice that the decay of A occurs with an apparent rate constant equal to $k_B + k_C$, the sum of rate constants for each reaction branch. Second, the ratio of product concentrations is independent of time. That is, at any time point the ratio $[B]/[C]$ is identical. This behavior is consistent with Equations (18.76) and (18.77) where this ratio of product concentrations is predicted to be

$$\frac{[B]}{[C]} = \frac{k_B}{k_C} \tag{18.78}$$

Equation (18.78) is a very interesting result. The equation states that as the rate constant for one of the reaction branches increases relative to the other, the final concentration of the corresponding product increases as well. Furthermore, notice that the ratio of the product concentrations in Equation (18.78) contains no time dependence; therefore, the product ratio will be the same throughout the course of the reaction.

Equation (18.78) demonstrates that the extent of product formation in a parallel reaction is dependent on the rate constants. Another way to view this behavior is with respect to probability; the larger the rate constant for a given process, the more likely that product will be formed. The **yield** $\Phi$ is defined as the probability that a given product will be formed by decay of the reactant:

$$\Phi_i = \frac{k_i}{\sum_n k_n} \tag{18.79}$$

In Equation (18.79), $k_i$ is the rate constant for the reaction leading to formation of the product of interest indicated by the subscript $i$. The denominator is the sum over all rate constants for the reaction branches. The total yield is the sum of the yields for forming each product, and it is normalized such that

$$\sum_i \Phi_i = 1 \tag{18.80}$$

In the example reaction depicted in Figure 18.12 where $k_B = 2k_C$, the yield for the formation of product C is

$$\Phi_C = \frac{k_C}{k_B + k_C} = \frac{k_C}{(2k_C) + k_C} = \frac{1}{3} \tag{18.81}$$

Because there are only two branches in this reaction, $\Phi_B = 2/3$. Inspection of Figure 18.12 reveals that $[B] = 2[C]$, which is consistent with the calculated yields.

---

**EXAMPLE PROBLEM 18.7**

In acidic conditions, benzyl penicillin (BP) undergoes the following parallel reaction:
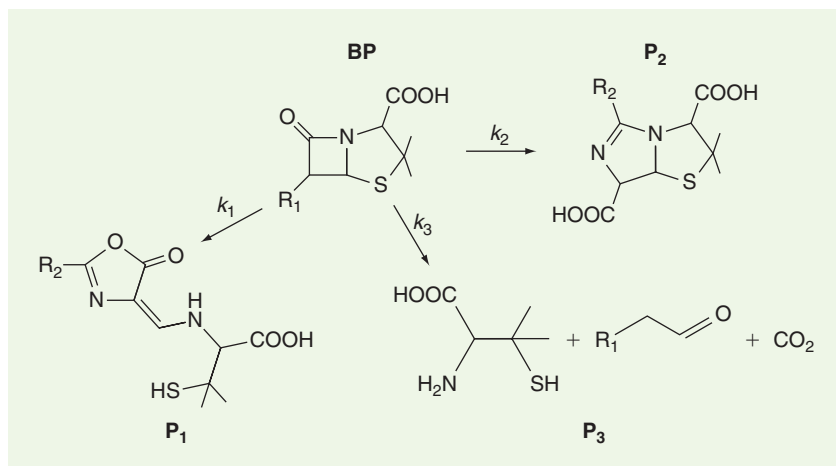
In the molecular structures, $R_1$ and $R_2$ indicate alkyl substituents. Imagine swallowing penicillin while in your stomach the pH is $\sim 3$. At this pH the rate constants for the processes at 22°C are $k_1 = 7.0 \times 10^{-4}$ s$^{-1}$, $k_2 = 4.1 \times 10^{-3}$ s$^{-1}$, and $k_3 = 5.7 \times 10^{-3}$ s$^{-1}$. What is the yield for $P_1$ formation?

#### Solution

Using Equation (18.79),

$$\Phi_{P_1} = \frac{k_1}{k_1 + k_2 + k_3} = \frac{7.0 \times 10^{-4}\ \text{s}^{-1}}{7.0 \times 10^{-4}\ \text{s}^{-1} + 4.1 \times 10^{-3}\ \text{s}^{-1} + 5.7 \times 10^{-3}\ \text{s}^{-1}}$$

$$= 0.067$$

Of the BP that undergoes acid-catalyzed dissociation, 6.7% will result in the formation of $P_1$.

# 18.9 Temperature Dependence of Rate Constants

As mentioned at the beginning of this chapter, rate constants ($k$) are generally temperature-dependent quantities. Experimentally, it is observed that for many reactions a plot of $\ln(k)$ versus $T^{-1}$ demonstrates linear or close to linear behavior. The following empirical relationship between temperature and $k$, first proposed by Arrhenius in the late 1800s, is known as the **Arrhenius expression:**

$$k = Ae^{-E_a/RT} \tag{18.82}$$

In Equation (18.82), the constant $A$ is referred to as the **frequency factor** or **Arrhenius preexponential factor,** and $E_a$ is the **activation energy** for the reaction. The units of the preexponential factor are identical to those of the rate constant and will vary depending on the order of the reaction. The activation energy is in units of energy mol$^{-1}$ (for example, kJ mol$^{-1}$). The natural log of Equation (18.82) results in the following expression:

$$\ln(k) = \ln(A) - \frac{E_a}{R}\frac{1}{T} \tag{18.83}$$

Equation (18.83) predicts that a plot of $\ln(k)$ versus $T^{-1}$ will yield a straight line with slope equal to $-E_a/R$ and $y$ intercept equal to $\ln(A)$. Example Problem 18.8 provides an application of Equation (18.83) to determine the Arrhenius parameters for a reaction.

### EXAMPLE PROBLEM 18.8

The temperature dependence of the acid-catalyzed hydrolysis of penicillin (illustrated in Example Problem 18.7) is investigated, and the dependence of $k_1$ on temperature is given in the following table. What is the activation energy and Arrhenius preexponential factor for this branch of the hydrolysis reaction?

| Temperature (°C) | $k_1$ (s$^{-1}$) |
| --- | --- |
| 22.2 | $7.0 \times 10^{-4}$ |
| 27.2 | $9.8 \times 10^{-4}$ |
| 33.7 | $1.6 \times 10^{-3}$ |
| 38.0 | $2.0 \times 10^{-3}$ |

**Solution**

A plot of $\ln(k_1)$ versus $T^{-1}$ is shown here:
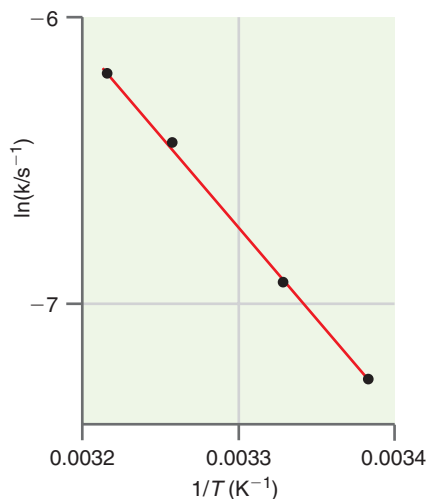


The data are indicated by the points, and the solid line corresponds to the linear least-squares fit to the data. The equation for the line is

$$\ln(k) = (-6300 \text{ K})\frac{1}{T} + 14.1$$

As shown in Equation (18.83), the slope of the line is equal to $-E_a/R$ such that

$$6300 \text{ K} = \frac{E_a}{R} \Rightarrow E_a = 52{,}400 \text{ J mol}^{-1} = 52.4 \text{ kJ mol}^{-1}$$

The $y$ intercept is equal to $\ln(A)$ such that

$$A = e^{14.1} = 1.33 \times 10^6 \text{ s}^{-1}$$

The origin of the energy term in the Arrhenius expression can be understood as follows. The activation energy corresponds to the energy needed for the chemical reaction to occur. Conceptually, we envision a chemical reaction as occurring along an energy profile as illustrated in Figure 18.13. If the energy content of the reactants is greater than the activation energy, the reaction can proceed. In Figure 18.13 Boltzmann distributions

**FIGURE 18.13**
A schematic drawing of the energy profile for a chemical reaction. Reactants must acquire sufficient energy to overcome the activation energy $E_a$ for the reaction to occur. The reaction coordinate represents the bonding and geometry changes that occur in the transformation of reactants into products. Shown here are Boltzmann distributions of molecular translational energy ($E_{trans}$) at 200 and 500 K. Notice that the fraction of molecules with translational energy greater than $E_a$ increase with temperature.
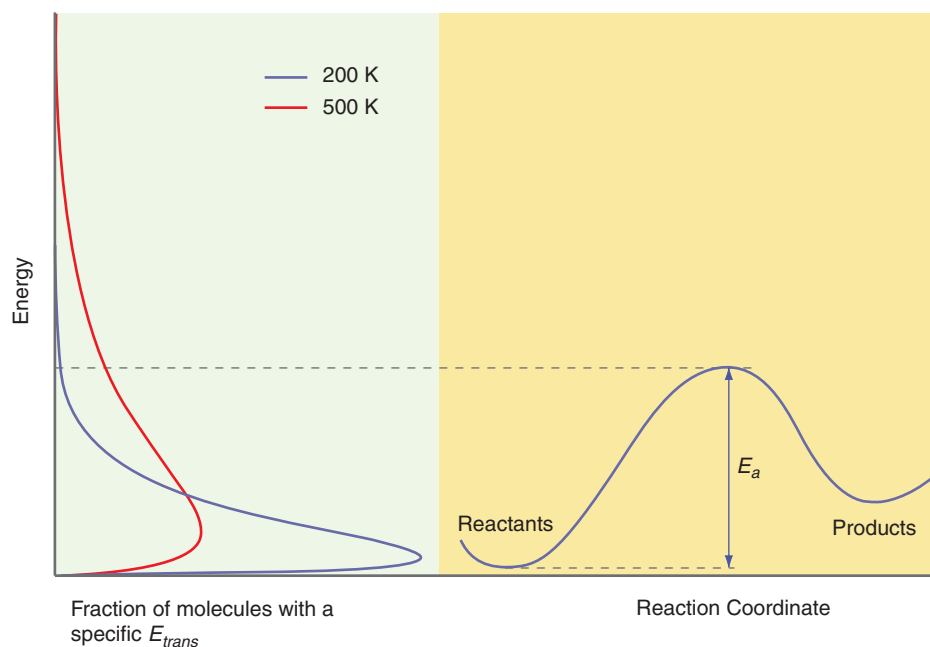
of translational energy at 200 K and 500 K are presented. Notice that the number of molecules with translational energy greater than $E_a$ increases with temperature. This behavior is captured in the exponential dependence on the activation energy, given by $\exp(-E_a/RT)$. At fixed temperature, as the activation energy for a reaction increases the fraction of molecules with sufficient energy to react will decrease, and this will be reflected as a decrease in the reaction rate.

Not all chemical reactions demonstrate Arrhenius behavior. Specifically, the inherent assumption in Equation (18.83) is that both $E_a$ and $A$ are temperature-independent quantities. There are many reactions for which a plot of $\ln(k)$ versus $T^{-1}$ does not yield a straight line, consistent with the temperature dependence of one or both of the Arrhenius parameters. Modern theories of reaction rates predict that the rate constant will demonstrate the following behavior:

$$k = aT^m e^{-E'/RT}$$

where $a$ and $E'$ are temperature-independent quantities, and $m$ can assume values such as 1, 1/2, and $-1/2$ depending on the details of the theory used to predict the rate constant. For example, in the upcoming section on activated complex theory (Section 18.14), a value of $m = 1$ is predicted. With this value for $m$, a plot of $\ln(k/T)$ versus $T^{-1}$ should yield a straight line with slope equal to $-E'/R$ and the $y$ intercept equal to $\ln(a)$. Although the limitations of the Arrhenius expression are well known, this relationship still provides an adequate description of the temperature dependence of reaction rate constants for a wide variety of reactions.

# 18.10 Reversible Reactions and Equilibrium

In the kinetic models discussed in earlier sections, it was assumed that once reactants form products, the opposite or "back" reaction does not occur. However, the **reaction coordinate** presented in Figure 18.14 suggests that, depending on the energetics of the reaction, such reactions can indeed occur. Specifically, the figure illustrates that reactants form products if they have sufficient energy to overcome the activation energy for the reaction. But what if the reaction coordinate is viewed from the product's perspective? Can the coordinate be followed in reverse, with products returning to reactants by overcoming the activation energy barrier from the product side $E_a'$ of the coordinate? Such **reversible reactions** are discussed in this section.

Consider the following reaction in which the forward reaction is first order in A, and the back reaction is first order in B:

$$A \underset{k_B}{\overset{k_A}{\rightleftharpoons}} B \qquad\qquad \textbf{(18.84)}$$
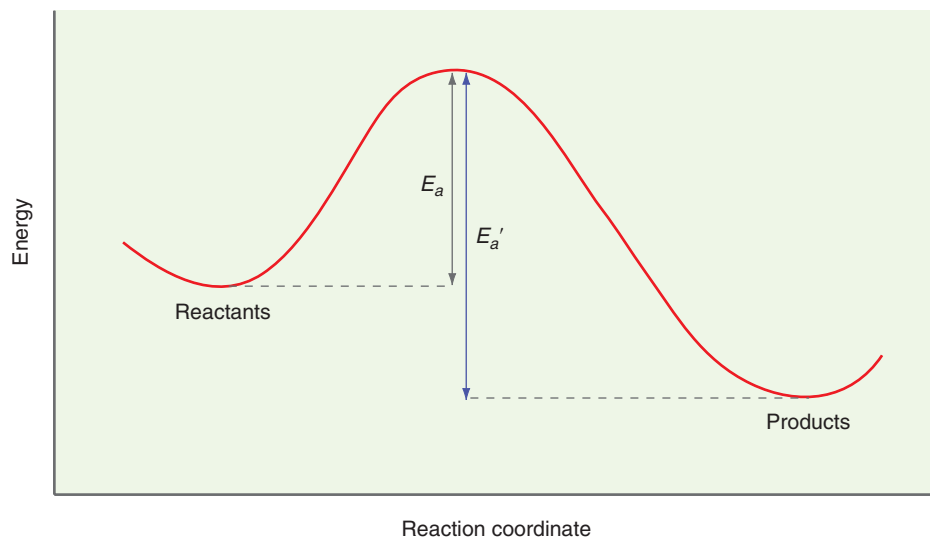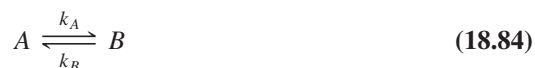


**FIGURE 18.14**
Reaction coordinate demonstrating the activation energy for reactants to form products $E_a$ and the back reaction in which products form reactants $E_a'$.

The forward and back rate constants are $k_A$ and $k_B$, respectively. Integrated rate law expressions can be obtained for this reaction starting with the differential rate expressions for the reactant and product:

$$\frac{d[A]}{dt} = -k_A[A] + k_B[B] \tag{18.85}$$

$$\frac{d[B]}{dt} = k_A[A] - k_B[B] \tag{18.86}$$

Equation (18.85) should be contrasted with the differential rate expression for first-order reactant decay given in Equation (18.26). Reactant decay is included through the $-k_A[A]$ term similar to first-order decay discussed earlier; however, a second term involving the formation of reactant by product decay $k_B[B]$ is now included. The initial conditions are identical to those employed in previous sections. Only reactant is present at the beginning of the reaction when $t = 0$. Also, the concentration of reactant and product for $t > 0$ must be equal to the initial concentration of reactant:

$$[A]_0 = [A] + [B] \tag{18.87}$$

With these initial conditions, Equation (18.85) can be integrated as follows:

$$\frac{d[A]}{dt} = -k_A[A] + k_B[B]$$
$$= -k_A[A] + k_B([A]_0 - [A])$$
$$= -[A](k_A + k_B) + k_B[A]_0$$

$$\int_{[A]_0}^{[A]} \frac{d[A]}{[A](k_A + k_B) - k_B[A]_0} = -\int_0^t dt \tag{18.88}$$

Equation (18.88) can be evaluated using the following standard integral:

$$\int \frac{dx}{(a + bx)} = \frac{1}{b}\ln(a + bx)$$

Using this relationship with the initial conditions specified earlier, the concentrations of reactant and products are

$$[A] = [A]_0 \frac{k_B + k_A e^{-(k_A + k_B)t}}{k_A + k_B} \tag{18.89}$$

$$[B] = [A]_0 \left(1 - \frac{k_B + k_A e^{-(k_A + k_B)t}}{k_A + k_B}\right) \tag{18.90}$$

Figure 18.15 presents the time dependence of [A] and [B] for the case where $k_A = 2k_B = 0.06 \text{ s}^{-1}$. Note that [A] undergoes exponential decay with an apparent rate constant equal to $k_A + k_B$, and [B] appears exponentially with an equivalent rate constant. If the back reaction were not present, [A] would be expected to decay to zero; however, the existence of the back reaction results in both [A] and [B] being nonzero at long times. The concentration of reactant and product at long times is defined as the equilibrium concentration. The equilibrium concentrations are equal to the limit of Equations (18.89) and (18.90) as time goes to infinity:

$$[A]_{eq} = \lim_{t \to \infty} [A] = [A]_0 \frac{k_B}{k_A + k_B} \tag{18.91}$$

$$[B]_{eq} = \lim_{t \to \infty} [B] = [A]_0 \left(1 - \frac{k_B}{k_A + k_B}\right) \tag{18.92}$$

Equations (18.91) and (18.92) demonstrate that the reactant and product concentrations reach a constant or equilibrium value that depends on the relative magnitude of the forward and back reaction rate constants.

In theory, one must wait an infinite amount of time before equilibrium is reached. Fortunately, in practice there will be a time after which the reactant and

product concentrations are sufficiently close to equilibrium, and the change in these concentrations with time is so modest that approximating the system as having reached equilibrium is reasonable. This time is indicated by $t_{eq}$ in Figure 18.15, where inspection of the figure demonstrates that the concentrations are at their equilibrium values for times $> t_{eq}$. After equilibrium has been established, the reactant and product concentrations are time independent such that

$$\frac{d[A]_{eq}}{dt} = \frac{d[B]_{eq}}{dt} = 0 \qquad (18.93)$$

The subscripts in Equation (18.93) indicate that equality applies only after equilibrium has been established. A common misconception is that Equation (18.93) states that at equilibrium the forward and back reaction rates are zero. Instead, at equilibrium the forward and back reaction rates are equal, but not zero, such that the macroscopic concentration of reactant or product does not evolve with time. That is, the forward and back reactions still occur, but they occur with equal rates at equilibrium. Using Equation (18.93) in combination with the differential rate expressions for the reactant [Equation (18.85)], we arrive at what is hopefully a familiar relationship:

$$\frac{d[A]_{eq}}{dt} = \frac{d[B]_{eq}}{dt} = 0 = -k_A[A]_{eq} + k_B[B]_{eq}$$

$$\frac{k_A}{k_B} = \frac{[B]_{eq}}{[A]_{eq}} = K_c \qquad (18.94)$$

In this equation, $K_c$ is the equilibrium constant defined in terms of concentrations. This quantity is identical to that first encountered in thermodynamics (Chapter 6) and statistical mechanics (Chapter 15). We now have a definition of equilibrium from the kinetic perspective; therefore, Equation (18.94) is a remarkable result in which the concept of equilibrium as described by these three different perspectives is connected into one deceptively simple equation. From the kinetic standpoint, $K_c$ is related to the ratio of forward and backward rate constants for the reaction. The greater the forward rate constant relative to that for the back reaction, the more equilibrium will favor products over reactants.

Figure 18.16 illustrates the methodology by which forward and backward rate constants can be determined. Specifically, measurement of the reactant decay kinetics (or equivalently the product formation kinetics) provides a measure of the apparent rate constant, $k_A + k_B$. The measurement of $K_c$, or the reactant and product concentrations at equilibrium, provides a measure of the ratio of the forward and backward rate constants.
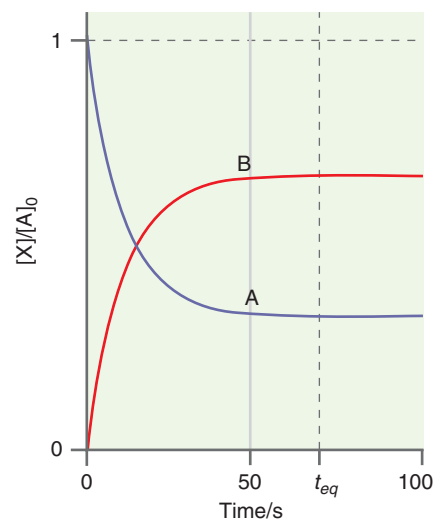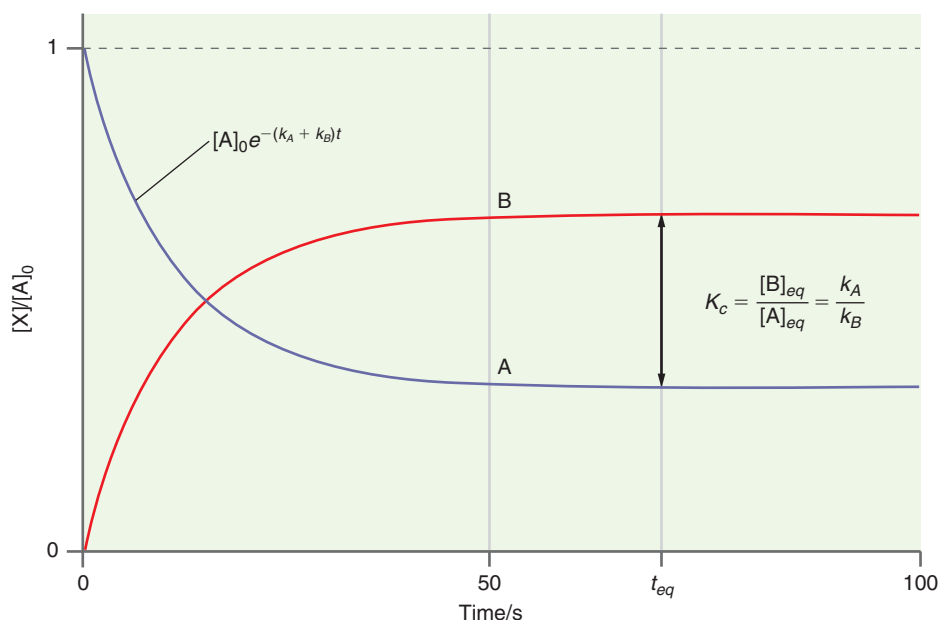


**FIGURE 18.15**

Time-dependent concentrations in which both forward and back reactions exist between reactant A and product B. In this example, $k_A = 2k_B = 0.06 \text{ s}^{-1}$. Note that the concentrations reach a constant value at longer times ($t \geq t_{eq}$) at which point the reaction reaches equilibrium.



**FIGURE 18.16**

Methodology for determining forward and backward rate constants. The apparent rate constant for reactant decay is equal to the sum of forward $k_A$ and backward $k_B$ rate constants. The equilibrium constant is equal to $k_A/k_B$. These two measurements provide a system of two equations and two unknowns that can be readily evaluated to produce $k_A$ and $k_B$.

Together, these measurements represent a system of two equations and two unknowns that can be readily solved to determine $k_A$ and $k_B$.

### EXAMPLE PROBLEM 18.9

Consider the interconversion of the "boat" and "chair" conformations of cyclohexane:
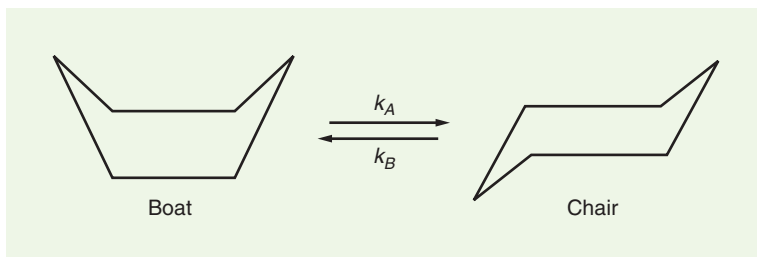


Boat        Chair

The reaction is first order in each direction, with an equilibrium constant of $10^4$. The activation energy for the conversion of the chair conformer to the boat conformer is 42 kJ/mol. Assuming an Arrhenius preexponential factor of $10^{12}$ s$^{-1}$, what is the expected observed reaction rate constant at 298 K if one were to initiate this reaction starting with only the boat conformer?

### Solution

Using the Arrhenius expression of Equation (18.82), $k_B$ is given by

$$k_B = Ae^{-E_a/RT} = 10^{12} \text{ s}^{-1}\exp\left[\frac{-42,000 \text{ J mol}^{-1}}{(8.314 \text{ J mol}^{-1} \text{ K}^{-1})(298 \text{ K})}\right]$$

$$= 4.34 \times 10^4 \text{ s}^{-1}$$

Using the equilibrium constant, $k_A$ can be determined as follows:

$$K_c = 10^4 = \frac{k_A}{k_B}$$

$$k_A = 10^4 \, k_B = 10^4(4.34 \times 10^4 \text{ s}^{-1}) = 4.34 \times 10^8 \text{ s}^{-1}$$

Finally, the apparent rate constant is simply the sum of $k_A$ and $k_B$:

$$k_{app} = k_A + k_B = 4.34 \times 10^8 \text{ s}^{-1}$$

SUPPLEMENTAL

# 18.11 Perturbation-Relaxation Methods

The previous section demonstrated that for reactions with appreciable forward and backward rate constants, concentrations approaching those at equilibrium will be established at some later time after initiation of the reaction. The forward and backward rate constants for such reactions can be determined by monitoring the evolution in reactant or product concentrations as equilibrium is approached and by measuring the concentrations at equilibrium. But what if the initial conditions for the reaction cannot be controlled? For example, what if it is impossible to sequester the reactants such that initiation of the reaction at a specified time is impossible? In such situations, application of the methodology described in the preceding section to determine forward and backward rate constants is not possible. However, if one can perturb the system by changing temperature, pressure, or concentration, the system will no longer be at equilibrium and will evolve until a new equilibrium is established. If the perturbation occurs on a

timescale that is rapid compared to the system relaxation, the kinetics of the relaxation can be monitored and related to the forward and backward rate constants. This is the conceptual idea behind perturbation methods and their application to chemical kinetics.

There are many perturbation techniques; however, the focus here is on **temperature jump** (or $T$-jump) methods to illustrate the type of information available using perturbation techniques. Consider again the following reaction in which both the forward and back reactions are first order:

$$A \underset{k_B}{\overset{k_A}{\rightleftharpoons}} B \qquad (18.95)$$

Next, a rapid change in temperature occurs such that the forward and backward rate constants are altered in accord with the Arrhenius expression of Equation (18.82), and a new equilibrium is established:

$$A \underset{k_B^+}{\overset{k_A^+}{\rightleftharpoons}} B \qquad (18.96)$$

The superscript $+$ in this expression indicates that the rate constants correspond to the conditions after the temperature jump. As described next, one can jump to a final temperature of interest so that the reaction can be characterized at this temperature. Following the temperature jump, the concentrations of reactants and products will evolve until the new equilibrium concentrations are reached. At the new equilibrium, the differential rate expression for the reactant is equal to zero so that

$$\frac{d[A]_{eq}}{dt} = 0 = -k_A^+[A]_{eq} + k_B^+[B]_{eq}$$

$$k_A^+[A]_{eq} = k_B^+[B]_{eq} \qquad (18.97)$$

The subscripts on the reactant and product concentrations represent the new equilibrium concentrations after the temperature jump. The evolution of reactant and product concentrations from the pre-temperature to post-temperature jump values can be expressed using a coefficient of reaction advancement (Section 18.2). Specifically, let the variable $\xi$ represent the extent to which the pre-temperature jump concentration is shifted away from the concentration for the post-temperature jump equilibrium:

$$[A] - \xi = [A]_{eq} \qquad (18.98)$$

$$[B] + \xi = [B]_{eq} \qquad (18.99)$$

Immediately after the temperature jump, the concentrations will evolve until equilibrium is reached. Using this idea, the differential rate expression describing the extent of reaction advancement is as follows:

$$\frac{d\xi}{dt} = -k_A^+[A] + k_B^+[B]$$

Notice in this equation that the forward and backward rate constants are the post-temperature jump values. Substitution of Equations (18.98) and (18.99) into the differential rate expression yields the following:

$$\frac{d\xi}{dt} = -k_A^+(\xi + [A]_{eq}) + k_B^+(-\xi + [B]_{eq})$$

$$= -k_A^+[A]_{eq} + k_B^+[B]_{eq} - \xi(k_A^+ + k_B^+)$$

$$= -\xi(k_A^+ + k_B^+) \qquad (18.100)$$

In the second step of the preceding equation, the first two terms cancel in accord with Equation (18.97). The relaxation time $\tau$ is defined as follows:

$$\tau = (k_A^+ + k_B^+)^{-1} \qquad (18.101)$$

**FIGURE 18.17**
Example of a temperature-jump experiment for a reaction in which the forward and backward rate processes are first order. The orange and light green portions of the graph indicate times before and after the temperature jump, respectively. After the temperature jump, [A] decreases with a time constant related to the sum of the forward and backward rate constants. The change between the pre-jump and post-jump equilibrium concentrations is given by $\xi_0$.
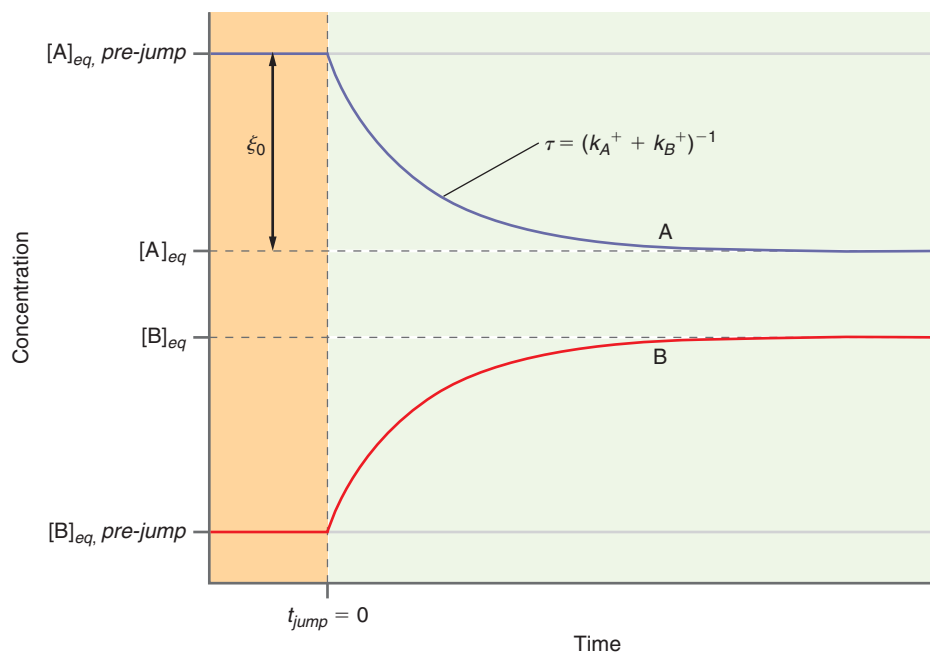


Employing the relaxation time, Equation (18.100) is readily evaluated:

$$\frac{d\xi}{dt} = -\frac{\xi}{\tau}$$

$$\int_{\xi_0}^{\xi} \frac{d\xi'}{\xi'} = -\frac{1}{\tau} \int_0^t dt'$$

$$\xi = \xi_0\, e^{-t/\tau} \qquad\qquad \textbf{(18.102)}$$

Equation (18.102) demonstrates that for this reaction the concentrations will change exponentially, and the relaxation time is the time it takes for the coefficient of reaction advancement to decay to $e^{-1}$ of its initial value. The timescale for relaxation after the temperature jump is related to the sum of the forward and backward rate constants. This information in combination with the equilibrium constant (given by measurement of $[A]_{eq}$ and $[B]_{eq}$) can be used to determine the individual values for the rate constants. Figure 18.17 presents a schematic of this process.

**SUPPLEMENTAL**

# 18.12 The Autoionization of Water: A Temperature-Jump Example

In the autoionization of water, the equilibrium of interest is the following:

$$H_2O(aq) \underset{k_r}{\overset{k_f}{\rightleftharpoons}} H^+(aq) + OH^-(aq) \qquad\qquad \textbf{(18.103)}$$
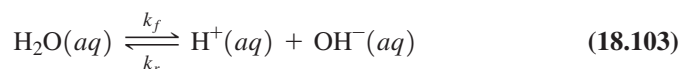
The reaction is first order in the forward direction and second order in the reverse direction. The differential rate expressions that describe the temporal evolution of $H_2O$ and $H^+$ concentrations are as follows:

$$\frac{d[H_2O]}{dt} = -k_f[H_2O] + k_r[H^+][OH^-] \qquad\qquad \textbf{(18.104)}$$

$$\frac{d[H^+]}{dt} = k_f[H_2O] - k_r[H^+][OH^-] \qquad\qquad \textbf{(18.105)}$$

Following a temperature jump to 298 K, the measured relaxation time constant was 37 $\mu$s. In addition, the pH of the solution is 7. Given this information, the forward and back rate

constants can be determined as follows. First, the equilibrium constant after the temperature jump is

$$\frac{k_f^+}{k_r^+} = \frac{[H^+]_{eq}[OH^-]_{eq}}{[H_2O]_{eq}} = K_c \qquad (18.106)$$

The differential rate expression for the extent of reaction advancement after the perturbation is given by

$$\frac{d\xi}{dt} = -k_f^+[H_2O] + k_r^+[H^+][OH^-]$$

$$= -k_f^+(\xi + [H_2O]_{eq}) + k_r^+(\xi - [H^+]_{eq})(\xi - [OH^-]_{eq})$$

$$= -k_f^+\left(\xi + \frac{k_r^+}{k_f^+}[H^+]_{eq}[OH^-]_{eq}\right) + k_r^+(\xi - [H^+]_{eq})(\xi - [OH^-]_{eq})$$

$$= -k_f^+\xi - k_r^+\xi([H^+]_{eq} + [OH^-]_{eq}) + O(\xi^2) \qquad (18.107)$$

The last term in Equation (18.107) represents terms on the order of $\xi^2$. If the extent of reaction advancement is small, corresponding to a small perturbation of the system temperature, then this term can be neglected, resulting in the following expression for the reaction advancement as a function of time:

$$\frac{d\xi}{dt} = -\xi(k_f^+ + k_r^+([H^+]_{eq} + [OH^-]_{eq})) \qquad (18.108)$$

Proceeding as before, the relaxation time is defined as

$$\frac{1}{\tau} = (k_f^+ + k_r^+([H^+]_{eq} + [OH^-]_{eq})) \qquad (18.109)$$

Substitution of Equation (18.109) into Equation (18.108) and integration yields an expression for the post-temperature jump evolution identical to that derived earlier in Equation (18.102). The parameters needed to determine the autoionization forward and backward rate constants are the expression for the relaxation time [Equation (18.109)] and the equilibrium constant. Recall that the experimental relaxation time was 37 $\mu$s (1 $\mu$s $= 10^{-6}$ s) such that

$$\frac{1}{3.7 \times 10^{-5}\,\text{s}} = (k_f^+ + k_r^+([H^+]_{eq} + [OH^-]_{eq})) \qquad (18.110)$$

In addition, the pH at equilibrium is 7.00 such that $[H^+] = [OH^-] = 1.0 \times 10^{-7}$ M. Finally, the concentration of water at 298 K is 55.5 M. Using this information, the ratio of the forward to back rate constants becomes

$$\frac{k_f^+}{k_r^+} = \frac{[H^+]_{eq}[OH^-]_{eq}}{[H_2O]_{eq}} = \frac{(1.0 \times 10^{-7}\,\text{M})(1.0 \times 10^{-7}\,\text{M})}{55.5\,\text{M}} = 1.8 \times 10^{-16}\,\text{M} \qquad (18.111)$$

Substitution of Equation (18.111) into Equation (18.110) yields the following value for the reverse rate constant:

$$\frac{1}{3.7 \times 10^{-5}\,\text{s}} = (k_f^+ + k_r^+([H^+]_{eq} + [OH^-]_{eq}))$$

$$= (1.8 \times 10^{-16}\,\text{M}(k_r^+) + k_r^+(2.0 \times 10^{-7}\,\text{M}))$$

$$\frac{1}{(3.7 \times 10^{-5}\,\text{s})(2.0 \times 10^{-7}\,\text{M})} = k_r^+$$

$$1.4 \times 10^{11}\,\text{M}^{-1}\,\text{s}^{-1} = k_r^+$$

Finally, the forward rate constant is

$$k^+ = (k_r^+)1.8 \times 10^{-16}\,\text{M} = (1.4 \times 10^{11}\,\text{M}^{-1}\,\text{s}^{-1})(1.8 \times 10^{-16}\,\text{M})$$

$$= 2.5 \times 10^{-5}\,\text{s}^{-1}$$

Notice the substantial difference between the forward and backward rate constants, consistent with the modest amount of autoionized species in water. In addition, the forward and reverse rate constants are temperature dependent, and the autoionization constant also demonstrates temperature dependence.

# 18.13 Potential Energy Surfaces

In the discussion of the Arrhenius equation, the energetics of the reaction were identified as an important factor determining the rate of a reaction. This connection between reaction kinetics and energetics is central to the concept of the potential energy surface. To illustrate this concept, consider the following bimolecular reaction:
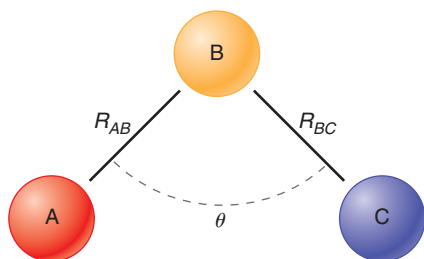
$$AB + C \rightarrow A + BC \qquad (18.112)$$

The diatomic species AB and BC are stable, but we will assume that the triatomic species ABC and the diatomic species AC are not formed during the course of the reaction. This reaction can be viewed as the interaction of three atoms, and the potential energy of this collection of atoms can be defined with respect to the relative positions in space. The geometric relationship between these species is generally defined with respect to the distance between two of the three atoms ($R_{AB}$ and $R_{BC}$) and the angle formed between these two distances, as illustrated in Figure 18.18.

The potential energy of the system can be expressed as a function of these coordinates. The variation of the potential energy with a change along these coordinates can then be presented as a graph or surface referred to as a **potential energy surface.** Formally, for our example reaction this surface would be four-dimensional (the three geometric coordinates and energy). The dimensionality of the problem can be reduced by considering the energetics of the reaction at a fixed value for one of the geometric coordinates. In our example reaction, the centers of A, B, and C must be aligned during the reaction such that $\theta = 180°$. With this constraint, the potential energy is reduced to a three-dimensional problem as shown in Figure 18.19. The graphs represent the variation in energy with displacement along $R_{AB}$ and $R_{BC}$ with the arrows indicating the direction of increased separation.

Figures 18.19a and 18.19b illustrate the three-dimensional potential energy surface, and the two minima in this surface corresponding to the stable diatomic molecules AB and BC. A more convenient way to view the potential energy surface is to use a two-dimensional **contour plot,** as illustrated in Figure 18.19c. One can think of this plot as a view straight down onto the three-dimensional surface presented in Figure 18.19. The lines on the contour plot connect regions of equal potential energy. On the lower left-hand region of the surface is a broad energetic plateau that corresponds to the energy when the three atoms are separated or the dissociated state A + B + C. The pathway corresponding to the reaction of B + C to form BC is indicated by the dashed line between points $a$ and $a'$. The cross section of the potential energy surface along this line is presented in Figure 18.19d, and this contour is simply the potential energy diagram for the diatomic molecule BC. The depth of the potential is equal to the dissociation energy of the diatomic, $D_e(BC)$, and the minimum along $R_{BC}$ corresponds to the equilibrium bond length of the diatomic. Figure 18.19e presents the corresponding diagram for the diatomic molecule AB, as indicated by the dashed line between points $b$ and $b'$ in Figure 18.19c.

The dashed line between points $c$ and $d$ in Figure 18.19c represents the system energy as C approaches AB and reacts to form BC and A under the constraint that $\theta = 180°$. This pathway represents the AB + C $\rightarrow$ A + BC reaction. The maximum in energy along this pathway is referred to as the **transition state** and is indicated by the double dagger symbol, ‡. The variation in energy as one proceeds from reactants to products along this reactive pathway can be plotted to construct a reaction coordinate diagram as presented in Figure 18.20. Note that the transition state corresponds to a maximum along the reaction coordinate; therefore, the activated complex is not a stable species (i.e., an intermediate) along the reaction coordinate.



**FIGURE 18.18**
Definition of geometric coordinates for the AB + C $\rightarrow$ A + BC reaction.

(a)

(b)

(c)

$R_e(BC)$

$R_{BC}$

A + BC

A + B + C

AB + C

$R_{AB}$  $R_e(AB)$

(d)

a'

c

$D_e(BC)$

a

$R_e(BC)$  $R_{BC}$

(e)

b'

d

$D_e(AB)$

b

$R_e(AB)$  $R_{AB}$
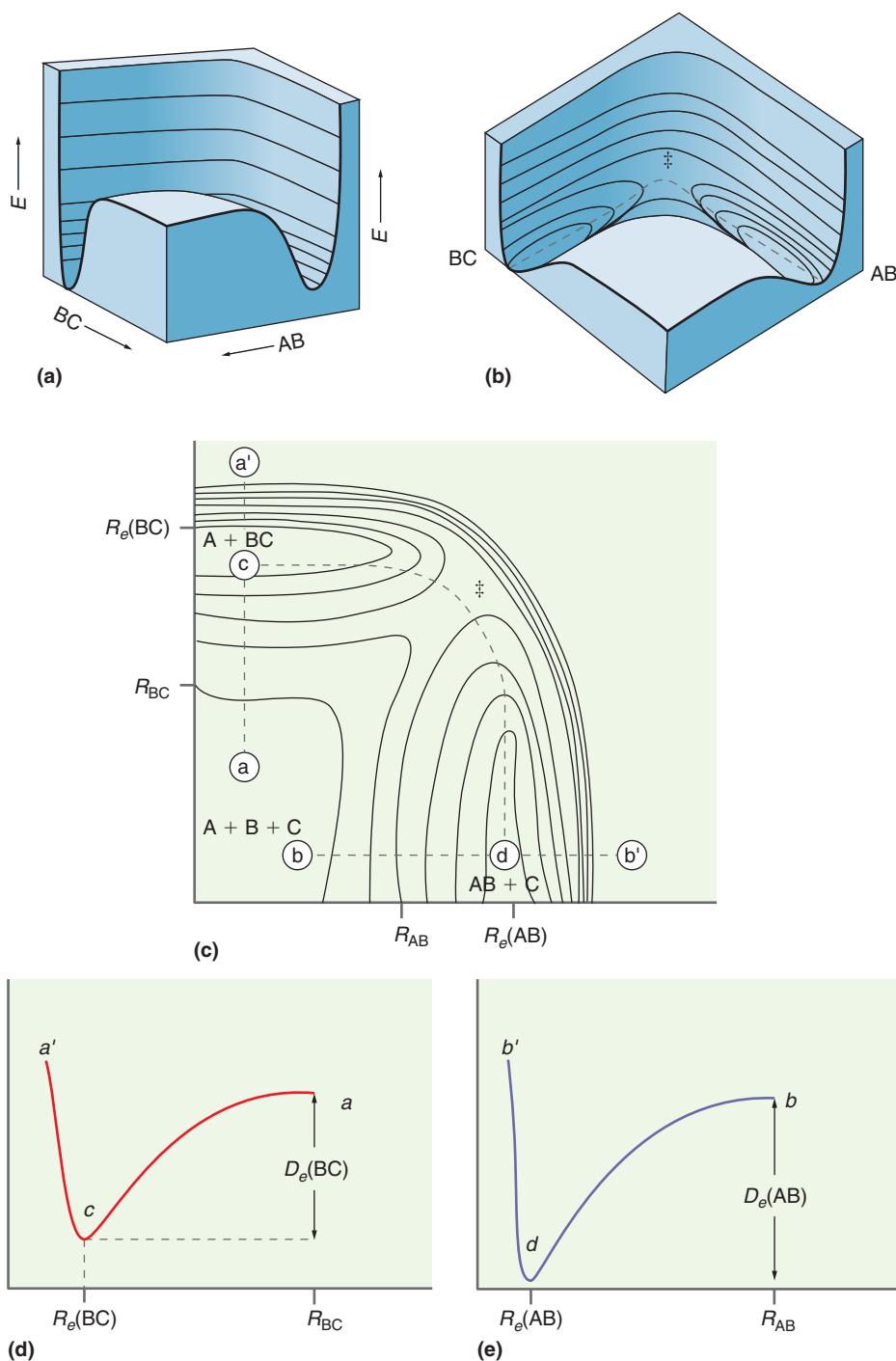
**FIGURE 18.19**

Illustration of a potential energy surface for the AB + C reaction at a colinear geometry ($\theta = 180°$ in Figure 18.18). **(a, b)** Three-dimensional views of the surface. **(c)** Contour plot of the surface with contours of equipotential energy. The curved dashed line represents one possible path of a reactive event, corresponding to its reaction coordinate. The transition state for this coordinate is indicated by the symbol ‡. **(d, e)** Cross sections of the potential energy surface along the lines $a'-a$ and $b'-b$, respectively. These two graphs correspond to the potential for two-body interactions of B with C, and A with B. [Adapted from J. H. Noggle, *Physical Chemistry*, 3rd Edition, © 1996. Reprinted and electronically reproduced by permission of Pearson Education, Inc., Upper Saddle River, New Jersey.]

The discussion of potential energy surfaces just presented suggests that the kinetics and product yields will depend on the energy content of the reactants and the relative orientation of reactants. This sensitivity can be explored using techniques of crossed-molecular beams. In this approach, reactants with well-defined energies are seeded into a molecular beam that intersects another beam of reactants at well-defined beam geometries. The products formed in the reaction can be analyzed in terms of their energetics, spatial distribution of the products, and beam geometry. This experimental information is then used to construct a potential energy surface (following a substantial amount of analysis). Crossed-molecular beam techniques have provided much insight into the nature of reactive pathways, and detailed, introductory references to this important area of research are provided at the end of this chapter.
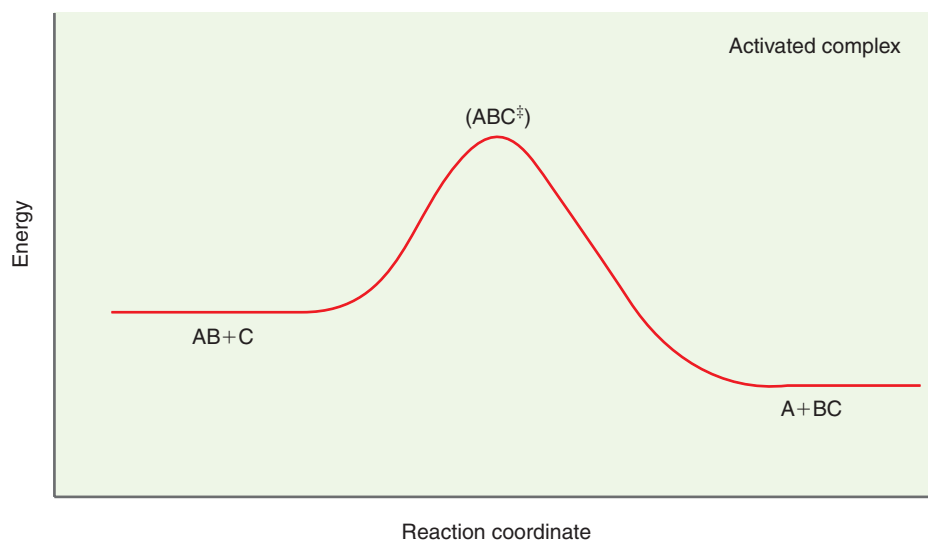
## 18.14 Activated Complex Theory

The concept of equilibrium is central to a theoretical description of reaction rates developed principally by Henry Eyring in the 1930s. This theory, known as **activated complex theory** or **transition state theory,** provides a theoretical description of reaction rates. To illustrate the conceptual ideas behind activated complex theory, consider the following bimolecular reaction:

$$A + B \overset{k}{\rightarrow} P \qquad \text{(18.113)}$$

Figure 18.21 illustrates the reaction coordinate for this process, where A and B react to form an activated complex that undergoes decay, resulting in product formation. The **activated complex** represents the system at the transition state. This complex is not stable and has a lifetime on the order of one to a few vibrational periods ($\sim 10^{-14}$ s). When this theory was first proposed, experiments were incapable of following reaction dynamics on such short timescales such that evidence for an activated complex corresponding to the transition state was not available. However, recent developments in experimental kinetics have allowed for the investigation of these transient species, and a few references to this work are provided at the end of this chapter.

Activated complex theory involves a few major assumptions. The primary assumption is that an equilibrium exists between the reactants and the activated complex. It is also assumed that the reaction coordinate describing decomposition of the activated complex can be mapped onto a single energetic degree of freedom of the activated complex. For example, if product formation involves the breaking of a bond, then the vibrational degree of freedom corresponding to bond stretching is taken to be the reactive coordinate.

With these approximations in mind, we can take the kinetic methods derived earlier in this chapter and develop an expression for the rate of product formation. For the example of the bimolecular reaction from Equation (18.113), the kinetic mechanism corresponding to the activated complex model described earlier is

$$A + B \underset{k_{-1}}{\overset{k_1}{\rightleftarrows}} AB^{\ddagger} \qquad \text{(18.114)}$$

$$AB^{\ddagger} \overset{k_2}{\rightarrow} P \qquad \text{(18.115)}$$

Equation (18.114) represents the equilibrium between reactants and the activated complex, and Equation (18.115) represents the decay of the activated complex to form product. With the assumption of an equilibrium between the reactants and the activated complex, the
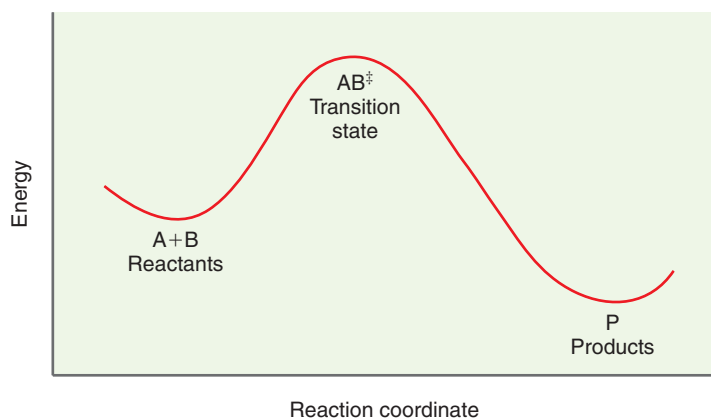
differential rate expression for one of the reactants (A in this case) is set equal to zero consistent with equilibrium, and an expression for $[AB^{\ddagger}]$ is obtained as follows:

$$\frac{d[A]}{dt} = 0 = -k_1[A][B] + k_{-1}[AB^{\ddagger}]$$

$$[AB^{\ddagger}] = \frac{k_1}{k_{-1}}[A][B] = \frac{K_c^{\ddagger}}{c^{\circ}}[A][B] \qquad \textbf{(18.116)}$$

In Equation (18.116), $K_c^{\ddagger}$ is the equilibrium constant involving the reactants and the activated complex, and it can be expressed in terms of the molecular partition functions of these species as described in Chapter 14. In addition, $c^{\circ}$ is the standard state concentration (typically 1 M), which appears in the following definition for $K_c^{\ddagger}$:

$$K_c^{\ddagger} = \frac{[AB^{\ddagger}]/c^{\circ}}{([A]/c^{\circ})([B]/c^{\circ})} = \frac{[AB^{\ddagger}]c^{\circ}}{[A][B]}$$

The rate of the reaction is equal to the rate of product formation, which by Equation (18.115) is equal to

$$R = \frac{d[P]}{dt} = k_2[AB^{\ddagger}] \qquad \textbf{(18.117)}$$

Substitution into Equation (18.117) of the expression for $[AB^{\ddagger}]$ provided in Equation (18.116) yields the following expression for the reaction rate:

$$R = \frac{d[P]}{dt} = \frac{k_2 K_c^{\ddagger}}{c^{\circ}}[A][B] \qquad \textbf{(18.118)}$$

Further evaluation of the reaction rate expression requires that $k_2$ be defined. This rate constant is associated with the rate of activated complex decay. Imagine that product formation requires the dissociation of a weak bond in the activated complex (since this bond eventually breaks, resulting in product formation). The activated complex is not stable, and the complex dissociates with motion along the corresponding bond-stretching coordinate. Therefore, $k_2$ is related to the vibrational frequency associated with bond stretching, $\nu$. The rate constant is exactly equal to $\nu$ only if every time an activated complex is formed, it dissociates, resulting in product formation. However, it is possible that the activated complex will instead revert back to reactants in which case only a fraction of the activated complexes formed will result in product formation. To account for this possibility, a term referred to as the transmission coefficient $\kappa$ is included in the definition of $k_2$:

$$k_2 = \kappa\nu \qquad \textbf{(18.119)}$$

With this definition of $k_2$, the reaction rate becomes

$$R = \frac{\kappa\nu K_c^{\ddagger}}{c^{\circ}}[A][B] \qquad \textbf{(18.120)}$$

One can express $K_c^{\ddagger}$ in terms of the partition function of reactants and the activated complex using the techniques outlined in Chapter 15. In addition, the partition function for the

activated complex can decompose into a product of partition functions corresponding to vibrational degree of freedom corresponding to the reaction coordinate and the remaining energetic degrees of freedom. Removing the partition function for the reactive coordinate from the expression of $K_c^{\ddagger}$ yields

$$K_c^{\ddagger} = q_{rc} \overline{K}_c^{\ddagger} = \frac{k_B T}{h\nu} \overline{K}_c^{\ddagger} \tag{18.121}$$

where $q_{rc}$ is the partition function associated with the energetic degree of freedom corresponding to the reactive coordinate, $\overline{K}_c^{\ddagger}$ is the remainder of the original equilibrium constant in the absence of $q_{rc}$, and $k_B$ is Boltzmann's constant. The final equality in Equation (18.121) is made by recognizing that the reactive vibrational coordinate corresponds to a weak bond where $h\nu \ll kT$, and the high-temperature approximation for $q_{rc}$ is valid. Substituting Equation (18.121) into Equation (18.120) yields the following expression for rate constant for product formation ($k$):

$$k = \kappa \frac{k_B T}{hc^{\circ}} \overline{K}_c^{\ddagger} \tag{18.122}$$

Equation (18.122) is the central result of activated complex theory, and it provides a connection between the rate constant for product formation and the molecular parameters for species involved in the reaction. Evaluation of this rate expression requires that one determine $\overline{K}_c^{\ddagger}$, which is related to the partition functions of the activated complex and reactants. The partition functions for the reactants can be readily determined; however, the partition function for the activated complex requires some thought.

The translational partition function for the complex can also be determined using the techniques described earlier, but determination of the rotational and vibrational partition functions requires some knowledge of the structure of the activated complex. The determination of the vibrational partition function is further complicated by the requirement that one of the vibrational degrees of freedom be designated as the reactive coordinate; however, identification of this coordinate may be far from trivial for an activated complex with more than one weak bond. At times, computational techniques can be used to provide insight into the structure of the activated complex and assist in determination of the partition function for this species. With these complications acknowledged, Equation (18.122) represents an important theoretical accomplishment in chemical reaction kinetics. Note that the presentation of activated complex theory provided here is a very rudimentary description of this field. Work continues to the present day to advance and refine this theory, and references are provided at the end of this chapter to review articles describing the significant advances in this field.

We end this discussion by connecting the results of activated complex theory to earlier thermodynamic descriptions of chemical reactions. Recall from thermodynamics that the equilibrium constant $K_c^{\ddagger}$ is related to the corresponding change in Gibbs energy using the following thermodynamic definition:

$$\Delta G^{\ddagger} = -RT \ln K_c^{\ddagger} \tag{18.123}$$

In this definition, $\Delta G^{\ddagger}$ is the difference in Gibbs energy between the transition state and reactants. With this definition for $K_c^{\ddagger}$, $k$ becomes (setting $\kappa = 1$ for convenience)

$$k = \frac{k_B T}{hc^{\circ}} e^{-\Delta G^{\ddagger}/RT} \tag{18.124}$$

In addition, $\Delta G^{\ddagger}$ can be related to the corresponding changes in enthalpy and entropy using

$$\Delta G^{\ddagger} = \Delta H^{\ddagger} - T\Delta S^{\ddagger} \tag{18.125}$$

Substituting Equation (18.125) into Equation (18.124) yields

$$k = \frac{k_B T}{hc^{\circ}} e^{\Delta S^{\ddagger}/R} e^{-\Delta H^{\ddagger}/RT} \tag{18.126}$$

Equation (18.126) is known as the **Eyring equation.** Notice that the temperature dependence of the reaction rate constant predicted by transition state theory is different than that assumed by the Arrhenius expression of Equation (18.82). In particular, the

preexponential term in the Eyring equation demonstrates temperature dependence as opposed to the temperature independence of the corresponding term in the Arrhenius expression. However, both the Eyring equation and the Arrhenius expression provide an expression for the temperature dependence of rate constants; therefore, one might expect that the parameters in the Eyring equation ($\Delta H^{\ddagger}$ and $\Delta S^{\ddagger}$) can be related to corresponding parameters in the Arrhenius expression ($E_a$ and $A$). To derive this relationship, we begin with a modification of Equation (18.82) where the Arrhenius activation energy is written as

$$E_a = RT^2 \left( \frac{d \ln k}{dT} \right) \tag{18.127}$$

Substituting for $k$ the expression given in Equation (18.122) yields

$$E_a = RT^2 \left( \frac{d}{dT} \ln \left( \frac{k_B T}{hc^{\circ}} \overline{K_c^{\ddagger}} \right) \right) = RT + RT^2 \left( \frac{d \ln \overline{K_c^{\ddagger}}}{dT} \right)$$

From thermodynamics the temperature derivative of $\ln(K_c)$ is equal to $\Delta U / RT^2$. Employing this definition to the previous equation results in the following:

$$E_a = RT + \Delta U^{\ddagger}$$

We also make use of the thermodynamic definition of enthalpy, $H = U + PV$, to write

$$\Delta U^{\ddagger} = \Delta H^{\ddagger} - \Delta(PV)^{\ddagger} \tag{18.128}$$

In Equation (18.128), the $\Delta(PV)^{\ddagger}$ term is related to the difference in the product $PV$ with respect to the activated complex and reactants. For a solution-phase reaction, $P$ is constant and the change in $V$ is negligible such that $\Delta U^{\ddagger} \approx \Delta H^{\ddagger}$ and the activation energy in terms of $\Delta H^{\ddagger}$ becomes

$$E_a = \Delta H^{\ddagger} + RT \text{ (solutions)} \tag{18.129}$$

Comparison of this result with Equation (18.126) demonstrates that the Arrhenius preexponential factor in this case is

$$A = \frac{ek_B T}{hc^{\circ}} e^{\Delta S^{\ddagger}/R} \text{ (solutions, bimolecular)} \tag{18.130}$$

For solution-phase unimolecular reactions once again $\Delta U^{\ddagger} \approx \Delta H^{\ddagger}$ and the activation energy for a unimolecular solution phase reaction is identical to Equation (18.129). All that changes relative to the bimolecular case is the Arrhenius preexponential factor losing the factor of $c^{\circ}$ (see Equation 18.116), resulting in

$$A = \frac{ek_B T}{h} e^{\Delta S^{\ddagger}/R} \text{ (solutions, unimolecular)} \tag{18.131}$$

For a gas-phase reaction, $\Delta(PV)^{\ddagger}$ in Equation (18.128) is proportional to the difference in the number of moles between the transition state and reactants. For a unimolecular ($\Delta n^{\ddagger} = 0$) and bimolecular ($\Delta n^{\ddagger} = -1$) reaction, $E_a$ and $A$ are given by

$$\text{gas, uni} \quad E_a = \Delta H^{\ddagger} + RT; \quad A = \frac{ek_B T}{h} e^{\Delta S^{\ddagger}/R} \tag{18.132}$$

$$\text{gas, bi} \quad E_a = \Delta H^{\ddagger} + 2RT; \quad A = \frac{e^2 k_B T}{hc^{\circ}} e^{\Delta S^{\ddagger}/R} \tag{18.133}$$

Notice now that both the Arrhenius activation energy and preexponential terms are expected to demonstrate temperature dependence. If $\Delta H^{\ddagger} \gg RT$, then the temperature dependence of $E_a$ will be modest. Also notice that if the enthalpy of the transition state is lower than that of the reactants, the reaction rate may become faster as temperature is decreased! However, the entropy difference between the transition state and reactants is also important in determining the rate. If this entropy difference is positive and the activation energy is near zero, the reaction rate is determined by entropic rather than enthalpic factors.

**EXAMPLE PROBLEM 18.10**

The thermal decomposition reaction of nitrosyl halides is important in tropospheric chemistry. For example, consider the decomposition of NOCl:

$$2 \text{ NOCl}(g) \rightarrow 2 \text{ NO}(g) + \text{Cl}_2(g)$$

The Arrhenius parameters for this reaction are $A = 1.00 \times 10^{13} \text{ M}^{-1} \text{ s}^{-1}$ and $E_a = 104.0 \text{ kJ mol}^{-1}$. Calculate $\Delta H^{\ddagger}$ and $\Delta S^{\ddagger}$ for this reaction with $T = 300.\text{ K}$.

**Solution**

This is a bimolecular reaction such that

$$\Delta H^{\ddagger} = E_a - 2RT = 104 \text{ kJ mol}^{-1} - 2(8.314 \text{ J mol}^{-1} \text{ K}^{-1})(300.\text{ K})$$

$$= 104.0 \text{ kJ mol}^{-1} - (4.99 \times 10^3 \text{ J mol}^{-1})\left(\frac{1 \text{ kJ}}{1000 \text{ J}}\right) = 99.0 \text{ kJ mol}^{-1}$$

$$\Delta S^{\ddagger} = R \ln\left(\frac{Ahc^{\circ}}{e^2 kT}\right)$$

$$= (8.314 \text{ J mol}^{-1} \text{ K}^{-1}) \ln\left(\frac{(1.00 \times 10^{13} \text{M}^{-1}\text{s}^{-1})(6.626 \times 10^{-34}\text{J s})(1 \text{ M})}{e^2(1.38 \times 10^{-23}\text{J K}^{-1})(300.\text{ K})}\right)$$

$$= -12.7 \text{ J mol}^{-1} \text{ K}^{-1}$$

One of the utilities of this calculation is that the sign and magnitude of $\Delta S^{\ddagger}$ provide information on the structure of the activated complex at the transition state relative to the reactants. The negative value in this example illustrates that the activated complex has a lower entropy (or is more ordered) than the reactants. This observation is consistent with a mechanism in which the two NOCl reactants form a complex that eventually decays to produce NO and Cl.

# 18.15 Diffusion Controlled Reactions

For bimolecular chemical reactions in solution, the presence of solvent molecules can result in reaction dynamics that differ significantly from those in the gas phase. For example, the activation energy and relative orientation of reacting species were identified as being key factors in defining the rate constant for the reaction in the previous section. Imagine a reaction occurring in solution as illustrated in Figure 18.22. Since the average kinetic energy of the reactants is $3/2 \, RT$, the average translational velocity is the same as in the gas phase. However, in solution the presence of the solvent molecules results in a number of solvent–solute collisions before the reactants collide. Subsequently, the uninterrupted approach of the reactants characteristic of a gas-phase reaction is replaced by the reactants undergoing diffusion in solution until they encounter each other. In this case, the rate of diffusion can determine the rate of reaction.

The role of diffusion in solution-phase chemistry can be described using the following kinetic scheme:

$$A + B \overset{k_d}{\rightarrow} AB \tag{18.134}$$

$$AB \overset{k_r}{\rightarrow} A + B \tag{18.135}$$

$$AB \overset{k_p}{\rightarrow} P \tag{18.136}$$

In this scheme, reactants A and B diffuse with rate constant $k_d$ until they make contact and form the intermediate complex AB. Once this complex is formed, dissociation can



**FIGURE 18.22**
Top: Reactants A and B approach each other and collide in the gas phase. Bottom: In solution, the reactants undergo a series of collisions with the solvent. In this case, the approach of the reactants is dependent on the rate of reactant diffusion in solution.

A — → ← — B
Gas phase

A    B
Solution phase

occur to re-form the separate reactants (with rate constant $k_r$), or the reaction can continue resulting in product formation (with rate constant $k_P$). The expression for the reaction rate consistent with this scheme is

$$R = k_p[AB] \tag{18.137}$$

Since AB is an intermediate, the steady-state approximation is employed to express the concentration of this species in terms of the reactants:

$$\frac{d[AB]}{dt} = 0 = k_d[A][B] - k_r[AB] - k_p[AB]$$

$$[AB] = \frac{k_d[A][B]}{k_r + k_p} \tag{18.138}$$

Using this expression for [AB] the reaction rate becomes

$$R = \frac{k_p k_d}{k_r + k_p}[A][B] \tag{18.139}$$

If the rate constant for product formation is much greater than the decay of the intermediate complex to re-form the reactants ($k_p \gg k_r$), the rate expression becomes

$$R = k_d[A][B] \tag{18.140}$$

This is the **diffusion-controlled limit** where diffusion for the reactants limits the rate of product formation. The rate constant for diffusion can be related to the diffusion coefficients for the reactants by

$$k_d = 4\pi N_A (r_A + r_B) D_{AB} \tag{18.141}$$

In Equation (18.141), $r_A$ and $r_B$ are the radii of the reactants, and $D_{AB}$ is the mutual diffusion coefficient equal to the sum of diffusion coefficients for the reactants ($D_{AB} = D_A + D_B$). For a spherical particle in solution the diffusion coefficient is related to the viscosity $\eta$ by the Stokes–Einstein equation (Chapter 17):

$$D = \frac{k_B T}{6\pi\eta r} \tag{18.142}$$

In Equation (18.142) $k$ is Boltzmann's constant, $T$ is temperature, $\eta$ is solvent viscosity, and $r$ is the particle radius. This equation predicts that the reaction rate constant should decrease linearly with an increase in solvent viscosity.

To provide some insight into the magnitude of diffusion-controlled rate constants, consider the protonation of acetate ($CH_3COO^-$) in aqueous solution. The diffusion coefficient of $CH_3COO^-$ is $1.1 \times 10^{-5}$ cm$^2$ s$^{-1}$ and of $H^+$ is $9.3 \times 10^{-5}$ cm$^2$ s$^{-1}$, and ($r_A + r_B$) is on the order of 5 Å for ions in solution. Assuming that this reaction is diffusion controlled, the rate constant for the reaction is $6.5 \times 10^{-11}$ cm$^3$ s$^{-1}$ per reactant pair. Using $N_A$ to convert this quantity to a molar value, $k_d = 3.9 \times 10^{10}$ M$^{-1}$ s$^{-1}$. Experimentally, the rate constants for acid/base neutralization reactions are greater than the diffusion-controlled limit due to Coulombic attraction of the ions accelerating the collisional rate beyond the diffusion-controlled limit. Another prediction of the diffusion-controlled limit is that the rate of reaction is dependent on the viscosity of solution.

The opposite limit for the reaction occurs when the rate constant for product formation is much smaller than the rate of complex dissociation. In this activation-controlled limit the expression for the reaction rate [(Equation (18.139)] is

$$R = \frac{k_p k_d}{k_r}[A][B] \tag{18.143}$$

In this limit, the rate of the reaction depends on the energetics of the reaction, which are contained in $k_p$.

**EXAMPLE PROBLEM 18.11**

In aqueous solution at 25°C and pH 7.4 the diffusion coefficient for hemoglobin (radius = 35 Å) is $7.6 \times 10^{-7}$ cm$^2$ s$^{-1}$, and the diffusion coefficient for $O_2$ (radius = 2.0 Å) is $2.2 \times 10^{-5}$ cm$^2$ s$^{-1}$. The rate constant for the binding of $O_2$ to hemoglobin is $4 \times 10^7$ M$^{-1}$ s$^{-1}$. Is this a diffusion-controlled reaction?

**Solution**

Assuming the reaction is diffusion controlled, the rate constant is expected to be

$$k_d = 4\pi N_A(r_A + r_B)D_{AB}$$
$$= 4\pi N_A(35 \times 10^{-8}\text{ cm} + 2.0 \times 10^{-8}\text{ cm})$$
$$(7.6 \times 10^{-7}\text{ cm}^2\text{ s}^{-1} + 2.2 \times 10^{-5}\text{ cm}^2\text{ s}^{-1})$$
$$= 6.4 \times 10^{10}\text{ M}^{-1}\text{ s}^{-1}$$

The diffusion-controlled rate constant is significantly greater than the experimentally measured rate constant; therefore, the binding of $O_2$ to hemoglobin is not diffusion controlled.

# Vocabulary

activated complex

activated complex theory

activation energy

Arrhenius expression

Arrhenius preexponential factor

chemical kinetics

chemical methods

contour plot

diffusion-controlled limit

elementary reaction step

Euler's method

Eyring equation

femtochemistry

first-order reaction

flash photolysis techniques

frequency factor

half-life

initial rate

integrated rate law expression

intermediate

isolation method

method of initial rates

molecularity

parallel reaction

perturbation-relaxation methods

physical methods

potential energy surface

rate constant

rate-determining step

rate law

rate of conversion

reaction coordinate

reaction mechanism

reaction order

reaction rate

reversible reaction

second-order reaction (type I)

second-order reaction (type II)

sequential reaction

steady-state approximation

stopped-flow techniques

temperature jump

transition state

transition state theory

yield

# Conceptual Problems

**Q18.1**   Why is the stoichiometry of a reaction generally not sufficient to determine reaction order?

**Q18.2**   What is the difference between the order of a reaction with respect to a given species and the overall order?

**Q18.3**   What is an elementary chemical step, and how is one used in kinetics?

**Q18.4**   What is the difference between chemical and physical methods for studying chemical kinetics?

**Q18.5**   What are the fastest timescales on which chemical reactions can be investigated? Describe three experimental techniques for investigation of chemical reactions.

**Q18.6**   What is the method of initial rates, and why is it used in chemical kinetics studies?

**Q18.7**   What is a rate law expression, and how is it determined?

**Q18.8**   What is the difference between a first-order reaction and a second-order reaction?

**Q18.9**   What is a half-life? Is the half-life for a first-order reaction dependent on concentration?

**Q18.10**   In a sequential reaction, what is an intermediate?

**Q18.11**   What is meant by the rate-determining step in a sequential reaction?

**Q18.12** What is the steady-state approximation, and when is this approximation employed?

**Q18.13** In a parallel reaction in which two products can be formed from the same reactant, what determines the extent to which one product will be formed over another?

**Q18.14** What is the kinetic definition of equilibrium?

**Q18.15** In a temperature-jump experiment, why does a change in temperature result in a corresponding change in equilibrium?

**Q18.16** What is a transition state? How is the concept of a transition state used in activated complex theory?

**Q18.17** What is meant by a diffusion-controlled reaction?

**Q18.18** What is a typical rate constant for a diffusion-controlled reaction in aqueous solution?

**Q18.19** What is the relationship between the parameters in the Arrhenius equation and in the Eyring equation?

# Numerical Problems

Problem numbers in **red** indicate that the solution to the problem is given in the *Student's Solutions Manual*.

**P18.1** Express the rate of reaction with respect to each species in the following reactions:

**a.** $2 NO(g) + O_2(g) \rightarrow N_2O_4(g)$

**b.** $H_2(g) + I_2(g) \rightarrow 2 HI(g)$

**c.** $ClO(g) + BrO(g) \rightarrow ClO_2(g) + Br(g)$
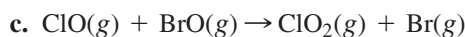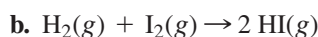
**P18.2** Consider the first-order decomposition of cyclobutane at 438°C at constant volume: $C_4H_8(g) \rightarrow 2C_2H_4(g)$

**a.** Express the rate of the reaction in terms of the change in total pressure as a function of time.

**b.** The rate constant for the reaction is $2.48 \times 10^{-4} \text{ s}^{-1}$. What is the half-life?

**c.** After initiation of the reaction, how long will it take for the initial pressure of $C_4H_8$ to drop to 90% of its initial value?

**P18.3** As discussed in the text, the total system pressure can be used to monitor the progress of a chemical reaction. Consider the following reaction: $SO_2Cl_2(g) \rightarrow SO_2(g) + Cl_2(g)$. The reaction is initiated, and the following data are obtained:

| Time (h) | 0 | 3 | 6 | 9 | 12 | 15 |
|---|---|---|---|---|---|---|
| $P_{Total}$ (kPa) | 11.07 | 14.79 | 17.26 | 18.90 | 19.99 | 20.71 |

**a.** Is the reaction first or second order with respect to $SO_2Cl_2$?

**b.** What is the rate constant for this reaction?

**P18.4** Consider the following reaction involving bromophenol blue (BPB) and $OH^-$: $HBPB(aq) + OH^-(aq) \rightarrow BPB^-(aq) + H_2O(l)$. The concentration of BPB can be monitored by following the absorption of this species and using the Beer–Lambert law. In this law, absorption $A$ and concentration are linearly related.

**a.** Express the reaction rate in terms of the change in absorbance as a function of time.

**b.** Let $A_o$ be the absorbance due to HBPB at the beginning of the reaction. Assuming that the reaction is first order with respect to both reactants, how is the absorbance of HBPB expected to change with time?

**c.** Given your answer to part (b), what plot would you construct to determine the rate constant for the reaction?

**P18.5** For the following rate expressions, state the order of the reaction with respect to each species, the total order of the reaction, and the units of the rate constant $k$:

**a.** $R = k[ClO][BrO]$

**b.** $R = k[NO]^2[O_2]$

**c.** $R = k\dfrac{[HI]^2[O_2]}{[H^+]^{1/2}}$

**P18.6** What is the overall order of the reaction corresponding to the following rate constants?

**a.** $k = 1.63 \times 10^{-4} \text{ M}^{-1} \text{ s}^{-1}$

**b.** $k = 1.63 \times 10^{-4} \text{ M}^{-2} \text{ s}^{-1}$

**c.** $k = 1.63 \times 10^{-4} \text{ M}^{-1/2} \text{ s}^{-1}$

**P18.7** The reaction rate as a function of initial reactant pressures was investigated for the reaction $2 NO(g) + 2 H_2(g) \rightarrow N_2(g) + 2 H_2O(g)$, and the following data were obtained:

| Run | $P_o$ H$_2$ (kPa) | $P_o$ NO (kPa) | Rate $(\text{kPa s}^{-1})$ |
|---|---|---|---|
| 1 | 53.3 | 40.0 | 0.137 |
| 2 | 53.3 | 20.3 | 0.033 |
| 3 | 38.5 | 53.3 | 0.213 |
| 4 | 19.6 | 53.3 | 0.105 |

What is the rate law expression for this reaction?

**P18.8** One loss mechanism for ozone in the atmosphere is the reaction with the $HO_2 \cdot$ radical:

$$HO_2 \cdot (g) + O_3(g) \rightarrow OH \cdot (g) + 2O_2(g)$$
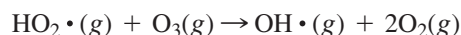
Using the following information, determine the rate law expression for this reaction:

| Rate $(\text{cm}^{-3} \text{ s}^{-1})$ | $[HO_2 \cdot] \, (\text{cm}^{-3})$ | $[O_3] \, (\text{cm}^{-3})$ |
|---|---|---|
| $1.9 \times 10^8$ | $1.0 \times 10^{11}$ | $1.0 \times 10^{12}$ |
| $9.5 \times 10^8$ | $1.0 \times 10^{11}$ | $5.0 \times 10^{12}$ |
| $5.7 \times 10^8$ | $3.0 \times 10^{11}$ | $1.0 \times 10^{12}$ |

**P18.9** The disaccharide lactose can be decomposed into its constituent sugars galactose and glucose. This decomposition can be accomplished through acid-based hydrolysis or by the enzyme lactase. Lactose intolerance in humans is due to the lack of lactase production by cells in the small intestine. However, the stomach is an acidic environment; therefore,

one might expect lactose hydrolysis to still be an efficient process. The following data were obtained on the rate of lactose decomposition as a function of acid and lactose concentration. Using this information, determine the rate law expression for the acid-based hydrolysis of lactose.

| Initial Rate $(M^{-1} s^{-1})$ | $[lactose]_0$ (M) | $[H^+]$ (M) |
|---|---|---|
| 0.00116 | 0.01 | 0.001 |
| 0.00232 | 0.02 | 0.001 |
| 0.00464 | 0.01 | 0.004 |

**P18.10**   (Challenging) The first-order thermal decomposition of chlorocyclohexane is as follows: $C_6H_{11}Cl(g) \rightarrow C_6H_{10}(g) + HCl(g)$. For a constant volume system the following total pressures were measured as a function of time:

| Time (s) | P (Torr) | Time (s) | P (Torr) |
|---|---|---|---|
| 3 | 237.2 | 24 | 332.1 |
| 6 | 255.3 | 27 | 341.1 |
| 9 | 271.3 | 30 | 349.3 |
| 12 | 285.8 | 33 | 356.9 |
| 15 | 299.0 | 36 | 363.7 |
| 18 | 311.2 | 39 | 369.9 |
| 21 | 322.2 | 42 | 375.5 |

**a.** Derive the following relationship for a first-order reaction: $P(t_2) - P(t_1) = (P(t_\infty) - P(t_0))e^{-kt_1}(1 - e^{-k(t_2-t_1)})$. In this relation, $P(t_1)$ and $P(t_2)$ are the pressures at two specific times; $P(t_0)$ is the initial pressure when the reaction is initiated, $P(t_\infty)$ is the pressure at the completion of the reaction, and $k$ is the rate constant for the reaction. To derive this relationship do the following:

i.   Given the first-order dependence of the reaction, write the expression for the pressure of chlorocyclohexane at a specific time $t_1$.

ii.   Write the expression for the pressure at another time $t_2$, which is equal to $t_1 + \Delta$where delta is a fixed quantity of time.

iii.   Write expressions for $P(t_\infty)-P(t_1)$ and $P(t_\infty)-P(t_2)$.

iv.   Subtract the two expressions from part (iii).

**b.** Using the natural log of the relationship from part (a) and the data provided in the table given earlier in this problem, determine the rate constant for the decomposition of chlorocyclohexane. (*Hint*: Transform the data in the table by defining $t_2-t_1$ to be a constant value, for example, 9 s.)

**P18.11**   You are given the following data for the decomposition of acetaldehyde:

| Initial Concentration (M) | $9.72 \times 10^{-3}$ | $4.56 \times 10^{-3}$ |
|---|---|---|
| Half-Life (s) | 328 | 685 |

Determine the order of the reaction and the rate constant for the reaction.

**P18.12**   Consider the schematic reaction $A \xrightarrow{k} P$.
**a.** If the reaction is one-half order with respect to A, what is the integrated rate law expression for this reaction?

**b.** What plot would you construct to determine the rate constant $k$ for the reaction?

**c.** What would be the half-life for this reaction? Will it depend on initial concentration of the reactant?

**P18.13**   A certain reaction is first order, and 540 s after initiation of the reaction, 32.5% of the reactant remains.

**a.** What is the rate constant for this reaction?

**b.** At what time after initiation of the reaction will 10% of the reactant remain?

**P18.14**   The half-life of $^{238}U$ is $4.5 \times 10^9$ years. How many disintegrations occur in 1 min for a 10 mg sample of this element?

**P18.15**   You are performing an experiment using $^3H$ (half-life = $4.5 \times 10^3$ days) labeled phenylalanine in which the five aromatic hydrogens are labeled. To perform the experiment, the initial activity cannot be lower than 10% of the initial activity when the sample was received. How long after receiving the sample can you wait before performing the experiment?

**P18.16**   One issue confronting the use of $^{14}C$ decay (half-life of 5760 years) to date materials is that of obtaining a standard. One approach to this issue is found in the field of dendrochronology or using tree rings to determine age. Using this approach, tree materials dating back 10,000 years have been identified. Assuming you had a sample of such a tree in which the number of decay events was 15.3 decays per minute before decomposition, what would the decays per minute be in the present day?

**P18.17**   A convenient source of gamma rays for radiation chemistry research is $^{60}Co$, which undergoes the following decay process: $^{60}_{27}Co \xrightarrow{k} {}^{60}_{28}Ni + \beta^- + \gamma$. The half-life of $^{60}Co$ is $1.9 \times 10^3$ days.

**a.** What is the rate constant for the decay process?

**b.** How long will it take for a sample of $^{60}Co$ to decay to half of its original concentration?

**P18.18**   The growth of a bacterial colony can be modeled as a first-order process in which the probability of cell division is linear with respect to time such that $dN/N = \zeta dt$, where $dN$ is the number of cells that divide in the time interval $dt$, and $\zeta$ is a constant.

**a.** Use the preceding expression to show that the number of cells in the colony is given by $N = N_0 e^{\zeta t}$, where $N$ is the number of cells in the colony and $N_0$ is the number of cells present at $t = 0$.

**b.** The generation time is the amount of time it takes for the number of cells to double. Using the answer to part (a), derive an expression for the generation time.

**c.** In milk at 37°C, the bacterium *Lactobacillus acidophilus* has a generation time of about 75 min. Construct a plot of the *acidophilus* concentration as a function of time for time intervals of 15, 30, 45, 60, 90, 120, and 150 min after a colony of size $N_0$ is introduced to a container of milk.

**P18.19** A technique for radioactively labeling proteins is electrophilic radioiodination in which an aromatic substitution of $^{131}$I onto a tyrosine residue is performed as follows:
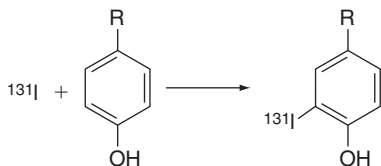


Using the activity of $^{131}$I, one can measure protein lifetimes in a variety of biological processes. $^{131}$I undergoes beta decay with a half-life of 8.02 days. Initially a protein labeled with $^{131}$I has a specific activity of 1.0 μCi, which corresponds to 37,000 decay events every second. The protein is suspended in aqueous solution and exposed to oxygen for 5 days. After isolating the protein from solution, the protein sample is found to have a specific activity of 0.32 μCi. Is oxygen reacting with the tyrosine residues of the protein, resulting in the loss of $^{131}$I?

**P18.20** Molybdenum-99 decays to form "metastable" technetium-99 ($^{99}$Tc) through beta decay. This isotope has a very long lifetime (half-life of 6 hours) compared to other nuclear isomers that undergo gamma decay. The gamma rays emitted when $^{99}$Tc decays are easily detected, which makes this species ideal for a variety of medical imaging applications such as single-photon emission computed tomography. At the beginning of this millennium, the decommissioning of two nuclear reactors created a critical shortage of $^{99}$Tc, and this shortage remains to be addressed (*Science* 331 (2011): 227). Imagine you are performing an imaging experiment with $^{99}$Tc in which you need 2 hours to obtain the image after injecting the isotope into the patient. How much of the $^{99}$Tc will have decayed during this time?

**P1821** Show that the ratio of the half-life to the one-quarter life, $t_{1/2}/t_{1/4}$, for a reaction that is $n$th order ($n > 1$) in reactant $A$ can be written as a function of $n$ alone (that is, there is no concentration dependence in the ratio). (Note: The one-quarter life is defined as the time at which the concentration is $1/4$ of the initial concentration.)

**P18.22** Given the following kinetic scheme and associated rate constants, determine the concentration profiles of all species using Euler's method. Assume that the reaction is initiated with only the reactant $A$ present at an initial concentration of 1 M. To perform this calculation, you may want to use a spreadsheet program such as Excel.

$$A \xrightarrow{k=1.5\times10^{-3}\text{ s}^{-1}} B$$

$$A \xrightarrow{k=2.5\times10^{-3}\text{ s}^{-1}} C \xrightarrow{k=1.8\times10^{-3}\text{ s}^{-1}} D$$
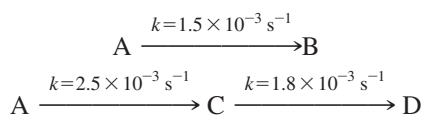
**P18.23** For the sequential reaction $A \xrightarrow{k_A} B \xrightarrow{k_B} C$, the rate constants are $k_A = 5 \times 10^6$ s$^{-1}$ and $k_B = 3 \times 10^6$ s$^{-1}$. Determine the time at which $[B]$ is at a maximum.

**P18.24** For the sequential reaction $A \xrightarrow{k_A} B \xrightarrow{k_B} C$, $k_A = 1.00 \times 10^{-3}$ s$^{-1}$. Using a computer spreadsheet program such as Excel, plot the concentration of each species for cases where $k_B = 10k_A$, $k_B = 1.5k_A$, and $k_B = 0.1k_A$. Assume that only the reactant is present when the reaction is initiated.

**P18.25** (Challenging) For the sequential reaction in Problem P18.21, plot the concentration of each species for the case where $k_B = k_A$. Can you use the analytical expression for [B] in this case?

**P18.26** For a type II second-order reaction, the reaction is 60% complete in 60 seconds when $[A]_0 = 0.1$ M and $[B]_0 = 0.5$ M.

**a.** What is the rate constant for this reaction?

**b.** Will the time for the reaction to reach 60% completion change if the initial reactant concentrations are decreased by a factor of 2?

**P18.27** Bacteriorhodopsin is a protein found in *Halobacterium halobium* that converts light energy into a transmembrane proton gradient that is used for ATP synthesis. After light is absorbed by the protein, the following initial reaction sequence occurs:

$$\text{Br} \xrightarrow{k_1=2.0\times10^{12}\text{ s}^{-1}} \text{J} \xrightarrow{k_2=3.3\times10^{11}\text{ s}^{-1}} \text{K}$$
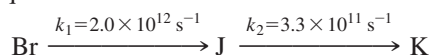
**a.** At what time will the maximum concentration of the intermediate J occur?

**b.** Construct plots of the concentration of each species versus time.

**P18.28** Bananas are somewhat radioactive due to the presence of substantial amounts of potassium. Potassium-40 decays by two different paths:

$$^{40}_{19}\text{K} \rightarrow {}^{40}_{20}\text{Ca} + \beta^- \ (89.3\%)$$

$$^{40}_{19}\text{K} \rightarrow {}^{40}_{18}\text{Ar} + \beta^+ \ (10.7\%)$$
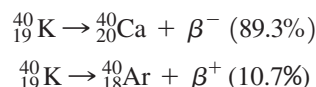
The half-life for potassium decay is $1.3 \times 10^9$ years. Determine the rate constants for the individual channels.

**P18.29** The bimolecular reaction of chlorine monoxide can result in the formation of three different combinations of products or product channels (the rate constant for each reaction is indicated):

$$\text{ClO}\cdot(g) + \text{ClO}\cdot(g) \rightarrow \text{Cl}_2(g) + \text{O}_2(g) \qquad k = 2.9 \times 10^6$$
$$\rightarrow \text{ClOO}\cdot(g) + \text{Cl}\cdot(g) \qquad k = 4.8 \times 10^6$$
$$\rightarrow \text{OClO}\cdot(g) + \text{Cl}\cdot(g) \qquad k = 2.1 \times 10^6$$
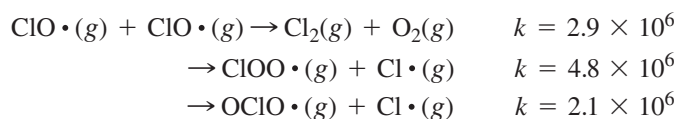
Determine the quantum yield for the three product channels.

**P18.30** In the stratosphere, the rate constant for the conversion of ozone to molecular oxygen by atomic chlorine is $\text{Cl}\cdot(g) + \text{O}_3(g) \rightarrow \text{ClO}\cdot(g) + \text{O}_2(g)$ [(half-life of 5760 years) k $= (1.7 \times 10^{10}\text{ M}^{-1}\text{s}^{-1})e^{-260K/T}$].

**a.** What is the rate of this reaction at 20 km where $[\text{Cl}] = 5 \times 10^{-17}$ M, $[\text{O}_3] = 8 \times 10^{-9}$ M, and $T = 220$ K?

**b.** The actual concentrations at 45 km are $[\text{Cl}] = 3 \times 10^{-15}$ M and $[\text{O}_3] = 8 \times 10^{-11}$ M. What is the rate of the reaction at this altitude where $T = 270$ K?

**c.** (Optional) Given the concentrations in part (a), what would you expect the concentrations at 20. km to be assuming that the gravity represents the operative force defining the potential energy?

**P18.31** An experiment is performed on the following parallel reaction:
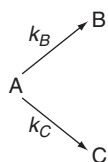


Two things are determined: (1) The yield for B at a given temperature is found to be 0.3 and (2) the rate constants are described well by an Arrhenius expression with the activation to B and C formation being 27 and 34 kJ mol$^{-1}$, respectively, and with identical preexponential factors. Demonstrate that these two statements are inconsistent with each other.

**P18.32** The reaction of atomic chlorine with ozone is the first step in the catalytic decomposition of stratospheric ozone by Cl • :

$$Cl \cdot (g) + O_3(g) \rightarrow ClO \cdot (g) + O_2(g)$$
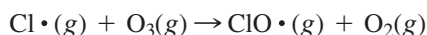
At 298 K the rate constant for this reaction is $6.7 \times 10^9 \, M^{-1} \, s^{-1}$. Experimentally, the Arrhenius pre-exponential factor was determined to be $1.4 \times 10^{10} \, M^{-1} \, s^{-1}$. Using this information determine the activation energy for this reaction.

**P18.33** In addition to Cl • , other halogens can potentially contribute to stratospheric ozone loss. For example, consider the reaction of Br • with ozone:

$$Br \cdot (g) + O_3(g) \rightarrow BrO \cdot (g) + O_2(g)$$
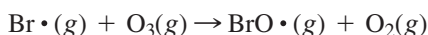
At 298 K the rate constant for this reaction is $1.2 \times 10^8 \, M^{-1} \, s^{-1}$, about a factor of 50 reduced from the Cl • value presented in the previous problem. Experimentally, the Arrhenius pre-exponential factor was determined to be $1.0 \times 10^{10} \, M^{-1} \, s^{-1}$.

**a.** Without doing any calculations, is the energy barrier for this reaction greater or less than that for Cl?

**b.** Calculate the activation energy for this reaction.

**P18.34** A standard "rule of thumb" for thermally activated reactions is that the reaction rate doubles for every 10 K increase in temperature. Is this statement true independent of the activation energy (assuming that the activation energy is positive and independent of temperature)?

**P18.35** Calculate the ratio of rate constants for two thermal reactions that have the same Arrhenius preexponential term but have activation energies that differ by 1.0, 10., and 30. kJ/mol for $T = 298$ K.

**P18.36** The conversion of $NO_2(g)$ to $NO(g)$ and $O_2(g)$ can occur through the following reaction:

$$NO_2(g) \rightarrow 2NO(g) + O_2(g)$$

The activation energy for this reaction is 111 kJ mol$^{-1}$ and the pre-exponential factor is $2.0 \times 10^{-9} \, M^{-1} \, s^{-1}$. Assume that these quantities are temperature independent.

**a.** What is the rate constant for this reaction at 298 K?

**b.** What is the rate constant for this reaction at the tropopause where T = 225 K.

**P18.37** The activation energy for a reaction is 50. J mol$^{-1}$. Determine the effect on the rate constant for this reaction with a change in temperature from 273 K to 298 K.

**P18.38** The rate constant for the reaction of hydrogen with iodine is $2.45 \times 10^{-4} \, M^{-1} \, s^{-1}$ at 302°C and $0.950 \, M^{-1} \, s^{-1}$ at 508°C.

**a.** Calculate the activation energy and Arrhenius preexponential factor for this reaction.

**b.** What is the value of the rate constant at 400.°C?

**P18.39** Consider the gas phase thermal decomposition of 1.0 atm of $(CH_3)_3COOC(CH_3)_3(g)$ to acetone $(CH_3)_2CO(g)$ and ethane $(C_2H_6)(g)$, which occurs with a rate constant of $0.0019 \, s^{-1}$. After initiation of the reaction, at what time would you expect the pressure to be 1.8 atm?

**P18.40** At 552.3 K, the rate constant for the thermal decomposition of $SO_2Cl_2$ is $1.02 \times 10^{-6} \, s^{-1}$. If the activation energy is 210. kJ mol$^{-1}$, calculate the Arrhenius preexponential factor and determine the rate constant at 600. K.

**P18.41** The melting of double-strand DNA into two single strands can be initiated using temperature-jump methods. Derive the expression for the $T$-jump relaxation time for the following equilibrium involving double-strand (DS) and single-strand (SS) DNA:

$$DS \underset{k_r}{\overset{k_f}{\rightleftharpoons}} 2SS$$
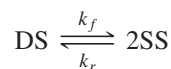
**P18.42** Consider the reaction

$$A + B \underset{k'}{\overset{k}{\rightleftharpoons}} P$$
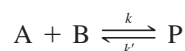
A temperature-jump experiment is performed where the relaxation time constant is measured to be 310 $\mu$s, resulting in an equilibrium where $K_{eq} = 0.70$ with $[P]_{eq} = 0.20$ M. What are $k$ and $k'$? (Watch the units!)

**P18.43** In the limit where the diffusion coefficients and radii of two reactants are equivalent, demonstrate that the rate constant for a diffusion controlled reaction can be written as

$$k_d = \frac{8RT}{3\eta}$$

**P18.44** In the following chapter, enzyme catalysis reactions will be extensively reviewed. The first step in these reactions involves the binding of a reactant molecule (referred to as a substrate) to a binding site on the enzyme. If this binding is extremely efficient (that is, equilibrium strongly favors the enzyme–substrate complex over separate enzyme and substrate) and the formation of product rapid, then the rate of catalysis could be diffusion limited. Estimate the expected rate constant for a diffusion controlled reaction using typical values for an enzyme ($D = 1.00 \times 10^{-7} \, cm^2 \, s^{-1}$ and $r = 40.0$ Å) and a small molecular substrate ($D = 1.00 \times 10^{-5} \, cm^2 \, s^{-1}$ and $r = 5.00$ Å).

**P18.45** Imidazole is a common molecular species in biological chemistry. For example, it constitutes the side chain of

the amino acid histidine. Imidazole can be protonated in solution as follows:
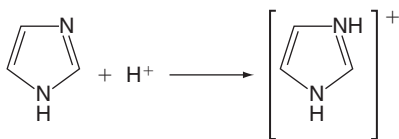


The rate constant for the protonation reaction is $5.5 \times 10^{10} \text{ M}^{-1} \text{ s}^{-1}$. Assuming that the reaction is diffusion controlled, estimate the diffusion coefficient of imidazole when $D(\text{H}^+) = 9.31 \times 10^{-5} \text{ cm}^2 \text{ s}^{-1}$, $r(\text{H}^+) \sim 1.0$ Å and $r$ (imidazole) $= 6.0$ Å. Use this information to predict the rate of deprotonation of imidazole by $\text{OH}^-$ ($D = 5.30 \times 10^{-5} \text{ cm}^2 \text{ s}^{-1}$ and $r = \sim 1.5$ Å).

**P18.46** Catalase is an enzyme that promotes the conversion of hydrogen peroxide ($\text{H}_2\text{O}_2$) into water and oxygen. The diffusion constant and radius for catalase are $6.0 \times 10^{-7} \text{ cm}^2 \text{ s}^{-1}$ and 51.2 Å. For hydrogen peroxide the corresponding values are $1.5 \times 10^{-5} \text{ cm}^2 \text{ s}^{-1}$ and $r \sim 2.0$ Å. The experimentally determined rate constant for the conversion of hydrogen peroxide by catalase is $5.0 \times 10^6 \text{ M}^{-1} \text{ s}^{-1}$. Is this a diffusion-controlled reaction?

**P18.47** The unimolecular decomposition of urea in aqueous solution is measured at two different temperatures, and the following data are observed:

| Trial Number | Temperature (°C) | $k$ ($\text{s}^{-1}$) |
|---|---|---|
| 1 | 60.0 | $1.20 \times 10^{-7}$ |
| 2 | 71.5 | $4.40 \times 10^{-7}$ |

**a.** Determine the Arrhenius parameters for this reaction.
**b.** Using these parameters, determine $\Delta H^{\ddagger}$ and $\Delta S^{\ddagger}$ as described by the Eyring equation.

**P18.48** The gas-phase decomposition of ethyl bromide is a first-order reaction, occurring with a rate constant that demonstrates the following dependence on temperature:

| Trial Number | Temperature (K) | $k$ ($\text{s}^{-1}$) |
|---|---|---|
| 1 | 800. | 0.0360 |
| 2 | 900. | 1.410 |

**a.** Determine the Arrhenius parameters for this reaction.
**b.** Using these parameters, determine $\Delta H^{\ddagger}$ and $\Delta S^{\ddagger}$ as described by the Eyring equation.

**P18.49** Hydrogen abstraction from hydrocarbons by atomic chlorine is a mechanism for $\text{Cl} \cdot$ loss in the atmosphere. Consider the reaction of $\text{Cl} \cdot$ with ethane:

$$\text{C}_2\text{H}_6(g) + \text{Cl} \cdot (g) \rightarrow \text{C}_2\text{H}_5 \cdot (g) + \text{HCl}(g)$$
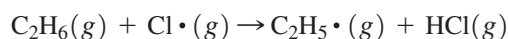
This reaction was studied in the laboratory, and the following data were obtained:

| T (K) | k ($\times 10^{-10} \text{ M}^{-2}\text{s}^{-1}$) |
|---|---|
| 270 | 3.43 |
| 370 | 3.77 |
| 470 | 3.99 |
| 570 | 4.13 |
| 670 | 4.23 |

**a.** Determine the Arrhenius parameters for this reaction.
**b.** At the tropopause (the boundary between the troposphere and stratosphere located approximately 11 km above the surface of Earth), the temperature is roughly 220 K. What do you expect the rate constant to be at this temperature?
**c.** Using the Arrhenius parameters obtained in part (a), determine the Eyring parameters $\Delta H^{\ddagger}$ and $\Delta S^{\ddagger}$ for this reaction at 220 K.

**P18.50** Consider the "unimolecular" isomerization of methylcyanide, a reaction that will be discussed in detail in Chapter 19: $\text{CH}_3\text{NC}(g) \rightarrow \text{CH}_3\text{CN}(g)$. The Arrhenius parameters for this reaction are $A = 2.5 \times 10^{16} \text{ s}^{-1}$ and $E_a = 272 \text{ kJ mol}^{-1}$. Determine the Eyring parameters $\Delta H^{\ddagger}$ and $\Delta S^{\ddagger}$ for this reaction with $T = 300.$ K.

**P18.51** Reactions involving hydroxyl radical ($\text{OH} \cdot$) are extremely important in atmospheric chemistry. The reaction of hydroxyl radical with molecular hydrogen is as follows:

$$\text{OH} \cdot (g) + \text{H}_2(g) \rightarrow \text{H}_2\text{O}(g) + \text{H} \cdot (g)$$
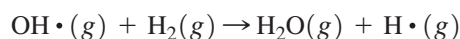
Determine the Eyring parameters $\Delta H^{\ddagger}$ and $\Delta S^{\ddagger}$ for this reaction where $A = 8.0 \times 10^{13} \text{ M}^{-1} \text{ s}^{-1}$ and $E_a = 42 \text{ kJ mol}^{-1}$.

**P18.52** Chlorine monoxide ($\text{ClO} \cdot$) demonstrates three bimolecular self-reactions:

$$Rxn_1: \text{ClO} \cdot (g) + \text{ClO} \cdot (g) \xrightarrow{k_1} \text{Cl}_2(g) + \text{O}_2(g)$$

$$Rxn_2: \text{ClO} \cdot (g) + \text{ClO} \cdot (g) \xrightarrow{k_2} \text{Cl} \cdot (g) + \text{ClOO} \cdot (g)$$

$$Rxn_3: \text{ClO} \cdot (g) + \text{ClO} \cdot (g) \xrightarrow{k_3} \text{Cl} \cdot (g) + \text{OClO} \cdot (g)$$
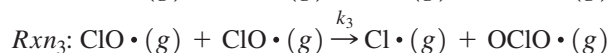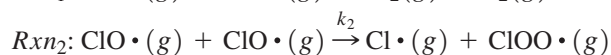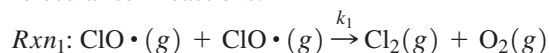
The following table provides the Arrhenius parameters for this reaction:

| | $A$ ($\text{M}^{-1} \text{ s}^{-1}$) | $E_a$ (kJ/mol) |
|---|---|---|
| $Rxn_1$ | $6.08 \times 10^8$ | 13.2 |
| $Rxn_2$ | $1.79 \times 10^{10}$ | 20.4 |
| $Rxn_3$ | $2.11 \times 10^8$ | 11.4 |

**a.** For which reaction is $\Delta H^{\ddagger}$ greatest and by how much relative to the next closest reaction?
**b.** For which reaction is $\Delta S^{\ddagger}$ the smallest and by how much relative to the next closest reaction?

# Computational Problems

More detailed instructions on carrying out these calculations using Spartan Physical Chemistry are found on the book website at *www.masteringchemistry.com.*

**C18.1** Chlorofluorocarbons are a source of atomic chlorine in the stratosphere. In this problem the energy needed to dissociate the C—Cl bond in $\text{CF}_3\text{Cl}$ will be determined.

**a.** Perform a Hartree–Fock 3-21G calculation on the freon $CF_3Cl$ and determine the minimum energy of this compound.

**b.** Select the C—Cl bond and calculate the ground-state potential energy surface along this coordinate by determining the energy of the compound for the following C—Cl bond lengths:

| $r_{CCl}$ (Å) | E (Hartree) | $r_{CCl}$ (Å) | E (Hartree) |
|---|---|---|---|
| 1.40 | | 2.40 | |
| 1.50 | | 2.60 | |
| 1.60 | | 2.80 | |
| 1.70 | | 3.00 | |
| 1.80 | | 4.00 | |
| 2.00 | | 5.00 | |
| 2.20 | | 6.00 | |

**c.** Using the difference between the minimum of the potential energy surface to the energy at 6.00 Å, determine the barrier to dissociation.

**d.** Assuming an Arrhenius preexponential factor of $10^{-12}$ s$^{-1}$, what is the expected rate constant for dissociation based on this calculation at 220 K? Is thermal dissociation of the C—Cl bond occurring to an appreciable extent in the stratosphere?

**C18.2** Consider the dissociation of the C—F bond in $CFCl_3$. Using a standard bond dissociation energy of 485 kJ mol$^{-1}$, what would be the effect on the predicted rate constant for dissociation if zero-point energy along the C—F stretch coordinate were ignored? Performing a Hartree–Fock 6-31G* calculation, determine the frequency of the vibrational mode dominated by C—F stretch character. Calculate the dissociation rate using the Arrhenius expression without consideration of zero-point energy by adding the zero-point energy to the standard dissociation energy. Assume $A = 10^{10}$ s$^{-1}$ and $T = 298$ K. Perform the corresponding calculation using the standard dissociation energy only. Does zero-point energy make a significant difference in the rate constant for this dissociation?

# Web-Based Simulations, Animations, and Problems

**W18.1** In this problem, concentration profiles as a function of rate constant are explored for the following sequential reaction scheme:

$$A \xrightarrow{k_a} B \xrightarrow{k_b} C$$
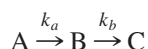
Students vary the rate constants $k_a$ and $k_b$ and explore the following behavior:

**a.** The variation in concentrations as the rate constants are varied.

**b.** Comparison of the maximum intermediate concentration time determined by simulation and through computation.

**c.** Visualization of the conditions under which the rate-limiting step approximation is valid.

**W18.2** In this simulation, the kinetic behavior of the following parallel reaction is studied:

$$A \xrightarrow{k_b} B; \quad A \xrightarrow{k_c} C$$
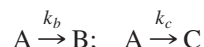
The variation in concentrations as a function of $k_b$ and $k_c$ is studied. In addition, the product yields for the reaction determined based on the relative values of $k_b$ and $k_c$ are compared to the simulation result.

# For Further Reading

Brooks, P. R. "Spectroscopy of Transition Region Species." *Chemical Reviews* 87 (1987): 167.

Callender, R. H., R. B. Dyer, R. Blimanshin, and W. H. Woodruff. "Fast Events in Protein Folding: The Time Evolution of a Primary Process." *Annual Review of Physical Chemistry* 49 (1998): 173.

Castellan, G. W. *Physical Chemistry*. Reading, MA: Addison-Wesley, 1983.

Eyring, H., S. H. Lin, and S. M. Lin. *Basic Chemical Kinetics*. New York: Wiley, 1980.

Frost, A. A., and R. G. Pearson. *Kinetics and Mechanism*. New York: Wiley, 1961.

Gagnon, E., P. Ranitovic, X.-M. Tong, C. L. Cocke, M. M. Murnane, H. C. Kapteyn, and A. S. Sandhu. "Soft X-Ray-Driven Femtosecond Molecular Dynamics." *Science* 317 (2007): 1374.

Hammes, G. G. *Thermodynamics and Kinetics for the Biological Sciences*. New York: Wiley, 2000.

Laidler, K. J. *Chemical Kinetics*. New York: Harper & Row, 1987.

Martin, J.-L., and M. H. Vos. "Femtosecond Biology." *Annual Review of Biophysical and Biomolecular Structure* 21 (1992): 1999.

Pannetier, G., and P. Souchay. *Chemical Kinetics*. Amsterdam: Elsevier, 1967.

Schoenlein, R. W., L. A. Peteanu, R. A. Mathies, and C. V. Shank. "The First Step in Vision: Femtosecond Isomerization of Rhodopsin." *Science* 254 (1991): 412.

Steinfeld, J. I., J. S. Francisco, and W. L. Hase. *Chemical Kinetics and Dynamics*. Prentice-Hall, Upper Saddle River, NJ: Prentice-Hall, 1999.

Truhlar, D. G., W. L. Hase, and J. T. Hynes. "Current Status in Transition State Theory." *Journal of Physical Chemistry* 87 (1983): 2642.

Vos, M. H., F. Rappaport, J.-C. Lambry, J. Breton, and J.-L. Martin. "Visualization of Coherent Nuclear Motion in a Membrane Protein by Femtosecond Spectroscopy." *Nature* 363 (1993): 320.

Zewail, H. "Laser Femtochemistry." *Science* 242 (1988): 1645.

# Complex Reaction Mechanisms

In this chapter, the chemical kinetic tools developed in the previous chapter are applied to complex reactions. Reaction mechanisms and their use in predicting reaction rate law expressions are explored. The preequilibrium approximation is presented and used in the evaluation of catalytic reactions including enzyme catalysis. In addition, homogeneous and heterogeneous catalytic processes are described. Reactions involving radicals, including polymerization and radical-initiated explosions, are discussed. The chapter concludes with an introduction to photochemistry. The unifying theme behind these apparently different topics is that all of the reaction mechanisms for these phenomena can be developed using the techniques of elementary chemical kinetics. Seemingly complex reactions can be decomposed into a series of well-defined kinetic steps, thereby providing substantial insight into the underlying chemical reaction dynamics.

## 19.1 Reaction Mechanisms and Rate Laws

**Reaction mechanisms** are defined as the collection of individual kinetic processes or steps involved in the transformation of reactants into products. The rate law expression for a chemical reaction, including the order of the reaction, is entirely dependent on the reaction mechanism. For a reaction mechanism to be valid, the rate-law expression predicted by the mechanism must agree with experiment. Consider the following reaction:

$$2 \, N_2O_5(g) \rightarrow 4 \, NO_2(g) \, + \, O_2(g) \tag{19.1}$$
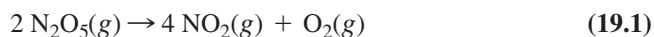
For the remainder of this section the phase of the species is suppressed for clarity. One possible mechanism for this reaction is a single step consisting of a bimolecular collision between two $N_2O_5$ molecules. A reaction mechanism that consists of a single elementary step is known as a **simple reaction.** The rate law predicted by this mechanism is second order with respect to $N_2O_5$. However, the experimentally determined rate law for this reaction is first order in $N_2O_5$, not second order. Therefore, the single-step mechanism cannot be correct. To explain the observed order dependence of the reaction rate, the following mechanism was proposed:

$$2\left\{ N_2O_5 \underset{k_{-1}}{\overset{k_1}{\rightleftharpoons}} NO_2 \, + \, NO_3 \right\} \tag{19.2}$$

$$\text{NO}_2 + \text{NO}_3 \xrightarrow{k_2} \text{NO}_2 + \text{O}_2 + \text{NO} \qquad (19.3)$$

$$\text{NO} + \text{NO}_3 \xrightarrow{k_3} 2\,\text{NO}_2 \qquad (19.4)$$
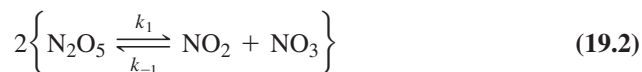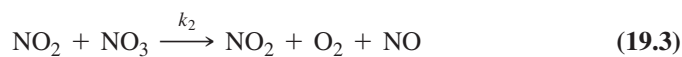
This mechanism is an example of a **complex reaction,** defined as a reaction that occurs in two or more elementary steps. In this mechanism, the first step, Equation (19.2), represents an equilibrium between $\text{N}_2\text{O}_5$ to $\text{NO}_2$ and $\text{NO}_3$. In the second step, Equation (19.3), the bimolecular reaction of $\text{NO}_2$ and $\text{NO}_3$ results in the dissociation of $\text{NO}_3$ to product NO and $\text{O}_2$. In the final step of the reaction, Equation (19.4), NO and $\text{NO}_3$ undergo a bimolecular reaction to produce $2\,\text{NO}_2$.

In addition to the reactant ($\text{N}_2\text{O}_5$) and overall reaction products ($\text{NO}_2$ and $\text{O}_2$), two other species appear in the mechanism (NO and $\text{NO}_3$) that are not in the overall reaction of Equation (19.1). These species are referred to as **reaction intermediates.** Reaction intermediates that are formed in one step of the mechanism must be consumed in a subsequent step. Given this requirement, step 1 of the reaction must occur twice in order to balance the $\text{NO}_3$ that appears in steps 2 and 3. Therefore, we have multiplied this reaction by 2 in Equation (19.2) to emphasize that it must occur twice for every occurrence of steps 2 and 3. The number of times a given step occurs in a reaction mechanism is referred to as the **stoichiometric number.** In the mechanism under discussion, step 1 has a stoichiometric number of 2, whereas the other two steps have stoichiometric numbers of 1. With correct stoichiometric numbers, the sum of the elementary reaction steps will produce an overall reaction that is stoichiometrically equivalent to the reaction of interest.

*For a reaction mechanism to be considered valid, the mechanism must be consistent with the experimentally determined rate law.* Using the mechanism depicted by Equations (19.2) through (19.4), the rate of the reaction is

$$R = -\frac{1}{2}\frac{d[\text{N}_2\text{O}_5]}{dt} = \frac{1}{2}\left(k_1[\text{N}_2\text{O}_5] - k_{-1}[\text{NO}_2][\text{NO}_3]\right) \qquad (19.5)$$

Notice that the stoichiometric number of the reaction is not included in the differential rate expression. Equation (19.5) corresponds to the loss of $\text{N}_2\text{O}_5$ by unimolecular decay and production by the bimolecular reaction of $\text{NO}_2$ with $\text{NO}_3$. As discussed earlier, NO and $\text{NO}_3$ are reaction intermediates. Writing the differential rate expression for these species and applying the steady-state approximation to the concentrations of both intermediates (Section 18.7.3) yields

$$\frac{d[\text{NO}]}{dt} = 0 = k_2[\text{NO}_2][\text{NO}_3] - k_3[\text{NO}][\text{NO}_3] \qquad (19.6)$$

$$\frac{d[\text{NO}_3]}{dt} = 0 = k_1[\text{N}_2\text{O}_5] - k_{-1}[\text{NO}_2][\text{NO}_3] - k_2[\text{NO}_2][\text{NO}_3] - k_3[\text{NO}][\text{NO}_3]$$
$$(19.7)$$

Equation (19.6) can be rewritten to produce the following expression for [NO]:

$$[\text{NO}] = \frac{k_2[\text{NO}_2]}{k_3} \qquad (19.8)$$

Substituting this result into Equation (19.7) yields

$$0 = k_1[\text{N}_2\text{O}_5] - k_{-1}[\text{NO}_2][\text{NO}_3] - k_2[\text{NO}_2][\text{NO}_3] - k_3\left(\frac{k_2[\text{NO}_2]}{k_3}\right)[\text{NO}_3]$$

$$0 = k_1[\text{N}_2\text{O}_5] - k_{-1}[\text{NO}_2][\text{NO}_3] - 2k_2[\text{NO}_2][\text{NO}_3]$$

$$\frac{k_1[\text{N}_2\text{O}_5]}{k_{-1} + 2k_2} = [\text{NO}_2][\text{NO}_3] \qquad (19.9)$$

Substituting Equation (19.9) into Equation (19.5) results in the following predicted rate law expression for this mechanism:

$$R = \frac{1}{2}(k_1[N_2O_5] - k_{-1}[NO_2][NO_3])$$

$$= \frac{1}{2}\left(k_1[N_2O_5] - k_{-1}\left(\frac{k_1[N_2O_5]}{k_{-1} + 2k_2}\right)\right)$$

$$= \frac{k_1k_2}{k_{-1} + 2k_2}[N_2O_5] = k_{eff}[N_2O_5] \qquad \textbf{(19.10)}$$

In Equation (19.10), the collection of rate constants multiplying $[N_2O_5]$ has been renamed $k_{eff}$. Equation (19.10) demonstrates that the mechanism is consistent with the experimentally observed first-order dependence on $[N_2O_5]$. However, as discussed in Chapter 18, the consistency of a reaction mechanism with the experimental order dependence of the reaction is not proof that the mechanism is absolutely correct but instead demonstrates that the mechanism is consistent with the experimentally determined order dependence.

The example just presented illustrates how reaction mechanisms are used to explain the order dependence of the reaction rate. A theme that reoccurs throughout this chapter is the relation between reaction mechanisms and elementary reaction steps. As we will see, the mechanisms for many complex reactions can be decomposed into a series of elementary steps, and the techniques developed in the previous chapter can be readily employed in the evaluation of these complex kinetic problems.

# 19.2 The Preequilibrium Approximation

The preequilibrium approximation is a central concept employed in the evaluation of reaction mechanisms. This approximation is used when equilibrium among a subset of species is established before product formation occurs. In this section, the preequilibrium approximation is defined. This approximation will prove to be extremely useful in subsequent sections.

## 19.2.1 General Solution

Consider the following reaction:

$$A + B \underset{k_r}{\overset{k_f}{\rightleftharpoons}} I \overset{k_p}{\rightarrow} P \qquad \textbf{(19.11)}$$

In Equation (19.11), forward and back rate constants link the reactants A and B with an intermediate species, I. Decay of I results in the formation of product, P. If the forward and backward reactions involving the reactants and intermediate are more rapid than the decay of the intermediate to form products, then the reaction of Equation (19.11) can be envisioned as occurring in two distinct steps:

1. First, equilibrium between the reactants and the intermediate is maintained during the course of the reaction.

2. The intermediate undergoes decay to form product.

This description of events is referred to as the **preequilibrium approximation.** The application of the preequilibrium approximation in evaluating reaction mechanisms containing equilibrium steps is performed as follows. The differential rate expression for the product is

$$\frac{d[P]}{dt} = k_p[I] \qquad \textbf{(19.12)}$$

In Equation (19.12), [I] can be rewritten by recognizing that this species is in equilibrium with the reactants; therefore,

$$\frac{[\text{I}]}{[\text{A}][\text{B}]} = \frac{k_f}{k_r} = K_c \tag{19.13}$$

$$[\text{I}] = K_c[\text{A}][\text{B}] \tag{19.14}$$

In the preceding equations, $K_c$ is the equilibrium constant expressed in terms of reactant and product concentrations. Substituting the definition of [I] provided by Equation (19.14) into Equation (19.12), the differential rate expression for the product becomes

$$\frac{d[\text{P}]}{dt} = k_p[\text{I}] = k_p K_c[\text{A}][\text{B}] = k_{eff}[\text{A}][\text{B}] \tag{19.15}$$

Equation (19.15) demonstrates that with the preequilibrium approximation, the predicted rate law is second order overall and first order with respect to both reactants (A and B). Finally, the rate constant for product formation is not simply $k_p$ but is instead the product of this rate constant with the equilibrium constant, which is in turn equal to the ratio of the forward and backward rate constants.

## 19.2.2 A Preequilibrium Example

The reaction of NO and $O_2$ to form product $NO_2$ provides an example in which the preequilibrium approximation provides insight into the mechanism of $NO_2$ formation. The specific reaction of interest is

$$2\,\text{NO}(g) + \text{O}_2(g) \rightarrow 2\,\text{NO}_2(g) \tag{19.16}$$
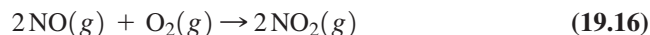
One possible mechanism for this reaction is that of a single elementary step corresponding to a trimolecular reaction of two NO molecules and one $O_2$ molecule. The experimental rate law for this reaction is second order in NO and first order in $O_2$, consistent with this mechanism. However, this mechanism was further evaluated by measuring the temperature dependence of the reaction rate. If correct, raising the temperature will increase the number of collisions, and the reaction rate should increase. However, as the temperature is increased, a *reduction* in the reaction rate is observed, proving that the trimolecular-collisional mechanism is incorrect. An alternative mechanism for this reaction was proposed:

$$2\,\text{NO} \underset{k_r}{\overset{k_f}{\rightleftharpoons}} \text{N}_2\text{O}_2 \tag{19.17}$$

$$\text{N}_2\text{O}_2 + \text{O}_2 \xrightarrow{k_p} 2\,\text{NO}_2 \tag{19.18}$$

In the first step of this mechanism, Equation (19.17), an equilibrium between NO and the dimer $N_2O_2$ is established rapidly compared to the rate of product formation. In the second step, Equation (19.18), a bimolecular reaction involving the dimer and $O_2$ results in the production of the $NO_2$ product. The stoichiometric number for each step is 1. To evaluate this mechanism, the preequilibrium approximation is applied to step 1 of the mechanism, and the concentration of $N_2O_2$ is expressed as

$$[\text{N}_2\text{O}_2] = \frac{k_f}{k_r}[\text{NO}]^2 = K_c[\text{NO}]^2 \tag{19.19}$$

Using the second step of the mechanism, the reaction rate is written as

$$R = \frac{1}{2}\frac{d[\text{NO}_2]}{dt} = k_p[\text{N}_2\text{O}_2][\text{O}_2] \tag{19.20}$$

Substitution of Equation (19.19) into the differential rate expression for [$NO_2$] yields

$$R = k_p[\text{N}_2\text{O}_2][\text{O}_2] = k_p K_c[\text{NO}]^2[\text{O}_2] = k_{eff}[\text{NO}]^2[\text{O}_2] \tag{19.21}$$

The rate law predicted by this mechanism is second order in NO and first order in $O_2$, consistent with experiment. Furthermore, the preequilibrium approximation provides an explanation for the temperature dependence of product formation. Specifically, the formation of $N_2O_2$ is an exothermic process such that an increase in temperature shifts the equilibrium between NO and $N_2O_2$ toward NO. As such, there is less $N_2O_2$ to react with $O_2$ such that the rate of $NO_2$ formation decreases with increased temperature.

# 19.3 The Lindemann Mechanism

The **Lindemann mechanism** for **unimolecular reactions** provides an elegant example of the relationship between kinetics and reaction mechanisms. This mechanism was developed to describe the observed concentration dependence in unimolecular dissociation reactions of the form

$$A \rightarrow fragments \tag{19.22}$$

In this reaction, a reactant molecule undergoes decomposition when the energy content of one or more vibrational modes is sufficient for decomposition to occur. The question is "how does the reactant acquire sufficient energy to undergo decomposition?" One possibility is that the reactant acquires sufficient energy to react through a bimolecular collision. Experimentally, however, the rate of decomposition demonstrates only first-order behavior at high reactant concentrations, and not second order as expected for a single-step bimolecular mechanism. Frederick Lindemann proposed another mechanism to explain the order dependence of the reaction with respect to reactant concentration.

The Lindemann mechanism involves two steps. First, reactants acquire sufficient energy to undergo reaction through a bimolecular collision:

$$A + A \xrightarrow{k_1} A^* + A \tag{19.23}$$
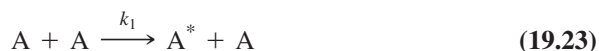
In this reaction, $A^*$ is the "activated" reactant that has received sufficient energy to undergo decomposition. The collisional partner of the activated reactant molecule leaves the collision with insufficient energy to decompose. In the second step of the Lindemann mechanism, the **activated reactant** undergoes one of two reactions: collision resulting in deactivation or decomposition resulting in product formation:

$$A^* + A \xrightarrow{k_{-1}} A + A \tag{19.24}$$

$$A^* \xrightarrow{k_2} P \tag{19.25}$$

The separation of the reaction into two steps is the key conceptual contribution of the Lindemann mechanism. Specifically, the mechanism implies that a separation in timescale exists between activation and deactivation/product formation. Inspection of the mechanism described by Equations (19.24) and (19.25) demonstrates that the only process resulting in product formation is the final decomposition step of Equation (19.25); therefore, the rate of product production is written as

$$\frac{d[P]}{dt} = k_2[A^*] \tag{19.26}$$

Evaluation of Equation (19.26) requires an expression for $[A^*]$ in terms of reactant concentration, $[A]$. Because $A^*$ is an intermediate species, the relationship between $[A^*]$ and $[A]$ is obtained by writing the differential rate expression for $[A^*]$ and applying the steady-state approximation:

$$\frac{d[A^*]}{dt} = k_1[A]^2 - k_{-1}[A][A^*] - k_2[A^*] = 0$$

$$[A^*] = \frac{k_1[A]^2}{(k_{-1}[A] + k_2)} \tag{19.27}$$

Substituting Equation (19.27) into Equation (19.26) results in the final differential rate expression for [P]:

$$\frac{d[P]}{dt} = \frac{k_1 k_2 [A]^2}{k_{-1}[A] + k_2} \tag{19.28}$$

Equation (19.28) is the central result of the Lindemann mechanism. It states that the observed order dependence on [A] depends on the relative magnitude of $k_{-1}[A]$ versus $k_2$. At high reactant concentrations, $k_{-1}[A] > k_2$ and Equation (19.28) reduces to

$$\frac{d[P]}{dt} = \frac{k_1 k_2}{k_{-1}}[A] \tag{19.29}$$

Equation (19.29) demonstrates that at high reactant concentrations or pressures (recall that $P_A/RT = n_A/V = [A]$) the rate of product formation will be first order in [A], consistent with experiment. Mechanistically, at high pressures activated molecules will be produced faster than decomposition occurs such that the rate of decomposition is the rate-limiting step in product formation. At low reactant concentrations $k_2 > k_{-1}[A]$ and Equation (19.28) becomes

$$\frac{d[P]}{dt} = k_1 [A]^2 \tag{19.30}$$

Equation (19.30) demonstrates that at low pressures the formation of activated complex becomes the rate-limiting step in the reaction and the rate of product formation is second order in [A].

The Lindemann mechanism can be generalized to describe a variety of unimolecular reactions through the following generic scheme:

$$A + M \underset{k_{-1}}{\overset{k_1}{\rightleftharpoons}} A^* + M \tag{19.31}$$

$$A^* \xrightarrow{k_2} P \tag{19.32}$$

In this mechanism, M is a collisional partner that can be the reactant itself (A) or some other species such as a nonreactive buffer gas added to the reaction. The rate of product formation can be written as follows:

$$\frac{d[P]}{dt} = \frac{k_1 k_2 [A][M]}{k_{-1}[M] + k_2} = k_{uni}[A] \tag{19.33}$$

In Equation (19.33), $k_{uni}$ is the apparent rate constant for the reaction defined as

$$k_{uni} = \frac{k_1 k_2 [M]}{k_{-1}[M] + k_2} \tag{19.34}$$

In the limit of high M concentrations, $k_{-1}[M] \gg k_2$ and $k_{uni} = k_1 k_2/k_{-1}$, resulting in an apparent rate constant that is independent of [M]. As [M] decreases, $k_{uni}$ will decrease until $k_2 > k_{-1}[M]$, at which point $k_{uni} = k_1[M]$ and the apparent rate demonstrates first-order dependence on M. Figure 19.1 presents a plot of the observed rate constant for the isomerization of methyl isocyanide versus pressure measured at 230.4°C by Schneider and Rabinovitch. The figure demonstrates that the predicted linear relationship between $k_{uni}$ and pressure at low pressure, which is consistent with the corresponding limiting behavior of Equation (19.34), is observed for this reaction. In addition, at high pressure $k_{uni}$ reaches a constant value, which is also consistent with the limiting behavior of Equation (19.34).

The Lindemann mechanism provides a detailed prediction of how the rate constant for a unimolecular reaction will vary with pressure or concentration. Inverting Equation (19.34), the relationship between $k_{uni}$ and reactant concentration becomes

$$\frac{1}{k_{uni}} = \frac{k_{-1}}{k_1 k_2} + \left(\frac{1}{k_1}\right)\frac{1}{[M]} \tag{19.35}$$
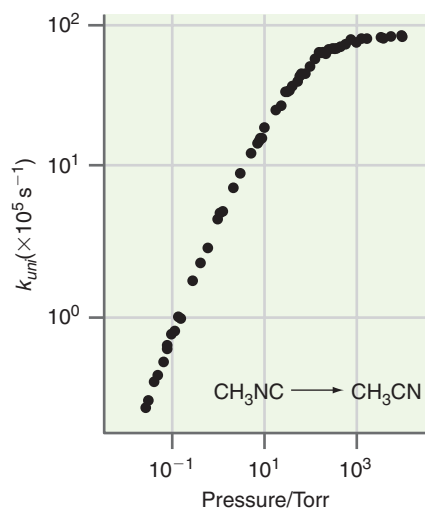


**FIGURE 19.1**
Pressure dependence of the observed rate constant for the unimolecular isomerization of methyl isocyanide.
[Data from Schneider and Rabinovitch, "Thermal Unimolecular Isomerization of Methyl Isocyanide - Fall-Off Behavior," *J. American Chemical Society* 84 (1962): 4225.]
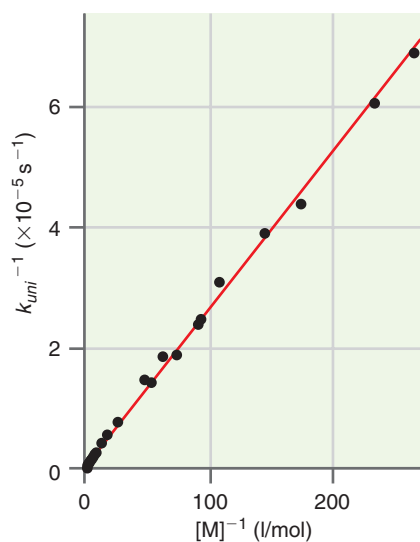


**FIGURE 19.2**
Plot of $k_{uni}^{-1}$ versus $[M]^{-1}$ for the unimolecular isomerization of methyl isocyanide at 230.4°C. The solid line is the best fit to the data.

Equation (19.35) predicts that a plot of $k_{uni}^{-1}$ versus $[M]^{-1}$ should yield a straight line with slope $1/k_1$ and $y$ intercept of $k_{-1}/k_1 k_2$. A plot of the data presented in Figure 19.1 employing Equation (19.35) is presented in Figure 19.2. The figure demonstrates that the expected linear relationship between $k_{uni}^{-1}$ and $[M]^{-1}$ that is observed for this reaction is consistent with the Lindemann mechanism. The solid line in the figure is the best fit to the data by a straight line. The slope of this line provides a value for $k_1$ of $4.16 \times 10^6 \text{ M}^{-1} \text{ s}^{-1}$, and the $y$ intercept in combination with the value for $k_1$ dictates that $k_{-1}/k_2 = 1.76 \times 10^5 \text{ M}^{-1}$.

# 19.4 Catalysis

A **catalyst** is a substance that participates in chemical reactions by increasing the reaction rate, yet the catalyst itself remains intact after the reaction is complete. The general function of a catalyst is to provide an additional mechanism by which reactants are converted to products. The presence of a new reaction mechanism involving the catalyst results in a second reaction coordinate that connects reactants and products. The activation energy along this second reaction coordinate will be lower in comparison to the uncatalyzed reaction; therefore, the overall reaction rate will increase. For example, consider Figure 19.3 in which a reaction involving the conversion of reactant A to product B with and without a catalyst is depicted. In the absence of a catalyst, the rate of product formation is given by rate $= r_0$. In the presence of the catalyst, a second pathway is created, and the reaction rate is now the sum of the original rate plus the rate for the catalyzed reaction, or $r_0 + r_c$.

An analogy for a catalyzed reaction is found in the electrical circuits depicted in Figure 19.3. In the "catalyzed" electrical circuit, a second, parallel pathway for current flow has been added, allowing for increased total current when compared to the "uncatalyzed" circuit. By analogy, the addition of the second, parallel pathway is equivalent to the alternative reaction mechanism involving the catalyst.

To be effective, a catalyst must combine with one or more of the reactants or with an intermediate species involved in the reaction. After the reaction has taken place, the catalyst is freed and can combine with another reactant or intermediate in a subsequent reaction. The catalyst is not consumed during the reaction, so a small amount of catalyst can participate in numerous reactions. The simplest mechanism describing a catalytic process is as follows:

$$\text{S} + \text{C} \underset{k_{-1}}{\overset{k_1}{\rightleftharpoons}} \text{SC} \tag{19.36}$$

$$\text{SC} \overset{k_2}{\longrightarrow} \text{P} + \text{C} \tag{19.37}$$
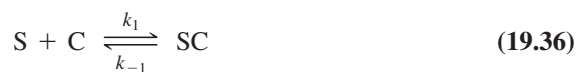
where S represents the reactant or substrate, C is the catalyst, and P is the product. The **substrate–catalyst complex** is represented by SC and is an intermediate species in this mechanism. The differential rate expression for product formation is

$$\frac{d[\text{P}]}{dt} = k_2[\text{SC}] \tag{19.38}$$

Given that SC is an intermediate, we write the differential rate expression for this species and apply the steady-state approximation:

$$\frac{d[\text{SC}]}{dt} = k_1[\text{S}][\text{C}] - k_{-1}[\text{SC}] - k_2[\text{SC}] = 0$$

$$[\text{SC}] = \frac{k_1[\text{S}][\text{C}]}{k_{-1} + k_2} = \frac{[\text{S}][\text{C}]}{K_m} \tag{19.39}$$

In Equation (19.39), $K_m$ is referred to as the **composite constant** and is defined as

$$K_m = \frac{k_{-1} + k_2}{k_1} \tag{19.40}$$
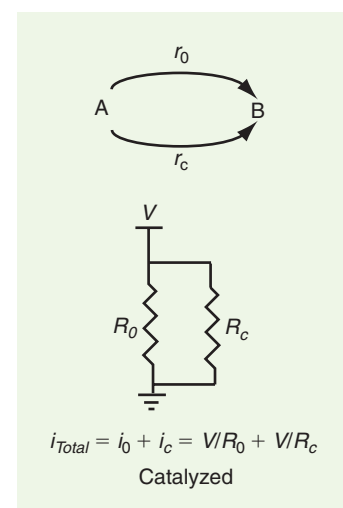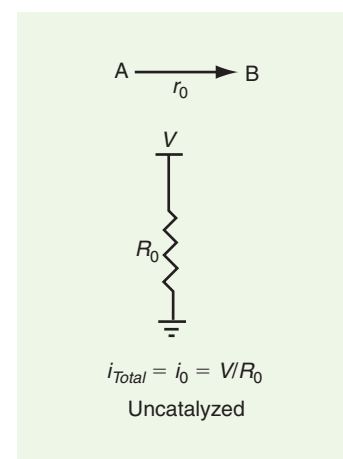


**FIGURE 19.3**
Illustration of catalysis. In the uncatalyzed reaction, the rate of reaction is given by $r_0$. In the catalyzed case, a new pathway is created by the presence of the catalyst with corresponding rate $r_c$. The total rate of reaction for the catalyzed case is $r_0 + r_c$. The analogous electrical circuits are also presented for comparison.

Substituting the expression for [SC] into Equation (19.38), the rate of product formation becomes

$$\frac{d[P]}{dt} = \frac{k_2[S][C]}{K_m} \tag{19.41}$$

Equation (19.41) illustrates that the rate of product formation is expected to increase linearly with both substrate and catalyst concentrations. This equation is difficult to evaluate over the entire course of the reaction because the concentrations of substrate and catalyst given in Equation (19.41) correspond to species not in the SC complex, and these concentrations can be quite difficult to measure. A more convenient measurement is to determine how much substrate and catalyst are present at the beginning of the reaction. Conservation of mass dictates the following relationship between these initial concentrations and the concentrations of all species present after the reaction is initiated:

$$[S]_0 = [S] + [SC] + [P] \tag{19.42}$$

$$[C]_0 = [C] + [SC] \tag{19.43}$$

Rearrangement of Equations (19.42) and (19.43) yields the following definitions for [S] and [C]:

$$[S] = [S]_0 - [SC] - [P] \tag{19.44}$$

$$[C] = [C]_0 - [SC] \tag{19.45}$$

Substituting these expressions into Equation (19.39) yields

$$K_m[SC] = [S][C] = ([S]_0 - [SC] - [P])([C]_0 - [SC])$$

$$0 = [[C]_0([S]_0 - [P])] - [SC]([S]_0 + [C]_0 - [P] + K_m) + [SC]^2 \tag{19.46}$$

Equation (19.46) can be evaluated as a quadratic equation to determine [SC]. However, two assumptions are generally employed at this point to simplify matters. First, through control of the initial substrate and catalyst concentrations, conditions can be employed such that [SC] is small. Therefore, the $[SC]^2$ term in Equation (19.46) can be neglected. Second, we confine ourselves to early stages of the reaction when little product has been formed; therefore, terms involving [P] can also be neglected. With these two approximations, Equation (19.46) is readily evaluated, providing the following expression for [SC]:

$$[SC] = \frac{[S]_0[C]_0}{[S]_0 + [C]_0 + K_m} \tag{19.47}$$

Substituting Equation (19.47) into Equation (19.38), the rate of the reaction becomes

$$R_0 = \frac{d[P]}{dt} = \frac{k_2[S]_0[C]_0}{[S]_0 + [C]_0 + K_m} \tag{19.48}$$

In Equation (19.48), the subscript on the rate indicates that this expression applies to the early-time or initial reaction rate. We next consider two limiting cases of Equation (19.48).

### 19.4.1 Case 1: [C]$_0$ ≪ [S]$_0$

The most common case in catalysis is when there is much more substrate present in comparison to catalyst. In this limit $[C]_0$ can be neglected in the denominator of Equation (19.48) and the rate becomes

$$R_0 = \frac{k_2[S]_0[C]_0}{[S]_0 + K_m} \tag{19.49}$$

For substrate concentrations where $[S]_0 < K_m$, the reaction rate should increase linearly with substrate concentration, with a slope equal to $k_2[C]_0/K_m$. Parameters such as $k_2$ and $K_m$ can be obtained by comparing experimental reaction rates to Equation (19.49). An alternative approach to determining these parameters is to invert Equation (19.49) to obtain the following relationship between the reaction rate and initial substrate concentration:

$$\frac{1}{R_0} = \left(\frac{K_m}{k_2[C]_0}\right)\frac{1}{[S]_0} + \frac{1}{k_2[C]_0} \tag{19.50}$$

Equation (19.50) demonstrates that a plot of the inverse of the initial reaction rate versus $[S]_0^{-1}$, referred to as a **reciprocal plot,** should yield a straight line. The $y$ intercept and slope of this line provide a measure of $K_m$ and $k_2$, assuming $[C]_0$ is known.

At elevated concentrations of substrate where $[S]_0 \gg K_m$, the denominator in Equation (19.49) can be approximated as $[S]_0$, resulting in the following expression for the reaction rate:

$$R_0 = k_2[C]_0 = R_{max} \tag{19.51}$$

In other words, the rate of reaction will reach a limiting value where the rate becomes zero order in substrate concentration. In this limit, the reaction rate can only be enhanced by increasing the amount of catalyst. An illustration of the variation in the reaction rate with initial substrate concentration predicted by Equations (19.49) and (19.50) is provided in Figure 19.4.

### 19.4.2 Case 2: $[C]_0 \gg [S]_0$

In this limit Equation (19.48) becomes

$$R_0 = \frac{k_2[S]_0[C]_0}{[C]_0 + K_m} \tag{19.52}$$

In this concentration limit, the reaction rate is first order in $[S]_0$ but can be first or zero order in $[C]_0$ depending on the magnitude of $[C]_0$ relative to $K_m$. In catalysis studies, this limit is generally avoided because the insight to be gained regarding the rate constants for the various reaction steps are more easily evaluated for the previously discussed Case 1. In addition, good catalysts can be expensive; therefore, employing excess catalyst in a reaction is not cost effective.

### 19.4.3 Michaelis–Menten Enzyme Kinetics

**Enzymes** are protein molecules that serve as catalysts in a wide variety of chemical reactions. Enzymes are noted for their reaction specificity, with nature having developed specific catalysts to facilitate the vast majority of biological reactions required for organism survival. An illustration enzyme with associated substrate is presented in Figure 19.5. The figure presents a space-filling model derived from a crystal structure of phospholipase $A_2$ (white) containing a bound substrate analogue (red). This enzyme catalyzes the hydrolysis of esters in phospholipids. The substrate analogue contains a stable phosphonate group in place of the enzyme-susceptible ester. The substrate analogue is resistant to enzymatic hydrolysis so that it does not suffer chemical breakdown during the structure determination process. With reactive substrate, ester hydrolysis occurs and the products of the reaction are released from the enzyme, resulting in regeneration of the free enzyme.

The kinetic mechanism of phospholipase $A_2$ catalysis can be described using the **Michaelis–Menten mechanism** of enzyme activity illustrated in Figure 19.6. The figure depicts the "lock-and-key" model for enzyme reactivity in which the substrate is bound to the active site of the enzyme where the reaction is catalyzed. The enzyme and substrate form the enzyme–substrate complex, which dissociates into product and uncomplexed enzyme. The interactions involved in creation of the enzyme–substrate
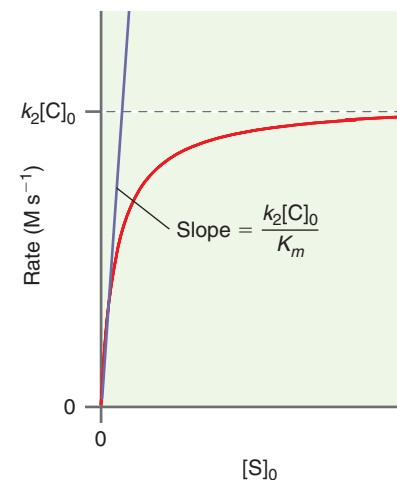


(a)
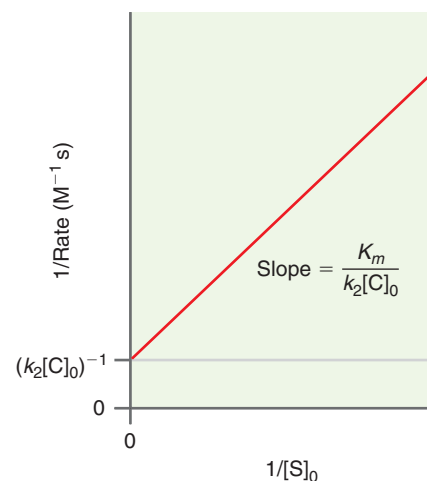


(b)

**FIGURE 19.4**
Illustration of the variation in the reaction rate with substrate concentration under Case 1 conditions as described in the text. **(a)** Plot of the initial reaction rate with respect to substrate concentration [Equation (19.49)]. At low substrate concentrations, the reaction rate increases linearly with substrate concentration. At high substrate concentrations, a maximum reaction rate of $k_2[C]_0$ is reached. **(b)** Reciprocal plot where the inverse of the reaction rate is plotted with respect to the inverse of substrate concentration [Equation (19.50)]. The $y$ intercept of this line is equal to the inverse of the maximum reaction rate, or $(k_2[C]_0)^{-1}$. The slope of the line is equal to $K_m(k_2[C]_0)^{-1}$; therefore, with the slope and $y$ intercept, $K_m$ can be determined.

complex are enzyme specific. For example, the active site may bind the substrate in more than one location, thereby creating geometric strain that promotes product formation. The enzyme may orient the substrate so that the reaction geometry is optimized. In summary, the details of enzyme-mediated chemistry are highly dependent on the reaction of interest. Rather than an exhaustive presentation of enzyme kinetics, our motivation here is to describe enzyme kinetics within the general framework of catalyzed reactions.

A schematic description of the mechanism illustrated in Figure 19.6 is as follows:

$$E + S \underset{k_{-1}}{\overset{k_1}{\rightleftharpoons}} ES \overset{k_2}{\longrightarrow} E + P \tag{19.53}$$
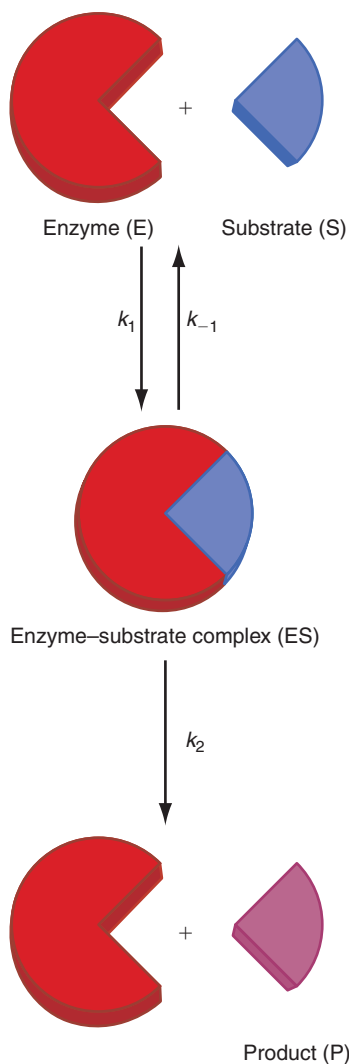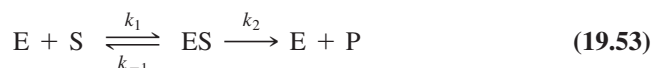
In this mechanism, E is enzyme, S is substrate, ES is the complex, and P is product. Comparison of the mechanism of Equation (19.53) to the general catalytic mechanism described earlier in Equations (19.36) and (19.37) demonstrates that this mechanism is identical to the general catalysis mechanism except that the catalyst C is now the enzyme E. In the limit where the initial substrate concentration is substantially greater than that of the enzyme ($[S]_0 \gg [E]_0$ or Case 1 conditions as described previously), the rate of product formation is given by

$$R_0 = \frac{k_2[S]_0[E]_0}{[S]_0 + K_m} \tag{19.54}$$

In enzyme kinetics the composite constant $K_m$ in Equation (19.54) is referred to as the **Michaelis constant** in enzyme kinetics, and Equation (19.54) is referred to as the **Michaelis–Menten rate law.** When $[S]_0 \gg K_m$, the Michaelis constant can be neglected, resulting in the following expression for the rate:

$$R_0 = k_2[E]_0 = R_{max} \tag{19.55}$$

Equation (19.55) demonstrates that the rate of product formation will plateau at some maximum value equal to the product of initial enzyme concentration and $k_2$, the rate constant for product formation, consistent with the behavior depicted in Figure 19.4. A reciprocal plot of the reaction rate can also be constructed by inverting Equation (19.54), which results in the **Lineweaver–Burk equation:**

$$\frac{1}{R_0} = \frac{1}{R_{max}} + \frac{K_m}{R_{max}} \frac{1}{[S]_0} \tag{19.56}$$

For the Michaelis–Menten mechanism to be consistent with experiment, a plot of the inverse of the initial rate with respect to $[S]_0^{-1}$ should yield a straight line from which the $y$ intercept and slope can be used to determine the maximum reaction rate and the Michaelis constant. This reciprocal plot is referred to as the **Lineweaver–Burk plot.** In addition, because $[E]_0$ is readily determined experimentally, the maximum rate can be used to determine $k_2$, referred to as the **turnover number** of the enzyme [Equation (19.55)]. The turnover number can be thought of as the maximum number of



Enzyme (E)        Substrate (S)

$k_1$    $k_{-1}$

Enzyme–substrate complex (ES)

$k_2$

Product (P)

**FIGURE 19.6**
Schematic of enzyme catalysis.

substrate molecules per unit time that can be converted into product. Most enzymes demonstrate turnover numbers between 1 and $10^5 \text{ s}^{-1}$ under physiological conditions.

### EXAMPLE PROBLEM 19.1

DeVoe and Kistiakowsky [*J. American Chemical Society* 83 (1961): 274] studied the kinetics of $CO_2$ hydration catalyzed by the enzyme carbonic anhydrase:

$$CO_2 + H_2O \Longrightarrow HCO_3^- + H^+$$
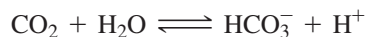
In this reaction, $CO_2$ is converted to bicarbonate ion. Bicarbonate is transported in the bloodstream and converted back to $CO_2$ in the lungs, a reaction that is also catalyzed by carbonic anhydrase. The following initial reaction rates for the hydration reaction were obtained for an initial enzyme concentration of 2.3 nM and temperature of 0.5°C:

| Rate (M s$^{-1}$) | [CO$_2$] (mM) |
|---|---|
| $2.78 \times 10^{-5}$ | 1.25 |
| $5.00 \times 10^{-5}$ | 2.5 |
| $8.33 \times 10^{-5}$ | 5.0 |
| $1.67 \times 10^{-4}$ | 20.0 |

Determine $K_m$ and $k_2$ for the enzyme at this temperature.

### Solution

The Lineweaver–Burk plot of the rate$^{-1}$ versus $[CO_2]^{-1}$ is shown here:
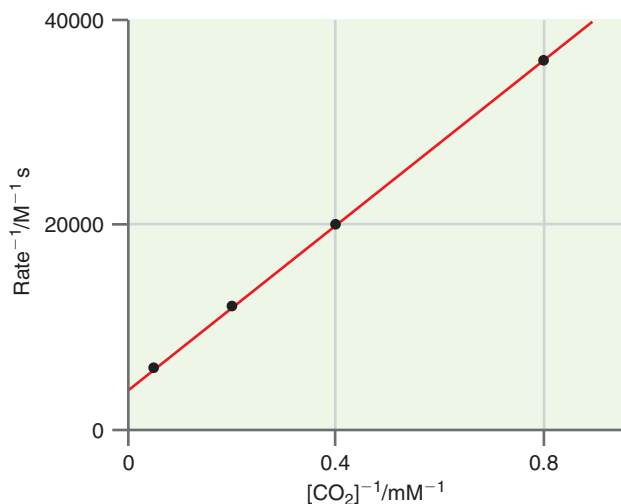


The $y$ intercept for the best fit line to the data is 4000 M$^{-1}$ s corresponding to $R_{max} = 2.5 \times 10^{-4}$ M s$^{-1}$. Using this value and $[E]_0 = 2.3$ nM, $k_2$ is

$$k_2 = \frac{R_{max}}{[E]_0} = \frac{2.5 \times 10^{-4} \text{ M s}^{-1}}{2.3 \times 10^{-9} \text{ M}} = 1.1 \times 10^5 \text{ s}^{-1}$$

Notice that the units of $k_2$, the turnover number, are consistent with a first-order process, in agreement with the Michaelis–Menten mechanism. The slope of the best fit line is 40 s such that, per Equation (19.56), $K_m$ is given by

$$K_m = slope \times R_{max} = (40 \text{ s})(2.5 \times 10^{-4} \text{ M s}^{-1})$$

$$= 10 \text{ mM}$$

In addition to the Lineweaver–Burk plot, $K_m$ can be estimated if the maximum rate is known. Specifically, if the initial rate is equal to one-half the maximum rate, Equation (19.54) reduces to

$$R_0 = \frac{k_2[S]_0[E]_0}{[S]_0 + K_m} = \frac{R_{max}[S]_0}{[S]_0 + K_m}$$

$$\frac{R_{max}}{2} = \frac{R_{max}[S]_0}{[S]_0 + K_m}$$

$$[S]_0 + K_m = 2[S]_0$$

$$K_m = [S]_0 \qquad (19.57)$$

Equation (19.57) demonstrates that when the initial rate is half the maximum rate, $K_m$ is equal to the initial substrate concentration. Therefore, $K_m$ can be determined by viewing a substrate saturation curve, as illustrated in Figure 19.7 for the carbonic-anhydrase catalyzed hydration of $CO_2$ discussed in Example Problem 19.1. The figure demonstrates that the initial rate is equal to half the maximum rate when $[S]_0 = 10$ mM. Therefore, the value of $K_m$ determined in this relatively simple approach is in excellent agreement with that determined from the Lineweaver–Burk plot. Notice in Figure 19.7 that the maximum rate depicted was that employed using the Lineweaver–Burk analysis as shown in the example problem. When employing this method to determine $K_m$, the high-substrate-concentration limit must be carefully explored to ensure that the reaction rate is indeed at a maximum.

### 19.4.4 Competitive Inhibition in Enzyme Catalysis

The activity of an enzyme can be affected by the introduction of species that structurally resemble the substrate and that can occupy the enzyme active site; however, once bound to the active site the molecules are nonreactive. Such molecules are referred to as **competitive inhibitors.** The phosphonated substrate bound to phospholipase $A_2$ in Figure 19.5 is an example of a competitive inhibitor. Competitive inhibition can be described using the following mechanism:

$$E + S \underset{k_{-1}}{\overset{k_1}{\rightleftharpoons}} ES \qquad (19.58)$$

$$ES \xrightarrow{k_2} E + P \qquad (19.59)$$

$$E + I \underset{k_{-3}}{\overset{k_3}{\rightleftharpoons}} EI \qquad (19.60)$$

In this mechanism, I is the inhibitor, EI is the enzyme–inhibitor complex, and the other species are identical to those employed in the standard enzyme kinetic scheme of Equation (19.53). How does the rate of reaction differ from the noninhibited case discussed earlier? To answer this question, we first define the initial enzyme concentration:

$$[E]_0 = [E] + [EI] + [ES] \qquad (19.61)$$
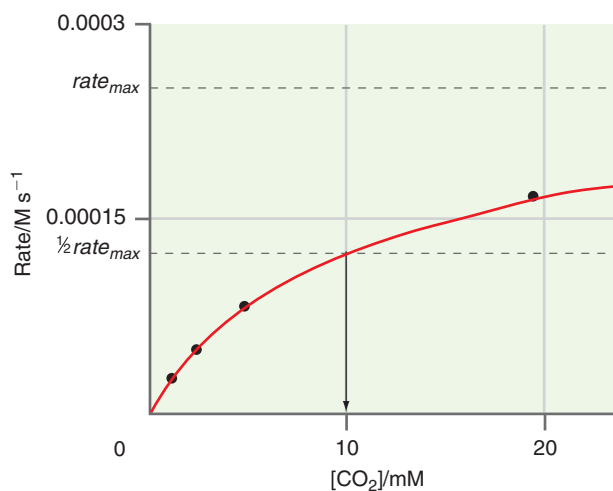


**FIGURE 19.7**

Determination of $K_m$ for the carbonic-anhydrase catalyzed hydration of $CO_2$. The substrate concentration at which the rate of reaction is equal to half that of the maximum rate is equal to $K_m$.

Next, assuming that $k_1$, $k_{-1}$, $k_3$, and $k_{-3} \gg k_2$ the preequilibrium approximation is applied using Equations (19.58) and (19.60), yielding

$$K_s = \frac{[E][S]}{[ES]} \approx K_m \qquad (19.62)$$

$$K_i = \frac{[E][I]}{[EI]} \qquad (19.63)$$

In Equation (19.62), the constant describing the enzyme and substrate is written as $K_m$ (Equation 19.40) when $k_{-1} \gg k_2$. With these relationships, Equation (19.61) can be written as

$$[E]_0 = \frac{K_m[ES]}{[S]} + \frac{[E][I]}{K_i} + [ES]$$

$$= \frac{K_m[ES]}{[S]} + \left(\frac{K_m[ES]}{[S]}\right)\frac{[I]}{K_i} + [ES]$$

$$= [ES]\left(\frac{K_m}{[S]} + \frac{K_m[I]}{[S]K_i} + 1\right) \qquad (19.64)$$

Solving Equation (19.64) for [ES] yields

$$[ES] = \frac{[E]_0}{1 + \dfrac{K_m}{[S]} + \dfrac{K_m[I]}{[S]K_i}} \qquad (19.65)$$

Finally, the rate of product formation is given by

$$R = \frac{d[P]}{dt} = k_2[ES] = \frac{k_2[E]_0}{1 + \dfrac{K_m}{[S]} + \dfrac{K_m[I]}{[S]K_i}} = \frac{k_2[S][E]_0}{[S] + K_m\left(1 + \dfrac{[I]}{K_i}\right)}$$

$$R \cong \frac{k_2[S]_0[E]_0}{[S]_0 + K_m\left(1 + \dfrac{[I]}{K_i}\right)} \qquad (19.66)$$

In Equation (19.66), the assumption that [ES] and [P] $\ll$ [S] has been employed so that $[S] \cong [S]_0$, consistent with the previous treatment of uninhibited catalysis. Comparison of Equation (19.66) to the corresponding expression for the uninhibited case of Equation (19.54) illustrates that with competitive inhibition, a new apparent Michaelis constant can be defined:

$$K_m^* = K_m\left(1 + \frac{[I]}{K_i}\right) \qquad (19.67)$$

Notice that $K_m^*$ reduces to $K_m$ in the absence of inhibitor ([I] = 0). Next, using the definition of maximum reaction rate defined earlier in Equation (19.55), the reaction rate in the case of competitive inhibition can be written as

$$R_0 \cong \frac{R_{max}[S]_0}{[S]_0 + K_m^*} \qquad (19.68)$$

In the presence of inhibitor, $K_m^* \geq K_m$, and more substrate is required to reach half the maximum rate in comparison to the uninhibited case. The effect of inhibition can also be observed in a Lineweaver–Burk plot of the following form:

$$\frac{1}{R_0} = \frac{1}{R_{max}} + \frac{K_m^*}{R_{max}}\frac{1}{[S]_0} \qquad (19.69)$$

Because $K_m^* > K_m$, the slope of the Lineweaver–Burk plot will be greater with inhibitor compared to the slope without inhibitor. Figure 19.8 presents an illustration of this effect.

(a)

(b)
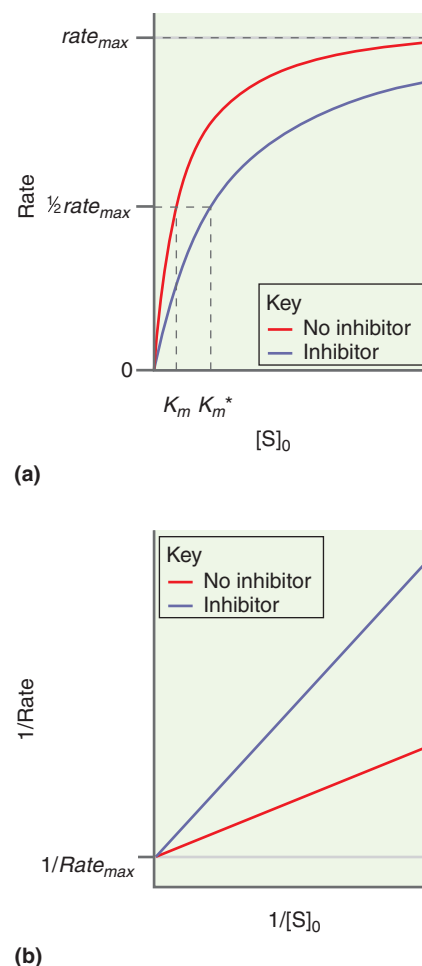
**FIGURE 19.8**
Comparison of enzymatic reaction rates in the presence and absence of a competitive inhibitor. **(a)** Plot of rate versus initial substrate concentration. The location of $K_m$ and $K_m^*$ is indicated. **(b)** Reciprocal plots ($1/R$ versus $1/[S]_0$). Notice that $1/R_{max}$ is identical in the presence and absence of a competitive inhibitor.

NH$_2$

SO$_2$

NH$_2$

**Sulfanilamide**

NH$_2$

CO$_2$H

**p-Aminobenzoic acid**
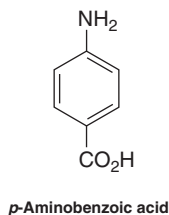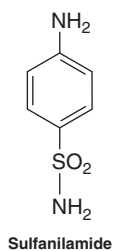
Competitive inhibition has been used in drug design for antiviral, antibacterial, and antitumor applications. Many drugs are molecules that serve as competitive inhibitors for enzymes required for viral, bacterial, or cellular replication. For example sulfanilamide (Figure 19.9) is a powerful antibacterial drug. This compound is similar to p-aminobenzoic acid, the substrate for the enzyme dihydropteroate synthetase that participates in the production of folate. When present, the enzyme in bacteria cannot produce folate, and the bacteria die. However, humans do not possess this enzyme; they obtain folate from other sources. Therefore, sulfanilamide is not toxic.

### 19.4.5 Homogeneous and Heterogeneous Catalysis

A **homogeneous catalyst** is a catalyst that exists in the same phase as the species involved in the reaction, and a **heterogeneous catalyst** exists in a different phase. Enzymes serve as an example of a homogeneous catalyst; they exist in solution and catalyze reactions that occur in solution. A famous example of gas-phase catalysis is the catalytic depletion of stratospheric ozone by atomic chlorine. In the mid-1970s, F. Sherwood Rowland and Mario Molina proposed that Cl atoms catalyze the decomposition of stratospheric ozone by the following mechanism:

$$Cl + O_3 \xrightarrow{k_1} ClO + O_2 \tag{19.70}$$

$$\underline{ClO + O \xrightarrow{k_2} Cl + O_2} \tag{19.71}$$

$$O_3 + O \rightarrow 2\,O_2 \tag{19.72}$$

In this mechanism, Cl reacts with ozone to produce chlorine monoxide (ClO) and molecular oxygen. The ClO undergoes a second reaction with atomic oxygen, largely formed by O$_3$ photolysis, resulting in the reformation of Cl and the product of O$_2$. The sum of these reactions leads to the net conversion of O$_3$ and O to 2 O$_2$. Notice that the Cl is not consumed in the net reaction.

The catalytic efficiency of Cl can be determined using standard techniques in kinetics. The experimentally determined rate law expression for the uncatalyzed reaction of Equation (19.72) is

$$R_{nc} = k_{nc}[O][O_3] \tag{19.73}$$

The stratospheric temperature where this reaction occurs is roughly 220 K, at which temperature $k_{nc}$ has a value of $3.30 \times 10^5\,M^{-1}\,s^{-1}$. For the Cl catalyzed decomposition of ozone, the rate constants at this temperature are $k_1 = 1.56 \times 10^{10}\,M^{-1}\,s^{-1}$ and $k_2 = 2.44 \times 10^{10}\,M^{-1}\,s^{-1}$. To employ these rates in determining the overall rate of reaction, the rate law expression for the catalytic mechanism must be determined. Notice that both Cl and ClO are intermediates in this mechanism. Applying the steady-state approximation, the concentration of intermediates is taken to be a constant such that

$$[Cl]_{total} = [Cl] + [ClO] \tag{19.74}$$

where $[Cl]_{total}$ is defined as the sum of reaction intermediate concentrations, a definition that will prove useful in deriving the rate law. In addition, the steady-state approximation is applied in evaluating the differential rate expression for [Cl] as follows:

$$\frac{d[Cl]}{dt} = 0 = -k_1[Cl][O_3] + k_2[ClO][O]$$

$$k_1[Cl][O_3] = k_2[ClO][O]$$

$$\frac{k_1[Cl][O_3]}{k_2[O]} = [ClO] \tag{19.75}$$

Substituting Equation (19.75) into Equation (19.74) yields the following expression for [Cl]:

$$[\text{Cl}] = \frac{k_2[\text{Cl}]_{total}[\text{O}]}{k_1[\text{O}_3] + k_2[\text{O}]} \tag{19.76}$$

Using Equation (19.76), the rate law expression for the catalytic mechanism is determined as follows:

$$R_{cat} = -\frac{d[\text{O}_3]}{dt} = k_1[\text{Cl}][\text{O}_3] = \frac{k_1 k_2[\text{Cl}]_{total}[\text{O}][\text{O}_3]}{k_1[\text{O}_3] + k_2[\text{O}]} \tag{19.77}$$

The composition of the stratosphere is such that $[\text{O}_3] \gg [\text{O}]$. Taken in combination with the numerical values for $k_1$ and $k_2$ presented earlier, the $k_2[\text{O}]$ term in the denominator of Equation (19.77) can be neglected, and the rate law expression for the catalyzed reaction becomes

$$R_{cat} = k_2[\text{Cl}]_{total}[\text{O}] \tag{19.78}$$

The ratio of catalyzed to uncatalyzed reaction rates is

$$\frac{R_{cat}}{R_{uc}} = \frac{k_2[\text{Cl}]_{total}}{k_{nc}[\text{O}_3]} \tag{19.79}$$

In the stratosphere $[\text{O}_3]$ is roughly $10^3$ greater than $[\text{Cl}]_{total}$, and Equation (19.79) becomes

$$\frac{R_{cat}}{R_{uc}} = \frac{k_2}{k_{nc}} \times 10^{-3} = \frac{2.44 \times 10^{10} \, \text{M}^{-1}\text{s}^{-1}}{3.30 \times 10^5 \, \text{M}^{-1}\text{s}^{-1}} \times 10^{-3} \approx 74$$

Therefore, through Cl-mediated catalysis, the rate of $O_3$ loss is roughly two orders of magnitude greater than the loss through the bimolecular reaction of $O_3$ and O directly.

Where does stratospheric Cl come from? Rowland and Molina proposed that a major source of Cl was from the photolysis of chlorofluorocarbons such as $CFCl_3$ and $CF_2Cl_2$, anthropogenic compounds that were common refrigerants at the time. These molecules are extremely robust, and when released into the atmosphere, they readily survive transport through the troposphere and into the stratosphere. Once in the stratosphere, these molecules can absorb a photon of light with sufficient energy to dissociate the C—Cl bond, and Cl is produced. This proposal served as the impetus to understand the details of stratospheric ozone depletion, and it led to the Montreal Protocol in which the vast majority of nations agreed to phase out the industrial use of chlorofluorocarbons.

Heterogeneous catalysts are extremely important in industrial chemistry. The majority of industrial catalysts are solids. For example, the synthesis of $NH_3$ from reactants $N_2$ and $H_2$ is catalyzed using Fe. This is an example of heterogeneous catalysis because the reactants and product are in the gas phase, but the catalyst is a solid. An important step in reactions involving solid catalysis is the adsorption of one or more of the reactants to the solid surface. First, we assume that the particles adsorb to the surface without changing their internal bonding, a process referred to as **physisorption.** A dynamic equilibrium exists between the free and surface-adsorbed species or adsorbate, and information regarding the kinetics of surface adsorption and desorption can be obtained by studying this equilibrium as a function of reactant pressure over the surface of the catalyst. A critical parameter in evaluating surface adsorption is the **fractional coverage** $\theta$ defined as

$$\theta = \frac{\text{Number of adsorption sites occupied}}{\text{Total number of adsorption sites}}$$

Figure 19.10 provides an illustration of a surface with a series of adsorption sites. Reactant molecules (given by the blue spheres) can exist in either the gas phase or be adsorbed to one of these sites. The fractional coverage is simply the fraction of adsorption sites occupied.

The fractional coverage can also be defined as $\theta = V_{adsorbed}/V_m$ where $V_{adsorbed}$ is the volume of adsorbate at a specific pressure and $V_m$ is the volume of adsorbate in the high-pressure limit corresponding to monolayer coverage.
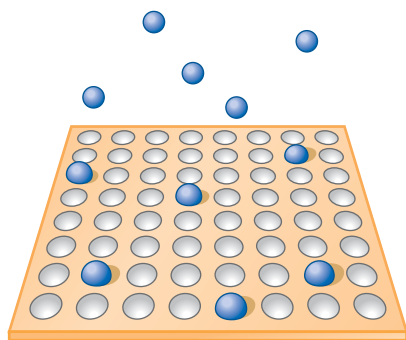
**FIGURE 19.10**
Illustration of fractional coverage $\theta$. The surface (orange parallelogram) contains a series of adsorption sites (white circles). The reactant (blue spheres) exists in an equilibrium between free reactants and adsorbates. The fractional coverage is the number of occupied adsorption sites divided by the total number of sites on the surface.

Studies of adsorption involve measuring the extent of adsorption or $\theta$ as a function of reactant-gas pressure at a specific temperature. The variation in $\theta$ with pressure at fixed temperature is called an **adsorption isotherm.** The simplest kinetic model describing the adsorption process is known as the **Langmuir model,** where adsorption is described by the following mechanism:

$$R(g) + M\ (surface) \underset{k_d}{\overset{k_a}{\rightleftharpoons}} RM\ (surface) \tag{19.80}$$

In Equation (19.80), R is reagent, M (surface) is an unoccupied adsorption site on the surface of the catalyst, RM (surface) is an occupied adsorption site, $k_a$ is the rate constant for adsorption, and $k_d$ is the rate constant for desorption. Three approximations are employed in the Langmuir model:

1. Adsorption is complete once monolayer coverage has been reached.
2. All adsorption sites are equivalent, and the surface is uniform.
3. Adsorption and desorption are uncooperative processes. The occupancy state of the adsorption site will not affect the probability of adsorption or desorption for adjacent sites.

With these approximations, the rate of change in $\theta$ will depend on the rate constant for adsorption $k_a$, reagent pressure $P$, and the number of vacant sites, which is equal to $N(1 - \theta)$ or the total number of adsorption sites $N$ times the fraction of sites that are open $(1 - \theta)$:

$$\left(\frac{d\theta}{dt}\right)_{abs} = k_a PN(1 - \theta) \tag{19.81}$$

The corresponding change in $\theta$ due to desorption is related to the rate constant for desorption $k_d$ and the number of occupied adsorption sites $N\theta$ as follows:

$$\left(\frac{d\theta}{dt}\right)_{des} = -k_d N\theta \tag{19.82}$$

At equilibrium, the change in fractional coverage with time is equal to zero so we can write

$$\frac{d\theta}{dt} = 0 = k_a PN(1 - \theta) - k_d N\theta$$

$$(k_a PN + k_d N)\theta = k_a PN$$

$$\theta = \frac{k_a P}{k_a P + k_d}$$

$$\theta = \frac{KP}{KP + 1} \tag{19.83}$$

where $K$ is the equilibrium constant defined as $k_a/k_d$. Equation (19.83) is the equation for the **Langmuir isotherm.** Figure 19.11 presents Langmuir isotherms for various values of $k_a/k_d$. Notice that as the rate constant for desorption increases relative to adsorption, higher pressures must be employed to reach $\theta = 1$, and this behavior can be understood based on the competition between the kinetics for adsorption and desorption. Correspondingly, if the rate constant for desorption is small, the coverage becomes independent of pressure for lower values of pressure.

In many instances adsorption is accompanied by dissociation of the adsorbate, a process that is referred to as **chemisorption** and described by the following mechanism:

$$R_2(g) + 2M\ (surface) \underset{k_d}{\overset{k_a}{\rightleftharpoons}} 2RM\ (surface)$$
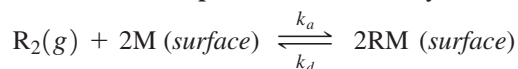
Kinetic analysis of this mechanism (see the end-of-chapter problems) yields the following expression for $\theta$:

$$\theta = \frac{(KP)^{1/2}}{1 + (KP)^{1/2}} \tag{19.84}$$



**FIGURE 19.11**
Langmuir isotherms for a range of $k_a/k_d$.

Inspection of Equation (19.84) reveals that the extent of surface coverage should demonstrate weaker pressure dependence compared to physisorption. Figure 19.12 provides a

comparison of the isotherms predicted using nondissociative and dissociative mechanisms corresponding to the same ratio of $k_a/k_d$. Finally, different Langmuir isotherms can be collected and evaluated over a range of temperatures to determine $K$ as a function of $T$. With this information, a van't Hoff plot of $\ln K$ versus $1/T$ should provide a straight line of slope $-\Delta H_{ads}/R$. Through this analysis, the enthalpy of adsorption $\Delta H_{ads}$ can be determined.

The assumptions employed in the Langmuir model may not be rigorously obeyed in real heterogeneous systems. First, surfaces are generally not uniform, resulting in the presence of more than one type of adsorption site. Second, the rate of adsorption and desorption may depend on the occupation state of nearby adsorption sites. Finally, it has been established that adsorbed molecules can diffuse on the surface and then adsorb corresponding to a kinetic process of adsorption that is more complicated than the Langmuir mechanism envisions.



**FIGURE 19.12**
Comparison of Langmuir isotherms for nondissociative and dissociative adsorption with $k_a/k_d = 0.5$ atm$^{-1}$.

### EXAMPLE PROBLEM 19.2

The following data were obtained for the adsorption of Kr on charcoal at 193.5 K. Using the Langmuir model, construct the adsorption isotherm, and determine $V_m$ and the equilibrium constant for adsorption/desorption.

| $V_{ads}$ (cm$^3$ g$^{-1}$) | $P$ (Torr) |
|---|---|
| 5.98 | 2.45 |
| 7.76 | 3.5 |
| 10.1 | 5.2 |
| 12.35 | 7.2 |
| 16.45 | 11.2 |
| 18.05 | 12.8 |
| 19.72 | 14.6 |
| 21.1 | 16.1 |

### Solution

The fractional coverage is related to the experimentally measured $V_{ads}$. The adsorption isotherm is given by a plot of $V_{ads}$ versus $P$, which can be compared to the behavior predicted by Equation (19.83) as illustrated here:



Although the comparison of the adsorption isotherm to Equation (19.83) illustrates that the Langmuir model is consistent with the adsorption of Kr on charcoal, determination of the Langmuir parameters is difficult because parameters such as $V_m$ are unknown. This information is more readily determined by using the reciprocal of Equation (19.83):

$$\frac{1}{V_{ads}} = \left(\frac{1}{KV_m}\right)\frac{1}{P} + \frac{1}{V_m}$$

This equation demonstrates that a plot of $(V_{ads})^{-1}$ versus $(P)^{-1}$ should yield a straight line with slope equal to $(KV_m)^{-1}$ and $y$ intercept equal to $(V_m)^{-1}$. A plot of the data in reciprocal form with the best fit line is shown next:
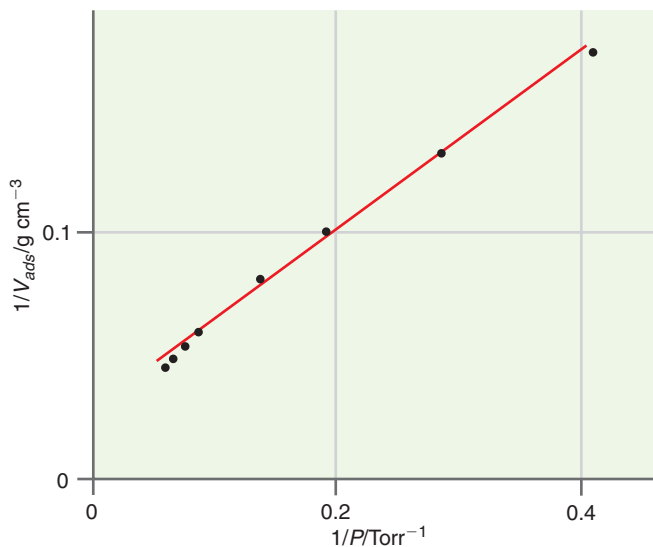


The $y$ intercept obtained from the best fit line is 0.0293 g cm$^{-3}$ such that $V_m = 34.1$ cm$^3$ g$^{-1}$. The slope of the best fit line is 0.3449 Torr g cm$^{-3}$. Using $V_m$ determined from the $y$ intercept, $K$ is found to be $8.38 \times 10^{-2}$ Torr$^{-1}$.

# 19.5 Radical-Chain Reactions

**Radicals** are chemical species that contain an unpaired electron. Due to the presence of the unpaired electron, radicals tend to be extremely reactive. In 1934, Rice and Herzfeld were able to demonstrate that the kinetic behavior of many organic reactions was consistent with the presence of radicals in the reaction mechanism. An example of a radical-mediated reaction is the thermal decomposition of ethane:

$$C_2H_6(g) \rightarrow C_2H_4(g) + H_2(g) \tag{19.85}$$
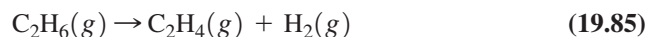
Small amounts of methane ($CH_4$) are also produced in this decomposition. The decomposition mechanism proposed by Rice and Herzfeld is as follows:

$$\text{Initiation} \qquad C_2H_6 \xrightarrow{k_1} 2\ CH_3\cdot \tag{19.86}$$

$$\text{Propagation} \qquad CH_3\cdot + C_2H_6 \xrightarrow{k_2} CH_4 + C_2H_5\cdot \tag{19.87}$$

$$C_2H_5\cdot \xrightarrow{k_3} C_2H_4 + H\cdot \tag{19.88}$$

$$H\cdot + C_2H_6 \xrightarrow{k_4} C_2H_5\cdot + H_2 \tag{19.89}$$

$$\text{Termination} \qquad H\cdot + C_2H_5\cdot \xrightarrow{k_5} C_2H_6 \tag{19.90}$$
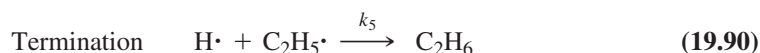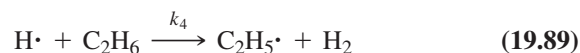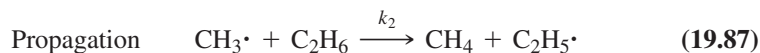
In this section, we include a dot ($\cdot$) in the formula of a compound to indicate that the species is a radical. The first elementary step in the mechanism involves the creation of two methyl radicals, referred to as an **initiation step** [Equation (19.86)]. In an initiation step, radicals are produced from a precursor species. The next three steps in the mechanism [Equations (19.87) through (19.89)] are referred to as **propagation steps** in which a radical reacts with another species to produce radical and nonradical products, and the radical products go on to participate in subsequent reactions. The final step in the mechanism is a **termination step** in which two radicals recombine to produce a nonradical product.

Although the mechanism of Equations (19.86) through (19.90) is clearly complex, the rate law expression predicted by this mechanism is remarkably simple. To derive this rate law, we begin with the differential rate expression for the disappearance of ethane:

$$-\frac{d[C_2H_6]}{dt} = k_1[C_2H_6] + k_2[C_2H_6][CH_3\cdot] + k_4[C_2H_6][H\cdot] - k_5[C_2H_5\cdot][H\cdot]$$

(19.91)

Because the methyl radical is a reactive intermediate, the steady-state approximation is applied to this species, resulting in the following expression for $[CH_3]$:

$$\frac{d[CH_3\cdot]}{dt} = 0 = 2k_1[C_2H_6] - k_2[C_2H_6][CH_3\cdot] \qquad (19.92)$$

$$[CH_3\cdot] = \frac{2k_1}{k_2} \qquad (19.93)$$

The factor of 2 in Equation (19.92) originates from the relationship between the reaction rate and the rate of $CH_3\cdot$ appearance as discussed in Chapter 18. Next, the steady-state approximation is applied to the differential rate expressions for the ethyl radical and atomic hydrogen since they are also reaction intermediates:

$$\frac{d[C_2H_5\cdot]}{dt} = 0 = k_2[CH_3\cdot][C_2H_6] - k_3[C_2H_5\cdot]$$

$$+ k_4[C_2H_6][H\cdot] - k_5[C_2H_5\cdot][H\cdot] \qquad (19.94)$$

$$\frac{d[H\cdot]}{dt} = 0 = k_3[C_2H_5\cdot] - k_4[C_2H_6][H\cdot] - k_5[C_2H_5\cdot][H\cdot] \qquad (19.95)$$

Adding Equations (19.94), (19.95), and (19.92) yields the following expression for $[H\cdot]$:

$$0 = 2k_1[C_2H_6] - 2k_5[C_2H_5\cdot][H\cdot]$$

$$[H\cdot] = \frac{k_1[C_2H_6]}{k_5[C_2H_5\cdot]} \qquad (19.96)$$

Substituting Equation (19.96) into Equation (19.95) yields

$$0 = k_3[C_2H_5\cdot] - k_4[C_2H_6]\left(\frac{k_1[C_2H_6]}{k_5[C_2H_5\cdot]}\right) - k_5[C_2H_5\cdot]\left(\frac{k_1[C_2H_6]}{k_5[C_2H_5\cdot]}\right)$$

$$0 = k_3[C_2H_5\cdot] - \frac{k_4k_1[C_2H_6]^2}{k_5[C_2H_5\cdot]} - k_1[C_2H_6]$$

$$0 = [C_2H_5\cdot]^2 - \frac{k_4k_1[C_2H_6]^2}{k_5k_3} - \frac{k_1}{k_3}[C_2H_6][C_2H_5\cdot] \qquad (19.97)$$

The last expression is a quadratic equation in $[C_2H_5\cdot]$ for which the solution yields the following expression for $[C_2H_5\cdot]$:

$$[C_2H_5\cdot] = [C_2H_6]\left[\frac{k_1}{2k_3} + \left(\left(\frac{k_1}{2k_3}\right)^2 + \left(\frac{k_1k_4}{k_3k_5}\right)\right)^{1/2}\right] \qquad (19.98)$$

Experimentally, the rate constant for initiation $k_1$ is small such that only the lowest power term in Equation (19.98) is appreciable such that

$$[C_2H_5\cdot] = \left(\frac{k_1k_4}{k_3k_5}\right)^{1/2}[C_2H_6] \qquad (19.99)$$

With Equation (19.99), $[H\cdot]$ from Equation (19.96) becomes

$$[H\cdot] = \frac{k_1[C_2H_6]}{k_5[C_2H_5\cdot]} = \frac{k_1}{k_5}\left(\frac{k_3k_5}{k_1k_4}\right)^{1/2} = \left(\frac{k_1k_3}{k_4k_5}\right)^{1/2} \qquad (19.100)$$

With the preceding definitions for $[H\cdot]$ and $[C_2H_5\cdot]$ in hand, the differential rate expression for the disappearance of ethane [Equation (19.91)] becomes

$$-\frac{d[C_2H_6]}{dt} = \left(k_2[CH_3\cdot] + \left(\frac{k_1k_3k_4}{k_5}\right)^{1/2}\right)[C_2H_6] \qquad \textbf{(19.101)}$$

Finally, using the definition of $[CH_3\cdot]$ in Equation (19.93) and ignoring higher powers of $k_1$, the final differential rate expression for $[C_2H_6]$ is

$$-\frac{d[C_2H_6]}{dt} = \left(\frac{k_1k_3k_4}{k_5}\right)^{1/2}[C_2H_6] \qquad \textbf{(19.102)}$$

Equation (19.102) predicts that the decay of ethane should be first order with respect to ethane, as is observed experimentally. The remarkable aspect of this result is that from a very complex mechanism a relatively simple rate expression is derived. In general, even the most complex Rice–Herzfeld radical mechanisms will yield orders of $1/2$, $1$, $3/2$, and $2$.

## EXAMPLE PROBLEM 19.3

Consider the following reaction of methane with molecular chlorine:

$$CH_4(g) + Cl_2(g) \rightarrow CH_3Cl(g) + HCl(g)$$
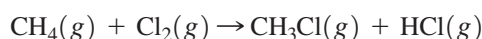
Experimental studies have shown that the rate law for this reaction is one-half order with respect to $Cl_2$. Is the following mechanism consistent with this behavior?

$$Cl_2 \xrightarrow{k_1} 2\,Cl\cdot$$

$$Cl\cdot + CH_4 \xrightarrow{k_2} HCl + CH_3\cdot$$

$$CH_3\cdot + Cl_2 \xrightarrow{k_3} CH_3Cl + Cl\cdot$$

$$Cl\cdot + Cl\cdot \xrightarrow{k_4} Cl_2$$
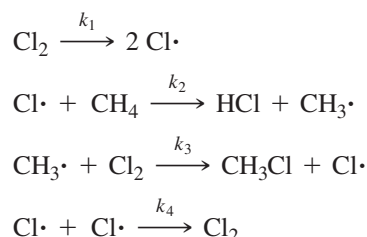
### Solution

The rate of reaction in terms of product HCl is given by

$$R = \frac{d[HCl]}{dt} = k_2[Cl\cdot][CH_4]$$

Because $Cl\cdot$ is a reaction intermediate, it cannot appear in the final rate law expression, and $Cl\cdot$ must be expressed in terms of $[CH_4]$ and $[Cl_2]$. The differential rate expressions for $[Cl\cdot]$ and $[CH_3Cl\cdot]$ are

$$\frac{d[Cl\cdot]}{dt} = 2k_1[Cl_2] - k_2[Cl\cdot][CH_4] + k_3[CH_3\cdot][Cl_2] - 2k_4[Cl\cdot]^2$$

$$\frac{d[CH_3\cdot]}{dt} = k_2[Cl\cdot][CH_4] - k_3[CH_3\cdot][Cl_2]$$

Applying the steady-state approximation to the expression for $[CH_3\cdot]$ yields

$$[CH_3\cdot] = \frac{k_2[Cl\cdot][CH_4]}{k_3[Cl_2]}$$

Next, we substitute this definition of $[CH_3\cdot]$ into the differential rate expression for $[Cl\cdot]$ and apply the steady-state approximation:

$$0 = 2k_1[Cl_2] - k_2[Cl\cdot][CH_4] + k_3[CH_3\cdot][Cl_2] - 2k_4[Cl\cdot]^2$$

$$0 = 2k_1[Cl_2] - k_2[Cl\cdot][CH_4] + k_3\left(\frac{k_2[Cl\cdot][CH_4]}{k_3[Cl_2]}\right)[Cl_2] - 2k_4[Cl\cdot]^2$$

$$0 = 2k_1[Cl_2] - 2k_4[Cl\cdot]^2$$

$$[Cl\cdot] = \left(\frac{k_1}{k_4}[Cl_2]\right)^{1/2}$$

With this result, the predicted rate law expression becomes

$$R = k_2[Cl\cdot][CH_4] = k_2\left(\frac{k_1}{k_4}\right)^{1/2}[CH_4][Cl_2]^{1/2}$$

The mechanism is consistent with the experimentally observed one-half order dependence on $[Cl_2]$.

# 19.6 Radical-Chain Polymerization

A very important class of radical reactions are **radical polymerization reactions.** In these processes, a monomer is activated through the reaction with a radical initiator, creating a monomer radical. Next, the monomer radical reacts with another monomer to create a radical dimer. The radical dimer then reacts with another monomer, and the process continues, resulting in formation of a **polymer chain.** The mechanism for chain polymerization is as follows. First, the activated monomer must be created in an initiation step:

$$I \xrightarrow{k_i} 2R\cdot \tag{19.103}$$

$$R\cdot + M \xrightarrow{k_1} M_1\cdot \tag{19.104}$$

In this step, the initiator I is transformed into radicals $R\cdot$ that react with a monomer to form an activated monomer $M_1\cdot$. The next mechanistic step is propagation, in which the activated monomer reacts with another monomer to form activated dimer, and the dimer undergoes subsequent reactions as follows:

$$M_1\cdot + M \xrightarrow{k_p} M_2\cdot \tag{19.105}$$

$$M_2\cdot + M \xrightarrow{k_p} M_3\cdot \tag{19.106}$$

$$M_{n-1}\cdot + M \xrightarrow{k_p} M_n\cdot \tag{19.107}$$
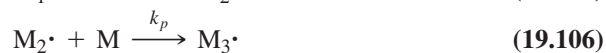
In the preceding equations, the subscript indicates the number of monomers contained in the polymer chain, and the rate constant for propagation $k_p$ is assumed to be independent of polymer size. The final step in the mechanism is termination in which two radical chains undergo reaction:

$$M_m\cdot + M_n\cdot \xrightarrow{k_t} M_{m+n} \tag{19.108}$$

The rate of activated monomer production is related to the rate of radical $(R\cdot)$ formation as follows:

$$\left(\frac{d[M\cdot]}{dt}\right)_{production} = 2\phi k_i[I] \tag{19.109}$$

where $\phi$ represents the probability that the initiator-generated radical $(R\cdot)$ will create a radical chain. Since active monomers combine to terminate polymerization [Equation (19.107)], the rate of activated monomer loss is equal to the rate of termination:

$$\left(\frac{d[M\cdot]}{dt}\right)_{decay} = -2k_t[M\cdot]^2 \tag{19.110}$$

The total differential rate expression for $[M\cdot]$ is given by the sum of Equations (19.109) and (19.110):

$$\frac{d[M\cdot]}{dt} = 2\phi k_i[I] - 2k_t[M\cdot]^2 \tag{19.111}$$

Because M· is an intermediate species, the steady-state approximation is applied to Equation (19.111), yielding the following:

$$[\text{M·}] = \left(\frac{\phi k_i}{k_t}\right)^{1/2}[\text{I}]^{1/2} \tag{19.112}$$

Finally, the monomer consumption is dominated by propagation such that the differential rate expression for [M] becomes

$$\frac{d[\text{M}]}{dt} = -k_p[\text{M·}][\text{M}]$$

$$= -k_p\left(\frac{\phi k_i}{k_t}\right)^{1/2}[\text{I}]^{1/2}[\text{M}] \tag{19.113}$$

Equation (19.113) demonstrates that the rate of monomer consumption is predicted to be overall 3/2 order, 1/2 order in initiator concentration, and first order in monomer concentration.

One measure of the efficiency of polymerization is the kinetic chain length $\nu$. This quantity is defined as the average number of monomers in the polymer chain per active center monomer produced. Consistent with this definition, $\nu$ can be expressed as the rate of monomer unit consumption divided by the rate of active monomer production:

$$\nu = \frac{k_p[\text{M·}][\text{M}]}{2\phi k_i[\text{I}]} = \frac{k_p[\text{M·}][\text{M}]}{2k_t[\text{M·}]^2} = \frac{k_p[\text{M}]}{2k_t[\text{M·}]} \tag{19.114}$$

Substitution of Equation (19.112) into Equation (19.114) provides the final expression for the kinetic chain length:

$$\nu = \frac{k_p[\text{M}]}{2k_t\left(\dfrac{\phi k_i}{k_t}\right)^{1/2}[\text{I}]^{1/2}} = \frac{k_p[\text{M}]}{2(\phi k_i k_t)^{1/2}[\text{I}]^{1/2}} \tag{19.115}$$

Equation (19.115) predicts that the kinetic chain length will increase as the rate constants for chain initiation or termination or the concentration of initiator are reduced. Therefore, polymerization is usually carried out at minimal initiator concentrations such that the number of activated monomers is kept small.

# 19.7 Explosions

Consider a highly exothermic reaction in which a significant amount of heat is liberated during the reaction. The reaction will proceed with a certain initial rate, but if the heat liberated during the reaction is not dissipated, the system temperature will rise, as will the rate of reaction. The final result of this process is a thermal explosion. A second type of explosion involves chain-branching reactions. In the previous section, the concentration of radical intermediate species was determined by applying the steady-state approximation. However, what if the concentrations of radical intermediate species were not constant with time? Two limits can be envisioned: either a significant reduction or increase in radical intermediate concentration as time proceeds. If the concentration of radical intermediates decreases with time, then the reaction will terminate. What if the concentration of reactive intermediates increases rapidly with time? From the mechanisms discussed thus far, an increase in radical intermediate concentration would lead to the creation of more radical species. In this case, the number of radical chains increases exponentially with time, leading to explosion.

A standard introductory chemistry demonstration is the ignition of a balloon containing hydrogen and oxygen. The balloon is ignited, and if the two gases are present in the correct stoichiometric ratio, an explosion occurs as evidenced by a loud bang and a number of startled students. The specific reaction is

$$2\,\text{H}_2(g) + \text{O}_2(g) \rightarrow 2\,\text{H}_2\text{O}(g) \tag{19.116}$$
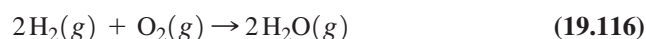
The reaction is deceptively simple, yet the mechanism of the reaction is not fully understood. Important mechanistic components of this reaction are

$$H_2 + O_2 \rightarrow 2 \, OH\cdot \tag{19.117}$$

$$H_2 + OH\cdot \rightarrow H\cdot + H_2O \tag{19.118}$$

$$H\cdot + O_2 \rightarrow OH\cdot + \cdot O\cdot \tag{19.119}$$

$$\cdot O\cdot + H_2 \rightarrow OH\cdot + H\cdot \tag{19.120}$$

$$H\cdot + O_2 + M \rightarrow HO_2\cdot + M^* \tag{19.121}$$

The first step in the mechanism, Equation (19.117), is an initiation step in which two hydroxyl radicals (OH·) are created. The radical is propagated in the second step, Equation (19.118). Steps 3 and 4, Equations (19.119) and (19.120), are referred to as **branching reactions,** in which a single radical species reacts to produce two radical species. As such, the number of reactive radicals increases twofold in these branching steps. These branching steps lead to a chain-branching explosion because the concentration of the reactive species grows rapidly in time.

The occurrence of explosions for this reaction is dependent on temperature and pressure, as shown in Figure 19.13. First, explosion will occur only if the temperature is greater than 460°C. At lower temperatures, the rates for the various radical-producing reactions are insufficient to support appreciable chain branching. In addition to temperature, the pressure must also be sufficiently high to support chain branching. If the pressure is low, radicals that are produced can diffuse to the walls of the vessel where they are destroyed. Under these conditions, the rates of radical production and decay are balanced such that branching is not prevalent and explosion does not occur. As the pressure is increased, the first explosion regime is reached in which the radicals can participate in branching reactions before reaching the container walls. A further increase in pressure results in the reaction returning to a controlled regime where the pressure is so great that radical–radical reactions reduce the number of reactive species present. The final reaction in the mechanism under discussion is an example of such a reaction. In this step, H· and $O_2$ react to produce $HO_2\cdot$, which does not contribute to the reaction. The formation of this species requires a three-body collision, with the third species, $M$, taking away excess energy such that the $HO_2\cdot$ radical is stable. Such reactions will occur only at elevated pressures. Finally, at highest pressures another explosive regime is encountered. This is a thermal explosive regime in which the dissipation of heat is insufficient to keep the system temperature from increasing rapidly, providing for explosive behavior.

The likelihood of undergoing an explosion is highly dependent on radical concentration. A generic scheme for chain-branching reactions is as follows:

$$A + B \xrightarrow{k_i} R\cdot \tag{19.122}$$

$$R\cdot \xrightarrow{k_b} \phi R\cdot + P_1 \tag{19.123}$$

$$R\cdot \xrightarrow{k_t} P_2 \tag{19.124}$$

In this scheme, the first step involves the reaction of reactants A and B, resulting in the formation of radical R·. The second step is chain branching in which the radical undergoes reaction to produce other radicals with a branching efficiency given by $\phi$. The final step of the mechanism is termination. Finally, the species $P_1$ and $P_2$ represent nonreactive products. The differential rate expression for $[R\cdot]$ consistent with this mechanism is as follows:

$$\frac{d[R\cdot]}{dt} = k_i[A][B] - k_b[R\cdot] + \phi k_b[R\cdot] - k_t[R\cdot]$$

$$= \Gamma + k_{eff}[R\cdot] \tag{19.125}$$

In Equation (19.125), the following definitions have been employed:

$$\Gamma = k_i[A][B]$$

$$k_{eff} = k_b(\phi - 1) - k_t$$
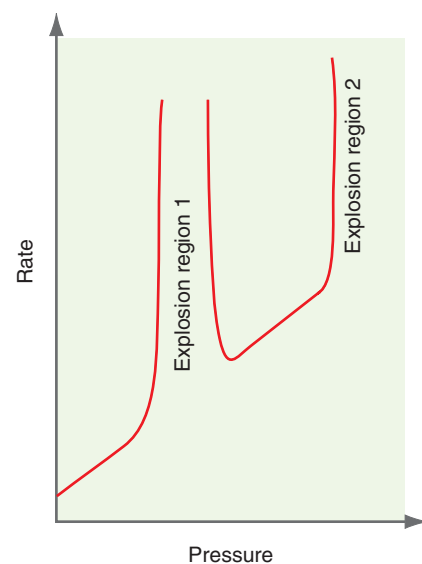


**FIGURE 19.13**
Schematic of an explosive reaction. As the pressure is increased, two explosive regimes are encountered. The region at lower pressures is due to chain-branching reactions, and the higher pressure region corresponds to a thermal explosion.

Equation (19.125) can be solved for $[R\cdot]$ to yield

$$[R\cdot] = \frac{\Gamma}{k_{eff}}(e^{k_{eff}t} - 1) \tag{19.126}$$

Equation (19.126) demonstrates that $[R\cdot]$ is dependent on $k_{eff}$. Two cases can be envisioned depending on the magnitude of $k_t$ in comparison to $k_b(\phi - 1)$. In the limit where $k_t \gg k_b(\phi - 1)$, termination dominates and Equation (19.126) becomes

$$\lim_{k_1 \gg k_b(\phi-1)}[R\cdot] = \frac{\Gamma}{k_t}(1 - e^{-k_t t}) \tag{19.127}$$

Equation (19.127) demonstrates that in this limit the radical concentration will reach a limiting value of $\Gamma/k_t$ at $t = \infty$. The interpretation of this limiting behavior is that $[R\cdot]$ will never become large enough to support branching, and explosion will not occur. The second limit occurs when $k_b(\phi-1) \gg k_t$ and branching dominates. In this limit, Equation (19.126) becomes

$$\lim_{k_b(\phi-1) \gg k_t}[R\cdot] = \frac{\Gamma}{k_b(\phi - 1)}(e^{k_b(\phi-1)t} - 1) \tag{19.128}$$

Equation (19.128) demonstrates that $[R\cdot]$ is predicted to increase exponentially corresponding to explosion. This simple mechanism illustrates the importance of efficient propagation/branching in promoting explosions in chain-branching reactions.

## 19.8 Feedback, Nonlinearity, and Oscillating Reactions

The discussion of chemical kinetics thus far has largely involved systems in which reactants combine to produce products, and the reaction proceeds until equilibrium (defined as an absence of macroscopic variation in reactant of product concentrations with time) is reached. However, there is a class of reactions that demonstrate periodic variation in concentration in space or in time. These reactions are referred to as **oscillating reactions.** Oscillating reactions are generally open systems kept from reaching equilibrium by supplying reactants or removing products from the reaction. Under these conditions, concentrations of reactants, products, and intermediates can demonstrate macroscopic variation in concentrations. Once viewed as an oddity, oscillating reactions are found in a wide variety of systems in biology (cellular energy, chemotaxis) and chemistry (combustion, film growth). All oscillating reactions involve two kinetic features: nonlinearity and feedback.

The previous section describing explosions and radical chemistry provided an example of feedback. Specifically, in the conversion of hydrogen and oxygen to water [Equation (19.116)] the first step in the mechanism involved the formation of hydroxyl radical:

$$H_2 + O_2 \rightarrow 2\,OH\cdot$$
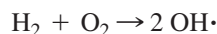
After formation, hydroxyl radical could in turn react with hydrogen:

$$H_2 + OH\cdot \rightarrow H\cdot + H_2O$$
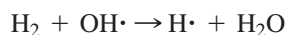
Notice that once the $OH\cdot$ intermediate is formed, this species reacts with $H_2$, which results in an increase in the rate of $H_2$ consumption and correspondingly the reaction rate. This is an example of **feedback,** where products formed in one step of the mechanism can influence the rate of other steps. Acceleration of the reaction rate (as described previously) is an example of positive feedback, and negative feedback occurs when the formation of a species results in a reduction in the reaction rate.

What does it mean for a chemical reaction to be **nonlinear**? To explore this concept, we return to the coefficient of reaction advancement ($\xi$). For the following reaction:

$$A + BC \rightarrow AB + C \tag{19.129}$$

We define $\xi$ with respect to A as follows:

$$\xi = \frac{[A]_0 - [A]}{[A]_0} \tag{19.130}$$

With this definition, $\xi$ has a value of 1 at the beginning of the reaction and 0 when A has been consumed. If we measure the rate of the reaction with BC in excess, then the reaction will be first-order in A and the reaction rate defined with respect to $\xi$ will be

$$\frac{d\xi}{dt} = k(1 - \xi) \tag{19.131}$$

This expression demonstrates that the reaction rate will initially be at a maximum and will decrease linearly as the reaction proceeds as shown in Figure 19.14. However, what if BC is not in excess and the reaction is second order? In this case the reaction rate becomes

$$\frac{d\xi}{dt} = k(1 - \xi)^2 \tag{19.132}$$

This expression dictates that the decrease in the reaction rate as $\xi$ increases will be non-linear as shown in Figure 19.14. Notice that nonlinear evolution of the reaction rate with $\xi$ is a relatively common aspect of chemical kinetics. In this simple example, the reaction had to simply be second order for the reaction to be nonlinear.

What happens if feedback and nonlinearity are combined? Returning back to the reaction of molecular hydrogen and oxygen, we would expect the rate of the reaction to increase as hydroxyl radical is formed, and then decrease as the reactants are consumed. We can model this behavior in terms of $\xi$ as follows:

$$\frac{d\xi}{dt} = k\xi(1 - \xi) \tag{19.133}$$

This expression can be directly related to the general relationship for quadratic **autocatalysis:**

$$A + B \xrightarrow{k} 2B \qquad R = k[A][B] \tag{19.134}$$

In this autocatalytic reaction we would expect the reaction rate to initially increase as the reaction proceeds due to the increase in [B]. As the reaction proceeds, [A] will eventually be depleted and the reaction rate will approach zero as $\xi$ approaches one. This evolution in the reaction rate for this autocatalytic reaction is shown in Figure 19.14.

Autocatalytic reactions provide the opportunity for concentrations and reaction rates to evolve in time, including oscillatory variation in these quantities. Perhaps the most famous example of a chemical reaction demonstrating oscillations is the
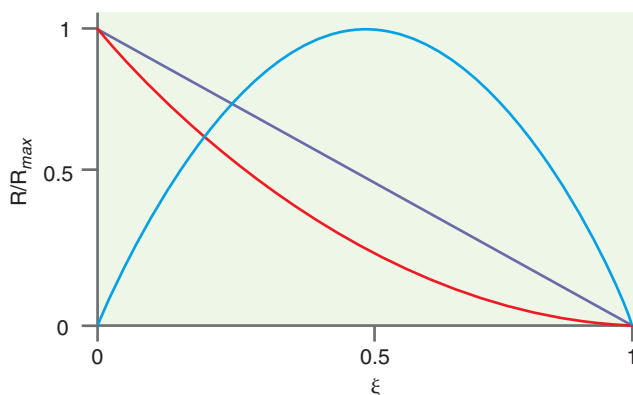


**FIGURE 19.14**
Illustration of the dependence of the reaction rate on the coefficient of reaction advancement ($\xi$). The purple curve represents linear dependence of the rate with $\xi$ (Equation 19.131), and the red curve demonstrates nonlinear dependence for a second-order reaction (Equation 19.132). The blue curve represents quadratic autocatalysis (Equation 19.133) where both feedback and nonlinear behavior result in a maximum in the reaction rate after the reaction has been initiated.

**FIGURE 19.15**
Image of the Belousov-Zhabotinsky (BZ) reaction. The variation in color is due to spatial differences in chemical composition, which vary in time and in space.

**Belousov-Zhabotinsky (BZ) reaction.** The feedback steps in the BZ reaction are the following:

$$BrO_3^- + HBrO_2 + H^+ \underset{k_{-1}}{\overset{k_1}{\rightleftharpoons}} 2 BrO_2 \cdot + H_2O \qquad (19.135)$$

$$BrO_2 \cdot + Ce(III) + H^+ \overset{k_2}{\longrightarrow} HBrO_2 + Ce(IV) \qquad (19.136)$$
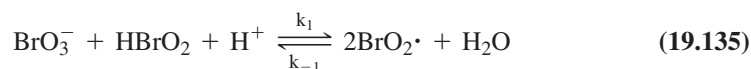
The feedback mechanism in this reaction involves $HBrO_2$, which reacts to yield two $BrO_2$ radicals, with these radicals forming the reactant $HBrO_2$ through the oxidation of Ce(III). If each of the $BrO_2$ radicals goes on to form $HBrO_2$, then the following net reaction occurs:

$$BrO_3^- + HBrO_2 + 3 H^+ + 2 Ce(III) \rightarrow 2 HBrO_2 + 2 Ce(IV) + H_2O \qquad (19.137)$$
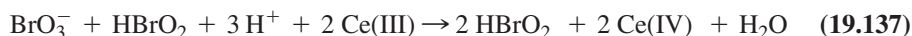
Comparison to Equation 19.134 reveals that this reaction is predicted to demonstrate quadratic autocatalysis. The dependence of the rate law on $HBrO_2$ can be further explored using basic kinetic tools. First, we can express the reaction rate with respect to $HBrO_2$ as follows:

$$R = \frac{d[HBrO_2]}{dt}$$

$$= -k_1[BrO_3^-][HBrO_2][H^+] + k_{-1}[BrO_2\cdot]^2 + k_2[BrO_2\cdot][Ce(III)][H^+] \quad (19.138)$$

Since the oxidation of Ce(III) is relatively slow, we can employ the preequilibrium approximation to derive an expression for $[BrO_2\cdot]$:

$$[BrO_2\cdot] = \left\{ \frac{k_1[BrO_3^-][HBrO_2][H^+]}{k_{-1}} \right\}^{1/2} \qquad (19.139)$$

Substituting this into the rate expression yields

$$R = \frac{d[HBrO_2]}{dt} = k_2 \left( \frac{k_1}{k_{-1}} \right)^{1/2} [BrO_3^-]^{1/2}[Ce(III)][H^+]^{3/2}[HBrO_2]^{1/2} \quad (19.140)$$

This rate expression is consistent with autocatalytic behavior as indicted by the positive exponent for $HBrO_2$, and half-order dependence. In contrast, if Fe(III)/Fe(IV) are used in place of Ce(III)/Ce(IV), the oxidation of Fe(III) is rapid and the steady-state approximation can be used to define $[BrO_2\cdot]$. In this case the rate law expression for the reaction demonstrates autocatalytic behavior that is first order in $HBrO_2$:

$$R = \frac{d[HBrO_2]}{dt} = k_1[BrO_3^-][H^+][HBrO_2] \qquad (19.141)$$

Autocatalysis can also lead to oscillatory behavior where concentrations of reactants and products demonstrate recurring maxima with time. Figure 19.15 presents a picture of a BZ reaction, where color variation is due to spatial variation in concentrations. The spatial patterns evolve with time since autocatalysis results in oscillations in concentrations with time and space.

The BZ reaction is rather complex. A simpler example of an oscillatory chemical reaction is the **Lotka-Volterra mechanism:**

$$A + X \overset{k_1}{\longrightarrow} 2X \qquad (19.142)$$

$$X + Y \overset{k_2}{\longrightarrow} 2Y \qquad (19.143)$$

$$Y \overset{k_3}{\longrightarrow} B \qquad (19.144)$$

The differential rate expressions for X and Y based on this mechanism are

$$\frac{d[X]}{dt} = 2 k_1[A][X] - k_2[X][Y] \qquad (19.145)$$

$$\frac{d[Y]}{dt} = 2 k_2[X][Y] - k_3[Y] \qquad (19.146)$$
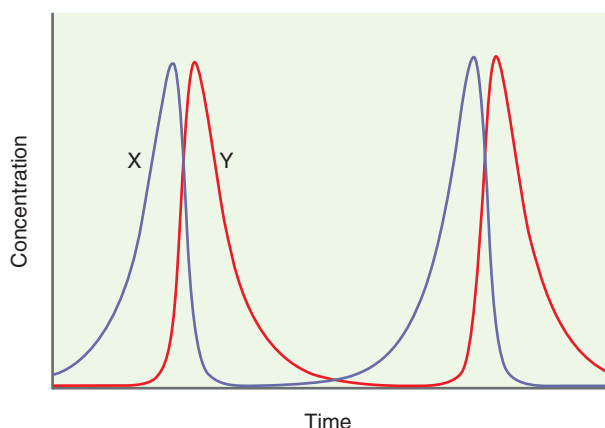
Imagine that the reaction is carried out by keeping the concentration of A ([A]) constant, which can be achieved by continuously supplying A as the reaction proceeds. Furthermore, notice that the reaction rate is not dependent on the concentration of the product B. Under these conditions the only concentrations relevant to the reaction rate are the intermediates [X] and [Y]. Using numerical methods (such as Euler's method described in Section 18.6) [X] and [Y] can be determined using the differential rate expressions above for a given set of rate constants and $[A]_0$. The results of this calculation are shown in Figure 19.16. Notice that [X] and [Y] oscillate, demonstrating periodic recurrences in time. Also, notice that the maximum in [Y] occurs after the maximum in [X]. Inspection of the mechanism reveals why this would be the case. The first step of the mechanism is autocatalytic with respect to X, resulting in an increase in rate of X production. However, once X is produced it reacts with Y in the second step of the mechanism. Since this second step is autocatalytic with respect to Y, the rate of Y production will increase, resulting in a depletion of X. Finally, the decay in Y to form the product B given by the third step of the mechanism provides for a decrease in [Y]. Although we have explored the Lotka-Volterra mechanism in a chemical context, the differential rate expressions represent a general class of differential equations referred to as "predator-prey" equations. In our example, X is the prey and Y is the predator. The initial increase in prey population promotes an increase in the predator population. Ultimately, the predators consume the prey, resulting in a decrease in the prey population. With a decrease in the prey population, the predator populations will decline. Finally, a decline in predators allows the prey population to increase, and the cycle starts over again. These equations have been used to describe oscillations in economic activity, wildlife populations, and the spread of disease.

# 19.9 Photochemistry

Photochemical processes involve the initiation of a chemical reaction through the absorption of a photon by an atom or molecule. In these reactions, photons can be thought of as reactants, and initiation of the reaction occurs when the photon is absorbed. Photochemical reactions are important in a wide variety of areas. The primary event in vision involves the absorption of a photon by the visual pigment rhodopsin. Photosynthesis involves the conversion of light energy into chemical energy by plants and bacteria. Finally, numerous photochemical reactions occur in the atmosphere (e.g., ozone production and decomposition) that are critical to life on Earth. As illustrated by these examples, photochemical reactions are an extremely important area of chemistry, and they are explored in this section.

## 19.9.1 Photophysical Processes

When a molecule absorbs a photon of light, the energy contained in the photon is transferred to the molecule. The amount of energy contained by a photon is given by the Planck equation:

$$E_{photon} = h\nu = \frac{hc}{\lambda} \qquad \textbf{(19.147)}$$

In Equation (19.147), $h$ is Planck's constant ($6.626 \times 10^{-34}$ J s), $c$ is the speed of light in a vacuum ($2.998 \times 10^8$ m s$^{-1}$), $\nu$ is the frequency of light, and $\lambda$ is the corresponding wavelength of light. A mole of photons is referred to as an einstein, and the energy contained by an einstein of photons is Avogadro's number times $E_{photon}$. The intensity of light is generally stated as energy per unit area per unit time. Because one joule per second is a watt, a typical intensity unit is W cm$^{-2}$.

The simplest photochemical process is the absorption of a photon by a reactant resulting in product formation:

$$ \text{A} \xrightarrow{h\nu} \text{P} \tag{19.148} $$

The rate of reactant photoexcitation is given by

$$ R = -\frac{d[\text{A}]}{dt} = \frac{I_{abs}1000}{l} \tag{19.149} $$

In Equation (19.149), $I_{abs}$ is the intensity of absorbed light in units of Einstein cm$^{-2}$ s$^{-1}$, $l$ is the path length of the sample in centimeters, and 1000 represents the conversion from cubic centimeters to liters such that the rate has appropriate units of M s$^{-1}$. In Equation (19.149), it is assumed that reactant excitation occurs through the absorption of a single photon. According to the Beer–Lambert law, the intensity of light transmitted through a sample ($I_{trans}$) is given by

$$ I_{trans} = I_0 10^{-\varepsilon l[\text{A}]} \tag{19.150} $$

where $I_0$ is the intensity of incident radiation, $\varepsilon$ is the **molar absorptivity** of species A, and [A] is the concentration of reactant. Recall that the molar absorptivity will vary with excitation wavelength. Because $I_{abs} = I_0 - I_{trans}$,

$$ I_{abs} = I_0(1 - 10^{-\varepsilon l[\text{A}]}) \tag{19.151} $$

The series expansion of the exponential term in Equation (19.151) is

$$ 10^{-\varepsilon l[\text{A}]} = 1 - 2.303\varepsilon l[\text{A}] + \frac{(2.303\varepsilon l[\text{A}])^2}{2!} - \cdots \tag{19.152} $$

If the concentration of reactant is kept small, only the first two terms in Equation (19.152) are appreciable, and substitution into Equation (19.151) yields

$$ I_{abs} = I_0(2.303)\varepsilon l[\text{A}] \tag{19.153} $$

Substitution of Equation (19.153) into the rate expression for reactant photoexcitation of Equation (19.149) and integration yield the following expression for [A]:

$$ [\text{A}] = [\text{A}]_0 e^{-I_0(2303)\varepsilon t} = [\text{A}]_0 e^{-kt} \tag{19.154} $$

Equation (19.154) demonstrates that the absorption of light will result in the decay of reactant concentration consistent with first-order kinetic behavior. Most photochemical reactions are first order in reactant concentration such that Equation (19.154) describes the evolution in reactant concentration for the majority of photochemical processes. At times it is more useful to discuss photochemical processes with respect to the number of molecules as opposed to concentration. This is precisely the limit one encounters when considering the **photochemistry** of individual molecules as presented later. In this case, Equation (19.149) becomes

$$ -\frac{d\text{A}}{dt} = I_0 \frac{2303\varepsilon}{N_A}\text{A} \tag{19.155} $$

where A represents the number of molecules of reactant and $N_A$ is Avogadro's number. Integrating Equation (19.155), we obtain

$$A = A_0 e^{-I_0(2303\varepsilon/N_A)t} = A_0 e^{-I_0\sigma_A t} \qquad \textbf{(19.156)}$$

where $\sigma_A$ is known as the **absorption cross section** and the rate constant for excitation $k_a$ is equal to $I_0\sigma_A$ with $I_0$ in units of photons $cm^{-2} s^{-1}$.

The absorption of light may occur when the photon energy is equal to the energy difference between two energy states of the molecule. A schematic of the processes that occur following photon absorption resulting in an electronic energy-level transition (or "electronic transition") is given in Figure 19.17. Such diagrams are referred to as **Jablonski diagrams** after Aleksander Jablonski, a Polish physicist who developed these diagrams for describing kinetic processes initiated by electronic transitions. In a Jablonski diagram, the vertical axis represents increasing energy. The electronic states depicted are the ground-state singlet $S_0$, first excited singlet $S_1$, and triplet $T_1$. In the singlet states, the electrons are spin paired such that the spin multiplicity is one (i.e., a "singlet"), and in the triplet state two electrons are unpaired such that the spin multiplicity is three (a "triplet"). The subscripts indicate the energy ordering of the states. Because triplets are generally formed by electronic excitation, the lowest energy triplet state is labeled $T_1$ as opposed to $T_0$ (the lowest energy spin configuration of molecular oxygen is a triplet, a famous exception to this generality). Finally, the lowest vibrational level for each electronic state is indicated by dark horizontal lines, with higher vibrational levels indicated by the lighter horizontal lines. In addition, a manifold of rotational states will exist for each vibrational level; however, the rotational energy levels have been suppressed for clarity in Figure 19.17.
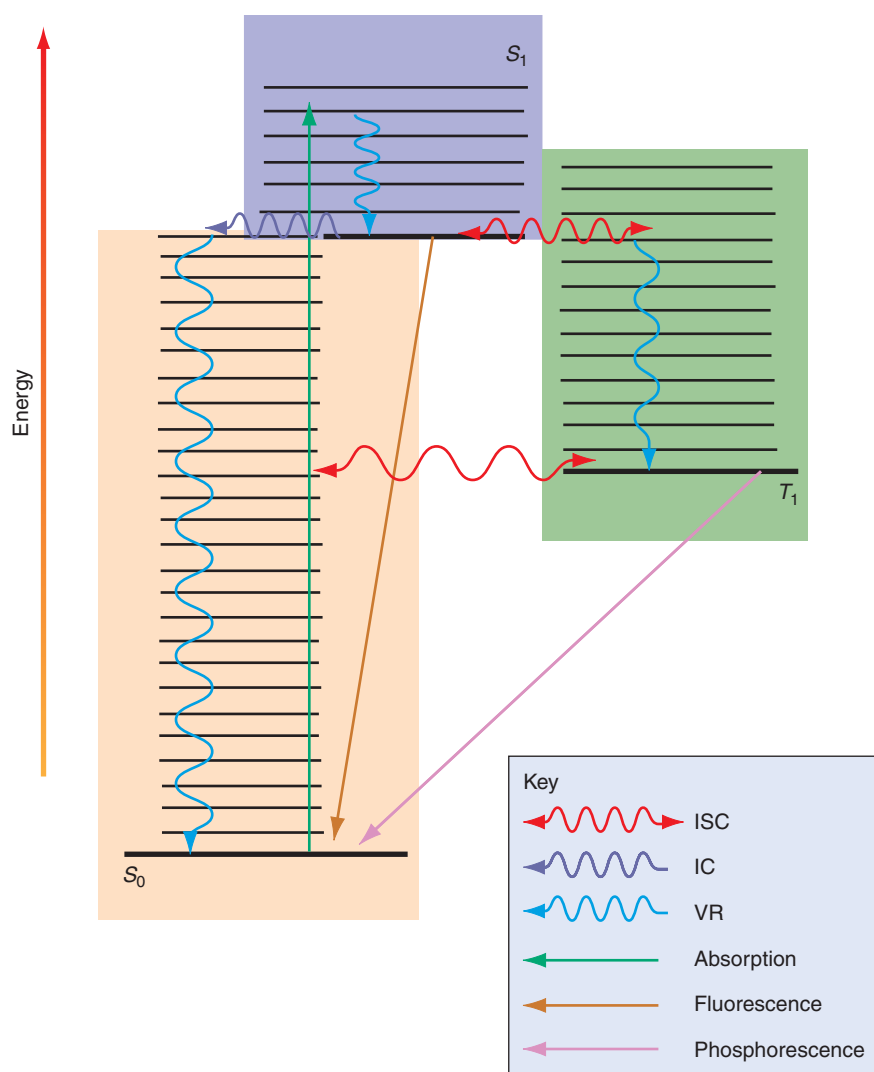


**FIGURE 19.17**
A Jablonski diagram depicting various photophysical processes, where $S_0$ is the ground electronic singlet state, $S_1$ is the first excited singlet state, and $T_1$ is the first excited triplet state. Radiative processes are indicated by the straight lines. The nonradiative processes of intersystem crossing (ISC), internal conversion (IC), and vibrational relaxation (VR) are indicated by the wavy lines.

The solid and wavy lines in Figure 19.17 represent a variety of processes that couple the electronic states. These processes, including the absorption of light and subsequent energetic relaxation pathways, are referred to as **photophysical processes** because the structure of the molecule remains unchanged. In fact, many of the processes of interest in "photochemistry" do not involve photochemical transformation of the reactant at all but are instead photophysical in nature. The absorption of light decreases the population in the lowest energy singlet state $S_0$, referred to as a depletion. Correspondingly, the population in the first excited singlet $S_1$ is increased. The absorption transition depicted in Figure 19.17 is to a higher vibrational level in $S_1$, with the probability of transition to a specific vibrational level determined by the Franck–Condon factor between the lowest energy vibrational level in $S_0$ and the vibrational states in $S_1$.

After populating $S_1$, thermal equilibration of the vibrational energy will occur, a process referred to as vibrational relaxation. Vibrational relaxation is extremely rapid ($\sim 100$ fs), and when complete, the vibrational state population in $S_1$ will be governed by the Boltzmann distribution. The vibrational energy-level spacings are assumed to be sufficiently large such that only the lowest vibrational level of $S_1$ is populated to a significant extent after equilibration. Decay of $S_1$ resulting in repopulation of $S_0$ can occur through one of three paths:

1. *Path 1*: Loss of excess electronic energy through the emission of a photon. Such processes are referred to as **radiative transitions.** The process by which photons are emitted in the radiative transitions between $S_1$ and $S_0$ is referred to as **fluorescence.** This process is equivalent to spontaneous emission.

2. *Path 2*: **Intersystem crossing** (ISC in Figure 19.14) resulting in population of $T_1$. This process involves a change in spin state, a process that is forbidden by quantum mechanics. As such, intersystem crossing is significantly slower than vibrational relaxation, but it is competitive with fluorescence in systems where the triplet state is populated to a significant extent. Following intersystem crossing, vibrational relaxation in the triplet vibrational manifold occurs, resulting in population of the lowest energy vibrational level. From this level, a second radiative transition can occur where $S_0$ is populated and the excess energy is released as a photon. This process is referred to as **phosphorescence.** Because the $T_1 - S_0$ transition also involves a change in spin, it is also forbidden by spin selection rules. Therefore, the rate for this process is slow, and phosphorescence occurs over longer timescales ($10^{-6}$ s to seconds) as compared to fluorescence ($\sim 10^{-9}$ s).

3. *Path 3*: Rather than undergoing a radiative transition, decay from $S_1$ to a high vibrational level of $S_0$ can occur followed by rapid vibrational relaxation. This process is referred to as **internal conversion** or nonradiative decay. Nonradiative decay can also occur through the triplet state by intersystem crossing to $S_0$ followed by vibrational relaxation.

From the viewpoint of kinetics, the absorption of light and subsequent relaxation processes can be viewed as a collection of reactions with corresponding rates. Figure 19.18 presents a modified version of the Jablonski diagram that focuses on these processes and corresponding rate constants. The individual processes, reactions, and notation for the reaction rates are provided in Table 19.1.

**TABLE 19.1    Photophysical Reactions and Corresponding Rate Expressions**

| Process | Reaction | Rate |
|---|---|---|
| Absorption/excitation | $S_0 + h\nu \rightarrow S_1$ | $k_a[S_0] \ (k_a = I_0 \sigma_A)$ |
| Fluorescence | $S_1 \rightarrow S_0 + h\nu$ | $k_f[S_1]$ |
| Internal conversion | $S_1 \rightarrow S_0$ | $k_{ic}[S_1]$ |
| Intersystem crossing | $S_1 \rightarrow T_1$ | $k_{isc}^S[S_1]$ |
| Phosphorescence | $T_1 \rightarrow S_0 + h\nu$ | $k_p[T_1]$ |
| Intersystem crossing | $T_1 \rightarrow S_0$ | $k_{isc}^T[T_1]$ |
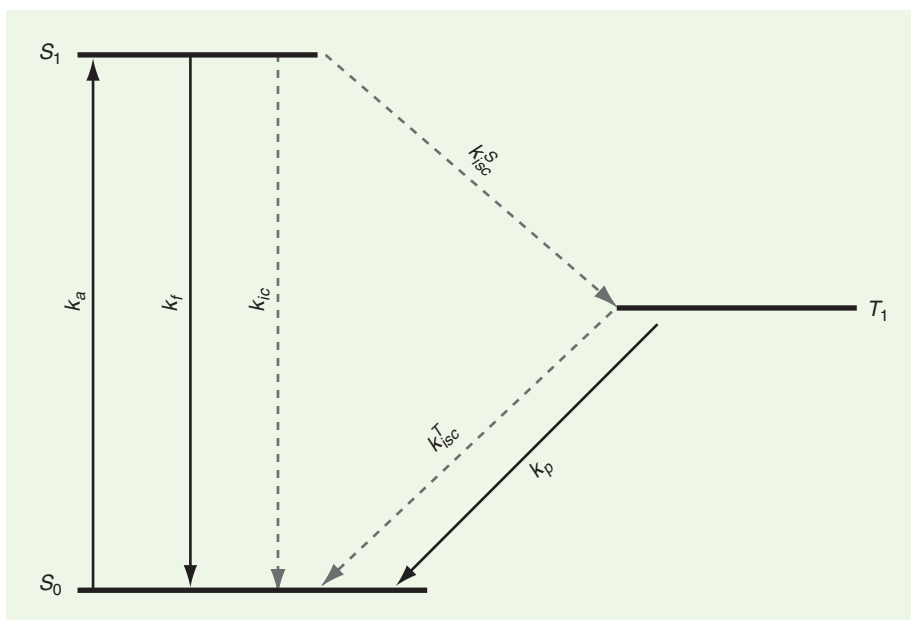
### 19.9.2 Fluorescence and Fluorescence Quenching

The photophysical processes outlined in Table 19.1 are present for any molecular system. To study excited state lifetimes, another photophysical process is introduced: **collisional quenching.** In this process, a collision occurs between a species Q and a molecule populating an excited electronic state. The result of the collision is the removal of energy from the molecule with the accompanying conversion of the molecule from $S_1$ to $S_0$:

$$S_1 + Q \xrightarrow{k_q} S_0 + Q \qquad (19.157)$$

The rate expression for this process is

$$R_q = k_q[S_1][Q] \qquad (19.158)$$

By studying the rate of collisional quenching as a function of [Q], it is possible to determine the $k_f$. To demonstrate this procedure, we begin by recognizing that in the kinetic scheme illustrated in Figure 19.18, $S_1$ can be considered an intermediate species. Under constant illumination, the concentration of this intermediate will not change. Therefore, we can write the differential rate expression for $S_1$ and apply the steady-state approximation:

$$\frac{d[S_1]}{dt} = 0 = k_a[S_0] - k_f[S_1] - k_{ic}[S_1] - k^S_{isc}[S_1] - k_q[S_1][Q] \qquad (19.159)$$

The **fluorescence lifetime** $\tau_f$ is defined as

$$\frac{1}{\tau_f} = k_f + k_{ic} + k^S_{isc} + k_q[Q] \qquad (19.160)$$

Using this definition of $\tau_f$, Equation (19.159) becomes

$$\frac{d[S_1]}{dt} = 0 = k_a[S_0] - \frac{[S_1]}{\tau_f} \qquad (19.161)$$

Equation (19.161) is readily solved for $[S_1]$:

$$[S_1] = k_a[S_0]\tau_f \qquad (19.162)$$

The fluorescence intensity $I_f$ depends on the rate of fluorescence given by

$$I_f = k_f[S_1] \tag{19.163}$$

Substituting Equation (19.162) into Equation (19.163) results in

$$I_f = k_a[S_0]k_f\tau_f \tag{19.164}$$

Inspection of the last two factors in Equation (19.164) illustrates the following relationship:

$$k_f\tau_f = \frac{k_f}{k_f + k_{ic} + k_{isc}^S + k_q[Q]} = \Phi_f \tag{19.165}$$

The product of the fluorescence rate constant and fluorescence lifetime is equivalent to the radiative rate constant divided by the sum of rate constants for all processes leading to the decay of $S_1$. In effect, $S_1$ decay can be viewed as a branching reaction, and the ratio of rate constants contained in Equation (19.165) can be rewritten as the quantum yield for fluorescence $\Phi_f$, similar to the definition of reaction yield provided in Section 18.8. The fluorescence quantum yield is also defined as the number of photons emitted as fluorescence divided by the number of photons absorbed. Comparison of this definition to Equation (19.165) demonstrates that the fluorescence quantum yield will be large for molecules in which $k_f$ is significantly greater than other rate constants corresponding to $S_1$ decay. Inverting Equation (19.164) and using the definition of $\tau_f$, the following expression is obtained:

$$\frac{1}{I_f} = \frac{1}{k_a[S_0]}\left(1 + \frac{k_{ic} + k_{isc}^S}{k_f}\right) + \frac{k_q[Q]}{k_a[S_0]k_f} \tag{19.166}$$

For a fluorophore with a quantum yield approaching unity, $k_f \gg k_{ic}$ and $k_{isc}^S$. In fluorescence quenching experiments, fluorescence intensity is measured as a function of $[Q]$. Measurements are generally performed by referencing to the fluorescence intensity observed in the absence of quencher $I_f^0$ such that

$$\frac{I_f^0}{I_f} = 1 + \frac{k_q}{k_f}[Q] \tag{19.167}$$

Equation (19.167) reveals that a plot of the fluorescence intensity ratio as a function of $[Q]$ will yield a straight line, with slope equal to $k_q/k_f$. Such plots are referred to as **Stern–Volmer plots,** an example of which is shown in Figure 19.19.

### 19.9.3 Measurement of $\tau_f$

In the development presented in the preceding subsection, it was assumed that the system of interest was subjected to continuous irradiation so that the steady-state approximation could be applied to $[S_1]$. However, it is often more convenient to photoexcite the system with a temporally short burst of photons or pulse of light. If the temporal duration of the pulse is short compared to the rate of $S_1$ decay, the decay of this state can be measured directly by monitoring the fluorescence intensity as a function of time. Optical pulses as short as 4 fs $(4 \times 10^{-15}\text{ s})$ can be produced that provide excitation on a timescale that is significantly shorter than the decay time of $S_1$.

After excitation by a temporally short optical pulse, the concentration of molecules in $[S_1]$ will be finite. In addition, the rate constant for excitation is zero because $I_0 = 0$; therefore, the differential rate expression for $S_1$ becomes

$$\frac{d[S_1]}{dt} = -k_f[S_1] - k_{ic}[S_1] - k_{isc}^S[S_1] - k_q[Q][S_1]$$

$$\frac{d[S_1]}{dt} = -\frac{[S_1]}{\tau_f} \tag{19.168}$$
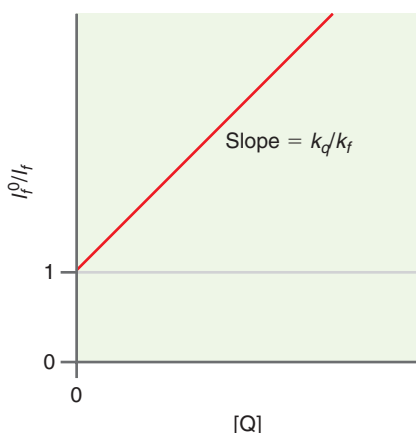


**FIGURE 19.19**
A Stern–Volmer plot. Intensity of fluorescence as a function of quencher concentration is plotted relative to the intensity in the absence of quencher. The slope of the line provides a measure of the quenching rate constant relative to the rate constant for fluorescence.

Equation (19.168) can be solved for $[S_1]$ resulting in

$$[S_1] = [S_1]_0 e^{-t/\tau_f} \tag{19.169}$$

Because the fluorescence intensity is linearly proportional to $[S_1]$ per Equation (19.163), Equation (19.169) predicts that the fluorescence intensity will undergo exponential decay with time constant $\tau_f$. In the limit where $k_f \gg k_{ic}$ and $k_f \gg k_{isc}^S$, $\tau_f$ can be approximated as follows:

$$\lim_{k_f \gg k_{ic}, k_{isc}^S} \tau_f = \frac{1}{k_f + k_q[Q]} \tag{19.170}$$

In this limit, measurement of the fluorescence lifetime at a known quencher concentration combined with the slope from a Stern–Volmer plot is sufficient to uniquely determine $k_f$ and $k_q$. Taking the reciprocal of Equation (19.170), we obtain

$$\frac{1}{\tau_f} = k_f + k_q[Q] \tag{19.171}$$

Equation (19.171) demonstrates that a plot of $(\tau_f)^{-1}$ versus $[Q]$ will yield a straight line with $y$ intercept equal to $k_f$ and slope equal to $k_q$.

### EXAMPLE PROBLEM 19.4

Thomaz and Stevens (in *Molecular Luminescence*, New York: W. A. Benjamin Inc, 1969) studied the fluorescence quenching of pyrene in solution. Using the following information, determine $k_f$ and $k_q$ for pyrene in the presence of the quencher $Br_6C_6$.

| $[Br_6C_6]$ (M) | $\tau_f$ (s) |
|---|---|
| 0.0005 | $2.66 \times 10^{-7}$ |
| 0.001 | $1.87 \times 10^{-7}$ |
| 0.002 | $1.17 \times 10^{-7}$ |
| 0.003 | $8.50 \times 10^{-8}$ |
| 0.005 | $5.51 \times 10^{-8}$ |

### Solution

Using Equation (19.171), a plot of $(\tau_f)^{-1}$ versus $[Q]$ for this system is as follows:
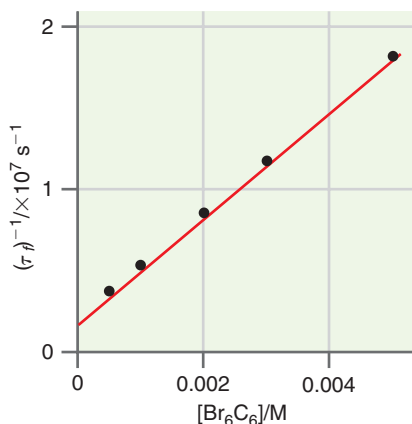


The best fit to the data by a straight line corresponds to a slope of $3.00 \times 10^9 \text{ s}^{-1}$, which is equal to $k_q$ by Equation (19.171), and a $y$ intercept of $1.98 \times 10^6 \text{ s}^{-1}$, which is equal to $k_f$.
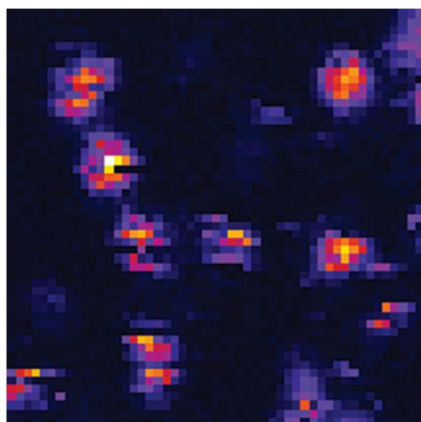
**FIGURE 19.20**
Microscope image of single Rhodamine B dye molecules on glass. Image was obtained using a confocal scanning microscope with the bright spots in the image corresponding to molecular fluorescence. The image dimension is 5 $\mu$m by 5 $\mu$m.

## 19.9.4 Single-Molecule Fluorescence

Equation (19.169) describes how the population of molecules in $S_1$ will change with time, and the fluorescence intensity is predicted to demonstrate exponential decay. This predicted behavior is for a collection, or ensemble, of molecules; however, recent spectroscopic techniques and advances in light detection have allowed for the detection of fluorescence from a single molecule. Figure 19.20 presents an image of single molecules obtained using a confocal scanning microscope. In a confocal microscope, the excitation source and image occur at identical focal distances such that fluorescence from sample areas not directly in focus can be rejected. Using this technique in combination with laser excitation and efficient detectors, it is possible to observe the fluorescence from a single molecule. In Figure 19.20, the bright features represent fluorescence from single molecules. The spatial dimension of these features is determined by the diameter of the light beam at the sample ($\sim$300 nm).

What does the fluorescence from a single molecule look like as a function of time? Instead of a population of molecules in $S_1$ being responsible for the emission, the fluorescence is derived from a single molecule. Figure 19.21 presents the observed fluorescence intensity from a single molecule with continuous photoexcitation. Fluorescence is observed after the light field is turned on, and the molecule cycles between $S_0$ and $S_1$ due to photoexcitation and subsequent relaxation via fluorescence. This regime of constant fluorescence intensity continues until the fluorescence abruptly stops. At this point, depopulation of the $S_1$ state results in the production of $T_1$ or some other state of the molecule that does not fluoresce. Eventually, fluorescence is again observed at later times corresponding to the eventual recovery of $S_0$ by relaxation from these other states, with excitation resulting in the repopulation of $S_1$ followed by fluorescence. This pattern continues until a catastrophic event occurs in which the structural integrity of the molecule is lost. This catastrophic event is referred to as photodestruction, and it results in irreversible photochemical conversion of the molecule to another, nonemissive species.

Clearly, the fluorescence behavior observed in Figure 19.21 is dramatically different than the behavior predicted for an ensemble of molecules. Current interest in this field involves the application of single-molecule techniques to elucidate behavior that is not reflected by the ensemble. Such studies are extremely useful for isolating molecular dynamics from an ensemble of molecules having inherently inhomogeneous behavior. In addition, molecules can be studied in isolation of the bulk, thereby providing a window into the connection between molecular and ensemble behavior.

## 19.9.5 Fluorescence Resonance Energy Transfer

Another fluorescence quenching technique involves the transfer of excitation from one chromophore to another thereby reducing the excited-state population of the initially photoexcited chromophore and correspondingly the fluorescence from this chromophore. This process, known as **fluorescence resonance energy transfer,** or FRET, has been extensively used to measure the structure and dynamics of many biological

**FIGURE 19.21**
Fluorescence from a single Rhodamine B dye molecule. Steady illumination of the single molecule occurs at $t_{on}$, resulting in fluorescence, $I_f$. The fluorescence continues until decay of the $S_1$ state leads to population of a nonfluorescent state. At the end of the time axis, a brief period of fluorescence is observed corresponding to decay of the nonfluorescent state to populate $S_0$ followed by photoexcitation, resulting in the population of $S_1$ and fluorescence. However, this second period of fluorescence ends abruptly due to photodestruction of the molecule as evidenced by the absence of fluorescence after the decay event ($t_{pd}$).
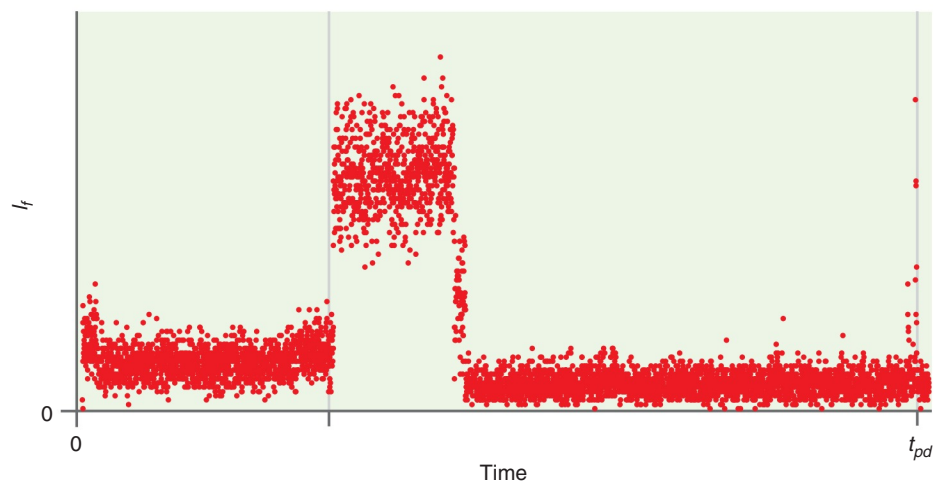
systems. The following mechanism can be employed to describe energy transfer between donor (D) and acceptor (A) chromophores:

$$D \xrightarrow{h\nu} D^* \tag{19.172}$$

$$D^* \xrightarrow{k_f} D \tag{19.173}$$

$$D^* \xrightarrow{k_{nr}} D \tag{19.174}$$

$$D^* + A \xrightarrow{k_{fret}} D + A^* \tag{19.175}$$

$$A^* \xrightarrow{k_{f'}} A \tag{19.176}$$
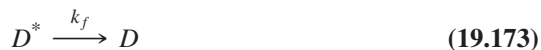
In this scheme, the donor is initially photoexcited, resulting in population of the first-excited singlet state. Decay from this state can occur through fluorescence, nonradiative decay (representing the sum of internal conversion and intersystem crossing), and resonant energy transfer to $A$ resulting in this species populating the first-excited singlet state ($A^*$). Decay of the acceptor excited-state occurs through fluorescence of this species. Proceeding as in the previous section, in the absence of $A$ the mechanism provides the following expression for the fluorescence quantum yield:

$$\Phi_f = \frac{k_f}{k_f + k_{nr}} \tag{19.177}$$

FRET experiments are generally performed with high-fluorescence quantum yield donors where $k_f \gg k_{nr}$. In the presence of $A$ the expression for the fluorescence quantum yield becomes

$$\Phi_{f \text{ w/fret}} = \frac{k_f}{k_f + k_{nr} + k_{fret}} \tag{19.178}$$

The efficiency of excitation transfer is related to the ratio of the fluorescence quantum yields as follows:

$$Eff = 1 - \frac{\Phi_{f \text{ w/fret}}}{\Phi_f} \tag{19.179}$$

This expression illustrates that as $k_{fret}$ becomes greater than $k_f$, the efficiency approaches unity.

What factors influence FRET efficiency? The theory for resonance energy transfer was first developed by T. Förster in the late 1940s. The central ideas inherent in Förster theory are that the efficiency of resonance energy transfer is dependent on the distance between the donor and acceptor, that the absorption band of the acceptor should overlap with the fluorescence band of the donor (that is, $S_0 - S_1$ energy gaps of the donor and acceptors are comparable), and that the relative orientation of the donor and acceptor pair will influence the efficiency of transfer. The distance dependence of the transfer efficiency predicted by Förster theory is

$$Eff = \frac{r_0^6}{r_0^6 + r^6} \tag{19.180}$$

In Equation (19.180), $r$ is the separation distance between donor and acceptor, and $r_0$ is a pair-dependent quantity that defines the distance at which the transfer efficiency is 0.5. The value of $r_0$ depends on the spectral overlap of the donor fluorescence and acceptor absorption as well as the relative orientation between donor and acceptor:

$$r_0(\text{Å}) = 8.79 \times 10^{-5} \left( \frac{\kappa^2 J \Phi_f}{n^4} \right)^{1/6} \tag{19.181}$$

In this expression, $\kappa$ depends on the relative orientation of the transition dipole moments, and is equal to 0 if they are perpendicular, 2 if they are parallel, and 1/3 for random orientation. Since $\kappa$ can be difficult to determine, the random-orientation value for this quantity is

**TABLE 19.2** Values of $R_0$ for FRET Pairs

| Donor | Acceptor | $r_0$ (Å) |
|---|---|---|
| EDANS | DABCYL | 33 |
| Pyrene | Coumarin | 39 |
| Dansyl | Octadecylrhodamine | 43 |
| IAEDANS | Fluorescein | 46 |
| Fluorescein | Tetramethylrhodamine | 55 |

IAEDANS = 5-(((2-iodoacetyl)amino)ethyl)amino)naphthalene-1-sulfonic acid

EDANS = 5-((2-aminoethyl)amino)naphthalene-1-sulfonic acid

DABCYL = 4-((4-(dimethylamino)phenyl)azo)benzoic acid, succinimidyl ester

generally assumed. Also in the expression for $r_0$, $\Phi_f$ is the fluorescence quantum yield of the donor, $n$ is the refractive index of the medium in which the transfer occurs, and $J$ is the overlap integral between the donor fluorescence and acceptor absorption expressed as:

$$J = \int \varepsilon_A(\lambda) F_D(\lambda) \lambda^4 d\lambda \qquad (19.182)$$

In this expression, $\varepsilon_A$ is the extinction coefficient of the acceptor, $F_D$ is the fluorescence spectrum of the donor, and the integral is performed over all wavelengths. The value of this integral, and correspondingly the value for $r_0$, will vary as a function of donor–acceptor pair. To illustrate the connection between donor emission, acceptor absorption, and the overlap integral, Figure 19.22 presents the emission and absorption for the fluorescein/tetramethylrhodamine (TMR) FRET pair, and provides an illustration of $J$ for this FRET pair.

A collection of FRET donor–acceptor pairs are presented in Table 19.2. When using FRET to measure distance, it is critical to choose a donor–acceptor pair whose $r_0$ is close to the length scale of interest. For distances where $r \gg r_0$, the FRET efficiency will be 0 so that the fluorescence quantum yield of the donor will be largely unaffected by the presence of the acceptor. In the other limit where $r_0 \gg r$, the quenching of the donor fluorescence from energy transfer will be extremely efficient and little emission from the donor will be observed. The overlap between the fluorescein emission and TMR absorption is shown.

### EXAMPLE PROBLEM 19.5

You are designing a FRET experiment to determine the magnitude of the structural change introduced by substrate binding to an enzyme. Using site-specific mutagenesis, you have constructed a mutant form of the enzyme that possesses a single tyrosine residue and a single tryptophan residue, and these residues are separated by 11 Å. You would like to determine if the distance between these residues changes with substrate binding. The fluorescence of tyrosine overlaps with the tryptophan absorption; therefore, these two amino acids form a FRET pair for which $r_0 = 9$ Å, determined using the absorption and emission spectra in combination with Equation (19.181). Calculate the FRET efficiency at 11 Å separation and how much this distance must increase in order for the efficiency to decrease by 20%, the experimental detection limit.

### Solution

Using the initial separation distance and $r_0$, the efficiency is determined as follows:

$$Eff = \frac{r_0^6}{r_0^6 + r^6} = \frac{(9 \text{ Å})^6}{(9 \text{ Å})^6 + (11 \text{ Å})^6} = 0.23$$

The detection limit corresponds to $Eff = 0.18$. Solving for $r$ yields:

$$Eff = 0.18 = \frac{r_0^6}{r_0^6 + r^6} = \frac{(9 \text{ Å})^6}{(9 \text{ Å})^6 + r^6}$$
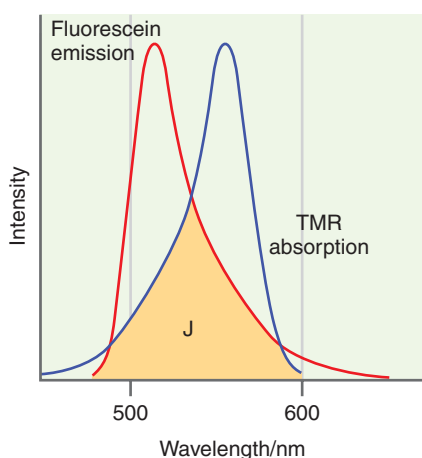


**FIGURE 19.22**
Illustration of the overlap integral ($J(\lambda)$) for the fluorescein/tetramethylrhodamine (TMR) FRET donor–acceptor pair.

$$\frac{(9\ \text{Å})^6}{0.18} = (9\ \text{Å})^6 + r^6$$

$$2.42 \times 10^6\ \text{Å}^6 = r^6$$

$$11.6\ \text{Å} = r$$

Notice that for this FRET pair the modification of the tyrosine–tryptophan separation accompanying substrate binding can be measured for a relatively limited change in $r$. This example illustrates the importance of choosing FRET pairs having $r_0$ values that are close to the length scale of interest.

An important application of resonant energy transfer involves light harvesting in photosynthetic pigments. The absorption of light is enabled by light-harvesting by antenna pigments contained in the thylakoid membranes of the chloroplast, the photosynthetic organelles of green plants and algae. These systems have evolved such that light primarily in the visible and near-infrared regions of the electromagnetic spectrum are absorbed corresponding to electronic transitions of the pigments. The most abundant plant pigments are chlorophylls $a$ and $b$ as illustrated in Figure 19.23. In addition, carotenoids such as $\beta$-carotene also serve as light-harvesting pigments. These light-harvesting pigments are organized into light-harvesting complexes. X-ray crystallographic studies have shown that the chlorophyll molecules are arranged in symmetric cyclical structures in the light-harvesting complexes. The structure of light-harvesting complex II consisting of chlorophyll and $\beta$-carotene is shown in Figure 19.23. This spatial arrangement of light-harvesting pigments provides for efficient inter-pigment transfer once a photon is absorbed and for transfer of this energy outside the light-harvesting complex.

The biological purpose of light-harvesting complexes is to absorb solar radiation and through resonance energy transfer deliver this energy to the reaction center. The intensity of sunlight is such that the probability of a chlorophyll molecule absorbing a photon is extremely modest. Incorporating numerous chlorophylls into a single light-harvesting complex provides for maximum collection efficiency. Resonance energy transfer results in the migration of absorbed photon energy from the light-harvesting complex to the reaction center as illustrated in Figure 19.24. Once the energy is transferred to the reaction center, it initiates an electron transfer process that is the start of

**FIGURE 19.23**
**Left.** Structures of photosynthetic light-harvesting pigments chlorophyll (a), $\beta$-carotene (b), and phycoerythrin (c). Chlorophylls $a$ and $b$ are the most abundant plant pigments. **Right.** X-ray crystal structure of the light-harvesting complex II of purple photosynthetic bacteria. The pigments, including bacteriochlorophyll (green) are held in this spatially complex arrangement by the surrounding protein (parts of which are shown in red and white).
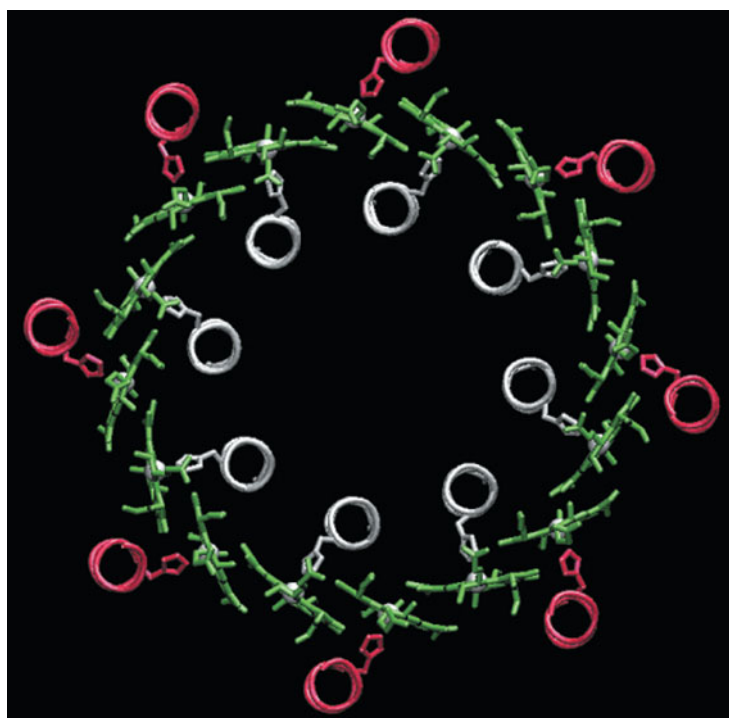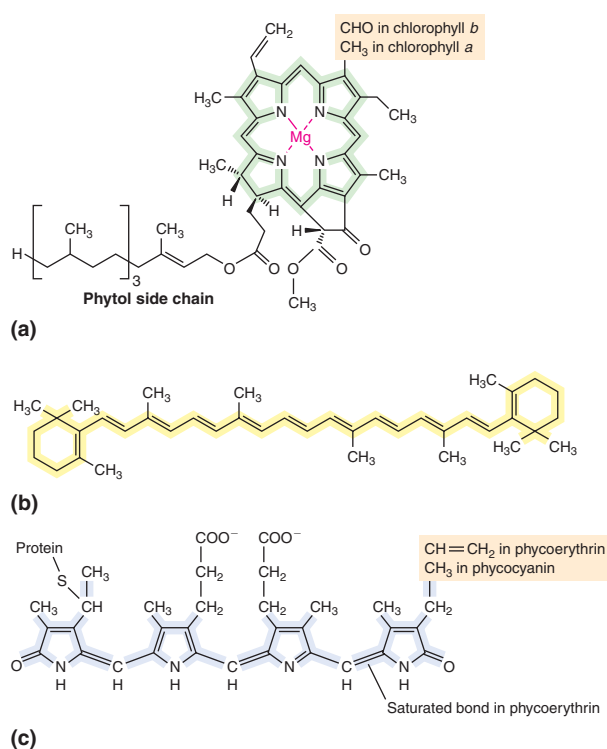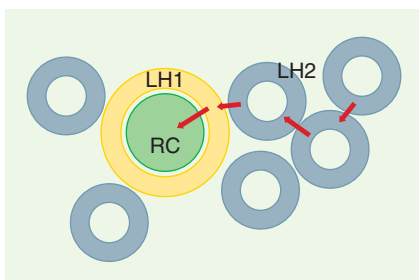


(a)

(b)

(c)

the chemical transformations involved in photosynthesis. This electron transfer reaction will be further explored in the upcoming section on electron transfer.

### 19.9.6 Photochemical Processes

As discussed earlier, photochemical processes are distinct from photophysical processes in that the absorption of a photon results in chemical transformation of the reactant. For a photochemical process that occurs through the first excited singlet state $S_1$, a photochemical reaction can be viewed kinetically as another reaction branch, resulting in the decay of $S_1$. The corresponding expression for the rate corresponding to this photochemical reaction branch is

$$R_{photochem.} = k^S_{photo}[S_1] \quad\quad \textbf{(19.183)}$$

where $k_{photo}$ is the rate constant for the photochemical reaction. For photochemical processes occurring through $T_1$, a rate expression similar to Equation (19.183) can be constructed as follows:

$$R_{photochem.} = k^T_{photo}[T_1] \quad\quad \textbf{(19.184)}$$

The absorption of a photon can also provide sufficient energy to initiate a chemical reaction. However, given the range of photophysical processes that occurs, absorption of a photon is not sufficient to guarantee that the photochemical reaction will occur. The extent of photochemistry is quantified by the overall **quantum yield** $\phi$, which is defined as the number of reactant molecules consumed in photochemical processes per photon absorbed. The overall quantum yield can be greater than one, as demonstrated by the photoinitiated decomposition of $HI(g)$ that proceeds by the following mechanism:

$$HI + h\nu \rightarrow H\cdot + I\cdot \quad\quad \textbf{(19.185)}$$

$$H\cdot + HI \rightarrow H_2 + I\cdot \quad\quad \textbf{(19.186)}$$

$$I\cdot + I\cdot \rightarrow I_2 \qu\quad \textbf{(19.187)}$$

In this mechanism, absorption of a photon results in the loss of two HI molecules such that $\phi = 2$. In general, the overall quantum yield can be determined experimentally by comparing the molecules of reactant lost to the number of photons absorbed as illustrated in Example Problem 19.6.

---

### EXAMPLE PROBLEM 19.6

The reactant 1,3-cyclohexadiene can be photochemically converted to *cis*-hexatriene. In an experiment, 2.5 mmol of cyclohexadiene are converted to *cis*-hexatriene when irradiated with 100. W of 280. nm light for 27.0 s. All of the light is absorbed by the sample. What is the overall quantum yield for this photochemical process?

#### Solution

First, the total photon energy absorbed by the sample, $E_{abs}$, is

$$E_{abs} = (power)\Delta t = (100. \, J\,s^{-1})(27.0 \, s) = 2.70 \times 10^3 \, J$$

Next, the photon energy at 280. nm is

$$E_{ph} = \frac{hc}{\lambda} = \frac{(6.626 \times 10^{-34} \, J\,s)(2.998 \times 10^8 \, m\,s^{-1})}{2.80 \times 10^{-7} \, m} = 7.10 \times 10^{-19} \, J$$

The total number of photons absorbed by the sample is therefore

$$\frac{E_{abs}}{E_{ph}} = \frac{2.70 \times 10^3 \, J}{7.10 \times 10^{-19} \, J \, photon^{-1}} = 3.80 \times 10^{21} \, photons$$

Dividing this result by Avogadro's number results in $6.31 \times 10^{-3}$ Einsteins or moles of photons. Therefore, the overall quantum yield is

$$\phi = \frac{moles_{react}}{moles_{photon}} = \frac{2.50 \times 10^{-3} \, mol}{6.31 \times 10^{-3} \, mol} = 0.396 \approx 0.40$$

# 19.10 Electron Transfer

**Electron transfer** reactions involve the exchange of charge between chemical species. These reactions are ubiquitous in biological chemistry. For example, photosynthesis involves electron transfer in biological energy transduction. In plants, the net reaction from photosynthesis is the conversion of $CO_2(g)$ and $H_2O(l)$ to form carbohydrates and molecular oxygen:

$$6CO_2(g) + 6H_2O(l) \rightarrow C_6H_{12}O_6(s) + 6O_2(g) \qquad \Delta G° = 2870 \text{ kJ}$$
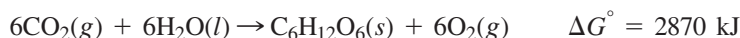
Photosynthesis also occurs in certain bacteria. For example, in green sulfur bacteria $H_2S$ serves as the reactant rather than water:

$$2H_2S(aq) + CO_2(g) \rightarrow CH_2O(g) + H_2O(l) + 2S(rh) \qquad \Delta G° = 88 \text{ kJ}$$
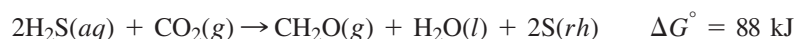
In these reactions, the carbon in $CO_2(g)$ is reduced and $H_2O/H_2S$ is oxidized such that net reactions involve the electron transfer. Although photosynthesis is based on a series of coupled reactions rather than the single-step reaction shown earlier, the net reactions do illustrate the importance of electron transfer in this process.

In the previous section we discussed the transfer of radiative energy from the light-harvesting complex to the photosynthetic reaction center. The radiative energy transferred to the reaction center is used to initiate an electron transfer reaction from a pair of chlorophyll molecules (known as the special pair) to a nearby pheophytin molecule (structurally similar to chlorophyll). This process is extremely fast, occurring in approximately 3 ps ($3 \times 10^{-12}$ s). A second electron transfer process occurs in which the electron on the pheophytin is transferred to a quinone in 200 ps. Ultimately, the electron is transferred to a second quinone in 100 μs. The electrons on the quinone are used to "split" water as follows:

$$2H_2O(l) \rightarrow O_2(g) + 4H^+(aq) + 4e^-$$
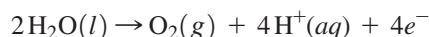
The electrons and hydrogen ions are transported in a series of sequential reactions ultimately resulting in the production of carbohydrate and molecular oxygen. The net effect of this transport is to create a transmembrane proton gradient that is used by the cell to drive ATP synthesis. Given the importance of electron transfer in photosynthesis and other areas of biological chemistry discussed earlier in the text, in this section we investigate simple kinetic models for charge transfer and explore **Marcus theory** for describing electron transfer processes.

## 19.10.1 Kinetic Model of Electron Transfer

Electron transfer involves the exchange of an electron from a donor molecule ($D$) to an acceptor molecule (A) resulting in donor oxidation ($D^+$) and reduction of the acceptor ($A^-$):

$$D + A \rightleftharpoons D^+ + A^- \tag{19.188}$$

The reaction mechanism employed to describe bimolecular electron transfer in solution is as follows. First, the donor and acceptor form the donor–acceptor complex by diffusing in solution until these species come in contact. Formation of the donor–acceptor complex is modeled as a reversible process; therefore,

$$D + A \underset{k_{d'}}{\overset{k_d}{\rightleftharpoons}} DA \tag{19.189}$$

In the next step of the mechanism, electron transfer from the donor to the acceptor occurs in the complex. In addition, the back-electron transfer process is also possible, corresponding to reformation of the donor–acceptor complex:

$$DA \underset{k_{b-et}}{\overset{k_{et}}{\rightleftharpoons}} D^+A^- \tag{19.190}$$

In the final step of the mechanism, the post-electron transfer complex separates to form isolated oxidized donor and reduced acceptor:

$$D^+A^- \xrightarrow{k_{sep}} D^+ + A^- \qquad (19.191)$$

The expression for the rate of reaction consistent with this mechanism is derived as follows. The last step of the mechanism results in the formation of products; therefore, the reaction rate can be written as

$$R = k_{sep}[D^+A^-] \qquad (19.192)$$

Writing the differential-rate expression for $D^+A^-$ and applying the steady-state approximation results in the following expression for $[D^+A^-]$:

$$\frac{d[D^+A^-]}{dt} = 0 = k_{et}[DA] - k_{b-et}[D^+A^-] - k_{sep}[D^+A^-]$$

$$[D^+A^-] = \frac{k_{et}[DA]}{k_{b-et} + k_{sep}} \qquad (19.193)$$

The donor–acceptor complex ($DA$) is also an intermediate; therefore, writing the differential rate expression for this species and applying the steady-state approximation yields

$$\frac{d[DA]}{dt} = 0 = k_d[D][A] - k_{d'}[DA] - k_{et}[DA] + k_{b-et}[D^+A^-]$$

$$[DA] = \frac{k_d[D][A] + k_{b-et}[D^+A^-]}{k_{d'} + k_{et}} \qquad (19.194)$$

Substituting this result into the expression for $[D^+A^-]$ results in the following:

$$[D^+A^-] = \frac{k_{et}[DA]}{k_{b-et} + k_{sep}} = \left(\frac{k_{et}}{k_{b-et} + k_{sep}}\right)\left(\frac{k_d[D][A] + k_{b-et}[D^+A^-]}{k_{d'} + k_{et}}\right)$$

$$[D^+A^-] = \frac{k_{et}k_d}{k_{b-et}k_{d'} + k_{sep}k_{d'} + k_{sep}k_{et}}[D][A] \qquad (19.195)$$

Using this expression for $[D^+A^-]$, the reaction rate becomes

$$R = \frac{k_{sep}k_{et}k_d}{k_{b-et}k_{d'} + k_{sep}k_{d'} + k_{sep}k_{et}}[D][A] \qquad (19.196)$$

The reaction is predicted to be first order with respect to both donor and acceptor concentrations (as expected), and the apparent microscopic rate constant is a composite of the microscopic rate constants for the various steps in the mechanism. If we assume that dissociation of the post-electron transfer complex is rapid compared to back-electron transfer $(k_{sep} \gg k_{b-et})$, then the reaction rate becomes

$$R = \frac{k_{et}k_d}{k_{d'} + k_{et}}[D][A] \qquad (19.197)$$

Finally, if the rate constant for electron transfer is sufficiently large relative to dissociation of the donor–acceptor complex $(k_{et} \gg k_{d'})$, then formation of the donor acceptor becomes the rate-limiting step and electron transfer becomes a diffusion-controlled reaction as described in the previous chapter. In the opposite limit $(k_{et} \ll k_{d'})$, electron transfer becomes the rate-limiting step and the expression for the reaction rate becomes

$$R_{k_{d'} \gg k_{et}} = k_{et}K_{d,d'}[D][A] = k_{exp}[D][A] \qquad (19.198)$$

In this expression, $K_{d,d'}$ is the equilibrium constant for the $D + A \rightleftharpoons DA$ step of the reaction mechanism described earlier, and $k_{exp}$ is the experimentally measured rate constant. In this limit, the rate of electron transfer is determined by the rate constant for the transfer process itself. This later limit is also representative of systems in which the donor and acceptor are already in contact (for example, by covalently linking the donor

and acceptor), and in many biological systems in which the electron donor and acceptor are held at a fixed distance by the surrounding protein matrix.

## 19.10.2  Marcus Theory

What factors determine the magnitude of the observed rate constant for electron transfer? The kinetic model for electron transfer presented earlier suggests two important factors in determining the value of $k_{exp}$. First, the model requires that donor and acceptor be in proximity before electron transfer can occur. Therefore, the rate constant should depend on the separation distance between the donor and acceptor. This distance dependence is expressed as

$$k_{exp} \propto e^{-\beta r} \tag{19.199}$$

In this expression, $\beta$ is a constant that varies as a function of the system of interest and the medium in which electron transfer occurs, and $r$ is the donor–acceptor separation distance. The second factor that influences the observed rate constant is thermodynamic in origin. If the charge transfer occurs over an energy barrier, we can refer back to transition state theory described in the previous chapter and model this barrier as the difference in free energy between the donor–acceptor complex and the activated complex corresponding to the free-energy maximum along the reaction coordinate connecting the donor–acceptor complex with the complex after electron transfer. Therefore, the experimentally observed rate constant for electron transfer depends on the Gibbs energy of activation $\Delta G^{\ddagger}$ as follows:

$$k_{exp} \propto e^{-\Delta G^{\ddagger}/kT} \tag{19.200}$$

Therefore, the rate constant for electron transfer can be written as

$$k_{exp} \propto e^{-\beta r} e^{-\Delta G^{\ddagger}/kT} \tag{19.201}$$

Rudolph Marcus received the Nobel Prize in Chemistry in 1992 for his contributions to defining this relationship and exploring the chemical factors that are important in determining the value of $\Delta G^{\ddagger}$. Specifically, Marcus noted that after electron transfer both the solvent and solute will undergo relaxation. For the solutes, the transfer of an electron will result in a change in bond order and the nuclei will relax to assume new equilibrium geometries. The solvent will rearrange in response to the change in charge distribution accompanying the formation of $D^{+}$ and $A^{-}$. Taking these factors into account, Marcus defined the Gibbs energy of activation in terms of the standard change in Gibbs energy accompanying the charge transfer ($DA \rightleftharpoons D^{+}A^{-}$) and the change in Gibbs energy accompanying relaxation of the solvent and solute, referred to as the **reorganization energy** or $\lambda$:

$$\Delta G^{\ddagger} = \frac{(\Delta G^{\circ} + \lambda)^2}{4\lambda} \tag{19.202}$$

The reorganization energy can be thought of as the Gibbs energy accompanying rearrangement of bonds in the donor and acceptor as well as solvent rearrangement of accompanying evolution along the electron-transfer reaction coordinate. This expression demonstrates that the Gibbs energy of activation will be at a minimum when $-\Delta G^{\circ} = \lambda$. If the separation distance of the donor and acceptor is fixed, then the experimentally observed rate constant will be greatest at this value of $\Delta G^{\circ}$. A sketch of $\ln(k_{exp})$ versus $-\Delta G^{\circ}$ is presented in Figure 19.25. The maximum in the rate constant occurs when $-\Delta G^{\circ} = \lambda$, but notice that the rate constant is predicted to decrease as the charge-transfer state decreases in free energy relative to the neutral state. This is the so-called Marcus inverted regime of electron transfer.

The connection between the rate constant for reaction and the Gibbs energy for the reactants and products is presented in Figure 19.26. Two curves are shown, one representing the neutral donor and acceptor, and the other representing the donor cation and acceptor anion formed as a result of electron transfer. The potential energy surfaces representing donor and acceptor configurations are parabolic, consistent with the quadratic dependence of energy with displacement along nuclear vibrational coordinates (i.e., $V(x) = 1/2\, kx^2$ where $k$ is the force constant of the bond and $x$ is displacement). The electron transfer occurs at the point along the reaction coordinate where the two
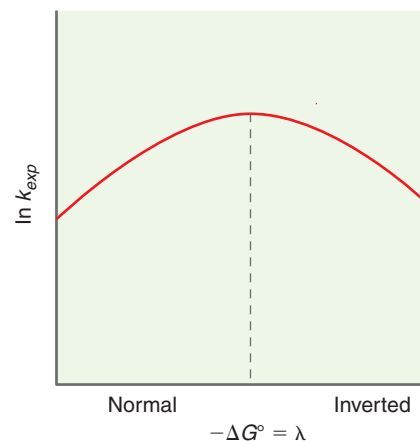


**FIGURE 19.25**

Illustration of the Marcus normal and inverted regimes. The experimentally measured rate constant is predicted to increase as the driving force for the reaction increases corresponding to the normal regime, and be at a maximum when $-\Delta G^{\circ} = \lambda$. As the driving force for the reaction increases beyond this point, the rate constant should decrease corresponding to the inverted regime.

**FIGURE 19.26**
Plots of the Gibbs energy versus the
reaction coordinate for electron transfer.
Three different values for $\Delta G°$ are
presented corresponding to the normal,
maximum, and inverted Marcus regimes.
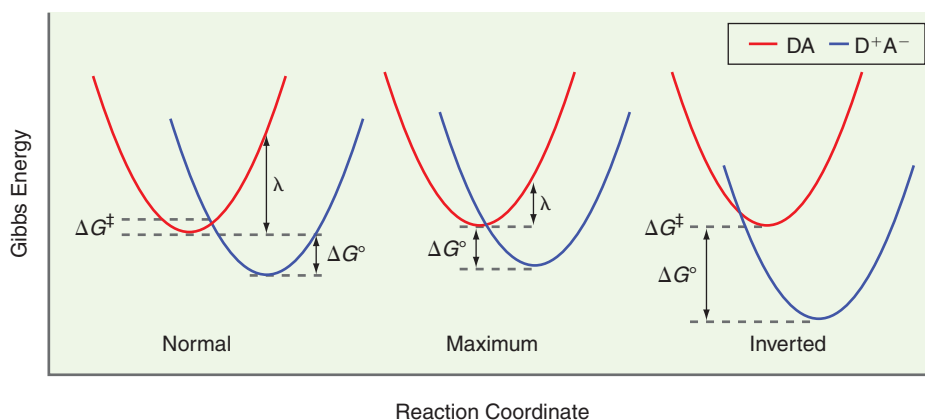


curves cross so that energy is conserved in the transfer. In addition, electron transfer is
considered to be rapid compared to nuclear motion; therefore, the transfer occurs at one
point along the reaction coordinate. In the normal regime, the value of $\Delta G°$ is such that
there is a barrier to electron transfer that must be overcome. This barrier corresponds to
$\Delta G^{\ddagger}$ as described earlier. As the Gibbs energy of the charge transfer state is reduced
relative to that of the reactant state, the thermodynamic driving force for the reaction
increases, and when $-\Delta G° = \lambda$, the electron transfer is predicted to be a barrierless
process corresponding to a maximum in the rate constant for electron transfer. A fur-
ther decrease in the Gibbs energy of the products relative to the reactants results in an
increased barrier to electron transfer and corresponding reduction in the reaction rate
constant, corresponding to the Marcus inverted regime.

A significant amount of experimental research has been performed to test the valid-
ity of Marcus theory, and in particular to obtain evidence for the inverted regime. One
successful demonstration of the inverted regime is illustrated in Figure 19.27. Here, the
biphenyl donor was connected to a variety of acceptors through a cyclohexane scaffold.
As the acceptor is changed, $\Delta G°$ is altered. The data clearly illustrate a decrease in the
observed rate constant for electron transfer with increased driving force for the reaction
beyond ~1.1 eV. For other systems inverted-regime behavior has not been observed.
In these systems, the participation of solute vibrational degrees of freedom in the elec-
tron transfer process decreases the barrier to formation of the activated complex in the
inverted regime; therefore, the rate constant remains close to the maximum value even
as the driving force for the reaction increases.

### EXAMPLE PROBLEM 19.7

The experimental results presented earlier demonstrate that a maximum in the rate
constant for electron transfer ($\sim 2.0 \times 10^9$ s$^{-1}$) occurs when $-\Delta G° = 1.20$ eV.
Given this observation, estimate the rate constant for electron transfer when
2-naphthoquinoyl is employed as the acceptor for which $-\Delta G° = 1.93$ eV.

#### Solution

The rate constant for electron transfer is predicted to be at a maximum when
$-\Delta G° = \lambda$; therefore, $\lambda = 1.20$ eV. Using this information, the barrier to electron
transfer is determined as follows:

$$\Delta G^{\ddagger} = \frac{(\Delta G° + \lambda)^2}{4\lambda} = \frac{(-1.93 \text{ eV} + 1.20 \text{ eV})^2}{4(1.20 \text{ eV})} = 0.111 \text{ eV}$$

With the barrier to electron transfer, the rate constant is estimated as follows:

$$\frac{k_{1.93 \text{ eV}}}{k_{\max}} = e^{-\Delta G^{\ddagger}/kT} = exp\left(-0.111 \text{ eV} \times \frac{1.60 \times 10^{-19} \text{J}}{\text{eV}} \middle/ \left(1.38 \times 10^{-23} \text{J K}^{-1}\right)(296 \text{ K})\right)$$

$$= 0.0129$$

$$k_{1.93 \text{ eV}} = k_{\max} (0.0129) = (2.0 \times 10^9 \text{ s}^{-1})(0.0129) = 2.6 \times 10^7 \text{ s}^{-1}$$
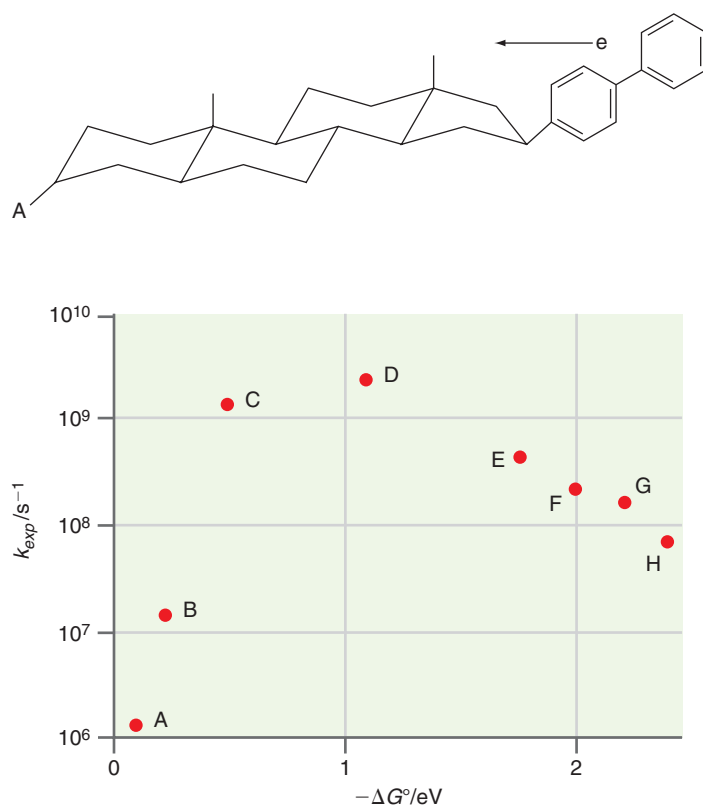
**FIGURE 19.27**
Experimental verification of the Marcus inverted regime in electron transfer. In this experiment, the electron transfer rates between the biphenyl donor and the various acceptors were measured in 2-methyltetrahydrofuran at 296 K. Notice that the rate constant reaches a maximum and then decreases as $-\Delta G°$ increases corresponding to an increase in driving force for the reaction. Figure adapted from Miller et al., *J. American Chemical Society*, 106 (1984): 3047.
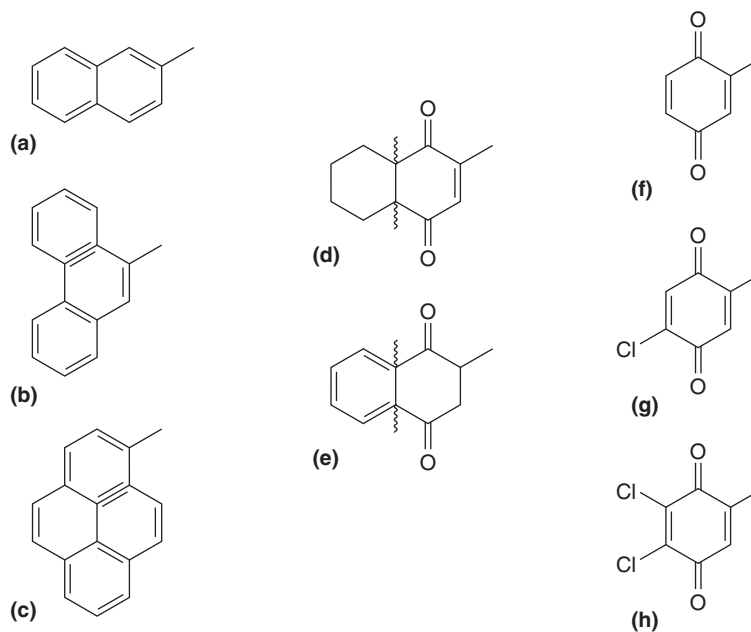
# Vocabulary

| | | |
|---|---|---|
| absorption cross section | Belousov-Zhabotinsky (BZ) reaction | collisional quenching |
| activated reactant | branching reaction | competitive inhibitor |
| adsorption isotherm | catalyst | complex reaction |
| autocatalysis | chemisorption | composite constant |

| | | |
|---|---|---|
| electron transfer | Lineweaver–Burk equation | propagation step |
| enzymes | Lineweaver–Burk plot | quantum yield |
| feedback | Lotka-Volterra mechanism | radiative transitions |
| fluorescence | Marcus theory | radical |
| fluorescence lifetime | Michaelis constant | radical polymerization reaction |
| fluorescence resonance energy transfer | Michaelis–Menten mechanism | reaction intermediate |
| fractional coverage | Michaelis–Menten rate law | reaction mechanism |
| heterogeneous catalyst | molar absorptivity | reciprocal plot |
| homogeneous catalyst | nonlinear reaction | reorganization energy |
| initiation step | oscillating reaction | simple reaction |
| internal conversion | phosphorescence | Stern–Volmer plot |
| intersystem crossing | photochemistry | stoichiometric number |
| Jablonski diagram | photophysical processes | substrate–catalyst complex |
| Langmuir isotherm | physisorption | termination step |
| Langmuir model | polymer chain | turnover number |
| Lindemann mechanism | preequilibrium approximation | unimolecular reactions |

# Conceptual Problems

**Q19.1** How is a simple reaction different from a complex reaction?

**Q19.2** For a reaction mechanism to be considered correct, what property must it demonstrate?

**Q19.3** What is a reaction intermediate? Can an intermediate be present in the rate law expression for the overall reaction?

**Q19.4** What is the preequilibrium approximation, and under what conditions is it considered valid?

**Q19.5** What is the main assumption in the Lindemann mechanism for unimolecular reactions?

**Q19.6** How is a catalyst defined, and how does such a species increase the reaction rate?

**Q19.7** What is an enzyme? What is the general mechanism describing enzyme catalysis?

**Q19.8** What is the Michaelis–Menten rate law? What is the maximum reaction rate predicated by this rate law?

**Q19.9** How is the standard enzyme kinetic scheme modified to incorporate competitive inhibition? What plot is used to establish competitive inhibition and to determine the kinetic parameters associated with inhibition?

**Q19.10** What is the difference between a homogeneous and a heterogeneous catalyst?

**Q19.11** What are the inherent assumptions in the Langmuir model of surface adsorption?

**Q19.12** What is a radical? What elementary steps are involved in a reaction mechanism involving radicals?

**Q19.13** In what ways are radical polymerization reactions similar to radical reactions in general?

**Q19.14** What is autocatalysis?

**Q19.15** What is an oscillating reaction?

**Q19.16** What is photochemistry? How does one calculate the energy of a photon?

**Q19.17** What depopulation pathways occur from the first excited singlet state? For the first excited triplet state?

**Q19.18** What is the expected variation in excited state lifetime with quencher concentration in a Stern–Volmer plot?

**Q19.19** What is the distance dependence for fluorescence resonance energy transfer predicted by the Förster model?

**Q19.20** What two factors influence the electron transfer rate constant according to Marcus theory?

# Numerical Problems

Problem numbers in **red** indicate that the solution to the problem is given in the *Student's Solutions Manual*.

**P19.1** A proposed mechanism for the formation of $N_2O_5(g)$ from $NO_2(g)$ and $O_3(g)$ is

$$NO_2(g) + O_3(g) \xrightarrow{k_1} NO_3(g) + O_2(g)$$

$$NO_2(g) + NO_3(g) + M(g) \xrightarrow{k_2} N_2O_5(g) + M(g)$$
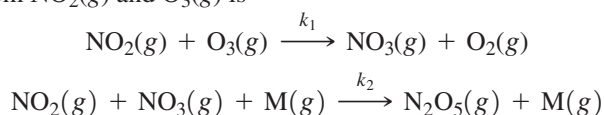
Determine the rate law expression for the production of $N_2O_5(g)$ given this mechanism.

**P19.2** The reaction of nitric oxide ($NO(g)$) with molecular hydrogen ($H_2(g)$) results in the production of molecular nitrogen and water as follows:

$$2NO(g) + 2H_2(g) \rightarrow N_2O(g) + 2H_2O(g)$$
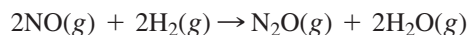
The experimentally-determined rate-law expression for this reaction is first order in $H_2(g)$ and second order in $NO(g)$.

**a.** Is the reaction as written consistent with the experimental order dependence for this reaction?

**b.** One potential mechanism for this reaction is as follows:

$$H_2(g) + 2NO(g) \xrightarrow{k_1} N_2O(g) + H_2O(g)$$

$$H_2(g) + N_2O(g) \xrightarrow{k_2} N_2(g) + H_2O(g)$$
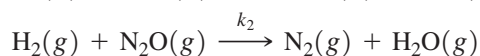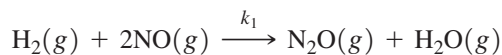
Is this mechanism consistent with the experimental rate law?

**c.** An alternative mechanism for the reaction is

$$2NO(g) \underset{k_{-1}}{\overset{k_1}{\rightleftharpoons}} N_2O_2(g) \text{ (fast)}$$

$$H_2(g) + N_2O_2(g) \xrightarrow{k_2} N_2O(g) + H_2O(g)$$

$$H_2(g) + N_2O(g) \xrightarrow{k_3} N_2(g) + H_2O(g)$$
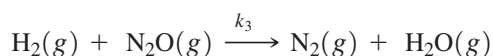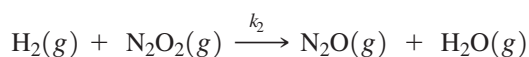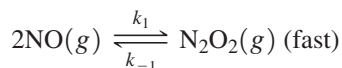
Show that this mechanism is consistent with the experimental rate law.

**P19.3** In the troposphere carbon monoxide and nitrogen dioxide undergo the following reaction:

$$NO_2(g) + CO(g) \rightarrow NO(g) + CO_2(g)$$
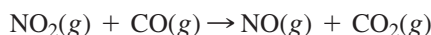
Experimentally, the rate law for the reaction is second order in $NO_2(g)$, and $NO_3(g)$ has been identified as an intermediate in this reaction. Construct a reaction mechanism that is consistent with these experimental observations.

**P19.4** The Rice–Herzfeld mechanism for the thermal decomposition of acetaldehyde ($CH_3CO(g)$) is

$$CH_3CHO(g) \xrightarrow{k_1} CH_3\cdot(g) + CHO\cdot(g)$$

$$CH_3\cdot(g) + CH_3CHO(g) \xrightarrow{k_2} CH_4(g) + CH_2CHO\cdot(g)$$

$$CH_2CHO\cdot(g) \xrightarrow{k_3} CO(g) + CH_3\cdot(g)$$

$$CH_3\cdot(g) + CH_3\cdot(g) \xrightarrow{k_4} C_2H_6(g)$$
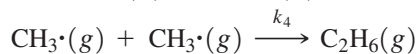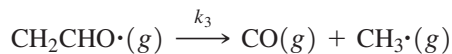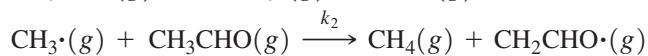
Using the steady-state approximation, determine the rate of methane ($CH_4(g)$) formation.

**P19.5** Consider the following mechanism for ozone thermal decomposition:

$$O_3(g) \underset{k_{-1}}{\overset{k_1}{\rightleftharpoons}} O_2(g) + O(g)$$

$$O_3(g) + O(g) \xrightarrow{k_2} 2O_2(g)$$
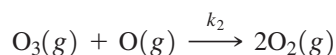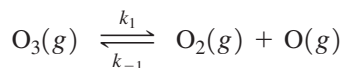
**a.** Derive the rate law expression for the loss of $O_3(g)$.

**b.** Under what conditions will the rate law expression for $O_3(g)$ decomposition be first order with respect to $O_3(g)$?

**P19.6** Consider the formation of double-stranded (DS) DNA from two complementary single strands (S and S′) through the following mechanism involving an intermediate helix (IH):

$$S + S' \underset{k_{-1}}{\overset{k_1}{\rightleftharpoons}} IH$$

$$IH \xrightarrow{k_2} DS$$
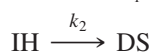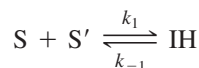
**a.** Derive the rate law expression for this reaction employing the preequilibrium approximation.

**b.** What is the corresponding rate-law expression for the reaction employing the steady state approximation for the intermediate IH?

**P19.7** The hydrogen–bromine reaction corresponds to the production of $HBr(g)$ from $H_2(g)$ and $Br_2(g)$ as follows: $H_2(g) + Br_2(g) \rightleftharpoons 2HBr(g)$. This reaction is famous for its complex rate law, determined by Bodenstein and Lind in 1906:

$$\frac{d[HBr]}{dt} = \frac{k[H_2][Br_2]^{1/2}}{1 + \dfrac{m[HBr]}{[Br_2]}}$$

where $k$ and $m$ are constants. It took 13 years for a likely mechanism of this reaction to be proposed, and this feat was accomplished simultaneously by Christiansen, Herzfeld, and Polyani. The mechanism is as follows:

$$Br_2(g) \underset{k_{-1}}{\overset{k_1}{\rightleftharpoons}} 2Br\cdot(g)$$

$$Br\cdot(g) + H_2(g) \xrightarrow{k_2} HBr(g) + H\cdot(g)$$

$$H\cdot(g) + Br_2(g) \xrightarrow{k_3} HBr(g) + Br\cdot(g)$$

$$HBr(g) + H\cdot(g) \xrightarrow{k_4} H_2(g) + Br\cdot(g)$$
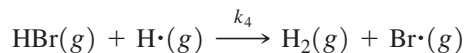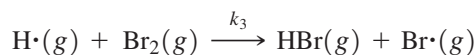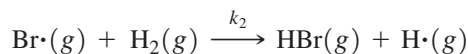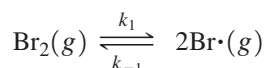
Construct the rate law expression for the hydrogen–bromine reaction by performing the following steps:

**a.** Write down the differential rate expression for [HBr].

**b.** Write down the differential rate expressions for [Br·] and [H·].

**c.** Because $Br\cdot(g)$ and $H\cdot(g)$ are reaction intermediates, apply the steady-state approximation to the result of part (b).

**d.** Add the two equations from part (c) to determine [Br·] in terms of [Br$_2$].

**e.** Substitute the expression for [Br·] back into the equation for [H·] derived in part (c) and solve for [H·].

**f.** Substitute the expressions for [Br·] and [H·] determined in part (e) into the differential rate expression for [HBr] to derive the rate law expression for the reaction.

**P19.8**

**a.** For the hydrogen–bromine reaction presented in Problem P19.7 imagine initiating the reaction with only $Br_2$ and $H_2$ present. Demonstrate that the rate law expression at $t = 0$ reduces to

$$\left(\frac{d[HBr]}{dt}\right)_{t=0} = 2k_2\left(\frac{k_1}{k_{-1}}\right)^{1/2}[H_2]_0[Br_2]_0^{1/2}$$

**b.** The activation energies for the rate constants are as follows:

| Rate Constant | $\Delta E_a$ (kJ/mol) |
|:---:|:---:|
| $k_1$ | 192 |
| $k_2$ | 0 |
| $k_{-1}$ | 74 |

What is the overall activation energy for this reaction?

**c.** How much will the rate of the reaction change if the temperature is increased to 400. K from 298 K?

**P19.9** For the reaction $I^-(aq) + OCl^-(aq) \rightleftharpoons OI^-(aq) + Cl^-(aq)$ occurring in aqueous solution, the following mechanism has been proposed:

$$OCl^-(aq) + H_2O(l) \underset{k_{-1}}{\overset{k_1}{\rightleftharpoons}} HOCl(aq) + OH^-(aq)$$

$$I^-(aq) + HOCl(aq) \overset{k_2}{\longrightarrow} HOI(aq) + Cl^-(aq)$$

$$HOI(aq) + OH^-(aq) \overset{k_3}{\longrightarrow} H_2O(l) + OI^-(aq)$$
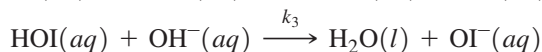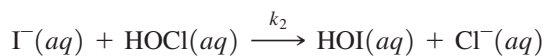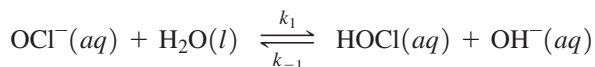
**a.** Derive the rate law expression for this reaction based on this mechanism. (*Hint:* [OH$^-$] should appear in the rate law.)

**b.** The initial rate of reaction was studied as a function of concentration by Chia and Connick [*J. Physical Chemistry* 63 (1959): 1518], and the following data were obtained:

| $[I^-]_0$ (M) | $[OCl^-]_0$ (M) | $[OH^-]_0$ (M) | Initial Rate (M s$^{-1}$) |
|---|---|---|---|
| $2.0 \times 10^{-3}$ | $1.5 \times 10^{-3}$ | 1.00 | $1.8 \times 10^{-4}$ |
| $4.0 \times 10^{-3}$ | $1.5 \times 10^{-3}$ | 1.00 | $3.6 \times 10^{-4}$ |
| $2.0 \times 10^{-3}$ | $3.0 \times 10^{-3}$ | 2.00 | $1.8 \times 10^{-4}$ |
| $4.0 \times 10^{-3}$ | $3.0 \times 10^{-3}$ | 1.00 | $7.2 \times 10^{-4}$ |

Is the predicted rate law expression derived from the mechanism consistent with these data?

**P19.10** Using the preequilibrium approximation, derive the predicted rate law expression for the following mechanism:

$$A_2 \underset{k_{-1}}{\overset{k_1}{\rightleftharpoons}} 2A$$

$$A + B \overset{k_2}{\longrightarrow} P$$
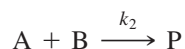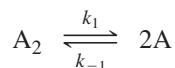
**P19.11** Consider the following mechanism, which results in the formation of product P:

$$A \underset{k_{-1}}{\overset{k_1}{\rightleftharpoons}} B \underset{k_{-2}}{\overset{k_2}{\rightleftharpoons}} C$$

$$B \overset{k_3}{\rightarrow} P$$
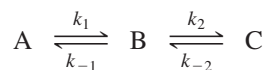
If only the species A is present at $t = 0$, what is the expression for the concentration of P as a function of time? You can apply the preequilibrium approximation in deriving your answer.

**P19.12** Consider the gas-phase isomerization of cyclopropane:

$$\begin{array}{c} CH_2 \\ \diagup \quad \diagdown \\ CH_2 \!-\! CH_2 \end{array} \longrightarrow CH_3CH\!=\!CH_2$$
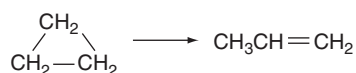
Are the following data of the observed rate constant as a function of pressure consistent with the Lindemann mechanism?

| P (Torr) | $k$ ($10^4$ s$^{-1}$) | P (Torr) | $k$ ($10^4$ s$^{-1}$) |
|---|---|---|---|
| 84.1 | 2.98 | 1.36 | 1.30 |
| 34.0 | 2.82 | 0.569 | 0.857 |
| 11.0 | 2.23 | 0.170 | 0.486 |
| 6.07 | 2.00 | 0.120 | 0.392 |
| 2.89 | 1.54 | 0.067 | 0.303 |

**P19.13** In the discussion of the Lindemann mechanism, it was assumed that the rate of activation by collision with another reactant molecule A was the same as collision with a nonreactant molecule M such as a buffer gas. What if the rates of activation for these two processes are different? In this case, the mechanism becomes

$$A + M \underset{k_{-1}}{\overset{k_1}{\rightleftharpoons}} A^* + M$$

$$A + A \underset{k_{-2}}{\overset{k_2}{\rightleftharpoons}} A^* + A$$

$$A^* \overset{k_3}{\longrightarrow} P$$
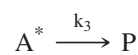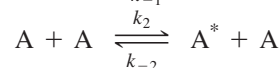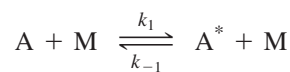
**a.** Demonstrate that the rate law expression for this mechanism is

$$R = \frac{k_3(k_1[A][M] + k_2[A]^2)}{k_{-1}[M] + k_{-2}[A] + k_{-3}}$$

**b.** Does this rate law reduce to the expected form when $[M] = 0$?

**P19.14** In the unimolecular isomerization of cyclobutane to butylene, the following values for $k_{uni}$ as a function of pressure were measured at 350 K:

| $P_0$ (Torr) | 110 | 210 | 390 | 760 |
|---|---|---|---|---|
| $k_{uni}$ (s$^{-1}$) | 9.58 | 10.3 | 10.8 | 11.1 |

Assuming that the Lindemann mechanism accurately describes this reaction, determine $k_1$ and the ratio $k_{-1}/k_2$.

**P19.15** Consider the collision-induced dissociation of $N_2O_5(g)$ via the following mechanism:

$$N_2O_5(g) + N_2O_5(g) \underset{k_{-1}}{\overset{k_1}{\rightleftharpoons}} N_2O_5(g)^* + N_2O_5(g)$$

$$N_2O_5(g)^* \overset{k_2}{\longrightarrow} NO_2(g) + NO_3(g)$$
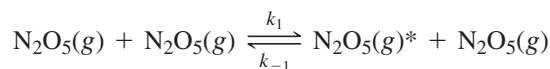
The asterisk in the first reaction indicates that the reactant is activated through collision. Experimentally it is found that the reaction can be either first or second order in $N_2O_5(g)$ depending on the concentration of this species. Derive a rate law expression for this reaction consistent with this observation.

**P19.16** The enzyme fumarase catalyzes the hydrolysis of fumarate: Fumarate$(aq) + H_2O(l) \rightarrow$ L-malate$(aq)$. The turnover number for this enzyme is $2.5 \times 10^3$ s$^{-1}$, and the Michaelis constant is $4.2 \times 10^{-6}$ M. What is the rate of fumarate

conversion if the initial enzyme concentration is $1 \times 10^{-6}$ M and the fumarate concentration is $2 \times 10^{-4}$ M?

**P19.17** The enzyme catalase catalyzes the decomposition of hydrogen peroxide. The following data are obtained regarding the rate of reaction as a function of substrate concentration:

| $[H_2O_2]_0$ (M) | 0.001 | 0.002 | 0.005 |
|---|---|---|---|
| Initial Rate (M s$^{-1}$) | $1.38 \times 10^{-3}$ | $2.67 \times 10^{-3}$ | $6.00 \times 10^{-3}$ |

The concentration of catalase is $3.50 \times 10^{-9}$ M. Use these data to determine $R_{max}$, $K_m$, and the turnover number for this enzyme.

**P19.18** Peptide bond hydrolysis is performed by a family of enzymes known as serine proteases. The name is derived from a highly conserved serine residue that is critical for enzyme function. One member of this enzyme class is chymotrypsin, which preferentially cleaves proteins at residue sites with hydrophobic side chains such as phenylalanine, leucine, and tyrosine. For example, *N*-benzoyl-tyrosylamide (NBT) and *N*-acetyl-tyrosylamide (NAT) are cleaved by chymotrypsin:
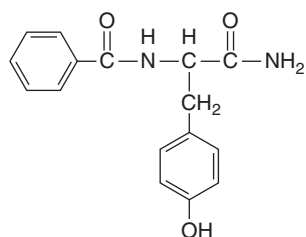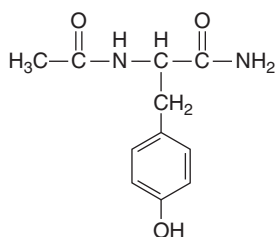


**N-benzoyl-tyrosylamide (NBT)**          **N-acetyl-tyrosylamide (NAT)**

**a.** The cleavage of NBT by chymotrypsin was studied and the following reaction rates were measured as a function of substrate concentration:

| [NBT] (mM) | 1.00 | 2.00 | 4.00 | 6.00 | 8.00 |
|---|---|---|---|---|---|
| $R_0$ (mM s$^{-1}$) | 0.040 | 0.062 | 0.082 | 0.099 | 0.107 |

Use these data to determine $K_m$ and $R_{max}$ for chymotrypsin with NBT as the substrate.

**b.** The cleavage of NAT is also studied and the following reaction rates versus substrate concentration were measured:

| [NAT] (mM) | 1.00 | 2.00 | 4.00 | 6.00 | 8.00 |
|---|---|---|---|---|---|
| $R_0$ (mM s$^{-1}$) | 0.004 | 0.008 | 0.016 | 0.022 | 0.028 |

Use these data to determine $K_m$ and $R_{max}$ for chymotrypsin with NAT as the substrate.

**P19.19** Protein tyrosine phosphatases (PTPases) are a general class of enzymes that are involved in a variety of disease processes including diabetes and obesity. In a study by Z.-Y. Zhang and coworkers [*J. Medicinal Chemistry* 43 (2000): 146], computational techniques were used to identify potential competitive inhibitors of a specific PTPase known as PTP1B. The

structure of one of the identified potential competitive inhibitors is shown here:
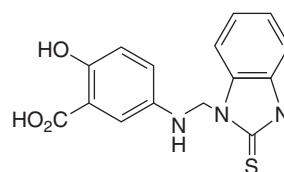


**PTP1B inhibitor**

The reaction rate was determined in the presence and absence of inhibitor $I$ and revealed the following initial reaction rates as a function of substrate concentration:

| [S] ($\mu$M) | $R_0$ ($\mu$M s$^{-1}$), [$I$] = 0 | $R_0$ ($\mu$M s$^{-1}$), [$I$] = 200 $\mu$M |
|---|---|---|
| 0.299 | 0.071 | 0.018 |
| 0.500 | 0.100 | 0.030 |
| 0.820 | 0.143 | 0.042 |
| 1.22 | 0.250 | 0.070 |
| 1.75 | 0.286 | 0.105 |
| 2.85 | 0.333 | 0.159 |
| 5.00 | 0.400 | 0.200 |
| 5.88 | 0.500 | 0.250 |

**a.** Determine $K_m$ and $R_{max}$ for PTP1B.

**b.** Demonstrate that the inhibition is competitive, and determine $K_i$.

**P19.20** The rate of reaction can be determined by measuring the change in optical rotation of the sample as a function of time if a reactant or product is chiral. This technique is especially useful for kinetic studies of enzyme catalysis involving sugars. For example, the enzyme invertase catalyzes the hydrolysis of sucrose, an optically active sugar. The initial reaction rates as a function of sucrose concentration are as follows:

| [Sucrose]$_0$ (M) | $R_0$ (M s$^{-1}$) |
|---|---|
| 0.029 | 0.182 |
| 0.059 | 0.266 |
| 0.088 | 0.310 |
| 0.117 | 0.330 |
| 0.175 | 0.362 |
| 0.234 | 0.361 |

Use these data to determine the Michaelis constant for invertase.

**P19.21** The enzyme glycogen synthase kinase $3\beta$(GSK-3$\beta$) plays a central role in Alzheimer's disease. The onset of Alzheimer's disease is accompanied by the production of highly phosphorylated forms of a protein referred to as "$\tau$." GSK-3$\beta$ contributes to the hyperphosphorylation of $\tau$ such that inhibiting the activity of this enzyme represents a pathway for the development of an Alzheimer's drug. A compound known as Ro 31-8220 is a competitive inhibitor of GSK-3$\beta$. The following data were obtained for the rate of GSK-3$\beta$ activity in the presence and

absence of Ro 31-8220 [A. Martinez et al., *J. Medicinal Chemistry* 45 (2002): 1292]:

| $[S](\mu M)$ | $R_0\ (\mu M\ s^{-1})$, $[I] = 0$ | $R_0\ (\mu M\ s^{-1})$, $[I] = 200\ \mu M$ |
|---|---|---|
| 66.7 | $4.17 \times 10^{-8}$ | $3.33 \times 10^{-8}$ |
| 40.0 | $3.97 \times 10^{-8}$ | $2.98 \times 10^{-8}$ |
| 20.0 | $3.62 \times 10^{-8}$ | $2.38 \times 10^{-8}$ |
| 13.3 | $3.27 \times 10^{-8}$ | $1.81 \times 10^{-8}$ |
| 10.0 | $2.98 \times 10^{-8}$ | $1.39 \times 10^{-8}$ |
| 6.67 | $2.31 \times 10^{-8}$ | $1.04 \times 10^{-8}$ |

Determine $K_m$ and $R_{max}$ for GSK-3$\beta$ and, using the data with the inhibitor, determine $K_m^*$ and $K_I$.

**P19.22** In the Michaelis–Menten mechanism, it is assumed that the formation of product from the enzyme–substrate complex is irreversible. However, consider the following modified version in which the product formation step is reversible:

$$E + S \underset{k_{-1}}{\overset{k_1}{\rightleftharpoons}} ES \underset{k_{-2}}{\overset{k_2}{\rightleftharpoons}} E + P$$

Derive the expression for the Michaelis constant for this mechanism in the limit where $[S]_0 \gg [E]_0$.

**P19.23** Reciprocal plots provide a relatively straightforward way to determine if an enzyme demonstrates Michaelis–Menten kinetics and to determine the corresponding kinetic parameters. However, the slope determined from these plots can require significant extrapolation to regions corresponding to low substrate concentrations. An alternative to the reciprocal plot is the Eadie–Hofstee plot in which the reaction rate is plotted versus the rate divided by the substrate concentration and the data are fit to a straight line.

**a.** Beginning with the general expression for the reaction rate given by the Michaelis–Menten mechanism:

$$R_0 = \frac{R_{max}[S]_0}{[S]_0 + K_m}$$

rearrange this equation to construct the following expression, which is the basis for the Eadie–Hofstee plot:

$$R_0 = R_{max} - K_m\left(\frac{R_0}{[S]_0}\right)$$

**b.** Using an Eadie–Hofstee plot, determine $R_{max}$ and $K_m$ for hydrolysis of sugar by the enzyme invertase using the following data:

| $[Sucrose]_0$ (M) | $R_0$ (M s$^{-1}$) |
|---|---|
| 0.029 | 0.182 |
| 0.059 | 0.266 |
| 0.088 | 0.310 |
| 0.117 | 0.330 |
| 0.175 | 0.362 |
| 0.234 | 0.361 |

**P19.24** Determine the predicted rate law expression for the following radical-chain reaction:

$$A_2 \xrightarrow{k_1} 2A\cdot$$

$$A\cdot \xrightarrow{k_2} B\cdot + C$$

$$A\cdot + B\cdot \xrightarrow{k_3} P$$

$$A\cdot + P \xrightarrow{k_4} B\cdot$$
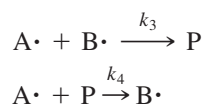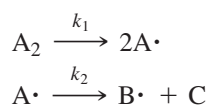
**P19.25** The overall reaction for the halogenation of a hydrocarbon (RH) using Br as the halogen is $RH(g) + Br_2(g) \rightarrow RBr(g) + HBr(g)$. The following mechanism has been proposed for this process:

$$Br_2(g) \xrightarrow{k_1} 2Br\cdot(g)$$

$$Br\cdot(g) + RH(g) \xrightarrow{k_2} R\cdot(g) + HBr(g)$$

$$R\cdot(g) + Br_2(g) \xrightarrow{k_3} RBr(g) + Br\cdot(g)$$

$$Br\cdot(g) + R\cdot(g) \xrightarrow{k_4} RBr(g)$$
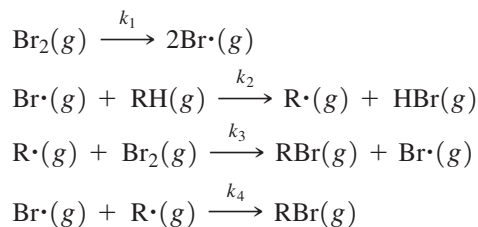
Determine the rate law predicted by this mechanism.

**P19.26** The chlorination of vinyl chloride, $C_2H_3Cl + Cl_2 \rightarrow C_2H_3Cl_3$, is believed to proceed by the following mechanism:

$$Cl_2 \xrightarrow{k_1} 2Cl\cdot$$

$$Cl\cdot + C_2H_3Cl \xrightarrow{k_2} C_2H_3Cl_2\cdot$$

$$C_2H_3Cl_2\cdot + Cl_2 \xrightarrow{k_3} C_2H_3Cl_3 + Cl\cdot$$

$$C_2H_3Cl_2\cdot + C_2H_3Cl_2\cdot \xrightarrow{k_4} \text{stable species}$$
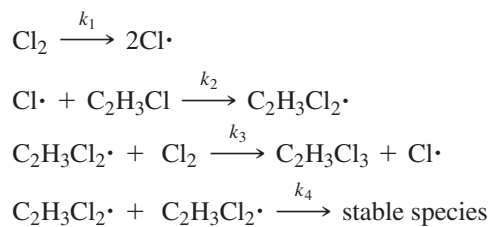
Derive the rate law expression for the chlorination of vinyl chloride based on this mechanism.

**P19.27** Determine the expression for fractional coverage as a function of pressure for the dissociative adsorption mechanism described in the text in which adsorption is accompanied by dissociation:

$$R_2(g) + 2M\ (surface) \underset{k_d}{\overset{k_a}{\rightleftharpoons}} 2RM\ (surface)$$
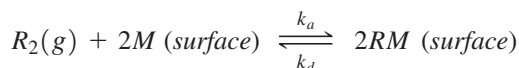
**P19.28** The adsorption of ethyl chloride on a sample of charcoal at 0°C measured at several different pressures is as follows:

| $P_{C_2H_5Cl}$ (**Torr**) | $V_{ads}$ (**mL**) |
|---|---|
| 20 | 3.0 |
| 50 | 3.8 |
| 100 | 4.3 |
| 200 | 4.7 |
| 300 | 4.8 |

Using the Langmuir isotherm, determine the fractional coverage at each pressure and $V_m$.

**P19.29** Given the limitations of the Langmuir model, many other empirical adsorption isotherms have been proposed to better reproduce observed adsorption behavior. One of these empirical isotherms is the Temkin isotherm:
$V_{adsorbed} = r \ln(sP)$, where $V$ is the volume of gas adsorbed, $P$ is pressure, and $r$ and $s$ are empirical constants.

**a.** Given the Temkin isotherm provided, what type of plot is expected to give a straight line?

**b.** Use your answer from part (a) to determine $r$ and $s$ for the data presented in Problem P19.24.

**P19.30**   Use the following data to determine the Langmuir adsorption parameters for nitrogen on mica:

| $V_{ads}$ (cm$^3$ g$^{-1}$) | $P$ (Torr) |
|---|---|
| 0.494 | $2.1 \times 10^{-3}$ |
| 0.782 | $4.60 \times 10^{-3}$ |
| 1.16 | $1.30 \times 10^{-2}$ |

**P19.31**   Many surface reactions require the adsorption of two or more different gases. For the case of two gases, assuming that the adsorption of a gas simply limits the number of surface sites available for adsorption, derive expressions for the fractional coverage of each gas.

**P19.32**   DNA microarrays or "chips" first appeared on the market in 1996. These chips are divided into square patches, with each patch having strands of DNA of the same sequence attached to a substrate. The patches are differentiated by differences in the DNA sequence. One can introduce DNA or mRNA of unknown sequence to the chip and monitor to which patches the introduced strands bind. This technique has a wide variety of applications in genome mapping and other areas.

Modeling the chip as a surface with binding sites, and modeling the attachment of DNA to a patch using the Langmuir model, what is the required difference in the Gibbs energy of binding needed to modify the fractional coverage on a given patch from 0.90 to 0.10 for two different DNA strands at the same concentration at 298 K? In performing this calculation replace pressure (P) with concentration (c) in the fractional-coverage expression. Also, recall that $K = \exp(-\Delta G/RT)$.

**P19.33**   Another type of autocatalytic reaction is referred to as cubic autocatalytic corresponding to the following elementary process:

$$A + 2B \rightarrow 3B$$

Write the rate law expression for this elementary process. What would you expect the corresponding differential rate expression in terms of $\xi$ (the coefficient of reaction advancement) to be?

**P19.34**   (Challenging) Cubic autocatalytic steps are important in a reaction mechanism referred to as the "brusselator" (named in honor of the research group in Brussels that initially discovered this mechanism):

$$A \xrightarrow{k_1} X$$
$$2X + Y \xrightarrow{k_2} 3X$$
$$B + X \xrightarrow{k_3} Y + C$$
$$X \xrightarrow{k_4} D$$
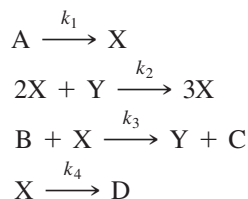
If [A] and [B] are held constant, this mechanism demonstrates interesting oscillatory behavior that we will explore in this problem.

**a.** Identify the autocatalytic species in this mechanism.

**b.** Write down the differential rate expressions for [X] and [Y].

**c.** Using these differential rate expressions, employ Euler's method (Section 18.6) to calculate [X] and [Y] versus time under the conditions $k_1 = 1.2$ s$^{-1}$, $k_2 = 0.5$ M$^{-2}$ s$^{-1}$, $k_3 = 3.0$ M$^{-1}$ s$^{-1}$, $k_4 = 1.2$ s$^{-1}$, and $[A]_0 = [B]_0 = 1$ M. Begin with $[X]_0 = 0.5$ M and $[Y]_0 = 0.1$ M. A plot of [Y] versus [X] should look like the top panel in the following figure.

**d.** Perform a second calculation identical to that in part (c), but with $[X]_0 = 3.0$ M and $[Y]_0 = 3.0$ M. A plot of [Y] versus [X] should look like the bottom panel in the following figure.

**e.** Compare the left and bottom panels in the following figure. Notice that the starting conditions for the reaction are different (indicated by the black spot). What DO the figures indicate regarding the oscillatory state the system evolves to?
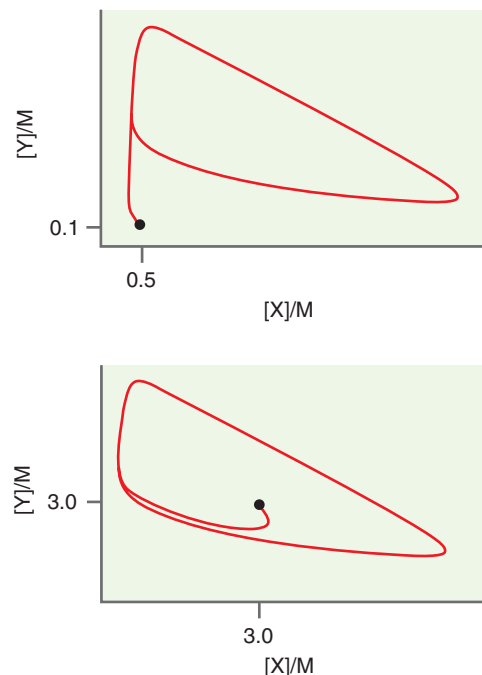


**P19.35**   The Kermack-McKendrick model was developed to explain the rapid rise and fall in the number of infected people during epidemics. This model involves the interaction of susceptible (S), infected (I), and recovered (R) people through the following mechanism:

$$S + I \xrightarrow{k_1} I + I$$
$$I \xrightarrow{k_2} R$$
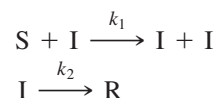
**a.** Write down the differential rate expressions for S, I, and R.

**b.** The key quantity in this mechanism is called the epidemiological threshold defined as the ratio of $[S]k_1/k_2$. When this ratio is greater than 1 the epidemic will spread; however, when the threshold is less than 1 the epidemic will die out. Based on the mechanism, explain why this behavior is observed.

**P19.36**   A sunburn is caused primarily by sunlight in what is known as the UVB band, or the wavelength range from 290 to 320 nm. The minimum dose of radiation needed to create a sunburn (erythema) is known as a MED (minimum erythema dose). The MED for a person of average resistance to burning is 50.0 mJ cm$^{-2}$.

**a.** Determine the number of 290. nm photons corresponding to the MED, assuming each photon is absorbed. Repeat this calculation for 320. nm photons.

**b.** At 20° latitude, the solar flux in the UVB band at the surface of the earth is 1.45 mW cm$^{-2}$. Assuming that each photon is absorbed, how long would a person with unprotected skin be able to stand in the sun before acquiring one MED?

**P19.37** A likely mechanism for the photolysis of acetaldehyde is

$$CH_3CHO(g) + h\nu \rightarrow CH_3\cdot(g) + CHO\cdot(g)$$

$$CH_3\cdot(g) + CH_3CHO(g) + \xrightarrow{k_1} CH_4(g) + CH_3CO\cdot(g)$$

$$CH_3CO\cdot(g) \xrightarrow{k_2} CO(g) + CH_3\cdot(g)$$

$$CH_3\cdot(g) + CH_3\cdot(g) \xrightarrow{k_3} C_2H_6(g)$$
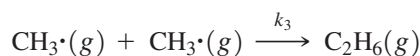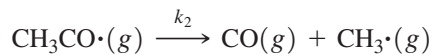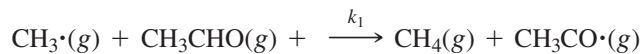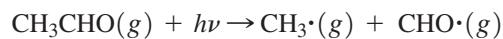
Derive the rate law expression for the formation of $CO(g)$ based on this mechanism.

**P19.38** If $\tau_f = 1 \times 10^{-10}$ s and $k_{ic} = 5 \times 10^8$ s$^{-1}$, what is $\phi_f$? Assume that the rate constants for intersystem crossing and quenching are sufficiently small that these processes can be neglected.

**P19.39** The quantum yield for $CO(g)$ production in the photolysis of gaseous acetone is unity for wavelengths between 250 and 320 nm. After 20.0 min of irradiation at 313 nm, 18.4 cm$^3$ of $CO(g)$ (measured at 1008 Pa and 22°C) is produced. Calculate the number of photons absorbed and the absorbed intensity in J s$^{-1}$.

**P19.40** If 10% of the energy of a 100. W incandescent bulb is in the form of visible light having an average wavelength of 600. nm, how many photons are emitted per second from the light bulb?

**P19.41** For phenanthrene, the measured lifetime of the triplet state $\tau_p$ is 3.3 s, the fluorescence quantum yield is 0.12, and the phosphorescence quantum yield is 0.13 in an alcohol-ether glass at 77 K. Assume that no quenching and no internal conversion from the singlet state occurs. Determine $k_p$, $k_{isc}^T$, and $k_{isc}^S/k_f$.

**P19.42** In this problem you will investigate the parameters involved in a single-molecule fluorescence experiment. Specifically, the incident photon power needed to see a single molecule with a reasonable signal-to-noise ratio will be determined.

a. Rhodamine dye molecules are typically employed in such experiments because their fluorescence quantum yields are large. What is the fluorescence quantum yield for Rhodamine B (a specific rhodamine dye) where $k_r = 1 \times 10^9$ s$^{-1}$ and $k_{ic} = 1 \times 10^8$ s$^{-1}$? You can ignore intersystem crossing and quenching in deriving this answer.

b. If care is taken in selecting the collection optics and detector for the experiment, a detection efficiency of 10% can be readily achieved. Furthermore, detector dark noise usually limits these experiments, and dark noise on the order of 10 counts s$^{-1}$ is typical. If we require a signal-to-noise ratio of 10:1, then we will need to detect 100 counts s$^{-1}$. Given the detection efficiency, a total emission rate of 1000 fluorescence photons s$^{-1}$ is required. Using the fluorescence quantum yield and a molar extinction coefficient for Rhodamine B of ~40,000 M$^{-1}$ cm$^{-1}$, what is the intensity of light needed in this experiment in terms of photons cm$^{-2}$ s$^{-1}$?

c. The smallest diameter focused spot one can obtain in a microscope using conventional refractive optics is approximately one-half the wavelength of incident light. Studies of Rhodamine B generally employ 532 nm light such that the focused-spot diameter is ~270 nm. Using this diameter, what incident power in watts is required for this experiment? Do not be surprised if this value is relatively modest.

**P19.43** A central issue in the design of aircraft is improving the lift of aircraft wings. To assist in the design of more efficient wings, wind-tunnel tests are performed in which the pressures at various parts of the wing are measured generally using only a few localized pressure sensors. Recently, pressure-sensitive paints have been developed to provide a more detailed view of wing pressure. In these paints, a luminescent molecule is dispersed into an oxygen-permeable paint and the aircraft wing is painted. The wing is placed into an airfoil, and luminescence from the paint is measured. The variation in $O_2$ pressure is measured by monitoring the luminescence intensity, with lower intensity demonstrating areas of higher $O_2$ pressure due to quenching.

a. The use of platinum octaethylporphyrin (PtOEP) as an oxygen sensor in pressure-sensitive paints was described by Gouterman and coworkers [*Review of Scientific Instruments* 61 (1990): 3340]. In this work, the following relationship between luminescence intensity and pressure was derived: $I_0/I = A + B(P/P_0)$, where $I_0$ is the fluorescence intensity at ambient pressure $P_0$, and $I$ is the fluorescence intensity at an arbitrary pressure $P$. Determine coefficients $A$ and $B$ in the preceding expression using the Stern–Volmer equation: $k_{total} = 1/\tau_l = k_l + k_q[Q]$. In this equation $\tau_l$ is the luminescence lifetime, $k_l$ is the luminescent rate constant, and $k_q$ is the quenching rate constant. In addition, the luminescent intensity ratio is equal to the ratio of luminescence quantum yields at ambient pressure $\Phi_0$ and an arbitrary pressure $\Phi$:

$$\Phi_0/\Phi = I_0/I.$$

b. Using the following calibration data of the intensity ratio versus pressure observed for PtOEP, determine $A$ and $B$:

| $I_0/I$ | $P/P_0$ | $I_0/I$ | $P/P_0$ |
|---------|---------|---------|---------|
| 1.0 | 1.0 | 0.65 | 0.46 |
| 0.9 | 0.86 | 0.61 | 0.40 |
| 0.87 | 0.80 | 0.55 | 0.34 |
| 0.83 | 0.75 | 0.50 | 0.28 |
| 0.77 | 0.65 | 0.46 | 0.20 |
| 0.70 | 0.53 | 0.35 | 0.10 |

c. At an ambient pressure of 1 atm, $I_0 = 50,000$ (arbitrary units) and 40,000 at the front and back of the wing. The wind tunnel is turned on to a speed of Mach 0.36, and the measured luminescence intensity is 65,000 and 45,000 at the respective locations. What is the pressure differential between the front and back of the wing?

**P19.44** Oxygen sensing is important in biological studies of many systems. The variation in oxygen content of sapwood trees was measured by del Hierro and coworkers

[*J. Experimental Biology* 53 (2002): 559] by monitoring the luminescence intensity of $[Ru(dpp)_3]^{2+}$ immobilized in a sol-gel that coats the end of an optical fiber implanted into the tree. As the oxygen content of the tree increases, the luminescence from the ruthenium complex is quenched. The quenching of $[Ru(dpp)_3]^{2+}$ by $O_2$ was measured by Bright and coworkers [*Applied Spectroscopy* 52 (1998): 750] and the following data were obtained:

| $I_0/I$ | $\%O_2$ |
|---------|---------|
| 3.6 | 12 |
| 4.8 | 20 |
| 7.8 | 47 |
| 12.2 | 100 |

**a.** Construct a Stern–Volmer plot using the data supplied in the table. For $[Ru(dpp)_3]^{2+}$ $k_r = 1.77 \times 10^5$ s$^{-1}$, what is $k_q$?

**b.** Comparison of the Stern–Volmer prediction to the quenching data led the authors to suggest that some of the $[Ru(dpp)_3]^{2+}$ molecules are located in sol-gel environments that are not equally accessible to $O_2$. What led the authors to this suggestion?

**P19.45**   The pyrene/coumarin FRET pair ($r_0 = 39$ Å) is used to study the fluctuations in enzyme structure during the course of a reaction. Computational studies suggest that the pair will be separated by 35 Å in one conformation and 46 Å in a second configuration. What is the expected difference in FRET efficiency between these two conformational states?

**P19.46**   In a FRET experiment designed to monitor conformational changes in T4 lysozyme, the fluorescence intensity fluctuates between 5000 and 10,000 counts per second. Assuming that 7500 counts represents a FRET efficiency of 0.5, what is the change in FRET pair separation distance during the reaction? For the tetramethylrhodamine/texas red FRET pair employed $r_0 = 50$. Å.

**P19.47**   One complication when using FRET is that fluctuations in the local environment can affect the $S_0-S_1$ energy gap for the donor or acceptor. Explain how this fluctuation would impact a FRET experiment.

**P19.48**   One can use FRET to follow the hybridization of two complimentary strands of DNA. When the two strands bind to form a double helix, FRET can occur from the donor to the acceptor allowing one to monitor the kinetics of helix formation (for an example of this technique see *Biochemistry* 34 (1995): 285). You are designing an experiment using a FRET

pair with $R_0 = 59.6$ Å. For B-form DNA the length of the helix increases 3.46 Å per residue. If you can accurately measure FRET efficiency down to 0.10, how many residues is the longest piece of DNA that you can study using this FRET pair?

**P19.49**   In Marcus theory for electron transfer, the reorganization energy is partitioned into solvent and solute contributions. Modeling the solvent as a dielectric continuum, the solvent reorganization energy is given by

$$\lambda_{sol} = \frac{(\Delta e)^2}{4\pi\varepsilon_0}\left(\frac{1}{d_1} + \frac{1}{d_2} - \frac{1}{r}\right)\left(\frac{1}{n^2} - \frac{1}{\varepsilon}\right)$$

where $\Delta e$ is the amount of charge transferred, $d_1$ and $d_2$ are the ionic diameters of ionic products, $r$ is the separation distance of the reactants, $n^2$ is the index of refraction of the surrounding medium, and $\varepsilon$ is the dielectric constant of the medium. In addition, $(4\pi\varepsilon_0)^{-1} = 8.99 \times 10^9$ J m C$^{-2}$.

**a.** For an electron transfer in water ($n = 1.33$ and $\varepsilon = 80.$), where the ionic diameters of both species are 6 Å and the separation distance is 15 Å, what is the expected solvent reorganization energy?

**b.** Redo the earlier calculation for the same reaction occurring in a protein. The dielectric constant of a protein is dependent on sequence, structure, and the amount of included water; however, a dielectric constant of 4 is generally assumed consistent with a hydrophobic environment. Using light-scattering measurements the dielectric constant of proteins has been estimated to be ~1.5.

**P19.50**   An experiment is performed in which the rate constant for electron transfer is measured as a function of distance by attaching an electron donor and acceptor to pieces of DNA of varying length. The measured rate constant for electron transfer as a function of separation distance is as follows:

| $k_{exp}$ (s$^{-1}$) | $2.10 \times 10^8$ | $2.01 \times 10^7$ | $2.07 \times 10^5$ | 204 |
|---|---|---|---|---|
| **Distance (Å)** | 14 | 17 | 23 | 32 |

**a.** Determine the value for $\beta$ that defines the dependence of the electron transfer rate constant on separation distance.

**b.** It has been proposed that DNA can serve as an electron "$\pi$-way" facilitating electron transfer over long distances. Using the rate constant at 17 Å presented in the table, what value of $\beta$ would result in the rate of electron transfer decreasing by only a factor of 10 at a separation distance of 23 Å?

# Web-Based Simulations, Animations, and Problems

**W19.1**   In this problem, the Lindemann mechanism for unimolecular rearrangements is investigated. Students will investigate the dependence of the reaction rate on reactant concentration and on the relative rate constants for the reaction. The turnover of the rate law from second order to first order as the reactant concentration is

increased is explored. Also, dependence of this turnover on the relative magnitudes of $k_{-1}$ [A] and $k_2$ is investigated.

**W19.2**   In this problem, Michaelis–Menten enzyme kinetics are investigated, specifically, the variation in reaction rate with substrate concentration for three enzymes having significantly different Michaelis–Menten

kinetic parameters. Students will investigate how the maximum reaction rate and overall kinetics depend on $K_m$ and turnover number. Finally, hand calculations of enzyme kinetic parameters performed by the students are compared to the results obtained by simulation.

**W19.3** In this problem, the Langmuir isotherms for non-dissociative and dissociative adsorption to a surface are investigated. Students study the dependence of the isotherms for these two adsorption processes on the adsorption/desorption rate constants and on adsorbate pressure.

# For Further Reading

*CRC Handbook of Photochemistry and Photophysics*. Boca Raton, FL: CRC Press, 1990.

Eyring, H., S. H. Lin, and S. M. Lin. *Basic Chemical Kinetics*. New York: Wiley, 1980.

Pannetier, G., and P. Souchay. *Chemical Kinetics*. Amsterdam: Elsevier, 1967.

Hammes, G. G. *Thermodynamics and Kinetics for the Biological Sciences*. New York: Wiley, 2000.

Fersht, A. *Enzyme Structure and Mechanism*. New York: W. H. Freeman, 1985.

Fersht, A. *Structure and Mechanism in Protein Science*. New York: W. H. Freeman, 1999.

Laidler, K. J. *Chemical Kinetics*. New York: Harper & Row, 1987.

Robinson, P. J., and K. A. Holbrook. *Unimolecular Reactions*. New York: Wiley, 1972.

Turro, N. J. *Modern Molecular Photochemistry*. Menlo Park, CA: Benjamin Cummings, 1978.

Simons, J. P. *Photochemistry and Spectroscopy*. New York Wiley, 1971.

Lim, E. G. *Molecular Luminescence*. Menlo Park, CA Benjamin Cummings, 1969.

Noggle, J. H. *Physical Chemistry*. New York: HarperCollins, 1996.

Scott, S. K. *Oscillations, Waves, and Chaos in Chemical Kinetics*. Oxford: Oxford University Press, 2004.

Data tables referenced throughout the text are listed here and appear either on the page number in parentheses or, if no page number is listed, in this appendix.

## Sources of Data

The most extensive databases for thermodynamic data (and the abbreviations listed with the tables) are as follows:

**HCP** Lide, D. R., Ed., *Handbook of Chemistry and Physics,* 83rd ed. CRC Press, Boca Raton, FL, 2002.

**NIST Chemistry Webbook** Linstrom, P. J., and W. G. Mallard, Eds., *NIST Chemistry Webbook: NIST Standard Reference Database Number 69*. National Institute of Standards and Technology, Gaithersburg, MD, retrieved from http://webbook.nist.gov.

Additional data sources used in the tables include the following:

**Bard** Bard, A. J., R. Parsons, and J. Jordan, *Standard Potentials in Aqueous Solution*. Marcel Dekker, New York, 1985.

**DAL** Blachnik, R., Ed., *D'Ans Lax Taschenbuch für Chemiker und Physiker*, 4th ed. Springer, Berlin, 1998.

**HP** Benenson, W., J. W. Harris, H. Stocker, and H. Lutz, *Handbook of Physics*. Springer, New York, 2002.

**HTTD** Lide, D. R., Ed., *CRC Handbook of Thermophysical and Thermochemical Data*. CRC Press, Boca Raton, FL, 1994.

**TDOC** Pedley, J. B., R. D. Naylor, and S. P. Kirby, *Thermochemical Data of Organic Compounds*. Chapman and Hall, London, 1977.

**TDPS** Barin, I., *Thermochemical Data of Pure Substances*. VCH Press, Weinheim, 1989.

**AS** Alberty, R. A., and R. S. Silbey, *Physical Chemistry*. John Wiley & Sons, New York, 1992.

## TABLE 2.3   Physical Properties of Selected Elements

Densities are shown for nongaseous elements under standard conditions.

| Substance | Atomic Weight | Melting Point (K) | Boiling Point (K) | $\rho°\,(\text{kg m}^{-3})$ | $C_{P,\,m}\,(\text{J K}^{-1}\,\text{mol}^{-1})$ | Oxidation States |
|---|---|---|---|---|---|---|
| Aluminum | 26.982 | 933.47 | 2792.15 | 2698.9 | 25.4 | 3 |
| Argon | 39.948 | 83.79 tp (69 kPa) | 87.30 | — | 20.79 | |
| Barium | 137.33 | 1000.15 | 2170.15 | 3620 | 28.07 | 2 |
| Boron | 10.811 | 2348.15 | 4273.15 | 2340 | 11.1 | 3 |
| Bromine | 79.904 | 265.95 | 331.95 | 3103 | 36.05 | 1, 3, 4, 5, 6 |
| Calcium | 40.078 | 1115.15 | 1757.15 | 1540 | 25.9 | 2 |
| Carbon | 12.011 | 4713.15 | | 3513 | 6.113 | 2, 4 |
| | | (12.4 GPa) | 4098.15 | (diamond) | (diamond) | |
| | | 4762.15 tp | (graphite) | 2250 | 8.527 | |
| | | (10.3 MPa) | | (graphite) | (graphite) | |
| Cesium | 132.91 | 301.65 | 944.15 | 1930 | 32.20 | 1 |
| Chlorine | 35.453 | 171.65 | 239.11 | — | 33.95 | 1, 3, 4, 5, 6, 7 |
| Copper | 63.546 | 1357.77 | 2835.15 | 8960 | 24.4 | 1, 2 |
| Fluorine | 18.998 | 53.48 tp | 85.03 | — | 31.30 | 1 |
| Gold | 196.97 | 1337.33 | 3129.15 | 19320 | 25.42 | 1, 3 |
| Helium | 4.0026 | 0.95 | 4.22 | — | 20.79 | |
| Hydrogen | 1.0079 | 13.81 | 20.28 | — | 28.84 | 1 |
| Iodine | 126.90 | 386.85 | 457.55 | 4933 | 54.44 | 1, 3, 5, 7 |
| Iron | 55.845 | 1811.15 | 3134.15 | 7874 | 25.10 | 2, 3 |
| Krypton | 83.80 | 115.77 tp (73.2 kPa) | 119.93 | — | 20.79 | |
| Lead | 207.2 | 600.61 | 2022.15 | 11343 | 26.44 | 2, 4 |
| Lithium | 6.941 | 453.65 | 1615.15 | 534 | 24.77 | 1 |
| Magnesium | 24.305 | 923.15 | 1363.15 | 1740 | 24.89 | 2 |
| Manganese | 54.938 | 1519.15 | 2334.15 | 7300 | 26.3 | 2, 3, 4, 6, 7 |
| Mercury | 200.59 | 234.31 | 629.88 | 13534 | 27.98 | 1, 2 |
| Molybdenum | 95.94 | 2896.15 | 4912.15 | 10222 | 23.90 | 2, 3, 4, 5, 6 |
| Neon | 20.180 | 24.54 tp (43 kPa) | 27.07 | — | 20.79 | |
| Nickel | 58.693 | 1728.15 | 3186 | 8902 | 26.07 | 2, 3 |
| Nitrogen | 14.007 | 63.15 | 77.36 | — | 29.12 | 1, 2, 3, 4, 5 |
| Oxygen | 15.999 | 54.36 | 90.20 | — | 29.38 | 1,2 |
| Palladium | 106.42 | 1828.05 | 3236.15 | 11995 | 25.98 | 2, 4 |
| Phosphorus (white) | 30.974 | 317.3 | 553.65 | 1823 | 23.84 | 3, 5 |
| Platinum | 195.08 | 2041.55 | 4098.15 | 21500 | 25.85 | 2, 4, 6 |
| Potassium | 39.098 | 336.65 | 1032.15 | 890 | 29.58 | 1 |
| Rhenium | 186.21 | 3459.15 | 5869.15 | 20800 | 25.31 | 2, 4, 5, 6, 7 |
| Rhodium | 102.91 | 2237.15 | 3968.15 | 12410 | 24.98 | 2, 3, 4 |
| Ruthenium | 101.07 | 2607.15 | 4423.15 | 12100 | 24.04 | 3, 4, 5, 6, 8 |
| Silicon | 28.086 | 1687.15 | 3538.15 | 2330 | 20.00 | 4 |
| Silver | 107.87 | 1234.93 | 2435.15 | 10500 | 25.35 | 1 |
| Sodium | 22.990 | 370.95 | 1156.15 | 971 | 28.24 | 1 |
| Sulfur | 32.066 | 388.36 | 717.75 | 1819 | 22.76 | 2, 4, 6 |
| Tin | 118.71 | 505.08 | 2879 | 7310 | 26.99 | 2, 4 |
| Titanium | 47.867 | 1941.15 | 3560.15 | 4506 | 25.05 | 2, 3, 4 |
| Vanadium | 50.942 | 2183.15 | 3680.15 | 6000 | 24.89 | 2, 3, 4, 5 |
| Xenon | 131.29 | 161.36 tp (81.6 kPa) | 165.03 | — | 20.79 | 2, 4, 6, 8 |
| Zinc | 65.39 | 692.68 | 1180.15 | 7135 | 25.40 | 2 |

*Sources:* HCP and DAL.

**TABLE 2.4   Physical Properties of Selected Compounds**

Densities are shown for nongaseous compounds under standard conditions.

| Formula | Name | Molecular Weight | Melting Point (K) | Boiling Point (K) | Density $\rho°$ (kg m$^{-3}$) | Heat Capacity $C_{P,m}$ (J K$^{-1}$ mol$^{-1}$) |
|---|---|---|---|---|---|---|
| $CO(g)$ | Carbon monoxide | 28.01 | 68.13 | 81.65 | — | 29.1 |
| $COCl_2(g)$ | Phosgene | 98.92 | 145.4 | 281 | — | |
| $CO_2(g)$ | Carbon dioxide | 44.01 | 216.6 tp | 194.75 | — | 37.1 |
| $D_2O(l)$ | Deuterium oxide | 20.03 | 277 | 374.6 | 1108 | |
| $HCl(g)$ | Hydrogen chloride | 36.46 | 158.98 | 188.15 | — | 29.1 |
| $HF(g)$ | Hydrogen fluoride | 20.01 | 189.8 | 293.15 | — | |
| $H_2O$ | Water | 18.02 | 273.15 | 373.15 | 998($l$) | 75.3($l$) |
| | | | | | 20°C | 36.2($s$) |
| | | | | | 917($s$) 0°C | |
| $H_2O_2(l)$ | Hydrogen peroxide | 34.01 | 272.72 | 423.35 | 1440 | 43.1 |
| $H_2SO_4(l)$ | Sulfuric acid | 98.08 | 283.46 | 610.15 | 1800 | |
| $KBr(s)$ | Potassium bromide | 119.00 | 1007.15 | 1708.15 | 2740 | 52.3 |
| $KCl(s)$ | Potassium chloride | 74.55 | 1044.15 | | 1988 | 51.3 |
| $KI(s)$ | Potassium iodide | 166.0 | 954.15 | 1596.15 | 3120 | 52.9 |
| $NaCl(s)$ | Sodium chloride | 58.44 | 1073.85 | 1738.15 | 2170 | 50.5 |
| $NH_3(g)$ | Ammonia | 17.03 | 195.42 | 239.82 | — | 35.1 |
| $SO_2(g)$ | Sulfur dioxide | 64.06 | 197.65 | 263.10 | — | 39.9 |
| $CCl_4(l)$ | Carbon tetrachloride | 153.82 | 250.3 | 349.8 | 1594 | 131.3 |
| $CH_4(g)$ | Methane | 16.04 | 90.75 | 111.65 | — | 35.7 |
| $HCOOH(l)$ | Formic acid | 46.03 | 281.45 | 374.15 | 1220 | 99.04 |
| $CH_3OH(l)$ | Methanol | 32.04 | 175.55 | 337.75 | 791.4 | 81.1 |
| $CH_3CHO(l)$ | Acetaldehyde | 44.05 | 150.15 | 293.25 | 783.4 | 89.0 |
| $CH_3COOH(l)$ | Acetic acid | 60.05 | 289.6 | 391.2 | 1044.6 | 123.1 |
| $CH_3COCH_3(l)$ | Acetone | 58.08 | 178.5 | 329.2 | 789.9 | 125.45 |
| $C_2H_5OH(l)$ | Ethanol | 46.07 | 158.8 | 351.5 | 789.3 | 112.3 |
| $C_3H_7OH(l)$ | 1-Propanol | 60.10 | 147.05 | 370.35 | 799.8 | 156.5 |
| $C_4H_{11}OH(l)$ | 1-Butanol | 74.12 | 183.35 | 390.85 | 809.8 | 176.9 |
| $C_5H_5NH_2(l)$ | Pyridine | 79.10 | 231.55 | 388.35 | 981.9 | 193 |
| $C_5H_{12}(l)$ | Pentane | 72.15 | 143.45 | 309.15 | 626.2 | 167.2 |
| $C_5H_{11}OH(l)$ | 1-Pentanol | 88.15 | 194.25 | 411.05 | 814.4 | 207.5 |
| $C_6H_{12}(l)$ | Cyclohexane | 84.16 | 279.6 | 353.9 | 773.9 | 156.0 |
| $C_6H_5CHO(l)$ | Benzaldehyde | 106.12 | 247.15 | 452.15 | 1041.5 | 172.0 |
| $C_6H_5COOH(s)$ | Benzoic acid | 122.12 | 395.55 | 522.35 | 1265.9 | 147.8 |
| $C_6H_5CH_3(l)$ | Toluene | 92.14 | 178.2 | 383.8 | 866.9 | 157.1 |
| $C_6H_5NH_2(l)$ | Aniline | 93.13 | 267 | 457 | 1021.7 | 194.1 |
| $C_6H_5OH(s)$ | Phenol | 94.11 | 314.05 | 454.95 | 1057.6 | 127.2 |
| $C_6H_6(l)$ | Benzene | 78.11 | 278.6 | 353.3 | 876.5 | 135.7 |
| $1,2\text{-}(CH_3)_2C_6H_5(l)$ | $o$-Xylene | 106.17 | 248 | 417.6 | 880.2 | 187.7 |
| $C_8H_{18}(l)$ | Octane | 114.23 | 216.35 | 398.75 | 698.6 | 254.7 |

*Sources:* HCP and TDOC.

**TABLE 2.5**   Molar Heat Capacity, $C_{P,m}$, of Gases in the Range 298–800 K

Given by

$$C_{P,m} \text{ (J K}^{-1}\text{ mol}^{-1}) = A(1) + A(2)\frac{T}{K} + A(3)\frac{T^2}{K^2} + A(4)\frac{T^3}{K^3}$$

Note that $C_{P,m}$ for solids and liquids at 298.15 K is listed in Tables 2.1 and 2.2.

| Name | Formula | $C_{P,m}$ (298.15 K) in J K$^{-1}$ mol$^{-1}$ | A(1) | A(2) | A(3) | A(4) |
|---|---|---|---|---|---|---|
| All monatomic gases | He, Ne, Ar, Xe, O, H, among others | 20.79 | 20.79 | | | |
| Bromine | Br$_2$ | 36.05 | 30.11 | 0.03353 | $-5.5009 \times 10^{-5}$ | $3.1711 \times 10^{-8}$ |
| Chlorine | Cl$_2$ | 33.95 | 22.85 | 0.06543 | $-1.2517 \times 10^{-4}$ | $1.1484 \times 10^{-7}$ |
| Carbon monoxide | CO | 29.14 | 31.08 | $-0.01452$ | $3.1415 \times 10^{-5}$ | $-1.4973 \times 10^{-8}$ |
| Carbon dioxide | CO$_2$ | 37.14 | 18.86 | 0.07937 | $-6.7834 \times 10^{-5}$ | $2.4426 \times 10^{-8}$ |
| Fluorine | F$_2$ | 31.30 | 23.06 | 0.03742 | $-3.6836 \times 10^{-5}$ | $1.351 \times 10^{-8}$ |
| Hydrogen | H$_2$ | 28.84 | 22.66 | 0.04381 | $-1.0835 \times 10^{-4}$ | $1.1710 \times 10^{-7}$ |
| Water | H$_2$O | 33.59 | 33.80 | $-0.00795$ | $2.8228 \times 10^{-5}$ | $-1.3115 \times 10^{-8}$ |
| Hydrogen bromide | HBr | 29.13 | 29.72 | $-0.00416$ | $7.3177 \times 10^{-6}$ | |
| Hydrogen chloride | HCl | 29.14 | 29.81 | $-0.00412$ | $6.2231 \times 10^{-6}$ | |
| Hydrogen fluoride | HF | 29.14 | 28.94 | 0.00152 | $-4.0674 \times 10^{-6}$ | $3.8970 \times 10^{-9}$ |
| Ammonia | NH$_3$ | 35.62 | 29.29 | 0.01103 | $4.2446 \times 10^{-5}$ | $-2.7706 \times 10^{-8}$ |
| Nitrogen | N$_2$ | 29.13 | 30.81 | $-0.01187$ | $2.3968 \times 10^{-5}$ | $-1.0176 \times 10^{-8}$ |
| Nitric oxide | NO | 29.86 | 33.58 | $-0.02593$ | $5.3326 \times 10^{-5}$ | $-2.7744 \times 10^{-8}$ |
| Nitrogen dioxide | NO$_2$ | 37.18 | 32.06 | $-0.00984$ | $1.3807 \times 10^{-4}$ | $-1.8157 \times 10^{-7}$ |
| Oxygen | O$_2$ | 29.38 | 32.83 | $-0.03633$ | $1.1532 \times 10^{-4}$ | $-1.2194 \times 10^{-7}$ |
| Sulfur dioxide | SO$_2$ | 39.83 | 26.07 | 0.05417 | $-2.6774 \times 10^{-5}$ | |
| Methane | CH$_4$ | 35.67 | 30.65 | $-0.01739$ | $1.3903 \times 10^{-4}$ | $8.1395 \times 10^{-8}$ |
| Methanol | CH$_3$OH | 44.07 | 26.53 | 0.03703 | $9.451 \times 10^{-5}$ | $-7.2006 \times 10^{-8}$ |
| Ethyne | C$_2$H$_2$ | 44.05 | 10.82 | 0.15889 | $-1.8447 \times 10^{-4}$ | $8.5291 \times 10^{-8}$ |
| Ethene | C$_2$H$_4$ | 42.86 | 8.39 | 0.12453 | $-2.5224 \times 10^{-5}$ | $-1.5679 \times 10^{-8}$ |
| Ethane | C$_2$H$_6$ | 52.38 | 6.82 | 0.16840 | $-5.2347 \times 10^{-5}$ | |
| Propane | C$_3$H$_8$ | 73.52 | 0.56 | 0.27559 | $-1.0355 \times 10^{-4}$ | |
| Butane | C$_4$H$_{10}$ | 101.01 | 172.02 | $-1.08574$ | $4.4887 \times 10^{-3}$ | $-6.5539 \times 10^{-6}$ |
| Pentane | C$_5$H$_{12}$ | 120.11 | 2.02 | 0.44729 | $-1.7174 \times 10^{-4}$ | |
| Benzene | C$_6$H$_6$ | 82.39 | $-46.48$ | 0.53735 | $-3.8303 \times 10^{-4}$ | $1.0184 \times 10^{-7}$ |
| Hexane | C$_6$H$_{12}$ | 142.13 | $-13.27$ | 0.61995 | $-3.5408 \times 10^{-4}$ | $7.6704 \times 10^{-8}$ |

*Sources:* HCP and HTTD.

## TABLE 2.6 Molar Heat Capacity, $C_{P,m}$, of Solids

$$C_{P,m} \text{ (J K}^{-1} \text{ mol}^{-1}) = A(1) + A(2)\frac{T}{K} + A(3)\frac{T^2}{K^2} + A(4)\frac{T^3}{K^3} + A(5)\frac{T^4}{K^4}$$

| Formula | Name | $C_{P,m}$ (298.15 K) (J K$^{-1}$ mol$^{-1}$) | A(1) | A(2) | A(3) | A(4) | A(5) | Range (K) |
|---|---|---|---|---|---|---|---|---|
| Ag | Silver | 25.35 | 26.12 | −0.0110 | $3.826 \times 10^{-5}$ | $3.750 \times 10^{-8}$ | $1.396 \times 10^{-11}$ | 290–800 |
| Al | Aluminum | 24.4 | 6.56 | 0.1153 | $-2.460 \times 10^{-4}$ | $1.941 \times 10^{-7}$ | | 200–450 |
| Au | Gold | 25.4 | 34.97 | −0.0768 | $2.117 \times 10^{-4}$ | $-2.350 \times 10^{-7}$ | $9.500 \times 10^{-11}$ | 290–800 |
| CsCl | Cesium chloride | 52.5 | 43.38 | 0.0467 | $-8.973 \times 10^{-5}$ | $1.421 \times 10^{-7}$ | $-8.237 \times 10^{-11}$ | 200–600 |
| CuSO$_4$ | Copper sulfate | 98.9 | −13.81 | 0.7036 | $-1.636 \times 10^{-3}$ | $2.176 \times 10^{-6}$ | $-1.182 \times 10^{-9}$ | 200–600 |
| Fe | Iron | 25.1 | −10.99 | 0.3353 | $-1.238 \times 10^{-3}$ | $2.163 \times 10^{-6}$ | $-1.407 \times 10^{-9}$ | 200–450 |
| NaCl | Sodium chloride | 50.5 | 25.19 | 0.1973 | $-6.011 \times 10^{-4}$ | $8.815 \times 10^{-7}$ | $-4.765 \times 10^{-10}$ | 200–600 |
| Si | Silicon | 20.0 | −6.25 | 0.1681 | $-3.437 \times 10^{-4}$ | $2.494 \times 10^{-7}$ | $6.667 \times 10^{-12}$ | 200–450 |
| C (graphite) | C | 8.5 | −12.19 | 0.1126 | $-1.947 \times 10^{-4}$ | $1.919 \times 10^{-7}$ | $-7.800 \times 10^{-11}$ | 290–600 |
| C$_6$H$_5$OH | Phenol | 127.4 | −5.97 | 1.0380 | $-6.467 \times 10^{-3}$ | $2.304 \times 10^{-5}$ | $-2.658 \times 10^{-8}$ | 100–314 |
| C$_{10}$H$_8$ | Naphthalene | 165.7 | −6.16 | 1.0383 | $-5.355 \times 10^{-3}$ | $1.891 \times 10^{-5}$ | $-2.053 \times 10^{-8}$ | 100–353 |
| C$_{14}$H$_{10}$ | Anthracene | 210.5 | 11.10 | 0.5816 | $2.790 \times 10^{-4}$ | | | 100–488 |

*Sources:* HCP and HTTD.

## TABLE 4.1 Thermodynamic Data for Inorganic Compounds at 298.15 K

| Substance | $\Delta H_f^\circ$ (kJ mol$^{-1}$) | $\Delta G_f^\circ$ (kJ mol$^{-1}$) | $S_m^\circ$ (J mol$^{-1}$ K$^{-1}$) | $C_{P,m}$ (J mol$^{-1}$ K$^{-1}$) | Atomic or Molecular Weight (amu) |
|---|---|---|---|---|---|
| **Aluminum** | | | | | |
| Al(s) | 0 | 0 | 28.3 | 24.4 | 26.98 |
| Al$_2$O$_3$(s) | −1675.7 | −1582.3 | 50.9 | 79.0 | 101.96 |
| Al$^{3+}$(aq) | −538.4 | −485.0 | −325 | | 26.98 |
| **Antimony** | | | | | |
| Sb(s) | 0 | 0 | 45.7 | 25.2 | 121.75 |
| **Argon** | | | | | |
| Ar(g) | 0 | 0 | 154.8 | 20.8 | 39.95 |
| **Barium** | | | | | |
| Ba(s) | 0 | 0 | 62.5 | 28.1 | 137.34 |
| BaO(s) | −548.0 | −520.3 | 72.1 | 47.3 | 153.34 |
| BaCO$_3$(s) | −1216.3 | −1137.6 | 112.1 | 85.4 | 197.35 |
| BaCl$_2$(s) | −856.6 | −810.3 | 123.7 | 75.1 | 208.25 |
| BaSO$_4$(s) | −1473.2 | −1362.3 | 132.2 | 101.8 | 233.40 |
| Ba$^{2+}$(aq) | −537.6 | −560.8 | 9.6 | | 137.34 |
| **Bromine** | | | | | |
| Br$_2$(l) | 0 | 0 | 152.2 | 75.7 | 159.82 |
| Br$_2$(g) | 30.9 | 3.1 | 245.5 | 36.0 | 159.82 |
| Br(g) | 111.9 | 82.4 | 175.0 | 20.8 | 79.91 |
| HBr(g) | −36.3 | −53.4 | 198.7 | 29.1 | 90.92 |
| Br$^-$(aq) | −121.6 | −104.0 | 82.4 | | 79.91 |

| Substance | $\Delta H_f^{\circ}$ (kJ mol$^{-1}$) | $\Delta G_f^{\circ}$ (kJ mol$^{-1}$) | $S_m^{\circ}$ (J mol$^{-1}$ K$^{-1}$) | $C_{P,\,m}$ (J mol$^{-1}$ K$^{-1}$) | Atomic or Molecular Weight (amu) |
|---|---|---|---|---|---|
| **Calcium** | | | | | |
| Ca(s) | 0 | 0 | 41.6 | 25.9 | 40.08 |
| CaCO$_3$(s) calcite | −1206.9 | −1128.8 | 92.9 | 83.5 | 100.09 |
| CaCl$_2$(s) | −795.4 | −748.8 | 104.6 | 72.9 | 110.99 |
| CaO(s) | −634.9 | −603.3 | 38.1 | 42.0 | 56.08 |
| CaSO$_4$(s) | −1434.5 | −1322.0 | 106.5 | 99.7 | 136.15 |
| Ca$^{2+}$(aq) | −542.8 | −553.6 | −53.1 | | 40.08 |
| **Carbon** | | | | | |
| Graphite(s) | 0 | 0 | 5.74 | 8.52 | 12.011 |
| Diamond(s) | 1.89 | 2.90 | 2.38 | 6.12 | 12.011 |
| C(g) | 716.7 | 671.2 | 158.1 | 20.8 | 12.011 |
| CO(g) | −110.5 | −137.2 | 197.7 | 29.1 | 28.011 |
| CO$_2$(g) | −393.5 | −394.4 | 213.8 | 37.1 | 44.010 |
| HCN(g) | 135.5 | 124.7 | 201.8 | 35.9 | 27.03 |
| CN$^-$(aq) | 150.6 | 172.4 | 94.1 | | 26.02 |
| HCO$_3^-$(aq) | −692.0 | −586.8 | 91.2 | | 61.02 |
| CO$_3^{2-}$(aq) | −675.2 | −527.8 | −50.0 | | 60.01 |
| **Chlorine** | | | | | |
| Cl$_2$(g) | 0 | 0 | 223.1 | 33.9 | 70.91 |
| Cl(g) | 121.3 | 105.7 | 165.2 | 21.8 | 35.45 |
| HCl(g) | −92.3 | −95.3 | 186.9 | 29.1 | 36.46 |
| ClO$_2$(g) | 104.6 | 105.1 | 256.8 | 45.6 | 67.45 |
| ClO$_4^-$(aq) | −128.1 | −8.52 | 184.0 | | 99.45 |
| Cl$^-$(aq) | −167.2 | −131.2 | 56.5 | | 35.45 |
| **Copper** | | | | | |
| Cu(s) | 0 | 0 | 33.2 | 24.4 | 63.54 |
| CuCl$_2$(s) | −220.1 | −175.7 | 108.1 | 71.9 | 134.55 |
| CuO(s) | −157.3 | −129.7 | 42.6 | 42.3 | 79.54 |
| Cu$_2$O(s) | −168.6 | −146.0 | 93.1 | 63.6 | 143.08 |
| CuSO$_4$(s) | −771.4 | −662.2 | 109.2 | 98.5 | 159.62 |
| Cu$^+$(aq) | 71.7 | 50.0 | 40.6 | | 63.54 |
| Cu$^{2+}$(aq) | 64.8 | 65.5 | −99.6 | | 63.54 |
| **Deuterium** | | | | | |
| D$_2$(g) | 0 | 0 | 145.0 | 29.2 | 4.028 |
| HD(g) | 0.32 | −1.46 | 143.8 | 29.2 | 3.022 |
| D$_2$O(g) | −249.2 | −234.5 | 198.3 | 34.3 | 20.028 |
| D$_2$O(l) | −294.6 | −243.4 | 75.94 | 84.4 | 20.028 |
| HDO(g) | −246.3 | −234.5 | 199.4 | 33.8 | 19.022 |
| HDO(l) | −289.9 | −241.9 | 79.3 | | 19.022 |
| **Fluorine** | | | | | |
| F$_2$(g) | 0 | 0 | 202.8 | 31.3 | 38.00 |
| F(g) | 79.4 | 62.3 | 158.8 | 22.7 | 19.00 |
| HF(g) | −273.3 | −275.4 | 173.8 | 29.1 | 20.01 |
| F$^-$(aq) | −332.6 | −278.8 | −13.8 | | 19.00 |
| **Gold** | | | | | |
| Au(s) | 0 | 0 | 47.4 | 25.4 | 196.97 |
| Au(g) | 366.1 | 326.3 | 180.5 | 20.8 | 197.97 |

(continued)

**TABLE 4.1 Thermodynamic Data for Inorganic Compounds at 298.15 K (continued)**

| Substance | $\Delta H_f^\circ$ (kJ mol$^{-1}$) | $\Delta G_f^\circ$ (kJ mol$^{-1}$) | $S_m^\circ$ (J mol$^{-1}$ K$^{-1}$) | $C_{P,\,m}$ (J mol$^{-1}$ K$^{-1}$) | Atomic or Molecular Weight (amu) |
|---|---|---|---|---|---|
| **Hydrogen** | | | | | |
| $H_2(g)$ | 0 | 0 | 130.7 | 28.8 | 2.016 |
| $H(g)$ | 218.0 | 203.3 | 114.7 | 20.8 | 1.008 |
| $OH(g)$ | 39.0 | 34.2 | 183.7 | 29.9 | 17.01 |
| $H_2O(g)$ | −241.8 | −228.6 | 188.8 | 33.6 | 18.015 |
| $H_2O(l)$ | −285.8 | −237.1 | 70.0 | 75.3 | 18.015 |
| $H_2O(s)$ | | | 48.0 | 36.2 (273 K) | 18.015 |
| $H_2O_2(g)$ | −136.3 | −105.6 | 232.7 | 43.1 | 34.015 |
| $H^+(aq)$ | 0 | 0 | 0 | | 1.008 |
| $OH^-(aq)$ | −230.0 | −157.24 | −10.9 | | 17.01 |
| **Iodine** | | | | | |
| $I_2(s)$ | 0 | 0 | 116.1 | 54.4 | 253.80 |
| $I_2(g)$ | 62.4 | 19.3 | 260.7 | 36.9 | 253.80 |
| $I(g)$ | 106.8 | 70.2 | 180.8 | 20.8 | 126.90 |
| $I^-(aq)$ | −55.2 | −51.6 | 111.3 | | 126.90 |
| **Iron** | | | | | |
| $Fe(s)$ | 0 | 0 | 27.3 | 25.1 | 55.85 |
| $Fe(g)$ | 416.3 | 370.7 | 180.5 | 25.7 | 55.85 |
| $Fe_2O_3(s)$ | −824.2 | −742.2 | 87.4 | 103.9 | 159.69 |
| $Fe_3O_4(s)$ | −1118.4 | −1015.4 | 146.4 | 150.7 | 231.54 |
| $FeSO_4(s)$ | −928.4 | −820.8 | 107.5 | 100.6 | 151.92 |
| $Fe^{2+}(aq)$ | −89.1 | −78.9 | −137.7 | | 55.85 |
| $Fe^{3+}(aq)$ | −48.5 | −4.7 | −315.9 | | 55.85 |
| **Lead** | | | | | |
| $Pb(s)$ | 0 | 0 | 64.8 | 26.4 | 207.19 |
| $Pb(g)$ | 195.2 | 162.2 | 175.4 | 20.8 | 207.19 |
| $PbO_2(s)$ | −277.4 | −217.3 | 68.6 | 64.6 | 239.19 |
| $PbSO_4(s)$ | −920.0 | −813.20 | 148.5 | 86.4 | 303.25 |
| $Pb^{2+}(aq)$ | 0.92 | −24.4 | 18.5 | | 207.19 |
| **Lithium** | | | | | |
| $Li(s)$ | 0 | 0 | 29.1 | 24.8 | 6.94 |
| $Li(g)$ | 159.3 | 126.6 | 138.8 | 20.8 | 6.94 |
| $LiH(s)$ | −90.5 | −68.3 | 20.0 | 27.9 | 7.94 |
| $LiH(g)$ | 140.6 | 117.8 | 170.9 | 29.7 | 7.94 |
| $Li^+(aq)$ | −278.5 | −293.3 | 13.4 | | 6.94 |
| **Magnesium** | | | | | |
| $Mg(s)$ | 0 | 0 | 32.7 | 24.9 | 24.31 |
| $Mg(g)$ | 147.1 | 112.5 | 148.6 | 20.8 | 24.31 |
| $MgO(s)$ | −601.6 | −569.3 | 27.0 | 37.2 | 40.31 |
| $MgSO_4(s)$ | −1284.9 | −1170.6 | 91.6 | 96.5 | 120.38 |
| $MgCl_2(s)$ | −641.3 | −591.8 | 89.6 | 71.4 | 95.22 |
| $MgCO_3(s)$ | −1095.8 | −1012.2 | 65.7 | 75.5 | 84.32 |
| $Mg^{2+}(aq)$ | −466.9 | −454.8 | −138.1 | | 24.31 |
| **Manganese** | | | | | |
| $Mn(s)$ | 0 | 0 | 32.0 | 26.3 | 54.94 |
| $Mn(g)$ | 280.7 | 238.5 | 173.7 | 20.8 | 54.94 |
| $MnO_2(s)$ | −520.0 | −465.1 | 53.1 | 54.1 | 86.94 |
| $Mn^{2+}(aq)$ | −220.8 | −228.1 | −73.6 | | 54.94 |
| $MnO_4^-(aq)$ | −541.4 | −447.2 | 191.2 | | 118.94 |

| Substance | $\Delta H_f^\circ$ (kJ mol$^{-1}$) | $\Delta G_f^\circ$ (kJ mol$^{-1}$) | $S_m^\circ$(J mol$^{-1}$ K$^{-1}$) | $C_{P,\,m}$ (J mol$^{-1}$ K$^{-1}$) | Atomic or Molecular Weight (amu) |
|---|---|---|---|---|---|
| **Mercury** | | | | | |
| Hg($l$) | 0 | 0 | 75.9 | 28.0 | 200.59 |
| Hg($g$) | 61.4 | 31.8 | 175.0 | 20.8 | 200.59 |
| Hg$_2$Cl$_2$($s$) | −265.4 | −210.7 | 191.6 | 101.9 | 472.09 |
| Hg$^{2+}$($aq$) | 170.2 | 164.4 | −36.2 | | 401.18 |
| Hg$_2^{2+}$($aq$) | 166.9 | 153.5 | 65.7 | | 401.18 |
| **Nickel** | | | | | |
| Ni($s$) | 0 | 0 | 29.9 | 26.1 | 58.71 |
| Ni($g$) | 429.7 | 384.5 | 182.2 | 23.4 | 58.71 |
| NiCl$_2$($s$) | −305.3 | −259.0 | 97.7 | 71.7 | 129.62 |
| NiO($s$) | −239.7 | −211.5 | 38.0 | 44.3 | 74.71 |
| NiSO$_4$($s$) | −872.9 | −759.7 | 92.0 | 138.0 | 154.77 |
| Ni$^{2+}$($aq$) | −54.0 | −45.6 | −128.9 | | 58.71 |
| **Nitrogen** | | | | | |
| N$_2$($g$) | 0 | 0 | 191.6 | 29.1 | 28.013 |
| N($g$) | 472.7 | 455.5 | 153.3 | 20.8 | 14.007 |
| NH$_3$($g$) | −45.9 | −16.5 | 192.8 | 35.1 | 17.03 |
| NO($g$) | 91.3 | 87.6 | 210.8 | 29.9 | 30.01 |
| N$_2$O($g$) | 81.6 | 103.7 | 220.0 | 38.6 | 44.01 |
| NO$_2$($g$) | 33.2 | 51.3 | 240.1 | 37.2 | 46.01 |
| NOCl($g$) | 51.7 | 66.1 | 261.7 | 44.7 | 65.46 |
| N$_2$O$_4$($g$) | 11.1 | 99.8 | 304.4 | 79.2 | 92.01 |
| N$_2$O$_4$($l$) | −19.5 | 97.5 | 209.2 | 142.7 | 92.01 |
| HNO$_3$($l$) | −174.1 | −80.7 | 155.6 | 109.9 | 63.01 |
| HNO$_3$($g$) | −133.9 | −73.5 | 266.9 | 54.1 | 63.01 |
| NO$_3^-$($aq$) | −207.4 | −111.3 | 146.4 | | 62.01 |
| NH$_4^+$($aq$) | −132.5 | −79.3 | 113.4 | | 18.04 |
| **Oxygen** | | | | | |
| O$_2$($g$) | 0 | 0 | 205.2 | 29.4 | 31.999 |
| O($g$) | 249.2 | 231.7 | 161.1 | 21.9 | 15.999 |
| O$_3$($g$) | 142.7 | 163.2 | 238.9 | 39.2 | 47.998 |
| OH($g$) | 39.0 | 34.22 | 183.7 | 29.9 | 17.01 |
| OH$^-$($aq$) | −230.0 | −157.2 | −10.9 | | 17.01 |
| **Phosphorus** | | | | | |
| P($s$) white | 0 | 0 | 41.1 | 23.8 | 30.97 |
| P($s$) red | −17.6 | −12.1 | 22.8 | 21.2 | 30.97 |
| P$_4$($g$) | 58.9 | 24.4 | 280.0 | 67.2 | 123.90 |
| PCl$_5$($g$) | −374.9 | −305.0 | 364.6 | 112.8 | 208.24 |
| PH$_3$($g$) | 5.4 | 13.5 | 210.2 | 37.1 | 34.00 |
| H$_3$PO$_4$($l$) | −1271.7 | −1123.6 | 150.8 | 145.0 | 94.97 |
| PO$_4^{3-}$($aq$) | −1277.4 | −1018.7 | −220.5 | | 91.97 |
| HPO$_4^{2-}$($aq$) | −1299.0 | −1089.2 | −33.5 | | 92.97 |
| H$_2$PO$_4^-$($aq$) | −1302.6 | −1130.2 | 92.5 | | 93.97 |
| **Potassium** | | | | | |
| K($s$) | 0 | 0 | 64.7 | 29.6 | 39.10 |
| K($g$) | 89.0 | 60.5 | 160.3 | 20.8 | 39.10 |
| KCl($s$) | −436.5 | −408.5 | 82.6 | 51.3 | 74.56 |
| K$_2$O($s$) | −361.5 | −322.8 | 102.0 | 77.4 | 94.20 |
| K$_2$SO$_4$($s$) | −1437.8 | −1321.4 | 175.6 | 131.5 | 174.27 |
| K$^+$($aq$) | −252.4 | −283.3 | 102.5 | | 39.10 |

(continued)

**TABLE 4.1** **Thermodynamic Data for Inorganic Compounds at 298.15 K (continued)**

| Substance | $\Delta H_f^\circ$ (kJ mol$^{-1}$) | $\Delta G_f^\circ$ (kJ mol$^{-1}$) | $S_m^\circ$ (J mol$^{-1}$ K$^{-1}$) | $C_{P,m}$ (J mol$^{-1}$ K$^{-1}$) | Atomic or Molecular Weight (amu) |
|---|---|---|---|---|---|
| **Silicon** | | | | | |
| Si($s$) | 0 | 0 | 18.8 | 20.0 | 28.09 |
| Si($g$) | 450.0 | 405.5 | 168.0 | 22.3 | 28.09 |
| SiCl$_4$($g$) | −662.7 | −622.8 | 330.9 | 90.3 | 169.70 |
| SiO$_2$(*quartz*) | −910.7 | −856.3 | 41.5 | 44.4 | 60.09 |
| **Silver** | | | | | |
| Ag($s$) | 0 | 0 | 42.6 | 25.4 | 107.87 |
| Ag($g$) | 284.9 | 246.0 | 173.0 | 20.8 | 107.87 |
| AgCl($s$) | −127.0 | −109.8 | 96.3 | 50.8 | 143.32 |
| AgNO$_2$($s$) | −44.4 | 19.8 | 140.6 | 93.0 | 153.88 |
| AgNO$_3$($s$) | −44.4 | 19.8 | 140.9 | 93.1 | 169.87 |
| Ag$_2$SO$_4$($s$) | −715.9 | −618.4 | 200.4 | 131.4 | 311.80 |
| Ag$^+$($aq$) | 105.6 | 77.1 | 72.7 | | 107.87 |
| **Sodium** | | | | | |
| Na($s$) | 0 | 0 | 51.3 | 28.2 | 22.99 |
| Na($g$) | 107.5 | 77.0 | 153.7 | 20.8 | 22.99 |
| NaCl($s$) | −411.2 | −384.1 | 72.1 | 50.5 | 58.44 |
| NaOH($s$) | −425.8 | −379.7 | 64.4 | 59.5 | 40.00 |
| Na$_2$SO$_4$($s$) | −1387.1 | −1270.2 | 149.6 | 128.2 | 142.04 |
| Na$^+$($aq$) | −240.1 | −261.9 | 59.0 | | 22.99 |
| **Sulfur** | | | | | |
| S(*rhombic*) | 0 | 0 | 32.1 | 22.6 | 32.06 |
| SF$_6$($g$) | −1220.5 | −1116.5 | 291.5 | 97.3 | 146.07 |
| H$_2$S($g$) | −20.6 | −33.4 | 205.8 | 34.2 | 34.09 |
| SO$_2$($g$) | −296.8 | −300.1 | 248.2 | 39.9 | 64.06 |
| SO$_3$($g$) | −395.7 | −371.1 | 256.8 | 50.7 | 80.06 |
| SO$_3^{2-}$($aq$) | −635.5 | −486.6 | −29.3 | | 80.06 |
| SO$_4^{2-}$($aq$) | −909.3 | −744.5 | 20.1 | | 96.06 |
| **Tin** | | | | | |
| Sn(*white*) | 0 | 0 | 51.2 | 27.0 | 118.69 |
| Sn($g$) | 301.2 | 266.2 | 168.5 | 21.3 | 118.69 |
| SnO$_2$($s$) | −577.6 | −515.8 | 49.0 | 52.6 | 150.69 |
| Sn$^{2+}$($aq$) | −8.9 | −27.2 | −16.7 | | 118.69 |
| **Titanium** | | | | | |
| Ti($s$) | 0 | 0 | 30.7 | 25.0 | 47.87 |
| Ti($g$) | 473.0 | 428.4 | 180.3 | 24.4 | 47.87 |
| TiCl$_4$($l$) | −804.2 | −737.2 | 252.4 | 145.2 | 189.69 |
| TiO$_2$($s$) | −944.0 | −888.8 | 50.6 | 55.0 | 79.88 |
| **Xenon** | | | | | |
| Xe($g$) | 0 | 0 | 169.7 | 20.8 | 131.30 |
| XeF$_4$($s$) | −261.5 | −123 | 146 | 118 | 207.29 |
| **Zinc** | | | | | |
| Zn($s$) | 0 | 0 | 41.6 | 25.4 | 65.37 |
| ZnCl$_2$($s$) | −415.1 | −369.4 | 111.5 | 71.3 | 136.28 |
| ZnO($s$) | −350.5 | −320.5 | 43.7 | 40.3 | 81.37 |
| ZnSO$_4$($s$) | −982.8 | −871.5 | 110.5 | 99.2 | 161.43 |
| Zn$^{2+}$($aq$) | −153.9 | −147.1 | −112.1 | | 65.37 |

*Sources:* HCP, HTTD, and TDPS.

**TABLE 4.2   Thermodynamic Data for Selected Organic Compounds at 298.15 K**

| Substance | Formula | Molecular Weight | $\Delta H_f^\circ$ (kJ mol$^{-1}$) | $\Delta H_{combustion}^\circ$ (kJ mol$^{-1}$) | $\Delta G_f^\circ$ (kJ mol$^{-1}$) | $S_m^\circ$ (J mol$^{-1}$ K$^{-1}$) | $C_{P,m}$ (J mol$^{-1}$ K$^{-1}$) |
|---|---|---|---|---|---|---|---|
| Carbon (graphite) | C | 12.011 | 0 | −393.5 | 0 | 5.74 | 8.52 |
| Carbon (diamond) | C | 12.011 | 1.89 | −395.4 | 2.90 | 2.38 | 6.12 |
| Carbon monoxide | CO | 28.01 | −110.5 | −283.0 | −137.2 | 197.7 | 29.1 |
| Carbon dioxide | CO$_2$ | 44.01 | −393.5 | | −394.4 | 213.8 | 37.1 |
| Acetaldehyde(*l*) | C$_2$H$_4$O | 44.05 | −192.2 | −1166.9 | −127.6 | 160.3 | 89.0 |
| Acetic acid(*l*) | C$_2$H$_4$O$_2$ | 60.05 | −484.3 | −874.2 | −389.9 | 159.8 | 124.3 |
| Acetone(*l*) | C$_3$H$_6$O | 58.08 | −248.4 | −1790 | −155.2 | 199.8 | 126.3 |
| Benzene(*l*) | C$_6$H$_6$ | 78.12 | 49.1 | −3268 | 124.5 | 173.4 | 136.0 |
| Benzene(*g*) | C$_6$H$_6$ | 78.12 | 82.9 | −3303 | 129.7 | 269.2 | 82.4 |
| Benzoic acid(*s*) | C$_7$H$_6$O$_2$ | 122.13 | −385.2 | −3227 | −245.5 | 167.6 | 146.8 |
| 1,3-Butadiene(*g*) | C$_4$H$_6$ | 54.09 | 110.0 | −2541 | | | 79.8 |
| *n*-Butane(*g*) | C$_4$H$_{10}$ | 58.13 | −125.7 | −2878 | −17.0 | 310.2 | 97.5 |
| 1-Butene(*g*) | C$_4$H$_8$ | 56.11 | −0.63 | −2718 | 71.1 | 305.7 | 85.7 |
| Carbon disulfide(*g*) | CS$_2$ | 76.14 | 116.9 | −1112 | 66.8 | 238.0 | 45.7 |
| Carbon tetrachloride(*l*) | CCl$_4$ | 153.82 | −128.2 | −360 | −62.5 | 214.4 | 133.9 |
| Carbon tetrachloride(*g*) | CCl$_4$ | 153.82 | −95.7 | | −58.2 | 309.7 | 83.4 |
| Cyclohexane(*l*) | C$_6$H$_{12}$ | 84.16 | −156.4 | −3920 | 26.8 | 204.5 | 154.9 |
| Cyclopentane(*l*) | C$_5$H$_{10}$ | 70.13 | −105.1 | −3291 | 38.8 | 204.5 | 128.8 |
| Cyclopropane(*g*) | C$_3$H$_6$ | 42.08 | 53.3 | −2091 | 104.5 | 237.5 | 55.6 |
| Dimethyl ether(*g*) | C$_2$H$_6$O | 131.6 | −184.1 | −1460 | −112.6 | 266.4 | 64.4 |
| Ethane(*g*) | C$_2$H$_6$ | 30.07 | −84.0 | −1561 | −32.0 | 229.2 | 52.5 |
| Ethanol(*l*) | C$_2$H$_6$O | 46.07 | −277.6 | −1367 | −174.8 | 160.7 | 112.3 |
| Ethanol(*g*) | C$_2$H$_6$O | 46.07 | −234.8 | −1367 | −167.9 | 281.6 | 65.6 |
| Ethene(*g*) | C$_2$H$_4$ | 28.05 | 52.4 | −1411 | 68.4 | 219.3 | 42.9 |
| Ethyne(*g*) | C$_2$H$_2$ | 26.04 | 227.4 | −1310 | 209.2 | 200.9 | 44 |
| Formaldehyde(*g*) | CH$_2$O | 30.03 | −108.6 | −571 | −102.5 | 218.8 | 35.4 |
| Formic acid(*l*) | CH$_2$O$_2$ | 46.03 | −425.0 | −255 | −361.4 | 129.0 | 99.0 |
| Formic acid(*g*) | CH$_2$O$_2$ | 46.03 | −378.7 | −256 | −351.0 | 248.7 | 45.2 |
| α-D-Glucose(*s*) | C$_6$H$_{12}$O$_6$ | 180.16 | −1273.1 | −2805 | −910.6 | 209.2 | 219.2 |
| *n*-Hexane(*l*) | C$_6$H$_{14}$ | 86.18 | −198.7 | −4163 | −4.0 | 296.0 | 195.6 |
| Hydrogen cyanide(*l*) | HCN | 27.03 | 108.9 | | 125.0 | 112.8 | 70.6 |
| Hydrogen cyanide(*g*) | HCN | 27.03 | 135.5 | | 124.7 | 201.8 | 35.9 |
| Methane(*g*) | CH$_4$ | 16.04 | −74.6 | −891 | −50.5 | 186.3 | 35.7 |
| Methanol(*l*) | CH$_4$O | 32.04 | −239.2 | −726 | −166.6 | 126.8 | 81.1 |
| Methanol(*g*) | CH$_4$O | 32.04 | −201.0 | −764 | −162.3 | 239.9 | 44.1 |
| Oxalic acid(*g*) | C$_2$H$_2$O$_4$ | 90.04 | −731.8 | −246 | −662.7 | 320.6 | 86.2 |
| *n*-Pentane(*g*) | C$_5$H$_{12}$ | 72.15 | −146.9 | −3509 | −8.2 | 349.1 | 120.1 |
| Phenol(*s*) | C$_6$H$_6$O | 94.11 | −165.1 | −3054 | −50.2 | 144.0 | 127.4 |
| Propane(*g*) | C$_3$H$_8$ | 44.10 | −103.8 | −2219 | −23.4 | 270.3 | 73.6 |
| Propene(*g*) | C$_3$H$_6$ | 42.08 | 20.0 | −2058 | 62.7 | 266.9 | 64.0 |
| Propyne(*g*) | C$_3$H$_4$ | 40.07 | 184.9 | −2058 | 194.5 | 248.2 | 60.7 |
| Pyridine(*l*) | C$_5$H$_5$N | 79.10 | 100.2 | −2782 | | 177.9 | 132.7 |
| Sucrose(*s*) | C$_{12}$H$_{22}$O$_{11}$ | 342.3 | −2226.1 | −5643 | −1544.6 | 360.2 | 424.3 |
| Thiophene(*l*) | C$_4$H$_4$S | 84.14 | 80.2 | −2829 | | 181.2 | 123.8 |
| Toluene(*g*) | C$_7$H$_8$ | 92.14 | 50.5 | −3910 | 122.3 | 320.8 | 104 |
| Urea(*s*) | C$_2$H$_4$N$_2$O | 60.06 | −333.1 | −635 | −197.4 | 104.3 | 92.8 |

*Sources:* HCP, HTTD, TDPS, and TDOC.

**TABLE 7.1 Second Virial Coefficients for Selected Gases in Units of cm³ mol⁻¹**

| | 200 K | 300 K | 400 K | 500 K | 600 K | 700 K |
|---|---|---|---|---|---|---|
| Benzene | | −1453 | −712 | −429 | −291 | −211 |
| $Cl_2$ | | −299 | −166 | −97 | −59 | −36 |
| $CO_2$ | | −126 | −61.7 | −30.5 | −12.6 | −1.18 |
| $H_2O$ | | −1126 | −356 | −175 | −104 | −67 |
| Heptane | | −2782 | −1233 | −702 | −452 | −304 |
| Kr | −117 | −51.0 | −23.0 | −7.75 | 1.78 | 8.33 |
| $N_2$ | −34.4 | −3.91 | 9.17 | 16.3 | 20.8 | 23.8 |
| Octane | | −4042 | −1704 | −936 | −583 | −375 |

*Source:* Calculated from HTTD.

**TABLE 7.2 Critical Constants of Selected Substances**

| Substance | Formula | $T_c$ (K) | $P_c$ (bar) | $10^3 V_c$ (L) | $z_c = \dfrac{P_c V_c}{RT_c}$ |
|---|---|---|---|---|---|
| Ammonia | $NH_3$ | 405.40 | 113.53 | 72.47 | 0.244 |
| Argon | Ar | 150.86 | 48.98 | 74.57 | 0.291 |
| Benzene | $C_6H_6$ | 562.05 | 48.95 | 256.00 | 0.268 |
| Bromine | $Br_2$ | 588.00 | 103.40 | 127.00 | 0.268 |
| Carbon dioxide | $CO_2$ | 304.13 | 73.75 | 94.07 | 0.274 |
| Carbon monoxide | CO | 132.91 | 34.99 | 93.10 | 0.295 |
| Ethane | $C_2H_6$ | 305.32 | 48.72 | 145.50 | 0.279 |
| Ethanol | $C_2H_5OH$ | 513.92 | 61.37 | 168.00 | 0.241 |
| Ethene | $C_2H_4$ | 282.34 | 50.41 | 131.1 | 0.281 |
| Ethyne | $C_2H_2$ | 308.30 | 61.38 | 112.20 | 0.269 |
| Fluorine | $F_2$ | 144.30 | 51.72 | 66.20 | 0.285 |
| Hydrogen | $H_2$ | 32.98 | 12.93 | 64.20 | 0.303 |
| Methane | $CH_4$ | 190.56 | 45.99 | 98.60 | 0.286 |
| Methanol | $CH_3OH$ | 512.50 | 80.84 | 117.00 | 0.221 |
| Nitrogen | $N_2$ | 126.20 | 33.98 | 90.10 | 0.292 |
| Oxygen | $O_2$ | 154.58 | 50.43 | 73.37 | 0.288 |
| Pentane | $C_5H_{12}$ | 469.70 | 33.70 | 311.00 | 0.268 |
| Propane | $C_3H_8$ | 369.83 | 42.48 | 200.00 | 0.276 |
| Pyridine | $C_5H_5N$ | 620.00 | 56.70 | 243.00 | 0.267 |
| Tetrachloromethane | $CCl_4$ | 556.60 | 45.16 | 276.00 | 0.269 |
| Water | $H_2O$ | 647.14 | 220.64 | 55.95 | 0.229 |
| Xenon | Xe | 289.74 | 58.40 | 118.00 | 0.286 |

*Sources:* HCP and DAL.

**TABLE 7.4** van der Waals and Redlich–Kwong Parameters for Selected Gases

| Substance | Formula | van der Waals | | Redlich–Kwong | |
| | | $a$ (dm$^6$ bar mol$^{-2}$) | $b$ (dm$^3$ mol$^{-1}$) | $a$ (dm$^6$ bar mol$^{-2}$ K$^{1/2}$) | $b$ (dm$^3$ mol$^{-1}$) |
|---|---|---|---|---|---|
| Ammonia | $NH_3$ | 4.225 | 0.0371 | 86.12 | 0.02572 |
| Argon | Ar | 1.355 | 0.0320 | 16.86 | 0.02219 |
| Benzene | $C_6H_6$ | 18.82 | 0.1193 | 452.0 | 0.08271 |
| Bromine | $Br_2$ | 9.75 | 0.0591 | 236.5 | 0.04085 |
| Carbon dioxide | $CO_2$ | 3.658 | 0.0429 | 64.63 | 0.02971 |
| Carbon monoxide | CO | 1.472 | 0.0395 | 17.20 | 0.02739 |
| Ethane | $C_2H_6$ | 5.580 | 0.0651 | 98.79 | 0.04514 |
| Ethanol | $C_2H_5OH$ | 12.56 | 0.0871 | 287.7 | 0.06021 |
| Ethene | $C_2H_4$ | 4.612 | 0.0582 | 78.51 | 0.04034 |
| Ethyne | $C_2H_2$ | 4.533 | 0.05240 | 80.65 | 0.03632 |
| Fluorine | $F_2$ | 1.171 | 0.0290 | 14.17 | 0.01993 |
| Hydrogen | $H_2$ | 0.2452 | 0.0265 | 1.427 | 0.01837 |
| Methane | $CH_4$ | 2.303 | 0.0431 | 32.20 | 0.02985 |
| Methanol | $CH_3OH$ | 9.476 | 0.0659 | 217.1 | 0.04561 |
| Nitrogen | $N_2$ | 1.370 | 0.0387 | 15.55 | 0.02675 |
| Oxygen | $O_2$ | 1.382 | 0.0319 | 17.40 | 0.02208 |
| Pentane | $C_5H_{12}$ | 19.09 | 0.1448 | 419.2 | 0.1004 |
| Propane | $C_3H_8$ | 9.39 | 0.0905 | 182.9 | 0.06271 |
| Pyridine | $C_5H_5N$ | 19.77 | 0.1137 | 498.8 | 0.07877 |
| Tetrachloromethane | $CCl_4$ | 20.01 | 0.1281 | 473.2 | 0.08793 |
| Water | $H_2O$ | 5.537 | 0.0305 | 142.6 | 0.02113 |
| Xenon | Xe | 4.192 | 0.0516 | 72.30 | 0.03574 |

*Source:* Calculated from critical constants.

**TABLE 8.1** Triple Point Pressures and Temperatures of Selected Substances

| Formula | Name | $T_{tp}$ (K) | $P_{tp}$ (Pa) |
|---|---|---|---|
| Ar | Argon | 83.806 | 68950 |
| $Br_2$ | Bromine | 280.4 | 5879 |
| $Cl_2$ | Chlorine | 172.17 | 1392 |
| HCl | Hydrogen chloride | 158.8 | |
| $H_2$ | Hydrogen | 13.8 | 7042 |
| $H_2O$ | Water | 273.16 | 611.73 |
| $H_2S$ | Hydrogen sulfide | 187.67 | 23180 |
| $NH_3$ | Ammonia | 195.41 | 6077 |
| Kr | Krypton | 115.8 | 72920 |
| NO | Nitrogen oxide | 109.54 | 21916 |
| $O_2$ | Oxygen | 54.36 | 146.33 |
| $SO_3$ | Sulfur trioxide | 289.94 | 21130 |
| Xe | Xenon | 161.4 | 81590 |
| $CH_4$ | Methane | 90.694 | 11696 |
| CO | Carbon monoxide | 68.15 | 15420 |
| $CO_2$ | Carbon dioxide | 216.58 | 518500 |
| $C_3H_6$ | Propene | 87.89 | $9.50 \times 10^{-4}$ |

*Sources:* HCP, HTTP, and DAL.

## TABLE 8.3 Vapor Pressure and Boiling Temperature of Liquids

$$\ln\frac{P(T)}{\text{Pa}} = A(1) - \frac{A(2)}{\frac{T}{K} + A(3)} \qquad T_{vap}(P) = \frac{A(2)}{A(1) - \ln\frac{P}{\text{Pa}}} - A(3)$$

| Molecular Formula | Name | $T_{vap}$ (K) | $A(1)$ | $A(2)$ | $A(3)$ | $10^{-3}P(298.15\text{ K})$ (Pa) | Range (K) |
|---|---|---|---|---|---|---|---|
| Ar | Argon | 87.28 | 22.946 | $1.0325 \times 10^3$ | 3.130 | — | 73–90 |
| Br$_2$ | Bromine | 331.9 | 20.729 | $2.5782 \times 10^3$ | $-51.77$ | 28.72 | 268–354 |
| HF | Hydrogen fluoride | 292.65 | 22.893 | $3.6178 \times 10^3$ | 25.627 | 122.90 | 273–303 |
| H$_2$O | Water | 373.15 | 23.195 | $3.8140 \times 10^3$ | $-46.290$ | | 353–393 |
| SO$_2$ | Sulfur dioxide | 263.12 | 21.661 | $2.3024 \times 10^3$ | $-35.960$ | | 195–280 |
| CCl$_4$ | Tetrachloromethane | 349.79 | 20.738 | $2.7923 \times 10^3$ | $-46.6667$ | 15.28 | 287–350 |
| CHCl$_3$ | Trichloromethane | 334.33 | 20.907 | $2.6961 \times 10^3$ | $-46.926$ | 26.24 | 263–335 |
| HCN | Hydrogen cyanide | 298.81 | 22.226 | $3.0606 \times 10^3$ | $-12.773$ | 98.84 | 257–316 |
| CH$_3$OH | Methanol | 337.70 | 23.593 | $3.6971 \times 10^3$ | $-31.317$ | 16.94 | 275–338 |
| CS$_2$ | Carbon disulfide | 319.38 | 20.801 | $2.6524 \times 10^3$ | $-33.40$ | 48.17 | 255–320 |
| C$_2$H$_5$OH | Ethanol | 351.45 | 23.58 | $3.6745 \times 10^3$ | $-46.702$ | 7.87 | 293–366 |
| C$_3$H$_6$ | Propene | 225.46 | 20.613 | $1.8152 \times 10^3$ | $-25.705$ | 1156.6 | 166–226 |
| C$_3$H$_8$ | Propane | 231.08 | 20.558 | $1.8513 \times 10^3$ | $-26.110$ | 948.10 | 95–370 |
| C$_4$H$_9$Br | 1-Bromobutane | 374.75 | 17.076 | $1.5848 \times 10^3$ | $-11.188$ | 5.26 | 195–300 |
| C$_4$H$_9$Cl | 1-Chlorobutane | 351.58 | 20.612 | $2.6881 \times 10^3$ | $-55.725$ | 13.68 | 256–352 |
| C$_5$H$_{11}$OH | 1-Pentanol | 411.133 | 20.729 | $2.5418 \times 10^3$ | $-134.93$ | 0.29 | 410–514 |
| C$_6$H$_5$Cl | Chlorobenzene | 404.837 | 20.964 | $3.2969 \times 10^3$ | $-55.515$ | 1.57 | 335–405 |
| C$_6$H$_5$I | Iodobenzene | 461.48 | 21.088 | $3.8136 \times 10^3$ | $-62.654$ | 0.13 | 298–462 |
| C$_6$H$_6$ | Benzene | 353.24 | 20.767 | $2.7738 \times 10^3$ | $-53.08$ | 12.69 | 294–378 |
| C$_6$H$_{14}$ | Hexane | 341.886 | 20.749 | $2.7081 \times 10^3$ | $-48.251$ | 20.17 | 286–343 |
| C$_6$H$_5$CHO | Benzaldehyde | 451.90 | 21.213 | $3.7271 \times 10^3$ | $-67.156$ | 0.17 | 311–481 |
| C$_6$H$_5$CH$_3$ | Toluene | 383.78 | 21.600 | $3.6266 \times 10^3$ | $-23.778$ | 3.80 | 360–580 |
| C$_{10}$H$_8$ | Naphthalene | 491.16 | 21.100 | $4.0526 \times 10^3$ | $-67.866$ | 0.01 | 353–453 |
| C$_{14}$H$_{10}$ | Anthracene | 614.0 | 21.965 | $5.8733 \times 10^3$ | $-51.394$ | | 496–615 |

*Sources:* HCP and HTTP.

## TABLE 8.4 Sublimation Pressure of Solids

$$\ln\frac{P(T)}{\text{Pa}} = A(1) - \frac{A(2)}{\frac{T}{K} + A(3)}$$

| Molecular Formula | Name | $A(1)$ | $A(2)$ | $A(3)$ | Range (K) |
|---|---|---|---|---|---|
| CCl$_4$ | Tetrachloromethane | 17.613 | $1.6431 \times 10^3$ | $-95.250$ | 232–250 |
| C$_6$H$_{14}$ | Hexane | 31.224 | $4.8186 \times 10^3$ | $-23.150$ | 168–178 |
| C$_6$H$_5$COOH | Benzoic acid | 14.870 | $4.7196 \times 10^3$ | | 293–314 |
| C$_{10}$H$_8$ | Naphthalene | 31.143 | $8.5750 \times 10^3$ | | 270–305 |
| C$_{14}$H$_{10}$ | Anthracene | 31.620 | $1.1378 \times 10^4$ | | 353–400 |

*Sources:* HCP and HTTP.

**TABLE 10.2**   **Dielectric Constants, $\varepsilon_r$, of Selected Liquids**

| Substance | Dielectric Constant | Substance | Dielectric Constant |
|---|---|---|---|
| Acetic acid | 6.2 | Heptane | 1.9 |
| Acetone | 21.0 | Isopropyl alcohol | 20.2 |
| Benzaldehyde | 17.8 | Methanol | 33.0 |
| Benzene | 2.3 | Nitrobenzene | 35.6 |
| Carbon tetrachloride | 2.2 | o-Xylene | 2.6 |
| Cyclohexane | 2.0 | Phenol | 12.4 |
| Ethanol | 25.3 | Toluene | 2.4 |
| Glycerol | 42.5 | Water (273 K) | 88.0 |
| 1-Hexanol | 13.0 | Water (373 K) | 55.3 |

*Source:* HCP.

**TABLE 10.3**   **Mean Activity Coefficients in Terms of Molalities at 298 K**

| Substance | 0.1 $m$ | 0.2 $m$ | 0.3 $m$ | 0.4 $m$ | 0.5 $m$ | 0.6 $m$ | 0.7 $m$ | 0.8 $m$ | 0.9 $m$ | 1.0 $m$ |
|---|---|---|---|---|---|---|---|---|---|---|
| $AgNO_3$ | 0.734 | 0.657 | 0.606 | 0.567 | 0.536 | 0.509 | 0.485 | 0.464 | 0.446 | 0.429 |
| $BaCl_2$ | 0.500 | 0.444 | 0.419 | 0.405 | 0.397 | 0.391 | 0.391 | 0.391 | 0.392 | 0.395 |
| $CaCl_2$ | 0.518 | 0.472 | 0.455 | 0.448 | 0.448 | 0.453 | 0.460 | 0.470 | 0.484 | 0.500 |
| $CuCl_2$ | 0.508 | 0.455 | 0.429 | 0.417 | 0.411 | 0.409 | 0.409 | 0.410 | 0.413 | 0.417 |
| $CuSO_4$ | 0.150 | 0.104 | 0.0829 | 0.0704 | 0.0620 | 0.0559 | 0.0512 | 0.0475 | 0.0446 | 0.0423 |
| HCl | 0.796 | 0.767 | 0.756 | 0.755 | 0.757 | 0.763 | 0.772 | 0.783 | 0.795 | 0.809 |
| $HNO_3$ | 0.791 | 0.754 | 0.735 | 0.725 | 0.720 | 0.717 | 0.717 | 0.718 | 0.721 | 0.724 |
| $H_2SO_4$ | 0.2655 | 0.2090 | 0.1826 |  | 0.1557 |  | 0.1417 |  |  | 0.1316 |
| KCl | 0.770 | 0.718 | 0.688 | 0.666 | 0.649 | 0.637 | 0.626 | 0.618 | 0.610 | 0.604 |
| KOH | 0.798 | 0.760 | 0.742 | 0.734 | 0.732 | 0.733 | 0.736 | 0.742 | 0.749 | 0.756 |
| $MgCl_2$ | 0.529 | 0.489 | 0.477 | 0.475 | 0.481 | 0.491 | 0.506 | 0.522 | 0.544 | 0.570 |
| $MgSO_4$ | 0.150 | 0.107 | 0.0874 | 0.0756 | 0.0675 | 0.0616 | 0.0571 | 0.0536 | 0.0508 | 0.0485 |
| NaCl | 0.778 | 0.735 | 0.710 | 0.693 | 0.681 | 0.673 | 0.667 | 0.662 | 0.659 | 0.657 |
| NaOH | 0.766 | 0.727 | 0.708 | 0.697 | 0.690 | 0.685 | 0.681 | 0.679 | 0.678 | 0.678 |
| $ZnSO_4$ | 0.150 | 0.140 | 0.0835 | 0.0714 | 0.0630 | 0.0569 | 0.0523 | 0.0487 | 0.0458 | 0.0435 |

*Source:* HCP.

**TABLE 11.1**   **Standard Reduction Potentials in Alphabetical Order**

| Reaction | $E°$ (V) | Reaction | $E°$ (V) |
|---|---|---|---|
| $Ag^+ + e^- \longrightarrow Ag$ | 0.7996 | $Au^{3+} + 2e^- \longrightarrow Au^+$ | 1.401 |
| $Ag^{2+} + e^- \longrightarrow Ag^+$ | 1.980 | $Au^{3+} + 3e^- \longrightarrow Au$ | 1.498 |
| $AgBr + e^- \longrightarrow Ag + Br^-$ | 0.07133 | $AuBr_2^- + e^- \longrightarrow Au + 2Br^-$ | 0.959 |
| $AgCl + e^- \longrightarrow Ag + Cl^-$ | 0.22233 | $AuCl_4^- + 3e^- \longrightarrow Au + 4Cl^-$ | 1.002 |
| $AgCN + e^- \longrightarrow Ag + CN^-$ | −0.017 | $Ba^{2+} + 2e^- \longrightarrow Ba$ | −2.912 |
| $AgF + e^- \longrightarrow Ag + F^-$ | 0.779 | $Be^{2+} + 2e^- \longrightarrow Be$ | −1.847 |
| $Ag_4[Fe(CN)_6] + 4e^- \longrightarrow 4\,Ag + [Fe(CN)_6]^{4-}$ | 0.1478 | $Bi^{3+} + 3e^- \longrightarrow Bi$ | 0.20 |
| $AgI + e^- \longrightarrow Ag + I^-$ | −0.15224 | $Br_2(aq) + 2e^- \longrightarrow 2\,Br^-$ | 1.0873 |
| $AgNO_2 + e^- \longrightarrow Ag + NO_2^-$ | 0.564 | $BrO^- + H_2O + 2e^- \longrightarrow Br^- + 2\,OH^-$ | 0.761 |
| $Al^{3+} + 3e^- \longrightarrow Al$ | −1.662 | $Ca^+ + e^- \longrightarrow Ca$ | −3.80 |
| $Au^+ + e^- \longrightarrow Au$ | 1.692 | $Ca^{2+} + 2e^- \longrightarrow Ca$ | −2.868 |

(continued)

**TABLE 11.1** Standard Reduction Potentials in Alphabetical Order (continued)

| Reaction | $E°$ (V) | Reaction | $E°$ (V) |
|---|---|---|---|
| $Cd^{2+} + 2e^- \longrightarrow Cd$ | −0.4030 | $In^{3+} + 3e^- \longrightarrow In$ | −0.3382 |
| $Cd(OH)_2 + 2e^- \longrightarrow Cd + 2\,OH^-$ | −0.809 | $K^+ + e^- \longrightarrow K$ | −2.931 |
| $CdSO_4 + 2e^- \longrightarrow Cd + SO_4^{2-}$ | −0.246 | $Li^+ + e^- \longrightarrow Li$ | −3.0401 |
| $Ce^{3+} + 3e^- \longrightarrow Ce$ | −2.483 | $Mg^{2+} + 2e^- \longrightarrow Mg$ | −2.372 |
| $Ce^{4+} + e^- \longrightarrow Ce^{3+}$ | 1.61 | $Mg(OH)_2 + 2e^- \longrightarrow Mg + 2\,OH^-$ | −2.690 |
| $Cl_2(g) + 2e^- \longrightarrow 2\,Cl^-$ | 1.35827 | $Mn^{2+} + 2e^- \longrightarrow Mn$ | −1.185 |
| $ClO_4^- + 2\,H^+ + 2e^- \longrightarrow ClO_3^- + H_2O$ | 1.189 | $Mn^{3+} + e^- \longrightarrow Mn^{2+}$ | 1.5415 |
| $ClO^- + H_2O + 2e^- \longrightarrow Cl^- + 2\,OH^-$ | .81 | $MnO_2 + 4\,H^+ + 2e^- \longrightarrow Mn^{2+} + 2\,H_2O$ | 1.224 |
| $ClO_4^- + H_2O + 2e^- \longrightarrow ClO_3^- + 2\,OH^-$ | 0.36 | $MnO_4^- + 4\,H^+ + 3e^- \longrightarrow MnO_2 + 2\,H_2O$ | 1.679 |
| $Co^{2+} + 2e^- \longrightarrow Co$ | −0.28 | $MnO_4^{2-} + 2\,H_2O + 2e^- \longrightarrow MnO_2 + 4\,OH^-$ | 0.595 |
| $Co^{3+} + e^- \longrightarrow Co^{2+}$ | 1.92 | $MnO_4^- + 8\,H^+ + 5e^- \longrightarrow Mn^{2+} + 4\,H_2O$ | 1.507 |
| $Cr^{2+} + 2e^- \longrightarrow Cr$ | −0.913 | $MnO_4^- + e^- \longrightarrow MnO_4^{2-}$ | 0.558 |
| $Cr^{3+} + e^- \longrightarrow Cr^{2+}$ | −0.407 | $2\,NO + 2\,H^+ + 2e^- \longrightarrow N_2O + H_2O$ | 1.591 |
| $Cr^{3+} + 3e^- \longrightarrow Cr$ | −0.744 | $HNO_2 + H^+ + e^- \longrightarrow NO + H_2O$ | 0.983 |
| $Cr_2O_7^{2-} + 14\,H^+ + 6e^- \longrightarrow 2\,Cr^{3+} + 7\,H_2O$ | 1.232 | $NO_2 + H_2O + 3e^- \longrightarrow NO + 2\,OH^-$ | −0.46 |
| $Cs^+ + e^- \longrightarrow Cs$ | −2.92 | $NO_3^- + 4\,H^+ + 3e^- \longrightarrow NO + 2\,H_2O$ | 0.957 |
| $Cu^+ + e^- \longrightarrow Cu$ | 0.521 | $NO_3^- + 2\,H^+ + e^- \longrightarrow NO_2^- + H_2O$ | 0.835 |
| $Cu^{2+} + e^- \longrightarrow Cu^+$ | 0.153 | $NO_3^- + H_2O + 2e^- \longrightarrow NO_2^- + 2\,OH^-$ | 0.10 |
| $Cu(OH)_2 + 2e^- \longrightarrow Cu + 2\,OH^-$ | −0.222 | $Na^+ + e^- \longrightarrow Na$ | −2.71 |
| $F_2 + 2\,H^+ + 2e^- \longrightarrow 2\,HF$ | 3.053 | $Ni^{2+} + 2e^- \longrightarrow Ni$ | −0.257 |
| $F_2 + 2e^- \longrightarrow 2\,F^-$ | 2.866 | $NiOOH + H_2O + e^- \longrightarrow Ni(OH)_2 + OH^-$ | 0.52 |
| $Fe^{2+} + 2e^- \longrightarrow Fe$ | −0.447 | $Ni(OH)_2 + 2e^- \longrightarrow Ni + 2\,OH^-$ | −0.72 |
| $Fe^{3+} + 3e^- \longrightarrow Fe$ | −0.030 | $NiO_2 + 2\,H_2O + 2e^- \longrightarrow Ni(OH)_2 + 2\,OH^-$ | 0.49 |
| $Fe^{3+} + e^- \longrightarrow Fe^{2+}$ | 0.771 | $NiO_2 + 4\,H^+ + 2e^- \longrightarrow Ni^{2+} + 2\,H_2O$ | 1.678 |
| $[Fe(CN)_6]^{3-} + e^- \longrightarrow [Fe(CN)_6]^{4-}$ | 0.358 | $O_2 + e^- \longrightarrow O_2^-$ | −0.56 |
| $2\,H^+ + 2e^- \longrightarrow H_2$ | 0 | $O_2 + 2\,H^+ + 2e^- \longrightarrow H_2O_2$ | 0.695 |
| $HBrO + H^+ + e^- \longrightarrow 1/2\,Br_2 + H_2O$ | 1.574 | $O_2 + 4\,H^+ + 4e^- \longrightarrow 2\,H_2O$ | 1.229 |
| $HClO + H^+ + e^- \longrightarrow 1/2\,Cl_2 + H_2O$ | 1.611 | $O_2 + 2\,H_2O + 2e^- \longrightarrow H_2O_2 + 2\,OH^-$ | −0.146 |
| $HClO_2 + 3\,H^+ + 3e^- \longrightarrow 1/2\,Cl_2 + 2\,H_2O$ | 1.628 | $O_2 + 2\,H_2O + 4e^- \longrightarrow 4\,OH^-$ | 0.401 |
| $HO_2 + H^+ + e^- \longrightarrow H_2O_2$ | 1.495 | $O_2 + H_2O + 2e^- \longrightarrow HO_2^- + OH^-$ | −0.076 |
| $HO_2 + H_2O + 2e^- \longrightarrow 3\,OH^-$ | 0.878 | $O_3 + 2\,H^+ + 2e^- \longrightarrow O_2 + H_2O$ | 2.07 |
| $2\,H_2O + 2e^- \longrightarrow H_2 + 2\,OH^-$ | −0.8277 | $O_3 + H_2O + 2e^- \longrightarrow O_2 + 2\,OH^-$ | 1.24 |
| $H_2O_2 + 2\,H^+ + 2e^- \longrightarrow 2\,H_2O$ | 1.776 | $Pb^{2+} + 2e^- \longrightarrow Pb$ | −0.1262 |
| $2\,H_2SO_3 + H^+ + 2e^- \longrightarrow H_2SO_4^- + 2\,H_2O$ | −0.056 | $Pb^{4+} + 2e^- \longrightarrow Pb^{2+}$ | 1.67 |
| $H_2SO_3 + 4\,H^+ + 4e^- \longrightarrow S + 3\,H_2O$ | 0.449 | $PbBr_2 + 2e^- \longrightarrow Pb + 2\,Br^-$ | −0.284 |
| $H_3PO_4 + 2\,H^+ + 2e^- \longrightarrow H_3PO_3 + H_2O$ | −0.276 | $PbCl_2 + 2e^- \longrightarrow Pb + 2\,Cl^-$ | −0.2675 |
| $Hg^{2+} + 2e^- \longrightarrow Hg$ | 0.851 | $PbO + H_2O + 2e^- \longrightarrow Pb + 2\,OH^-$ | −0.580 |
| $Hg_2^{2+} + 2e^- \longrightarrow 2\,Hg$ | 0.7973 | $PbO_2 + 4\,H^+ + 2e^- \longrightarrow Pb^{2+} + 2\,H_2O$ | 1.455 |
| $Hg_2Cl_2 + 2e^- \longrightarrow 2\,Hg + 2\,Cl^-$ | 0.26808 | $PbO_2 + SO_4^{2-} + 4\,H^+ + 2e^- \longrightarrow PbSO_4 + 2\,H_2O$ | 1.6913 |
| $Hg_2SO_4 + 2e^- \longrightarrow 2\,Hg + SO_4^{2-}$ | 0.6125 | $PbSO_4 + 2e^- \longrightarrow Pb + SO_4^{2-}$ | −0.3505 |
| $I_2 + 2e^- \longrightarrow 2\,I^-$ | 0.5355 | $Pd^{2+} + 2e^- \longrightarrow Pd$ | 0.951 |
| $I_3^- + 2e^- \longrightarrow 3\,I^-$ | 0.536 | $Pt^{2+} + 2e^- \longrightarrow Pt$ | 1.118 |
| $In^+ + e^- \longrightarrow In$ | −0.14 | $[PtCl_4]^{2-} + 2e^- \longrightarrow Pt + 4\,Cl^-$ | 0.755 |
| $In^{2+} + e^- \longrightarrow In^+$ | −0.40 | $[PtCl_6]^{2-} + 2e^- \longrightarrow [PtCl_4]^{2-} + 2\,Cl^-$ | 0.68 |

| Reaction | $E°$ (V) | Reaction | $E°$ (V) |
|---|---|---|---|
| $Pt(OH)_2 + 2e^- \longrightarrow Pt + 2\,OH^-$ | 0.14 | $Sn^{2+} + 2e^- \longrightarrow Sn$ | −0.1375 |
| $Rb^+ + e^- \longrightarrow Rb$ | −2.98 | $Sn^{4+} + 2e^- \longrightarrow Sn^{2+}$ | 0.151 |
| $Re^{3+} + 3e^- \longrightarrow Re$ | 0.300 | $Ti^{2+} + 2e^- \longrightarrow Ti$ | −1.630 |
| $S + 2e^- \longrightarrow S^{2-}$ | −0.47627 | $Ti^{3+} + e^- \longrightarrow Ti^{2+}$ | −0.9 |
| $S + 2\,H^+ + 2e^- \longrightarrow H_2S(aq)$ | 0.142 | $TiO_2 + 4\,H^+ + 2e^- \longrightarrow Ti^{2+} + 2\,H_2O$ | −0.502 |
| $S_2O_6^{2-} + 4\,H^+ + 2e^- \longrightarrow 2\,H_2SO_3$ | 0.564 | $Zn^{2+} + 2e^- \longrightarrow Zn$ | −0.7618 |
| $S_2O_6^{2-} + 2e^- + 2\,H^+ \longrightarrow 2\,HSO_3^-$ | 0.464 | $ZnO_2^{2-} + 2\,H_2O + 2e^- \longrightarrow Zn + 4\,OH^-$ | −1.215 |
| $S_2O_8^{2-} + 2e^- \longrightarrow 2\,SO_4^{2-}$ | 2.010 | $Zr(OH)_2 + H_2O + 4e^- \longrightarrow Zr + 4\,OH^-$ | −2.36 |

*Source:* HCP and Bard.

## TABLE 11.2   Standard Reduction Potentials Ordered by Reduction Potential

| Reaction | $E°$ (V) | Reaction | $E°$ (V) |
|---|---|---|---|
| $Ca^+ + e^- \longrightarrow Ca$ | −3.80 | $Cd^{2+} + 2e^- \longrightarrow Cd$ | −0.4030 |
| $Li^+ + e^- \longrightarrow Li$ | −3.0401 | $In^{2+} + e^- \longrightarrow In^+$ | −0.40 |
| $Rb^+ + e^- \longrightarrow Rb$ | −2.98 | $PbSO_4 + 2e^- \longrightarrow Pb + SO_4^{2-}$ | −0.3505 |
| $K^+ + e^- \longrightarrow K$ | −2.931 | $In^{3+} + 3e^- \longrightarrow In$ | −0.3382 |
| $Cs^+ + e^- \longrightarrow Cs$ | −2.92 | $PbBr_2 + 2e^- \longrightarrow Pb + 2\,Br^-$ | −0.284 |
| $Ba^{2+} + 2e^- \longrightarrow Ba$ | −2.912 | $Co^{2+} + 2e^- \longrightarrow Co$ | −0.28 |
| $Ca^{2+} + 2e^- \longrightarrow Ca$ | −2.868 | $H_3PO_4 + 2\,H^+ + 2e^- \longrightarrow H_3PO_3 + H_2O$ | −0.276 |
| $Na^+ + e^- \longrightarrow Na$ | −2.71 | $PbCl_2 + 2e^- \longrightarrow Pb + 2\,Cl^-$ | −0.2675 |
| $Mg(OH)_2 + 2e^- \longrightarrow Mg + 2\,OH^-$ | −2.690 | $Ni^{2+} + 2e^- \longrightarrow Ni$ | −0.257 |
| $Ce^{3+} + 3e^- \longrightarrow Ce$ | −2.483 | $CdSO_4 + 2e^- \longrightarrow Cd + SO_4^{2-}$ | −0.246 |
| $Mg^{2+} + 2e^- \longrightarrow Mg$ | −2.372 | $Cu(OH)_2 + 2e^- \longrightarrow Cu + 2\,OH^-$ | −0.222 |
| $Zr(OH)_2 + H_2O + 4e^- \longrightarrow Zr + 4\,OH^-$ | −2.36 | $AgI + e^- \longrightarrow Ag + I^-$ | −0.15224 |
| $Be^{2+} + 2e^- \longrightarrow Be$ | −1.847 | $O_2 + 2\,H_2O + 2e^- \longrightarrow H_2O_2 + 2\,OH^-$ | −0.146 |
| $Al^{3+} + 3e^- \longrightarrow Al$ | −1.662 | $In^+ + e^- \longrightarrow In$ | −0.14 |
| $Ti^{2+} + 2e^- \longrightarrow Ti$ | −1.630 | $Sn^{2+} + 2e^- \longrightarrow Sn$ | −0.1375 |
| $ZnO_2^{2-} + 2\,H_2O + 2e^- \longrightarrow Zn + 4\,OH^-$ | −1.215 | $Pb^{2+} + 2e^- \longrightarrow Pb$ | −0.1262 |
| $Mn^{2+} + 2e^- \longrightarrow Mn$ | −1.185 | $O_2 + H_2O + 2e^- \longrightarrow HO_2^- + OH^-$ | −0.076 |
| $Cr^{2+} + 2e^- \longrightarrow Cr$ | −0.913 | $2\,H_2SO_3 + H^+ + 2e^- \longrightarrow H_2SO_4^- + 2\,H_2O$ | −0.056 |
| $Ti^{3+} + e^- \longrightarrow Ti^{2+}$ | −0.9 | $Fe^{3+} + 3e^- \longrightarrow Fe$ | −0.030 |
| $2\,H_2O + 2e^- \longrightarrow H_2 + 2\,OH^-$ | −0.8277 | $AgCN + e^- \longrightarrow Ag + CN^-$ | −0.017 |
| $Cd(OH)_2 + 2e^- \longrightarrow Cd + 2\,OH^-$ | −0.809 | $2\,H^+ + 2e^- \longrightarrow H_2$ | 0 |
| $Zn^{2+} + 2e^- \longrightarrow Zn$ | −0.7618 | $AgBr + e^- \longrightarrow Ag + Br^-$ | 0.07133 |
| $Cr^{3+} + 3e^- \longrightarrow Cr$ | −0.744 | $NO_3^- + H_2O + 2e^- \longrightarrow NO_2^- + 2\,OH^-$ | 0.10 |
| $Ni(OH)_2 + 2e^- \longrightarrow Ni + 2\,OH^-$ | −0.72 | $Pt(OH)_2 + 2e^- \longrightarrow Pt + 2\,OH^-$ | 0.14 |
| $PbO + H_2O + 2e^- \longrightarrow Pb + 2\,OH^-$ | −0.580 | $S + 2\,H^+ + 2e^- \longrightarrow H_2S1aq2$ | 0.142 |
| $O_2 + e^- \longrightarrow O_2^-$ | −0.56 | $Ag_4[Fe(CN)_6] + 4e^- \longrightarrow 4\,Ag + [Fe(CN)_6]^{4-}$ | 0.1478 |
| $TiO_2 + 4\,H^+ + 2e^- \longrightarrow Ti^{2+} + 2\,H_2O$ | −0.502 | $Sn^{4+} + 2e^- \longrightarrow Sn^{2+}$ | 0.151 |
| $S + 2e^- \longrightarrow S^{2-}$ | −0.47627 | $Cu^{2+} + e^- \longrightarrow Cu^+$ | 0.153 |
| $NO_2 + H_2O + 3e^- \longrightarrow NO + 2\,OH^-$ | −0.46 | $Bi^{3+} + 3e^- \longrightarrow Bi$ | 0.20 |
| $Fe^{2+} + 2e^- \longrightarrow Fe$ | −0.447 | $AgCl + e^- \longrightarrow Ag + Cl^-$ | 0.22233 |
| $Cr^{3+} + e^- \longrightarrow Cr^{2+}$ | −0.407 | $Hg_2Cl_2 + 2e^- \longrightarrow 2\,Hg + 2\,Cl^-$ | 0.26808 |

(continued)

**TABLE 11.2 Standard Reduction Potentials Ordered by Reduction Potential (continued)**

| Reaction | $E°$ (V) | Reaction | $E°$ (V) |
|---|---|---|---|
| $Re^{3+} + 3e^- \longrightarrow Re$ | 0.300 | $AuCl_4 + 3e^- \longrightarrow Au + 4\,Cl^-$ | 1.002 |
| $[Fe(CN)_6]^{3-} + e^- \longrightarrow [Fe(CN)_6]^{4-}$ | 0.358 | $Br_2(aq) + 2e^- \longrightarrow 2\,Br^-$ | 1.0873 |
| $ClO_4^- + H_2O + 2e^- \longrightarrow ClO_3^- + 2\,OH^-$ | 0.36 | $Pt^{2+} + 2e^- \longrightarrow Pt$ | 1.118 |
| $O_2 + 2\,H_2O + 4e^- \longrightarrow 4OH^-$ | 0.401 | $ClO_4^- + 2\,H^+ + 2e^- \longrightarrow ClO_3^- + H_2O$ | 1.189 |
| $H_2SO_3 + 4\,H^+ + 4e^- \longrightarrow S + 3\,H_2O$ | 0.449 | $MnO_2 + 4\,H^+ + 2e^- \longrightarrow Mn^{2+} + 2\,H_2O$ | 1.224 |
| $S_2O_6^{2-} + 2e^- + 2\,H^+ \longrightarrow 2\,HSO_3^-$ | 0.464 | $O_2 + 4\,H^+ + 4e^- \longrightarrow 2\,H_2O$ | 1.229 |
| $NiO_2 + 2\,H_2O + 2e^- \longrightarrow Ni(OH)_2 + 2\,OH^-$ | 0.49 | $Cr_2O_7^{2-} + 14\,H^+ + 6e^- \longrightarrow 2Cr^{3+} + 7\,H_2O$ | 1.232 |
| $NiOOH + H_2O + e^- \longrightarrow Ni(OH)_2 + OH^-$ | 0.52 | $O_3 + H_2O + 2e^- \longrightarrow O_2 + 2\,OH^-$ | 1.24 |
| $Cu^+ + e^- \longrightarrow Cu$ | 0.521 | $Cl_2(g) + 2e^- \longrightarrow 2\,Cl^-$ | 1.35827 |
| $I_2 + 2e^- \longrightarrow 2\,I^-$ | 0.5355 | $Au^{3+} + 2e^- \longrightarrow Au^+$ | 1.401 |
| $I_3^- + 2e^- \longrightarrow 3\,I^-$ | 0.536 | $PbO_2 + 4\,H^+ + 2e^- \longrightarrow Pb^{2+} + 2\,H_2O$ | 1.455 |
| $MnO_4^- + e^- \longrightarrow MnO_4^{2-}$ | 0.558 | $HO_2 + H^+ + e^- \longrightarrow H_2O_2$ | 1.495 |
| $AgNO_2 + e^- \longrightarrow Ag + NO_2^-$ | 0.564 | $Au^{3+} + 3e^- \longrightarrow Au$ | 1.498 |
| $S_2O_6^{2-} + 4\,H^+ + 2e^- \longrightarrow 2\,H_2SO_3$ | 0.564 | $MnO_4^- + 8\,H^+ + 5e^- \longrightarrow Mn^{2+} + 4\,H_2O$ | 1.507 |
| $MnO_4^{2-} + 2\,H_2O + 2e^- \longrightarrow MnO_2 + 4\,OH^-$ | 0.595 | $Mn^{3+} + e^- \longrightarrow Mn^{2+}$ | 1.5415 |
| $Hg_2SO_4 + 2e^- \longrightarrow 2\,Hg + SO_4^{2-}$ | 0.6125 | $HBrO + H^+ + e^- \longrightarrow 1/2\,Br_2 + H_2O$ | 1.574 |
| $[PtCl_6]^{2-} + 2e^- \longrightarrow [PtCl_4]^{2-} + 2\,Cl^-$ | 0.68 | $2\,NO + 2\,H^+ + 2e^- \longrightarrow N_2O + H_2O$ | 1.591 |
| $O_2 + 2\,H^+ + 2e^- \longrightarrow H_2O_2$ | 0.695 | $Ce^{4+} + e^- \longrightarrow Ce^{3+}$ | 1.61 |
| $[PtCl_4]^{2-} + 2e^- \longrightarrow Pt + 4\,Cl^-$ | 0.755 | $HClO + H^+ + e^- \longrightarrow 1/2\,Cl_2 + H_2O$ | 1.611 |
| $BrO^- + H_2O + 2e^- \longrightarrow Br^- + 2\,OH^-$ | 0.761 | $HClO_2 + 3\,H^+ + 3e^- \longrightarrow 1/2\,Cl_2 + 2\,H_2O$ | 1.628 |
| $Fe^{3+} + e^- \longrightarrow Fe^{2+}$ | 0.771 | $Pb^{4+} + 2e^- \longrightarrow Pb^{2+}$ | 1.67 |
| $AgF + e^- \longrightarrow Ag + F^-$ | 0.779 | $NiO_2 + 4\,H^+ + 2e^- \longrightarrow Ni^{2+} + 2\,H_2O$ | 1.678 |
| $Hg_2^{2+} + 2e^- \longrightarrow 2\,Hg$ | 0.7973 | $MnO_4^- + 4\,H^+ + 3e^- \longrightarrow MnO_2 + 2\,H_2O$ | 1.679 |
| $Ag^+ + e^- \longrightarrow Ag$ | 0.7996 | $PbO_2 + SO_4^{2-} + 4\,H^+ + 2e^- \longrightarrow PbSO_4 + 2\,H_2O$ | 1.6913 |
| $ClO^- + H_2O + 2e^- \longrightarrow Cl^- + 2\,OH^-$ | 0.81 | $Au^+ + e^- \longrightarrow Au$ | 1.692 |
| $NO_3^- + 2\,H^+ + e^- \longrightarrow NO_2^- + H_2O$ | 0.835 | $H_2O_2 + 2\,H^+ + 2e^- \longrightarrow 2\,H_2O$ | 1.776 |
| $Hg^{2+} + 2e^- \longrightarrow Hg$ | 0.851 | $Co^{3+} + e^- \longrightarrow Co^{2+}$ | 1.92 |
| $HO_2 + H_2O + 2e^- \longrightarrow 3\,OH^-$ | 0.878 | $Ag^{2+} + e^- \longrightarrow Ag^+$ | 1.980 |
| $Pd^{2+} + 2e^- \longrightarrow Pd$ | 0.951 | $S_2O_8^{2-} + 2e^- \longrightarrow 2\,SO_4^{2-}$ | 2.010 |
| $NO_3^- + 4\,H^+ + 3e^- \longrightarrow NO + 2\,H_2O$ | 0.957 | $O_3 + 2\,H^+ + 2e^- \longrightarrow O_2 + H_2O$ | 2.076 |
| $AuBr_2 + e^- \longrightarrow Au + 2\,Br^-$ | 0.959 | $F_2 + 2e^- \longrightarrow 2F^-$ | 2.866 |
| $HNO_2 + H^+ + e^- \longrightarrow NO + H_2O$ | 0.983 | $F_2 + 2\,H^+ + 2e^- \longrightarrow 2\,HF$ | 3.053 |

*Sources:* HCP and Bard.

## B.1 Working with Complex Numbers and Complex Functions

Imaginary numbers can be written in the form

$$z = a + ib \tag{B.1}$$

where $a$ and $b$ are real numbers and $i = \sqrt{-1}$. It is useful to represent complex numbers in the complex plane shown in Figure B.1. The vertical and horizontal axes correspond to the imaginary and real parts of $z$, respectively.

In the representation shown in Figure B.1, a complex number corresponds to a point in the complex plane. Note the similarity to the polar coordinate system. Because of this analogy, a complex number can be represented either as the pair $(a, b)$, or by the radius vector $r$ and the angle $\theta$. From Figure B.1, it can be seen that

$$r = \sqrt{a^2 + b^2} \quad \text{and} \quad \theta = \cos^{-1}\frac{a}{r} = \sin^{-1}\frac{b}{r} = \tan^{-1}\frac{b}{a} \tag{B.2}$$



**FIGURE B.1**

Using the relations between $a$, $b$, and $r$ as well as the Euler relation $e^{i\theta} = \cos\theta + i\sin\theta$, a complex number can be represented in either of two equivalent ways:

$$a + ib = r\cos\theta + r\sin\theta = re^{i\theta} = \sqrt{a^2 + b^2}\exp[i\tan^{-1}(b/a)] \tag{B.3}$$

If a complex number is represented in one way, it can easily be converted to the other way. For example, we express the complex number $6 - 7i$ in the form $re^{i\theta}$. The magnitude of the radius vector $r$ is given by $\sqrt{6^2 + 7^2} = \sqrt{85}$. The phase is given by $\tan\theta = (-7/6)$ or $\theta = \tan^{-1}(-7/6)$. Therefore, we can write $6 - 7i$ as $\sqrt{85}\exp[i\tan^{-1}(-7/6)]$.

In a second example, we convert the complex number $2e^{i\pi/2}$, which is in the $re^{i\theta}$ notation, to the $a + ib$ notation. Using the relation $e^{i\alpha} = \exp(i\alpha) = \cos\alpha + i\sin\alpha$, we can write $2e^{i\pi/2}$ as

$$2\left(\cos\frac{\pi}{2} + i\sin\frac{\pi}{2}\right) = 2(0 + i) = 2i$$

The complex conjugate of a complex number $z$ is designated by $z^*$ and is obtained by changing the sign of $i$, wherever it appears in the complex number. For example, if $z = (3 - \sqrt{5}i)e^{i\sqrt{2}\phi}$, then $z^* = (3 + \sqrt{5}i)e^{-i\sqrt{2}\phi}$. The magnitude of a complex number is defined by $\sqrt{zz^*}$ and is always a real number. This is the case for the previous example:

$$zz^* = (3 - \sqrt{5}i)e^{i\sqrt{2}\phi}(3 + \sqrt{5}i)e^{-i\sqrt{2}\phi}$$
$$= (3 - \sqrt{5}i)(3 + \sqrt{5}i)e^{i\sqrt{2}\phi - i\sqrt{2}\phi} = 14 \tag{B.4}$$

Note also that $zz^* = a^2 + b^2$.

Complex numbers can be added, multiplied, and divided just like real numbers. A few examples follow:

$$(3 + \sqrt{2}i) + (1 - \sqrt{3}i) = [4 + (\sqrt{2} - \sqrt{3})i]$$
$$(3 + \sqrt{2}i)(1 - \sqrt{3}i) = 3 - 3\sqrt{3}i + \sqrt{2}i - \sqrt{6}i^2$$
$$= (3 + \sqrt{6}) + (\sqrt{2} - 3\sqrt{3})i$$
$$\frac{(3 + \sqrt{2}i)}{(1 - \sqrt{3}i)} = \frac{(3 + \sqrt{2}i)}{(1 - \sqrt{3}i)}\frac{(1 + \sqrt{3}i)}{(1 + \sqrt{3}i)}$$
$$= \frac{3 + 3\sqrt{3}i + \sqrt{2}i + \sqrt{6}i^2}{4}$$
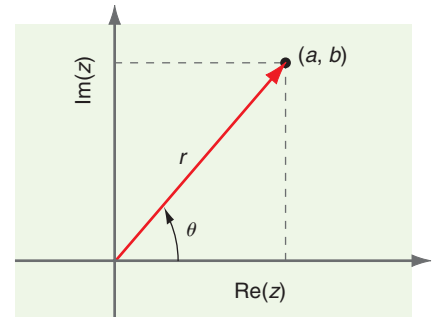
**571**
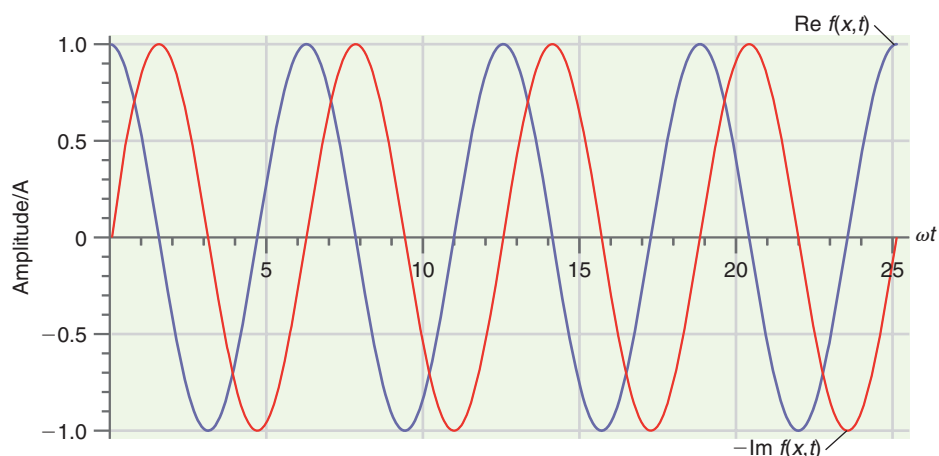
**FIGURE B.2**

$$= \frac{(3 - \sqrt{6}) + (3\sqrt{3} + \sqrt{2})i}{4}$$

Functions can depend on a complex variable. It is convenient to represent a plane traveling wave usually written in the form

$$\psi(x, t) = A \sin(kx - \omega t) \tag{B.5}$$

in the complex form

$$Ae^{i(kx - \omega t)} = A \cos(kx - \omega t) - iA \sin(kx - \omega t) \tag{B.6}$$

Note that

$$\psi(x, t) = -\mathrm{Im} Ae^{i(kx - \omega t)} \tag{B.7}$$

The reason for working with the complex form rather than the real form of a function is that calculations such as differentiation and integration can be carried out more easily. Waves in classical physics have real amplitudes, because their amplitudes are linked directly to observables. For example, the amplitude of a sound wave is the local pressure that arises from the expansion or compression of the medium through which the wave passes. However, in quantum mechanics, observables are related to $|\psi(x, t)|^2$ rather than $\psi(x, t)$. Because $|\psi(x, t)|^2$ is always real, $\psi(x, t)$ can be complex, and the observables associated with the wave function are still real.

For the complex function $f(x, t) = Ae^{i(kx - \omega t)}$, $zz^* = \psi(x, t)\psi^*(x, t) = Ae^{i(kx - \omega t)}A^*e^{-i(kx - \omega t)} = AA^*$, so that the magnitude of the function is a constant and does not depend on $t$ or $x$. As Figure B.2 shows, the real and imaginary parts of $Ae^{i(kx - \omega t)}$ depend differently on the variables $x$ and $t$; they are phase shifted by $\pi/2$. The figure shows the amplitudes of the real and imaginary parts as a function of $\omega t$ for $x = 0$.
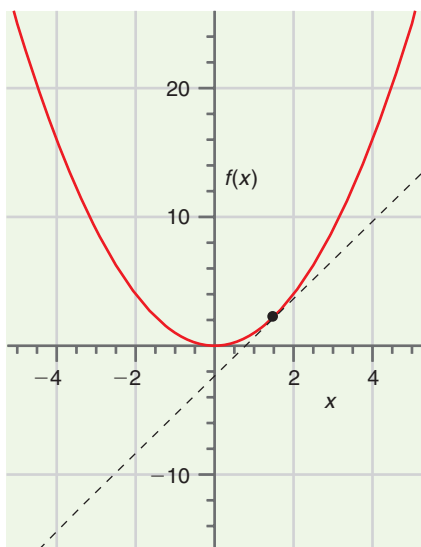
# B.2 Differential Calculus

## B.2.1 THE FIRST DERIVATIVE OF A FUNCTION

The derivative of a function has as its physical interpretation the slope of the function evaluated at the position of interest. For example, the slope of the function $y = x^2$ at the point $x = 1.5$ is indicated by the line tangent to the curve shown in Figure B.3.

Mathematically, the first derivative of a function $f(x)$ is denoted $f'(x)$ or $df(x)/dx$. It is defined by

$$\frac{df(x)}{dx} = \lim_{h \to 0} \frac{f(x + h) - f(x)}{h} \tag{B.8}$$



**FIGURE B.3**

For the function of interest,

$$\frac{df(x)}{dx} = \lim_{h \to 0} \frac{(x+h)^2 - (x)^2}{h}$$

$$= \lim_{h \to 0} \frac{2hx + h^2}{h} = \lim_{h \to 0} 2x + h = 2x \tag{B.9}$$

In order for $df(x)/dx$ to be defined over an interval in $x$, $f(x)$ must be continuous over the interval.

Based on this example, $df(x)/dx$ can be calculated if $f(x)$ is known. Several useful rules for differentiating commonly encountered functions are listed next:

$$\frac{d(ax^n)}{dx} = anx^{n-1}, \quad \text{where } a \text{ is a constant and } n > 0 \tag{B.10}$$

For example, $d(\sqrt{3}x^{4/3})/dx = (4/3)\sqrt{3}x^{1/3}$

$$\frac{d(ae^{bx})}{dx} = abe^{bx}, \quad \text{where } a \text{ and } b \text{ are constants} \tag{B.11}$$

For example, $d(5e^{3\sqrt{2}x})/dx = 15\sqrt{2}e^{3\sqrt{2}x}$

$$\frac{d(ae^{bx})}{dx} = abe^{bx}, \quad \text{where } a \text{ and } b \text{ are constants}$$

$$\frac{d(a \sin x)}{dx} = a \cos x, \quad \text{where } a \text{ is a constant}$$

$$\frac{d(a \cos x)}{dx} = -a \sin x, \quad \text{where } a \text{ is a constant} \tag{B.12}$$

Two useful rules in evaluating the derivative of a function that is itself the sum or product of two functions are as follows:

$$\frac{d[f(x) + g(x)]}{dx} = \frac{df(x)}{dx} + \frac{dg(x)}{dx} \tag{B.13}$$

For example,

$$\frac{d(x^3 + \sin x)}{dx} = \frac{dx^3}{dx} + \frac{d \sin x}{dx} = 3x^2 + \cos x$$

$$\frac{d[f(x)g(x)]}{dx} = g(x)\frac{df(x)}{dx} + f(x)\frac{dg(x)}{dx} \tag{B.14}$$

For example,

$$\frac{d[\sin(x)\cos(x)]}{dx} = \cos(x)\frac{d \sin(x)}{dx} + \sin(x)\frac{d \cos(x)}{dx}$$

$$= \cos^2 x - \sin^2 x$$

## B.2.2   THE RECIPROCAL RULE AND THE QUOTIENT RULE

How is the first derivative calculated if the function to be differentiated does not have a simple form such as those listed in the preceding section? In many cases, the derivative can be found by using the product and quotient rules stated here:

$$\frac{d\left(\dfrac{1}{f(x)}\right)}{dx} = -\frac{1}{[f(x)]^2}\frac{df(x)}{dx} \tag{B.15}$$

For example,

$$\frac{d\left(\dfrac{1}{\sin x}\right)}{dx} = -\frac{1}{\sin^2 x}\frac{d\sin x}{dx} = \frac{-\cos x}{\sin^2 x}$$

$$\frac{d\left[\dfrac{f(x)}{g(x)}\right]}{dx} = \frac{g(x)\dfrac{df(x)}{dx} - f(x)\dfrac{dg(x)}{dx}}{[g(x)]^2} \tag{B.16}$$

For example,

$$\frac{d\left(\dfrac{x^2}{\sin x}\right)}{dx} = \frac{2x\sin x - x^2\cos x}{\sin^2 x}$$

### B.2.3   THE CHAIN RULE

In this section, we deal with the differentiation of more complicated functions. Suppose that $y = f(u)$ and $u = g(x)$. From the previous section, we know how to calculate $df(u)/du$. How do we calculate $df(u)/dx$? The answer to this question is stated as the chain rule:

$$\frac{df(u)}{dx} = \frac{df(u)}{du}\frac{du}{dx} \tag{B.17}$$

Several examples illustrating the chain rule follow:

$$\frac{d\sin(3x)}{dx} = \frac{d\sin(3x)}{d(3x)}\frac{d(3x)}{dx} = 3\cos(3x)$$

$$\frac{d\ln(x^2)}{dx} = \frac{d\ln(x^2)}{d(x^2)}\frac{d(x^2)}{dx} = \frac{2x}{x^2} = \frac{2}{x}$$

$$\frac{d\left(x+\dfrac{1}{x}\right)^{-4}}{dx} = \frac{d\left(x+\dfrac{1}{x}\right)^{-4}}{d\left(x+\dfrac{1}{x}\right)}\frac{d\left(x+\dfrac{1}{x}\right)}{dx} = -4\left(x+\frac{1}{x}\right)^{-5}\left(1-\frac{1}{x^2}\right)$$

$$\frac{d\exp(ax^2)}{dx} = \frac{d\exp(ax^2)}{d(ax^2)}\frac{d(ax^2)}{dx} = 2ax\exp(ax^2), \quad \text{where } a \text{ is a constant}$$

### B.2.4   HIGHER ORDER DERIVATIVES: MAXIMA, MINIMA, AND INFLECTION POINTS

A function $f(x)$ can have higher order derivatives in addition to the first derivative. The second derivative of a function is the slope of a graph of the slope of the function versus the variable. Mathematically,

$$\frac{d^2 f(x)}{dx^2} = \frac{d}{dx}\left(\frac{df(x)}{dx}\right) \tag{B.18}$$

For example,

$$\frac{d^2\exp(ax^2)}{dx^2} = \frac{d}{dx}\left[\frac{d\exp(ax^2)}{dx}\right] = \frac{d[2ax\exp(ax^2)]}{dx}$$

$$= 2a\exp(ax^2) + 4a^2 x^2\exp(ax^2), \quad \text{where } a \text{ is a constant}$$

The second derivative is useful in identifying where a function has its minimum or maximum value within a range of the variable, as shown next.

Because the first derivative is zero at a local maximum or minimum, $df(x)/dx = 0$ at the values $x_{max}$ and $x_{min}$. Consider the function $f(x) = x^3 - 5x$ shown in Figure B.4 over the range $-2.5 \le x \le 2.5$.

By taking the derivative of this function and setting it equal to zero, we find the minima and maxima of this function in the range

$$\frac{d(x^3 - 5x)}{dx} = 3x^2 - 5 = 0, \quad \text{which has the solutions } x = \pm\sqrt{\frac{5}{3}} = 1.291$$

The maxima and minima can also be determined by graphing the derivative and finding the zero crossings as shown in Figure B.5.

Graphing the function clearly shows that the function has one maximum and one minimum in the range specified. What criterion can be used to distinguish between these extrema if the function is not graphed? The sign of the second derivative, evaluated at the point for which the first derivative is zero, can be used to distinguish between a maximum and a minimum:

$$\frac{d^2f(x)}{dx^2} = \frac{d}{dx}\left[\frac{df(x)}{dx}\right] < 0 \quad \text{for a maximum}$$

$$\frac{d^2f(x)}{dx^2} = \frac{d}{dx}\left[\frac{df(x)}{dx}\right] > 0 \quad \text{for a minimum} \qquad \text{(B.19)}$$

We return to the function graphed earlier and calculate the second derivative:

$$\frac{d^2(x^3 - 5x)}{dx^2} = \frac{d}{dx}\left[\frac{d(x^3 - 5x)}{dx}\right] = \frac{d(3x^2 - 5)}{dx} = 6x$$

By evaluating

$$\frac{d^2f(x)}{dx^2} \text{ at } x = \pm\sqrt{\frac{5}{3}} = \pm 1.291$$

we see that $x = 1.291$ corresponds to the minimum, and $x = -1.291$ corresponds to the maximum.

If a function has an inflection point in the interval of interest, then

$$\frac{df(x)}{dx} = 0 \quad \text{and} \quad \frac{d^2f(x)}{dx^2} = 0 \qquad \text{(B.20)}$$

An example for an inflection point is $x = 0$ for $f(x) = x^3$. A graph of this function in the interval $-2 \le x \le 2$ is shown in Figure B.6. As you can verify,

$$\frac{dx^3}{dx} = 3x^2 = 0 \text{ at } x = 0 \quad \text{and} \quad \frac{d^2(x^3)}{dx^2} = 6x = 0 \text{ at } x = 0$$

## B.2.5  MAXIMIZING A FUNCTION SUBJECT TO A CONSTRAINT

A frequently encountered problem is that of maximizing a function relative to a constraint. We first outline how to carry out a constrained maximization, and subsequently apply the method to maximizing the volume of a cylinder while minimizing its area. The theoretical framework for solving this problem originated with the French mathematician Lagrange, and the method is known as Lagrange's method of undetermined multipliers. We wish to maximize the function $f(x, y)$ subject to the constraint that $\phi(x, y) - C = 0$, where $C$ is a constant. For example, you may want to maximize the area $A$ of a rectangle while minimizing its circumference $C$. In this case, $f(x, y) = A(x, y) = xy$ and $\phi(x, y) = C(x, y) = 2(x + y)$, where $x$ and $y$ are the length and width of the rectangle. The total differentials of these functions are given by Equation (B.21):

$$df = \left(\frac{\partial f}{\partial x}\right)_y dx + \left(\frac{\partial f}{\partial y}\right)_x dy = 0 \quad \text{and} \quad d\phi = \left(\frac{\partial \phi}{\partial x}\right)_y dx + \left(\frac{\partial \phi}{\partial y}\right)_x dy = 0$$

$$\text{(B.21)}$$
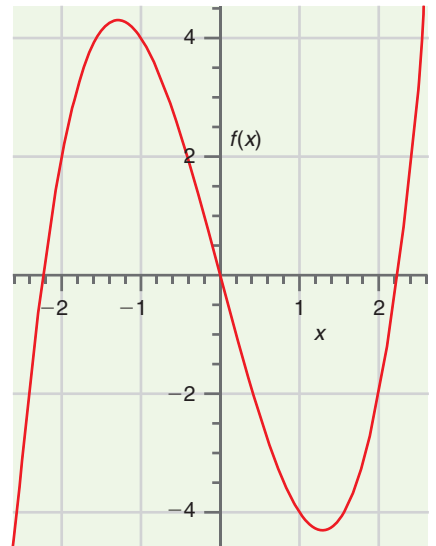


**FIGURE B.4**
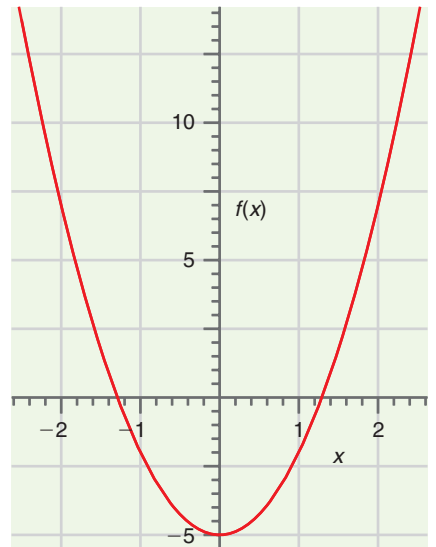


**FIGURE B.5**
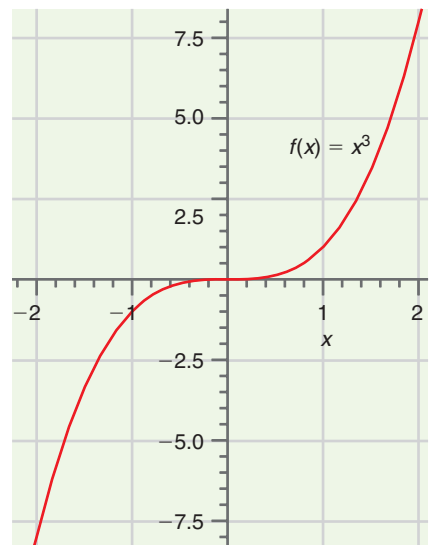


**FIGURE B.6**

If $x$ and $y$ were independent variables (there is no constraining relationship), the maximization problem would be identical to those dealt with earlier. However, because $d\phi = 0$ also needs to be satisfied, $x$ and $y$ are not independent variables. In this case, Lagrange found that the appropriate function to minimize is $f - \lambda\phi$, where $\lambda$ is an undetermined multiplier. He showed that each of the expressions in the square brackets in the differential given by Equation (B.22) can be maximized independently. A separate multiplier is required for each constraint:

$$df = \left[\left(\frac{\partial f}{\partial x}\right)_y - \lambda\left(\frac{\partial \phi}{\partial x}\right)_y\right]dx + \left[\left(\frac{\partial f}{\partial y}\right)_x - \lambda\left(\frac{\partial \phi}{\partial y}\right)_x\right]dy \tag{B.22}$$

We next use this method to maximize the volume $V$ of a cylindrical can subject to the constraint that its exterior area $A$ be minimized. The functions $f$ and $\phi$ are given by

$$V = f(r,h) = \pi r^2 h \quad \text{and} \quad A = \phi(r,h) = 2\pi r^2 + 2\pi r h \tag{B.23}$$

Calculating the partial derivatives and using Equation (B.22), we have

$$\left(\frac{\partial f(r,h)}{r}\right)_h = 2\pi r h \quad \left(\frac{\partial f(r,h)}{h}\right)_r = \pi r^2$$

$$\left(\frac{\partial \phi(r,h)}{r}\right)_h = 4\pi r + 2\pi h \quad \left(\frac{\partial \phi(r,h)}{h}\right)_r = 2\pi r$$

$$(2\pi r h - \lambda[4\pi r + 2\pi h])dr = 0 \quad \text{and} \quad (\pi r^2 - \lambda 2\pi r)dh = 0 \tag{B.24}$$

Eliminating $\lambda$ from these two equations gives

$$\frac{2\pi r h}{4\pi r + 2\pi h} = \frac{\pi r^2}{2\pi r} \tag{B.25}$$

Solving for $h$ in terms of $r$ gives the result $h = 2r$. Note that there is no need to determine the value of multiplier $\lambda$. Perhaps you have noticed that beverage cans do not follow this relationship between $r$ and $h$. Can you think of factors other than minimizing the amount of metal used in the can that might be important in this case?

# B.3 Series Expansions of Functions

## B.3.1 CONVERGENT INFINITE SERIES

Physical chemists often express functions of interest in the form of an infinite series. For this application, the series must converge. Consider the series

$$a_0 + a_1 x + a_2 x^2 + a_3 x^3 + \cdots a_n x^n + \cdots \tag{B.26}$$

How can we determine if such a series converges? A useful convergence criterion is the ratio test. If the absolute ratio of successive terms (designated $u_{n-1}$ and $u_n$) is less than 1 as $n \to \infty$, the series converges. We consider the series of Equation (B.26) with (a) $a_n = n!$ and (b) $a_n = 1/n!$, and apply the ratio test as shown in Equations (B.27a and b).

$$(a)\ \lim_{n\to\infty}\left|\frac{u_n}{u_{n-1}}\right| = \left|\frac{n!x^n}{(n-1)!x^{n-1}}\right| = \lim_{n\to\infty}|nx| > 1 \text{ unless } x = 0 \tag{B.27a}$$

$$(b)\ \lim_{n\to\infty}\left|\frac{u_n}{u_{n-1}}\right| = \left|\frac{x^n/n!}{x^{n-1}/(n-1)!}\right| = \lim_{n\to\infty}\left|\frac{x}{n}\right| < 1 \text{ for all } x \tag{B.27b}$$

We see that the infinite series converges if $a_n = 1/n!$ but diverges if $a_n = n!$.

The power series is a particularly important form of a series that is frequently used to fit experimental data to a functional form. It has the form

$$a_0 + a_1 x + a_2 x^2 + a_3 x^3 + a_1 x + a_4 x^4 + \cdots = \sum_{n=0}^{\infty} a_n x^n \tag{B.28}$$

Fitting a data set to a series with a large number of terms is impractical, and to be useful, the series should contain as few terms as possible to satisfy the desired accuracy. For

example, the function $\sin x$ can be fit to a power series over the interval $0 \leq x \leq 1.5$ by the following truncated power series

$$\sin x \approx -1.20835 \times 10^{-3} + 1.02102x - 0.0607398x^2 - 0.11779x^3$$

$$\sin x \approx -8.86688 \times 10^{-5} + 0.996755x + 0.0175769x^2$$
$$-0.200644x^3 - 0.027618x^4 \tag{B.29}$$

The coefficients in Equation (B.29) have been determined using a least squares fitting routine. The first series includes terms in $x$ up to $x^3$, and is accurate to within 2% over the interval. The second series includes terms up to $x^4$, and is accurate to within 0.1% over the interval. Including more terms will increase the accuracy further.

A special case of a power series is the geometric series, in which successive terms are related by a constant factor. An example of a geometric series and its sum is given in Equation (B.30). Using the ratio criterion of Equation (B.27), convince yourself that this series converges for $|x| < 1$.

$$a(1 + x + x^2 + x^3 + \cdots) = \frac{a}{1 - x}, \quad \text{for } |x| < 1 \tag{B.30}$$

## B.3.2  REPRESENTING FUNCTIONS IN THE FORM OF INFINITE SERIES

Assume that you have a function in the form $f(x)$ and wish to express it as a power series in $x$ of the form

$$f(x) = a_0 + a_1x + a_2x^2 + a_3x^3 + \cdots \tag{B.31}$$

To do so, we need a way to find the set of coefficients $(a_0, a_1, a_2, a_3, \cdots)$. How can this be done?

If the functional form $f(x)$ is known, the function can be expanded about a point of interest using the Taylor-Maclaurin expansion. In the vicinity of $x = a$, the function can be expanded in the series

$$f(x) = f(a) + \left(\frac{df(x)}{dx}\right)_{x=a}(x - a) + \frac{1}{2!}\left(\frac{d^2f(x)}{dx^2}\right)_{x=a}(x - a)^2$$
$$+ \frac{1}{3!}\left(\frac{d^3f(x)}{dx^3}\right)_{x=a}(x - a)^3 + \cdots \tag{B.32}$$

For example, consider the expansion of $f(x) = e^x$ about $x = 0$. Because $(d^ne^x/dx^n)_{x=0} = 1$ for all values of $n$, the Taylor-Maclaurin expansion for $e^x$ about $x = 0$ is

$$f(x) = 1 + x + \frac{1}{2!}x^2 + \frac{1}{3!}x^3 + \cdots \tag{B.33}$$

Similarly, the Taylor-Maclaurin expansion for $\ln(1 + x)$ is found by evaluating the derivatives in turn:

$$\frac{d \ln(1 + x)}{dx} = \frac{1}{1 + x}$$

$$\frac{d^2 \ln(1 + x)}{dx^2} = \frac{d}{dx}\frac{1}{(1 + x)} = -\frac{1}{(1 + x)^2}$$

$$\frac{d^3 \ln(1 + x)}{dx^3} = -\frac{d}{dx}\frac{1}{(1 + x)^2} = \frac{2}{(1 + x)^3}$$

$$\frac{d^4 \ln(1 + x)}{dx^4} = \frac{d}{dx}\frac{2}{(1 + x)^3} = \frac{-6}{(1 + x)^4}$$

Each of these derivatives must be evaluated at $x = 0$.

Using these results, the Taylor-Maclaurin expansion for $\ln(1 + x)$ about $x = 0$ is

$$f(x) = x - \frac{x^2}{2!} + \frac{2x^3}{3!} - \frac{6x^4}{4!} + \cdots = x - \frac{x^2}{2} + \frac{x^3}{3} - \frac{x^4}{4} + \cdots \tag{B.34}$$

$f(x)$



$n=2$



$n=5$



$n=10$
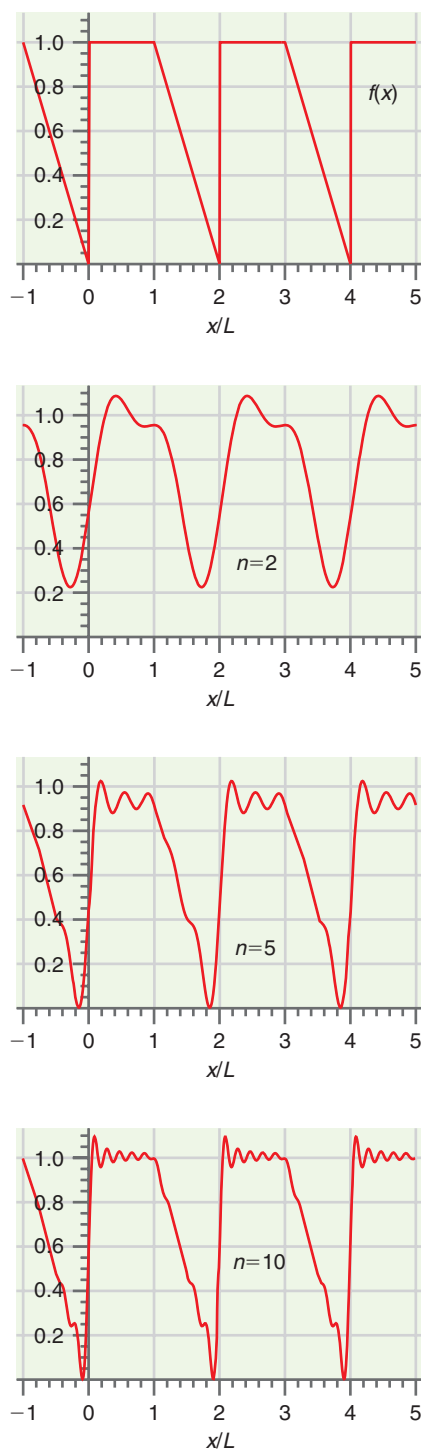
**FIGURE B.7**

The number of terms that must be included to adequately represent the function depends on the value of $x$. For $-1 \ll x \ll 1$, the series converges rapidly and, to a very good approximation, we can truncate the Taylor-Maclaurin series after the first one or two terms involving the variable. For the two functions just considered, it is reasonable to write $e^x \approx 1 + x$ and $\ln(1 \pm x) \approx \pm x$ if $-1 \ll x \ll 1$.

A second widely used series is the Fourier sine and cosine series. This series can be used to expand functions that are periodic over an interval $-L \le x \le L$ by the series

$$f(x) = \frac{1}{2}b_0 + \sum_n b_n \cos\frac{n\pi x}{L} + \sum_n a_n \sin\frac{n\pi x}{L} \tag{B.35}$$

A Fourier series is an infinite series, and the coefficients $a_n$ and $b_n$ can be calculated using the equations

$$a_n = \frac{1}{L}\int_{-L}^{+L} f(x)\sin\frac{n\pi x}{L}\,dx \quad\text{and}\quad b_n = \frac{1}{L}\int_{-L}^{+L} f(x)\cos\frac{n\pi x}{L}\,dx \tag{B.36}$$

The usefulness of the Fourier series is that a function can often be approximated by a few terms, depending on the accuracy desired.

For functions that are either even or odd with respect to the variable $x$, only either the sine or the cosine terms will appear in the series. For even functions, $f(-x) = f(x)$, and for odd functions, $f(-x) = -f(x)$. Because $\sin(-x) = -\sin(x)$ and $\cos(-x) = \cos(x)$, all coefficients $a_n$ are zero for an even function, and all coefficients $b_n$ are zero for an odd function. Note that Equation (B.29) is not an odd function of $x$ because the function was only fit over the interval $0 \le x \le 1.5$.

Whereas the coefficients for the Taylor-Maclaurin series can be readily calculated, those for the Fourier series require more effort. To avoid mathematical detail here, the Fourier coefficients $a_n$ and $b_n$ are not explicitly calculated for a model function. The coefficients can be easily calculated using a program such as *Mathematica*. Our focus here is to show that periodic functions can be approximated to a reasonable degree by using the first few terms in a Fourier series, rather than to carry out the calculations.

To demonstrate the usefulness of expanding a function in a Fourier series, consider the function

$$f(x) = 1 \quad\text{for } 0 \le x \le L$$

$$f(x) = -x \quad\text{for } -L \le x \le 0 \tag{B.37}$$

which is periodic in the interval $-L \le x \le L$, in a Fourier series. This function is a demanding function to expand in a Fourier series because the function is discontinuous at $x = 0$ and the slope is discontinuous at $x = 0$ and $x = 1$. The function and the approximate functions obtained by truncating the series at $n = 2$, $n = 5$, and $n = 10$ are shown in Figure B.7. The agreement between the truncated series and the function is reasonably good for $n = 10$. The oscillations seen near $x/L = 0$ are due to the discontinuity in the function. More terms in the series are required to obtain a good fit if the function changes rapidly in a small interval.

# B.4 Integral Calculus

## B.4.1 DEFINITE AND INDEFINITE INTEGRALS

In many areas of physical chemistry, the property of interest is the integral of a function over an interval in the variable of interest. For example, the total probability of finding a particle within an interval $0 \le x \le a$ is the integral of the probability density $P(x)$ over the interval

$$P_{total} = \int_0^a P(x)\,dx \tag{B.38}$$

Geometrically, the integral of a function over an integral is the area under the curve describing the function. For example, the integral $\int_{-2.3}^{2.3}(x^3 - 5x)\,dx$ is the sum of the

areas of the individual rectangles in Figure B.8 in the limit within which the width of the rectangles approaches zero. If the rectangles lie below the zero line, the incremental area is negative; if the rectangles lie above the zero line, the incremental area is positive. In this case the total area is zero because the total negative area equals the total positive area. This is the case because $f(x)$ is an odd function of $x$.

The integral can also be understood as an antiderivative. From this point of view, the integral symbol is defined by the relation

$$f(x) = \int \frac{df(x)}{dx} dx \qquad \text{(B.39)}$$

and the function that appears under the integral sign is called the integrand. Interpreting the integral in terms of area, we evaluate a definite integral, and the interval over which the integration occurs is specified. The interval is not specified for an indefinite integral.

The geometrical interpretation is often useful in obtaining an integral from experimental data when the functional form of the integrand is not known. For our purposes, the interpretation of the integral as an antiderivative is more useful. The value of the indefinite integral $\int (x^3 - 5x)\, dx$ is that function which, when differentiated, gives the integrand. Using the rules for differentiation discussed earlier, you can verify that

$$\int (x^3 - 5x)\, dx = \frac{x^4}{4} - \frac{5x^2}{2} + C \qquad \text{(B.40)}$$



**FIGURE B.8**

Note the constant that appears in the evaluation of every indefinite integral. By differentiating the function obtained upon integration, you should convince yourself that any constant will lead to the same integrand. In contrast, a definite integral has no constant of integration. If we evaluate the definite integral

$$\int_{-2.3}^{2.3} (x^3 - 5x)\, dx = \left( \frac{x^4}{4} - \frac{5x^2}{2} + C \right)_{x=2.3} - \left( \frac{x^4}{4} - \frac{5x^2}{2} + C \right)_{x=-2.3} \qquad \text{(B.41)}$$

we see that the constant of integration cancels. Because the function obtained upon integration is an even function of $x$, $\int_{-2.3}^{2.3} (x^3 - 5x)\, dx = 0$, just as we saw in the geometric interpretation of the integral.

It is useful for the student of physical chemistry to commit the integrals listed next to memory, because they are encountered frequently. These integrals are directly related to the derivatives discussed in Section B.2:

$$\int df(x) = f(x) + C$$

$$\int x^n\, dx = \frac{x^{n+1}}{n+1} + C$$

$$\int \frac{dx}{x} = \ln x + C$$

$$\int e^{ax} = \frac{e^{ax}}{a} + C, \quad \text{where } a \text{ is a constant}$$

$$\int \sin x\, dx = -\cos x + C$$

$$\int \cos x\, dx = \sin x + C$$

However, the primary tool for the physical chemist in evaluating integrals is a good set of integral tables. The integrals that are most frequently used in elementary quantum mechanics are listed here; the first group lists indefinite integrals:

$$\int (\sin ax)\, dx = -\frac{1}{a}\cos ax + C$$

$$\int (\cos ax)\, dx = \frac{1}{a}\sin ax + C$$
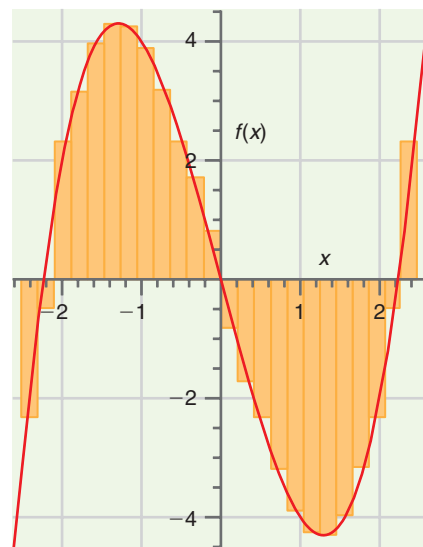
$$\int (\sin^2 ax)\, dx = \frac{1}{2}x - \frac{1}{4a}\sin 2ax + C$$

$$\int (\cos^2 ax)\, dx = \frac{1}{2}x + \frac{1}{4a}\sin 2ax + C$$

$$\int (x^2 \sin^2 ax)\, dx = \frac{1}{6}x^3 - \left(\frac{1}{4a}x^2 - \frac{1}{8a^3}\right)\sin 2ax - \frac{1}{4a^2}x \cos 2ax + C$$

$$\int (x^2 \cos^2 ax)\, dx = \frac{1}{6}x^3 + \left(\frac{1}{4a}x^2 - \frac{1}{8a^3}\right)\sin 2ax + \frac{1}{4a^2}x \cos 2ax + C$$

$$\int (\sin^3 ax)\, dx = -\frac{3 \cos ax}{4a} + \frac{\cos 3ax}{12a} + C$$

$$\int x^2 (\sin ax)\, dx = \frac{(a^2x^2 - 2)\cos ax}{a^3} + \frac{2x \sin ax}{a^2} + C$$

$$\int x^2 (\cos ax)\, dx = \frac{(a^2x^2 - 2)\sin ax}{a^3} + \frac{2x \cos ax}{a^2} + C$$

$$\int x^m e^{ax}\, dx = \frac{x^m e^{ax}}{a} - \frac{m}{a}\int x^{m-1} e^{ax}\, dx + C$$

$$\int \frac{e^{ax}}{x^m}\, dx = -\frac{1}{m-1}\frac{e^{ax}}{x^{m-1}} + \frac{a}{m-1}\int \frac{e^{ax}}{x^{m-1}}\, dx + C$$

The following group lists definite integrals.

$$\int_0^a \sin\left(\frac{n\pi x}{a}\right) \times \sin\left(\frac{m\pi x}{a}\right) dx = \int_0^a \cos\left(\frac{n\pi x}{a}\right) \times \cos\left(\frac{m\pi x}{a}\right) dx = \frac{a}{2}\delta_{mn}$$

$$\int_0^a \left[\sin\left(\frac{n\pi x}{a}\right)\right] \times \left[\cos\left(\frac{n\pi x}{a}\right)\right] dx = 0$$

$$\int_0^\pi \sin^2 mx\, dx = \int_0^\pi \cos^2 mx\, dx = \frac{\pi}{2}$$

$$\int_0^\infty \frac{\sin x}{\sqrt{x}}\, dx = \int_0^\infty \frac{\cos x}{\sqrt{x}}\, dx = \sqrt{\frac{\pi}{2}}$$

$$\int_0^\infty x^n e^{-ax}\, dx = \frac{n!}{a^{n+1}} \quad (a > 0, n \text{ positive integer})$$

$$\int_0^\infty x^{2n} e^{-ax^2}\, dx = \frac{1\cdot 3\cdot 5\cdots(2n-1)}{2^{n+1}a^n}\sqrt{\frac{\pi}{a}} \quad (a > 0, n \text{ positive integer})$$

$$\int_0^\infty x^{2n+1} e^{-ax^2}\, dx = \frac{n!}{2\,a^{n+1}} \quad (a > 0, n \text{ positive integer})$$

$$\int_0^\infty e^{-ax^2}\, dx = \left(\frac{\pi}{4a}\right)^{1/2}$$

In the first integral above, $\delta_{mn} = 1$ if $m = n$, and 0 if $m \neq n$.

## B.4.2   MULTIPLE INTEGRALS AND SPHERICAL COORDINATES

In the previous section, integration with respect to a single variable was discussed. Often, however, integration occurs over two or three variables. For example, the wave functions for the particle in a two-dimensional box are given by

$$\psi_{n_x n_y}(x, y) = N \sin \frac{n_x \pi x}{a} \sin \frac{n_y \pi y}{b} \tag{B.42}$$

In normalizing a wave function, the integral of $|\psi_{n_x n_y}(x,y)|^2$ is required to equal 1 over the range $0 \leq x \leq a$ and $0 \leq y \leq b$. This requires solving the double integral

$$\int_0^b dy \int_0^a \left( N \sin \frac{n_x \pi x}{a} \sin \frac{n_y \pi y}{b} \right)^2 dx = 1 \tag{B.43}$$

to determine the normalization constant $N$. We sequentially integrate over the variables $x$ and $y$ or vice versa using the list of indefinite integrals from the previous section.

$$\int_0^b dy \int_0^a \left( N \sin \frac{n_x \pi x}{a} \sin \frac{n_y \pi y}{b} \right)^2 dx$$

$$= \left[ \frac{1}{2}x - \frac{a}{4n\pi} \sin \frac{2n_x \pi x}{a} \right]_{x=0}^{x=a} \times N^2 \int_0^b \left( \sin \frac{n_y \pi y}{b} \right)^2 dy$$

$$1 = \left[ \frac{1}{2}a - \frac{a}{4n\pi} (\sin 2n_x \pi - 0) \right] \times N^2 \int_0^b \left( \sin \frac{n_y \pi y}{b} \right)^2 dy$$

$$1 = N^2 \left[ \frac{1}{2}a - \frac{a}{4n\pi} (\sin 2n_x \pi - 0) \right] \times \left[ \frac{1}{2}b - \frac{a}{4n\pi} (\sin 2n_y \pi - 0) \right] = \frac{N^2 ab}{4}$$

$$N = \frac{2}{\sqrt{ab}}$$

Convince yourself that the normalization constant for the wave functions of the three-dimensional particle in the box

$$\psi_{n_x n_y n_z}(x, y, z) = N \sin \frac{n_x \pi x}{a} \sin \frac{n_y \pi y}{b} \sin \frac{n_z \pi z}{c} \tag{B.44}$$

has the value $N = 2\sqrt{2}/\sqrt{abc}$.

   Up to this point, we have considered functions of a single variable. This restricts us to dealing with a single spatial dimension. The extension to three independent variables becomes important in describing three-dimensional systems. The three-dimensional system of most importance to us is the atom. Closed-shell atoms are spherically symmetric, so we might expect atomic wave functions to be best described by spherical coordinates. Therefore, you should become familiar with integrations in this coordinate system. In transforming from spherical coordinates $r$, $\theta$, and $\phi$ to Cartesian coordinates $x$, $y$, and $z$, the following relationships are used:

$$x = r \sin \theta \cos \phi$$
$$y = r \sin \theta \sin \phi \tag{B.45}$$
$$z = r \cos \theta$$

These relationships are depicted in Figure B.9. For small increments in the variables $r$, $\theta$, and $\phi$, the volume element depicted in this figure is a rectangular solid of volume

$$dV = (r \sin \theta \, d\phi)(dr)(r \, d\theta) = r^2 \sin \theta \, dr \, d\theta \, d\phi \tag{B.46}$$

Note in particular that the volume element in spherical coordinates is not $dr \, d\theta \, d\phi$ in analogy with the volume element $dx \, dy \, dz$ in Cartesian coordinates.
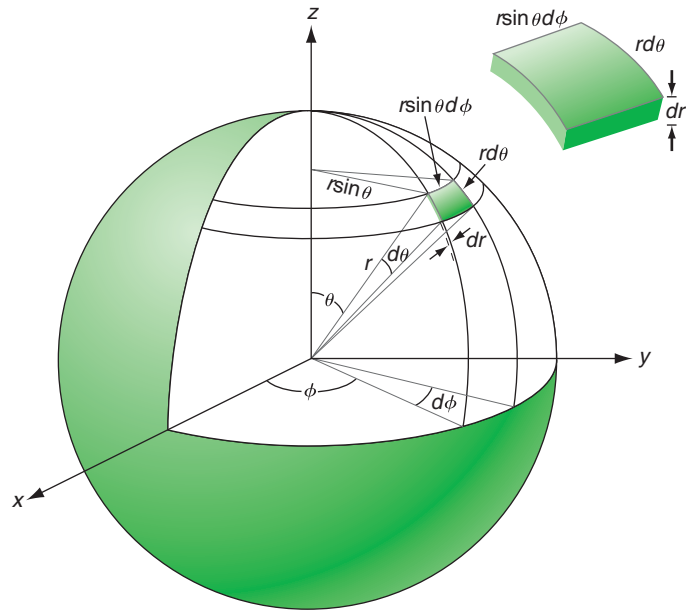
**FIGURE B.9**

In transforming from Cartesian coordinates $x$, $y$, and $z$ to the spherical coordinates $r$, $\theta$, and $\phi$, these relationships are used:

$$r = \sqrt{x^2 + y^2 + z^2} \quad \theta = \cos^{-1}\frac{z}{\sqrt{x^2 + y^2 + z^2}} \quad \text{and} \quad \phi = \tan^{-1}\frac{y}{x} \quad \textbf{(B.47)}$$

What is the appropriate range of variables to integrate over all space in spherical coordinates? If we imagine the radius vector scanning over the range $0 \le \theta \le \pi$; $0 \le \phi \le 2\pi$, the whole angular space is scanned. If we combine this range of $\theta$ and $\phi$ with $0 \le r \le \infty$, all of the three-dimensional space is scanned. Note that $r = \sqrt{x^2 + y^2 + z^2}$ is always positive.

To illustrate the process of integration in spherical coordinates, we normalize the function $e^{-r}\cos\theta$ over the interval $0 \le r \le \infty$; $0 \le \theta \le \pi$; $0 \le \phi \le 2\pi$:

$$N^2 \int_0^{2\pi} d\phi \int_0^{\pi} \sin\theta\, d\theta \int_0^{\infty} (e^{-r}\cos\theta)^2 r^2\, dr = N^2 \int_0^{2\pi} d\phi \int_0^{\pi} \cos^2\theta \sin\theta\, d\theta \int_0^{\infty} r^2 e^{-2r}\, dr = 1$$

It is most convenient to integrate first over $\phi$, giving

$$2\pi N^2 \int_0^{\pi} \cos^2\theta \sin\theta\, d\theta \int_0^{\infty} r^2 e^{-2r}\, dr = 1$$

We next integrate over $\theta$, giving

$$2\pi N^2 \left[ \frac{-\cos^3\pi + \cos^3 0}{3} \right] \times \int_0^{\infty} r^2 e^{-2r}\, dr = \frac{4\pi N^2}{3} \int_0^{\infty} r^2 e^{-2r}\, dr = 1$$

We finally integrate over $r$ using the standard integral

$$\int_0^{\infty} x^n e^{-ax}\, dx = \frac{n!}{a^{n+1}} \quad (a > 0,\, n \text{ positive integer})$$

The result is

$$\frac{4\pi N^2}{3} \int_0^{\infty} r^2 e^{-2r}\, dr = \frac{4\pi N^2}{3}\frac{2!}{8} = 1 \quad \text{or} \quad N = \sqrt{\frac{3}{\pi}}$$

We conclude that the normalized wave function is $\sqrt{3/\pi}\, e^{-r}\cos\theta$.

# B.5 Vectors

The use of vectors occur frequently in physical chemistry. Consider circular motion of a particle at constant speed in two dimensions, as depicted in Figure B.10. The particle is moving in a counterclockwise direction on the ring-like orbit. At any instant in time, its position, velocity, and acceleration can be measured. The two aspects to these measurements are the magnitude and the direction of each of these observables. Whereas a scalar quantity such as speed has only a magnitude, a vector has both a magnitude and a direction.

For the particular case under consideration, the position vectors $\mathbf{r}_1$ and $\mathbf{r}_2$ extend outward from the origin and terminate at the position of the particle. The velocities $\mathbf{v}_1$ and $\mathbf{v}_2$ are related to the position vector as $\mathbf{v} = \lim_{\Delta t \to 0} [\mathbf{r}(t + \Delta t) - \mathbf{r}(t)]/\Delta t$. Therefore, the velocity vector is perpendicular to the position vector. The acceleration vector is defined by $\mathbf{a} = \lim_{\Delta t \to 0} [\mathbf{v}(t + \Delta t) - \mathbf{v}(t)]/\Delta t$. As we see in part (b) of Figure B.10, $\mathbf{a}$ is perpendicular to $\mathbf{v}$, and is antiparallel to $\mathbf{r}$. As this example of a relatively simple motion shows, vectors are needed to describe the situation properly by keeping track of both the magnitude and direction of each of the observables of interest. For this reason, it is important to be able to work with vectors.

In three-dimensional Cartesian coordinates, any vector can be written in the form

$$\mathbf{r} = x_1\mathbf{i} + y_1\mathbf{j} + z_1\mathbf{k} \tag{B.48}$$

where $\mathbf{i}$, $\mathbf{j}$, and $\mathbf{k}$ are the mutually perpendicular vectors of unit length along the $x$, $y$, and $z$ axes, respectively, and $x_1$, $y_1$, and $z_1$ are numbers. The length of a vector is defined by the equation

$$|\mathbf{r}| = \sqrt{x_1^2 + y_1^2 + z_1^2} \tag{B.49}$$

This vector is depicted in the three-dimensional coordinate system shown in Figure B.11.

By definition, the angle $\theta$ is measured from the $z$ axis, and the angle $\phi$ is measured in the $xy$ plane from the $x$ axis. The angles $\theta$ and $\phi$ are related to $x_1$, $y_1$, and $z_1$ by

$$\theta = \cos^{-1}\frac{z_1}{\sqrt{x_1^2 + y_1^2 + z_1^2}} \quad \text{and} \quad \phi = \tan^{-1}\frac{y_1}{x_1} \tag{B.50}$$

We next consider the addition and subtraction of two vectors. Two vectors $\mathbf{a} = x\mathbf{i} + y\mathbf{j} + z\mathbf{k}$ and $\mathbf{b} = x'\mathbf{i} + y'\mathbf{j} + z'\mathbf{k}$ can be added or subtracted according to the equations

$$\mathbf{a} \pm \mathbf{b} = (x \pm x')\mathbf{i} + (y \pm y')\mathbf{j} + (z \pm z')\mathbf{k} \tag{B.51}$$

The addition and subtraction of vectors can also be depicted graphically, as done in Figure B.12.

The multiplication of two vectors can occur in either of two forms. Scalar multiplication of $\mathbf{a}$ and $\mathbf{b}$, also called the dot product of $\mathbf{a}$ and $\mathbf{b}$, is defined by

$$\mathbf{a} \cdot \mathbf{b} = |\mathbf{a}||\mathbf{b}| \cos \alpha \tag{B.52}$$

where $\alpha$ is the angle between the vectors. For $\mathbf{a} = 3\mathbf{i} + 1\mathbf{j} - 2\mathbf{k}$ and $\mathbf{b} = 2\mathbf{i} + -1\mathbf{j} + 4\mathbf{k}$, the vectors in the previous equation can be expanded in terms of their unit vectors:

$$\mathbf{a} \cdot \mathbf{b} = (3\mathbf{i} + 1\mathbf{j} - 2\mathbf{k}) \cdot (2\mathbf{i} + -1\mathbf{j} + 4\mathbf{k})$$
$$= 3\mathbf{i} \cdot 2\mathbf{i} + 3\mathbf{i} \cdot (-1\mathbf{j}) + 3\mathbf{i} \cdot 4\mathbf{k} + 1\mathbf{j} \cdot 2\mathbf{i} + 1\mathbf{j} \cdot (-1\mathbf{j})$$
$$+ 1\mathbf{j} \cdot 4\mathbf{k} - 2\mathbf{k} \cdot 2\mathbf{i} - 2\mathbf{k} \cdot (-1\mathbf{j}) - 2\mathbf{k} \cdot 4\mathbf{k}$$

However, because $\mathbf{i}$, $\mathbf{j}$, and $\mathbf{k}$ are mutually perpendicular vectors of unit length, $\mathbf{i} \cdot \mathbf{i} = \mathbf{j} \cdot \mathbf{j} = \mathbf{k} \cdot \mathbf{k} = 1$ and $\mathbf{i} \cdot \mathbf{j} = \mathbf{i} \cdot \mathbf{k} = \mathbf{j} \cdot \mathbf{k} = 0$. Therefore, $\mathbf{a} \cdot \mathbf{b} = 3\mathbf{i} \cdot 2\mathbf{i} + 1\mathbf{j} \cdot (-1\mathbf{j}) - 2\mathbf{k} \cdot 4\mathbf{k} = -3$.
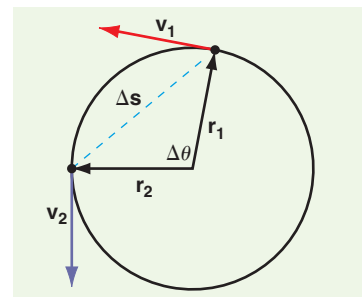
(a)
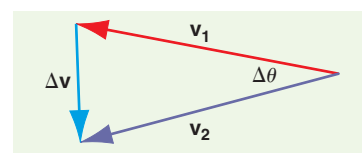
(b)

**FIGURE B.10**
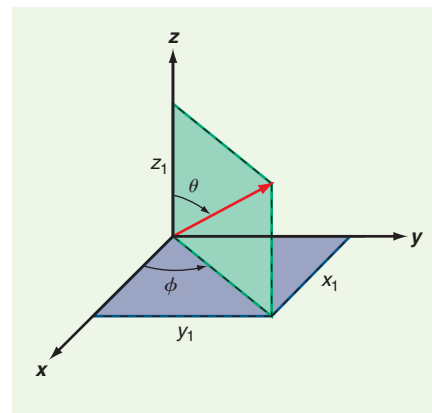
**FIGURE B.11**
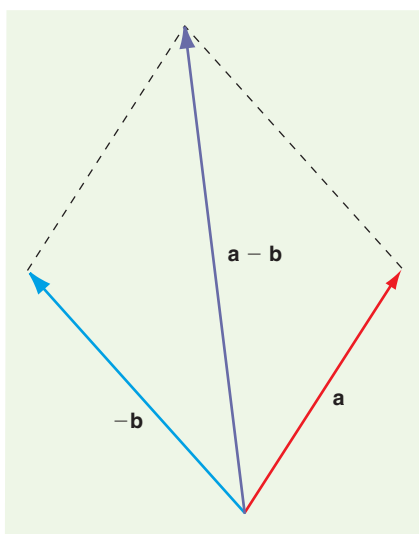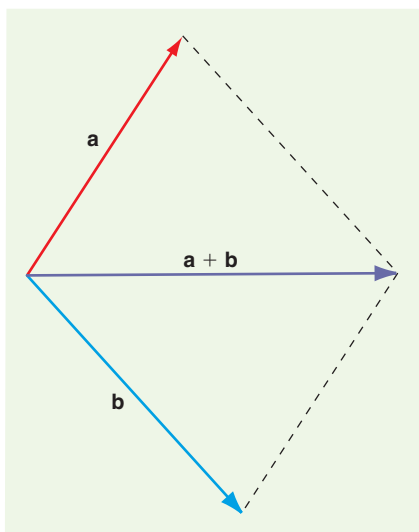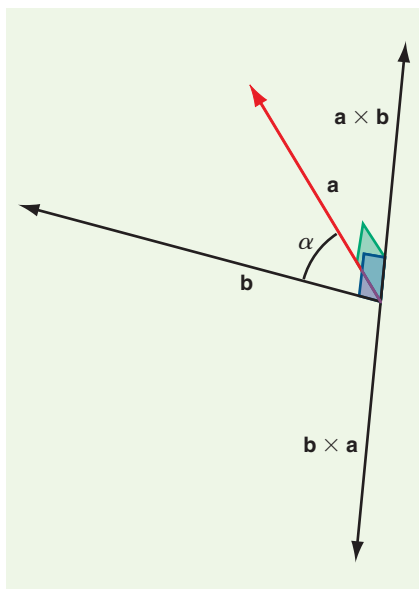
The other form in which vectors are multiplied is the vector product, also called the cross product. The vector multiplication of two vectors results in a vector, whereas the scalar multiplication of two vectors results in a scalar. The cross product is defined by the equation

$$\mathbf{a} \times \mathbf{b} = \mathbf{c}|\mathbf{a}||\mathbf{b}| \sin \alpha \tag{B.53}$$

Note that $\mathbf{a} \times \mathbf{b} = -\mathbf{b} \times \mathbf{a}$ as shown in Figure B.13. By contrast, $\mathbf{a} \cdot \mathbf{b} = \mathbf{b} \cdot \mathbf{a}$.

In Equation (B.53), $\mathbf{c}$ is a vector of unit length that is perpendicular to the plane containing $\mathbf{a}$ and $\mathbf{b}$ and has a positive direction found by using the right-hand rule (see Chapter 7 in *Quantum Chemistry and Spectroscopy*) and $\alpha$ is the angle between $\mathbf{a}$ and $\mathbf{b}$.

The cross product between two three-dimensional vectors $\mathbf{a}$ and $\mathbf{b}$ is given by

$$
\begin{aligned}
\mathbf{a} \times \mathbf{b} &= (a_x\mathbf{i} + a_y\mathbf{j} + a_z\mathbf{k}) \times (b_x\mathbf{i} + b_y\mathbf{j} + b_z\mathbf{k}) \\
&= a_x\mathbf{i} \times b_x\mathbf{i} + a_x\mathbf{i} \times b_y\mathbf{j} + a_x\mathbf{i} \times b_z\mathbf{k} + a_y\mathbf{j} \times b_x\mathbf{i} + a_y\mathbf{j} \times b_y\mathbf{j} \\
&\quad + a_y\mathbf{j} \times b_z\mathbf{k} + a_z\mathbf{k} \times b_x\mathbf{i} + a_z\mathbf{k} \times b_y\mathbf{j} + a_z\mathbf{k} \times b_z\mathbf{k}
\end{aligned} \tag{B.54}
$$

However, using the definition of the cross product in Equation (B.53),

$$\mathbf{i} \times \mathbf{i} = \mathbf{j} \times \mathbf{j} = \mathbf{k} \times \mathbf{k} = 0, \quad \mathbf{i} \times \mathbf{j} = \mathbf{k}, \quad \mathbf{i} \times \mathbf{k} = -\mathbf{j}$$
$$\mathbf{j} \times \mathbf{i} = -\mathbf{k}, \quad \mathbf{j} \times \mathbf{k} = \mathbf{i}, \quad \mathbf{k} \times \mathbf{i} = \mathbf{j}, \quad \mathbf{k} \times \mathbf{j} = -\mathbf{i}$$

Therefore, Equation (B.54) simplifies to

$$\mathbf{a} \times \mathbf{b} = (a_yb_z - a_zb_y)\mathbf{i} + (a_zb_x - a_xb_z)\mathbf{j} + (a_xb_y - a_yb_x)\mathbf{k} \tag{B.55}$$

As we will see in Section B.7, there is a simple way to calculate cross products using determinants.

The angular momentum $\mathbf{l} = \mathbf{r} \times \mathbf{p}$ is of particular interest in quantum chemistry, because $s$, $p$, and $d$ electrons are distinguished by their orbital angular momentum. For the example of the particle rotating on a ring depicted at the beginning of this section, the angular momentum vector is pointing upward in a direction perpendicular to the plane of the page. In analogy to Equation (B.55),

$$\mathbf{l} = \mathbf{r} \times \mathbf{p} = (yp_z - zp_y)\mathbf{i} + (zp_x - xp_z)\mathbf{j} + (xp_y - yp_x)\mathbf{k}$$



**FIGURE B.12**



**FIGURE B.13**

# B.6 Partial Derivatives

In this section, we discuss the differential calculus of functions that depend on several independent variables. Consider the volume of a cylinder of radius $r$ and height $h$, for which

$$V = f(r, h) = \pi r^2 h \tag{B.56}$$

where $V$ can be written as a function of the two variables $r$ and $h$. The change in $V$ with a change in $r$ or $h$ is given by the partial derivatives

$$\left(\frac{\partial V}{\partial r}\right)_h = \lim_{\Delta r \to 0} \frac{V(r + \Delta r, h) - V(r, h)}{\Delta r} = 2\pi rh$$

$$\left(\frac{\partial V}{\partial h}\right)_r = \lim_{\Delta h \to 0} \frac{V(r, h + \Delta h) - V(r, h)}{\Delta h} = \pi r^2 \tag{B.57}$$

The subscript $h$ in $(\partial V/\partial r)_h$ reminds us that $h$ is being held constant in the differentiation. The partial derivatives in Equation (B.57) allow us to determine how a function changes when one of the variables changes. How does $V$ change if the values of both variables change? In this case, $V$ changes to $V + dV$ where

$$dV = \left(\frac{\partial V}{\partial r}\right)_h dr + \left(\frac{\partial V}{\partial h}\right)_r dh \tag{B.58}$$

These partial derivatives are useful in calculating the error in the function that results from errors in measurements of the individual variables. For example, the relative error in the volume of the cylinder is given by

$$\frac{dV}{V} = \frac{1}{V}\left[\left(\frac{\partial V}{\partial r}\right)_h dr + \left(\frac{\partial V}{\partial h}\right)_r dh\right] = \frac{1}{\pi r^2 h}[2\pi rh\, dr + \pi r^2 dh] = \frac{2dr}{r} + \frac{dh}{h}$$

This equation shows that a given relative error in $r$ generates twice the relative error in $V$ as a relative error in $h$ of the same size.

We can also take second or higher derivatives with respect to either variable. The mixed second partial derivatives are of particular interest. The mixed partial derivatives of $V$ are given by

$$\left(\frac{\partial}{\partial h}\left(\frac{\partial V}{\partial r}\right)_h\right)_r = \left(\partial\left(\frac{\partial[\pi r^2 h]}{\partial r}\right)_h \middle/ \partial h\right)_r = \left(\frac{\partial[2\pi rh]}{\partial h}\right)_r = 2\pi r$$

$$\left(\frac{\partial}{\partial r}\left(\frac{\partial V}{\partial h}\right)_r\right)_h = \left(\partial\left(\frac{\partial[\pi r^2 h]}{\partial h}\right)_r \middle/ \partial r\right)_h = \left(\frac{\partial[\pi r^2]}{\partial r}\right)_h = 2\pi r \qquad \textbf{(B.59)}$$

For the specific case of $V$, the order in which the function is differentiated does not affect the outcome. Such a function is called a state function. Therefore, for any state function $f$ of the variables $x$ and $y$,

$$\left(\frac{\partial}{\partial y}\left(\frac{\partial f(x,y)}{\partial x}\right)_y\right)_x = \left(\frac{\partial}{\partial x}\left(\frac{\partial f(x,y)}{\partial y}\right)_x\right)_y \qquad \textbf{(B.60)}$$

Because Equation (B.60) is satisfied by all state functions $f$ it can be used to determine if a function $f$ is a state function.

We demonstrate how to calculate the partial derivatives

$$\left(\frac{\partial f}{\partial x}\right)_y, \left(\frac{\partial f}{\partial y}\right)_x, \left(\frac{\partial^2 f}{\partial x^2}\right)_y, \left(\frac{\partial^2 f}{\partial y^2}\right)_x, \left(\partial\left(\frac{\partial f}{\partial x}\right)_y \middle/ \partial y\right)_x, \text{and} \left(\partial\left(\frac{\partial f}{\partial y}\right)_x \middle/ \partial x\right)_y$$

for the function $f(x,y) = ye^{ax} + xy\cos x + y\ln xy$, where $a$ is a real constant:

$$\left(\frac{\partial f}{\partial x}\right)_y = aye^{ax} + \frac{y}{x} + y\cos x - xy\sin x,$$

$$\left(\frac{\partial f}{\partial y}\right)_x = 1 + e^{ax} + x\cos x + \ln xy$$

$$\left(\frac{\partial^2 f}{\partial x^2}\right)_y = a^2 ye^{ax} - \frac{y}{x^2} - 2y\sin x - xy\cos x, \left(\frac{\partial^2 f}{\partial y^2}\right)_x = \frac{1}{y}$$

$$\left(\partial\left(\frac{\partial f}{\partial x}\right)_y \middle/ \partial y\right)_x = ae^{ax} + \frac{1}{x} + \cos x - x\sin x,$$

$$\left(\partial\left(\frac{\partial f}{\partial y}\right)_x \middle/ \partial x\right)_y = ae^{ax} + \frac{1}{x} + \cos x - x\sin x$$

Because we have shown that

$$\left(\partial\left(\frac{\partial f}{\partial x}\right)_y \middle/ \partial y\right)_x = \left(\partial\left(\frac{\partial f}{\partial y}\right)_x \middle/ \partial x\right)_y$$

$f(x, y)$ is a state function of the variables $x$ and $y$.

Whereas the partial derivatives tell us how the function changes if the value of one of the variables is changed, the total differential tells us how the function changes when all of the variables are changed simultaneously. The total differential of the function $f(x, y)$ is defined by

$$df = \left(\frac{\partial f}{\partial x}\right)_y dx + \left(\frac{\partial f}{\partial y}\right)_x dy \qquad \textbf{(B.61)}$$

The total differential of the function used earlier is calculated as follows:

$$df = \left( aye^{ax} + \frac{y}{x} + y\cos x - xy\sin x \right) dx + \left( 1 + e^{ax} + x\cos x + \log xy \right) dy$$

Two other important results from multivariate differential calculus are used frequently. For a function $z = f(x,y)$, which can be rearranged to $x = g(y,z)$ or $y = h(x,z)$,

$$\left( \frac{\partial x}{\partial y} \right)_z = \frac{1}{\left( \dfrac{\partial y}{\partial x} \right)_z} \tag{B.62}$$

The other important result that is used frequently is the cyclic rule:

$$\left( \frac{\partial x}{\partial y} \right)_z \left( \frac{\partial y}{\partial z} \right)_x \left( \frac{\partial z}{\partial x} \right)_y = -1 \tag{B.63}$$

Consider an additional example of calculating partial derivatives for a function encountered in quantum mechanics. The Schrödinger equation for the hydrogen atom takes the form

$$-\frac{\hbar^2}{2\mu} \left[ \frac{1}{r^2} \frac{\partial}{\partial r}\left( r^2 \frac{\partial \psi(r,\theta,\phi)}{\partial r} \right) + \frac{1}{r^2 \sin\theta} \frac{\partial}{\partial \theta}\left( \sin\theta \frac{\partial \psi(r,\theta,\phi)}{\partial \theta} \right) + \frac{1}{r^2 \sin\theta} \frac{\partial^2 \psi(r,\theta,\phi)}{\partial \phi^2} \right]$$

$$-\frac{e^2}{4\pi\varepsilon_0 r} \psi(r,\theta,\phi) = E\psi(r,\theta,\phi)$$

Note that each of the first three terms on the left side of the equation involves partial differentiation with respect to one of the variables $r$, $\theta$, and $\phi$ in turn. Two of the solutions to this differential equation are $(r/a_0)e^{-r/2a_0}\sin\theta e^{\pm i\phi}$. Each of these terms is evaluated separately to demonstrate how partial derivatives are taken in quantum mechanics. Although this is a more complex exercise than those presented earlier, it provides good practice in partial differentiation. For the first term, the partial derivative is taken with respect to $r$:

$$-\frac{\hbar^2}{2\mu} \frac{1}{\sqrt{64\pi}} \left( \frac{1}{a_0} \right)^{3/2} \left[ \frac{1}{r^2} \frac{\partial}{\partial r}\left( r^2 \frac{\partial\left( \dfrac{r}{a_0}e^{-r/2a_0}\sin\theta e^{\pm i\phi} \right)}{\partial r} \right) \right]$$

$$= -\frac{\hbar^2}{2\mu} \frac{1}{\sqrt{64\pi}} \left( \frac{1}{a_0} \right)^{3/2} \sin\theta e^{\pm i\phi} \left[ \frac{1}{r^2} \frac{\partial}{\partial r}\left( r^2 \frac{\partial\left( \dfrac{r}{a_0}e^{-r/2a_0} \right)}{\partial r} \right) \right]$$

$$= -\frac{\hbar^2}{2\mu} \frac{1}{\sqrt{64\pi}} \left( \frac{1}{a_0} \right)^{3/2} \sin\theta e^{\pm i\phi} \left[ \frac{1}{r^2} \frac{\partial}{\partial r}\left( r^2 \left( \frac{1}{a_0}e^{-r/2a_0} - (r/2a_0^2)e^{-r/2a_0} \right) \right) \right]$$

$$= -\frac{\hbar^2}{2\mu} \frac{1}{\sqrt{64\pi}} \left( \frac{1}{a_0} \right)^{3/2} \sin\theta e^{\pm i\phi} \left[ \frac{1}{r^2}\left( \begin{array}{c} -r^2\dfrac{e^{-r/2a_0}}{a_0^2} + r^3\dfrac{e^{-r/2a_0}}{4a_0^3} + 2r\dfrac{e^{-r/2a_0}}{a_0} \\ -2r^2\dfrac{e^{-r/2a_0}}{a_0^2} \end{array} \right) \right]$$

$$= -\frac{\hbar^2}{2\mu} \frac{1}{\sqrt{64\pi}} \left( \frac{1}{a_0} \right)^{3/2} \sin\theta e^{\pm i\phi} e^{-r/2a_0} \frac{(8a_0^2 - 8a_0 r + r^2)}{4a_0^3 r}$$

Partial differentiation with respect to $\theta$ is easier, because the terms that depend on $r$ and $\phi$ are constant:

$$-\frac{\hbar^2}{2\mu} \frac{1}{\sqrt{64\pi}} \left( \frac{1}{a_0} \right)^{3/2} \left[ \frac{1}{r^2 \sin\theta} \frac{\partial}{\partial\theta}\left( \sin\theta \frac{\partial\left( \dfrac{r}{a_0}e^{-r/2a_0}\sin\theta e^{\pm i\phi} \right)}{\partial\theta} \right) \right]$$

$$= -\frac{\hbar^2}{2\mu} \frac{1}{\sqrt{64\pi}} \left( \frac{1}{a_0} \right)^{3/2} \frac{r}{a_0}e^{-r/2a_0}e^{\pm i\phi} \left[ \frac{1}{r^2 \sin\theta} \frac{\partial}{\partial\theta}\left( \sin\theta \frac{\partial(\sin\theta)}{\partial\theta} \right) \right]$$

$$
= -\frac{\hbar^2}{2\mu} \frac{1}{\sqrt{64\pi}} \left(\frac{1}{a_0}\right)^{3/2} \frac{r}{a_0} e^{-r/2a_0} e^{\pm i\phi} \left[\frac{1}{r^2 \sin\theta} \frac{\partial}{\partial\theta}(\sin\theta\cos\theta)\right]
$$

$$
= -\frac{\hbar^2}{2\mu} \frac{1}{\sqrt{64\pi}} \left(\frac{1}{a_0}\right)^{3/2} \frac{r}{a_0} e^{-r/2a_0} e^{\pm i\theta} \left[\frac{1}{r^2 \sin\theta}(\cos^2\theta - \sin^2\theta)\right]
$$

Partial differentiation with respect to $\phi$ is also not difficult, because the terms that depend on $r$ and $\theta$ are constant:

$$
-\frac{\hbar^2}{2\mu} \frac{1}{\sqrt{64\pi}} \left(\frac{1}{a_0}\right)^{3/2} \left[\frac{1}{r^2 \sin\theta} \frac{\partial^2 \frac{r}{a_0} e^{-r/2a_0} \sin\theta \, e^{\pm i\phi}}{\partial\phi^2}\right]
$$

$$
= -\frac{\hbar^2}{2\mu} \frac{1}{\sqrt{64\pi}} \left(\frac{1}{a_0}\right)^{3/2} \frac{r}{a_0} e^{-r/2a_0} \frac{1}{r^2}\left[\frac{\partial^2 e^{\pm i\phi}}{\partial\phi^2}\right]
$$

$$
= \frac{\hbar^2}{2\mu} \frac{1}{\sqrt{64\pi}} \left(\frac{1}{a_0}\right)^{3/2} \frac{r}{a_0} e^{-r/2a_0} \frac{1}{r^2}\left[e^{\pm i\phi}\right]
$$

# B.7 Working with Determinants

A determinant of $n$th order is a square $n \times n$ array of numbers symbolically enclosed by vertical lines. A fifth-order determinant is shown here with the conventional indexing of the elements of the array:

$$
\begin{vmatrix}
a_{11} & a_{12} & a_{13} & a_{14} & a_{15} \\
a_{21} & a_{22} & a_{23} & a_{24} & a_{25} \\
a_{31} & a_{32} & a_{33} & a_{34} & a_{35} \\
a_{41} & a_{42} & a_{43} & a_{44} & a_{45} \\
a_{51} & a_{52} & a_{53} & a_{54} & a_{55}
\end{vmatrix}
\tag{B.64}
$$

A $2 \times 2$ determinant has a value that is defined in Equation (B.65). It is obtained by multiplying the elements in the diagonal connected by a line with a negative slope and subtracting from this the product of the elements in the diagonal connected by a line with a positive slope.

$$
\begin{vmatrix}
a_{11} & a_{12} \\
a_{21} & a_{22}
\end{vmatrix} = a_{11}a_{22} - a_{12}a_{21}
\tag{B.65}
$$

The value of a higher order determinant is obtained by expanding the determinant in terms of determinants of lower order. This is done using the method of cofactors. We illustrate the use of method of cofactors by reducing a $3 \times 3$ determinant to a sum of $2 \times 2$ determinants. Any row or column can be used in the reduction process. We use the first row of the determinant in the reduction. The recipe is spelled out in this equation:

$$
\begin{vmatrix}
a_{11} & a_{12} & a_{13} \\
a_{21} & a_{22} & a_{23} \\
a_{31} & a_{32} & a_{33}
\end{vmatrix} = (-1)^{1+1}a_{11}\begin{vmatrix} a_{22} & a_{23} \\ a_{32} & a_{33} \end{vmatrix} + (-1)^{1+2}a_{12}\begin{vmatrix} a_{21} & a_{23} \\ a_{31} & a_{33} \end{vmatrix}
$$

$$
+ (-1)^{1+3}a_{13}\begin{vmatrix} a_{21} & a_{22} \\ a_{31} & a_{32} \end{vmatrix}
$$

$$
= a_{11}\begin{vmatrix} a_{22} & a_{23} \\ a_{32} & a_{33} \end{vmatrix} - a_{12}\begin{vmatrix} a_{21} & a_{23} \\ a_{31} & a_{33} \end{vmatrix} + a_{13}\begin{vmatrix} a_{21} & a_{22} \\ a_{31} & a_{32} \end{vmatrix}
\tag{B.66}
$$

Each term in the sum results from the product of one of the three elements of the first row, $(-1)^{m+n}$, where $m$ and $n$ are the indices of the row and column designating the element, respectively, and the $2 \times 2$ determinant obtained by omitting the entire row and column to which the element used in the reduction belongs. The product $(-1)^{m+n}$ and the $2 \times 2$

determinant are called the cofactor of the element used in the reduction. For example, the value of the following $3 \times 3$ determinant is found using the cofactors of the second row:

$$\begin{vmatrix} 1 & 3 & 4 \\ 2 & -1 & 6 \\ -1 & 7 & 5 \end{vmatrix} = (-1)^{2+1}2\begin{vmatrix} 3 & 4 \\ 7 & 5 \end{vmatrix} + (-1)^{2+2}(-1)\begin{vmatrix} 1 & 4 \\ -1 & 5 \end{vmatrix} + (-1)^{2+3}6\begin{vmatrix} 1 & 3 \\ -1 & 7 \end{vmatrix}$$

$$= -1 \times 2 \times (-13) + 1 \times (-1) \times 9 + (-1) \times 6 \times 10 = -43$$

If the initial determinant is of a higher order than 3, multiple sequential reductions as outlined earlier will reduce it in order by one in each step until a sum of $2 \times 2$ determinants is obtained.

The main usefulness for determinants is in solving a system of linear equations. Such a system of equations is obtained in evaluating the energies of a set of molecular orbitals obtained by combining a set of atomic orbitals. Before illustrating this method, we list some important properties of determinants that we will need in solving a set of simultaneous equations.

**Property I** The value of a determinant is not altered if each row in turn is made into a column or vice versa as long as the original order is kept. By this we mean that the $n$th row becomes the $n$th column. This property can be illustrated using $2 \times 2$ and $3 \times 3$ determinants:

$$\begin{vmatrix} 2 & 1 \\ 3 & -1 \end{vmatrix} = \begin{vmatrix} 2 & 3 \\ 1 & -1 \end{vmatrix} = -5 \quad \text{and} \quad \begin{vmatrix} 1 & 3 & 4 \\ 2 & -1 & 6 \\ -1 & 7 & 5 \end{vmatrix} = \begin{vmatrix} 1 & 2 & -1 \\ 3 & -1 & 7 \\ 4 & 6 & 5 \end{vmatrix} = -43$$

**Property II** If any two rows or columns are interchanged, the sign of the value of the determinant is changed. For example,

$$\begin{vmatrix} 2 & 1 \\ 3 & -1 \end{vmatrix} = -5, \text{ but } \begin{vmatrix} 1 & 2 \\ -1 & 3 \end{vmatrix} = +5 \quad \text{and}$$

$$\begin{vmatrix} 1 & 3 & 4 \\ 2 & -1 & 6 \\ -1 & 7 & 5 \end{vmatrix} = -43, \text{ but } \begin{vmatrix} 2 & -1 & 6 \\ 1 & 3 & 4 \\ -1 & 7 & 5 \end{vmatrix} = +43$$

**Property III** If two rows or columns of a determinant are identical, the value of the determinant is zero. For example,

$$\begin{vmatrix} 2 & 1 \\ 2 & 1 \end{vmatrix} = 2 - 2 = 0 \text{ and}$$

$$\begin{vmatrix} 1 & 1 & 4 \\ 2 & 2 & 6 \\ -1 & -1 & 5 \end{vmatrix} = (-1)^{2+1}2\begin{vmatrix} 1 & 4 \\ -1 & 5 \end{vmatrix} + (-1)^{2+2}2\begin{vmatrix} 1 & 4 \\ -1 & 5 \end{vmatrix}$$

$$+ (-1)^{2+3}6\begin{vmatrix} 1 & 1 \\ -1 & -1 \end{vmatrix}$$

$$= -1 \times 2 \times 9 + 1 \times 2 \times 9 + (-1) \times 6 \times 0 = 0$$

**Property IV** If each element of a row or column is multiplied by a constant, the value of the determinant is multiplied by that constant. For example,

$$\begin{vmatrix} 2 & 1 \\ 3 & -1 \end{vmatrix} = -5 \text{ and } \begin{vmatrix} 8 & 4 \\ 3 & -1 \end{vmatrix} = -20 \quad \text{and}$$

$$\begin{vmatrix} 1 & 2 & -1 \\ 3 & -1 & 7 \\ 4 & 6 & 5 \end{vmatrix} = -43 \text{ and } \begin{vmatrix} 1 & 3\sqrt{2} & 4 \\ 2 & -\sqrt{2} & 6 \\ -1 & 7\sqrt{2} & 5 \end{vmatrix} = -43\sqrt{2}$$

**Property V**   The value of a determinant is unchanged if a row or column multiplied by an arbitrary number is added to another row or column. For example,

$$\begin{vmatrix} 2 & 1 \\ 3 & -1 \end{vmatrix} = \begin{vmatrix} 2+1 & 1 \\ 3-1 & -1 \end{vmatrix} = \begin{vmatrix} 2 & 1 \\ 3 & -1 \end{vmatrix} = -5 \quad \text{and}$$

$$\begin{vmatrix} 1 & 3 & 4 \\ 2 & -1 & 6 \\ -1 & 7 & 5 \end{vmatrix} = \begin{vmatrix} 1 & 3 & 4 \\ 2-1 & -1+7 & 6+5 \\ -1 & 7 & 5 \end{vmatrix} = \begin{vmatrix} 1 & 3 & 4 \\ 2 & -1 & 6 \\ -1 & 7 & 5 \end{vmatrix} = -43$$

How are determinants useful? This question can be answered by illustrating how determinants can be used to solve a set of linear equations:

$$x + y + z = 10$$

$$3x + 4y - z = 12$$

$$-x + 2y + 5z = 26 \tag{B.67}$$

This set of equations is solved by first constructing the $3 \times 3$ determinant that is the array of the coefficients of $x$, $y$, and $z$:

$$\mathbf{D}_{coefficients} = \begin{vmatrix} 1 & 1 & 1 \\ 3 & 4 & -1 \\ -1 & 2 & 5 \end{vmatrix} \tag{B.68}$$

Now imagine that we multiply the first column by $x$. This changes the value of the determinant as stated in Property IV:

$$\begin{vmatrix} 1x & 1 & 1 \\ 3x & 4 & -1 \\ -1x & 2 & 5 \end{vmatrix} = x\mathbf{D}_{coefficients} \tag{B.69}$$

We next add to the first column of $x D_{coefficients}$ the second column of $\mathbf{D}_{coefficients}$ multiplied by $y$, and the third column multiplied by $z$. According to Properties IV and V, the value of the determinant is unchanged. Therefore,

$$\mathbf{D}_{c1} = \begin{vmatrix} 1 & 1 & 1 \\ 3 & 4 & -1 \\ -1 & 2 & 5 \end{vmatrix} = \begin{vmatrix} x+y+z & 1 & 1 \\ 3x+4y-z & 4 & -1 \\ -x+2y+5z & 2 & 5 \end{vmatrix} = \begin{vmatrix} 10 & 1 & 1 \\ 12 & 4 & -1 \\ 26 & 2 & 5 \end{vmatrix} = x\mathbf{D}_{coefficients} \tag{B.70}$$

To obtain the third determinant in the previous equation, the individual equations in Equation (B.67) are used to substitute the constants for the algebraic expression in the preceding determinants. From the previous equation, we conclude that

$$x = \frac{\mathbf{D}_{c1}}{\mathbf{D}_{coefficients}} = \frac{\begin{vmatrix} 10 & 1 & 1 \\ 12 & 4 & -1 \\ 26 & 2 & 5 \end{vmatrix}}{\begin{vmatrix} 1 & 1 & 1 \\ 3 & 4 & -1 \\ -1 & 2 & 5 \end{vmatrix}} = 3$$

To determine $y$ and $z$, the exact same procedure can be followed, but we substitute instead in columns 2 and 3, respectively. The first step in each case is to multiply all elements of the second (third) row by $y(z)$. If we do so, we obtain the determinants $\mathbf{D}_{c2}$ and $\mathbf{D}_{c3}$:

$$\mathbf{D}_{c2} = \begin{vmatrix} 1 & 10 & 1 \\ 3 & 12 & -1 \\ -1 & 26 & 5 \end{vmatrix} \quad \text{and} \quad \mathbf{D}_{c3} = \begin{vmatrix} 1 & 1 & 10 \\ 3 & 4 & 12 \\ -1 & 2 & 26 \end{vmatrix}$$

and we conclude that

$$y = \frac{\mathbf{D}_{c2}}{\mathbf{D}_{coefficients}} = \frac{\begin{vmatrix} 1 & 10 & 1 \\ 3 & 12 & -1 \\ -1 & 26 & 5 \\ 1 & 1 & 1 \\ 3 & 4 & -1 \\ -1 & 2 & 5 \end{vmatrix}}{} = 2 \quad \text{and}$$

$$z = \frac{\mathbf{D}_{c3}}{\mathbf{D}_{coefficients}} = \frac{\begin{vmatrix} 1 & 1 & 10 \\ 3 & 4 & 12 \\ -1 & 2 & 26 \\ 1 & 1 & 1 \\ 3 & 4 & -1 \\ -1 & 2 & 5 \end{vmatrix}}{} = 5$$

This method of solving a set of simultaneous linear equations is known as Cramer's method.

If the constants in the set of equations are all zero, as in Equations B.71a and B.71b,

$$x + y + z = 0$$
$$3x + 4y - z = 0 \qquad \qquad \textbf{(B.71a)}$$
$$-x + 2y + 5z = 0$$

$$3x - y + 2z = 0$$
$$-x + y - z = 0$$
$$(1 + \sqrt{2})x + (1 - \sqrt{2})y + \sqrt{2}z = 0 \qquad \textbf{(B.71b)}$$

the determinants $\mathbf{D}_{c1}$, $\mathbf{D}_{c2}$, and $\mathbf{D}_{c3}$ all have the value zero. An obvious set of solutions is $x = 0$, $y = 0$ and $z = 0$. For most problems in physics and chemistry, this set of solutions is not physically meaningful and is referred to as the set of trivial solutions. A set of nontrivial solutions only exists if the equation $\mathbf{D}_{coefficients} = 0$ is satisfied. There is no nontrivial solution to the set of Equation (B.71a) because $\mathbf{D}_{coefficients} \neq 0$. There is a set of nontrivial solutions to the set of Equations (B.71b), because $\mathbf{D}_{coefficients} = 0$ in this case.

Determinants offer a convenient way to calculate the cross product of two vectors, as discussed in Section B.5. The following recipe is used:

$$\mathbf{a} \times \mathbf{b} = \begin{vmatrix} \mathbf{i} & \mathbf{j} & \mathbf{k} \\ a_x & a_y & a_z \\ b_x & b_y & b_z \end{vmatrix} = \mathbf{i}\begin{vmatrix} a_y & a_z \\ b_y & b_z \end{vmatrix} - \mathbf{j}\begin{vmatrix} a_x & a_z \\ b_x & b_z \end{vmatrix} + \mathbf{k}\begin{vmatrix} a_x & a_y \\ b_x & b_y \end{vmatrix}$$
$$= (a_y b_z - a_z b_y)\mathbf{i} + (a_z b_x - a_x b_z)\mathbf{j} + (a_x b_y - a_y b_x)\mathbf{k} \quad \textbf{(B.72)}$$

Note that by referring to Property II, you can show that $\mathbf{b} \times \mathbf{a} = -\mathbf{a} \times \mathbf{b}$.

# B.8 Working with Matrices

Physical chemists find widespread use for matrices. Matrices can be used to represent symmetry operations in the application of group theory to problems concerning molecular symmetry. They can also be used to obtain the energies of molecular orbitals formed through the linear combination of atomic orbitals. We next illustrate the use of matrices for representing the rotation operation that is frequently encountered in molecular symmetry considerations.

Consider the rotation of a three-dimensional vector about the $z$ axis. Because the $z$ component of the vector is unaffected by this operation, we need only consider the effect of the rotation operation on the two-dimensional vector formed by the projection of the

three-dimensional vector on the $xy$ plane. The transformation can be represented by $(x_1, y_1, z_1) \rightarrow (x_2, y_2, z_1)$. The effect of the operation on the $x$ and $y$ components of the vector is shown in Figure B.14.

Next, relationships are derived among $(x_1, y_1, z_1)$, $(x_2, y_2, z_1)$, the magnitude of the radius vector $r$, and the angles $\alpha$ and $\beta$, based on the preceding figure. The magnitude of the radius vector $r$ is

$$r = \sqrt{x_1^2 + y_1^2 + z_1^2} = \sqrt{x_2^2 + y_2^2 + z_1^2} \tag{B.73}$$

Although the values of $x$ and $y$ change in the rotation, $r$ is unaffected by this operation. The relationships between $x$, $y$, $r$, $\alpha$, and $\beta$ are given by

$$\theta = 180° - \alpha - \beta$$
$$x_1 = r \cos \alpha, \qquad y_1 = r \sin \alpha$$
$$x_2 = -r \cos \beta, \qquad y_1 = r \sin \beta \tag{B.74}$$

In the following discussion, these identities are used:

$$\cos(\alpha \pm \beta) = \cos \alpha \cos \beta \pm \sin \alpha \sin \beta$$
$$\sin(\alpha \pm \beta) = \sin \alpha \cos \beta \pm \cos \alpha \sin \beta \tag{B.75}$$

From Figure B.14, the following relationship between $x_2$ and $x_1$ and $y_1$ can be derived using the identities of Equation (B.75):

$$\begin{aligned}
x_2 &= -r \cos \beta = -r \cos(180° - \alpha - \theta) \\
&= r \sin 180° \sin(-\theta - \alpha) - r \cos 180° \cos(-\theta - \alpha) \\
&= r \cos(-\theta - \alpha) = r \cos(\theta + \alpha) = r \cos \theta \cos \alpha - r \sin \theta \sin \alpha \\
&= x_1 \cos \theta - y_1 \sin \theta
\end{aligned} \tag{B.76}$$

Using the same procedure, the following relationship between $y_2$ and $x_1$ and $y_1$ can be derived:

$$y_2 = x_1 \sin \theta + y_1 \cos \theta \tag{B.77}$$

Next, these results are combined to write the following equations relating $x_2$, $y_2$, and $z_2$ to $x_1$, $y_1$, and $z_1$:

$$x_2 = x_1 \cos \theta - y_1 \sin \theta$$
$$y_2 = x_1 \sin \theta + y_1 \cos \theta$$
$$z_2 = 0x_1 + 0y_1 + z_1 \tag{B.78}$$

At this point, the concept of a matrix can be introduced. An $n \times m$ matrix is an array of numbers, functions, or operators that can undergo mathematical operations such as addition and multiplication with one another. The operation of interest to us in considering rotation about the $z$ axis is matrix multiplication. We illustrate how matrices, which are designated in bold script, such as $\mathbf{A}$, are multiplied using $2 \times 2$ matrices as an example.

$$\mathbf{AB} = \begin{pmatrix} a_{11} & a_{12} \\ a_{21} & a_{22} \end{pmatrix} \begin{pmatrix} b_{11} & b_{12} \\ b_{21} & b_{22} \end{pmatrix} = \begin{pmatrix} a_{11}b_{11} + a_{12}b_{21} & a_{11}b_{12} + a_{12}b_{22} \\ a_{21}b_{11} + a_{22}b_{21} & a_{21}b_{12} + a_{22}b_{22} \end{pmatrix} \tag{B.79}$$

Using numerical examples,

$$\begin{pmatrix} 2 & 1 \\ -3 & 4 \end{pmatrix} \begin{pmatrix} 1 & 6 \\ 2 & -1 \end{pmatrix} = \begin{pmatrix} 4 & 11 \\ 5 & -22 \end{pmatrix} \quad \text{and} \quad \begin{pmatrix} 1 & 6 \\ 2 & -1 \end{pmatrix} \begin{pmatrix} 1 \\ -1 \end{pmatrix} = \begin{pmatrix} -5 \\ 3 \end{pmatrix}$$

Now consider the initial and final coordinates $(x_1, y_1, z_1)$ and $(x_2, y_2, z_1)$ as $3 \times 1$ matrices $(x_1, y_1, z_1)$ and $(x_2, y_2, z_1)$. In that case, the set of simultaneous equations of Equation (B.78) can be written as

$$\begin{pmatrix} x_2 \\ y_2 \\ z_2 \end{pmatrix} = \begin{pmatrix} \cos \theta & -\sin \theta & 0 \\ \sin \theta & \cos \theta & 0 \\ 0 & 0 & 1 \end{pmatrix} \begin{pmatrix} x_1 \\ y_1 \\ z_1 \end{pmatrix} \tag{B.80}$$
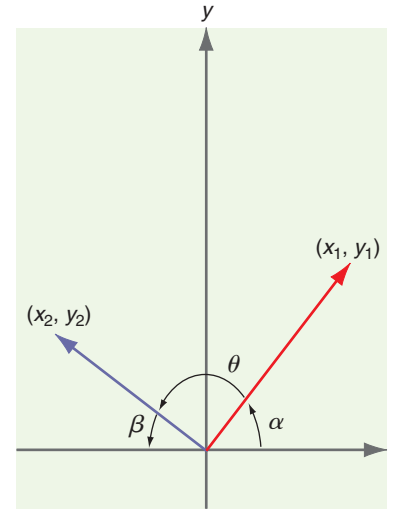


**FIGURE B.14**

We see that we can represent the operator for rotation about the $z$ axis, $R_z$, as the following $3 \times 3$ matrix:

$$\mathbf{R_z} = \begin{pmatrix} \cos\theta & -\sin\theta & 0 \\ \sin\theta & \cos\theta & 0 \\ 0 & 0 & 1 \end{pmatrix} \tag{B.81}$$

The rotation operator for 180° and 120° rotation can be obtained by evaluating the sine and cosine functions at the appropriate values of $\theta$. These rotation operators have the form

$$\begin{pmatrix} -1 & 0 & 0 \\ 0 & -1 & 0 \\ 0 & 0 & 1 \end{pmatrix} \text{ and } \begin{pmatrix} 1/2 & -\sqrt{3}/2 & 0 \\ \sqrt{3}/2 & 1/2 & 0 \\ 0 & 0 & 1 \end{pmatrix}, \text{ respectively} \tag{B.82}$$

One special matrix, the identity matrix designated $\mathbf{I}$, deserves additional mention. The identity matrix corresponds to an operation in which nothing is changed. The matrix that corresponds to the transformation $(x_1, y_1, z_1) \rightarrow (x_2, y_2, z_2)$ expressed in equation form as

$$\begin{aligned} x_2 &= x_1 + 0y_1 + 0z_1 \\ y_2 &= 0x_1 + y_1 + 0z_1 \\ z_2 &= 0x_1 + 0y_1 + z_1 \end{aligned} \tag{B.83}$$

is the identity matrix

$$\mathbf{I} = \begin{pmatrix} 1 & 0 & 0 \\ 0 & 1 & 0 \\ 0 & 0 & 1 \end{pmatrix}$$

The identity matrix is an example of a diagonal matrix. It has this name because only the diagonal elements are nonzero. In the identity matrix of order $n \times n$ all diagonal elements have the value one.

The operation that results from the sequential operation of two individual operations represented by matrices $\mathbf{A}$ and $\mathbf{B}$ is the products of the matrices: $\mathbf{C} = \mathbf{AB}$. An interesting case illustrating this relationship is counterclockwise rotation through an angle $\theta$ followed by clockwise rotation through the same angle, which corresponds to rotation by $-\theta$. Because $\cos(-\theta) = \cos\theta$ and $\sin\theta = -\sin\theta$, the rotation matrix for $-\theta$ must be

$$\mathbf{R_{-z}} = \begin{pmatrix} \cos\theta & \sin\theta & 0 \\ -\sin\theta & \cos\theta & 0 \\ 0 & 0 & 1 \end{pmatrix} \tag{B.84}$$

Because the sequential operations leave the vector unchanged, it must be the case that $\mathbf{R_z R_{-z}} = \mathbf{R_{-z} R_z} = \mathbf{I}$. We verify here that the first of these relations is obeyed:

$$\begin{aligned} \mathbf{R_z R_{-z}} &= \begin{pmatrix} \cos\theta & -\sin\theta & 0 \\ \sin\theta & \cos\theta & 0 \\ 0 & 0 & 1 \end{pmatrix}\begin{pmatrix} \cos\theta & \sin\theta & 0 \\ -\sin\theta & \cos\theta & 0 \\ 0 & 0 & 1 \end{pmatrix} \\ &= \begin{pmatrix} \cos^2\theta + \sin^2\theta + 0 & \sin\theta\cos\theta - \sin\theta\cos\theta + 0 & 0 \\ \sin\theta\cos\theta - \sin\theta\cos\theta + 0 & \cos^2\theta + \sin^2\theta + 0 & 0 \\ 0 & 0 & 1 \end{pmatrix} \\ &= \begin{pmatrix} 1 & 0 & 0 \\ 0 & 1 & 0 \\ 0 & 0 & 1 \end{pmatrix} \end{aligned} \tag{B.85}$$

Any matrix $\mathbf{B}$ that satisfies the relationship $\mathbf{AB} = \mathbf{BA} = \mathbf{I}$ is called the inverse matrix of $\mathbf{A}$ and is designated $\mathbf{A}^{-1}$. Inverse matrices play an important role in finding the energies of a set of molecular orbitals that is a linear combination of atomic orbitals.

# Answers to Selected End-of-Chapter Problems

Numerical answers to problems are included here. Complete solutions to selected problems can be found in the *Student's Solutions Manual*.

## Chapter 1

**P1.1**  $1.27 \times 10^6$

**P1.2**  $2.33 \times 10^3$ L

**P1.3**  26.9 bar

**P1.4**  $x_{CO_2} = 0.235$, $x_{H_2O} = 0.314$, $x_{O_2} = 0.451$

**P1.5**  32.0%

**P1.6**  $1.11 \times 10^{21}$

**P1.7**  8.37 g

**P1.8**  37.9 L

**P1.9**  a.  $N_2$ 67.8%, $O_2$ 18.2%, Ar 0.869%, and $H_2O$ 13.1%

  b.  20.6 L

  c.  0.981

**P1.10**  $3.7 \times 10^3$

**P1.11**  34.6 bar

**P1.12**  $3.66 \times 10^5$ Pa

**P1.13**  $x_{H_2}^\circ = 0.366$; $x_{O_2}^\circ = 0.634$

**P1.14**  0.280 moles

**P1.16**  18.6 L

**P1.17**  0.27

**P1.18**  a.  $2.18 \times 10^{-2}$ bar

  b.  $x_{O_2} = 0.0136$, $x_{N_2} = 0.805$, $x_{CO} = 0.181$

  $P_{O_2} = 2.97 \times 10^{-4}$ bar, $P_{N_2} = 1.76 \times 10^{-2}$ bar

  $P_{CO} = 3.94 \times 10^{-3}$ bar

**P1.19**  21.4 bar

**P1.20**  a.  $3.86 \times 10^4$ Pa

  b.  $6.68 \times 10^4$ without mixing

  $1.49 \times 10^5$ with mixing

**P1.21**  0.149 L

**P1.22**  $2.20 \times 10^{-2}$ L

**P1.23**  $7.95 \times 10^4$ Pa

**P1.24**  91

**P1.25**  $2.69 \times 10^{25}$

**P1.26**  a.  $P_{H_2} = 2.48 \times 10^6$ Pa; $P_{O_2} = 1.52 \times 10^5$ Pa

  $P_{total} = 2.64 \times 10^6$ Pa

  mol % $H_2 = 94.2\%$; mol % $O_2 = 5.78\%$

  b.  $P_{N_2} = 1.34 \times 10^5$ Pa; $P_{O_2} = 8.23 \times 10^4$ Pa

  $P_{total} = 2.17 \times 10^5$ Pa

  mol % $N_2 = 62.0\%$, mol % $O_2 = 38.0\%$

  c.  $P_{NH_3} = 1.63 \times 10^5$ Pa; $P_{CH_4} = 2.06 \times 10^5$ Pa

  $P_{total} = 3.69 \times 10^5$ Pa

  mol % $NH_3 = 44.2\%$, mol % $CH_4 = 55.8\%$

**P1.27**  0.557

**P1.28**  $1.36 \times 10^3$ K

**P1.29**  34.8 L

**P1.30**  0.0040

**P1.31**  $x_{O_2} = 0.295$,  $x_{H_2} = 0.705$

**P1.32**  0.0919 atm mol$^{-1}$ °C$^{-1}$, 265.0 °C

**P1.33**  2.37 L

**P1.34**  $V_{N_2} = 0.0521$ L, $V_{CO_2} = 0.312$ L

  $V_{total} = 0.364$ L

**P1.35**  $6.44 \times 10^8$ L

**P1.36**  77.2 amu

## Chapter 2

**P2.1**  $7.82 \times 10^3$ J, 0.642 m

**P2.2**  $q = 0$, $w = \Delta U = 838$ J, $\Delta H = 1.40 \times 10^3$ J

**P2.3**  a.  $w = -754$ J, $\Delta U$ and $\Delta H = 0$, $q = -w = 754$ J

  b.  $\Delta U = -1.68 \times 10^3$ J,

  $w = 0, q = \Delta U = -1.68 \times 10^3$ J

  $\Delta H = -2.81 \times 10^3$ J

  $\Delta U_{total} = -1.68 \times 10^3$ J

  $w_{total} = -754$ J, $q_{total} = -930.$ J

  $\Delta H_{total} = -2.81 \times 10^3$ J

**P2.4**  15 g

**P2.5**  30. m

**P2.6**  a.  $-2.64 \times 10^3$ J,   b.  $-4.55 \times 10^3$ J

**P2.7**  $q = 0$; $\Delta U = w = -4.90 \times 10^3$J, $\Delta H = -8.17 \times 10^3$ J

**P2.8**  $w = -4.68 \times 10^3$ J, 1.06 bar

**P2.9**  $w = -0.172$ J

  $q = 34.6 \times 10^3$ J

  $\Delta H = 34.6 \times 10^3$ J

  $\Delta U = 34.6 \times 10^3$ J

**P2.10**  0.46 J

**P2.11**  a.  418 K, $w = 4.63 \times 10^3$ J

  b.  954 K, $30.4 \times 10^3$ J

**P2.12**  $q = 0$, $\Delta U = w = -1300.$ J, $\Delta H = -2.17 \times 10^3$ J

**P2.13**  322 K

**P2.14**  a.  $-3.76 \times 10^3$ J,   b.  $-1.82 \times 10^3$ J

**P2.15**  $134.0 \times 10^3$ Pa, $129.7 \times 10^3$ Pa

**P2.16**  $1.12 \times 10^3$ K, $q = 0$, $w = \Delta U = 22.7 \times 10^3$ J

  $\Delta H = 3.79 \times 10^4$ J

**P2.17**  301 K

**P2.19**  step 1: 0, step 2: $-22.0 \times 10^3$ J, step 3: $8.90 \times 10^3$ J,

  cycle: $-13.1 \times 10^3$ J

**P2.20** $w = 3.58 \times 10^3$ J

$q = 0$

$\Delta H = 5.00 \times 10^3$ J

$\Delta U = 3.58 \times 10^3$ J

**P2.21** $-35.6 \times 10^3$ J

**P2.22** $T_f = 168$ K

$q = 0$

$w = \Delta U = -8.40 \times 10^3$ J

$\Delta H = -10.8 \times 10^3$ J

**P2.23** $q = 0$

a. $T_f = 213$ K, b. 248 K

a. $w = -2.66 \times 10^3$ J, b. $-3.17 \times 10^3$ J

a. $\Delta H = -4.44 \times 10^3$ J, b. $-4.44 \times 10^3$ J

a. $\Delta U = -2.66 \times 10^3$ J, b. $-3.17 \times 10^3$ J

**P2.24** a. $-17.393 \times 10^3$ J,

b. $-17.675 \times 10^3$ J, $-1.57\%$

**P2.25** 0.60 K

**P2.26** a. $\Delta U = \Delta H = 0$, $w = -q = -1.27 \times 10^3$ J

b. $w = 0$,

$q = \Delta U = -1.14 \times 10^3$ J, $\Delta H = -1.91 \times 10^3$ J

For the overall process, $w = -1.27 \times 10^3$ J,

$q = 130.$ J, $\Delta U = -1.14 \times 10^3$ J, and

$\Delta H = -1.91 \times 10^3$ J

**P2.27** a. $P_1 = 5.83 \times 10^5$ Pa, $w = -6.44 \times 10^3$ J

$\Delta U = 0$ and $\Delta H = 0$

$q = -w = 6.44 \times 10^3$ J

b. $P_2 = 7.35 \times 10^5$ Pa, $\Delta U = 2.29 \times 10^3$ J

$w = 0$, $q = 2.29 \times 10^3$ J

$\Delta H = 3.81 \times 10^3$ J

overall:

$q = 8.73 \times 10^3$ J, $w = -6.44 \times 10^3$ J

$\Delta U = 2.29 \times 10^3$ J, $\Delta H = 3.81 \times 10^3$ J

**P2.28** $q = 0$, $\Delta U = w = -4.90 \times 10^3$ J, $\Delta H = -8.16 \times 10^3$ J

**P2.29** 408 K

**P2.30** $\Delta U = -1.77 \times 10^3$ J, $\Delta H = q_P = -2.96 \times 10^3$ J

$w = 1.18 \times 10^3$ J

**P2.31** 5.6 K

**P2.32** $18.9 \times 10^3$ J, $7.30 \times 10^3$ J, 0

**P2.33** 251 K

**P2.34** a. $-19.2$ K

b. 0 K

c. 18.0 K

**P2.35** a. 158 K b. 204 K

**P2.36** $-1190$ J

**P2.37** $\Delta H = 5.88 \times 10^4$ J, $\Delta U = 4.78 \times 10^4$ J

**P2.38** $w = 0$, $\Delta U = q = 1.31 \times 10^4$ J, $\Delta H = 1.83 \times 10^4$ J

**P2.39** c. 984 kg, $1.38 \times 10^3$ kg

**P2.41** 0.35 kg

**P2.42** $2.2 \times 10^{-19}$ J

**P2.43** $w = 1.22 \times 10^4$ J, $\Delta U = 0$ and $\Delta H = 0$

$q = -1.22 \times 10^4$ J

**P2.44** 0.99 J

# Chapter 3

**P3.3** $\Delta H = q = 8.58 \times 10^4$ J

$\Delta U = 7.18 \times 10^4$ J;

$w = -1.39 \times 10^4$ J

**P3.5** 292 K

**P3.6** 93.4 bar

**P3.8** 369 K

**P3.9** $1.78 \times 10^3$ J, 0

**P3.11** 314 K

**P3.12** $q = \Delta H = 8.51 \times 10^4$ J;

$w = -8.85 \times 10^3$ J

$\Delta U = 7.62 \times 10^4$ J

# Chapter 4

**P4.1** SiF 596 kJ mol$^{-1}$, 593 kJ mol$^{-1}$

SiCl 398 kJ mol$^{-1}$, 396 kJ mol$^{-1}$

CF 489 kJ mol$^{-1}$, 487 kJ mol$^{-1}$

NF 279 kJ mol$^{-1}$, 276 kJ mol$^{-1}$

OF 215 kJ mol$^{-1}$, 213 kJ mol$^{-1}$

HF 568 kJ mol$^{-1}$, 565 kJ mol$^{-1}$

**P4.2** $-49.39$ kJ mol$^{-1}$

**P4.3** $\Delta U_f - 361$ kJ mol$^{-1}$; $\Delta H_f^\circ = -362$ kJ mol$^{-1}$

**P4.4** 91.7 kJ mol$^{-1}$

**P4.5** $\Delta H = 5.80 \times 10^{17}$ kJ yr$^{-1}$

**P4.7** a. 416 kJ mol$^{-1}$, 413 kJ mol$^{-1}$

b. 329 kJ mol$^{-1}$, 329 kJ mol$^{-1}$

c. 589 kJ mol$^{-1}$, 588 kJ mol$^{-1}$

**P4.8** a. 428.22 kJ mol$^{-1}$, 425.74 kJ mol$^{-1}$

b. 926.98 kJ mol$^{-1}$, 922.02 kJ mol$^{-1}$

c. 498.76 kJ mol$^{-1}$, 498.28 kJ mol$^{-1}$

**P4.9** $-182.9$ kJ mol$^{-1}$

**P4.11** 134.68 kJ mol$^{-1}$

**P4.12** a. $-73.0$ kJ mol$^{-1}$;

b. $-804$ kJ mol$^{-1}$

**P4.13** $\Delta H_{combustion} = -3268$ kJ mol$^{-1}$

$\Delta U_{reaction} = -3264$ kJ mol$^{-1}$; 0.0122

**P4.14**   $-59.8$ kJ mol$^{-1}$

**P4.15**   $6.64 \times 10^3$ J °C$^{-1}$

**P4.16**   $\Delta H = 7.89 \times 10^{17}$ kJ yr$^{-1}$

**P4.17**   a.   $-1815$ kJ mol$^{-1}$, $-1817.5$ kJ mol$^{-1}$

   b.   $-116.2$ kJ mol$^{-1}$, $-113.7$ kJ mol$^{-1}$

   c.   62.6 kJ mol$^{-1}$, 52.7 kJ mol$^{-1}$

   d.   $-111.6$ kJ mol$^{-1}$, $-111.6$ kJ mol$^{-1}$

   e.   205.9 kJ mol$^{-1}$, 200.9 kJ mol$^{-1}$

   f.   $-172.8$ kJ mol$^{-1}$, $-167.8$ kJ mol$^{-1}$

**P4.18**   $-2.4 \times 10^3$ J mol$^{-1}$, 5.1%

**P4.19**   a.   696.8 kJ mol$^{-1}$

   b.   $-1165.1$ kJ mol$^{-1}$

   c.   $-816.7$ kJ mol$^{-1}$

**P4.20**   a.   $\Delta H_{combustion} = -1.364 \times 10^3$ kJ mol$^{-1}$

   b.   $\Delta H_f^\circ = -280.0.$ kJ mol$^{-1}$

**P4.21**   $-812.2$ kJ mol$^{-1}$

**P4.22**   a.   $\Delta U = \Delta H = -5.635 \times 10^3$ kJ mol$^{-1}$

      $\Delta H = -5.635 \times 10^3$ kJ mol$^{-1}$

   b.   $\Delta H_f^\circ = -2.231 \times 10^3$ kJ mol$^{-1}$

   c.   $1.19 \times 10^3$ J K$^{-1}$

**P4.23**   $-1811$ kJ mol$^{-1}$

**P4.24**   $-20.6$ kJ mol$^{-1}$, $-178.2$ kJ mol$^{-1}$

**P4.25**   180 kJ mol$^{-1}$

**P4.26**   $-393.6$ kJ mol$^{-1}$

**P4.27**   15.3 kJ mol$^{-1}$, 13.1%

**P4.28**   $-266.3$ kJ mol$^{-1}$, $-824.2$ kJ mol$^{-1}$

**P4.29**   415.8 kJ mol$^{-1}$, 1.2%

**P4.30**   $-134$ kJ mol$^{-1}$, $\approx 0\%$

**P4.31**   49.6 kJ mol$^{-1}$

**P4.32**   356.5 kJ mol$^{-1}$

**P4.33**   49 g

**P4.34**   1.8

**P4.35**   6.5°C

# Chapter 5

**P5.1**   At 298.15 K,

   $\Delta S = -262.4$ J K$^{-1}$ mol$^{-1}$

   $\Delta H = 2803$ kJ mol$^{-1}$

   $\Delta S_{surroundings} = -9.40 \times 10^3$ J K$^{-1}$ mol$^{-1}$

   $\Delta S_{universe} = -9.66 \times 10^3$ J K$^{-1}$ mol$^{-1}$

   At 310. K,

   $\Delta S = -273.4$ J K$^{-1}$ mol$^{-1}$

   $\Delta H = 2799$ kJ mol$^{-1}$

   $\Delta S_{surroundings} = -9.03 \times 10^3$ J K$^{-1}$ mol$^{-1}$

   $\Delta S_{universe} = -9.30 \times 10^3$ J K$^{-1}$ mol$^{-1}$

**P5.2**   a.   0.627,      b.   0.398,      c.   110.7

**P5.3**   $1.57 \times 10^6$ g per day

**P5.4**   $4.85 \times 10^8$ J

**P5.5**   57.2 J K$^{-1}$

**P5.6**   a.   $w = -6.83 \times 10^3$ J, $\Delta U = 10.2 \times 10^3$ J

      $q = \Delta H = 17.1 \times 10^3$ J, $\Delta S = 36.4$ J K$^{-1}$

   b.   $w = 0$, $\Delta U = q = 10.2 \times 10^3$ J

      $\Delta H = 17.1 \times 10^3$ J, $\Delta S = 21.8$ J K$^{-1}$

   c.   $\Delta U = \Delta H = 0$;

      $w_{reversible} = -q = -6.37 \times 10^3$ J

      $\Delta S = 20.6$ J K$^{-1}$

**P5.7**   a.   $V_c = 113$ L;   $V_d = 33.0$ L

   b.   $w_{ab} = -9.44 \times 10^3$ J, $w_{bc} = -11.2 \times 10^3$ J

      $w_{cd} = 3.96 \times 10^3$ J, $w_{da} = 11.2 \times 10^3$ J

      $w_{total} = -5.49 \times 10^3$ J

   c.   0.581, 1.72 kJ

**P5.8**   $\Delta S = 256$ kJ k$^{-1}$ week$^{-1}$

**P5.9**   a.   $\Delta S_{surroundings} = 0$, $\Delta S = 0$, $\Delta S_{total} = 0$. not spontaneous.

   b.   $\Delta S = 30.9$ J K$^{-1}$, $\Delta S_{surroundings} = 0$

      $\Delta S_{total} = 30.9$ J K$^{-1}$, spontaneous.

   c.   $\Delta S = 30.9$ J K$^{-1}$

      $\Delta S_{surroundings} = -30.9$ J K$^{-1}$

      $\Delta S_{total} = 0$, not spontaneous

**P5.10**   0.538, 0.661

**P5.11**   $\Delta U = -17.9 \times 10^3$ J, $\Delta H = -25.0 \times 10^3$ J

   $\Delta S = -80.5$ J K$^{-1}$

**P5.12**   27.9 J K$^{-1}$

**P5.13**   $-0.0765$ J K$^{-1}$, $-0.0765$ J K$^{-1}$

**P5.14**   $-191.2$ J K$^{-1}$ mol$^{-1}$

**P5.15**   $-2.5$ K

**P5.16**   a.   $q = 0$, $\Delta U = w = -4.96 \times 10^3$ J

      $\Delta H = -8.26 \times 10^3$ J, $\Delta S = 0$

   b.   $q = 0$

      $\Delta U = w = -3.72 \times 10^3$ J, $\Delta H = -6.19 \times 10^3$ J

      $\Delta S = 10.1$ J K$^{-1}$

   c.   $w = 0$, $\Delta U = \Delta H = 0$, $q = 0$;

      $\Delta S = 34.3$ J K$^{-1}$

**P5.17**   2.4

**P5.18**   $a \rightarrow b$: $\Delta U = \Delta H = 0$, $q = -w = 9.44 \times 10^3$ J

   $b \rightarrow c$: $\Delta U = w = -11.2 \times 10^3$ J, $q = 0$

   $\Delta H = -15.6 \times 10^3$ J

   $c \rightarrow d$: $\Delta U = \Delta H = 0$, $q = -w = -3.96 \times 10^3$ J

   $d \rightarrow a$: $\Delta U = w = 11.2 \times 10^3$ J, $q = 0$

   $\Delta H = 15.6 \times 10^3$ J

   $q_{total} = 5.49 \times 10^3$ J $= -w_{total}$

   $\Delta U_{total} = \Delta H_{total} = 0$

**P5.19** a. $1.0 \text{ J K}^{-1} \text{ mol}^{-1}$, b. $3.14 \text{ J K}^{-1} \text{ mol}^{-1}$

    c. $\Delta S_{transition} = 8.24 \text{ J K}^{-1} \text{ mol}^{-1}$

    $\Delta S_{fusion} = 25.1 \text{ J K}^{-1} \text{ mol}^{-1}$

**P5.20** $\Delta U = 49.7 \text{ J}$, $w = -5.55 \times 10^3 \text{ J}$

    $\Delta H = 85.2 \text{ J}$, $q = 5.59 \times 10^3 \text{ J}$, $\Delta S = 18.8 \text{ J K}^{-1}$

**P5.21** $104.5 \text{ J K}^{-1} \text{ mol}^{-1}$

**P5.22** $\Delta H = 3.75 \text{ kJ}$, $\Delta S = 12.1 \text{ J K}^{-1}$

**P5.23** a. $105 \text{ J K}^{-1}$,      b. $74.8 \text{ J K}^{-1}$

**P5.25** $50.1 \text{ J K}^{-1} \text{ mol}^{-1}$

**P5.26** $3.0 \text{ J K}^{-1}$

**P5.27** $\Delta S = 175 \text{ J K}^{-1} \text{ mol}^{-1}$

    $\Delta S_{suroundings} = 225 \text{ J K}^{-1} \text{ mol}^{-1}$

    and $\Delta S_{total} = 400. \text{ J K}^{-1} \text{ mol}^{-1}$

**P5.28** $\Delta S = 53.0 \text{ J K}^{-1}$, $\Delta S_{suroundings} = -143 \text{ J K}^{-1}$

    and $\Delta S_{universe} = -90.0 \text{ J K}^{-1}$

**P5.29** $\Delta S = -21.48 \text{ J K}^{-1}$, $\Delta S_{surroundings} = 21.78 \text{ J K}^{-1}$

    $\Delta S_{total} = 0.30 \text{ J K}^{-1}$

**P5.30** $\Delta S = -1.66 \times 10^6 \text{ J K}^{-1}$

    $\Delta S_{suroundings} = 2.03 \times 10^6 \text{ J K}^{-1}$

    and $\Delta S_{universe} = 3.72 \times 10^5 \text{ J K}^{-1}$

**P5.31** $135.1 \text{ J K}^{-1} \text{ mol}$

**P5.32** a. $\Delta S_{total} = \Delta S + \Delta S_{surroundings} = 0 + 0 = 0$. not spontaneous.

    b. $\Delta S_{total} = \Delta S + \Delta S_{surroundings} = 10.1 \text{ J K}^{-1} + 0 = 10.1 \text{ J K}^{-1}$. spontaneous.

**P5.33** $773 \text{ J s}^{-1}$

**P5.34** $a \rightarrow b$: $\Delta S = -\Delta S_{surroundings} = 12.8 \text{ J K}^{-1}$

    $\Delta S_{total} = 0$

    $b \rightarrow c$: $\Delta S = -\Delta S_{surroundings} = 0$, $\Delta S_{total} = 0$

    $c \rightarrow d$: $\Delta S = -\Delta S_{surroundings} = -12.8 \text{ J K}^{-1}$

    $\Delta S_{total} = 0$

    $d \rightarrow a$: $\Delta S = -\Delta S_{surroundings} = 0$, $\Delta S_{total} = 0$ to within the round-off error.

    For the cycle, $\Delta S = \Delta S_{surroundings} = \Delta S_{total} = 0$ to within the round-off error.

**P5.35** $\Delta H = 5.65 \times 10^3 \text{ J}$, $\Delta S = 17.9 \text{ J K}^{-1}$

**P5.36** $\Delta S_{surroundings} = -20.6 \text{ J K}^{-1}$

    $\Delta S_{total} = 0$, not spontaneous

**P5.37** $206 \text{ J K}^{-1}$

**P5.38** $32.6 \text{ J K}^{-1} \text{ mol}^{-1}$

**P5.39** a. $2.71 \text{ J K}^{-1}$;      b. $154 \text{ J K}^{-1}$

**P5.40** $26.0 \text{ J K}^{-1}$

**P5.41** $135.2 \text{ J K}^{-1} \text{ mol}^{-1}$

**P5.42** $19.4 \text{ m}^2$

**P5.43** a. $q = 0$

    $\Delta U = w = -3.56 \times 10^3 \text{ J}$, $\Delta H = -4.98 \times 10^3 \text{ J}$

    $\Delta S = 0$, $\Delta S_{surroundings} = 0$, $\Delta S_{total} = 0$.

    b. $w = 0$, $\Delta U = q = 3.56 \times 10^3 \text{ J}$, $\Delta H = 4.98 \times 10^3 \text{ J}$

    $\Delta S = 16.0 \text{ J K}^{-1}$

    c. $\Delta H = \Delta U = 0$, $w = -q = 4.40 \times 10^3 \text{ J}$

    $\Delta S = -16.0 \text{ J K}^{-1}$

    For the cycle,

    $w_{cycle} = 840. \text{ J}$, $q_{cycle} = -840. \text{ J}$

    $\Delta U_{cycle} = 0$, $\Delta H_{cycle} = 0$;

    $\Delta S_{cycle} = 0$

**P5.44** $\Delta S = 620 \text{ J K}^{-1} \text{ mol}^{-1}$

**P5.45** a. $108.5 \text{ J mol}^{-1} \text{ K}^{-1}$

    b. $25.7 \times 10^3 \text{ J mol}^{-1}$

# Chapter 6

**P6.1** $\Delta G_{combustion} = -3203 \times 10^3 \text{ kJ mol}^{-1}$

    $\Delta A_{combustion} = -3199 \times 10^3 \text{ kJ mol}^{-1}$

**P6.2** $2.29 \times 10^6$ at 298 K and $2.37 \times 10^2$ at 490. K

**P6.3** b. $2.11 \times 10^{-2}$

    c. 1.96 moles of $N_2(g)$, 3.88 moles of $H_2(g)$, and 1.58 moles of $NH_3(g)$

**P6.4** a. 0.379 at 700. K, 1.28 at 800. K

    b. $\Delta H_R^\circ = 56.7 \times 10^3 \text{ J mol}^{-1}$;

    $\Delta G_R^\circ (298.15 \text{ K}) = 35.0 \times 10^3 \text{ J mol}^{-1}$

**P6.5** c. $4.0 \times 10^3$ bar

**P6.6** a. 0.141,      b. $2.01 \times 10^{-18}$

    c. $101 \text{ kJ mol}^{-1}$

**P6.7** graphite $173 \text{ J mol}^{-1}$, He: $14.3 \text{ kJ mol}^{-1}$, 82.9

**P6.8** a. $15.0 \text{ kJ mol}^{-1}$

    b. $2.97 \times 10^{-3}$

**P6.9** b. 0.55,     d. 0.72

**P6.10** $4.76 \times 10^6$

**P6.11** a. 0.464; $\Delta G_R^\circ = 7.28 \times 10^3 \text{ J mol}^{-1}$

    b. $-28.6 \text{ kJ mol}^{-1}$

**P6.12** $132.9 \text{ kJ mol}^{-1}$

**P6.13** a. $2.10 \times 10^{-2}$,    b. 0.0969 bar

**P6.14** $8.56 \times 10^3 \text{ J}$

**P6.15** a. $275 \text{ kJ mol}^{-1}$

    b. $5.42 \times 10^{-49}$

**P6.16** $\Delta A = w_{rev} = -0.015 \text{ J}$

    $\Delta S = 1.61 \times 10^{-4} \text{ J K}^{-1}$

    $\Delta U = -0.035 \text{ J}$

**P6.17** $-65.0 \times 10^3 \text{ J mol}^{-1}$

**P6.18** $-40.99 \text{ kJ g}^{-1}$, $-117.6 \text{ kJ g}^{-1}$

**P6.19** $1.2 \times 10^3 \text{ K}$, 0.43 Torr

**P6.20** $-9.54 \times 10^3 \text{ J}$

**P6.21** c. 0.0820, 0.0273,     d. $-1.49\%$

**P6.22**   $-17.9 \times 10^3$ J, 51.4 J K$^{-1}$

**P6.23**   178 g

**P6.24**   a.   $\Delta H_R^\circ = -19.0$ kJ mol$^{-1}$

   $\Delta G_R^\circ (700.°C) = 3.03$ kJ mol$^{-1}$

   $\Delta S_R^\circ (700.°C) = -22.6$ J mol$^{-1}$ K$^{-1}$

   b.   $x_{CO_2} = 0.408, \quad x_{CO} = 0.592$

**P6.27**   9.00, $-58.8 \times 10^3$ J mol$^{-1}$

**P6.28**   539 K, 1.03 $\times$ 10$^4$

**P6.29**   $-215.2 \times 10^3$ J mol$^{-1}$, $-5.8\%$

**P6.30**   0.241

**P6.31**   $-1363$ kJ mol$^{-1}$, $-1364$ kJ mol$^{-1}$

**P6.32**   $-257.2 \times 10^3$ J mol$^{-1}$ at 298.15 K;

   $-231.1 \times 10^3$ J mol$^{-1}$ at 600. K

**P6.33**   a.   $-11.7 \times 10^3$ J, $-11.7 \times 10^3$ J

   b.   same as a.

**P6.34**   a.   $-34.3$ kJ;   b. $-47.3$ kJ;

   c.   $-13.0$ kJ

**P6.35**   b.   23.3 Pa;

   c.   39.5 Pa

**P6.36**   c.   $9.32 \times 10^{-33}$ at 600. K and $3.30 \times 10^{-29}$ at 700. K,

   d.   $9.32 \times 10^{-33}$ for 1.00 bar and

   $2.10 \times 10^{-32}$ for 2.00 bar

**P6.37**   28.0 kJ mol$^{-1}$

**P6.38**   a.   $K_P (700. K) = 3.85, K_P (800. K) = 1.56$

   b.   $\Delta H_R^\circ = -42.0$ kJ mol$^{-1}$
   $\Delta G_R^\circ (700 K) = -7.85$ kJ mol$^{-1}$
   $\Delta G_R^\circ (800 K) = -2.97$ kJ mol$^{-1}$
   $\Delta S_R^\circ (700 K) = -48.7$ J mol$^{-1}$ K$^{-1}$
   $\Delta S_R^\circ (800 K) = -48.7$ J mol$^{-1}$ K$^{-1}$

   c.   $-27.4$ kJ mol$^{-1}$

**P6.39**   $-0.015$ J

**P6.40**   $-126$ kJ mol$^{-1}$ at 298.15 K, $-128$ kJ mol$^{-1}$ at 310. K

# Chapter 7

**P7.1**   $b = 3.97 \times 10^{-5}$ m$^3$ mol$^{-1}$

   $a = 6.43 \times 10^{-2}$ m$^6$ Pa mol$^{-2}$

**P7.2**   a.   $R = 0.0833$ L bar K$^{-1}$ mol$^{-1}$
   $a = 5.56$ L$^2$ bar mol$^{-2}$, $b = 0.0305$ L mol$^{-1}$
   b.   $a = 5.53$ L$^2$ bar mol$^{-2}$, $b = 0.0305$ L mol$^{-1}$

**P7.4**   310. K ideal gas, 309 K van der Waals

**P7.5**   670. K, 127 bar

**P7.6**   $a = 0.692$ L$^2$ bar mol$^{-2}$, $\quad b = 0.0537$ L mol$^{-1}$
   $V_m = 24.8$ L

**P7.7**   $\gamma = 0.414, 0.357, 0.436, 0.755$, and 1.86
   at 150., 250., 350., 450., and 550. bar, respectively.

**P7.8**   $V_m = 0.0167$ L mol$^{-1}$, $z = 0.942$

**P7.9**   ideal gas: 4.65 mol L$^{-1}$, vdW gas, 4.25 mol L$^{-1}$

**P7.10**   ideal gas: $-16.9 \times 10^3$ J, vdW gas: $-16.8 \times 10^3$ J, 1.2%

**P7.12**   $1.62 \times 10^{-10}$ m

**P7.14**   0.399 L mol$^{-1}$, $-8.9\%$

**P7.17**   $b = 0.04286$ dm$^3$ mol$^{-1}$

   $a = 3.657$ dm$^6$ bar mol$^{-2}$

**P7.18**   $a = 14.29$ dm$^6$ bar K$^{\frac{1}{2}}$ mol$^{-2}$

   $b = 0.02010$ dm$^3$ mol$^{-1}$

**P7.19**   ideal gas: 0.521 L, vdW gas: 0.180 L

**P7.22**   $\rho_{idealgas} = 224$ g L$^{-1}$, $\rho_{vdW} = 216$ g L$^{-1}$

**P7.24**   ideal gas 371 bar

   vdW: 408 bar, R-K: 407 bar

**P7.25**   ideal gas: 0.344 L mol$^{-1}$

   vdW gas: 0.129 L mol$^{-1}$

   R-K gas: 0.115 L mol$^{-1}$

**P7.26**   111 K, 426 K, 643 K

# Chapter 8

**P8.1**   32.3 kJ mol$^{-1}$

**P8.2**   a.   351 K

   b.   $\Delta H_{vaporization} (351 K) = 40.6$ kJ mol$^{-1}$

   $\Delta H_{vaporization} (298 K) = 43.0$ kJ mol$^{-1}$

**P8.4**   $\Delta H_{sublimation} = 33.2$ kJ mol$^{-1}$

   $\Delta H_{vaporization} = 30.0$ kJ mol$^{-1}$

   $\Delta H_{fusion} = 3.2$ kJ mol$^{-1}$

   342 K, $6.70 \times 10^4$ Pa

**P8.7**   $2.89 \times 10^{-9}$ J

**P8.8**   a.   582 bar

   b.   $2.2 \times 10^2$ bar

   c.   $-1.5$ °C

**P8.10**   $1.04 \times 10^4$ Pa

**P8.11**   $\Delta H_{sublimation} = 53.4$ kJ mol$^{-1}$

   $\Delta H_{vaporization} = 31.8$ kJ mol$^{-1}$

   $\Delta H_{fusion} = 21.6$ kJ mol$^{-1}$

   193 K, 18.7 Pa

**P8.13**   1.95 atm

**P8.14**   425 Pa

**P8.16**   51.1 kJ mol$^{-1}$

**P8.17**   a. 26.6 Torr,   b. 25.2 Torr

**P8.19**   23.5 kJ mol$^{-1}$

**P8.20**   $T_{b,normal} = 342.8$ K, $T_{b,standard} = 343.4$ K

**P8.21**   a. 0.583 bar,   b. 0.553 bar

**P8.22**   $1.76 \times 10^4$ Pa

**P8.23**   $6.78 \times 10^4$ Pa

**P8.24** $\Delta H_{sublimation} = 18.4 \text{ kJ mol}^{-1}$

$\Delta H_{vaporization} = 14.4 \text{ kJ mol}^{-1}, \Delta H_{fusion} = 4.0 \text{ kJ mol}^{-1}$

$T_{triple} = 117 \text{ K}, P_{triple} = 33.5 \text{ Torr}$

**P8.25** 344 K

**P8.26** a. $7.77 \times 10^6 \text{ Pa}$

b. $3.53 \times 10^5 \text{ Pa}$

**P8.27** $2.33 \times 10^4 \text{ Pa}, 1.39$

**P8.28** $27.4 \text{ kJ mol}^{-1}$

**P8.31** $4.40 \text{ kJ mol}^{-1}$

**P8.33** $-0.717 \text{ K at } 100. \text{ bar and } -3.58 \text{ K at } 500. \text{ bar}$

**P8.34** a. $\Delta H_{vaporization} = 32.1 \times 10^3 \text{ J mol}^{-1}$

$\Delta H_{sublimation} = 37.4 \times 10^3 \text{ J mol}^{-1}$

b. $5.4 \times 10^3 \text{ J mol}^{-1}$

c. $349.5 \text{ K}, 91.8 \text{ J mol}^{-1} \text{K}^{-1}$

d. $T_{tp} = 264 \text{ K}, P_{tp} = 2.84 \times 10^3 \text{ Pa}$

**P8.35** $3567 \text{ Pa K}^{-1}, 3564 \text{ Pa K}^{-1}, 0.061\%$

**P8.36** $38.4 \text{ J K}^{-1}\text{mol}^{-1}, 16.4 \times 10^3 \text{J mol}^{-1}$

**P8.37** $360. \text{ K}, 1.89 \times 10^4 \text{ Pa}$

**P8.38** $27.1 \text{ kJ mol}^{-1}$

**P8.39** $1.51 \times 10^3 \text{ Pa}$

**P8.40** a. $49.5 \text{ J mol}^{-1}$

b. $267 \text{ J mol}^{-1}$

**P8.41** $2.62 \times 10^4 \text{ Pa}$

**P8.42** a. 56.1 Torr

b. 52.5 Torr

**P8.43** $-3.5°\text{C}$

**P8.44** $142 \text{ K}, 2.94 \times 10^3 \text{ Torr}$

$\Delta H_{sublimation} = 10.1 \times 10^3 \text{ J mol}^{-1}$

$\Delta H_{vaporization} = 9.38 \times 10^3 \text{ J mol}^{-1}$

$\Delta H_{fusion} = 0.69 \times 10^3 \text{ J mol}^{-1}$

**P8.45** gas only 868 L, liquid only 0.0200 L

# Chapter 9

**P9.2** $a_A = 0.489, \gamma_A = 1.58, a_B = 1.00, \gamma_B = 1.45$

**P9.4** a. 0.697, b. 0.893

**P9.5** $-8.0 \text{ cm}^3$

**P9.6** $57.9 \text{ cm}^3 \text{ mol}^{-1}$

**P9.7** $1.45 \times 10^3 \text{ g mol}^{-1}$

**P9.8** 170 Torr

**P9.9** 0.312

**P9.10** $7.14 \times 10^{-3}\text{g}, 2.67 \times 10^{-3} \text{ g}$

**P9.11** a. 25.0 Torr, 0.500

b. $Z_{EB} = (1 - Z_{EC}) = 0.39$

**P9.12** a. $P_A = 27.0 \text{ Torr}, P_B = 28.0 \text{ Torr}$

b. $P_A = 41.4 \text{ Torr}, P_B = 21.0 \text{ Torr}$

**P9.14** $1.86 \text{ K kg mol}^{-1}$

**P9.15** a. for ethanol $a_1 = 0.9504, \gamma_1 = 1.055$, for isooctane

$a_2 = 1.411, \gamma_2 = 14.20$

b. 121.8 Torr

**P9.16** $2.68 \times 10^{-6} \text{ mol L}^{-1}$

**P9.17** $5.6 \times 10^{-9} \text{ M}$

**P9.19** $P_a^* = 0.874 \text{ bar}, P_B^* = 0.608 \text{ bar}$

**P9.20** 413 Torr

**P9.21** 61.9 Torr

**P9.22** $-0.10 \text{ L}$

**P9.24** 0.466

**P9.25** $123 \text{ g mol}^{-1}$

**P9.26** $6.15 \text{ m}, 6.01 \times 10^4 \text{ Pa}$

**P9.27** 0.116 bar

**P9.28** $x_{bromo} = 0.769, y_{bromo} = 0.561$

**P9.29** 0.450

**P9.30** a. $2.65 \times 10^3 \text{ Torr}$

b. 0.525

c. $Z_{chloro} = 0.614$

**P9.31** $K = 9.5 \times 10^4 \text{ M}^{-1}$

$N = 0.12$

**P9.32** $a_{CS_2}^R = 0.872, \gamma_{CS_2}^R = 1.21, a_{CS_2}^H = 0.255, \gamma_{CS_2}^H = 0.353$

**P9.33** $M = 41.3 \text{ g mol}^{-1}, \Delta T_f = -1.16 \text{ K}, \dfrac{P_{benzene}}{P_{benzene}^*} = 0.983$

$\pi = 4.93 \times 10^5 \text{ Pa}$

# Chapter 10

**P10.3** a. 0.91, b. 0.895, c. 0.641

**P10.4** a. $0.119 \text{ mol kg}^{-1}$

b. $0.0750 \text{ mol kg}^{-1}$

c. $0.0750 \text{ mol kg}^{-1}$

d. $0.171 \text{ mol kg}^{-1}$

**P10.5** a. 48%, b. 60.%, c. 51%

**P10.6** 0.0547

**P10.7** $0.150 \text{ } m \text{ } 1.13\%, 1.50 \text{ } m \text{ } 0.372\%,$

Ignoring ionic interactions $0.150 \text{ } m \text{ } 1.07\%, 1.50 \text{ } m \text{ } 0.341\%$

**P10.8** a. 0.144, b. 0.0663, c. 0.155

**P10.9** a. 10.6%, b. 5.92%, c. 4.37%

**P10.10** $\Delta H_R^° = 17 \text{ kJ mol}^{-1}, \Delta G_R^° = 16.5 \text{ kJ mol}^{-1}$

**P10.12** $-426 \times 10^3 \text{ J mol}^{-1}$

**P10.13** $0.321 \text{ mol kg}^{-1}$

**P10.14** $I = 0.072 \text{ mol kg}^{-1}, \gamma_\pm = 0.389, a_\pm = 0.0106$

**P10.16** 0.41 nm

**P10.17** a. $6.28 \times 10^{-5} \text{ mol L}^{-1}$

b. $1.22 \times 10^{-5} \text{ mol kg}^{-1}$

**P10.20** $0.239 \text{ mol kg}^{-1}, 0.0539$

**P10.21** a. 5.44%, b. 10.9%

**P10.22**   a.   51.5%,        b. 42.5%

**P10.23**   1.4 nm

**P10.24**   $I = 0.215 \text{ mol kg}^{-1}$

$\gamma_\pm = 0.114$

$a_\pm = 0.00740$

**P10.25**   $I = 0.105 \text{ mol kg}^{-1}$

$\gamma_\pm = 0.320$

$a_\pm = 0.0128$

**P10.26**   a.   $0.225 \text{ mol kg}^{-1}$

b.   $0.0750 \text{ mol kg}^{-1}$

c.   $0.300 \text{ mol kg}^{-1}$

d.   $0.450 \text{ mol kg}^{-1}$

**P10.27**   a.   $5.5 \times 10^{-3} \text{ mol kg}^{-1}$

b.   $8.7 \times 10^{-3} \text{ mol kg}^{-1}$

c.   $5.5 \times 10^{-3} \text{ mol kg}^{-1}$

**P10.28**   $\Delta H_R^\circ = -65.4 \text{ kJ mol}^{-1}, \Delta G_R^\circ = -55.7 \text{ kJ mol}^{-1}$

**P10.29**   4.39, 4.63

**P10.30**   0.791

# Chapter 11

**P11.1**   a. $2.65 \times 10^6$

b. $-36.7 \text{ kJ mol}^{-1}$

**P11.2**   $-103.8 \text{ kJ mol}^{-1}$

**P11.3**   $-131.2 \text{ kJ mol}^{-1}$

**P11.4**   $0.7680 \text{ V}, 1.38 \times 10^{21}$

**P11.5**   a. 1.216 V,   b. 1.172 V

$-3.73 \%$

**P11.6**   a. $0.337 \text{ V}, 2.47 \times 10^{11}$

**P11.7**   a. 1.108 V,   b. 1.099 V, $-0.804 \%$

**P11.8**   $2.413 \text{ V}, 7.44 \times 10^{77}$

**P11.9**   $-131.1 \text{ kJ mol}^{-1}$

**P11.10**   $1.42 \text{ V}, 8.55 \times 10^{-5} \text{V K}^{-1}$

**P11.11**   $1.154 \text{ V}, 6.61 \times 10^{35}, 204.5 \text{ kJ mol}^{-1}$

**P11.12**   $\Delta G_R = -33.4 \text{ kJ mol}^{-1}, \Delta S_R = -29.9 \text{ J mol}^{-1} \text{ K}^{-1}$
$\Delta H_R = -43.1 \text{ kJ mol}^{-1}$

**P11.13**   $-210.7 \text{ kJ mol}^{-1}, 7.21 \times 10^{36}, -210.374 \text{ kJ mol}^{-1}$

**P11.15**   a. $1.11 \times 10^8$,        b. $6.67 \times 10^{-56}$

**P11.16**   0.769

**P11.17**   c. $-1108 \text{ kJ}$

**P11.18**   a. 1.110 V,    b. $Zn^{2+}$: 0.733, $Cu^{2+}$: 0.626,    c. 1.108 V

**P11.19**   $\Delta G_R^\circ = -219.0 \text{ kJ mol}^{-1}, \Delta S_R^\circ = -7.91 \text{ J K}^{-1}$
$\Delta H_R^\circ = -221.4 \text{ kJ mol}^{-1}$

**P11.20**   $-0.913 \text{ V}$

**P11.21**   $\Delta G_R = -370.1 \text{ kJ mol}^{-1}, -370.6 \text{ kJ mol}^{-1}$
$\Delta S_R = 15.4 \text{ J mol}^{-1}\text{K}^{-1}, 25.4 \text{ J mol}^{-1}\text{K}^{-1}$
$\Delta H_R = -365.8 \text{ kJ mol}^{-1}, -362.8 \text{ kJ mol}^{-1}$

**P11.22**   $1.10 \times 10^{-11}$

**P11.24**   $-713.2 \text{ kJ mol}^{-1}, 9.06 \times 10^{124}$

**P11.25**   $4.16 \times 10^{-4}$

**P11.26**   $8.28 \times 10^{-84}, -1.22869 \text{ V}$

**P11.28**   a.   9.95,   b.   0.100

**P11.29**   $4.90 \times 10^{-13}$

**P11.30**   a.   $6.56 \times 10^{-81}$,   b.    $7.62 \times 10^{-14}$

# Chapter 12

**P12.1**   a.   4/52

b.   1/52

c.   12/52 and 3/52, respectively

**P12.2**   a.   0.002

b.   $1.52 \times 10^{-6}$

**P12.3**   a.   1/6

b.   1/9

c.   21/36

**P12.4**   a.   8/49

b.   6/49

c.   23/49

**P12.5**   a.   $10^7$

b.   160

c.   $1.6 \times 10^9$

**P12.6**   a.   $2.56 \times 10^{10}$

b.   $5.08 \times 10^9$

**P12.7**   a.   0.372

b.   0.569

**P12.8**   a.   0.06

b.   0.0006

**P12.9**   a.   720

b.   360

c.   1

d.   $3.73 \times 10^{16}$

**P12.10**   120

**P12.11**   a.   1

b.   15

c.   1

d.   $1.03 \times 10^{10}$

**P12.12**   a.   $4.57 \times 10^5$

b.   $1.76 \times 10^4$

c.   $3.59 \times 10^5$

**P12.13**   a.   $9.52 \times 10^{-7}$

b.   $9.52 \times 10^{-7}$

c.   $1.27 \times 10^{-6}$ and $3.77 \times 10^{-7}$

**P12.14**   a.   $1.0 \times 10^{-5}$

b.   $2.2 \times 10^{-8}$

c.   $3.0 \times 10^{-6}$

**P12.15** 0.004

**P12.16** a. $4.52 \times 10^{-8}$

b. $1.04 \times 10^{-6}$

c. $8.66 \times 10^{-9}$

**P12.17** a. bosons: 220; fermions: 45

b. bosons: $1.72 \times 10^5$; fermions: $1.62 \times 10^5$

**P12.18** a. $7.41 \times 10^{11}$

b. $2.97 \times 10^{10}$

c. $2.04 \times 10^6$

**P12.19** a. $9.77 \times 10^{-4}$

b. 0.044

c. 0.246

d. 0.044

**P12.20** a. $1.69 \times 10^{-5}$

b. $3.05 \times 10^{-3}$

c. 0.137

d. 0.195

**P12.21** a. $9.54 \times 10^{-7}$

b. 0.176

c. 0.015

**P12.22** a. $(n)(n-1)$

b. $(n)(n-1)(n-2)\dots(n/2+1)/(n+2)!$

**P12.24** $1.91

**P12.25** b. $\ln(2)/k$

**P12.26** a. $9.6 \times 10^{-6}$ s

b. 0.37

**P12.27** c $182 \text{ J mol}^{-1}$

**P12.28** c. case 1: 0.245; case 2: 0.618

**P12.29** a. $2/a$

b. $a/2$

c. $a^2(1/3 - 1/2\pi^2)$

d. $a^2(1/12 - 1/2\pi^2)$

**P12.30** a. $(m/2\pi kT)^{1/2}$

b. 0

c. $kT/m$

d. $kT/m$

**P12.31** $\langle x \rangle = 0$

**P12.32** $1.6 \times 10^4$ m

**P12.33** $x_{mp} = (a)^{1/2}$

**P12.34** a. 0

b. 1/3

**P12.35** a. 0.175

b. 0.0653

c. 0.0563

# Chapter 13

**P13.1** b. $\exp(693)$

c. $\exp(673)$

**P13.2** $10^{694}$

**P13.4** 0.25

**P13.5** a. $2.6 \times 10^6$

b. 5148

**P13.8** $P_{N_2} = 0.230$ atm; $P_{O_2} = 0.052$ atm

**P13.9** a. 250 K

b. 180 K

**P13.10** a. 250 K

b. 180 K

**P13.11** a. $6.07 \times 10^{-20}$ J

b. Set C

**P13.12** a. $500. \text{ cm}^{-1}$

$W = 1287$

b. $500. \text{ cm}^{-1}$

$W = 2860$

c. $500. \text{ cm}^{-1}$

$W = 858$

**P13.13** limiting value is 0.333

**P13.14** 721 K

**P13.15** 4152 K

**P13.16** 1.28, 5.80

**P13.17** 0.781, 0.00294

**P13.18** 25,300 K

**P13.19** 0.999998

**P13.20** $a_- = 0.333334$

$a_0 = 0.333333$

$a_+ = 0.333333$

**P13.22** 432 K

**P13.23** 1090 K

**P13.24** At 300 K, $p = 0.074$ $F_2$ equivalent at 523 K

At 1000 K, $p = 0.249$ $F_2$ equivalent at 1740 K

**P13.25** $1.06 \times 10^{-9}$

**P13.27** $5.85 \times 10^4$

**P13.29** At 100 K, $p = 0.149$

At 500 K, $p = 0.414$

At 200 K, $p = 0.479$

**P13.30** b. 10,300 K

**P13.31** 1780 K

# Chapter 14

**P14.1** $H_2$: $2.77 \times 10^{26}$

$N_2$: $1.43 \times 10^{28}$

**P14.2** $q_T = 5.66 \times 10^{29}$

$q_T\left(^{37}Cl_2\right) = 1.087 \times q_T\left(^{35}Cl_2\right)$

**P14.3** $q_T = 4.46 \times 10^{24}$

**P14.4** $q_T(Ar) = 2.44 \times 10^{29}, T = 590.$ K

**P14.5** 0.0680 K

**P14.6** $3.90 \times 10^{17}$

**P14.7** $4.38 \times 10^{4}$

**P14.8** $1.99 \times 10^{5}$

**P14.9** a. 1

b. 2

c. 2

d. 12

e. 2

**P14.10** $CCl_4$: 12

$CFCl_3$: 3

$CF_2Cl_2$: 2

$CF_3Cl$: 3

**P14.11** rotational: HD; translational: $D_2$

**P14.12** $H_2$: 1.00; HD: 1.22

**P14.13** $q_R = 401$

**P14.14** $q_R = 424$

**P14.15** a. no

b. no

c. yes

d. yes

**P14.16** 5840

**P14.17** $3.77 \times 10^{4}$

**P14.18** a. 616 K

b. $J = 5-6$

**P14.19** $J = 19-20$ transition

**P14.20** 4 to 5

**P14.21** $q_R = 5.02$; by summation $q_R = 20.6$

**P14.22** 0.419012 cm$^{-1}$, $q_R = 494$

**P14.23** a. 

| $J$ | $P_J$ |
|---|---|
| 0 | 0.041 |
| 1 | 0.113 |
| 2 | 0.160 |
| 3 | 0.175 |
| 4 | 0.167 |
| 5 | 0.132 |
| 6 | 0.095 |
| 7 | 0.062 |
| 8 | 0.037 |
| 9 | 0.019 |

b. 

| $J$ | $P_J$ |
|---|---|
| 0 | 0.043 |
| 1 | 0.117 |
| 2 | 0.116 |
| 3 | 0.179 |
| 4 | 0.163 |
| 5 | 0.131 |
| 6 | 0.093 |
| 7 | 0.059 |
| 8 | 0.034 |
| 9 | 0.018 |

**P14.24** a. $B_A = B_B = B_C = 5.27$ cm$^{-1}$

b. yes

**P14.25** 0.418 K

**P14.26** 300 K: $q_V = 1, p_0 = 1$

3000 K: $q_V = 1.32, p_0 = 0.762$

**P14.27** 1820

**P14.28** IF: 300 K: $q_V = 1.06, p_0 = 0.946, p_1 = 0.051,$
$p_2 = 0.003$
3000 K: $q_V = 3.94, p_0 = 0.254, p_1 = 0.189, p_2 = 0.141$
IBr: 300 K: $q_V = 1.38, p_0 = 0.725, p_1 = 0.199,$
$p_2 = 0.055$
3000 K: $q_V = 8.26, p_0 = 0.121, p_1 = 0.106, p_2 = 0.094$

**P14.29** $q_V = 1.67$

**P14.30** $q_V = 1.10$

**P14.31** $q_V = 1.69$

**P14.32** $q_V = 4.09$

**P14.33** $p_0 = 1, p_1 = 0$

**P14.34** a. 1601 cm$^{-1}$

**P14.35** a. $q_V = 1.00$

b. 1710 K

**P14.37** 453 cm$^{-1}$

**P14.39** a. $q = L/\Lambda$

b. $q = V/\Lambda^3$

**P14.41** a. $q_v = 1, q_r = 1.29$

b. $q_v = 1, q_r = 1.26$

**P14.42** $q_E = 10.2$

**P14.43** a. $q_E = 4.77$

b. 2320 K

**P14.44** a. $q_E = 3.11$

b. 251 K

**P14.45** $q_E = 1.00$

**P14.46** $q = 1.71 \times 10^{34}$

**P14.47** $q = 1.30 \times 10^{29}$

**P14.48** $q_R = 265$

# Chapter 15

**P15.2** 655 K

**P15.3** Ensemble b

**P15.4** 1310 K

**P15.5** $NkT$

**P15.6** $U = \frac{1}{2}NkT; C_V = \frac{1}{2}Nk$

**P15.8**

| Molecule | $\theta_R$ (K) | High $T$? | $\theta_V$ (K) | High $T$? |
|---|---|---|---|---|
| $H^{35}Cl$ | 15.2 | No | 4150 | No |
| $^{12}C^{16}O$ | 2.78 | Yes | 3120 | No |
| $^{39}KI$ | 0.088 | Yes | 233 | No |
| CsI | 0.035 | Yes | 173 | No |

**P15.9** 1.71 kJ mol$^{-1}$

**P15.10** 307 J mol$^{-1}$

**P15.12** 3.72 kJ mol$^{-1}$

**P15.13** 6.20 kJ mol$^{-1}$

**P15.14** $U_R$ are equivalent.
$U_V(\text{BrCl}) - U_V(\text{BrF}) = 434$ J mol$^{-1}$

**P15.16** $C_V$ values (J mol$^{-1}$K$^{-1}$) are as follows:

| | **298 K** | **500 K** | **1000 K** |
|---|---|---|---|
| 2041 cm$^{-1}$ | 0.042 | 0.808 | 4.24 |
| 712 cm$^{-1}$ | 3.37 | 5.93 | 7.62 |
| 3329 cm$^{-1}$ | 0.00 | 0.048 | 1.56 |
| Total | 6.78 | 12.7 | 21.0 |

**P15.17** $(0.751)R$

**P15.18** $(0.0586)R$

**P15.19** $n(1.85$ J mol$^{-1}$ K$^{-1})$

**P15.20** c. 352 m s$^{-1}$

**P15.21** b. 24.6 J mol$^{-1}$ K$^{-1}$

**P15.22** 7.82 J mol$^{-1}$ K$^{-1}$

**P15.25** 200 K: 122 J mol$^{-1}$ K$^{-1}$; 300 K: 128 J mol$^{-1}$ K$^{-1}$;
500 K: 135 J mol$^{-1}$ K$^{-1}$

**P15.26** $1.28 \times 10^{-10}$ m

**P15.27** 219 J mol$^{-1}$ K$^{-1}$

**P15.28** 256 J mol$^{-1}$ K$^{-1}$

**P15.29** 176 J mol$^{-1}$ K$^{-1}$

**P15.30** 191 J mol$^{-1}$ K$^{-1}$, 260 J mol$^{-1}$ K$^{-1}$

**P15.31** 186 J mol$^{-1}$ K$^{-1}$

**P15.33** 49.1 J mol$^{-1}$ K$^{-1}$

**P15.34** 79.5 J mol$^{-1}$ K$^{-1}$

**P15.35** 211 J mol$^{-1}$ K$^{-1}$

**P15.38** 11.5 J mol$^{-1}$ K$^{-1}$

**P15.39** a. $R \ln 2$  b. $R \ln 4$
c. $R \ln 2$  d. 0

**P15.43** Ne: $-40.0$ kJ mol$^{-1}$; Kr: $-45.3$ kJ mol$^{-1}$

**P15.45** $-57.2$ kJ mol$^{-1}$

**P15.46** $G_{R,m}^{\circ} = -15.4$ kJ mol$^{-1}$; $G_{V,m}^{\circ} = -0.30$ kJ mol$^{-1}$

**P15.47** $2.25 \times 10^{-9}$

**P15.49** 0.824

**P15.50** $0.977 \exp(-2720)$

**P15.51** a. 143.4 mJ mol$^{-1}$
b. 28.0

# Chapter 16

**P16.2**

| | $\nu_{mp}$ (m s$^{-1}$) | $\nu_{ave}$ (m s$^{-1}$) | $\nu_{rms}$ (m s$^{-1}$) |
|---|---|---|---|
| Ne | 495 | 559 | 607 |
| Kr | 243 | 274 | 298 |
| CH$_4$ | 555 | 626 | 680 |
| C$_2$H$_6$ | 406 | 458 | 497 |
| C$_{60}$ | 82.9 | 93.6 | 102 |

**P16.3**

| | $\nu_{mp}$ (m s$^{-1}$) | $\nu_{ave}$ (m s$^{-1}$) | $\nu_{rms}$ (m s$^{-1}$) |
|---|---|---|---|
| 300. K | 395 | 446 | 484 |
| 500. K | 510 | 575 | 624 |

$\nu(\text{H}_2) = (3.98)\nu(\text{O}_2)$

**P16.4**

| | **H$_2$O** | **HOD** | **D$_2$O** |
|---|---|---|---|
| $\nu_{ave}$ (m s$^{-1}$) | 592 | 576 | 562 |

**P16.5** $\nu_{ave}(\text{CCl}_4) = 202$ m s$^{-1}$; $\nu_{ave}(\text{O}_2) = 444$ m s$^{-1}$;
$KE_{ave} = 6.17 \times 10^{-21}$ J for both

**P16.6** 444 m for O$_2$; 274 m for Kr

**P16.7** a. $5.66 \times 10^{-4}$ s
b. $2.11 \times 10^{-3}$ s
c. 0.534

**P16.8** $\dfrac{\nu_{ave}}{\nu_{mp}} = \dfrac{2}{\sqrt{\pi}}; \dfrac{\nu_{rms}}{\nu_{mp}} = \sqrt{\dfrac{3}{2}}$

**P16.9** 81.5 K (both cases)

**P16.10** 1240 K

**P16.11** 0.843 and 0.157, respectively.

**P16.12** a. Ne: 828 m s$^{-1}$, Kr: 406 m s$^{-1}$, Ar: 589 m s$^{-1}$
b. 2100 K

**P16.13** 0.392

**P16.14** a. $2.10 \times 10^5$ K
b. $3.00 \times 10^4$ K

**P16.15** 298 K: 0.132, 500 K: 0.071

**P16.16** b. 557 m s$^{-1}$

**P16.23**   $1.47 \times 10^{24}$ collisions s$^{-1}$

**P16.24**   a.   4.97 s

b.   $6.03 \times 10^{-4}$ kg

**P16.25**   $6 \times 10^{11}$ collisions s$^{-1}$

**P16.26**   a.   $2.73 \times 10^{23}$ collisions s$^{-1}$

b.   $3.60 \times 10^{14}$ collisions s$^{-1}$

**P16.27**   $1 \times 10^{-5}$ m$^2$

**P16.28**   a.   $7 \times 10^{9}$ collisions s$^{-1}$

b.   0.38 atm

c.   $1.3 \times 10^{-7}$ m

**P16.29**   a.   $2.18 \times 10^{-7}$ m

b.   $7.78 \times 10^{-5}$ m

**P16.30**   a.   $8.44 \times 10^{34}$ m$^{-3}$ s$^{-1}$

b.   1380 K

**P16.31**   a.   $z_{11} = 9.35 \times 10^3$ s$^{-1}$, $\lambda = 0.051$ m

b.   $z_{11} = 9.35 \times 10^{-4}$ s$^{-1}$, $\lambda = 5.1 \times 10^5$ m

**P16.32**   a.   $1.60 \times 10^{-7}$ m

b.   $1.60 \times 10^{-5}$ m

c.   $1.60 \times 10^{-2}$ m

**P16.33**   Ne: $2.0 \times 10^{-7}$ m, Kr: $9.3 \times 10^{-8}$ m, CH$_4$: $1.0 \times 10^{-7}$ m

**P16.34**   $4.6 \times 10^{-4}$ Torr

**P16.36**   a.   $1.00 \times 10^8$ s$^{-1}$

b.   $1.87 \times 10^{28}$ m$^{-3}$ s$^{-1}$

c.   $4.40 \times 10^{-6}$ m

# Chapter 17

**P17.1**   0.318 nm$^2$

**P17.2**   $1.06 \times 10^{-5}$ m$^2$ s$^{-1}$

**P17.3**   a.   0.368 nm$^2$

b.   0.265 nm$^2$

**P17.4**   a.   319 s

b.   $6.13 \times 10^{-10}$ s

**P17.5**   a.   $1.60 \times 10^{-3}$ s

b.   $2.40 \times 10^{-3}$ s

**P17.6**   b.   $2.58 \times 10^{-5}$ m

**P17.7**   a.   $-9.60$ J s$^{-1}$

b.   $-33.6$ J s$^{-1}$

c.   $-22.8$ J s$^{-1}$

**P17.8**   No. $\kappa_{Ar} = (2.09)\kappa_{Kr}$

**P17.9**   $-1.80 \times 10^{-4}$ W cm$^{-2}$

**P17.10**   a.   0.0052 J K$^{-1}$ m$^{-1}$ s$^{-1}$

b.   0.0025 J K$^{-1}$ m$^{-1}$ s$^{-1}$

c.   0.0051 J K$^{-1}$ m$^{-1}$ s$^{-1}$

**P17.11**   $1.5 \times 10^{-19}$ m$^2$

**P17.12**   $1.6 \times 10^{-19}$ m$^2$

**P17.13**   c. $1.5 \times 10^{-19}$ m$^2$

**P17.14**   a. 1.14

b. 0.659

**P17.15**   1.33

**P17.16**   a.   $6.22 \times 10^{-19}$ m$^2$

b.   0.00389 J K$^{-1}$ m$^{-1}$ s$^{-1}$

**P17.17**   a.   $2.05 \times 10^{-3}$ m$^3$ s$^{-1}$

b.   $1.88 \times 10^{-3}$ m$^3$ s$^{-1}$

**P17.18**   a.   37.3 m s$^{-1}$

b.   0.893 m s$^{-1}$

**P17.19**   D$_2$: 119 $\mu$P, HD 103 $\mu$P

**P17.20**   1.89 cP

**P17.21**   22 s

**P17.22**   b.   $1.34 \times 10^{-5}$ m$^2$ s$^{-1}$

**P17.23**   b.   $6.59 \times 10^{-3}$ J K$^{-1}$ m$^{-1}$ s$^{-1}$

c.   $1.47 \times 10^{-2}$ J K$^{-1}$ m$^{-1}$ s$^{-1}$

**P17.24**   $E = 10.7$ kJ mol$^{-1}$, A $= 8.26 \times 10^{-3}$

**P17.25**   4.07 Pa

**P17.26**   0.265 L s$^{-1}$

**P17.27**   a.   1.89 nm

b.   16.8 kg mol$^{-1}$

**P17.28**   $f = 7.25 \times 10^{-8}$ g s$^{-1}$, $r = 3.85$ nm

**P17.29**   a. catalase: 238 kg mol$^{-1}$, alcohol dehyd.: 74.2 kg mol$^{-1}$

b. $3.10 \times 10^4$ s

**P17.30**   a.   $1.69 \times 10^{-13}$ s

b.   1.90 nm

**P17.31**   77.7 kg mol$^{-1}$

**P17.32**   $3.75 \times 10^{20}$ electrons

**P17.33**   0.0125 S m$^2$ mol$^{-1}$

**P17.34**   Strong electrolyte;   $\Lambda_m^\circ = 0.0125$ S m$^2$ mol$^{-1}$

**P17.35**   $\Lambda_m^\circ = 0.00898$ S m$^2$ mol$^{-1}$

**P17.37**   10 steps: $4.39 \times 10^{-2}$, 20 steps: $7.39 \times 10^{-2}$, 100 steps: $6.66 \times 10^{-2}$

**P17.38**   $1.17 \times 10^{-10}$ m$^2$ s$^{-1}$

**P17.39**   a.   $4.4810 \times 10^{-2}$ S m$^{-1}$ ohm

b.   $4.3395 \times 10^{-6}$ S m$^{-1}$

**P17.40**   b.   $K = 1.00 \times 10^{-14}$

# Chapter 18

**P18.2**   b. $2.79 \times 10^3$ s

c. 425 s

**P18.3**   First order, $k = 3.79 \times 10^{-5}$ s$^{-1}$

**P18.5**
a. First order with respect to (wrt) ClO

First order wrt BrO

Second order overall

Units of $k$: $M^{-1} s^{-1}$

b. Second order wrt NO

First order wrt $O_2$

Third order overall

Units of $k$: $M^{-2} s^{-1}$

c. Second order wrt HI

First order wrt $O_2$

$-1/2$ order wrt $H^+$

2.5 order overall

Units of $k$: $M^{-3/2} s^{-1}$

**P18.6**
a. Second

b. Third

c. 1.5

**P18.7** Second order wrt $NO_2$

First order wrt $H_2$

$k = 1.61 \times 10^{-6} kPa^{-2} s^{-1}$

**P18.8** $K = 1.9 \times 10^{-15} molec^{-1} cu^3 s^{-1}$

**P18.9** $R = 116 M^{-1} s^{-1} [Lactose][H^+]$

**P18.11** Second order

$k = 0.317 M^{-1} s^{-1}$

**P18.13**
a. $k = 2.08 \times 10^{-3} s^{-1}$

b. $t = 1.11 \times 10^3 s$

**P18.14** $1.43 \times 10^{24}$

**P18.15** $1.50 \times 10^4$ days

**P18.16** 4.61 decay $min^{-1}$

**P18.17**
a. $k = 3.65 \times 10^{-4} day^{-1}$

b. $1.90 \times 10^3$ days

**P18.20** 20%

**P18.23** $2.6 \times 10^{-7} s$

**P18.26**
a. $k = 0.03 M^{-1} s^{-1}$

b. 120 s

**P18.27**
a. $1.08 \times 10^{-12} s$

**P18.28** $k_1 = 4.76 \times 10^{-10} yr^{-1}$ and $k_2 = 5.70 \times 10^{-11} yr^{-1}$

**P18.29** $\Phi_1 = 0.30, \Phi_2 = 0.49, \Phi_3 = 0.21$

**P18.30**
a. Rate $= 2.1 \times 10^{-15} M s^{-1}$

b. Rate $= 1.6 \times 10^{-15} M s^{-1}$

c. $[Cl] = 1.1 \times 10^{-18} M$

$[O_3] = 4.2 \times 10^{-11} M$

**P18.32** 1800 J $mol^{-1}$

**P18.33**
b. 11 kJ $mol^{-1}$

**P18.36**
a. $7.0 \times 10^{-11} M^{-1} S^{-1}$

b. $3.5 \times 10^{-11} M^{-1} S^{-1}$

**P18.37** 0.15

**P18.38**
a. $E_a = 1.50 \times 10^5 J mol^{-1}, A = 1.02 \times 10^{10} M^{-1} s^{-1}$

b. $k = 0.0234 M$

**P18.39** 269 s

**P18.40** $A = 7.38 \times 10^{13} s^{-1}, k = 3.86 \times 10^{-5} s^{-1}$

**P18.42** $1800 s^{-1}$ and

$1300 M^{-1} s^{-1}$

**P18.44** $3.44 \times 10^{10} M^{-1} s^{-1}$

**P18.45** $D_{imid} = 1.1 \times 10^{-5} cm^2 s^{-1}, k = 3.6 \times 10^{10} M^{-1} s^{-1}$

**P18.46** No. $k = 6.3 \times 10^{10} M^{-1} s^{-1}$ for diffusion limited

**P18.47**
a. $E_a = 108 kJ mol^{-1}, A = 1.05 \times 10^{10} s^{-1}$

b. $\Delta S^{\ddagger} = -62.3 J mol^{-1} K^{-1}; \Delta H^{\ddagger} = 105 kJ mol^{-1}$

**P18.48**
a. $E_a = 219 kJ mol^{-1}, A = 7.20 \times 10^{12} s^{-1}$

b. $\Delta S^{\ddagger} = -15.3 J mol^{-1} K^{-1}; \Delta H^{\ddagger} = 212 kJ mol^{-1}$

**P18.49**
a. $E_a = 790 J mol^{-1}, A = 4.88 \times 10^{10} M^{-1} s^{-1}$

b. $k = 3.17 \times 10^{10} M^{-1} s^{-1}$

c. $\Delta S^{\ddagger} = -57.9 J mol^{-1} K^{-1}; \Delta H^{\ddagger} = -2.87 kJ mol^{-1}$

**P18.50** $\Delta S^{\ddagger} = 60.6 J mol^{-1} K^{-1}; \Delta H^{\ddagger} = 270 kJ mol^{-1}$

**P18.51** $\Delta S^{\ddagger} = 4.57 J mol^{-1} K^{-1}; \Delta H^{\ddagger} = 37.0 kJ mol^{-1}$

# Chapter 19

**P19.8**
b. 59 kJ $mol^{-1}$

c. 434

**P19.14** $k_1 = 1.19 \times 10^4 M^{-1} s^{-1}; k_1/k_2 = 1.05 \times 10^3 M^{-1}$

**P19.16** $2.45 \times 10^{-3} M s^{-1}$

**P19.17** $R_{max} = 3.75 \times 10^{-2} M s^{-1}$

$K_m = 2.63 \times 10^{-2} M$

$k_2 = 1.08 \times 10^7 s^{-1}$

**P19.18**
a. $K_m = 2.42 mM, R_{max} = 0.137 mM s^{-1}$

b. $K_m = 73.3 mM, R_{max} = 0.0298 mM s^{-1}$

**P19.19**
a. $K_M = 2.5 \times 10^{-6} M$

$R_M = 6.5 \times 10^{-7} Ms^{-1}$

b. $K_M = 1.3 \times 10^{-5} M$

$R_M = 7.9 \times 10^{-7} Ms^{-1}$

$K_I = 4.8 \times 10^{-5} M$

**P19.20** 0.0431 M

**P19.21** $K_m = 6.49 \mu M, R_{max} = 4.74 \times 10^{-8} \mu M s^{-1}$,

$K_m* = 24.9 \mu M$,

$K_i = 70.4 \mu M$

**P19.23** $K_m = 0.0392 M, R_{max} = 0.437 M s^{-1}$

**P19.28**

| $P$ (atm) | $\theta$ |
|---|---|
| 20. | 0.595 |
| 50. | 0.754 |
| 100. | 0.853 |
| 200. | 0.932 |
| 300. | 0.952 |

**P19.29**  $r = 0.674$ mL, $s = 4.99$ Torr$^{-1}$

**P19.30**  $V_m = 1.56$ cm$^3$ g$^{-1}$, $K = 220$ Torr$^{-1}$

**P19.32**  11 kJ mol$^{-1}$

**P19.36**  a.  at 298 nm: $7.29 \times 10^{16}$ photons cm$^{-2}$;
at 320 nm: $8.05 \times 10^{16}$ photons cm$^{-2}$

b.  34.5 s

**P19.38**  0.95

**P19.39**  $4.55 \times 10^{18}$ photons, $I = 2.41 \times 10^{-3}$ J s$^{-1}$

**P19.40**  $3.02 \times 10^{19}$ photons s$^{-1}$

**P19.41**  $k_{isc}^S/k_f = 7.33$, $k_P = 3.88 \times 10^{-2}$ s$^{-1}$, $k_{isc}^T = 0.260$ s$^{-1}$

**P19.42**  a.  0.91

b.  $7.2 \times 10^{18}$ photons cm$^{-2}$ s$^{-1}$

c.  1.5 nW

**P19.43**  b.  $A = 0.312$, $B = 0.697$

c.  $-0.172$ atm

**P19.44**  $k_q = 1.71 \times 10^4$ %O$_2$ $^{-1}$ s$^{-1}$

**P19.45**  0.39

**P19.46**  12 Å

**P19.48**  25 residues

**P19.49**  a.  $3.4 \times 10^{-19}$ J

b.  $1.2 \times 10^{-19}$ J

**P19.50**  a.  0.768 Å$^{-1}$

b.  0.384 Å$^{-1}$

*This page intentionally left blank*

# Credits

## Cover

Artwork courtesy of the artist, Kim Kopp; photo credit: Frank Huster.

## Chapter 5

**Page 114:** AP Photo/Frank Franklin II; Imaginechina via AP Images.

## Chapter 6

**Page 153:** Photo courtesy of Professor Dr. Rolf Jurgen Behm/University of Ulm. From T. Diemant, T. Hager, H.E. Hoster, H. Rauscher, and R.J. Behm, *Surf. Sci.* 141(2003) 137, fig. 1a.

## Chapter 11

**Page 281:** Courtesy of Dr. D.M. Kolb, Department of Electrochemistry, University of Ulm.
**Page 282:** Courtesy of Dr. D.M. Kolb, Department of Electrochemistry, University of Ulm.
**Page 283:** Courtesy of Dr. D.M. Kolb, Department of Electrochemistry, University of Ulm; Photo courtesy of Professor Dr. Rolf Jurgen Behm/University of Ulm. Magnussen et al. "In-Situ Atomic-Scale Studies of the Mechanisms and Dynamics of Metal STM." *Electrochemica Acta* 46 (2001): 3725–3733, Figure 1.
**Page 284:** Courtesy of Dr. D.M. Kolb, Department of Electrochemistry, University of Ulm; Photo courtesy of Professor Dr. Rolf Jurgen Behm/University of Ulm. Magnussen et al. "In-Situ Atomic-Scale Studies of the Mechanisms and Dynamics of Metal STM." *Electrochemica Acta* 46 (2001): 3725–3733, Figure 2.
**Page 287:** Trimmer, A.L., Hudson, J.L., Kock, M., and Schuster, R. *Applied Physics Letters* 82 (2003): 3327. Copyright 2003, American Institute of Physics; Kock, M. et al. *Electrochemica Acta* 48, nos. 20–22 (30 September 2003): Figure 7, p. 3218; Trimmer, A.L., Hudson, J.L., Kock, M., and Schuster, R. *Applied Physics Letters* 82 (2003): 3327. Copyright 2003, American Institute of Physics.

## Chapter 19

**Page 526:** Copyright © 1991 Richard Megna - Fundamental Photographs.

*This page intentionally left blank*

# Index

## Values of Selected Physical Constants

| Constant | Symbol | Value |
|---|---|---|
| Atomic mass constant | amu | $1.660\,538921 \times 10^{-27}$ kg |
| Avogadro's constant | $N_A$ | $6.022\,14129 \times 10^{23}$ mol$^{-1}$ |
| Bohr magneton | $\mu_B = e\hbar/2m_e$ | $9.274\,00968 \times 10^{-24}$ J T$^{-1}$ |
| Bohr radius | $a_0 = 4\pi\varepsilon_0\hbar^2/m_e e^2$ | $5.291\,772\,1092 \times 10^{-11}$ m |
| Boltzmann constant | $k_B$ | $1.380\,6488 \times 10^{-23}$ J K$^{-1}$ |
| | | $0.695\,03476$ cm$^{-1}$ |
| Electron rest mass | $m_e$ | $9.109\,38291 \times 10^{-31}$ kg |
| Faraday constant | $F$ | $9.64853365 \times 10^{4}$ C mol$^{-1}$ |
| Gravitational constant | $G$ | $6.67384 \times 10^{-11}$ m$^3$ kg$^{-1}$ s$^{-2}$ |
| Standard acceleration of gravity | $G_n$ | $9.80665$ m s$^{-2}$ |
| Molar gas constant | $R$ | $8.3144621$ J K$^{-1}$ mol$^{-1}$ |
| | | $0.083\,144621$ dm$^3$ bar K$^{-1}$ mol$^{-1}$ |
| | | $0.082\,0578$ dm$^3$ atm K$^{-1}$ mol$^{-1}$ |
| Molar volume, ideal gas | | |
| (1 bar, 0°C) | | $22.710953$ L mol$^{-1}$ |
| (1 atm, 0°C) | | $22.413968$ L mol$^{-1}$ |
| Nuclear magneton | $\mu_N = e\hbar/2m_p$ | $5.050\,78353 \times 10^{-27}$ J T$^{-1}$ |
| Permittivity of vacuum | $\varepsilon_0$ | $8.854\,187\,817 \times 10^{-12}$ C$^2$ J$^{-1}$ m$^{-1}$ |
| Planck constant | $h$ | $6.626\,069\,57 \times 10^{-34}$ J s |
| | $\hbar$ | $1.054\,571726 \times 10^{-34}$ J s |
| Proton charge | $e$ | $1.602\,176\,565 \times 10^{-19}$ C |
| Proton magnetogyric ratio | $\gamma_P$ | $2.675\,221\,28 \times 10^8$ s$^{-1}$ T$^{-1}$ |
| Proton rest mass | $m_P$ | $1.672\,621\,777 \times 10^{-27}$ kg |
| Rydberg constant for infinite nuclear mass | $R_\infty = m_e e^4/8\varepsilon_0^2 h^2$ | $2.179\,8736 \times 10^{-18}$ J |
| | | $109\,73731.568\,539$ m$^{-1}$ |
| Rydberg constant for H | $R_H$ | $109677.581$ cm$^{-1}$ |
| Speed of light in vacuum | $c$ | $2.99\,792\,458 \times 10^8$ m s$^{-1}$ |
| Stefan-Boltzmann constant | $\sigma = 2\pi^5 k_B^4/15h^3 c^2$ | $5.670\,373 \times 10^{-8}$ J m$^{-2}$ K$^{-4}$ s$^{-1}$ |

## SI Prefixes

| Fraction | Prefix | Symbol | Fraction | Prefix | Symbol |
|---|---|---|---|---|---|
| $10^{-1}$ | deci | d | $10$ | deca | da |
| $10^{-2}$ | centi | c | $10^2$ | hecto | h |
| $10^{-3}$ | milli | m | $10^3$ | kilo | k |
| $10^{-6}$ | micro | $\mu$ | $10^6$ | mega | M |
| $10^{-9}$ | nano | n | $10^9$ | giga | G |
| $10^{-12}$ | pico | p | $10^{12}$ | tera | T |
| $10^{-15}$ | femto | f | $10^{15}$ | peta | P |
| $10^{-18}$ | atto | a | $10^{18}$ | exa | E |

## Greek Alphabet

| | | | | | | | | |
|---|---|---|---|---|---|---|---|---|
| Alpha | A | $\alpha$ | Iota | I | $\iota$ | Rho | P | $\rho$ |
| Beta | B | $\beta$ | Kappa | K | $\kappa$ | Sigma | $\Sigma$ | $\sigma$ |
| Gamma | $\Gamma$ | $\gamma$ | Lambda | $\Lambda$ | $\lambda$ | Tau | T | $\tau$ |
| Delta | $\Delta$ | $\delta$ | Mu | M | $\mu$ | Upsilon | $\Upsilon$ | $\upsilon$ |
| Epsilon | E | $\varepsilon$ | Nu | N | $\nu$ | Phi | $\Phi$ | $\phi$ |
| Zeta | Z | $\zeta$ | Xi | $\Xi$ | $\xi$ | Chi | X | $\chi$ |
| Eta | H | $\eta$ | Omicron | O | $o$ | Psi | $\Psi$ | $\psi$ |
| Theta | $\Theta$ | $\theta$ | Pi | $\Pi$ | $\pi$ | Omega | $\Omega$ | $\omega$ |

## Conversion Table for Units

*Length*

| | | |
|---|---|---|
| meter (SI unit) | m | |
| centimeter | cm | $= 10^{-2}$ m |
| ångström | Å | $= 10^{-10}$ m |
| micron | $\mu$ | $= 10^{-6}$ m |

*Volume*

| | | |
|---|---|---|
| cubic meter (SI unit) | m$^3$ | |
| liter | L | $= $ dm$^3 = 10^{-3}$ m$^3$ |

*Mass*

| | | |
|---|---|---|
| kilogram (SI unit) | kg | |
| gram | g | $= 10^{-3}$ kg |
| metric ton | t | $= 1000$ kg |

*Energy*

| | | |
|---|---|---|
| joule (SI unit) | J | |
| erg | erg | $= 10^{-7}$ J |
| rydberg | Ry | $= 2.179\ 87 \times 10^{-18}$ J |
| electron volt | eV | $= 1.602\ 176\ 565 \times 10^{-19}$ J |
| inverse centimeter | cm$^{-1}$ | $= 1.986\ 455\ 684 \times 10^{-23}$ J |
| calorie (thermochemical) | Cal | $= 4.184$ J |
| liter atmosphere | l atm | $= 101.325$ J |

*Pressure*

| | | |
|---|---|---|
| pascal (SI unit) | Pa | |
| atmosphere | atm | $= 101325$ Pa |
| bar | bar | $= 10^5$ Pa |
| torr | Torr | $= 133.322$ Pa |
| pounds per square inch | psi | $= 6.894\ 757 \times 10^3$ Pa |

*Power*

| | | |
|---|---|---|
| watt (SI unit) | W | |
| horsepower | hp | $= 745.7$ W |

*Angle*

| | | |
|---|---|---|
| radian (SI unit) | rad | |
| degree | ° | $= \dfrac{2\pi}{360}$ rad $= \left(\dfrac{1}{57.295\ 78}\right)$ rad |

*Electrical dipole moment*

| | | |
|---|---|---|
| C m (SI unit) | | |
| debye | D | $= 3.335\ 64 \times 10^{-30}$ C m |

## Masses and Natural Abundances for Selected Isotopes

| Nuclide | Symbol | Mass (amu) | Percent Abundance |
|---------|--------|------------|-------------------|
| H | $^1$H | 1.0078 | 99.985 |
| | $^2$H | 2.0140 | 0.015 |
| He | $^3$He | 3.0160 | 0.00013 |
| | $^4$He | 4.0026 | 100 |
| Li | $^6$Li | 6.0151 | 7.42 |
| | $^7$Li | 7.0160 | 92.58 |
| B | $^{10}$B | 10.0129 | 19.78 |
| | $^{11}$B | 11.0093 | 80.22 |
| C | $^{12}$C | 12 (exact) | 98.89 |
| | $^{13}$C | 13.0034 | 1.11 |
| N | $^{14}$N | 14.0031 | 99.63 |
| | $^{15}$N | 15.0001 | 0.37 |
| O | $^{16}$O | 15.9949 | 99.76 |
| | $^{17}$O | 16.9991 | 0.037 |
| | $^{18}$O | 17.9992 | 0.204 |
| F | $^{19}$F | 18.9984 | 100 |
| P | $^{31}$P | 30.9738 | 100 |
| S | $^{32}$S | 31.9721 | 95.0 |
| | $^{33}$S | 32.9715 | 0.76 |
| | $^{34}$S | 33.9679 | 4.22 |
| Cl | $^{35}$Cl | 34.9688 | 75.53 |
| | $^{37}$Cl | 36.9651 | 24.4 |
| Br | $^{79}$Br | 79.9183 | 50.54 |
| | $^{81}$Br | 80.9163 | 49.46 |
| I | $^{127}$I | 126.9045 | 100 |

Periodic Table of the Elements

group

1 — atomic number
H — symbol
1.0079 — atomic mass

period — 1

Main groups

**Legend:**
- Metals
  - one kind of positively charged ion
  - multiple kinds of positively charged ions
- Semi-Metals
- Non-Metals
- Alkali Metals
- Alkaline Earths
- Halogens
- Noble Gases

Transition metals

| 1 | 2 | 3 | 4 | 5 | 6 | 7 | 8 | 9 | 10 | 11 | 12 | 13 | 14 | 15 | 16 | 17 | 18 |
|---|---|---|---|---|---|---|---|---|---|---|---|---|---|---|---|---|---|
| 1 **H** 1.0079 | | | | | | | | | | | | | | | | | 2 **He** 4.003 |
| 3 **Li** 6.941 | 4 **Be** 9.012 | | | | | | | | | | | 5 **B** 10.81 | 6 **C** 12.01 | 7 **N** 14.01 | 8 **O** 16.00 | 9 **F** 19.00 | 10 **Ne** 20.18 |
| 11 **Na** 22.99 | 12 **Mg** 24.31 | | | | | | | | | | | 13 **Al** 26.98 | 14 **Si** 28.09 | 15 **P** 30.97 | 16 **S** 32.07 | 17 **Cl** 35.45 | 18 **Ar** 39.95 |
| 19 **K** 39.10 | 20 **Ca** 40.08 | 21 **Sc** 44.96 | 22 **Ti** 47.87 | 23 **V** 50.94 | 24 **Cr** 52.00 | 25 **Mn** 54.94 | 26 **Fe** 55.85 | 27 **Co** 58.93 | 28 **Ni** 58.68 | 29 **Cu** 63.55 | 30 **Zn** 65.39 | 31 **Ga** 69.72 | 32 **Ge** 72.61 | 33 **As** 74.92 | 34 **Se** 78.96 | 35 **Br** 79.90 | 36 **Kr** 83.80 |
| 37 **Rb** 85.47 | 38 **Sr** 87.62 | 39 **Y** 88.91 | 40 **Zr** 91.22 | 41 **Nb** 92.91 | 42 **Mo** 95.94 | 43 **Tc** (98) | 44 **Ru** 101.07 | 45 **Rh** 102.91 | 46 **Pd** 106.42 | 47 **Ag** 107.87 | 48 **Cd** 112.41 | 49 **In** 114.82 | 50 **Sn** 118.71 | 51 **Sb** 121.76 | 52 **Te** 127.60 | 53 **I** 126.90 | 54 **Xe** 131.29 |
| 55 **Cs** 132.91 | 56 **Ba** 137.33 | 57 **La** 138.91 | 72 **Hf** 178.49 | 73 **Ta** 180.95 | 74 **W** 183.84 | 75 **Re** 186.21 | 76 **Os** 190.23 | 77 **Ir** 192.22 | 78 **Pt** 195.08 | 79 **Au** 196.97 | 80 **Hg** 200.59 | 81 **Tl** 204.38 | 82 **Pb** 207.2 | 83 **Bi** 208.98 | 84 **Po** (209) | 85 **At** (210) | 86 **Rn** (222) |
| 87 **Fr** (223) | 88 **Ra** (226) | 89 **Ac** (227) | 104 **Rf** (261) | 105 **Db** (262) | 106 **Sg** (263) | 107 **Bh** (262) | 108 **Hs** (265) | 109 **Mt** (266) | 110 **Ds** (271) | 111 **Rg** (272) | 112 **Cn** (285) | 113 **Uut** (284) | 114 **Uuq** (289) | 115 **Uup** (288) | 116 **Uuh** (293) | | 118 **Uuo** (294) |

**Lanthanides**

| 58 **Ce** 140.12 | 59 **Pr** 140.91 | 60 **Nd** 144.24 | 61 **Pm** (145) | 62 **Sm** 150.36 | 63 **Eu** 151.96 | 64 **Gd** 157.25 | 65 **Tb** 158.93 | 66 **Dy** 162.50 | 67 **Ho** 164.93 | 68 **Er** 167.26 | 69 **Tm** 168.93 | 70 **Yb** 173.04 | 71 **Lu** 174.97 |
|---|---|---|---|---|---|---|---|---|---|---|---|---|---|

**Actinides**

| 90 **Th** 232.04 | 91 **Pa** 231.04 | 92 **U** 238.03 | 93 **Np** (237) | 94 **Pu** (244) | 95 **Am** (243) | 96 **Cm** (247) | 97 **Bk** (247) | 98 **Cf** (251) | 99 **Es** (252) | 100 **Fm** (257) | 101 **Md** (258) | 102 **No** (259) | 103 **Lr** (262) |
|---|---|---|---|---|---|---|---|---|---|---|---|---|---|